Scientific Programming

Decision Support System for Developing Smart and Intelligent Applications

Lead Guest Editor: Muhammad Usman
Guest Editors: Muhammad Zakarya and Abid Yahya

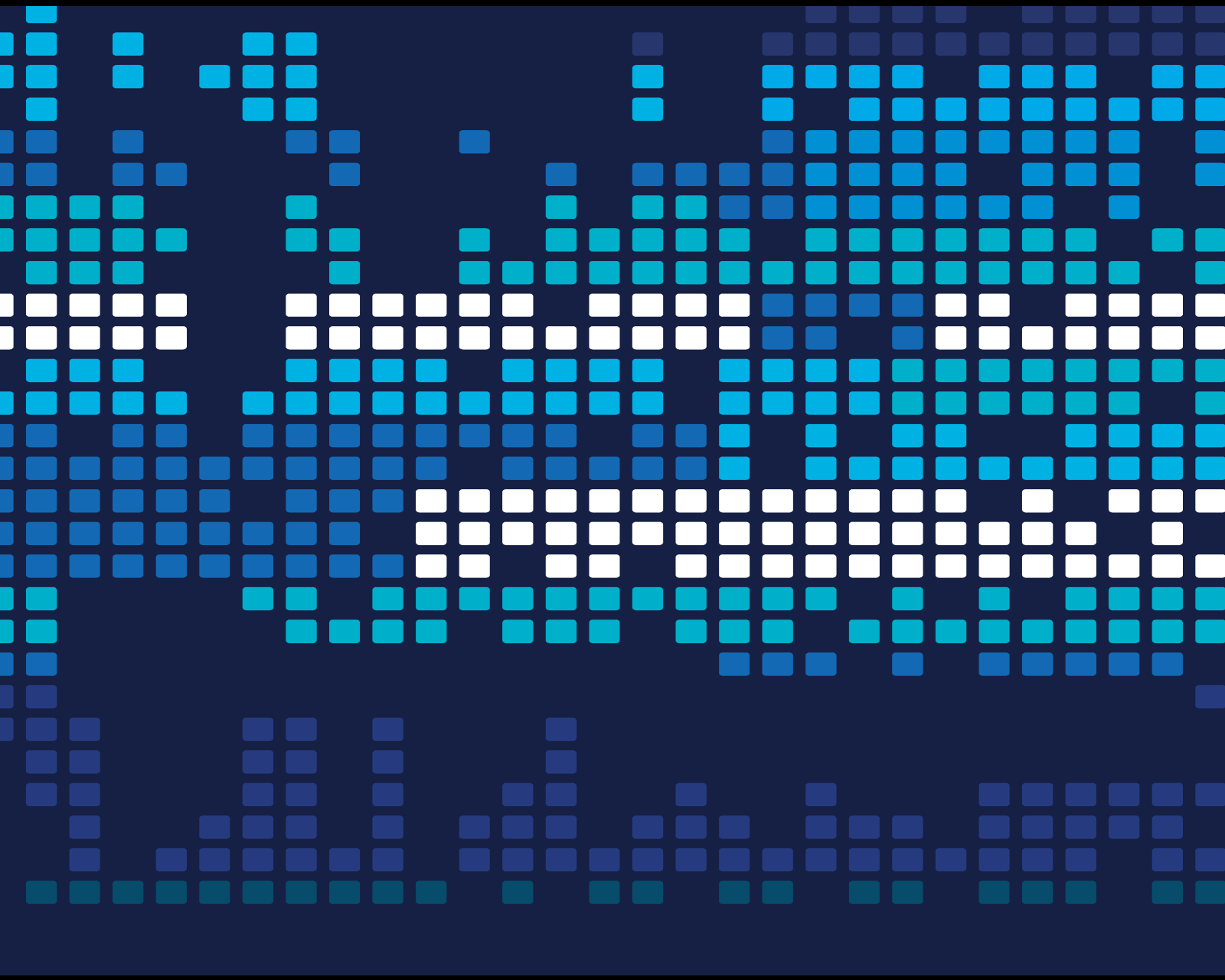

Decision Support System for Developing Smart and Intelligent Applications

Scientific Programming

Decision Support System for Developing Smart and Intelligent Applications

Lead Guest Editor: Muhammad Usman
Guest Editors: Muhammad Zakarya and Abid Yahya

Contents

Contents

Contents

Hindawi
Scientific Programming
Volume 2023, Article ID 9769278, 1 page
https://doi.org/10.1155/2023/9769278

Retraction

Retracted: Construction of a Six-Pronge Intelligent Physical Education Classroom Model in Colleges and Universities

Scientific Programming

Received 26 September 2023; Accepted 26 September 2023; Published 27 September 2023

This article has been retracted by Hindawi following an investigation undertaken by the publisher [1]. This investigation has uncovered evidence of one or more of the following indicators of systematic manipulation of the publication process:

(1) Discrepancies in scope
(2) Discrepancies in the description of the research reported
(3) Discrepancies between the availability of data and the research described
(4) Inappropriate citations
(5) Incoherent, meaningless and/or irrelevant content included in the article
(6) Peer-review manipulation

The presence of these indicators undermines our confidence in the integrity of the article's content and we cannot, therefore, vouch for its reliability. Please note that this notice is intended solely to alert readers that the content of this article is unreliable. We have not investigated whether authors were aware of or involved in the systematic manipulation of the publication process.

In addition, our investigation has also shown that one or more of the following human-subject reporting requirements has not been met in this article: ethical approval by an Institutional Review Board (IRB) committee or equivalent, patient/participant consent to participate, and/or agreement to publish patient/participant details (where relevant).

Wiley and Hindawi regrets that the usual quality checks did not identify these issues before publication and have since put additional measures in place to safeguard research integrity.

We wish to credit our own Research Integrity and Research Publishing teams and anonymous and named external researchers and research integrity experts for contributing to this investigation.

The corresponding author, as the representative of all authors, has been given the opportunity to register their agreement or disagreement to this retraction. We have kept a record of any response received.

References

[1] L. Zhou and Q. Tang, "Construction of a Six-Pronge Intelligent Physical Education Classroom Model in Colleges and Universities," *Scientific Programming*, vol. 2022, Article ID 9003864, 11 pages, 2022.

Hindawi
Scientific Programming
Volume 2022, Article ID 1027211, 21 pages
https://doi.org/10.1155/2022/1027211

Research Article

Intelligent System Construction Paths for Digitalization Process of Real Economy: A Study from the Perspective of Artificial Intelligence and Platform Leverage

Huayao Zhang, Jing Wen, Xiaoling Chen, Yuqing Ge, and Yuting Chen

School of Management, Zhejiang University of Technology, Hangzhou, Zhejiang 310023, China

Correspondence should be addressed to Jing Wen; wenjing83@zjut.edu.cn

Received 13 March 2022; Revised 30 March 2022; Accepted 4 April 2022; Published 14 September 2022

Academic Editor: Muhammad Zakarya

This study studies the internal driving force and system construction issues in the integration of information technology and traditional business. Established on theory of platform leverage in the value creation, we use causal analysis and case studies to explore two closely related questions with data of 31 digital platforms (including 21 focal cases and 10 reference cases): (i) what is the value creation mechanism of these digital platforms? and (ii) how does the value creation mechanism affect the construction path of the system? The study identified three typical value creation mechanism configurations, i.e., innovation-driven, business integration, and data-driven, and then explained the system construction paths of these three configurations. We observed that the production and innovation leverages are the general construction drivers of the platform. However, the transaction leverage is only significant in a small number of platforms; that is, the role of network effects can be observed. These findings can deepen our understanding of platform theory in the digitalization of the real economy and explain why network effects cannot be the source of competitive advantage within the economic digitalization scenarios. We believe that it is of great significance to the digital transformation practice of the economy.

1. Introduction

With the deep integration of information technologies such as the Internet of things (IoT), cloud computing, and big data with traditional business models, the digitization of the real economy is changing the competitive landscapes in many industries and ultimately completely reshaping the market and society [1–3]. In the process of digital transformation, the practice of forming a cross-organizational coordination system based on digital platforms and driving the digital transformation of access enterprises [4] has spread across various real economic fields such as manufacturing, distribution, and professional services, representing the current mainstream phenomenon of the digital transformation. However, the process of digital transformation in real economy has similar structural characteristics to the classic Internet economy whose typical characteristic is individual access. Furthermore, it exhibits completely different economic characteristics, which leads to frequent difficulties in platform patterns based on experience logic. Exploring its inherent principles will not only help reduce the huge waste of resources and business opportunities for enterprises but also be the key to the smooth implementation of digital transformation strategy in China and even all over in world.

Exploring the inherent principles of cross-organizational coordination system cannot ignore the basic characteristics of organizational coordination, which determines the construction logic of the entire system. The current research on digital transformation in Industry 4.0 and information systems generally agrees that the system has two basic characteristics: firstly, the integration process is the combination of information systems and enterprise operation systems [5–7]; secondly, it is difficult to see the economic benefits of digitalization in the short term [8]. The above two characteristics make the value creation ability of digital platforms become the key to system construction [9].

The value creation ability of the platform in organizational coordination is the role of leverage, intending to emphasize that the platform can achieve leverage beyond the conventional input-output ratio through certain measures [10]. The authors proposed three leverages based on combing different schools of research, that is transaction leverage, production leverage, and innovation leverage. The current mainstream of construction logic in platform system believes that traction leverage is the core value creation mechanism of the platform. Transaction leverage reflects the role of positive network effect (In the discussion context of platform competitive advantage, platform entrepreneurship, and other issues, network effects generally refer to positive effects, such as and Evans [11]; that is, when a market involves different customer groups, the number of individuals in different customer groups determines the value of the market [12].) that represents the core view of market intermediary stream and has a profound impact on practice [10–13]. The market intermediary stream can be reviewed as the affiliation of platform construction, and construction logic corresponding to the view of affiliation is called the structure view [14]. The structural perspective leads the system construction logic of the platform to digital transformation, focuses on the fit between the platform and the users of platform and even other stakeholders, and emphasizes the importance of strategic attention to different users of platform [14, 15]. Although the structural view has received extensive attention, there is a lack of comprehensive discussion on the impact of the two basic characteristics in digitization, and it is still difficult to systematically answer two basic theoretical questions: (1) what value-creating mechanisms do digital platforms in different industries have? (2) How does the value creation mechanism affect the construction path of the system? These two issues are closely related and are the core of understanding the laws of digitalization of the real economy and determine the direction and focus of resource investment in practice.

Platforms are everywhere, including all the patterns of Internet within an organization or interorganizations [16], and the complexity of the system and the diversity of system patterns make it difficult to conduct research using a single case study approach. This study will adopt a hybrid research method of fuzzy set qualitative comparative analysis (fsQCA) and case study. We firstly use fsQCA as an auxiliary method [17] to classify multiple cases and use case study to link the complex and diverse platform context with the effect of system construction. The major contributions of this study are as follows:

(i) investigate the internal driving force and system construction issues in the integration of information technology and traditional business

(ii) We use causal analysis and case studies to explore (i) what is the value creation mechanism of these digital platforms and (ii) how does the value creation mechanism affect the construction path of the system

(iii) We discuss the dynamic mechanism and construction path of the system in the digital transformation process

The following sections are carried out in the following order: Section 2 reviews the literature on the leverage of platform value creation and the digital characteristics of the real economy and identifies research questions; Section 3 introduces research design and case selection; Sections 4 and 5 introduce the steps and findings of fsQCA and case studies, show the causal logic configuration of the platform value found by fsQCA, and analyze the system construction paths under different logic configurations; Section 6 is the discussion; and finally, Section 7 concludes this study.

2. Theoretical Background

2.1. Leverage of Value Creation in Platform. "Platform" is used to describe the management phenomenon of individual products, product systems, industry supply chains, markets, industries, and even clusters [18] and is sometimes referred to as platform strategy [14]. Researchers generally believe that modularity and mutual benefit are two core characteristics of platforms [15], and they are the source of value creation in platform. Organizational stream reviews that the organizational resources and capability structures should be shared [19]. The product family stream represents that economic advantages are created in supporting flexibility in product development and product functionality [20]. The market intermediation stream emphasizes the efficiency of two-sided market in connecting supply and demand [12]. Platform ecosystem stream identifies the specialization and complementarity embodied in sharing core technologies [21], which are the result of the combined effects of modularity and mutual benefits. Three leverages are put forward based on two characteristics of the value creation mechanism, among which, the transaction leverage is mainly based on the classic research of the market intermediary stream, the production leverage is mainly based on the classic research of the organization and product family stream, and the innovation leverage is mainly based on the classic research of the platform ecosystem stream [10]. The definitions and dimensions of various leverages are detailed in Table 1.

The basic feature of digitization is that platform operators use information systems to provide digital service activities for various users [30]. We used CiteSpace to analyze the Web of Science literature around the related literature and found that there are two perspectives that discussed the potentials brought by digital information technology and the advantages generated by integration, that is, information technology perspective and digital service perspective, both of which provided rich insights for understanding leverages (see Table 1).

2.1.1. Trade Leverage. The information technology perspective literature treats digital platforms as software-based platforms [35], representing that the reprogrammability, data homogeneity, and self-referentiality of digital technologies provide technical support for the realization of a two-sided market structure [23]. With such support, value is created for transactions between supply and demand (or multiple parties) by directly matching supply and demand,

Table 1: Three leverages in digitalization.

	Transaction leverage	Production leverage	Innovation leverage
Definition	Improve transaction efficiency and reduce search costs based on manipulation of pricing and governance including market availability, pricing mechanism, and entry mechanism	Use interfaces and standards to share resources to motivate economies of scale and scope including production (including service) quality/efficiency, production organization, and production methods	Use interfaces and standards to share resources to facilitate the creation of new goods and services including product/service quality and new product/service business process
Information technology perspective	(i) The layered network architecture provided by digital technologies supports the multi-/bilateral market structure of the physical world [22, 23]	(i) The widespread use of IoT components promotes monitoring, control optimization, and autonomy, promotes new business generation, and improves management efficiency [1, 24, 25]	(i) Digital artifacts lead to changes in the time and space boundaries of innovation, promote knowledge sharing and collaborative changes, and shape distributed innovation (ii) The modular and complementary architecture of the digital platform facilitates collaboration between the platform and access parties [26–29]
Digital service perspective	Data help service providers reduce market friction by matching two different players searching for each other [22, 30–32]	Effective data analysis can improve services or execute data-driven algorithmic decision-making processes more efficiently [7, 33, 34]	Data can fuel open innovation, or expand business models to new customer groups [32]

Note. The division and definition of leverage are based on Thomas et al.

suggesting possible transactions, or providing powerful search capabilities [36]. The literature from the perspective of digital services believes that digital services are a data-intensive process [37], which works by accessing different data sources to form an intelligent autonomous system with users, providing platform with the opportunity to create data streams and create opportunities for further development of value-added services [30]. It has been proved that the logical structure of two-sided markets correlates with emerging opportunities created by data [32], and data help reduce market friction in matching participants [36]. The above research shows that IT and digital services themselves contain the basis for the generation of transaction leverage and do not necessarily rely on platform operators to achieve through pricing mechanisms and entry mechanisms.

2.1.2. Production Leverage. The role of information system in production is closely connected to new technological hardware. The widespread use of IoT components not only provides value in terms of monitoring, control, optimization, and autonomy [1], making the real world more personalized and efficient, and enabling the creation of value-added services [24], but also greatly improves the management efficiency of industrial processes in enterprises [25]. The large amount of user/product-generated data is the key to creating value [33], and companies can use effective data analysis to provide better services or more efficient decision-making processes to gain competitive advantage [7, 34]. Therefore, the generation of production leverage is not only based on the combination of modular and complementary but also depends on the productivity brought by digital systems and data.

2.1.3. Innovation Leverage. Existing literature has pointed out that digital infrastructure enhances the innovation capability of enterprises through two functions [28]: firstly, digital technology leads to changes in the time and space boundaries of innovation, enabling the innovation process to spread across time and space, promoting knowledge sharing, collaborative paradigm change, and the emergence of a distributed innovation landscape [26]; secondly, the boundaries and interface functions of digital platforms change the function of boundaries, turning boundaries between complementary companies from barriers to point of penetration for resource connections [27], facilitating cross-organizational collaboration and the creation of new products [26, 28, 29]. From a data service perspective, the data in the platform can be used as a trigger to enhance the value capture mechanism of entire system [32], which can facilitate the open innovation of the platform or expand the business model to new customer groups [32]. On the one hand, these findings show that the digital system has changed the principles of innovation, and on the other hand, the emergence of multi-/bilateral market structure is not necessarily the result of the increase in the number of access parties, but may be an endogenous value-added method of the system.

2.2. System Construction Characteristics in Digitization of the Real Economy

2.2.1. Influencing Factors in Platform Context. The digitization of real economy is characterized by the fusion of information systems and business operating systems [30]. The result of digitalization is a complex cyber-physical system [38]. The factors from the business operating system and other factors in the progress of integration of IT system and operation system will exert significant impacts on digitalization, which results in the uniqueness of the system construction. The platform context refers to the characteristics of platform that affect the leverages [6], including various factors impacting digitization. Combing the research

of information technology and platform governance, we can see that the platform context involves both information technology and enterprise operations. Digitization means the deep integration of information technology and daily operations of enterprises, which requires digital platforms to penetrate business processes. Therefore, the system construction process is regarded as a process of human-machine integration and business integration [39, 40]. The newest research also highly emphasizes the role of the two integrations in the progress of digitization. According to Accenture research, 86% of senior managers believe that the use of digital technologies at the personal level is important to digitization ("accessed" "title="https://www.accenture.com/us-en/insights/technology/technology-trends-2021, accessed"">https://www.accenture.com/us-en/insights/technology/technology-trends-2021, accessed to 20.3.2021). In digital transformation, research mostly emphasizes the role of new technologies in integrating different processes and activities [41]. Achieving digitization requires recombining digital assets with other organizational resources to transform the way business. Digitalization can enhance the value creation through continuously sensing and seizing market opportunities as demonstrated in [9, 19].

In addition, the platform context involves the factors of all parties involved in the platform system. The platform system is a value co-creation system composed of platform operators and various users, and they are the key subjects that influence leverages [9]. From the perspective of system operation, the ability to provide high-quality digital services is an important prerequisite for the generation of leverages. For example, the triggering role of data in the capture of system value will provide advantages for the digital companies which already have certain amount of business [32]. However, this triggering effect needs sufficient data resources and the abilities of data mining, which reflects the resource endowment in the progress of platform's growth. From the perspective of users, since digitization often requires a certain amount of investment, for example, the digitalization in industries may represent the transformation of production lines, but it is difficult to achieve economic results in the short term, so it faces the "digital paradox" [42]. The users may have higher requirements than strategic fit [14] when participating in digitalization. Due to the particularity of the digitization of real economy, the impact from the platform context may be complex and diverse.

2.2.2. Measurement of System Construction. The digitization of the real economy is also characterized by a long economic return cycle, which limits the use of financial indicators to measure transformation results. On the one hand, digitalization comes with high installation costs and long payback periods [42], and many companies are willing to accept short-term losses in exchange for long-term growth [9]. On the other hand, the various improvements brought about by digital technologies are often more attractive, and new business models are often placed on higher expectations than the direct economic effects. Digitalization can dynamically adjust production processes through process monitoring and leverage transformative digital metrics to provide finer-grained insights [9], which will bring new business models to enterprises [19].

In terms of the characteristics of digitalization, the quick response enthusiasm of users can reflect the system construction effect much better. The essence of digitization is the realization of complex solutions in integration [30], which will pose huge challenges to the knowledge and capabilities of platform owners [41]. The active interaction and response of users will facilitate the sharing of more resources, knowledge, and skills [6] and promote the digitalization process.

It can be seen from the above research that leverage is an inherent feature of the platform, and the three leverages coexist in a platform context. However, due to the differentiated platform contexts, different combinations of leverage may be used to promote system interaction and then have an impact on system construction. The following research will provide the following possibilities: firstly, the leverage is examined through the effect of constructing digital platform system; secondly, the platform context factors through clarifying leverages will be found; and finally, we will identify different system construction paths with different leverages. However, as far as the current research is concerned, there are still a series of issues to be studied in the research topics related to the value creation mechanism and system construction in the digitalization of real economy, such as what different leverage combinations are mainly present in the value creation mechanism? what is the platform context for various value creation mechanisms? and what are the significant influencing factors in the platform context? From the platform environment to value creation to system interaction, what are the key driving forces in different value creation mechanisms? The key to revealing this series of problems lies in how to classify complex and diverse platform contexts.

3. Methodology

We view the digital platforms as a set of creating value through multi-agent collaboration. According to the principles of set theory (open set and pair set axioms), there are several subsets reflecting the diversity of contexts. fsQCA can support the research of relatively large amount of cases and find various configurations. fsQCA has been affirmed by mainstream journals all over the world [43], and its logical basis is finding the unique phenomenon in comparison [44]. faQCA reduces complexity in limited diversity cases, provides a framework for case comparison, and explores the patterns of configuration types [17].

This study will use fsQCA and case study jointly to find the value creation mechanisms. The reasons are as follows: firstly, the combination of leverages reflects the specific mechanisms of platform value creation, and fsQCA has the advantages of finding regularities in a specific combination [17]. When performing configuration analysis, it can identify a typical case. fsQCA can also present a framework of combination between different leverages and provide opportunities of inducing commonness and finally clearly

Table 2: Overview of the research methods.

Research method selection	fsQCA	Case study
The purpose of analysis	(i) Distinguish and analyze the connection of value creation mechanisms (explore whether the notion of affiliation is a realistic system-building logic) (ii) Establish a causal logic configuration to provide a basis for case interpretation	(i) Identify characteristics, dynamics, and building path of configurations (ii) Answer why affiliation is not the construction logic of in reality
The resources of research	(i) Construct variable value (ii) Describe each case	(i) Construct logic configuration (ii) Describe each case
The output of research	(i) The logic relation of value creation mechanism (ii) The framework of logic configuration	(i) The characteristics of platform configuration (ii) The driving forces and paths of system construction

show the commonness of logical configurations. Based on the above analysis of fsQCA, it is found that the multi-case analysis can show the relationship between the characteristics of platform context in the logical configuration, the value creation mechanism configuration, and the system construction result, thus showing the digital realization path. The internal logical relationship of the two methods is shown in Table 2. The entire analysis process includes many cross-stage iterations. For example, when problems are encountered in the consistency check in fsQCA, additional research on conflict cases is required to confirm the accuracy of assignments. The case study will observe the robustness of typical case studies and the commonness of cases through dynamically adjusting the case scope and criteria of consistency.

There are two sources of the analyzed cases in this study: one is the 8 first-hand cases developed by authors, and the other is 23 second-hand cases recorded in China Management Case Sharing Center (Three conditions are required to be met when selecting case base cases: (1) the keywords contain "platform (ecosystem)," "digital transformation," and "digital information system"; (2) there are substantial expressions of three types of leverages and system construction effects; and (3) there is a commitment to the authenticity of the information.). The cases tracked by the author's team have records of multiple rounds of field investigations and interviews. In addition to the case text, the second-hand cases are supplemented with other second-hand data and confirmatory research. There is no significant difference in the completeness of information between the two sources of cases.

In terms of case selection, we follow the classification of platforms proposed by 44 and focus on supply chain platforms (case codes starting with B) and industrial platforms (case codes starting with C), both of which represent the collaborative relationship between platform operators and users. At the same time, 10 intra-enterprise platforms are added for reference (the case code starts with A) (The cases for reference help to play an opposing reference role in indicator assignment, consistency checking, and case subset discovery. The research and data analysis process for the reference case is the same as that for the focus case. Reference cases include A-HMZY, A-XADT, A-KTZN, A-ZKXC, A-ZHCG, A-FSK, A-LBJT, A-MCYP, A-HBJT, and A-BLJT.). It can be seen from Table 3 that production or professional services in the supply chain platform are common features, while professional services in the industrial platform are the main manifestation, both of which reflect the basic characteristics of the business integration. In terms of functional positioning, 6 of 9 supply chain platforms have transaction functions, while only 3 of 12 industrial platforms have transaction functions. The case information and details are shown in Table 3.

4. fsQCA

4.1. Variable Assignment. This study identifies antecedent variables and configuration output variables according to the constructs and dimensions presented in the well-known theory of the platform leverage in the value creation [10]. In addition to the three leverage effects, as discussed earlier, the antecedent variables also add the platform type (Platform_type) as a control variable to eliminate the influence of the type gap, and the configuration output variable adopts the construction effect; see Table 4 for further details.

The fuzzy assignment of research indicators is the basis of the analysis. In fact, this requires a comprehensive and complete understanding of all cases. In this research, we use the quartile assignment method, which is put forward by Ragin [45]. This method mainly includes three steps: (1) review the whole cases, extract the materials for indexes, make tables for each case, and merge the materials according to the dimensions; (2) set the key points (0.33, 0.67) according to the quartile method and identify case groups; and (3) sort the cases within the group and assign subjective numbers to the indicators. The fuzzy assignment process of the indicators is shown in Table 5. Further details on this method are illustrated in Ragin [45].

4.2. Logical Relationship of Leverages. This study uses transaction leverage to reflect network effects, as transaction leverage reflects the information matching and search value brought about by (virtual) two-sided market [22]. However, because "the number of users of one group affecting the willingness of other groups to access" in the concept of network effect [12] is an abstract description, it is difficult to

Table 3: Information of cases.

No.	Case code	Case description	Case sources	Platform functions
1	B-GBWJ	Digitally empowered internal platform/stationery manufacturing in R&D design, manufacturing, service marketing	Second-hand case Communication investigation	Transaction manufacturing
2	B-MYZS	A shared manufacturing platform aiming at outputting cloud services of the whole value chain/covering multiple manufacturing industries	Second-hand case Communication investigation	Manufacturing
3	B-QHW	Transaction, collaboration, and sharing platform of industrial chain resources in the chemical industry/chemical product transaction, industry information, legal services, etc.	Second-hand case	Transaction service
4	B-PM	Construction industry platform based on BIM technology/BIM software and construction solutions for the construction industry	Second-hand case field investigation	Personal services
5	B-ZSZK	Industrial Internet platform based on data services/covering transportation and multi-manufacturing industries	Second-hand case Communication investigation	Transaction manufacturing
6	B-ZTGF	Underground engineering whole industry chain platform/shield machine leasing, engineer sharing, equipment part trading, shield tunneling construction, etc.	Second-hand case	Transaction service manufacturing
7	B-HCB	"Internet + logistics" sharing platform/vehicle-cargo matching, after-vehicle services, and three major business systems of finance	Second-hand case Communication investigation	Transaction Services
8	B-ZCQC	Collaborative design and lean manufacturing enterprise platform/rail transit equipment manufacturing	Second-hand case Communication investigation	Manufacturing
9	B HYJT	Production and trading platform of the whole industry chain of chemical fiber textile industry/chemical industry	Field investigation	Manufacturing transaction
10	C-MHS	Chemical industry B2B platform/chemical industry information transaction service	Second-hand case	Transaction services
11	C-ZBJW	"Big data+" crowdsourcing service platform/intellectual property, finance and taxation, finance, printing	Second-hand case	Professional services
12	C-HLB	Advertising creative vertical service crowdsourcing platform/brand case, technology development, and other services	Second-hand case	Professional services
13	C-HMW	Whole industry chain solution B2B innovation platform/new services such as cloud computing and information services	Second-hand case	Professional services
14	C-AJSH	One-stop home improvement service platform/home improvement process and services	Second-hand case	Professional services
15	C-YSJJ	C2F cloud home online customization platform/custom furniture whole process and service	Second-hand case Communication investigation	Professional services
16	C-NBCX	Customized service industrial Internet platform/textile intelligent manufacturing online and services	Second-hand case	Manufacturing services
17	C-SYB	Capacity sharing intelligent manufacturing platform/full-process service of metal and plastic processing and production	Field investigation	Professional service
18	C-ZFW	Textile industry idle capacity service platform/textile industry upstream and downstream enterprise transactions	Field investigation	Transaction
19	C-SZZN	AI service and business platform/"intelligent + artificial" model legal consultation and AI + RPA digital employee service	Field investigation	Professional service
20	C-XLMY	Psychological counseling service platform based on artificial intelligence/"intelligent + artificial" mode of psychological counseling service	Field investigation	Professional service
21	X-XBB	A comprehensive service platform for the luggage industry/industry chain capacity sharing service aiming at building the whole industry chain ecosystem of luggage and leather goods	Field investigation	Transaction

Note. *Production function: the access terminal is a platform function that dynamically identifies the data source and can go deep into the machine level; transaction function: the access terminal is a platform function that statically identifies the data source and mainly promotes transactions; professional service functions: platform functions that provide professional services based on industry professional activities; the distinction between transaction and professional service functions is based on whether professional activities continue to exist in the transaction.

Table 4: Variables.

Types of variables	Definitions and dimensions	Explanation
Leverage	Transaction leverage (match): improves transaction efficiency through information retrieval and matching capabilities (i) Market availability: improves the availability of market information and improves transaction efficiency through information technology (ii) Pricing mechanism: improves transaction efficiency through pricing mechanism and means Production leverage (production): achieving economies of scale and scope based on recombination of assets/resources in production, generating leverage (i) Product quality/efficiency: digitization improves product/service design quality or reduces cost and development time through reutilization of production resources (ii) Organizational constructor: digitization changes organizational structures, reorganizes supply chains, or generates new ways of organizing business Innovation leverage (innovation): the collection of assets drives innovation and the realization of complementary economies and the creation of new products/services (i) Product quality: digitalization improves product performance and service quality through efficient use of knowledge (ii) New product: digitization facilitates the development of new products or services (iii) Business model innovation (It is difficult to distinguish production methods and organizational processes in the data from cases, and they both reflect the content of business model innovation so this study uses business model innovation as a dimension of innovation leverage.): digitization changes the way value is created by innovating business processes/connections Platform type: the degree of extension from within the enterprise to the industry (in the actual measurement, the assignment range is first determined according to the type of platform; that is, the internal platform of the enterprise is less than 0.33, the industry chain platform is between 0.33 and 0.67, and the industrial platform is greater than 0.67)	Antecedent variables
The outcome of system construction	Outcome: the extension of users' acceptance (in this study, the quartile method is used to measure the resistance encountered in the digitalization. Less than 0.33 represents there are obvious twists and turns in the progress of digitalization; from 0.33 to 0.67 means the process is basically smooth when encountering obstacles; more than 0.67 suggests there is no obstacle in the progress of digitalization)	*Output variables*

find data in cases, while transaction leverage defines the specific activities or means of realization. The research explores the following questions in turn: (1) is transaction leverage an important value-creating mechanism in reality? A key point in the indicator value is 0.67, and a leverage variable above this value means that the system is being built substantially. The assignments of each dimension are combined according to the logical OR algorithm, which reflects the strength of various leverages in a case (As long as there is a strong leverage in one dimension, it indicates that the leverage is strong. The calculation method is as follows: $a = \max(a_1, a_2, \ldots, a_m)$). When the transaction leverage exceeds the key point of 0.67, it means that the transaction leverage is an important value creation mechanism. (2) Is trading leverage an antecedent or a consequence of system construction? The causal relationship between transaction leverage and "production + innovation leverage" is tested, respectively, and then, the logical relationship between transaction leverage and "production + innovation leverage" is analyzed with transaction leverage as the outcome variable.

Firstly, a significance analysis on each leverage is performed. Figure 1 shows the numbers of the three leverages for each case. In terms of quantity, among 21 cases, only four cases (QHW, ZTGF, HCB, and MHS) have transaction leverages. Exceeding the key point means that the network effect promotes the system construction, but correspondingly, there are 16 cases where the production leverage or innovation leverage has played a promoting role, and there are 3 cases (GBWJ, ZFW, and XBB) that show no leverage to reach the substantial influence line of 0.67. Notably, in three of four cases where the transaction leverage exceeded the key point, the production and/or innovation leverage also exceeded the key point, which leads us to speculate that the transaction leverage may be the result of other leverages. According to the view of affiliation (the intermediary market stream in Thomas et al. 10), transaction leverage is the core value creation mechanism of platforms, and correspondingly, the logic or effects of production leverage and innovation leverage represent competing hypotheses. The mean value of transaction leverage of 0.57 means that no significant impact is achieved, while the corresponding numbers of production leverage and innovation leverage both exceed the key point of 0.67, and the logical OR effect reaches 0.76. This shows that transaction leverage is not an important value-creating mechanism, and the competitive view of affiliation can be more realistically supported. Compared with network effect logic, it is more realistic to overcome real difficulties in digitalization through production leverage or innovation leverage.

Furthermore, the causal relationship between transaction leverage and "production + innovation leverage" is tested, respectively, and then, the logical relationship

Table 5: Fuzzy assignment of indicators.

	The first step	The second step	第三步
contents	I) Classifying and integrate case data According to the materials collected in the independent case material table, the expressions that best reflect the characteristics of the case indicators are classified one by one according to the variable dimensions.	I) Identifying the key points Comprehensively understand the meaning of the expressions, sort them in order of impact strength, and find out whether there is a significant impact on the cut-off point and whether it has a substantial impact on the system construction.°	I) Assigning indexes Independently compare each expression in the three groups identified by the two key points, and assign corresponding numbers according to the strengthof the effect
examples	I) *Product quality/efficiency* II) Changed the status quo of exchanging overtime for economic benefits... It only takes 7 days to complete the customization, and the minimum cost is only 2,000 yuan (A-KTZN) III) Through the big data of freight transportation...realize intelligent vehicle and cargo matching, intelligent real -time scheduling...improve the operation efficiency of road logistics, and reasonably change the flow and direction of transportation capacity (B-HCB) IV) Deeply solve...multi-party collaboration problems, improve the work efficiency of construction enterprises, provide...solutions (B-PM) I) The first house interior measurement software to optimize the design process... Improve service efficiency and reduce labor costs (C-YSJJ) II) "Remote shop inspection system" greatly improves the efficiency, ... 6 shop inspection tasks can be completed every day, which improves the efficiency (A-MCYP) III) Using the big data of the platform, subcontract the total order of the brand to the appropriate processing factory... The order can be completed in as little as 3 days (C-SYB)	Key point: 0.33 The dividing line between the low and middle segments, the difference in is whether a realistic and credible significant impact can be found Key point: 0.67 The boundary between the middle section and the high section, the difference in impact is whether it has a substantial impact on the system construction	0-0.33 0.33-0.67 0.67-1
Notes:	I) Generally, it is the expression that best reflects the core business, or the expression that has a substantive effect in the corresponding material of the indicator.	I) The attention of this step should be placed on judging which influence level the material belongs to; II) The key point is not to divide the material sequence into three equal parts, it should be judged according to the material.	I) The assignment within the group does not need to be uniform, and the order and size should be judged according to the actual content.

between transaction leverage and "production + innovation leverage" is analyzed with transaction leverage as the outcome variable. Table 2 is two-dimensional diagram based on the above analysis. When the causality hypothesis is satisfied, the points representing the case will be uniformly distributed on one side of the diagonal, and the consistency test value is close to 1; on the contrary, when the points are randomly scattered on both sides of the diagonal, then the assumption cannot be satisfied. It is generally considered that the consistency level is an ideal level when it exceeds 0.9.

As shown in Figure 2, except that the results of Figure 2(a) do not support the causality hypothesis, Figures 2(b) and 2(c) both support the assumption that the X condition is a sufficient condition for the Y result [17]. This shows that the concept of affiliation perspective of system construction cannot be supported, while the competitive hypothesis is strongly supported. The data support that transaction leverage is the result of the value creation activities of production and innovation leverage, indicating that transaction leverage is not the antecedent of system construction, but the result of system construction. We propose the following proposition based on the above analysis.

Proposition 1. *In the digital platform formed by the digitization of the real economy, the network effect is not a means to promote the system construction, but the result of system construction.*

4.3. Configuration Analysis. The fsQCA configuration analysis determines the identification of the characteristics of platform context and discovers the paths of system construction. It mainly includes the following steps: (1) carrying out logical operations on different dimensions of each leverage according to the logic and merging variables to eliminate vacancies; (2) calibrating data (fsQCA is an analysis based on the principle of set theory, so it is also a formal system. The numerical structure after logical merging

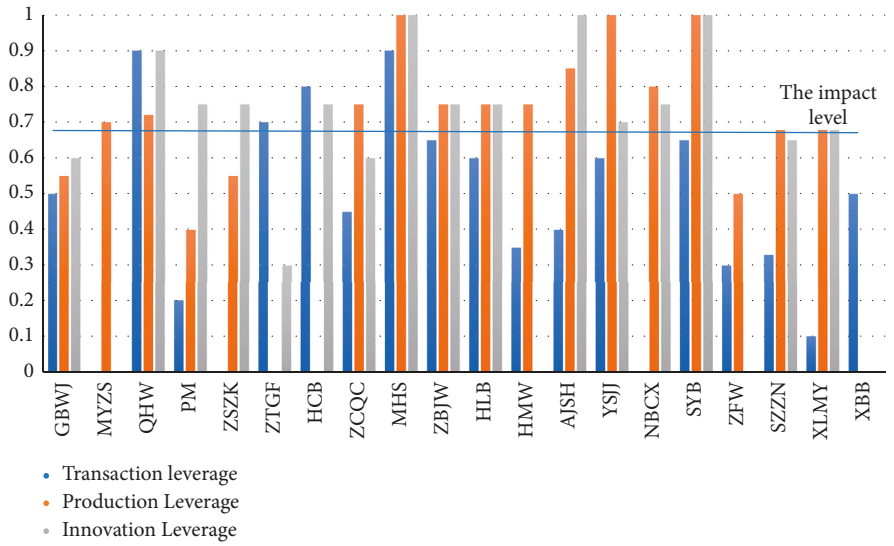

Figure 1: Significant comparison of three leverages.

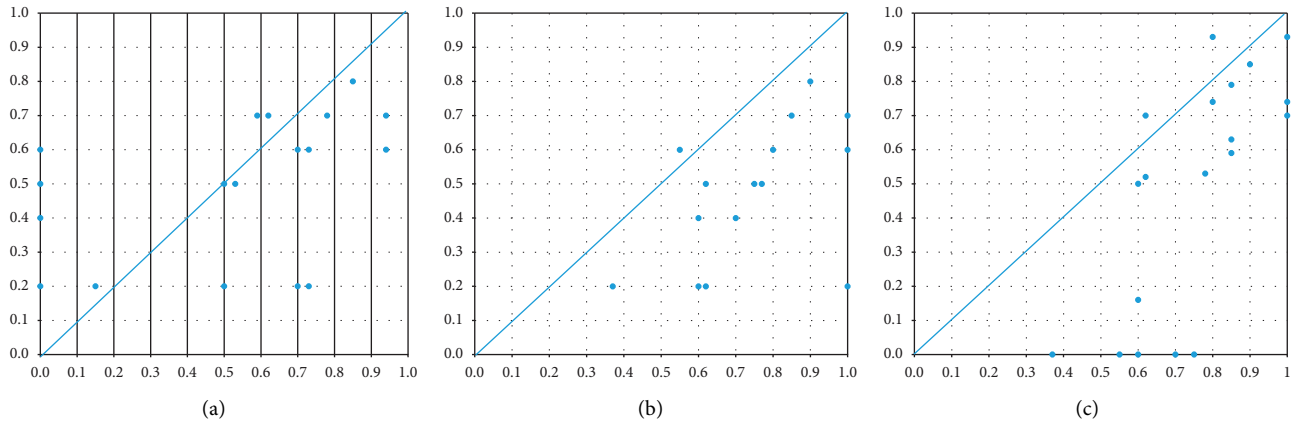

Figure 2: Two-dimensional logic verification of transaction leverage. (a) X: match. Y: outcome. Consist. $X \geq Y$: 0.5336. (b) X: Production and Innovation. Y: outcome. Consist. $X \geq Y$: 0.9946. (c) X: Pro.andInno. Y: match. Consist. $X \geq Y$: 0.9774.

has changed, and it is difficult to ensure the basic symmetry relative to the intermediate value. The calibration maps 0.67 to 0.5, 0, and 1, which remains unchanged.); (3) adjusting the case selection range and consistency criteria for standard configuration analysis, and comparing the results to ensure the robustness of the analysis results; (4) conducting additional investigations and assignment corrections for contradictory cases; and (5) configuration analysis and identifying antecedent combinations and corresponding cases. Among them, in the analysis of step 3, the test coverage of transaction leverage as a logical output is high (97.8%), but the consistency is not high, which indicates the existence of different subsets. Therefore, we transform different levels of consistency to compare output from standard configuration analysis to enhance robustness (The exploration found that better results can be obtained with a lower consistency standard, and the intra-enterprise platform and no two-sided market can be removed through the "~Platform_type" variable. Therefore, the final output is based on the analysis of 31 cases.).

The process of configuration analysis is also the process of identifying and deleting inappropriate cases: (1) there are three cases who did not generate a bilateral structure, that is, MYZS, PM, and ZSZK, so they are not included in the final case studies. The identified configurations included all cases that have developed into a two-sided market structure, which ensures the rationality of the discussion of transaction leverage; (2) among the four subsets generated by the configuration analysis, there is one subset (including ZFW and XBB) that shows completely different characteristics from other cases, because both of them are only online trading platforms in the industry, and they have not been integrated with the business as of the time of the survey, which is difficult to reflect the actual research purpose, so we will not discuss these two cases.

Table 6 presents different value creation configurations (According to the exploratory analysis, this table removes the configuration with the "~Platform_type" antecedent condition in the consistency level of 0.735 and the intermediate solution results in the full case set (this category

Table 6: Platform system construction truth table and typical cases.

No.	Assumptions and implications	Coverage	Consistency	Typical case (membership degree greater than 0.5)
I	Innovation ∗ match	0.462	0.754	C-MHS, B-HCB, B-QHW, B-ZTGF, C-ZBJW, C-SYB, C-YSJJ, B-GBWJ, C-HLB, B-ZCQC, C-AJSH
II	Production ∗ innovation	0.589	0.702	C-MHS, C-YSJJ, C-SYB, C-AJSH, C-NBCX, B-ZCQC, C-ZBJW, C-HLB, B-QHW, C-SZZN, C-XLMY, C-HYJT
III	Production ∗ platform_type ∗ match	0.373	0.761	C-MHS, C-SYB, C-YSJJ, C-ZBJW, C-HLB, B-QHW, C-AJSH, C-HMW

shows the reference case and the one that does not produce a bilateral platform structure), which brings into view all cases that generate the business characteristics of a bilateral structure. Not shown in the table is a subset that did not achieve integration with the business.), showing different combinations of leverages in different subsets. Subset I has good innovation leverage and transaction leverage, subset II has good production leverage and innovation leverage, and subset III has good production leverage and transaction leverage. The significance of the three subsets is that it allows us to distinguish different platform contexts in all cases, examine the origin of transaction leverage and reasons why it cannot work, and deeply analyze the dynamic mechanism in system construction. The three subsets are both overlapping and different, which shows that the complexity of the value creation mechanism of the platform cannot be explained by a single leverage. This also explains the reason why most of the system constructions that seek to use network effect logic will get into trouble in reality.

5. Case Study

5.1. Identifying the Characteristics of Platform Context. The main purpose of the case analysis is to analyze typical cases in the configuration under the guidance of the logical relationship shown in each configuration. The major steps in the case analysis are as follows. Firstly, key platform characteristics are identified. Each group of cases is analyzed one by one, the factors that promote the system construction in the platform environment characteristics are realized, and the factors in the platform system that are conducive to human-machine integration (named human-machine integration), and the factors in the platform system that are conducive to the integration of platform services and supplier business (named as business integration), and the factors in the platform system that are conducive to promoting the value-added of the platform (named as system value-added) are obtained. These three factors are the key factors that promote the construction of the system. Figure 3 represents the progress of configurations inducing the data. The secondary theme (C1–C5) reflects the characteristic factors from the platform owners and users (In addition to the significant influence of the characteristics of users in the business integration, the influence of the platform operator in the other two aspects has absolute advantages.).

5.2. Identifying the Path System Construction. The second step of case analysis is to complete the induction of subset features and identifying system construction path based on identifying key cases. Based on the logical antecedent variables hinted by the three configuration subsets, we analyze in the following way: how does the production leverage and innovation leverage in configuration I promote transaction leverage and system construction? What is the reason why the transaction leverage of configuration II is not significant enough? What characteristics make the transaction leverage of configuration III significant? The exploration led us to discover respectively the strong role of innovative use of information technology in system construction, the reasons for business integration that inhibited the generation of transaction leverage, but also promoted system construction, and the remarkable characteristics of data-driven facilitated system construction. Through multi-case analysis, we put them in the most suitable classifications and name three new subsets with no intersection as innovation-driven path, business-driven path, and data-driven path.

For the convenience of induction, different symbols are used to mark the impacts of the characteristics of platform context: "●" means that it has a substantial impact on the system construction, "◎" means that it has a significant impact but has not reached a substantial level, and "○" means not mentioned or the influence is not enough to reach a significant level. These three symbols reflect the order of influence from strong to weak; blank means there is inconsistency in the performance of typical cases within the group; and "⟶" means causal dynamic relationship. Note that this notation method is used in the following Tables 7.

5.2.1. Innovation-Driven Path. The "innovation" here in Tables 8 and 9 refers to the technology and means of innovative business development through information technology, with the purpose of achieving production efficiency and product/service improvement. The logical framework characteristic of the innovation-driven subset is that it has good innovation leverage and transaction leverage. The newest digital technology is the key to solving business problems, and digital platforms often give better play to its technological advantages. This huge advantage of technological progress has played a role that cannot be ignored in digital transformation. Table 7 presents three representative cases, which demonstrate this feature well.

The cases in this configuration all demonstrate the great role of advanced digital technology and digital systems in system construction. This configuration subset has obvious characteristics in terms of human-machine integration and business integration, which is an important reason for good innovation leverage and transaction leverage, and is reflected in the innovation-driven path of platform value co-creation.

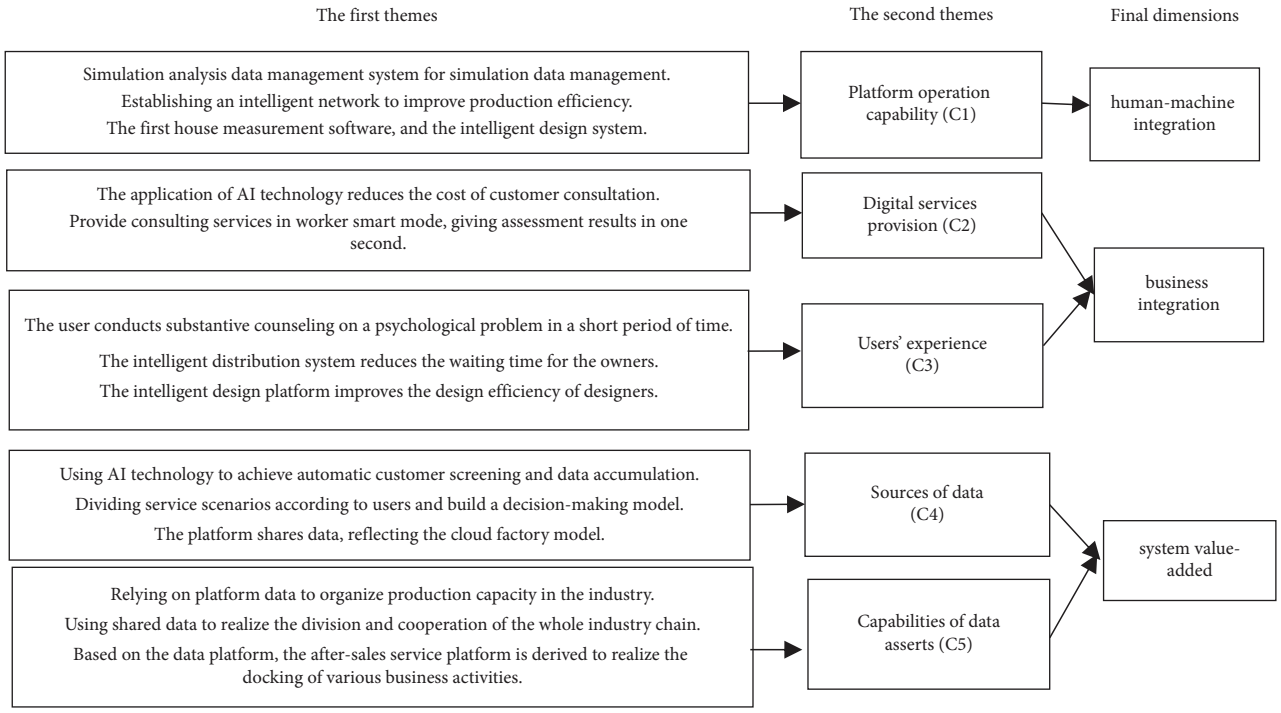

Figure 3: Data structure diagram.

Human-machine integration and business integration have resulted in significant innovation-driven effects in terms of production methods, product quality, production organization, and business model innovation. The excellent platform operation ability enables ZCQC to develop simulation data system and GBWJ to use big data technology test equipment, which bring the improvement on production and efficiency for these two companies. Digital service provision and the users' experience have promoted YSJJ to adopt a distributed production method, realize the synergy of the whole production value chain, achieve a huge efficiency improvement in organizing production, and promote business model innovation. The characteristics of good human-machine integration and business integration not only improve the users' experience but also bring more potential users and improve market availability. For example, the development of CRRC B2B trading platform of ZCQC is directly related to the good experience in the adoption of technologies such as simulation data systems; the good experience in the adoption of data systems and other technologies is directly related to the improvement of transaction efficiency of YSJJ, which is also related to the experience of using new data technologies on the design platform. Overall, it is the performance and experience improvements brought about by digital technology that drives the systematic construction of the platform.

5.2.2. Business Integration Path. Digital services are the integration of technologies and processes from different knowledge domains across enterprise boundaries [25]. This has brought great challenges to the capabilities of enterprises, especially those entrepreneurs who have invested in the industry with cross-border ideas and technology outside the industry. This configuration is also an extension of the previous configuration. The logical framework of this subset is characterized by good production leverage and innovation leverage, reflecting the difference between new business cases and incumbent platform owners, and explaining the reason why transaction leverage did not work in this configuration. The three representative cases listed in Table 8 are all entrepreneurial platform cases, reflecting platform owners need to go deep into the business for value creation due to the professionalism of knowledge, which also limits transaction leverage.

Entrepreneurs rely on advanced digital technology to solve the problems that plague traditional industries and go deep into the business to create value for customers with complementary suppliers. Three conditions are required: the basic is owning and being able to make a digital platform system work well. For example, XLMY gets substantive consultation in a short time, and SYB can subcontract the business skillfully. Both of which rely on digital facilities to provide customers with products and services with higher efficiency and higher quality and generate platform value, which is a fundamental characteristic of entrepreneurial success. However, the basis of providing professional services is the need to be highly familiar with the business the platforms are engaged in and to be involved in the business from beginning to end. These characteristics limit the platform's transaction matching function. For example, HLB establishes marketing platform to help the authors to finish the works, and the engineers of SYB need to deeply analyze each order received by the platform, which limits their ability to assist and accept orders.

The cases of configuration all go through a trial-and-error process of attracting customers by relying on matching

Table 7: Innovation-driven path.

Case	Characteristics of platform					Leverage		Data from cases
	C1	C2	C3	C4	C5	Transaction	Production	Innovation	
B-ZCQC	●	●	●	◎	◎	◎	●	●	Case summary: relying on the improvement of production efficiency and quality, the platform business volume is generated, and the capital operation management platform and the material circulation platform are derived. "...Work station system rhythm, centering on quality, efficiency and benefit, from... etc. To eliminate waste and continue to improve" (C2/C3 ⟶ production method); "all products have achieved full three-dimensional design, ... improve in order to improve the efficiency and quality of simulation analysis, establish a unified, standardized, efficient and collaborative business process in key business links such as ..." (C1/C2/C3 ⟶ product quality); "the accumulation of business volume generates a large amount of platform funds. Upstream and downstream of the industrial chain, build an e-commerce platform for the global rail transit field, and strive to create a B2B trading platform for waste and recycled materials" (C1/C2/C3/C4 ⟶ market availability)
C-HMW	●	●	●	○	○	○	●	●	Case summary: based on the intelligent digital network, the improvement of product quality and efficiency, the improvement of production organization, and the construction of industrial Internet system are derived. "Building an intelligent network, reducing the cost of each node in the enterprise and the industrial chain, improving communication efficiency, achieving high end-to-end integration, and ultimately improving production efficiency"; "...intelligent transformation project, reducing production personnel by 66 people and reducing the proportion of copying 50%...a 10.8x increase." (C1/C2/C3 ⟶ product quality/efficiency); "integrate advanced technologies such as the Internet of things, edge computing, big data, artificial intelligence. Integrate and optimize industrial resources. Launch on the basis of the industrial Internet application service platform...." (C1/C2/C3 ⟶ new products, business model innovation)
C-YSJJ	●	●	●	○	○	○	●	●	Case summary: relying on advanced digital technology and systems, it has achieved a comprehensive improvement in product quality/efficiency, production organization, production methods, and business processes, attracting users to the platform. "The first building interior measurement software, optimizing the design process...improving service efficiency adopting an intelligent design system to improve the designer's design efficiency" (C1/C2/C3 ⟶ product quality/efficiency); "using distributed production methods, synergistically integrate upstream and downstream enterprise resources to realize the synergy of the whole product value chain" (C1/C2/C3 ⟶ production organization); "designers and customers based on the platform's massive data... Accurately and quickly grasp customer needs.... The first FIM home furnishing information model meet different needs" (C1/C2/C3 ⟶ business model innovation; C1/c2/C3 ⟶ transaction efficiency)

Table 7: Continued.

Case	Characteristics of platform					Leverage			Data from cases
	C1	C2	C3	C4	C5	Transaction	Production	Innovation	
Commonness	●	●	●				●	●	Logical framework features: good innovation leverage and trading leverage. The good human-machine integration (C1) and business integration (C2/C3) of the platform promote the production and innovation levers, promote the comprehensive digital determination of the access users, and drive more access, thereby promoting the construction of the system. Among them, the advanced nature of new technology is the key premise of the dynamic mechanism of the whole system

transactions, but ultimately solve the difficult problem of system construction by integrating professional teams into the business and realizing the integration of information technology and business. The common point between the business integration path and the innovation path is that both types of configurations appear in different groups in Table 5 at the same time. The difference is that the business integration path has a typical "cross-border" feature, while the innovation-driven approach represents the new technologies adopted in the industry. Differences in business foundations lead to differences in construction paths.

5.2.3. Data-Driven Path. The digital service of the platform is a data-intensive process, which creates opportunities for further development of value-added services, and has proved to be easy to derive the logical structure of the two-sided market, which brings the possibility for the incumbent enterprises to completely build a multilateral platform and finally finish the digital transformation. The logical framework characteristics of this subset are that it has good production leverage, transaction leverage, and relatively difficult organizational interactions. The three representative cases listed in Table 9 are typical representatives of this configuration.

The common feature of this group of representative cases is the companies that have accumulated business at first and then with the help of new products or services derived from data accumulation finally form a multilateral platform. This model needs to deal with two challenges. One is how to solve the problem of business digitalization. Due to the complexity of the business, it is necessary to rely on very rich industry experience to meet this challenge. For example, NBCX developed HP2-52C automatic computerized flat knitting machine; ZTGF handles the supply and demand information of shield owners and demanders, and QHW provides product customization, formulation technology consulting services, etc., all of which are inseparable from a deep understanding of the industry. The second is how to solve the problem of sufficient business volume. In the final construction of the trading platform of each case, only sufficient business volume can generate a large amount of data accumulation, which provides conditions for value-added services based on data analysis. The coexistence of the two conditions not only challenges the capabilities of the platform owners but also leads to more and more complex systems. It is necessary to distinguish various complex services and establish a multilateral market with limited scale but various types. QHW is very a good example. QHW forms the business platformization of 7 service products in 3 major sectors. Although the scale is objective in terms of total volume, with the complexity of the business, the operating cost of the platform will also increase rapidly.

5.3. Comparison of Paths. The third step of the case study is to compare the system construction paths and obtain the different influence mechanisms of the complex platform context on the system construction path. The three configurations rely on different value creation mechanisms to realize the system construction, in which the factors influencing leverage are different, and the dynamic mechanisms of the influencing factors to induce the value creation mechanisms are also different. The key inducing mechanisms of the three paths are different: in innovation-driven path, the production, and/or innovation leverage are the key factors that affect the subjective evaluation for users; in the business integration path, the platform owners solve business problems for the business supplier to generate production and/or innovation leverage, while in the data-driven path, system value-added is the premise of production and innovation leverage. The contexts of platforms of the three paths have both commonalities and differences: firstly, a well-operated digital platform system (C1) is an indispensable basic condition for all construction paths and is the premise of human-machine integration, business integration, and system productivity; secondly, it is also a basic premise to be able to solve problems in digital services based on this system (C2); the users' experience (C3) in business integration is also a commonality condition, though the inducing mechanism is different (such as innovation-driven and business integration-driven). The difference is that data-driven comes from mature systems, and it also places higher demands on the scale (C4) and capability (C5) of the digital system itself.

However, transaction leverage is not a key driver in any of the three paths. The reason is that transaction leverage reflects the advantages in connection structure and

Table 8: Business integration path.

Cases	Characteristics of platform					Leverages			Data from cases
	C1	C2	C3	C4	C5	Transaction	Production	Innovation	
C-XLMY	●	●	●	◎	◎	◎	●	●	Case summary: use AI technology to match customers, solve the difficult problems of traditional psychological counseling, improve service efficiency, generate professional services, and promote value creation. "The application of AI technology can greatly reduce the cost of customer consultation. . .. Users can enter substantive consultation for a certain psychological problem in a short period of time." (*C1/C2/C3 ⟶ production quality/efficiency*); research and development of psychological companionship and marketing robots. . .. Launched the "21 days to help you get out of lovelorn predicament" service. (*C2/C3 ⟶ new products*); "embed AI technology into the platform to realize automatic screening and data accumulation of customers, and the platform will automatically guide professional consultants" (*C1/C2/C3/C4/C5 ⟶ business model innovation*)
C-HLB	●	●	●	○	○	○	●	●	Case summary: the platform builds its own professional team, goes deep into the business content level, relies on the digital platform to provide platform customers with products and services with higher efficiency and higher quality, and generate platform value. "The self-built design team matches the creators who live on the platform, and cooperates with the creator's progress, . . . to complete the design in only 23 hours" (*C2/C3 ⟶ product quality*); "the self-built marketing creative team helps the creators complete the work., internalize the industry knowledge into the platform, and improve the service quality of the platform" (*C1/C2/C3 ⟶ production organization*); "provide customized package services for customers and provide comprehensive consulting services." (*C1/C2/C3 ⟶ business model innovation*)
C-SYB	●	●	●	◎	◎	○	●	●	Case summary: the platform builds its own technology research and development department, enters the production process of the manufacturing industry, and relies on digital technology and systems to achieve service and product innovation and generate platform value. "Using the platform's big data, subcontract the total order of the brand to the appropriate processing factory. . .. The fastest production can be realized in 3 days" (*C1/C2/C4/C5 ⟶ production quality/efficiency*); "on the platform the process research and development department was established internally, and the customer's products were split, and within two weeks. . .. Completed the tasks that competitors dared not take up" *(C2/C3 ⟶ production organization)*; "modularize production capacity and respond quickly according to customer needs." *(C2/C3 ⟶ business model innovation)* ". . .rely on data to organize the production capacity in the industry instead of the traditional way. . ." (*C1/C2/C3/C4/C5 ⟶ business model innovation*)

Table 8: Continued.

Cases	Characteristics of platform					Leverages			Data from cases
	C1	C2	C3	C4	C5	Transaction	Production	Innovation	
Commonness	●	●	●				●	●	Logical framework characteristics: good production levers and innovation levers. The entrepreneurial platform relies on operating a self-built digital platform system (CI), replacing traditional business forms (C2/C3) (psychological consultation, legal consultation, advertising creativity, processing services, etc.), solving matching problems in business development, relying on production, and the role of innovation leverage promotes the smooth development of business (C2/C3) and promotes the construction of the platform system. "Cross-boundary" integration is its basic feature

connection technology and is not enough to solve the obstacles that platforms provide digital services to users in digitalization. The machine integration and the business integration are the resistances for the network effect to exert influences. Even if these obstacles are resolved, as in the case of the data-driven path, since the platform owners have a broader vision (data volume) and sharper perception (data analysis capability) than users, the network between users is also not the dynamics for system construction. The network effects of the interaction between the two are also not the driving force of the system construction. According to the transaction leverage emphasized in affiliation and the production and innovation levers that embody the competitive dynamic mechanism, the system construction paths of the three configurations are shown in Figure 4.

Figure 4 shows that human-machine integration and business integration promoting production leverage and innovation leverage are a common feature of the three configurations, which reflects the dynamic mechanisms shown in Tables 7–9. Among the two paths in which transaction leverage does not play a significant role, innovation-driven approach has better transaction leverage generation than the business integration path. The reason is that the characteristics of business integration limit the generation of transaction leverage. In the data-driven path where transaction leverage plays a significant role, the production leverage and innovation leverage that promote the increased volume of business and the data accumulation and data analysis capabilities that promote the play of transaction leverage are the main reasons. The assertion is not only confirmed by the causal connection between the data in the case analysis but also supported by the qualitative data information and the consistency test results of fsQCA, which shows the inappropriateness of promoting the digital transformation of the real economy by pursuing network effects in reality. From the above findings, the following propositions can be obtained:

Proposition 2. *In the digital platform formed by the digitization of the real economy, the production leverage and the innovation leverage are the main driving mechanisms for promoting the construction of the platform system. Human-machine integration, business integration, and data-driven are important platform context characteristics that lead to the production leverage and innovation leverage.*

Proposition 3. *In the digital platform formed by the digitization of the real economy, the deep integration of business is an important reason for inhibiting the generation of transaction leverage.*

Proposition 4. *In the digital platform formed by the digitization of the real economy, the generation of transaction leverage is premised on production leverage and/or innovation leverage, and data accumulation and data analysis capabilities are necessary conditions for transaction leverage to function.*

6. Discussion

6.1. Theoretical Contributions. The affiliation view of the platform (or the intermediary market stream) considers network effects to be the core source of a platform's competitive advantage. Under the influence of this theory, its strategic guidance tends to focus on aggregate volume, general governance, and community enhancement, and Eisenmann et al. [13], Evans et al. [11], Rochet, and Tirole [12] are the main sources of influence for this theoretical claim. The structural view formed by Adner [14] as the main representative and supplemented by Jacobides et al. [15] emphasizes the importance of users in system construction. The shift from the view of affiliation view to structure of structure view implies a shift from emphasizing the platform itself to emphasizing the impact of the business context. However, in this shift, the powerful influence of digital technology itself, the context characteristics of platform, and the complex dynamics of system construction are also not reflected, so a structural view remains difficult to answer for the complexities of platform value creation mechanisms in digitization. This study uses a large number of facts to show that the theory of affiliation view is not feasible in the real digital transformation and also identifies different situations

Table 9: Data-driven system construction path.

Case	Platform features					Leverages			Data from cases
	C1	C2	C3	C4	C5	Transaction	Production	Innovation	
C-NBCX	●	●	●	●	●	●	●	●	Case summary: based on the foundation of enterprise research and development, improve production technology, promote model transformation, and form an industry platform. "Development of HP2-52C fully automatic computerized flat knitting machine to realize fully automatic manufacturing to greatly shorten the production cycle" (*C2 ⟶ production quality/efficiency*); "integrate industry-leading enterprises and technical resources customized according to specific needs Production. . .. Formulate application system solutions to help customers reduce costs and increase efficiency" (*C1/C2/C3 ⟶ production organization*); "realize data sharing, and the cloud factory model realizes the division of labor and collaboration across the entire industry chain" (*C4/C5 ⟶ business model innovation ⟶ market availability*)
B-ZTGF	●	●	●	●	●	●	●	●	Case summary: based on the digital transformation of the shield business, a more efficient production form has been generated, and a multi-/bilateral market structure has been derived. "Through the shield cloud platform to achieve zero-distance contact between management personnel and the site. . .. Using the accumulated experience of experts and engineers to solve various difficult problems in construction in a timely manner feeding back the experience in construction technology and technological innovation on the technological innovation of shield machine equipment" (*C1/C2/C3 ⟶ production organization/business model innovation*); ". . .getting through the supply and demand information of shield machine owners and demanders through offline contracts to achieve the platform online and offline. Linkage financial institutions can provide financial security the 'work service mall e-commerce platform' for shield machine equipment parts trading, providing one-stop comprehensive solutions" (*C1/C2/C3/C4/C5 ⟶ market availability*)
B-QHW	●	●	●	●	●	●	●	●	Case summary: solve the tedious problems in the actual connection, generate an effective production form, and derive a complex multilateral platform model. ". . .Rihuahui information sharing platform, on the basis of product customization and formula technical consulting services provided by the platform, quickly customize the production of disinfection and sterilization products" (*C1/C2/C3 ⟶ business model innovation*); "the first-hand market the information is sent to the R&D side, and the formulas, products, etc. researched by the platform are matched. . .. Continue to launch innovative businesses, and have launched 7 service products in 3 major sectors, covering. . ." (*C4/C5 ⟶ new products*); "make upstream and downstream companies are more transparent, convenient and efficient, simplifying the transaction process" (*C4/C5 ⟶ market availability*)
Commonness	●	●	●	●	●	●	●	●	Logical framework features: good production leverage, transaction leverage, and highly difficult organizational interactions. With the foundation of human-machine integration and business integration (C1/C2/C3), based on the ability of data accumulation and data analysis (C4/C5), it can realize the leverage value of production and innovation and then gradually promote the value creation mechanism of transaction leverage. A mature system and sufficient traffic are the basic characteristics

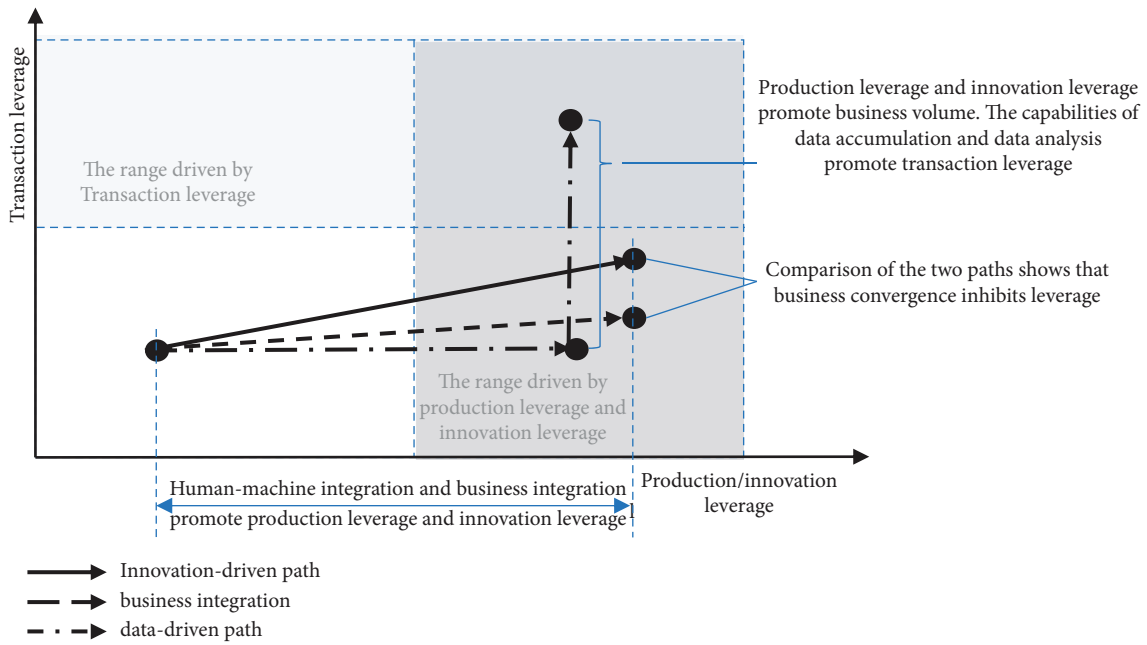

Figure 4: System construction path of the three platform value lever configurations.

Table 10: Theoretical contributions.

System construction paths	Findings	Theoretical contributions	Typical cases
Innovation-driven path	Rely on advanced digital technologies and systems to promote production leverage and innovation leverage, create value for users, and facilitate system construction. Preconditions are as follows: (i) Advanced digital technologies and systems (ii) Production efficiency improvement and product innovation	The structure view only provides a perspective, but it is still not enough to answer the value creation mechanisms and process of the platform. This theory gives the answer from the perspective of digital technology and innovation	ZCQC GBWJ HMW YSJJ AJSH
Business integration-driven path	Solve industry problems with advanced digital technologies and systems, and go deep into the business to create value for customers with complementary suppliers. Preconditions are as follows: (i) Digital technology to solve industry problems (ii) In-depth integration of business and suppliers	The affiliation view is only suitable for the situation where the platform participates in the value creation of complementary advantages with unscaled resources, and there is a theoretical blind spot. This theory explains the mechanism and realization path of the platform participating in the value creation with scaled resources under the complex industry matching situation	XLMY SZZN HLB SYB
Data-driven path	Relying on a certain scale of business volume and digital systems to achieve data accumulation, relying on analytical capabilities to derive new products or services, forming a multilateral platform. Preconditions are as follows: (i) Digital systems with good human-machine and business integration (ii) A certain scale of business volume (iii) Data accumulation and analysis ability	Platform complexity is an important factor limiting the value creation ability of platforms, and the subordination and structure views have not paid attention to this impact. This theory emphasizes that intrinsic value creation is the foundation and provides the premise, motivation, and process for the growth of the platform system	NBCX ZTGF QHW HYJT HCB

of innovation-driven, business integration, and data-driven and develops the structure view (see Table 10).

6.1.1. Theoretical Contributions of Innovation-Driven Path. The structure view believes that, unlike e-commerce and social media and other consumer-oriented Internet, most digital transformation has "strong connection characteristics" [14]; that is, the connection of platforms does not provide an "accidental connection possibility," but a substantial investing in service solutions leads to a relatively stable relationship between service recipients and providers. This theoretical claim explains why value co-creation activities by users in digital transformation are difficult. This

study finds that production leverage and innovation leverage act to address the user's dilemma when accessing the platform. A realistic and feasible path is to rely on advanced digital technologies and digital systems to promote the leveraging of production and innovation and create value for users. When the leverage is strong enough, the users can easily intuitively feel the advantages of accessing the platform, and potential users can easily access the system under the demonstration effect, thus solving the problem of value co-creation. In this case, two antecedents are indispensable: (1) advanced digital technologies and digital systems and (2) production efficiency improvement and product innovation.

The innovation-driven path shows that digital systems have the triple advantages of transaction leverage, production leverage, and innovation leverage. Although the convenience of modular complementarity is implied in itself, the adoption of digital technologies and systems often faces huge system integration difficulties in implementation. Advantages are not inevitable. In the system construction, the integration of digital technology and traditional technology is accompanied by various innovations. If the new digital technologies and system can be successfully controlled, it will bring enough efficiency improvement and become the driving force to attract more access users to access the platform. The innovation-driven path gives the power sources of the platform approach from the perspective of the combination of digital technologies and business domains. The structure view put forward by Adner [14] is still not enough to answer the motivation and process of system construction, and this study emphasizes the importance of new technologies and provides a path of system construction through improving the efficiency and added product/service.

6.1.2. Theoretical Contribution of the Business Integration Path. The platform theory of affiliation view believes that increasing the number of users is the way to obtain a competitive advantage. The implicit premise is that there is friction in the transaction, resulting in transaction costs, and the platform has information and professional advantages in the transaction. Low-cost replication leads to system advantages, which embodies the alternative economic logic proposed by Garud and Kumaraswamy [46]; that is, the transaction led by the platform owners achieves economies of scale and scope in the process of replacing direct transactions between the two parties. The finding of this study is different from the phenomenon observed in the view of affiliation. The professional advantage of platform is a professional technical activity. It relies on advanced digital technologies to solve the problems that plague traditional businesses in the industry and goes deep into the business to work with complementary suppliers to create value for customers, not just deal matching.

There are two antecedents to business integration path: (1) advanced digital technologies solve industrial problems and (2) deep integration into business. The first condition produces substitution advantages, and the second condition enables platform owners and professional service providers to achieve economies of scale and scope in the division of labor and cooperation. However, differences in transaction activity and technical expertise lead to differences in the conditions for creating network effects. According to the division of resource types by Wassmer and Dussauge [47], due to the powerful capability of information search and matching in digital technology, the resources that facilitate transactions are scale-free resources in digital systems; that is, they are reused and resourced. It does not affect the ability of resources to create value, so the bottleneck of system value creation lies in the inability to attract more users, rather than the lack of the system's ability to process transactions. However, in the case of creating service value in the progress of business, the digital system provides a combination of platform capabilities and professional service provider capabilities. This activity no longer has the attribute of no scale, which limits the possibility of creating value through transaction capabilities. In this case, it is difficult to observe the significance of the network effect, and the method of expanding the access of the platform is often futile. This finding reveals the fundamental difference between the digital transformation platform that goes deep into the business and the classic Internet platform studied from the view of affiliation; that is, the complex business characteristics lead to the platform requiring the intervention of scaled resources in transaction matching, which limits the scope of the platform's asset scope economy and inhibits the role of transaction leverage.

6.1.3. Theoretical Contributions of Data-Driven Path. Digital service is a data-intensive activity that can create value-added services, reduce market friction, and create conditions for transaction leverage. However, digital services have the characteristics of cross-enterprise boundaries, which bring challenges to the knowledge and capabilities of service providers and bring about challenges to the knowledge and capabilities of service providers. Suppressing the willingness of service recipients to accept, this situation will make the generation of transaction leverage face uncertainty. This study shows that successful data driving firstly occurs in the digital platform system built by enterprises. The realization of digital transformation helps in data accumulation and relies on digital analysis to derive new products or services, forming a multilateral platform. The realization of this approach depends on three antecedents: (1) a digital system integrating human-machine and business; (2) a certain scale of business volume; and (3) data accumulation and analysis capabilities.

Different from the view of affiliation, which emphasizes the creation of users' numbers and platform governance, and also different from the view of structure, the data-driven multilateral platforms reveal the importance of data in the multilateral structure and the endogenous dynamics of digital platforms. As summarized by Mikalef et al. [34], data have been increasingly confirmed as an emerging source of production means and capabilities in the digital context [48]. However, we found that the three antecedent conditions are indispensable and demonstrated the complexity of systems through sufficient realistic materials (similar evidence such as

the formulation of hypermodule platforms). It is this complexity that places high demands on industry experience and data analysis capabilities. This study reveals the preconditions for the value creation of digital platforms, points out the inhibitory role of transaction leverage, and emphasizes that the construction of digital platform system construction is an endogenous growth process. The difference between our findings and the view of affiliation is that it emphasizes that solving problems in service is the foundation of generating value, rather than establishing external relationships. The difference from the view of structure is that this study gives the premise, motivation, and process of system growth.

6.2. Practical Contributions. The practical inspiration of this study is that it clearly shows the importance of building platform internal force in the process of digital transformation, rather than focusing on the potential structure. In particular, for the entrepreneurships with platform as the organizational structure, the system construction should not overemphasize the platform's customer volume, but choose an appropriate platform path according to the specific platform context, strengthen its own capacities, and use the capabilities endowed by digital technologies and digital systems to enhance the value perception of users through innovation, business specialization, and data-driven methods. The construction of a digital platform system is a process of endogenous growth. Solving problems in services and discovering intrinsic value is fundamental. For example, the value of digital systems is reflected through internal innovation, and value is created in solving practical problems. The enterprises should fully exploit the service quality improvement potential endowed by digital assets to enable platform users to achieve improved benefits. The specific inspirations are as follows:

(i) Firstly, human-machine integration and business integration through innovation-driven role are promoted. Digital technologies and digital platforms are advanced forms to replace traditional business forms, but their efficiency and innovation cannot be taken for granted. The enterprises should actively build internal capabilities, effectively harness the value creation potential endowed by new technologies and systems, and give full play to digital technologies and digital systems in production. The active role in innovation and promotion of human-machine integration and business integration in platform access is an effective way to effectively solve the concerns of platform users.

(ii) Secondly, value in deep business participation is created. The digital transformation of traditional industries is not to solve simple matching and docking problems. Platform owners, especially entrepreneurs, should focus on relying on the advantages of digital technologies in solving traditional problems and creating values in the specialization of participating businesses and cooperation with suppliers, rather than blindly expanding the number of users.

(iii) Thirdly, the platform's own digital capacities are strengthened. Digital services are often accompanied by the generation of a large amount of data. Active digital analysis capabilities and digital application capabilities are not only the premise to ensure the effective operation of the platform but also the capability basis for derivative value-added services and multi-/bilateral markets. Therefore, strengthening digital capacity building is an effective means to effectively achieve digital transformation and enhance the platform's advantages.

6.3. Limitations. The cross-platform perspective and a large number of platforms ptovide this study with strong power of factor discovery and verification capabilities. However, with the limitations of concerns and phenomena, this study also has two limitations: (1) from the point of view of concerns, this study focuses on the system comparison of cross-platform contexts. The too wide vision makes it impossible to introduce and analyze in detail in this study, and it is difficult to introduce in detail the process of exploring the causal connection of factors under different environmental configurations; (2) from the phenomenon of concern, this study focuses on the process of deep integration of information technologies and business systems, resulting in the measurement of variables and the selection of cases are consistent with this research phenomenon, and the conclusion may have a certain deviation from the mature platform. Nonetheless, the potential for theoretical discovery arising from multi-context comparison and induction is undeniable, and if further analysis of the three logical configurations identified in this study is conducted, it will provide a deeper theoretical understanding and practice of the platform approach in digitization transformation.

7. Conclusions and Future Work

This study uses a large number of cases in industries where the information technology is integrated with industries in China and discusses the dynamic mechanism and construction path of the system construction in the digital transformation from the perspective of the leverages of platform method. The study found that production leverage and innovation leverage are the general construction drivers of platform, and transaction leverage is only significant in a small number of platforms; that is, the role of network effects can be observed. There are many reasons why transaction leverage is difficult to become the main driving force, but from the perspective of system characteristics, the digitization of the real economy requires the human-machine integration and business integration between the digital platforms and users, which leads to the complexity of digital system and generate economic characteristics that differ from classic Internet platforms. In complex manifestations, successful digital transformation reflects the typical configuration characteristics of innovation-driven, business

integration, and data-driven. In the three configurations, on the one hand, the system requirements of human-machine integration and business integration make the platform owners and business providers deeply integrated, and it is difficult to exert transaction leverage; on the other hand, in the situation where transaction leverage can be observed, either the result of business integration often promotes the play of production leverage and innovation leverage, which is reflected in the characteristics of innovation-driven, or the mature system derives a multilateral platform through the value-added of digital services, and its essence is that the transaction leverage is still triggered by production leverage and innovation leverage. Therefore, in the complex manifestations of digitization, network effects are difficult to become the core driving force of the platform approach.

Data Availability

Data are available on request from the corresponding author.

Conflicts of Interest

The authors declare that they have no conflicts of interest for publication of this work.

Acknowledgments

This study was funded by the National Natural Science Foundation of China: Research on the Growth Mechanism of Cross-Border Entrants: the Perspective of Niche Competition (71702168); National Social Science Major Project: Research on the Mechanism and Path of Digital Industry Innovation in Collaborative Promotion of Technical Standards and Intellectual Property (19ZDA078); and project supported by the Science Foundation: Model, Benefit Evaluation and Sustainable Optimization of Shared Manufacturing Value Network (20BGL013).

References

[1] M. E. Porter and J. E. Heppelmann, "How smart, connected products are transforming companies," *Harvard Business Review*, vol. 93, no. 10, pp. 96–114, 2015.

[2] P. Rippa and G. Secundo, "Digital academic entrepreneurship: the potential of digital technologies on academic entrepreneurship," *Technological Forecasting and Social Change*, vol. 146, pp. 900–911, 2019.

[3] I. M. Sebastian, J. W. Ross, and C. Beath, "How big old companies navigate digital transformation," *Strategic Information Management*, pp. 133–150, Routledge, 2020.

[4] D. H. Olsen, T. R. Eikebrokk, and K. Aspø, "How big old companies navigate digital transformation," *Responsible Design, Implementation and Use of Information and Communication Technology*, vol. 37, Article ID 12066, pp. 126–137, 2020.

[5] C. Matt, T. Hess, and A. Benlian, "Digital transformation strategies," *Business & Information Systems Engineering*, vol. 57, no. 5, pp. 339–343, 2015.

[6] A. Sklyar, C. Kowalkowski, B. Tronvoll, and D Sorhammar, "Organizing for digital servitization: a service ecosystem perspective," *Journal of Business Research*, vol. 104, pp. 450–460, 2019.

[7] G. Vial, "Understanding digital transformation: a review and a research agenda," *The Journal of Strategic Information Systems*, vol. 28, no. 2, pp. 118–144, 2019.

[8] H. Gebauer, E. Fleisch, C. Lamprecht, and F. Wortmann, "Growth paths for overcoming the digitalization paradox," *Business Horizons*, vol. 63, no. 3, pp. 313–323, 2020.

[9] P. C. Verhoef, T. Broekhuizen, Y. Bart et al., "Digital transformation: a multidisciplinary reflection and research agenda," *Journal of Business Research*, vol. 122, pp. 889–901, 2021.

[10] L. D. W. Thomas, E. Autio, and D. M. Gann, "Architectural leverage: putting platforms in context," *Academy of Management Perspectives*, vol. 28, no. 2, pp. 198–219, 2014.

[11] D. S. Evans, "How catalysts ignite: the economics of platform-based start-ups," *Platforms, markets and innovation*, vol. 5, pp. 99–128, 2009.

[12] J. C. Rochet and J. Tirole, "Platform competition in two-sided markets," *Journal of the European Economic Association*, vol. 1, no. 4, pp. 990–1029, 2003.

[13] T. Eisenmann, G. Parker, and M. W. V. Alstyne, "Strategies for two-sided markets," *Harvard Business Review*, vol. 84, no. 10, pp. 92–103, 2006.

[14] R. Adner, "Ecosystem as structure: an actionable construct for strategy," *Journal of Management*, vol. 43, no. 1, pp. 39–58, 2017.

[15] M. G. Jacobides, C. Cennamo, and A. Gawer, "Towards a theory of ecosystems," *Strategic Management Journal*, vol. 39, no. 8, pp. 2255–2276, 2018.

[16] A. Gawer and M. A. Cusumano, "Industry platforms and ecosystem innovation," *Journal of Product Innovation Management*, vol. 31, no. 3, pp. 417–433, 2014.

[17] C. C. Ragin, *Redesigning Social Inquiry*, University of Chicago Press, Chicago, Illinois, 2009.

[18] A. Gawer and R. Henderson, "Platform owner entry and innovation in complementary markets: evidence from Intel," *Journal of Economics and Management Strategy*, vol. 16, no. 1, pp. 1–34, 2009.

[19] D. J. Teece, G. Pisano, and A. Shuen, "Dynamic capabilities and strategic management," *Strategic Management Journal*, vol. 18, no. 7, pp. 509–533, 1997.

[20] T. W. Simpson, "Product platform design and customization: s," *Artificial Intelligence for Engineering Design, Analysis and Manufacturing*, vol. 18, no. 1, pp. 3–20, 2004.

[21] M. Cusumano, "Technology strategy and managementThe evolution of platform thinking," *Communications of the ACM*, vol. 53, no. 1, pp. 32–34, 2010.

[22] D. S. Evans and R. Schmalensee, *The Antitrust Analysis of Multi-Sided Platform Businesses*, National Bureau of Economic Research, MA, USA, 2013.

[23] Y. Yoo, O. Henfridsson, and K. Lyytinen, "Research commentary—the new organizing logic of digital innovation: an agenda for information systems research," *Information Systems Research*, vol. 21, no. 4, pp. 724–735, 2010.

[24] P. Brody and V. Pureswaran, "The next digital gold rush: how the internet of things will create liquid, transparent markets," *Strategy & Leadership*, vol. 43, no. 1, pp. 36–41, 2015.

[25] S. Leminen, M. Rajahonka, M. Westerlund, and R. Wendelin, "The future of the Internet of Things: toward heterarchical ecosystems and service business models," *Journal of Business & Industrial Marketing*, vol. 33, no. 6, pp. 749–767, 2018.

[26] S. Nambisan, M. Wright, and M. Feldman, "The digital transformation of innovation and entrepreneurship: progress,

challenges and key themes," *Research Policy*, vol. 48, no. 8, pp. 103773–104111, 2019.
[27] E. Baraldi, J. F. Proença, T. Proença, and L. M. D. Castro, "The supplier's side of outsourcing: t," *Industrial Marketing Management*, vol. 43, no. 4, pp. 553–563, 2014.
[28] P. Constantinides, O. Henfridsson, and G. G. Parker, "Introduction—platforms and infrastructures in the digital age," *Information Systems Research*, vol. 29, no. 2, pp. 381–400, 2018.
[29] A. Hein, M. Schreieck, T. Riasanow et al., "Digital platform ecosystems," *Electronic Markets*, vol. 30, no. 1, pp. 87–98, 2020.
[30] M. Kohtamäki, V. Parida, P. Oghazi, H. Gebauer, and T. Baines, "Digital servitization business models in ecosystems: a theory of the firm," *Journal of Business Research*, vol. 104, pp. 380–392, 2019.
[31] K. Menon, H. Kärkkäinen, and T. Wuest, "Industrial internet platform provider and end-user perceptions of platform openness impacts," *Industry & Innovation*, vol. 27, no. 4, pp. 363–389, 2020.
[32] D. Trabucchi, T. Buganza, and E. Pellizzoni, "Give Away Your Digital Services: leveraging Big Data to Capture Value New models that capture the value embedded in the data generated by digital services may make it viable for companies to offer those services for free," *Research-Technology Management*, vol. 60, no. 2, pp. 43–52, 2017.
[33] A. Rymaszewska, P. Helo, and A. Gunasekaran, "IoT powered servitization of manufacturing – an exploratory case study," *International Journal of Production Economics*, vol. 192, pp. 92–105, 2017.
[34] P. Mikalef, I. O. Pappas, J. Krogstie, and M. Giannakos, "Big data analytics capabilities: a systematic literature review and research agenda," *Information Systems and E-Business Management*, vol. 16, no. 3, pp. 547–578, 2018.
[35] S. Nambisan and M. Sawhney, *Academy of Management Perspectives*, vol. 25, no. 3, pp. 40–57, 2011.
[36] D. S. Evans and R. Schmalensee, *Matchmakers: The New Economics of Multisided Platforms*, Harvard Business Review Press, MA, USA, 2016.
[37] D. Opresnik and M. Taisch, "The value of Big Data in servitization," *International Journal of Production Economics*, vol. 165, pp. 174–184, 2015.
[38] A. Napoleone, M. Macchi, and A. Pozzetti, "A review on the characteristics of cyber-physical systems for the future smart factories," *Journal of Manufacturing Systems*, vol. 54, pp. 305–335, 2020.
[39] J. Lee and N. Moray, "Trust, control strategies and allocation of function in human-machine systems," *Ergonomics*, vol. 35, no. 10, pp. 1243–1270, 1992.
[40] P. Sen and B. K. Chakrabarti, *Sociophysics: An introduction*, Oxford University Press, Oxford, United Kingdom, 2014.
[41] A. G. Frank, G. H. S. Mendes, N. F. Ayala, and A. Ghezzi, "Servitization and Industry 4.0 convergence in the digital transformation of product firms: a business model innovation perspective," *Technological Forecasting and Social Change*, vol. 141, pp. 341–351, 2019.
[42] J. Gebauer, J. Füller, and R. Pezzei, "The dark and the bright side of co-creation: t," *Journal of Business Research*, vol. 66, no. 9, pp. 1516–1527, 2013.
[43] S. Furnari, D. Crilly, V. F. Misangyi, G. Thomas, C. P. Fiss, and V. A. Ruth, "Capturing causal complexity: heuristics for configurational theorizing," *Academy of Management Review*, vol. 2, pp. 2–50, 2020.
[44] K. D. Bailey, *Typologies and Taxonomies: An Introduction to Classification Techniques*, Sage, CA, USA, 1994.
[45] C. C. Ragin, *Health Services Research*, vol. 34, no. 5 Pt 2, pp. 1137–1151, 1999.
[46] R. Garud and A. Kumaraswamy, "Technological and organizational designs for realizing economies of substitution," *Strategic Management Journal*, vol. 16, no. S1, pp. 93–109, 1995.
[47] U. Wassmer and P. Dussauge, "Value creation in alliance portfolios: the benefits and costs of network resource interdependencies," *European Management Review*, vol. 8, no. 1, pp. 47–64, 2011.
[48] M. Ghasemaghaei, K. Hassanein, and O. Turel, "Increasing firm agility through the use of data analytics: the role of fit," *Decision Support Systems*, vol. 101, pp. 95–105, 2017.

Hindawi
Scientific Programming
Volume 2022, Article ID 5886648, 10 pages
https://doi.org/10.1155/2022/5886648

Research Article

Psychological Factors and Innovation Performance of Scientific and Technological Personnel: The Mediating Role of Proactive Behavior and the Moderating Role of Organizational Support

Chunhui Li

Guangzhou Huashang Vocational College, Guangzhou, Guangdong 511300, China

Correspondence should be addressed to Chunhui Li; lichunhui@gzhsvc.edu.cn

Received 7 April 2022; Revised 16 May 2022; Accepted 2 June 2022; Published 7 July 2022

Academic Editor: Muhammad Usman

The personal innovation of scientific and technological personnel not only provides the fundamental power for the innovation of enterprises, but also lays a solid foundation for enterprises innovation. In current study total 1050 scientific and technical staff questionnaires, empirical analysis of individual psychological contracts, psychological capital on personal proactive behavior of the employees, and a unique performance mechanism were used. The result can be drawn that the psychological contract of an individual and psychological capital factors on personal proactive behavior are more meaningfully and positively linked to innovation performance, intermediary between individual innovation performance, organizational support in individual psychological contracts, psychological capital, and proactive behavior.

1. Introduction

With the in-depth development of Internet technology and economic globalization, the business environment of enterprises is increasingly dynamic and changeable, and innovation has become a necessary means and an important way for enterprises to grow and obtain sustainable competitive advantages [1]. The personal innovation of employees not only provides the fundamental driving force for the innovation of the enterprise but also lays a solid foundation for enterprise innovation [2]. The proactive behavior of employees is closely related to innovation [3] and is an important driving factor for innovation [4]. Reasonable development and management of it can provide effective ways to stimulate employees' positive energy and break through innovation dilemmas [5]. Being risky and dangerous, individuals, on the other hand, should avoid proactive behavior. What are the internal psychological factors that encourage individual employees to implement such risky inputs? What is the relationship between proactive behaviours and innovation performance? How can organizations effectively stimulate and support employees? The proactive behaviours of guiding employees are still in short supply and need to be clarified.

This paper takes scientific and technological personnel of high-tech enterprises in the Guangdong and Hong Kong, Macau Dawan District, as research objects, and explores the relationship between individual psychological factors, organizational support, proactive behavior, and individual innovation performance by constructing an empirical research framework, providing new knowledge for proactive behavior theory and practical reference for enterprise managers.

Following are review and assumptions.

1.1. Psychological Factors of Scientific and Technological Personnel and Individual Innovation Performance. Amabile believed that individual innovation performance "refers to the useful and novel ideas put forward by employees for the problems they encounter in the process of work" [6]. Han et al. thought innovation performance could be discussed and studied from innovation willingness, innovation action, and innovation promotion [7]. Pieterse

et al. pointed out that the innovation performance of employees was generated by a series of processes such as problem identification, generation of new ideas, planning, and expansion of new ideas [8]. Yu et al. proposed that employee innovation performance referred to novel and useful ideas, products, processes, services, or methods generated in the process of interaction between employees and organizations [9]. In summary, individual innovation performance is the result of innovative ideas proposed by employees to improve corporate performance.

Innovation performance is an externalization process that may occur after the external environment acts on individual employees through selective perception [10]. When the psychological needs of employees are met, it may be easier to promote the improvement of innovation performance. Therefore, understanding the psychological factors of corporate employees is very important. This topic mainly studies the psychological contract and psychological capital of individual employees.

Psychological contract was put forward by Argyris in the 1960s [11]. Different scholars have different understanding of psychological contract. Levinson and others believed that psychological contract is the expectation of each other that the organization and employees have agreed in advance in the employment relationship [12]. Schein believed that psychological contract was "the expectation not written between each member of the organization working at any time and different supervisors and other members of the organization" [13]. Kotter believed that psychological contract was "an implicit contract with specific expected pay and expected return between individuals and organizations" [14]. Dunahee and Wangler believed that psychological contract was "The psychological agreement between employees and organizations that binds them together" [15]. The above scholars define the psychological contract between the organization and employees. Other scholars, such as Rousseau, believed that psychological contract was "employee's expectations for employers and their mutual responsibility and obligations" [16]. Turnley and others believed "The psychological contract consists of the cognition of the obligations that employees think the organization should perform for them and the cognition of the obligations that they should perform for the company" [17]. These scholars only looked at the psychological contract with the organization from the perspective of individual employees, which was also the perspective of this study.

Zhang and Liao divided psychological contract into transaction contract, relationship contract, and development contract [18]. Xue et al. pointed out that material incentive in transaction contract, employee promotion in relationship contract, and emotional appeal were the psychological contract factors affecting employee performance [19]. Wang et al. empirically believed that the psychological contract had a significant forward impact on performance [20]. Luthans' definition of psychological capital was widely accepted. Luthans et al. pointed out that "psychological capital is the psychological state that individuals display in line with the standard of positive organizational behavior" [21]. In 2007, Luthans revised the definition of psychological capital were "the self-efficacy, hope, toughness and optimistic psychological state of the individual in the process of growth and development" [22]. An empirical study such as that by Sweetman et al. pointed out that the overall psychological capital and various dimensions had a significant positive impact on innovation performance [23]. Wu and You believed that employees' positive psychological state would have a positive impact on enterprise innovation performance [24]; Shen found that the psychological capital had a positive effect on innovation performance, and the knowledge acquisition had played an intermediary effect between psychological capital and innovation performance [25]. In the study of Xu and Li with Tu Youyou's research object, the root theory is used to find that psychological capital had positive significance for innovation performance [26].

In summary, we think that psychological contract and psychological capital factors of scientific and technological personnel can positively predict the individual innovation performance of employees. Therefore, it can be assumed that

H1: psychological factors of science and technology personnel are significantly positively correlated with innovation performance

H1a: psychological contract is significantly positively correlated with innovation performance

H1b: psychological capital is significantly positively correlated with innovation performance

1.2. Innovation Performance and Individual Proactive Behavior. Different scholars defined different perspectives on proactive behavior, such as "proactive behavior is the work behavior of employees independent, expected, and proactive" [27]; "it is an employee's intentional behavior that is future oriented and tries to change their situation" [28]; it is the behavior of employees spontaneously, intended to change or improve their own conditions or situation [29];"it is a tendency to stabilize the environmental changes in the employee, which can actively complete the work, willing to change the environment in a timely manner, not by environmental constraints" [30]. To sum up, proactive behavior is a future-oriented and spontaneous change behavior of individual employees, which can positively predict the individual innovation performance of employees, so it can be assumed that

H2: proactive behavior is significantly positively correlated with individual innovation performance

1.3. Psychological Factors and Proactive Behavior of Scientific and Technological Personnel. According to Hou et al., employees' psychological contracts were in good shape and situation, which could encourage them to actively invest more, thereby stimulating individual innovation behavior [31] and enhancing employees' ability to predict events in the future organizational environment [32]. It developed the value hidden in positive psychology, enhancing employees' pressure resistance, promoting innovation to become an internal requirement of enterprise employees, and reshaping

the value hidden in positive psychology with more confidence and work achievements [33]. Li and Li believed that psychological contract could make employees think their work was full of meaning or feel good about themselves so that employees would actively assume more responsibilities, stimulated inspiration and obtained new ideas in continuous exploration and enterprising [34]. Dong and Gao confirmed that the psychological capital as a positive psychological state, the confidence, hope, optimism, and toughness dimension of the psychological capital, enabled the employees to have an internal incentive so that they experienced positive intrinsic emotions [35].

To sum up, we think psychological contract and psychological capital factors of scientific and technical personnel are able to positively predict employee's proactive behavior, so we assume the following:

H3: psychological factors of scientific and technical personnel are significantly positively correlated with proactive behavior

H3a: psychological contract is significantly positively correlated with proactive behavior

H3b: psychological capital is significantly positively correlated with proactive behavior

1.4. A Mediation Role of Proactive Behavior. Hou et al. showed that intrinsic motivation and psychological contract were the most direct antecedents of innovation performance, and psychological contract also indirectly affected innovation performance through the intermediate role of intrinsic motivation [36]. Zhang research showed that cultivating and improving psychological capital could enable enterprise employees to meet their competency, autonomy, and relationship needs so as to stimulate internal work motivation and produce innovative performance [37]. Xiong et al. believed that positive psychological capital would promote employees to continuously shape themselves, actively cultivated good psychological quality, enthusiastically and optimistically tapped their potential in career development, and constantly pursued self-realization. In this process, innovation had become a derivative of their personal development, thus improving individual innovation performance [38].

To sum up, we believe that individual psychological contract and psychological capital will have an impact on individual employees' innovation performance through the intermediary of individual proactive behavior. So we assume that

H4: proactive behavior mediates the relationship between individual psychological factors and innovation performance

H4a: proactive behavior mediates the relationship between psychological contract and innovation performance

H4b: proactive behavior mediates the relationship between psychological capital and innovation performance

1.5. Regulatory Role of Organizational Support. Environmental factors would have an important impact on individual performance. As an important environmental factor of employee innovation, organizational support may play an intervention role in the promotion of proactive behavior, innovation performance, and innovation performance by individual psychological factors. Eisenberge et al. thought that organizational support referred to "the overall feeling of employees in an organization to how much the organization values their contributions and cares about their welfare" [39]. Ling et al. believed that "Organizational Support is the view of employees to treat them to contribute and care about their interests" [40]. Mckenny et al. found that organization support included respect (emotion) support, benefit support, and toolbery support in three dimensions [41]. According to the social exchange theory, an organization's support for an employee's work attitude and performance has a favorable impact. Employees believe that organizational support can raise employees' expectations for the outcomes of their hard work and emphasize the favorable impact of the reciprocity principle on their work attitudes. The greater the impact on employee's individual psychological contract and psychological capital, the more beneficial will be employee's behavior to the organization. Ajzen et al. [42] pointed out that when employees felt organizational support, they would have the responsibility and obligation to repay the enterprise and worked with higher focus and enthusiasm, which made it easier to produce positive behavior and attitude, resulting in higher innovation performance.

In conclusion, we believe that organizational support will play a regulatory role in individual psychological contract, psychological capital factors, proactive behavior, and individual innovation performance. So we assume that

H5: organizational support moderates the relationship between individual innovation performance and psychological factors

H5a: organizational support moderates the relationship between innovation performance and psychological contract

H5b: organizational support moderates the relationship between innovative performance and psychological capital

H6: organizational support moderates the relationship between innovation performance and proactive behavior

H7: organizational support moderates the relationship between proactive behavior and individual psychological factor

H7a: organizational support moderates the relationship between proactive behavior and psychological contract

H7b: organizational support moderates the relationship between proactive behavior and psychological capital

In summary, the research framework is shown in Figure 1.

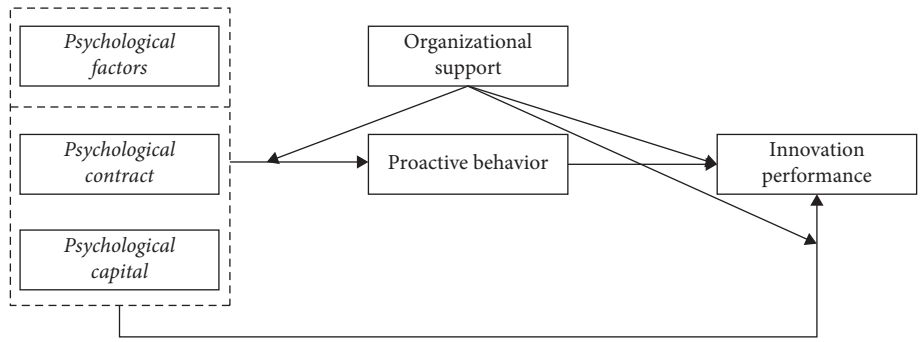

Figure 1: Research framework.

Table 1: Sample demographic characteristics.

Value	Detail	Numb	Percentage of total number of people	Variable	Detail	Numb	Percentage of total number of people
Sex	Male	550	52.38	Age	$Y \leq 25$	20	1.9
					$25 < Y \leq 35$	380	36.19
	Female	500	47.62		$35 < Y \leq 45$	500	47.62
					$45 < Y$	150	14.29
Education	Specialist	20	1.9	Length of service	$Y \leq 1$	30	2.86
	Undergraduate	280	26.67		$1 < Y \leq 5$	160	15.24
	Master	690	65.71		$5 < Y \leq 10$	210	20.0
	PHD	60	5.72		$10 < Y$	650	61.9

2. Research Design

2.1. Samples. We surveyed university teachers and high-tech enterprises in the Greater Bay Area. We investigated through the "Questionnaire Star" network platform and sent QR codes to students, friends, and acquaintances through WeChat to collect 1,050 answers. The recovery rate was 90.0% and the effective rate is 100%.

The final valid sample population statistics are shown in Table 1.

2.2. Research Tools. Based on the existing maturity scale, the questionnaire is adjusted properly, and all variables are measured using the 5-point Likert method.

Individual psychological factors: psychological contract mainly refers to the scale developed by Li [43] and Rousseau [16]. Psychological capital is mainly referred to the psychological capital quantitative number developed by Luthans [22] (Psychological Capistionnaire, referred to as PCQ).

Organizational support: for reference, Ling et al. [40] and Eisenberger et al. [39] developed scale.

Individual proactive behavior: the scale prepared by Parker et al. [29].

Individual innovation performance: the scale prepared by Han et al. [7] and Janssen et al. [44].

3. Data Analysis

3.1. Reliability Analysis. The Cronbach's A coefficient is used to assess the measurement item's reliability. Table 2 shows that Cronbach's A coefficient of psychological contract was 0.672, which is higher than 0.6, indicating that the research data was reliable. Psychological capital, organizational support, proactive behavior, and innovation performance all had Cronbach's A coefficient values of 0.829, 0.861, 0.823, and 0.881, respectively, all of which were greater than 0.8, indicating that the research data was reliable and could be used for future analysis.

Table 2: Cronbach's A coefficient test value.

Scale	Cases	Cronbach's value
Psychological contract	2	0.672
Psychological capital	3	0.829
Organization support	3	0.861
Proactive behavior	3	0.823
Innovation performance	4	0.881

3.2. Validity Analysis. Bartlett sphericity and KMO test were used for validity verification. From Table 3, psychological capital KMO value was 0.711, greater than 0.7, a good description was better; organization supports KMO value was 0.696, proactive behavior KMO value was 0.685, greater than 0.6, explain degree acceptance. Innovative performance KMO value was 0.802, greater than 0.8, with very good validity. There were only 2 psychological contract studies, and the KMO value was 0.5 in any case. The Bartlett sphericity test of psychological contract, psychological capital, proactive behavior, organizational support, and innovation performance all reached 0.01 significance level, suitable for factor analysis, indicating good validity of research items.

Table 3: KMO and Bartlett test values.

		Psychological contract	Psychological capital	Organization support	Proactive behavior	Innovation performance
KMO		0.500	0.711	0.696	0.685	0.802
Bartlett sphericity test	Approximate chi-square	32.199	117.702	155.640	120.646	242.078
	df	1	3	3	3	6
	p	<0.01	<0.01	<0.01	<0.01	<0.01

3.3. Analysis of Homology Deviation. Confirmatory factor analysis is used to examine the homogeneous deviation (CMV) (CFA). It means that all measurement items (measurement items relating to all variables) are grouped together and analysed as a single factor. If the model's fitting indicator, such as the χ^2/df, RMSEA, RMR, and CFI, does not meet the required standard, it shows that the model's fitting is poor, and all measurements should not be the same as one factor. As a result, the data passes the Common Method Divergence (CMV) test, indicating that there is no homology deviation.

This time put all 15 measurement items into one factor for CFA analysis, and the model fitting indicator was obtained as shown in Table 4:

Table 4 shows that the χ^2/df is 5.089, higher than standard (<3), and the four indicators of CFI, GFI, NFI, and NNFI are all lower than 0.7. The standard value of obvious deviation (>0.9), the RMSEA is higher than 0.10, and the RMR is higher than 0.05, also indicating the deviation standard value. Other indicators, for example, AGFI, PGFI, IFI, and PNFI, are all less than 0.7, and the severity deviation is higher than 0.9, and thus, the model fit quality is very bad, that is, the research scale data cannot be focused into a factor, namely, it shows that there is no homologous deviation problem.

3.4. Data Analysis. To investigate the relationship between the two variables, conduct a Pearson correlation study on each variable and utilise the Pearson correlation factor to describe the strength of the relevant association and relationship. The specific correlation coefficient values are shown in Table 5.

From Table 5, we can see that psychological contract, psychological capital, organizational support, proactive behavior, and entrepreneurial performance are all positive numbers greater than 0.4, and the significance of 0.01 levels, thus explaining the above 5 items have a significant positive correlation between each other.

3.5. Correlation and Mediating Effect Test. The main research variables have a link, according to Pearson correlation analysis. Based on this, the stepwise regression approach is used to further test the variables' relationships, revealing the causal link and mechanism of effect between variables.

Model 1 takes a psychological contract, psychological capital as an argument, and atrial behavior as a result of returning to variables to verify the relationship between psychological contract and psychological capital on innovative proactive behavior.

Model 2 uses a psychological contract, psychological capital as an argument, and innovative performance as a result of returning due to variables, to verify the relationship between psychological contract and psychological capital on innovation performance. After adding proactive behavior to Model 2; after Model 3 joins the proactive behavior based on the model, it is still based on innovative performance as a variable, verifying psychological contract, psychological capital, and proactive behavior on innovation performance; finally using step-by-step regression analysis mediating role.

From Table 6 Model 2, the psychological contract and the proactive performance return coefficient value is 0.142, the T value is 2.093, and it is remarkable at 0.05 level, indicating the psychological contract is significantly positive influence, so that H1a is established; the psychological capital and innovative performance regression coefficient is 0.385, the T value is 4.772, and it is remarkable at 0.01 level, indicating the psychological capital is significantly positive influence, so that H1b is established, then H1: psychological factors of science and technology personnel are significantly positively correlated with innovation performance must also be established.

From Table 6 Model 3, the F value change exhibits significance ($p < 0.05$) on the basis of Model 2, which means that the model is explained after the proactive behavior is added. In addition, the R^2 is rising from 0.352 to 0.586, meaning proactive behavior can be an explanation of 23.4% for innovative performance. Specifically, the proactive behavior regression coefficient value is 0.676 and has a significant property ($T = 7.404$, $p < 0.01$), meaning proactive behavior has a positive influence relationship of innovation performance. Therefore, it is assumed that H2 is established.

From Table 6 Model 1, it is known that the psychological contract and the proactive behavior return coefficient value is 0.182, the T value is 3.010, and it is remarkable at 0.01 level, indicating the psychological contract is significantly positive and influential, so it is assumed that H3a is established; the number of psychological capital and proactive behavior is 0.452, the T value is 6.297, and it is s remarkable at 0.01 level, indicating the psychological capital is significantly positive and influential. Therefore, assuming that H3b is established, then H3 must also be established. Therefore, it is assumed that H4a: proactive behavior mediates the relationship between psychological contract and innovation performance, and H4b: proactive behavior mediates the relationship between psychological capital and innovation performance. Then H4 is established.

Table 4: CFA analysis model fitting index.

Index	χ^2	df	p	χ^2/df	GFI	RMSEA	RMR	CFI	NFI	NNFI
Judge standard	—	—	>0.05	<3	>0.9	<0.10	<0.05	>0.9	>0.9	>0.9
Value	457.972	90	0.00	5.089	0.577	0.197	0.101	0.592	0.545	0.524
Other index	TLI	AGFI	IFI	PGFI	PNFI	SRMR	AIC	BIC		
Judge level	>0.9	>0.9	>0.9	>0.9	>0.9	<0.1	The smaller the better	The smaller the better		
Value	0.524	0.436	0.599	0.433	0.468	0.138	3240.873	3320.492		

Table 5: Pearson values of research variables.

	Psychological contract	Psychologica l capital	Organization support	Proactive behavior	Innovation performance
Psychological contract	1				
Psychological capital	0.481**	1			
Organization support	0.805**	0.465**	1		
Proactive behavior	0.492**	0.643**	0.596**	1	
Innovation performance	0.415**	0.553**	0.439**	0.749**	1

*$p < 0.05$; **$p < 0.01$.

Table 6: Mediation effect model of proactive behavior.

	Model 1 Proactive behavior	Model 2 Innovation performance	Model 3 Innovation performance
Psychological capital	0.452 (6.297**)	0.385 (4.772**)	0.080 (1.038)
Psychological contract	0.182 (3.010**)	0.142 (2.093*)	0.019 (0.339)
Proactive behavior			0.676 (7.404**)
R^2	0.473	0.352	0.586
Adjust R^2	0.441	0.313	0.556
F value	$F(6, 98) = 14.689$, $p < 0.01$	$F(6, 98) = 8.883$, $p < 0.01$	$F(7, 97) = 19.628$, $p < 0.01$

*$p < 0.05$, **$p < 0.01$, the value outside the bracket is the regression coefficient b value, and the value inside the bracket is the T value.

From Table 6 Model 3, it is also known that after joining the previous behavior on a Model 2, although proactive behavior has a significant positive impact relationship to innovation performance, the regression coefficient of psychological contract becomes 0.019, the T value is 0.339, which is not significant at 0.05, indicating the psychological contract is no longer influenced by innovation performance. The regression coefficient of psychological capital becomes 0.080, the T value is 1.038, and it is not significant at 0.05, indicating that psychological capital no longer positively affects innovation performance, As a result, proactive behavior may be demonstrated to play a totally mediating role in psychological contracts, psychological capital, and inventive performance. Therefore, assuming that H4a: proactive behavior mediates the relationship between psychological contract and innovation performance and H4b: proactive behavior mediates the relationship between psychological capital and innovation performance is established. Then H4: proactive behavior mediates the relationship between individual psychological factors and innovation performance must also be established.

3.6. Test of Regulating Effect

3.6.1. Organization Support Adjustment Effect Inspection between Innovation Performance and Individual Psychological Factors. Table 7 shows that independent variables of Model 4 are psychological capital, psychological contract, and dependent variable are innovation performance. In Model 5, the regulatory variable organizational support is added on Model 4. In Model 6, the product term of psychological contract and organizational support is added on Model 5, and in Model 7, the product term of psychological capital and organizational support is added on Model 5.

As can be seen from Model 6 in Table 7, the F value of Model 5 to Model 6 changes significantly ($p = 0.004 < 0.01$), and the interaction item between psychological contract and organizational support shows significant ($t = 2.941$, $p = 0.004 < 0.01$), which means the influence range of adjustment variable organizational support is significantly different at different levels, when psychological contract affects innovation performance. So H5a: organizational support moderates the relationship between innovation performance and psychological contract.

As can be seen from Model 7 in Table 7, F value from Model 5 to Model 7 changes significantly ($p = 0.002 < 0.01$), and the interactive item supported by organizational support and psychological capital has shown significance ($T = 3.225$, $p = 0.002 < 0.01$), which means that when psychological capital affects proactive behavior, the moderating variable organizational support has significant differences at different levels. So the hypothesis H5b: organizational support moderates the relationship between innovative performance

Table 7: Moderating effect model of organizational support between individual psychological factors and innovation performance.

	Model 4	Model 5	Model 6	Model 7
Psychological capital	0.385 (4.772**)	0.361 (4.448**)	0.339 (4.324**)	0.372 (4.795**)
Psychological contract	0.142 (2.093*)	0.009 (0.085)	0.016 (0.166)	0.000 (0.002)
Organizational support		0.186 (1.724)	0.211 (2.028*)	0.181 (1.757)
Psychological contract * organizational support			0.161 (2.941**)	
Psychological capital * organizational support				0.267 (3.225**)
R^2	0.352	0.372	0.423	0.433
Adjust R^2	0.313	0.326	0.375	0.386
F value	$F(6, 98) = 8.883,\ p < 0.01$	$F(7, 97) = 8.192,\ p < 0.01$	$F(8, 96) = 8.814,\ p < 0.01$	$F(8, 96) = 9.163,\ p < 0.01$
$\triangle R^2$	0.352	0.019	0.052	0.061
$\triangle F$ value	$F(6, 98) = 8.883,\ p < 0.01$	$F(1, 97) = 2.973,\ p = 0.088$	$F(1, 96) = 8.647,\ p = 0.004$	$F(1, 96) = 10.400,\ p = 0.002$

Dependent variable: innovation performance. $^{*}p < 0.05$, $^{**}p < 0.01$, the value outside the bracket is the value of regression coefficient b, and the value inside the bracket is the value of T.

Table 8: Moderating effect model of organizational support between individual proactive behavior and innovation performance.

	Model 8	Model 9	Model 10
Proactive behavior	0.749 (11.258**)	0.752 (8.930**)	0.753 (8.913**)
Organizational support		−0.003 (−0.053)	−0.010 (−0.147)
Proactive behavior * organizational support			0.043 (0.584)
R^2	0.580	0.580	0.582
Adjust R^2	0.559	0.554	0.551
F value	$F(5, 99) = 27.356,\ p < 0.01$	$F(6, 98) = 22.567,\ p < 0.01$	$F(7, 97) = 19.262,\ p < 0.01$
$\triangle R^2$	0.580	0.000	0.001
$\triangle F$ value	$F(5, 99) = 27.356,\ p < 0.01$	$F(1, 98) = 0.003,\ p = 958$	$F(1, 97) = 0.341,\ p = 0.560$

Dependent variable: innovation performance. $^{*}p < 0.05$, $^{**}p < 0.01$, the value outside the bracket is the value of regression coefficient b, and the value inside the bracket is the value of T.

and psychological capital. So assumed that H5: organizational support moderates the relationship between individual innovation performance and psychological factors are also established.

3.6.2. Organization Support Adjustment Effect Inspection between Innovation Performance and Individual Proactive Behavior. Model 8's dependent variable innovation performance and independent variable proactive behavior are shown in Table 8, while Model 9 adds the support of regulatory variable organization to Model 8 and Model 10 adds the product term of interaction term, proactive behavior, and organization support to Model 9.

According to Model 10 in Table 8, the change of F value from Model 9 to Model 10 is not significant ($p = 0.560 > 0.05$), and the interaction between psychological contract and organizational support is not significant ($t = 0.584$, $p = 0.560 > 0.05$). From the comparison between Model 8 and Model 10, it can be observed that when proactive behavior has an influence on innovation performance, the adjustment variable organizational support has the same impact range at various levels. Assume that H6 has been established.

3.6.3. Organization Support Adjustment Effect Inspection between Individual Psychological Factors and Proactive Behavior. According to Table 9, the independent variables of Model 11 are psychological contract, psychological capital, and dependent variable proactive behavior. Model 12 adds the regulatory variable organizational support on Model 11, Model 13 adds the product term of interaction term, psychological contract and organizational support on Model 12, and Model 14 adds the product term of interaction term, psychological capital, and organizational support based on Model 12.

According to Model 13 in Table 9, the F value from Model 12 to Model 13 changes significantly ($p = 0.001 < 0.01$), and the interaction items between psychological contract and organizational support show significant ($t = 3.339$, $p = 0.001 < 0.01$), which means that when psychological contract affects proactive behavior, the influence range of regulatory variable organizational support is significantly different at different levels. Therefore, assumed that H7a: organizational support moderates the relationship between proactive behavior and psychological contract is established.

According to Model 14 in Table 9, the F value from Model 12 to Model 14 changes significantly ($p = 0.006 < 0.01$), and the interaction item between psychological capital and organizational support shows significant ($t = 2.798$, $p = 0.006 < 0.01$). It suggests that the effect range of regulatory variable organizational support on proactive behavior is considerably varied at various levels

Table 9: Moderating effect model of organizational support between individual psychological factors and proactive behavior.

	Model 11	Model 12	Model 13	Model 14
Psychological capital	0.452(6.297**)	0.406(5.961**)	0.386(5.925**)	0.414(6.284**)
Psychological contract	0.182(3.010**)	−0.073(−0.843)	−0.065(−0.798)	−0.079(−0.947)
Organizational support		0.354(3.916**)	0.378(4.378**)	0.351(4.010**)
Psychological contract * organizational support			0.152(3.339**)	
Psychological capital * organizational support				0.197(2.798**)
R^2	0.473	0.545	0.593	0.580
Adjust R^2	0.441	0.513	0.559	0.545
F value	$F(6,98) = 14.689$, $p < 0.01$	$F(7,97) = 16.624$, $p < 0.01$	$F(8,96) = 17.461$, $p < 0.01$	$F(8,96) = 16.549$, $p < 0.01$
$\triangle R^2$	0.473	0.072	0.047	0.034
$\triangle F$ value	$F(6,98) = 14.689$, $p < 0.01$	$F(1,97) = 15.339$, $p < 0.01$	$F(1,96) = 11.149$, $p = 0.001$	$F(1,96) = 7.830$, $p = 0.006$

Dependent variable: proactive behavior. $^{*}p < 0.05$, $^{**}p < 0.01$, the value outside the bracket is the value of regression coefficient b, and the value inside the bracket is the value of T.

when psychological capital is involved. As a result, it is demonstrated that H7b: organizational support moderates the link between proactive behavior and psychological capital. It is also true that H7: organizational support moderates the relationship between proactive behavior and individual psychological factor.

4. Conclusions

Enterprises can use psychological contract and psychological capital to stimulate employees' proactive behavior and enhance individual innovation performance. Enterprise managers hide the positive psychology of technology employees through psychological contracts and psychological capital development. This research integrates psychological contract and psychological capital. It has been confirmed that the psychological capital and psychological contract are positively correlated with individual proactive behavior and innovation performance. The proactive behavior is also positively correlated with individual innovation performance. Through organizational support, businesses may encourage proactive behavior among employees and improve individual innovation performance. It motivates employees to take the initiative to improve their individual innovation performance by instilling proactive behavior in them. The results show that the proactive behavior mediates the relationship between individual psychological capital, psychological contract factor, individual innovation performance, and organizational support. The employee's individual innovation performance is improved by strengthens the influence of individual proactive behavior of employees. Since such behaviours are not purely passive, therefore, if companies want to improve the individual innovation performance, the key is to stimulate employees' proactive behaviours and then they can improve the individual innovation performance.

The collection of questions parallel to other work can lead to lessen the risk of deviating from the same source approach, in future by adopting combination of horizontal and vertical field survey method the persuasiveness of work might be obtained. The current research only worked on psychological factors and organizational support on proactive behavior and innovation performance. More factors, such as job characteristics, should be added in future research to make the analysis more comprehensive and detailed.

Data Availability

The data used to support the findings of this study are included within the article.

Conflicts of Interest

The authors declare that they have no competing interest.

Acknowledgments

This study was supported by Guangdong Provincial Department of Education Research Platform 2018 Characteristic Innovation Topics Science and Technology Personnel Proactive Behavior Development and Innovation Performance-Taking Guangdong and Hong Kong, Macau Dawan District High-tech Enterprises as an Example (2018GWTSCX05).

References

[1] T. C. Shao, *Profiling Organizational Climate as an Indicator of Readiness for Innovation at a Selected institute of Technology in Taiwan*, The University of South Dakota, Vermillion, SD, USA, 2002.

[2] Y. Gu and J. Peng, "The influence of organizational innovation atmosphere on employee innovation behaviour: the mediating role of innovation self-efficacy," *Nankai Management Review*, vol. 13, no. 01, pp. 30–41, 2010.

[3] S. J. Ashford, N. P. Rothbard, S. K. Piderit, and J. E. Dutton, "Out on a limb: the role of context and impression management in selling gender-equity issues," *Administrative Science Quarterly*, vol. 43, no. 1, pp. 23–57, 1998.

[4] K. L. Unsworth and S. K. Parker, *Promoting a Proactive and Innovative Workforce for the New Workplace*, John Wiley & Sons, Hoboken, NJ, USA, 2003.
[5] X. Li and L. Su, "Context and review of research on employee proactive behaviour in the context of innovation," *Science of Science and Management of Science and Technology*, vol. 33, no. 12, pp. 144–152, 2012.
[6] T. M. Amabile, "The social psychology of Creativity: a componential conceptualization," *Journal of Personality and Social Psychology*, vol. 45, no. 2, pp. 357–377, 1993.
[7] Yi. Han, J. Liao, and L. Long, "Construction and empirical study of employee work performance structure model [J]," *Journal of Management Science*, no. 05, pp. 62–77, 2007.
[8] A. N. Pieterse, D. Van Knippenberg, M. Schippers, and D. Stam, "Transformational and transactional leadership and innovative behaviour: the moderating role of psychological empowerment," *Journal of Organizational Behaviour*, vol. 31, no. 4, pp. 609–623, 2010.
[9] W. Yu, Y. Fan, J. Zhang, and M. Yi, "Will the heterogeneity of values promote the production of innovation performance? -The mediated moderating effect of supportive organizational climate and feedback-seeking behavior," *Forecast*, vol. 34, no. 02, pp. 14–21, 2015.
[10] Q. Tao and T. Gao, "Social innovation: source, research context and theoretical framework [J]," *Foreign Economics and Management*, vol. 41, no. 6, pp. 85–104, 2019.
[11] C. Argyris, *Understanding Organizational Behaviour*, Dorsey Press, Homeward, IL, USA, 1960.
[12] H. Levinson, C. R. Price, K. J. Munden, and C. M. Solley, *Men, Management and Mental Health*, Harvard University Press, Cambridge. MA, USA, 1962.
[13] E. H. Schein, *Organizational Psychology*, Prentice-Hall, Englewood Cliffs, NJ, USA, 1965.
[14] J. P. Kotter, "The psychological contract: managing the joining-up process," *California Management Review*, vol. 15, no. 3, pp. 91–99, 1973.
[15] M. H. Dunahee and L. A. Wangler, "The Psychological Contract: a conceptual structure for management/employee relations," *Personnel Journal*, vol. 53, pp. 518–526, 1974.
[16] D. M. Rousseau, "Psychological and implied contracts in organizations," *Employee Responsibilities and Rights Journal*, vol. 2, no. 2, pp. 121–139, 1989.
[17] W. H. Turnley, M. C. Bolino, and S. W. Lester, "The effects of psychological contract breach on union ommitment," *Journal of Occupational*, vol. 6, pp. 37–39, 2004.
[18] S. Zhang and J. Liao, "Psychological contract of enterprise employees: exploration of the difference between state-owned enterprises and private enterprises," *Business Economics and Management*, no. 6, pp. 26–33, 2008.
[19] R. Xue, He Zhao, and X. Li, "An empirical study on the relationship between psychological contracts and employee performance--take communication enterprises as an example," *Finance and Accounting Newsletter*, vol. 717, no. 25, pp. 29–32, 2016.
[20] S. Wang, H. Wang, and F. Li, "A study on the relationship between psychological contract and the performance of university scientific research innovation teams--taking work embeddedness as an intermediary variable," *Journal of Yangzhou University (Agricultural and Life Science Edition)*, no. 4, pp. 51–55, 2016.
[21] F. Luthans, B. J. Avolio, F. O. Walumbwa, and W. Li, "The psychological capital of Chinese workers: exploring the relationship with performance," *Management and Organization Review*, vol. 1, pp. 247–269, 2005.
[22] S. F. Lu, *Psychological Capital: Building Human Competitive Advantages. Li Chaoping*, China Light Industry Press, Beijing, China, 2007.
[23] D. Sweetman, J. B. Luthans, F. Avey, and B. C. Luthans, "Relationship between positive psychological capital and creative performance," *Canadian Journal of Administrative Sciences - Revue Canadienne des Sciences de l Administration*, vol. 28, no. 1, pp. 4–13, 2011.
[24] Q. Wu and D. You, "Cross-level analysis of employee psychological capital, organizational innovation atmosphere and technological innovation performance," *Systems Engineering*, vol. 29, no. 01, pp. 69–77, 2011.
[25] W. Shen, "The influence of civil servants' psychological capital and knowledge acquisition on innovation performance and the intermediary mechanism," *China Human Resources Development*, no. 09, pp. 70–73+84, 2015.
[26] L. Xu and L. Li, "Analysis of the psychological capital and innovative performance relationship of nobel prize in China - an analysis of the case of Tu Youyou," *Journal of Science and Technology Progress and Countermeasures*, vol. 33, no. 07, pp. 1–6, 2016.
[27] S. J. Crant, "Proactive behavior in organizations," *Journal of Management*, vol. 26, no. 3, pp. 435–462, 2000.
[28] D. J. Campbell, "The proactive employee: managing workplace initiative," *Academy of Management Perspectives*, vol. 14, no. 3, pp. 52–66, 2000.
[29] S. K. Parker, T. D. Wall, and J. Cordery, "Future work design research and practice: towards an elaborated model of work design," *Journal of Occupational and Organizational Psychology*, vol. 74, no. 4, pp. 413–440, 2001.
[30] F. D. Belschak, D. N. Den Hartog, and D. Fay, "Exploring positive, negative and context-dependent aspects of proactive behaviours at work," *Journal of Occupational and Organizational Psychology*, vol. 83, no. 2, pp. 267–273, 2010.
[31] E. Hou, S. Chen, and Q. Chang, "The impact of knowledge workers' psychological capital on innovation performance: the intermediary of psychological contract," *Science of Science and Management of Science and Technology*, vol. 33, no. 06, pp. 149–155, 2012.
[32] Z. X. Chen, A. S. Tsui, and L. F. Zhong, "Reactions to psychological contract breach: a dual perspective," *Journal of Organizational Behavior*, vol. 29, no. 5, pp. 527–548, 2008.
[33] Q. Xu, "Research on the influence of Chinese enterprise employees' psychological capital on work values," Master's degree thesis, Tsinghua University, Beijing, China, 2013.
[34] W. Li and J. Li, "The relationship between psychological empowerment and employees' innovative behavior: the mediating role of a new perspective of psychological contract," *Industrial Technology Economics*, vol. 35, no. 10, pp. 78–84, 2016.
[35] Y. Dong and J. Gao, "The influence of psychological capital on the innovation initiative of employees," *Academic Exchange*, no. 11, pp. 122–125, 2016.
[36] E. Hou, S. Chen, and Q. Chang, "Research on the relationship between the psychological capital, intrinsic motivation and innovation performance of enterprise knowledge employees," *Journal of Dalian University of Technolgy*, vol. 33, no. 2, pp. 65–70, 2012.
[37] H. Zhang, "An empirical study on the impact of psychological capital on innovation performance," *Management World*, no. 10, pp. 170-171, 2013.
[38] Z. Xiong, Y. Zhu, and Y. Zhang, "Research on the impact of human capital, social capital and psychological capital on the new generation of knowledge workers' innovative

performance--based on the mediation of job satisfaction and the adjustment of job characteristics," *Journal of Hunan University*, no. 6, pp. 79–87, 2018.

[39] R. Eisenberger, R. Huntington, S. Huntington, and D. Sowa, "Perceived organizational support," *Journal of Applied Psychology*, vol. 71, no. 2, pp. 500–507, 1986.

[40] W. Ling, H. Yang, and L. Fang, "Organizational support of enterprise employees," *Psychological Bulletin*, vol. 38, no. 2, pp. 281–287, 2006.

[41] A. F. McKenny, J. c Short, and G. T. Payne, "Using computer-aided text analysis to elevate constructs," *Organizational Research Methods*, vol. 16, no. 1, pp. 152–184, 2013.

[42] I. Ajzen and M. Fishbein, *Understanding Attitudes and Predicting Social Behavior*, Prentice-Hall, Englewood Cliffs, NJ, USA, 1980.

[43] Li. Yuan, *Research on the Structure and Related Factors of Employee Psychological Contract*, Capital Normal University, Beijing, China, 2002.

[44] C. E. Janssen, L. L. Gilson, and T. C. Blum, "Interactive effects of growth need strength, work context, and job complexity on self-reported creative performance," *Academy of Management Journal*, vol. 52, no. 3, pp. 349–505, 2004.

Hindawi
Scientific Programming
Volume 2022, Article ID 1691400, 12 pages
https://doi.org/10.1155/2022/1691400

Research Article

Research on Marketing Strategy of Railway Passenger Travel Behaviour Analysis in Competitive Section

Xiaopei Hao,[1] **Jiansheng Zhu**,[2] **Xinhua Shan**,[2] **and Wen Li**[2]

[1]*China Academy of Railway Sciences, Beijing 100081, China*
[2]*Institute of Computing Technologies, China Academy of Railway Sciences, Beijing 100081, China*

Correspondence should be addressed to Jiansheng Zhu; zhujiansheng@rails.cn

Received 2 April 2022; Revised 9 May 2022; Accepted 16 May 2022; Published 1 June 2022

Academic Editor: Muhammad Usman

The deep mining of passengers' travel data can identify competitive segments and gain insights into passengers' characteristics and differentiated demands. This can not only effectively support precise marketing strategy adjustment of railway transport but also improve its competitiveness in the passenger transportation market. In this paper, hidden railway travel behaviour is introduced and integrated with railway travel behaviour to create a complete passenger travel chain, based on existing distance-based competitive segment recognition methods. The loyalty index values of passengers are calculated using this travel chain to identify competitive segments. Furthermore, passenger classification and grouping currently ignore social relationships as well as personal travel characteristics. Therefore, a novel passenger grouping method is proposed; it integrates individuals' travel characteristics and social relations. Individual travel labels are created for travellers based on their travel data. Social relation topologies, such as ticketing relation, the relation of travelling together, and benefit relation via point redemption, can be extracted using these labels. Social relation traits can be retrieved using graph attention networks and multigraph fusion. Finally, travellers are categorised based on their individual travel characteristics. As an example, and a case study, the grouping of Guangzhou–Shanghai passengers in 2020 is taken which shows that the suggested method has the potential to improve both the precision and the feasibility of grouping railway passengers. As a result, new ideas for passenger grouping in railway marketing might be offered.

1. Introduction

Passengers who have a travel demand select appropriate trip plans according to their characteristics in conjunction with various factors related to transportation services, like safety, comfort, convenience, speed, punctuality, and cost-effectiveness. To assist railway passenger transportation administration departments in formulating customised and personalised service strategies based on the travel characteristics of diverse groups, we need to accurately and effectively define the competitive segments of different transportation modes, profoundly investigate the vehicle selection behaviours of passengers, quantitatively analyse the individual factors influencing passengers' travel choices and their social relations in travel, gain insights into the characteristics and differentiated demands of passengers, and finally divide passengers into different groups. This may further promote the passenger service mode innovation, service strategy transformation, and service quality improvement of railway transportation. Theoretical bases can also be provided for railway passenger transport enterprises to reasonably design train service products and implement precision marketing activities.

Regarding the different transportation modes in China's passenger service market, diverse marketing strategies are selected for various segments to meet passengers' demands and attract passengers, thus improving their market competitiveness. In this context, effective recognition of the competitive segments of various transportation means is the basis on which railway passenger service enterprises analyse the advantages of their competitors, discover their weaknesses, and optimise their marketing strategies. According to Dobruszkes et al. [1], supplies are dynamically adjusted by European aviation companies in line with the running time of G-series high-speed trains. The longer the running time, the greater the number of supplies. Supplies are specifically

at the minimum for running times within 2–2.5 h (corresponding travel distance: approximately 500 km). Through a comparative analysis of the superiorities of the passenger transportation means in Taiwan, Cheng [2] stated that civil aviation, G-series high-speed train travel, and highway travel are primarily suitable for distances of 700 km and above, 200–700 km, and 200 km and below, respectively. According to Zhang et al. [3], the travel distance is a crucial aspect that influences passengers' travel decisions. The 600–1,000 km segment is the most competitive between G-series high-speed trains and civil aviation, while the segment with the highest competition is approximately 1,000 km. Due to the vastness of China's territory, imbalanced economic development between various areas, and changes in passenger composition within segments, distance-based division and categorisation of competitive segment may have several drawbacks.

Group segmentation is a foundation of marketing strategy optimisation. In essence, it aims to learn user characteristics, demands, and objectives by analysing historical data to provide users with customised service strategies, maximise benefits, and optimise service quality. For example, in the intuitive target market selection method of Chou et al. [4], the personal features of individuals are established based on demographic variables to identify potential customers. In another approach, the categories and prices of products purchased by customers are analysed to calculate consumer buying behaviour similarity. The simulated annealing algorithm is applied in a behaviour-based customer segmentation model (Yan et al. [5]). According to Holly, self-organising neural networks may also be used for customer segmentation, depending on the particular features of the customers (Rushmeier et al. [6]). Qian [7] created a mixture regression model to investigate how passengers rate safety, comfort, speed, frequency, punctuality, prices, and convenience; he used the expectation maximisation algorithm to evaluate regression coefficients and calculate the distribution probability of passengers. Bayesian statistics is used for this purpose resulting in passenger group segmentation. The recency, frequency, monetary (RFM) model for customer value judgement was introduced and combined with the analytic hierarchy process and fuzzy clustering to segment passengers into five categories and analyse their potential transformation classes; the resulting model was used to identify customer values (Li [8]). The multiclass twin support vector machine (MTWSVM) has been thoroughly explored and experimentally verified to perform well in multiclass classification problems (Zhang et al. [9]). However, the existing travel behaviour research data are mostly collected by means of questionnaire surveys. Questions in these questionnaires usually have certain shortcomings, such as lack of detailed information. Furthermore, although customer segmentation models principally consider the personal features of customers, they neglect the social relations of these individuals. This makes it unlikely for such models to describe customer characteristics comprehensively based on vectors and thereby compromises the performance of the model.

In this study, a passenger railway travel chain that depends on passenger railway travel data is constructed. Hidden railway travel behaviour is introduced to perfect the railway travel chain and then analysed to recognise relevant competitive segments and calculate the railway travel loyalty indices of passengers. Afterwards, we focus on the grouping of railway passengers in competitive segments to analyse their individual travel characteristics and establish social networks during their travels. The loyalty indices of passengers serve as an initial strategy of group segmentation, and the graph attention mechanism is adopted to build a group recognition model. Through passenger group segmentation for competitive segments, passenger transport products are reasonably designed for different competitive segments of railways, and personalised marketing strategies can be made. As a result, passenger experience is improved, and theoretical support is provided for railway resource utilisation efficiency.

2. Travel Chain Analysis

2.1. Travel Chains. Travel, a door-to-door traffic behaviour performed to achieve a certain trip goal, is defined by a set of behaviours that include information such as departure time, departure location, destination, mode of transportation, and journey distance [10]. A travel chain represents the entire passenger travel process. It is made up of connecting links that are placed according to the departure time of a travel behaviour. Generally, passengers select appropriate transportation means to achieve their trip purposes and generate complete travel chains for themselves.

The data involved in this study are primarily derived from the real-name system and travel information of railway passengers from Guangzhou to Shanghai. Because of data limitations, no complete travel chains can be formed from the data of passengers who go on tours by multiple modes of transportation. Therefore, hidden railway travel behaviour is introduced, and urban transport is ignored to generate complete travel chains for these passengers. Travel data from 2020 are ranked based on riding time to construct the travel chains of passengers, as shown in Table 1. A travel chain (LC) is formed through an end-to-end connection between the railway travel behaviour and the hidden railway travel behaviour, which are, respectively, defined as TB_j = (train_date, start_time, start_city, to_city) and OB_j = [start_date, stop_time, start_city, to_city]. Integrity (CP) signifies whether the railway travel behaviour of a passenger constitutes a complete travel chain, that is, whether the destination city of the j th trip by train is the departure city selected for the $(j + 1)$th trip by train. TBH is the number of hidden railway travels. It represents the least number of trips that need to be increased when a passenger produces a complete travel chain based on a railway trip. Loyalty to the railway industry, which is denoted by LOY_i, indicates the probability of passenger i to complete intercity displacement by train, and it is expressed as

$$LOY_i = \frac{TBR_i}{TBR_i + TBH_i} * 100, \tag{1}$$

where TBR_i stands for the total number of times passenger i travels by train in a travel chain.

Table 1: Railway passenger travel chain in 2020.

ID	LC	CP	TBH	LOY	ODY	DDY
P_1	(20200119, 1846, Hangzhou, Nanjing, 322 km) -> [20200814, 20200816, Nanjing, Suzhou, 297 km] -> (20200212, 1046, Suzhou, Hangzhou, 692 km) -> (20200718, 0910, Hangzhou, Hefei, 443 km) -> (20200719, 1504, Hefei, Hangzhou, 439 km) -> (20200720, 1739, Hangzhou, Nanjing, 322 km) -> (20200807, 2019, Nanjing, Suzhou, 297 km) -> (20200921, 1304, Suzhou, Hangzhou, 692 km)	No	1	87.5	(Nanjing, Suzhou, 50)	(250 km–350 km, 75)
P_2	(20201004, 1816, Jinhua, Cangnan) -> (20201005, 1730, Cangnan, Jinhua)	Yes	0	100	No	No
P_3	(20200605, 1849, Hangzhou, Jiaxing, 79 km) -> (20200607, 1127, Jiaxing, Hangzhou, 78 km) -> (20201006, 0944, Hangzhou, Yuyao) -> (20201006, 1928, Yuyao, Hangzhou) -> (20201107, 1529, Hangzhou, Jiaxing, 79 km) -> (20201108, 1429, Jiaxing, Hangzhou, 78 km)	Yes	0	100	No	No
P_4	(20200810, 1413, Jiaxing, Hangzhou, 78 km) -> (20200810, 1501, Hangzhou, Jinhua) -> [20200810, 20200814, Jinhua, Hangzhou, 153 km] -> (20200814, 1308, Hangzhou, Jinhua) -> [20200814, 20200816, Jinhua, Quzhou, 110 km] -> (20200816, 2240, Quzhou, Zhuzhou, 666 km) -> (20200822, 2156, Zhuzhou, Hangzhou, 932 km) -> (20200823, 2050, Hangzhou, Jiaxing, 79 km) -> (20200827, 1457, Jiaxing, Hangzhou, 78 km) -> (20200827, 1532, Hangzhou, Quzhou, 263 km) -> [20200827, 20200830, Quzhou, Hangzhou, 260 km] -> (20200830, 2141, Hangzhou, Jiaxing, 79 km) -> (20201115, 1523, Jiaxing, Hangzhou, 78 km) -> (20201115, 1614, Hangzhou, Liling, 887 km) -> (20201116, 1533, Liling, Jinhua, 704 km) -> (20201116, 2050, Jinhua, Hangzhou, 153 km)	No	3	81.25	(Jinhua, Hangzhou, 50) (Jinhua, Quzhou, 0)	(150 km–2000 km, 50) (50 km–100 km)
P_5	(20200820, 1832, Hefei, Yangzhou, 143 km) -> (20200824, 1506, Yangzhou, Shanghai, 324 km) -> (20200824, 1828, Shanghai, Hangzhou, 163 km)	No	0	100	No	No

$\mathrm{ODY}(F,T)_i$, loyalty to a segment, signifies the probability of passenger i, who has a travel demand in segment (F,T) (the segment from departure F to destination T) to select a railway. It is determined as

$$\mathrm{ODY}(F,T)_i = \frac{\mathrm{TBR}(F,T)_i}{\mathrm{TBR}(F,T)_i + \mathrm{TBH}(F,T)_i} * 100, \quad (2)$$

where $\mathrm{TBR}(F,T)_i$ is the total number of times passenger i takes a train in segment (F,T) belonging to his/her travel chain and $\mathrm{TBH}(F,T)_i$ represents the number of times a hidden railway travel behaviour occurs in segment (F,T).

$\mathrm{DDY}(D_f,D_t)_i$, loyalty to travel distance, is the probability of passenger P_i, who has a travel demand to take a train over the trip distances of D_t and D_f. They can be calculated by

$$\mathrm{DDY}\left(D_f,D_t\right)_i = \frac{\mathrm{TBR}(F,T)_i}{\mathrm{TBR}(F,T)_i + \mathrm{TBH}(F,T)_i} * 100, \quad D_f \le D(F,T) \le D_t, \quad (3)$$

where D_f and D_t are the maximum and minimum travel distances, respectively. The travel distances, $TBR(F,T)_i$ and $TBH(F,T)_i$, must be within the range of $[D_f,D_t)$.

According to Table 1, the travel chain (TC_1) of passenger P_1 consists of seven railway travel behaviours. TB_1 represents a travel behaviour involving departure by train from Hangzhou at 18:46, 19 January 2020, and arrival in Nanjing; TB_2 is a travel behaviour involving departure from Suzhou at 10:46, 12 February 2020, and arrival in Hangzhou; TB_3 refers to a departure from Hangzhou at 9:10, 18 July 2020, and arrival in Hefei; TB_4 means that the passenger leaves Hefei at 15:04, 19 July 2020, for Hangzhou; TB_5 stands for departure from Hangzhou at 17:39, 23 July 2020, and arrival in Nanjing; TB_6 means a departure from Nanjing at 20:19, 7 August 2020, and arrival in Suzhou; TB_7 involves leaving Suzhou at 13:04, 21 September 2020, and arriving in Hangzhou. Analysis shows that in the travel chain of passenger P_1, the destination city of TB_1 is not the departure city of TB_2. This reveals that this passenger chooses another mode of transportation to complete his/her travel from Nanjing to Suzhou. In other words, at least one travel behaviour from Nanjing to Suzhou is absent. Therefore, the number of occurrences of hidden railway travel is 1. Considering that 8 is the number of times of travel in a complete travel chain, the number of trips completed by train is 7. From equation (1), the passenger's loyalty to travelling by train is 87.5. Moreover, the hidden railway travel behaviour of this passenger occurs in the segment from Nanjing to Suzhou; hence, either the number of occurrences of railway travel or that of hidden railway travel is 1 in this segment. According to equation (2), loyalty

to the segment of a hidden railway travel behaviour is 50. Equation (3) is utilised to determine the passenger's loyalty to a travel distance of 250–350 km, which is 75.

2.2. Analyses of Competitive Segments. The proportion of a hidden railway travel behaviour in a segment can effectively show whether the passenger service products designed for this segment are reasonable, whether the service quality needs to be further enhanced and whether its marketing strategies should be optimised. A large proportion indicates that the existing railway passenger services in the segment fail to meet the travel demands of most passengers. The greater the proportion, the lower the competitiveness of this segment. In this study, the proportions of hidden railway travel behaviours reflect the competitiveness of competitive segments, as expressed by

$$\mathrm{TBHP}(F,T) = \frac{\sum_{i=1}^{n} \mathrm{TBH}_i}{\sum_{i=1}^{n} \left(\mathrm{TBR}_i + \mathrm{TBH}_i\right)}, \tag{4}$$

where $\mathrm{TBHP}(F,T)$ represents the competition intensity from a departure city (F) to a destination city (T); $\sum_{i=1}^{n} TBH_i$ is the number of occurrences of all hidden railway travel behaviours in the segment; and $\sum_{i=1}^{n} TBR_i + TBH_i$ is the sum of the total number of occurrences of railway travel behaviour and that of hidden railway travel behaviour in the segment.

Spark is used to analyse data related to the railway travel behaviour of all passengers in 2020. Being an open source, Apache Spark is a distributed processing system for big data workloads. On this basis, the proportions of hidden railway travel behaviours in segments of different distances are obtained, as shown in Figure 1. An increase in the travel distance is clearly accompanied by a drop followed by an increase in the competition intensity. When the competition intensity of a segment with a travel distance of no more than 50 km exceeds 10%, highways characterised by flexibility, simplicity, and convenience become the main competitors of railways. At travel distances over 1,350 km, the corresponding competition intensity can be raised accordingly. In such segments, flights become the main competitors of railways because of their high speed, safety, and other benefits. The competition is less intense when the travel distance varies from 150 to 1,000 km; therefore, this can be regarded as the dominant segment where railways are superior to other modes of transportation.

3. Construction of Passengers' Travel Behaviour Characteristics

This section presents discussions that are based on railway ticketing data and oriented by the passenger transportation market, and aviation marketing strategies are used as reference. From the perspectives of passengers' personal characteristics and social relations, it aims to fulfil the mining, clustering, regrouping, and deep fusion of digital railway passenger transportation resources. Furthermore, different passenger groups can be segmented, which may help gain insights into the associations between passengers' characteristics and their selection of transportation means.

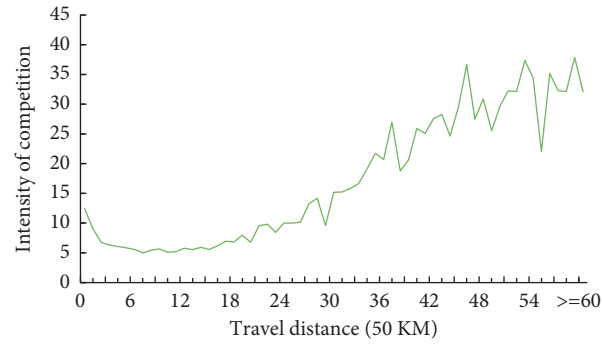

Figure 1: Relationship of travel distance (50 km) and competition intensity.

Hopefully, a data basis can be provided for model improvement, theory refinement, the research process, and the optimisation method.

3.1. Travel Characteristics of Individuals. In the CRNet ticketing system, feature data associated with individual passengers can be divided into two categories: demographic data (about natural attributes) and travel behaviour data. The former relates to information already stored in the system, such as gender, age, and residence. These data are often known as static data since they rarely change and have a relatively constant data structure. A sequence of behaviour records made during a trip, such as ticket booking, travel, ticket check, and inbound/outbound data, fall under the latter group. They are also known as dynamic data because of their high frequency of occurrence. Passengers are shown using multiple data dimensions based on these two kinds of data. As given in Figure 2, the static and dynamic characteristics of passengers are generated with abstract semantic labels that are easy to understand, thus producing a full view of passenger information [11].

3.2. Social Relations. Most passengers in a transportation system do not make decisions on their own, including how their travel requests are generated, how their travel routes are planned, and how their travel times and modes are decided. Passengers are influenced by their social relationships in addition to their preferences and traffic situations.

Since the 12306 Internet ticketing system went online in 2012, massive data capable of embodying social relations have been accumulated by its unique business process. Based on these data, we can extract ticketing relations, relations of travelling together, and relation of benefits by the point redemption mechanism.

3.2.1. Ticketing Relation. This is a relation between a purchaser and a passenger. A single ticketing relation includes the following information: ticket purchaser, passenger, ticket purchasing time, ticket price per kilometre, and number of tickets. Here, $G(i, j)$ represents a behavioural sequence of a ticketing relation in which passenger i buys a ticket for passenger j; $G(i, j)[k] = (b_k, gt_k, atp_j[k])$ denotes a record

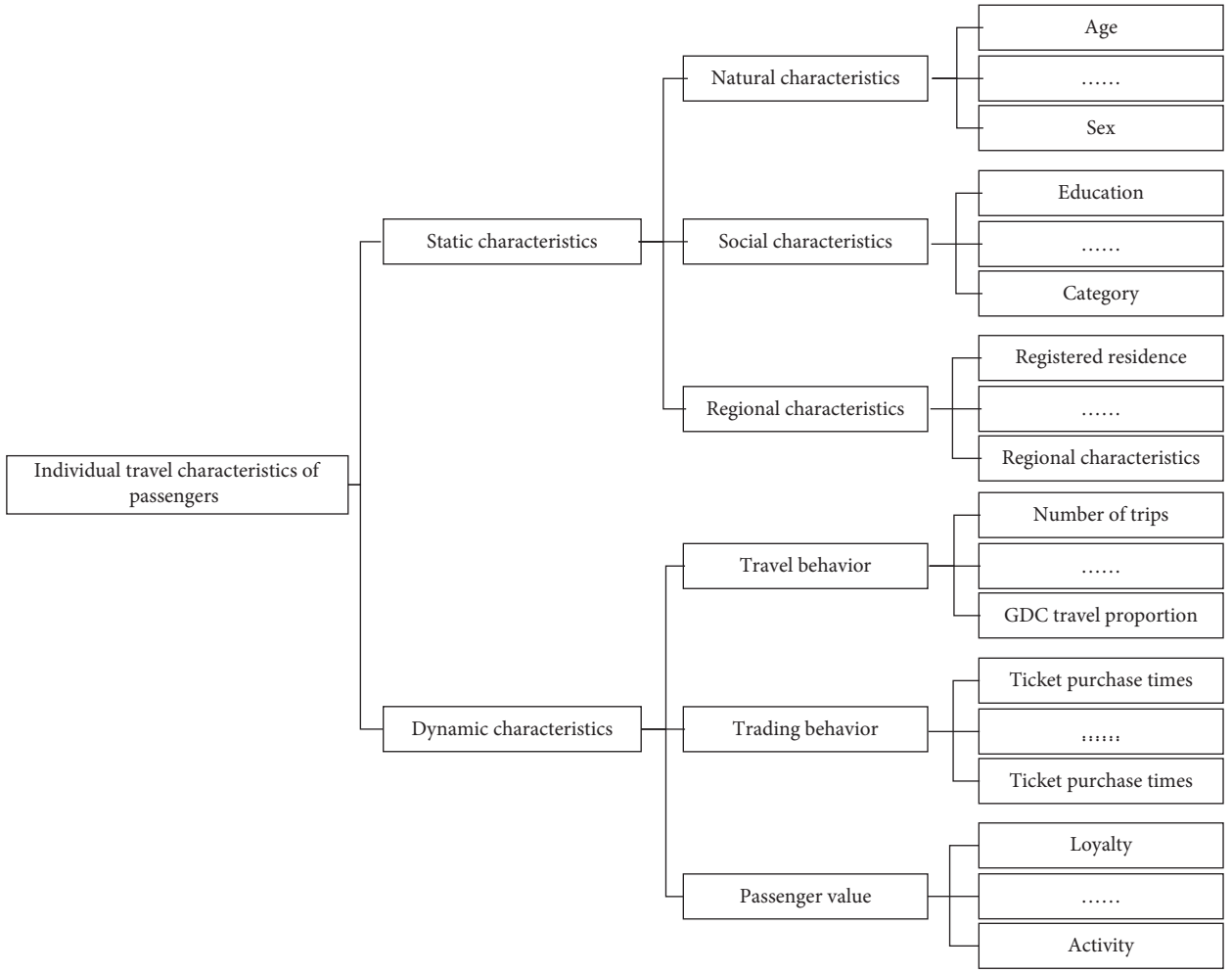

Figure 2: Travel characteristics of individuals.

of the k th ticket purchasing behaviour, where b_k stands for the number of tickets purchased, gt_k the time of buying a ticket, and $atp_j[k]$ the ticket price per kilometre. In accordance with the sequence of a passenger's ticketing relation, the weight of this relation is determined as

$$wr_{i,j}^{g} = \sum_{k} w_g[k] = \frac{1}{\sqrt{b_k \times atp_j[k]} \times \left((ct - gt_k)/(ct - ft)\right)}, \quad (5)$$

where $w_g[k]$ is the weight generated by passenger i when buying a ticket for passenger j the k th time, ct is the current time, and ft is the start date of the sample data. The weight of the ticketing relation is time sensitive and may attenuate as the time window increases.

The 12306 Internet ticketing system has 600 million registered users. According to an analysis of the number of their frequent contact persons (Figure 3), only 34% of these registered users have a single-frequency contact (i.e., the user himself/herself), whereas ticketing relations can be found among over 60% of the passengers when they buy tickets.

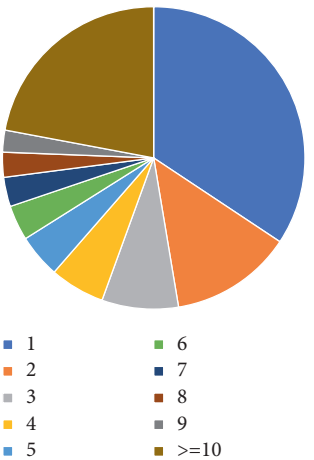

Figure 3: Distribution proportions of the number of frequent contacts.

3.2.2. Relation of Travelling Together. The relation of travelling together exists in passengers under the same ticket booking order, including the specific passengers, riding time, ticket price per kilometre, and number of passengers travelling together. Here, $C(i, j)$ is a behavioural sequence in which passenger i buys a ticket for passenger j; $C(i, j)[k] =$

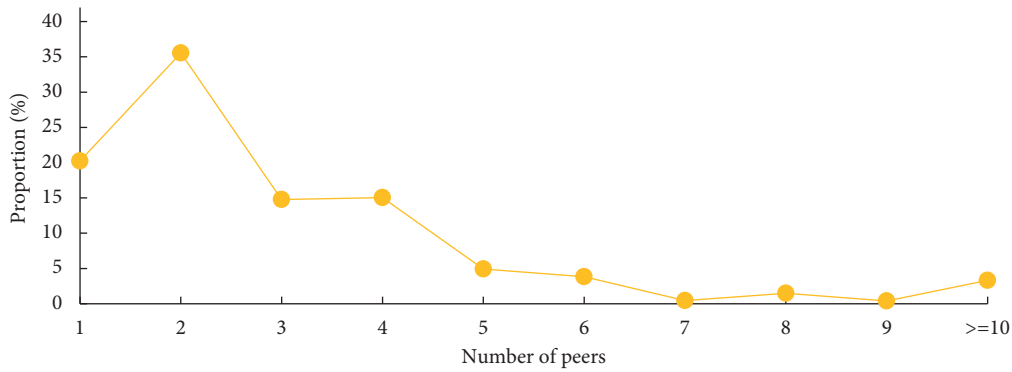

Figure 4: Distribution proportions of the number of passengers travelling together.

$(c_k, t_k, atp_j[k])$ represents a record of the k th ticket purchasing behaviour, where c_k stands for the number of passengers travelling together, t_k for the riding time, and $atp_j[k]$ for the ticket price per kilometre. Depending on the sequence of a relation of travelling together, the weight of this relation can be calculated according to

$$wr^c_{i,j} = \sum_k w_c[k] = \frac{1}{\sqrt{c_k \times atp_j[k]} \times \left((ct - t_k)/(ct - ft)\right)}, \tag{6}$$

where $w_c[k]$ is the weight of the fact that passenger i travels together with passenger j for the k th time.

The number of passengers falling into the same online order numbers in 2020 is statistically analysed, and the results are presented in Figure 4. Only 20% of the passengers travelled alone that year, and a relation of travelling together is found among the remaining passengers.

3.2.3. Benefit Relation by Point Redemption Mechanism. This relation means that the purchaser buys a ticket for another passenger through point redemption. A single benefit relation by the point redemption mechanism consists of the following information: the purchaser, the other passenger, riding time, and ticket price per kilometre. Here, $S(i, j)$ is a sequence representing the act of passenger i buying a ticket for passenger j through point redemption; $S(i, j)[k] = (t_k, atp_j[k])$ is a record of the k th ticket purchasing behaviour based on the point redemption mechanism, where t_k stands for the riding time and $atp_j[k]$ for the ticket price per kilometre. Depending on the sequence of this relation, the corresponding weight is computed according to

$$wr^s_{i,j} = \sum_k w_s[k] = \frac{1}{\sqrt{atp_j[k]} \times \left((ct - t_k)/(ct - ft)\right)}, \tag{7}$$

where $w_s[k]$ is the weight of passenger i buying a ticket for passenger j for the k th time by point redemption.

The benefit relations between purchasers and other passengers in orders made through point redemption in 2020 are analysed, as presented in Figure 5. Nearly 30% of the purchasers paid using their points for other passengers in 2020, thus forming a benefit relation with these passengers by the point redemption mechanism.

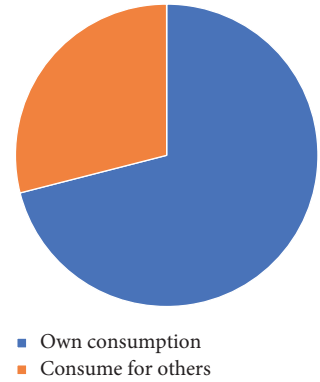

Figure 5: Distribution proportions of the benefit relation by the point redemption mechanism.

3.2.4. Passenger Classification. The railway trips of a passenger are related to their loyalties to railway travel, hidden travel segments, and travel distance. In this paper, passengers of a certain segment are grouped, and the importance of their loyalties is ranked as follows: $O\ DY > LOY > D\ D\ Y$. According to equation (8), LY, passengers' loyalty to a segment, can be calculated in combination with weights and diverse loyalty indices.

$$LY = 0.5 * O\ DY + 0.3 * L\ DY + 0.2 * D\ D\ Y. \tag{8}$$

Based on their indices, passengers are divided into the following groups: low loyalty (0–10), moderate loyalty (11–50), high loyalty (51–80), and very high loyalty (81–100).

4. Railway Passenger Grouping Model

A passenger grouping model integrating social relations is presented based on the travel characteristics and social relations of individual passengers. This model is made up of a personal travel characteristics fusion layer, a social relation fusion layer, an activation layer, and a group categorisation layer, as illustrated in Figure 6. Passengers' personal qualities are initially chosen as input. The feature fusion layer is then used to achieve personal feature vector fusion, and dimensionality reduction is used to lower the complexity of the corresponding algorithm. Following that, a social network topology is built based on passenger social relationships. The

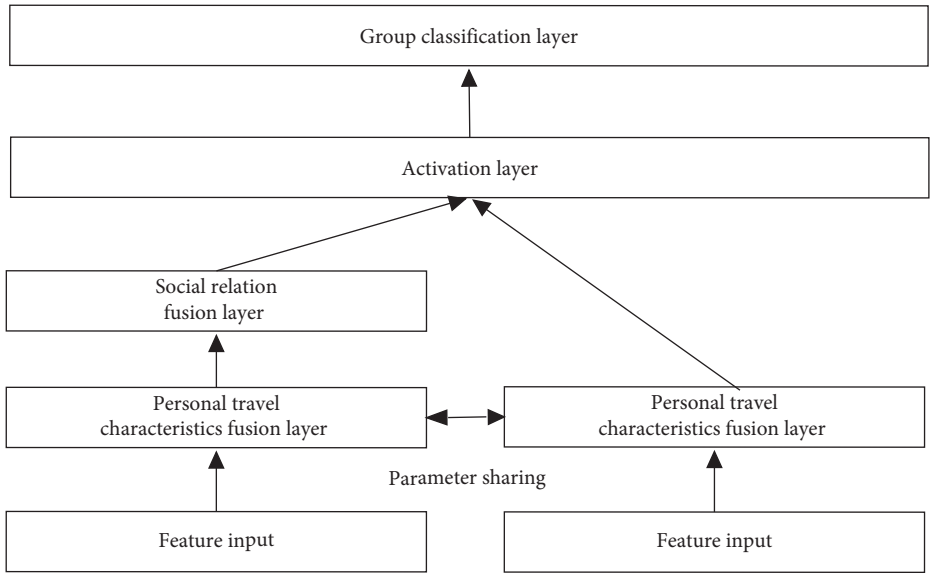

Figure 6: Structure of the graph attention network (GAT) with social relation fusion.

social relation fusion layer receives this topology, as well as the fused personal travel characteristics, as input. This approach is expected to realise feature information interaction between a goal node and a neighbouring node. In addition, the activation layer is designed to acquire the target values of passenger grouping from the passengers' personal characteristics and passengers' characteristics fused with the neighbouring node.

4.1. Personal Feature Fusion Layer. The number of personal travel characteristics already exceeds 2,000 in the user portrait system of railway passengers, which covers redundant and noisy information. This may not only interfere with subsequent data analysis but also affect the algorithm complexity, increase the computation overhead, and eventually influence the accuracy and efficiency of classification. Therefore, an autoencoder is introduced based on feature dimension reduction as the personal feature fusion layer. By virtue of this encoder, data in the high-dimensional feature space of passengers can be mapped to a low-dimensional space to reconstruct the passengers' personal features [12] and acquire the essential structural features of their characteristics. To decrease model complexity and improve training efficiency, personal features are processed through the personal feature fusion layer during personal feature processing and social relation fusion, in addition to parameter sharing.

$$\overrightarrow{f}_i' = \text{Autoencoder}\left(\overrightarrow{f}_i\right), \overrightarrow{f}_i' \in \mathbb{R}^{P'}, \overrightarrow{f}_i \in \mathbb{R}^{P}, \quad (9)$$

where $\overrightarrow{f}_i$ refers to the original feature vector of passenger i, P the number of original features, $\overrightarrow{f}_i'$ the feature vector of passenger i after feature fusion, and P' the number of fused features.

4.2. Social Relation Fusion Layer. The structure of the social relation fusion layer is presented in Figure 7. It consists of three social relation networks and a multigraph feature fusion process.

4.2.1. Social Relation Network. A social network may clearly embody the intended ticketing relation, relation of travelling together, and benefit relation via the point redemption method. Furthermore, the social network of railway passengers is represented by three undirected weighted graphs, namely, $G^g = (P, E^g, F', Wr^g)$, $G^c = (P, E^c, F', Wr^c)$, and $G^s = (P, E^s, F', Wr^s)$, where G^g, G^c, and G^s are the graphs of the ticketing relation, relation of travelling together, and benefit relation by the point redemption mechanism, respectively; P is the set of all railway passengers; E^g, E^c, and E^s are the sets of the ticketing relation, relation of travelling together, and benefit relation by the point redemption mechanism, respectively; F' is the set of the personal travel characteristics of all passengers after feature fusion; Wr^g, the weight of the ticketing relation, comprises $wr^g_{i,j}$; and finally, Wr^c and Wr^s are the weights of the travelling together relation and the benefit relation, respectively (the former is formed by $wr^c_{i,j}$, whereas the latter is composed of $wr^s_{i,j}$).

The 12306 Internet ticketing system has over 600 million registered users. The number of passengers is nearly 900 million. Moreover, there are some abnormal accounts. For these reasons, the relations of travelling together and ticketing are rather complicated for some passengers. In addition, a large difference lies in the number of neighbouring nodes around each node. As the passenger nodes possess a great number of neighbouring nodes, samples are taken from these neighbouring nodes to improve model training efficiency. We assume that the number of neighbouring nodes is N, and the corresponding sampling prescription is as follows.

When $N \leq 20$, all nodes are treated as social relation network nodes. As for $N > 20$, the nodes need to be classified based on the number of times of ticketing and the number of

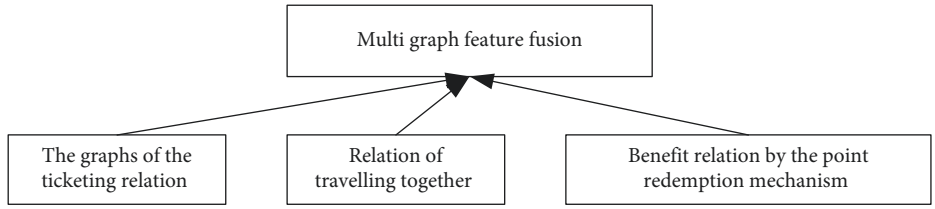

Figure 7: Structure of the GAT.

times of railway travel. For each category, the nodes are ordered based on the number of times and divided into three intervals with proportions of 40%, 40%, and 20% (N_1, N_2, and N_3, respectively). The neighbouring nodes in each interval are sampled in a ratio of $20/N$, and the number of neighbouring node samples can be expressed in $N = N_1 + N_2 + N_3$.

4.2.2. GAT Layer. In the GAT, the inherent normalised functions are replaced with an attention mechanism to assign a weight to each passenger node. During the updating of the hidden layer, the nodes and neighbouring nodes are aggregated according to the magnitude of weights [13].

In the present study, three types of social relations are included. For the relation of ticketing, for example, a feature vector set of target passengers and their neighbouring nodes is used as the input of the GAT layer, which can be written as

$$f' = \left\{\overrightarrow{f_o}', \overrightarrow{f_1}', \ldots, \overrightarrow{f_N}'\right\} \overrightarrow{f_i}' \in \mathbb{R}^{P'}, \tag{10}$$

where f' is the feature vector set of nodes (passengers' personal characteristics), $\overrightarrow{f_o}'$ the feature vector set of target nodes, $\overrightarrow{f_i}'$ the feature vector set of the i th neighbouring node of the target node, N the number of neighbouring nodes associated with the target node, and P' the number of passengers' features after fusion.

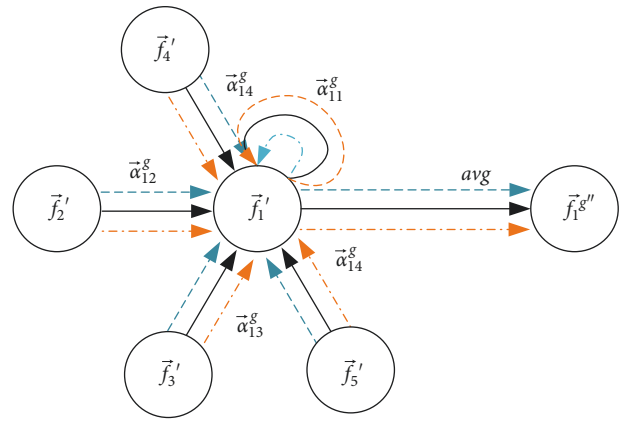

Figure 8: Multigraph attention mechanism.

A graph attention coefficient is constructed to output target node features that contain neighbouring node features. The corresponding computational formula is

$$e^{g} = a^{g}\left(W^{g}\overrightarrow{f}_i', W^{g}\overrightarrow{f}_j'\right), \tag{11}$$

$$\alpha_{ij}^{g} = \text{soft max}\left(e_{ij}^{g}\right) = \frac{\exp\left(\text{LeakyReLU}\left(a^{g\,T}\left[W^{g}\overrightarrow{f}_i', W^{g}\overrightarrow{f}_j'\right]\right)\right)}{\sum_{k\in N+i}\exp\left(\text{LeakyRe}LU\left(a^{g\,T}\left[W^{g}\overrightarrow{f}_i', W^{g}\overrightarrow{f}_k'\right]\right)\right)}. \tag{12}$$

In equation (11), W^{g} is a shared parameter in the network of ticketing relations, and it is used for feature enhancement. $a^{g}(\cdot)$ represents the importance of the target and neighbouring nodes in this network. In equation (12), α_{ij}^{g} is an attention coefficient of nodes i to j, and LeakyReLU to an activation function.

After the normalised attention coefficient is obtained, linear combinations of the corresponding features are calculated and then selected as the final output features of each node. In this paper, multigraph attention is introduced. The multigraph attention mechanism can be utilised to determine the attention coefficients of surrounding nodes, thus stabilising the learning process of the model. An update process for the hidden state is depicted in Figure 8.

Regarding the computational results subjected to K independent attention mechanisms, K-means is adopted and takes the place of a connection. Its computational formula is

$$f_i^{\,g''} = \sigma\left(\frac{1}{K^{g}}\sum_{k=1}^{K^{g}}\sum_{j\in L_i}\alpha_{ij}^{g\,k}W^{g\,k}\overrightarrow{f}_j'\right), \tag{13}$$

where $f_i^{\,g''}$ is a feature vector after a fusion between a target passenger and information of neighbouring nodes in a ticketing relation network formed by this passenger, K^{g} stands for the serial number of an independent attention mechanism, $\sigma(\cdot)$ stands for the activation function, and $\alpha_{ij}^{g\,k}$ stands for the attention coefficient of passenger i relative to passenger j in the network of ticketing relations.

With the use of the abovementioned calculation processes, the ticketing relation network feature fusion, feature fusion $f_i{}^{c''}$ of the relation of travelling together, and feature fusion $f_i{}^{s''}$ of the benefit relation by the point redemption mechanism are obtained.

4.2.3. Multigraph Feature Fusion. A fully connected layer is established for the multigraph fusion of $f_i{}^{g''}$, $f_i{}^{c''}$, and $f_i{}^{s''}$ (vectors of features incorporating social relations), which can be expressed as

$$f_{\mathrm{PSC}\,i} = W_{ps}\left(f_i{}^{g''}, f_i{}^{c''}, f_i{}^{s''}\right), \tag{14}$$

where $f_{PSC\,i}$ is the target passenger feature undergoing fusion with multiple social relations and W_{ps} is a training parameter that denotes the importance of the three relation-generating features.

4.3. Activation Layer. Node feature vectors that incorporate the ticketing, travelling together, and benefit relations are obtained through training by the GAT layer. Personal feature vectors are also acquired through training by the personal feature fusion layer. Afterwards, the node and personal feature vectors are aggregated to generate the final feature vector, which is then transferred to the activation layer. In this way, different groups can be obtained as

$$\widehat{f} = \tanh\left[f_{\mathrm{PIC}} \cdot f_{\mathrm{psc}}\right], \tag{15}$$

$$q(c) = \mathrm{soft\,max}\left(W_q \widehat{f} + b_q\right). \tag{16}$$

In equation (15), f_{PIC}, f_{PIC} stands for the feature vectors outputted from the personal feature fusion layer, f_{psc} for the feature vectors outputted from the social relation fusion layer, and $\widehat{f}$ for the final feature vector of the target passenger. In equation (16), c is the class label of passengers and $q(\cdot)$ is the predicted passenger group.

4.4. Model Training. The methodology divides passengers into four categories based on the passenger loyalty indices. Vectors of passengers' personal travel characteristics are developed based on passenger portraits of railway transportation through supervised training. A network of travellers' social interactions is formed using information from common contacts and online orders (among other things), and then used as the model input through rule-based pruning. Additionally, relevant cross-entropy loss functions are minimised via L_2 normalisation to fulfil model training. The corresponding computational formula is

$$L_{\mathrm{loss}} = -\sum_{c \in C} \widehat{q}_c \cdot \ln q_c + \lambda \sum_{\theta \in \Theta} \theta^2, \tag{17}$$

where $\widehat{q}_c$ and q_c represent the actual class labels of passenger groups and their model-predicted class labels, respectively, and λ stands for the normalised parameter L_2 and Θ for the set of model parameters.

Table 2: Loyalty-based distribution of Guangzhou–Shanghai passengers in 2020.

Passenger types	Class labels	Loyalty ranges	Proportions (%)
Low loyalty	1	0–10	44
Moderate loyalty	2	10–50	22
High loyalty	3	50–80	13
Very high loyalty	4	80–100	21

5. Case Study and Experiments

This section descries the overall result of current study.

5.1. Data Description. The dataset for the case study in this paper is the real-name information of railway passengers and their travel data, both of which underwent masking in 2020. As seen in Section 2.2, competition may become increasingly fierce once the travel distance exceeds 1,500 km. Moreover, passengers in the segment from Guangzhou to Shanghai (travel distance: 1,800 km) are adopted as the research object. An analysis of the travel chain of passengers in 2020 shows a total of 401,300 passengers (railway travel and hidden railway travel behaviours) from Guangzhou to Shanghai. Their loyalty indices are calculated for passenger segmentation. Here, numerals 1, 2, 3, and 4 are the model output of different groups, as shown in Table 2.

For reducing the model complexity, 14 travel features are selected from passengers and listed in Table 3. Features with a large span are normalised and then combined with a social relation network constructed for the 401,300 passengers to serve as the model input.

5.2. Experimental Design. Two experiments are designed for this study: an accuracy test and a compatibility test. Five common classification models (Table 4) are introduced in the accuracy tests for training comparison and accuracy evaluation of the Guangzhou-Shanghai passenger grouping. The compatibility test focuses on grouping prediction for the passengers from January to October 2021 based on the model training of the 2020 passenger data and an analysis of the time-varying performance of the passenger grouping model.

Here, k-fold cross-validation [16] is used to eliminate statistical errors incurred by the use of different training subsets. The dataset is randomly divided into k groups; for model construction, one group is used successively as the test dataset, and the remaining $k - 1$ groups are regarded as training sets. Based on the data size of the experimental samples, the training datasets are randomly classified into five groups.

5.3. Evaluation Indices. Accuracy, precision, recall, and harmonic mean F1 are primarily selected as comprehensive evaluation indices of the passenger grouping model to assess the accuracy of the passenger grouping results.

Table 3: Passenger feature selection.

Serial nos.	Features	Categories	Descriptions
1	Students or not	Enumeration	0: no, 1: yes
2	Business persons or not	Enumeration	0: no, 1: yes
3	Sex	Enumeration	0: male, 1: female
4	Age	Numerical values	Normalisation
5	Number of times of local train ticket booking	Numerical values	Normalisation
6	Number of times of D-series high-speed train ticket booking	Numerical values	Normalisation
7	Number of times of taking local trains	Numerical values	Normalisation
8	Number of times of taking D-series high-speed trains	Numerical values	Normalisation
9	Proportion of passengers taking D-series high-speed trains	Numerical values	Actual values
10	Proportion of passengers purchasing D-series high-speed trains	Numerical values	Actual values
11	Proportion of passengers taking premium seats	Numerical values	Normalisation
12	Proportion of passengers forming a relation of travelling together	Numerical values	Actual values

Table 4: Grouping algorithm description.

Algorithms	Description
Random forest	An algorithm integrating multiple decision trees through ideas of ensemble learning to achieve classification
XGBoost [14]	A gradient boosting decision tree that combines multiple weak classifiers accumulatively into a strong classifier to minimise the objective loss function
MTWSVMs	Primarily fulfilling multiclass problems
LightGBM [15]	A distributed classification algorithm implementing GBDT enabling highly efficient training over large-scale data with low memory cost and high accuracy
DNN	Deep learning

$$\begin{aligned} \text{Accuracy} &= \frac{\text{TP} + \text{TN}}{\text{P} + \text{N}}, \\ \text{Precision} &= \frac{\text{TP}}{\text{TP} + \text{FP}}, \\ \text{Re call} &= \frac{\text{TP}}{\text{TP} + \text{FN}}, \\ \text{F1} &= \frac{2 \times \text{Precision} \times \text{Recall}}{\text{Precision} + \text{Recall}}. \end{aligned} \tag{18}$$

In comparison with deep learning models, machine learning models, such as random forest, XGBoost, MTWSVMs, and LightGBM, have lower complexity, fewer training parameters, and shorter training times. However, the classification accuracy of machine learning models is poor. Training time is, therefore, not considered a model evaluation index in this experiment.

5.4. Experimental Results and Analyses. Through threshold adjustment, optimal results of various classification methods are obtained based on the training datasets. The values of the model evaluation indices are determined as well. For each passenger grouping model, the corresponding indices are averaged via fivefold cross-validation. The results are listed in Table 5.

According to Table 5, random forest has the worst accuracy and precision; XGBoost, MTWSVMs, and LightGBM outperform it to a certain extent in terms of these indices. The performance of the proposed model is superior to that of the other models. In some cases, the proposed model even performs the best, followed by DNN. The overall tendency of the proposed model for recall is the same as that for accuracy and precision. According to the F1 values, there are 85% commonalities in the passenger characteristics reflected in the proposed passenger grouping model. Hence, the passenger grouping of the proposed model is highly accurate.

Table 5: Comparison of model-based experiments.

Models	Evaluation indices			
	Accuracy	Precision	Recall	F1
Random forest	59.83	60.13	83.21	69.81
XGBoost	62.63	62.93	84.92	72.28
MTWSVMs	64.36	65.23	85.82	74.12
LightGBM	63.62	65.68	83.91	73.68
DNN	71.42	72.82	88.64	79.95
Proposed algorithm	82.54	84.73	92.36	88.38

The 2021 testing data are separated into 10 parts by month, and passenger groups are predicted using these parts. Figure 9 shows the prediction results, with the x-axis representing the months and the y-axis representing the F1 values. The F1 values of all models gradually decrease with time, and passenger grouping effects turn worse. Previous data training models are no longer sufficient to meet the future segmentation needs of passengers' attributes in this case. The longer the interval from the training time, the worse the passenger grouping results. In particular, the F1 values of random forest and LightGBM are already below 50% in October 2021, showing the worst adaptation. Concerning all tests, the proposed model produces F1 values no less than 70, proving that it is well applicable to future data.

In summary, travel characteristic selection and knowledge extraction are important factors influencing the results of passenger grouping. The features of the random forest model are comparatively static and simple; it ignores feature

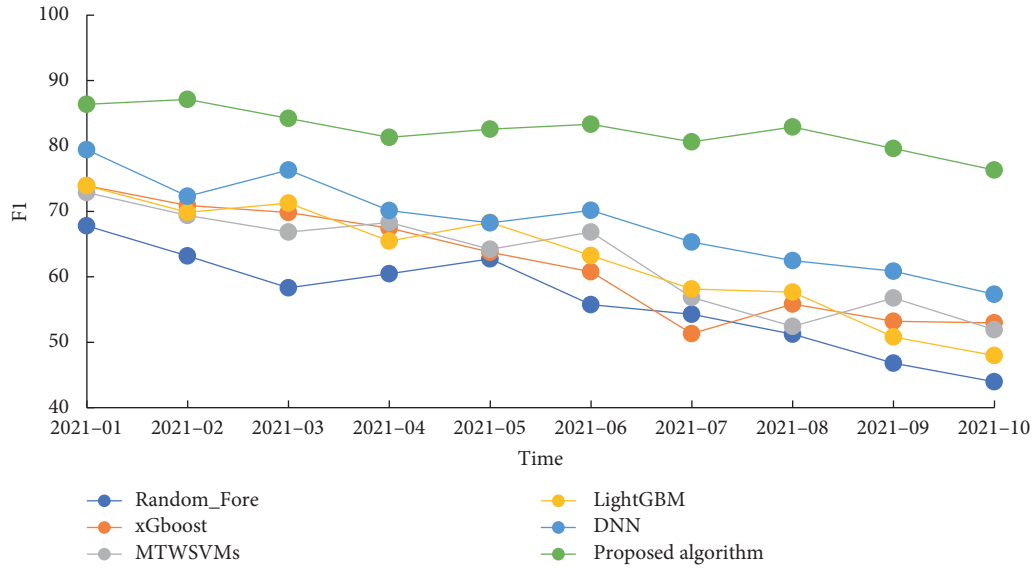

Figure 9: F1 variation prediction of future data based on six approaches.

correlations and produces the worst grouping results under the same conditions. The XGBoost model performs well in terms of prediction precision when applied to low-/medium-dimensional data, but it fails to adapt to large-scale feature inputs. Given a large sample size and large numbers of features and classes, the number of subclassifiers of MTWSVMs exponentially rises, thus excessively increasing the complexity of the corresponding classification system. In this scenario, large quantities of passengers cannot be grouped. The LightGBM model is highly susceptible to noisy information. Finally, DNN can perform feature fusion for passengers' travel characteristics, thereby reducing feature processing complexity and improving model accuracy. Regarding the proposed passenger grouping algorithm, the fusion of social relations and personal features is completed, and the model can correctly extract common features of various passenger groups. From the perspectives of effects, accuracy, and adaptation, the proposed algorithm outperforms the abovementioned existing models.

6. Conclusions

To create a comprehensive travel chain for passengers, hidden railway travel behaviour is introduced and integrated with railway travel behaviour. Passengers' indices of loyalty to railway travel, hidden railway travel segments, and travel distance are determined independently based on passengers' specific information, such as the number of instances of hidden railway travel behaviour, number of railway travels, travel distances, and travel segments. Furthermore, the ratios of segments featuring hidden railway travel behaviour are determined in order to disclose the degree of competition in various segments. The competition is at its peak when the journey distance exceeds 1,350 kilometres, according to the findings. The competition intensity is comparatively low for travel distances of 150 to 1,000 km, and the railway clearly outperforms. As a result, passengers' personal travel characteristics are determined from the dimensions of time and space established on their travel behaviour and real-name data. Furthermore, the point redemption system creates a social relation network of passengers based on their ticketing, travelling together, and benefit relations. Finally, the loyalty of passengers is determined by determining their devotion to railway travel, hidden railway travel segments, and travel distance. The passengers are then divided into four categories based on their level of loyalty: 0–10, 10–50, 50–80, and 80–100.

An autoencoder is employed in addition to the suggested passenger grouping model to minimise the dimensionality of passenger attributes and reduce algorithm complexity. To vectorise the social relations, a graph attention mechanism and a multigraph fusion mechanism are also used. To complete passenger grouping, a fusion of social relation vectors and feature dimensionality reduction outcomes is obtained. The experimental dataset is made up of data from Guangzhou–Shanghai travellers in 2020, which is then trained, tested, and matched to existing classification models including random forest, XGBoost, MTWSVMs, LightGBM, and DNN. According to the findings, the developed passenger grouping model, which adds social ties, beats the other models in terms of accuracy and adaption [17].

Data Availability

The data supporting the results of this study can be obtained from the railway department as reasonably required.

Conflicts of Interest

The authors declare that they have no conflicts of interest.

Acknowledgments

This project was supported by the Major Scientific and Technological Research Project of China National Railway Group Limited: N2021X034.

References

[1] F. Dobruszkes, C. Dehon, and M. Givoni, "Does European high-speed rail affect the current level of air services? An EU-wide analysis," *Transportation Research Part A: Policy and Practice*, vol. 69, no. nov, pp. 461–475, 2014.

[2] Y.-H. Cheng, "High-speed rail in Taiwan: new experience and issues for future development," *Transport Policy*, vol. 17, no. 2, pp. 51–63, 2010.

[3] X. Zhang, W. X. Luan, and Q. Cai, "Research on the competition between High?Speed rail and air transport," *Journal of Dalian University of Technolgy*, vol. 32, no. 1, p. 4246, 2011.

[4] P. B. Chou, E. Grossman, and D. Gunopulos, "Identifying prospective customer," in *Proceedings of the Six ACM SIGKDD International Conference on Knowledge Discovery and Date Mining*, pp. 447–456, ACM Press, Boston,MAsUSA, 2000.

[5] X.-bin An, L. I. Yi-jun, and Q. Ye, "Research on customer segmentation based on purchase behaviors," *Computer Integrated Manufacturing Systems*, vol. 11, no. 12, pp. 1769–1774, 2005.

[6] H. Rushmeier, R. Lawrence, and A. George, "Case study: visuaiizing customer segmentation produced by self organizing maps," in *Proceedings of the Visualization '97 (Cat. No. 97CB36155)*, pp. 463–466, Phoenix, AZ, USA, October 1997.

[7] B Qian, .. *Research on Revenue Management for Dedicated Passenger Line Based on Passenger Choice-Behavior*, Southwest Jiaotong University, Sichuan, China, 2014.

[8] L. Li, *Research on the Revenue Optimization of High-Speed Railway Basedon Passenger Behavior Analysis*, CHINA ACADEMY OF RAILWAY SCIENCES, Beijing, China, 2017.

[9] R. Zhang, M. A. Yu, and B.-ru Zhao, "Passenger choice behavior of high-speed rail and airline between beijing and Shanghai," *Journal of Transportation Systems Engineering and Information Technology*, vol. 000, no. 001, pp. 223–228, 2016.

[10] L. I. An-juna, D. Wang, and P. E. N. G. Qi-yuan, "Regional intercity railway planning method based on individual travel path," *Journal of Transportation Systems Engineering and Information Technology*, vol. 21, no. 2, pp. 30–36, 2021.

[11] C. Yu and H. Lv, "Research on passenger transport marketing strategy based on big data railway passenger portrait," *Journal of the China Railway Society*, vol. 42, no. 8, pp. 23–28, 2020.

[12] F. Yuan, L. Zhang, J. Shi, X. Xia, and G. Li, "Theories and applications of auto-encoder neural networks: a literature survey," *Chinese Journal of Computers*, vol. 42, no. 1, pp. 203–230, 2019.

[13] P. Velickovic, G. Cucurull, A. Casanova, A. Romero, P. Lio, and Y. Bengio, "Graphattention networks," 2017, https://arxiv.org/abs/1710.10903.

[14] H. Li and Y. Zhu, "Xgboost algorithm optimization based on gradient distribution harmonized strategy," *Journal of Computer Applications*, vol. 40, no. 6, pp. 1633–1637, 2020.

[15] D. I. N. G. Shi-Fei, J. Zhang, X.-K. Zhang, and Y. X. An, "Survey on multi class twin support vector machines," *Journal of Software*, vol. 029, no. 001, pp. 89–108, 2018.

[16] G. Ke, Q. Meng, and T. Finley, *LightGBM: A Highly Efficient Gradient Boosting Decision Tree*, in *Proceedings of the 31st Conference on Neural Information Processing Systems (NIPS 2017)*, pp. 1–9, Long Beach, CA, USA, December 2017.

Hindawi
Scientific Programming
Volume 2022, Article ID 6480380, 14 pages
https://doi.org/10.1155/2022/6480380

Research Article

Theoretical and Simulation Studies of Transverse Beam Size Effects on Optical Transition Radiation in Prewave Zone

Haofeng Liu[1,2] **and Fang Fang**[3]

[1]*The College of Nuclear Technology and Automation Engineering, Chengdu University of Technology, Chengdu, Sichuan 610000, China*
[2]*National Institute of Measurement and Testing Technology, Chengdu, Sichuan 610000, China*
[3]*Key Laboratory of Applied Nuclear Techniques in Geosciences Sichuan, Chengdu University of Technology, Chengdu, Sichuan 610000, China*

Correspondence should be addressed to Fang Fang; ff@cdut.edu.cn

Received 6 March 2022; Revised 19 March 2022; Accepted 13 May 2022; Published 30 May 2022

Academic Editor: Muhammad Zakarya

Optical transition radiation (OTR) has been studied and applied on the beam diagnostics for decades. The potential implication of OTR also includes THz radiation sources. Therefore, the theoretical analysis and simulation tools have become indispensable for the OTR study. Moreover, the OTR theory, for the wave zone (far-field approximation), has been widely used in the literature. However, these theories for the prewave zone have been proposed on the basis of single electron approximation. In this study, we developed a theory with consideration of the electron beam structure based on Kirchhoff's method for studying the effect of beam transverse size on the angular distribution of the OTR in prewave zone. The proposed formalism involves complicated convolution integral of functions and the dimensions of integrand are not low. To perform such integral, we developed a Fortran program for quasi-monte Carlo method, which is robust and suitable for high dimensional integration. The disadvantage of this method is that a large amount of samplings may need to be employed to achieve good convergence. Therefore, in order to get the radiation angular profile, we need to perform such integration for different observation angles that might be computationally intensive. Therefore, we parallelize the program with the Message Passing Interface (MPI) programming concepts. To verify the theoretical calculations, few two-dimensional FDTD simulations were carried out that show the validity of the proposed model. The proposed theory and numerical tool would be used to predict radiation properties of the NSRRC THz coherent transition radiation (CTR) in the prewave zone.

1. Introduction

When an electron traverses across an interface of two different media, radiation is emitted. This phenomenon is called transition radiation (TR) and was theoretically predicted by Ginzburg and Frank in 1946. Their approach to tackle this problem is based on solving the electromagnetic wave equations directly with consideration of boundary conditions at the interface [1–3] and provided solutions in wave zone (far-field). It is often called optical transition radiation (OTR). If the wavelength is not shorter than that of the visible light, OTR from metallic foils have been used for electron beam diagnostics for decades [4–6]. In such applications, metallic foils are considered as perfect conductors and the Ginzburg-Frank formula has been widely used for the theoretical prediction of the radiation properties. Alternative to their approach, as suggested by Fermi [7], the velocity fields of the incident electron are decomposed into Fourier components of waves such that the problem can be modeled as scattering of waves by the interface. Kirschhoff's method can be used to solve this scattering problem [8, 9]. With this integral formalism, one may find that the condition for far-field approximation holds when the observation distance $r_0 >> \gamma^2\lambda$. In this regard, the radiation source is the surface current on conductor which is induced by the electric field from incident

electron; the size, or more specifically the cut-off size, is of the order γ^{λ} because the asymptotic behavior of particle field falls off with radial distance d perpendicular to the trajectory that is proportional to $\exp(-2\pi d/\beta\gamma\lambda)$. Due to the finite source size, the prewave zone can be defined as $\gamma^2\lambda > r_0 >> \gamma\lambda$. The behaviors of the OTR in this region, such as spectral angular distribution, are quite different from those in wave zone [10, 11].

The OTR properties in the prewave zone attracts much attention in applications, such as beam profile monitoring and generation of THz radiation in high energy accelerators because the far-field condition may not be satisfied [12, 13]. However, far-field approximation is usually used in the experimental designs [14]. On the other hand, as pointed out by Orlandi et al., beam transverse size would affect the behavior of the angular spectrum and may be an important issue for beam diagnostic. In their work, the authors stated that the bunch size effects for normal incident beam of OTR in far-field were studied [15–18]. For a bunch with Gaussian distribution $\exp(-(x^2 + y^2/2\sigma_{\perp}^2))\exp(-(z^2/2\sigma_{\parallel}^2))$, the OTR angular spectrum is proportional to $\mathscr{F}_{\perp}(\lambda,\theta)\mathscr{F}_{\parallel}(\lambda)I_e(\lambda,\theta)\mathfrak{N}$, where I_e is the OTR angular spectrum of single particle with normal incidence. Moreover, $\mathscr{F}_{\perp}(\lambda,\theta)$ and $\mathscr{F}_{\parallel}(\lambda)$ are transverse and longitudinal form factors, respectively. We intend to design a theory with consideration of the electron beam structure based on Kirchhoff's method for studying the effect of beam transverse size on the angular distribution of the OTR in prewave zone. The proposed formalism involves complicated convolution integral of functions and the dimensions of integrand are not low. To perform such integral, we developed a Fortran program for quasi-monte Carlo method, which is robust and suitable for high dimensional integration.

In this research, based on Kirchhoff's method, a theoretical formalism for the prewave zone OTR is proposed to study the beam size effects. A two-dimensional numerical simulation code based on finite difference time domain (FDTD) method is used to verify the theoretical predictions. The theory would be used to predict radiation properties of the NSRRC THz coherent transition radiation (CTR) in the prewave zone [11]. We will review Kirchhoff's method, and the pseudo-photons from a bunch of electrons are also introduced and illustrated in detail. After that, a theory for prewave OTR from a bunch of electrons with oblique incidence is derived. Basic concepts about FDTD are introduced, and the simulation model to verify the theory is described. The effects of beam transverse size on prewave zone OTR are discussed, and the simulation verifications of the case with normal incidence are presented as well (using a case study). The major contributions of this research are as follows.

(i) We developed a theory with consideration of the electron beam structure based on Kirchhoff's method for studying the effect of beam transverse size on the angular distribution of OTR in prewave zone.

(ii) We developed a Fortran program for quasi-monte Carlo method, which is robust and suitable for high dimensional integration.

(iii) The developed Fortran program is then used to tackle the complex numerical integration problem.

(iv) We parallelize the program with MPI programming interface.

The rest of the paper is organized as follows. In Section 2, we offer an overview of the materials, methods, and theories. Section 3 is about the datasets and evaluation metrics using simulations. Moreover, experimental details are also presented. In Section 4, results are discussed. Moreover, a case study is also discussed. Finally, Section 5 concludes this paper and offers several directions for further research and investigation.

2. Related Work, Theories, and Models

In this chapter, we will first review Kirchhoff's method for plane conducting target. Based on superposition principle, the velocity fields form a bunch of electrons which are discussed. With velocity fields from a bunch of electrons, a formalism for prewave zone OTR from electron bunch with oblique incidence is derived. The beam size effects in prewave zone and wave zone are also discussed [19].

2.1. Kirchhoff's Method for OTR. In this section, we would review the theoretical treatment proposed by Karlovets [20]. The coordinate system in original work is in left-hand coordinate system and we will follow this convention.

2.1.1. Kirchhoff's Method for Plane Conductor. Consider an OTR system (Figure 1), in which the perfect conducting plane target is situated at $z = 0$, and an electron bunch moves with an incident angle α relative to z-axis. To construct the scattering theory for such system, we can start with Green's identity.

$$\int_V f\nabla^2 g - g\nabla^2 f \,\mathrm{d}V = \oint_S \hat{n}\cdot(f\nabla g - g\nabla f)\mathrm{d}S, \tag{1}$$

where f and g are smooth function, V is a volume in space, S is the boundary enclosing V, and $\hat{n}$ is the unit direction normal to S. By the method of image, a suitable choice of Green's function for this system is determined through using the following equation:

$$g = -\frac{\exp\left(ik\left|\mathbf{r}-\mathbf{r}_0\right|\right)}{\left|\mathbf{r}-\mathbf{r}_0\right|} + \frac{\exp\left(ik\left|\mathbf{r}-\mathbf{r}_0'\right|\right)}{\left|\mathbf{r}-\mathbf{r}_0'\right|}, \tag{2}$$

where $\mathbf{r}_0'$ is the mirror image of $\mathbf{r}_0$ with respect to plane at $z = 0$. If we put $f = E_i^R$ we can get the fields relation for each component of $\mathbf{E^R}$. To apply the integral equation to scattering problem, we can make $\mathbf{E}^R(\mathbf{r}_0,\omega) = \mathbf{E}(\mathbf{r}_0,\omega) - \mathbf{E}^0(\mathbf{r}_0,\omega)$ and this yields

$$\mathbf{E}^R(\mathbf{r}_0,\omega) = \frac{1}{4\pi}\int \mathbf{E}^0(\mathbf{r},\omega)(\hat{n}\cdot\nabla g)\mathrm{d}S, \tag{3}$$

where $\mathbf{E}$ and $\mathbf{E_0}$ are total field and incident field. With the boundary conditions of perfect conducting plane, $E_{x,y}(\mathbf{r},\omega)|_S = 0$, we can further conclude

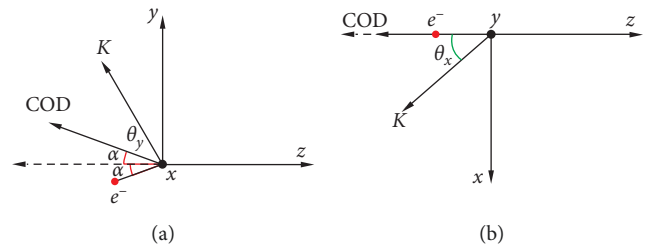

Figure 1: Projections of the coordinate system on y-z and x-z plans. (a) Projection on y-z plan. (b) Projection on x-z plan.

$$E^R_{x,y}(\mathbf{r}_0,\omega) = -\frac{1}{4\pi}\int E^0_{x,y}(\mathbf{r},\omega)(\hat{n}\cdot\nabla g)\mathrm{d}S. \tag{4}$$

For $r_0 >> r$, we have

$$(\hat{n}\cdot\nabla g)|_S \approx 2ikz_0\frac{\exp\left(ik|\mathbf{r}_0-\mathbf{r}|\right)}{|\mathbf{r}_0-\mathbf{r}|}, \tag{5}$$

and therefore the radiation fields (scattered field) become as illustrated by

$$E^R_{x,y}(\mathbf{r}_0,\omega) = -\frac{2ikz_0}{4\pi}\int E^0_{x,y}(\mathbf{r},\omega)\frac{\exp\left(ik|\mathbf{r}_0-\mathbf{r}|\right)}{|\mathbf{r}_0-\mathbf{r}|}\mathrm{d}S. \tag{6}$$

2.1.2. Radiation Field in Observer's Frame. An electron bunch moves with an incident angle α relative to z-axis (Figure 1). Because OTR can be considered as the particle's fields scattered by the target, it may obey the optical law of reflection. Therefore, one should put the center of detector (COD) with angle α relative to z-axis. The position of observer can be described with θ_x and θ_y relative to COD, and the coordinates transformation between observer's frame and target's frame (k) can be characterized by the two consecutive rotations, as given by

$$\mathscr{R}_y\cdot\mathscr{R}_x = \begin{pmatrix}\cos\theta_x & 0 & \sin\theta_x\\ 0 & 1 & 0\\ -\sin\theta_x & 0 & \cos\theta_x\end{pmatrix}\begin{pmatrix}1 & 0 & 0\\ 0 & \cos(\alpha+\theta_y) & -\sin(\alpha+\theta_y)\\ 0 & -\sin(\alpha+\theta_y) & \cos(\alpha+\theta_y)\end{pmatrix}, \tag{7}$$

and the radiation fields transformation between these two frames is illustrated as

$$\mathbf{E}^R_k = \begin{pmatrix}\cos\theta_x & \sin(\alpha+\theta_y)\sin\theta_x & \cos(\alpha+\theta_y)\sin\theta_x\\ 0 & \cos(\alpha+\theta_y) & \sin(\alpha+\theta_y)\\ -\sin\theta_x & -\sin(\alpha+\theta_y)\cos\theta_x & \cos(\alpha+\theta_y)\cos\theta_x\end{pmatrix}\cdot\mathbf{E}^R. \tag{8}$$

Assuming that the longitudinal component in the observer's frame is absent, we get

$$\begin{aligned}E^R_{x_k} &= E^R_x,\\ E^R_{y_k} &= \frac{E^R_y}{\cos(\alpha+\theta_y)} + E^R_x\tan\theta_x\tan(\alpha+\theta_y).\end{aligned} \tag{9}$$

With the fields in observer's frame, the radiation energy spectrum can be calculated with the following equation:

$$\frac{W}{\mathrm{d}\omega\mathrm{d}\Omega} = cr_0^2\left(\left|E_{x_k}\right|^2+\left|E_{y_k}\right|^2\right). \tag{10}$$

2.2. Velocity Field from a Bunch of Electrons. When investigating the interaction between matter and electrically charged particle, which has a uniform velocity, one may consider this problem as scattering. The moving fields from the charge particle are scattered by the media. This concept was proposed by Fermi [21]. When tackling a scattering problem, one normally considers the incident fields in frequency domain. Therefore, we can transform the velocity fields into the frequency domain through the well-known Fourier decomposition method [21]. For the velocity fields from single electron moving along $+z_e$ direction, we have

$$\begin{aligned}E^e_{x_e} &= \frac{e\omega}{\pi v^2\gamma}\frac{x_e}{\sqrt{x_e^2+y_e^2}}K_1\left(\frac{\omega\sqrt{x_e^2+y_e^2}}{v\gamma}\right)\exp\left(i\frac{\omega z_e}{v}\right),\\ E^e_{y_e} &= \frac{e\omega}{\pi v^2\gamma}\frac{y_e}{\sqrt{x_e^2+y_e^2}}K_1\left(\frac{\omega\sqrt{x_e^2+y_e^2}}{v\gamma}\right)\exp\left(i\frac{\omega z_e}{v}\right),\\ E^e_{z_e} &= -\frac{e\omega}{\pi v^2\gamma}\frac{i}{\gamma}K_0\left(\frac{\omega\sqrt{x_e^2+y_e^2}}{v\gamma}\right)\exp\left(i\frac{\omega z_e}{v}\right).\end{aligned} \tag{11}$$

When an electron moves in z_e direction in space with constant velocity, then there exists a time t_0, such that this electron would arrive the plane $z_e = 0$ when $t = t_0$. If this electron has a deviation in transverse coordinate, say for example (x_0, y_0), the velocity fields in the time domain can be written as given by

$$E^e_{x_e,y_e,z_e}(x_e-x_0, y_e-y_0, z_e, t-t_0). \tag{12}$$

For a bunch of electrons moving along z_e direction with constant velocity v having the distribution $\mathrm{NB}_\perp(x',y')B_\parallel(t')$, where N is the number of electrons in this bunch, $B_\perp(x',y')$ and $B_\parallel(t')$ are longitudinal and transverse distribution, respectively. It should be noted that the velocity fields from this bunch are, based on superposition of the fields from each electrons, illustrated through the followingequation:

$$E^b_{x_e,y_e,z_e} = N\iiint B_\perp(x', y')B_\parallel(t')E^e_{x_e,y_e,z_e} (x_e - x', y_e - y', z_e, t - t')\mathrm{d}x\prime\mathrm{d}y\prime\mathrm{d}t'. \tag{13}$$

The fields in the frequency domain are

$$E^b_{x_e,y_e,z_e} = N\mathscr{F}_\parallel \int\int B_\perp(x', y')E^e_{x_e,y_e,z_e}(x_e - x', y_e - y', z_e, \omega)\mathrm{d}x'\mathrm{d}y', \tag{14}$$

where $\mathscr{F}_\parallel = \int B_\parallel(t')\exp(i\omega t')\mathrm{d}t'$ is the longitudinal form factor for this bunch. The incident fields in the scattering formalism are represented in the target frame, and we may want to express the fields from electron bunch (the incident source) in such frame. For the OTR system, we consider (refer to Figure 1), the transformation between electron's frame and target's frame is

$$\begin{aligned} x_e &= x, \\ y_e &= y\cos\alpha - z\sin\alpha, \\ z_e &= y\sin\alpha + z\cos\alpha, \\ E^b_x &= E^b_{x_e}, \\ E^b_y &= E^b_{y_e}\cos\alpha + E^b_{z_e}\sin\alpha, \\ E^b_z &= -E^b_{z_e}\sin\alpha + E^b_{z_e}\cos\alpha, \end{aligned} \tag{15}$$

and velocity fields from this electron bunch in the target's frame are

$$\begin{aligned} E^b_x(x_e, y_e, z_e, \omega) &= E^b_{x_e}(x, y\cos\alpha - z\sin\alpha, z\cos\alpha + y\sin\alpha, \omega), \\ E^b_y(x_e, y_e, z_e, \omega) &= E^b_{y_e}(x, y\cos\alpha - z\sin\alpha, z\cos\alpha \\ &\quad + y\sin\alpha, \omega)\cos\alpha n + E^b_{z_e}(x, y\cos \\ &\quad \alpha - z\sin\alpha, z\cos\alpha + y\sin\alpha, \omega)\sin\alpha, \\ E^b_z(x_e, y_e, z_e, \omega) &= -E^b_{z_e}(x, y\cos\alpha - z\sin\alpha, z\cos\alpha \\ &\quad + y\sin\alpha, \omega)\sin\alpha + E^b_{z_e}(x, y\cos \\ &\quad \alpha - z\sin\alpha, z\cos\alpha + y\sin\alpha, \omega)\cos\alpha. \end{aligned} \tag{16}$$

2.3. OTR from a Bunch of Electrons. To formulate the problem of OTR from electron bunch, we begin with equation (6) and use the velocity fields from electron bunch (equation (16)) as the incident field. This yields the radiation fields in the target's frame

$$\begin{aligned} E^R_x(\mathbf{r}_0, \omega) &= -\frac{2ikz_0}{4\pi}\int E^b_{x_e}(x, y\cos\alpha - z\sin\alpha, z\cos\alpha \\ &\quad + y\sin\alpha, \omega)\frac{\exp\left(ik|\mathbf{r}_0 - \mathbf{r}|\right)}{|\mathbf{r}_0 - \mathbf{r}|}\mathrm{d}S, \\ E^R_y(\mathbf{r}_0, \omega) &= -\frac{2ikz_0}{4\pi}\int\left[E^b_{y_e}(x, y\cos\alpha - z\sin\alpha, z\cos\alpha \right. \\ &\quad + y\sin\alpha, \omega)\cos\alpha + E^b_{z_e}(x, y\cos \\ &\quad \left.\alpha - z\sin\alpha, z\cos\alpha + y\sin\alpha, \omega)\sin\alpha\right] \\ &\quad \frac{\exp\left(ik|\mathbf{r}_0 - \mathbf{r}|\right)}{|\mathbf{r}_0 - \mathbf{r}|}d. \end{aligned} \tag{17}$$

Transforming to observer's frame by using equation (9), we get

$$\begin{aligned} E^R_{x_k} &= E^R_x \\ &= -\frac{2ikz_0}{4\pi}\int E^b_{x_e}(x, y, z, \omega)\frac{\exp\left(ik|\mathbf{r}_0 - \mathbf{r}|\right)}{|\mathbf{r}_0 - \mathbf{r}|}\mathrm{d}S \\ E^R_{y_k} &= \frac{E^R_y}{\cos\left(\alpha + \theta_y\right)} + E^R_x\tan\theta_x\tan\left(\alpha + \theta_y\right), \\ &= -\frac{2ikz_0}{4\pi} \\ &\quad \int\left[\frac{1}{\cos\left(\alpha + \theta_y\right)}\begin{pmatrix} E^b_{y_e}(x, y\cos\alpha - z\sin\alpha, z\cos\alpha + y\sin\alpha, \omega)\cos\alpha \\ +E^b_{z_e}(x, y\cos\alpha - z\sin\alpha, z\cos\alpha + y\sin\alpha, \omega)\sin\alpha \end{pmatrix}\right. \\ &\quad \left. +E^b_{x_e}(x, y, z, \omega)\tan\theta_x\tan\left(\alpha + \theta_y\right)\right] \\ &\quad \frac{\exp\left(ik|\mathbf{r}_0 - \mathbf{r}|\right)}{|\mathbf{r}_0 - \mathbf{r}|}\mathrm{d}S. \end{aligned} \tag{18}$$

The following formula can be calculated by equations (11) and (16):

$$E_{x_k}^R = N\mathscr{F}_\parallel \frac{2ie}{\beta\gamma\lambda^2}\frac{\cos(\alpha+\theta_y)}{r_0}\iiiint b_\perp(x',y')\frac{\overline{x}}{\sqrt{\overline{x}^2+\overline{y}^2\cos^2\alpha}}K_1\left[\frac{2\pi}{\beta\gamma\lambda}\sqrt{\overline{x}^2+\overline{y}^2\cos^2\alpha}\right]\exp(i\phi)\mathrm{d}\overline{x}\mathrm{d}\overline{y}\mathrm{d}x'\mathrm{d}y',$$

$$E_{y_k}^R = N\mathscr{F}_\parallel \frac{2ie}{\beta\gamma\lambda^2}\frac{\cos\theta_x}{r_0}\iiiint b_\perp(x',y')\left\{K_1\left[\frac{2\pi}{\beta\gamma\lambda}\sqrt{\overline{x}^2+\overline{y}^2\cos^2\alpha}\right]\frac{\overline{y}\cos^2\alpha+\overline{x}\tan\theta_x\sin(\alpha+\theta_y)}{\sqrt{\overline{x}^2+\overline{y}^2\cos^2\alpha}}\right.$$
$$\left.-\frac{i}{\gamma}K_0\left[\frac{2\pi}{\beta\gamma\lambda}\sqrt{\overline{x}^2+\overline{y}^2\cos^2\alpha}\right]\sin\alpha\right\}\exp(i\phi)\mathrm{d}\overline{x}\mathrm{d}\overline{y}\mathrm{d}x'dy', \tag{19}$$

$$\phi = k\sqrt{(\overline{x}+x'-x_0)^2+\left(\overline{y}+\frac{y'}{\cos\alpha}-y_0\right)^2+z_0^2}+\frac{k(\overline{y}+(y'/\cos\alpha))\sin\alpha}{\beta}.$$

With the radiation fields, one can calculate the radiation energy with (10).

2.4. Numerical Integration. In the numerical calculation, an electron bunch with the Gaussian distribution is considered, and we calculate the radiation fields in the plane of incidence. In this case and transforming the variables to polar coordinate, (19) becomes $\overline{\rho}^2 = \overline{x}^2+\overline{y}^2\cos^2\alpha$ and $\rho' = x'^2+y'^2$; this yields

$$E_{x_k}^R = \mathscr{F}_\parallel \frac{2ie}{\beta\gamma\lambda^2}\frac{1}{\sqrt{2\sigma_\perp^2}}\frac{1}{r_0}\frac{\cos(\alpha+\theta_y)}{\cos\alpha}\iiiint \overline{\rho}\rho'\exp\left(-\frac{\rho'^2}{2\sigma_\perp^2}\right)K_1\left[\frac{2\pi}{\beta\gamma\lambda}\overline{\rho}\right]\exp(ik\Phi)\mathrm{d}\overline{\rho}\mathrm{d}\rho'\mathrm{d}\overline{\phi}\mathrm{d}\phi,'$$

$$E_{y_k}^R = \mathscr{F}_\parallel \frac{2ie}{\beta\gamma\lambda^2}\frac{1}{\sqrt{2\sigma_\perp^2}}\frac{1}{r_0}\frac{\cos\theta_x}{\cos\alpha}\iiiint \overline{\rho}\rho'\exp\left(-\frac{\rho'^2}{2\sigma_\perp^2}\right)\left\{K_1\left[\frac{2\pi}{\beta\gamma\lambda}\overline{\rho}\right]\cos\alpha\sin\overline{\phi}\right.$$
$$\left.-\frac{i}{\gamma}K_0\left[\frac{2\pi}{\beta\gamma\lambda}\overline{\rho}\right]\sin\alpha\right\}\exp(ik\Phi)\mathrm{d}\overline{\rho}\mathrm{d}\rho'\mathrm{d}\overline{\phi}\mathrm{d}\phi,' \tag{20}$$

$$\Phi = r_0-\frac{1}{\cos\alpha}\left(\overline{\rho}\sin\overline{\phi}+\rho'\sin\phi'\right)\left(\sin(\alpha+\theta_y)-\frac{\sin\alpha}{\beta}\right)+\frac{1}{2r_0}\left\{\left(\overline{\rho}\cos\overline{\phi}+\rho'\cos\phi'\right)^2\right.$$
$$\left.+\frac{1}{\cos^2\alpha}\left(\overline{\rho}\sin\overline{\phi}+\rho'\sin\phi'\right)^2\cos^2(\alpha+\theta_y)\right\}.$$

$\mathscr{F}_\parallel = 1/\sqrt{2\sigma_\parallel^2}\sqrt{2\pi\sigma_\parallel^2}\exp(-(\sigma_\parallel^2\omega^2/2))$.

To get the angular profile of the prewave OTR from electron bunch, one needs to evaluate equation (19). However, the integrands in equation (19) involve complicated convolution of functions and are not low dimensional. It might be difficult to find the interpolating functions which are easy to evaluate. To tackle this numerical integration, we use Monte Carlo method, which is robust and suitable for high dimensional integrations. The disadvantage of this method is that a large amount of points may, in general, be needed to achieve good convergence. We developed a code with Fortran. In this code, instead of pseudo-random sequence, Sobol sequence is implemented, which is of low discrepancy and can lead to better rate of convergence [22]. To get the angular profile, we need to perform such integration for different angles. This is a time-consuming task, and therefore we parallelize this implementation code with the MPI programming interface and model. This will reduce the time needed to reach particular decisions. The detailed description for the algorithm and source code are given later in the appendices.

3. Simulations and Experiments

To verify the results from theoretical calculation, simulations based on finite difference time domain method (FDTD) are performed. In this paper, concepts of FDTD method are surveyed, and the simulation model based on FDTD for OTR is described after that.

3.1. Finite Difference Time Domain Method. The FDTD method is a widespread method for computational electromagnetism and was proposed by Yee. We would review some key concepts of FDTD method for two-dimensional system [23]. In isotropic medium, the time evolution of electromagnetic fields can be fully characterized by Maxwell's equations and constitutive relations.

$$\begin{aligned} \nabla \times \mathbf{E} + \frac{\partial \mathbf{B}}{\partial t} &= 0, \\ \frac{\partial \mathbf{D}}{\partial t} - \nabla \times \mathbf{H} &= \mathbf{J}, \\ \mathbf{B} &= \mu \mathbf{H}, \\ \mathbf{D} &= \epsilon \mathbf{E}. \end{aligned} \tag{21}$$

For two-dimensional system with the coordinate (x, y), the fields behavior can be split into transverse electric (TE_z) mode

$$\begin{aligned} H_x &= H_y = 0, \\ E_z &= 0, \\ -\mu \frac{\partial H_z}{\partial t} &= \frac{\partial E_x}{\partial y} - \frac{\partial E_y}{\partial x} \epsilon \frac{\partial E_x}{\partial t} \frac{\partial H_z}{\partial y} - J_x, \\ \epsilon \frac{\partial E_y}{\partial t} &= -\frac{\partial H_z}{\partial x} - J_y n, \end{aligned} \tag{22}$$

and transverse magnetic (TM_z) mode

$$\begin{aligned} E_x &= E_y = 0, \\ H_z &= 0, \\ \epsilon \frac{\partial E_z}{\partial t} &= \frac{\partial H_y}{\partial x} - \frac{\partial H_x}{\partial y} - J_z, \\ \mu \frac{\partial H_x}{\partial t} &= -\frac{\partial E_z}{\partial y}, \\ \mu \frac{\partial H_y}{\partial t} &= \frac{\partial E_z}{\partial x}. \end{aligned} \tag{23}$$

One may then use central difference scheme to discretize Maxwell's equation and get the following discretization for TE_z mode and for TM_z mode (Figure 2).

In most cases, the electromagnetic problems are considered in unbounded regions. It might mean that we have to generate the simulation domain as large as possible to avoid the finite boundary effect. However, this is inefficient or even impossible in practice. One of the most common ways is to create a lossy medium outside the physical domain, and the waves are damped inside this medium. Besides, we also require that the absorbing layer to be reflectionless to the incident waves with all kinds of incident angles. This is the so-called perfectly matched layer. In the FDTD code, the uniaxial perfectly matched layer (UPML) is implemented. The layer is based on the anisotropic medium [24], and the interface between this medium and free space can be reflectionless with suitable choice of the material properties. In this subsection, we will follow and go through briefly the construction of this medium.

Consider a two-dimensional space is divided into region 1 ($x < 0$) and region 2 ($x > 0$). Region 1 is isotropic space with the propagating incident wave

$$\mathbf{H}_{inc} = \mathbf{H}_0 \exp\left(-jk_{1x}x - jk_{1y}y\right), \tag{24}$$

which propagates toward region 2. The region 2 is full of anisotropic medium which is characterized by

$$\epsilon_2 = \epsilon_2 \begin{pmatrix} a & 0 & 0 \\ 0 & b & 0 \\ 0 & 0 & b \end{pmatrix}, \mu_2 = \mu_2 \begin{pmatrix} c & 0 & 0 \\ 0 & d & 0 \\ 0 & 0 & d \end{pmatrix}. \tag{25}$$

The Maxwell equations in this medium are

$$\begin{aligned} \nabla \times \mathbf{E} &= -j\omega\mu_2 \mathbf{H}, \\ \nabla \times \mathbf{H} &= j\omega\epsilon_2 \mathbf{E}. \end{aligned} \tag{26}$$

We consider here the case for $\mathbf{TE_z}$. To calculate the reflection coefficient, we write down the plane wave in both regions

$$\begin{aligned} \mathbf{H}_1 &= \hat{z} H_0 \left(1 + \Gamma \exp\left(2jk_{1x}x\right)\right) \exp\left(-jk_{1x}x - jk_{1y}y\right), \\ \mathbf{E}_1 &= H_0 \left[-\hat{x} \frac{k_{1y}}{\omega\epsilon_1} \left(1 + \Gamma \exp\left(2jk_{1x}x\right)\right) \right. \\ &\quad \left. + \hat{y} \frac{k_{1x}}{\omega\epsilon_1} \left(1 - \Gamma \exp\left(2jk_{1x}x\right)\right) \right] \exp\left(-jk_{1x}x - jk_{1y}y\right), \\ \mathbf{H}_2 &= \hat{z} H_0 T \exp\left(-jk_{2x}x - jk_{2y}y\right), \\ \mathbf{E}_2 &= H_0 \left[-\hat{x} \frac{k_{2y}}{\omega\epsilon_2 a} + \hat{y} \frac{k_{2x}}{\omega\epsilon_2 b} \right] T \exp\left(-jk_{1x}x - jk_{1y}y\right), \end{aligned} \tag{27}$$

where Γ and T are reflection and transmission coefficient. By using the tangential boundary conditions

$$\begin{aligned} \mathbf{H}_{1\parallel} &= \mathbf{H}_{2\parallel}, \\ \mathbf{E}_{1\parallel} &= \mathbf{E}_{2\parallel}, \end{aligned} \tag{28}$$

we can solve the reflection and transmission coefficient

$$\Gamma = \frac{k_{1x} - k_{2x} b^{-1}}{k_{1x} + k_{2x} b^{-1}}, \tag{29}$$

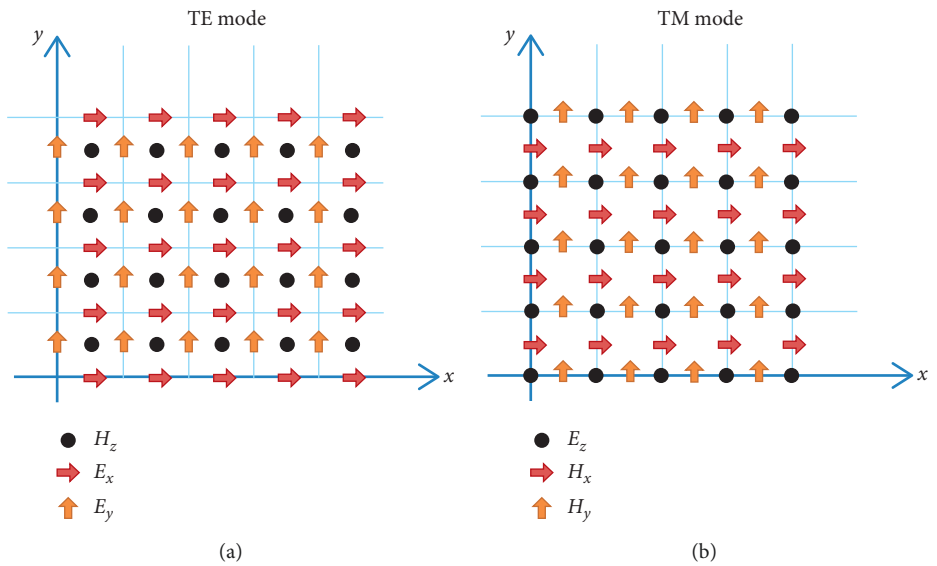

Figure 2: Two-dimension Yee grid for both TE and TM modes. (a) TE mode for 2D Yee grid. (b) TM mode for 2D Yee grid.

and also get Snell's law

$$k_{2x} = \sqrt{k_2^2 b\, d - \left(k_{1y}\right)^2 a^{-1} b}. \tag{30}$$

If $\epsilon_1 = \epsilon_2, \mu_1 = \mu_2, d = b$ and $a^{-1} = b$, then $k_1 = k_2$ and $k_{2x} = bk_{1x}$

Substituting into reflection coefficient, we can see that the interface is reflectionless for any angles of incidence wave.

So far we have discussed the UPML, which is reflectionless for the boundary normal to x direction and attenuates the wave propagating in x direction. We also need to consider the case for y direction. In general, Maxwell's equation in UPML can be expressed as

$$\begin{aligned} \nabla \times \mathbf{E} &= -j\omega\mu s\mathbf{H}, \\ \nabla \times \mathbf{H} &= j\omega\epsilon s^{\mathrm{t}}\mathbf{E}, \end{aligned} \tag{31}$$

where s is

$$s^{\mathrm{t}} = \begin{pmatrix} s_x^{-1} s_y s_z & 0 & 0 \\ 0 & s_x s_y^{-1} s_z & 0 \\ 0 & 0 & s_x s_y s_z^{-1} \end{pmatrix}. \tag{32}$$

For two-dimension case, we have three kinds of material properties for UPML (Figure 3):

(i) Boundary normal to x direction ($R1$): set $\sigma_y = \sigma_z = 0$.

(ii) Boundary normal to y direction ($R1$): set $\sigma_x = \sigma_z = 0$.

(iii) Overlapping region ($R3$): set $\sigma_z = 0$.

3.2. Simulation for OTR with Normal Incidence. Although the theoretical model developed in previous chapter can be applied for the electron bunch with oblique incidence, we only perform the simulation for the electron bunch with normal incidence. In this case, the spectral angular distribution of OTR is azimuthal symmetry and the simulation

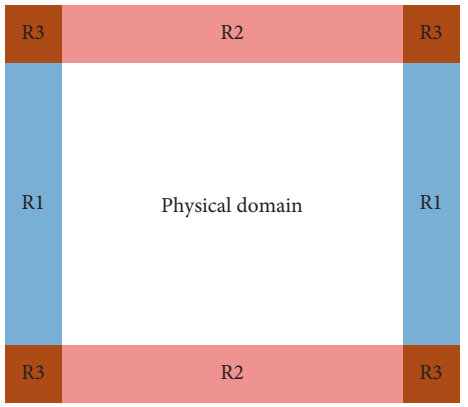

Figure 3: UPML in two-dimension simulation.

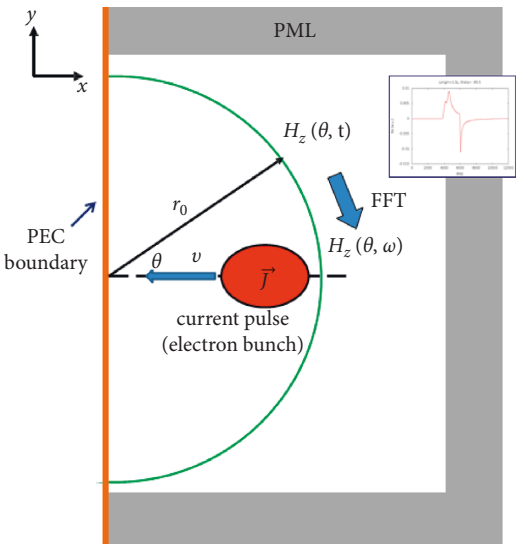

Figure 4: Simulation setup for OTR from normal incidence of electron bunch.

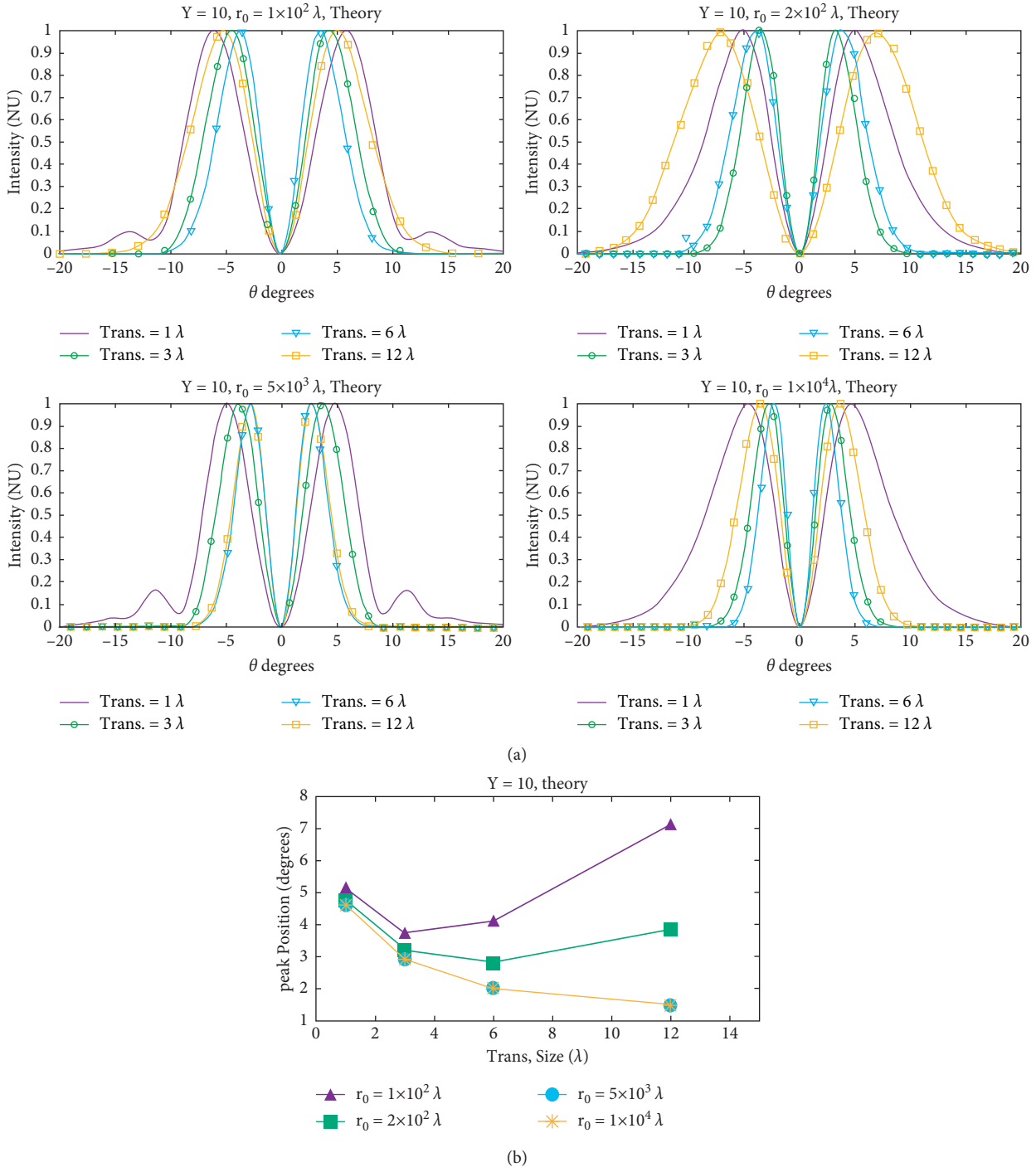

Figure 5: Angular distributions for various beam transverse sizes at different observation distances. (b) Peak positions for profiles from (a).

model can be reduced to two dimensions. Our simulation model is based on two-dimensional FDTD. The code we use in this study is written in Fortran with MPI parallelization and is developed by Dr. Toseo Moritaka. The simulation setup is showed in Figure 4.

Once the current pulse moves across the PEC boundary, OTR will be generated and then propagates toward the right hand side. The time signals for H_z fields situated at semicircular arc will be recorded. By using FFT, we can transform the time signals for each angle to specific frequency. The absolute square of the fields from different angles in frequency domain is corresponding to the angular distribution of radiation.

4. Results and Discussion

4.1. Theoretical Calculations. In this section, we show the radiation angular distribution from electron bunch with

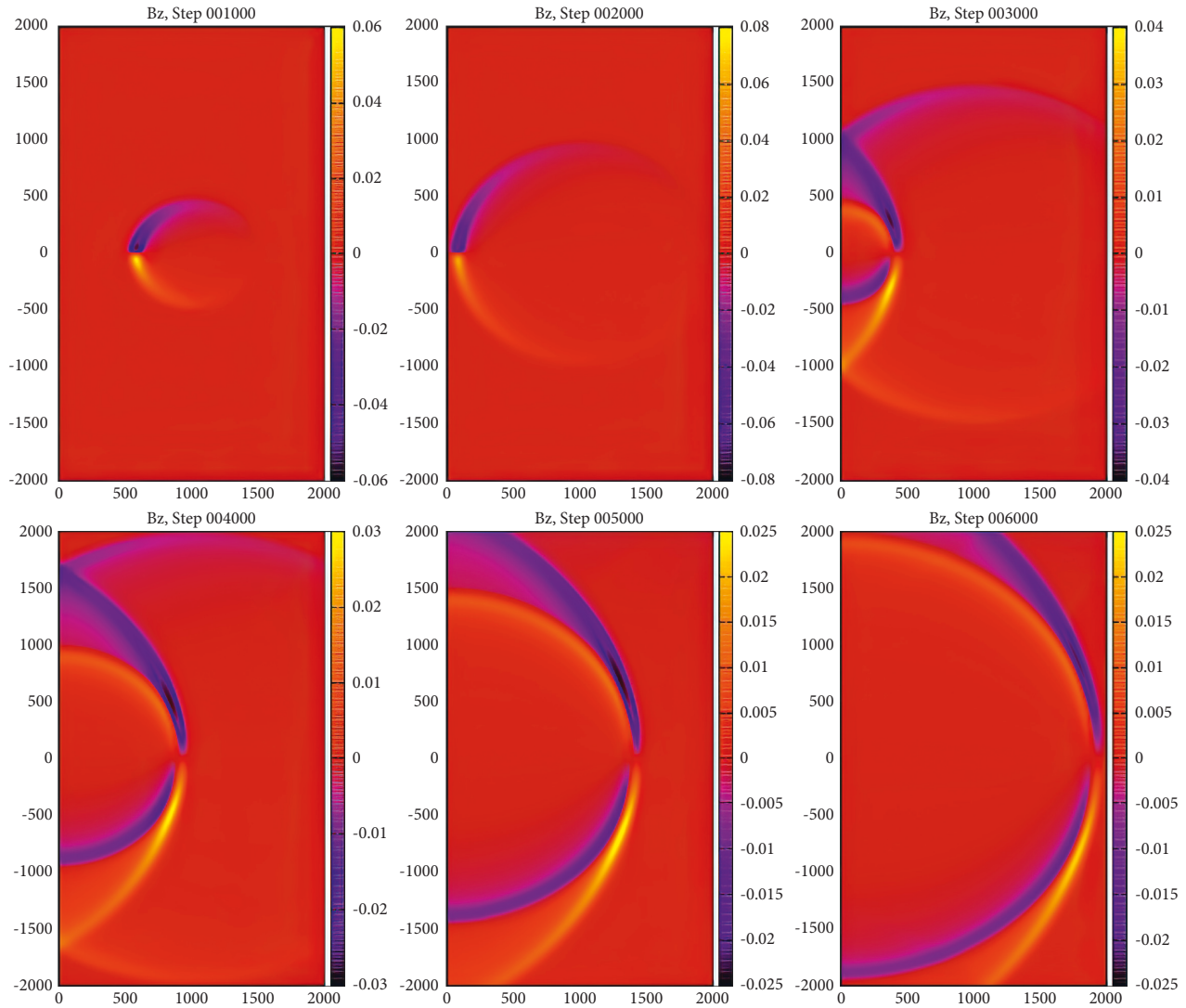

Figure 6: Heat maps of B_z field in full simulation domain.

normal incidence. We also compare the angular distributions in wave zone with the angular distributions in prewave zone.

4.1.1. Wave Zone vs. Prewave Zone. We studied the angular distributions from various transverse beam sizes at different observation distances. The outcomes are shown in Figure 5. We can firstly observe that the angular distributions change significantly with distance and become constant when the distance is large enough, such as $r_0 = 5 \times 10^3 \lambda$ and $r_0 = 1 \times 10^4 \lambda$. Besides, we can also observe that in wave zone the larger the beam transverse size is, the narrower the angular distribution is. However, this trend can not happen in the prewave zone. Taking angular distributions at $r_0 = 1 \times 10^2 \lambda$, for example, when the beam transverse size is increasing, the distribution will firstly narrow down and then broaden with the passage of time. This shows that the angular distributions in prewave zone are more sensitive to transverse beam size.

4.2. Simulations. To verify the theory, few two-dimensional FDTD simulations were performed. This should be remembered that in this study: we only verified OTR from electron bunch with normal incidence. In this case, the radiation angular distribution is azimuthal symmetry, and the simulation model can be reduced to two dimensions (Figure 6).

4.2.1. Evolution of B_z Field in Full Simulation Domain

4.2.2. Simulations vs. Theory. To verify the theory, we performed the simulation for bunch with normal incidence and compared it with the results from theory. The obtained results and findings are shown in Figure 7.

We can see the results from simulation qualitatively match the prediction form theory: in the prewave zone, say $r_0 = 1 \times 10^2 \lambda$, the angular distribution from larger beam transverse size can be broader than that from smaller beam transverse size. Also, as the distance increases, like

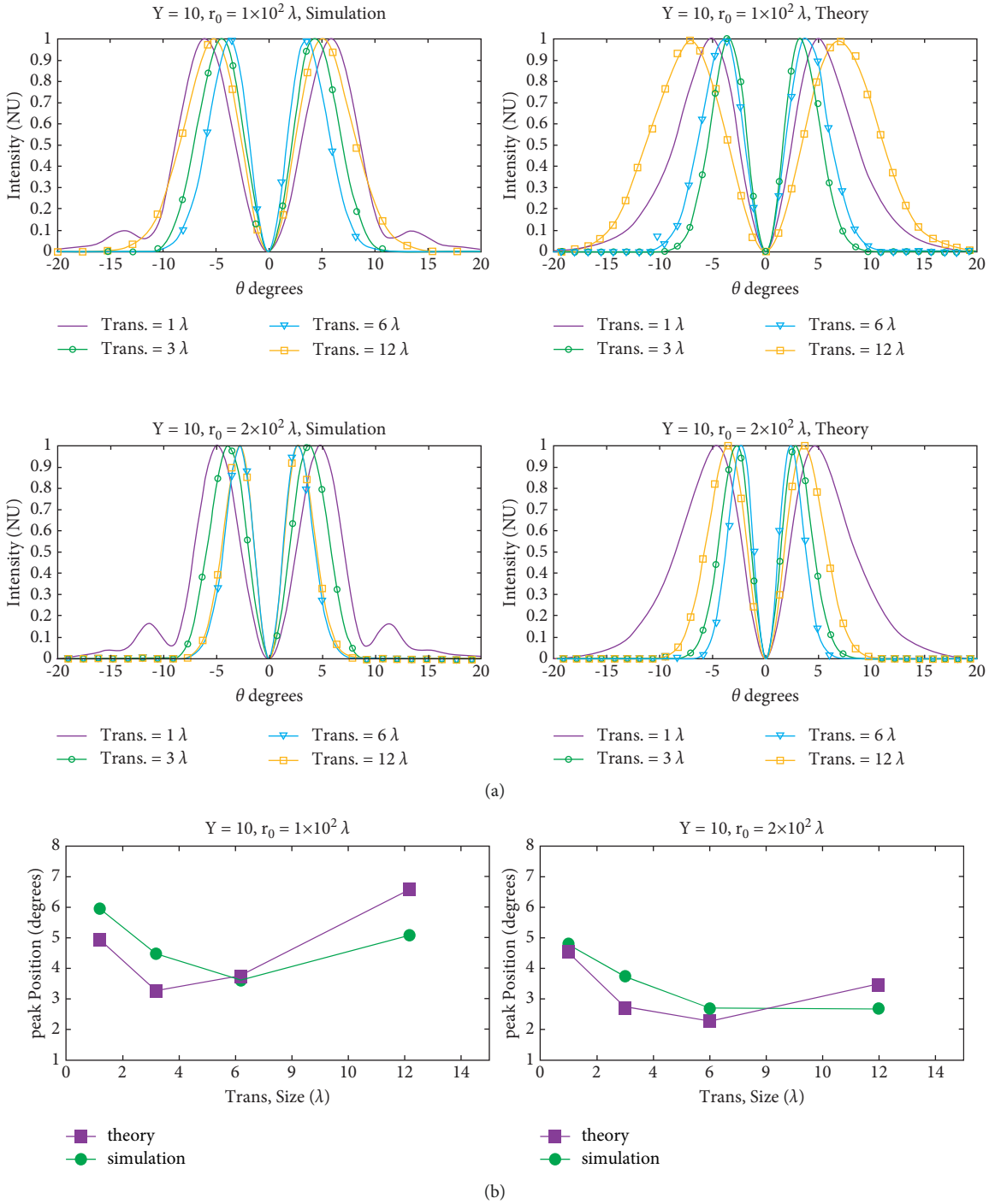

Figure 7: Comparison of angular spectrums between simulation and theory. (b) Peak positions for profiles from (a).

$r_0 = 2 \times 10^2 \lambda$, this broadening effect reduces, and the behavior of angular distributions is more similar to the behavior in wave zone.

4.3. Oblique Incidence. The angular distributions become asymmetric when a bunch with oblique incidence is considered. In wave zone, the asymmetry is more severe as the transverse beam size is large. In the prewave zone, however, the location in center of detector does have value (as shown in Figures 8 and 9); the value becomes large when the transverse beam size becomes large.

The above results can be understood from a simple physical diagram as shown in Figure 10.

4.4. Case Study. Although people normally consider a beam with incident angle of 45 degrees, in practice, however, in this study we consider the angular distribution from different incident angles. When a beam with incident angle is

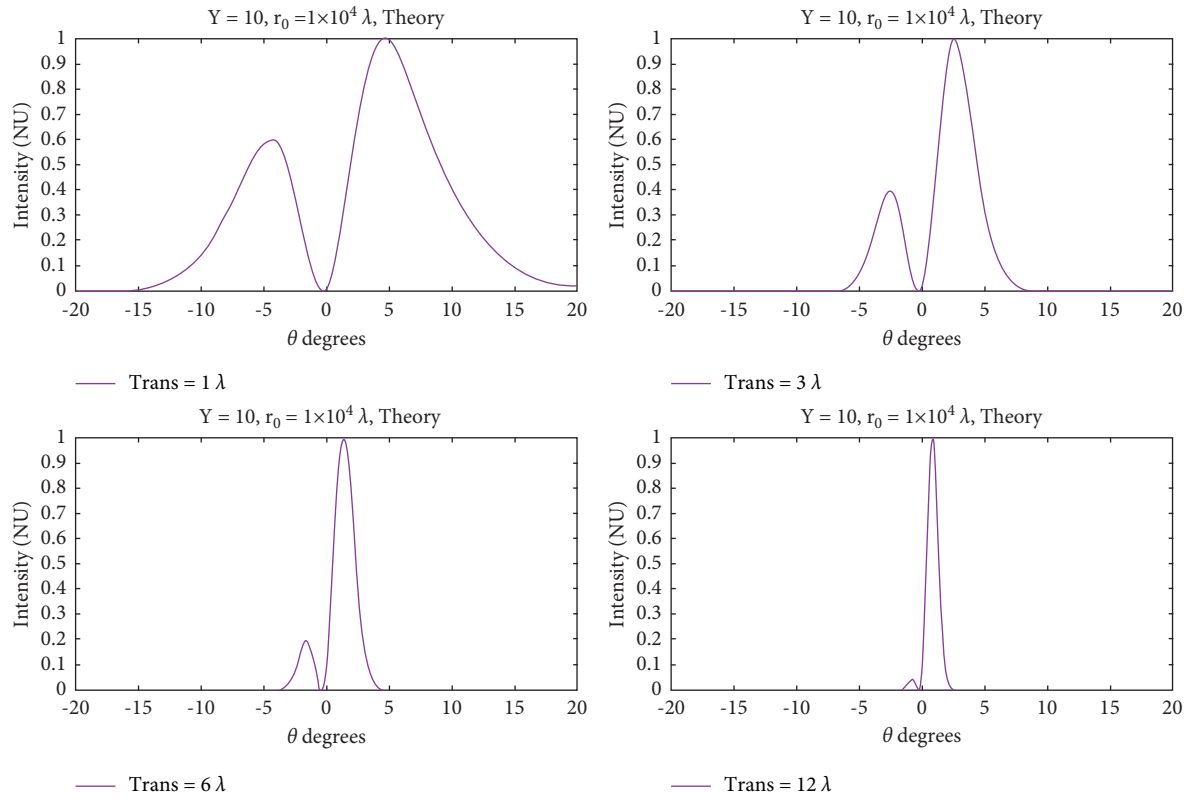

Figure 8: Angular distributions with $\alpha = \pi/4$ in wave zone.

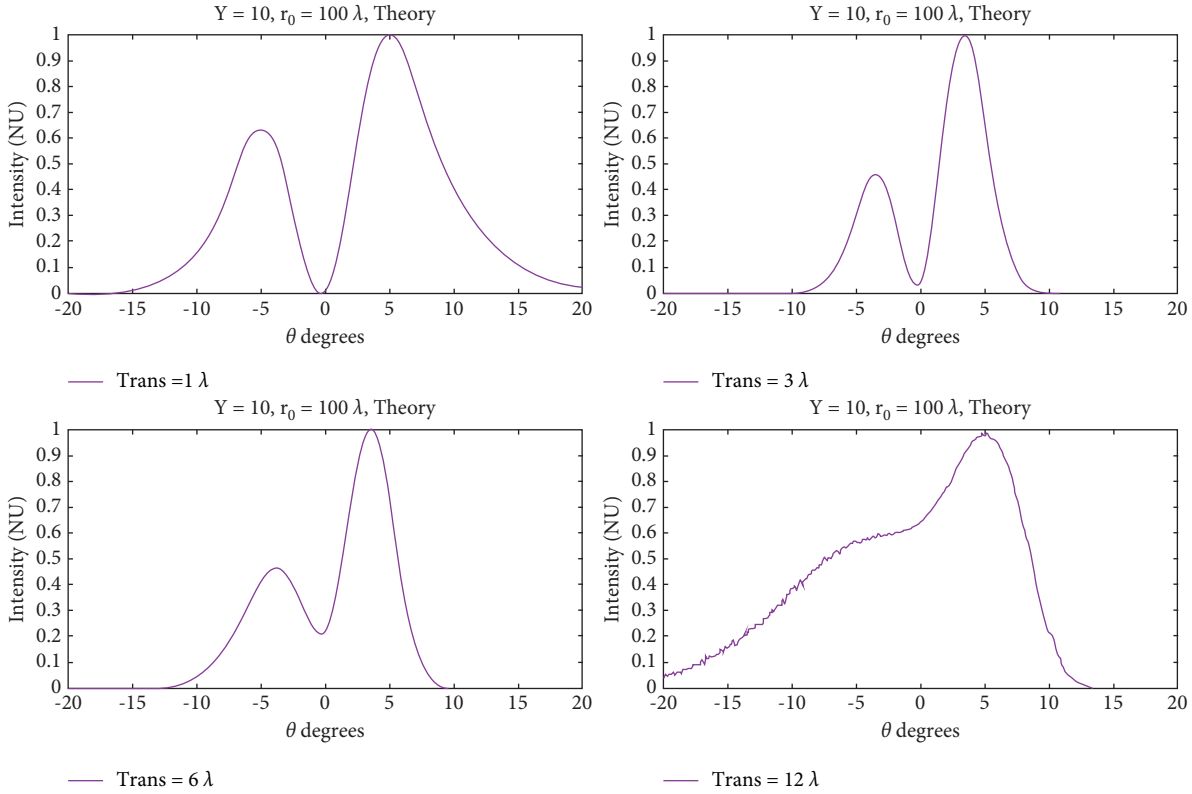

Figure 9: Angular distributions with $\alpha = \pi/4$ in prewave zone.

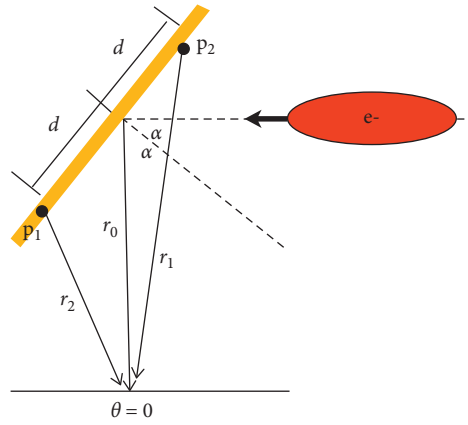

Figure 10: A simple picture for OTR from electron bunch.

Table 1: Parameters from HBI group, NSRRC.

Project	Numerical value
Energy	30 Mev
Transverse beam size (rms)	2 mm
Observation distance	1 m

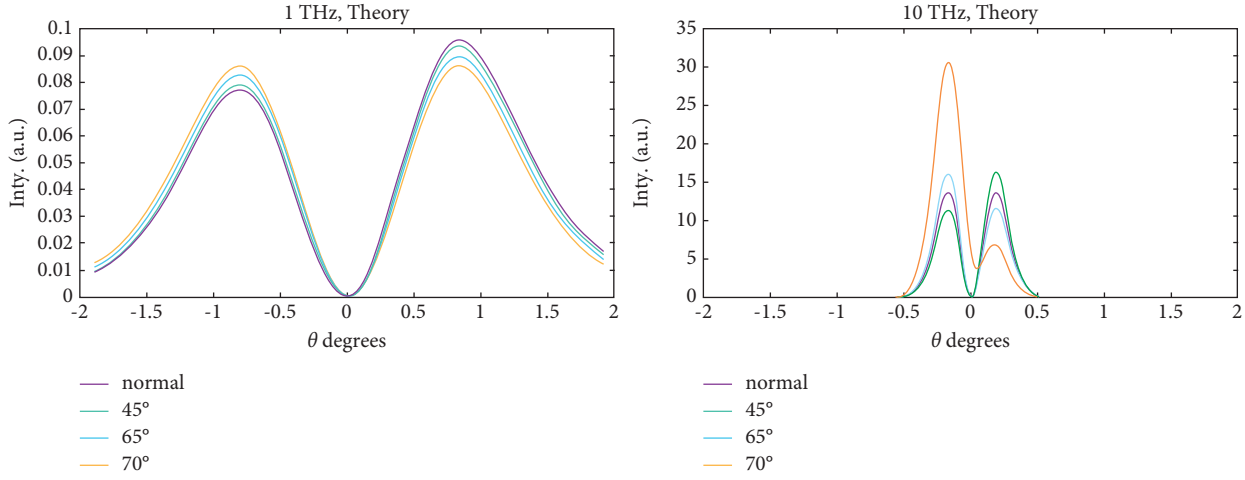

Figure 11: Angular distributions with different observation angles.

considered, the angular distributions become asymmetric, as reported in Table 1 below.

For 1 THz case, we can see that the asymmetry of angular distribution becomes severe as the incident angle is increased (as shown in Figure 11). For 10 THz case, when the incident angle is increased, the asymmetry pattern changes. The cause of such asymmetric angular distributions can be understood from a simple diagram as depicted in Figure 12.

In the above figure, we assume that θ_2 and θ_1 are the position with peak value, where $\theta_2 > 0$ and $\theta_2 < 0$. We can easily see the phase difference of the radiations from p_1 and p_2 is different at θ_2 and θ_1. This causes asymmetric angular distributions.

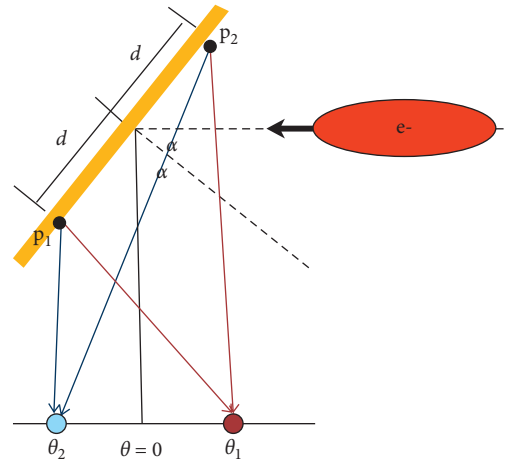

Figure 12: Simple picture of asymmetric angular distributions.

5. Conclusions and Future Work

In this study, we proposed a theory treating prewave zone OTR with the consideration of beam structure. In the proposed theory, the beam transverse size effect can be simplified to transverse form factor when wave zone approximation is considered. A parallelized numerical integration code based on quasi-Monte Carlo method was developed to perform the complicated integration. We demonstrated, theoretically, that the angular distributions in the prewave zone are more sensitive than those in the wave zone. The simulations also provide consistent findings and results. The provided formalism theory and numerical tool could be useful for the prediction of radiation properties for the OTR experiment in prewave zone. The disadvantage of this method is that a large amount of samplings may need to be employed to achieve good convergence. In the future, we will investigate more robust technique to improve the performance and convergence speed using various parallelism concepts like the one used in this paper, i.e., MPI. Similarly, statistical methods should be used to find accurate mapping and excluding similar samples that could potentially decrease the convergence speed.

Data Availability

The data can be requested from the corresponding author.

Conflicts of Interest

The authors declare that they have no conflicts of interest.

Acknowledgments

This study was supported by the National Natural Science Foundation of China, 41774140, project title: Research on Soil Radon Measurement Technology and Abnormal Information Extraction Method in Uranium Exploration; National Natural Science Foundation of China, 11675028, project title: Research on Digital Shaping Algorithm and Real-Time Processing Technology of Nuclear Pulse Signal; and National Key R&D Program, 2018YFC0603304, project title: Development of Neutron Gamma Logging Methods and Instruments for Rock-Forming Elements.

References

[1] M. L. Ter Mikaelian and L. S. Osborne, "High energy electromagnetic Processes in condensed media," *Physics Today*, vol. 26, no. 3, pp. 69–71, 1973.

[2] L. D. Landau, E. M. Lifshitz, J. B. Sykes, J. S. Bell, and E. H. Dill, "Electrodynamics of continuous media," *Physics Today*, vol. 14, no. 10, pp. 48–50, 1961.

[3] G. Wang, L. Deng, and Z. Zheng, "Study on the Transmission Characteristics of Epithermal Electron Beam by Using Transition Radiation," *High Power Laser and Particle Beam*, 2007.

[4] G. Wang, Li Deng, and Z. Zheng, "Study on the transmission characteristics of epithermal electron beam by using transition radiation," *Intense laser and particle beam*, vol. 19, no. 2, pp. 241–244, 2007.

[5] C. Ma, G. Wang, and T. Chen, "Comparative study of hot electron transit radiation and high energy proton emission," *Journal of Shanxi Normal University Natural Science Edition*, vol. 31, no. 03, pp. 346–349, 2008.

[6] J. G. Yang, Z. Zhang, S. F. Chen, C. J. Liu, and Y. Z. Lin, "Application of transit radiation in high current electron beam diagnosis," *Chinese Physics C*, vol. 29, no. 3, pp. 305–311, 2005.

[7] Q. Yu, "Theoretical Simulation and Experimental Study on Thomson Scattering and Transition Radiation of Laser Plasma," *Institute of Physics in Chinese Academy of Sciences*, vol. 16, 2005.

[8] C. G. Wang, Z. J. Zheng, Y. Q. Gu, T. Chen, and T. Zhang, "Study on the transport process of hot electrons in solid targets by using transition radiation," *Acta Physica Sinica*, vol. 48, no. 02, pp. 982–987, 2007.

[9] X. Luo, L. C. Lao, J. X. Wang et al., "Longitudinal length measurement of PS level electron beam in superconducting accelerator by microwave zero phase method," *Atomic Energy Science and Technology*, vol. 53, no. 006, pp. 1147–1152, 2019.

[10] A. Sampath, X. Davoine, S. Corde et al., "Extremely dense gamma-ray pulses in electron beam-multifoil collisions," *Physical Review Letters*, vol. 126, Article ID 064801, 2021.

[11] A. Curcio, M. Bergamaschi, R. Corsini et al., "Diffractive shadowing of coherent polarization radiation," *Physics Letters A*, vol. 391, Article ID 127135, 2021.

[12] X. Tan, X. Weng, W. Kun, T. Zhang, and X. Wu, *Picosecond Pulsed Electron Beam Measurement Device and Method Based on Optical Transition Radiation*, IEEE, Sanya, China, 2019.

[13] X. Qian, K. Chen, and C. Sheng, "Study of tunable enhanced terahertz transition radiation based on graphene," *Chinese Science: Physics, mechanics, astronomy*, vol. 16, no. 6, pp. 1–8, 2019.

[14] A. Curcio, M. Bergamaschi, R. Corsini et al., "Noninvasive bunch length measurements exploiting Cherenkov diffraction radiation," *Physical Review Accelerators and Beams*, vol. 23, Article ID 022802, 2020.

[15] S. Yao, L. Su, and S. Zhou, "Transition radiation energy in a coupled elastic layer with an inclined interface," *Acta Mechanica Sinica*, vol. 52, no. 1, 2020.

[16] F. An, Y. Lei, C. Yu, S. Yang, J. Lei, and Y. Xu, "Mechanism and Research on stimulated radiation of materials based on light," *Journal of Suihua University*, vol. 40, no. 12, pp. 163–165, 2020.

[17] G. Wang and Z. Zheng, "Back surface transition radiation in the interaction between femtosecond laser and solid target," *China laser*, vol. 35, no. 4, 2008.

[18] S. Liu and Y. Sun, "Relationship between spontaneous emission and stimulated emission in free electron laser with transit radiation," *Acta Physica Sinica*, vol. 000, no. 009, pp. 1505–1509, 1988.

[19] K. Fedorov, P. Karataev, Y. Saveliev et al., "Development of longitudinal beam profile monitor based on Coherent Transition Radiation effect for CLARA accelerator," *Journal of Instrumentation*, vol. 15, Article ID C06008, 2020.

[20] J. Wolfenden, R. B. Fiorito, and C. P. Welsch, "A novel simulation and analysis algorithm for high resolution optical transition radiation imaging," *Optics Express*, vol. 27, pp. 2988–2999, 2019.

[21] Y. Zheng and L. Chen, "A new method for measuring optical properties of optical transition radiation," *Acta Photonica Sinica*, vol. 67, 2009.
[22] Y. Yang, Z. Zhao, and I O. Anisimov, "Electromagnetic radiation excited by modulated electron beam in space plasma," *Journal of Radio Science*, vol. 021, no. 003, pp. 305–309, 2006.
[23] T. Chen and Z. Li, "Measurement of free electron laser clustering by coherent transition radiation," *Journal of Southwest University of science and Technology (NATURAL SCIENCE EDITION)*, vol. 21, no. 3, pp. 75–78, 2006.
[24] G. Wang and Z. Zheng, "Back surface transition radiation in the interaction between femtosecond laser and solid target," *China laser*, vol. 35, no. 4, p. 524, 2008.

Hindawi
Scientific Programming
Volume 2022, Article ID 4668147, 12 pages
https://doi.org/10.1155/2022/4668147

Research Article

Effect of English Reading on the Cultivation of College Students' Humanistic Spirit Based on Embedded Sensor System

Lingtuo Wang,[1] Xiaobin Li ,[2] and Yufang Jiao[3]

[1]*Department of Foreign Languages, Shanghai University of Finance and Economics Zhejiang College, Jinhua 321013, Zhejiang, China*
[2]*School of Foreign Languages, Zhijiang College of Zhejiang University of Technology, Shaoxing 312030, Zhejiang, China*
[3]*School of Japanese Studies, Shanghai International Studies University, Hongkou 200083, Shanghai, China*

Correspondence should be addressed to Xiaobin Li; lxb@zjc.zjut.edu.cn

Received 17 March 2022; Revised 2 May 2022; Accepted 12 May 2022; Published 26 May 2022

Academic Editor: Muhammad Usman

With the development of information technology in recent years, people have integrated English reading with information technology, which is conducive to improving the ability of English reading and cultivating the humanistic spirit of college students. This paper aims to study how to play the role of English reading in the cultivation of college students' humanistic spirit based on the embedded sensor system. This paper proposes an embedded speech recognition technology algorithm and a speech recognition technology algorithm based on dynamic time warping. Speech recognition technology is conducive to the improvement of English reading efficiency, as well as improving the reading interest of college students. The experimental results of this paper show that the speed of English development has become faster and faster in recent years, from 30% in 2011 to 55% in 2020. Although it fluctuates in the middle, the overall trend is upward. People pay more and more attention to English, and the proportion of English reading is gradually increasing, from about 20% in 2011 to about 41%. Therefore, it can be known that the importance of English reading is getting higher and higher, and it is necessary to cultivate the humanistic spirit of college students through English reading.

1. Introduction

With the advancement of science and technology, human beings have entered the information age. Computers and various embedded digital devices play a very important role in this prosperous digital age. Speech recognition is a technology for humans to convey information and a technology for machines to read sound signals and convert them into words and commands. After years of development, speech recognition has come a long way, showing great application possibilities.

With the development of computers, the indispensable mobile devices in people's lives continue to increase. In order to make these devices operate more conveniently and naturally, embedded application software based on speech recognition technology is required. Research in this area is becoming increasingly popular, and manual manipulations can be replaced with voice manipulations.

The innovation of this paper is as follows: (1) This paper introduces the theoretical knowledge of embedded sensor system and humanistic spirit cultivation. This paper also uses the embedded speech recognition technology to analyze how the embedded sensor system promotes the effect of English reading on the cultivation of college students' humanistic spirit. (2) This paper expounds the embedded speech recognition technology based on time warping. This paper finds that speech recognition technology can effectively promote English reading through experiments so as to effectively cultivate the humanistic spirit of college students.

2. Related Work

With the vigorous development of education in recent years, people are paying more and more attention to English reading. Shao et al. discovered an embedded high-temperature sensor for intelligent aeroengines and other intelligent mechanical

systems. This high-temperature sensor is directly constructed on the surface of aeroengine turbine blades through micromachining technology. But sensor fabrication faces two major challenges: high-temperature electrical insulation and curved soft lithography. They conducted a series of elaborate high-temperature experiments to study the accuracy and precision of high-temperature characterization. The results show that the temperature in a high-temperature system can cause inherent errors in high-temperature measurements. The scholars conducted high-temperature experiments, but they did not list the experimental data and comparative data [1]. Bouain found that multisensor architectures are widely used to better sense the environment of intelligent vehicles. Using multiple sensors to handle perception tasks in rich environments is a natural solution. Most of the research work has focused on perception-based task implementation, and little attention has been paid to custom embedded design. He proposed a multisensor data fusion embedded design for ranging sensors for vehicle perception tasks. The scholar proposed embedded sensors to sense vehicles but did not prove the feasibility of this method [2]. Duan found that the country proposed the activity-based teaching method in English reading teaching. With the development of the times, the demand for English teachers is changing because educators attach great importance to the application of modern information technology and activity-based. Therefore, around how to use the English activity method in reading teaching, he designed three learning activities. The scholar designed three learning activities, but he did not give a specific introduction to the three activities, so the authenticity of these three activities could not be verified [3]. Wu found that, in English reading teaching, it is necessary to promote the development of students' thinking quality. This is an important part of the key competencies in the English subject. However, the current English reading teaching over-emphasizes the input of language knowledge, the extraction of basic information, and the application of reading strategies, while ignoring the cultivation of students' thinking quality. Therefore, how to cultivate students' thinking quality in English reading teaching has become an important problem to be solved urgently. Although the scholar proposed that thinking quality is an urgent problem to be solved, he did not mention how to solve this problem [4]. Zhou demonstrated the limitations of traditional English reading teaching methods. He further explored the feasibility and effectiveness of multimedia teaching in junior high school English reading teaching. It includes the design of reading teaching activities and the application and evaluation of multimedia in the classroom teaching process. He provided students with efficient learning methods. But he did not elaborate on the shortcomings of traditional English reading teaching [5]. Munandar and Srimurni's research aimed to analyze the effectiveness of embedded systems in improving students' reading comprehension. They did research on this and found that teachers face some problems in teaching reading comprehension to their students. To find out, they employed an experimental approach to quantitative research. After statistical acquisition and interpretation of the data, they concluded that the directional reading activity method can improve students' reading comprehension ability. At the same time, studies have found that this strategy can also increase and enhance students' vocabulary and reading skills. However, the scholar's quantitative research did not describe it in detail, resulting in an unrealistic and reliable conclusion [6]. Alenezi found that reading is an essential strategic and lifelong skill necessary for learning success. His research examines foreign language students' knowledge and beliefs about strategies for reading comprehension in English. He also intended to determine whether there is a significant correlation between students' basic knowledge of English reading comprehension strategies and their beliefs about reading comprehension strategies. His research uses a quantitative approach, with data collected using a forty-item questionnaire. The scholar used a questionnaire method to study the relationship between basic knowledge and beliefs but did not reach a conclusion [7].

3. Method Based on Embedded Speech Recognition Technology

3.1. Concept of English Reading and Humanistic Spirit Cultivation. The information age that people are living in now is an age of all kinds of data and information flooding, and it is also an age full of problems. While enriching people's lives, people must constantly analyze, judge, and choose. Huge information can easily affect students' cognition. Faced with a variety of viewpoints, it is repeatedly emphasized in education that students "reject blind obedience." The key to not blind obedience is to cultivate the thinking habit of critical thinking; that is to say, students must actively cultivate the humanistic spirit [8]. The degree of emphasis that college students place on textbook knowledge and humanistic spirit is shown in Table 1.

As shown in Table 1, in 2015, 86% of college students believed that knowledge was more important, and only 14% of college students believed that the cultivation of humanistic spirit was also very important. The formation of comprehensive language ability is based on the overall development of students' learning skills, language knowledge, emotional attitudes, learning strategies, and cultural awareness. With the continuous development of modern education, humanistic spirit has become a hot topic in the field of education. As a language, English must also undertake the important task of cultivating students' humanitarian spirit in education, so as to promote students' development and cultivate students with more comprehensive and high-quality talents [9, 10]. The schematic diagram of the embedded English learning system is shown in Figure 1.

As shown in Figure 1, the 21st century is the age of knowledge and information. With the rapid development of

Table 1: The degree that college students attach importance to textbook knowledge and humanistic spirit.

Year	Knowledge (%)	Human spirit (%)
2015	86	14
2016	84	16
2017	80	20
2018	85	15

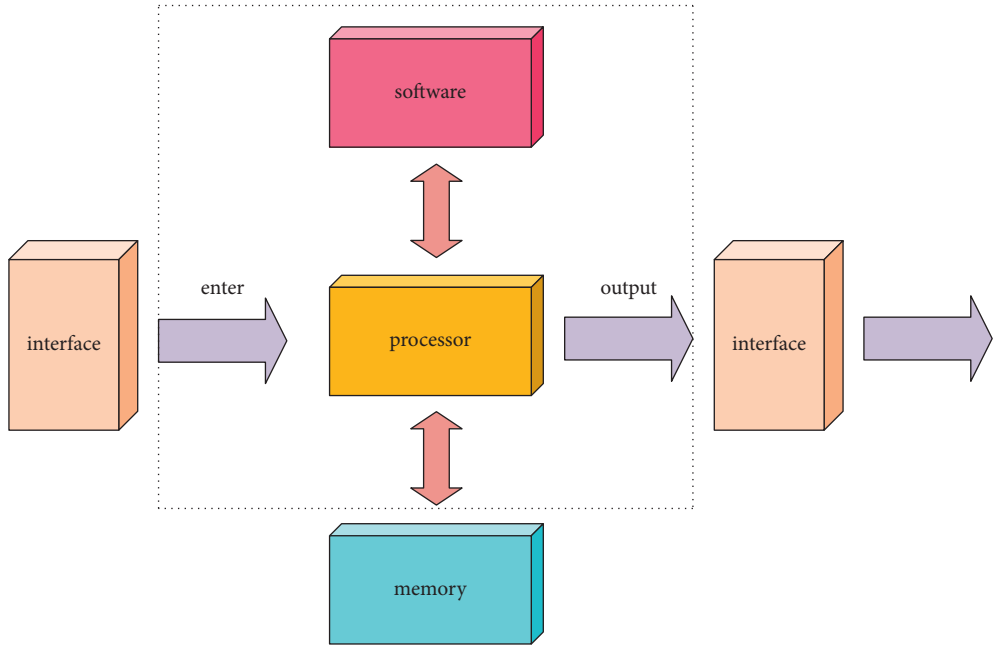

Figure 1: Schematic diagram of the embedded English learning system.

embedded technology, the functions of learning machines are not limited to the scope of electronic dictionaries. Learning machines can learn a variety of topics at the same time, and their functions are also more powerful [11]. A wireless sensor network is a task-oriented wireless self-organizing network composed of multiple nodes, as shown in Figure 2.

As shown in Figure 2, a wireless sensor network consists of multiple sensor nodes dispersed in high density, and each sensor node has specific functions of data collection, processing, and wireless communication [12]. Embedded generally refers to embedded systems. Embedded systems consist of hardware and software. It is a device that can operate independently. Its software content only includes the software operating environment and its operating system. The hardware content includes various aspects, including signal processor, memory, and communication module. The sensor node structure is shown in Figure 3.

As shown in Figure 3, embedded wireless sensor networks can also play a great role in the field of education. For example, a learning machine equipped with a wireless communication module can automatically form a network for the educational process, including educational interaction and resource sharing. Wireless sensor network is a distributed sensor network. At its tip are sensors that can sense and inspect the outside world. Sensors in WSN

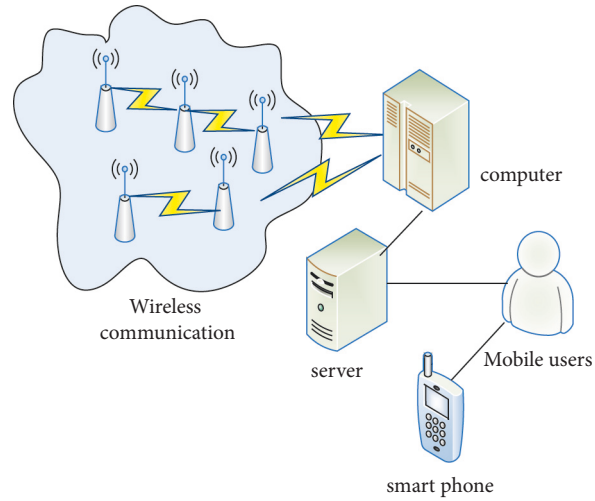

Figure 2: Schematic diagram of wireless sensor network and application.

communicate wirelessly. Therefore, the network settings are flexible, and the device location can be changed at any time. It can also be wired or wirelessly connected to the Internet. It is a multihop self-organizing network formed by wireless communication. In the framework of China's core literacy,

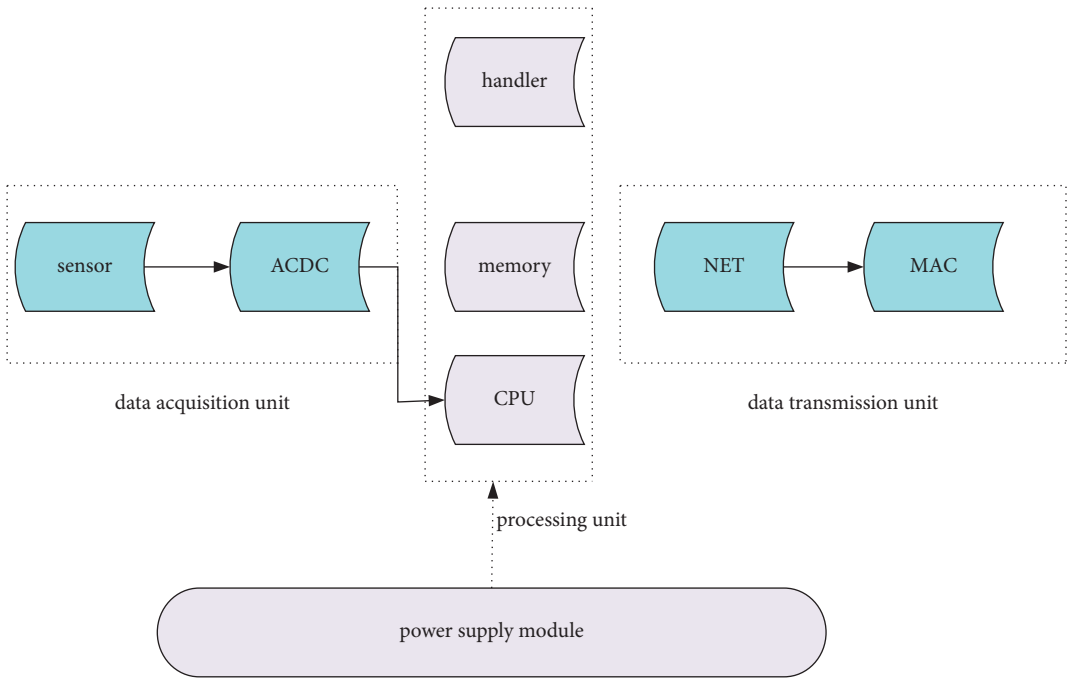

Figure 3: Sensor node structure.

the ability to "critical and question" is an interdisciplinary ability that requires joint efforts and implementation in all fields [13]. In the English subject, the English course will undertake the task of cultivating students' basic English ability and developing students' thinking ability. Regarding the reading ability students should have, the curriculum standards are students' comprehension, prediction, judgment, and generalization of reading. Reasonable prediction, rigorous inference, and wise judgment are inseparable from the support of critical thinking [14].

The English reading process is an interaction between visual and nonvisual information. Visual information refers to everything that uses literal symbols to convey meaning through surface structures, such as basic words and interpretations of texts. Nonvisual information contains world general knowledge and specific knowledge, and it is more important than visual information [15]. English reading is shown in Figure 4.

As shown in Figure 4, English reading is a complex cognitive activity. In the process of reading, the reader does not passively accept knowledge but reorganizes the process of language based on his own understanding of knowledge, experience and the meaning of the text. Therefore, in the complete reading process, comprehension must be included. English critical reading meets the requirements of the core competence of English subjects, as well as the requirements of the development of the times and the development of students' thinking [16]. This helps promote the development of students' critical thinking and enhance their deep understanding of reading materials. The application of speech recognition technology is shown in Figure 5.

As shown in Figure 5, any technology can help to further expand the living space of human beings and promote the way of life of human beings. In general, the direction of speech recognition is to serve humans better. To achieve this goal, speech recognition technology also needs to make leaps in the areas, and most speech recognition modes are based on one language. If the user inputs multiple languages such as Chinese and English, the accuracy of speech recognition will drop significantly [17]. To overcome this problem, this paper adopts a mixed language mode approach which becomes the topic of speech recognition research today [18].

3.2. Speech Recognition Algorithm Based on Dynamic Time Warping (DTW). Dynamic time warping is a nonlinear method that combines the computation of time warping and distance measurements. Its purpose is to convert the time-varying features of words into consistent time periods [19]. This algorithm is based on the concept of dynamic programming, which is an early classic algorithm for speech recognition. It is generally used to identify isolated words with a small vocabulary. Dynamic time warping is shown in Figure 6.

As shown in Figure 6, the dynamic time warping algorithm is a dynamic programming algorithm that calculates the similarity of two time series, especially series of different lengths. It is mainly used in time-series data, such as isolated word speech recognition, gesture recognition, data mining, and information retrieval. Each intersection in the grid represents the intersection between the test mode frame and the training mode frame. The goal of the DTW algorithm is to find a path through several grid points in this grid. The grid points that the path passes through are the frame numbers of the test and reference templates used for distance calculation [20]. In order to make the path not too inclined, the DTW algorithm gives the following constraints during dynamic warping, and the boundary conditions are formula (1):

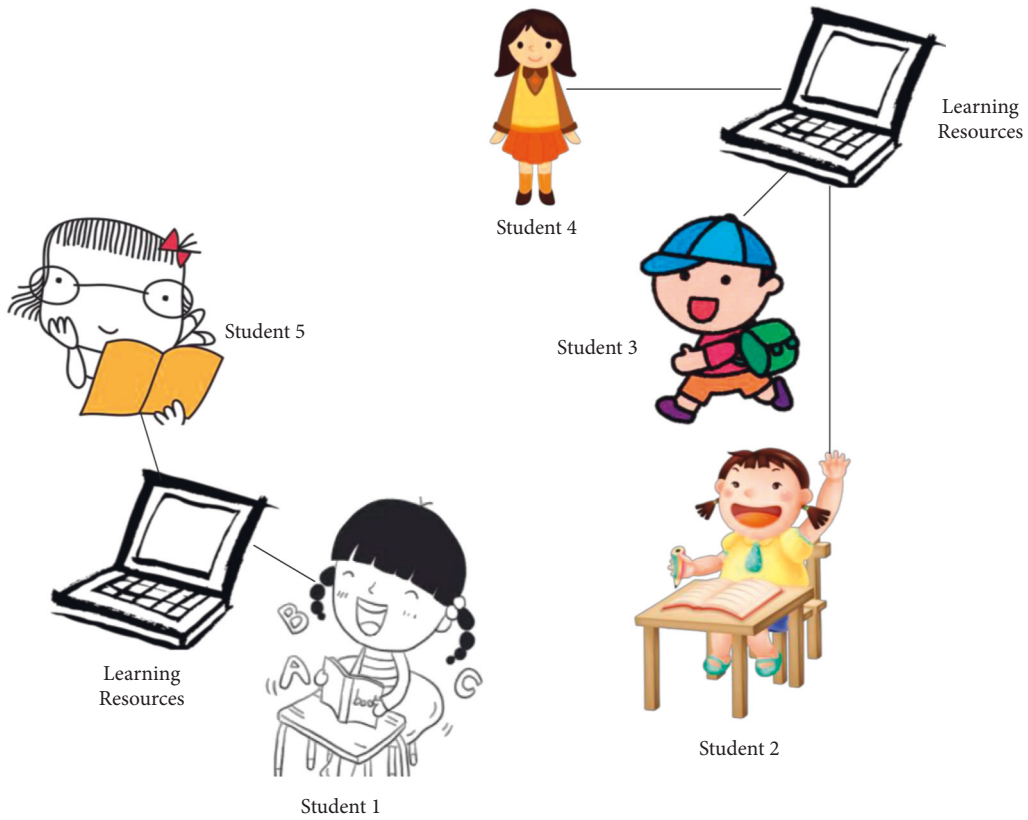

Figure 4: How to read in English.

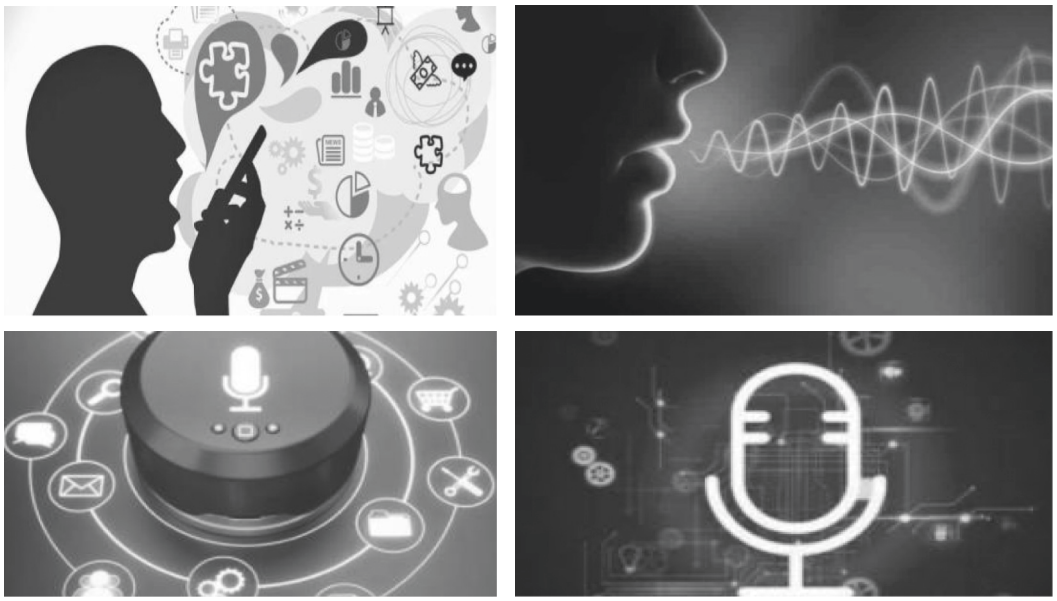

Figure 5: Applications of speech recognition technology.

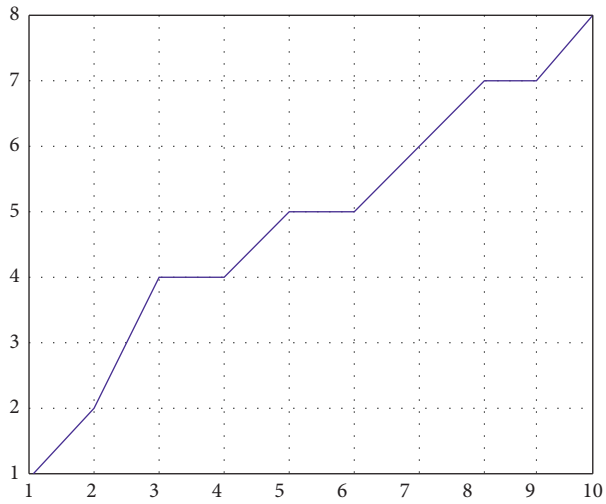

Figure 6: DTW algorithm search path.

$$w(1) = 1,\ w(N) = M. \tag{1}$$

Assuming that the reference template feature vector sequence in the template library is $a_1, a_2, \ldots, a_n$, then the DTW algorithm satisfies formula (2):

$$D = \min \sum_{n=1}^{N} d[n, w, (n)]. \tag{2}$$

$d[n, w(n)]$ is the distance between the input vector of the nth frame and the reference vector of the mth frame, and D is the distance measure of the two voices. The preprocessing part of the speech signal includes normalization and preemphasis. Normalization is a way of simplifying the calculation; that is, the dimensional expression is transformed into a dimensionless expression and becomes a scalar. This method is often used in various calculations. Because the volume of speech affects the energy value of each speech frame, the energy is normalized to exclude differences in the volume of each person's speech [21]. The specific method is as formula (3):

$$b[n] = \frac{(x_{\max} - a[n])}{\left|X_{\max} - X_{\min}\right|}. \tag{3}$$

Among them, $X_{\max}$ represents the maximum amplitude of the speech signal, and $X_{\min}$ represents the minimum amplitude.

High-frequency loss occurs after the speech is emitted from the lips. In order to make up for these high-frequency losses, preemphasis processing is required here, the sound signal of each frame will be emphasized at high frequencies and filtered with a high-frequency filter, and the high-efficiency filter is mainly used to capture particulate dust above 0.5 um and various suspended solids, as the end filter of various filtration systems, such as formula (4):

$$H(z) = 1 - a \times z^{-1}, \tag{4}$$

where a is between 0.9 and 1, and the preemphasized signal $S_2(n)$ is formula (5):

$$S_2(n) = S(n) - a \times s(n-1). \tag{5}$$

Spectral leakage occurs due to direct truncation of the signal (with a rectangular window). In order to improve the situation of spectral leakage, a nonrectangular window is added. It is generally a plus Hamming window. Because the amplitude-frequency characteristic of the Hamming window is that the side lobe attenuation is large, the attenuation of the main lobe peak and the first side lobe peak can reach 43 db. The specific windowing method is as follows: people set a speech signal as $S(n) = 0, 1, \ldots, n$. The expression of the Hamming window is shown in formula (6):

$$W(n, a) = (1 - a) - a\cos\left(\frac{2pm}{N-1}\right). \tag{6}$$

Then after windowing (multiplied by Hamming window), the speech signal is converted into $\cos(2pm/N - 1)$. The value of a is between 0 and 1. If the value of a is different, the corresponding Hamming window will also be different. Generally speaking, the larger the value of a, the flatter the shape of the Hamming window. The shape change of the Hamming window under different values is shown in Figure 7.

As shown in Figure 7, training is actually the process of extracting a common template feature from multiple input signals as training samples. Generally speaking, when there are more samples and the difference between samples is less than a critical value, the obtained template is the most reliable. That is, such a template best matches the actual standard value. The more reliable a template is, the higher the accuracy of template matching is. Template matching is one of the most primitive and basic pattern recognition methods. It studies where the pattern of a specific object is located in the image and then recognizes the object. This is a matching problem. It is the most basic and most commonly used matching method in image processing.

When performing template matching, the dynamic time warping algorithm makes the accumulated distance on the path as shown in formula (7):

$$D[T(n), R(m)] = \sum_{i=1}^{p} (t_i - r_i)^2. \tag{7}$$

Among them, T represents the input template, R represents the reference template, t and r are the feature coefficients of the frames corresponding to the input template and the reference template, respectively, and P is the order of the feature coefficients.

The distance matrix can be obtained by performing Euclidean operation on the corresponding frame of the input template and the reference template, and then combined with the defined forward direction, that is, the local decision function, the accumulated distance matrix can be obtained. Euclidean space is a special metric space that plays a role in the definition of manifolds that include Euclidean and non-Euclidean geometries.

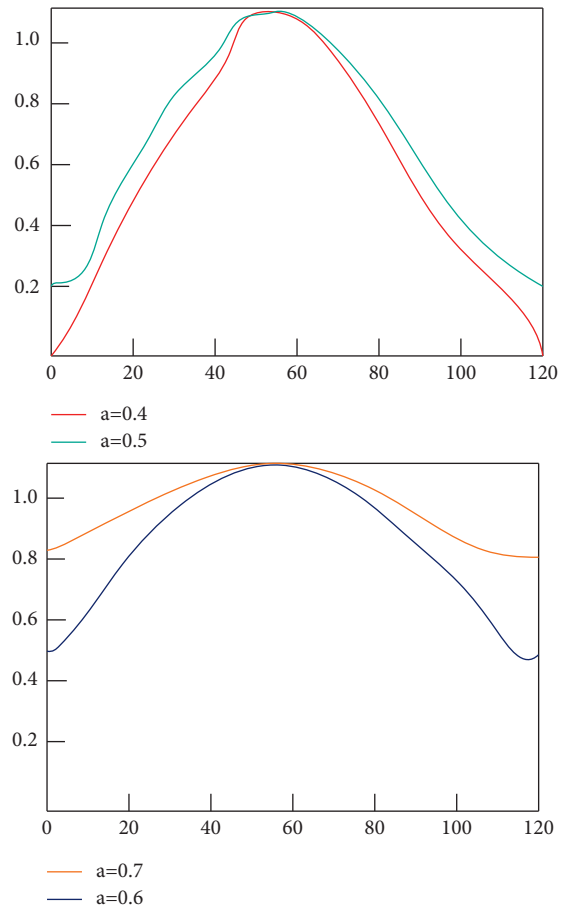

Figure 7: Different a values correspond to different Hamming windows.

3.3. Embedded Speech Recognition Based on Kalman Filter. Kalman filtering is a filtering method that uses the minimum mean square error prediction error as the criterion to perform linear unbiased estimation of speech signals from noise-contaminated observation signals. Kalman filtering is a method of using a linear system of state equations. It is an algorithm that optimally estimates the system state through the system input and output observation data. Since the observation data includes the influence of noise and interference in the system, the optimal estimation can also be regarded as a filtering process. The speech signal can be represented as an all-pole linear output self-recursive process driven by white noise. Under the assumption of short-term stationary, a pure speech signal can establish the L-order AR model, that is, formula (8):

$$s(n) = \sum_{i=1}^{L} a_i n \times s(n-i) + \omega(n), \tag{8}$$

where $a_i n$ is the linear prediction coefficient, $\omega(n)$ is the mean value of 0, the variance is δ^2 white Gaussian noise, and $S(n)$ is the clean speech signal. Based on the analysis, the mathematical model of the speech signal $b(n)$ with additive noise can be described as formula (9):

$$b(n) = s(n) + v(n), \tag{9}$$

where $s(n)$ is the clean speech signal, $v(n)$ is the additive background noise with mean 0 and variance δ^2, and $s(n)$ and $v(n)$ are uncorrelated. In theoretical analysis, the variance δ^2 must be known, but in practical applications, δ^2 is unknown, and the usual practice is to use the first frame of the speech signal to estimate. The improved Kalman fast filtering algorithm is shown in formula (10):

$$K(n) = \frac{R_s(n)}{(R_s(n) + R_v(n))}. \tag{10}$$

Since the judgment threshold is inferred from the observation data, there is a certain error, and the forgetting factor can be used to reduce the error. Then, the judgment threshold is updated as in formula (11):

$$U = (1-d) \times U + d \times \mathrm{P}_v(n). \tag{11}$$

The forgetting factor is a weighting factor in the error measure function. The purpose of introducing it is to give different weights to the original data and the new data so that the algorithm has the ability to respond quickly to the change of the input process characteristics. Here, the characteristic of the forgetting factor can also be used to reduce the error. When the background noise changes from large to small, the determination threshold U can be changed from large to small.

Two signal-to-noise ratios need to be calculated for comparison. The signal-to-noise ratio of a current speech frame is such as formula (12):

$$SNRI(n) = 10 \times \log_{10}\left(\frac{\delta_r{}^2(n) - \delta_r{}^2(n)}{\delta_r{}^2(n)}\right). \tag{12}$$

The other is the signal-to-noise of the entire speech signal such as formula (13):

$$\mathrm{SNRI}(n) = 10 \times \log_{10}\left(\frac{\delta_s{}^2(n) - \delta_s{}^2(n)}{\delta_s{}^2(n)}\right). \tag{13}$$

When $\mathrm{SNR1}(n)$ is less than or equal to $\mathrm{SNR0}(n)$ or $\mathrm{SNR}(n)$ is less than 0, people can think that this speech frame is very likely to be noise.

3.4. Hidden Markov Algorithms. As a statistical model, Hidden Markov Model (HMM) originated in the 1980s. Hidden Markov Models can describe not only static random processes but also dynamic transitions between these random processes. In this way, a speech signal can be better described. Hidden Markov Model, as a statistical analysis model, was founded in the 1970s. It was spread and developed in the 1980s, and it has become an important direction of signal processing. It has been successfully used in speech recognition, behavior recognition, text recognition, and fault diagnosis. Therefore, compared to traditional template-based models, Hidden Markov Models are more widely cited in today's speech processing field. The HMM model is composed of multiple states. With the change of time, each state may change and exist in one state. Each

observation vector has an output probability corresponding to a different state. The HMM model is shown in Figure 8.

As shown in Figure 8, compared with other current recognition algorithms, the advantage of the HMM method is that it is easy to use other pieces of information such as speech and language models. It has the unique advantage of continuous speech recognition. However, the downside is the complex computation and long training sequence, namely, formula (14):

$$A = \begin{pmatrix} a_{11} & a_{1n} \\ a_{n1} & a_{nn} \end{pmatrix}, \tag{14}$$

where a_{nn} is the transition probability when transitioning from state S_i to state S_j. The set of initial state probabilities of the system $\pi = [\pi_t]$, π_t represents the probability that the initial state is S_i, that is, formula (15):

$$\pi_t = p[S_1 = S_i], \ (1 \le i \le N). \tag{15}$$

Therefore, a model can be denoted as an octet model, and using this model, a sequence of observations can be generated.

The excitation source of the excitation model includes silence and sound, and the silent signal is the output of a linear system excited by a series of white noises. The voiced signal is generated by a periodic pulse generator, and the period depends on the fundamental frequency and the sampling frequency. The transfer function refers to the ratio of the Laplace transform of the linear system response to the Laplace transform of the excitation under zero initial conditions. Its transfer function is formula (16):

$$H_v(z) = G(z)V(z)R(z). \tag{16}$$

Among them, $G(z)$ is the transfer function of the glottal pulse, $V(z)$ is the transfer function of the vocal tract model generator, and $R(z)$ is the transfer function of the radiation model.

The glottal vein is a term used in linguistic research to describe the effect of the manipulation of the vocal folds on the quality of the voice during speech. From a mechanical point of view, the glottal pulse is generated by the flap of tissue in the vocal fold area and its gap, and it is collectively referred to as the glottis. In order to make the excitation signal of the voiced sound have the actual waveform of the glottal pulse, it is necessary to pass a glottal pulse model filter, which is transformed into formula (17):

$$G(z) = \frac{1}{\left(1 - g_1 z^{-2}\right)\left(-g_2 z^{-2}\right)}. \tag{17}$$

Among them, g_1 and g_2 are very close, so the unvoiced signal can be simulated as random white noise. $V(z)$ in the channel model is the channel transfer function, and its expression is formula (18):

$$V(z) = \frac{1}{1 - \sum_{k=1}^{N} a_k z^{-k}}. \tag{18}$$

In the radiation model is a first-order high-pass filter whose expression is formula (19):

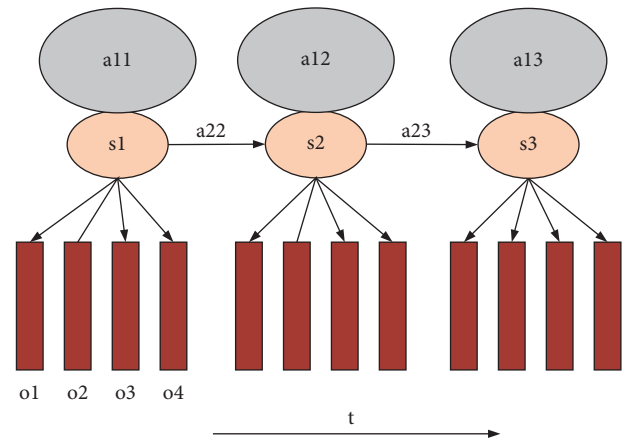

Figure 8: Relationship between HMM and speech parameters.

$$R(z) = R_0\left(1 - z^{-1}\right). \tag{19}$$

Voice signal is a kind of data with a large capacity. Under the premise that both identification and storage are calculated locally, the hardware resources of the embedded system are required to be configured relatively high, such as processor chip specifications, memory capacity, and peripheral circuit interface. As an analog signal carrying specific information, voice has become an important means of obtaining and disseminating information in people's social life. The purpose of speech signal processing is to extract effective speech information in a complex speech environment. The impact of environmental interference on the signal in the process of speech transmission cannot be underestimated, so the antinoise capability of speech signal processing has become an important research direction.

Today, many users enrich their lives through voice technology, using voice technology to command computers. It converts text into voice and reads aloud. However, the computer still needs a lot of training to recognize the user's speech. Aside from the influence of the speaker itself, the most important factor is ambient noise. In noisy public places, the human ear can automatically notice sound sources that require attention. However, the electronic device does not have this self-filtering function and cannot identify the effective information of the audio source. Currently, the best way to use speech recognition technology in a noisy environment is of course with an antinoise microphone, but that is not possible for most users. If an antinoise microphone is installed in the device, that will add significantly to the cost. Therefore, how to overcome this speech recognition problem is still a difficult task.

3.5. Cultivation of Humanistic Spirit and Implementation in Teaching. In modern academic circles, the spirit of humanism is formed through introspection and perception of the heart that depends on the foundations of language, literature, history, philosophy, music, art, and so on. It includes morals, feelings, attitudes, values, freedom, self-awareness, and social laws combined with real-life situations. It defines it as criticism, transcendence, judgment, and

reflection on the meaning and value of life. Humanity is a goal based on the full realization of life and full free development. It is a cultural spirit and life norm that combines the principles of ultimate concern and realistic concern for the value of life.

In the new century, China promotes innovative education in an all-round way, insists on taking quality education as the core, and insists on taking moral education and "learning to be a man" as the guiding ideology of quality education. High-quality educational content includes knowledge, ability, ideology and morality, and healthy personality. Its core is to let the people who receive education grow up healthily and harmoniously and attaches great importance to students' learning "people-oriented." The cultivation of humanistic spirit is regarded as the central content of humanistic education. The characteristics of the humanistic spirit are shown in Figure 9.

As shown in Figure 9, the modern humanistic spirit can be said to be a free humanistic spirit. It is a human consciousness that respects human value and dignity, safeguards human rights, and realizes human goals and ideals. But this free humanistic spirit must be built on an orderly humanistic platform, and it is a rule that everyone should follow. Therefore, the humanistic spirit emphasizes the free development of human interests and pursuits and the full development of human creativity. It emphasizes people's own improvement and continuous self-improvement, people's self-realization, and people's personality independence and subjectivity.

In general, education in China is mainly based on scientific guidance, which is conducive to the transmission and development of knowledge. But because it ignores cognition and emotion, it will bring a series of problems accordingly. As a language, especially as a foreign language, English is a very practical subject. But in educational practice, people still misunderstand it. Its practicality has not attracted enough attention, mainly reflected in the following aspects.

From the perspective of educational goals, modern education regards the cultivation of high-tech and high-intelligence talents as the ultimate educational goal. Therefore, foreign language education is often the same as physics, chemistry, and mathematics education, ignoring the accumulation of students' emotional experience.

From the perspective of teaching methods, because the importance of knowledge is overemphasized, the subjective initiative of students is ignored. The teaching method is simplified to the pure knowledge education method, and the monotonous teaching method will seriously weaken the students' enthusiasm for learning and make the students completely become the "filler" of knowledge.

Students lack a lot of language knowledge and practical ability. To make matters worse, many students lose interest and confidence in continuing their studies. It also lacks virtue, responsibility, and affection, which is the complete opposite of what is advocated for the human spirit. Therefore, we must actively promote the cultivation of humanitarian spirit and implement emotional education in English education.

4. Experiment and Analysis on the Effect of English Reading on the Cultivation of Humanistic Spirit

4.1. Experimental Analysis Based on Time Warped Template Matching. There are 5 training samples in this experiment, and the experiment is divided into external test (A template) and internal test (B template). They refer to untrained and trained recordings, respectively. The sampling frequency of these voice signals is 16 kHz, and the sampling size is 8 bits. This paper randomly selects 10 times from the same experimenter's training sample speech (i.e., a single sample) for matching test.

From the experimental data in Tables 2 and 3, it can be seen that, under the condition that other conditions remain unchanged, in general, the richer the speech signal participating in the training, the more accurate the template obtained so that the recognition accuracy is also relatively high.

Human society has entered the 21st century; with the economic globalization and the informatization of social life, the importance of English has become more and more significant. Many countries regard English education as an important part of basic education and place it in an important position. After more than ten years of English learning in primary and secondary schools, many students have only learned fragmented language knowledge without corresponding humanistic quality. They only have the basic knowledge of culture and no cultural background. Some have distinct personal views, but they do not have complete values and worldviews. The development trend of English and the percentage of English reading from 2011 to 2021 are shown in Figure 10.

As shown in Figure 10, economic globalization and informatization of social life have challenged traditional English education, and traditional English education has exposed many problems. Among them, the lack of humanistic spirit is a problem that cannot be ignored. At present, the tendency for examination-oriented education in many parts of China is still serious. As a pure examination-oriented tool, English subjects in senior high schools cannot give full play to the emotional education function of English subjects. If it only pays attention to the knowledge given in education and ignores the students' feelings, attitudes, personality, interests, and other nonknowledge factors, it can only cultivate a student who cannot develop in an all-round way.

4.2. Cultivation Strategies for Students' Humanistic Literacy in College English Reading

4.2.1. Combining with Information Technology. Language not only contains the historical and cultural background of a country but also contains the accumulation of the country's values, ways of thinking, way of life, and spiritual levels. Therefore, it is indispensable to infiltrate humanistic education in college English reading. Careful reading is an

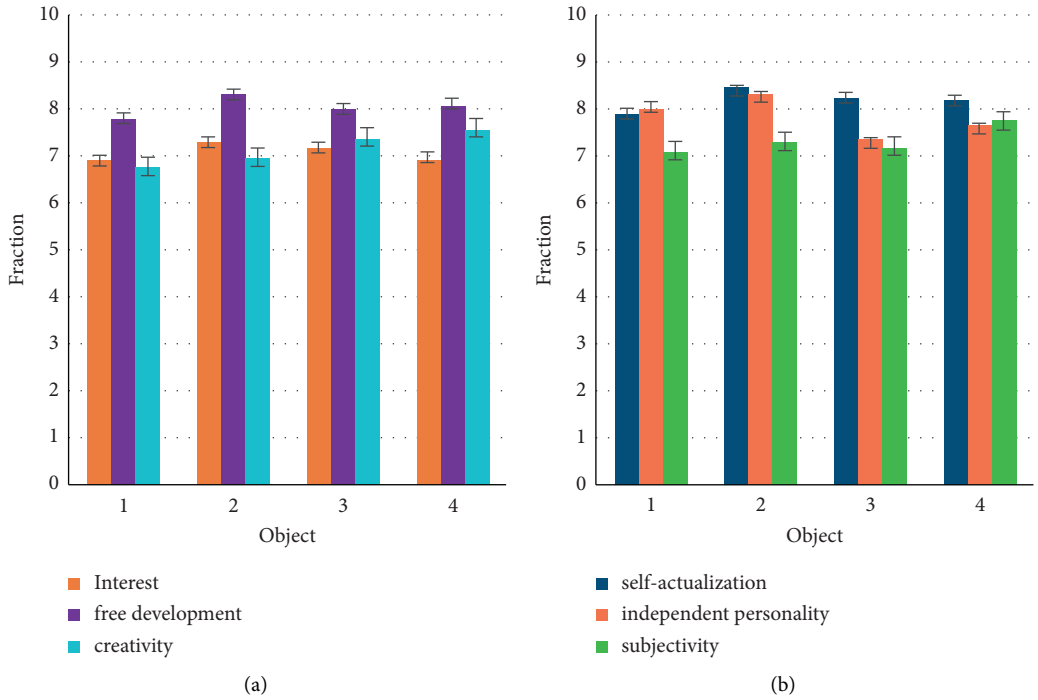

Figure 9: Characteristics of humanistic spirit.

Table 2: External test (A template) correct rate.

Experimenter	Template A correct times/total times	Total times	Correct rate (%)
a	10	10	100
b	10	10	100
c	9	10	90
d	9	10	90
e	7	10	70

Table 3: Internal test (B template) accuracy rate.

Experimenter	Template A correct times/total times	Total times	Correct rate (%)
a	20	20	100
b	18	20	90
c	16	20	80
d	17	20	85
e	18	20	90

important part of the reading curriculum in the classroom, allowing students to think deeply and improve cultural outcomes. Teachers guide students to pay attention to the deep meaning of words in context and guide students to explore the author's attitudes and perspectives. Then, this paper grasps the main structure of the article and the logical relationship between paragraphs from a macroperspective and mines the text theme. On the basis of a complete understanding of the language and structure of the text, students can communicate based on their background knowledge and the text, making it conflict.

4.2.2. Actively Changing Concepts and Improving Students' Initiative in English Reading. English reading is an important method to cultivate students' humanistic spirit. Only when the teacher recognizes its importance can students love English reading, improve the quality, and promote the internalization of students. In order for students to better understand the importance of English reading, teachers should first change their concepts. It regards English reading as an important part of English education and firmly believes that extracurricular reading will directly affect the effect of English learning.

Figure 10: English development trends and percentage of English reading, 2011–2021: (a) 2011–2021 English development trend and (b) 2011–2021 percentage of English reading.

4.2.3. Enriching the Content of Extracurricular Reading, Recommending Necessary Reading Lists, and Corresponding Reading Resources. It is necessary to practice instruction on students' reading outside the classroom. Teachers must include extracurricular readings each semester in their educational plan. It provides students with a specific reading list and selects English newspapers, magazines, online resources, original literary works, original rewriting, and other extracurricular reading materials for students. For extracurricular reading, it should let students divide into categories, or let students read some touching quotations, and so on. Second, students can arrange extracurricular reading content according to the actual situation and go to the library or bookstore to find their favorite books. In English education, teachers must pay great attention to the subject status of each student, give full play to their abilities, and improve the students' overall English proficiency.

5. Conclusion

The concept of humanistic education has a great influence on modern education, and the cultivation of humanistic spirit helps to improve the comprehensive quality of English majors. At present, the lack of humanistic spirit education is the real problem faced by college English majors. It seriously hinders the overall growth of students. Therefore, this paper mainly focuses on how to use the embedded system to improve the effect of English reading on the cultivation of humanistic spirit. This paper gives a detailed explanation of the embedded system and the theoretical knowledge of humanistic spirit cultivation so as to achieve the purpose of echoing the topic. In the method part, based on speech recognition technology, this paper proposes a speech recognition technology algorithm based on dynamic time warping (DTW) and embedded speech recognition based on the Kalman filter. As we all know, English reading is achieved by learning machines and various tools to achieve higher reading efficiency. Therefore, speech recognition has also become very important. This paper also summarizes the problems existing in the cultivation of humanistic spirit. In the experimental part, this paper analyzes the development trend of English in recent years and the proportion of English reading in English. This paper finds that people are paying more and more attention to English and paying more and more attention to English reading. At the end of the experiment, some suggestions are given for the cultivation of humanistic literacy of college English reading middle school students. All in all, it is very meaningful to improve the cultivation of humanistic spirit through English reading.

Data Availability

The experimental data used to support the findings of this study are available from the corresponding author upon request.

Conflicts of Interest

The authors declare that they have no conflicts of interest to report regarding the present study.

Acknowledgments

This work was supported by the General Project of Shanghai University of Finance and Economics Zhejiang College "Research on the Construction of College Students' Humanistic Spirit" (2017), Zhejiang Provincial Cultural and Tourism Research and Innovation Project (2020KYY009), and Humanities and Social Science Research Fund of Zhejiang University of Technology (GZ20511200009) "Research on the Construction of Emergency Language Service System in Public Events."

References

[1] J. Shao, L. Duan, Q. Wang, F. Zheng, and G. Ding, "Fabrication and high temperature characterization by MEMS embedded sensor," *Chinese Journal of Sensors and Actuators*, vol. 30, no. 9, pp. 1352–1358, 2017.

[2] M. Bouain, K. M. Li, K. M. A. Ali, D. Berdjag, N. Fakhfakh, and R. B. Atitallah, "An embedded multi-sensor data fusion design for vehicle perception tasks," *Journal of Communications*, vol. 13, no. 1, pp. 8–14, 2018.

[3] X. Duan, "The application of activity-based method in English reading teaching in senior high school," *Region-Educational Research and Reviews*, vol. 3, no. 2, pp. 60–64, 2021.

[4] J. Wu, "The research on the English reading teaching mode aiming at the improvement of thinking quality," *Region-Educational Research and Reviews*, vol. 3, no. 2, pp. 40–43, 2021.

[5] Q. Zhou, "The application of TBLT to English reading teaching in junior high school," *Region - Educational Research and Reviews*, vol. 3, no. 2, pp. 52–55, 2021.

[6] I. Munandar and S. Srimurni, "Directed reading activity (dra) application in English reading comprehension classroom," *Jurnal As-Salam*, vol. 5, no. 1, pp. 90–100, 2021.

[7] S. Alenezi, "Investigating Saudi EFL students' knowledge and beliefs related to English reading comprehension," *Arab World English Journal*, vol. 12, no. 1, pp. 339–356, 2021.

[8] D. Junior, J. M. Vianna, H. Oliveira, E. F. Coelho, and F. Z. Werneck, "Talent development in basketball: a perspective from Brazilian coaches," *Revista de Psicologia del Deporte*, vol. 30, no. 2, pp. 165–173, 2021.

[9] J. Mutanga, G. Kaisara, K. Yakobi, and S. O. Atiku, "Exploring push and pull factors for talent development and retention: implications for practice," *Development and Learning in Organizations*, vol. 35, no. 3, pp. 1–3, 2021.

[10] S. Yao, "The cultivation of students' humanistic quality in college English teaching," *Journal of Hubei University of Science and Technology*, vol. 35, no. 4, pp. 84–86, 2015.

[11] L. Pylvs and P. Nokelainen, "Finnish WorldSkills achievers' vocational talent development and school-to-work pathways," *International Journal for Research in Vocational Education and Training*, vol. 4, no. 2, pp. 95–116, 2017.

[12] T. Duberman and P. Erdahl, "Applying industry talent development best practices to advance your board: lessons learned from industry to accelerate board performance," *Board Leadership*, vol. 2021, no. 176, pp. 4–8, 2021.

[13] D. Z. Qin and J. R. Qin, "A study of STEAM interdisciplinary integration mode from the perspective of key competencies," *Theory and Practice of Education*, vol. 38, no. 22, pp. 52–56, 2018.

[14] Z. Ahmad, "The effect of teacher attitudes on students' English reading proficiency," *Shanlax International Journal of English*, vol. 8, no. 4, pp. 25–34, 2020.

[15] M. Haqiqiyah, "The predictability of English reading skill from Indonesian reading skill and English knowledge at students of sman 1 pademawu-pamekasan," *Al-Insyiroh: Jurnal Studi Keislaman*, vol. 6, no. 2, pp. 1–19, 2020.

[16] F. Li and X. Li, "On the practice of college English reading and writing course from the perspective of POA theory," *Open Journal of Modern Linguistics*, vol. 10, no. 5, pp. 560–568, 2020.

[17] Y. Zhang, "Developing EFL students' critical thinking competence in English reading class," *Creative Education*, vol. 11, no. 7, pp. 1145–1151, 2020.

[18] Y. Yue, "Integrating PAD class to college English reading teaching," *Open Access Library Journal*, vol. 08, no. 6, pp. 1–8, 2021.

[19] J.-Y. Baek, K. H. Rha, and K.-H. Rha, "Analyzing the effectiveness of a film-based class in a college setting: how can a language-culture integrated English reading class be implemented," *Foreign Languages Education*, vol. 28, no. 1, pp. 123–143, 2021.

[20] D. R. Bolla, J. J. Jijesh, M. S. Pramod, and Shivashankar, "Real-time data fusion applications in embedded sensor network using TATAS," *Indian Journal of Science and Technology*, vol. 10, no. 13, pp. 1–7, 2017.

[21] D. K. Choi, Y. U. Lim, and S. H. Lee, "Fabrication and evaluation of a drag-force type dual flow sensor with an embedded temperature sensor," *Microsystem Technologies*, vol. 24, no. 4, pp. 1975–1985, 2018.

Hindawi
Scientific Programming
Volume 2022, Article ID 8121161, 12 pages
https://doi.org/10.1155/2022/8121161

Research Article

Application of Internet of Things Technology in Student Management Evaluation System

Jiaming Zhu,[1] **Zhi Li**,[2] **Jing Fu**,[3] **Fangcheng He**,[4] **Xiaoling Mou**,[1] **and Pengjv Wu**[5]

[1]*School of Foreign Languages and Literatures, Chongqing University of Education, Chongqing 400065, China*
[2]*School of Artificial Intelligence, Chongqing University of Education, Chongqing 400065, China*
[3]*School of Mathematics Physics and Big Data, Chongqing University of Science and Technology, Chongqing 400127, China*
[4]*Students Affairs Office, Chongqing University of Education, Chongqing 400065, China*
[5]*College of Arts, Chongqing Three Gorges University, Chongqing 403428, China*

Correspondence should be addressed to Jiaming Zhu; zhujm@cque.edu.cn

Received 19 March 2022; Revised 1 May 2022; Accepted 9 May 2022; Published 23 May 2022

Academic Editor: Muhammad Usman

In modern society, the rapid development of the knowledge economy makes education become the core resource of a country's economic and social modernization development. Under this circumstance, student management has been paid more and more attention by people. This paper aims to study how to use the internet of things technology to study the student management evaluation system. This paper proposes a data mining algorithm based on the internet of things technology and proposes a decision tree method and an association rule algorithm based on the data mining algorithm. The experimental results of this paper show that the student growth rate in 2018 increased from 10% to 33% in 2019 and then from 21% in 2020 to 35% in 2021. It can be seen that with the development of the economy, the enrollment rate is also increasing, and the number of people who can go to college has increased rapidly. This also increases the difficulty of student management, making teachers' work more arduous, and the complexity of the amount of information leads to a drop in the efficiency of student management. However, the student management evaluation system based on the internet of things technology is beneficial to solving this problem.

1. Introduction

Student management occupies a large proportion in school management, and many schools in today's society still use manual methods for student management. However, as schools continue to expand in size and the number of students continues to increase, manual methods that are inefficient and prone to errors are no longer suitable for the needs of day-to-day school management. Designing and developing a student management system with computer technology and database can realize student management, and automation is an urgent necessity for the student management department. The internet of things technology has originated in the media field and is the third revolution of the information technology industry. The internet of things refers to the connection of any object with the network through the information sensing equipment and according to the agreed protocol, and the objects exchange and communicate information through the information dissemination medium to realize intelligent identification, positioning, tracking, supervision, and other functions.

At present, one of the important directions of student management informatization research is how to explore the potential knowledge in student data and fully explore the value of data in the system, so as to help decision-makers manage and adjust and finally achieve the purpose of cultivating talents in the new era with high efficiency and individuality. The association rule mining algorithm can find the correlation between students' performance, activity, practice, psychology, and other data from a large amount of data and reveal the problems existing in student training and teaching. By mining the results, students' growth can be predicted; the students can be scientifically evaluated; and the characteristics of different students can be fully considered. By mining the results, it is possible to predict the growth of students, conduct a scientific evaluation of

students, fully consider the characteristics of various students, and provide more personalized education.

The innovations of this paper are: (1) this paper introduces the theoretical knowledge of the internet of things technology and the student management evaluation system and uses the decision tree classification algorithm based on the internet of things technology to analyze the importance of the internet of things technology in the application of the student management evaluation system. (2) This paper expounds on the strategy tree classification algorithm and the tomographic analysis algorithm. Through experiments, it is found that the student management evaluation system based on the internet of things technology makes the work efficiency of student management higher.

2. Related Work

With the development of education in recent years, the management of students has become more and more difficult. Verma et al. found that internet of things (IoT) technology allows educators and managers to turn data into actionable insights, and educational organizations leverage solutions such as cloud computing on IoT platforms. Verma et al. proposed a five-layer framework to facilitate the automated assessment of student achievement based on the concept of intelligent computing, providing real-time perception and automatic analysis for the system. The five-layer framework proposed by Verma et al. has not been described, which makes the concept of the framework difficult to understand [1]. Ramirez-Noriega et al. found that assessing students' knowledge acquisition is the main task of intelligent tutoring system (ITS). They put forward a proposal to infer the knowledge level of students, gave the general structure of ITS, and proposed an evaluation module based on the Bayesian network; the evaluation module can infer many problems through the relationship of the Bayesian network. They mentioned that the module can find problems; then how to solve the problem is the most important [2]. Papa et al. found that from previous models and strategies used to study academic performance in college students, it is clear that none of them assess T-shaped degrees. The research they provides employs well-established models and strategies to show the monitoring of college students' first-year performance in response to the growing demand for professionals with this characteristic. They did not prove that their proposed strategy is mature and reliable [3]. Nizam found that the most important goal of colleges today is to increase student flexibility and productivity. He mainly discusses the impact of the student exchange process (SEP) on the campus management system (CMS), and for the final impact, he recommends a flexible system design to enhance educational benefits between universities. He makes suggestions, but what exactly is the specific suggestion and is the design real? [4]. He et al. found deep learning to be a promising approach to extracting accurate information from raw sensor data from IoT devices deployed in complex environments. Therefore, they first introduced deep learning for IoT into the edge computing environment. A novel offloading strategy is also designed, and the evaluation results show that this method outperforms other optimization solutions in IoT deep learning. Why He et al. bring deep learning into the edge computing environment is because the connection between the two should be expounded [5]. Hopkins and Hawking find that with the advancement of communication technology, global corporate activities continue to evolve, and many companies are implementing global information systems in order to improve their global operations. In this regard, however, companies face many complexities when implementing them. Although he sees many difficulties in implementing a global system, he does not specify the specific manifestations of the complexity [6].

3. Data Mining Algorithm Based on IoT Technology

3.1. Development of Data Mining. Human beings have more data; human beings have entered the era of big data; and the problem of information explosion has also been exposed. At the same time, computer technology has also made rapid progress [7]. In such an environment, data mining technology emerged. It is a generalized data technology, which has been widely used and developed in many fields and integrates related technologies in many fields. Data mining technology is a technology that can "mine" the knowledge rules that are valuable to users from a large amount of data [8]. Considering the data itself, usually, data mining needs eight steps, including data cleaning, data transformation, data mining implementation process, pattern evaluation, knowledge representation, and so on. The process of data mining is shown in Figure 1.

As shown in Figure 1, the management business of colleges and universities has entered the digital information age from the previous manual mode. Student management is an important part of management in colleges and universities [9]. Students use the information management system of a comprehensive professional school to improve their management level. In recent years, the number of students has increased dramatically with the heightened attention to education. The difficulty of student management has also increased greatly. The growth trend of students in recent years is shown in Figure 2.

As shown in Figure 2, the growth trend of students is getting faster and faster, the student management work lacks a sound management model, and the teacher cannot do a good job in the management work driven by the management model. At the same time, the teacher's understanding of the students' ideological and living conditions is not thorough enough, which affects the management efficiency. And one of the important techniques of data mining is association rule mining. The application of association rule mining technology to the student management of colleges and universities can help schools obtain information hidden in student data and then become an important way for schools to obtain more valuable information [10]. IoT technology is shown in Figure 3.

As shown in Figure 3, association rule mining technology provides more scientific and accurate evaluation

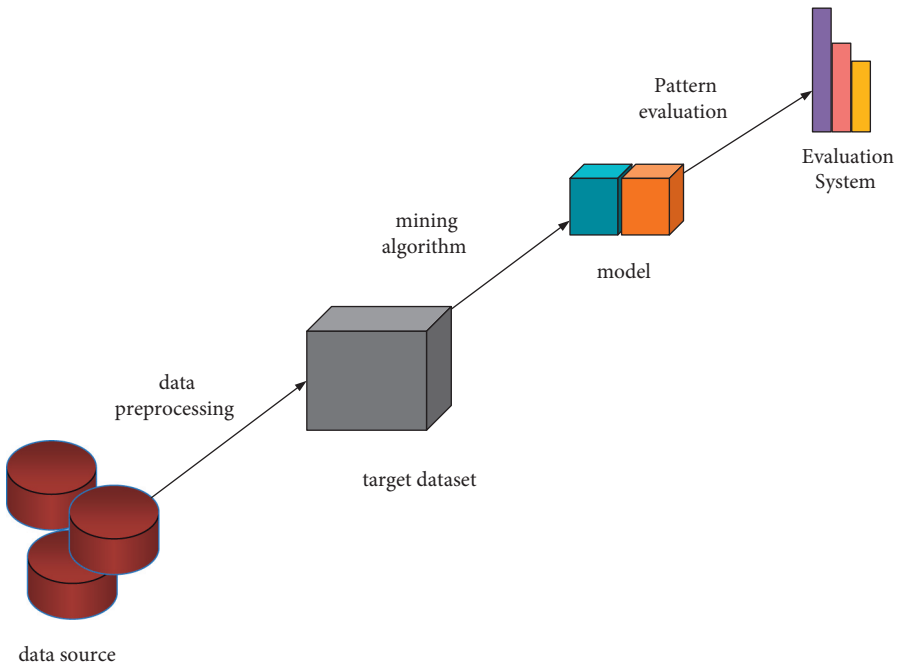

Figure 1: The process of data mining.

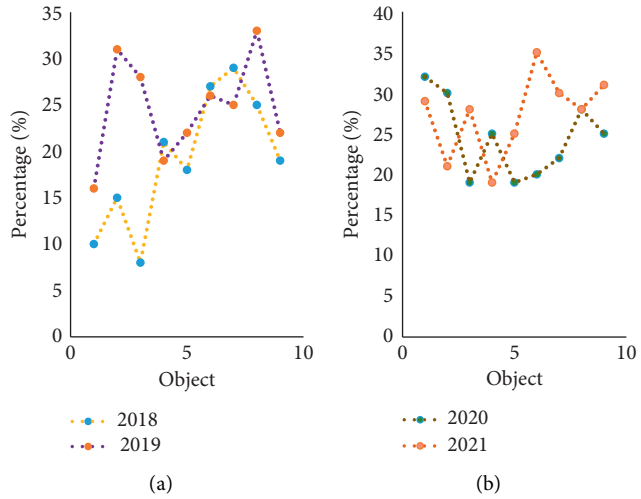

Figure 2: Student growth trends 2018–2021: (a) 2018–2019 student growth trends and (b) 2020–2021 student growth trends.

results, provides positive guidance, and finally achieves efficient and personalized talent training and improves the quality of talent training [11].

The precise definition of the internet of things has not yet been formed. It is generally believed that the internet of things is a network that connects items with the Internet through various sensing devices to exchange and communicate information to achieve intelligent identification, positioning, tracking, monitoring, and management [12]. The application areas of the internet of things are shown in Figure 4.

As shown in Figure 4, with the development of colleges, the reform of student management has gradually deepened, and the learning environment and living environment on campus are getting better and better, but the relationship between students and between students and schools is becoming more and more complicated. Daily life management and education management are also becoming more and more diverse, and all IoT technologies are playing an increasingly important role in student management [13]. Through the internet of things technology, students' psychological, language, action, and other information can be obtained in a short time. This is very helpful in strengthening the management of a small number of students, and it also plays a big role in dealing with some emergencies.

3.2. Decision Tree Classification Algorithm Based on Data Mining. The decision tree algorithm is the most concerned

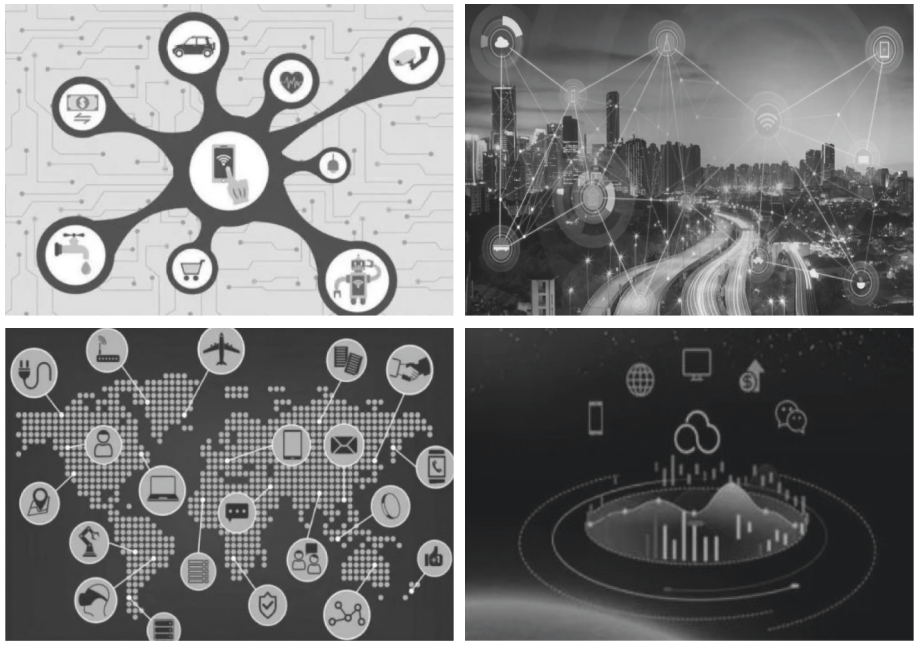

Figure 3: IoT technology.

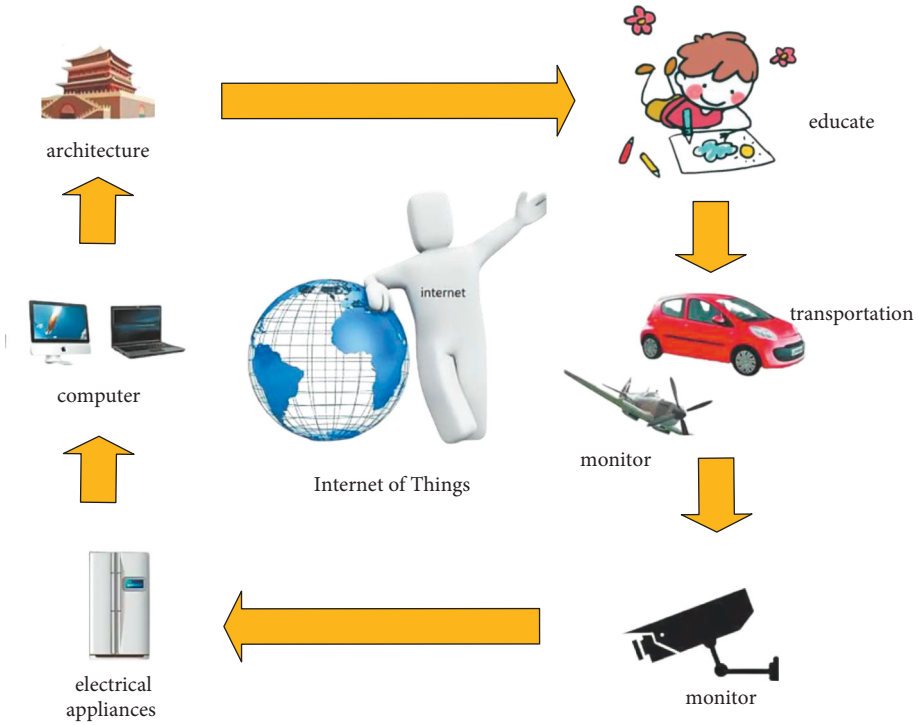

Figure 4: Application areas of IoT.

classification algorithm in data mining. The reason why this algorithm is highly valued in the fields of data mining, artificial intelligence, and machine learning is that the decision tree algorithm has many special advantages over other algorithms. The decision tree algorithm is easy to understand, and the mechanism is simple to explain. The decision tree algorithm can be used for small data sets, and the time complexity is small, which is the logarithm of the data points used to train the decision tree. Compared to other algorithms that intelligently analyze one type of variable, the decision tree algorithm can handle numbers and categories of data. The structure diagram of the decision tree algorithm is shown in Figure 5.

As shown in Figure 5, the first is that its structure is very simple and easy to understand, and the corresponding classification mode is also very easy to convert into

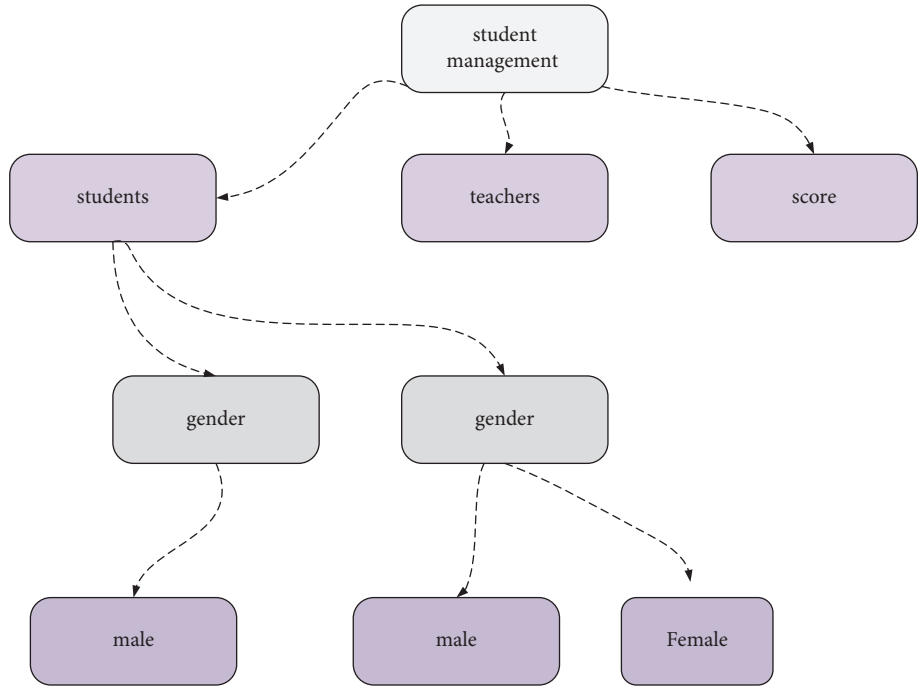

Figure 5: Decision tree algorithm structure diagram.

corresponding classification rules. Second, the decision tree algorithm has a high classification accuracy for the data [14].

3.2.1. ID3 Algorithm. ID3 algorithm is a greedy algorithm used to construct decision trees. The ID3 algorithm has originated from the concept learning system (CLS) and takes the decreasing speed of information entropy as the criterion for selecting test attributes. That is to say, at each node, the attribute with the highest information gain that has not been used for division is selected as the division criterion, and then this process is continued until the generated decision tree can perfectly classify the training samples. Before introducing the ID3 algorithm, first introduce the relevant knowledge of information theory to facilitate the understanding of the algorithm, as follows:

Information entropy represents the uncertainty of the whole information sent by the information source, which is defined as follows:

$$H(A) = -\sum_{i=1}^{r} p(x_i) I(x_i). \tag{1}$$

Conditional entropy $H(A|B)$ represents the uncertainty of the recipient of information B when it receives information A. If the A information is represented by x_i, the B information is represented by y_i, and $p(x_i|y_i)$ is the probability that A is x_i when B is y_i; then the formula is

$$H(A|B) = -\sum_{i=1} p(x_i|y_i) \mathrm{Log}_2 p(x_i|y_i). \tag{2}$$

The average mutual information represents the magnitude of the signal A that the signal B can provide, and $I(A|B)$ is expressed as follows:

$$I(A|B) = H(A) - H(A|B). \tag{3}$$

The key to constructing a decision tree by the ID3 algorithm is the calculation of information gain. Information gain is defined as the difference between the original information demand and the new demand. In probability theory and information theory, information gain is asymmetric and used to measure the difference between two probability distributions P and Q. The calculation process is as follows:

The desired information needed to classify groups in D, that is, the information entropy of D, is

$$\mathrm{Info}(D) = -\sum_{j=1}^{k} p\left(C_j\right) \mathrm{Log}_2 p\left(C_j\right). \tag{4}$$

The formula for calculating the category conditional entropy classified by attribute A is

$$\mathrm{Info}_A(D) = -\sum_{i=1}^{m} \frac{|D_i|}{|D|} \mathrm{Info}(D_i), \tag{5}$$

where $|D_i|/|D|$ acts as the weight of the ith partition and $\mathrm{Info}(D_i)$ is the expected information required for group classification in the subset D_i partitioned by the value x_i of attribute A.

The ID3 algorithm is suitable for the processing of discrete attribute values. In the case of discrete attributes, the hierarchical structure of the decision tree model is used to show that those attributes have a greater effect on the decision attributes [15].

3.2.2. Optimization of Association Rules for Decision Tree Algorithm. Judging from the existing decision tree

algorithms, most algorithm researches focus on the measurement of attribute selection or improve the pruning algorithm. However, in many cases, due to the influence of various factors, such as the redundancy of original data attributes, insufficient information, and so on, the constructed decision tree is always unsatisfactory [16]. The effect of the association rule algorithm on massive data mining is obvious. Using an association rule algorithm to mine knowledge is convenient and easy to understand. Therefore, the research on mining association rules algorithm is also a major field of attention of scholars. However, the number of association rules mined by many association rule algorithms is always astonishingly large, which is bound to be unfavorable to the mining results. Therefore, in order to construct new attributes through association rules, it is extremely important to select which rules to construct [17].

After the approximate exact rule algorithm generates a series of rules, the rule antecedents are integrated into new attributes and added to the original data set. In computer science and operations research, an approximation algorithm is an algorithm used to find approximate methods to solve optimization problems.

The value of the new attribute ABR_1 is as follows:

$$\mathrm{ABR}_1 = \begin{cases} 1, & if, X_1 = a_{11}, X_2 = a_{31}, X_3 = a_{31}, \\ 0, & \text{else.} \end{cases} \tag{6}$$

Obviously, the approximate exact rule mining algorithm generally produces more than one approximate exact rule, and the generated new attributes will also become many correspondingly, so if all of them are added to the original data set, it will inevitably cause data set attribute redundancy. To avoid this situation, each new attribute must be evaluated to determine whether it has any value for classification. In this paper, combining the idea of information gain, an evaluation criterion called "approximate information gain" is given [18].

First, take the candidate attribute ABR_i to be evaluated as the root node of a decision tree and calculate the information content of the root node as follows:

$$G_{\mathrm{root}} = -\sum_{j=1}^{n} \frac{n_j}{N} \mathrm{Log}_2 \frac{n_j}{N}. \tag{7}$$

When classifying the sample data with the attribute ABR_i to be evaluated, the number of data records with attribute $\mathrm{ABR}_i = 1$ is denoted as N_1, which is calculated by the following formula:

$$N_1 = N * \frac{\sup(R_i)}{\mathrm{conf}(R_i)}. \tag{8}$$

In the data record of attribute $\mathrm{ABR}_i = 1$, the number of records of category attribute $B = b_i$ is N_2, which is calculated as follows:

$$N_2 = N * \sup(R_i). \tag{9}$$

In the records with attribute $\mathrm{ABR}_i = 1$, the number of records with the value b_i of category attribute B is unknown. Because an approximate exact algorithm is used to generate approximate exact rules, the amount of information contained in this type of data is ignored here [19]. Therefore, the amount of information contained in the records that meet $\mathrm{ABR}_i = 1$ in the data set is

$$G_1 = \frac{N_1}{N} \left[-\frac{N_2}{N_1} \mathrm{Log}_2 \frac{N_2}{N_1} \right]. \tag{10}$$

3.2.3. C4.5 Algorithm and Improvement. C4.5 is a family of algorithms used in classification problems in machine learning and data mining. Its goal is supervised learning: given a data set, each tuple in it can be described by a set of attribute values, and each tuple belongs to one of the mutually exclusive categories. The goal of C4.5 is to learn to find a mapping from attribute values to categories, and this mapping can be used to classify new entities with unknown categories. In the decision tree C4.5 algorithm, the test condition for attribute selection in the decision tree model is the information gain rate, and the amount of classification information required for a specified data sample is given as follows:

$$\mathrm{Info}(D) = -\sum_{i=1}^{m} p_i \log_2(p_i), \tag{11}$$

where p_i is the proportion of C_i in the sample, which can generally be calculated by C_i/d.

On the basis of information gain, the information gain rate is developed. When the sample is divided based on the value of attribute A, $\mathrm{SplitInfo}_A(D)$ is the concept of entropy; entropy generally refers to a measure of the state of certain material systems; and the degree to which certain material system states may appear. It is also used by the social sciences as a metaphor for the degree of certain states of human society, such as

$$\mathrm{SplitInfo}_A(D) = -\sum_{j=1}^{v} p_j \log_2 p_j, \tag{12}$$

where p_j is the proportion of samples with the same value a_j on A, which can generally be calculated by d_j/d. Finally, the information gain rate formula of attribute A divided data set is obtained, such as

$$\mathrm{GainRatio}(A) = \frac{\mathrm{Info}(D) - \mathrm{Info}_A(D)}{\mathrm{SplitInfo}_A(D)}. \tag{13}$$

The gain rate of attribute A is defined as $\mathrm{GainRatio}(A)$ is as

$$\mathrm{GainRatio}(A) = \frac{\mathrm{Gain}(A)}{\mathrm{SplitInfo}_A(D)}. \tag{14}$$

After an in-depth study of the C4.5 algorithm, it is found that C4.5 does not handle the phenomenon of overfitting enough and sometimes fails to achieve satisfactory results in terms of accuracy [20, 21]. Therefore, this paper improves the decision tree algorithm. In order to reduce the information entropy of unimportant attributes, a balance coefficient is imported into the calculation process, and the precision of the generated decision tree model becomes higher.

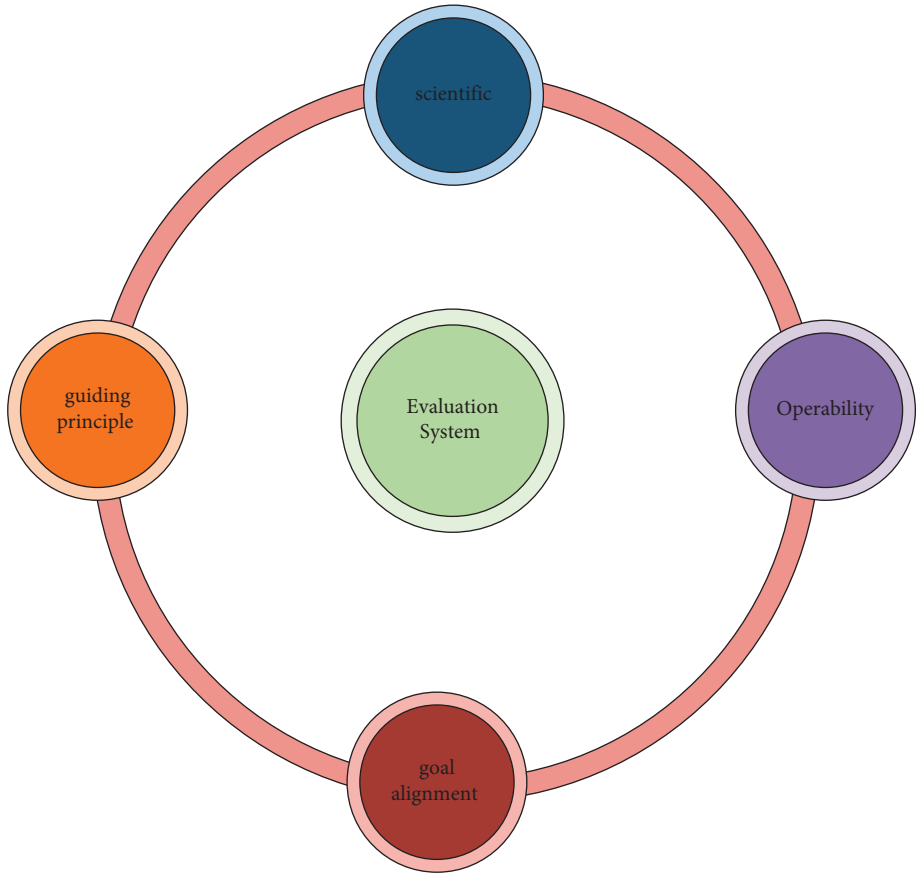

Figure 6: Construction principles of the evaluation system.

According to the characteristics of student evaluation, the balance coefficient ω is set for the evaluation index concerned. The larger ω is, the more interested the user is in this attribute. In order to study the equilibrium degree that should be achieved when the total reflux operation is used to complete a certain separation task, the concept of equilibrium degree coefficient is proposed. When the balance coefficient of all attributes is 0, the result is still the original information gain rate. After introducing the balance coefficient, the formula of the information gain rate becomes

$$\mathrm{Info}_{A\omega}(D) = -\sum_{i=1}^{m}\left(\frac{D_i}{D} + \omega\right)\mathrm{Info}(D_i). \tag{15}$$

By adding the balance coefficient, the improved algorithm can overcome the fact that the evaluation indicators that some users pay attention to are farther from the root node than the nonconcerned indicators in reality so that the decision tree implementation has a higher reference value in a specific environment.

3.3. Construction and Design of Student Evaluation System

3.3.1. Construction Principles of the Evaluation System. Because there are many factors involved in student evaluation and their importance is not the same, it is difficult to obtain an accurate and comprehensive evaluation of students' comprehensive quality. Therefore, the key to constructing a student evaluation system is to reflect the characteristics of the quality of contemporary college students, and these characteristics can just reflect the students' specialties and abilities in all aspects. The purpose of student evaluation is the guiding ideology and purpose of the whole implementation process, which determines the development direction of student evaluation and the final goal to be achieved. At the same time, when building a student evaluation system, the following principles need to be followed, as shown in Figure 6.

The principle of scientificity: as shown in Figure 6, student evaluation of students as a practical activity for judging the quality of students should be guided and restricted by educational scientific theory, and the evaluation system is a concrete manifestation of the guiding and restrictive role. The formulation of the evaluation system not only reflects the objective laws of student education but also follows the laws of talent requirements.

The principle of independence: it is the basic requirement for formulating the index system. There are many factors in the comprehensive quality of college students, each of which is relatively independent, which can reflect the information of all aspects of the students.

The principle of goal consistency: it means that the designed evaluation index must be consistent with the evaluation goal, and the competition index cannot be

configured on the same project. The principle of consistency includes the consistency of calculation methods, space-time boundaries, and measurement units.

3.3.2. Steps of Analytic Hierarchy Process

Analytic hierarchy process (AHP) refers to a decision-making method that decomposes the elements that are always related to decision-making into goals, criteria, programs, and other levels and then conducts qualitative and quantitative analysis on this basis. After determining the evaluation indicators of the student evaluation system, people need to determine the relative weights of each indicator. The relevant methods include empirical judgment, Delphi, and AHP. Because AHP has the characteristics of convenient calculation and concise, practical, and rigorous mathematical theory, this paper adopts AHP to determine the weight of the index.

The construction of the judgment matrix is an important step of the AHP. Experts compare all the indicators at the same level, judge their relative importance according to the scaling method, and quantify the judgment results to form the judgment matrix. In order to quantify the judgment result, the calibration method is usually used. After the comparison and quantization are completed, the judgment matrix of the following form can be obtained as follows:

$$X = \begin{bmatrix} x_{11} & x_{12} & x_{1n} \\ x_{21} & x_{22} & x_{2n} \\ x_{n1} & x_{n1} & x_{nm} \end{bmatrix}. \tag{16}$$

To calculate the weights, the judgment matrix needs to be operated and normalized, and there are two common methods: the sum-product method and the square root method. Since the sum-product method is simple to calculate and has sufficient accuracy, this paper adopts the sum-product method to calculate the weight; when using the AHP to calculate the weights of indicators at all levels, the sum-product method is used to find the maximum eigenroot and eigenvector; and the calculation process is divided into the following three steps:

The judgment matrix is normalized, that is, divided by the sum of each column, so that the sum of each column is 1; the formula is

$$y_{ij} = \frac{x_{ij}}{\sum_{i=1}^{n} x_{ij}}. \tag{17}$$

Summing over each row is

$$v_i = \sum_{j=1}^{n} y_{ij}. \tag{18}$$

Calculating the eigenvectors of the matrix, the weight vectors are calculated as follows:

$$w_i = \frac{v_i}{\sum_{i=1}^{n} v_i}. \tag{19}$$

Consistency test of the judgment matrix: generally speaking, if any two elements in the judgment matrix have the relationship of $x_{ij} = (x_{ik}/x_{kj})$, the judgment matrix has complete consistency.

3.3.2. Calculation Example of Index Weight. Solicited the opinions of the teachers, counselors, and relevant experts of the School of Computer Science on the weights of various indicators, used the Delphi method to analyze and weigh the weight opinions, and obtained the final judgment results. Delphi method, also called the expert investigation method, is essentially a feedback anonymous inquiry method. The general process is to sort out, summarize, and count after obtaining the opinions of experts on the problems to be predicted and then anonymously feed them back to the experts, then ask for opinions again, focus again, and feed back again, until getting a consensus, as shown in Table 1.

According to Table 1, the judgment matrix A can be obtained as follows:

$$X = \begin{bmatrix} 1 & 1/5 & 2 & 1/3 \\ 5 & 1 & 5 & 2 \\ 1/2 & 1/5 & 1 & 1/5 \\ 3 & 1/2 & 5 & 1 \end{bmatrix}. \tag{20}$$

Similarly, the judgment matrix and relative weight calculation method between other levels are the same as above. Through the calculation and integration test of AHP, the components of the complete evaluation index of college student management can be obtained.

3.4. Design and Implementation of Student Comprehensive Information Management Evaluation System. The comprehensive student information management system realizes the complete information management of students from enrollment to graduation, including student status, grades, rewards, and punishments. This system realizes data sharing with other systems under the digital campus platform, which effectively avoids the "information island."

A comprehensive student information management system based on B/S mode, which integrates accuracy, efficiency, security, and ease of use, is designed and developed. It solves a series of problems such as low efficiency, low accuracy, and inability to share data caused by the original manual management, so as to make student information management networked and improve the level of student management informatization.

The basic process of student management is as follows: after the freshmen are enrolled, the counselor will enter the student information, and the educational administration personnel will arrange the student number and register the student status after reviewing the student information. Every semester, teachers enter students' grades, and counselors enter students' reward and punishment information, generate a make-up exam plan and register student status and enrollment change information at the same time.

The student management system is very important for the decision-makers and managers of the school; it provides the users with sufficient information and quick query means.

Table 1: Calculation of indicator weights.

U	Ideological and moral quality	Knowledge ability quality	Physical and mental quality	Practical innovation quality
Ideological and moral quality	1	1/5	2	1/3
Knowledge ability quality	5	1	5	2
Physical and mental quality	1/2	1/5	1	1/5
Practical innovation quality	3	1/2	5	1

With the continuous improvement of science and technology, computer science is becoming more and more mature, and its powerful functions have been deeply recognized by people. It has entered various fields of human society and played an increasingly important role. According to the needs of different users for system functions, the system functions are divided into five modules: basic information, student status management, achievement management, graduation management, and data analysis, as shown in Figure 7.

As shown in Figure 7, the score management module includes score entry, score review, make-up test plan management, and score query statistics. Teachers are responsible for entering the test scores for the courses they are responsible for. Academic administrators are responsible for reviewing grades and generating make-up exam plans. Students can check their grades only after the academic administrator has reviewed the grades.

Academic administrators can count the average score and pass rate by class, and the data analysis module includes student information data mining. Using the student information data in the database, through the data mining algorithm, the comprehensive intelligent analysis of the students is realized. The workflow of the system is shown in Figure 8.

As shown in Figure 8, in order to restrict illegal users from using the system, users must perform identity identification when logging in, and legitimate users are allowed to log in. After successful login, they are transferred to the corresponding processing module according to different levels. It draws a more objective evaluation of the student management work of each department and makes a statistical analysis of each department and each assessment item.

There are two ways to log in to the system: one is through the unified login portal on the home page of the digital campus platform, and the other is to directly enter the network address of the system in the browser, which is realized through the login page. After the above two methods successfully log in to the system, if need to enter other business systems of the digital campus platform, do not need to enter the user name and password again, which realizes unified verification.

4. Experiment and Analysis of C4.5 Algorithm Comparison before and after Improvement

Before using the decision tree model, it is necessary to test the decision tree model; the purpose is to test the accuracy of

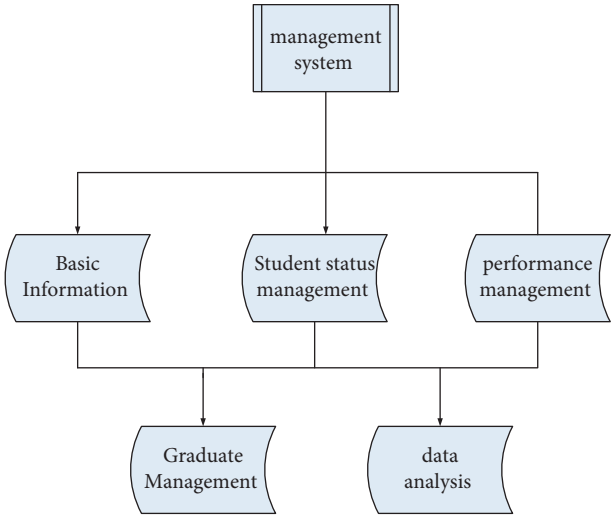

Figure 7: Functional module diagram of student integrated information management system.

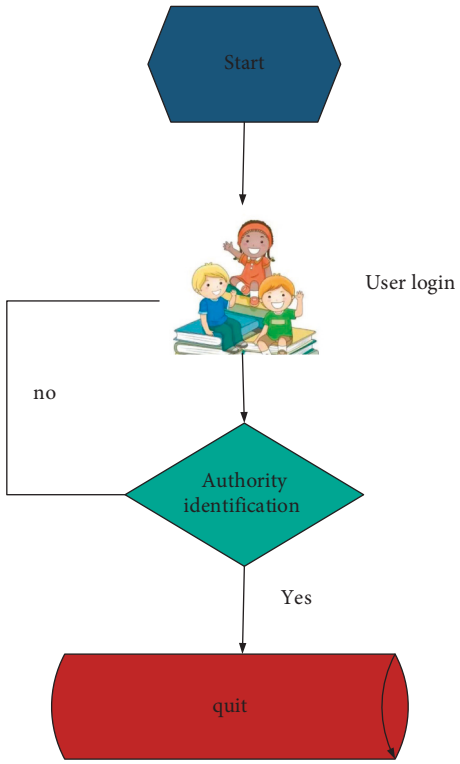

Figure 8: Workflow of the management system.

Table 2: Decision tree model tests.

Sample category	Number of samples	Number of correct identifications	Correct rate (%)	Average recognition rate (%)
Excellent	50	43	86	93.2
Good	100	95	95	93.2
Qualified	150	148	98.6	93.2

Table 3: Comparison of the classification results of the two algorithms.

Model	C4.5 algorithmic model	Improved decision tree algorithm model
Tree level	6	6
Number of leaf nodes	12	9
Leaf node sample proportion average	(18/12)/18∗100% = 8.3%	(15/9)/15∗100% = 10.7%

Table 4: Basic information of UCI data set.

Data set	Number of samples	Number of attributes	Number of categories
Annealing	50	8	4
Balance scale	40	3	2
Glass	30	7	6

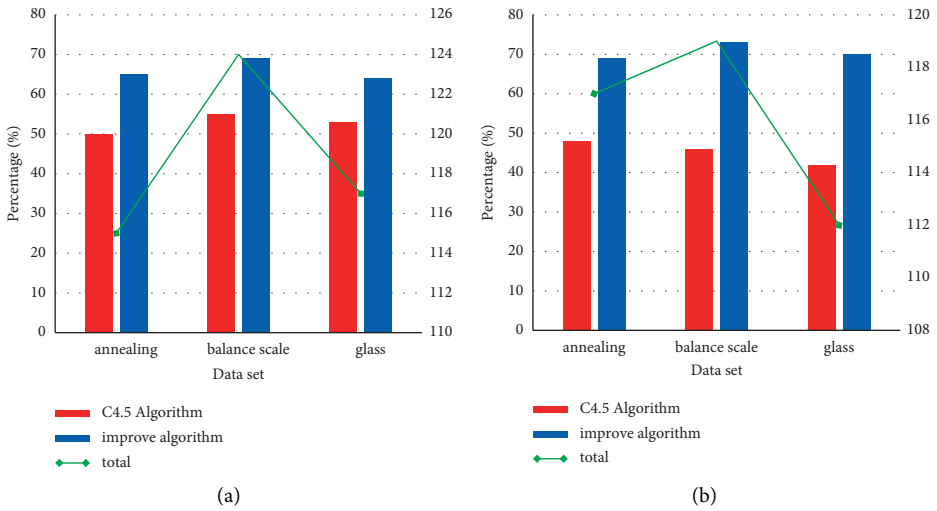

Figure 9: The accuracy of the C4.5 algorithm and the improved algorithm at different experimental stages: (a) the accuracy comparison between the C4.5 algorithm and the improved algorithm in the first five experiments and (b) the accuracy comparison between the C4.5 algorithm and the improved algorithm in the last five experiments.

the decision tree model, to judge whether the decision tree model is effective and whether it can obtain valuable results and apply it to practical work. In this example, the obtained decision tree model is verified with the test data set, and the detailed results are shown in Table 2.

It can be seen from Table 2 that the accuracy rates of the three categories of excellent, good, and qualified are 86%, 95%, and 98.6%, respectively, and the average recognition rate is 93.2%, and the obtained accuracy meets the actual requirements. It can be considered that the decision tree model is effective. In addition, with the increase in sample data, the correct recognition rate of the decision tree model will be further improved.

Using the improved C4.5 algorithm tree, the number of leaf nodes will be reduced, and the number of samples of some leaf nodes will also increase. By adopting the improved C4.5 algorithm, the classification results will be more accurate and reasonable, which is convenient for decision-makers to make correct decisions, as shown in Table 3.

As shown in Table 3, given that the selected sample data set is relatively small, in order to better verify the effect of the algorithm, people use the three data sets of annealing, balance scale, and glass in the UCI database for experimental verification. Table 4 gives the basic situation of the UCI data set.

As shown in Table 4, the execution efficiency of the decision tree model is very high, which is very suitable for the training set of data volume comparison. The decision tree model has very good scalability and can be easily combined with most databases to realize the processing of various data types.

This paper compares and analyzes the accuracy of the C4.5 algorithm and the improved algorithm in different experimental stages through experiments, as shown in Figure 9.

It can be seen from Figure 9 that the improved algorithm is significantly better than the C4.5 algorithm in the classification of the three data sets. It can be seen that the improved algorithm merges branches with relatively high entropy values, that is, merges those branches with little or no contribution to classification. This method effectively controls the generation of fragments and limits the occurrence of overfitting to a certain extent. After setting the balance coefficient, the entropy value of some attributes is reduced, which is beneficial to improving the accuracy of decision tree construction.

5. Conclusion

This paper uses the internet of things technology to automatically obtain student attendance information and realizes the digital task of the daily management of students according to the needs of student information management. The development of a student management evaluation system can reduce the intensity of teachers' daily management work and improve work efficiency. This paper has carried out rich discussions around the internet of things technology and the theoretical knowledge of the student management evaluation system. In the method part, based on the internet of things, an association rule mining algorithm and a decision tree algorithm are proposed, and experiments are carried out on the C4.5 algorithm. It is found that the improved C4.5 can improve the accuracy of decision tree classification, which is also conducive to mining students' information, so as to better manage and evaluate. The traditional student management evaluation system is based on manual work, which is very complex and has a large workload, but it makes the evaluation more accurate and fast. Therefore, this paper is very meaningful to study the student management evaluation system based on the internet of things technology.

Data Availability

No data were used to support this study.

Conflicts of Interest

The authors declare that there are no conflicts of interest.

References

[1] P. Verma, S. K. Sood, and S. Kalra, "Smart computing based student performance evaluation framework for engineering education," *Computer Applications in Engineering Education*, vol. 25, no. 6, pp. 977–991, 2017.

[2] A. Ramírez-Noriega, R. Juárez-Ramírez, and Y. Martínez-Ramírez, "Evaluation module based on bayesian networks to intelligent tutoring systems," *International Journal of Information Management*, vol. 37, no. 1, pp. 1488–1498, 2017.

[3] F. Papa, Castro V D, P. Becker, E. Marcos, and L Olsina, "Evaluation of Students' Performance on a T-Shaped Degree," *IEEE Transactions on Education*, vol. 64, pp. 1–10, 2021.

[4] A. Nizam, "Evaluation and improvement of the credit transfer models in the student exchange process," *The International Journal of Information and Learning Technology*, vol. 37, no. 1–2, pp. 1–13, 2019.

[5] L. He, K. Ota, and M. Dong, "Learning IoT in edge: deep learning for the Internet of Things with edge computing," *IEEE Network*, vol. 32, no. 1, pp. 96–101, 2018.

[6] J. Hopkins and P. Hawking, "Big data analytics and IoT in logistics: a case study," *International Journal of Logistics Management*, vol. 29, no. 6, p. 00, 2018.

[7] A. Molassiotis, W. Russell, J. Hughes, M. Breckons, M. Lloydwilliams, and J Richardson, "The effectiveness and cost-effectiveness of acupressure for the control and management of chemotherapy-related acute and delayed nausea," *Health Technol Assess*, vol. 17, pp. 1–114, 2018.

[8] G. Feng, M. Fan, and Y. Chen, "'Analysis and prediction of students' academic performance based on educational data mining," *IEEE Access*, vol. 10, no. 2, pp. 19558–19571, 2022.

[9] W. J. Hou, "Transformation of college students management methods in education," *Jiangsu Higher Education*, vol. 19, no. 9, pp. 107–110, 2019.

[10] K. Wen and Y. Fang, "Daily information management system for postgraduates to check in and out of the dormitory based on mobile edge computing," *Mobile Information Systems*, vol. 2021, no. 8, Article ID 5167395, 12 pages, 2021.

[11] A. R. Al-Ali, I. A. Zualkernan, M. Rashid, R. Gupta, and M Alikarar, "A smart home energy management system using IoT and big data analytics approach," *IEEE Transactions on Consumer Electronics*, vol. 63, pp. 426–434, 2018.

[12] Hammi M T, Hammi B, Bellot P, and Bellot P, "Serhrouchni A. Bubbles of Trust: a decentralized Blockchain-based authentication system for IoT," *Computers & Security*, vol. 78, pp. 126–142, 2018.

[13] N. Songsom, P. Nilsook, and P. Wannapiroon, "The synthesis of the student relationship management system using the Internet of Things to collect the digital footprint for higher education institutions," *International Journal of Online and Biomedical Engineering (iJOE)*, vol. 15, no. 06, pp. 99–112, 2019.

[14] F L Wu, X R Liu, Y D Wang, X L Li, and M Zhou, "Research on Evaluation Model of Hospital Informatization Level Based on Decision Tree Algorithm," *Security and Communication Networks*, vol. 2022, 9 pages, 2022.

[15] M. Ammar, G. Russello, and B. Crispo, "Internet of Things: a survey on the security of IoT frameworks," *Journal of Information Security and Applications*, vol. 38, no. FEB, pp. 8–27, 2018.

[16] C. Sisavath and L. Yu, "Design and implementation of security system for smart home based on IOT technology," *Procedia Computer Science*, vol. 183, no. 2, pp. 4–13, 2021.

[17] A. Abu-Saa, M. Al-Emran, and K. Shaalan, "Factors affecting students' performance in higher education: a systematic review of predictive data mining techniques," *Technology, Knowledge and Learning*, vol. 24, no. 4, pp. 567–598, 2019.

[18] A. Calma and C. Dickson-Deane, "The student as customer and quality in higher education," *International Journal of*

Educational Management, vol. 34, no. 8, pp. 1221–1235, 2020.

[19] F. Mcleay, A. Robson, and M. Yusoff, "New applications for importance-performance analysis (IPA) in higher education," *The Journal of Management Development*, vol. 36, no. 6, pp. 780–800, 2017.

[20] O. Palombi, F. Jouanot, N. Nziengam, B. Omidvar-Tehrani, M. C. Rousset, and A. Sanchez, "OntoSIDES: Ontology-based student progress monitoring on the national evaluation system of French Medical Schools," *Artificial Intelligence in Medicine*, vol. 96, pp. 59–67, 2019.

[21] B. Oguguo, F. A. Nannim, J. J. Agah, Y. Zheng, and Z. J. Chen, "Effect of learning management system on Student's performance in educational measurement and evaluation," *Education and Information Technologies*, vol. 26, pp. 1–13, 2021.

Hindawi
Scientific Programming
Volume 2022, Article ID 7727915, 11 pages
https://doi.org/10.1155/2022/7727915

Research Article

Application of Offensive and Defensive Linkage in a Virtual Football Game in the Internet of Things Decision-Making System

Hongtao Chen

School of Physical Education and Health, Yulin Normal University, Yulin 537000, Guangxi, China

Correspondence should be addressed to Hongtao Chen; 20040580@ylu.edu.cn

Received 8 March 2022; Revised 23 April 2022; Accepted 28 April 2022; Published 16 May 2022

Academic Editor: Muhammad Usman

Football is a popular sport in the world. Playing football can not only exercise the body and improve physical fitness but also learn some offensive and defensive skills. Football games are popular events all over the world. With the development of science and technology, virtual football games have also become popular. The virtual football game is an entertainment project that combines computer technology and virtual reality technology to analyze the attack and defense relationship in the virtual football game. It can understand the decision-making mechanism and apply the decision-making mechanism to the Internet of Things decision-making system, which will be able to make accurate and fast decisions like virtual players. This is also the content of this paper. This paper proposes a decision system based on virtual football, applies the system to the Internet of Things, and shows that the data of the system fluctuate within 1.5%, that is, the calculation accuracy of the system model is as high as 98.5%, with high calculation stability, high accuracy, and certain reliability.

1. Introduction

The Internet of Things is a comprehensive development technology formed by the integration of multiple disciplines, and its core technologies mainly include AI, sensor technology, radio frequency identification technology, and GPS navigation technology. The development of it and the intelligent system is mainly to simulate the human brain system, nervous system, information system, and behavior system. The improvement of artificial intelligence technology has produced the so-called virtual reality technology. As a realistic embodiment of imitating all human activities, VR has been paid much attention by researchers, and gradually started to study virtual football.

In order to integrate the Internet of Things and virtual football games, researchers need a new object research and development platform. In the process of better scientific research, it can also save research costs. The football game is now used as the research object carrier, mainly because of the inherent combat nature of the team, the individual players' football control ability, the physical confrontation in the game, and the frequent occurrence of emergencies in the game. In view of the characteristics, the virtual football simulation system is produced. The virtual football system mainly refers to the use of virtual reality technology through computer programming to realize the compilation of virtual football characteristics, the transmission of information between virtual players and the control of football in the game. It is a system that competes with the opposing team through cooperation in the virtual arena and wins the game. The application of Internet of Things technology and virtual reality technology in the simulation of football games has important research significance and practical value for the integration and innovation of the two technologies.

The decision-making system is a system studied by the decision theory, which generally consists of three parts: input, output, and internal structure. Its mathematical model describes the state evolution formula and output formula of the research object and reflects the goals required by decision makers. In this way, only after a reasonable objective function is formulated, it is possible to obtain the optimal decision. As a ubiquitous activity of human beings, decision-making is based on a specific object system (decision-making system). This decision-making system

generally includes basic elements such as decision makers, decision-making objects, decision-making information, decision-making theories and methods, and decision-making results. It is the core of the modern scientific decision-making system. It is necessary to study the Internet of Things decision-making system to take measures more efficiently, improve work efficiency, or reduce security incidents.

The innovation of this article lies in the integration of the overall optimization strategy and the individual optimization on the basis of the existing virtual human technology research and decision-making. Therefore, on the basis of the theoretical research, this paper abstracts the mathematical model of the simulation system of virtual reality technology in football games. The model can increase players' enthusiasm for the game and gain a detailed understanding of game strategy decisions. It can well reflect the situation of the real football game and better deal with the emergencies in the game.

2. Related Work

With the rapid development of the Internet of Things technology, many fields use its fast and efficient characteristics to make data decisions. Among them, Pegoraro et al. proposed and discussed a novel DSSE (i.e., adaptive distributed system state estimation) solution that relies on distributed decision points and leverages the cloud-based IoT paradigm. So far, DSSE procedures have used fixed settings independent of the actual value of the measurement accuracy, which is actually affected by the actual health of the network. The proposed DSSE is innovative with respect to previous literature studies in that it can adaptively use the updated accuracy of the measurement device. The information used in the estimation process and the execution rate will be updated as indicated by the appropriate local metrics. These metrics are designed to detect possible changes in the health of the distribution network. Specifically, the variation and variation trend of the rms voltage value obtained by the phasor measurement unit (PMU) is used to trigger the variation in DSSE. If a dynamic change is detected, the measurement data are sent to the DSSE at a higher rate for the estimation process to update the precision values to be considered in the estimation. The proposed system relies on a cloud-based IoT platform designed to integrate various measurement devices, such as PMUs and smart meters. The results obtained on the bus system demonstrate the effectiveness of the proposed method, which is very efficient both in the estimation process and in the use of communication resources [1]. Suryaprakash et al. proposed a human-machine interface through a distance-based fuzzy algorithm that utilizes the user's domain knowledge to construct rules through context awareness and a decision support system. The developed system is based on Linux OS, the algorithms are developed using python and the results are stored on the Internet via FHEM API for IoT application Raspberry Pi *B*+ toolbox and mobile SSH setup using Wi-Fi modem. Using this app, Suryaprakash et al. can be accessed through the home automation system by connecting to the IP address of the web server, and the voice assistance module can also help the patient to control the device through voice control. Suryaprakash et al. believed that this efficient algorithmic decision-making and voice-assisted automation can produce better results in the real world automating things [2]. Early warning systems (EWS) are core type of data-driven Internet of Things (IoT) systems for environmental disaster risk and impact management. Potential benefits of EWS using semantic types include the following: easier plug-and-play of sensors and data sources, simpler, richer, and more dynamic metadata-driven data analysis, and easier service interoperability and coordination. The challenges faced during the practical deployment of semantic EWS are the need for scalable time-sensitive data exchange and processing (especially involving heterogeneous data sources) and the need to be resilient to changing ICT resource constraints in crisis areas. Based on the multisemantic representation model, Poslad et al. proposed a novel IoT EWS system framework to deal with the challenges faced in the actual deployment process. Poslad et al. used heavyweight semantics for the top-level W3C web ontology language ontology model, which describes a multilayered knowledge base and semantic-driven decision support and workflow orchestration. This approach can be validated by identifying system-related metrics and case studies involving a high-level prototype system of semantic EWS (integrated with a deployed EWS infrastructure) [3]. Fukuda et al. attempted to develop a new type of prosthetic control system based on the Internet of Things (IoT) paradigm. The method proposed by Fukuda et al. was able to exploit not only information from the user's muscle activity and prosthetic hand state but also extensive data obtained from objects and objects in the environment. Sensor data can be static features, dynamic states, or even contextual information for operations. The fusion of these sensor data forms a rich information base to support multi-DOF and dexterous prosthetic hands. It is expected that more reliable reasoning and more autonomous control decisions can be developed using IoT-based control systems. The method proposed by Fukuda et al. is validated by a case study using an object with a simple sensor unit and a Myo armband for electromyography (EMG) signals [4]. Data are essential to help decision-making. If the authenticity of the data is low, the choice is less likely to be correct. The Internet of Things (IoT) inevitably involves mistakes, irregularities, flaws, tricks, and model guesswork in big data. Improving data accuracy is critical to addressing these difficulties. Revathy and Canessane summarized the key qualities and difficulties of IoT that affect data processing and decision-making. Revathy and Canessane audited scenarios for estimating and upgrading data accuracy and mining uncertain data streams. Revathy and Canessane makes five recommendations for advancing truly big IoT data surveys in the future. The recommendations relate to the heterogeneity and appropriateness of IoT data, fundamental leadership for autonomy, the idea of developing conscious and regional lean, and data cleansing and processing procedures for IoT. Moreover, Revathy and Canessane proposed edge gadgets and data management methods for protection, customization and security [5]. The Internet of Things (IoT)-

connected societies and systems represent a huge paradigm shift. Siryani et al. proposed a framework for decision support systems (DSS) operating in the IoT ecosystem. DSS leverages advanced analytics capabilities of smart meter (ESM) network communication quality data to improve cost forecasting for smart meter field operations and provide actionable decision recommendations on whether to dispatch technicians to customer locations to resolve ESM issues. He empirically evaluates models using datasets from commercial networks. Siryani et al. demonstrated the effectiveness of his method with a complete Bayesian network prediction model and compares it with three machine learning prediction model classifiers, that is, (1) naive Bayes; (2) random forest; (3) and decision tree. The results show that Siryani et al.'s method produces statistically significant estimates and that DSS will improve the cost efficiency of ESM network operation and maintenance [6]. The research and experiments of the scholars have provided a strong theoretical basis and authenticity for the decision-making of the Internet of Things, but further refinement is needed in the algorithm. This paper analyzes the algorithm based on the attack and defense connection in the virtual football game, and the proposed scheme has practical feasibility, accuracy, and efficiency.

3. Offensive and Defensive Decision-Making Scheme Based on a Virtual Football Game

3.1. Offensive and Defensive Linkages in Virtual Football Matches

3.1.1. Virtual Football Game. When people try to explain a concept, they usually define it with the help of another concept. It is believed that if this way of definition continues, some concepts will be reached eventually. These concepts are so simple and straightforward that there is no other meaning in logic. Observing the proposition that "football is a game", we will find that people's interpretation of football is very consistent with the process of explaining other concepts. If "0" means "football", "1" is "game", if the concept of "game" is still abstract. It must be further explained with the help of the concept of "2" or "3", so that the concept of "football" is more directly and concretely accepted by us. Since "football is a game", the next question is "what is a football game?". Obviously, it is very difficult to directly define the football game. This is largely due to the complexity, dynamics, and unpredictability of processes and outcomes of football games. However, it seems easier to form an intuitive understanding to explain the football game, which involves "what is in the football game". That is, it constitutes what people call a football game. According to different angles, the football game can be composed of two aspects. First of all, the individual player is the basic element of the game. Although the football game is centered on the ball, the decisive factor affecting the process and result of the game is the players on the field. From this point of view, the football game can be decomposed into two parts, the individual and the whole [7, 8]. There are many studies on these two parts. The research on individual ability involves the player's technique, physical fitness, and intelligence, while the overall research mainly covers three aspects: formation, play, and position analysis. The general formation for a football match is shown in Figure 1.

3.1.2. Importance of Offense and Defense. The division of various parts of a football game is the first step that people take in the process of understanding the game, and it reflects people's current fundamental understanding of football issues, that is, football views. Observing any training session, one can clearly see the profound impact of this concept on the training content. A training session is carried out from two perspectives, the individual and the whole. The technical training and physical fitness training in the preparation activities are aimed at improving the personal ability of the players. The tactical coordination drill, formation movement, and group confrontation are the main forms of overall training. However, individual and overall training is always combined with the game scene. A player's individual ability usually refers to a player's ability to handle situations in an offensive and defensive environment. Passing and receiving, shooting, and ball-handling abilities are the reflection of individual abilities in offense. Steals, balls, and clearances are the embodiment of personal ability in defense. Compared with the training of personal ability, the training of overall tactics, formation and play style will inevitably incorporate offensive and defensive elements. The wing tactical training includes both wing attack tactics training and wing defense training. Correspondingly, set-pieces appear in both offense and defense. Therefore, offense and defense are still indispensable factors in set-piece training [9, 10]. Figure 2 shows the tactical arrangement and decision-making in a football match.

3.1.3. Role of Offense and Defense in the Game. Offense and defense are the eternal themes of football games. Some teams advocate offense and believe that only scoring goals can bring the possibility of winning for the team, and some even put forward the view that "offense is the best defense", which fully reflects the importance of offense in the game [11]. Those who hold this opinion can indeed provide convincing evidence, with the data summarizing the rankings and goals and losses of the top three teams in the Europa League for the 2021–2022 season. Table 1 shows the Premier League standings, Table 2 shows the Serie A standings, Table 3 shows the Bundesliga standings, and Table 4 shows the Ligue 1 standings. These data fully demonstrate the important role of offense for the team to win and even win the league championship.

In the 2021–2022 European football season, the champions and runners-up of the Premier League, Serie A, Bundesliga, and Ligue 1 ultimately belong to the teams with the strongest attacking power. The characteristics of Serie A : Most teams have a slower pace, and most teams are not competitive for the championship, but whether it is a strong team or a weak team, they all pay attention to the defensive mode. The characteristics of the Premier League: The competition in the Premier League is more intense year by

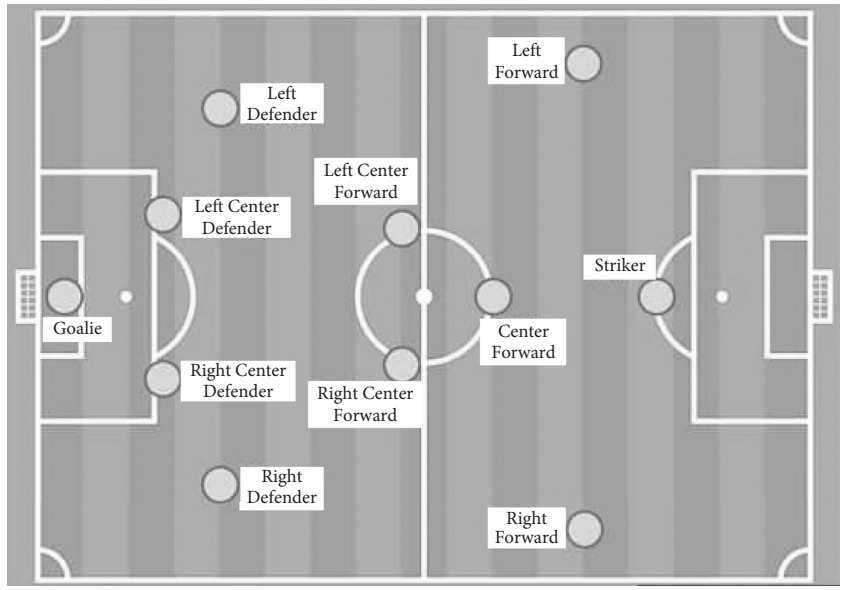

Figure 1: Stadium formation layout.

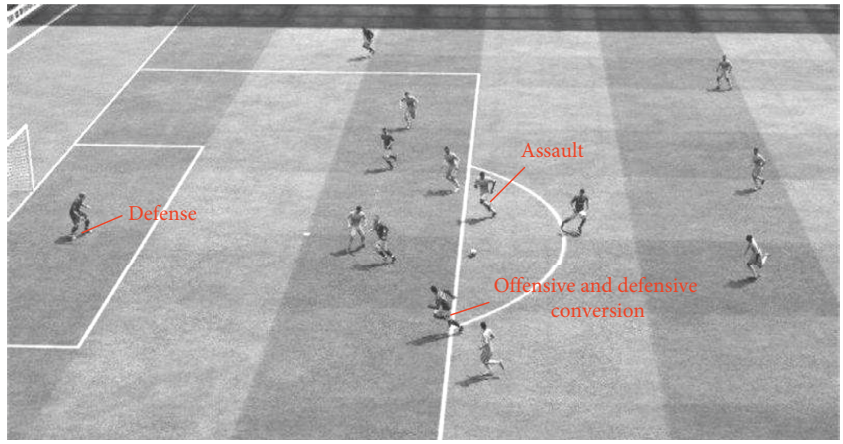

(a)

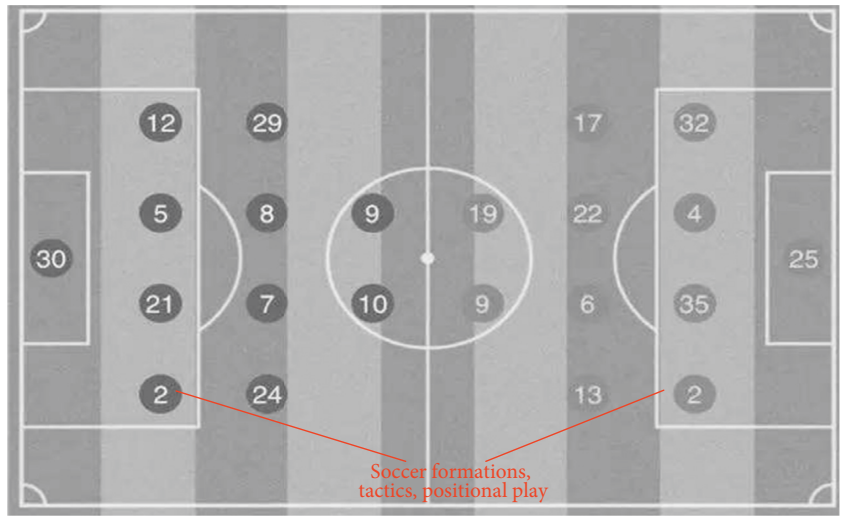

(b)

Figure 2: Football tactics and decisions. (a) Moment of football match. (b) Match formation and player placement.

Table 1: 2021–2022 Premier League standings.

Team	Goal	Conceded	Goal difference	Victory	Ranking
Manchester City	63	17	46	20	1
Liverpool	64	20	44	17	2
Chelsea	49	18	31	14	3

Table 2: 2021–2022 Italian Serie A standings.

Team	Goal	Conceded	Goal difference	Victory	Ranking
AC Milan	52	28	24	17	1
Inter Milan	55	22	33	16	2
Naples	46	17	29	16	3

Table 3: 2021–2022 Bundesliga standings.

Team	Goal	Conceded	Goal difference	Victory	Ranking
Bayern Gurney	74	26	48	18	1
Dortmund	63	36	27	16	2
Leverkusen	60	39	21	12	3

Table 4: 2021–2022 French Premier League standings.

Team	Goal	Conceded	Goal difference	Victory	Ranking
Paris Saint-Germain	53	22	31	18	1
Marseille	48	23	46	13	2
Nice	47	21	45	14	3

year, creating more big-name players. The high salary has also attracted many stars, the scene is relatively hot, the rhythm of playing is relatively fast, the mid-to-long distance coordination is relatively good, and the short-range short pass can be used with individual teams. The characteristics of the Bundesliga: Each team is more inclined to the technical flow. With the decline of Bayern's dominance year by year, each team has begun to maintain a certain degree of competitiveness for the championship. At the same time, the referee's law enforcement level is relatively high, and there are few disputes. 's penalty. The characteristics of Ligue 1: Compared with other league teams, Ligue 1 teams prefer to develop their own players. Among them, there are many African players with good skills, but they are not famous. At the same time, the team cooperates with discipline and the organization is not so good, so the scenes are often gorgeous, but there are few goals. And as can be seen from Table 3, the Bayern Munich team in the Bundesliga is very aggressive, scoring 74 goals, 11 more than the second place. This is enough to show that the offense plays a decisive role in the team's victory [12].

It can also be seen from the data that the top three teams not only score the most goals but also concede fewer goals. As shown in Table 1, the number of goals scored by Manchester City and Liverpool is similar. Manchester City scored 1 goal less, but Manchester City conceded fewer goals than Liverpool, and its ranking is higher than Liverpool. This law fully explains the role of defense in the game, and the data of consecutive seasons in Serie A point to this trend, which proves that defense has a significant impact on the process and results of football matches [13, 14].

3.1.4. Offensive and Defensive Contact. Links exist on both ends of the offensive and defensive end. In the moment of offense and defense, contact always has an important impact on both offense and defense. In all situations in the game, one side is on offense and the other side is on defense. From the point of view of the attacking side, breaking the connection of the defending side with the connection between the players of the own side is the key factor for success in the attack. If the attacking side establishes a close enough connection, and the defending side is relatively loose, then the attacking side is likely to take advantage of this advantage to create scoring opportunities [15].

From the standpoint of the defender, a certain scene in the game can also be analyzed accordingly. If the team members are at a disadvantage in the local confrontation, the action to be taken must be to delay the opponent's attack and buy the necessary time for the teammates to establish contact in this area. If the offensive and defensive sides form an evenly matched situation in a local area, the action that the defensive side needs to take is to maintain contact with each other, control the offensive players, and try to cut off the contact between the ball carrier and other players [16].

3.1.5. Establish effective contacts. Usually, players can establish and maintain contact through observation, communication and movement. Observation is the subjective behavior of players to understand the game, and it is the direct way for players to obtain game information. Communication is the main way players exchange information during the game, including verbal reminders and body language expressions. Running is the most basic way a player moves in a game. Almost all coaches are emphasizing the importance of running in the process of competition, and they even believe that active running is the premise of all tactics and the guarantee of team victory [17, 18].

3.2. Internet of Things. The Internet of Things is also known as the "Internet of Everything". It is a huge network formed by the combination of various information detection equipment and the Internet. The goal is to realize the interconnection of people, machines, and things anytime, anywhere. The Internet of Things serves the society with "things" or the physical world as the data source and is a data-centric network. It covers a wide range, including satellite positioning, video surveillance, driving recorders, intelligent identification, education and medical care,

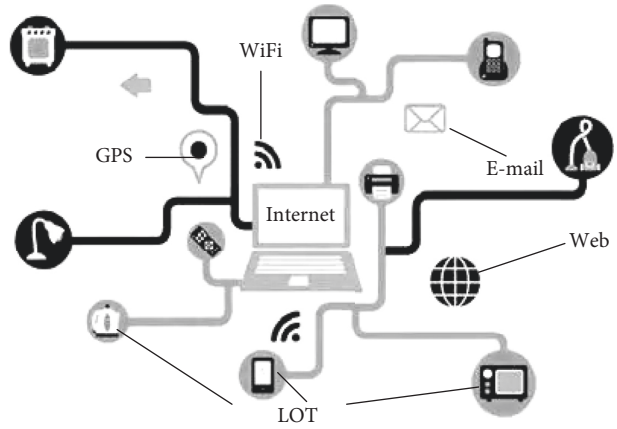

Figure 3: Schematic diagram of IoT concepts.

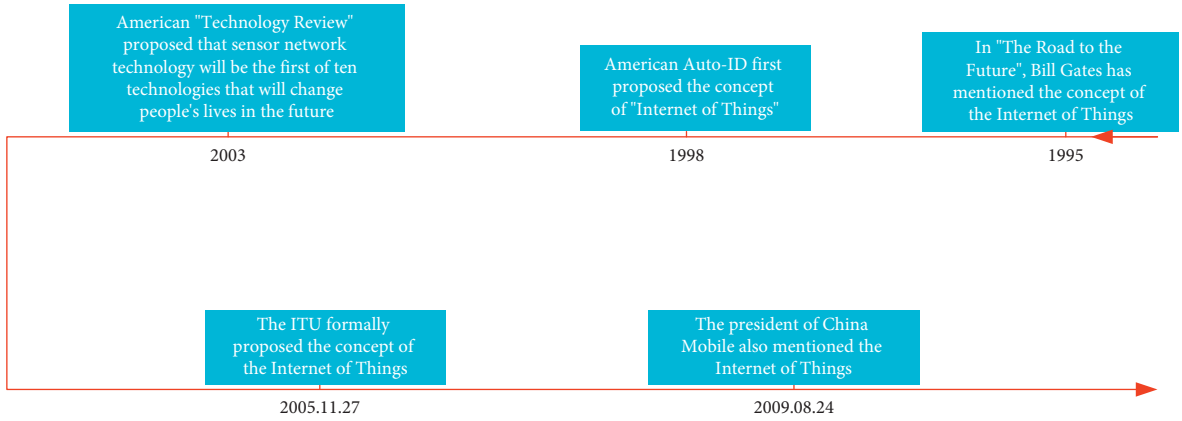

Figure 4: Evolution of IoT.

entertainment and leisure, and many other fields. Its data volume is large, and the current big data include billions of records and petabyte-level data volume. Its update speed is fast, and the Internet of Things big data flow at a speed of hundreds of thousands of pieces of data per second [19]. The IoT data model is usually not one step from IoT devices to big data, but after one or more levels of processing and aggregation, big data are formed, and the convergence point in the middle is called small data. In other words, IoT devices are first aggregated to small data nodes, and then aggregated into big data. Its specific meaning can be shown in Figure 3.

The source and development process of the Internet of Things is shown in Figure 4. From the initial Internet in 1969 to the concept of the Internet of Things in 2005, it has experienced 36 years of development. It has only been more than 10 years since the concept of the Internet of Things was proposed to its popularization. The rapid development of the Internet of Things has greatly facilitated people's work and life.

The key technologies of the Internet of Things mainly include radio frequency identification technology, sensor technology, M2M system framework, and cloud computing. The RFID technology enables items to "talk", which gives the Internet of Things a feature that can be tracked. The goal of the sensor technology is to integrate the acquisition, processing, and execution of information to form a multifunctional microsystem. It is integrated into a large-scale system, thereby greatly improving the level of automation, intelligence, and reliability of the system. M2M is a networked application and service centered on the intelligent interaction of machine terminals, which will enable objects to realize intelligent control. Cloud computing aims to integrate multiple relatively low-cost computing entities into a perfect system with powerful computing power through the network. Moreover, with the help of advanced business models, end users can get these powerful computing services.

The application field of the Internet of Things involves all aspects and is applied in infrastructure fields such as industry, agriculture, environment, transportation, logistics, and security. It effectively promotes the intelligent development of these aspects, making the limited resources more rational use and distribution, thereby improving the efficiency and benefit of the industry. Its application in fields is closely related to life, such as home furnishing, medical health, education, finance and service industry, tourism, and so on. It has greatly improved in terms of service scope, service method, and service quality, which greatly improves people's quality of life.

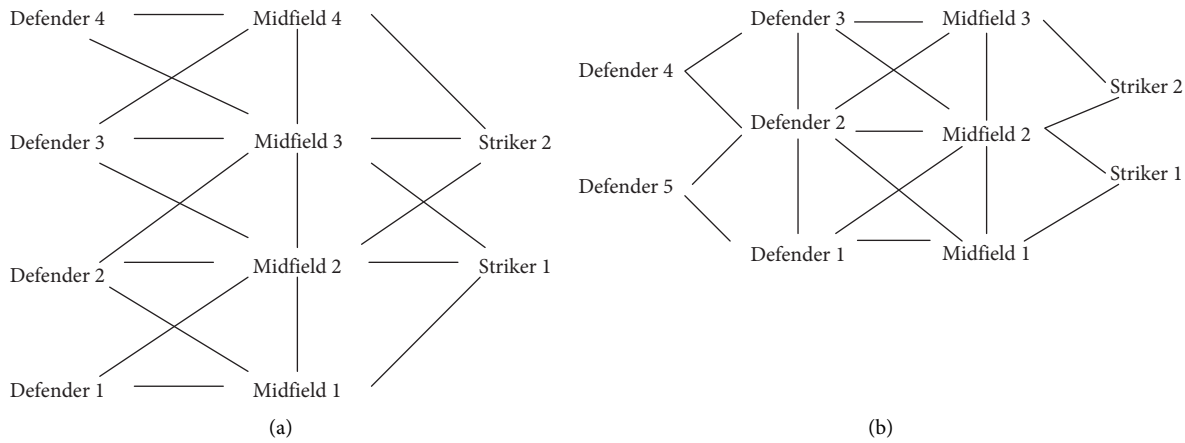

Figure 5: Passing relationship diagram between players of different formations. (a) Classic 2-4-4 formation. (b) 2-3-3-2 defensive formation.

3.3. Decision System

3.3.1. Concept. The behavior of virtual football players mainly includes decision-making and control operations. The behavior and ball-controlling methods of players on the virtual arena are determined by decision-making. The effectiveness of decision-making needs to change according to the situation and real-time changes of the virtual arena. The IoT decision framework provides a structured approach to creating a robust IoT product strategy. The IoT decision framework is about strategic decisions. The IoT decision framework helps users understand where decisions need to be made and ensures consistency across all strategic business decisions, technology, and more. The IoT decision framework is even more important because a product or service that communicates over a network goes through several different layers of technical complexity.

3.3.2. Decision-Making Strategies. For football, its decision-making strategies are divided into low-level decision-making strategies and high-level decision-making strategies. For the team, the high-level strategy library reflects the core strategy of the team. It guides all players of the team to cooperate to implement the formation and tactics in the strategy library, which is similar to the role of the coach in the actual game. The low-level strategy library is to establish different low-level strategy libraries for different player roles, and the different tasks of each role determine the football strategy in the game [20]. Figure 5 displays a diagram of the passing relationship between players of different formations.

3.3.3. Decision-Making Algorithm. The distance and behavior between players are used as the basis for decision-making. Assuming that the distance between the football and the player is dis(ball, player), and the ball control distance is set to CONST_DIST, then when formula (1) is satisfied, it means that the ball control is lost:

$$\text{dis}(\text{ball}, \text{player}) \leq \text{CONST\_DIST}. \tag{1}$$

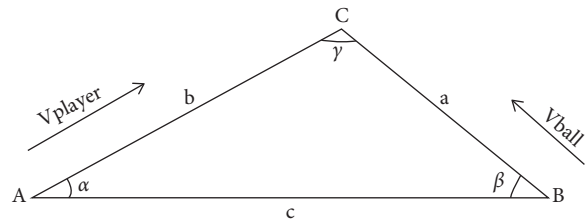

Figure 6: Schematic diagram of players grabbing the ball.

When dis(ball, player) > CONST_DIST, it is assumed that the last three players have possession of the ball, as shown in Figure 6.

According to the triangular cosine law:

$$b^2 = c^2 + a^2 - 2\cos\beta. \tag{2}$$

According to the relationship between distance and speed, there are the following conditions:

$$\begin{aligned} \beta &= \overline{V_{\text{ball}}} \Lambda \overline{BA}, \\ \frac{a}{b} &= \frac{\left|\overline{V_{\text{ball}}}\right|}{\left|\overline{V_{\text{player}}}\right|}, \\ c &= |\overline{BA}|. \end{aligned} \tag{3}$$

According to this, the player who has the earliest possession of the ball and the position of possession can be obtained.

The player movement path can be described as follows:

$$p(t) = a_0 + a_1 t + a_2 t^2 + a_3 t^3. \tag{4}$$

Guidance can be obtained:

$$\dot{p}(t) = \frac{\mathrm{d}p}{\mathrm{d}t} = a_1 + a_2 t + a_3 t^2. \tag{5}$$

Substitute $t = 0$, 1 into the formula, respectively, to obtain:

$$\begin{bmatrix} a_0 \\ a_1 \\ a_2 \\ a_3 \end{bmatrix} = \begin{bmatrix} 1001 \\ 0010 \\ -33-2-1 \\ 2-211 \end{bmatrix} \begin{bmatrix} p(0) \\ p(1) \\ \dot{p}(0) \\ \dot{p}(1) \end{bmatrix}. \tag{6}$$

Then, the expression is as follows:

$$p(t) = \begin{bmatrix} 1tt^2t^3 \end{bmatrix} \begin{bmatrix} 1001 \\ 0010 \\ -33-2-1 \\ 2-211 \end{bmatrix} \begin{bmatrix} p(0) \\ p(1) \\ \dot{p}(0) \\ \dot{p}(1) \end{bmatrix}. \tag{7}$$

Soccer sports model:

$$\begin{aligned} \left(V_x^{t+T}, V_y^{t+T}\right) &= \left(V_x^t, V_y^t\right) + \left(a_x, a_y\right) \cdot T, \\ \left(S_x^{t+T}, S_y^{t+T}\right) &= \frac{\left(V_x^t, V_y^t\right) + \left(V_x^{t+T}, V_y^{t+T}\right)}{2} \\ &\quad \cdot T = \left(V_x^t, V_y^t\right) \cdot T + \frac{1}{2}\left(a_x, a_y\right) \cdot T^2, \\ \left(\left(P_x^{t+T}, P_y^{t+T}\right) &= \left(P_x^t, P_y^t\right) + \left(S_x^{t+T}, S_y^{t+T}\right), \end{aligned} \tag{8}$$

where V is the speed, S is the distance, and P is the position.

If the motion acceleration is ignored in the model, the velocity can be calculated as follows:

$$\left(S_x^{t+T}, S_y^{t+T}\right) = \left(V_x^t, V_y^t\right) \cdot T. \tag{9}$$

The distance the player runs is as follows:

$$S(t) = \begin{cases} 0, & t = o \\ S(t-T) + \sqrt{S_x^{t2} + S_y^{t22}}, & t > 0 \end{cases}. \tag{10}$$

Assuming that the collision distance between the two players is, if the distance is less than this, it means that the players collide and have the same spatial position, that is:

$$\mathrm{Dis}(\mathrm{Player1}, \mathrm{Player2}) < \varepsilon. \tag{11}$$

When the ball-handling player gets the ball, his next step can be represented by the activation function as follows:

$$n_{ij}(t) = \frac{1}{\mathrm{d}_{ij}}, \tag{12}$$

where d_{ij} represents the distance from i to j during the player's travel.

In the process of traveling, the information obtained between i and j is as follows:

$$\begin{aligned} \tau_{ij}(t+n) &= (1-\rho) \cdot \tau_{ij}(t) + \Delta\tau_{ij}(t), \\ \Delta\tau_{ij}(t) &= \sum_{k=1}^{m} \Delta\tau_{ijij}^{\ k}(t), \end{aligned} \tag{13}$$

where ρ is the information disappearance coefficient and $\Delta\tau_{ij}$ is the information increment.

U is used to represent the offensive potential energy of the ball-handling side, U_{art} is used to represent the total potential energy of the arena, $U_{\mathrm{goal}}(x)$ represents the attractive potential energy, and $U_{obs}(\mathrm{x})$ represents the repulsive potential energy, then it can be expressed as follows:

$$U_{\mathrm{art}}(x) = U_{\mathrm{goal}}(x) + U_{\mathrm{obs}}(x). \tag{14}$$

Among them, the attractive potential energy:

$$U_{\mathrm{goal}}(x) = \frac{1}{2} k_p \left(\frac{1}{x - x_{\mathrm{goal}}}\right)^2. \tag{15}$$

Repulsive potential energy:

$$U_{\mathrm{obs}}(x) = \begin{cases} \frac{1}{2}\omega\left(\frac{1}{\rho} - \frac{1}{\rho_0}\right)^2, & \rho \le \rho_0 \\ 0, & \rho > \rho_0 \end{cases}. \tag{16}$$

4. Design and Application of Decision-Making System Based on Virtual Football

4.1. System Design. In the design process of the framework, the overall framework is divided into four modules, namely, entity module, situation module, strategy module, and monitor module. The software structure included in each module is shown in Figure 7.

The situation module state is similar to the entity information on the field such as the physical state of the player and the football path as the main maintenance object. At the same time, the objects monitored by the monitor system are moving objects that can be imaged or animated. Due to the position and moving speed of football and players, it just meets the research object criteria of the surveillance system. It uses the abstract method defined by run() to implement overloading in the entity class. In order to update the motion state of players and footballs, the subclass overloading process is determined according to the motion laws of different research objects. In the state class, each entity instance in the entity module is often used as the reference object, and each entity instance is simultaneously referenced by multiple entities to form the state class. The state class provides a getter to collect the game information of the game through the monitor module. It introduces it into the module interface, in order to keep abreast of the situation on the field, find the collision problem in the field, and make processing decisions in the first time. This needs to establish a separate circuit program in the state class, start the program in the simulated state class, and perform simulated manipulation [21].

The abstract decision maker class used in the strategy module is an abstract form of decision makers, which can provide decision makers with some decision-making information. The execute abstract method it describes must be implemented in all its concrete subclasses. The derived global decision maker class is suitable for the global decision of the actual team, and the individual decision maker class is suitable for a specific individual decision of a player in the game. Due to the differences in the division of labor among players on the field, the individual decision maker divides all players into four categories: Goalie DM for goalkeeper

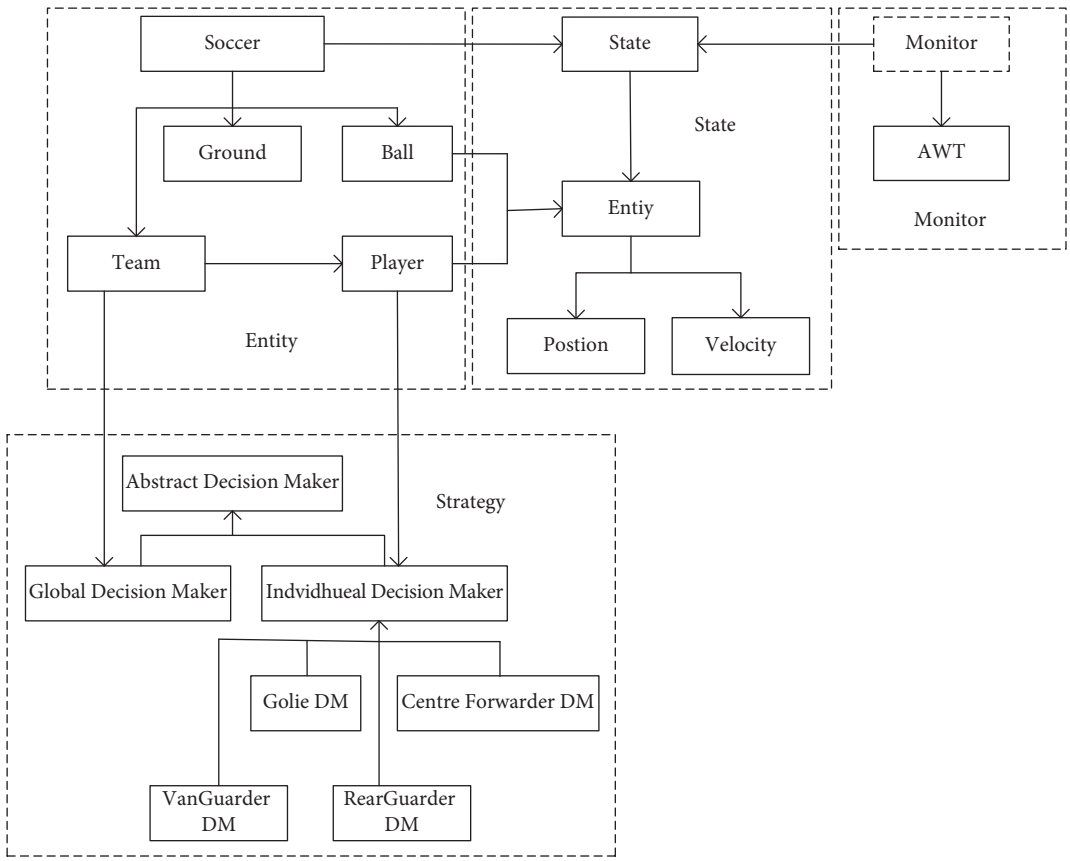

Figure 7: IoT system framework based on virtual football.

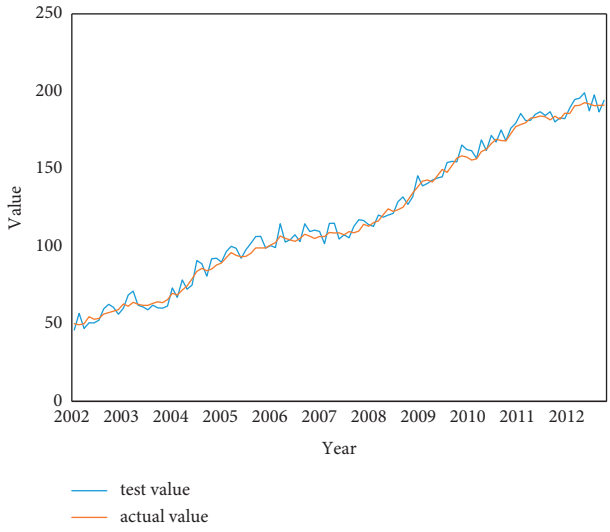

Figure 8: Fit plot of training versus actual values.

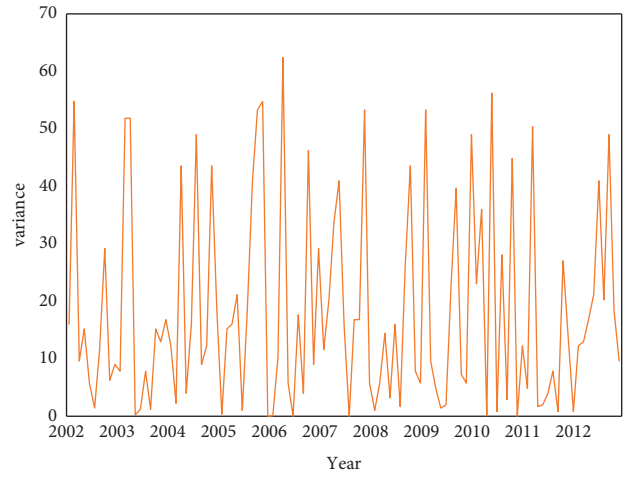

Figure 9: Training error values.

decision-making, Rear Guarder DM for defender decision-making, Centre Forwarder DM for midfield decision-making, and Van Guarder DM for forward decision-making.

4.2. System Testing and Data Analysis. The IoT Decision Framework focuses on six key decision areas in any IoT product. These decision areas include user experience, data, business, technology, security, standards, and regulations. Aiming at the offensive and defensive relationship between players, this paper applies the designed decision-making system to data prediction and processing to make decisions.

In this paper, for an Internet of Things system, we use the designed decision system to predict its data and make corresponding decisions to increase the output. The data volume of the Internet of Things in the past 10 years is shown

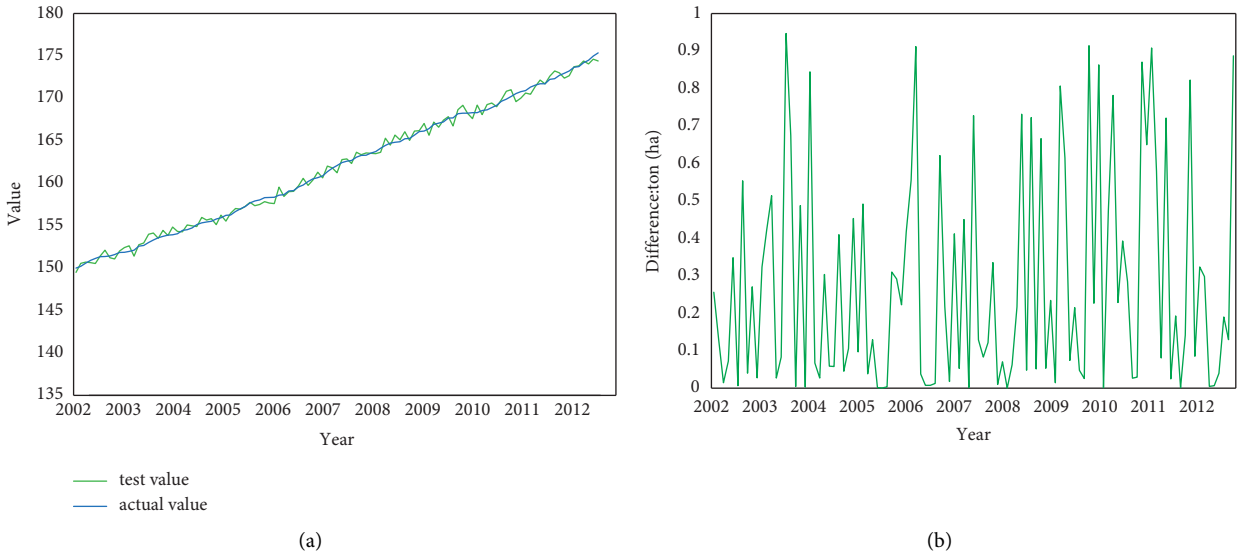

Figure 10: Test results. (a) Comparison of test value and actual value. (b) Test error value.

in Figure 8, and these data are trained to fit the trained and actual values.

As can be seen from Figure 8, although there are still many errors compared with the training data displayed according to the Internet of Things, the two fitting degrees are still quite high, and the overall trend is consistent. In order to understand the error more easily, the error diagram is made as shown in Figure 9.

As can be seen from Figure 9, the magnitude of the training variance values are between 65, compared with the maximum value of 200, and the error is less than 5%, so there is sufficient accuracy after training.

Therefore, this is further tested, and the test and actual results are obtained, as shown in Figure 10.

As can be seen from Figure 10, the final test result fluctuates in the variance value within 1, and the error is not more than 1.5%. That is to say, the calculation accuracy of the system model on the data decision of the Internet of Things is as high as 98.5%, with high calculation stability, high accuracy and certain reliability.

5. Discussion

In order to create a realistic and effective decision-making system about virtual football games, this paper still needs to work hard from the following three aspects:

(1) This paper considers the player's action process during the game, but there is no analysis and research on the warm-up action and physical state of the player before the official start of the game.

(2) In the process of formulating decision-making strategies, this paper only analyzes the actions and thinking of the ball-controlling members in detail. However, this paper does not conduct a detailed study on the activities of other team members. Perhaps, sudden actions such as physical collisions by non-ball-possessing members often affect the progress of the game.

(3) The static formation in the decision-making system is not perfect, and the information in the player's personal strategy database is not clear and accurate, and needs to be further improved.

6. Conclusion

This paper first summarizes the research purpose and content of this paper in the abstract part and introduces the background meaning and some key content of this paper in the introduction part. Second, some scholars' research results on the main content of this paper are listed in the related work part, so as to understand the relationship between the content of the virtual football game and the offense and defense.

In the theoretical research part, this paper first focuses on the attack-defense connection of virtual football games. It includes its virtual football game, the importance of offense and defense, the role of offense and defense in the game, the link between offense and defense, and the establishment of effective links. Second, this paper introduces the Internet of Things, including its concept and development process. Finally, this paper introduces the decision-making system, including its concept, decision-making strategy, and decision-making algorithm.

In the experimental test, this paper first introduces the overall structure of the decision-making system based on virtual football and introduces the particularly important situation module and strategy module in detail. Second, this paper conducts data training on the system according to the collected data of the Internet of Things. After obtaining sufficient training accuracy, the system test is carried out. Finally, the test results are described in this paper with the help of charts. The final result shows that the overall

architecture of the decision-making system based on virtual football in this paper has high calculation accuracy, high calculation stability, and high accuracy for IoT decision-making data, and the system has a certain reliability.

Data Availability

No data were used to support this study.

Conflicts of Interest

There are no conflicts of interest with any financial organizations regarding the material reported in this manuscript.

References

[1] P. A. Pegoraro, A. Meloni, L. Atzori, P. Castello, and S. Sulis, "PMU-based distribution system state estimation with adaptive accuracy exploiting local decision metrics and IoT paradigm," *IEEE Transactions on Instrumentation and Measurement*, vol. 66, no. 4, pp. 704–714, 2017.

[2] S. Suryaprakash, M. Mathankumar, and R. Ramachandran, "IOT based home automation system through adaptive decision making fuzzy algorithm," *Research Journal of Engineering & Technology*, vol. 8, no. 3, pp. 268–272, 2017.

[3] S. Poslad, S. E. Middleton, F. Chaves, R. Tao, O. Necmioglu, and U. Bügel, "A semantic IoT early warning system for natural environment crisis management," *IEEE Transactions on Emerging Topics in Computing*, vol. 3, no. 2, pp. 246–257, 2017.

[4] O. Fukuda, Y. Takahashi, N. Bu, and H. Okumura, "Development of an IoT-based prosthetic control system," *Journal of Robotics and Mechatronics*, vol. 29, no. 6, pp. 1049–1056, 2017.

[5] R. Revathy and R. A. Canessane, "IoT based decision making system to improve veracity of big data," *International Journal of Engineering & Technology*, vol. 7, no. 3, pp. 63–65, 2018.

[6] J. Siryani, B. Tanju, and T. J. Eveleigh, "A machine learning decision-support system improves the internet of things' smart meter operations," *IEEE Internet of Things Journal*, vol. 4, no. 4, pp. 1056–1066, 2017.

[7] S. R. Mugunthan, "Decision tree based interference recognition for fog enabled IOT architecture," *Journal of Trends in Computer Science and Smart Technology*, vol. 2, no. 1, pp. 15–25, 2020.

[8] M. A. Al-Jarrah, Y. Ma, A. A. Dweik, O. A. Dobre, and E. Alsusa, "Decision fusion for IoT-based wireless sensor networks," *IEEE Internet of Things Journal*, vol. 7, no. 2, pp. 1313–1326, 2020.

[9] G. Xu, Y. Zhao, L. Jiao et al., "Tt-SVD: An efficient sparse decision-making model with two-way trust recommendation in the AI-enabled IoT systems," *IEEE Internet of Things Journal*, vol. 8, no. 12, pp. 9559–9567, 2021.

[10] M. M. TKarthick, "Fog assisted IoT basedmedical cyber system for cardiovascular diseases affected patients," *Concurrency and Computation: Practice and Experience*, vol. 31, no. 12, Article ID e4861, 2019.

[11] J. A. Jiang, J. C. Wang, H. S. Wu et al., "A novel sensor placement strategy for an IoT-based power grid monitoring system," *IEEE Internet of Things Journal*, vol. 7, no. 8, pp. 7773–7782, 2020.

[12] K. Hameed, I. S. Bajwa, S. Ramzan, W. Anwar, and A. Khan, "An intelligent IoT based healthcare system using fuzzy neural networks," *Scientific Programming*, vol. 2020, no. 6, 15 pages, Article ID 8836927, 2020.

[13] P. Kaur, R. Kumar, and M. Kumar, "A healthcare monitoring system using random forest and internet of things (IoT)," *Multimedia Tools and Applications*, vol. 78, no. 14, Article ID 19905, 2019.

[14] F. Giannino, S. Esposito, M. Diano, S. Cuomo, and G. Toraldo, "A predictive Decision Support System (DSS) for a microalgae production plant based on Internet of Things paradigm," *Concurrency and Computation: Practice and Experience*, vol. 30, no. 15, Article ID e4476, 2018.

[15] S. Choochotkaew, H. Yamaguchi, and T. Higashino, "Two-tier VoI prioritization system on requirement-based data streaming toward IoT," *Mobile Information Systems*, vol. 2017, Article ID 7892545, 16 pages, 2017.

[16] R. Kumar, C. Rogall, S. Thiede, C. Herrmann, and K. S. Sangwan, "Development of a decision support system for 3D printing processes based on cyber physical production systems," *Procedia CIRP*, vol. 98, no. 1, pp. 348–353, 2021.

[17] A. Aldahiri, B. Alrashed, and W. Hussain, "Trends in using IoT with machine learning in health prediction system," *Forecasting*, vol. 3, no. 1, pp. 181–207, 2021.

[18] M. S. Munir, I. S. Bajwa, A. Ashraf, R. Rashid, and W. Anwar, "Intelligent and smart irrigation system using edge computing and IoT[J]," *Complexity*, vol. 2021, no. 2, 16 pages, Article ID 6691571, 2021.

[19] Q. Hao, S. Nazir, X. Gao, L. Ma, and M. Ilyas, "A review on multicriteria decision support system and industrial internet of things for source code transformation," *Scientific Programming*, vol. 2021, no. 2, 9 pages, Article ID 6661272, 2021.

[20] N. Surantha and H. Herman, "Smart hydroculture control system based ON iot and fuzzy logic," *International journal of innovative computing, information & control: IJICIC*, vol. 16, no. 1, pp. 207–221, 2020.

[21] D. N. Le, L. L. Tuan, and M. Tuan, "Smart-building management system: an Internet-of-Things (IoT) application business model in Vietnam," *Technological Forecasting and Social Change*, vol. 141, pp. 22–35, 2019.

Hindawi
Scientific Programming
Volume 2022, Article ID 1026926, 9 pages
https://doi.org/10.1155/2022/1026926

Research Article

A Study on the Translation of Cultural Classics Based on Deep Learning Methods

Yanqing Zhang, Jianying Lou, and Zhiqi Cheng

School of Foreign Languages, Hebei University of Economics and Business, Shijiazhuang, Hebei 050000, China

Correspondence should be addressed to Jianying Lou; 201410022@heuet.edu.cn

Received 22 March 2022; Revised 11 April 2022; Accepted 16 April 2022; Published 9 May 2022

Academic Editor: Muhammad Zakarya

China's cultural classics have high artistic and ideological values in the world, which implies China's historical heritage and the inheritance of the cultural situation of the Chinese nation for thousands of years. At present, with the rapid development of China's economy, especially in the development environment of cultural globalization, China's traditional cultural classics have attracted worldwide attention along with historical and cultural treasures. In fact, other countries need to translate cultural classics out of their love for China's cultural classics or academic research. However, there are a large number of cultural classics in China. According to relevant data, there are approximately 35,000 kinds of cultural classics, out of which only 0.2% are translated into foreign languages. In order to make China's excellent cultural classics known to the world and let more people in other countries understand Chinese culture, this paper studies the translation of cultural classics through in-depth learning. Firstly, this paper introduces the basic concept of deep learning and proposes an algorithm that deeply studies the convolution layer and pool layer. Secondly, the algorithm establishes a deep learning model that calculates and counts the text information of ancient books through explicit intertextuality. Thirdly, the model carries out automatic text translation and lists the analysis process of cultural classics translation based on intertextuality, so as to study cultural classics translation. The obtained results can promote the development of cultural classics translation in China. For the translation of complex cultural classics, the effects of the three models are tested experimentally, of which the sequence model (seq) is the best. This model is fast and simple to extract the text of literary classics.

1. Introduction

The rapid development of cultural classics translation has attracted the attention of experts and scholars at academia, industries, and research organizations, and it studies the translation theory of cultural classics from the perspectives of various dimensions, including "culture," "language," and "communication" [1]. In fact, there are many contents involved in the translation of cultural classics. Since the text in China's language and culture is composed of paragraphs, texts, words, and sentences, it is necessary to count, retrieve, and extract the contents of cultural classics before translation. Furthermore, these have been translated in the established cultural monolingual and parallel bilingual corpus [2]. At the same time, there are complex classical Chinese poetry and other contents in cultural classics and the amount of data to be analyzed are huge. Therefore, the state-of-the-art computational learning techniques such as machine learning, artificial intelligence, and deep learning can be used for similar data analysis and manipulations.

This paper uses a deep learning method to analyze the text data in cultural classics and suggests a learning algorithm that calculates the explicit intertextual data in cultural classics. Furthermore, the proposed algorithm compares the text data and finds the same number of words between two sentences. Subsequently, we use text translation index to realize automatic text translation. However, China's classical translation is more complex, which can only be assisted by computer translation to further analyze the intertextuality between each sentence of the original text and the historical text in cultural classics, so as to judge the meaning of cultural classics in history and culture.

In this paper, we analyze the data of cultural classics based on the deep learning algorithm, compare the historical intertextuality of each sentence in cultural classics by using text translation index, and establish intertextuality matrix to analyze the content of cultural classics. Moreover, we analyze the sentences of cultural classics according to the intertextuality text translation index process and improve the spatial vector model based on the sequence model. Using this model, we can measure the intertextuality of the text in cultural classics, analyze the similarity between each extension, and improve the accuracy of the cultural classics translation. The main innovations of this study are as follows:

(i) Analyze the data of cultural classics based on a deep learning algorithm, compare the historical intertextuality of each sentence in cultural classics by using a text translation index, and establish intertextuality matrix to analyze the content of cultural classics

(ii) Analyze the sentences of cultural classics according to the intertextuality text translation index process and improve the spatial vector model based on the sequence model

(iii) For the translation of complex cultural classics, the effects of three models are tested experimentally, of which the sequence model (seq) is the best

The remaining part of the paper is structured as follows: we discuss some of the recent state-of-the-art methods in Section 2. A deep learning-based algorithm is suggested in Section 3. We discuss the convolution neural networks and proposed a model for text translation. In Section 4, we discuss the translation of cultural classics based on the suggested deep learning algorithm. The obtained results are elaborated in Section 5. Finally, we conclude this discussion along with directions for future research in Section 6.

2. Related Work

The Republic of China began to translate Chinese cultural classics as early as 647 AD and translated the Tao Te Ching into Sanskrit, opening the door for Chinese cultural classics to go outside of China [3]. Chinese cultural classics were firstly translated into english and spreaded into west countries at the end of 16th century. In 1588, Manila, the Philippines, translated the "Mingxin Baojian" into Spanish, which opened the prelude to the western translation of Chinese cultural classics in China [4]. Li and Jiang provided a platform for westerners to better understand China in their Chinese series, which includes all aspects of history, language and literature, religion, politics, and geography and has become a link between Chinese and Western cultures [5]. Ricci and Luo Mingjian et al. translated Chinese cultural classics, both of which translated the "four books." Up to now, Luo Mingjian's translations have been kept in national libraries such as in Rome and Italy [6].

In this period, all the Latin translations were hand-copied and only a few were printed. As the earliest western translation of cultural classics in China, the translation had little impact over the entire world. Thoreau, a famous American writer in the 19th century, read Chinese Confucian classics and absorbed the Confucian thought of "peace and contentment." In the process of constructing American culture, Thoreau firmly believed in the thought of "peace and contentment" and began to question the popular materialism in the United States. Under the influence of Thoreau, the United States began to accept Chinese ecological literature and cultural classics [7]. Sun studied the influence of medieval classics on the development of Japan and spread China's ancient classics to Japan through multiple channels and different ways. During the prosperous Tang Dynasty, Chinese classics were widely spread and distributed across Japan, directly affecting Japanese culture and education, politics, economy, literature, and art [8].

From the perspective of medical administration, Li and Teng studied the contents of medical administration in the Taiping imperial survey of the Song Dynasty, which fully reflects the contribution of ancient medical literature and history books to human medical development [9]. Pang and Hou introduced the Chinese traditional cultural classics to the whole world and let them feel the charm of Chinese cultural classics. In addition, they also put forward the concept of ecological translation and established the translation ecology of Chinese traditional cultural classics [10]. In the era of "Chinese literature going global," Zhao, starting from the theory of translation multisubjectivity, combined with the view of Chinese context cultural poetics, chose Mencius as an example to fully reflect the multibody of different translators in China [11]. Starting from the development of guided reading education, Liu et al. integrated the Chinese cultural classics and used them in setting courses, recommending books, teaching materials, etc. In essence, this plays a guiding role and integrates science and technology, national history, and traditional culture as the development background of guided reading of Chinese cultural classics in the new era [12–14].

3. Deep Learning-Based Algorithm

3.1. Concept of the Convolutional Neural Network (CNN). When exploring the deep learning algorithm, researchers analyzed it deeply on the basis of convolutional neural network [15]. Deep learning is a feedforward neural network with deep level and convolution operation. It has strong representation and fitting ability and can classify the input information according to the translation invariance of the hierarchical structure [16]. Through continuous and in-depth research, neural networks for different scenarios have appeared, namely, the RNN network and the CNN network. The two layers involved within the deep learning framework are the (i) convolution layer and (ii) pool layer.

3.1.1. The Convolution Layer. A basic component of the convolution neural network is the convolution layer. The function of convolution layer is to realize feature extraction. This method is similar to convolution in signal processing. It uses the small convolution kernel to slide in an image area,

uses the convolution kernel on pixels in the corresponding area of the image, and outputs the results through linear superposition [17]. The following equation determines the convolution calculation formula:

$$\int_{-\infty}^{\infty} f(\tau) g(x-\tau) d_{\tau}. \quad (1)$$

The physical meaning of the convolution is the result of multiple inputs in the superposition system acting together at a certain time. In formula (1), $f(\tau)$ is the original pixel of the image and all pixels are combined into a complete image. Similarly, $g(x)$ represents the action point, which is widely used as the definition of the convolution kernel. Superimposing two kinds of linearity is the convolution result [18]. Figure 1 shows that $7 * 7(I)$ is the input content and $3 * 3(K)$ is the convolution kernel. The two, i.e., I and K, interact to form the final result in the form of $I * K$.

There are many convolution layers in the convolution neural network, and there are a large number of convolution units in the convolution layer. The purpose of convolution operation on each layer of the convolution neural network is to extract various types of features. The convolution in the front row is used to extract low-level features from the image, such as lines and edges, and deep convolution is used to extract more complex features from the image [19].

Similarly, the main function of the convolution kernel convolution operation is to extract image features, and different image blocks are obtained under the calculation of the convolution kernel. This paper chooses to extract image edge features, for example, analysis [20]. First, the first-order differential and second-order differential are described in detail, and the first-order differential is defined by the following formula:

$$\frac{\partial f}{\partial x} = f(x+1) - f(x). \quad (2)$$

The second-order differential is defined by the following formula:

$$\frac{\partial^2 f}{\partial x^2} = f(x+1) - f(x) - 2f(x). \quad (3)$$

The rotation invariant filter is used in the convolution neural network. Based on this filter, the fixed image filtering result can be obtained by rotating the image arbitrarily. The second-order differential operator is more sensitive to the edge image. Here, the rotation invariant differential operator is selected to explain [21, 22]. For two-dimensional images, the derivation process of the Prass operator can be described by the differential operator. First, the second-order differential of x is calculated by the following formula:

$$\frac{\partial^2 f}{\partial x^2} = f(x+1, y) - f(x-1, y) - 2f(x, y). \quad (4)$$

The Laplace operator is obtained by summing the second-order differential of y and the second-order differential of x, which is similar to the convolution kernel. The Laplacian is a differential operator, which is used in the sudden change of image gray level. The sharpening result can be obtained by superimposing the original image and the operator.

3.1.2. The Pooling Layer. The convolution layer outputs the characteristic map from the convolution neural network. The pooling layer follows the convolution layer. The essence of the pooling layer is to select the characteristic process. The two common types of the pooling layer are (i) the maximum pooling layer and (ii) the average pooling layer. The following analysis description is related to the process of selecting the maximum pooling layer [23].

Let x be the $p \times q$ matrix, the elements in the matrix are represented by x_{ij}, the size of the convolution kernel is 2×2, and 1 is the step size of the pooling layer, and the pool operation is completed by the following formula:

$$y_{ij} = \max\left(x_{i,j}, x_{i,j+1}, x_{i+1,j}, x_{i+1,j+1}\right). \quad (5)$$

Here, $j \le q - 2$ and $j \le p - 2$ correspond to the calculation process of the pooling layer in the form of an image.

As shown in Figure 2, the analysis shows that the step size of the maximum pool layer is 2 and the filtering is $2 * 2$. The result obtained by maximizing the $4 * 4$ area in the upper left corner of the operation diagram is 6, that is, the maximum value of the four numbers on the right in the diagram. According to the same principle, the other areas are 3, 4, and 8 and finally constitute the characteristics of the pooling layer.

The function of the pooling layer is to remove all redundant data and retain only key data, which can better deal with the problem of more parameters on the convolutional neural network. Due to more parameters, it will definitely increase the computational complexity. In addition, the pooling layer can enhance the spatial translation and the deformation and scale invariance. The essence of the pooling layer is the information filtering process. During this period, some data will be lost to optimize the computing performance.

3.2. Deep Learning-Based Model. When designing the traditional CNN model, it is necessary to increase the channels or layers to improve the performance. However, increasing the number of channels and layers will lead to more complex parameters that will be required during the training process. The increase of the number of network parameters will lead to the overfitting phenomenon of the network, as well as computational training time [24]. Therefore, the number of cells per layer is not ideal or the number of cells per layer is not increased.

In this paper, the sparse hierarchical structure is used to expand the learning feature interval. Moreover, the size of a single convolution scale is different, which can reduce the amount of information calculation and better express the sparse structure [25]. Compared with the receptive field, multiscale convolution can learn a variety of change characteristics according to the change of receptive field. Figure 3 shows that the structure on inception V1 is used here, and the size of convolutional kernel is 3×3, 1×1, and 5×5,

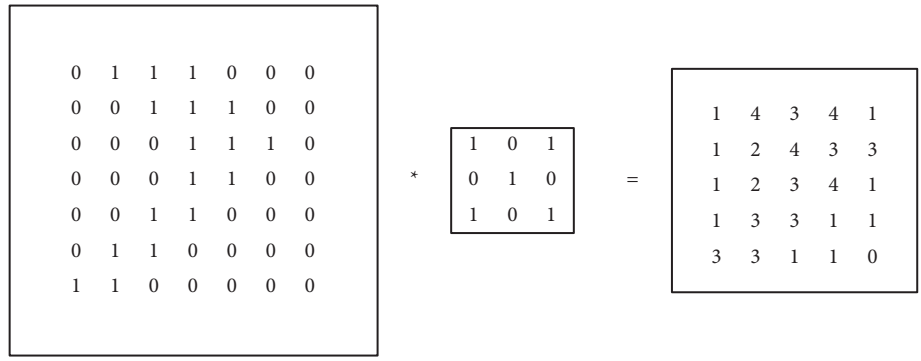

Figure 1: Convolution kernel operation process.

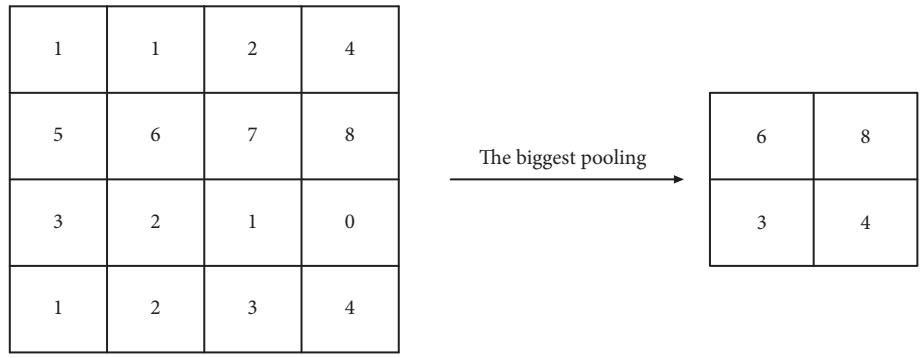

Figure 2: Maximum pool process image.

which is used to generate the multiscale convolution layer. In this figure, constrained convolution is used to process backward 3×3, 1×1, and 5×5. Next, we feed them in the convolution layer and integrate the input characteristic map of each layer to complete the maximum pool operation and 7×7 convolution operation [26].

4. Translation of Cultural Classics Based on Deep Learning

4.1. Explicit Intertextuality Statistics. This paper studies the translation of cultural classics based on in-depth learning, compares the text information to find the explicit intertextuality, and selects a fixed measure to solve it. The higher level is implicit intertextuality. We should understand the meaning of the text from the context and the meaning of the text. It should be noted that intertextuality calculation can quantify the explicit intertextuality in cultural classics and, therefore, may provide relevant clues for understanding the implicit intertextuality in cultural classics.

When measuring the explicit intertextuality, the number of the same words between two sentences should be calculated. In addition, the measurement method should be used to deal with two sentences in two cultural classics. In the experiment, this paper selects the text classics "xucha Jing" and "Cha Jing" as the object, adopts a variety of vector similarity measures as text intertextuality for operation, and lists the measurement definitions, as shown in Table 1.

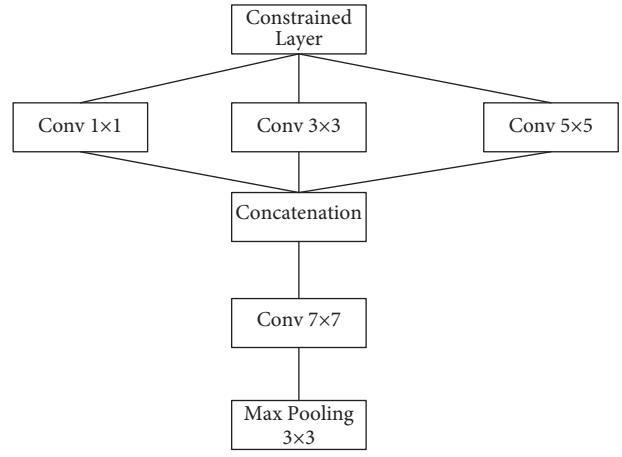

Figure 3: Multiscale convolution.

If a sentence is regarded as a vector composed of multiple words or phrases, the statistical value between each vector is the intertextuality measurement result between different sentences. Note that X and Y represent vectors, the corresponding length of each vector is represented by $|x|$ and $|y|$, to represent the number of elements contained in the vector, and the common dimension of X and Y is represented by $|X \cap Y|$. This paper calculates the longest common subsequence in two sentences. The following is the process of calculating the longest common sequence [14].

Table 1: Mathematical model of statistical measurement of intertextuality.

Measurement of intertextuality	Deiss coefficient	Matching coefficient	Full confidence	Cosine
Mathematical model	$2 * \lvert X \cap Y\rvert / \lvert X\rvert + \lvert Y\rvert$	$\lvert X \cap Y\rvert$	$\lvert X \cap Y\rvert / \mathrm{Max}(\lvert X\rvert, \lvert Y\rvert)$	$\lvert X \cap Y\rvert / \sqrt{\lvert X\rvert * \lvert Y\rvert}$

Suppose that the intertextual matrix of $X = \{X_1, X_2, ..., X_m\}$ statement and $Y = \{y_1, y_2, ..., y_n\}$ statement is as follows:

$$D = \begin{bmatrix} d_{11}d_{12} \cdots\cdots d_{1n} \\ d_{21}d_{22} \cdots\cdots d_{2n} \\ d_{31}d_{32} \cdots\cdots d_{3n} \\ \cdots \\ d_{m1}d_{m2} \cdots\cdots d_{\mathrm{mn}} \end{bmatrix},$$

$$\text{also } di\ j = \begin{cases} 1, & \text{if the } i-\text{th element of } X \text{ is equal to the } j-\text{th element,} \\ 0, & \text{other situations.} \end{cases} \tag{6}$$

Based on the intertextual matrix DIJ of the above two sentences, the maximum matching subsequence between them is obtained by using the dynamic programming algorithm. The purpose of calculating the maximum matching subsequence is to find the ideal collocation between the words of two sentences and to find the elements without common columns and rows in the matrix to the greatest extent. The maximum matching subsequence is calculated by the dynamic programming algorithm, and the calculation formula is as follows:

$$\begin{cases} \mathrm{Intertestality}(D) = M_{m,n}, \\ M_{i,j} = \max d_{\mathrm{ik}} + M_{i-1,k-1}, \max\left\{d_{\mathrm{kj}} + M_{k-1,j-1}\right\}, \\ M_{i,j} = \max\{d_k 1\}, (i = 1, j = 1). \end{cases} \tag{7}$$

Here, $M_{m,n}$ represents the objective function of the dynamic programming and Intertestality (D) represents the similarity function.

4.2. Text Translation Index. Automatic text translation is very important compared with the translation of cultural classics, and the interpretation of classics is difficult. Here, we can make full use of computers to complete the auxiliary translation of cultural classics [27]. The text translation index is used to automatically select a highly referential original sentence on a fixed measurement standard. Similarly, intertextuality is used to comprehensively explain the correlation and influence between texts. Moreover, translation provides a coherent and accurate data reference. Each text has the function of guidance and reference to form intertextuality. In addition, there are many sentences with mutual reference and meme origin in the same text, so the content of text intertextuality mapping is mainly divided into two parts: (i) intertextuality within the text and (ii) intertextuality before the text. The two intertextual measurement types can provide an important basis for the understanding and translation of the original text. We provide further details on both text intertextuality mapping in a subsequent discussion:

(i) Intertextuality between texts: two different texts need to calculate their intertextuality. It is assumed that there are n sentences in the original text and m sentences in the historical text. The intertextuality of the two sentences is combined to form the following intertextuality matrix $A(n * m)$:

$$A = \begin{bmatrix} a_{11}a_{12} \cdots\cdots a_{1n} \\ a_{21}a_{22} \cdots\cdots a_{2n} \\ a_{31}a_{32} \cdots\cdots a_{3n} \\ \cdots \\ a_{m1}a_{m2} \cdots\cdots a_{\mathrm{mn}} \end{bmatrix}. \tag{8}$$

(ii) Intertextuality in the text: assuming that there are n sentences in the original text, the original text has some intertextuality, and the original text itself can also become an intertextuality matrix, which is shown as follows:

$$\begin{matrix} a_{11} & a_{12} & \cdots & a_{1n} \\ a_{21} & a_{22} & \cdots & a_{2n} \\ \cdots & \cdots & \cdots & \cdots \\ a_{n1} & a_{n1} & \cdots & a_{\mathrm{nm}} \end{matrix}. \tag{9}$$

Each of the above-given elements represents the intertextuality between the basis in the original text and the basis in the historical text, and a_{ij} represents the intertextuality between the i sentence in the original text and the j sentence in the historical text. According to the intertextuality matrix, the sentence representing the original text in each line and the corresponding historical text index can be obtained. The elements of each line can be arranged according to the intertextuality level and the qualified queue output, that is, the translation index of the original sentence. According to the intertextuality matrix, the values of most elements are 0, so the matrix is a sparse matrix, which is saved in the form of linked list and an array, as shown in Figure 4.

Each node in Figure 4 represents the corresponding statement, where a_i represents the target statement, that is, the translation statement. Furthermore, the node on the right represents the intertextuality index, or all reference nodes with intertextuality not 0. This should be kept in mind that the node that does not calculate the value of 0 can be ignored.

Note that a_{ij} is a diagonal element, and the result is always 1, which means that, at the same time, it cannot provide new understanding information. However, this value is not considered when queuing. Another feature of the matrix is based on the diagonal symmetry matrix $a_{ij} = a_{ji}$. Since the similarity between sentences i and j in the original text is equal to that between sentences j and i, the value of the

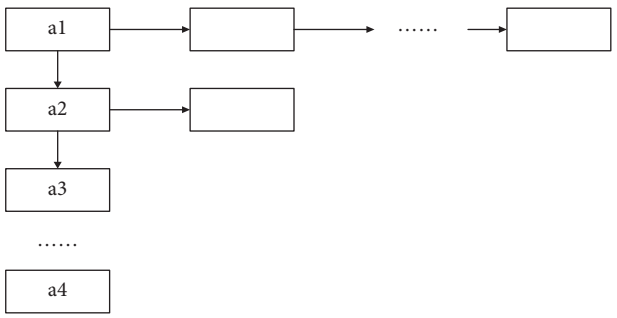

Figure 4: Storage structure of the intertextuality matrix.

triangular matrix should be taken into account when solving and the amount of calculation can be reduced by half.

5. Research and Analysis of Cultural Classics Translation Based on Deep Learning

5.1. Analysis of Cultural Classics Translation Based on Deep Learning. The following steps illustrate the construction process of the cultural classics translation index based on in-depth learning:

(1) Building a library and importing ancient books and documents

(2) Preprocessing data in the literature

(3) Dividing the document into retrieval units, usually sentences

(4) Building the inverted index

(5) Searching the function

(6) Parsing the input sentence and then decomposing it into multiple retrieval units

(7) Searching the inverted table according to the search unit in the input sentence

(8) Calculating the intertextuality between the sentences in the S search set and the input sentences

(9) Arranging the sentences in the search set according to the size of intertextuality, which becomes a list of search sets and is provided to users.

The intertextuality is calculated by the vector space model, and then, the improved model in the text is used to calculate the intertextuality for further comparative analysis. The evaluation results obtained by different models are calculated according to the ratio. In the evaluation, it is judged according to the recall and accuracy rates and then the F value is used to measure the values of the two parameters. The following are the basic definitions:

$$\begin{aligned}\text{accuracy} &= \frac{\text{the number of units forming intertextuality in the query structure of the search result kernel}}{\text{the number of all units in the search result} \times 100\%},\\ \text{recall rate} &= \frac{\text{the number of units forming intertextuality in the query structure of the search result kernel}}{\text{and the total number of units forming intertextuality in the query set} \times 100\%},\\ F &= \frac{2 \times P \times R}{P + R}.\end{aligned} \tag{10}$$

This paper sets up three groups of experiments. First, we use the vector space model (VSM) model to calculate a group of experiments (VSM) based on the $rf * iaf$ weighted value method. Secondly, we use the improved lexical semantic similarity method to complete a group of experiments (sem). Finally, we use the sequence model to complete a group of experiments (seq). The results obtained using the three groups are shown in Figure 5:

According to the experimental results, as shown in Figure 5, the effect of the VSM benchmark test is ideal. Similarly, the result obtained by using the improved similarity calculation method (sem) is not significant. However, the sequence model (seq) has the best effect. By comparing the three models in Figure 5, it can be concluded that the vector space model can more simply represent the results obtained. For the problems in the VSM model, this paper calculates them by expanding the semantic information word similarity and analyzes them by using the sequence model.

5.2. Corpus Intertextual Translation Analysis. The texts of cultural classics show a crisscross intertextual relevance. The text language in cultural classics is relatively classical and concise, which contains China's history, culture, and connotation [28]. Due to a large number of early intertextual texts in a target text, there are multidimensional recognition and compound diachrony, which increases the difficulty of translating cultural classics, and there will be defects or information errors during code switching. Therefore, when translating this kind of cultural classics with strong intertextuality, translators do not start from the original text but first analyze and then further translate on the basis of the previous intertextuality. During the long-term spread of the text, this will be affected by various factors and deformed. The translator should compare and analyze multiple versions. In addition, the texts of cultural classics are often cited by others, which are cited, infiltrated, and developed during their circulation.

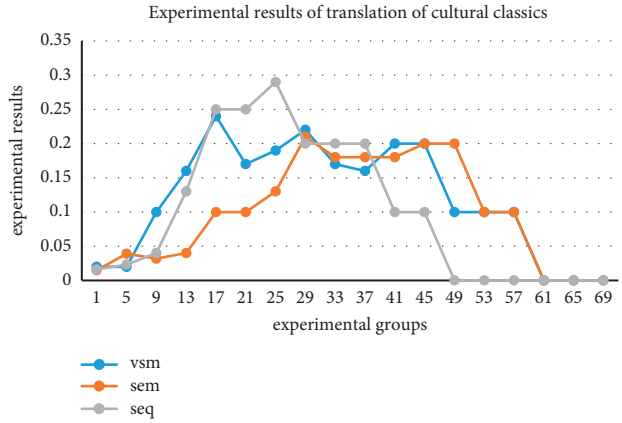

Figure 5: Experimental results.

Searching the corpus can help the translator complete the basic translation work. When translating cultural classics, intertextual markers are important elements in the text. Intertextual markers are shown in Figure 6.

Bilingual parallel corpus means that there are a large number of electronic databases of marked original texts and corresponding translated texts. The two texts can be kept corresponding to each other in terms of paragraphs, texts, vocabulary, and sentences. The tea classic and its translation can be established by extracting the above information through using the deep learning algorithm in the computer and then making statistics and retrieval classics of tea's monolingual and parallel bilingual corpus of tea culture. After that, the monolingual corpus retrieval software is used to master the text characteristics of the English translation version of the book of tea, and the text information is counted by the deep learning algorithm. The specific information is listed in Table 2.

In Table 2, there are 128273120 tokens in the English translation version of the tea classics. The standard class character ratio (STTR) and the class character ratio (TTR) are 46.367 and 25.93, respectively. One thousand words are used as a unit to count the above data. The total number of paragraphs obtained when all the title information is retained is 340, and the number of pure paragraphs left after all the titles are removed is 314. It can be concluded that in the statistical data, the TTR and STTR values of the English translation version of the tea classic are low and there are many repeated words in the phrases or sentences. They are tested and searched manually, including a large number of professional terms related to the tea culture.

Since the total shape symbols in ancient Chinese are less than 1000, it is difficult to count them all. Starting from the language characteristics, the number of shape symbols in English is more than twice that in the Chinese language. It is concluded from the paragraphs that the translator intends to correspond to the paragraphs in the ancient Chinese book of tea, so the number of paragraphs is roughly the same. There is a very low repetition rate of category symbols in the book of tea. In the bilingual version, the category symbols with frequency 1 and frequency 2 account for 86% and 84% of the whole category symbols, respectively. Table 3 shows the proportion statistics of the low-frequency words and text.

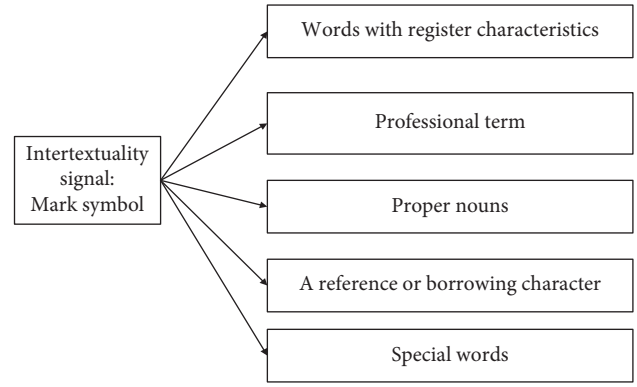

Figure 6: Intertextuality marker character.

Table 2: Stylistic information statistics of the book of tea.

Text file	The classic of tea text
File size	74291
Tokens (running words) in the text	12827
Type/token ratio (TTR)	46.367
Standardized TTR	25.93
Paragraphs	314/340

Table 3: Proportion statistics of low-frequency words and texts.

	Ancient Han	English
Freq. = 1	278	492
Freq. = 2	58	108
Low-frequency part character %	334/389 = 86%	598/710 = 84%

6. Conclusions and Future Work

With the rapid development of the society and the rapid change of science and technology, the field of international translation has also been paid attention to, which has been gradually developed. Through the translation of cultural classics, we can understand the historical, cultural, and humanistic information of a particular country of interest. During this period, we should strengthen the translation quality, translation process, and translation environment of

cultural classics. When studying the translation of cultural classics, this paper uses the deep learning algorithm analysis and establishes the mathematical model of intertextuality statistical measurement. Moreover, the paper constructs the text translation index. For the translation of complex cultural classics, the effects of three models are tested experimentally, of which the sequence model (seq) is the best. This model is fast and simple to extract the text of literary classics. Based on the analysis of the intertextual relevance features crisscross in the cultural classics, the text is divided into sentences, paragraphs, and words. Finally, they are judged by comparing the contents of the previous intertextual text, so as to improve the accuracy of the cultural classics translation.

In the near future, we will aim to create and build more impactful deep learning-based text identification and translation models, which will end in enriched exactness and correctness. Accordingly, deep learning approaches are very time-consuming, which are dependent over the amount of data, and as a result, training a model may take longer periods. Therefore, new strategies, such as data aggregation, can be created to improve algorithm performance in terms of training the model and reduced prediction durations. In addition to the CNN, other techniques like LSTM, graph convolutional network (GCN), ResNet, and even the impact of attention networks can be researched in the near future. Although the Relu function was employed in this research, we believe that alternative functions might provide different results. As a result, a good piece of future work will be to look at a variety of comparable functions.

Data Availability

Data are available on request to the corresponding author.

Conflicts of Interest

The authors declare that they have no conflicts of interest.

Acknowledgments

The work was supported by the Hebei Social Science Fund Project: A Study of the Translation and Dissemination of the Classical Yanzhao Culture (HB20XW015).

References

[1] T. F. Bao, "From "image thinking," represented by "image thinking" -Reflection on "Image thinking" and the English Translation of Tao Te Ching," *Forum on Chinese Culture*, vol. 8, no. 8, pp. 5–15, 2017.

[2] A. B. Confucius, "A Chinese christian prophet? The translation of Chinese classics by the Priest Joaquim Guerra and the religious dialogue in 20th century," *International Communication of Chinese Culture*, vol. 7, no. 4, pp. 485–498, 2020.

[3] A. X. Wang, "The exchange of art, images and artistic techniques between China and Europe in the 17th and 18th centuries," *International Communication of Chinese Culture*, vol. 8, no. 1, pp. 103–119, 2021.

[4] Y. Yan, "On the introduction and translation of Chinese classics published in the English periodicals :A case study of ming xin bao jian," *Journal of Huaihai Institute of Technology (Natural Sciences Edition)*, vol. 16, no. 9, pp. 82–86, 2018.

[5] H. J. Li and F. M. Jiang, "On introduction and translation of the Chinese classics in Chinese repository," *Shandong Foreign Languages Teaching Journal*, vol. 37, no. 6, pp. 101–107, 2016.

[6] Y. Luo, "A new study on the manuscript of the "four books" by Luo mingjian, a jesuit," *Foreign Language Teaching and Research*, vol. 53, no. 2, pp. 284–295, 2021.

[7] M. T. Hue, "The influence of confucianism: a narrative study of Hong Kong teachers' understanding and practices of school guidance and counselling," *British Journal of Guidance & Counselling*, vol. 36, no. 3, pp. 303–316, 2008.

[8] P. Sun, "The influence of ancient Chinese classics on the development of Japanese culture -taking the analects of confucius and the introduction of Tang dynasty Chinese classics as examples," *Journal of Changchun Normal University (Humanities and Social Sciences)*, vol. 40, no. 4, pp. 184–187, 2021.

[9] J. W. Li and J. L. Teng, "Metaphors of medicine and politics in Literary and historical books and their contemporary enlightenment -Taking Taiping Imperial Review·Ministry of Disease as the center," *Journal of Hefei Normal University*, vol. 39, no. 2, pp. 56–59, 2021.

[10] B. K. Pang and D. H. Hou, "Construction of Chinese traditional literature translation system from the perspective of ecological translation," *Journal of Educational Institute of Jilin Province*, vol. 36, no. 8, pp. 168–171, 2020.

[11] X. Zhao, "Multi-subjectivity in the translation strategy of classic books in the new period inspired by the cultural poetics of Chinese context: a case study of mencius fa translation," *Journal of Shanxi Coal-mining Administrators College*, vol. 33, no. 3, pp. 94–96, 2020.

[12] W. S. Liu and Y. T. Ou, "The status quo and future of guided reading education of Chinese cultural classics," *Journal of Chuzhou University*, vol. 22, no. 6, pp. 75–79, 2021.

[13] J. Li and A. J. C. Sun, "A survey on deep learning for named entity recognition," *IEEE Transactions on Knowledge and Data Engineering*, vol. 34, no. 1, pp. 50–70, 2022.

[14] S. Pouyanfar and S. Y. H. Y. M. P. M.-L. S.-C. S. S. Sadiq, "A survey on deep learning," *ACM Computing Surveys*, vol. 51, no. 5, pp. 1–36, 2019.

[15] A. Saeedi, M. Saeedi, A. Maghsoudi, and A. Shalbaf, "Major depressive disorder diagnosis based on effective connectivity in EEG signals: a convolutional neural network and long short-term memory approach," *Cognitive Neurodynamics*, vol. 15, no. 2, pp. 239–252, 2021.

[16] B. Shi, X. Bai, and C. Yao, "An end-to-end trainable neural network for image-based sequence recognition and its application to scene text recognition," *IEEE Transactions on Pattern Analysis and Machine Intelligence*, vol. 39, no. 11, pp. 2298–2304, 2017.

[17] H. Zhang and Q. B. B. Zheng, "A financial ticket image intelligent recognition system based on deep learning," *Knowledge-Based Systems*, vol. 222, no. 2021, Article ID 106955, 2021.

[18] A. Ali, Y. Zhu, and M. Zakarya, "Exploiting dynamic spatio-temporal graph convolutional neural networks for citywide traffic flows prediction," *Neural Networks*, vol. 145, no. 2022, pp. 233–247, 2022.

[19] Z. W. Ren, Q. S. Sun, B. Wu, X. Q. Zhang, and W. Z. Yan, "Learning latent low-rank and sparse embedding for robust image feature extraction," *IEEE Transactions on Image Processing: A Publication of the IEEE Signal Processing Society*, vol. 29, no. 1, pp. 2094–2107, 2020.

[20] S. Dong, P. Wang, and K. Abbas, "A survey on deep learning and its applications," *Computer Science Review*, vol. 40, no. 2021, Article ID 100379, 2021.

[21] H. Vartiainen, M. Tedre, and T. Valtonen, "Learning machine learning with very young children: who is teaching whom?" *International journal of child-computer interaction*, vol. 25, Article ID 100182, 2020.

[22] S. J. Qin and L. H. Chiang, "Advances and opportunities in machine learning for process data analytics," *Computers & Chemical Engineering*, vol. 126, pp. 465–473, 2019.

[23] S. Mao, D. Rajan, and L. T. Chia, "Deep residual pooling network for texture recognition," *Pattern Recognition*, vol. 112, no. 5, Article ID 107817, 2021.

[24] A. Maffei, J. M. Haut, M. E. Paoletti, J. L. Plaza, and A. Plaza, "A single model CNN for h image d," *IEEE Transactions on Geoscience and Remote Sensing*, vol. 58, no. 4, pp. 2516–2529, 2020.

[25] F. L. Galvo, S. Guimares, and A. X. Falco, "Image segmentation using dense and sparse hierarchies of superpixels," *Pattern Recognition*, vol. 108, no. 1, Article ID 107532, 2020.

[26] F. Gu, F. O'Sullivan, D. A. Mankoff, and D. A Mankoff, "Quantitation of multiple injection dynamic PET scans: an investigation of the benefits of pooling data from separate scans when mapping kinetics," *Physics in Medicine and Biology*, vol. 66, no. 13, Article ID 135010, 2021.

[27] R. M. Andrianjaka, R. Hajarisena, I. Mihaela, M. I. Thomas, and R. N. Raft, "Automatic generation of Web service for the Praxeme software aspect from the ReLEL requirements model," *Procedia Computer Science*, vol. 184, no. 1, pp. 791–796, 2021.

[28] A. Katsuta and K. Yamamoto, "Lexical simplification by unsupervised machine translation," *International Journal of Asian Language Processing*, vol. 30, no. 02, pp. 81–94, 2020.

Hindawi
Scientific Programming
Volume 2022, Article ID 9583803, 10 pages
https://doi.org/10.1155/2022/9583803

Research Article

Informatization of National Public Service Fitness in Constructing a Smart City Using Big Data

Xinjun Dong,[1] **Feng Yi**,[1] **and Zhenzhong Wang**[2]

[1]*Sports Department of Jiangsu University of Technology, Changzhou, Jiangsu 213001, China*
[2]*Department of Physical Education of Hubei University of Science and Technology, Xianning, Hubei 437100, China*

Correspondence should be addressed to Zhenzhong Wang; wangzhenzhong@hbust.edu.cn

Received 26 March 2022; Revised 15 April 2022; Accepted 20 April 2022; Published 9 May 2022

Academic Editor: Muhammad Zakarya

The public service system of national fitness is the condition and guarantee for the public to participate in various fitness activities. In order to effectively integrate the existing national fitness service resources and to improve the efficiency of the public service supply, this paper aims to study the informatization of building national fitness public services in smart city under the background of big data. Firstly, we build a public service information platform of national fitness in the smart city, consisting of different modules, and then describe each module in detail. Secondly, we consider different types of fitness projects and establish the database structure model of network resources. Thirdly, we obtain the multitree cascade system of the national fitness and the heterogeneous data model of the national fitness benefit index by using high-dimensional statistical analysis method. Combined with the national fitness behavior, data mining, and support vector machine (SVM), the objective function of data mining statistical decision-making is established. Finally, the well-known particle swarm optimization (PSO) method is used to optimize the target parameters so as to realize the national fitness, big data mining, and feature analysis. The simulation results show that the proposed model has superior performance, as it can realize heterogeneous data mining of the national fitness benefit index. In addition, we quantitatively analyze the promoting effect of the national fitness on the physical quality and health level of the public.

1. Introduction

With the gradual development and progress of computer networks and information technology, the important concept of smart city supported by modern information technology and big data has emerged and has been widely used in many fields. Among them, the national fitness service is the main component of the health service system. The cause of national fitness is mainly for the public. It advocates scientific fitness so as to form a healthy lifestyle. It aims to enhance the physical quality of the public, serve the physical health of the public, and promote the development of the public. In fact, the main aim is to enrich the spiritual life of the public, promote the rapid development of the economy as well as society, and enhance the comprehensive strength of the country. Therefore, national fitness is mainly related to the physical and mental health and happy life of the public. It is an important symbol of comprehensive national strength and social civilization and progress. Overall, the national fitness is assumed an important part of building a well-off society. Vigorously advocating the development of national fitness and doing a good job of national fitness are of great and far-reaching strategic significance for improving the physical quality of the public. Subsequently, this may help in accelerating the reform and development of China's sports industry at a new starting point.

Similarly, vigorously developing national fitness and advocating the use of sports fitness activities to improve the physique of the whole people and the distance between national fitness and the public have gradually narrowed. Moreover, sports have gradually become an important part of the social public life, whereas the number of people participating in sports activities has gradually increased. In addition, the physical quality of the whole people has been significantly improved, and the level of physical health has been gradually improved. Besides, big data, Internet of

things, information technology, computer networks, and machine learning-based learning methods can be used to better explore this field of research. In order to effectively integrate the existing national fitness service resources and to improve the efficiency of the public service supply, this paper aims to study the informatization of building national fitness public services in smart city under the background of big data. We believe that this area of research has remained relatively less explored in the existing literature.

In this paper, we firstly build the public service information platform of national fitness in smart city under big data. Then, we introduce the major modules in the platform in detail and build the heterogeneous data model of the national fitness benefit index. Next, we optimize the target parameters by using the particle swarm optimization (PSO) method to realize the big data mining and feature analysis of national fitness. Our evaluation and experimental results demonstrate that the proposed method can effectively integrate the current national fitness service resources and improve the efficiency of public service supply. The major innovations of this paper are as follows:

(i) we build the public service information platform of national fitness in smart city under the big data environment

(ii) introduce the major modules in the platform in detail and build the heterogeneous data model of the national fitness benefit index in order to optimize the target parameters by using the particle swarm optimization (PSO) method and

(iii) we show that the proposed method can effectively integrate the current national fitness service resources and improve the efficiency of public service supply.

The remaining of the paper is organized as follows. In Section 2, state-of-the-art-related work is illustrated. In Section 3, we build a smart city public service information platform for national fitness that is based on the well-known particle swarm algorithm. A mathematical proof of the model is illustrated in Section 4. Implementation and results of the proposed model based on the particle swarm algorithm are discussed in Section 5. Finally, we conclude this study along with future research directions in Section 6.

2. Related Work

In recent years, the informatization construction of national fitness service in the construction of smart city has had a good start and development momentum. Local and regional national fitness guidance websites and platform systems have achieved some results, therefore making national fitness more convenient. Zhang et al. proposed a description algorithm based on the national fitness trajectory [1]. The extracted interest points form the fitness trajectory through the optical flow field. The movement change value is calculated, in detail, through the interest points of the national fitness trajectory. The calculation results are added to the calculation process of the description operator. On the data set of the national fitness service, the calculated value is used to judge the change in fitness information. The codebook is selected according to the change degree of fitness information. In addition, the national fitness data samples are classified, and the experiment is carried out on the deep exercise data set. The simulation results show that the description algorithm based on the national fitness trajectory information has stronger robustness and better performance than other methods, but this method does not improve the efficiency of service resource supply [1].

In order to improve the efficiency of the supply of public services for national fitness, Huang et al. proposed a neural network based on the combination of normalized neural network and neural network with long-term and short-term memory [2]. The normalized idea of the national fitness is introduced, and the fitness data samples, which are input into the network training, are normalized and sent to the long-term and short-term memory (LSTM) neural network. This method is through the national fitness service network model of space-time double flow. The fitness video image is used as the network input, and the fitness behavior recognition results obtained in the space-time dual flow network are weighted and fused. Finally, the recognition results of the national fitness service are obtained. The experimental results show that the spatiotemporal dual-flow neural network method designed in the literature can effectively improve the efficiency of the public services in national fitness behavior; however, the whole process is more complex and less useable [2].

In view of the poor resource integration of the current national fitness service, which leads to the problem of being unable to effectively identify the fitness action, Ma et al. put forward the recognition method of the national fitness behavior [3]. The authors adopted the improved fitness movement dense track and choose the fitness action video as the basic action sequence. Next, they encode its fitness action as the fitness action feature sequence of PA and use affine propagation to turn it into the index sequence. Based on the mining of the sequence patterns, the sequence models of different fitness behaviors are formed. Moreover, the models are efficiently studied, whereas the comparative features, matching features, and sequence set features of fitness service sequences are calculated to form the function of fitness action scoring. In fact, the linear discriminant analysis is introduced to classify and learn the fitness action scoring system so as to complete the fitness exercise recognition and experiment on the corresponding data set. The experimental results show that in the face of various fitness actions, the proposed method can effectively improve the accuracy of the fitness action recognition. Similarly, the model can effectively integrate the national fitness resources, but the supply efficiency of fitness public services is low [3].

Li et al. proposed a model along with the rapid development of various microelectronic technologies, and through the information construction of public fitness services for all, the proposed model is of great significance to the physical quality of the public [4]. In order to investigate that how to improve the integration of service resources and considering the characteristics of fitness mode, the authors

proposed a human fitness mode recognition method based on the CNN and Mogrifier LSTM models. The recognition of human fitness mode mainly extracts the relevant features of the original fitness data through the CNN approach, while Mogrifier LSTM is used to replace the full connection layer, mine the dependence of local relevant features, and identify common fitness actions such as walking and running in fitness. Experimental evaluation shows that compared with some other methods, the recognition accuracy of the proposed method has increased significantly, which also proves the superiority of the CNN algorithm; however, there are also complex processes that reduce the integration of national fitness resources [4].

3. Smart City Public Service Information Platform for National Fitness

The main purpose of the national fitness public service information platform is to activate users in the national fitness service platform in the form of platform points. Users can use different fitness operations on the platform to obtain points and share points with each other. After obtaining points, users can consume them on the fitness service platform. The point consumption can also be used to exchange for other value-added services. Figure 1 shows the relevant contents on the national fitness public service platform [5, 6]. Various modules of the platform are discussed in subsequent subsections.

3.1. Personnel Analysis. The relevant personnel who establish the public service platform for national fitness include (i) athletes, (ii) fitness coaches, and (iii) referees. Figure 2 shows the personnel analysis of the national fitness service platform. On this fitness service platform, the public can search relevant information such as fitness venues, fitness equipment, and activity equipment. Relevant personnel on the service platform use the service to obtain points, which can be consumed after superposition [7, 8].

The main data of the national fitness users include users' basic data such as name, gender, height, and weight.

3.2. Site Analysis. The venues of the national fitness public service platform include common public venues (such as parks, badminton halls, and other fee-paying sports venues), and semiopen venues mainly include school sports venues or sports venues built by enterprises. Figure 3 shows the analysis model of public service venues for the national fitness [9, 10].

The national fitness service information platform collects the venue data including the type and charging standard of the venue as well as the time period of use of the sports venue. Moreover, it displays these data according to the venue category, quantity, and venue type and records the resource data of the sports venue and the venue to the fitness service platform for unified management [11, 12].

3.3. Platform Content Analysis. The operation content of the national fitness service information platform is ecological services and value-added services including (i) the leasing of fitness equipment, (ii) the purchase of fitness equipment, (iii) the introduction of sports items as well as routine sports training, and (iv) various event performance activities. Figure 4 shows the key contents of the informatization construction of the public services for national fitness.

3.4. Planning Platform. The main contents of the information platform construction of the national fitness service in smart city are small programs and official account terminals. After the completion of the fitness service platform, the front end contains multiple modules such as sports columns, events, and personal centers, and the back end includes different modules such as the management of system architecture, the management of authority, and the management of venues [13, 14]. Figure 5 shows the overall planning content of the platform construction.

4. Informatization of the National Fitness Public Service under Big Data

4.1. Mathematical Model Construction of National Fitness Benefit Index Mining. Combined with the above construction of the national fitness public service information platform of the smart city, the mathematical model of national fitness benefit index mining is established in this section. In order to master the improvement degree of physical function of different groups by national fitness exercise, we realize big data mining in order to establish a mathematical model for the index of national fitness benefit. The proposed model ensures to increase endurance, improve coordination, control the ability of different parts of the body, and make the public strong [15, 16]. In the establishment of the mathematical model, different types of fitness items are comprehensively considered, and the vector of positioning state estimation of the data target position is expressed using the following formula:

$$\alpha = (\alpha_1, \alpha_2, \ldots, \alpha_n) \neq 0. \tag{1}$$

According to the goal of the national fitness plan, the heterogeneous data of the diversified national fitness benefit index are provided to different servers. When scheduling the heterogeneous data information resources of the national fitness benefit index, $s_j^{(k)}$ represents the linear input of the system and $y_j^{(k)}$ represents the reversible invariance output, which is expressed through the following equation:

$$\begin{aligned} x^{(k)} &= \left[x_1^{(k)}, x_2^{(k)}, \ldots x_{N_{k-1}}^{(k)}\right]^T, \\ s^{(k)} &= \left[s_1^{(k)}, s_2^{(k)}, \ldots s_{N_k}^{(k)}\right]^T, \\ y^{(k)} &= \left[y_1^{(k)}, y_2^{(k)}, \ldots y_{N_k}^{(k)}\right]^T. \end{aligned} \tag{2}$$

Then, under national fitness, we investigate the time-frequency characteristics of cardiopulmonary function data and use the characteristics as the medium to portray the

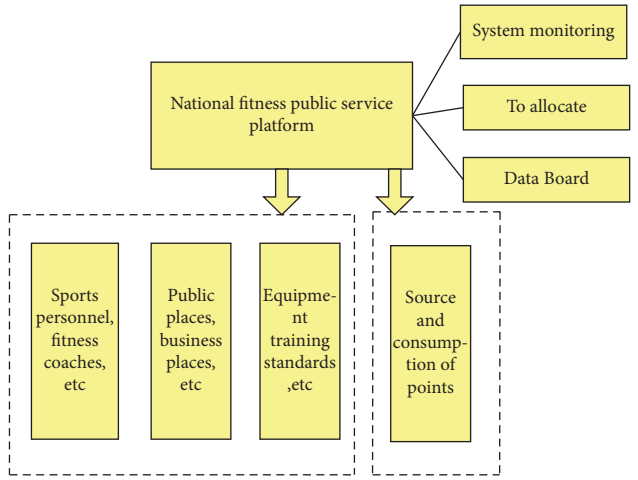

Figure 1: Main contents of the national fitness public service platform.

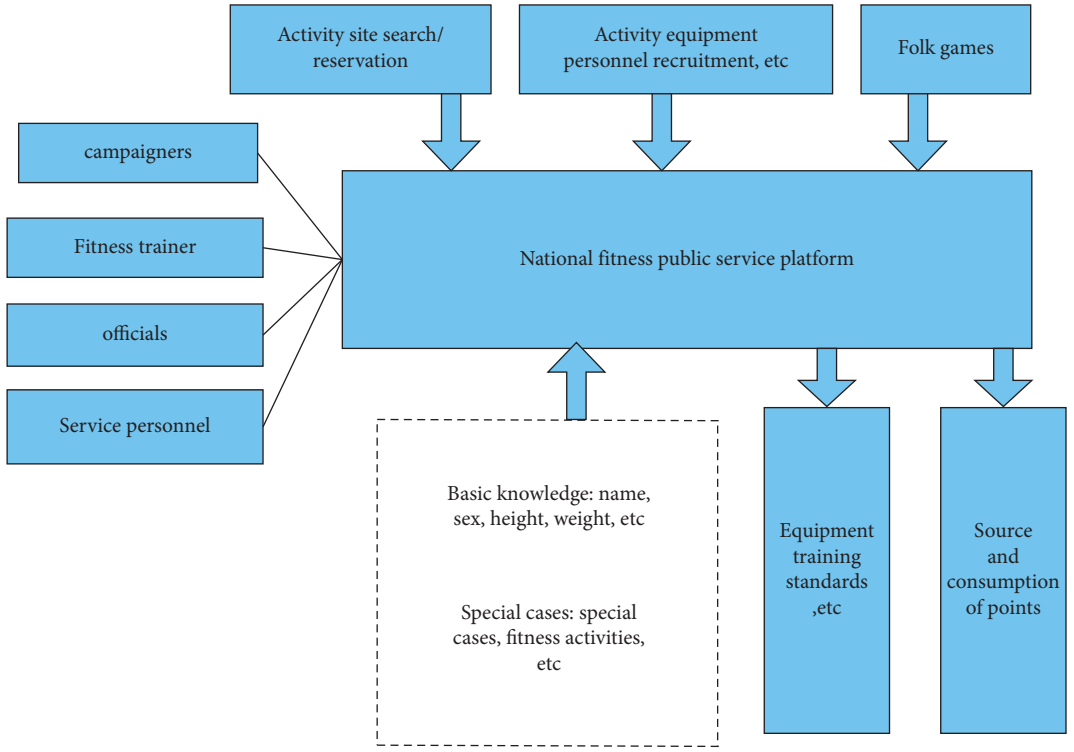

Figure 2: Personnel analysis of national fitness public service platform.

cardiopulmonary function data's original features. Assuming that the data range is N discrete points, $A = \{a_1, \ldots, a_N\}$, the national fitness benefit index's average time is computed as follows:

$$t_m = \frac{1}{G_x} t|x(t)|^2. \tag{3}$$

The mean value of the frequency is expressed as illustrated by the following formula:

$$v_m = \frac{1}{G_x} v|x(v)|^2. \tag{4}$$

From the above formula, the index system of the national fitness benefit based on the linear model or equivalent approximate linear model is obtained.

Based on the data investigation and data sample collection, the detailed promotion relationship between national fitness training and the social public health benefit index is analyzed; meanwhile, the improvement degree of national fitness training on different physical functions is also grasped [17, 18]. Based on multivariate statistical analysis and PCA analysis method, the storage structure fractal of the national fitness benefit index is carried out. The

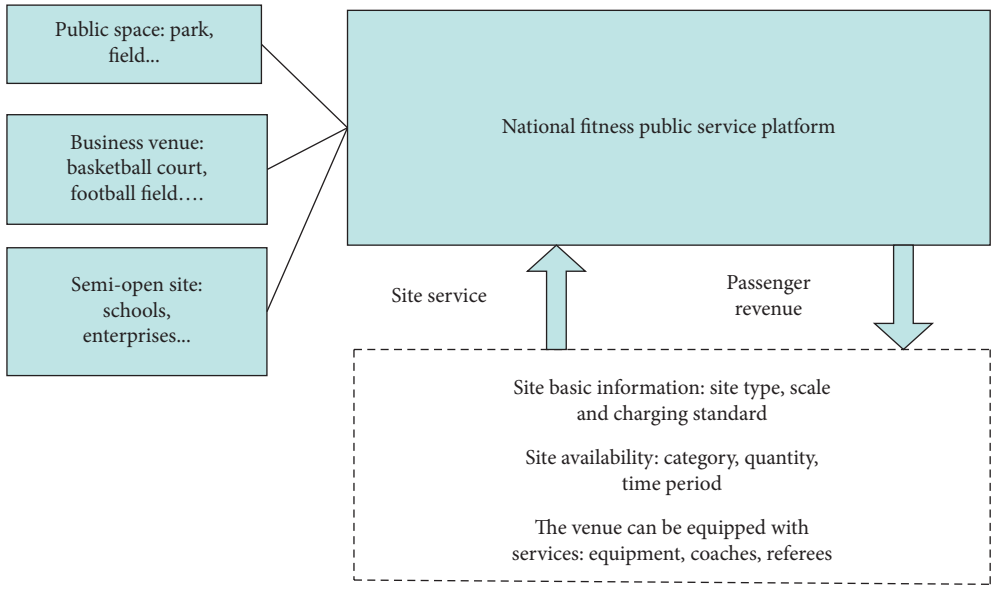

Figure 3: Site analysis of national fitness public service platform.

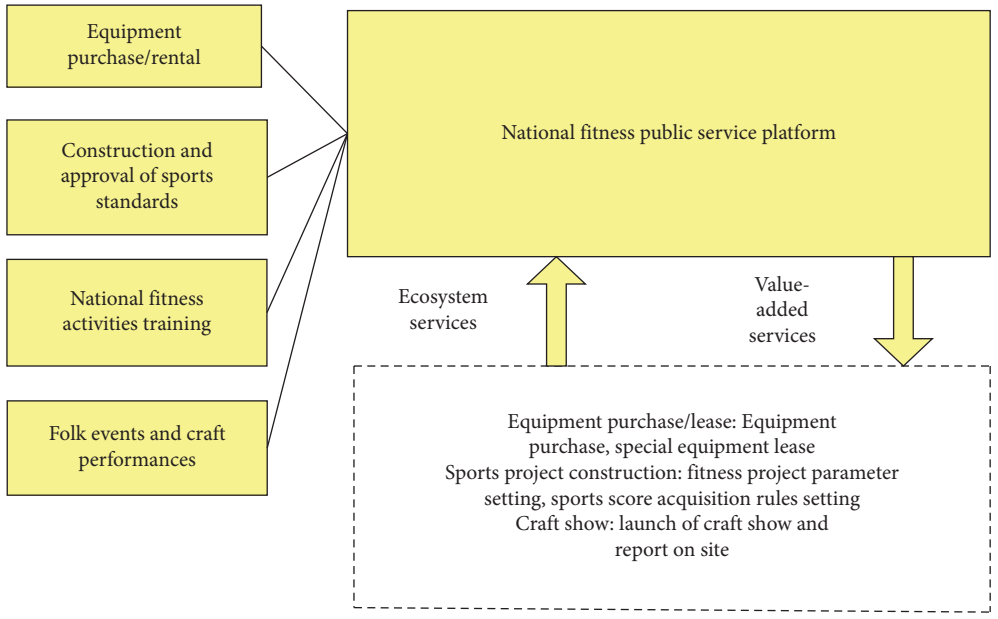

Figure 4: Content analysis of the national fitness public service platform.

matrix C for calculating the covariance of the information storage structure of the fitness benefit index is expressed as

$$C = \frac{1}{N}[X - \overline{X}_l][X - \overline{X}_l]^T. \tag{5}$$

Subsequently, we build a nonlinear dynamic system to fit the impact factors and complete the fitting of the index parameters of the national fitness benefit index. The fitting model can be expressed as

$$\begin{aligned} Z_\beta X &= C\left\{F \in \frac{U}{R} | c(F, X) \le \beta\right\}, \\ Z_\beta X &= U\left\{F \in \frac{U}{R} | c(F, X) \le 1 - \beta\right\}. \end{aligned} \tag{6}$$

This should be noted that the number of principal components must be chosen based on the degree of cumulative variance contribution, and the group of universal impact factors must be included. The relevant principal components m can be utilized as the main components to be selected when the cumulative contribution rate exceeds a particular quantity. It provides a resource database for achieving the heterogeneous data mining model of the national fitness benefit index using the aforesaid fractal design.

4.2. Analysis Model of Fitness Behavior Characteristics Based on Data Mining. Combined with the national fitness benefit index model constructed above, the support vector machine

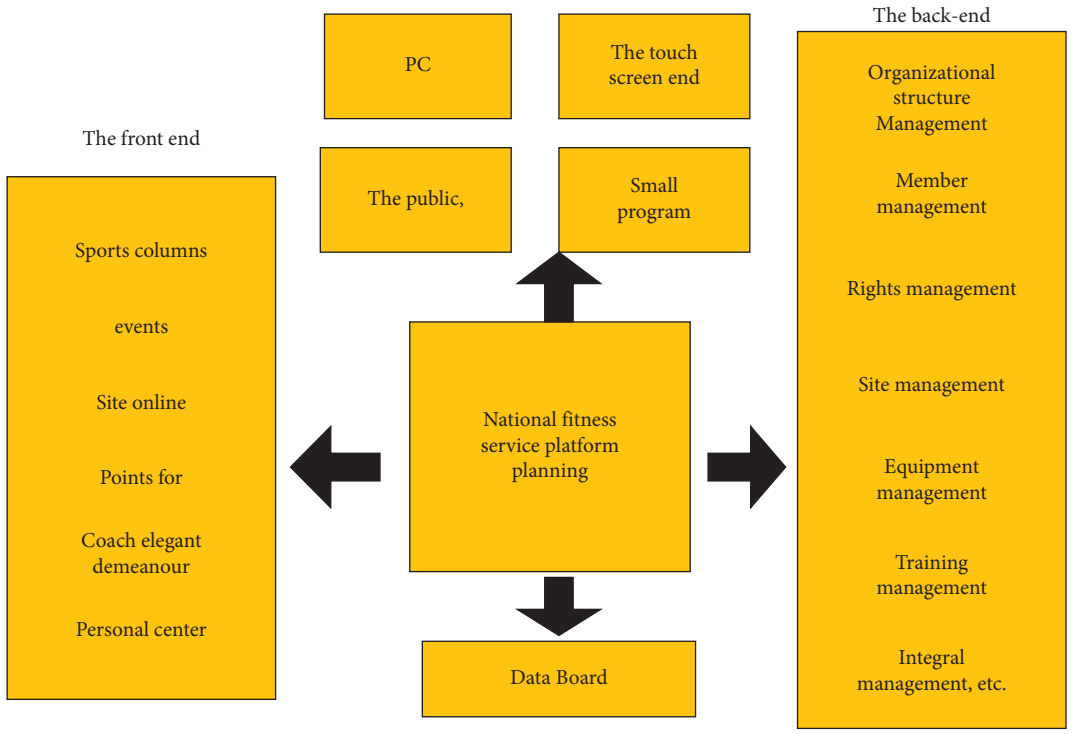

Figure 5: Overall planning of the national fitness platform construction.

(SVM) of the particle swarm optimization (PSO) is used to mine the information of big data of fitness behavior. The process of particle swarm flight is expressed as follows:

$$\begin{cases} v_t = wv_{t-1} + c_1 \text{rand}_1 \cdot (P_{\text{best}} - x_{t-1}) + c_2 \text{rand}_2 \cdot (g_{\text{best}} - x_{t-1}), \\ x_t = x_{t-1} + v_t. \end{cases} \tag{7}$$

In formula (7), v_t represents the running speed of the fitness behavior particles, x_t represents the fitness value of particles, c_1 and c_2 represent the optimal learning operator, and rand_1 and rand_2 represent the random number between $[0, 1]$, respectively. The objective function of constructing the statistical decision-making of the national fitness behavior data mining is expressed as given by the following formula:

$$\begin{cases} x_{i\,d}^{t+1} = \omega x_{i\,d}^{t} + c_1 r_1 \left(P_{a\,d} - x_{i\,d}^{t}\right) + c_2 r_2 \left(P_{g\,d} - x_{i\,d}^{t}\right), \\ P_{a\,d} = \dfrac{1}{m} \sum_{i=1}^{m} P_{i\,d}. \end{cases} \tag{8}$$

In formula (8), $P_{a\,d}$ represents the average value of the individual optimal position of the particle swarm.

The specific individual extreme value P_{best} of the fitness behavior is obtained by using the weighting technique of inertia weight (perhaps the dynamic), and the objective function of the population fitness is premeditated to enhance and improve the parameters values of the objective function of data mining. Therefore, the iterative formula for the particle swarm crossover and mutation is expressed as follows:

$$l_i(k) = (1 - \rho) l_i(k - 1) + \gamma f_i P_i(k). \tag{9}$$

In formula (9), $P_i(k)$ characterizes the movement probability of the i particle at a particular time k, and f_i characterizes the function of X_i which is an error back-propagation. Under the constraints and limitations of the convergence conditions, the optimization procedure of the particle swarm optimization crossover is updated according to the following formula:

$$\begin{cases} v_{i\,d}^{i+1} = \omega v_{i\,d}^{i} + c_1 r_1 \left(P_{i\,d} - x_{i\,d}^{i}\right) + c_2 r_2 \left(P_{g\,d} - x_{i\,d}^{i}\right), \\ x_{i\,d}^{i+1} = x_{i\,d}^{i} + v_{i\,d}^{i+1}. \end{cases} \tag{10}$$

By solving the above optimization problem in the variation process through the data characteristics, we can mine the national fitness behavior data, decompose the fitness behavior characteristics of all particles and fitness functions, and then calculate the state function of the fitness behavior data distribution. Through the stability functional, we can get

$$\min_{Q} \frac{1}{2} \left\| Q|_{\Omega} - P|_{\Omega} \right\|_F^2 + \mu \|Q\|. \tag{11}$$

We adjust the μ value to boost and improve the fitness of public service behavior of national fitness. Moreover, this should be noted that the selection of μ value must meet the following requirements:

$$\left\| Q|_{\Omega} - P|_{\Omega} \right\|_F^2 \approx \mu(\Omega)\sigma^2. \tag{12}$$

Suppose $\mu = (\sqrt{n_1} + \sqrt{n_2})\sqrt{p}$ and n_1 and n_2 are the parameters of the global optimization problem of the fitness

behavior, which characterizes the total quantity of the particle swarm in the data mining training of the national fitness behavior. This should be noted that the optimal value of the fitness behavior data mining is searched in a d-dimensional space. In carrying out the above procedure, the search step of each gradient descent direction could be achieved by using the updated iterative data of the particle swarm optimization, which can be expressed as illustrated in the following formula:

$$\operatorname{dist}(i,j) = \sqrt{\sum_{k=1}^{d}\left(x_{ik}-x_{jk}\right)^2 + \left(f\left(X_i\right)-f\left(X_j\right)\right)^2}. \tag{13}$$

Considering the global optimization of the national fitness $\min\{f(x)\}$, then the fitness rate of the national fitness behavior data mining is expressed as

$$\operatorname{Mdist}F_g = \frac{\sum_{i=1}^{N}\operatorname{dist}\left(i,F_g\right)}{N}. \tag{14}$$

Next, we set the threshold of particle swarm to ξ. Note that when the global optimum (i.e., the optimal value) is not altered in the exact time during the search process, then the moving step S can be used to determine the distinct values (optimal) with the smallest fitness. This should be kept in mind that the position of the i particle at time $k+1$ is expressed with the following formula (18):

$$x_i(k+1) = x_i(k) + s\left(\frac{x_j(k)-x_i(k)}{\left\|x_j(k)-x_i(k)\right\|}\right). \tag{15}$$

During the subsequent process, we input the weight and use the fitness function to assess and determine the particle mean square error (MSE). The calculation expression of the national fitness information data mining error is as follows:

$$\begin{aligned} E &= \sum_{j=1}^{q}\frac{E_j}{(q*k)}, \\ E_j &= \sum_{k}\varepsilon_k^2 = \sum_{k}\left(d_k-c_k\right)^2. \end{aligned} \tag{16}$$

In the above formula (16), q characterizes the total quantity of the input samples of national fitness data, ε_k represents the data mining distribution position vector of the national fitness behavior, and d_k represents the optimal (individual) and the global optimal extremum of the productivity layer, respectively. During the entire process of the iterative search, the weight of each particle can be calculated through adjusting the individual optimization and global optimization.

$$w_k^i = w_{k-1}^i\frac{p\left(z_k/x_k^i\right)p\left(x_k^i/x_{k-1}^i\right)}{q\left(x_k^i/x_{k-1}^i\right)}. \tag{17}$$

The particle swarm optimization (PSO) method is, therefore, adopted in order to enhance and boost the national fitness mining objective function and its associated parameters so as to precisely analyze and mine the big data of national fitness behavior. The characteristic function is expressed as

$$r = \frac{M^{-1}\sum_i j_i k_i - \left[M^{-1}\sum_i 1/2\left(j_i+k_i\right)\right]^2}{M^{-1}\sum_i 1/2\left(j_i^2+k_i^2\right) - \left[M^{-1}\sum_i 1/2\left(j_i+k_i\right)\right]^2}. \tag{18}$$

Finally, we analyze the static features of the data mining for national fitness behavior features and obtain the vector of particle velocity and the optimal (individual) position according to the particle optimization, which are expressed as

$$P = \min\left\{\sum_{i=1}^{\xi}P_i, 1\right\} = [x(n), x(n-1), \ldots, x(n-L+1)]^T. \tag{19}$$

From the above discussion, it is concluded that the process of data mining of the national fitness behavior characteristics is

$$\min\left(w,\xi,\xi^*\right) = X\frac{1}{2}\|w\|^2 + YC\sum_{i=1}^{n}\left(\xi_1+\xi_i^*\right). \tag{20}$$

$$\text{s.t. } H_i(z)\begin{cases} y_i - w^T\Phi(x) - b \le \varepsilon + \xi_i^*, \\ -y_i - w^T\Phi(x) + b \le \varepsilon + \xi_i, \\ \xi_i^*, \xi_i \ge 0. \end{cases} \tag{21}$$

In formulas (20) and (21), X represents the updated balance factor of the particle swarm (algorithm), Y represents the data mining load, and $H_i(z)$ represents the decision function with fuzzy data distribution of national fitness behavior characteristics, respectively [19, 20]. The above process completes the research on the informatization of national fitness public service in the construction of smart city [21].

5. Analysis of the Experimental Results

In order to verify the superior performance of information resource integration of national fitness public services and improve supply efficiency in the construction of smart city under big data, several simulation experiments were carried out. In the simulation experiment, the population of national fitness accounts for more than 30% of the total population, of which 60% of urban residents participate in the fitness activities in different types of sports clubs. The heterogeneous data mining test of the national fitness benefit index includes more than ten sports fitness projects, with a total of 500 fitness college students. Table 1 shows the experimental environment, system configuration, and experimental parameters along with hardware and software tools. Table 2 shows the time of national fitness behavior data mining between the proposed method and the traditional method.

It can be perceived from the detail shown in Table 2 that the data mining time of national fitness behavior data by using the method proposed in this paper is considerably faster than that by using the traditional method. Therefore, it shows that using this method can adaptively adjust the

Table 1: Description of the experimental environment and parameters.

Project	Parameter description and system settings
Node	One management node and 19 computing nodes
The operating system	Windows 7
The simulation environment	MATLAB 2017
The CPU mode	Automatically adjust CPU frequency based on task
The PC configuration	Intel(R)i5-2450M

Table 2: Time of national fitness behavior data mining using different methods.

Different methods for	Mining time/s
Method in this paper	70 s
The traditional method	110 s

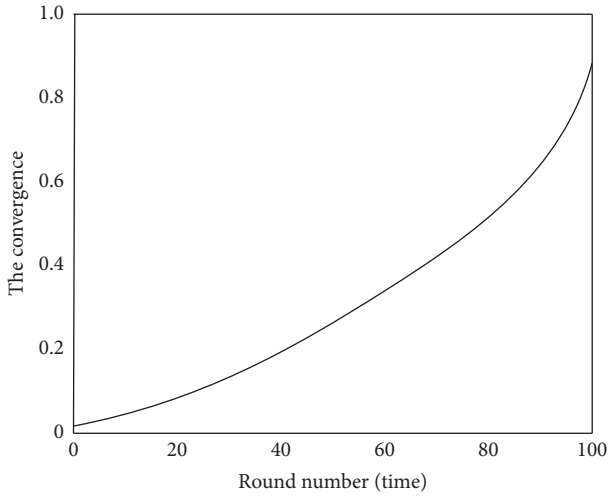

Figure 6: Convergence curve of the data mining algorithm.

Table 3: Overall performance of the data mining under different methods.

Different methods	Accuracy/%	Error rate/%	Reliability/%
Method in this paper	98	0.1	71
The traditional method	80	0.5	97

weight and realize the adaptive convergence of the data mining and big data. The convergence curve of the data mining algorithm is shown in Figure 6. Table 3 shows the overall performance, in terms of accuracy, error rate, and reliability, of the data mining under different methods.

Based on the analysis of Table 3 and Figure 6, using the heterogeneous data mining of the national fitness benefit index, we can get the relationship model of the promotion for the national fitness sports training on the social public health benefit index and master the improvement degree of the national fitness sports on the physical function of different groups. The accuracy and robustness of the data mining are also higher than other competing approaches. Figure 7 shows the comparison of the supply efficiency of public services for national fitness between the method, proposed in this paper, and other state-of-the-art methods proposed in the literature [1, 2].

By analyzing Figure 7, it can be seen that with the increase of data, the supply efficiency of the national fitness service proposed in [1] fluctuates significantly less and has been low. Moreover, the supply efficiency curve of the method proposed in [2] fluctuates more and is higher than that of the method proposed in [1]; however, the overall supply efficiency of the national fitness service is still lower than that of the method proposed in this paper. This shows that the method proposed in this paper can effectively integrate the current national fitness service resources and has good application value.

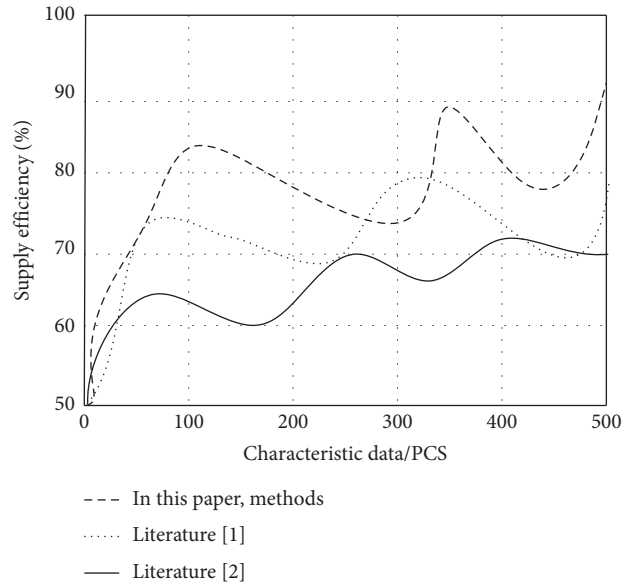

Figure 7: Efficiency of the national fitness service supply using different methods.

6. Conclusions and Future Work

In this paper, we firstly, developed a public service information platform of national fitness in smart city under big data. Then, we introduced the major modules in the platform in detail and proposed the heterogeneous data model of the national fitness benefit index. Next, we optimized the target parameters by using the particle swarm optimization (PSO) method to realize the big data mining and feature analysis of national fitness. Through evaluation and experimental results, we demonstrated that the proposed method can effectively integrate the current national fitness service resources and improve the efficiency of public service supply. Smart city construction under the big data is both an opportunity and a challenge. Through this opportunity, we will vigorously develop the cause of national fitness so that the public can obtain diversified and scientific information on national fitness public services. The national fitness informatization is the main support for constructing a hale and hearty country and an important prerequisite for the public to hanker for a healthier life.

No matter how smart cities will be built and developed, in the future, national fitness is a significant support for constructing a hale and hearty China and an inexorable prerequisite for the people to hanker for an improved and healthier life. The informatization of public service for national fitness must seize the opportunity and should not be limited to independent development but also integrate with different fields. In the future, with the support of the information technology, we will promote the informatization construction of public services for national fitness. In doing so, the government will play its leading role, increase capital investment, innovate development mode, improve service supply efficiency, and effectively improve the public service mechanism for national fitness. We will also investigate machine learning and other state-of-the-art technologies like Internet of things, edge computing methods, and their integration in the proposed method in order to increase accuracy and reliability.

Data Availability

Data are available on request from the corresponding author.

Conflicts of Interest

The authors declare that they have no conflicts of interest in this work.

Acknowledgments

This research received funding from the following sources: (1) 2019 Ministry of Education Humanities and Social Sciences Youth Fund Project: Research on the path and mechanism of China's rural community public sports service structural reform in the new era, project approval No. 19YJC890007, and (2) 2021 Study on the Countermeasures of rural public sports service in Xianning City, project approval No. 2021NJZD04.

References

[1] G. T. Zhang, Z. Gao, and H. Zhang, "Human action description algorithm based on depth motion trajectory information," *Journal of Optoelectronics - Laser*, vol. 28, no. 1, pp. 100–107, 2017.

[2] Y. W. Huang and C. L. Wang, "Human behavior recognition algorithm based on deep learning," *Application of Electronic Technique*, vol. 44, no. 10, pp. 1–5, 2018.

[3] X. M. Ma, N. G. Feng, and Y. Y. Wang, "Body motion recognition based on moving feature coupled bag-of-sequence," *Computer Engineering and Design*, vol. 39, no. 10, pp. 3220–3227, 2018.

[4] H. Li, Z. Y. Yu, and Y. C. Yin, "Human motion pattern recognition algorithm based on CNN-Mogrifier LSTM," *Electronic Measurement Technology*, vol. 44, no. 21, pp. 95–100, 2021.

[5] J. Y. Lin and Y. H. Zhang, "Research on marketing strategy of supermonkey fitness club based on internet positioning theory," *Contemporary Sports Technology*, vol. 11, no. 32, pp. 137–141, 2021.

[6] L. Xiao, "Design of mobile app system for exercise fitness evaluation," *Microcomputer Applications*, vol. 36, no. 10, pp. 119–121, 2020.

[7] L. Yu, X. Liu, X. Yu, X. Yu, and Y. Cai, "ADP-ribosylhydrolases: from DNA damage repair to COVID-19," *Journal of Zhejiang University - Science B*, vol. 22, no. 1, pp. 21–30, 2021.

[8] T. X. Guo, Q. R. Hu, and J. W. Li, "Fitness action recognition method based on human skeleton feature encoding," *Journal of Computer Applications*, vol. 41, no. 5, pp. 1458–1464, 2021.

[9] P. Wang, "Design and implementation of multi class fitness service client based on cloud services," *Electronic Design Engineering*, vol. 25, no. 14, pp. 32–35, 2017.

[10] L. Xu, Q. J. Wang, and W. T. Meng, "Internal demands and path selection of school sports venues in the era of big data to serve the national fitness wisdom governance," *Journal of Shandong Institute of Physical Education and Sports*, vol. 37, no. 5, pp. 73–82, 2021.

[11] G. P. Martin, P. Carter, and M. Dent, "Major health service transformation and the public voice: conflict, challenge or complicity?" *Journal of Health Services Research and Policy*, vol. 23, no. 1, pp. 28–35, 2018.

[12] J. Lasky, A. Kashem, S. H. Brann et al., "Do public health service increased risk donor lungs negatively affect survival outcomes?" *The Journal of Heart and Lung Transplantation*, vol. 39, no. 4, p. S382, 2020.

[13] E. H. D. Davi and M. A. D. T. Bruns, "Para ficar em cima do salto: a construção do corpo travesti na perspectiva Merleau-Pontyana," *PHENOMENOLOGICAL STUDIES - Revista da Abordagem Gestáltica*, vol. 23, no. 2, pp. 158–166, 2017.

[14] L. Lawson and L. Andrew, "Body" building: expanding Arkansas's standard for holographic wills," *Arkansas Law Review*, vol. 71, no. 4, p. 3, 2018.

[15] J. M. Labuz, C. Moraes, D. R. Mertz, B. M. Leung, and S. Takayama, "Building an experimental model of the human body with non-physiological parameters," *Technology*, vol. 05, no. 01, pp. 42–59, 2017.

[16] Y.-M. Jung and Y.-H. Seo, "Effect of autonomous fitness movement of obese middle-aged women to improve lifestyle-related disease factors," *Korean Journal of Sports Science*, vol. 26, no. 6, pp. 1151–1156, 2017.

[17] Y. Negra, H. Chaabene, S. Sammoud et al., "Effects of plyometric training on physical fitness in prepuberal soccer athletes," *International Journal of Sports Medicine*, vol. 38, no. 05, pp. 370–377, 2017.

[18] S. Youm, Y. Jeon, S.-H. Park, and W. Zhu, "RFID-based automatic scoring system for physical fitness testing," *IEEE Systems Journal*, vol. 9, no. 2, pp. 326–334, 2015.

[19] C. Helma, T. Cramer, S. Kramer, and L. De Raedt, "Data mining and machine learning techniques for the identification of mutagenicity inducing substructures and structure-activity relationships of noncongeneric compounds," *ChemInform*, vol. 35, no. 39, pp. 1402–1411, 2004.

[20] F. Zhang, "Prediction and evaluation of urban eco-sports tourism behavior using data mining technology," in *Proceedings of the 2019 4th International Conference on Big Data and Computing*, pp. 68–71, IEEE, Guangzhou, China, May 2019.

[21] M. A. Serdar, B. B. Can, M. Kilercik et al., "Analysis of changes in parathyroid hormone and 25 (OH) vitamin D levels with respect to age, gender and season: a data mining study," *Journal of Medical Biochemistry*, vol. 36, no. 1, pp. 73–83, 2017.

Hindawi
Scientific Programming
Volume 2023, Article ID 9769278, 1 page
https://doi.org/10.1155/2023/9769278

Retraction

Retracted: Construction of a Six-Pronge Intelligent Physical Education Classroom Model in Colleges and Universities

Scientific Programming

Received 26 September 2023; Accepted 26 September 2023; Published 27 September 2023

This article has been retracted by Hindawi following an investigation undertaken by the publisher [1]. This investigation has uncovered evidence of one or more of the following indicators of systematic manipulation of the publication process:

(1) Discrepancies in scope
(2) Discrepancies in the description of the research reported
(3) Discrepancies between the availability of data and the research described
(4) Inappropriate citations
(5) Incoherent, meaningless and/or irrelevant content included in the article
(6) Peer-review manipulation

The presence of these indicators undermines our confidence in the integrity of the article's content and we cannot, therefore, vouch for its reliability. Please note that this notice is intended solely to alert readers that the content of this article is unreliable. We have not investigated whether authors were aware of or involved in the systematic manipulation of the publication process.

In addition, our investigation has also shown that one or more of the following human-subject reporting requirements has not been met in this article: ethical approval by an Institutional Review Board (IRB) committee or equivalent, patient/participant consent to participate, and/or agreement to publish patient/participant details (where relevant).

Wiley and Hindawi regrets that the usual quality checks did not identify these issues before publication and have since put additional measures in place to safeguard research integrity.

We wish to credit our own Research Integrity and Research Publishing teams and anonymous and named external researchers and research integrity experts for contributing to this investigation.

The corresponding author, as the representative of all authors, has been given the opportunity to register their agreement or disagreement to this retraction. We have kept a record of any response received.

References

[1] L. Zhou and Q. Tang, "Construction of a Six-Pronge Intelligent Physical Education Classroom Model in Colleges and Universities," *Scientific Programming*, vol. 2022, Article ID 9003864, 11 pages, 2022.

Hindawi
Scientific Programming
Volume 2022, Article ID 9003864, 11 pages
https://doi.org/10.1155/2022/9003864

Research Article

Construction of a Six-Pronge Intelligent Physical Education Classroom Model in Colleges and Universities

Lihua Zhou[1] **and Qiang Tang**[2]

[1]*Department of Physical Education, Xiangtan University, Xiangtan, Hunan 411105, China*
[2]*Physical Education Teaching and Research Group, Mingde Tianzhong Middle School, Changsha, Hunan 410029, China*

Correspondence should be addressed to Lihua Zhou; zlh1818@xtu.edu.cn

Received 28 March 2022; Revised 15 April 2022; Accepted 21 April 2022; Published 6 May 2022

Academic Editor: Muhammad Zakarya

A main form of information construction in colleges and universities is smart campus, which is a new model based on the improvement and perfection of digital campus construction. The development of smart campus is inseparable from the support of technologies such as Internet of Things (IoTs), cloud computing, and big data. By perceiving the teaching environment and intelligently identifying the characteristics of teachers and students, it can be used as a basis to improve the physical education, teaching environment, and digital teaching space, that is, an intelligent and diversified teaching environment for college teachers and students. In this study, we introduce an intelligent teaching mode into physical education classroom, construct the "six-pronge" intelligent classroom model, and apply the model by setting up a control and an experimental group to study the application effects of the proposed model in physical education teaching. The control group consists of the students who do not adopt the teaching mode, while students in the experimental group use the intelligent physical education teaching model. Through a comparative analysis, students' physical education classroom teaching atmosphere, students' learning interest and learning attitude, the proposed intelligent physical education classroom model are tested and verified. The analysis results show that after implementation of the "six-pronged" intelligent physical education classroom model, the physical education classroom atmosphere is active, and students have strong interest in learning and correct learning attitude. We believe that the model can help students complete pre-class preparation, in class teaching and after class practice supervision, and obtain a lot of knowledge about physical training. In addition, the model can help to cultivate students' lifelong physical education learning and exercise habits, and greatly improve the quality of physical education classroom teaching in colleges.

1. Introduction

In the world, colleges and universities are the cradle of cultivating national talents. However, due to the high pressure of schoolwork, Chinese students generally lack physical exercise. They have not formed the habit of physical exercise since childhood and do not pay attention to physical education after entering colleges and universities. They believe that physical education is not a compulsory course, which makes the physical quality of Chinese college students poor. For this problem, colleges and universities need to strengthen physical education curriculum teaching. In addition, the traditional physical education teaching mode in colleges and universities cannot keep up with the development of the times and technologies [1]. Therefore, it is essential to account for state-of-the-art technologies that should be integrated into the classrooms for better quality education and student experiences, as well as, teachers' practices.

With the rapid development of information technology, experts all over the world began to focus on exploring the field of smart classrooms [2, 3]. Furthermore, in the era of wisdom, the rapid development of cloud computing technology, big data, Internet of Things (IoTs), and other emerging computational technologies has accelerated the reform stage of intelligent physical education classroom. In this paper, we construct a "six-pronge" intelligent physical education classroom model to change the current situation of physical education teaching and diversify the previous

single physical education classroom model. The "six-pronge" intelligent sports classroom model is centered on six stages, that is, (i) the "student-centered" three levels, (ii) three platforms, (iii) three modules, (iv) the student sports classroom teaching system, (v) the off campus training group, and (vi) the closed-loop practice teaching quality monitoring system. Moreover, the "six-pronge" teaching quality assurance system for the construction of the teaching staff ensures that teachers are constantly focusing on the quality of classroom teaching.

Moreover, this paper constructs a "six-pronge" smart classroom system centered on students' activities, which uses sensor-based human motion patterns to identify students' sports actions, and teachers guide. Subsequently, we analyze the sensor-based data according to students' sports data, which is conducive to students' after-school training and classroom content consolidation [2]. We also build an intelligent physical education classroom model, for colleges and universities, on the intelligent terminal equipment platform. We apply the developed model to the physical education classroom in colleges and universities, analyze and apply the teaching model to college students, and randomly select students who do not use the teaching model. Through a comparative analysis, we analyze the interest of physical education classroom teaching atmosphere, students' learning interest and learning attitude, and analyze the role of intelligent physical education classroom model. The following are the main contributions of the research presented in this paper:

(i) we introduce the intelligent teaching mode into the physical education classroom and constructs the "six-pronged" intelligent physical education classroom model in colleges and universities, and apply the model in the physical education classroom teaching in colleges and universities.

(ii) we build an intelligent physical education classroom model in colleges and universities on the intelligent terminal equipment platform, apply the model to the physical education classroom in colleges and universities.

(iii) by setting up a control and an experimental group to study the application effects of physical education classroom model in physical education teaching, in which the control group is the students who do not adopt the teaching mode, and the experimental group is the students who use the intelligent physical education teaching model.

The rest of the manuscript is structured as follows: In Section 2, we briefly discuss state-of-the-art research work within the domain of intelligent teaching models. Section 3 talks over the "Six-pronge" an intelligent physical education classroom system in colleges and universities. Construction of an intelligent physical education classroom model is elaborated in Section 4. Experimental results and analysis of the "six-pronge" intelligent physical education classroom are discussed in the subsequent Section 5. Finally, Section 6 summarizes this manuscript while offering several directions for more research and investigation.

2. Related Work

Smart physical education classroom is an important part of smart classrooms. With the rapid development of information technology, experts all over the world began to focus on exploring the field of smart classrooms [3]. Aversi-Ferreira et al. analyzed a similar model and observed that the current distance education is only in one-way teaching and network courseware, which is difficult to support the interaction between teachers and students in the classroom. Therefore, the authors put forward a new demonstration mode and distance teaching, which can realize the interaction between virtual scenes, teachers, and students. Focusing on the design of intelligent teachers, the authors put forward a variety of ways on how to use virtual reality technology in distance teaching [4]. Faria et al. also analyzed the current teaching situation of installing intelligent devices in Israeli national schools. Students have high-learning enthusiasm in the classroom and can give full play to teachers' ability. In addition, the authors also studied students' learning status in the smart classroom environment and analyzed various advantages and disadvantages of the applications of smart classrooms for students in teaching institutes [5].

From the perspectives of reflective thinking, student negotiation, function design, and ease of use, Mabassa et al. investigated and observed students' preference for teaching classroom in intelligent classroom learning, and come to the conclusion that the developed instrument is used as a reliable tool to judge college students' preference for intelligent classroom learning environment [6]. Similarly, other scholars also analyzed from the two aspects of classrooms: (i) wisdom, and (ii) intelligent classroom. Liu et al. analyzed from the two points of informatization and education, fundamentally changing the traditional "knowledge classroom" into "intelligent classroom," so as to strengthen students' intelligent ability [5]. Guo et al. pointed out that smart classroom is inseparable from the support of new technology environment. A new classroom teaching model is established for the purpose of cultivating students' wisdom [7]. Liu et al. proposed that smart classroom is based on constructivism learning theory, which trains students to master learning wisdom according to the new generation of information technology, highlights the individual differences of different students, and strengthens the emotional communication between teachers and students [8].

Wang et al. pointed out that under the rapid development of informatization, the concept of intelligent classroom was put forward and applied, and integrated with education and teaching [9]. Zeng et al. propose to carry out geography classroom education in the smart classroom based on iPad. Compared with traditional multimedia environment teaching, it can effectively improve students' interest in learning geography, enhance students' attention, better understand and master knowledge, and improve students' autonomous learning abilities [10]. Shao put forward that smart classroom is consistent with the requirements of the current new curriculum reforms in different colleges, universities, and teaching institutes [11]. They believe that the

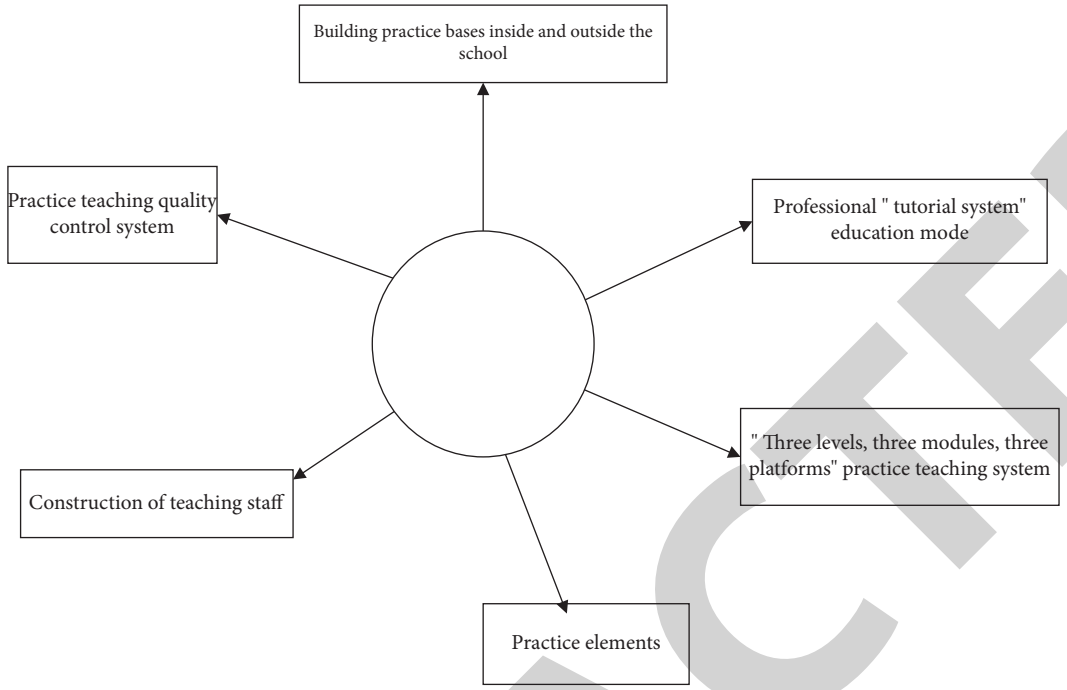

Figure 1: The "six-pronge" physical education classroom teaching quality assurance system.

application of smart classroom concept in physical education teaching strategy can fully show the interest, innovation, and sense of experience of physical education teaching [12].

Bai proposed several smart classroom methods and approaches which are based on e-book package. In addition, the authors have analyzed the smart learning content, evaluation methods, and basic composition on the created smart classroom system to form a complete system [13]. Based on the in-depth analysis of the technical characteristics of smart classroom, Wang and Zheng designed the latest learning model of smart classroom and applied it in practice [14]. Hu et al. launched the smart classroom teaching mode of "three stages and ten steps." The core of this mode is to organically combine the teaching mode with information technology and test the advantages of the teaching mode through experiments [15]. Wang and Zhao divided the system's functional requirements on the basis of big data and cloud computing platform. Their proposed model can design online classroom modules and improve the interactivity of video transmission, significantly [16].

3. "Six-Pronge" Intelligent Physical Education Classroom System in Colleges and Universities

3.1. Building a "Six-Pronge" Smart Classroom System. This paper adopts the "six-pronge" concept and the student-centered smart classroom system to replace the traditional "teacher-centered" education model [17]. Based on students' innovative and practical abilities, set up curriculum project cards, open implementation projects, graduation projects, and extracurricular scientific and technological works. In order to improve the practicality of students' physical education classroom and strengthen the professionalism of training, a layered and modular system is established to cultivate students' strong innovative thinking and practical abilities. The proposed modular system consists of three platforms: (i) in school classroom, (ii) extracurricular, and (iii) out of school classroom. In order to standardize the management and improve the quality of teaching, we establish two systems, that is, (a) the teaching-quality monitoring system, and (b) the teaching evaluation quality system. The main purpose of the system is to ensure the quality of daily physical education, and put forward the "three levels, three platforms and three modules" student physical education classroom teaching system, the training system outside the school, the closed-loop practice teaching quality monitoring system, and the "six-pronge" sports classroom teaching quality assurance system [18]. The proposed model is shown in Figure 1.

3.2. Human Motion Pattern Recognition Based on Sensor. In this study, the human movement pattern recognition method based on sensor is used to collect and recognize students' physical education classroom actions. The proposed system is more accurate than the traditional naked eye recognition and judgment method of teachers. Moreover, it can master the data of students' learning physical actions, intensity, training degree, and so on. The essence of this recognition mode is to use sensors to collect students' physical education classroom data, train the recognizer that meets the requirements of the recognition system according to the collected data, and finally recognize human motion data on the successfully trained recognizer. The recognition process includes various stages such as collecting the data, preprocessing the collected data, selecting, and extracting

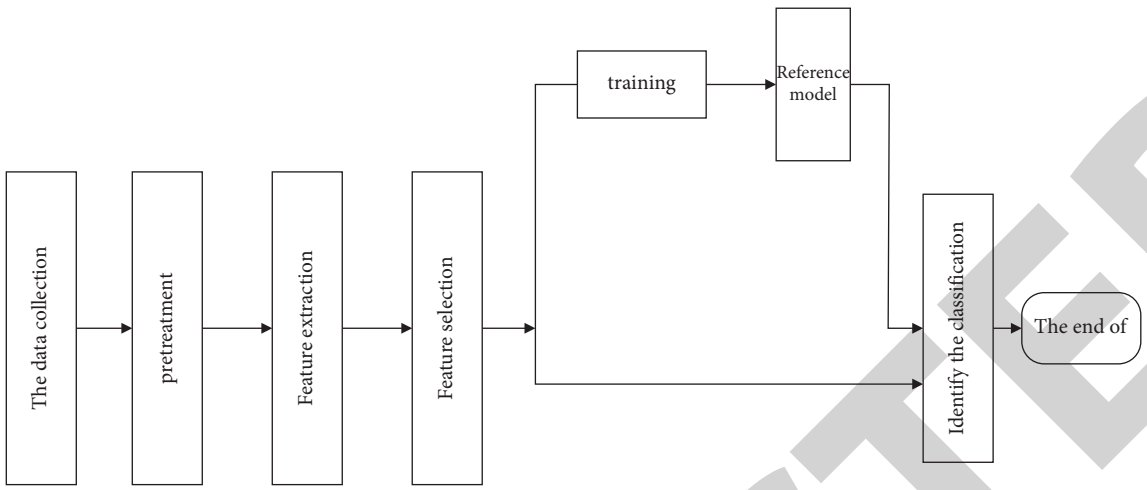

Figure 2: Human motion pattern recognition process.

features (using feature extraction from learning systems), and selecting recognizer. The specific process is shown in Figure 2.

In this study, 11 kinds of characteristic acceleration signals on X-axis, Y-axis, and Z-axis in frequency domain and time domain are extracted. The process of eigenvalue extraction algorithm is described in detail below. The Ai represents the i sampling value of any axis in X-axis, Y-axis, and Z-axis acceleration signals, and its relationship is represented by $A \in \{X, Y, Z\}$, where n represents the window length.

3.2.1. Mean Calculation Formula.

$$\mu_A = \frac{1}{n}\sum_{i=1}^{n} A_i. \tag{1}$$

The DC component of acceleration signal is the main meaning of mean value, which is used to show the difference of characteristics of different motion signals.

3.2.2. Calculation Formula of Standard Deviation.

$$\sigma_A = \sqrt{\frac{1}{n-1}\sum_{i=1}^{n}(A_i - \mu_A)^2}. \tag{2}$$

The mean value of acceleration data in the window is represented by μ_A. The standard deviation is the most widely used statistical feature, which can directly reflect the dispersion degree of acceleration compared with the average value [19]. At the same time, the standard deviation is in positive proportion to the intensity of human movement.

3.2.3. Energy Calculation Formula

$$E_A = \sum_{i=1}^{n} |A_i|^2. \tag{3}$$

The acceleration data energy in the window is represented by E_A, and the energy consumption of human motion in the window time is explained through the energy characteristics. For example, compared with running at the same time, running consumes more energy, so it can be accurately distinguished by energy characteristics.

3.2.4. Calculation Formula of Crest Factor.

$$A_{CrFr} = \frac{0.5(A_{\max} - A_{\min})}{\sqrt{1/n\sum_{i=1}^{n} A_i^2}}. \tag{4}$$

The highest and lowest values on the acceleration signal in the window are represented by A_{max} and A_{min}, respectively. The peak factor of the acceleration signal is A_{CrFr}r, and the peak factor is the ratio between waveform peak and effective value, which can effectively express the intensity of human movement.

3.2.5. Kurtosis Calculation Formula.

$$A_K = \frac{1}{n\sigma_A^4}\sum_{i=1}^{n}(A_i - \mu_A)^4. \tag{5}$$

The variance and mean value of the acceleration signal in the window are determined by σ_A and μ_A, respectively. According to the value obtained from formula (5), the steepness of the acceleration signal curve waveform can be reflected.

3.2.6. Skewness Calculation Formula

$$A_{SK} = \frac{n}{(n-1)(n-2)\sigma_A^3}\sum_{i=1}^{n}(A_i - \mu_A)^3. \tag{6}$$

The variance of the acceleration signal in the window is determined and represented by σ_A, the mean value is represented by μ_A, and the skewness of acceleration signal in the window is represented by ask. Furthermore, according to the

skewness result, the skew direction, and asymmetry degree of the data distribution can be judged. The skewness value is either positive or negative as the discussion follows. In case, if the acceleration signal value in the window is lower than the average value, then it indicates that the skewness result of the value is negative, otherwise, the skewness result value is positive and vice versa.

3.3. Analysis of "Six-Pronge" Physical Education Classroom Teaching Resource System. Based on the field of deep learning, the most important thing in the process of teachers' physical education classroom teaching is teachers' key ability, which involves teachers' personal physical education skills, teaching attitude, and personal knowledge reserve. Therefore, in the in-depth teaching environment, teachers should have digital survival ability, scientific and technological integration ability, lifelong learning ability, and professional teaching ability. On the basis of this ability, the quality of the physical education classroom teaching can be guaranteed. The key abilities of teachers are directly related to the cultivation and realization of the "six-pronge" of physical education classroom teaching. In addition, teaching institute such as colleges and universities can collect resources inside and outside the classroom in order to provide students with physical education teaching environment. Similarly, they can contact large-scale sports venues outside the school to establish cooperative relations, and they provide venues [20].

Schools provide teaching resources to jointly complete physical education teaching training, so that students are not limited to the teaching methods of traditional classroom books, teaching materials, and theoretical knowledge. It can let students really get in touch with all kinds of sports and avoid some students being unable to train on the spot due to less contact with sports. At the same time, when cultivating students' "six-pronge" sports teaching, by combining teachers' theoretical knowledge and students' independent display, each student can show the sports learned in sports classroom teaching. After that, the teachers will guide each student's sports activities and evaluate the nonstandard actions in the process of students' sports training. In addition, teachers focus on explaining the difficulties of physical training and let students know the essentials of movement by demonstration. Moreover, schools, colleges, and universities could adopt diversified teaching methods in the physical education classroom, hire professional teachers to teach the sports that need to be studied in the university, and strengthen the strength and professionalism of the schoolteacher team.

Carrying out physical education classroom teaching in this way (as described above) can improve the sports professionalism of students. This should be noted that physical education classroom teaching is not only a simple skill training but also combined with in class and out of class resources to cultivate students' "six-pronge" ability, so that students can apply their theoretical knowledge to practical physical training in physical education classroom. Besides the above-illustrated scenarios, students can also participate in college community activities or physical education competitions to improve their personal sports capabilities.

4. Construction of Intelligent Physical Education Classroom Model

4.1. Intelligent Terminal Equipment Platform. Intelligent terminal equipment platform refers to a variety of different types of terminal equipment tools, which is an important tool for teachers to carry out intelligent physical education classroom teaching [21]. The main function of the platform is to collect data from sensors, and use the Internet medium to transmit data to the health cloud management platform. In addition, it can intuitively feedback the cloud data analysis results. Teaching institutes including colleges and universities can build an intelligent terminal platform according to the actual situation. Through this platform, students' physique, sports capabilities, and sports performance can be tested and entered. At the same time, the platform is also an intelligent fitness equipment, which can monitor students' center jump, speed, sports ability, and other data in real time. These are some of the most important basis for judging students' physical qualities. As a result of the above model, all physical education teachers classify students according to students' physical exercise data and adopt different teaching methods for different groups of students. This will essentially help to realize accurate teaching for different types of students, improve students' enthusiasm to participate in physical education classroom, let students complete physical training under their affordable physical education classroom teaching methods, and give full play to the advantages of each student.

4.2. Subject Structure of Intelligent Physical Education Classroom in Colleges and Universities. The construction of an intelligent physical education classroom in colleges and universities belongs to system engineering, which should be realized with the support of big data, cloud computing, Internet of Things (IoTs), Internet medium, and other emerging technologies. Based on the intelligent service platform of "cloud, museum, and end," the theoretical knowledge of the physical education classroom is pushed, and the information management mode is adopted to evaluate the process of intelligent physical education classroom teaching [22]. Starting from the overall structure characteristics of smart physical education classroom, this paper constructs smart physical education classroom in a bottom-up way. The proposed intelligent smart physical education in the context of smart classrooms is as shown in Figure 3. The platform consists of four different layers: (i) foundation layer, (ii) data processing layer, (iii) end-user service layer, and (iv) teaching realization layer. Discussion around these layers can be found in subsequent sections.

4.3. Constructing Intelligent Physical Education Classroom Model in Colleges and Universities. Compared with the traditional physical education classroom-teaching mode, the intelligent physical education classroom teaching proposed in this study is significantly different [23]. The main purpose of the traditional physical education classroom is to tell the theoretical knowledge in the classroom, and then carry out

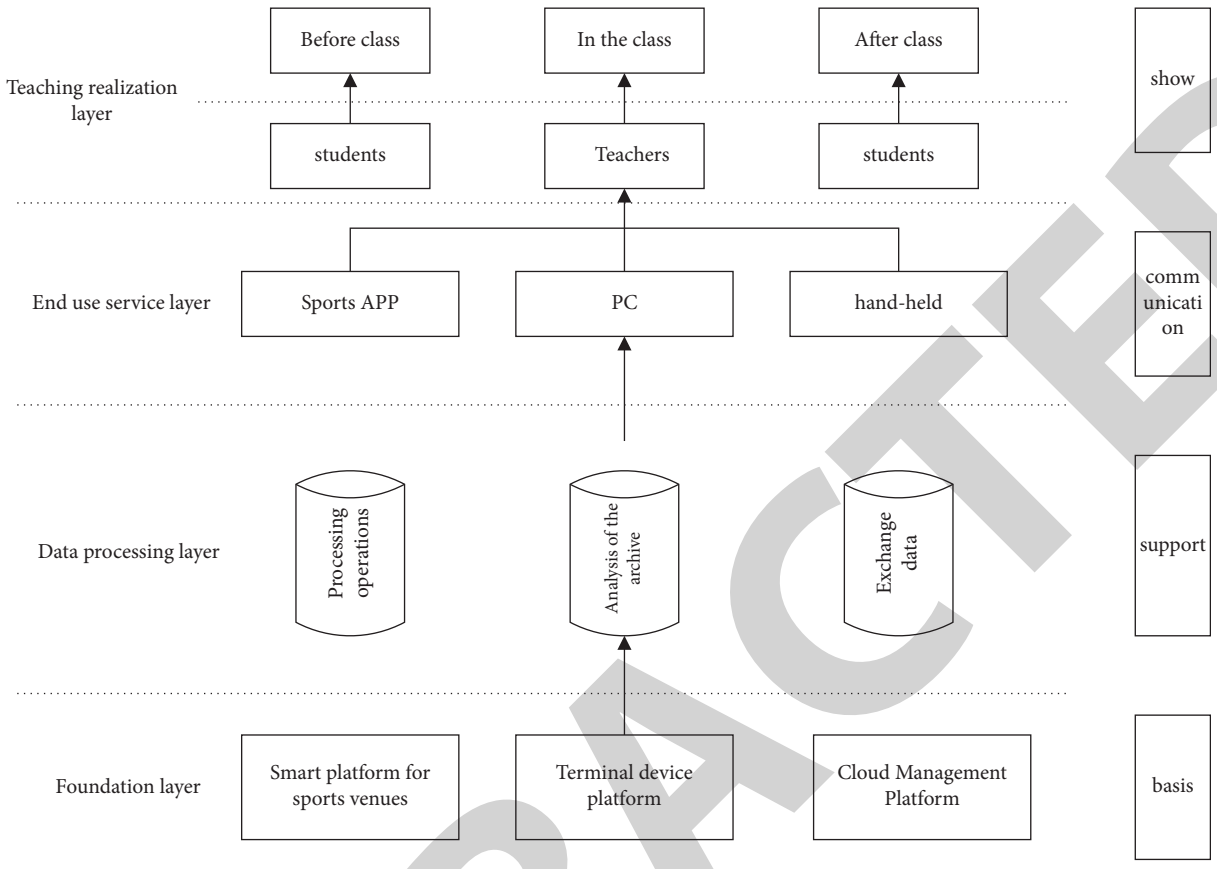

Figure 3: Main structure of intelligent physical education classroom in colleges and universities.

teaching and intelligent physical education classroom. By using information technology to enrich the classroom content and applying big data technology to intelligently reform the physical education classroom, evaluate the students' preview before class, determine teaching by learning, real-time monitor the training during and after class, and give full play to the students' subjectivity and initiative [24]. Moreover, pay attention to the individual differences of each student, teach students according to their aptitude, and evaluate the students' physical education classroom learning process. Combined with the characteristics of smart physical education classroom, the smart physical education classroom teaching model is established and divided into three stages, namely, (i) pre-class preparation, (ii) in class teaching, and (iii) after-class training. Figure 4 shows the smart physical education classroom teaching structure model.

This study establishes an intelligent college physical education classroom on the information platform, in the context of smart classrooms. Moreover, it extends physical education classroom education to before and after the class, promotes the mutual communication between students and teachers and realizes the sharing of all kinds of resources. Before teaching, teachers can design the teaching mode according to the data processing cloud information. Students can obtain the teacher's class content from the terminal and preview it in advance. After preview, students' initiative in the physical education classroom can be improved, and they can also follow the teacher's teaching ideas. In the course, teachers use intelligent devices to understand students' learning status in real time, conduct differential teaching for different types of students based on real-time information, and monitor students' exercise intensity. Middle-school students in physical education classroom can also learn physical education knowledge independently and communicate training essentials with other students. After the physical education classroom teaching, teachers use the intelligent platform to reasonably arrange the after-school training tasks, and take online counseling for the places where students are not clear. In addition, students can exercise independently after class so as to master the classroom teaching content, strengthen the physical education classroom teaching results, and cultivate students to develop good physical exercise habits.

5. Analysis of the "Six-Pronge" Intelligent Physical Education Classroom

According to the "six-pronge" intelligent physical education classroom model established above, the practical application effect is analyzed by means of questionnaire [25]. Taking the students of aerobics course as the research object, the "six-pronge" intelligent physical education classroom model is implemented in a university for one semester, and the practical application effect of the model is tested at the end of

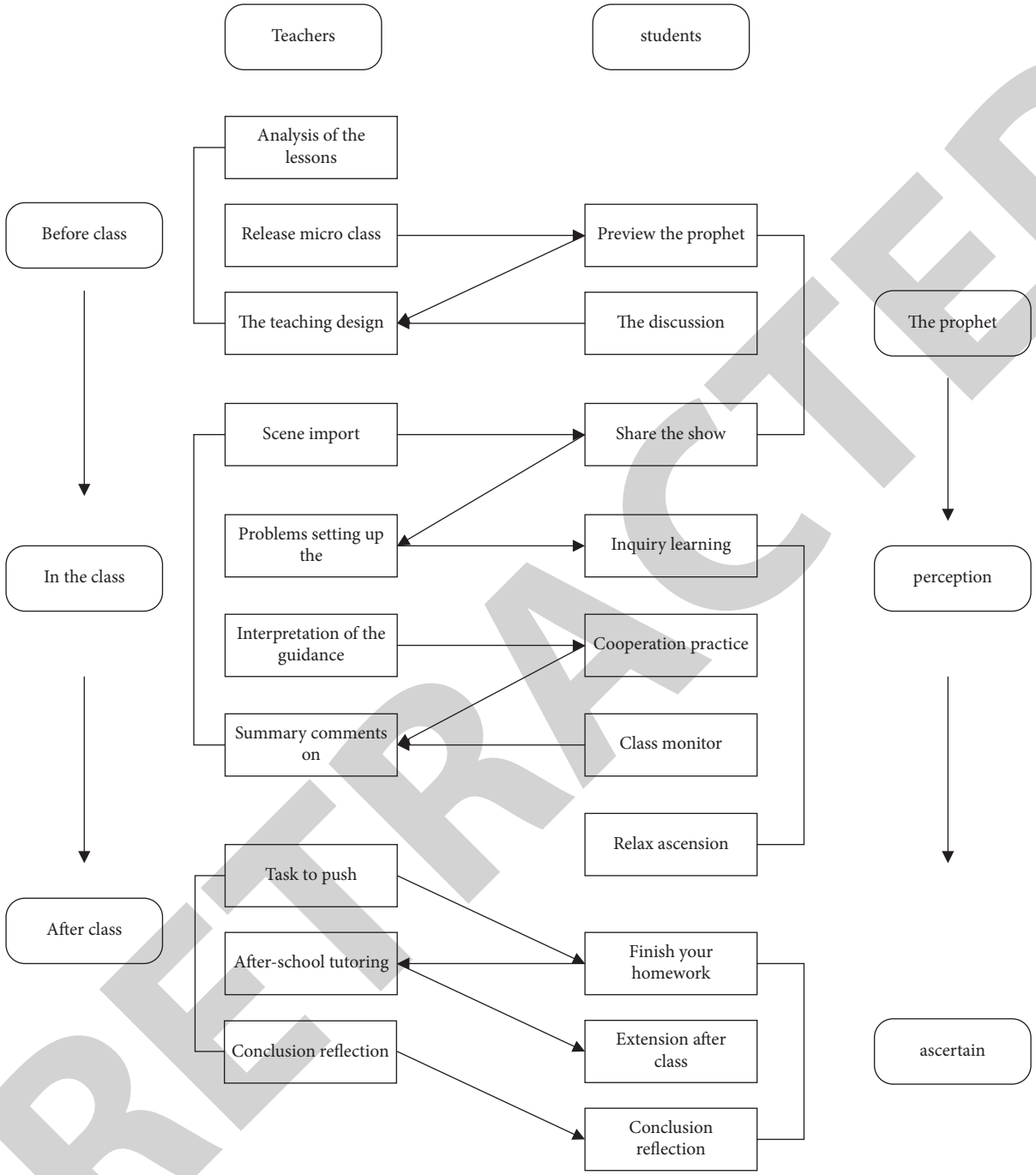

Figure 4: Intelligent physical education classroom teaching structure model.

the semester. Approximately, 40 students were randomly selected for the questionnaire survey. The 40 students were in the experimental group, and a total of 40 questionnaires were distributed. Then, 40 students who did not carry out the "six-pronge" intelligent physical education classroom teaching in colleges and universities were randomly selected as the control group. Thus, 40 questionnaires were distributed, and all questionnaire reports were recovered. The degree coefficient of the questionnaire exceeded 0.8, indicating that the data has high reliability and can be used in later analysis. Tables 1 and 2 illustrate the reliability test results of the questionnaire in the experimental group and the control group, respectively.

5.1. Analysis of Classroom Teaching Atmosphere Feeling. The students in the experimental group use smart phones to answer the questions raised by the students in the physical education classroom. The students record videos for each other. The classroom atmosphere is active and interesting. They correct each other's physical training movement problems so that the students can grow together in the physical

Table 1: Reliability test results of questionnaire survey in the experimental group.

Questionnaire object	Number of questionnaires returned	The effective volume	The correlation coefficient
Aerobics course students	40	40	$R = 0.832$

Table 2: Reliability test results of questionnaire survey in the control group.

Questionnaire object	Number of questionnaires returned	The effective volume	The correlation coefficient
Aerobics course students	40	40	$R = 0.856$

education classroom. The control group still adopts the traditional teaching mode in the physical education classroom. The teachers tell the theoretical knowledge and the students practice in groups. In the process of group practice, some students do not practice seriously and appear lazy. Only a few students train according to the requirements of the teachers. The whole classroom atmosphere is rigid, and there is less communication between students. This study investigates and analyzes the evaluation and analysis results of the students in the experimental group and the control group on the sports classroom atmosphere, and draws the following Figure 5 to show the analysis results of the sports classroom atmosphere. The vast majority of the experimental group has a good experience of this new teaching mode, and the teaching atmosphere is ideal, which can stimulate students' interest in learning. More than 50% of the students in the control group said that the physical education classroom atmosphere is not active and cannot raise their interest in learning.

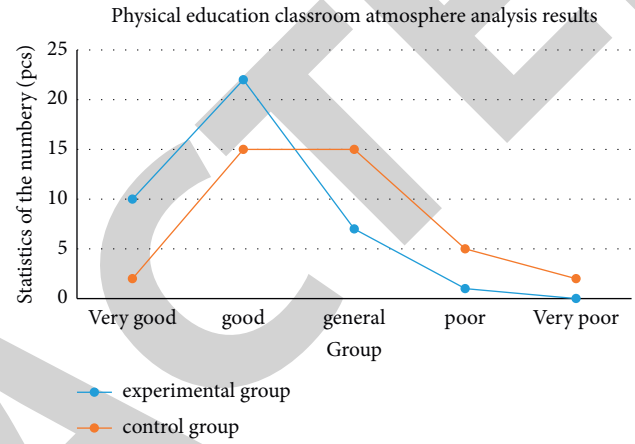

Figure 5: Analysis results of physical education classroom atmosphere.

5.2. A Comparative Analysis of Students' Learning Interest and Learning Attitude. After one semester of the "six-pronge" smart physical education classroom teaching, the students in the experimental group analyzed their interest in physical education courses. The data results are shown in Figure 6. A total of 21 people in the experimental group showed significant improvement in learning interest, while only 8 people in the control group. Because each student's learning ability, physical fitness, and personal experience are different; therefore, individual differences are observed. After comparison, the improvement of students' learning interest in the experimental group is much higher than that in the control group.

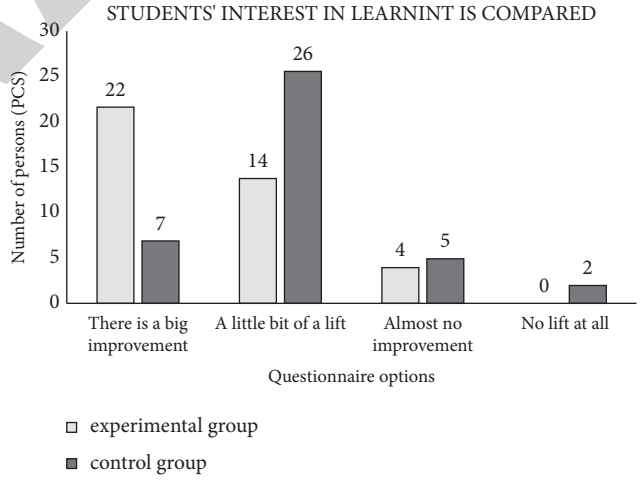

Figure 6: Comparison results of students' learning interests.

This study analyzes the changes of students' physical education learning attitude after colleges and universities use the proposed "six-pronge" intelligent physical education classroom model. This includes taking the initiative to communicate with other students and teachers whether to preview physical education courses in advance, whether to practice after the class, and whether to take physical training as a way of personal exercise. The statistics of students' learning attitude in the experimental group are listed in Table 3 and the survey results of the students in the control group are shown in Table 4. The results show that compared with the control group, the experimental group has more communication times, more active classroom atmosphere, and more mutual communication with teachers [26]. The experimental group submits physical training assignments through the intelligent physical education classroom platform, and the teachers will score according to the students' completion. After physical education teaching, the students in the experimental group and the control group were asked again whether they would like to continue reading and exercise in the later stage or not. Most of the students in the experimental group expressed interest in the physical education and would take the initiative to learn and exercise later, while the students in the control group were observed less interested.

5.3. Analysis on the Role of Intelligent Physical Education Classroom Model. Based on the "six-pronge" intelligent physical education classroom model constructed above, this

Table 3: Analysis of students' learning attitude in the experimental group.

The experimental group	A often	B occasionally	C almost not	D never
Take the initiative to communicate with other students and teachers	19 (48.7%)	15 (37.9%)	5 (12.6%)	1 (2.3%)
Whether to prepare physical education courses in advance	27 (65.4%)	12 (28.4%)	4 (7.6%)	0 (0%)
Do you practice after class?	18 (43.2%)	17 (41.2%)	3 (7.6%)	4 (11.2%)
Whether physical training as a personal exercise	6 (15.2%)	24 (58.4%)	8 (21.3%)	4 (7.6%)

Table 4: Analysis of students' learning attitude in the control group.

The experimental group	A often	B occasionally	C almost not	D never
Take the initiative to communicate with other students and teachers	9 (21.6%)	8 (22.6%)	14 (32.5%)	11 (25.2%)
Whether to prepare physical education courses in advance	2 (5.4%)	11 (28.1%)	19 (45.6%)	9 (22.6%)
Do you practice after class?	0 (0%)	4 (7.6%)	14 (32.6%)	24 (62.6%)
Whether physical training as a personal exercise	4 (7.8%)	7 (15.4%)	20 (47.3%)	13 (30.2%)

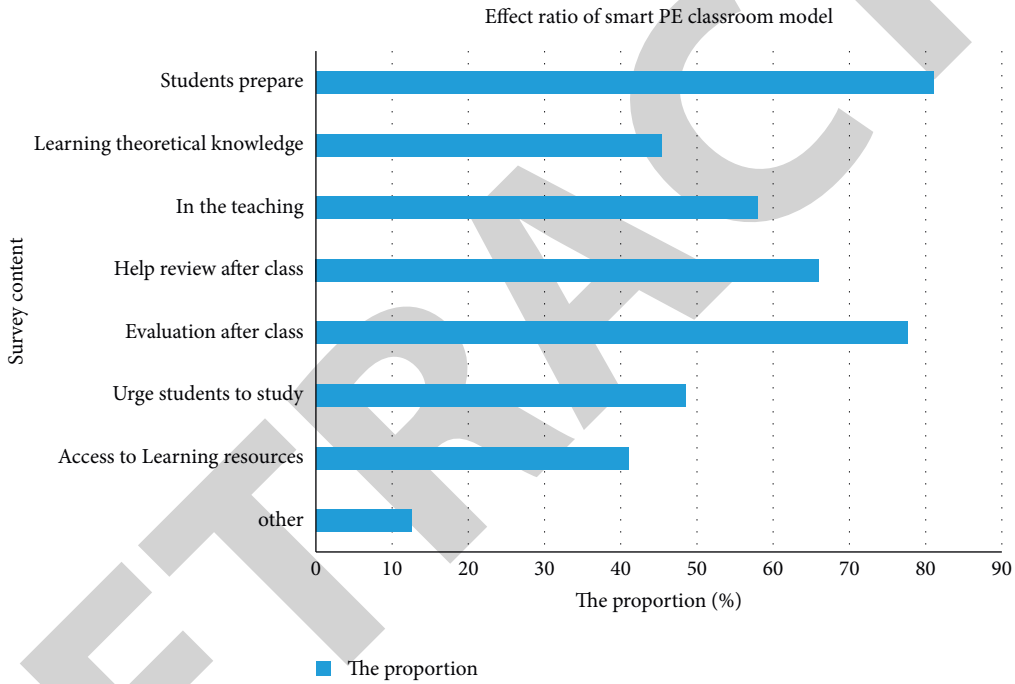

Figure 7: Role proportion of intelligent physical education classroom model.

study analyzes its role in college physical education classroom. According to the survey results of the students who participated in the survey, the obvious effects are to simplify the pre-class preparation process, facilitate after-class evaluation, simplify after-class review, and facilitate teachers' classroom teaching. The corresponding proportions of each role are 81, 77.6, 66, and 58%, respectively. Moreover, the proportion of the intelligent physical education classroom that can effectively urge learning is 48.5, and 41% help find more learning resources. The details of the outcomes are shown in Figure 7

6. Conclusions and Future Work

Nowadays, in the era of wisdom, rapid development of cloud computing, big data, Internet, and other technologies has accelerated the reform stage of intelligent physical education classroom in colleges and universities. Under the enlightenment of smart classroom and smart education, colleges and universities gradually open the reform mode, and introduce the smart education mode into physical education classroom teaching. In this study, we designed a "six-pronge" smart physical education classroom system in colleges and universities, and clarified the "six-pronge" teaching content. Moreover, we used the human body movement pattern based on sensors to identify the training of students in physical education classroom, and obtained the accurate movement of students. Teachers can guide students' training according to the data. Teaching institutes like colleges and universities should build intelligent terminal equipment platforms according to their own situations, establish the main structure of the college smart sports classroom, and establish a smart sports classroom-teaching model on this basis [27].

To verify the effectiveness of the proposed model, this paper investigated and analyzed the students who use smart sports classroom in colleges and universities, and sets up a control group. Approximately, 40 students were randomly selected to analyze their feelings of classroom-teaching atmosphere, students' learning interest, and learning attitude, and the role of smart sports classroom model. The results showed that the students in the experimental group are higher than those in the control group in all aspects, which fully reflects the practical application effect of smart sports classroom in colleges and universities. We believe that our intelligent model can provide an important practical basis for the construction of smart sports classroom in colleges and universities. In the future, we will use more advanced learning algorithms so that the model can be integrated for accurate results. Similarly, the experimental and control groups have few students that could be increased for generalization of the obtained outcomes. Additional evaluation metrics should be used to strengthen the research findings. As a future work, we will work on the real implementation of the proposed intelligent model in teaching institutes [28]. However, before that, the model training times, as well as, prediction durations should be investigated. This could be related to the number of students in each group and the amount of data collected from the sensors.

Data Availability

Data are available on request from the corresponding author.

Conflicts of Interest

The authors declare that they have no conflicts of interest.

References

[1] A. Boonsem and T. Chaoensupmanee, "Determining the factors of teaching effectiveness for physical education," *International Education Studies*, vol. 13, no. 3, p. 43, 2020.

[2] C. De, A. Wignall, V. Giannoudis, and A. Jimenez, "Perioperative outcomes and predictors of mortality in COVID-19 positive patients with hip fractures: a multicentre study in the UK," *Indian Journal of Orthopaedics*, vol. 54, no. S2, pp. 386–396, 2020.

[3] B. Bruya and M. Ardelt, "Fostering wisdom in the classroom, part 1," *Teaching Philosophy*, vol. 41, no. 3, pp. 239–253, 2018.

[4] T. A. Aversi-Ferreira, K. Cordeiro-De-Oliveira, S. Lima, and W. Santos, "The perceptions of students and instructor in a graduate mathematical modeling class: an experience with remote education," *Research, Society and Development*, vol. 10, no. 6, Article ID e2310615223, 2021.

[5] G. Faria, M. F. Peres, O. M. d. S. Neto, and C. A. G. d. au, "An educational didactic machine to improve the learning process of motor protection mechanisms in electrical engineering high education," *IEEE Revista Iberoamericana de Tecnologias del Aprendizaje*, vol. 15, no. 4, pp. 253–261, 2020.

[6] D. S. Mabassa, G. Lembe, and A. Koulombo, "Teaching of physical education: focus on the teaching preferences of teachers of brazzaville," *Open Journal of Social Sciences*, vol. 8, no. 7, pp. 99–111, 2020.

[7] S. L. Guo and J. D. Wang, "Study on the new classroom teaching mode based on learning," *Journal of Huainan Vocational & Technical College*, vol. 19, no. 4, pp. 84-85, 2019.

[8] X. S. Liu, "Discussion on the value and strategy of junior middle school information technology training students' digital learning ability," *Chinese and Foreign Communication*, vol. 28, no. 6, pp. 705-706, 2021.

[9] L. Wang and X. J. Bao, "Design and practice of online teaching process structure based on the concept of intelligent classroom," *Journal of Chifeng University*, vol. 34, no. 12, pp. 166–168, 2018.

[10] C. G. Zeng, "Follow the law of junior middle school students' cognitive development, improve the teaching effect of geography classroom education," *Secondary School Curriculum Coaching(Teaching Research)*, vol. 13, no. 8, p. 74, 2019.

[11] M. Kwet and P. Prinsloo, "The "smart" classroom: a new Frontier in the age of the smart university," *Teaching in Higher Education*, vol. 25, no. 4, pp. 510–526, 2020.

[12] J. Shao, "Analysis of sports teaching strategy in junior middle school based on sports skill cultivation," *DuYuXie*, vol. 18, no. 11, p. 251, 2021.

[13] A. Q. Bai, "Research on the construction of wisdom classroom in primary and secondary schools based on electronic schoolbag," *Software Guide*, vol. 16, no. 11, pp. 35-36, 2017.

[14] Y. Y. Wang and Y. H. Zheng, "Educational context awareness for smart classroom:value positioning, characteristic model and practice framework," *E-education Research*, vol. 42, no. 11, pp. 84–91, 2021.

[15] Y. H Zhang and J. R. Zhang, "Research on intelligent classroom teaching mode of vocational education cloud platform," *Wuxian Hulian Keji*, vol. 18, no. 22, pp. 132-133, 2021.

[16] J. Wang and B. Zhao, "Intelligent system for interactive online education based on cloud big data analytics," *Journal of Intelligent and Fuzzy Systems*, vol. 40, no. 1, pp. 1–11, 2020.

[17] X. T. You, "Construction of appraisal system for informationalized teaching ability of vocational education teachers based on smart class," *Journal of Nanning Polytechnic*, vol. 23, no. 1, pp. 59–62, 2018.

[18] P. P. Jin and Q. Zhou, "The reconstruction and practice strategies of views on talent of higher education in the popularization stage," *Contemporary Education and Culture*, vol. 13, no. 6, pp. 93–101, 2021.

[19] W.-l. Shang, "Application of machine learning and Internet of things techniques in evaluation of English teaching effect in colleges," *Computational Intelligence and Neuroscience*, vol. 2022, Article ID 7643006, 9 pages, 2022.

[20] M. Tedre and T. Toivonen, "Teaching machine learning in K-12 classroom: pedagogical and technological trajectories for artificial intelligence education," *IEEE Access*, vol. 9, no. 2021, pp. 110558–110572, 2021.

[21] L. J. Chen, A. Wang, and Y. F. Chen, "Design of cloud service platform for intelligent drug sales equipment under intelligent medical," *Machine Building & Automation*, vol. 50, no. 4, pp. 128–131, 2021.

[22] L. Ma, "An immersive context teaching method for college English based on artificial intelligence and machine learning in virtual reality technology," *Mobile Information Systems*, vol. 2021, Article ID 2637439, 7 pages, 2021.

[23] P. Chen, X. D. Li, and X. A. Chen, "A comparative study on the implementation effect of smart classroom teaching mode and traditional classroom teaching mode of college PE optional course under the background of education informatization," *Western China Quality Education*, vol. 7, no. 1, pp. 110–112, 2021.

Hindawi
Scientific Programming
Volume 2022, Article ID 1225634, 9 pages
https://doi.org/10.1155/2022/1225634

Research Article

Evaluation of English Subjective Questions Based on Deep Neural Networks

Shali Zhao

Nanchang Vocational University, Nanchang, Jiangxi 330500, China

Correspondence should be addressed to Shali Zhao; 202072128@yangtzeu.edu.cn

Received 21 March 2022; Revised 15 April 2022; Accepted 21 April 2022; Published 5 May 2022

Academic Editor: Muhammad Zakarya

In the background of artificial intelligence (AI) era, deep neural networks (DNNs) also have a far-reaching impact on all walks of life. For the field of education, the integration of deep neural network technology and language teaching is more in-depth. Targeting at the problems of high costs and low efficiency of manual evaluation, this paper aims to study the evaluation of the English subjective questions by using deep neural networks. Firstly, the surface features of the English character information, including English antisense, negative information, semantic features, word frequency, sentences length, and words order, are combined; and the calculation method of the English sentence similarity based on multifeature fusion is established through the analytic hierarchy process (AHP). Secondly, the English text recognition is composed of long and short memory lost by aggregation cross entropy. The introduction of aggregation cross entropy can effectively improve the accuracy of text recognition. Finally, the evaluation model based on deep neural network is used to evaluate the English subjective questions. The experimental results, in terms of accuracy, recall rate, and effectiveness of the automatic recognition, show that the proposed method has high accuracy and can effectively improve the quality of the English teaching and realize a personalized teaching approach.

1. Introduction

The Republic of China holds many English tests every year, and through so many years of practice, the correction of English test papers has a relatively mature and comprehensive process. Among them, the correction of objective questions has been mechanized for many years, but the subjective questions are still corrected and marked manually. Manual correction has many disadvantages, such as the concentration of correction teachers or evaluators, the prevention of teachers' violations, and the provision of marking venues. In addition, due to these issues, the evaluation process will consume a lot of human and material resources. At the same time, in order to ensure the fairness of the evaluation results of the English subjective questions, each test paper must be evaluated by several teachers at the same time, which will greatly increase the workload of the English teachers.

With the gradual advancement of modern educational English classroom design, the learning environment of the English teaching and learning is changing rapidly. These challenges promote the innovation and reform of the English learning methods. According to the English teaching, from the initial need to rely on the oral English teacher to learn English pronunciation, to the later use of tape recorder or phonograph to practice English listening, there are also modern multimedia teaching laboratories and corresponding technologies, which have played an important role in the process of English teaching. However, after in-depth research, it can be found that technology rarely has an impact on the English writing and teaching. The traditional evaluation systems have always been to solve the problem of pain points in English writing evaluation, accurate, timely, and comprehensive English evaluation feedback. However, classroom cooperation does not have efficient teaching means, and students' writing ability cannot be effectively improved. Although the emergence of automatic scoring system has effectively solved the problem of timeliness, however, the current existing scoring systems generally have some problems, such as low scoring accuracy, certain

loopholes in scoring rules, and single feedback effect, which limits the development of English subjective questions evaluation. Moreover, most of these systems are aimed at native English users, but they do not deal with the situation of nonnative English-speaking countries, in particular, where great efforts are required to encode the English grammar. Therefore, they are not suitable for Chinese users.

In this paper, we develop a scoring system for the evaluation of the English subjective questions based on the deep neural networks. First of all, we use the similarity calculation method of the English sentences based on multifeature fusion, and then the aggregation cross entropy approach is introduced to identify the English subjective questions. Finally, the subjective questions evaluation model based on deep neural network is adopted. Moreover, compared with other English subjective question evaluation methods, the results show that not only is the proposed method better than other methods in evaluation accuracy, but the recognition recall rate and recognition effectiveness rate are also better than other methods. This can effectively reduce teachers' teaching tasks and improve the feedback effect. The innovations of this paper are as follows:

(i) This paper aims to study the evaluation of English subjective questions by using deep neural network

(ii) We firstly use the similarity calculation method of English sentences based on multifeature fusion

(iii) The surface features of English character information are combined, and the calculation method of English sentence similarity based on multifeature fusion is established by using analytic hierarchy process

(iv) The aggregation cross entropy approach is introduced to accurately identify the English subjective questions

(v) English text recognition is composed of long and short memory lost by aggregation cross entropy

The remaining of this manuscript is structured as follows. Section 2 describes state-of-the-art related work. Key techniques of English subjective question evaluation are illustrated in Section 3. An evaluation model based on deep neural network is suggested in Section 4. Experimental evaluation and results are discussed in Section 5. Finally, Section 6 concludes the paper along with directions for further research.

2. Related Work

Foreign automatic evaluation systems for the English subjective questions have been developed for many years and have been very mature and applied to large-scale examinations. Most of these systems are aimed at native English users, but they do not deal with the situation of nonnative English-speaking countries. Therefore, they are not suitable for Chinese users. Domestic research in this area started relatively late, but some corresponding methods are also put forward. Liu et al. explained that, with the continuous development of artificial intelligence technology, the evaluation of English objective questions has been gradually handed over to the computer for processing [1]. However, in the process of scoring English subjective questions, it is easy to be affected by the subjective influence of the marking teacher, and the high-intensity marking work is easy to make mistakes. Aiming at this type of problems, an intelligent scoring method of English subjective questions based on deep learning is proposed. The intelligent analysis method based on big data can quickly compare students' handwritten answers with correct answers, so as to realize the correct evaluation and automatic scoring of subjective questions. However, these methods have the problems of low scoring accuracies [1].

In order to realize the automation of English online examination, Chen and Liu suggested a model of English subjective questions evaluation based on the concept of sentence similarity [2]. Firstly, from the similarity of three types of text features such as (a) English keywords; (b) semantics; and (c) syntax, the possibility of English subjective questions evaluation is analyzed. Next, the data of answers are cleaned and classified, and the main steps of automatic evaluation are followed. These steps are as follows: (i) build a multifeature sentence recognition calculation model, (ii) take semantics as the core, (iii) make a comparative analysis of the English subjective questions based on the comprehensive similarity of multifeatures, (iv) theoretically improve the accuracy of the English subjective question evaluation, and (v) take the automatic evaluation system for English subjective questions as the prototype. Experimental outcomes show that the proposed calculation method of sentence acquaintance can evaluate the English subjective questions in the form of an intelligent evaluation system. Although the suggested model has good development prospects, however, on the whole, the accuracy is low [2].

Song and Wang proposed an English subjective questions scoring system based on word segmentation algorithm [3]. This method introduces word segmentation in detail and improves and studies the existing algorithms. The proposed method uses the combination of word segmentation technology and text similarity to automatically evaluate English subjective questions, from the recognition degree of text length and text word line, and then combined with influencing factors to form a comprehensive similarity. In the results using the main characteristics of the comprehensive examination subjects, three influencing factors were scientifically set to test the test paper [4]. The test paper questions were four subjective questions, and the standard answers were controlled within 100 words. Approximately, 50 electronic test papers were recovered from each experiment. The experimental results were compared with the experimental results of the original algorithm. The experimental results showed that the gap between the optimized evaluation algorithm and the original algorithm was relatively small; however, there is still room for improvement [3].

Wang et al. also suggested a scoring system [5], but, according to the existing subjective question evaluation method, it cannot effectively identify professional terms. Moreover, it is easy to omit the semantic relationship between texts in the process of scoring, resulting in a large

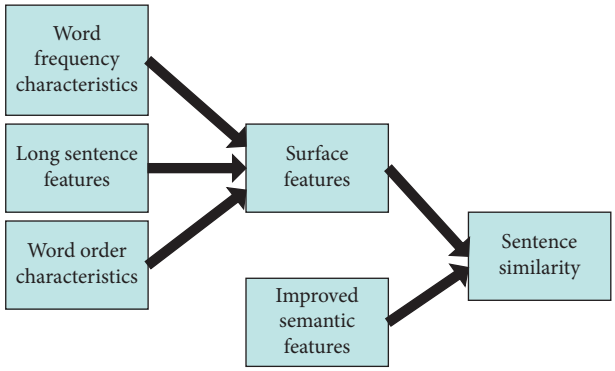

Figure 1: Calculation flow of similarity of multifeature sentences.

difference between the scoring results and the manual scoring results. Due to this problem, the proposed scoring system cannot effectively meet the basic requirements of the real examination. To solve these problems, a subjective question evaluation method based on domain ontology and dependency syntax is proposed in the same work [5]. This method integrates various factors such as distance similarity, information similarity, and common words similarity and introduces the domain ontology into the process of subjective questions scoring [6]. The main purpose of the proposal is to improve the effectiveness of subjective questions scoring results. Experimental results show that compared with existing methods, the proposed method is closer to the manual scoring method in subjective questions evaluation. However, because the process is too complex, therefore, it has impacts on the accuracy of review [5].

3. Key Techniques for English Subjective Questions Evaluation

3.1. English Sentence Similarity Method Based on Multifeature Fusion

3.1.1. Similarity of Multifeature Fusion. On the basis of improving the semantic features, this paper comprehensively considers the word frequency, sentence length, and English word order of English sentences and puts forward the similarity calculation of English sentences based on multifeature fusion. In fact, this can effectively improve the accuracy of similarity calculation of the English sentences [7, 8]. The specific calculation flow is shown in Figure 1.

Suppose S_1 and S_2 are two sentences waiting to calculate the similarity, the feature similarity based on the surface of the sentence is $\mathrm{sim}_{sf}(S_1, S_2)$, and the semantic feature similarity based on the English sentence is $\mathrm{sim}_{\mathrm{sem}}(S_1, S_2)$. The weighted fusion of the two feature similarities shows that the final similarity of the sentence is $\mathrm{sim}(S_1, S_2)$. The calculation process can be divided into three steps.

Step 1. Calculate the similarity of S_1 and S_2 surface features.

The features of sentence surface include word frequency, sentence length, and word order. The calculation process of the similarity is given as follows. The vector based spatial model method makes the calculation method of English sentence similarity based on word frequency, which mainly represents the sentence as a sentence, but mutually independent words form a vector, and uses the cosine value of the angle between the two vectors to calculate the similarity in English sentences. S_1 and S_2 are effectively mapped into the space of n vector, expressed as $S_1 = (w_1, w_2, \ldots, w_n)$ and $S_2 = (w_1', w_2', \ldots, w_n')$. The feature similarity based on English word frequency is expressed as

$$\mathrm{sim}_{sf_1}(S_1, S_2) = \frac{\sum_i^n w_i \times w_i'}{\sqrt{\sum_{i=1}^n w_i^2 \times \sum_{i=1}^n w_i'^2}}. \tag{1}$$

In formula (1), $w_i = tf_{T_i} \times i\ df_{T_i}$, where tf_{T_i} represents the frequency of the English word T_i in S_1, $i\ df_{T_i}$ represents the index of inverse text frequency, M represents the total number of English sentences in the corpus, and m represents the number of English words and T_i sentences included in the corpus.

Step 2. Interpolation.

The interpolation between the length of two sentences can reflect the similarity of English sentences [9, 10]. Generally, the similarity of English sentences can be inversely proportional to the interpolation of two sentence lengths. Assuming that the length of S_1 is $l(S_1)$ and the length of S_2 is $l(S_2)$, the feature similarity based on English sentences is expressed as

$$\mathrm{sim}_{sf_2}(S_1, S_2) = 1 - \frac{\left|l(S_1) - l(S_2)\right|}{\left|l(S_1) + l(S_2)\right|}. \tag{2}$$

For the same words in two sentences, the sequential relationship of word position must be considered. The reverse order number of the same words in two sentences can be used as a measure to express the similarity of the two sentences. If $f_r(S_1, S_2)$ is the reverse order number of the sequence composed of the same words in S_1 and S_2 in S_2, $f_{mr}(S_1, S_2)$ represents the largest reverse order number in the sequence of the same number of times in S_1 and S_2. Based on word order feature, similarity is expressed as

$$f_r(S_1, S_2) S_1 S_2 f_{mr}(S_1, S_2)$$

$$\mathrm{sim}_{sf_3}(S_1, S_2) = \begin{cases} 1 - \dfrac{f_r(S_1, S_2)}{f_{mr}(S_1, S_2)} f_{mr}(S_1, S_2) > 0 \\ 0 f_{mr}(S_1, S_2) = 0 \end{cases}. \tag{3}$$

Step 3. Weighted summation.

By weighted summation of the distribution weights of the similar calculation structures of the above three features of English sentences, it can be obtained that the similarity based on English sentences is expressed as

$$\mathrm{sim}_{sf}(S_1, S_2) = \sum_{i=1}^{n=3} a_i \times sim_{sf_i}(S_1, S_2). \tag{4}$$

In formula (4), a_i is expressed as an adjustable parameter, and $\sum_{i=1}^{n=3} a_i = 1$ and $a_i \geq 0$ are satisfied. The similarity of

the English sentences is calculated by combining the sentence features, and the final similarity of the two English sentences is expressed as

$$\mathrm{sim}(S_1, S_2) = b \times \mathrm{sim}_{sf}(S_1, S_2) + c \times \mathrm{sim}_{\mathrm{sem}}(S_1, S_2). \quad (5)$$

In formula (5), b represents the features based on the surface of the English sentences, c represents the improved semantic features, and the similarity value of English sentences meets $b + c = 1$, $b \geq 0, c \geq 0$.

3.1.2. Calculation of English Features Weights Based on Analytic Hierarchy Process. The analytic hierarchy process (AHP) is a decision-making method combining quantitative calculation and qualitative analysis [11]. It mainly decomposes the complex multifactor decision-making problem into the problem of mutual comparison and weight calculation between different levels of self-factors. This paper uses analytic hierarchy process to select the feature weight of the English sentences [12, 13].

We construct the hierarchical structure model of English sentence similarity and construct the structural model of the English sentence similarity according to the hierarchical structure system of analytic hierarchy process, which is shown in Figure 2.

The comparison matrix is established [14]. The comparison matrix is established according to the relative importance of different sentence features in the criterion layer, which is represented in Table 1.

Among the surface features of English sentences, the feature of word frequency is an important factor affecting the similarity of English sentences, which is very important [15, 16]. The characteristics of English sentence length and word order have roughly the same influence on English sentences, so the degree of importance is also the same [17].

3.1.3. The Consistency Test. Indicators of consistency are expressed as given in the following formula:

$$\mathrm{CI} = \frac{\lambda_{\max} - e}{n - 1}. \quad (6)$$

In formula (6), e represents the dimension of vector; that is, $\mathrm{CI} \geq 0$. The smaller the value of CI, the greater the consistency and vice versa. The CI is calculated as 0 according to formula (6), which indicates that the consistency is met.

After the CI value is obtained, the index RI of the random consistency must be defined prior to RI. The ratio formula of consistency is expressed as

$$\mathrm{CR} = \frac{\mathrm{CI}}{\mathrm{RI}}. \quad (7)$$

According to formula (7), it can be calculated that CR is 0 and its value is less than 0.1. Therefore, the weight vector $W = [0.750, 0.125, 0.125]$; that is, the similarity weight of English sentences based on word frequency feature is $a_1 = 0.750$, the similarity weight of English sentences based on sentence length feature is $a_2 = 0.125$, and the similarity weight of English sentences based on word order feature is $a = 0.125$. It is concluded that the weight of English sentence similarity based on surface features is $b = 0.833$, and the weight of improved English sentence similarity based on semantic features is $c = 0.1667$.

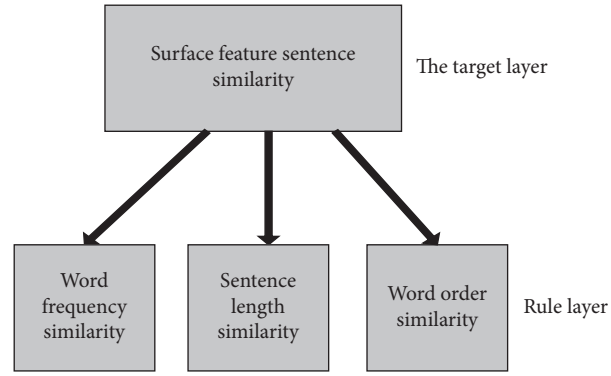

Figure 2: Hierarchical model of sentence similarity.

Table 1: Comparison matrix.

	Word frequency similarity	Sentence length similarity	Word order similarity
Word frequency similarity	1	6	6
Sentence length similarity	1/6	1	1
Word order similarity	1/6	1	1

3.2. Recognition of English Subjective Questions Based on Deep Learning. Combined with the above multifeature fusion, the loss of aggregation cross entropy is replaced by the attention mechanism. When calculating different types of English characters, it is not necessary to consider the feature order [11]. The network is used to accurately predict and mark the number of characters in each category in English subjective questions to minimize the loss function. The calculation formula is expressed as follows:

$$P(N_k | k, I; w). \quad (8)$$

In formula (8), $P(N_k|k, I; w)$ represents the prediction results of English characters, and the occurrence times of English characters of category k are equal to the probability of the given times of English labels under the condition of N^k [18, 19].

The feature sequence dimension of subjective questions is $(T \times K)$, where T represents the length of the sequence and K represents the number of categories of English characters. This paper defines that the feature sequence vector of the English sentence output is Y, the feature vector of English words at time t is y^t, and the prediction probability of English words of category k at time t is y_k^t. The total probability of category K in the whole English character sequence is $\sum_{t=1}^{T} y_k^t$.

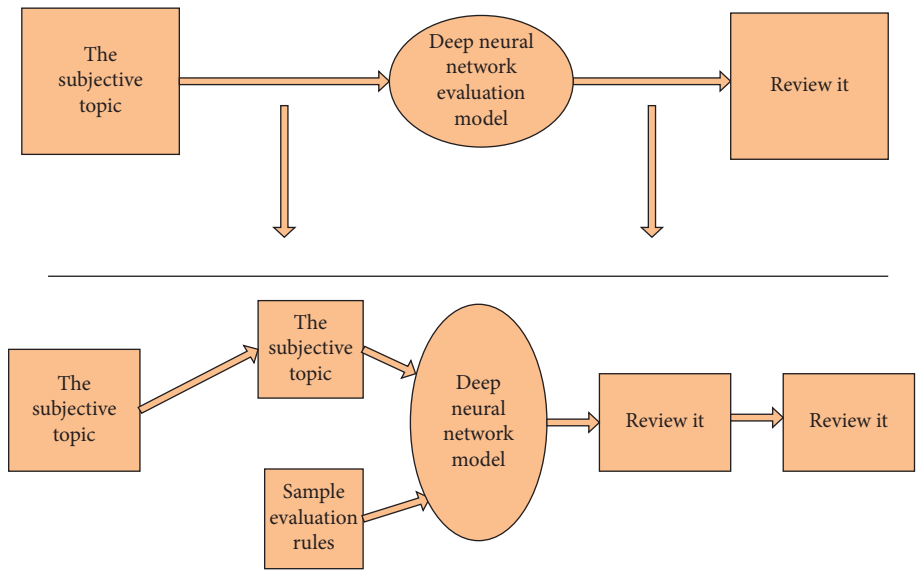

Figure 3: The overall framework of the review model.

Next, we adjust the lost English character function from the perspective of regression problem, and the calculation formula is expressed by the following equation:

$$L(w) = \frac{1}{2} \sum_{(I,S)\in Q} \sum_{k=1}^{|c^{\epsilon}|} \left(N^k - y^k\right)^2. \tag{9}$$

In formula (9), T represents the length of the predicted English text, $|S|$ represents the length of the label English text, and $(T - |S|)$ represents the number of white space characters in the English string; that is, $N_{\epsilon} = T - |S|$.

In order to avoid the disappearance of gradients, the cumulative probability of the k English character yk is normalized to $\overline{y}k = yk/T$, and the number of English characters N^k is normalized to $\overline{N}_k = \overline{N}_k/T$. The entropy of the intersection between $\overline{y}$ and $\overline{N}$ can be expressed as

$$L(I,S) = -\sum_{k=1}^{|C^{\epsilon}|} \overline{N}_k 1 n \overline{y} k. \tag{10}$$

As a final stage, in the final output probability matrix, the final sequence of the English text characters is obtained by greedy search method, so as to complete the recognition of English subjective questions.

4. Evaluation Model Based on Deep Neural Network

Based on the discussion of various mathematical models presented in the above section, we integrate them all to design a review model in this section. Combined with the above multifeature fusion English sentence similarity calculation and binary English subjective questions recognition, a review model based on deep neural network is constructed. Figure 3 shows the overall framework of the review model [20, 21]. The framework is composed of three layers: (i) the LSTM network layer; (ii) self-characteristic layer; and (iii) the full link layer. A detailed discussion of all layers is sketched in the subsequent sections.

The LSTM network layer:

The calculation formula of embedding English words into sequences and transferring them to the long and short memory network is

$$ht = \mathrm{LSTM}\left(h_{(t-1)}, xt\right). \tag{11}$$

In formula (11), xt and ht represent the vector of English word input at time t, respectively. The deep neural network model controls the data flow of English sentences in recursive operation through output, input, and forgetting gates. The following formula describes the depth neural network function:

$$ht = ot \circ \tanh(ct). \tag{12}$$

At time t, the deep neural network outputs a hidden vector ht, which reflects the English semantic content of English subjective questions at t.

Self-characteristic layer:

This layer mainly describes how to extract the self-features of English sentences from vectors obtained from deep neural network. The English subjective questions vector ei and distance English data information vector disti have internal relations between adjacent sentences of English subjective questions. These relations are described in the network model. It should be noted that he is the hidden layer of English subjective questions, het is the vector of position, hd is the hidden layer of distance information, and hdt is the vector of hd in position. Suppose d represents the length of English sentences [22, 23]. Calculating the similarity between the position t of the vector in the subjective question

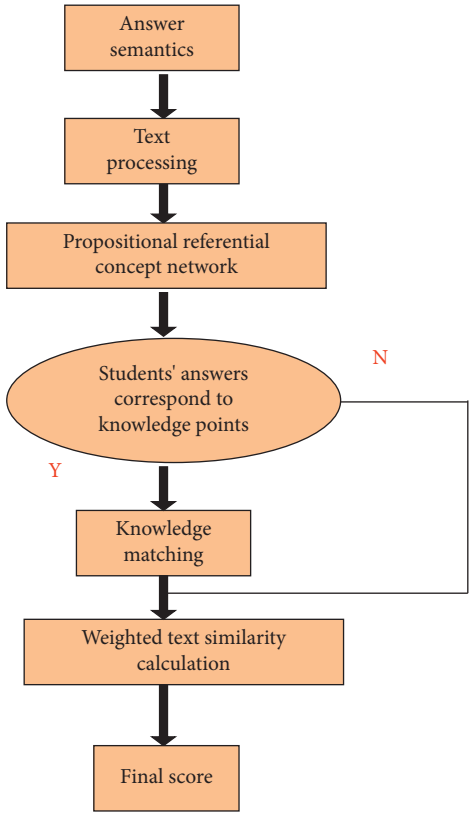

Figure 4: Flow chart of subjective question scoring.

and the sentence at $t + d$ can be called the feature in the similarity of English sentences, which can be calculated as described by the following formula:

$$\text{inner} - \text{feature} = \frac{\text{het} \cdot \text{het} + \delta}{|\text{het}| \cdot |\text{het} + \delta|}. \tag{13}$$

In addition, the similarity of the sentences of the vectors he and hd at the same position t of the subjective question is calculated, which is called the cross feature, and the calculation formula is expressed by the following equation:

$$\text{cross} - \text{feature} = \frac{\text{het} \cdot \text{het}}{|\text{het}| \cdot |\text{het}|}. \tag{14}$$

Both subjective in questions features and cross features are connected with vectors and directly input into the next layer. In addition to the internal and cross features of English subjective questions, there are also two outputs in this layer, the hidden layer of the paper and the hidden layer of distance information. The different layers of the car are treated differently. One is to directly take the vector of the last position of he and hd, and the second is to take the vector of the mean value in the corresponding time [24, 25]. Name these two vectors he – vector- and hd – vector. The vector is input into the full link layer.

The full link layer:

Four vectors are obtained from the characteristic layer of subjective questions, which are he – vector, hd – vector, inner – feature, and cross – feature. Connect these vectors into a vector. Then, input the vector to the Softmax layer.

Table 2: Experimental environment.

The name of the	Configuration
Python	3.6.5
PyTorch	1.2.0
The operating system	Ubuntu 16.04.6 LTS
The CPU model	Intel(R) Core(TM) i7-7820X CPU@3.60GHz
GPU model	TITAN Xp_12G
CUDA version	10.1

Table 3: Sentence similarity comparison results.

Different methods for	Sentence similarity (%)
Methods in this paper	0.88
Literature [1]	0.75
Literature [3]	0.65

The Softmax layer mainly classifies the English data output of the full link layer. The classification is mainly realized by equation and expressed by the following formula:

$$s(x) = \text{sigmoid}(w \cdot x + b). \tag{15}$$

In formula (15), x represents the vector of English data input, w represents the weight vector of English words, and b represents the offset of English words. Figure 4 visualizes the flow chart of subjective question scoring.

5. Analysis of Experimental Results

To evaluate the performance of the scoring method, the method is implemented in Python language, and the learning library used is PyTorch. The specific environment configuration of the experiment is shown in Table 2. This paper takes the test paper of the operating system course as the experimental material, selects 100 test papers of the test, inputs the English subjective questions into the computer, and also inputs the results of manual marking. When the results of manual marking are entered, each test question will be scored by two teachers, so as to improve the accuracy of manual marking. Among the answers of 100 test questions, 20 are randomly selected, with a full score of 20, as the test case, and the other 80 are used as the training set of system application, so as to make comparative analysis in all aspects.

Table 3 shows the comparison of sentence similarity in English subjective questions. As can be seen from Table 3, the similarity of English subjective questions sentences in the method proposed in this paper is significantly higher than that in the traditional model methods suggested in [1, 3]. Furthermore, the proposed method can improve the accuracy of English subjective questions evaluation.

5.1. Evaluation of the Accuracy. Accuracy is an important parameter to evaluate the English subjective question evaluation based on deep neural network described in this paper. It is expressed by formulas (16) and (17) to

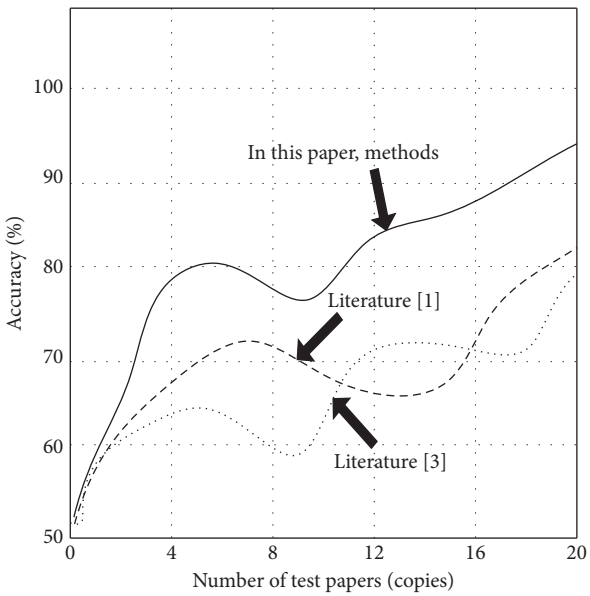

Figure 5: Comparison of rating accuracy of different methods.

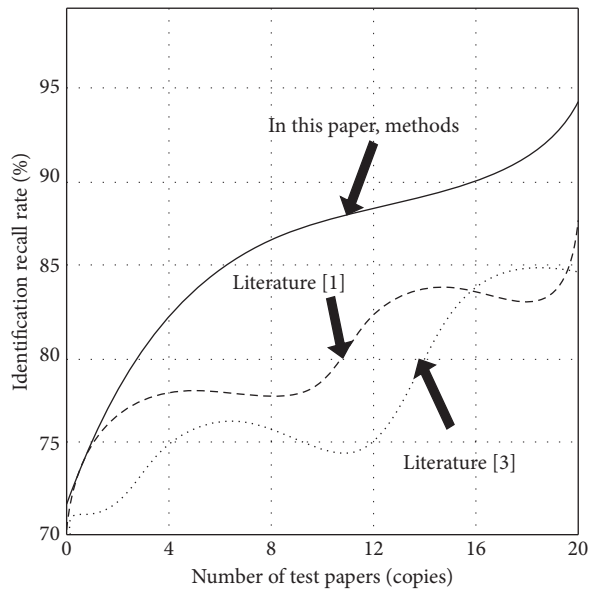

Figure 6: Comparison of recognition recall rates of different methods.

comprehensively evaluate the accuracy of subjective questions evaluation:

$$\text{Single answer accuracy}\left(V_i\right) = 1 - \frac{|\text{Manual scoring} - \text{Machine scoring}|}{\text{Full score of title}}, \tag{16}$$

$$\text{Comprehensive accuracy} = \sum_{i=t}^{N} \frac{V_i}{N}. \tag{17}$$

In formulas (16) and (17), V_i represents the accuracy of single answer evaluation, and N represents the total number of test papers.

5.2. Recall Rate of Subjective Questions Evaluation and Identification Results. The recall rate represents the number of results obtained by subjective question identification method, which is expressed by the following formula:

$$L = \frac{\theta_i}{\theta_a} * 100\%. \tag{18}$$

In formula (18), θ_i represents correctly identified information, and θ_a represents the information to be identified.

5.3. Effective Measurement of Automatic Recognition. This index mainly indicates the efficiency of the subjective questions recognition. According to this index, the effect of subjective questions recognition can be clarified, which is expressed by the following formula:

$$S' = \frac{2 * L * Q}{L + Q} * 100\%. \tag{19}$$

This paper selects the methods proposed in this paper based on deep neural network, methods suggested in [1, 3] for analysis, and compares the evaluation accuracy of the three methods, the recall rate of recognition results, and the effectiveness of automatic recognition. The results, in terms of accuracy, recall rate, and effectiveness of automatic recognition, are shown in Figures 5–7, respectively.

A detailed analysis of the data shown in Figure 5 shows that the effects of different methods are effectively reflected in this index experiment. The methods proposed in the text have relatively high accuracy in the evaluation of subjective questions and can evaluate multiple character information, while the methods proposed in [1, 3] can only evaluate a small amount of subjective questions and cannot analyze and recognize all character information of the subjective questions with high accuracy. This shows that the evaluation accuracy of the method proposed in this paper is high.

After verifying the accuracy of subjective questions evaluation, the recall rate of subjective questions recognition is verified and analyzed. According to the experimental results, as shown in Figure 6, it can be seen that there are great differences in the recall rate of subjective questions recognition of the three methods. The recall rate of recognition results based on deep neural network proposed in [1] and text is better, and it can recognize a variety of English

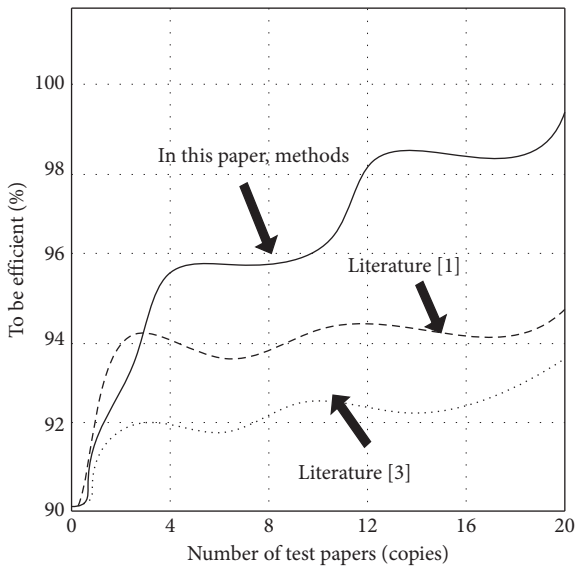

Figure 7: Comparison of the efficiency of different identification methods.

text information. The recall rate of the recognition results of the method proposed in [3] is relatively low, and it cannot recognize all the characters of subjective questions. Therefore, this method cannot get good recognition results [26]. Combined with the above results, the effective measures of the automatic recognition of subjective questions in different methods are studied, which is shown in Figure 7.

The evaluation system of English subjective questions is a kind of artificial intelligence technology. It has the characteristics of timely feedback, comprehensive feedback, and objectivity of feedback. It can effectively reduce the workload of teachers, meet the needs of English learners to improve their subjective questions answering ability, assist teachers to complete English teaching activities, improve the quality of English teaching, and realize personalized English teaching. Therefore, this paper makes an in-depth study on English subjective questions evaluation based on deep neural network.

6. Conclusions and Future Work

The evaluation system of English subjective questions is a kind of artificial intelligence technology. It has the characteristics of timely feedback, comprehensive feedback, and objectivity of feedback. It can effectively reduce the workload of teachers, meet the needs of English learners to improve their subjective question answering ability, assist teachers to complete English teaching activities, improve the quality of English teaching, and realize personalized English teaching. Therefore, in this paper we studied an in-depth analysis on English subjective questions evaluation and proposed a scoring system based on the deep neural networks. The results, in terms of accuracy, recall rate, and effectiveness of automatic recognition, verified the validity of the proposed model.

In the future, we will consider other features of the English language and text and other more advance machine learning methods to improve the accuracy and robustness of the scoring system. Moreover, the grammar should be taken into account when designing automatic text recognition and review systems. Finally, the attention network and LSTM models along with aggregation methods should be used to minimize the training time of the model [6, 27]. The computational time would essentially increase through either increasing the number of features from the English language perspective or increasing the amount of data for learning purposes. In the future, we will study the impact of the learning process on the accuracy of the automatic text recognition and training times.

Data Availability

Data are available upon request from the corresponding author.

Conflicts of Interest

The author declares that there are no conflicts of interest.

References

[1] C. G. Liu, F. Q. Yu, R. S. Ma et al., "[Study on *Cep63* expression and apoptosis of thyroid papillary carcinoma cell lines TPC-1]," *Zhonghua er bi yan hou tou jing wai ke za zhi = Chinese journal of otorhinolaryngology head and neck surgery, Internet of things technologies*, vol. 11, no. 1, pp. 62–68, 2021.

[2] X. W. Chen and D. B. Liu, "Research on automatic marking system of subjective questions based on sentence similarity," *Engineering Journal of Wuhan University*, vol. 51, no. 7, pp. 654–658, 2018.

[3] X. Y. Song and C. A. Wang, "Automatic scoring algorithm for subjective questions based on Chinese word segmentation," *Journal of Hebei North University (Natural Science Edition)*, vol. 33, no. 9, pp. 7–11, 2017.

[4] W. Weihong and T. Jiaoyang, "Research on license plate recognition algorithms based on deep learning in complex environment," *IEEE Access*, vol. 8, Article ID 91661, 2020.

[5] J. S. Wang, W. W. Guo, and Z. Y. Tang, "Automatic scoring method for subjective questions based on domain ontology and dependency parsing," *Journal of Guizhou University*, vol. 37, no. 6, pp. 79–84, 2020.

[6] B. Shi, X. Bai, and C. Yao, "An end-to-end trainable neural network for image-based sequence recognition and its application to scene text recognition," *IEEE Transactions on Pattern Analysis and Machine Intelligence*, vol. 39, no. 11, pp. 2298–2304, 2017.

[7] H. J. Luo and X. H. Ke, "Automated scoring Chinese subjective responses based on improved-LDA," *Computer Science*, vol. 44, no. z2, pp. 102–105, 2017.

[8] Z. L. Li, Y. Q. Cheng, and H. L. Jia, "Photoshop subjective examination questions marking method based on image contrast," *Computer Engineering and Applications*, vol. 54, no. 23, pp. 150–155, 2018.

[9] Q. T. Xu, L. F. Zhang, and X. H. Zhu, "An automatic scoring method for subjective questions using semantic technologies and LSTM," *Journal of Guangxi Normal University*, vol. 39, no. 2, pp. 51–61, 2021.

[10] J. K. Li, J. Y. Han, and Y. Wang, "Automatic grading of subjective qusetions based on similarity fusion algorithm,"

Journal of Tianjin University of Science & Technology, vol. 34, no. 1, pp. 76–80, 2019.

[11] A. Ali, Y. Zhu, and M. Zakarya, "Exploiting dynamic spatio-temporal graph convolutional neural networks for citywide traffic flows prediction," *Neural Networks*, vol. 145, no. 2022, pp. 233–247, 2022.

[12] S. Y. Hong, "Research on key technologies of Mandarin intelligent evaluation based on deep neural network," *Journal of Anhui Vocational College of Electrontcs and Information Technology*, vol. 20, no. 2, pp. 1–5, 2021.

[13] A. Chen, W. Tong, and Y. Q. Zhou, "Duplicate formula detection based on deep convolutional neural network," *Computer Science*, vol. 47, no. z2, pp. 409–415, 2020.

[14] F. Wang, Y. Lu, J. Li, and J. Ni, "Evaluating environmentally sustainable development based on the PSR framework and variable weigh analytic hierarchy process," *International Journal of Environmental Research and Public Health*, vol. 18, no. 6, p. 2836, 2021.

[15] M. Pasquier, C. Chéron, G. Barbier, C. Dugas, A. Lardon, and M. Descarreaux, "Learning spinal manipulation: objective and subjective assessment of performance," *Journal of Manipulative and Physiological Therapeutics*, vol. 43, no. 3, pp. 189–196, 2020.

[16] A. Maestro, I. Herruzo, D. Varillas-Delgado, and C. Martín-Saborido, "Subjective assessment reported by patients shows differences between single-bundle and double-bundle anterior cruciate ligament reconstruction, systematic review and meta-analysis," *Scientific Reports*, vol. 11, no. 1, Article ID 15385, 2021.

[17] A. Ali, Y. Zhu, and M. Zakarya, "A data aggregation based approach to exploit dynamic spatio-temporal correlations for citywide crowd flows prediction in fog computing," *Multimedia Tools and Applications*, vol. 80, no. 20, Article ID 31401, 2021.

[18] S. Schrder, "A subjective assessment of the participation of parkinsonss disease-support-groups of patients for their health literacy," *Sprache · Stimme · Geh?R*, vol. 44, no. 2, pp. 101-102, 2020.

[19] A. Ludwin, M. Coelho Neto, I. Ludwin et al., W. P. Martins, OC29.04: T-shaped uterus by Congenital Uterine Malformation by Experts (CUME): agreement of subjective assessment among top expert," *Ultrasound in Obstetrics and Gynecology*, vol. 54, no. S1, p. 76, 2019.

[20] M. Hoshikawa, S. Uchida, and Y. Hirano, "A subjective assessment of the prevalence and factors associated with poor sleep quality amongst elite Japanese athletes," *Sports Medicine - Open*, vol. 4, no. 1, p. 10, 2018.

[21] E. M. Wu, T. Y. El Ahmadieh, B. Kafka et al., "Clinical outcomes of normal pressure hydrocephalus in 116 patients: objective versus subjective assessment," *Journal of Neurosurgery*, vol. 132, no. 6, pp. 1757–1763, 2020.

[22] C. M. Sears, M. G. Nittala, C. Jayadev et al., "Comparison of subjective assessment and precise quantitative assessment of lesion distribution in diabetic retinopathy," *JAMA ophthalmology*, vol. 136, no. 4, pp. 365–371, 2018.

[23] S. Nam, D. Fels, and M. Chignell, "Toward a subjective assessment system for closed captioning quality," *SMPTE Motion Imaging Journal*, vol. 130, no. 3, pp. 35–44, 2021.

[24] P. Perez, L. Janowski, N. Garcia, and M. Pinson, "Subjective Assessment Experiments That Recruit Few Observers With Repetitions (FOWR)," *IEEE Transactions on Multimedia*, vol. 99, p. 1, 2021.

[25] N. Pagliarecci, F. Zimmer, A. Birouche, and M. Basset, "Test methodology for the vehicle-tire handling performance evaluation: objectification of driver's subjective assessment," *IFAC-PapersOnLine*, vol. 53, no. 2, Article ID 14394, 2020.

[26] S. Pouyanfar, S. Sadiq, Y. Yan et al., "A survey on deep learning," *ACM Computing Surveys*, vol. 51, no. 5, pp. 1–36, 2019.

[27] J. Li, A. Sun, J. Han, and C. Li, "A survey on deep learning for named entity recognition," *IEEE Transactions on Knowledge and Data Engineering*, vol. 34, no. 1, pp. 50–70, 2022.

Hindawi
Scientific Programming
Volume 2022, Article ID 3678090, 13 pages
https://doi.org/10.1155/2022/3678090

Research Article

Visual Space System Design in Digital Media Art Design

Mengyao Wang,[1,2] Jingyu Wang,[3] and Chuan Zhang[3]

[1]*School of Sino-British Digital Media (Digital Media) Art, Luxun Academy of Fine Arts, Dalian 116650, Liaoning, China*
[2]*Institute of Textile & Fashion Design, Luxun Academy of Fine Arts, Shenyang 110004, Liaoning, China*
[3]*Chinese Painting College, Luxun Academy of Fine Arts, Shenyang 110004, Liaoning, China*

Correspondence should be addressed to Chuan Zhang; zhangchuan@lumei.edu.cn

Received 1 March 2022; Revised 12 April 2022; Accepted 15 April 2022; Published 28 April 2022

Academic Editor: Abid Yahya

With the development of the economy, graphic design has become one of the main forms of commercial advertising. Designers design different graphic design schemes for different layouts and design requirements, which puts forward new requirements for graphic design process work. With the advancement of technology, graphic design (or visual communication design) supported by digital media technology is not limited to print media, and network media is also included. This research mainly discusses the visual space system in digital media art design. It can be said that the reconstructed space under virtual reality is based on interaction, has an immersive and imaginative space, and is combined with narrative to a certain extent to create a new form of expression for the information expression of space design. This paper first interprets the concept of "space" from psychology, painting art, and film art produced. Then explain the particularity of digital media art design, and it uses the design works to explain the content of the exposition. Connecting digital technology can bring people the uniqueness of aesthetics. This paper makes related theoretical research on the design practice of visual space. In this paper, visual perception in psychology is introduced into design thinking. The concept of visual space is not only expressed in art and culture but also involves the concept of space and time in physics and the scientific research theory of visual perception in psychology. It breaks through the level of perceptual cognition of space in art design. 31.85% of the respondents think that visual space design is attractive. Now is the era of new media interaction. The development of interactive technology and devices has brought infinite possibilities to visual communication design. We cannot accurately say its future development and changes. Because of the emergence of new technologies and media, visual communication design is also expanding its own types of works, and it is constantly developing and improving through the study of people's emotions and the combination of design and technology. This research has positive significance for the development of the visuospatial system. The advancement of digital media technology has enriched the means of expression in space design creation and expanded people's living spaces. Through the combination of modern digital media technology at multiple levels and multiple channels, various new spaces can be created to further meet the new needs of contemporary people.

1. Introduction

Under the influence of the modern digital media environment, visual art is based on the successful experience of different industries, using the most scientific media technology and advanced creative methods to develop visual art. The combination of contemporary digital media and visual art has produced new media technology, which can be regarded as the main means of the visual art innovation. Entering the twenty-first century, digital new media art has become the most common design method applied in the contemporary exhibition industry. Advanced digital technology has made the modern display industry more modern, and the display methods have also changed from single to richer.

This article analyzes and sorts out the development of digital media art, displays design at home and abroad at this stage, and provides some ideas for the development and application of domestic digital media art in display design. This has positive significance for the research of China's

digital media art industry. The process of creating visual art provides new meaning for visual art, and this new concept greatly expands the innovative vision in the field of visual art. Digital media art breaks through the artistic techniques of traditional film. In the current application process of digital media art, the application of simulation technology to express traditional artistic effects has the advantage of rendering scenes compared with the existing application methods.

The traditional display of static pictures, cultural relics, and text can no longer enlarge the amount of information the audience can get and cannot satisfy the audience's viewing experience. Therefore, digital display design requires practitioners to master the characteristics and advantages of print communication, video communication, electronic communication, and new media communication and organically combine traditional media and new media to achieve an optimal combination. Based on the theory of visual communication design, through the analysis and research of different ideological themes in the development of Chinese and Western painting art, it discusses that people's understanding of "space" is constantly changing. This change reflects that people's cognition of self, cognition of nature, and cognition of the universe are also constantly improving, and the aesthetic experience brought by visual space has a deeper meaning. Through the study of digital media, it is clear that visual communication is endowed with new forms and characteristics in the new design environment. From the perspective of human visual perception, a more scientific and rational analysis of the visual design elements in the visual communication design is carried out, and based on this, the unique realization method and expression form of the visual space design in the digital media art design are demonstrated. "Space" is endowed with a new form of expression and brings a different aesthetic experience and more concretely expresses the aesthetic experience brought by visual space through design practice. Digital media art has been recognized by more scholars and the public with its unique charm. The application of new technologies has changed the style of exhibitions in the past. What is more valuable is that the application of new technologies has made exhibitions that were originally impossible for human beings to become a reality, bringing strange feelings and satisfaction to the visitors. Facing the ever-changing development of new media art, as researchers, we need practitioners to work hard and think constantly.

2. Related Work

The widespread use of digital interactive technology and the widespread use of film reorganization spaces in the context of digital media have produced significant changes in film development. Peicheva D believes that we must continue to accept different types of challenges and continue to innovate digital communication products in various fields of society. Aims: "Mapping" promotes major theoretical efforts and applied practice in all aspects of digital media literacy, as well as exploring its dimensions and predictions in society, more effective methods need to be identified to engage, encourage, and motivate students to utilize high-quality theoretical and applied knowledge and skills [1]. Forestal believes that the problem of the virus exemplifies the challenges of building democratic communities [2]. Romer and Moreno believe that digital media provides more opportunities for marketing and social communication of risky products and behaviors [3]. Reyna et al. believe that literacy traditionally means the accessibility of these tools has changed and the general public can afford them [4]. Oklobdija and Popesku believe that information technology has led to many changes [5]. In today's digital age, with the emergence of "off-desktop" technologies such as virtual environment, augmented reality, mixed reality, and computer interaction, the design and art creation and development of multichannel human-computer interaction have become an important research direction. Human-computer interaction based on "vision" is particularly valued in art and scientific circles.

3. Visual Space System Design Method in Digital Media Art Design

3.1. Attributes of Visual Elements and Their Roles in Spatial Expression

3.1.1. Shape. Shapes are independent contours or surfaces that appear as regular or irregular polygons and closed curvilinear layouts. The shape itself presents visual stimuli and can be flat-like, with areas of the picture parallel and flush on a two-dimensional surface. But it is also possible to use the axes implicit in the shape or the combination of shapes to give the shape a sense of direction, thus creating depth and presenting a three-dimensional appearance. In multimedia art design, shapes are mostly completed by software. When computers recognize and express shapes, even complex shapes are derived from simple basic geometric shapes. Seemingly complex organisms are also obtained by intersecting, subtracting, and adding multiple basic geometric shapes [6].

3.1.2. Vein/Texture. Through the manipulation of various sizes, repetitions, densities, lightness, and shapes, two-dimensional planes can appear three-dimensional, and vein on three-dimensional surfaces can bring a tactile experience. The vein is a quality of modeling, and pattern can be regarded as texture if the unit is small enough. A pattern is a graphic design that is repeated in regular units. As long as the cells that make up the cluster are large enough to be discerned by the naked eye, it is no longer considered texture. Materials have solid texture features, which involve size, shape, orientation, and proportion. The texture appears as an intertwined appearance, derived from patterns. Generally, high-density regular or irregular units can form texture. Like color, texture also aids cognition and memory because it provides visual and tactile feedback that influences how people understand and interpret an image or object.

3.1.3. Dimensions. The size of the object depends on several variables, depending on the context. Factors such as points, lines, surfaces, shapes, colors, brightness, texture, and

orientation all determine the perception of size. For a point to look like a point, it must be placed against a large enough background so that it can appear small. Otherwise, the point will turn into a shape, and the apparent length and width will constitute visual-spatial cues. In the picture, large shapes will appear closer than small lines, and thick lines will appear closer than thin lines. Gradients from small to large can symbolize or suggest motion effects. In general, the lack of contrast in the size relationship of the object will result in a static picture with visual directional movement. Color and lightness play an important role in the sense of size relationship. Light and bright colors make objects appear larger, while deep and dark colors make them smaller.

3.1.4. Color. Color in physics means that light with different wavelengths shines on an object, part of the light wave is absorbed by the object, part of the light wave is reflected, and the reflected light wave is received by the human eye. Since wavelengths between 0.39 and 0.77 μm are visible to the human eye, different objects have colors in the human eye.

(S_R, S_G, S_B, S_A) is used to represent the blending parameter of the fragment; (D_R, D_G, D_B, D_A) is used to represent the target blending parameter; and the color value can be obtained through the blending operation [7]:

$$V_Y = S_R R + D_R R + D_G G + S_G A + D_B A + S_B B. \tag{1}$$

Given $n+1$ control points at positions P_K [8]:

$$P_K = (X_K, Y_K, Z_K). \tag{2}$$

The expression of the curve is [9]

$$P(U) = \sum B_K^N(U) P_K. \tag{3}$$

The mixing function $B_K^N(U)$ is a Bernstein polynomial [10]:

$$B_K^N(U) = C_{N,K}(1-U)^{N-K} U^K,$$
$$C_{N,K}\begin{pmatrix} N \\ K \end{pmatrix} = \frac{N!}{K!(N-K)!}. \tag{4}$$

Using a new variable t to replace the variable u, the calculation formula of the B-spline curve is [11]

$$P(t) = \sum p_k N(t), \tag{5}$$

where p_k is a set of $n+1$ control points [12].

$$N_{K,D}(t) = \frac{t - t_k}{t_{k+d-1} - t_k} N_{K,D-1}(t) + \frac{t_{k+d} - t_k}{t_{k+d-1} - t_k} N_{K+1,D-1}(t). \tag{6}$$

3.2. Fusion of Information in Human and Space Design under Digital Media

3.2.1. Symbiotic Relationship. The human body itself is the medium for disseminating information, an indispensable medium for people to feel the world and understand the world, and the basic way for people to express their thoughts and spread information. Modern performance artists also use the characteristics of "body media" to the extreme. Under the influence of digital media, people's dependence on electronic media is increasing day by day, and the way to know the world will come from the media rather than personal experience. While people widely use new information processors, they greatly enhance their own subjective initiative. The state of digital media art space is shown in Figure 1.

3.2.2. Interactivity. The development of digital media technology has provided the possibility for the interaction between people, people and things, and things in space design, and this interaction makes the readers, listeners, and audiences in the traditional sense increasingly change to participants. At present, the academic visual space system refers to the image system of various visual expression elements such as graphics, characters, colors, materials, and so on as a means to express the image, content, nature, direction, and other functions of the design in a specific space.

The vector formula of the Hermite curve segment between the two control points p_k and $p_{k+1}$is [13]

$$H(U) = AU^3 + BU^2 + CU + D. \tag{7}$$

Its equivalent matrix formula is [14]

$$H(U) = \begin{bmatrix} U^3 & U^2 & U & 1 \end{bmatrix} \cdot \begin{bmatrix} A & B & C & D \end{bmatrix}, \tag{8}$$

where the four parameters A, B, C, and D can be calculated from the boundary conditions of the Hermite curve segment, and the boundary conditions are [15]

$$\begin{aligned} H(0) &= P_K, \\ H(1) &= P_{K+1}, \\ H'(0) &= \Delta P_K, \\ H'(1) &= \Delta P_{K+1}. \end{aligned} \tag{9}$$

3.3. Reconstruction Trend of Virtual Space and Real Space

3.3.1. Immersion of Space. Virtual reality strives to make people feel as if they are on the scene through a certain form of presentation, which is of great significance to the formation of spatial immersion. A successful VR presentation or work can give participants a sense of escaping their real world and immersing themselves in another environment. This sense of immersion must be produced by the sensory organs alone, rather than by the psychological imagination, which is a kind of shock of the space to the participants' senses.

3.3.2. The Imagination of Space. The imaginative nature of virtual reality is that participants make associations, judgments and inferences based on the information they obtain in the virtual space (including the feedback information on

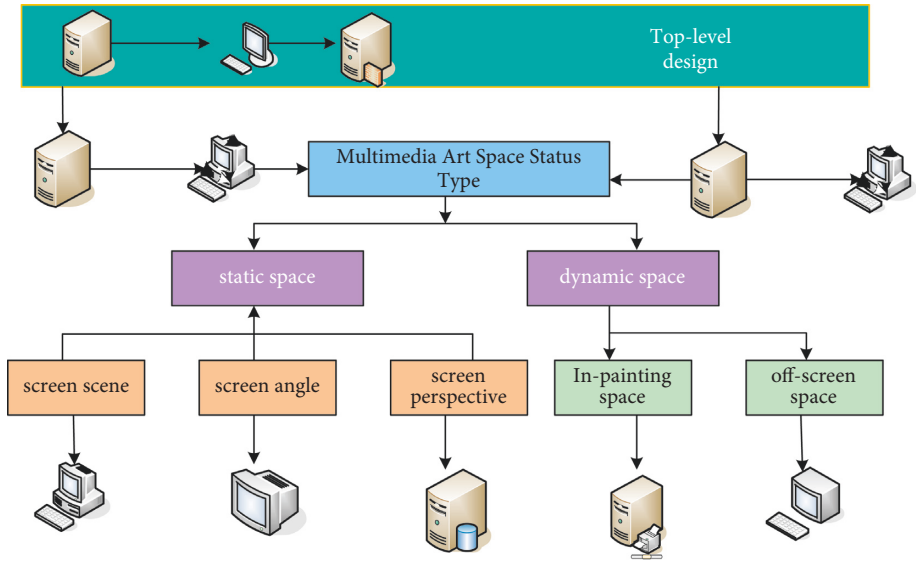

Figure 1: State of the digital media art space.

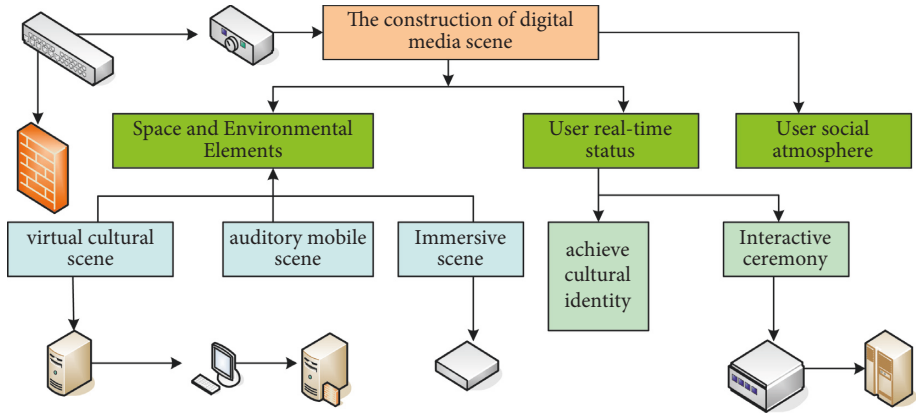

Figure 2: Construction of digital media art.

their own behavior) and make associations with the changes in the situation to obtain more information.

3.3.3. Reconstruction and Functional Change of Space. The space formed by virtual reality changes the relationship between the real space and the virtual space, that is, the virtual space can be a special part of the real space, a parallel world of the real space, or a nest of the virtual space and the real space. At this time, the virtual space is still based on the real world and does not really exist. The reconstruction of the virtual space and the real space has also changed its functionality, and the physical space, which is the basis of space at the beginning, has no special function. The survival needs of human beings gave birth to buildings, and the space has the function of living. The development of economy and culture gave birth to display culture, and the space has the function of display, and then people's imagination demand breeds virtual space. At this time, the space does not really exist, and people reach the satisfaction of their imagination after accepting the information in the space. When the narrative plot is more moving and believable, the immersion is stronger. Different participants intervene in the development of narrative plots and make interactive choices, which can also lead to the discontinuity and difference of spatial narratives, and then promote the participants to give feedback after interacting in the virtual space. The construction of digital media art is shown in Figure 2.

3.4. Construction Method and Performance of Image Element Space. The picture element is one of the most common elements in multimedia works, and its space can be divided into two. One is the space within the picture, that is, the scene in the picture we use (photographic work or other picture materials) itself constitutes the still three-dimensional space within the picture. Of course, this kind of space is the space that already exists when we obtain the picture data, and it is not changed by us. But this requires us to control the performance of the space in the shooting of reproducing the real space. The second is the space outside the picture, that is, the spatial structure of the interface of

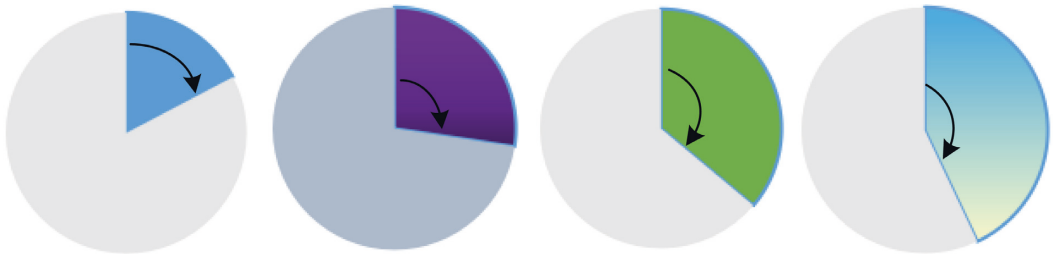

Figure 3: Brand image of a watch store.

multimedia works. The space is completely controlled by the designer, looking for the appropriate position to place pictures in the three-dimensional virtual dynamic space, making it one of the elements that constitute the overall space. The space is also a core part of multimedia art space design.

3.4.1. The Space inside the Picture. The picture element used in multimedia works, in terms of its performance in the multimedia virtual space, is a completely static two-dimensional state element and does not have a sense of volume.

3.4.2. The Space outside the Picture. The space outside the picture element in the multimedia work is the virtual three-dimensional space where the interface of the multimedia work is located. This space is a virtual three-dimensional space that is in motion. The space inside the picture is not interfered with by us, but the space outside the picture can be organized and arranged arbitrarily by us, and the core of the multimedia space form design is also here. For example, the brand image of a watch store is shown in Figure 3. In the form of a timer in a 20-minute period, it is constantly moving according to the color, the fan chart of the hour hand movement, the time, and the month, to convey the vitality of the brand and the variety of products. There will be a corresponding display visual space in the store to promote the brand culture, which can also better attract the attention of consumers.

3.5. Construction Method and Performance of Text Element Space. The spatial forms of text elements in multimedia works are divided into two-dimensional plane and three-dimensional. Regardless of whether it is a two-dimensional plane or a three-dimensional three-dimensional text element, it can be static or moving, and the text element in any state expresses the existence of space in its unique way. In multimedia design works, text mainly includes title and explanatory text, and its form is reflected by text type, font size, font color, layout and paragraph attributes between texts, some variants produced by fonts, and artistic processing effects.

3.5.1. Two-Dimensional Plane Text Elements. The text element in the two-dimensional plane state usually appears in its own inherent state and occupies its own space in multimedia works. However, this space is not emphasized too much, and the main function of the text element is to interpret the meaning of the picture. But, in some special effects, two-dimensional plane files can also achieve simple visual effects through some special methods and processing. For example, use projections or use text elements as textures to attach to 3D objects.

3.5.2. Three-Dimensional Text Elements. In the process of editing and creating multimedia works of art, we can directly build the text into a three-dimensional three-dimensional mode text style through three-dimensional software. Through the method of volume perspective, a sense of volume is established for it so that the text itself has an independent sense of visual space before it is used in multimedia works.

The weight difference D_i between $\mathrm{d}l_i$ and $\mathrm{d}l_j$ on the i-th scan line is defined as follows [16]:

$$D_{\mathrm{i}} = \frac{1}{Ml_i}\sum_{j=1}^{Ml_i}\mathrm{d}l_{i,j} - \frac{1}{Ml_{ri}}\sum_{j=1}^{Ml_i}\mathrm{d}l_{ri,rj}, \tag{10}$$

where Ml_i and Ml_{ri} represent the number of distance elements contained within $\mathrm{d}l_i$ and $\mathrm{d}l_j$, respectively [17].

$$p(\alpha) = A\,\exp[b\,\cos(\alpha)], \tag{11}$$

where b is a parameter used to adjust the degree of diffusion of the distribution and A is a normalization constant term [18].

3.6. The Construction Method and Performance of Sound Element Space-Time. Speech and all other information related to sound are sensed by hearing, so hearing is also one of the most important sense organs of human beings. Sound has also become a source of information, which uses a special transmission method to form a new art form. Digital media art is an emerging audiovisual art form, and its sound is an important digital media design element. And when we design some special multimedia works, sometimes, we use sound as the main object of digital media art design.

Classification of sounds in multimedia works:

(1) Voice time and space

Voice is the most expressive and colorful voice in reality. Vocal music makes the potential of voice fully and freely exerted, and theatrical performance makes

the voice artistic. The vitality of language is manifested in rich words. In life, we almost rely on instinct to achieve pronunciation. When they are happy, they speak very fast and have a high tone; when they are sad, they speak slowly, and their voices are low; and when they are crying and angry because their emotions are extremely unstable, the intensity, rhythm, and pitch of their voices show different time and space states. In the design of digital media artworks, voice is mainly expressed in the explanation of the content of its multimedia pages, forming a voice-over. It does not happen by the characters in the picture but only explains the meaning of the picture and the knowledge structure expressed by the work. Therefore, the voice in the digital media art design will not reflect too much of a single picture but is mostly used for the appearance of page transitions, which plays the role of prompting the page time and space to change.

(2) Sound effect space-time

Sound effects are all the sound effects in the big environment of nature, including motion, machinery, environment, nature, and other sounds. It is the most temporally expressive sound effect of all sound elements. For example, for the movement of the car from far to near, we will match the corresponding sound effects in the picture. We can see the car from far to near, and we can also audibly judge that the car is getting closer and closer to us. We can also use sound effects to hint at the spatiotemporal changes in page transitions. For example, the sound of waterfalls first enters hearing and then enters vision. This use of time and space brings us psychological-emotional changes or stimulates interest in the work itself.

(3) Music Time and Space

Music is the art of time, and the space-time created by music is an illusionary psychological space-time, which brings us a kind of psychological space-time feeling, a time-space about emotion. And what voice and sound bring us is the real environment space-time structure in the real sense. Here, we can use music to deepen the impression of the multimedia subject, render the theme atmosphere, and arouse the viewer's strong emotional inclination. In the time and space of art, music is an art that communicates with human hearts, expresses emotions, and cannot be expressed in words. It is also the most abstract and unique time art that can give people a huge imagination space. Therefore, we can use music to express rapid and subtle changes such as movement and stillness, end and change, tension and stillness, and so on to construct and set off the time and space of digital media art and to trigger people's various feelings about life. Music is an important element in the design of digital media art, and it has a huge appeal, making people immersed in the rhythm and rhythm given by the music. These characteristics of its music make us use music to render the atmosphere of the entire space-time environment and express the main emotion when we create multimedia works. When combined with its pictures, it presents richer temporal and spatial content.

The information amount X_L of a vertex with a steering angle of α is calculated as follows [19]:

$$X_L = -\log_2(\alpha). \tag{12}$$

The amount of information corresponding to rigid points (corner points) and soft points (sampling points) is calculated as follows [20]:

$$\begin{aligned} X_g &= -\sum_{i=1} \log_2\ p(\alpha), \\ X_r &= -\sum_{j=1} \log_2\ p(\alpha). \end{aligned} \tag{13}$$

Finally, the rigid-soft contrast of icon G is calculated as follows [21]:

$$G_B = \frac{I_S}{I_S + I_H}. \tag{14}$$

Let C_{out} and C_{in} denote the rigid-flex contrast of the outer boundary (if present in G) and inner boundary, respectively, and they are calculated as follows:

$$C_{\text{out}} = \frac{I_{\text{out}}}{(I_{\text{Hout}} + I_{\text{Sout}})}, \tag{15}$$

$$C_{\text{in}} = \frac{I_{\text{in}}}{(I_{\text{in}} + I_{\text{in}})}. \tag{16}$$

3.7. The Performance Time and Space of the Combination of Sound and Picture. The time and space environment is represented by a combination of audio and visual total hue calculation:

$$f_2 = \{i | h(i) > m \cdot \chi\}. \tag{17}$$

The image unevenness coefficient J_Y is

$$J_Y = \frac{(E_{\max} - E_{\min})}{(E_{\max} + E_{\min})}. \tag{18}$$

Correcting the L value:

$$L = L' + n_1 + n_1 + n_1 + \cdots + n_{m-1}. \tag{19}$$

By simplifying:

$$L = L' + (m-1) \times \overline{n} = L + (n-1) \times k \times \overline{l}, \tag{20}$$

where $\overline{l}$ is the span average.

4. Visual Space System Design Results in Digital Media Art Design

First, we use the boxplot tool to count the distribution of the average manual scores and contrast. Each central blue rectangle spans from the first quartile to the third quartile

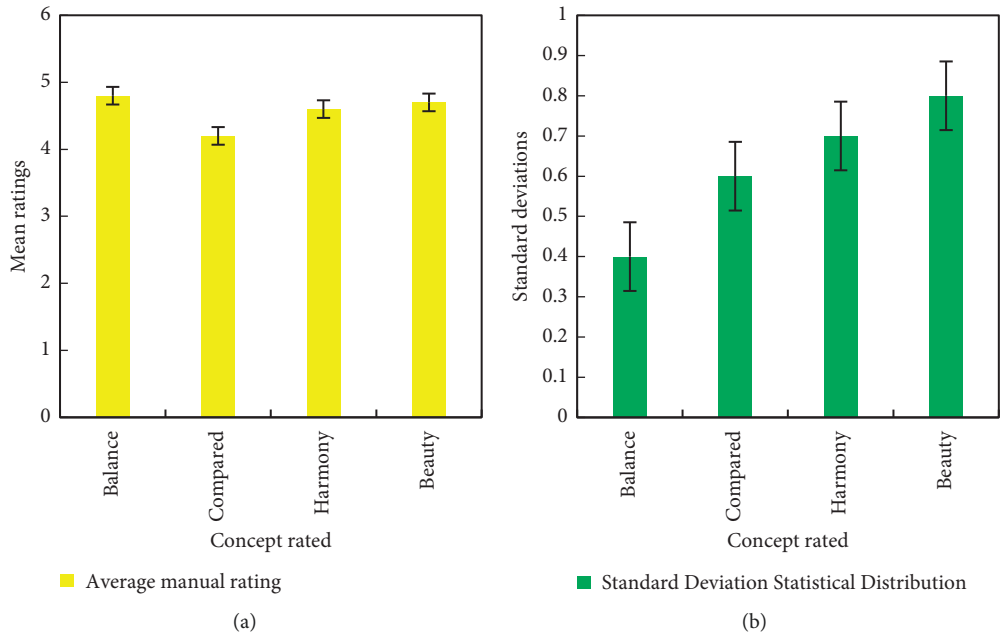

Figure 4: Comparison of 60 icons for balance, contrast, harmony, and aesthetics: (a) average human scoring and (b) standard deviation statistical distribution.

Table 1: Requirements and description of its development and operating environment.

Serial number	Name	Instruction
1	Operating system	Microsoft Windows 7, 64 bit operating system
2	RAM	The minimum requirement is 4 GB memory and the recommended 8 GB memory
3	3D modeling software	3ds max 2016 (64 bit)
4	Texture making software	Photoshop CS6 (64 bit)
5	Application development software	Unity 2017.2.3 (64 bit)

(average human scores are shown in Figure 4(a)). The graph shows the overall variation range (minimum to maximum value), the central variation range, and the typical value (median). The average human score of the 60 icons was used as the human evaluation score and aesthetic perception. In addition, we also counted the statistical distribution of the standard deviation of the manual scoring of the 60 icons in terms of balance, contrast, harmony, and aesthetics (the statistical distribution of the standard deviation is shown in Figure 4(b)). The standard deviation of the manual scoring of all icons is less than 0.9, which indicates that the variation of the manual scoring of all testers is small, which further ensures the high reliability and consistency of the manual scoring of all testers.

This design is a virtual reality indoor scene application. Since many 3D models with compact layouts need to be built using 3D modeling software in the development process, the requirements for the computer's 3D graphics computing capability are high. The development and operating environment requirements and descriptions are shown in Table 1.

According to the overall demand of the event, the plan is directly measured and drawn on the spot, then the layout is discussed, and finally, the safest, reliable, and cost-effective construction plan is determined. The construction part is divided into the following parts: light show projection wooden structure background, light show equipment hoisting rack, and AV audio lighting equipment. The construction schedule is shown in Table 2.

The construction of the M museum pays great attention to the development of the museum under the new situation. The museum not only has an educational interactive area but also pays attention to the experience and feelings of visitors in the design of the exhibition. It not only has exhibits and pictures, but even modern technology will be used as a form of expression to design a variety of media display projects. On the first floor of the museum, a digital projection hall and an interactive multimedia hall are established. The digital projection hall adopts a full-view ultrawide screen as a digital projection for playing high-definition digital movies and three-dimensional movies. The interactive multimedia hall is equipped with high-configuration computers and high-definition digital playback equipment. The exhibition area emphasizes making visitors feel like they are in the real world and conveys the information of the exhibits in an experiential and interactive way. The exhibition on the first floor of the M museum is shown in Figure 5.

The origin of the two-dimensional coordinate system is set at the upper left corner of the marker; the X-axis is the horizontal direction; and the Y-axis is the vertical direction.

Table 2: Construction period arrangement.

Matter	Time period	Number of vehicles	Number of people
Electrical construction	September 28, 09:00–10:00	1 car	3 people
Background construction	September 28, 09:00–29 12:00	1 car, 3 trucks	20 people
Truss frame construction	September 28, 09:00–14:00	1 car, 2 trucks	10 people
Projection lighting and sound system	September 28, 10:00–22:00	1 car, 2 trucks	10 people

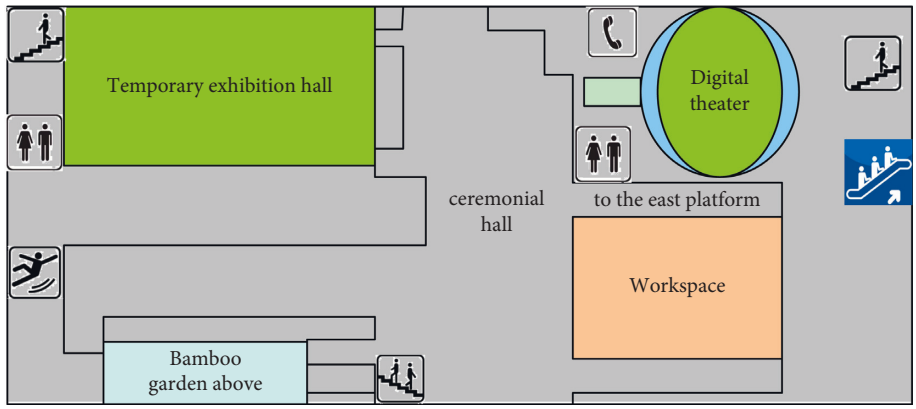

Figure 5: Exhibition on the first floor of the M museum.

Table 3: Raw pixel coordinates.

Color	Raw pixel coordinates	3D coordinates	Number of people	Color	3D coordinates
Red	(90, 810) (290, 921)	(−108.68, −13.12) (−71.71,−61.87)	Yellow	(840, 810) (1040, 921)	(76.17, −13.12) (47.71, −61.87)
Blue	(471, 810) (671, 921)	(−41.28, 13.12) (−12.31, 61.87)	Green	(1211, 810) (1411, 921)	(76.17, −13.12) (109.10, −61.87)

The pixel is (1,500, 1,050); the virtual key size is set to (200, 75); the Vuforia SDK adopts the right-hand coordinate system; and the center point (0, 0, 0) of the marker is used as the origin of the three-dimensional coordinate system. The X-axis is positive to the right; the Y-axis takes the marker plane as a reference, and the upward is positive; and the Z-axis takes the marker plane as a reference point and is perpendicular to the marker plane, and the upward is positive. The original pixel coordinates are based on the left and right diagonal coordinates of the virtual button rectangle. The original pixel coordinates are shown in Table 3.

The design survey questionnaire surveys relevant domestic designers and conducts a statistical analysis on the status and views of today's dynamic logo development. Questionnaires are distributed online and on-site so that the coverage is wide, and online distribution is convenient for designers to answer questions and saves time and paper. In the process of answering the field distribution, there are some related questions that can be exchanged in person and in a timely manner. The questionnaire was issued from January 24, 2018, to March 12, 2018, and 80% of the designers surveyed were from design majors (professional statistics are shown in Figure 6(a)). Among the designers, 52.46% are between 26 and 30 years old, and 39.34% are between 18 and 25 years old. Among them, 8.2% are over 35 years old (the age statistics of designers are shown in Figure 6(b)). It can be seen that the people engaged in dynamic logo design are generally young, with rich imagination and innovation passion.

The number of domestic dynamic logos is relatively small, and the data on the types of logos usually designed shows that 16.39% are text-based logos, and 16.39% are image-graphic logos (the statistics of text-based and image-graphic logos are shown in Figure 7(a)). Among them, 14.75% are geometric symbols; 47.54% are graphics combined with text; and only 4.92% are dynamic symbols (the statistics of geometric graphics and graphics combined with dynamic symbols are shown in Figure 7(b)). It can be seen that most of the logo designs are a combination of graphics and text, and there are fewer dynamic logo designs. Compared with static logos, dynamic logos more comprehensively show the spirit of enterprise. The development potential of a dynamic logo is great; the designer has few dynamic logo projects; and the experience is not rich enough, which is also one of the factors behind the slow development of the dynamic logo. Therefore, as a designer, we should strive to improve our own technology and knowledge and better apply dynamic logos to appropriate corporate branding.

In addition to meeting the basic aesthetic requirements, the use of digital media art in the display space is particularly important. The data on the direction that a dynamic logo

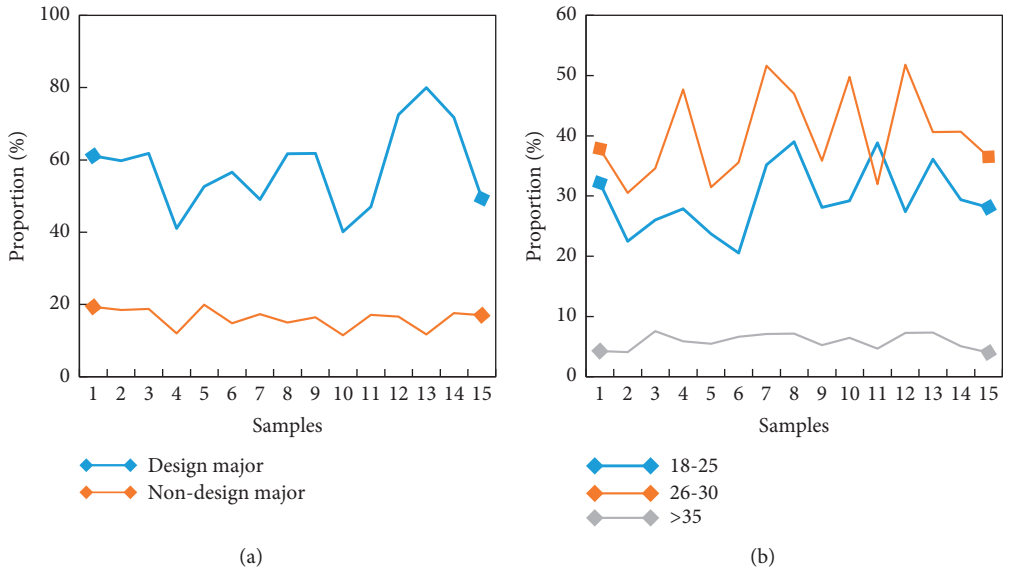

Figure 6: Designer statistics: (a) professional statistics and (b) designer age statistics.

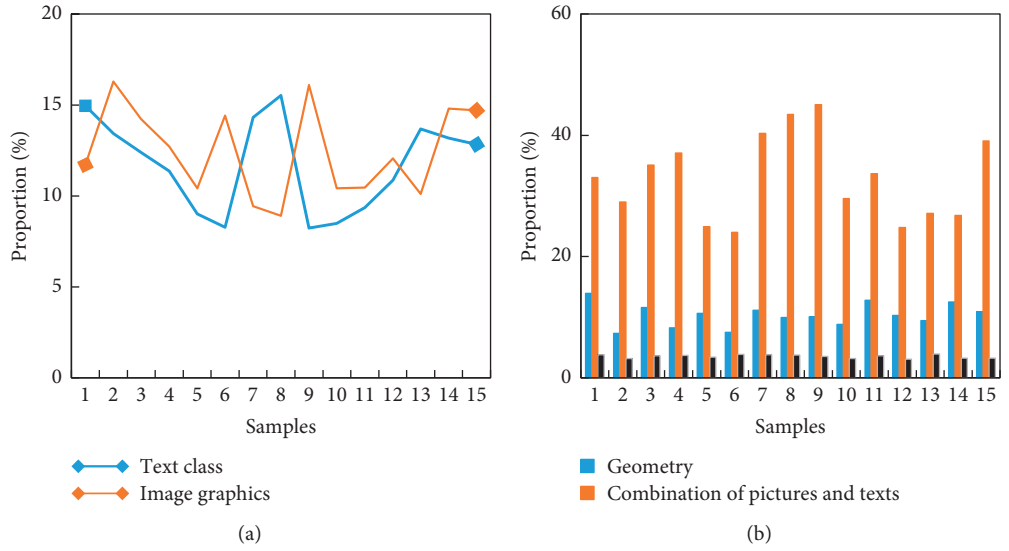

Figure 7: Logo design type data statistics: (a) statistics of text and image-graphic signs and (b) geometric figures, graphics and text combination, and dynamic logo statistics.

focuses on show that 68.85% of designers believe that good creativity is the most important aspect (color, shape, and style statistics are shown in Figure 8(a)). A creative dynamic logo can effectively attract the audience and leave a deep impression on the audience during the display process. In this way, while promoting the corporate image, it can leave a good reputation among the audience (meaning, creativity, practicality, and fashion statistics are shown in Figure 8(b)). When designing dynamic logos, designers should pay attention to the creative design part and take into account elements such as color, style, fashion, and shape. Creativity is the core soul of a dynamic logo, and it is also the most intuitive point of color. To attract the attention of the audience the first time and leave a deep impression, the creative point is very important.

Figure 9 shows the effect of digital media art on future corporate image propaganda. Among the designers, 75.41% believe that there is a promotion effect, which shows that the designers are very optimistic about the development prospects of digital media art. The designer's confidence in the development of digital media art is directly related to the completion and specific application of digital media art, and it has a positive effect on popularization.

According to the data analysis of CNNIC (China Internet Information Center), the main body of digital media in China is 10–39 years old, accounting for 78.1%. There are three main groups in the population structure: students

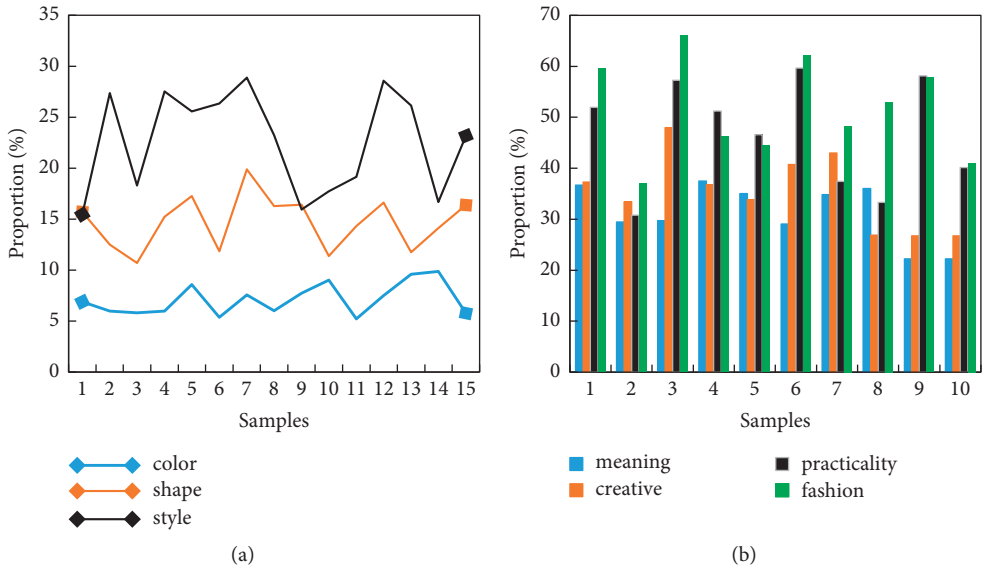

Figure 8: Statistical aspects of dynamic logo design focus: (a) statistics of text and image-graphic signs and (b) geometric figures, graphics and text combination, and dynamic logo statistics.

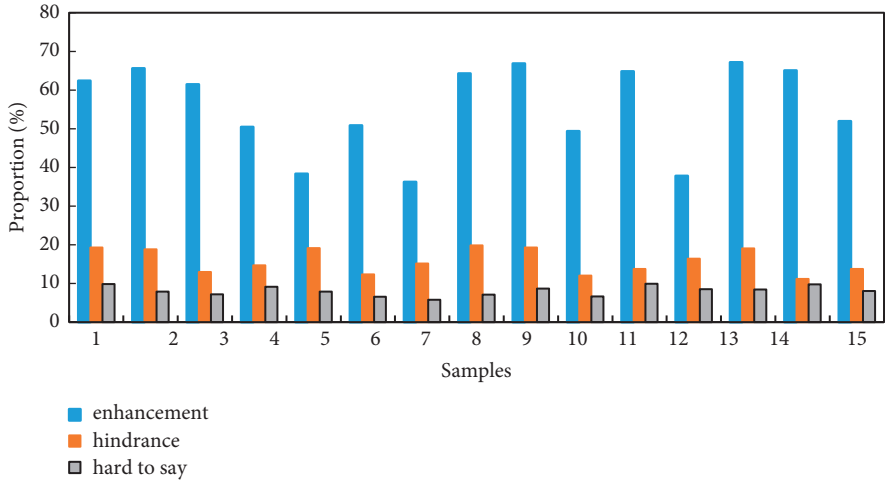

Figure 9: Statistics on the effect of digital media art on future corporate image promotion.

account for 23.8% of the total, self-employed and freelancers account for 22.3% of the total, and employees of public institutions and enterprises account for 14.2% of the total. Therefore, the main group of respondents is set as 18–35-year-old college students, office workers, and young self-employed freelancers. Figure 10 shows the population structure statistics of digital media.

Most of the dynamic logo designs are displayed on digital media, and there is a lot of room for display. The commonly seen dynamic logo display form is shown in Figure 11. According to the data, 80.33% of dynamic signs are displayed and played in the virtual display space of network media. The development of dynamic signs is closely related to the application of digital media art. As the main body of publicizing corporate image, relying on digital media display is too limited. For example, the art museum not only considers the dynamic logo display in the virtual digital space but also uses the form of installation art to display the dynamic logo in the actual space in order to enrich the art museum itself and image promotion. This breaks through the application of the single display space and enriches the dynamic logo display itself, which plays a good role in publicity. At present, it is the initial stage of the development of dynamic signs, which is mainly based on network media display, and the actual plane and environmental display space are used as a way to comprehensively publicize the image of enterprises in the future.

The statistics of favorite aspects of visual space design are shown in Figure 12. Among the respondents, 31.85% think that interesting and unusual styles are attractive; 31.21% think that creativity is the most attractive; and 17.17% think that the texture effect is more attractive. It can be seen that the public thinks that the visual space design that is creative

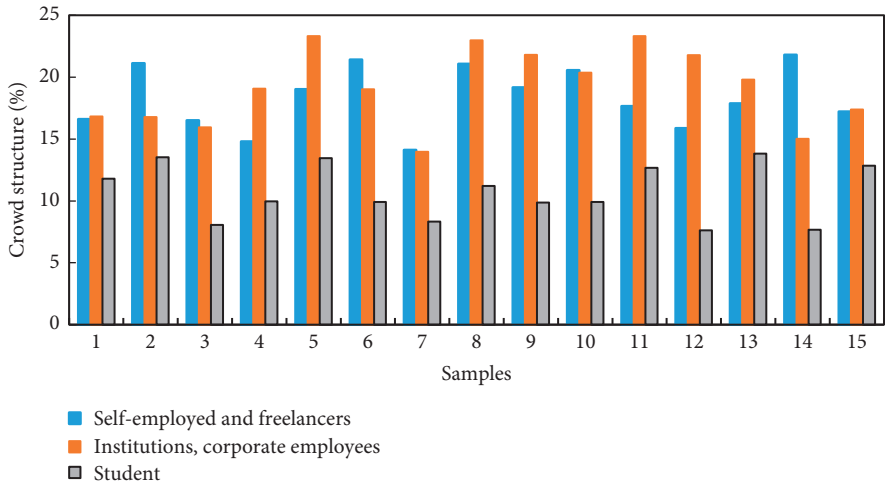

Figure 10: Crowd structure statistics of digital media.

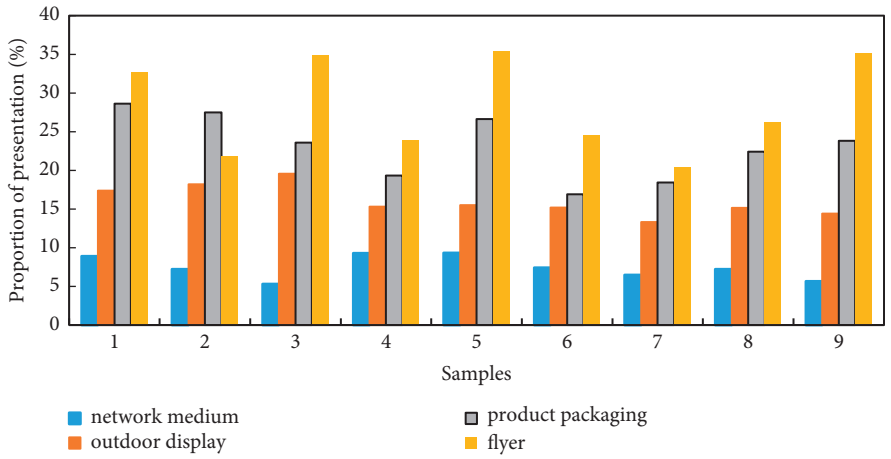

Figure 11: Dynamic logo display form.

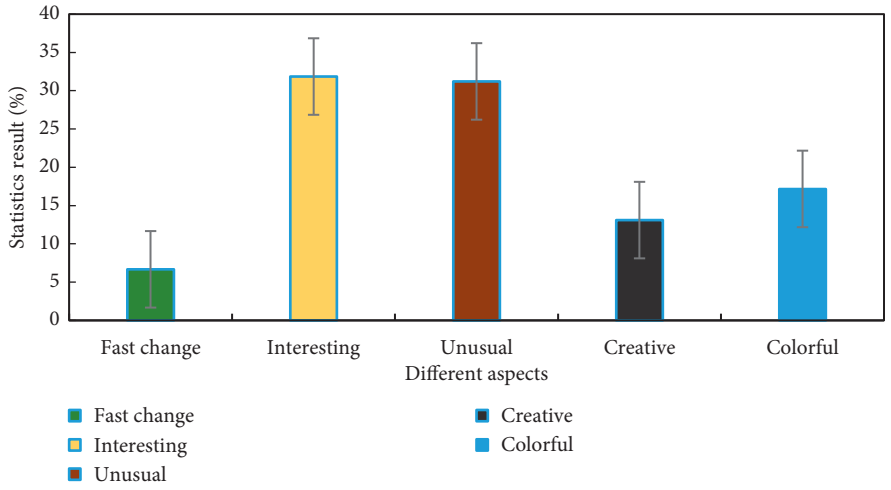

Figure 12: Favorite aspects of visual space design.

and distinctive and has a good display effect attracts people's attention. In the process of designing dynamic logos, we should pay attention to the appeals and aesthetic preferences of the public so that information can be more effectively conveyed during the display process and the brand culture can be better promoted.

5. Discussion

Digital media art is virtual, and the biggest feature of digital media art is digital. The virtuality of today's media art is achieved through the pervasiveness of computers in everyday life, helping realize the wider world. At the same time, the continuous development of computer technology has created a whole new movie world. Digital media art is commonly used in the shooting and production of film and telefilm. The application of digital media art in these fields can be excellent in shooting different scenes and effects. In movies, digital technology is used to create new scenes and virtual environments that do not exist in real life.

From visual communication to interactive art, from two-dimensional plane to three-dimensional, from printing art to an interactive display, from traditional to avant-garde, behind the development of information communication is the huge influence brought by the progress of science and technology. The development of new media interactive art has opened a new horizon for visual communication design [22]. No matter what field it is in, good works need to be integrated into emotions, and through humanized design, the original intention of creation can be restored to the maximum extent.

Network media is centered on digital technology, which has a huge impact on the design methods and thinking in visual communication design. It makes the design no longer limited to the two-dimensional plane composition, the organization structure, time, and movement of the three-dimensional space are also added to the visual elements, and the content layout also develops from static to dynamic and interactive layout. In such a design environment, the design forms that can bring people visual stimulation and aesthetic experience have attracted much attention. The expression of visual space in digital media art is also full of creativity.

The design of the subtitles fully emphasizes the visual art of the film. The design of subtitles is an important content and part of a movie. It is a form of expression in visual art that expresses aesthetics and emotions and expresses personal emotions independently. Subtitles can convey theatrical content through visual arts images and can also broadcast TV content without sound.

6. Conclusion

Digital copying has become the dominant copying method. Music and sound can be synthesized by computer, not only to restore the original high-quality sound effect but also to avoid the noise produced by existing external sound receiving equipment. Not only has the digital audio processing method become an appropriate term to reflect the feeling of replacing the visual image, but the priority sound also tightly controls the rhythm of the plot while giving designers more creative space. The main communication method in the context of digital media is visual communication, which is different from other communication methods. The dissemination of visual arts is a new way of disseminating information. Therefore, the dissemination of content will be richer, more complete, expressive, and attractive. Different from the traditional visual art communication methods, the visual art in the digital media environment has very important characteristics, which are mainly manifested in the visual art communication under the background of digital media represented by digital equipment and communication. Therefore, the dissemination of visual arts has the characteristics of media, and the dynamic characteristics of the transmitted media become more obvious. Digital media can innovate and develop display art from different perspectives, jointly improve the level of China's display industry, make the application of display design innovative and develop, and make the specific practical research of display design rise to comprehensive theoretical research. Ultimately, the application development of the display industry and other industries will be promoted through the development of digital media art.

Data Availability

No data were used to support this research.

Conflicts of Interest

The authors declare that they have no potential competing interests in our paper.

Authors' Contributions

All authors have read the manuscript and approved for publication.

References

[1] D. Peicheva and V. Milenkova, "Knowledge society and digital media literacy: foundations for social inclusion and realization in Bulgaria1n context[J]," *Calitatea Vietii*, vol. 28, no. 1, pp. 50–74, 2017.

[2] J. Forestal, "The architecture of political spaces: trolls, digital media, and deweyan democracy," *American Political Science Review*, vol. 111, no. 1, pp. 149–161, 2017.

[3] D. Romer and M. Moreno, "Digital media and risks for adolescent substance abuse and problematic gambling," *Pediatrics*, vol. 140, no. 2, pp. S102–S106, 2017.

[4] J. Reyna, J. Hanham, and P. Meier, "The Internet explosion, digital media principles and implications to communicate effectively in the digital space," *E-Learning and Digital Media*, vol. 15, no. 1, pp. 36–52, 2018.

[5] S. Oklobdija and J. Popesku, "The link between digital media and making travel choices," *Marketing*, vol. 48, no. 2, pp. 75–85, 2017.

[6] L. Zhang, "The visual elements in film poster design based on photoshop," in *Big Data Analytics for Cyber-Physical System in Smart City. BDCPS 2019*, M. Atiquzzaman, N. Yen, and Z. Xu, Eds., vol. 1117, pp. 1620–1625, Springer, Shenyang, China, 2020.

[7] T. Allmer and E. Bulut, "Academic labour, digital media and capitalism (combined PDF of all articles)," *tripleC: Communication, Capitalism & Critique. Open Access Journal for a Global Sustainable Information Society*, vol. 16, no. 1, pp. 44–240, 2018.

[8] R. M. Crotty, "Book review: gabriele Balbi and Paolo Magaudda, A history of digital media: an intermedia and global

perspective," *Mobile Media & Communication*, vol. 9, no. 1, pp. 151-152, 2021.

[9] W. Li and L. Ye, "224 digital media use and sleep in college students during COVID-19 pandemic," *Sleep*, vol. 44, pp. A89–A90, 2021.

[10] J. Reyna, J. Hanham, and P. Meier, "A taxonomy of digital media types for Learner-Generated Digital Media assignments," *E-Learning and Digital Media*, vol. 14, no. 6, pp. 309–322, 2017.

[11] L. N. cube and A. Salawu, *African Language Digital Media and Communication*, Routledge, vol. 34, no. 1, , pp. 1–4, New York, NY, USA, 2019.

[12] C. Arrieta-Castillo and Y. Berdasco-Gancedo, "Brexit and female leadership in Spanish digital media from a linguistic perspective. The case of Theresa May's decline," *Communications Society*, vol. 33, no. 2, pp. 243–257, 2020.

[13] S. Ren, K. He, R. Girshick, and J. Sun, "Faster R-CNN: towards real-time object detection with region proposal networks," *IEEE Transactions on Pattern Analysis and Machine Intelligence*, vol. 39, no. 6, pp. 1137–1149, 2017.

[14] J. Donahue, L. A. Hendricks, M. Rohrbach et al., "Long-term recurrent convolutional networks for visual recognition and description," *IEEE Transactions on Pattern Analysis and Machine Intelligence*, vol. 39, no. 4, pp. 677–691, 2017.

[15] S. S. S. Kruthiventi, K. Ayush, and R. V. Babu, "DeepFix: a fully convolutional neural network for predicting human eye fixations," *IEEE Transactions on Image Processing*, vol. 26, no. 9, pp. 4446–4456, 2017.

[16] D. G. Martin, "Discriminative scale space tracking," *IEEE Transactions on Pattern Analysis and Machine Intelligence*, vol. 39, no. 8, pp. 1561–1575, 2017.

[17] C. Forster, Z. Zhang, M. Gassner, M. Werlberger, and D Scaramuzza, "SVO: semidirect visual odometry for monocular and multicamera systems," *IEEE Transactions on Robotics*, vol. 33, no. 2, pp. 249–265, 2017.

[18] F. Han, B. Reily, W. Hoff, and H Zhang, "Space-time representation of people based on 3D skeletal data: a review," *Computer Vision and Image Understanding*, vol. 158, no. C, pp. 85–105, 2017.

[19] L. Li and H. W. Shen, "Image-based streamline generation and rendering," *IEEE Transactions on Visualization and Computer Graphics*, vol. 13, no. 3, pp. 630–640, 2017.

[20] Y. Wei, Y. Zhao, C. Lu et al., "Cross-modal retrieval with CNN visual features: a new baseline," *IEEE Transactions on Cybernetics*, vol. 47, no. 2, pp. 1–12, 2016.

[21] M. Muszkieta, "A variational approach to edge detection," *Inverse Problems and Imaging*, vol. 10, no. 2, pp. 499–517, 2017.

[22] D. Shao, "Art design methods based on big data analysis," in *Big Data Analytics for Cyber-Physical System in Smart City. BDCPS 2019*, M. Atiquzzaman, N. Yen, and Z. Xu, Eds., vol. 1117, pp. 584–589, Springer, Singapore, 2020.

Hindawi
Scientific Programming
Volume 2022, Article ID 4642995, 10 pages
https://doi.org/10.1155/2022/4642995

Research Article

A Pest Intrusion Detection in Chinese Beehive Culture Using Deep Learning

Chao Liu and Shouying Lin

Fujian Agriculture and Forestry University, Fuzhou, Fujian 350002, China

Correspondence should be addressed to Shouying Lin; 1191264001@fafu.edu.cn

Received 24 March 2022; Revised 14 April 2022; Accepted 18 April 2022; Published 28 April 2022

Academic Editor: Muhammad Zakarya

At present, the quality of material life and richness of the Chinese residents have been improved. Some people have high requirements for quality of their personal lives and put forward the problem of health preservation. Honey, as a nutritious food, is deeply loved by people. There are a large number of trace elements in honey, such as VC, VA, VD, VB1, and VB2. The honey from the Chinese honeybee has a very high nutritional value and plays an important role in the pollination and reproduction of some plants. Therefore, the Chinese honeybee plays a very significant role in the ecological environment. Moreover, it is protected as the main species resource of the country, which also fully proves the importance of the Chinese honeybee. Chinese bees can survive in various ecological and geographical environments in China and have strong heat as well as cold resistance. They can survive in the hot environment in the south and withstand the dynamics of severe cold in the north. At the same time, they can make full use of a small number of honey sources and have strong resistance to a variety of diseases and pests. In fact, there will be a variety of insect invasion problems in the beehive culture of Chinese bees, and it is necessary to accurately detect various diseases and pests during the breeding of Chinese bees. However, there are a large amount of insect invasion and various disease sources in the breeding stage of the Chinese bees. Therefore, in this paper, we use a deep learning algorithm to detect the insect invasion of the Chinese beehive culture and analyze the bee colonies in six bee farms in the province of Sichuan. In addition, we measure the common insect and disease indexes of the Chinese bee and analyze the parasitism rate, microsporidia infection rate, virus infection rate, and virus infection titer of bee colonies in overwintering and spring breeding. The experimental results show that the anti-insect invasion situation of bees in the six bee farms is significantly different; however, the antimite ability is basically the same.

1. Introduction

The problem of insect invasion during beehive breeding has always been a problem faced by the beekeeping industries. Globally, this has also hindered the development of the beekeeping industries. There are four kinds of parasitic insects in bee diseases and insect pests, which are (i) fungi, (ii) viruses, (iii) microsporidia, and (iv) bacteria. According to relevant data, the annual loss of bee colony breeding caused by diseases and insect pests in China exceeds 30%, and the economic loss caused by honey production reduction reaches hundreds of millions of yuan [1]. Especially in recent years, China has paid attention to the quality and safety of honey products and gradually improved the standard of chemical drug detection materials. Chinese bee can survive in various ecological and geographical environments in China. It has strong heat resistance and cold resistance. It can survive in the hot environment in the south and withstand the dynamics of severe cold in the north. At the same time, it can make full use of a small number of honey sources and show strong resistance to a variety of diseases and pests. However, there will be a variety of insect invasion problems in the beehive culture of Chinese bees, and it is necessary to accurately detect various diseases and pests during the breeding of Chinese bees. However, there are a large amount of insect invasion and various disease sources in the breeding stage of Chinese bees that should be detected accurately. In terms of detection, machine learning-based prediction approaches have been well studied in the state-of-the-art literature. Various mechanisms and

computational learning methods have been suggested to early detect similar diseases and reduce the losses of the bee industries [2, 3].

In this paper, we use the deep learning algorithm to detect the insect invasion of the Chinese beehive culture [4]. For the problem of insect invasion in Chinese beehive culture, this paper selects the deep learning algorithm for detection and analysis. It is one of the learning algorithms based on the human brain, such as the deep learning algorithm of the human brain, which uses the neural network to analyze and simulate the data. By combining with low-level features, it forms an abstract high-level representation of features and attributes. This paper uses a deep learning algorithm to simulate and analyze the problem of insect invasion in the process of Chinese beehive culture, summarizes various types of insect pests and diseases, analyzes the main types of insect pests and diseases attacking Chinese bees in hive culture in six farms, and studies the anti-insect and disease ability of Chinese bees in each stage.

In this paper, the process of intrusion algorithm based on deep learning is described in detail. Moreover, the operation process of the convolutional neural network (CNN) is introduced, and the intrusion detection technology is analyzed. Furthermore, the paper introduces the standard hive and ecological hive of Chinese beehive breeding and lists the detection technology of Chinese bee pest invasion. Through the analysis of six bee farms of Chinese beehive breeding in Sichuan province, the parasitic rate of bee mites and microsporidium spores is measured. Similarly, the virus infection rate and infection titer are calculated, and the invasion of Chinese bee pests in six bee farms in different periods are detected. The analysis shows that the virus infection is high. Furthermore, there are great differences in the invasion of insects such as microsporidia, and the parasitism of bee mites is basically the same. The main innovations of this paper are as follows:

(i) The process of intrusion detection algorithm based on deep learning is described in detail

(ii) The operation process of the convolutional neural network (CNN) model is introduced, and the intrusion detection technology is analyzed

(iii) We introduce the standard hive and ecological hive of Chinese beehive breeding and lists the detection technology of Chinese bee pest invasion

The remaining of the paper is structured as follows: In Section 2, we discuss some related work from the existing literature. We provide a brief summary of each approach that has been studied to detect honeybee diseases. In Section 3, we suggest an intrusion detection algorithm based on the deep learning method. Section 4 is about the pest intrusion detection in Chinese beehive culture. Section 5 is about the experimental results. Moreover, an analysis of insect invasion detection in Chinese beehive culture is also provided in this section. Finally, Section 6 summarizes the paper and discusses directions for further research.

2. Related Work

Beehive is the main tool for breeding bees and is also the habitat for bees to reproduce. Moreover, various honey products produced by bees are also stored in beehives [2]. Various researchers have proposed different methods related to the beehive. Sun et al. pointed out that the style and size of beehives directly affect the survival and later reproduction of bees, which is conducive to the scientific management and breeding of beekeepers and greatly improves the economic benefits of the bee breeding [3]. Zhang pointed out that Chinese bees mostly live and grow in a cave nesting way in the natural environment. Other scholars pointed out that breeders use old beehives made of wickers, adobe, wooden boxes, and hollow trees to domesticate Chinese bees and make them adapt to life in beehives [4]. However, these kinds of artificial beehive also incur problems in the process of breeding Chinese bees. For example, most of them are made by themselves, and there is no standardized basis for reference. In addition, it is difficult to build nests and take honey, which is not conducive to the large-scale breeding of the Chinese bees, which hinders the development of the Chinese bee breeding industry and hits the enthusiasm of beekeepers [5].

Xu et al. used the Italian bee Langs live frame hive method to breed the Chinese bees, and remarkable results were achieved. At the same time, more than ten kinds of Chinese bee live frame hives were invented to maintain the stable development of China's beekeeping industry [6]. Wang et al. pointed out that beehives directly affect the honey production of bees, and the number of bee colonies and honey production are different with different types of beehives [7]. For example, the superimposed beehive is based on reducing the capacity of a single Lang's beehive and adding the number of relay boxes, so that the bee colony has a very strong swarm potential and is convenient to form a mature bee colony. Su et al. readjusted the nest frame, bee path, and quantity of Lang's hive according to the breeding mode of the Chinese bee in Guangxi. After improvement, it has a wide range of applications in the market and is also loved by the majority of farms, especially for commercial breeding of the Chinese bee [8].

It is well-understood that the honeybee is the main economic insect. The main disease of a bee colony in the world is microcystis. Sener's research data show that the two honeybee microbroods are very similar in morphology, and there are only differences in size. Moreover, *N. apis* is approximately $6.0 \times 3.0\,\mu$m and *N. ceranae* is basically $4.7 \times 2.7\,\mu$m or so [9]. Chemurot et al. used a transmission electron microscope to identify *N. apis* and *N. ceranae* based on the polar coil, and the authors believe that a scanning electron microscope can accurately measure the length and diameter of the microbrood [10]. Yudakhina measured that the size of honeybee microbrood in the Oriental Honeybee colony was approximately $4.68 \times 2.19\,\mu$m. According to the data, it is speculated that the microsporidium in the Chinese bee may be *N. ceranae* [11].

3. Intrusion Detection Algorithm Based on Deep Learning

3.1. Deep Learning Algorithm Concept. Deep learning algorithms are widely used in computational and machine learning methods. These algorithms are used to deal with the problem of deep extraction of the data features [12]. When using artificial neural networks (ANNs) to deal with some very simple problems, there are only two key neurons, namely, (i) input signal neurons and (ii) output signal neurons. However, deep learning algorithms are not a double-layer structure. In fact, they try to hide a large number of linear or nonlinear elements in the double-layer structure, which can better process the input data (as shown in Figure 1).

Deep learning is an important part of the machine learning methods. In fact, deep learning is used to represent the multilayer network structure model. It simulates the basic characteristics of neurons processing and transmitting information through neural learning, which is shown in Figure 1 [13]. In general, multiple nodes are connected in the neural network calculation model, which shows the following two basic characteristics:

(1) It effectively deals with the problem of weighted input value between each node and adjacent nodes

(2) The weight has a direct impact on the transmission data strength between nodes, and the algorithm weight is adjusted by self-learning

The essence of deep learning is to represent some features on abstract data or very complex functions by using hierarchical and multilayer linear networks. During image processing, it is shown to train a large number of experimental samples to obtain learning image features. These can be obtained in the process known as feature extraction.

3.2. Convolutional Neural Network (CNN). Generally, $f(x) * g(x)$ represents the convolution process. Formula (1) is a continuous one-dimensional convolution solution equation, and formula (2) is a discrete one-dimensional convolution solution equation.

$$f(x) * g(x) = \int_{-\infty}^{+\infty} f(\tau) g(x - \tau) d\tau, \tag{1}$$

$$f(x) * g(x) = \sum_{i=-\infty}^{+\infty} f(i) g(x - i). \tag{2}$$

In the previous formulas, f represents input and G represents the kernel function. In most scenarios, convolution uses mathematical language to explain the signals obtained from the real world. People collect signals in the real world by superposition or coupling, and the essence of superposition or coupling is convolution. That is, u represents the signal collected by people from U1 and U2, whereas the UN original signal is obtained by the convolution process. For example, the sound heard can be regarded as the result of convolution between the student source and the propagation medium. Similarly, the seismic information received by the seismic sensor can be regarded as the result of convolution between the shock wave formed by the seismic source and the propagation medium of the array element. In addition, the image obtained by a remote sensing sensor is obtained by convolution of the ground object and the light source. The signals generated after collecting and convoluting ground object signals, microwave signals, and light sources are remote sensing images [14]. Based on the theory of convolution between signals and ground objects, people can get the required signal deconvolution from the ground objects [15].

3.3. Intrusion Detection Technology. The intrusion detection system can monitor the traffic on the network and the log data stored in the computer and judge whether there is a malicious attack through analyzing various characteristics of the data [16]. The main components of the proposed intrusion detection system are hardware and software. Figure 2 shows the deployment model of the intrusion detection system.

4. Pest Intrusion Detection in the Chinese Beehive Culture

4.1. Chinese Beehive

4.1.1. Standard Beehive. The standard beehive uses a standard 7-frame box with a thickness of about 2.5 cm. During the breeding of the Chinese bees, the relay box can be added according to the demand. The standard nest foundation, nest frame, and partition board are installed in the middle of the box. The top is covered with a box cover and cloth [17]. Finally, asbestos tile, straw, and wheat straw are covered on the cover, which are used to prevent rain and to shade from the natural disasters. Figure 3 shows a typical view of the standard box of the Chinese bee.

4.1.2. Ecological Beehive. According to the nature of the beehive, it can be called an ecological beehive. The basic principle of the beehive is to save space, produce honey with high maturity and quality, and cultivate strong bee colonies [18]. The components of the ecological beehive include multiple boxes, box covers, and box bottoms. Generally, the height, thickness, and width of the box are 10 cm, 3 cm, and 30 cm, respectively. It is a square wooden box with no cover at the top and bottom. After fixing and overlapping, a complete box is formed [19]. The box cover is made of a wooden board, with a length and width of 40 cm and a thickness of 3 cm. It is fixed on the top box, and asbestos tiles, straw, and wheat straw are covered on the box cover to prevent rain and to shade from the natural disasters. The length, width, and thickness of the box bottom formwork are 50 cm, 40 cm, and 3 cm, respectively. Four wooden strips with a width of 3 cm are used to nail into a square frame with an outer 30 cm. The number of ecological hives required is determined according to the number of cultured bees.

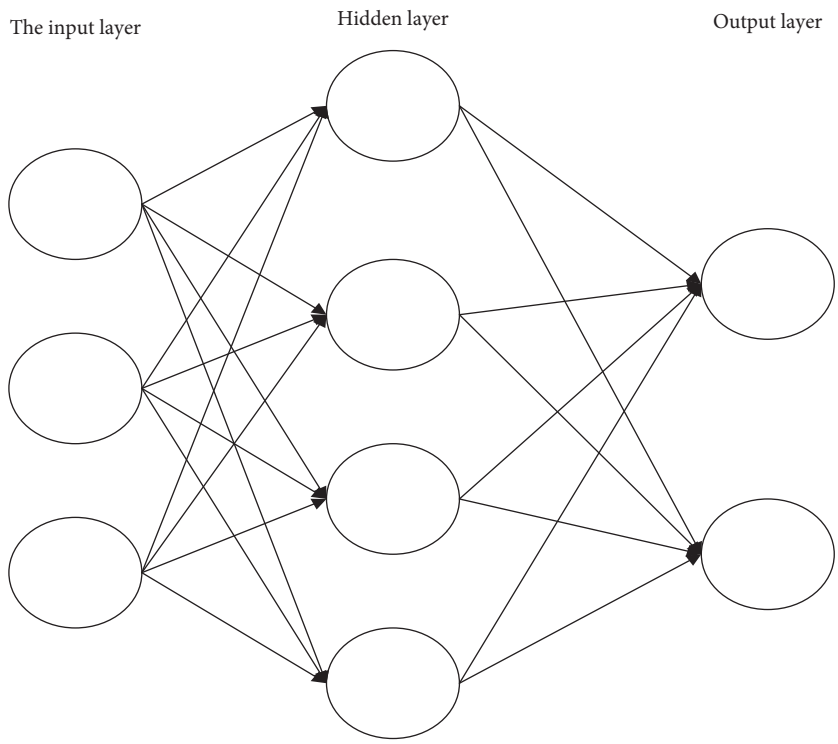

Figure 1: Neural network model.

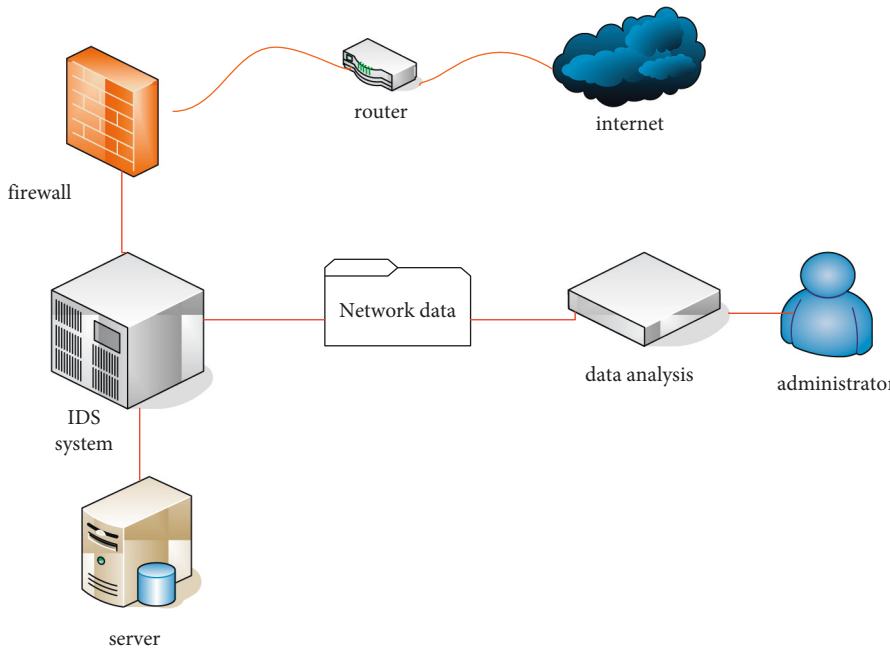

Figure 2: Deployment of the intrusion detection system.

Usually, an ecological hive is composed of three boxes, which is shown in Figure 4.

4.2. Techniques and Tools for Rapid Diagnosis of Chinese Bee Pest Invasion. In fact, each bee is small and most bees have the same external symptoms after diseases and insect pests. At present, the methods for diagnosing bee diseases are only used in the laboratory, which are described in detail, as illustrated in Table 1. The detection methods used include serological detection, microscopic examination, and molecular biology examination. In particular, the honeybee virus did not cause obvious symptoms for a long time after the invasion of diseases and pests, resulting in the formation of low-concentration recessive infection in the honeybee population. If the external environment meets the

Figure 3: Standard Chinese beehive.

Figure 4: Ecological Chinese beehive.

requirements, it will activate a large number of insect invasions, help them replicate rapidly in the host cells, improve the pathogenicity, and form a large-scale lethal honeybee virus. In most environments, there will be multiple compound infections or cross-infection transmission of different pathogens in a bee colony. The researchers proposed that *Varroa* mites can spread and carry the KBV virus [12, 20]. The harm caused by parasitic *Varroa* mites is serious after the number reaches medium scale, becoming a virus with high lethality. Therefore, once the honeybee epidemic appears on a large scale, due to the lack of directly applied systems or diagnostic and prediction tools, it is difficult for honeybee farmers to use effective measures to diagnose and control, so as to form the epidemic in various regions. At the same time, bee farmers will use various drugs to reduce the number of bee deaths, hoping that a drug can play a therapeutic role [21]. These drugs will remain in honey products, resulting in safety and quality problems of the bee products.

4.3. Pest Intrusion Detection in Chinese Beehive Culture

4.3.1. Test Colony. In this paper, six bee farms in six counties and cities, including Ya'an, Shimian, Xichang, Baoxing, Pingchang, and Mingshan, were selected as test colonies. The bee colonies and honey samples collected were transported to the Sichuan livestock and Poultry Quality Inspection Center in October 2019. After the selected test, colonies were sent to the Sichuan Inspection Center, where they were replaced with new beehives prepared before, and the test sites were placed alternately at random, in terms of number, and each colony was managed.

4.3.2. Measurement Index. In this paper, six bee colonies were sampled and measured on December 12, 2019, and March 12, 2020. The basic indicators selected in the determination of the bee colonies are (i) the number of microsporidia spores, (ii) the parasitic rate of bee mites, (iii) virus infection titer, and (iv) virus infection rate [22].

4.3.3. Test Method

(i) *Parasitism Rate of Bee Mites.* Approximately, 50 adult worker bees were randomly taken out from the outer nest spleen and partition of each bee colony, and the worker bees were frozen paralyzed. The parasitism rate of the bee mites at different sampling points can be obtained by checking the number of bee mites on them and calculating the ratio between the total number of bee mites and the total number of seals. After calculating the average value of the two sampling points, the parasitism rate of the bee mites in this bee colony can be obtained. During the overwintering period, all bee colonies were treated with mites to ensure that the bee colonies can survive the winter safely. The effect of bee colony mite control during overwintering was checked, and all bee colonies were treated during this time period [23].

(ii) *Microsporidium Spores*. A total of 15 adult worker bees were randomly taken from the outer nest spleen and partition of each bee colony, the abdomen of 30 bees was cut off, and 30 ml of purified water was put into it for grinding. After mixing evenly, we dropped the ground liquid in the middle of the blood cell counting plate. Moreover, we selected 10 × in order to calculate the number of microsporidia spores with a 40x microscope. Finally, we counted each bee colony three times and averaged the three times to obtain the number of microsporidia spores of each bee in each bee colony [24].

Table 1: Diagnostic methods of bee pests.

Name of pest and disease	Pathogen	Diagnosis way
Chronic paralysis	Chronic bee paralysis virus	Serology, electron microscopy, and PCR
Microsporidiosis	Honeybee microsporidia	Microscopy, PRC method, and immunological method
American larva rancid and rancid	*Bacillus* larva	Bacterial culture, serology, PRC method, and microscopic examination
Putrid disease of European larva	Honeybee	Bacterial culture, microscopy, and PCR

(iii) *Virus Infection Rate and Titer.* A total of 15 adult worker bees were randomly taken out from the outer nest spleen and partition of each colony. The number of bees in each colony was 30. They were frozen with liquid nitrogen and then ground. Then, 100 mg powder was taken out, and the total RNA was extracted with RNA Extraction Kit and passed through ReverTra Ace@qPCR RT Master Mix reverse transcription kit which can obtain cDNA. Next, we use SYBR@Green detection of infection titer and infection rate of viruses in honeybees with the real-time PCR MasterMix fluorescent quantitative PCR reagent. The viruses are CBPV, BQCV, DWV, IAPV, and SBV, respectively [25]. According to the plasmid standard curve, initially established by the Sichuan bee laboratory, the absolute quantification of the virus was judged and the calculation formulas are as follows:

$$\begin{aligned} Y_{BQCV} &= -3.1936X + 38.691, \\ R^2 &= 0.9968, \\ Y_{CBPV} &= -3.2896X + 46.0193, \\ R^2 &= 0.9911, \\ Y_{BQCV} &= -3.2103X + 37.832, \\ R^2 &= 0.9969, \\ Y_{BQCV} &= -3.3269X + 46.284, \\ R^2 &= 0.9908, \\ Y_{DWV} &= -3.3214X + 40.736, \\ R^2 &= 0.9996, \\ Y_{IAPV} &= -3.2713X + 39.028, \\ R^2 &= 0.9956, \\ Y_{SBV} &= -3.3721X + 48.623, \\ R^2 &= 0.9939. \end{aligned} \tag{3}$$

Here, y is the C_T value obtained through detection, X represents the number of virus log copies, and the virus infection titer is represented by 10^xcopies.

4.3.4. Statistical Analysis. In this paper, the number of adult bees, microsporidium spores, daughter spleen, and virus infection titer in bee colony were analyzed by factor variance, and multiple comparisons were made by the Tukey method in one-way ANOVA. Moreover, the Chi square test is used to study the virus infection rate and bee mite infection rate. Similarly, SPSS 20.0 software is used for statistical analysis. From the statistical test and 95% confidence interval point of view, if the P value is less than 0.05, there will be a very significant difference [20].

5. Analysis of Insect Invasion Detection in Chinese Beehive Culture

5.1. Swarm Mobilization. In this paper, six bee breeding bases in the Sichuan Province are selected to analyze the pest intrusion detection in the Chinese beehive breeding based on the deep learning algorithm, and the data on the day when the test bee colony enters the site are listed in Table 2. Among the 30 bee colonies, only four bee colonies in Ya'an bee farm have 11 nests and all the remaining other bee colonies have 10 nests [26]. The number of daughter spleens of each bee colony in different bee farms is very different from that of bee rats. The nest spleen of bee colonies in Ya'an, Shaoxing, Changxing, and Lanxi bee farms is symmetrical. Because there are a large number of nest spleens in the Ya'an bee farm, the number of daughter spleens and bees is significantly higher than that in other bee farms. However, on the Chunan bee farm, the spleen of the bee colony is less [27]. The number of bees on the Jiangshan bee farm is less, and the number of daughter spleens is also less than that in other bee farms.

To sum up, there is no significant difference in the number of daughter spleens and brush collars among bees on different bee farms ($P > 0.05$). Furthermore, there is no significant difference between the number of daughter spleens ($P < 0.001$) and the number of adult bees ($P < 0.001$) in each bee farm after entering the site. The colony potential in different bee farms during the spring breeding and overwintering is basically the same, which is shown in Figure 5.

5.2. Analysis of the Parasitism Rate of Bee Mites. The overwintering period is in the month of December every year. The bee colony in each bee farm checks the number of bee mites of adult bees and calculates the parasitism rate of bee mites. The result is that the average parasitism rate of bee mites on the Jiangshan bee farm is higher than that on other bee farms, but the difference is quite small ($P > 0.05$). The specific data are shown in Figure 6. Since honeybees can thoroughly control mites in honeybee colonies during the overwintering periods, the number of bee mites in honeybees is small before sampling in March. The surface inspection results of adult bees show that there are no bee mites, indicating that the parasitic rate of bee mites in all honeybee colonies is 0.

Table 2: Testing the basic situation of swarm mobilization.

Apiary	Determining the central colony number	Number of nests and spleens	Quantity (foot frame)	Number of spleens and children (foot frame)
Changxing	4	10	8	3
	10	10	6.5	3.5
	16	10	5	2.5
	22	10	6	1.5
	22	10	4	
	Mean ± standard deviation	10 ± 0.0	5.9 ± 1.5	2.7 ± 0.8
YaAn	5	10	9	4
	11	10	8	4.5
	17	10	8	5
	23	10	9	5
	17	10	9	4.5
	Mean ± standard deviation	10 ± 0.0	9.9 ± 0.5	4.4 ± 0.2

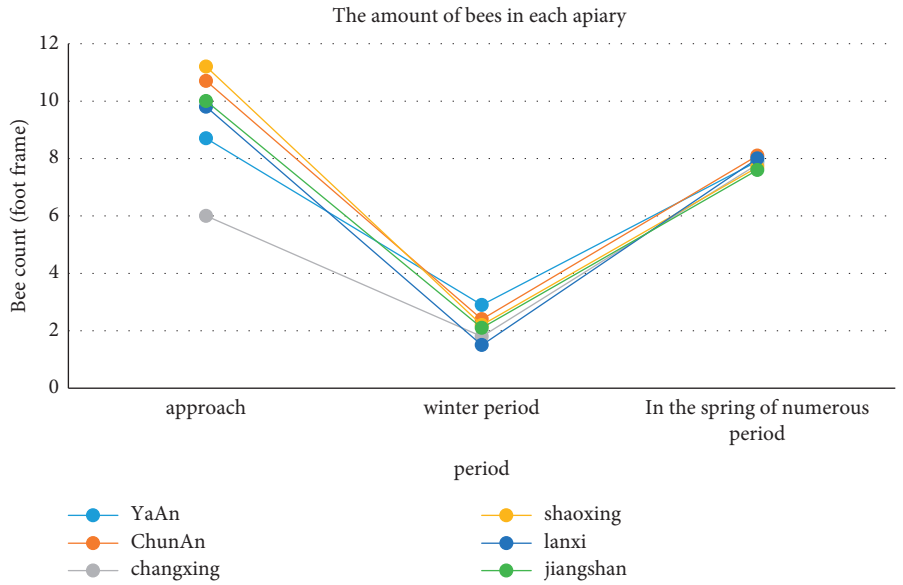

Figure 5: The number of bees in different areas in different time periods.

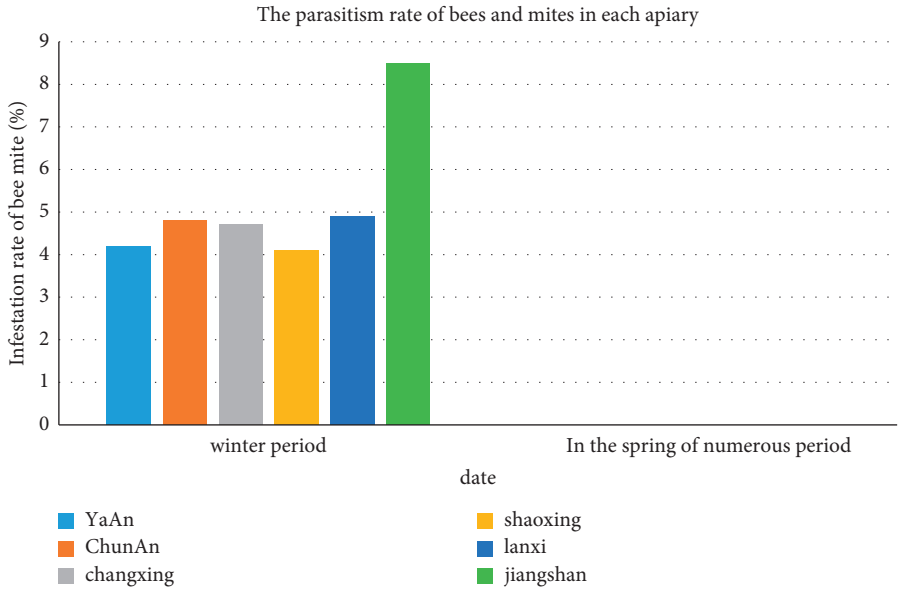

Figure 6: Parasitism rate of bee mites in different bee colonies.

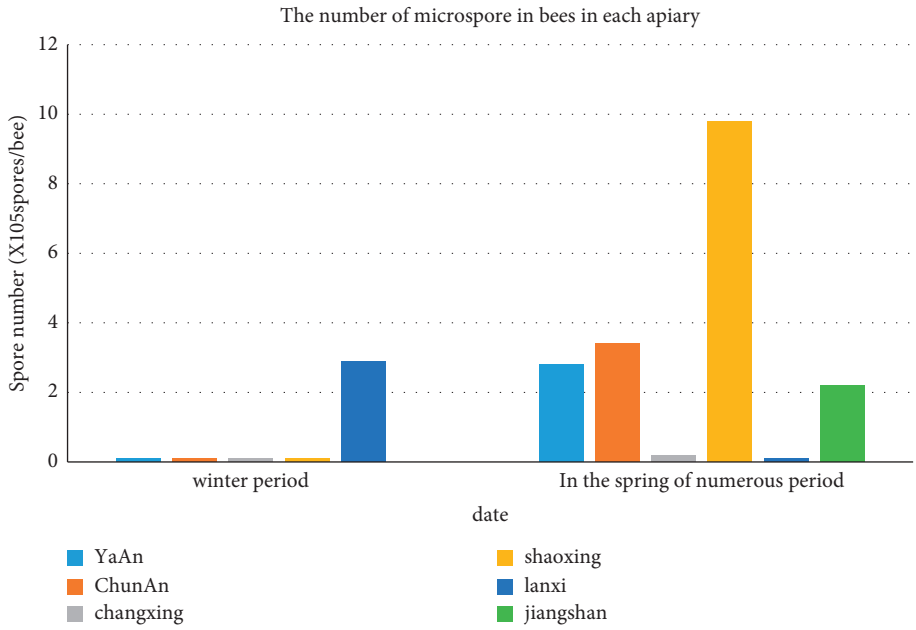

Figure 7: Number of microsporidian spores in bees in various bee farms.

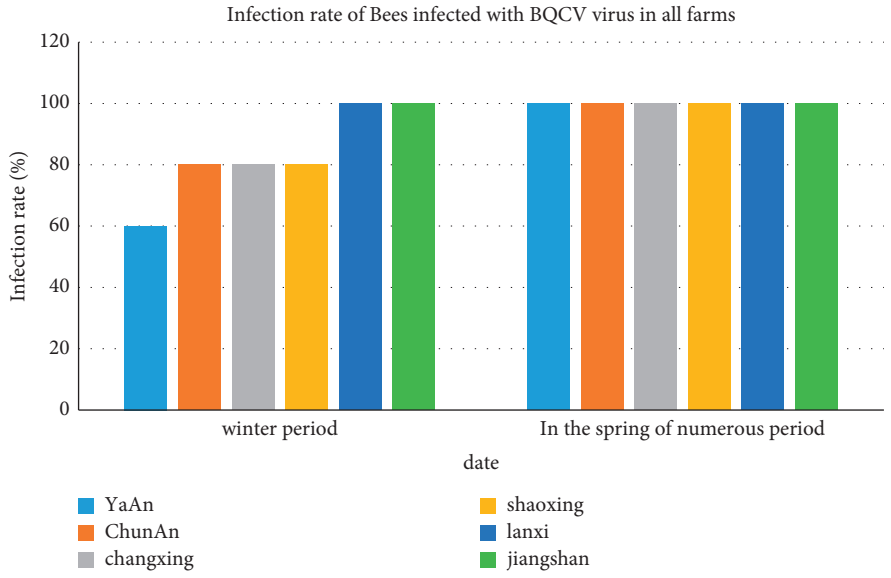

Figure 8: Infection rate of bees infected with the bqcv virus in various farms.

5.3. Analysis of the Microsporidian Infection. During the overwintering period in December, the number of microsporidia spores in the bee colony ranged from 0 to 7.0×10^5/bee intervals. It was observed that five groups of the bees in Xichang bee colony were not infected with microsporidia. The detection of microsporidia infection in each group of bees in Ya'an bee farm is very serious. After calculation, the average number of spores infected by each bee is 2.7×10^5, which was higher than that of other bee farms ($P < 0.05$). Figure 7 shows the number of infected spores of the bees in other bee farms. In March of the next year, the number of microsporidia infected spores in the bee colony in spring was 0 to 2.3×10^6/bee. Excluding Ya'an bee farm, the number of microsporidia in the body of bees in the remaining five bee farms remained elevated. In particular, the average number of spores in each bee body in Baoxing bee farm increased rapidly from 0.2×10^5 in the overwintering period to 9.1×10^5 in the spring breeding period, which was higher than that in Shaoxing and Ya'an bee farms. Moreover, there was no significant difference in the remaining bee farms.

5.4. Analysis of the Virus Infection Rate. During the overwintering period in December and the spring breeding period in March, five common viruses appear in each Chinese beehive farm, namely, bqcv, DWV, CBPV, SBV, and IAPV. The infection rate of the bqcv virus in each bee farm is shown in Figure 8. During the overwintering period of bees in each

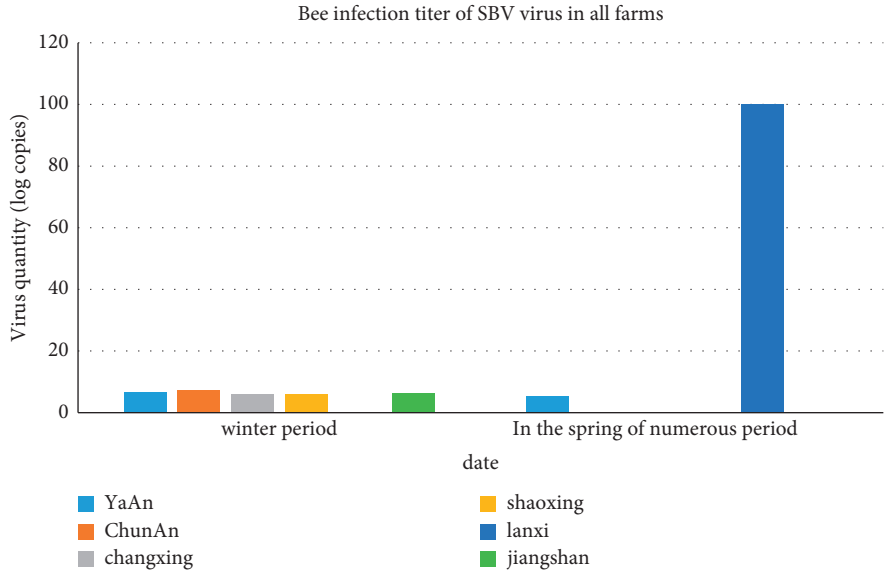

Figure 9: Infection titer of bee infected with SBV virus in all farms.

bee farm, the infection rate of bee colonies infected with the bqcv virus is high, which can reach as high as 60% to 100%. Similarly, the infection rate of the CBPV virus is 80% to 100%, the infection rate of the DWV virus is 100%, and the infection rate of the IAPV virus is 20% to 80%. This should be noted that the lowest infection rate is by the SBV virus. From the overwintering period to the spring breeding period, the bee farms did not contain the bqcv virus and the infection rate of the other four viruses continued to decrease, significantly. In the spring breeding period, the infection rate of the bee colony infected with the IAPV virus in the Mingshan farm is approximately 60%, which is higher than that in ordinary farms (0%). The infection rate of bee DWV virus in the Xichang farm is 100%, which is higher than that in the Baoxing farm.

5.5. Virus Infection Titer Analysis. By measuring the virus titer of infected species in six bee farms, selected in this paper, the infection titer infected with the bqcv virus is shown in Figure 9. When each bee farm is in the overwintering period, only the SBV virus infection titer varies greatly. It could be easily observed that only the Ya'an farm is not infected with the SBV virus, which is lower than the other five farms. The SBV virus infection titer of bees in the farms is much higher than that in Changxing and Lanxi farms [28]. During the breeding period, only five bees in Mingshan could not be detected to be infected with the SBV virus.

6. Conclusions and Future Work

Bees are social insects, and the external environment directly affects the health status of bee breeding groups. Therefore, when detecting the invasion of Chinese beehive breeding pests, we should select the best area and complete it based on the deep learning algorithm. Through the analysis of virus infection and microsporidia infection in six Chinese beehive breeding plants in the province of Sichuan, we observed that the parasitism of bee mites is basically the same. During the study, the bees in each bee farm have no strong natural antibee mite ability. At the same time, the degree of microsporidia infection in each bee colony is also very different. Microsporidia infection in some bee farms is very serious. In addition, each bee farm also has a serious phenomenon of virus infection; however, the antivirus ability is basically the same. This phenomenon is directly related to the parasites such as microsporidia and bee mites. In this paper, we analyzed the virus infection and insect invasion of bees in six Chinese bee farms by using the intrusion detection of the deep learning algorithm, so as to provide insect protection methods for bee breeding and management in the future. This will help to better prevent and control the infection degree of microsporidia and bee mites and improve the ability of bee breeding to resist diseases and insect pests.

In the future, we will propose other intrusion detection algorithms using more sophisticated deep learning methods such as graphical convolution network (GCN) and attention based networks. This is also well-understood that learning based prediction mechanisms are typically grounded on the dataset. In other words, the deep learning based prediction algorithm training may take expressively longer periods if the size of the data set is huge and vice versa. Therefore, it is essential to keep the performance aspect in mind when designing similar algorithms. In the future, we will consider reducing the computational time needed to train the model either through aggregation methods or using more robust algorithms. Finally, the impacts of hot, cold, winter, and spring weathers should be further investigated.

Data Availability

The data used to support the study are included in the paper.

Conflicts of Interest

The authors declare that there are no conflicts of interest for the publication of this paper.

References

[1] V. A. Ricigliano, K. E. Ihle, and S. T. Williams, "Nutrigenetic comparison of two Varroa-resistant honey bee stocks fed pollen and spirulina microalgae," *Apidologie*, vol. 52, no. 4, pp. 873–886, 2021.

[2] Y. Zhao, G. Deng, L. Zhang, N. Di, X. Jiang, and Z. Li, "Based investigate of beehive sound to detect air pollutants by machine learning," *Ecological Informatics*, vol. 61, Article ID 101246, 2021.

[3] Y. H. Sun, Z. J. Zhao, C. Kong, and J. S. Li, "The analysis of the influencing factors of the bee breeding income in shandong province-based on the perspective of cost of bee breeding," *Journal of Qingdao Agricultural University (Social Science Edition)*, vol. 31, pp. 23–26, 2019.

[4] H. Y. Zhang, "Honeybee with a nest "whole relocation" to collect bees," *Journal of Bee*, vol. 39, pp. 34-35, 2019.

[5] C. S. Zhou, "Cover the beehives with old outer tires," *Journal of Bee*, vol. 40, 25 pages, 2020.

[6] Y. Z. Xu, X. P. Wei, L. Lin, W. C. Zho, Q. W. Lin, and M. H. Jia, "Comparative experiment of different types of beehives rearing (PART I) -Also on production of matching shallow successive beehives," *Journal of Bee*, vol. 38, pp. 19–22, 2018.

[7] C. X. Wang, H. Y. Hu, R. H. Zhang, Y. Liu, and Z. L. Liu, "Study on application of honeybee activity enhancer on sweet cherry," *Journal of Henan Agricultural Sciences*, vol. 50, pp. 125–129, 2021.

[8] D. Y. Su, S. Y. Pu, and Q. Y. Zhu, "Analysis of rural entrepreneurial model of college students based on cooperative platform- A case study of Ya 'an Duoying Bee Breeding Cooperative," *Rural Economy and Science-Technology*, vol. 30, pp. 44–47, 2019.

[9] A. Sener, Y. Erkin, A. Sener, A. Tasdogen, E. Dokumaci, and Z. Elar, "Comparação in vitro da permeabilidade de filtros epidurais antibacterianos e triagem por microscopia eletrônica de varredura," *Brazilian Journal of Anesthesiology*, vol. 65, no. 6, pp. 491–496, 2015.

[10] M. Chemurot, L. De Smet, M. Brunain, R. De Rycke, and D. C. De Graaf, "Nosema neumanni n. sp. (Microsporidia, Nosematidae), a new microsporidian parasite of honeybees, *Apis mellifera* in Uganda," *European Journal of Protistology*, vol. 61, pp. 13–19, 2017.

[11] M. A. Yudakhina, "Influence of coniferous-wormwood extract on the viability of bee colonies in Eastern Siberia," *IOP Conference Series: Earth and Environmental Science*, vol. 421, no. 8, Article ID 082015, 2020.

[12] T. Sun, B. Zhou, L. Lai, and J. Pei, "Sequence-based prediction of protein protein interaction using a deep-learning algorithm," *BMC Bioinformatics*, vol. 18, no. 1, p. 277, 2017.

[13] X. Wang and M. Sun, "A novel prediction model of multilayer symbolic pattern network: based on causation entropy," *Physica A: Statistical Mechanics and Its Applications*, vol. 575, Article ID 126045, 2021.

[14] A. Ali, Y. Zhu, and M. Zakarya, "Exploiting dynamic spatio-temporal graph convolutional neural networks for citywide traffic flows prediction," *Neural Networks*, vol. 145, pp. 233–247, 2022.

[15] A. Ali, Y. Zhu, and M. Zakarya, "A data aggregation based approach to exploit dynamic spatio-temporal correlations for citywide crowd flows prediction in fog computing," *Multimedia Tools and Applications*, vol. 80, no. 20, Article ID 31401, 2021.

[16] A. S. Talita, O. S. Nataza, Z. Rustam, and P. Swarm, "Naïve bayes classifier and particle swarm optimization feature selection method for classifying intrusion detection system dataset," *Journal of Physics: Conference Series*, vol. 1752, no. 1, Article ID 012021, 2021.

[17] S. Abbas, Q. Nasir, D. Nouichi et al., "Improving security of the Internet of Things via RF fingerprinting based device identification system," *Neural Computing & Applications*, vol. 33, no. 21, Article ID 14753, 2021.

[18] H. Zhang, L. K. Cai, Y. B. Liu, Y. W. Zhang, and H. X. Jiang, "A new beehive and elaborative beekeeping technique for *Apis cerana* cerana," *Journal of Bee*, vol. 39, pp. 5–7, 2019.

[19] K. Anum, K. A. Nasir, K. F. Gul, A. Mazhar, S. Junaid, and K. A. U. Rehman, "Secure-CamFlow: a device-oriented security model to assist information flow control systems in cloud environments for IoTs," *Concurrency and Computation: Practice and Experience*, vol. 31, no. 8, Article ID e4729, 2019.

[20] Z. W. Hu, J. Yang, C. H. Miao, X. Q. Huang, and S. A. Yang, "Malformation grade of western honeybee, *Apis mellifera*, infected by mite, Varroa destructor," *Acta Agriculturae Zhejiangensis*, vol. 32, pp. 1187–1195, 2020.

[21] B. Yu, "Beehive sound: can it indicate the response of honey bees to chemicals in or out of the beehive," *Research sequare*, 2022.

[22] L. Swanson, T. Li, and R. Rinnan, "Contrasting responses of major and minor volatile compounds to warming and gall-infestation in the Arctic willow Salix myrsinites," *The Science of the Total Environment*, vol. 793, Article ID 148516, 2021.

[23] A. David, "Galbraith, L. Zachary. Investigating the viral ecology of global bee communities with high-throughput metagenomics," *Scientific Reports*, vol. 8, p. 8879, 2018.

[24] B. Y. Zheng and B. A. Zhao, "Effect of Sacbrood virus infection on nutritional and immune responses of *Apis cerana* cerana (Hymenoptera: apidae)," *Acta Entomologica Sinica*, vol. 62, pp. 1054–1064, 2019.

[25] A. Tripathi, A. K. Singh, K. N. Singh, K. K. Singh, P. Choudhary, and P. C. Vashist, "2 Food security and farming through IoT and machine learning," *Internet of Things and Machine Learning in Agriculture*, vol. 36, pp. 21–40, 2021.

[26] X. J. Xiang and Y. Q. Zhou, "Improvement and system development of moving target detection algorithm for the field of agricultural video surveillance," *Journal of Chinese Agricultural Mechanization*, vol. 42, pp. 166–174, 2021.

[27] D. Braga, A. Madureira, F. Scotti, V. Piuri, and A. Abraham, "An intelligent monitoring system for assessing bee hive health," *IEEE Access*, vol. 9, Article ID 89009, 2021.

[28] M. Zahid, X. Jiang, and S. M. Puswal, "Pests, parasitoids, and predators: can they degrade the sociality of a honeybee colony, and be assessed via acoustically monitored systems," *J Entomol Zool Stud*, vol. 8.3, pp. 1248–1260, 2020.

Hindawi
Scientific Programming
Volume 2022, Article ID 1188402, 9 pages
https://doi.org/10.1155/2022/1188402

Research Article

The Study Based on Intelligent Big Data Technology for Water Resources Audit

Yuhui Wang

School of Accounting, Harbin University of Commerce, Harbin150028, Heilongjiang, China

Correspondence should be addressed to Yuhui Wang; adacc@21cn.com

Received 6 January 2022; Revised 2 February 2022; Accepted 28 March 2022; Published 26 April 2022

Academic Editor: Muhammad Usman

The fast progress of science and technology has given immense ease to our lives, but it is also steadily destroying the environment in which we live. Environmental auditing was developed to safeguard the Earth we rely on for our existence, and subsequently, sustainable development was introduced to protect the planet we rely on for survival. Even though the quality of the natural environment is continuously increasing, it should not be taken for granted at this time. Therefore, in this paper, we study water resources auditing and sustainable development technologies based on AI-based big data. Specifically, we use an AI-based big data approach to construct the audit indicators of water resources and summarize the sustainable development technology of water resources. Finally, the proposed approach is used for case implementation. The experimental result shows that the BOD removal rate is about 95%, and the removal process is basically the same as removing COD.

1. Introduction

As individuals devote more and more attention to maintaining the ecological environment, an increasing number of academics devote more and more attention to the conservation of water resources [1–3]. As a result of pressing issues such as poor natural resource utilization rates in the manufacturing process and severe environmental contamination, natural resource auditing and environmental auditing have earned the backing of national policymakers [4]. The performance audit of natural resources follows the needs of contemporary development and the fundamental national circumstances of our country [5, 6].

Water resources auditing and sustainable development technologies have been the subjects of much investigation by many researchers [7–9]. Hranovska et al. [10] proposed a data-packet-based analytical approach for establishing environmental performance indicators by examining the shortcomings of current indicators, which was accepted by the scientific community. Different firms might undertake horizontal comparisons regarding a given environmental quality or characteristic set. Lipiwattanakarn et al. [11] analyzed and investigated environmental performance indicators from the standpoint of long-term sustainability. Environmental performance auditing, as used by Xu W et al. [12], is an audit activity that assists the audited department in resolving the present challenge in environmental management. The particular method is that audit institutions and auditors at all levels adhere to applicable regulations and National standards while reviewing, supervising, and evaluating funds utilized by the audited unit for building and management projects. Although academic circles have a wealth of studies on water resources auditing and sustainable development technologies, there are comparatively few studies on water resources auditing and sustainable development technologies based on computer information technology. As a result, the study on water resources audit and sustainable development technology based on computer information technology is critical.

In this paper, we first provide a brief introduction to the process of water resources protection in China, then construct a framework for water resources audit based on computer information technology and the water resources performance audit evaluation index, followed by a study of water resources sustainable development technology, and

finally use a village in this province as an example for planning and renovation.

2. Water Resources Audit and Sustainable Development Technology Based on Computer Information Technology

2.1. Water Resources Protection Work Process

2.1.1. Five Stages of Government Water Resources Protection. Through numerous policies and programs for water resource preservation, the national government has been steadily implementing these measures in recent years. Figure 1 depicts the country's water resources protection development process during the last 10 years. The pattern is as follows:

(1) Establish water resources management system

We can provide the most restrictive standards for the water resources management system in the history of the world, if necessary. It has established "red lines" in three areas: water resources development and exploitation, water efficiency regulation, and water function zones, all of which are intended to keep pollution to a minimum [13].

(2) Promote the construction of a water-saving society

The promotion of the development of a water-saving society [14] is the most effective way to address the core issue of my country's water resources. Most notably, this is manifested in the following ways: adjustment of the price system for residents' domestic water and agricultural water; technical transformation of industries with high water consumption, including the recommendation of water-saving equipment; centralized treatment of sewage; and utilization of seawater after desalination, among other things [15].

(3) Ecological civilization construction

Water ecological civilization and evaluation standards have been developed, focusing on integrating ecological civilization with the development, governance, distribution, utilization, and protection of water resources. Guiding opinions have also been issued on the construction of water ecological civilizations and evaluation standards. A few examples of specific metrics are [16] suggesting watersheds and regional rivers, lakes, and reservoirs; improving the distribution of water resources and creating a contemporary water resources network; improving the ecological architecture of local watersheds, among other things [17].

(4) Special plan for water resources pollution prevention and control

In 2015, the state announced the implementation of an action plan for water pollution prevention and control, including the general criteria for water pollution prevention and control and the targets to be achieved at different stages. The target requirements are that, by 2030, excellent water quality in the seven major domestic river basins will account for 70% or more of the total water quality, urban black and odorous water bodies will account for less than 10% of total water quality, and the high-quality water source of urban drinking water will account for more than 93% of total water quality. Table 1 contains the pertinent information.

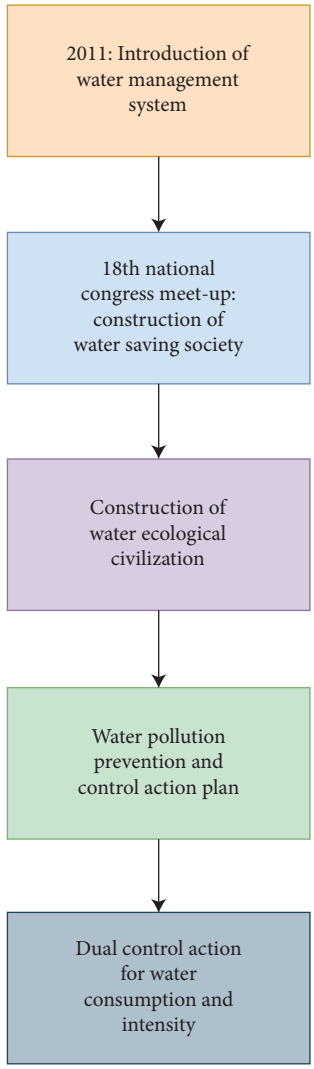

Figure 1: Five stages of water resources protection.

(5) Dual control action

The "Thirteenth Five-Year Plan" specifies in detail the total amount of water that will be used. Groundwater extraction should be centered on governance, and an early warning system should be put in place, according to the national yearly water consumption plan, which is limited to 670 billion cubic meters.

2.1.2. Effectiveness of Implementation of Water Resources Protection Measures. The work on water resources protection and management has yielded some significant results:

Table 1: Phased improvement targets for the water environment in 2020.

Seven key river basins	Excellent water quality	>70%
City drinking water	High-quality water	>93%
Groundwater	Very poor water quality	≈15%
Coastal waters	Excellent water quality	≈70%
Urban black and smelly water	Black smelly water	<10%

innovation in the water resources management system has essentially formed a water resources spatial allocation system with the pulse of water flow and built a modern ecological city with a good environment; through green buildings and urban drainage pipelines, water resources are used for storage, purification, and resource utilization, as well as for drought prevention and drainage, among other things.

2.2. Construction of Water Resources Audit Framework Based on Computer Information Technology

2.2.1. Water Resources Management Performance Audit Object. The freshwater resources under consideration in this article are those that can be utilized and controlled by people, namely, those that are accessible to humans. Generally speaking, water resources audits are concerned with the application of water resources management policies, the use of money, the advantages of water resources project management, the enhancement of water quality, and the social benefits of water resources management. It is possible to separate water resources management performance audit items into four categories, as shown in Figure 2: systems administration, financial administration, development of projects, and information disclosure.

Water resource accounting information and water resource situation information are the two most essential parts of information disclosure; the first is accounting information, and the second is situation information. The project's construction is split into two sections: the construction project and the water pollution prevention and control project. The construction project is the first of the two components. Aspects of the usage of money are represented by sewage treatment fees and the conversion of funds allocated for water pollution prevention and control into capital sewage charges. Regulations, policies, and environmental management systems are the most important aspects of system management. In reality, there are pollutant discharge permit systems, emission reduction liability systems, and other such systems in place.

2.2.2. Water Resources Management Performance Audit Objectives. The goals of a performance audit of water resources management may be broken down into the following categories:

(1) Authenticity

If the data and materials under evaluation are not genuine, then all of the audit findings acquired will be incorrect and have no significance whatsoever. Therefore, guaranteeing the validity of data and materials is a precondition for auditing to take place.

(2) Legality

A succession of government documentation, such as appropriate rules and regulations, must be followed in order for all water resources management efforts to be successful.

(3) Economical

Economic objectives are concerned with whether water resources management is consistent with the notion of conservation and if funds are being used in a scientifically sound manner. In the process of water resources management, not only must the quality be met, but it must also be ensured that the investment costs are kept to a bare minimum.

(4) Efficiency

The most important aspect of efficiency is the ability to do the most useful work at the lowest possible cost. Evaluation of water resource auditing efficiency is mostly dependent on investment and return, including whether or not the investment generates a high-quality return, among other factors.

(5) Effectiveness

The effectiveness of water resources relates to whether or not the performance audit of water resources is up to the standards, whether or not the intended outcomes are obtained, and whether or not the water resources are effective once they have been managed and administered.

2.2.3. Water Resources Management Performance Audit Program Based on Computer Information Technology. In the water management performance audit program, auditors collect data using computer information technology, which is divided into four phases: the audit preparation phase, the audit implementation phase, the audit report phase, and the audit trail phase. The audit preparation phase is the first of these phases.

(1) Audit preparation stage

To prepare for this stage, auditors must first understand the audited unit's water resources management strategy, resource allocation, and other related issues and then assess the risks associated with the audit and draft an audit plan. The audit preparation phase is continued until the audit notification is given, at which point it is terminated.

(2) Audit implementation stage

The audit of water resources is primarily concerned with this stage. The audit implementation stage is defined as the period between the time of entry into the audited unit and the time of withdrawal. It is essential to determine how each project will be implemented, collect and analyze audit data from the unit, and evaluate water resources management using performance audit indicators throughout this stage.

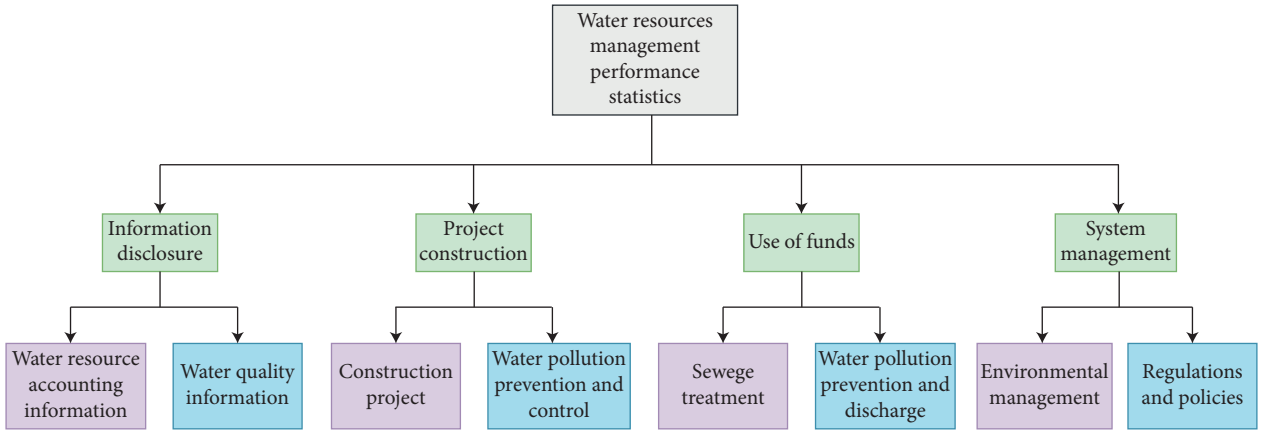

Figure 2: Scope of water resources management performance audit objects.

(3) Audit report stage

The audit report stage refers to the period from leaving the audited unit to completing the water resource audit work. The auditor analyzes the various evidence and documents obtained, evaluates the unit's work, discusses with the responsible department, calculates final scores, and makes corresponding recommendations based on the data results.

(4) Audit trail stage

The auditors will forward the violations of laws and regulations that have been investigated to the appropriate departments for proper handling in accordance with the law, and they will track and understand the rectification of the measures taken by governments and relevant departments at all levels until the completion of the rectification has been confirmed by the auditors.

2.2.4. Water Resources Management Performance Audit Method. There are generally the following methods in water resource management performance auditing:

(1) Audit methods of superiors and subordinates

The higher-level agency audits the water resources managed by the lower-level agency. Under normal circumstances, this cross-audit organization mode is usually adopted. That is, under the leadership of the previous agency, two or more auditing agencies separately audit the water resources management of their own agencies.

(2) The same level audit method

The same level audit refers to the audit of the water resources management of the government at the same level.

(3) Cooperative audit

The term "cooperative audit" refers to the process in which two or more audit subjects work together to complete the audit. Consider how the use of cooperative auditing may assist in promoting cross-border water resource concerns while auditing certain cross-basin water resource management.

2.3. Construction of Water Resources Performance Audit Evaluation Indicators Based on Computer Information Technology

2.3.1. Principles for Constructing Water Resources Performance Audit Evaluation Indicators

(1) Relevance principle

The user's expectations can only be addressed by configuring indicators that are relevant to the topic; hence, the relevance principle is the most fundamental concept. After the water audit is completed, the final results are utilized to increase work efficiency and better finish the task to accomplish the audit goals.

(2) Scientific principles

Indicators should be representative and used in conjunction with current computer information technology to gather data; if data is challenging to get, comparable indicators may be used instead of them. When picking indicators, they must be scientific in nature and capable of objectively reflecting the outcomes of the water resources audit, making the audit results more scientific and more accurate in their interpretation.

(3) The principle of combining flexibility and stability

Because the water resource situation in each location is unique, it is possible to pick the most suitable index according to the current circumstances while generating the index, which allows for more flexibility. When building indicators, we must also consider the stability of the resulting data. The scope of indicator assessment should be comprehensive so that when assessing, there is a primarily uniform indication to measure comparison and evaluation when comparing and evaluating indicators.

(4) The principle of combining qualitative and quantitative

The combination of qualitative and quantitative indicators may make the indicators more scientific from various viewpoints and can be used to audit water resources more entirely than either method alone. When there is no quantification of the indicator data, a qualitative and qualitative approach may be utilized for stratified scoring, and the median value is then employed as the assessment criterion.

(5) Principle of full disclosure

When developing water resources audit evaluation indicators, it is essential to include all of the relevant information about the government's water environment-related activities so that the general public can understand the government's relevant situation in terms of water resource protection and management.

2.3.2. Construction of Driving Force Indicators. Driving force indicators refer to the reasons that promote changes in the water resource environment. The reasons can be political, ecological, or social. The economic drive mainly refers to the adverse effects on the environment when the town is reopened for some economic activities, which drives the protection of the environment by the whole population; the social drive refers to the people's requirements for water quality; the ecological drive should reflect the postgovernment effectiveness.

2.3.3. Construction of Pressure Indicators. The index of pressure is the most important aspect of the overall assessment index. Stress indicators may show changes in pressure generated by human actions in the environment, and they can help individuals understand how to reduce stress more intuitively.

2.3.4. Construction of Status Indicators. Indicators of water resource status include the outcome element under pressure, which refers to the typical changes in water resources as a consequence of economic, ecological, and social pressures. Ideally, state indicators should capture all of the present features of water resources, such as hydrological parameters and water quality.

2.3.5. Construction of Response Indicators. The response index serves as the focal point for the whole assessment system. It might serve as a reflection of the government's efforts to manage water resources. It can be observed from the response index that the department is aware of and places a high value on the environment around water resources management. When the audited unit has assumed corresponding responsibilities for ecological development, the ecological response reflects whether or not it is responding to a national call and making efforts and contributions to ecological restoration; when the audited unit has responded to the masses, the economic response reflects whether or not it has assumed corresponding responsibilities for ecological development. This is in response to the mindset of urban water resources governance.

2.3.6. Construction of Impact Indicators. The impact indicator serves as a form of feedback loop for the reaction indicator and the impact indicator. The feedback is the change in the environment that occurs when the audited unit implements a set of water resource management policies and procedures. It can be determined whether or not the actions taken by the audited unit will have a significant impact on the existing situation.

2.4. Sustainable Development Technology of Water Resources

2.4.1. Water Supply Security Technology.

(1) Drinking water safety guarantee technology

Uncontaminated drinking water may be cleaned using standard treatment procedures to eliminate turbidity in the raw water and destroy microorganisms that are present in the water supply system. Precipitation, sand filtering, and chlorination disinfection are the three phases that make up the regular treatment procedure.

(2) Micro-polluted water source treatment technology

Because traditional water purification procedures can no longer efficiently treat micro-polluted water sources, new technologies for treating micro-polluted water sources have been developed, with promising results.

2.4.2. Sewage Treatment and Reuse Technology.

(1) Urban sewage treatment and reuse

In most cases, relatively developed methods are employed, such as the traditional Martian sludge process and the oxidation ditch method. Examples include the following: according to the government, it is essential to expedite the building of urban sewage treatment facilities while also choosing cost-efficient, acceptable, and effective treatment methods and boosting the rate of sewage treatment as well as the rate of reclaimed water consumption.

(2) Industrial wastewater treatment

Because the water quality and quantity of wastewater in each industry are different, different industrial wastewater treatment processes should also adopt different technological processes. Tannery wastewater treatment includes a single treatment process and a comprehensive treatment process. The only process used for this type of wastewater treatment is physicochemical + SBR + air flotation. First, the chromium-containing wastewater is precipitated to remove the precipitable solids in the water, and then alkali can be added to precipitate the chromium, and then through the concentration and dehydration process, the precipitated solids are further processed,

and the abovementioned wastewater after the chromium recovery enters the integrated wastewater treatment system.

2.4.3. Remediation Technology for Polluted Water Bodies. Water restoration technology is primarily defined as the process of implementing physical, chemical, and biological technological procedures on a contaminated water body in order to lower the amount or concentration of pollutants in the water body until the water body is fully safe to drink.

2.4.4. Water Saving Technology.

(1) Agricultural water-saving technology

Technology for delivering water via low-pressure pipelines is known as "pipe irrigation," and low-pressure pipeline water delivery technology is a water-saving technique that uses low-pressure water pipelines to transport water directly to field furrows and borders to irrigate crops while reducing water leakage and evaporation losses during transportation. Among the many benefits of this water-saving technology is its ability to save water, save energy, and be simple to administer. The investment is also relatively modest, the land utilization rate is increased, machine farming and maintenance are simple, and the irrigation efficiency may be considerably enhanced.

Drop irrigation, which is shown in the video, is a water-saving technique that involves delivering water directly to crop roots using a series of plastic pipe systems to reduce water use. Each faucet drips water directly onto the surface of the roots, which allows it to penetrate deeper into the soil and nourish the plants.

(2) Industrial water-saving technology

Because water has the advantages of being easy to use, having a large heat capacity, being easily transported through pipelines, and having good chemical stability, many industries use it as a cooling substance in their manufacturing processes, either directly or indirectly. Circulating cooling water-saving technology, the implementation of cooling water recycling, particularly indirect cooling water recycling, and improving the cooling water recycling rate have become the primary goals of industrial water conservation.

(3) Building water-saving technology

To conserve water, make use of water-saving household appliances in the home. The facility's faucets, showers, toilet flushing equipment, and tap water pipelines are the most critical water-saving appliances and equipment in the structure. Using water-saving appliances for a short time and with a restricted quantity of water is the most effective technique for conserving water.

2.4.5. Rainwater Utilization Technology. It is primarily based on the ecological system composed of soil, plants, and microorganisms to purify rainwater in urban areas, which can help maintain the natural ecology of cities, reduce energy consumption caused by artificial rainwater treatment, and achieve better economic, social, and environmental benefits.

3. Construction of Water Resources Sustainable Development Case

It is believed that the river flowing through the village region is part of the Yangtze. Among them are the Qingxi and Huatang rivers, which are permanent rivers on the Tibetan Plateau. From the Yangtze River, it runs down to Chaohu Lake, emptying into several rivers. Floods are a common occurrence in the city during the wet season, despite having enormous water supplies. The community is surrounded by water on all sides, and the rainfall will eventually flow into a neighboring river when it has been collected and treated.

3.1. Sewage Volume Measurement. The following is the estimation principle for sewage volume: the region's population and water consumption status should be thoroughly researched, and the sewage volume of the area should be adequately assessed. The per capita comprehensive water consumption indicator approach should estimate the sewage volume for plots that do not have data on their water use.

The following is the method for calculating the average daily sewage volume in cities and municipalities based on population density:

$$Q = \frac{nQ_1 \times K_1 \times L}{K_2 \times 1000}, \tag{1}$$

where Q is the average daily total sewage, n is the number of people, Q_1 is the highest daily domestic water quota for stockholders, K_1 is the domestic sewage discharge coefficient, L is the permeability coefficient, and K_2 is the daily variation coefficient of water supply.

The formula for the compliance rate of pollution source treatment is as follows:

$$R = \frac{H_1}{H_2} \times 100\%, \tag{2}$$

where R is the pollution source treatment compliance rate, H_1 is the number of pollution sources that meet the standard after treatment, and H_2 is the total number of pollution sources.

3.2. Sewage Treatment Design. The indicators of sewage water quality are shown in Table 2.

Analysis of sewage water quality characteristics is as follows:

The biological treatment method used in sewage, particularly the nitrogen and phosphorus removal procedures, has stricter criteria for the amount and balance of contaminants in the influent than other treatment processes used in wastewater. Table 3 contains an index list of the influent water quality ratios based on the water quality.

Table 2: Domestic sewage water quality of a village in this province.

Index	COD (mg/L)	BOD (mg/L)	NH + -N (mg/L)	TP (mg/L)	PH
Ranges	150~350	100~200	20~45	3.0~5.8	6.5~8.4

Table 3: List of water quality ratio indicators.

Project	BOD_5/COD_{cr}	BOD_5/TN	BOD_5/TP
Value	0.61	7.54	54.1
Index	>0.45	>3	>20

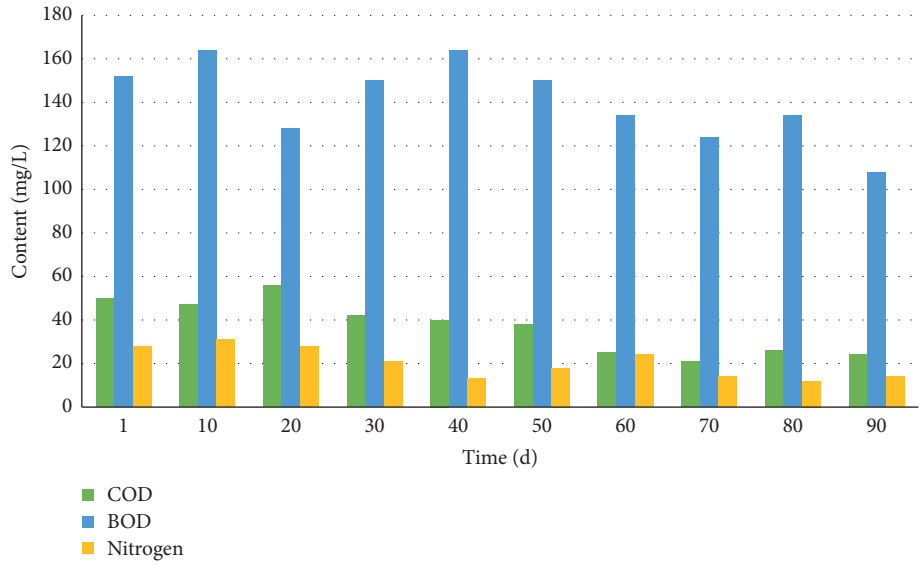

Figure 3: COD, BOD, and total nitrogen removal.

(1) BOD_5/COD_{cr}

This indicator is used to determine whether or not sewage is biodegradable. This indicator has a value of 0.61 in this region, and it may be purified by biological treatment. The biological treatment method used in this study will be used for sewage treatment.

(2) BOD_5/TN

Most of the time, this indicator is used to determine the biological denitrification performance of waterbodies. The greater the value of this finding, the greater the rate of denitrification. According to the index in this region, the nitrogen removal rate may be assured, showing that it fits the standards for biological nitrogen removal.

(3) BOD_5/TP

This indicator is primarily used to assess the efficacy of water bodies in removing phosphorus. The biological phosphorus removal procedure may be used in this project, depending on the quality of the wastewater determined by the analysis.

4. Project Construction Results

Following the project's successful completion, the water quality of the area's influent and effluent was tested. The results revealed that the COD, ammonia nitrogen, total nitrogen, total phosphorus, and suspended solids of the effluent in the area had all decreased significantly over the previous year. Figure 3 depicts a particular instance in which this is the case.

Figure 3 shows that the COD, BOD, and total nitrogen levels all fall significantly, and the effluent meets the required standards. Figure 3 shows that the gel layer of the treatment facility takes around 20 days to create and that the effluent quality starts to stabilize once the gel layer has been established. The removal rate of COD may be increased to 90% by using anoxic tank degradation in conjunction with membrane tank filtration. As seen in Figure 4, the clearance rate of COD and BOD is calculated.

From Figure 4, it can be seen that the BOD removal rate is around 90% and that the removal method is much the same as the COD removal process. As a result of the

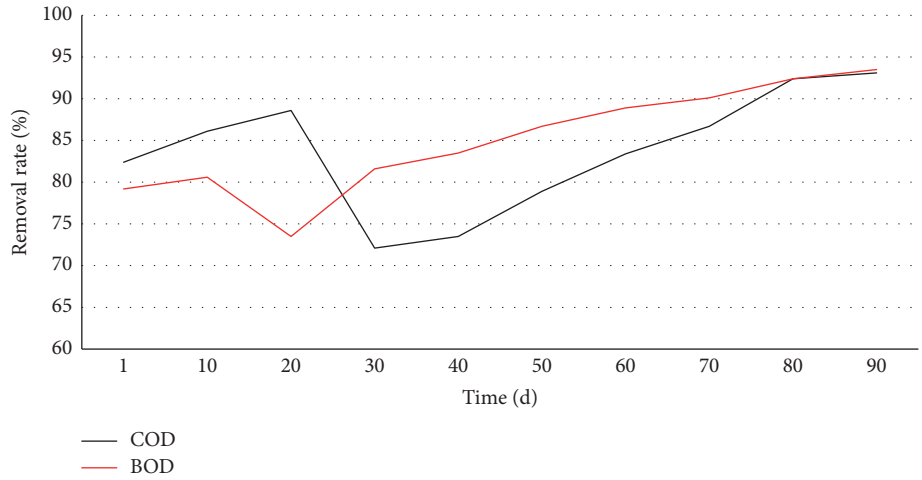

Figure 4: COD and BOD removal rate.

operation of the anoxic pool, COD will first convert BOD before being evacuated. The MBR technique is effective in removing ammonia and nitrogen from water sources. The operation of the filler biofilm in the anoxic tank results in the removal of about 80% of the total nitrogen produced.

5. Conclusions

As the role of government auditing in environmental oversight continues to expand, an increasing number of audit practices will conduct water resources environmental audits and encourage the system's improvement. Environmental degradation and contamination of water resources have become more prominent, necessitating the inclusion of environmental performance audits in audit work. In this paper, we propose an approach for water resource audits, summarize the sustainable development technology of water resources, and finally carry out case implementation. The practice has shown that the project can minimize the damage to the original ecological water environment in the process of rural economic development, improve the ground penetration rate of rainwater and the accumulation of rainwater resources, purify the rural green space, and also be a source of water for rural production and living [18].

Data Availability

The data underlying the results presented in the study are available within the manuscript.

Conflicts of Interest

There are no potential conflicts of interest in our paper, and all authors have seen the manuscript and approved to submit to the journal. The authors confirm that the content of the manuscript has not been published or submitted for publication elsewhere.

References

[1] К. Мельник, "Audit subject formalization in sustainable development," *Problems of Theory and Methodology of Accounting Control and Analysis*, vol. 3, pp. 34–39, 2019.

[2] K. Subramanian, S. S. Chopra, C. M. Wharton et al., "Mapping the food waste-energy-water-emissions nexus at commercial kitchens: a systems approach for a more sustainable food service sector," *Journal of Cleaner Production*, vol. 300, no. 600, Article ID 126856, 2021.

[3] D. P. Bhattarai and N. M. Shakya, "Conjunctive use of water resources in sustainable development of agriculture in t," *Journal of the Institute of Engineering*, vol. 15, no. 2, pp. 210–217, 2019.

[4] S. R. Jan, T. U. S. Syed, J. Ziaullah, and S. Yasin, "An innovative approach to investigate various software testing techniques and strategies," *International Journal of Scientific Research in Science, Engineering and Technology (IJSRSET)*, vol. 2, pp. 682–689, 2016.

[5] K. Burgers, "Production meter testing is key to a successful water audit," *Opflow*, vol. 46, no. 4, pp. 16–19, 2020.

[6] M. Mathew, S. George, R. Menon, and J. Tharakan, "City scale water audit of a pilgrimage town in South India," *International Journal of Water Resources and Environmental Engineering*, vol. 13, no. 1, pp. 88–96, 2021.

[7] S. T. U. Shah, F. Badshah, F. Dad, N. Amin, and M. A. Jan, "Cloud-assisted IoT-based smart respiratory monitoring system for asthma patients," in *Applications of Intelligent Technologies in Healthcare*, Springer, New York, NY, USA, 2019.

[8] S. T. U. Shah, H. Yar, I. Khan, M. Ikram, and H. Khan, "Internet of things-based healthcare: recent advances and challenges," *Applications of Intelligent Technologies in Healthcare*, pp. 153–162, 2019.

[9] F. Dad, N. Amin, S. T. Shah, F. Badshah, and Z. U. Rahman, "Optimal path selection using dijkstra's algorithm in cluster-based LEACH protocol," *Journal of Applied Environmental and Biological Sciences*, vol. 7, no. 2, pp. 194–198, 2017.

[10] L. M. Hranovska, R. A. Kyseliova, and D. L. Hranovsky, "Introduction principles of the environmental management and audit into the water sector in Ukraine," *Balanced Nature Management*, vol. 4, pp. 27–36, 2018.
[11] S. Lipiwattanakarn, S. Kaewsang, C. Makpiboon, and J. A. Changklom, "Water quality audit in drinking water distribution networks," *Journal of Water Resources Planning and Management*, vol. 147, no. 3, Article ID 04020113, 2021.
[12] W. Xu, Z. Zhong, D. Proverbs, and S. Y. Xiong, "Enhancing the resilience of the management of water resources in the agricultural supply chain," *Water*, vol. 13, no. 12, 1619 pages, 2021.
[13] A. K. Hua, "Applied structural equation model in sustainable development of water resources management," *Journal of Water and Land Development*, vol. 42, no. 1, pp. 83–90, 2019.
[14] S. T. U. Shah, J. Li, Z. Guo, G. Li, and Q. Zhou, "DDFL: a deep dual function learning-based model for recommender systems," in *Proceedings of the International Conference on Database Systems for Advanced Applications*, September 2020.
[15] M. Guo, Z. Jiang, Y. Bu, and J. Cheng, "Supporting sustainable development of water resources: a social welfare maximization game model," *International Journal of Environmental Research and Public Health*, vol. 16, no. 16, 2896 pages, 2019.
[16] F. Badshah, S. T. U. Shah, S. R. Jan, and I. U. Rahman, "Communication between multiple processes on same device using TCP/IP suite," in *PInternational Conference on Communication, Computing and Digital Systems (C-CODE)*, March2017.
[17] M. F. Zaragoza-Martí, "The legal-territorial perspective in the new models of water governance: the Spanish regulations," *International Journal of Sustainable Development and Planning*, vol. 14, no. 03, pp. 216–225, 2019.
[18] Y. Wang, X. Liu, L. Shi et al., "Sustainable development of water resources and food security in northwest China," *Chinese Journal of Engineering Science*, vol. 21, no. 5, pp. 38–44, 2019.

Hindawi
Scientific Programming
Volume 2022, Article ID 2680366, 8 pages
https://doi.org/10.1155/2022/2680366

Research Article

Optimization of University Financial Services Using the Blockchain Technology

Guixing Yang [1,2]

[1]*Fuzhou Technology and Business University, Fuzhou, Fujian 350001, China*
[2]*North-Chiang Mai University, Chiangmai 50000, Thailand*

Correspondence should be addressed to Guixing Yang; jjxy007@fjnu.edu.cn

Received 21 March 2022; Revised 10 April 2022; Accepted 15 April 2022; Published 26 April 2022

Academic Editor: Muhammad Zakarya

At present, the financial work of most colleges and universities is facing the dilemma of low intelligence level. The financial sharing mode of colleges and universities using blockchain technology can effectively supervise their financial management while solving the problems of high costs related to financial sharing services, hidden dangers of data security, and low efficiency. Therefore, this paper makes an in-depth study on the application of blockchain technology and the financial sharing service mode of colleges and universities. Firstly, the University Financial Sharing Service Center platform based on blockchain technology is constructed. Furthermore, each module of the service center platform is described. Combined with the constructed platform, university finance is deeply mined by using the mining algorithm based on certain association rules, which is convenient for effective management. Finally, an artificial intelligence algorithm is used to adaptively optimize financial management. Similarly, the planning model and fitting algorithm of the least square method are used to control the risk of the financial management so as to realize the optimization of the financial sharing service mode. The experiment results demonstrate that the proposed method can effectively improve the efficiency of the financial sharing service and reduce the potential safety problems and costs of financial management.

1. Introduction

The level of financial management in colleges and universities will have a direct impact on the effectiveness of their strategy for decision-making across the institutes. With the gradual development of China's higher education, the scale of university resources is also gradually expanding, and the requirements for the optimization of financial management systems have become even more. Some problems, such as difficult reimbursement, cumbersome process, low efficiency, too weak data analysis, and poor fund supervision, seriously perplex the relevant personnel of financial management in all colleges and universities. The traditional financial management system cannot meet the needs of gradually increasing business volume and the supply of financial information. Therefore, the optimization and upgrading of financial management systems are imminent and essential. In fact, the rapid development of blockchain technology brings new ideas and new directions to solve the current financial management problems of colleges and universities. The effective application of blockchain technology can provide an important guarantee for the information security and accuracy of financial data in colleges and universities. Furthermore, this will also improve the financial management system of colleges and universities so as to help improve the intelligent level of financial management, data, and information. Subsequently, this will strengthen the management of financial budget, optimize the efficiency of funds use, strengthen revenue and expenditure supervision, improve the transparency of financial budget and the efficiency of audit, and improve performance management. Therefore, using blockchain technology to optimize the financial management systems of colleges and universities is of great benefit to improve the efficiency of financial accounting, the fine management of finance, and the overall level of financial services. However, this should be taken into account in such a way so that the financial management systems of colleges and universities can meet

the needs of scientific research and better serve the strategic decision-making of colleges and universities.

In this paper, we use blockchain technology in order to build the central platform of the university financial sharing service mode and introduce the major modules in detail. Moreover, to manage the university finance based on association rules, a mining algorithm is suggested. Finally, we use an artificial intelligence algorithm to effectively control the risk of financial informatization so as to complete the optimization of the financial sharing service mode. The method proposed in this paper is compared with other state-of-the-art methods. Our empirical evaluation suggests that the proposed method is superior to other methods in terms of cost, data security risks, and financial management efficiency and has good application value. The major contributions of this research can be summarized as follows:

(i) An in-depth study is provided on the application of the blockchain technology to the financial sharing service mode of colleges and universities;

(ii) The university financial sharing service center platform based on the blockchain technology is constructed, and each module of the service center platform is described;

(iii) Combined with the constructed platform, the university finance is deeply mined by using the mining algorithm based on association rules;

(iv) An artificial intelligence algorithm is used to adaptively optimize the financial management;

(v) The planning model and fitting algorithm of the least square method are used to control the risk of the financial management of colleges and universities.

The rest of the manuscript is structured in the following manner. In Section 2, we provide a brief description of the related work and state-of-the-art methods. Construction of University Financial Sharing Service Center based on blockchain technology is illustrated in Section 3. In Section 4, the discussion over the optimization of the University Financial Sharing Service Mode based on blockchain technology is further elaborated. Analysis of experimental results and discussion are sketched in Section 5. Finally, the paper idea, along with obtained results, is summarized in Section 6. Several directions for further research are also presented in this section.

2. Related Work

At present, with the national support for higher education and with the rapid development of the social economy, the traditional financial management model cannot effectively meet the growing business management needs and has become the main factor restricting the development of education, teaching, and scientific research in colleges and universities. Gao et al. proposed an early warning method for university financial management based on the chaotic particle swarm optimization (PSO) technique. Firstly, this paper analyzes the early warning principle of financial management in detail and finds out the change in the law of financial management early warning in colleges and universities. Moreover, it establishes and describes the model, obtains the early warning classifier of financial management in colleges and universities, and introduces the chaotic particle swarm optimization (PSO) algorithm into it. The proposed algorithm optimizes the parameters of the early warning classifier of financial management in colleges and universities and finally carries out the simulation experiment of financial management early warning in colleges and universities. The experimental results show that, for the traditional early warning methods of financial management in colleges and universities, the accuracy of financial management early warning in colleges and universities based on the chaotic particle swarm optimization has been significantly improved. Moreover, the proposed model can early warn the financial management of colleges and universities in an effective time so as to solve some problems existing in the early warning of financial management in colleges and universities. Although it has a high application value, it has the problem of high economic cost [1].

A new combination of support vector machine (SVM) and Zhus is proposed in [2]. Firstly, the authors preprocess the financial data of colleges and universities, extract the data, and then model the data set. Then, the gray wolf optimization algorithm is improved by using the algorithm of differential evolution so as to improve the global search ability of the financial management. In fact, the authors solve the problem with the same approach because they believe that the gray wolf algorithm is easy to fall into local optimization and then realize the optimization of SVM parameters. Finally, the AdaBoost algorithm is used to improve the ability of financial data information classification of degwo-svm model. The experimental results show that the financial management prediction model based on the AdaBoost and SVM combination has significant dilemma prediction advantages. Compared with other algorithms and methods, the accuracy of the financial management data classification is significantly improved, but there are hidden dangers of data security [2].

Aiming at the complex and nonlinear characteristics of university financial data, a university financial early warning model based on a chaotic long drosophila algorithm and optimized regression neural network is proposed by Zhao et al. [3]. Firstly, the Logistic chaotic map is introduced to modify the initial value of FOA, and then the FOA step size is modified to a dynamic step size based on the optimal initial value so as to find the optimal spread value. Finally, the data predicted by the financial management are comprehensively analyzed, and representative comprehensive indicators are selected. The improved drosophila algorithm has a better ability for global optimization and rapid convergence of financial information and improves the accuracy of GRNN's financial management prediction. The simulation results show that, compared with other models, this model can effectively improve the accuracy of the financial management early warning in colleges and universities and has a high degree of fit with financial data. However, due to the complexity of the process, there are hidden dangers in financial data [3].

Guo et al. suggested a model aiming at constructing the evaluation model of scientific and financial risk in colleges and universities. The theory of support vector machine (SVM) is introduced into the evaluation process of financial data in colleges and universities. Using support vector machine to solve small sample data and nonlinear problems, it has strong generalization ability and constructs the evaluation algorithm model of a support vector machine. In order to effectively improve the performance of the support vector machine, the cuckoo search algorithm is used to optimize the support vector machine so as to improve the accuracy of vector machine detection. The feasibility of the model is verified by the financial data of a university. The verification results demonstrate that the financial data evaluation model based on the support vector machine has high accuracy and can effectively solve the nonlinear problem of financial data. Although it has good application value, there is still the problem of asymmetric data information [4].

3. Construction of University Financial Sharing Service Center Based on the Blockchain Technology

According to the analysis, a university financial sharing service mode platform based on blockchain technology and application has been established. A schematic diagram of the platform is shown in Figure 1. The platform consists of three layers: (i) service layer; (ii) application layer; (iii) base layer. These layers are responsible for providing different services that are described in the following sections.

3.1. Login of Terminal Equipment. Using the distributed system characteristics of the blockchain technology, students and teaching staff can log in by using a computer or mobile intelligent terminal with the help of their student card or staff ID card, respectively. Different accounts are described in detail. After logging in the role, apply for the business process according to the relevant options of the mobile client received by the front desk, and submit the transaction to the control module of the financial shared service platform to classify the financial data [5, 6].

3.2. Control Module of Financial Management Service Platform. The main control module of the service platform is composed of multiple modules, including the control module of personnel list, bachelor's degree, project research, document image, and so on. The mobile client of the platform generates vouchers according to the scanner method and transmits the original accounting vouchers established in the business process to the service platform of the Financial Sharing Center. The module of interconnection control between banks and universities. After students make an online payment, financial institutions can automatically generate vouchers and submit them to the service platform of the Financial Sharing Center, which is mainly used for accounting processing. The module of cost budget is composed of three parts: (i) the cost budget of special funds,

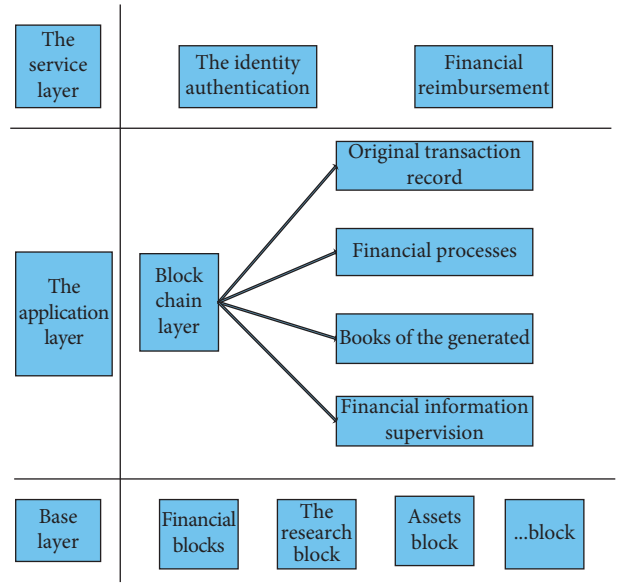

Figure 1: Financial sharing service model platform of colleges and universities.

(ii) the comprehensive cost budget of campus, and (iii) scientific research expenses. It mainly includes budget management, the system of adjustment and internal control, and the control module of official card clearing. Among them, the official card is a new transaction mode, and the teaching staff can use the official card to settle the travel expenses, conference expenses, and purchase expenses. The control module of financial statements is combined with the tables in various teaching fields of colleges and universities to integrate the financial reports of colleges and universities [7, 8].

3.3. Interactive Service of Financial Capital and Data Information. The interactive service platform of data information content in colleges and universities has connection points, which are used to describe the management authority of character information content in detail. The university financial sharing service platform is connected with the university budget management platform to promote the scientific and reasonable management of university finance [9, 10]. Furthermore, it can help to integrate different management systems inside and outside the university into the university financial sharing service platform to complete the university resource sharing and prevent the problem of information asymmetry [11, 12].

3.4. Auxiliary Management and Decision Support. The application platform supporting management decision-making is the financial data analysis layer, which is composed of the overall data analysis system [13]. The analysis system of early warning information data and the intelligent management system of system software. According to the data analysis system, based on the financial statements of colleges and universities, this paper makes a detailed analysis of the investment adjustment and change of college resources and

the ownership structure so as to find out whether the asset investment of colleges and universities is effective [14]. The analysis system of early warning information data comprehensively analyzes the specific revenue and expenditure situation and cost budget of colleges and universities so as to ensure the scientization of financial expenditure of colleges and universities. The intelligent management system of the system software implements the management method for the Financial Shared Service Platform of colleges and universities so that the financial shared service resource information can be shared and the relevant contents of confidential information can be effectively maintained [15, 16]. Figure 2 shows the application framework of Financial Sharing in colleges and universities.

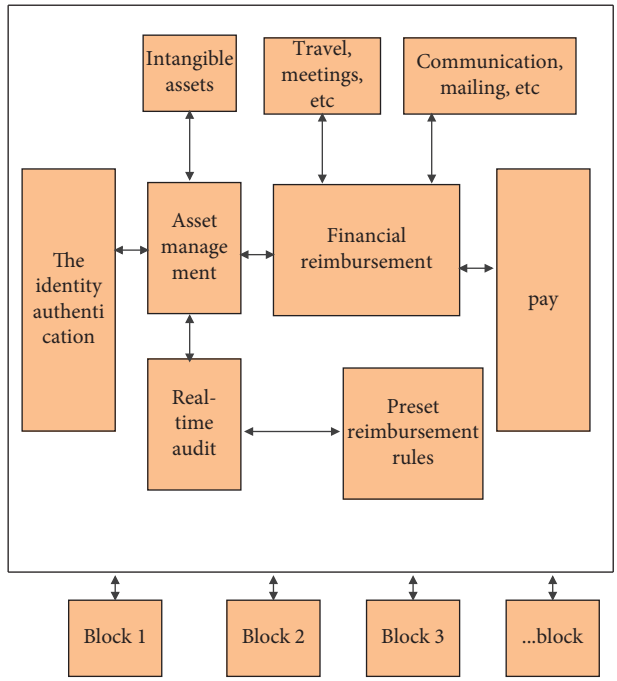

Figure 2: Application framework of financial sharing in colleges and universities.

4. Optimization of University Financial Sharing Service Mode Based on the Blockchain Technology

4.1. Financial Information Management Based on Association Rule Mining Algorithm. The $HG\ D$ mainly refers to the percentage of financial information item set in the overall database, which is recorded as $h(i)$. The $DK\ L$ refers to the union of item sets in the overall data. Suppose that in the financial information item set $I(I = (i_1, i_2, \cdots, i_n))$, any financial item i has a weight [17]. We can use this weight to measure the importance of the financial item in the overall set. The greater the weight, the more prominent the importance of the item and vice versa. On this premise, the financial items in the set are sorted according to the weight, and the information arrangement and combination from large to small are obtained, which finally forms a linear ordered set [18, 19]. The entire process of deep mining of university financial information based on association rule mining is shown in Figure 3.

Next, we use the above platform and to represent the information elements in the financial item set I. If $z \prec x$, it means that z is ahead of x. If the support of Z weighting is defined as $M(z) \times HG\ D(z)$, it means that the minimum weighted support of the project is as follows:

$$\mathrm{HGD(z)} = \frac{f_s - f_a(\mathrm{z})}{D}. \tag{1}$$

In formula (1), $HG\ D(\mathrm{z})$ represents the number of times that element z is found in financial management data, D represents the number of financial data, f_s represents the weighted frequent item set, and $f_a(\mathrm{z})$ represents the factor of weighted support calculation.

According to formula (1), the minimum weighted support of university finance is calculated. On this basis, the confidence of financial data is calculated according to the data mining algorithm of association rules. If $z, x \in I$ $z \cap x = \varnothing$, the confidence of $z \Rightarrow x$ can be defined as follows:

$$D(z \Rightarrow x) = \frac{k(z \cup x)}{n(x)}. \tag{2}$$

In formula (2), $k(z \cup x)$ represents the number of times two financial items appear together in the data, and $n(x)$ represents the correlation degree of the data; and $D(z \Rightarrow x)$ represents the confidence of $z \Rightarrow x$.

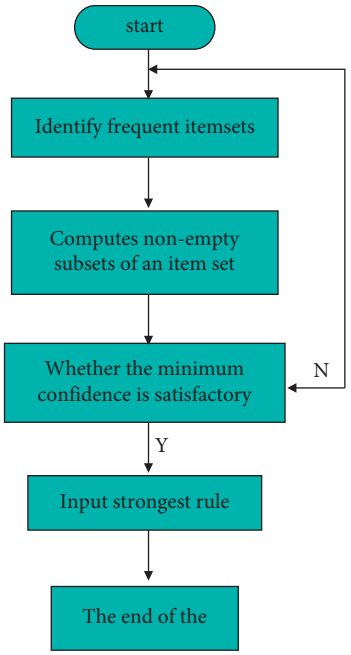

Figure 3: Financial information in-depth mining process.

According to the above formula calculation, we find out the problems of frequent item sets in university financial information and clarify the principle of reliable relationship in university financial information so as to complete the in-depth mining of financial information and provide an effective basis for university financial information management [20, 21].

On the basis of mining the financial information of colleges and universities, through the mining algorithm of association rules, a database of financial information management is constructed to manage the financial information of colleges and universities. The business logic, along with several operations of the database, is shown in Figure 4. The specific information contained in the financial information database is represented as given by Table 1.

In order to realize the information and data sharing of financial management in colleges and universities, we should formulate a unified interface management engine and carry out unified allocation.

The interface of the system is defined to provide the function of data exchange for the financial system because the financial information of colleges and universities is easily affected by noise in the process of exchange. Therefore, the data mining algorithm of association rules is used to standardize the format of financial data exchange, which can be expressed as follows:

$$G = K|v| \cdot \frac{m}{b_t}. \tag{3}$$

In formula (3), G represents the information of financial data exchange, $K|v|$ represents the center of financial data, b_t represents the conversion factor of data, and m represents the parameters of data storage.

On the premise of completing the construction of the above financial database, according to the database definition of financial information management in colleges and universities, the field names, types, and widths involved in all financial databases are defined, which are expressed as given below:

$$j = \frac{d''}{\sum_{i=1} c \Rightarrow b}. \tag{4}$$

In formula (4), j represents the integration parameters in the financial data set, $\sum_{i=1} c$ represents the parameters defined in the data, b represents the set factor of the financial data set, and d'' represents the information of the database.

The main purpose of defining the field name, type, and width involved in the university financial database is to maintain the database so as to complete the construction of the university financial database [22, 23]. Using the above process to complete the financial management of colleges and universities based on the data mining algorithm of association rules.

4.2. Risk Factor Control Algorithm of Financial Informatization Based on Artificial Intelligence. Combined with the above financial information management of colleges and universities, a limited set of horizontal evaluations of risk factor control of financial informatization in colleges and universities is constructed, which is expressed as follows:

$$f_{1g-M}(z) = \left(f_{1g}(z)h_x * f_{1g}(z)h_y * f_{1g}(z)\right). \tag{5}$$

In formula (5), $f_{1g}(z)$ represents the analysis value of the risk factor control of financial informatization in colleges and universities. Under the constraints and conditions of financial cash flow and financial redundancy, combined with financial policy and financial correlation factors, this paper analyzes the control model of financial informatization risk factors of financial informatization management and obtains the statistics as illustrated by the following formula:

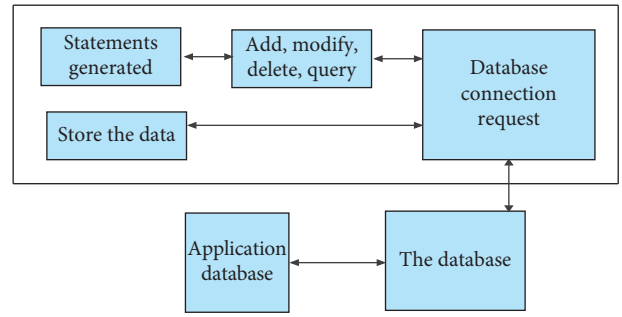

Figure 4: Database business logic.

$$C_{xx}(j\tau) = \sum_{r=1}^{t} \left\| W_i^T x_{ir} - W_i^T x_{irq} \right\|^2 B_{irq}. \tag{6}$$

In formula (6), x_{ir} represents the characteristic component of risk factor control of university financial informatization, x_{irp} represents the characteristic quantity of fuzzy state of university financial informatization risk factor control, and W_i represents the coefficient of sample regression [13].

Using artificial intelligence control method to control the risk factors of the financial informatization in colleges and universities, it is concluded that the main process of the risk factor control artificial intelligence learning is stated as follows:

$$X_i = \left(\alpha_c^{[1]}, \alpha_c^{[2]}, \alpha_c^{[3]}\right). \tag{7}$$

The artificial intelligence learning algorithm is used to adaptively optimize the risk factor control of financial informatization in colleges and universities [12]. Combined with the least square programming model, the risk factor control constraint rules of financial informatization in colleges and universities are expressed as follows:

$$\min(f) = \sum_{i=1}^{m} \sum_{j=1}^{n} C_{ij} X_{ij}, \quad \begin{cases} \sum_{j=1}^{m} X_{ij} = a_i, i = 1, 2 \cdots m, \\ \sum_{j=1}^{m} X_{ij} = b_i, j = 1, 2 \cdots m, \\ X_{ij} \geq 0, i = 1, 2 \cdots m, j = 1, 2 \cdots m. \end{cases} \tag{8}$$

In fact, we adopt the extreme learning method to train the adaptive control level of the risk factors of financial informatization in colleges and universities [11]. Under the learning condition of artificial intelligence, the adaptive learning model of risk factors control of financial informatization in colleges and universities is expressed as follows:

Table 1: Basic database information.

Financial personnel information	Financial account information	Confidential information	Subsidiary accounts
Staff name	Mnemonic code	Debit amount	Abstract
Date of birth	Subject area	Certificate status	Payment method
The title	Course name	Proof number	The balance of
Financial unit	Number of units	Proof of size	Entry number
Gender	The balance of direction	Audit	The settlement date
The user name	Inventory account	The date	The unit price

$$G_i = \sum_j \alpha_j y_i y_j K\left(x_i, x_j\right) + y_i b - 1. \tag{9}$$

Through the above steps, the adaptive control of risk factors of financial informatization in colleges and universities is realized. The formula of optimal control output is expressed as follows:

$$Q' = k\frac{G_i X_i}{M_{Du\ p}}. \tag{10}$$

Combined with the above analysis, the least square programming model and fitting algorithm are used to control the risk factors of university financial informatization so as to complete the optimization of the University Financial Sharing Service mode based on the blockchain technology [24, 25].

5. Analysis of Experimental Results

In order to test the optimization effect of University Financial Sharing mode based on the blockchain technology, empirical analysis is carried out. Table 2 shows the experimental environment data along with parameters. We select some historical data from the financial management system of a university as the data related to the research object. In order to make the results more convincing, we carry out five experiments. The sample distribution of the data is shown in Table 3.

Figure 5 shows the efficiency comparison between the financial information management based on the association rule mining algorithm proposed in this paper and the traditional financial information management.

Through the analysis of Figure 5, it can be seen that the efficiency of financial information management of the mining algorithm based on the association rules proposed in this paper is higher than that of the traditional financial management information methods. A series of five experiments have been carried out, which shows that using the method proposed in this paper can effectively improve the efficiency of the Financial Shared Service Mode in colleges and universities. Figure 6 shows the risk comparison of college financial data between the college financial risk factor control method based on artificial intelligence proposed in this paper and the methods proposed in [1, 2].

From the data analysis, as shown in Figure 6, it can be seen that the data risk of the method proposed in [1] has been very high with the increase in financial data information. Although the method proposed in [2] is not particularly high initially, the risk curve fluctuates greatly with the increase of financial data information. This indicates that

Table 2: Experimental environment data.

The name of the	Configuration
The operating system	Windows 7
The CPU processor	Intel core I5 8400 processor
CPU frequency	2.8 GHz
The development environment	Eclipse
Development of language	Java
The database	SQL Server2018

Table 3: Sample data of financial management simulation experiment.

The serial number	The training set	The test set
1	1200	500
2	1300	500
3	1200	500
4	1200	500
5	1300	500

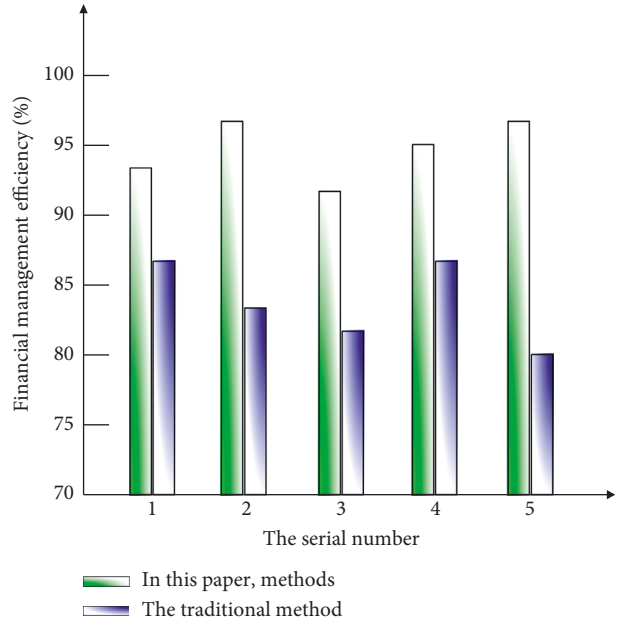

Figure 5: Comparison of financial management efficiency under different methods.

there is a certain risk in financial data information. The risk of the college financial risk factor control method based on artificial intelligence is lower than the other two methods at the beginning. Although the risk curve of financial data information fluctuates to a certain extent, it is still lower than the other two methods. This shows that the data security risk

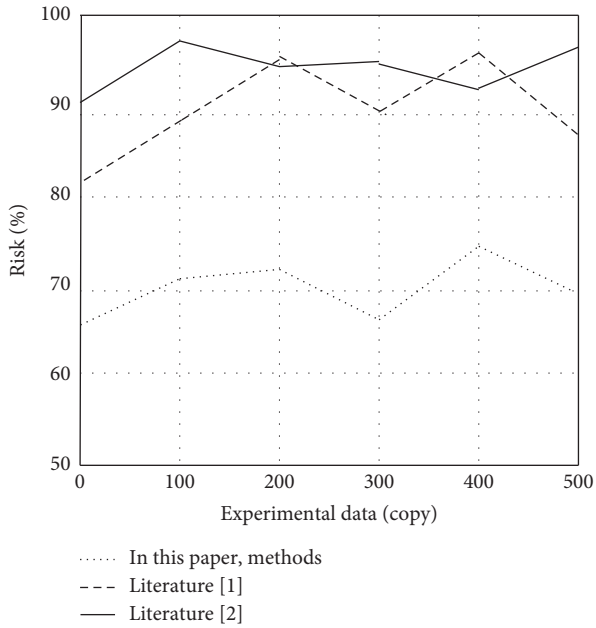

Figure 6: Risk comparison of financial data with different methods.

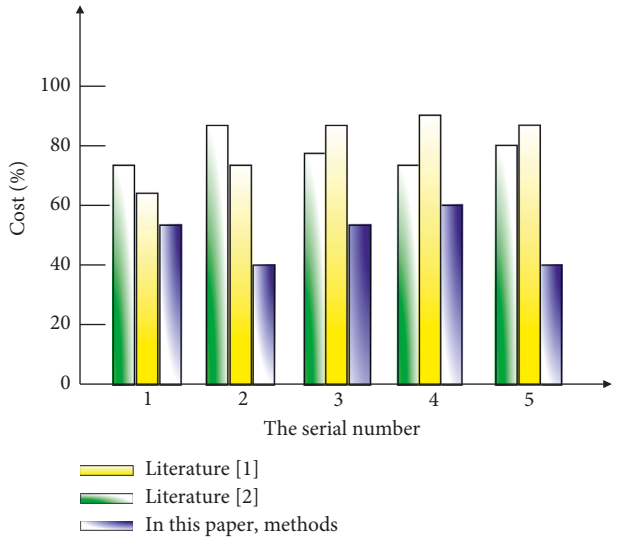

Figure 7: Comparison of financial management costs of different methods.

of the University Financial Sharing Service Center proposed in this paper is significantly low.

Figure 7 shows the cost comparison between the university financial sharing service method based on the blockchain technology proposed in this paper and the two methods proposed in [1, 2].

As can be seen from the experimental data in Figure 7, the cost of university financial management of the methods proposed in [1, 2] is significantly higher than that of the methods proposed in this paper. Through five experiments, the cost of university financial management in each experiment is higher than that of the methods proposed in this paper, which shows that the methods proposed in this paper can effectively reduce the cost of university financial shared services.

6. Conclusions and Future Work

In the era of intelligence, information technology and computer network technology show a trend of rapid development. There is an urgent need to improve the financial management ability and service level of colleges and universities. In this paper, combined with the constructed platform, university finance is deeply mined by using the mining algorithm based on certain association rules, which is convenient for effective management. Finally, an artificial intelligence algorithm is used to adaptively optimize financial management. Similarly, the planning model and fitting algorithm of the least square method are used to control the risk of the financial management so as to realize the optimization of the financial sharing service mode. The application of the blockchain technology in the financial sharing service mode of colleges and universities can effectively promote the transformation of financial functions of colleges and universities from accounting to financial management decision-making so as to effectively improve the efficiency of the Financial Sharing Service mode of colleges and universities and reduce the cost of financial management. In the future, we will integrate machine learning methods such as SVM and CNN within the proposed blockchain model. In terms of SVM, a cuckoo search algorithm could be integrated to obtain higher effectiveness.

Data Availability

The data can be made available upon request.

Conflicts of Interest

The authors declare that they have no conflicts of interest to publish this work.

Acknowledgments

This paper was supported by the 2020 Education and Scientific Research Project of Young and middle-aged Teachers in Fujian Province, Project No.: JAS20486, Project name: Application research of Accounting and Finance Integration based on block chain technology, and 2021 Provincial New Liberal Arts Research and Reform Practice Project, project name: New Liberal Arts Construction Practice in applied Undergraduate Economics and Management Law Field.

References

[1] X. Q. Gao, "Financial management early warning method based on chaos particle swarm optimization neural network," *Microcomputer Applications*, vol. 37, no. 5, pp. 119–121, 2021.

[2] C. S. Zhu, H. X. Tian, and W. F. Feng, "Financial distress prediction based on Adaboost algorithm combined with DEGWO-SVM," *Journal of Lanzhou University of Technology*, vol. 47, no. 6, pp. 100–107, 2021.

[3] N. N. Zhao, Y. X. Wang, and Y. B. Wang, "Application of GRNN optimized by LVFOA in the financial warning," *Computer Systems & Applications*, vol. 26, no. 6, pp. 17–25, 2017.

[4] W. J. Guo and H. Jin, "Design and simulation of financial data evaluation algorithm based on support vector machine," *Electronic Design Engineering*, vol. 29, no. 18, pp. 17–20, 2021.
[5] H. Q. Tang, "Optimization design of enterprise financial sharing mode based on blockchain technology: taking enterprises in xiamen city as an example," *Fujian Jiangxia Xueyuan Xuebao*, vol. 9, no. 5, pp. 32–38, 2019.
[6] Y. Yang, "Enterprise budget management problem and optimization path based on financial sharing mode," *ZHISHI JINGJI*, vol. 578, no. 15, pp. 112-113, 2021.
[7] K. Huang, "Optimization path of accounting business process of large group enterprises based on financial sharing mode," *Chief Financial Officer*, vol. 16, no. 2, pp. 96-97, 2020.
[8] L. Xiao, "Optimization of hospital financial management under the mode of financial sharing," *Modern Scientific Instruments*, vol. 38, no. 2, pp. 271–275, 2021.
[9] Y. W. He and X. D. Zheng, "On optimization of sales collection management under the financial sharing mode of real estate group: taking company A as an example," *Journal of Tongling University*, vol. 20, no. 3, pp. 39–42, 2021.
[10] J. L. Lai, "Financial sharing service mode of manufacturing enterprises driven by information technology in higher colleges," *Journal of Hubei Open Vocational College*, vol. 34, no. 21, pp. 31–35, 2021.
[11] L. Udayanga, N. Gunathilaka, M. C. M. Iqbal, M. M. M. Najim, K Pahalagedara, and W. Abeyewickreme, "Empirical optimization of risk thresholds for dengue: an approach towards entomological management of Aedes mosquitoes based on larval indices in the Kandy District of Sri Lanka," *Parasites & Vectors*, vol. 11, no. 1, p. 368, 2018.
[12] S. Yedida, "Optimization of repairable systems with repairman's multiple vacations," *International Journal of Quality & Reliability Management*, vol. 35, no. 1, pp. 266–290, 2018.
[13] B. V. Bojinov, "Current issues of financial management information technology in universities," *SSRN Electronic Journal*, vol. 13, no. 1, pp. 30–36, 2017.
[14] T. T. P. Asmara and L. Abubakar, "Juridical study on the optimization of cash waqf management by islamic banking in Indonesia," *PADJADJARAN Jurnal Ilmu Hukum (Journal of Law)*, vol. 6, no. 3, pp. 427–445, 2019.
[15] V. Chang, P. Baudier, H. Zhang, Q. Xu, J. Zhang, and M. Arami, "How Blockchain can impact financial services - the overview, challenges and recommendations from expert interviewees," *Technological Forecasting and Social Change*, vol. 158, p. 120166, 2020.
[16] L. Wang and Y. Wang, "Supply chain financial service management system based on block chain IoT data sharing and edge computing," *Alexandria Engineering Journal*, vol. 61, no. 1, pp. 147–158, 2022.
[17] V. V. Kozlov, T. V. Tomashevska, and N. I. Kuznetsov, "Using of optimization models in financial decision support systems," *Statistics of Ukraine*, vol. 88, no. 1, pp. 75–83, 2020.
[18] N. V. Vafiadis and T. T. Taefi, "Differentiating Blockchain Technology to Optimize the Processes Quality in Industry 4.0," in *Proceedings of the IEEE 5th World Forum on Internet of Things (WF-IoT)*, Limerick, Ireland, 2019.
[19] C. Yan, J. Zhu, Y. Ouyang, and X. Zeng, "Marketing method and system optimization based on the financial blockchain of the internet of things," *Wireless Communications and Mobile Computing*, vol. 2021, pp. 1–11, 2021.
[20] W. Amedzro St-Hilaire and P. Boisselier, "The coordinated strategy for the optimization of the interaction level of business model," *Journal of Economic and Administrative Sciences*, vol. 35, no. 2, pp. 79–93, 2019.
[21] J. M. Romo, "A closed-form solution for outperfomance options with stochastic correlation and stochastic volatility," *Journal of Industrial and Management Optimization*, vol. 11, no. 4, pp. 1185–1209, 2017.
[22] T. Alharbi, "Deployment of blockchain technology in software defined networks: a survey," *IEEE Access*, vol. 8, pp. 9146–9156, 2020.
[23] S. Faiza and Z. Muhammad, "Credit ratings and liquidity risk for the optimization of debt maturity structure," *Journal of Risk and Financial Management*, vol. 11, no. 2, p. 24, 2018.
[24] L. V. Pavão, C. Pozo, C. B. B. Costa, M. A. S. S. Ravagnani, and L. Jiménez, "Financial risks management of heat exchanger networks under uncertain utility costs via multi-objective optimization," *Energy*, vol. 139, no. 15, pp. 98–117, 2017.
[25] C. Antal, T. Cioara, M. Antal et al., "Blockchain based decentralized local energy flexibility market," *Energy Reports*, vol. 7, no. 9, pp. 5269–5288, 2021.

Hindawi
Scientific Programming
Volume 2022, Article ID 8400206, 9 pages
https://doi.org/10.1155/2022/8400206

Research Article

Application of Prediction Model Using Parallel Computing in Music Cultural Facilities

Jing Zhang

School of Music and Dance, Qiqihar University, Qiqihar, Heilongjiang 161006, China

Correspondence should be addressed to Jing Zhang; 02038@qqhru.edu.cn

Received 18 March 2022; Revised 7 April 2022; Accepted 11 April 2022; Published 26 April 2022

Academic Editor: Muhammad Zakarya

The important carrier of urban music and cultural activities is urban music and cultural facilities. In today's environment of rapid urban development and continuous acceleration of people's pace of life, the previous problems of music and cultural facilities with out-of-order combination, unbalanced layout and distorted scale cannot meet the basic music and cultural needs put forward by citizens. Therefore, more and more people begin to expect a reasonable layout of music and cultural facilities in their living environment. For this problem, this paper uses the prediction model of parallel computing when applying music and cultural facilities. The proposed model takes Chongqing as the research object and analyzes the construction of music and cultural facilities in various districts of the Chongqing. We investigate the specific number of music and cultural facilities in various districts and the surrounding population. Furthermore, we study whether the equipped music and cultural facilities meet people's actual needs. Form our evaluation, it is concluded that certain districts of the Chongqing have rich educational facilities, while other districts have a very balanced distribution of music and cultural facilities, and there are different degrees of imbalance in music and cultural facilities in other regions. Through analyzing the fairness of music and cultural facilities, the Lorentz curve of music and cultural facilities is drawn based on the population proportion of each region, and the Gini fairness coefficient is calculated to be 0.53. The attractiveness of the music and cultural facilities in Chongqing is analyzed according to the road traffic and public transportation of each region.

1. Introduction

With the rapid improvement of people's quality of life and level, while economic development can ensure people's basic life and physiological needs, some people begin to pursue cultural enjoyment. Music plays a special role in shaping the city's economy and culture. Each city's music culture is different, which is directly related to the city's history, region, and culture. This paper selects the parallel computing prediction model to generate an abstract computing model by abstracting the basic characteristics of music cultural facilities. At the same time, the parallel computing model provides basic software pages and hardware for parallel computing music cultural facilities, which can accurately analyze music cultural facilities, improve urban cultural atmosphere, and build a metropolis with music characteristics.

In today's environment of rapid urban improvement and unremitting speeding up of people's pace of life, the preceding problems of music and cultural facilities with out-of-order combination, unbalanced layout, and distorted scale cannot meet the basic music and cultural needs put forward by citizens. Therefore, more and more people begin to expect a reasonable layout of music and cultural facilities in their living environment. For this problem, certain prediction models, which are based on the parallel computing, have been suggested. These models could analyze the construction of music and cultural facilities in various districts, and investigate the specific number of music and cultural facilities in various districts and the surrounding population. There has been rich literature that investigates whether the equipped music and cultural facilities meet people's actual needs. However, due to the huge amount of data, parallel computing is not utilized. There are many types of predictive

control algorithms and different expression types. However, they all have the same three basic functions, namely, (i) rolling optimization, (ii) model prediction, and (iii) feedback correction [1]. The basic concept of the model predictive control (MPC) refers to the prediction model and measurement information at a particular time k. In subsequent step, the controller predicts the subsequent dynamic behavior of the system and solves the open-loop control sequence based on the preset constraints and open-loop performance objective function.

In this paper, the prediction model of parallel computing is used in music cultural facilities for analysis. Through briefly introducing the basic principle of prediction model control and mathematical calculation method, the parallel computing process is explained, and the algorithm is applied to music cultural facilities. We also establish the optimal layout model of music and cultural facilities, analyze the components and types of music and cultural facilities, judge the situation of urban construction of music and cultural facilities through the model and attraction model of music and cultural facilities, and point out the imbalance [1]. The main innovations of this paper are as follows:

(i) A prediction model based on the well-known parallel computing is used in music cultural facilities for analysis

(ii) Introduce the basic principles of prediction model control and mathematical calculation method, a parallel computing-based algorithm is applied to music cultural facilities

(iii) Analyze the components and types of music and cultural facilities, judge the situation of urban construction through the equity and attraction model, and point out the imbalance

The remaining of the article is organized in the following manner. In section 2, state-of-the-art-related work is illustrated. In section 3, a prediction model is proposed that is based on the well-known parallel computing platform. A mathematical proof of the model is also illustrated. Moreover, we also offer a brief introduction of the parallel computing. In section 4, the optimal layout model of music and cultural facilities is discussed. Applications of the proposed prediction model based on parallel computing in music cultural facilities are discussed in section 5. Finally, we conclude this study along with future research directions in section 6.

2. Related Work

The model predictive control (MPC) is an advanced control technology that is based on explicit process model. The main purpose of the MPC is to predict and estimate the future process behavior by combining measurable information and process dynamic model. Furthermore, it reduces the gap between the predicted process response and design response [2]. Nowadays, parallel computing technology is widely used in many intensive application fields. American scholars choose Cray XD 1 supercomputer manufactured by Cray company to study the parallel system of processing unit matrix operation based on general processor hybrid design and FPGA [3]. Subsequently, the American scholars put forward a parallel algorithm of matrix multiplication used in shared memory system and cluster environment [4]. Wang R et al. proposed a master-slave distributed matrix multiplication parallel computing system based on PCI interconnection and FPGA as processing unit [5]. Shuangxia et al. and other experts studied the parallel matrix algorithm based on heap multiprocessor [6]. According to the concept given by CX A. Almasi et al., parallel computing platform is a system formed by interconnecting multiple processing units with a certain structure.

The communication ability between units in the system is strong, and a large number of calculations can be realized through cooperation [7]. At the same time, some experts conducted research on cultural facilities. For example, Shi JR et al. deeply studied the feedback process and driving force of cultural innovation and transformation projects of French tobacco factories. As a result, the authors put forward the replacement mode of industrial heritage and cultural facilities [8]. Chang et al. believed that tourists pay most attention to the cultural facilities, so it is necessary to strengthen facility management to improve tourists' attention. Managers should also strengthen facility management and greatly improve the service level of facilities to meet the basic needs of the tourists [9]. Fei et al. proposed that the memorial hall has strong autonomy, opening-up ability, and high degree of transformation service equipment from the demand, which carries the main connotation of the city and residential area. In fact, this is also the foundation of establishing urban culture and serves as an important spatial carrier for people's cultural exchange [10].

Simone et al. proposed that the cultural facilities, as an important part, form an urban smart intensive area [11]. Similarly, Jia et al. pointed out from the degree and output of the cultural consumption in Europe that cultural facilities are the main measures to strengthen urban capital and display urban image. Both the higher education people and the middle class will consume around cultural facilities, and they are the main group of cultural consumption [12]. When studying Singapore, Kharvari et al. pointed out that the city attaches great importance to the cultural construction and the improvement of cultural facilities, which is an important driving force for innovation and development in the region. During the parallel development of cultural and educational facilities, the layout of cultural facilities also has a direct impact on people's living areas [13].

Chinese scholars use temporal and spatial differentiation to analyze the comprehensive cultural facilities in the urban area of Beijing, and study the factors of cultural facilities distributed in different stages in Beijing from the time dimension. The comprehensive cultural facilities involve economic, transportation, and densely populated areas, which could essentially help in providing the necessary conditions for the aggregation of cultural facilities [14].

3. Prediction Model Based on Parallel Computing

3.1. Overview of Model Predictive Control. In the 1960s, a new computer control algorithm, that is, model predictive control (MPC), was proposed in the industrial field of Europe and America. Moreover, MPC is combined with industrial practice to form a control mode. The MPC mode has low requirements for model accuracy and can be used in non-minimum phase systems and time-delay objects. Similarly, it has good tracking performance and is more ideal than the traditional adaptive control and optimal control. In fact, the MPC can be applied in more complex industrial engineering control to meet the basic needs of the environment. Model predictive control can deal with control problems with constraints easily and flexibly, and has become the core of theoretical circles and industrial fields at home and abroad. The following figure is a 1-bit model predictive control system diagram in which u (t|t) represents the use of model predictive controller in the controlled output of the system, y(t) represents the system response, and y_{ref} represents the system response track set in advance which is shown in Figure 1. Therefore, the basic characteristics of model predictive control can be summarized as: (i) rolling optimization, (ii) predictive model, and (iii) feedback correction.

3.2. Basic Principles of the Model Predictive Control (MPC). There are many types of predictive control algorithms and different expression types. However, they all have the same three basic functions, namely, (i) rolling optimization, (ii) model prediction, and (iii) feedback correction [15]. The basic concept of the model predictive control refers to the prediction model and measurement information at time k. The controller predicts the subsequent dynamic behavior of the system in the [k, $k+p$] time domain and solves the open-loop control sequence based on the preset constraints and open-loop performance objective function in [k, $k+m$] ($m<p$), as shown in Figure 2. The first open-loop control sequence element is applied to the physical system. Moreover, the k+1 time is optimized according to the new measurement information in order to find a new control sequence. Figure 2 shows the basic principles of the model predictive control, where m is the control area and p is the predictive time domain.

3.3. Mathematical Description of Model Predictive Control. The traditional MPC algorithm is an open-loop prediction. The following is the basic mathematical form of the open-loop optimization problem of the model predictive control:

$$\min_{\Delta U(k)} J(y(k), \Delta U(k)), \quad \text{s.t. } y(k+1) = f(y(k), u(k), d(k)), \tag{1}$$

$$\text{s.t. } y(k+1) = f(y(k), u(k), d(k)), \tag{2}$$

$$y(k) \in Y, \quad k \geq 0, \tag{3}$$

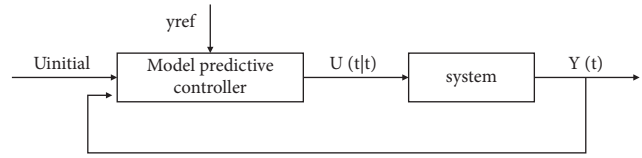

Figure 1: Model predictive control system.

$$u(k) \in U, \quad k \geq 0, \tag{4}$$

$$\Delta u(k) \in \Delta U, \quad k \geq 0. \tag{5}$$

Here, we would like to highlight the entire process in three steps:

(1) In formula (6), J represents the control performance index function, and the performance index commonly used in MPC is the quadratic objective function. The basic form is represented by the following equation [16]:

$$J = \sum_{i=1}^{P} \|y(k+i|k) - r(k+i)\|_Q^2 + \sum_{i=0}^{m} \|\Delta u(k+i-1)\|_R^2. \tag{6}$$

The above formula m represents the control time domain, p represents the prediction time domain, usually $m<p$; R represents the control increment weighting matrix, and Q represents the prediction error weighting matrix. The first direction in this form of performance index is the sum of the squares of the later p different sampling time prediction outputs minus the given value or time-varying reference trajectory difference; the second term is to accumulate all the values of the gain of the next m control variables.

$$\Delta U(k) \triangleq [\Delta u(k) \Delta u(k+1), \ldots, \Delta u(k+m-1)]^T. \tag{7}$$

Formula (7) is a sequence of control increments, which is an independent variable of the optimization problem.

(2) Formula (2) is the discrete model of the controlled system, where $y(k) \in R^p$ represents the output vector, $y(k) \in R^p$ represents the input vector, and $d(k) \in R^d$ represents the measurable interference vector [17]. The commonly used form of the model is convolution model, including step response model and impulse response model. The model has its own integrator convolution model, state space model, and Volterra model.

(3) Formula (3) is the output constraint, formula (4) is the control constraint, and formula (5) is the control gain constraint. Based on the predictive control principle, calculate all sampling times and solve the optimization problem. The results are as follows:

$$\Delta U^*(k) = [\Delta u^*(k), \Delta u^*(k+1), \ldots, \Delta u^*(k+m-1)]^T. \tag{8}$$

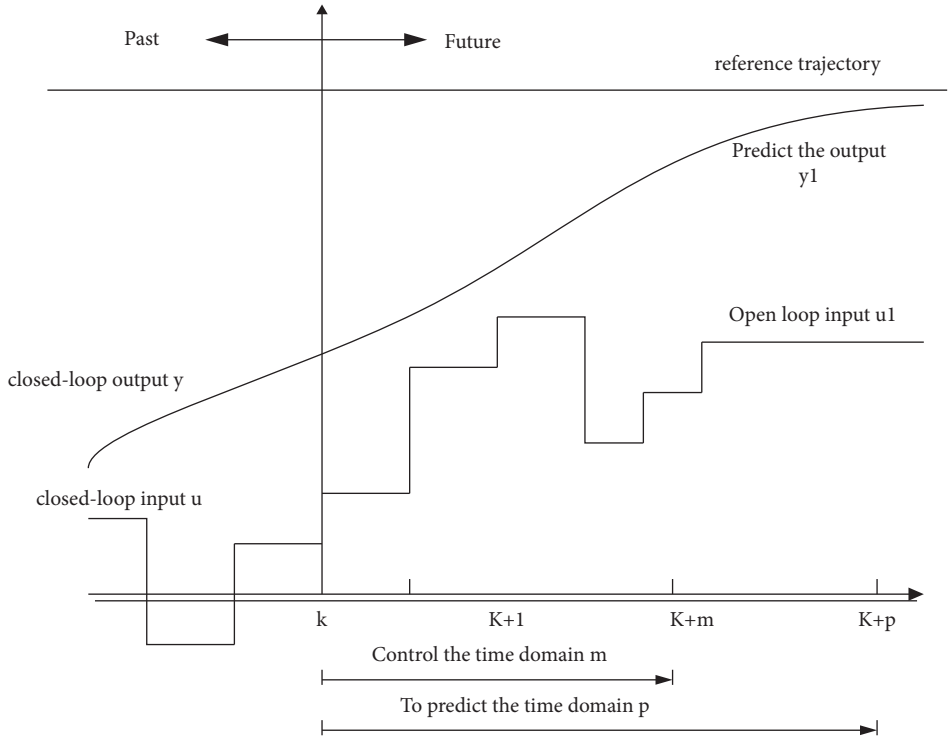

Figure 2: Schematic diagram of model predictive control.

The control increment sequence ΔU^* is used in the system, and $\Delta u^*(k+1)$ is calculated based on the new measurement results at the next sampling time.

3.4. Parallel Computing. Figure 3 shows the parallel computing architecture. The system is applicable to the relationship between the structures of multi-FPGA or DSP parallel computers. The common types of FPGA and DSP parallel computers are array machines, pipelined machines, and multiprocessor systems [7]. The pipelined technology is used to improve the speed of multiple parallel computing based on pipeline and data throughput. Similarly, the array machine is a kind of SIMD architecture (single input multiple data). Associative memory processor and systolic array machine were first proposed in the early 1980s. Its remarkable feature is that under the same control, a large number of PES are operated in parallel by synchronous locking mode to realize large-scale computing jobs. In the design of some array machines, the recursive operation, multiplication and addition calculation, and matrix multiplication operation often used in digital signal processing become multiple PES, and then, all PES are connected according to a certain law, so as to quickly improve the calculation speed.

4. Optimal Layout Model of Music and Cultural Facilities

Music culture has become an emerging industry under the environment of rapid development of cultural undertakings and economy, and finally become a brand-new music culture industry. Music culture facilities are the main material space carrier of music culture, which enriches the industrial content and realizes the expansion of industrial linkage [18]. As an emerging industry, the rapid development of music culture industry should be combined with the ways of industrial development and diversified binding with coordinated development, so as to increase the industrial share in the market and strengthen industrial publicity. We upgrade the traditional music culture and form an industry, so as to show the development space and importance of music culture. There is a direct relationship between music cultural value and social benefits, and industrial value is related to the development of economic benefits. It can be seen that music culture and industry complement each other and develop together. The rapid development of music culture industry has a certain driving effect on the cultural development and economic improvement of the region, and will also develop into a pillar industry in a certain region.

4.1. Composition Type of Music and Cultural Facilities. Based on the groups and functions of urban music and cultural facilities, this paper redivides them into several types. The common types of music and cultural facilities are (i) recreation, (ii) education, (iii) community, (iv) performance, and (v) commerce. The educational type mainly includes training institutions, piano companies, schools, etc. The recreational types mainly include gardening, fountains, streets, etc. Similarly, the performances mainly include theatres, concert halls, clubs, and opera courts, and the community type mainly includes cultural stations and activity centers. The commercial type mainly includes hotels,

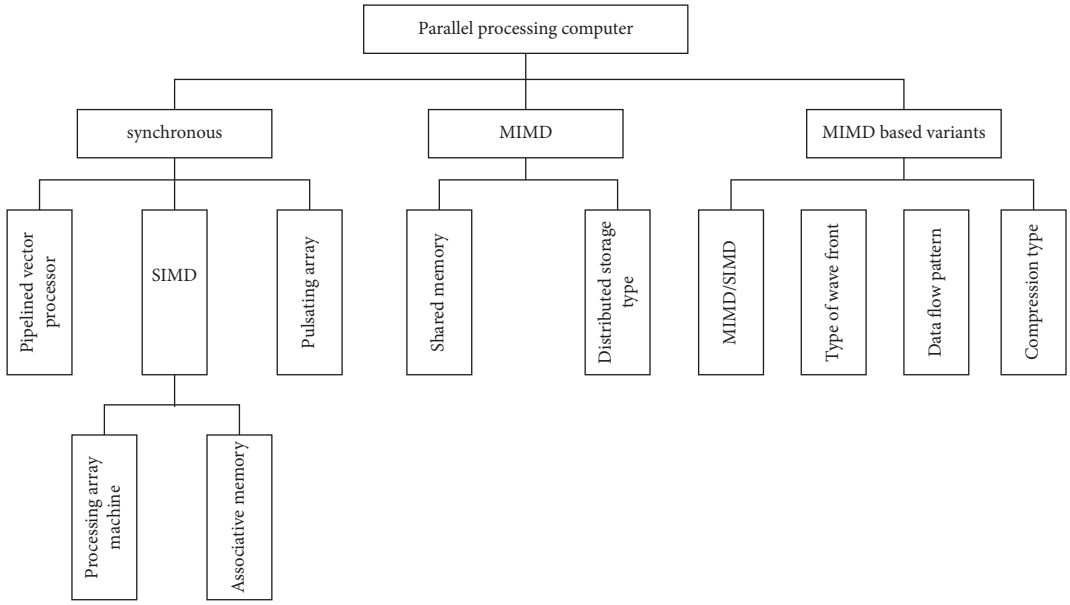

Figure 3: Duncan classification of parallel computing architecture.

bars, and KTV. Further details of the composition types are shown in Table 1.

4.2. Equity Model of Music Cultural Facilities. In the process of studying the space of music and cultural facilities, the most important thing is to analyze the relationship between citizens and facilities. The difference and connection between them are expressed according to the spatial distance. The characteristic results are very objective. On this basis, the layout of music and cultural facilities is analyzed from the needs of both sides and the factors affecting the spatial distribution. From the perspective of practical users, the distance between the arranged music culture settings and consumers is short. This means that the time for customers to arrive at music culture facilities is short, and the satisfaction is higher.

Lorentz curve is a kind of "fairness curve" in statistics. Usually, the "Lorentz curve" is used to express the fairness between the capital allocation and social income. This calculation can objectively judge whether a country's income allocation is balanced or not. Based on different types of social regions and strata, the capital or income is divided into multiple levels, which are arranged and superimposed in order, according to the size of the share. It is expressed on the ordinate, and the abscissa is the superimposed population. Based on this, the points are connected to form a Lorentz curve (as shown in Figure 4). The broken line with an angle of 45° is selected as the average line. There is an unfair problem of social income allocation in all countries. If there is an unfair phenomenon, there will be a prominent radian on the Lorentz curve. Generally, the arc below the fair line is a Lorentz curve, which shows a relatively tortuous curve on the abscissa. According to the radian size, it indicates the proximity between the configuration and the average value. If the arc is large, it indicates that the configuration is seriously unbalanced. Figure 4 demonstrates the schematic diagram of the Lorentz curve.

Table 1: Types of music and cultural facilities.

Type	Content
Educational	Training institutions, music shops, schools
Open type	Gardening, fountains, streets
Performance type	Theatre, concert hall, club, and opera garden
Local community	Cultural station, activity center
Business type	Restaurants, bars, KTV

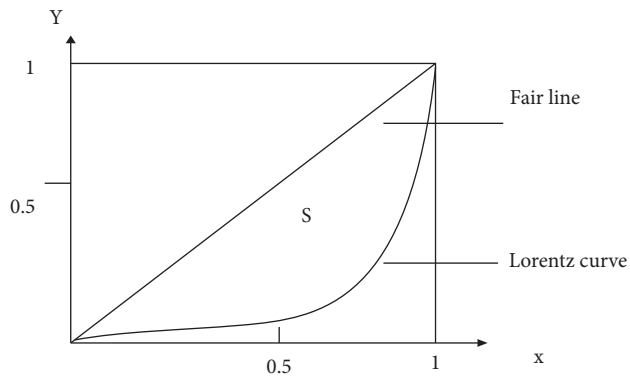

Figure 4: Schematic diagram of Lorentz curve.

4.3. Attraction Model of Music Cultural Facilities. Lagrange extended the law of universal gravitation and put forward the concept of gravitational potential. In the early 1950s, scholars in the social and economic fields believed that the connection between regions and cities was attractive based on this concept. From the perspective of urban facilities, the vast majority of facilities have strong attraction to

practical users. After the basic needs of users are obtained, the attraction also reflects the attraction and aggregation of the relevant facilities. At present, the research on attraction focuses on reducing the transaction costs, flexible layout, and basic behavior of facility users. Note that i and j are two existing fixed points, and there is a positive correlation among the established relationship between the two points. This should be noted that the activity relationship of i indicates that the separation coefficient between the two places is a positive correlation, which is expressed by the following formula:

$$Aij \propto Ei, \quad A \propto \frac{1}{f\left(t_{ij}\right)}. \tag{9}$$

The following conclusions can be drawn:

$$A_{ij} = \frac{Ei}{d_{ij}^{\beta}}, \quad i = 1, 2, 3, \ldots, \; j = 1, 2, 3, \ldots. \tag{10}$$

In the above formula, A_{ij} represents the operation potential between location i and location j; d_{ij} represents the time length or spatial distance between two locations i and j; β represents the impedance coefficient; and E_j represents the operation level of location j. Keeping these parameters in mind, then the total attraction of location i is calculated by the following formula:

$$A_i = \sum_j A_{ij} = \sum_j \frac{E_j}{d_{ij}^{\beta}}. \tag{11}$$

Based on this, the attraction formula is used in music and cultural facilities to calculate the attraction of the people affected by music and cultural facilities in a certain area. Note that Ei refers to the scale of building the i^{th} music and cultural facility. Moreover, D represents the spatial relationship between the music and cultural facilities and citizens, usually taking the shortest distance between them. Similarly, P is the impedance coefficient, that is, dependent on the attraction—the higher the value of Ai, the stronger the attraction and vice versa.

5. Application of Prediction Model Based on Parallel Computing in Music Cultural Facilities

5.1. Analysis on the Composition of Music and Cultural Facilities. When studying the applications of prediction model based on parallel computing in music cultural facilities, this paper selects Chongqing as the main research object for analysis. Based on the composition types of music and cultural facilities, suggested and proposed above, Chongqing music and cultural facilities are sorted out and divided into (i) recreation type, (ii) education type, (iii) performance type, (iv) commercial type, and (v) community type. According to the proportion of different types, the types of music and cultural facilities in Chongqing are mainly commercial and educational, accounting for a higher proportion compared with the three types of performance, recreation, and community. However, these three types are more similar to people's life, which is conducive to establishing a good image of the music and culture in Chongqing district. According to the data, as shown in Figure 5, and its analysis, we observed that the types of music and cultural facilities in the Chongqing district are unevenly distributed and lack a certain number of public welfare and open music culture.

This paper investigates the music and cultural facilities in the main administrative regions of the Chongqing city. The results show that the administrative regions with large population have a large number of facilities. There are many educational facilities in the Jiangbei district, but the allocation of other types of facilities is uneven. Moreover, the distribution of music and cultural facilities in Yuzhong district is relatively balanced. Because the area has complete large-scale music and cultural facilities and performance facilities, therefore, it can meet various basic needs of holding concerts. After analysis, it is concluded that in the market-free leading environment, music and cultural facilities will be deployed with commercial and educational facilities, and the line environment with certain optimization measures will redistribute the system on the basis of configuration, which will greatly improve the quality and efficiency of facilities [19, 20]. The actual distribution of music and cultural facilities in each district of the Chongqing is shown in Figure 6.

5.2. Equity Analysis of Music Cultural Facilities. When analyzing the fairness of music and cultural facilities, this paper first obtains the proportion of the total population of each region and the proportion of music and cultural facilities in the total amount of the city. In the second step, this arranges all data from small to large scale according to the proportion data of the music and cultural facilities built in each street. In the third step, we draw the Lorentz curve of the proportion of population and music and cultural facilities, as shown in Figure 7. The abscissa of the curve is the cumulative value of the proportion of population in each district of Chongqing, and the ordinate is the cumulative value of the proportion of music and cultural facilities built in each district of the Chongqing city. Next, we draw the Lorentz curve of the music and cultural facilities in Chongqing according to the population distribution according to the data. Based on the above data, the Gini equity coefficient, of the music and cultural facilities in each region of the Chongqing according to population distribution, is 0.53.

The Lorentz curve of music and cultural facilities drawn based on the population proportion in Figure 7 above can be obtained through comprehensive analysis of the Gini coefficient. The Gini coefficient of music and cultural facilities accumulated in Chongqing based on the population proportion is 0.53, indicating that Chongqing has serious unfair problems in the construction of music and cultural facilities in various districts, especially in the construction of fewer music and cultural facilities, with a large gap [21–23]. This shows that the music and cultural facilities built in Chongqing are seriously unbalanced.

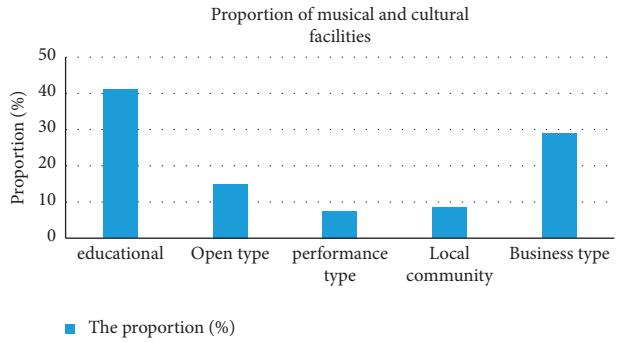

Figure 5: Proportion of types of music and cultural facilities.

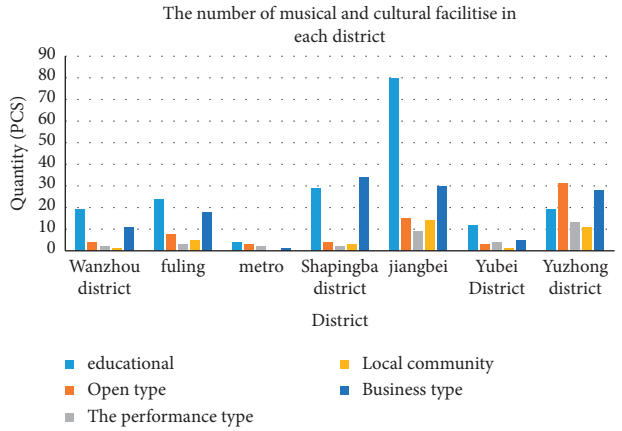

Figure 6: Quantity of various types of music and cultural facilities in each district.

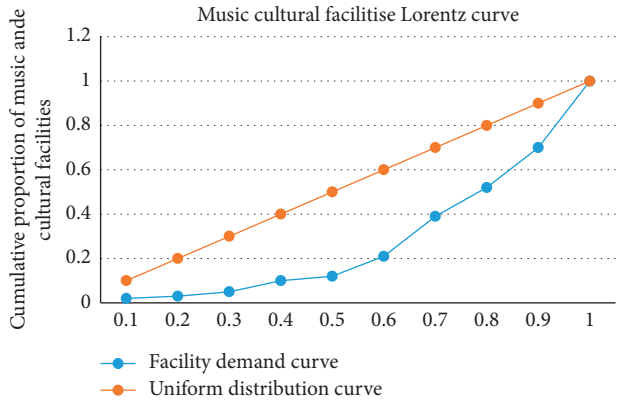

Figure 7: Lorentz curve of music and cultural facilities based on population proportion.

Through analyzing and observing the data, as shown in Figure 7, it can be seen that most of the music and cultural facilities in Chongqing are distributed in the central urban area. This distribution mode is unreasonable, resulting in less music and cultural facilities in areas far away from the city center, and the surrounding people cannot enjoy the edification of music and culture, resulting in a serious imbalance of music and cultural facilities in various districts. At the same time, only four districts in the central urban area of Chongqing have built large-scale music and cultural facilities, and no music and cultural facilities have been built in other districts [24]. Therefore, in order to strengthen and improve the service capacity of music and cultural facilities in Chongqing, we must first invest a lot of money in services of music and cultural facilities to improve the resource level of music and cultural facilities as a whole; in addition, we should also talk about the balanced distribution of resources of music and cultural facilities in each region, reduce the imbalance, and make services of the music and cultural facilities between each region relatively fair [25].

5.3. Analysis on the Attraction of Music Cultural Facilities. A main part of the analysis of the spatial layout of facilities is to analyze the attraction of music and cultural facilities. This paper uses the attraction model to reflect the demand and service level of music and cultural facilities, and intuitively shows that the service capacity provided to music and cultural facilities is further weakened with the extension of citizens' travel time, which usually shows a state of continuous decline. Here, Harvard model is selected as the attraction calculation model of music and cultural facilities, and the expected time of citizens to music and cultural facilities is calculated based on urban road traffic. According to the predetermined visits of music and cultural facilities, the service level and attraction of music and cultural facilities can be quantified, so as to accurately reflect the service capacity of music and cultural facilities, and the blind spots and problems existing in the layout of music and cultural facilities can be fully reflected in the objective calculation results. Based on the combination of current urban roads, traffic resistance, and the time of music and cultural facilities, five minutes is selected as the basic time to study the expected visits of music and cultural facilities [26]. The following is the basic calculation formula:

$$E_i = \sum_{i=1}^{m} \left(\frac{S_j C_i}{D_{ij}^{\lambda} \sum_{j=1}^{n} Sj / D_{ij}^{\lambda}} \right). \tag{12}$$

In the above formula, Sj represents the area of the block j, and D_{ij}^{λ} is the distance between the music and cultural facilities i and j roads, λ represents the resistance coefficient, which is approximately 1.5; Ci is the specific number of people arriving at the music facility i; m represents the number of accessible areas; and n represents the number of music and cultural facilities. The pre-access rate Di can be calculated by the following formula:

$$D_i = \frac{Ei}{p}. \tag{13}$$

In the above formula (13), D_i represents the previsit rate, p represents the total number of people in the region, and Ei represents the previsit volume. The above formula shows that the relationship between the attraction of music and cultural facilities and the accessible area is positive, and it is also positive with the number of people in the region, but inversely proportional to the travel time [27]. In this way, the

Table 2: The road speed (km/h).

Mode of transport	Arterial road	One road	Branch
Nonmotor vehicles	13	13	13
Public transport	26	21	16
A motor vehicle	41	41	31

Table 3: Expected visit rate of music and cultural facilities under public transport mode.

The time interval	0-5 min	0–10 min	0–15 min	0–20 min
Expected visit rate	0.46	0.96	1.27	1.45
Standard deviation	0.12	0.19	0.35	0.61

market orientation rate and previsit rate are calculated. The driving speeds of different road grades are listed in Table 2, and the expected access rate of music and cultural facilities under public transportation is listed in Table 3.

6. Conclusions and Future Work

With the rapid development of science and technology and the expansion of urban scale, more and more people begin to pay attention to the construction of urban cultural facilities and study the practical application of music cultural facilities according to the cultural facilities configured in urban planning. Music culture has been concerned by all sectors of society, experts, and scholars. Music culture has been integrated into people's daily life and has become the main medium of leisure life. Only by combining scientific urban planning and music culture can we fully reflect the scientificity and preciseness of music culture. Through applying the prediction model based on parallel computing in music cultural facilities, this paper summarizes the basic principle of model predictive control and parallel computing process, establishes the optimal layout model of music cultural facilities, and analyzes the composition types of music cultural facilities.

Taking Chongqing as the main research object, this paper analyzes the allocation of music and cultural facilities in various districts of Chongqing, lists the types and specific quantities of music and cultural facilities in various districts, analyzes the fairness and attraction of music and cultural facilities equipped in different regions, draws the Lorentz curve of music and cultural facilities based on the proportion of population, and comes to the conclusion that the Gini coefficient of music and cultural facilities in Chongqing is 0.53. In the future, we will consider other parallel computing, prediction models, and artificial intelligence techniques to investigate the topic well. Moreover, the more data should be used to generalize the outcomes of this research. Other evaluation metrics should be used to evaluate the performance of the proposed prediction model. In the meanwhile, prediction methods are usually dependent on a dataset, and model training might take a long time if the dataset is vast. To lessen the amount of time it takes to train the model, we will look at adopting aggregation approaches or more robust parallel computing enabled prediction algorithms.

Data Availability

Data are available on request from the corresponding author.

Conflicts of Interest

The authors declare that they have no conflicts of interest for publication of this work.

References

[1] R. Indriyani and D. L. Widaningrum, "A spatial equity assessment of the public facilities in the greater Jakarta area using Moran's I spatial autocorrelation," *IOP Conference Series: Earth and Environmental Science*, vol. 749, no. 1, Article ID 012090, 2021.

[2] T. Wang, H. Gao, and J. Qiu, "A combined adaptive neural network and nonlinear model predictive control for multirate networked industrial process control," *IEEE Transactions on Neural Networks and Learning Systems*, vol. 27, no. 2, pp. 416–425, 2017.

[3] S. Wang, J. Housden, T. Bai et al., "Robotic intra-operative ultrasound:virtual environments and parallel systems," *Acta Automatica Sinica: English edition*, vol. 8, no. 5, 2021.

[4] H. Khaleghzadeh, M. Fahad, A. Shahid, R. R. Manumachu, and A. Lastovetsky, "Bi-objective optimization of data-parallel applications on heterogeneous HPC platforms for performance and energy through workload distribution," *IEEE Transactions on Parallel and Distributed Systems*, vol. 32, no. 3, pp. 543–560, 2021.

[5] R. Wang, C. Chen, J. Lee, and E. Darve, "PBBFMM3D: a parallel black-box algorithm for kernel matrix-vector multiplication," *Journal of Parallel and Distributed Computing*, vol. 154, no. 1, pp. 64–73, 2021.

[6] B. Shuangxia, S. Shaomei, L. Shiyang, J. Wang, B. Li, and E. Neretin, "UAV maneuvering decision-making algorithm based on twin delayed deep deterministic policy gradient algorithm," *Journal of Artificial Intelligence Technology*, vol. 2, no. 1, 2022.

[7] K. I. Kiy, D. A. Anokhin, and A. V. Podoprosvetov, "A software system for processing images with parallel computing," *Programming and Computer Software*, vol. 46, no. 6, pp. 406–417, 2020.

[8] J. R. Shi, W. U. Jie, H. U. Zhe-Rong, and Z. Xiu-min, "Green corridor of rust belt: theory and practice of organic growth in three-dimensional space of industrial heritage," *Ecological Economy: English edition*, vol. 17, no. 1, 2021.

[9] Y. P. Chang and K. P. Hung, "Development and validation of a tourist experience scale for cultural and creative industries parks," *Journal of Destination Marketing & Management*, vol. 20, no. 1, Article ID 100560, 2021.

[10] W. U. Fei and W. Xiao, "Research on design methods of poetry city cultural and creative products based on regional culture," *Landscape Studies: English version*, vol. 13, no. 4, 2021.

[11] S. Porru, F. E. Misso, F. E. Pani, and C. Repetto, "Smart mobility and public transport:Opportunities and challenges in rural and urban areas," *Journal of Traffic and Transportation Engineering*, vol. 37, no. 1, pp. 93–102, 2020.

[12] M. J. Jia and S. F. Wang, "Group development of cultural facilities in stock area development era, guangzhou," *The Planner*, vol. 37, no. 17, pp. 80–85, 2021.
[13] F. Kharvari and M. Rostami-Moez, "Assessment of occupant adaptive behavior and visual comfort in educational facilities: a cross-sectional field survey," *Energy for Sustainable Development*, vol. 61, no. 6, pp. 153–167, 2021.
[14] E. Anedda, G. Carletto, G. Gilli, and D. Traversi, "Monitoring of air microbial contaminations in different bioenergy facilities using cultural and biomolecular methods," *International Journal of Environmental Research and Public Health*, vol. 16, no. 14, p. 2546, 2019.
[15] Y. Zhang, Y. M. Zhang, and X. H. Wang, "Peak current predictive control algorithm for boost converters," *Journal of Beijing University of Technology*, vol. 47, no. 1, pp. 24–31, 2021.
[16] T. Liu, H. Luo, O. Kaynak, and S. Yin, "A novel control-performance-oriented data-driven fault classification approach," *IEEE Systems Journal*, vol. 14, no. 2, pp. 1830–1839, 2020.
[17] R. Yang, W. X. Zheng, and Y. Yu, "Event-triggered sliding mode control of discrete-time two-dimensional systems in Roesser model," *Automatica*, vol. 114, no. 5, Article ID 108813, 2020.
[18] R. A. Rehfeldt, I. Tyndall, and J. Belisle, "Music as a cultural inheritance system: a contextual-behavioral model of symbolism, meaning, and the value of music," *Behavior and Social Issues*, vol. 30, no. 1, pp. 749–773, 2021.
[19] Y. R. Pandeya and J. Lee, "Deep learning-based late fusion of multimodal information for emotion classification of music video," *Multimedia Tools and Applications*, vol. 80, no. 2, pp. 2887–2905, 2021.
[20] M. Nuccio and E. Bertacchini, "Data-driven arts and cultural organizations: opportunity or chimera?" *European Planning Studies*, vol. 47, pp. 1–18, 2021.
[21] A. Ali, Y. Zhu, and M. Zakarya, "A data aggregation based approach to exploit dynamic spatio-temporal correlations for citywide crowd flows prediction in fog computing," *Multimedia Tools and Applications*, vol. 80, no. 20, 31433 pages, 2021.
[22] J. L. Jin, X. G. Xu, Y. Cui, R. Zhou, C. Wu, and L. Zhang, "Water resources spatial equilibrium evaluation method based on connection number and Lorenz curve," *Advances in Water Science*, vol. 32, no. 3, pp. 387–395, 2021.
[23] S. Abbas, Q. Nasir, D. Nouichi et al., "Improving security of the Internet of Things via RF fingerprinting based device identification system," *Neural Computing & Applications*, vol. 33, no. 21, Article ID 14769, 2021.
[24] A. Khurshid, A. N. Khan, F. G. Khan, M. Ali, J. Shuja, and A. U. R. Khan, "Secure CamFlow: a device-oriented security model to assist information flow control systems in cloud environments for IoTs," *Concurrency and Computation: Practice and Experience*, vol. 31, no. 8, 2019.
[25] A. Ali, Y. Zhu, and M. Zakarya, "Exploiting dynamic spatio-temporal graph convolutional neural networks for citywide traffic flows prediction," *Neural Networks*, vol. 145, pp. 233–247, 2022.
[26] H. Zheng, D. Liu, and Y. Liu, "Design and research on automatic recognition system of sports dance movement based on computer vision and parallel computing," *Microprocessors and Microsystems*, vol. 80, Article ID 103648, 2021.
[27] B. Ji, Y. Wang, K. Song et al., "A survey of computational intelligence for 6G: key technologies, applications and trends," *IEEE Transactions on Industrial Informatics*, vol. 17, no. 10, pp. 7145–7154, 2021.

Hindawi
Scientific Programming
Volume 2022, Article ID 1837512, 10 pages
https://doi.org/10.1155/2022/1837512

Research Article

Construction of a College Physical Education Teaching Model Using Multiple Intelligences Theory

Ming Xie and Xiaoqin Xu

Hunan International Economics University, Department of Physical Education, Changsha, Hunan 410205, China

Correspondence should be addressed to Xiaoqin Xu; linskned@hnu.edu.cn

Received 18 March 2022; Revised 6 April 2022; Accepted 11 April 2022; Published 25 April 2022

Academic Editor: Muhammad Zakarya

In recent years, China has comprehensively carried out and implemented the "national fitness campaign." Sports have been integrated into everyone's daily life. As a place for cultivating talents, colleges and universities have also begun to reform the physical education teaching mode and cultivate a number of talents with strong competition ability, teaching ability, and adaptability to the society. With the deepening of the reform of physical education teaching mode in colleges and universities, some colleges and universities have introduced the theory of multiple intelligences. By analyzing the concept and content of the theory of multiple intelligences and comparing it with the traditional physical education teaching mode, it fully reflects the advantages of the theory of multiple intelligences in physical education teaching. This paper uses fuzzy mathematics and fuzzy set algorithm to build a teaching model based on the theory of multiple intelligences. Moreover, we study the innovative methods of college physical education teaching, take college physical basketball teaching as the research object, and analyze the students' sports technology, students' teaching practice ability, and students' thinking ability based on the theory of multiple intelligences. Experimental outcomes show that the teaching method guided by the theory of multiple intelligences was designed for the intelligent characteristics of the students in the experimental group, and the teachers and students communicated with each other during the teaching period, which significantly improved the students' thinking ability.

1. Introduction

Some western countries have formed a complete theoretical system by using the theory of multiple intelligences in educational reform [1]. At present, China is also further deepening education reform. The theory of multiple intelligences is a good interpretation of quality education, which is also an important theoretical basis for education reform and promotes China's shell process reform. After the introduction of multiple intelligences theory in China, it has been valued by many experts and scholars and put into teaching practice. This paper uses the theory of multiple intelligences to construct the college physical education teaching model, which is of great significance to the development of college physical education in China. The theory of multiple intelligences explains intelligence well. Human intelligence belongs to diversity, not one or two, but a combination of multiple and independent. This theory is also recognized by experts in the field of education. This should be kept in mind that the multiple intelligences theory is a research achievement related to human intelligence. It has formed a mature and complete theoretical system and is now widely used in the fields of pedagogy and psychology.

A single presentation of theoretical knowledge in class will make students feel bored and uninterested. The application of multiple intelligences theory in college physical education can formulate corresponding teaching plans according to the individual differences of each student, which can greatly improve the teaching quality and achieve remarkable teaching results, which is of great value for cultivating high-quality talents. In this paper, we introduce the theory of multiple intelligences into college physical education and explain the main contents and characteristics of the theory in detail. We then compare and analyze the

differences between traditional teaching and multiple intelligences teaching so as to highlight the advantages of multiple intelligences teaching. Moreover, through combining fuzzy mathematics algorithm and fuzzy transformation method, this paper constructs an efficient physical education teaching mode based on multiple intelligences theory and analyzes the differences between multiple intelligences theory and traditional teaching mode from three aspects: (i) sports technology, (ii) teaching practice ability, and (iii) students' thinking ability [2].

The setting of the control group and the experimental group shows that there is a significant difference (statistical) in students' sports technology ($P < 0.01$). Based on the multiple teaching theory, teaching takes students' learning style and personality characteristics as the core and formulates a suitable teaching mode according to students' intelligence characteristics. There was a significant difference in the scores of teaching practice ability ($P < 0.01$). Because teachers carefully designed teaching methods, contents, and forms during teaching, students' teaching practice ability was strengthened. There was a significant difference in the scores of students' thinking ability ($P < 0.05$), which was due to the fact that the teaching method guided by the theory of multiple intelligences was designed for the intelligent characteristics of the students in the experimental group. Moreover, this means that the teachers and students communicated with each other during the teaching period, which significantly improved the students' thinking ability. The main innovations and contributions of the research conducted in this paper are as follows:

(i) This paper introduces the theory of multiple intelligences into college physical education and explains the main contents and characteristics of the theory in detail

(ii) It compares and analyzes the differences between traditional teaching and multiple intelligences teaching so as to highlight the advantages of multiple intelligences teaching

(iii) Combining fuzzy mathematics algorithm and fuzzy transformation method, this paper constructs an efficient physical education teaching mode based on multiple intelligences theory

(iv) It analyzes the differences between multiple intelligences theory and traditional teaching mode from three aspects: (a) sports technology, (b) teaching practice ability, and (c) students' thinking ability

The remaining of the paper is structured as follows. We discuss some of the recent state-of-the-art methods in Section 2. Section 3 is devoted to the theory of multiple intelligences. We discuss the convolution neural networks and proposed a model for text translation. In Section 4, we discuss the construction of the college physical education teaching model based on multiple intelligences theory. A teaching model is suggested. Section 5 illustrates the analysis of basketball teaching effect based on the multiple intelligences theory and the proposed teaching model. Finally, we conclude this discussion along with directions for future research in Section 6.

2. Related Work

In the last century, people have begun to realize the importance of intelligence and change the traditional cognition of intelligence [3]. Elkholy's knowledge construction theory is used as the theoretical basis for studying the brain's natural learning ability and generates intelligent psychological test tools, such as IQ test [4]. Al Qatawneh described the content of multiple intelligences and curriculum in detail. Moreover, the authors described the combination mode between curriculum and multiple intelligences in a very vivid way through figures and examples. In addition, they have also analyzed various intelligence training methods and students' intelligence education so as to better apply this theory in the curriculum [5]. Dewi referred to the theory of multiple intelligences and learning style to have a more diversified understanding of the students' learning characteristics and intelligence and used a variety of teaching styles and optimal teaching strategies to carry out targeted education [6]. China has also introduced the theory of multiple intelligences to improve China's quality of education because the theory of multiple intelligences reflects the characteristics of modern science, meets the requirements of China's educational reform, and is an important theoretical basis for China's educational reform.

Wang put forward the theory of multiple intelligences as an important basis for evaluating physical education teaching, which reflects the evaluation process of physical education teaching from multiple perspectives [7]. Zhao proposed that the problems in the evaluation of physical education teaching in colleges and universities in China can be supplemented by the theory of multiple intelligences evaluation (MIEM). The application of the multiple intelligences evaluation model in physical education teaching evaluation can better meet the requirements of the concept of teaching quality [8]. Xu research pointed out that multiple intelligences theory is more conducive to physical education teaching in learning and research [9]. Hu believes that the use of multiple intelligences theory in cultivating college students' physical ability is a new teaching model. However, there are still many problems in practical application, which need to be discussed later, especially the investigation of students' physical exercise after graduation [10].

Wei explained, from eight various aspects, that the process of applying multiple intelligences theory in student work plays a guiding role in students' entrepreneurship and scientific research [11]. Lu analyzed the use of multiple intelligences theory in English teaching from the perspective of teaching and pointed out that multiple intelligences theory should integrate teaching environment resources. Moreover, this should also integrate teaching resources by arranging classrooms, building campus culture and network environment, and paying attention to processing teaching contents and guiding students' employment [12, 13]. By summarizing various problems in the ideological and political courses in colleges and universities, Zhang proposed and recommended applying the theory of multiple intelligences to the ideological and political courses in colleges and universities. The authors also suggest designing the

ideological and political teaching strategy based on the theory of multiple intelligences [14, 15].

Ding affirmed the positive role of using the theory of multiple intelligences in colleges and universities and proposed that students can better understand the structure of intelligence by using the theory of multiple intelligences. One of the main reasons to support this claim is that the multiple intelligences theory is convenient for the cultivation and expansion of students' intelligence and conscious initiative [16, 17].

3. Based on the Theory of Multiple Intelligences

3.1. Content of Multiple Intelligences Theory. In the book "The Structure of Intelligence: The Theory of Multiple Intelligences" written by Gardner, it is proposed that a person has at least 8 kinds of intelligence [18]. These various kinds are shown in Figure 1.

Moreover, the content of multiple intelligences theory involves eight aspects that can be grouped by the intelligent species, content, and cultivating way, which are described in detail as illustrated in Table 1.

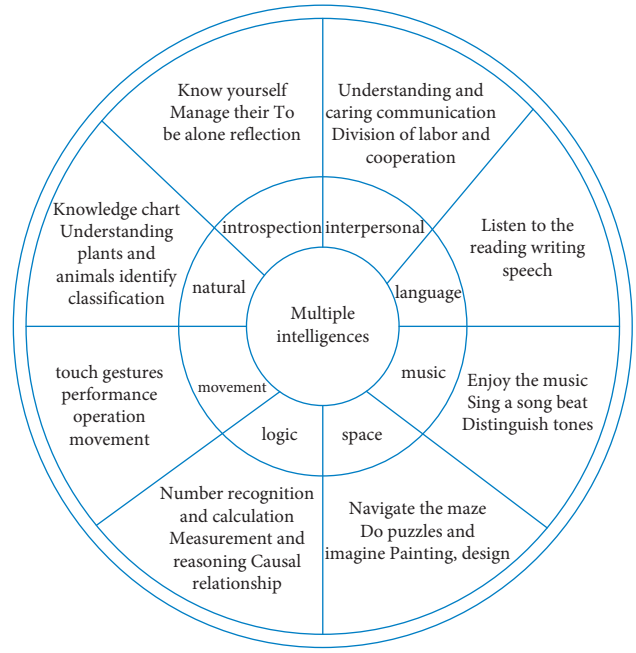

Figure 1: Composition of multiple intelligences theory.

3.2. Characteristics of Multiple Intelligences Theory

3.2.1. Individual Intelligence Difference. In the theory of multiple intelligences, it is pointed out that all people have eight kinds of intelligence. The intelligence of each person does not appear independently. It is flexibly combined in various ways to form an intelligent individual, and there are great differences among individuals. Based on this difference, all people have different intelligence. Even if the same intelligence is different in everyone, it is impossible to judge the individual IQ by an accurate standard [19]. Each student should be treated differently during teaching, and it is not allowed to evaluate the quality of students from a certain intelligence. During the period of teaching reform, we should fully integrate the core content of multiple intelligences theory and cultivate a large number of talents with strong comprehensive ability for the country [20].

3.2.2. Intelligence Emphasizes Individual Development. Based on Gardner's theory of multiple intelligences, modern multiple society does not simply judge talents from mathematical logic ability and language ability but pays more attention to the ability to deal with practical problems [21]. It is also the main trend of modern education reform. It is not only the traditional cultivation of students' mathematical logic ability and language ability but also students' individuality that guide students to improve their ability to deal with practical problems and innovate product effects [22].

3.2.3. Diversified View of Intelligence. Each individual intelligence is not judged from the aspects of mathematical logic ability and speech intelligence. It is a differentiation of individual manifestations integrating a variety of different abilities. Gardner pointed out that intelligence is multidimensional and its expression is independent. The intelligence of each individual will change with the accumulation of growth and experience and will also be affected by the environment. There are abilities other than eight kinds of intelligence [23, 24]. Therefore, we should analyze intelligence with multidimensional thinking. During the teaching period, it is necessary for modern teachers to analyze the intelligence of students for each student's characteristics, analyze the intelligence characteristics of each individual, and study students' intelligence from a multidimensional perspective.

3.3. Differences between Multiple Intelligences Teaching and Traditional Teaching. The purpose of formulating teaching methods is to complete teaching tasks and the means used in the activities participated by teachers and students. In fact, the teaching activities of both parties, that is, teacher and student, include teachers' teaching methods and students' learning methods [25]. During the teaching period, adopt scientific teaching methods to strengthen the teaching effect and complete multiple teaching objectives. Through comparing the theory of multiple intelligences with traditional teaching, the differences between the two teaching modes against certain aspects of the intelligence are studied and listed in Table 2.

4. The Construction of a Teaching Model for College Physical Education Based on the Theory of Multiple Intelligences

4.1. Fuzzy Mathematics Algorithm of College Physical Education Teaching Mode. In reality, the concepts of incompleteness, uncertainty, and inconsistency belong to fuzzy characteristics. Different fuzzy characteristics can be studied by corresponding fuzzy theories and methods. Their theories

Table 1: Content of multiple intelligences theory along with descriptions.

Intelligent species	Content	Cultivating way
Verbal intelligence	Ear sensitivity to word pronunciation, structure, meaning, and usage	Verbally stating that it happened
Music intelligence	Appreciate and form treble, rhythm, and sound quality, and appreciate different forms of music expression	Music works, recorded programs, and works display
Logic-mathematical intelligence	Sensitivity to mathematical model or logic, accurate discrimination, and reasoning ability of the model	Scientific theory, scientific discovery, category system, and mathematical calculation
Visual-spatial intelligence	Be able to accurately observe the visual-spatial world and initially transform perceptual ability	Navigation system, artwork, and architectural design
Action of intelligent	The ability to control limb movement and be proficient in target processing	Sports performances, handicrafts, drama works, and sculpture works
Intrapersonal intelligence	The ability to distinguish multiple emotions and master personal advantages and disadvantages	Psychological theory, religious system, and ritual
Interpersonal intelligence	The ability to accurately distinguish other people's emotions, tempers, wishes, and motives	Social institutions and political documents
Natural observation	The ability to accurately distinguish various animals and the ability to distinguish similar things	Herbal knowledge and folk classification

Table 2: Compare multiple intelligences with traditional intelligent teaching methods.

Intelligence	Multiple intelligences teaching method	Traditional intelligent teaching method
Speech language intelligence	Support students to participate in the teacher's teaching process and explain the demonstration actions in detail	The teacher explains the students' passive listening
Visual air switch relationship intelligence	Multiface demonstration teaching and intuitive teaching	Single teacher demonstration teaching
Music rhythm intelligence	Play suitable music teaching, strengthen students' sense of rhythm, and improve their interest in learning	Only warm up with music before and after class
Body movement intelligence	Make use of learning to let students be proficient in sports skills and exercise independently	The teacher teaches the action, and the students practice with the action
Interpersonal intelligence	Cooperative learning, group practice, and teachers' guidance on mistakes	Students practice according to a certain standard
Self-cognitive intelligence	Before the end of the class, students summarize the learning contents of this class and reflect on the problems	Teachers' unified evaluation of students

mainly include the combination of fuzzy logic and fuzzy. The following is the mathematical definition of fuzzy set [26].

Definition 1. Let u represent the universe; then the mapping μ: $U \longrightarrow [0, 1]$ from u to $[0, 1]$ can define a fuzzy subset A of universe U. Formulas (1) and (2) represent a fuzzy set on universe U:

$$A = \{\mu_A(\mu_1)/\mu_1, \mu_A(\mu_2)/\mu_2, \mu_A(\mu_3)/\mu_3 \ldots\ldots\}, \quad (1)$$

$$A = \{\mu_A(\mu_1)/\mu_1 + \mu_A(\mu_2)/\mu_2 + \mu_A(\mu_3)/\mu_3 \ldots\ldots\}. \quad (2)$$

For some finite domains, fuzzy set a is represented by the following ways:

$$A = \{\mu_A(\mu_1), \mu_A(\mu_2), \mu_A(\mu_3), \ldots\ldots, \mu_A(\mu_n)\}. \quad (3)$$

Fuzzy set is used when it is difficult to accurately define classification and element attributes. Refer to the degree of belonging of this element to any set, and its standard is the value of 0–1. If μ a (μ) is close to 1, it indicates that this element has high membership in the set; otherwise, it indicates that this element has low membership in the set. The following basic concepts are extended.

Define that fuzzy sets are equal: if A and B are different, for universe u, then $\mu \in U$ has two functions $\mu_A(\mu) = \mu_B(\mu)$, indicating that A fuzzy set is equal to B fuzzy set; that is, $A = B$.

The relationship between fuzzy sets is inclusion. Assuming that both A and B belong to F(U), if all have μA(x) ≤ μB(x), it can be concluded that fuzzy set B is included in fuzzy set A; that is, $A \subseteq B$. If there are special cases, $B \subseteq A$ is also true, and finally, A and B are equal.

4.2. Fuzzy Transformation Method of College Physical Education Teaching Mode. The fuzzy transformation method is a method of fuzzy comprehensive evaluation based on the matrix change mode [27]. R represents the fuzzy judgment matrix, A represents the weighting vector, and the comprehensive value of all elements in the weighting vector A is 1; that is, $\sum a_i = 1$. The calculation formula is shown by the following:

$$b_j = \vee\left(a_i \wedge r_{ij}\right)(j = 1, 2, 3, \ldots, m). \quad (4)$$

Regardless of the value of r_{ij} in the above formula, the result of $a_i \wedge r_{ij}$ is smaller than that of a_i. According to this analysis, a_i cannot weight the results but only limits some results and filtering. During the later calculation, the principle of taking the larger one is applied, and the highest one among the various $a_i \wedge r_{ij}$ results is always selected so as

to better exhaust gas factors and completely retain important factors [28]. Based on the above settings, the multiplication method will take the small instead, and its calculation formula is as follows:

$$b_j = \vee\left(a_i r_{ij}\right)(j = 1, 2, 3, ..., m). \quad (5)$$

The a_i function here is different from the above. It has no partial suppression or filtering function and only has weighting function. The following calculation formula also follows the principle of taking the larger one, and a is difficult to enter b_j. It is fully proved that the main factor is still the core part. Then the following is the calculation formula of the algorithm that will take the larger one instead of the larger one:

$$b_j = \sum_{i=1}^{n} \left(a_i \wedge r_{ij}\right)(j = 1, 2, 3, ..., m). \quad (6)$$

There is also a certain difference between a_i and multiplication instead of the minimization method. Its basic function is partial limit and filtering. All three factors in this method can obtain corresponding participation opportunities; that is, the role of the main factor is not significant [29]. The following is the weighted average algorithm formula:

$$b_j = \sum_{i=1}^{n} \left(a_i r_{ij}\right)(j = 1, 2, 3, ..., m). \quad (7)$$

4.3. Innovation of College Physical Education Based on the Theory of Multiple Intelligences. Physical education is related to the all-round development of students. The use of physical education can improve students' physical quality, develop students' potential intelligence, and realize the all-round development of personal ability. However, China's colleges and universities do not pay attention to the teaching of physical education, and the opening time is relatively short, which has not formed a complete teaching mode. Most colleges and universities' hardware facilities cannot meet the requirements, such as tennis courts, equipment, and teachers. In terms of software facilities, physical education teaching methods, teaching innovation, teaching content, and teaching evaluation also form a systematic theoretical system. The innovation of physical education teaching in colleges and universities involves many contents. This paper innovates physical education teaching based on the theory of multiple intelligences, which is shown in Figure 2.

4.4. Construction of Teaching Model Based on Multiple Intelligences Theory. The theory of multiple intelligences is used in college teaching practice, in which "observation" is to comprehensively collect students' learning data in the task situation environment. In addition, the evaluation task should aim at students' mastering and learning more knowledge and ability. The explanation includes the reasoning and analysis of observed phenomena and data, as well as the content of classroom evaluation to promote students' skill learning and students' knowledge. The three elements can be regarded as a closed cycle and interrelated process. Cognition corresponds to learning objectives. Observation is the search for evidence related to students' development, and interpretation is the effective feedback of students' evidence. As shown in Figure 3, the teaching model based on multiple intelligences theory is shown.

5. Analysis of Basketball Teaching Effect Based on Multiple Intelligences Theory

5.1. Analysis of Students' Sports Technology. This paper studies the construction of the college physical education teaching model based on multiple intelligences theory and takes college basketball teaching as the research object. Among them, "sports technology" refers to the way in which athletes' physical ability can effectively play and complete each action. Moreover, the sports skill refers to the ability to complete the specified action with a certain technology. During basketball teaching in colleges and universities, sports technology is not only the key to basketball teaching but also an important teaching mode. Therefore, based on the teaching mode guided by multiple intelligences theory, this paper analyzes sports technology and grasps the important role of multiple intelligences theory in basketball teaching composition. To do so, we set up a control group and an experimental group to compare the students' technical test scores. Figure 4 shows the learning technology scores of the two groups of students in the teaching experiment. Similarly, Table 3 shows the technical examination results of the two groups of students after the test teaching experiment.

According to the above Figure 4, the technical test scores of the students in the experimental group are mainly 83–73 and 94–84, respectively, and $P < 0.01$ can be obtained from the data in Table 3. The P value shows that the students in the control group and the experimental group have great differences in technical scores, which proves that the technical level of colleges and universities using multiple intelligences theory in basketball teaching is high. This is due to the fact that basketball teaching using multiple intelligences teaching theory can highlight students' personality characteristics and learning style. Starting from a variety of intelligent characteristics, corresponding teaching modes are adopted for different students. After observation, it is convenient for students to master the action structure, have a deeper understanding of the key parts of the technology, and experience the key points of technology through combining with their own characteristics. This essentially helps in making students more confident and interested in learning basketball.

5.2. Analysis of Students' Teaching Practice Ability. Teachers teach by organizing students to carry out interactive activities. Practice is not only the main channel of people's innovation but also the test of the results and level of innovative activities. Teaching activities are embodied in a certain form of teaching organization during teaching practice. As the main carrier and medium of teaching activities, teaching organization can ensure teachers carry out classroom teaching smoothly. In order to explore the influence of multiple intelligences theory on the effect of

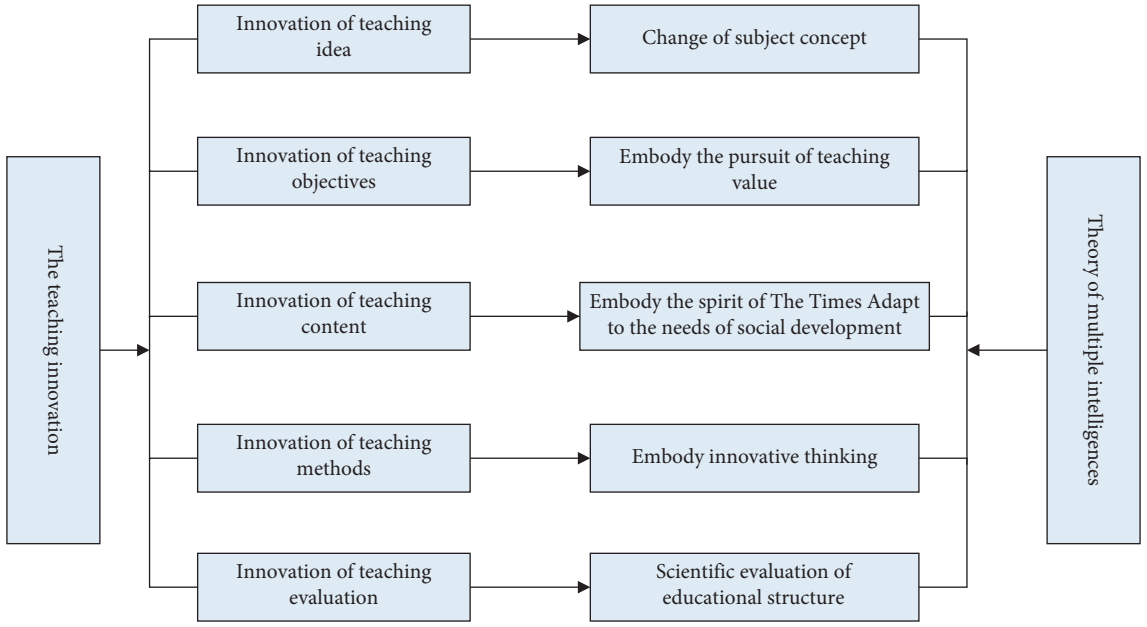

Figure 2: Innovation of college physical education based on the theory of multiple intelligences.

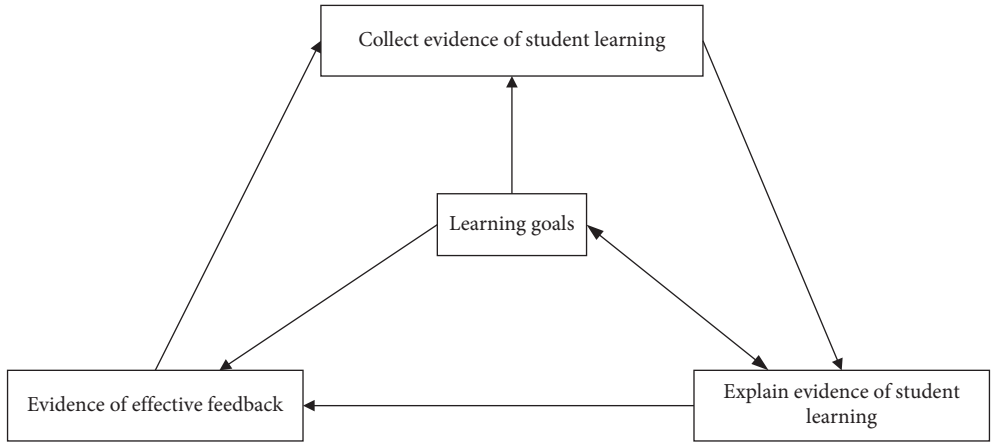

Figure 3: Teaching model based on the theory of multiple intelligences.

college basketball teaching, the index of students is assessed in the teaching experiment, and the experimental group and the control group are set to compare the students' scores. The teaching practice ability is assessed from three aspects: 30 demonstration skills, 40 explanation skills, and 30 organization teaching. The distribution results of the two groups of students' teaching practice ability after the teaching experiment are shown in Figure 5. Table 4 shows the comparison of the two groups of students' teaching practice ability after the teaching experiment.

Analysis of the data in Figure 5 shows that, during the teaching process, most of the students' practical ability scores of the experimental group are in the 95–90 division, and the students' practical ability scores of the control group are in the 77–72 division. According to the data in Table 4, the value of $P < 0.01$ fully shows that there is a great difference in practical ability between the control group and the experimental group. In terms of teaching practice ability, the students in the experimental group were significantly higher than those in the control group. This is because, based on the system control theory, teaching itself belongs to a controllable closed-loop system. The components of the system have multiple subsystems and a large number of teaching-related factors. Through the effective control of the teaching subfactors, the teaching tasks and objectives are realized and used during the basketball teaching. Teachers should design teaching methods, teaching contents, and teaching forms based on the characteristics of students so as to realize combination and optimization. Their manifestations should focus on physical activities and cultivate students' action technology. The designed teaching activities should be implemented in conjunction with various intelligent teaching methods. Because some technical actions cannot be explained in the actual teaching process, therefore they can

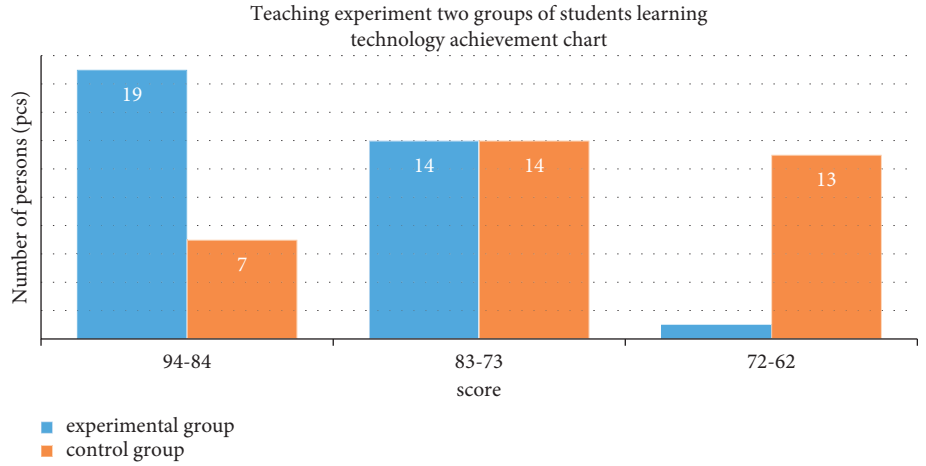

Figure 4: Achievement chart of learning technology of two groups of students in teaching experiment.

Table 3: After the teaching experiment, the results of the technical examination of the two groups of students were compared.

Group	$\overline{x}$	S	T	Sig	P
Experience group ($N = 33$)	86.27	5.13	6.21	0.00	<0.01
Control group ($N = 34$)	75.69	7.62			

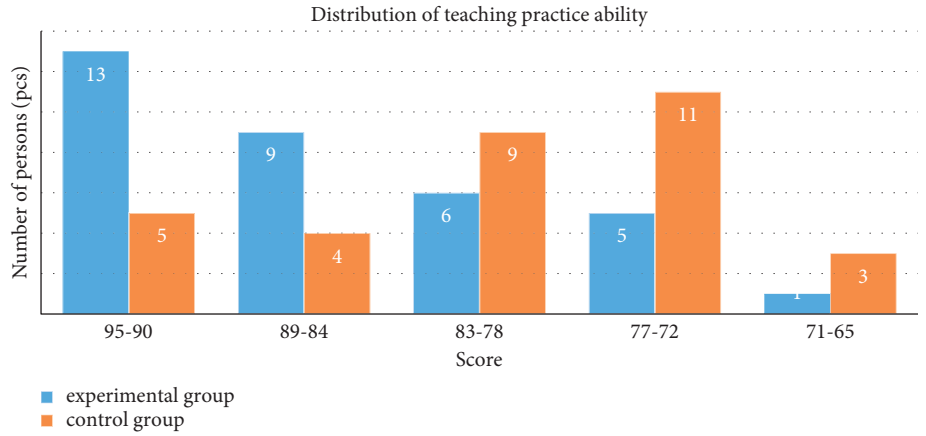

Figure 5: Distribution chart of students' teaching practice ability after teaching experiment.

only be demonstrated by teachers for many times. Students master the skills through observation and practice for many times. Students can quickly grasp the feedback information in a short period of time and realize the technical action of innovation and improvement.

5.3. Analysis of Students' Thinking Ability. Thinking is the source of human invention and creation. Students' learning activities should also use thinking flexibly. The key to improving students' learning ability is to strengthen their thinking ability [30]. Therefore, during the traditional physical education teaching in colleges and universities, teachers take students' sports technology as the core and do not pay attention to students' ability to observe, study, analyze, raise, and deal with problems. Therefore, under the guidance of multiple intelligences teaching theory, colleges and universities choose to observe, analyze, raise, and deal with problems as the test content. Teachers explain to all students and evaluate students. Figure 6 shows the results of the analysis of the thinking ability of the two groups of students in the teaching experiment. Moreover, Table 5 shows the results of the examination of the thinking ability of the two groups of students after the teaching experiment.

According to the results of students' thinking ability shown in Figure 6, most of the students in the experimental group scored 89–84 points, while the students in the control group scored 77–72 points. The information in Table 5 shows that the value of $P < 0.05$, which indicates that the thinking ability of the students in the control group and the

Table 4: After the teaching experiment, the test results of the comparison of the scores of the two groups of students' teaching practice ability.

Group	$\overline{x}$	S	T	Sig	P
Experience group ($N = 33$)	86.94	5.98	5.51	0.00	<0.01
Control group ($N = 34$)	79.02	6.24			

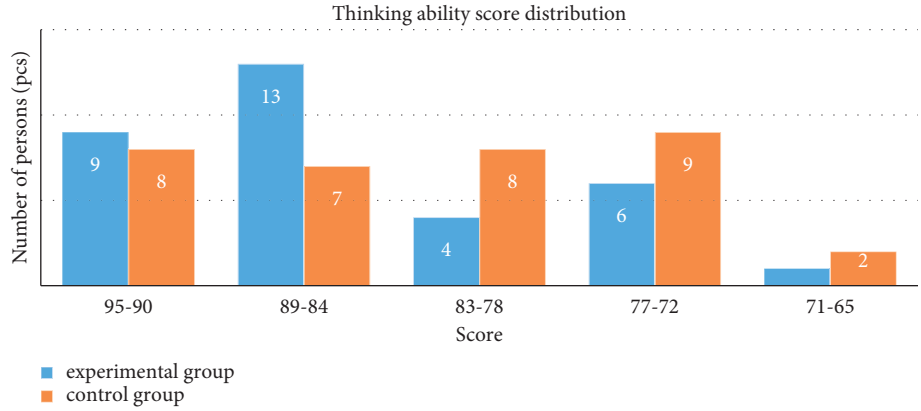

Figure 6: Distribution chart of students' thinking ability after teaching experiment.

Table 5: After the teaching experiment, the two groups of students' thinking ability scores were compared and tested.

Group	$\overline{x}$	S	T	Sig.	P
Experience group ($N = 33$)	87.53	6.46	2.36	0.041	<0.05
Control group ($N = 34$)	84.22	7.51			

experimental group is different. Subsequently, this also fully proves that colleges and universities can greatly improve students' thinking ability by using the theory of multiple intelligences in basketball teaching. The factor leading to this result is that the multiple intelligences theory designs the teaching scheme based on the intelligent characteristics of the students in the experimental group (control and experiment groups) and pays attention to improving the students' intelligence so as to supplement the lack of students' intelligence and double the students' self-confidence during learning.

6. Conclusions and Future Work

This paper adopts the theory of multiple intelligences in the study of college physical education teaching mode, which fully reflects the characteristics of multiple intelligences structure in teaching. The traditional teaching mode pays attention to theory. A single presentation of theoretical knowledge in class will make students feel bored and uninterested. The application of multiple intelligences theory in college physical education can formulate corresponding teaching plans according to the individual differences of each student, which can greatly improve the teaching quality and achieve remarkable teaching results, which is of great value for cultivating high-quality talents. This paper chooses college basketball teaching as the main research object and uses the multiple teaching theory to analyze the influence of college basketball teaching on students' sports technology, practical ability, and thinking ability, which can effectively strengthen students' initiative and enthusiasm for learning basketball. Experimental outcomes show that the teaching method guided by the theory of multiple intelligences was designed for the intelligent characteristics of the students in the experimental group, and the teachers and students communicated with each other during the teaching period, which significantly improved the students' thinking ability.

We will build a more powerful teaching model based on state-of-the-art algorithms in the future, which will result in improved accuracy. Deep learning approaches, therefore, are time expensive, and model training might take a long period. As a result, techniques such as aggregation can be utilized to increase the algorithm's performance in terms of training and prediction time. Other approaches, such as graph convolutional network (GCN), LSTM, ResNet, and attention networks, can be researched in the near future in addition to CNN. The ReLU function was used to get the results in this paper; however, other functions would produce different results. As a result, we will look into

several functions. The network depth, kernel size, and filter number study restrictions might also be a viable alternative for further enhancement of the proposed teaching model.

Data Availability

Data are available upon request from the corresponding author.

Conflicts of Interest

The authors declare that they have no conflicts of interest regarding the publication of this work.

References

[1] M. Ferrero, M. A. Vadillo, and S. P. León, "A valid evaluation of the theory of multiple intelligences is not yet possible: problems of methodological quality for intervention studies," *Intelligence*, vol. 88, no. 4, p. 101566, 2021.

[2] A. Vbl, A. Acag, and A. Cb, "Associations among psychological satisfaction in physical education, sports practice, and health indicators with physical activity: direct and indirect ways in a structural equation model proposal [J]," *International Journal of Pediatrics and Adolescent Medicine*, vol. 8, no. 4, pp. 246–252, 2021.

[3] K. Arun and S. Kumar, "Cognitive science and artificial intelligence for human cognition and communication [J]," *IEEE Consumer Electronics Magazine*, vol. 9, no. 1, pp. 72-73, 2020.

[4] W. Elkholy, M. El-Menshawy, J. Bentahar, M. Elqortobi, A. Laarej, and R. Dssouli, "Model checking intelligent avionics systems for test cases generation using multi-agent systems," *Expert Systems with Applications*, vol. 156, no. 3, p. 113458, 2020.

[5] S. S. Al-Qatawneh, N. R. Alsalhi, M. E. Eltahir, and O. A. Siddig, "The representation of multiple intelligences in an intermediate Arabic-language textbook, and teachers' awareness of them in Jordanian schools," *Heliyon*, vol. 7, no. 5, p. e07004, 2021.

[6] N. C. Dewi and fnm Martini, "Worksheet based on multiple intelligences for improving student's result," *Journal of Physics: Conference Series*, vol. 1567, no. 4, p. 042017, 2020.

[7] M. Y. Wang, "Evaluation of physical education teaching in the perspective of fractal theory [J]," *Shandong Sports Science & Technology*, vol. 39, no. 1, pp. 70–75, 2017.

[8] Y. J. Zhao, "Analysis on the present situation and trend of college PE teaching evaluation [J]," *The Guide of Science & Education*, vol. 11, no. 12, p. 236, 2019.

[9] H. Z. Xu and Y. J. Zhao, "Tasks and measures of physical education reform in colleges and universities in China in the new era," vol. 3, no. 3, pp. 98–103, 2022.

[10] X. Q. Hu and Y. Tang, "PE examination in the senior high school entrance examination: functions, problems and solutions [J]," *Journal of Beijing Sport University*, vol. 44, no. 93, pp. 67–75, 2021.

[11] Y. L. Wei and B. F. Shi, "Research on the cultivation of entrepreneurial ability of university students in minority areas under participatory Teaching [J]," *Education and Vocation*, vol. 18, no. 10, pp. 89–93, 2018.

[12] M. G. Lu and P. J. Shi, "Research on interdisciplinary practice teaching based on campus ecological environment resources: a case study of biology and geography in senior high school [J]," *Journal of Teaching and Management*, vol. 12, no. 3, pp. 62–65, 2019.

[13] M. Zakarya, I. Ur Rahman, and A. A. Khan, "Energy crisis, global warming & IT industry: can the IT professionals make it better some day? A review," in *Proceedings of the International Conference on Emerging Technologies*, IEEE, Islamabad, Pakistan, 2012.

[14] Y. Zhang, "Research on strategies of promoting ideological and political education through experimental teaching [J]," *Experimental Technology and Management*, vol. 34, no. 10, pp. 174-175, 2017.

[15] J. Wang, "Analysis of physical education quality evaluation model in colleges and universities based on big data analysis," in *Proceedings of the The International Conference on Cyber Security Intelligence and Analytics*, Springer, Haikou, China, 2020.

[16] X. W. Ding and K. Li, "Self-shaping of teachers in the new era of ideological and political lessons [J]," *Ideology and Politics Teaching*, vol. 8, no. 8, pp. 87–90, 2019.

[17] Y. Zhou, "Construction and application of college English multiple intelligence teaching model based on internet of things," *Mathematical Problems in Engineering*, vol. 2022, 2022.

[18] K. Wijekumar, B. J. Meyer, P. Lei, A. L. Beerwinkle, and M. Joshi, "Supplementing teacher knowledge using web-based Intelligent Tutoring System for the Text Structure Strategy to improve content area reading comprehension with fourth- and fifth-grade struggling readers," *Dyslexia*, vol. 26, no. 2, pp. 120–136, 2020.

[19] Z. Chen and Q. Chen, "Optimization of teaching evaluation system for football professional teachers based on multi-evaluation model," *Complexity*, vol. 2021, 2021.

[20] N. Feng and J. Liu, "Exploration on integrating mathematical games with classroom teaching based on multiple intelligence theory [J]," *Research in Teaching*, vol. 41, no. 5, pp. 27-28, 2019.

[21] M. Wang, "Design of college physical education teaching system based on artificial intelligence technology," *Journal of Physics: Conference Series*, vol. 1852, 2021.

[22] Z. C. Ren, A. Chen, and X. Zhao, "Strengthen mathematical reading ability test to show the foundation of logical thinking [J]," *Bulletin des Sciences Mathematics*, vol. 57, no. 7, pp. 8–13, 2018.

[23] A. A. Khan, "HeporCloud: an energy and performance efficient resource orchestrator for hybrid heterogeneous cloud computing environments," *Journal of Network and Computer Applications*, vol. 173, p. 102869, 2021.

[24] S. Abbas, Q. Nasir, D. Nouichi et al., "Improving security of the Internet of Things via RF fingerprinting based device identification system," *Neural Computing & Applications*, vol. 33, no. 21, pp. 14753–14769, 2021.

[25] A. Khurshid, A. N. Khan, F. G. Khan, M. Ali, J. Shuja, and A. u. R. Khan, "Secure-CamFlow: a device-oriented security model to assist information flow control systems in cloud environments for IoTs," *Concurrency and Computation: Practice and Experience*, vol. 31, no. 8, p. e4729, 2019.

[26] F. Li and Y. J. Chen, "Design and simulation of online mathematics course intelligent matching algorithm based on fuzzy clustering [J]," *Modern Electronics Technique*, vol. 44, no. 16, pp. 125–128, 2021.

[27] B. Q. Lv, J. J. Zhang, and Z. P. Li, "Fuzzy partical swarm optimization based on filled function and transformation function [J]," *Acta Automatica Sinica*, vol. 44, no. 1, pp. 74–86, 2018.

[28] L.-E. Díaz-Posada, S.-P. Varela-Londoño, and L.-P. Rodríguez-Burgos, "Multiple intelligences and curriculum implementation: progress, trends and opportunities," *Revista de Psicodidáctica*, vol. 22, pp. 69–83, 2017.

[29] Z. Yangsheng, "An AI based design of student performance prediction and evaluation system in college physical education," *Journal of Intelligent and Fuzzy Systems*, vol. 40, no. 2, pp. 3271–3279, 2021.

[30] G. J. Li, "Research on teacher literacy based on cultivating students' higher order thinking ability [J]," *Theory and Practice of Education*, vol. 41, no. 26, pp. 40–43, 2021.

Hindawi
Scientific Programming
Volume 2022, Article ID 6152558, 13 pages
https://doi.org/10.1155/2022/6152558

Research Article

Application of Digital 3D Printing Technology in Ceramic Art Creation

Mian Wang, Xinyu Zhao, and Dan Sun

Lu Xun Academy of Fine Arts, Shenyang 110004, Liaoning, China

Correspondence should be addressed to Dan Sun; sundan@lumei.edu.cn

Received 25 February 2022; Revised 5 April 2022; Accepted 11 April 2022; Published 21 April 2022

Academic Editor: Muhammad Usman

3D printing technology is a modern technical means and process based on three-dimensional molding, digital manufacturing, reverse engineering, and other emerging fields. 3D printing ceramics is one of the diversified designs of modern ceramics. At the same time, with the development of 5G technology, the platform access method will make 3D printing easier and more common. The purpose of this paper is to study the printing, preparation, and sintering processes of ceramic materials based on 3D printing technology and realize the rapid prototyping of ceramic parts, which can meet the requirements of low-cost, single-piece, and small-batch processing. This paper proposes to focus on the research on materials, design methods, and technological processes suitable for ceramic 3D printing technology from the perspective of the integration of art and science. By using 3D printing technology to perform geometric functions, mixing, recombination, and other cutting-edge tasks, the composite design of works is enhanced. The experimental results show that in the high temperature sintering stage, 1600°C is the holding temperature, the heating rate is 0.5°C/min, and the holding time is 600 min, and the sintering effect of ceramic parts is better. The measured shrinkage rate of the ceramic sample does not exceed 16%, the porosity is 47%, the bulk density is 2.27 g/cm^3, and the density is 53.2%. The results show that the ceramic parts prepared by this process can meet the basic performance requirements.

1. Introduction

As an engineering material, the history of ceramics can be traced back to BC. People mixed clay, sand, and water, kneaded them into specific shapes, and fired them to obtain original ceramic products. After the Industrial Revolution, ceramic materials began to be used in electric power, machinery, and other fields because of their excellent insulation and heat insulation. Since the 20th century, with the emergence of special ceramics, piezoelectric ceramics, and bioceramics, ceramic materials have become another popular material after metals and polymer materials. They are widely used in machinery, aerospace, medicine, electronics, and many other fields. The traditional production process of ceramics is divided into three stages: batching, molding, and firing. In the molding process, injection molding and rolling are the main methods. These two methods require high-precision molds to assist ceramic molding, and the processing of the mold itself is very complicated. This leads to a long production cycle, low production efficiency, and a low yield of traditional ceramics. In addition, due to the existence of the mold, it cannot achieve low-cost, single-piece, and small-batch processing, and it is difficult to meet the processing requirements of modern ceramics.

The 3D printing technology developed in recent years is different from the method of "subtraction" used in the traditional processing technology. Instead, it starts from nothing and uses the form of adding materials to accumulate objects layer by layer. The processing speed is fast, and the production cost is low. For processing parts with complex structures, such as hollowing out and complex heterosexual structures, 3D printing technology is far superior to traditional processing techniques. Therefore, using 3D printing technology to process ceramic materials can not only solve the problem of the long processing cycle of ceramic products but also use its technical characteristics to produce special structural ceramics that cannot be obtained by traditional processing technology. It has broad market application prospects and practical value.

The innovations of this paper are as follows: (1) This paper analyzes and compares different surface-forming

processes. Based on the constrained liquid surface method, this paper designs and builds a prototype of surface molding ceramic printing, which solves the problem of coating and printing high-viscosity ceramic paste. At the same time, this paper completes the construction and debugging of the control system of the experimental prototype and uses photosensitive resin for printing tests. (2) In this paper, the sintering temperature curve suitable for ceramic parts is given, and the changes in the components of ceramic parts during the sintering process are analyzed. The influence of sintering temperature on the density and sintering shrinkage of the parts is analyzed, and finally, ceramic parts that can meet the basic performance requirements are obtained.

2. Related Work

Bone has a strong self-healing ability, but bone defects that exceed a certain critical size will not heal themselves and require intervention to achieve complete healing. Mishra A characterized the material properties of 3D-printed apatite scaffolds, which were then tested by in situ implantation of horse tubers in vivo for 6 months [1]. While this type of implant has been extensively tested in vitro, there are limited in vivo data and even fewer in relevant large animal models. Sing et al. aimed to review additive manufacturing processes for ceramic materials, focusing on the partial and complete melting of ceramic powders by high-energy laser beams without the use of binders. They first introduced selective laser sintering or melting (SLS/SLM) technology. They then analyzed the results of silica (SiO2), zirconia (ZrO2), and ceramic-reinforced metal matrix composites processed by direct laser sintering and fusion. In the current state of technology, it remains a challenge for them to directly use SLS/SLM to fabricate dense ceramic components. They discussed the key challenges encountered in the direct laser melting of ceramics. They include the deposition of ceramic powder layers, the interaction between the laser and powder particles, the dynamic melting and consolidation mechanisms of the process, and the presence of residual stresses in ceramics processed by SLS/SLM [2]. Despite the challenges, SLS/SLM has potential in ceramic manufacturing. Today, 3D printing with ceramics is a promising direction for the development of additive technology. Dolgin et al. developed an alumina- and wax-based ceramic paste printing technique. They modeled and manufactured a ceramic paste printing extruder, selected the composition of the paste, made a paste for printing, and sintered it. It measured the sintering parameters and physical and mechanical properties of the product and used a scanning electron microscope to study the microstructure of the printed product [3]. The purpose of Rolling's study was to examine the perceptions of wearable accessory designers using 3D printing (3DP) technology. He conducted 16 semistructured interviews with 3DP wearable accessory designers around the world. The findings show that 3DP is easier than traditional production methods. Plastics are the easiest materials to print on, while steel and ceramics are harder to print. His research supported learning-friendly 3DP educational programs, software programs, and materials, educational resources needed in materials, and the creation of affordable higher quality printers [4]. Yang et al. introduced the preparation method, development status, and application fields of ceramic 3D printing. They reviewed recent advances in direct 3D printing and stereolithography of oxide (Al2O3, ZrO2) and nonoxide (Si3N4, SiC) ceramic suspensions. He demonstrated the influence of the molding method on the properties of ceramics and gave an outlook on the development of 3D printing [5]. Xlabc et al. synthesized a UV-curable ZrO2-Al2O3 composite ceramic slurry based on SLA-3D printing technology and 3D printed the corresponding ceramic green body. He finally made ZrO2-Al2O3 composite ceramic parts through subsequent degreasing processes. At a sintering temperature of 1500°C and a holding time of 60 min, the actual density, hardness, and fracture toughness of the ceramics can reach 3.75 g/cm, 14.1 GPa, and 4.05 MPam1/2, respectively [6]. However, when the sintering temperature is lower than 1500°C, the lower driving force makes the grains not fully developed, resulting in low ceramic density and poor mechanical properties.

3. 3D Printing Technology

3D printing technology is a product of this digital age, and the application of this technology has brought new fields to the entire manufacturing industry. It has accurate and efficient molding efficiency, and it can also print shapes that are difficult to achieve in traditional manufacturing through layered accumulation [7]. 3D printing application areas are shown in Figure 1.

As shown in Figure 1, 3D printing has emerged in the fields of medical applications, architectural design, parts printing, toys and animation, daily necessities, and the automotive industry. Therefore, using 3D printing technology to process ceramic materials can not only solve the problem of the long processing cycle of ceramic products but also use its technical characteristics to produce special structural ceramics that cannot be obtained by traditional processing technology. It has broad market application prospects and practical value.

3.1. Process of 3D Printing Ceramics. The whole process of ceramic 3D printing is mainly divided into two stages. The first stage is the model preparation and slicing computer-aided design stage. The second stage is the process of 3D printer printing and ceramic firing. Figure 2 shows the flow of the 3D ceramic printing process.

As can be seen from Figure 2, after considering the characteristics of 3D printing technology, the appearance of the final work was determined, and 3DsMAX was used for 3D digital modeling to adjust and control the "triangular face value" of the 3D model. By printing with a 3D printer, it fixes parameter errors during the printing process and performs post-surface treatment and glazing on the printed works.

3.1.1. Preparation of the Printer before Modeling and Printing. Import the model file processed by slicing into the printer, and then start the preparation before the printer

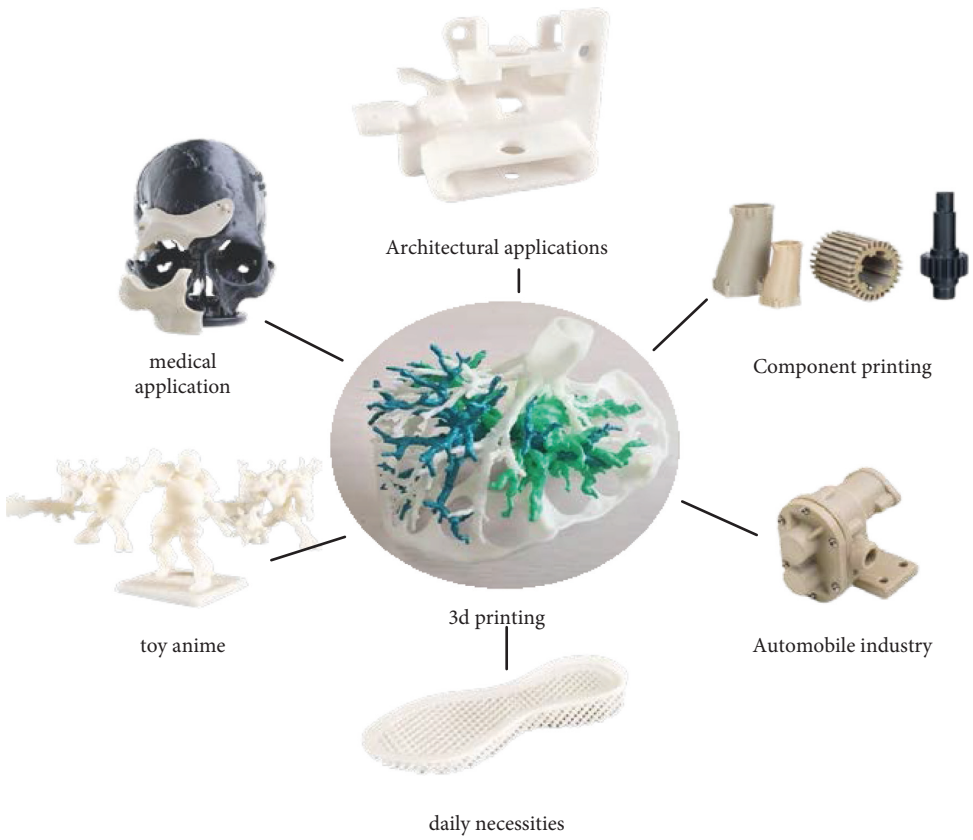

Figure 1: 3D printing application fields.

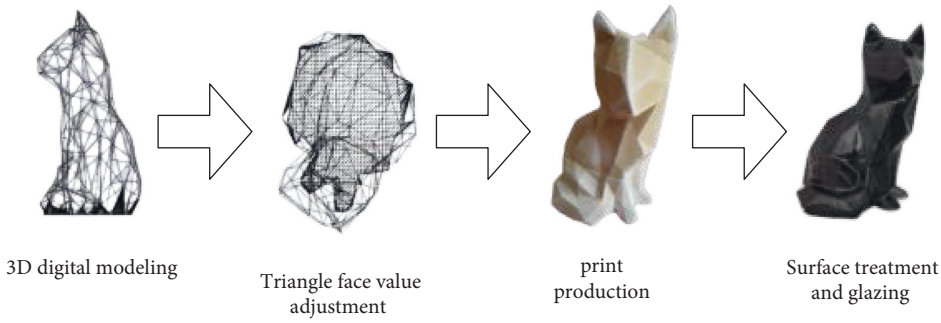

Figure 2: 3D printing ceramic process flow.

prints; then load the vacuum mud, adjust the air pressure, and push the mud into the extruder. The gas pressure is related to the pipe length of the mud-conveying material. The longer the mud pipe, the stronger the thrust required to push the mud material, and the higher the pressure. The adjustment range is 0.3 kpa–0.7 kap [8]. The pushing air pressure has a great influence on ceramic 3D printing. When the pressure is low and the thrust is insufficient, the extruded mud will obviously be broken, which will affect the printing. When the pressure is too high, the extruded mud flow will increase, which will affect the accuracy of ceramic modeling and printing and will cause certain damage to the interface parts of the printer. The air pressure used in all experiments in this paper was 0.5 kPa. In this paper, a flat plate covered with plastic film is used as the plane of the printing model to facilitate the movement of the printed body. The ceramic body will shrink during the drying process, so the printed body will generate shrinkage force at the bottom surface of the body in contact with the plane. As a base for printing, lightweight, absorbent paper is used to fill ceramic shapes.

3.1.2. Ceramic Modeling 3D Printing Molding Process. Before the ceramic model starts printing, the printer extrusion head is automatically homed. It runs the print operation from the origin, which will print a circle of mud on the outside of the first layer of the shape, checking whether the air pressure is stable and whether the distance between the extrusion head and the printing platform is appropriate by observing the smooth process of mud discharge [9, 10].

Then the process of printing and forming is officially started. The printing at the bottom is carried out in such a way that the shape surrounds the inner line and fills the line between each layer. The filling direction is 90 degrees. The lowering of the printing platform is controlled by the rotation of the screw, and the circles of lines are arranged to rise up, thereby stacking into a three-dimensional shape. The printing parameters that can be adjusted during the printing process are the printing speed and the size of the mud flow. The speed adjustment is mainly used for accurate printing and height modeling. When the printing reaches a certain height, the shaking of the blank is reduced by reducing the printing speed so as to avoid the tipping of the blank [11]. The control of the mud flow is to control the density of the overall shape. During the filling and printing process of the bottom and the increase in the mud flow at the junction between the bottom and the side wall, the bottom can be more compact and less prone to cracking and deformation. When printing with delicate patterns, the mud flow can be slightly reduced, making the line patterns more uniform and clear.

3.1.3. Trimming and Firing of the Printed Body. The shape of ceramic 3D printing is a clay body, which needs to be turned into a ceramic product through a firing process. Because the green body is formed by superimposing layers of mud strips, the surface will form layers of horizontal textures. In order to make a ceramic shape with a smooth surface, the surface of the green body is polished with tools such as sponge sand after printing. It forms a ceramic product with a smooth surface after glazing and firing. In terms of the use of glazes, most of the glazes sold on the market can be applied to the green body formed by ceramic 3D printing [12, 13]. In terms of the firing process of the 3D printing green body, the interlayer strength of the ceramic green body formed by 3D printing is relatively low, and it is easy to cause the phenomenon of cooling and cold cracking when combined with the firing of the glaze. This problem can be solved by slow cooling during the cooling process. When firing a ceramic model with a filling structure inside, it is necessary to pay attention to making ventilation holes on the molding bottom plate to discharge the internal gas and to reduce the heating rate during the firing process to avoid the phenomenon of frying.

3.2. 3D Printing Algorithm. Taking the blank at the front end of the current 3D printing path as a unit body and taking q_x and q_{x+d_x} as the heat flow for importing and exporting the unit body, respectively, S_c is the term of convection loss, and S_1 is the term of heat conduction between the uncured slurry and the cured body after extrusion. Deduced according to the heat conduction process, the change in heat in the unit with time is shown as

$$\begin{aligned} d\frac{\partial p}{\partial t}d_x &= \left(q_x - q_{x+d_x}\right)l - S_c l d_x - S_1 l d_x \\ &= k\frac{\partial^2 T}{\partial x^2} l d_x - S_c l d_x - S_1 l d_x. \end{aligned} \tag{1}$$

Here, d is the density, P is the specific enthalpy, t is the time, and k is the thermal conductivity: T is the average temperature of the unit body section, and x is the nozzle coordinate during the 3D printing process [14]. From this formula, the governing formula of the unit body can be obtained, as shown in formulas (2)–(4):

$$d\frac{\partial p}{\partial t} = k\frac{\partial^2 T}{\partial x^2} l d_x - S_c - S_1, \tag{2}$$

$$S_c = \frac{h}{h_g}\left(T - T_\infty\right), \tag{3}$$

$$S_1 = \frac{K}{w^2}\left(T - T_{\text{neigh}}\right). \tag{4}$$

Here, h is the convective heat transfer coefficient, h_g is the height of the printing path, T is the temperature when the paste is extruded, T_∞ is the ambient temperature, w is the width of the unit body, and T_{neigh} is the temperature of the adjacent layer at the printing nozzle.

$$-k\frac{\partial t}{\partial n} = h\left(T - T_\infty\right). \tag{5}$$

In the formula, n is the normal vector of the nozzle position.

The model determines the temperature change in the green body with time at different positions along the stacking path during the 3D printing process, thereby judging the solidification of the green body [15]. The integral of the temperature difference between the slurry temperature and the freezing point over time is defined as the bonding potential so as to judge the bonding strength between the green layers:

$$O = \int_o^q \left(T_M - T_C\right)\mathrm{d}_t, \tag{6}$$

where O is the bonding potential, T_M is the temperature of the uncured slurry, T_C is the curing temperature value, t is the time, and q is the integral variable. The bonding potential takes into account both the effective bonding time (the time from extrusion to curing of the slurry) and the strength of molecular diffusion determined by the temperature difference. It is used to judge the bonding quality between layers in 3D printing. The larger the temperature difference, the stronger the bonding potential, and the stronger the bonding between the green bodies. The model has very important guiding significance for the preliminary determination of process parameters such as molding temperature [16]. In the experiment, the influence of temperature on the wettability between the layers of the green body was analyzed, and f_{wetting} (0~1) was used to represent the degree of wetting between the adjacent layers of the green body. Its calculation formula is

$$f_{\text{wetting}} = \frac{\mathrm{d}_B}{\mathrm{d}F}. \tag{7}$$

The contour offset is actually the parallel offset of the inner and outer contours of the model along different

directions. The key problem is how to realize the offset of the inner and outer contours to generate scan lines so that the 3D printer can rapidly manufacture [17, 18]. In actual production, this is very similar to tool interpolation in CNC machining. Tool interpolation is divided into two types: shortened and nonshortened.

In order to make this algorithm more universal, the temporary coordinate system xoy is taken, and the coordinate origin is at the intersection point V_i of the two line segments. Line segments $V_{i-1}V_i$ and V_iV_{i+1} are any two adjacent line segments on the contour ring [19]. $\overrightarrow{L_i}$ and $\overrightarrow{L_{i+1}}$ are the vector forms of $V_{i-1}V_i$ and V_iV_{i+1}. $\overrightarrow{l_i}$, and $\overrightarrow{l_{i+1}}$ are the unit vectors of $\overrightarrow{L_i}$ and $\overrightarrow{L_{i+1}}$ in the coordinate system xoy, respectively.

$$\begin{cases} \overrightarrow{l_i} = \alpha \overrightarrow{i} + \beta \overrightarrow{j}, \\ \overrightarrow{l_{i+1}} = \alpha_{i+1} \overrightarrow{i} + \beta_{i+1} \overrightarrow{j}, \end{cases} \tag{8}$$

where

$$\begin{aligned} \alpha_i &= \frac{x_i - x_{i-1}}{\sqrt{(x_i - x_{i-1})^2 + (y_i - y_{i-1})^2}}, \\ \beta_i &= \frac{y_i - y_{i-1}}{\sqrt{(x_i - x_{i-1})^2 + (y_i - y_{i-1})^2}}, \\ \alpha_{i+1} &= \frac{x_{i+1} - x_i}{\sqrt{(x_{i+1} - x_i)^2 + (y_{i+1} - y_i)^2}}, \\ \beta_{i+1} &= \frac{y_{i+1} - y_i}{\sqrt{(x_{i+1} - x_i)^2 + (y_{i+1} - y_i)^2}}. \end{aligned} \tag{9}$$

$V_{i-1}(x_{i-1}, y_{i-1})$, $V_i(x_i, y_i)$, and $V_{i+1}(x_{i+1}, y_{i+1})$ are the coordinates of V_{i-1}, V_i, and V_{i+1} in the original coordinate system XOY, respectively [20]. According to the definition of the direction of the contour ring, the straight line formula after the line segments $\overrightarrow{L_i}$ and $\overrightarrow{L_{i+1}}$ are offset by a D value can be obtained as

$$\begin{cases} -\beta_i x + \alpha_i y = -D, \\ -\beta_{i+1} x + \alpha_{i+1} y = -D. \end{cases} \tag{10}$$

Because the straight lines L_i' and L_{i+1}' are not parallel (otherwise, L_i' and L_{i+1}' are on the same straight line), solving formula (10) with $\alpha_i\beta_{i+1} - \alpha_{i+1}\beta_i \neq 0$ can obtain the coordinate value of the new intersection in the coordinate system xoy after the two line segments are offset:

$$\begin{cases} x = \dfrac{(\alpha_{i+1} - \alpha_i)D}{\begin{vmatrix} \alpha_i & \beta_i \\ \alpha_{i+1} & \beta_{i+1} \end{vmatrix}}, \\ y = \dfrac{(\beta_{i+1} - \beta_i)D}{\begin{vmatrix} \alpha_i & \beta_i \\ \alpha_{i+1} & \beta_{i+1} \end{vmatrix}}. \end{cases} \tag{11}$$

Transforming it to the original coordinate system XOY can get the coordinate value of the new intersection:

$$\begin{cases} X = x_i + x, \\ Y = y_i + y. \end{cases} \tag{12}$$

In this way, by calculating the new intersection points of each adjacent line segment in the contour ring after offset one by one, the shape and position of the offset contour ring can be determined, and the contour offset filling line can be formed. The new intersection coordinates of the line and the arc are

$$\begin{cases} x = \alpha_i(\alpha_i x_0 + \beta_i y_0) - r\beta_i + S\alpha_i\sqrt{(R+r)^2 - (\alpha_i y_0 - \beta_i x_0 - r)^2}, \\ y = \beta_i(\alpha_i x_0 + \beta_i y_0) + r\alpha_i + S\beta_i\sqrt{(R+r)^2 - (\alpha_i y_0 - \beta_i x_0 - r)^2}, \end{cases} \tag{13}$$

where r is the tool radius, (x_0, y_0) is the center coordinate of the arc, and R is the arc radius. Here, $s = -\text{sign}(\alpha_i x_0, \beta_i y_0)$, and the intersection point can be obtained by substituting S into formula (13).

The photocuring performance of ceramic paste refers to the curing ability after being exposed to light [21]. For pure photosensitive resin, its photocuring performance includes two indicators: curing depth and curing reaction critical energy (light intensity); the relationship between the two is shown in formula (14):

The photosensitive resin curing thickness formula is

$$C_d = D_p \ln \frac{E}{E_c}. \tag{14}$$

Here, C_d is the curing depth, E is the incident light intensity of the light projected by the projector, E_c is the critical light intensity when the resin undergoes a curing reaction, and D_p is the projection depth coefficient, a decimal, which is a characteristic of the photosensitive resin itself [22]. When the photosensitive resin is cured by specific light irradiation, the oligomer in the photosensitive resin absorbs the energy of photons and undergoes a photocuring chemical reaction. The photocuring process follows the basic law of photochemical reaction, as shown in the formula:

$$I = I_0 e^{-kl}. \tag{15}$$

Formula (15) shows that the light intensity decreases exponentially with the transmission depth. For the ceramic slurry, when the light irradiates the ceramic powder, reflection and refraction will occur. It also needs to take into account the effect of ceramic particles on light, so the formula is corrected for light, and the scattering formula of the ceramic slurry can be obtained as shown in the following formula:

$$D_p = \frac{2d_{50}}{3\widetilde{Q}} * \frac{n_0^2}{\Delta n^2}. \tag{16}$$

Here, d_{50} is the average particle size of the ceramic powder; Δn is the difference between the refractive index n_p of the ceramic powder and the refractive index n_0 of the

photosensitive resin, a decimal; $\widetilde{Q}$ is the scattering coefficient, a decimal, depending on the solid content of the slurry and the wavelength of the light.

4. Design and Construction of Experimental Platform for 3D Printing Ceramic Technology

4.1. 3D Printing Processing Technology

4.1.1. Principle of 3D Printing. Surface molding 3D printing is to project the sliced image of the model to be printed on the surface of the photosensitive resin in the form of a mask through optical equipment such as a projector. The photosensitive resin in the image is cured by irradiation, thereby achieving selective molding of the cured layer. The object slice images are projected, cured, and finally stacked into printed parts.

4.1.2. Classification of 3D Printing Processing Technology. According to the positional relationship between the light source and the printing surface, the surface molding 3D printing process can be divided into the upper projection ceremony surface molding process and the lower projection ceremony surface molding process. The structure of the upper projection ceremony surface molding equipment is shown in Figure 3.

As shown in Figure 3, the working cycle of the upper projection ceremony surface forming process is generally divided into four processes:

(1) Use the modeling software to draw the model of the part to be printed.

(2) Using slicing software, slice the model to obtain the slice pattern of the model.

(3) When the projector is working, the mask pattern of the printed part is projected onto the surface of the photosensitive resin. At this time, the resin of the printing base is cured, formed, and adhered to the printing base.

(4) The Z-axis sliding table moves down and moves a distance of a layer thickness. After the resin liquid level is leveled, the projector is turned on again, and the resin between the cured layer and the liquid surface is cured under the projection of the next layer of the sliced image.

Since the projector is placed on the top, the resin liquid level is not restricted, so this technology is also called the free liquid surface process.

4.1.3. Forming Process of the Lower Projection Ceremony Surface. The bottom-mounted projection ceremony surface-forming equipment is similar to the top-mounted structure, except that the projector is located the processing plane, as shown in Figure 4.

It can be seen from Figure 4 that in the forming process of the lower projection ceremony surface, the projection light is irradiated from the resin disc. The photosensitive resin cured by light has only a part of the resin bound under the printing base, and the height of the cured resin is equal to the thickness of the printed layer. This technique is also called the constrained surface process. After printing a layer, the Z-axis slide moves up instead of moving down. Since the resin under the printing base is cured by light and adheres to the base, after printing a layer, the slide table moves up, allowing the resin to flow into the gap, and then a printing cycle can be completed.

4.1.4. Comparison of Two Surface-Forming Processes. In the top-mounted projection ceremony process, the sliding table is lowered by a distance of one layer thickness to ensure that the distance between the cured layer and the resin liquid surface is still one layer thickness at this time. In the underprojection ceremony process, the processed parts are adhered to the bottom of the printing base. Therefore, after the printing base moves upward for a certain distance, the descending distance should be one layer thickness less than the ascending distance to ensure that the distance between the processed layer and the bottom of the resin disc is one layer thickness.

4.2. Improvement of Surface-Forming Process Suitable for Ceramic Slurry. According to the comparison in the previous section, considering the particularity of the ceramic slurry, it is difficult to guarantee the accuracy of the cured layer if the overhead projection ceremony technique is used. In addition, the viscosity of the ceramic slurry is high, resulting in poor surface-processing quality and unsatisfactory printing effect. It adopts the lower projection ceremony surface forming process, and its structure needs to be improved to meet the printing requirements of high-viscosity paste.

4.2.1. Improvement of Bottom Glass of Resin Tank. When a layer of printing is completed, the printing base moves upward. Since the cured layer is tightly adhered to the glass at the bottom of the resin tank, it is difficult to separate the cured layer from the glass when lifting. In severe cases, it can also cause the resin tank to tilt, destroying the structure of the printer. Therefore, laying the Teflon film on the bottom glass of the resin tank can effectively reduce the separation resistance of the cured layer and the resin tank because of its low friction coefficient, good wear resistance, and no reaction with the resin, thereby protecting the bottom glass.

4.2.2. Improvement of the Separation Process between the Cured Part and the Resin Tank during Printing. In traditional printing equipment, after the resin is cured by light, the Z-axis slide is lifted. At this time, the cured layer is double-bonded by the upper printing base and the bottom surface of the resin tank, and it is difficult to ensure that each layer is firmly adhered, considering the separation of the printed part from the resin tank. The longitudinal adhesive separation force is much greater than the tangential adhesive

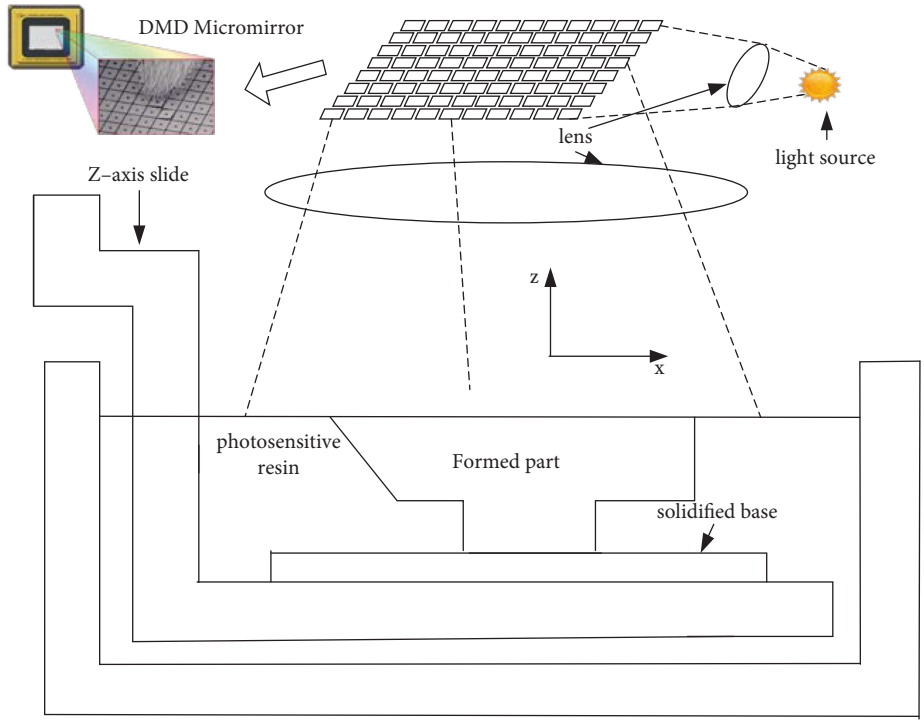

Figure 3: Top-mounted projection ceremony surface-forming equipment.

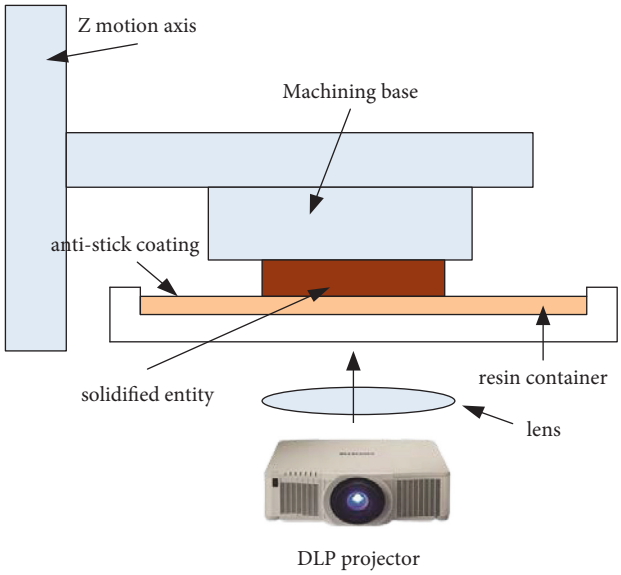

Figure 4: The lower projection ceremony surface-forming equipment.

separation force. The improved resin disk structure is shown in Figure 5.

As can be seen from Figure 5, the resin tank was changed into a disc shape, and semicircular PDMS (polydimethylsiloxane) was laid on one side. When the resin is cured, the resin disk is first rotated by 180° and then the *Z*-axis is moved upward. Due to the existence of the height difference, the cured layer will not be bonded by the glass. At this time, lifting the *Z*-axis slide table can ensure that the printed part is firmly adhered to the printing base. At the same time, during the spinning process, the resistance is greatly reduced due to the existence of the Teflon film, and the PDMS can also protect the plexiglass from impact.

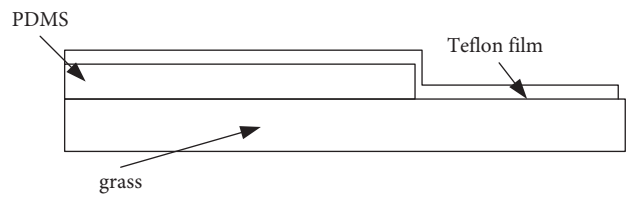

Figure 5: Schematic diagram of the improved resin disk structure.

4.3. Construction of Prototype 3D Printing of Ceramic Materials. The improved 3D printer model of ceramic material is divided into three parts: a hardware system, control system, and software system. The hardware system includes a resin disk-rotating device, *Z*-axis-lifting device, scraper-coating device, and projection device. The control system includes the control system of the lower computer of the printer. The software system includes printer control software and model slice software.

5. Rheological Properties and Dispersion of Silicon Carbide Ceramic Slurry

5.1. Effect of Carbon Black Content on Slurry Rheological Properties and Dispersion. In reactive sintering, carbon black acts as a carbon source to provide liquid silicon reaction sites that can fill voids in the green body. The amount of carbon black added will affect the structure and properties of the reaction sintered silicon carbide. Therefore, it is meaningful

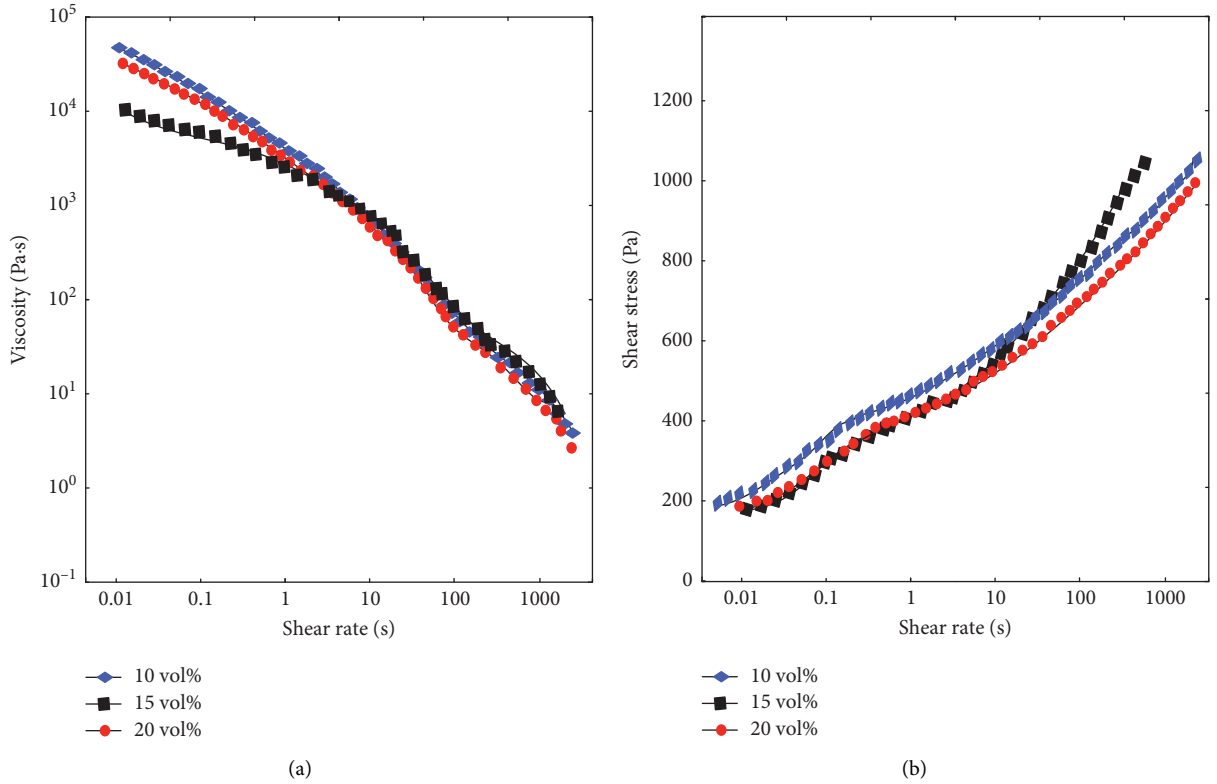

Figure 6: Shear rate of slurry under different carbon black contents. (a) Viscosity curve and (b) shear stress curve.

to study the effect of the amount of carbon black added on the paste direct-writing printing. The shear rates of the slurries with different carbon black contents are shown in Figure 6.

Figure 6 shows the shear rate–shear viscosity curves and shear rate–shear stress curves of slurries with different carbon black contents at shear rates of 0.01–1000 s when the chopped carbon fiber content is 20 vol %. It is not difficult to find that the slurry exhibits similar viscosity behavior under different carbon black contents; the viscosity decreases with the increase in the shear rate, and the shear stress gradually increases with the increase in the shear rate. It shows that the prepared slurries are all shear-thinning slurries. The reason for this phenomenon is that under the high shear rate of the slurry, the internal particles are driven by the shear force to move rapidly. The slurry is uniformly dispersed and has no large agglomeration, so the movement of the particles will not be hindered by each other. The figure shows that the difference in viscosity of the slurry with different carbon black contents is not obvious. When the shear rate is less than 10 s, the slurries with different carbon black contents maintain stable shear stress. When the shear rate is more than 10 s, the shear stress increases sharply, and the slurry with a carbon black content of 20 vol % exhibits the lowest shear rate. The reason for this phenomenon may be that the binder is not completely wrapped on the surface of the ceramic powder and carbon black, but the introduction of carbon black has a certain lubricating effect. The viscoelasticity of the slurry with different carbon black contents was further studied; the amplitude sweep test was carried out at a frequency of 1 Hz, and the curve of shear stress modulus and its corresponding shear stress were obtained as shown in Figure 7.

From Figure 7, it can be found that under low shear stress, the slurries with different carbon black contents all exhibit a distinct linear viscoelastic region. With the increase in shear stress, the slurry appeared shear-thinning. The slurry with a carbon black content of 20 vol % first reached the flow point under a shear stress of 25 Pa, and the slurry was transformed from a colloid to a fluid state. The slurry with 15 vol % carbon black content has the highest initial modulus, and the slurry with 10 vol % and 15 vol % carbon black content shows similar flow points, where the shear stress is about 44 Pa. This means that the slurry with high carbon black content requires less extrusion pressure during the direct writing process, making it easier to achieve extrusion of the slurry. The uniform dispersion of the silicon carbide ceramic composite slurry can reduce the extrusion pressure during the direct writing process of the slurry. The microscopic morphologies of the slurries with different carbon black contents after drying are shown in Figure 8.

It can be seen from Figure 8 that the silicon carbide powder has a weak agglomeration and the chopped carbon fibers are distributed evenly, which avoids the needle clogging caused by the agglomeration of the chopped carbon fibers during extrusion.

5.2. Preparation Technology of Ceramic Slurry. First, the vertical printing base is raised, and the ceramic slurry to be tested is poured into the resin tray; the printer resin tray is

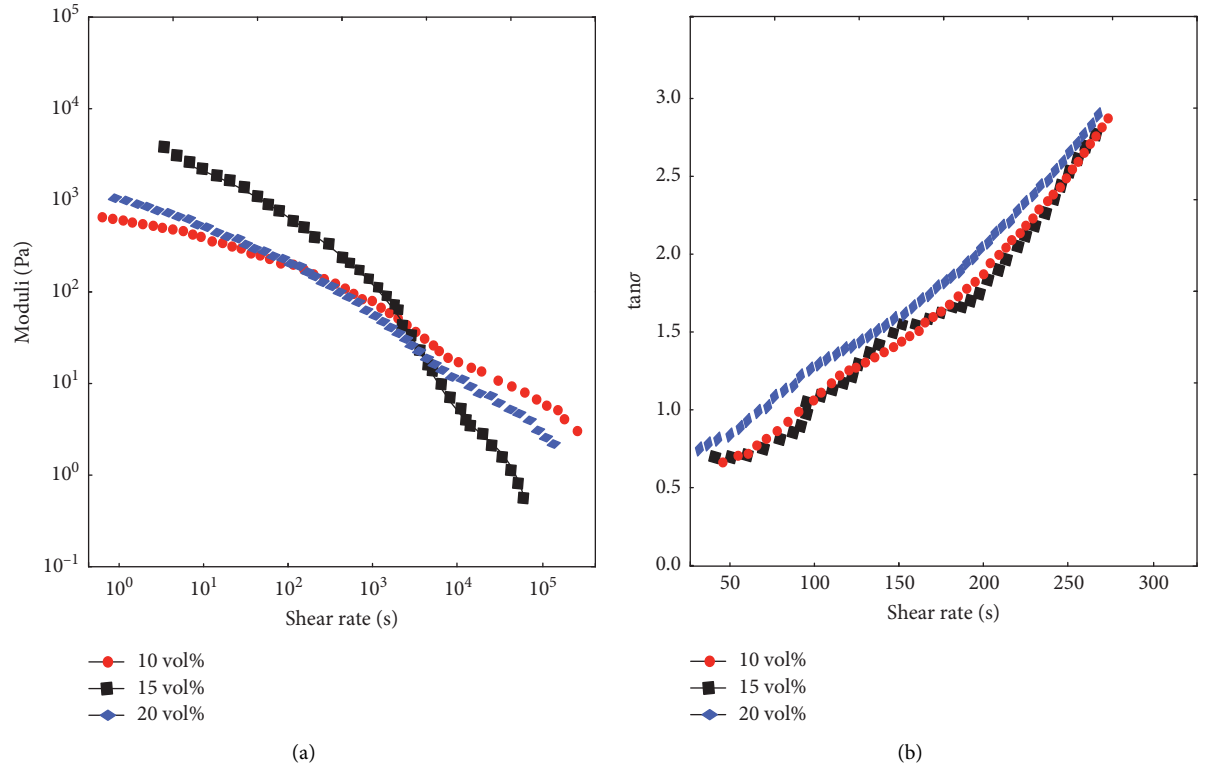

Figure 7: Shear stress of slurries with different carbon black contents. (a) Modulus curve and (b) loss factor curve.

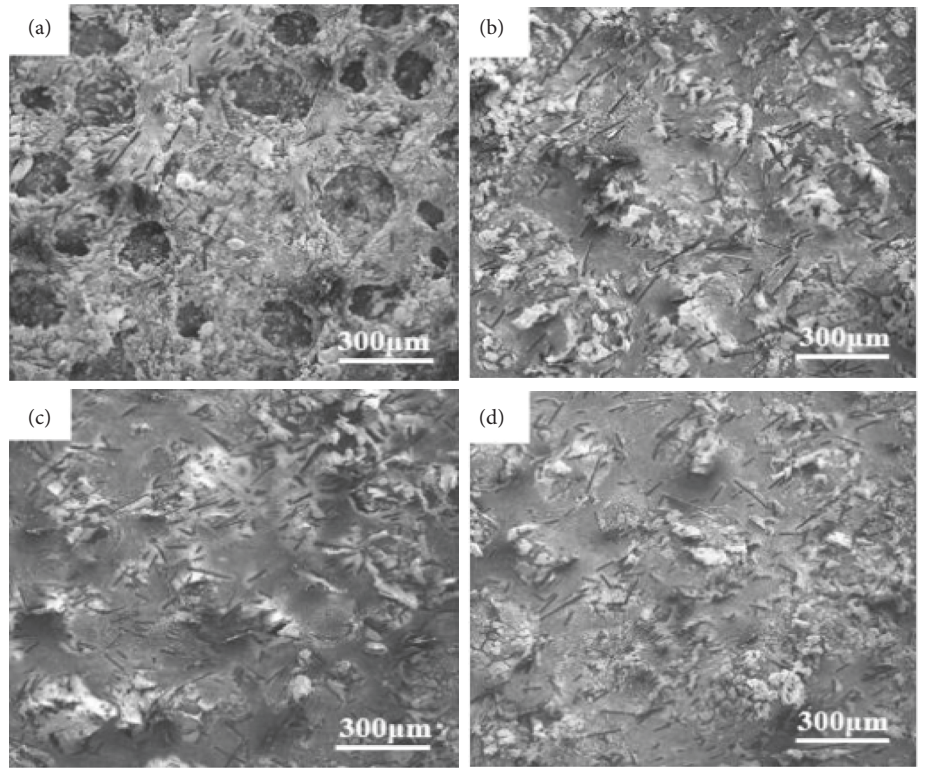

Figure 8: Dispersion morphologies of dry slurries with different carbon black contents. (a) 0 vol %; (b) 10 vol %; (c) 15 vol %; (d) 20 vol %.

turned on, which uses a scraper to smooth the slurry; the projector is turned on, a 10×10 mm square pattern is projected, the exposure time is set to 10 s, and then a screw micrometer is used to measure the cured layer thickness of each paste. The statistics are shown in Table 1.

It can be seen from Table 1 that for alumina ceramic slurry, when the solid phase content is the same, the smaller the powder particle size, the smaller the solidification depth. When the particle size of the powder is the same, the lower the solid content, the greater the solidification depth. According to the curing depth of the ceramic paste, it can guide the selection of printing layer thickness when printing ceramic parts. It can increase the printing speed by appropriately increasing the printing layer thickness. When the layer thickness cannot exceed the maximum curing depth of the paste, appropriately reducing the printing layer thickness can improve the printing quality, but the printing is slower. In addition, the layer thickness is set too low, and the precision of the lead screw of the vertical slide table is difficult to guarantee.

Since the photosensitive resin is a mixture, the specific decomposition temperature cannot be determined, so different degreasing temperature sections are set for degreasing experiments. The square ceramic green body obtained in the step is the experimental object. The parameters of the part degreasing and sintering stage are shown in Table 2.

As can be seen from Table 2, starting from room temperature, the temperature is heated to 300°C at a rate of 1°C/min and incubated for 120 min. The temperature was raised to 500°C at a rate of 1°C/min and maintained for 120 min. The temperature was raised to 800°C at a rate of 19°C/min and maintained for 120 min. The temperature was raised to 1000°C at a rate of 1°C/min, and the temperature was maintained for 120 min. During the cooling stage, the temperature was cooled to room temperature at 2°C/min, and the size and quality of the ceramic parts after sintering at different degreasing temperatures were measured. The ceramic parts obtained by degreasing and high temperature sintering were measured. Various parameters need to be measured and calculated to judge the printing and sintering effect. The firing shrinkage of ceramic parts in three directions at different sintering temperatures is calculated as shown in Table 3.

It can be seen from Table 3 that with the increase in sintering temperature, the firing shrinkage of ceramic parts increases gradually. The reason is that the sintering driving force required for sintering ceramic parts is the surface-free energy of alumina particles. The higher the sintering temperature, the higher the sintering degree, and the greater the firing shrinkage of the ceramic. At a sintering temperature of 1600°C, the alumina square sample with a solid content of 60% has a shrinkage rate of 15% to 16% in three directions. In addition, there is little difference in each direction, and it can be considered that the interior of the part is completely sintered and isotropic. In the high temperature sintering stage, 1600°C is the holding temperature, the heating rate is 0.5°C/min, and the holding time is 600 min. The sintering effect of ceramic parts is better. The measured shrinkage rate of the ceramic sample does not exceed 16%, the porosity is 47%, the bulk density is 2.27 g/cm^3, and the density is 53.2%. The results show that the ceramic parts prepared by this process can meet the basic performance requirements.

Table 1: The curing depth of ceramic slurry with different solid contents.

Solid phase content (%)	Particle size	Curing depth (mm)
50	5 pum	0.811
50	1 μum	0.772
50	50 nm	0.546
50	10 nm	0.293
60	5 μum	0.764
60	1 μum	0.603
60	50 nm	0.376

Table 2: Parameters of part degreasing and sintering stage.

Temperature (°C)	Length (L/mm)	Width (W/mm)	Width (W/mm)	Width (W/mm)
20	25.17	25.03	5.05	2.63
300	25.15	25.00	5.02	2.61
500	25.08	24.98	4.82	2.41
800	24.97	24.91	4.76	1.51
1000	24.96	24.91	4.76	1.49

Table 3: Sintering shrinkage of ceramic parts at different sintering temperatures.

Sintering temperature (C)	Firing shrinkage (%)		
	X	*Y*	*Z*
1400	7.9	7.6	7.7
1500	12.6	12.3	13.1
1600	15.8	15.7	16.1

5.3. Influence of Chopped Carbon Fiber Content on the Rheological Properties and Dispersion of the Slurry. Figure 9 shows the shear rate–viscosity curve and shear rate–shear stress curve of the silicon carbide ceramic slurry with different contents of chopped carbon fibers at a shear rate of 0.01–1000 s.

It can be seen from Figure 9 that within the test range, after adding chopped carbon fibers with different contents, the silicon carbide ceramic slurry showed a state of shear thinning. As the shear rate increases, the shear stress of the slurry first increases and then decreases. The viscosity of the slurry decreased gradually with the increase in the amount of chopped carbon fiber added; the viscosity with 20 vol % chopped carbon fiber content was the smallest, and the decrease in the viscosity increased. This is due to the gradual decrease in the binder on the individual chopped carbon fibers in the package as the content of chopped carbon fibers increases. The chopped carbon fibers provide more voids for the ceramic particles in the slurry, resulting in a reduced spacing between particles. The intermolecular attraction is weakened, which makes the slurry more prone to slipping of chopped carbon fibers under the action of shearing force. Therefore, the viscosity reduction in the pulp with high

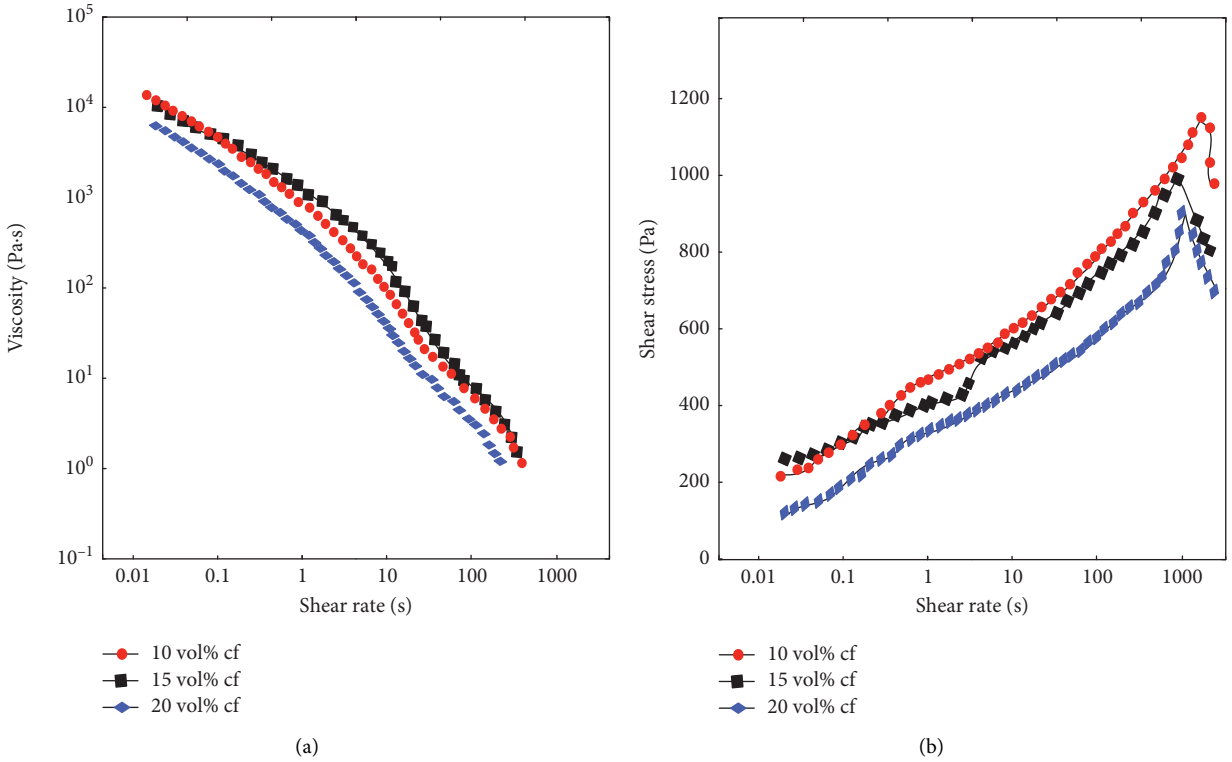

Figure 9: Shear rate under different Cr contents. (a) Viscosity curve and (b) shear stress curve.

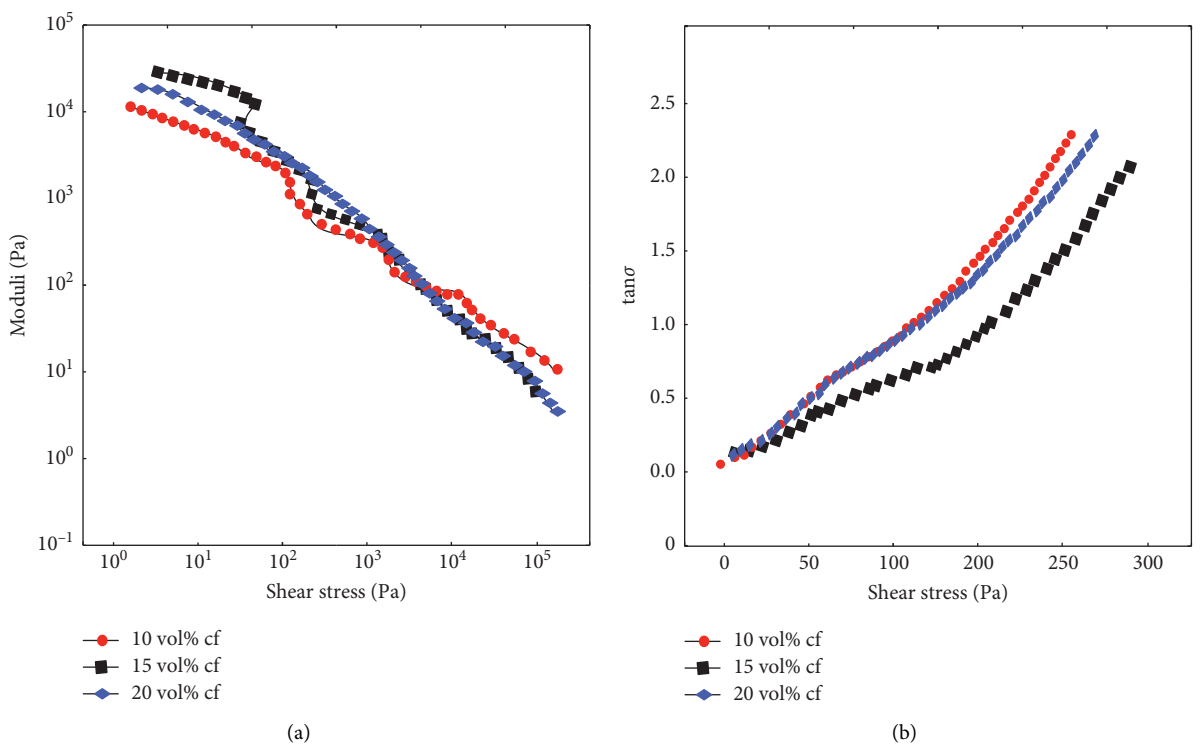

Figure 10: Shear stress under different Cr contents. (a) Modulus curve and (b) loss factor curve.

chopped carbon fiber content is larger. Figure 10 shows the shear stress–modulus curves and shear stress–loss factor curves of SiC ceramic slurries with different chopped carbon fiber contents after scanning at a frequency of 1 Hz.

Figure 10 shows the viscoelastic region's gel–fluid transition characteristics of shear-thinning fluids. Without the addition of chopped carbon fibers, the pulp exhibited the highest storage and dissipation modulus. With the increase in chopped carbon fiber content, the yield stress value of the pulp decreases, and the tanδ value also tends to increase under the same shear stress. This indicates that pulp with high chopped carbon fiber content has a lower modulus and is more prone to gel–fluid transition. Because the chopped carbon fiber has a high aspect ratio, the binder is difficult to wrap around the surface of the fiber, and the bonding effect is weak. The weakening of the coating effect of the binder on the surface of the chopped carbon fibers and the "bridging" effect of the short fibers themselves in the slurry make the chopped carbon fibers more prone to random shear slip under high shear stress.

6. Conclusion

Using 3D printing technology to process ceramic materials has advantages that are difficult to compare with traditional ceramic processing methods. It has fast processing speed and high forming precision and can realize manufacturing complex structural ceramic parts and the mass production of nonstandard parts. It has great practical value in the current application of ceramic materials. This paper focuses on the research on the processing technology of ceramic materials based on surface forming 3D printing technology. It mainly includes the research on the surface molding 3D printing process, the research on the preparation process of ceramic slurry suitable for surface molding 3D printing technology, and the research on the ceramic green body printing and sintering process. At present, the sintering degree is judged by the quality, size, and surface state of the sintered sample, and the sintering state can be accurately judged by observing the internal microscopic electron microscope image of the sample; in addition, the sintering process curve can be further optimized.

Data Availability

No data were used to support this study.

Conflicts of Interest

There are no potential competing interests in our paper. All authors have reviewed the article and have approved submission to your journal.

References

[1] A. Mishra and V. Srivastava, "Biomaterials and 3D printing techniques used in the medical field[J]," *Journal of Medical Engineering & Technology*, vol. 45, no. 4, pp. 1–13, 2021.

[2] S. L. Sing, W. Y. Yeong, F. E. Wiria et al., "Direct selective laser sintering and melting of ceramics: a review," *Rapid Prototyping Journal*, vol. 23, no. 3, pp. 611–623, 2017.

[3] A. S. Dolgin, A. I. Makogon, and S. P. Bogdanov, "Development of 3D printing technology with ceramic paste and study of properties of printed corundum products," *Materials Science Forum*, vol. 1040, pp. 178–184, 2021.

[4] V. Rolling, "Wearable accessory designers' perceptions using 3D printing technology," *International Journal of Fashion Design Technology and Education*, vol. 3, no. 1, pp. 1–9, 2021.

[5] M. M. Yang, X. D. Luo, and Z. P. Xie, "Review of 3D printing technology of ceramic," *Rengong Jingti Xuebao/Journal of Synthetic Crystals*, vol. 46, no. 1, pp. 183–186, 2017.

[6] D. Xlabc, D. Bzabc, D. Hxabc, and C. Huang, "The preparation of ZrO 2 -Al 2 O 3 composite ceramic by SLA-3D printing and sintering processing," *Ceramics International*, vol. 46, no. 1, pp. 937–944, 2020.

[7] T. Chittenden, "Printed pots and computerized coils: the place of 3D printing in ceramic practice," *Craft Research*, vol. 9, no. 1, pp. 9–40, 2018.

[8] M. K. Romanov and L. I. Zhuravleva, "Analysis of the technological and economic expediency of using additive technologies in manufacturing ceramic parts," *Glass and Ceramics*, vol. 76, no. 9-10, pp. 328–333, 2020.

[9] H. Shao, J. He, T. Lin, Z. Zhang, Y. Zhang, and S. Liu, "3D gel-printing of hydroxyapatite scaffold for bone tissue engineering," *Ceramics International*, vol. 45, no. 1, pp. 1163–1170, 2019.

[10] J. Zhang, L. Wei, X. Meng, F. Yu, N. Yang, and S. Liu, "Digital light processing-stereolithography three-dimensional printing of yttria-stabilized zirconia," *Ceramics International*, vol. 46, no. 7, pp. 8745–8753, 2020.

[11] G. S. Shin, H. K. Kweon, Y. G. Kang, and W. T. Oh, "Ceramic direct rapid tooling with FDM 3D printing technology," *The Korean Society of Manufacturing Process Engineers*, vol. 18, no. 7, pp. 83–89, 2019.

[12] A. Fleisher, D. Zolotaryov, A. Kovalevsky et al., "Reaction bonding of silicon carbides by Binder Jet 3D-Printing, phenolic resin binder impregnation and capillary liquid silicon infiltration," *Ceramics International*, vol. 45, no. 14, pp. 18023–18029, 2019.

[13] N. Shahrubudin, T. C. Lee, and R. Ramlan, "An overview of critical success factors for implementing 3D printing technology in manufacturing firms," *Journal of Applied Engineering Sciences*, vol. 17, no. 618, pp. 378–384, 2019.

[14] L. Yang, S. Tang, G. Li et al., "Layered extrusion forming of complex ceramic structures using starch as removable support," *Ceramics International*, vol. 45, no. 17, pp. 21843–21850, 2019.

[15] D. Zhu, R. Chu, X. Zhang, and E. Cheng, "Progress in mechanism of ceramics inkjet printing," *Journal of Mechanical Engineering*, vol. 53, no. 13, pp. 108–117, 2017.

[16] B. Wda, L. Shan, W. Gong et al., "Thermal conductivities and mechanical properties of AlN ceramics fabricated by three dimensional printing," *Journal of the European Ceramic Society*, vol. 40, no. 10, pp. 3535–3540, 2020.

[17] A. Safonov, S. Chugunov, A. Tikhonov, M. Gusev, and I. Akhatov, "Numerical simulation of sintering for 3D-printed ceramics via SOVS model," *Ceramics International*, vol. 45, no. 15, pp. 19027–19035, 2019.

[18] S. Kanazawa, W. Imagawa, S. Matsunari, and S. Akamine, "Ionic wind devices prepared by a 3D printer," *International Journal of Plasma Environmental Science and Technology*, vol. 11, no. 1, pp. 38–42, 2017.

[19] M. Arango, Y. Zhang, R. Li, G. Doerk, and L. Wiegart, "In-operando study of shape retention and microstructure development in a hydrolyzing sol-gel ink during 3D-printing," *ACS Applied Materials & Interfaces*, vol. 12, no. 45, pp. 51044–51056, 2020.

[20] X. Xu, S. Zhou, J. Wu, Q. Zhang, Y. Zhang, and G Zhu, "Preparation of highly dispersive solid microspherical α-Al2O3 powder with a hydrophobic surface for stereolithography-based 3D printing technology," *Ceramics International*, vol. 46, no. 2, pp. 1895–1906, 2020.

[21] A. Yz, C. Pla, D. B. Peng, Z. Yong, and C. Jimin, "Investigation on 3D printing ZrO 2 implant abutment and its fatigue performance simulation," *Ceramics International*, vol. 47, no. 1, pp. 1053–1062, 2021.

[22] X. Meng, M. Ren, Y. Zhuang, Y. Qu, L. Jiang, and Z Li, "Application experience and patient feedback analysis of 3D printed afo with different materials: a random crossover study," *BioMed Research International*, vol. 2021, no. 6, 6 pages, Article ID 8493505, 2021.

Hindawi
Scientific Programming
Volume 2022, Article ID 8429597, 12 pages
https://doi.org/10.1155/2022/8429597

Research Article

Relationship between Physical Training and Tactical Training in Sports Training Relying on Boosting and Bagging Algorithms

Kaining Liu,[1] **Xinwen Li**,[1] **and Christine A. Rochester**[2]

[1]*Department of Physical Education, University of Electronic Science and Technology of China, Chengdu, Sichuan 610054, China*
[2]*Department of Exercise Science, Physical Education and Recreation of Colorado State University- Pueblo, Pueblo, CO 81001, USA*

Correspondence should be addressed to Kaining Liu; liukaining@uestc.edu.cn

Received 21 February 2022; Revised 27 March 2022; Accepted 4 April 2022; Published 16 April 2022

Academic Editor: Muhammad Usman

With the development of sports, competition is becoming more and more confrontational and modern sports are developing in the direction of fast speed, fast rhythm, good skills, and high-altitude combat. And, this development requires good conditions and technology as a guarantee. Sports denote a competitive physical activity, which follows four aspects of competition: technology is the foundation, tactics are the means, the body is the cornerstone, and the psychology is the decisive point. Among these four factors, if the athlete does not have a good body, all techniques and know-how are empty talks. In this paper, two algorithms are introduced to track the athletes' physical training and tactical training videos and the relevant data in the game are counted to obtain the physical indicators required by the athletes in each position. In a certain game, the sprint distance in the first round was 1979 m, the high-speed running distance was 2426 m, the high-intensity running distance was 4398 m, and the jogging distance was 1267 m.

1. Introduction

With the improvement of human safety awareness in social life and the demand for intelligent sensing and measurement systems, moving target tracking technology has been widely developed and applied and has become an important research area in the field of computer vision. Using moving object video tracking, the task is to further determine the position of moving objects in each frame based on the conditional and temporal correlations of video information.

In daily training, it is very important to train the athlete's technique, tactics, and physical fitness. The focus of training should not be shifted to physical training because of poor physical fitness. In the long run, this will lead to a decline in the technical level of the athletes and lack of strategic thinking and only a good state will not win the game, so it is very important to study the relationship between tactical training and physical training.

Regarding sports training, relevant scientists have done the following research. Ahmadi A proposed a novel on the walking motion analysis framework. It is envisaged that the proposed framework can be used for accurate and automated physical activity classification and reliable sports technique assessment in a variety of unconstrained settings for injury management and performance improvement [1]. Tong and Li proposed an exploratory hybrid structural equation modeling framework for functional training decision-making in competitive sports training. The training environment will allow competitors to weigh their choices, decisions, and mistakes. It provides modest evidence of improved reaction times due to the decision learning module [2]. Kumyaito proposes an individualized athletic training program that specifies an individualized performance training schedule to optimize athlete performance. The results show that by applying the genetic algorithm modified by the constraint method, an optimized exercise training plan can be realized and finally the goal of improving the sports performance can be achieved [3]. The purpose of the Pérez–Turpin study was to determine the results of the analysis of men's single and double outdoor

badminton matches and to determine the relationship between technical and tactical aspects in a study organized by the Badminton World Federation. It confirms the applicability of computer symbolic analysis in determining the properties of outdoor beach badminton [4]. Sobko et al. developed and experimentally confirmed the use of video manuals in youth basketball referee season sports training. With the help of this manual, it is possible to determine the level of sophistication of young basketball referees and their psychophysiological abilities. The results showed that the technical, physical, and functional readiness indicators of basketball referees in the experimental group were significantly improved [5]. Shao introduced the auxiliary decision support system for college students' physical training. He introduced network security methods and designed a decision support system for sports training based on network security. The designed sports training decision support system based on the improved association rule prior algorithm has good applicability and efficiency [6]. Martinescu-Bdlan and Macovei proposed that the training process and the adaptation of the body are a multifactorial process. The body's adaptation to these factors is directly related to the methods and means used. During the training process, a series of principles and rules must be followed, which help ensure the correct operation of the athlete's training system [7]. Wei et al. reviewed the existing artificial intelligence application research. Based on the basic concepts of artificial intelligence and related research results, the study discussed three specific cases of artificial intelligence application in sports training. It explores the close relationship between artificial intelligence technology and sports training and highlights the advantages of artificial intelligence, including utilization, convenience, and innovation [8]. Aiming at the problem of low classification accuracy caused by the randomness of objective motion in sports training videos, Xu studied a deep learning-based sports training video classification model. The experimental results show that the model can effectively solve the problem of target movement randomness and the classification speed is faster [9]. Taking the diving team as an example, Zhao expounds on the role and significance of scientific training in developing competitive sports in ordinary colleges and universities and puts forward suggestions on the establishment, organization, and implementation of scientific training. The training of the diving team shows that scientific and systematic training is an important guarantee for the cultivation of high-level student athletes in ordinary colleges and universities [10]. Zhang et al. proposed a decision support model for motion training based on association rules. They used the posterior probability setting to reveal the weights of the discriminative power of attribute terms and set the classification performance to reflect the weights of the three measures that evaluate credit contribution. Effective sports training enables coaches to formulate corresponding countermeasures and achieve scientific management [11]. Ba takes sports videos as the analysis object and uses quadratic interpolation to improve it because of the large error between the RSSI value and the actual value when the positioning algorithm uses linear interpolation to calculate virtual tags. The results show that the algorithm of this study has a certain practical effect [12]. Reutskaya and Poltoratskaya studied the static stability characteristics of skiers during the exercise training phase. They recruited skiers who had gone through different stages of athletic training. It reveals the characteristics of the static stability of skiers in different sports training stages and helps to determine the standards and scales for the differential assessment of the development level of skiers' static stability in different sports training stages [13]. Based on the characteristics of athletes, Ma developed and designed a monitoring system for athletes' training process based on mobile artificial intelligence terminal technology. He uses GPS to obtain real-time location information of athletes and provides real-time guidance for athletes, revealing the changing laws of various indicators of athletes during training [14]. Reutskaya and Poltoratskaya studied the plausibility of skiers' movements in different sports training stages. Comparative characterization of the speed components of skiers in time trials showed that skiers experienced significant reductions in cycle frequency and cycle length during the athletic training phase. The higher movement velocity is maintained by the velocity component of the movement technique [15]. These methods provide some references for research, but due to the short time and small sample size of the relevant research, this research has not been recognized by the public.

The innovation of this paper is that two algorithms are introduced, the flow chart of the target tracking algorithm is obtained, and the target tracking of the athletes in the competition and training is carried out to obtain the data required for the research. In this paper, the average center position error and average overlap rate of the tracking results are obtained and analyzed. In this paper, the physical indicators of athletes in various positions are detected and the physical characteristics of athletes in various positions are summarized and analyzed.

2. Methods on the Relationship between Physical Training and Tactical Training

2.1. Boosting and Bagging Algorithms. A boosting algorithm is a mechanical algorithm that can be used to reduce bias in learning. Most addition algorithms involve reusing less-learned classifications and adding the results to the state-of-the-art learned rank. During the mixing process, different weights are usually provided according to the accuracy of their classification. After weak learners are added, the data are usually weighted to confirm the classification of previously classified data points [16].

Boosting is a machine learning technique that can be used for regression and classification problems. The lifting algorithm is essentially an iterative algorithm. In this technology, a weak classification prediction model (such as a decision tree) is generated at each step, and weighted accumulation is performed to achieve the purpose of continuously using a weak classifier to make up for the previous weak classifier. Figure 1 shows a schematic diagram of the boosting process of the Boosting algorithm.

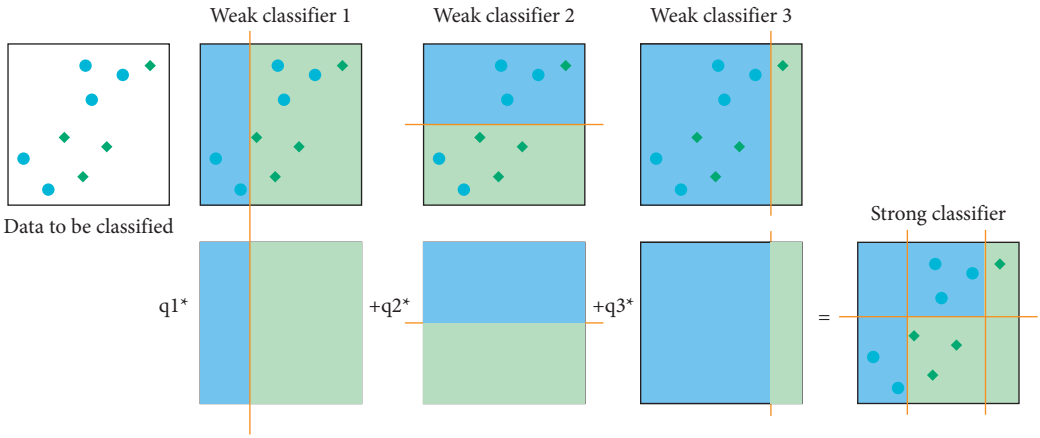

Figure 1: Schematic diagram of the boosting process of the Boosting algorithm.

In the training loop process, weighting the misclassified samples is an effective way to speed up the training. Since the weak classifier with a high accuracy rate in training has a larger weight, there will be more and more correctly classified samples in a new round of training. Training samples with smaller weights have less effect on the new round of training; that is, each new round of training focuses on training misclassified samples. The weak classifiers in actual training are the same, but the actual training data used by the weak classifiers are different. Usually, each dimension of the feature vector is used to form a weak classifier [17].

Suppose the desired final prediction model is

$$F(m) = \sum_{u=1}^{M} \eta_u r_u(m), \tag{1}$$

where $r(m)$ is the basis function.

The loss function of $F(m)$ is

$$P(n, F(\vec{m})) = \frac{1}{2}(n - F(\vec{m}))^2, \tag{2}$$

where n is the actual value and $F(m)$ is the predictive value.

We find the optimal step size using linear search.

$$\zeta_a = \arg\min \sum_{u=1}^{b} P(n_u, F_{a-1}(m_u))\,\xi, \tag{3}$$

where ξ is the step size of gradient descent.

The residual formula is

$$w_{ua} = \left[\frac{\partial P(n_u, F(m_u))}{\partial F(m_u)}\right]. \tag{4}$$

We give a certain type of deterministic prediction.

$$t_a(m) = \sum_{v=1}^{V} y_{va} I(m \in R_{va}), \tag{5}$$

where y_{va} is the predicted value of the sample in the region.

We calculate the learning rate using linear search.

$$\begin{aligned} F_a(m) &= F_{a-1}(m) + \zeta_a t_a(m), \\ \zeta_m &= \arg\min_{\zeta} \sum_{u=1}^{b} P(n_u, F_{b-1}(m_u) + \zeta \cdot t_b(m_u)), \end{aligned} \tag{6}$$

where $F(m)$ is the hypothetical optimal function, n_u is the weight, and P is the loss function.

We predict the best predictive model.

$$\begin{aligned} F_a(m) &= F_{a-1}(m) + \sum_{v=1}^{V} \zeta_{va} I, \\ \zeta_{va} &= \arg\min_{\zeta} \sum_{m \in R_{va}} P(n_u, F_{a-1}(m) + \zeta \cdot t_a(m)). \end{aligned} \tag{7}$$

Bagging algorithm is a group learning algorithm in machine learning. The Bagging algorithm can be combined with other classification and regression algorithms to improve its accuracy and stability and at the same time reduce the variance of the results to avoid overfitting. The algorithm is a technique that reduces common errors by combining multiple types. The main idea is to train several models separately and then select all models for test results. This is an example of a traditional machine learning method called model averaging, and the technique used in this example is called the aggregation method.

The Bagging algorithm is a method to improve the accuracy of weak sorting algorithms by creating a set of prediction functions and then combining them concretely into prediction functions. It is a framing algorithm that involves primarily processing of a subset of the model and then training the model using a weak ranking algorithm to create a basic set of classifications. A multilayer neural network is an artificial neural network that develops and maps regions of input vectors to regions of output vectors. MLP neural systems have the ability to solve linear and integral problems and are well suited for solving classical problems. Bagging algorithms are suitable for integration with unstable analysis algorithms. Unstable learning disabilities generally include neural networks and decision trees. Instability is when there is a small change in the

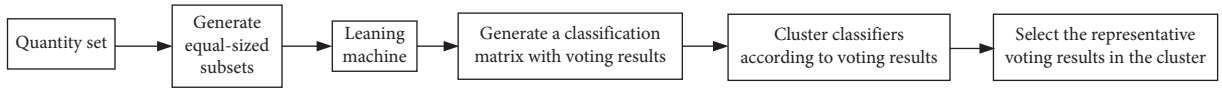

Figure 2: Schematic diagram of the algorithm.

ensemble of training models, and the results of the model can change dramatically. Thus, training with two different training sets results in different classifications that may have similar accuracies but with different parameters (e.g., initial neural system weights), resulting in differences in inclusion. By choosing this classification prediction, transport reduces common errors by minimizing the variance produced by the main classification. Bagging algorithms, on the other hand, can train weak classes to create strong classes in a special way.

The specific implementation method is as follows:

$$E_{\text{training}} = \left(m^{u}_{\text{training}}, m^{u}_{\text{training}}\right), \quad u = 1, 2, \ldots N, \tag{8}$$

where N is the number of samples in the original training set, m^{u}_{training} is the input volume of the sample, and n^{u}_{training} is the actual load value.

The final prediction result is

$$\widehat{n}_{\text{test}} = \frac{1}{S}\sum_{s=1}^{S} n^{s}_{\text{test}}, \tag{9}$$

where S is the number of neural network models and n^{s}_{test} is the forecast load.

$$q_u = \frac{AUD_u}{\sum_{v=1}^{R} AUD_v},$$

$$L(m) = \arg\max \sum_{u=1}^{R} q_u h_u(m), \tag{10}$$

$$g_u = \frac{AUD_u}{\sum_{v} AUD_v},$$

where q is the integrated classifier and $h_u(m)$ represents the weights of base classifiers.

$$G(q_0) = \frac{B\left|f(l_0) = q_0 \Lambda f(l_u) = q_u\right|\left|l_u - l_0\right| = 1|}{8B\left|f(l_0) = q_0\right|}, \tag{11}$$

where G represents the samples forming the training set and B stands for training individual learners.

The schematic diagram of the algorithm is shown in Figure 2.

The offline boosting algorithm prepares a large number of positive and negative samples in advance and obtains the classifier through offline training. Its training time is relatively long, the prepared samples cannot cover all the situations in the actual scene, and it is prone to drift. The online boosting algorithm is trained once with a sample, and the classifier is obtained by online training. It can update the classifier online according to the changes in the actual scene, and the training period is short.

2.2. Physical Training and Tactical Training. Physical fitness refers to the athletic ability of an athlete's body. It is one of the indispensable components of competitive athletic ability, and it is also the comprehensive athletic ability required by various bodies to improve athletes' competition performance and technical and tactical levels. Physical exercise refers to the training of the physical ability to exercise continuously for a long time under stressful and tense conditions, even in sports. The purpose of physical exercise is to create physical and mental adaptation to the human body by increasing the load of adaptive training and exercise for various organs and systems of the human body. It improves the athletic ability of the human body and cultivates the will of the athletes to train hard and fight tenaciously.

General strength training is a comprehensive strength training that uses a variety of nonspecific training methods to improve an athlete's physical fitness, improve form, and manage nonspecific athletic strategies, skills, and knowledge. It creates special conditions for improving sports technology. Specific training suggestions and training methods should be closely related to specific characteristics. It promotes the development of important athletic qualities in specific sports. Using training methods that can directly improve specific qualities, training closely related to a specific sport acquires knowledge and skills related to specific techniques and skills and helps to improve the performance and technical level of a specific sport. When planning a general physical activity, people are not developing and improving all body parts, systems, organs, and exercises comprehensively and vigorously but are doing exercises based on an individual's specific circumstances and needs. Special sports must be scientifically and rationally compiled through special education content. Different training directions have different demands on the body, so general training cannot replace specific training.

General physical training and special physical training should be arranged reasonably. General physical training can comprehensively develop athletes' athletic qualities such as strength, endurance, speed, agility, coordination, and flexibility. It improves the function of various organ systems of athletes, so that the athletes' bodies can develop in a balanced way. At the same time, it improves the fitness level of athletes through general physical training. The purpose of special physical training is to make the physical fitness obtained by athletes directly serve to improve sports performance. General physical fitness training serves for special physical fitness training, while special physical fitness training directly serves to improve the overall competitive level of athletes.

When choosing a training method, it should be similar to the technical movements with certain biomechanical characteristics and the physical training should not be separated from the training of overall characteristics such as technology, tactics, and psychology. Physical training does not have to be an isolated educational system. In the training process, if it is separated from techniques and tactics, it does not meet the requirements of being closely integrated with certain sports and the expected training effect cannot be achieved. For athletes, psychology and intelligence are especially important. Physical training often includes a lot of exercise, which can easily lead to insufficient mental endurance of athletes. Therefore, athletes should be aware of the importance of training, combining science and training, so that training is not easy or boring.

When determining the relationship between general training and special training in the training process, coaches should design a training content that varies from team to individual. In terms of time arrangement, it is recommended that coaches plan physical training according to factors such as competition time and athletes' physiological periods. Combined with the special characteristics, this article obtains some special physical training content. The content differing from person to person means that different training contents are arranged for different athletes. The physical function of each athlete cannot be exactly the same. Therefore, when performing physical training, it should be different from person to person and cannot be generalized. Only in this way, physical training can achieve better training effects; otherwise, it will reduce the physical fitness level of athletes.

The plasticity of each athletic quality is different, and there is a rapid growth period. Therefore, when training, we should grasp the favorable opportunity according to the sensitive period of different physical qualities, so that the relevant characteristics can be developed accordingly. Sensitivity to the development of sports quality means that any sport at a certain age, based on the natural growth and development of children and adolescents, develops rapidly and is in the best development period. Training should use this time in advance to fully develop the athletic qualities that meet the needs of specific sports or directly serve specific purposes and lay a solid foundation for good results.

Competitive sports are an important part of sports. It is a social sports activity with sports competition as its main feature and the main goal of creating excellent sports results and winning competitions. Competitive sports are gradually formed and developed in the process of human development. Competitive sports have also established a relatively complete management system in the process of development. It contains four parts: athlete selection, sports training, sports competition, and competitive sports management. There are four major elements of modern competitive ability: technology is the foundation, tactics are the means, the body is the cornerstone, and the psychology is the decisive point.

Because physical training is an energy-intensive training, some forms of training are also boring, which is why athletes often feel tired during training. Therefore, in daily training, it is necessary to strengthen the education of athletes' emotions and qualities and to improve athletes' awareness of the importance of physical education. Coaches should adopt effective training methods to increase athletes' interest in training and reduce athletes' mentality of training fatigue. And, coaches should make players clearly aware of the importance of physical fitness [18].

Before the test, you should understand the athlete's health status and be adequately prepared for the safety hazards that the test may bring. For example, if the athlete's waist injury has not healed, the maximum strength and sitting forward flexion tests can be temporarily suspended. In addition, it is necessary to check in advance whether the test equipment and environment are potentially dangerous during the test, etc. In test combinations and multiple tests, the recovery time can be determined by the athlete's pulse and experience. It should be noted that after the index test reflecting the extreme state of the athlete, the athlete should be given sufficient recovery time so as not to affect the subsequent test results.

The human body is an organic whole, a complete system. Therefore, the general physical fitness and the specific physical fitness of athletes are interrelated, influencing, and interdependent. General physical qualities include endurance, speed, strength, agility, flexibility, and coordination. Endurance is one of the important indicators of athlete's physical fitness. There are many sports such as ball games, cycling, swimming, mountaineering, middle-distance running, and race walking in track and field sports. The improvement of technical level and the achievement of competition results often depend on the level of endurance. And, some sports that do not require high aerobic endurance, such as weightlifting, diving, and gymnastics, will also have higher requirements for specific endurance. Good endurance is also an important prerequisite for accelerating physical recovery after heavy-duty training. Endurance quality can be divided into many types according to different standards, and different training methods should be used in training for different types of endurance.

3. Experiments on the Relationship between Physical Training and Tactical Training

The development of machine learning theory has had a profound impact on related fields, especially in research fields that require big data processing. Therefore, cluster learning, as an important discipline in machine learning, has had a significant impact in the fields of model analysis and computer vision. Boosting and Bagging algorithms are two common swarm learning algorithms. Initially, both algorithms were trained offline with a large number of models, so we can use them directly. Since offline training takes time, the algorithm changes after training and new models cannot be added later to update and improve classification skills. The proposed algorithm model is used to track the target of the athletes, so as to better perform physical training and tactical training. Figure 3 shows the flow chart of the target tracking algorithm.

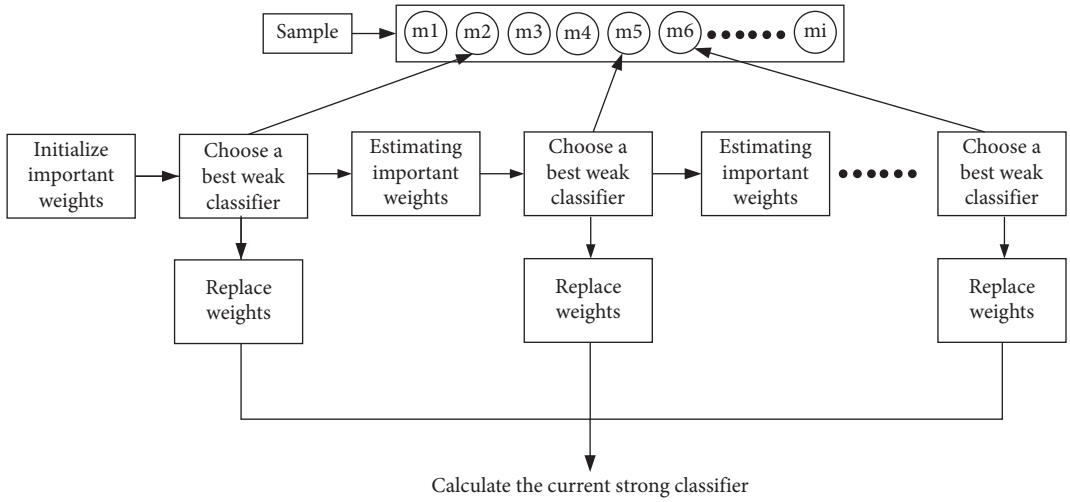

Figure 3: Target tracking algorithm flow chart.

The online boosting moving target tracking algorithm is a target tracking algorithm based on statistical learning, which regards the target tracking problem as a two-class problem of the target and background. Moreover, it does not describe the appearance of the target by establishing a complex model and then uses the model-matching method to track the target but to find a decision boundary that can effectively distinguish the target from the background. Then, it uses this decision boundary to get the specific location of the tracking target. The main principle is to first obtain a set of weak classifiers by online training and linearly combine these weak classifiers into a final strong classifier according to their corresponding voting weights. Then, it uses this strong classifier to evaluate each rectangular block in the search area of the current frame picture and returns a confidence value. After all rectangular blocks are evaluated, a confidence matrix will be obtained, in which the maximum confidence value is found and the corresponding rectangular block is the target to be tracked. Finally, if the target is tracked in the current frame, in order to adapt to the changes of the target appearance and background environment, all the weak classifiers are updated online using the current frame image.

The advantage of the online boosting algorithm is that the tracking problem is considered as an evaluation problem and the appropriate target attributes are selected in real time according to the changes of the tracking target. However, the main problem with this approach is that due to other conditions such as occlusion, any change in the target features may lead to an increase in the number of errors and accumulate errors after long-term execution. The experimental analysis shows that the selector in the online boosting algorithm increases the weight, which leads to the offset. However, the shutdown monitoring problem actually only affects the local region, not the global region [19]. The framework of the target tracking system is shown in Figure 4.

In the principle of online boosting, first, the selector chooses the weakest level with the least error, determines the appropriate voting weight, and continues to transfer the critical weight to the next selector. The previous steps take into account the influence of all elements and whether the result is correct or the weight of one selector in front affects the weight of the next selector. But, the selector result affects only local regions, not all regions. If the function selected by the previous selector is good, no matter whether the function selected by the latter selector is good or bad, the corresponding weight must be reduced. If there is a problem with the previous function of the next selector, this causes the corresponding selector weight to drop rapidly [20]. The average weight of selectors is shown in Table 1.

The corresponding weight of the selector drops rapidly, and the weight of the previous selectors determines the performance of the final classifier. Therefore, when the weights of the previous selectors are wrong, the drift of the tracking target is inevitable. Online adaptive learning target

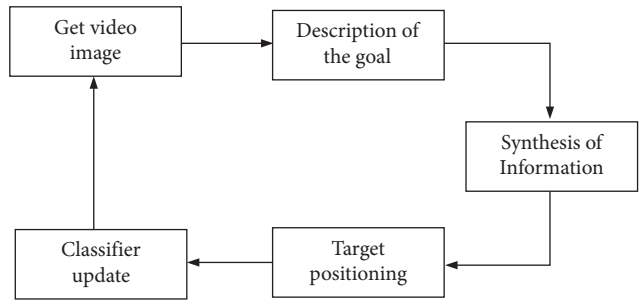

Figure 4: Framework of the object tracking system.

Table 1: Average weight of selectors.

Selector number	Selector's corresponding weight			
1–4	6.5123	4.5245	3.1729	2.3489
5–8	1.8712	1.4561	1.1523	0.9192
9–12	0.7842	0.6726	0.5208	0.5249
13–16	0.4331	0.3162	0.5337	0.3344
17–20	0.2291	0.4757	0.2327	0.2345

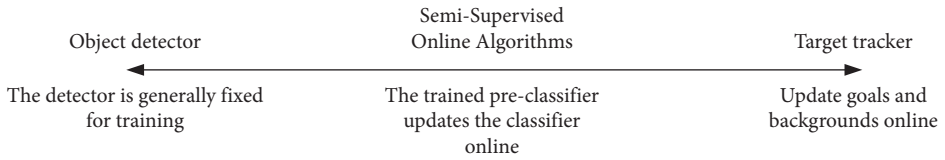

Figure 5: Object tracker with a detector.

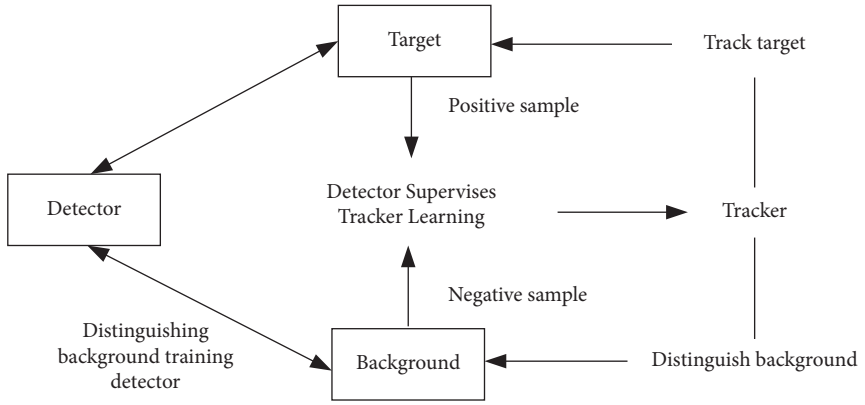

Figure 6: The relationship between detectors and tracking.

tracking often suffers from target drift, which is mainly caused by errors introduced by the tracker each time the tracker is updated. Figure 5 shows a schematic diagram of an object tracker with a detector.

In order to detect the target and adapt to changes in the target scene, etc., the update of the detector should be more sure that it is the correct target tracked before, so that it can be used as a positive sample to update the detector. With a "more confident object" detector, it can be used to identify false objects in some indistinguishable scenes. The relationship between the detector and tracking is shown in Figure 6.

The tracking rate to the target is tested with a large amount of video data, as shown in Table 2 for the experimental results.

The average center position error is the average of the pixel offsets between the center point position of the tracked target block and the center point position of the real target block in all frames of the video sequence. The tracking success rate is the ratio of the number of successful tracking frames to the total number of frames in all frames of the video sequence.

$$AE = \frac{\sum_{u=1}^{B} \sqrt{(m_{tu} - m_{ru})^2 + (n_{tu} - n_{ru})^2}}{B}, \quad (12)$$

where B is the total number of frames in the video sequence, (m_{tu}, n_{tu}) denotes the coordinates of the center point of the target block, and (m_{ru}, n_{ru}) denotes the coordinates of the center point of the real target block.

For detailed quantitative and qualitative analysis and comparison, Table 3 shows the average center position error of the tracking results.

The average center position error of the SB algorithm is reduced by 61.4% compared with the OB algorithm, and the center position error is reduced by 48.8% compared with the CT algorithm.

Table 2: The experimental results of the tracking rate to the target.

Video sequence	BST tracking rate	Our tracking rate
Running video	0.864	0.946
Walking video	0.683	0.884
Squat video	0.23	0.993
Physical training video	0.894	0.924
Tactical training videos	0.485	0.752

Table 3: Average center position error of tracking results.

Frame number	CT algorithm	OB algorithm	SB algorithm
832	25	39	21
365	45	62	30
175	60	69	15
Average	43	57	22

Table 4: Average overlap rate of tracking results.

Frame number	CT algorithm	OB algorithm	SB algorithm
832	74	43	77
365	56	37	50
175	30	25	83
Average	50	35	70

The average overlap rate of the tracking results is shown in Table 4.

The average tracking overlap rate of the SB algorithm is more than double rate of the OB algorithm and 28.5% higher than that of the CT algorithm.

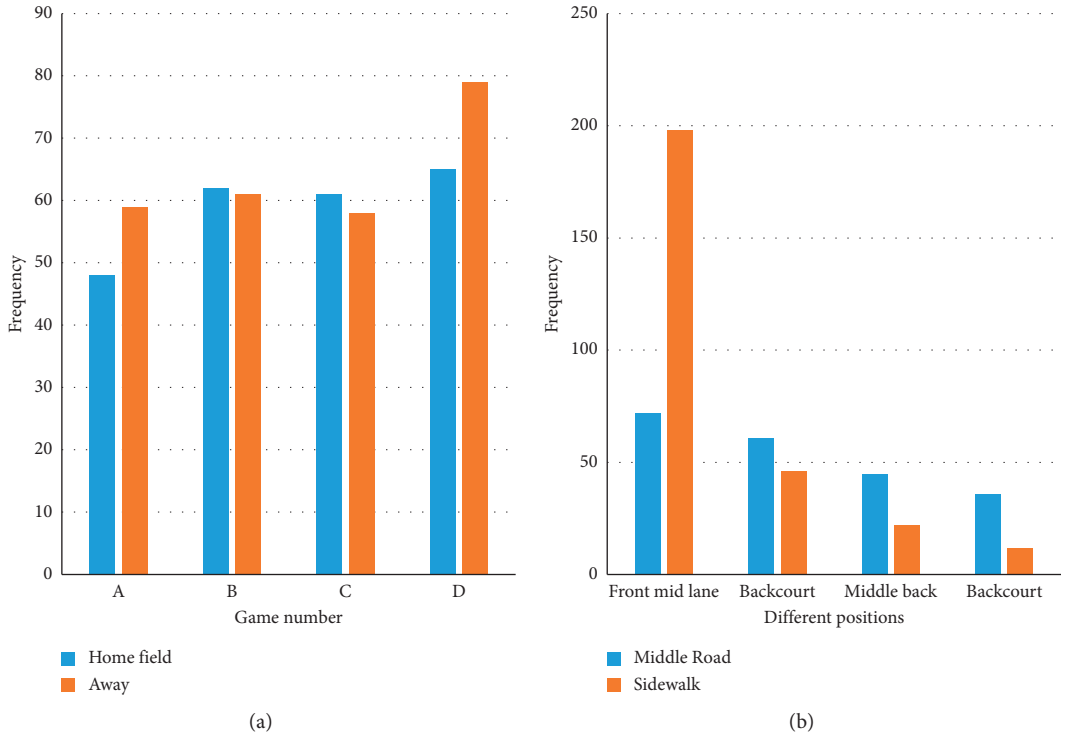

Figure 7: Comparison of the number of passes in different positions.

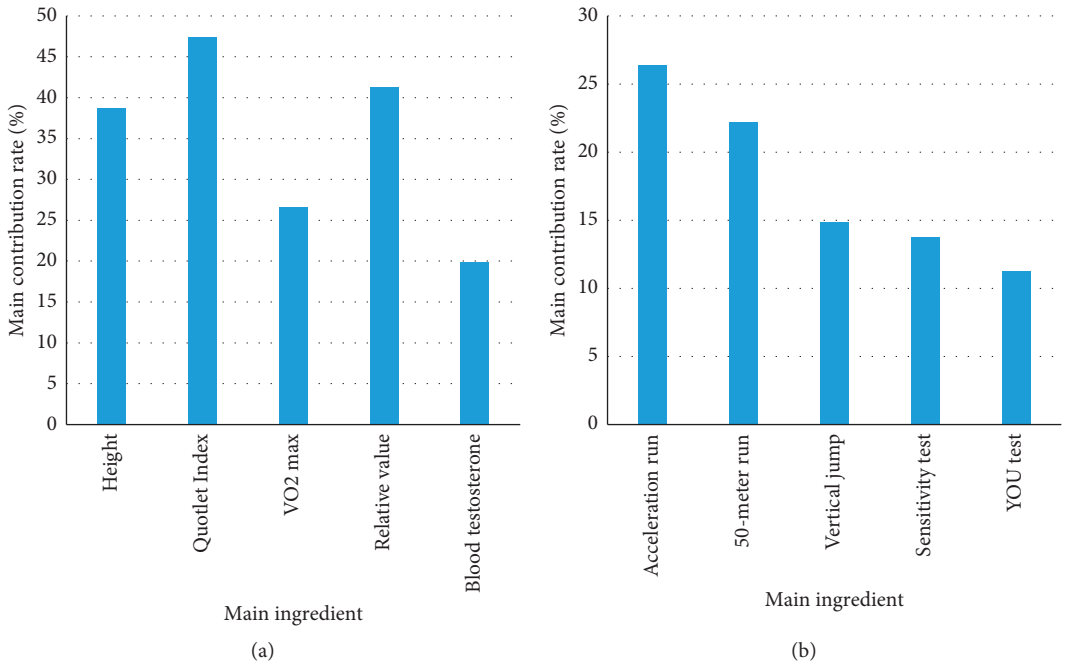

Figure 8: Physical structure characteristics and hierarchical model of frontcourt players.

3.1. Target Identification for Each Athlete in the Athlete's Physical Training Videos and Tactical Training Videos. Tactical awareness can be manifested in the fact that in order to defeat the opponent in the fierce confrontation and for flexible tactical application, according to the actual situation of the two sides on the field, the players correctly use the technology, rationally control their actions, and have a certain purpose. An athlete's instantaneous decision-making ability on the spot is a full reflection of whether a player has truly grown up and whether he has rich on-the-spot

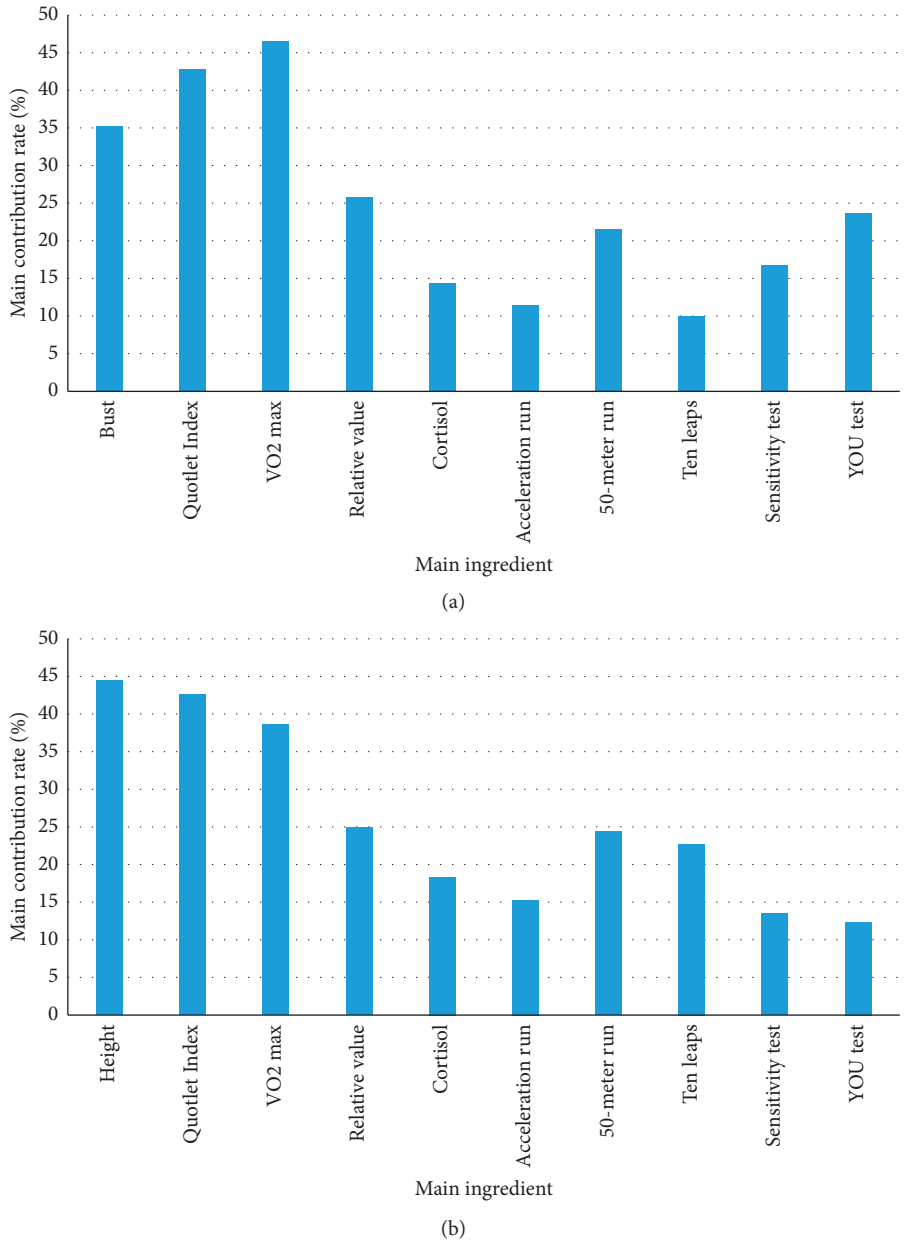

Figure 9: Physical characteristics of midfielders.

experience. Figure 7 shows the comparison of the number of passes in different positions by players in the four games.

No matter where the athlete is on the court, when he makes a tactical decision to pass the ball, he must first observe the movement of his own players and the distribution of the players on the court in different areas. The selection of the passing objects shows a certain degree of preference and orderliness. Before Kongka passes the ball, the priority is to observe the positional distribution and movement of the players in the center, followed by the connection or support of the players on the wing.

Many behaviors of the players in the game have a certain purpose. All the actions of the players in the offense have a certain tactical purpose in a sense. However, the purpose of this activity of the players begins before their tactical activities. Before the players make any tactical action, there will be subjective considerations and predictions about the positions of teammates and defenders on the field, the possible neutral positions on the field, the crossover of teammates in different positions, and which position players will most threaten the opponent's goal after receiving the ball. Under the domination of tactical guiding ideology, football players consciously change their tactical behaviors to maximize their own advantages and, at the same time, compress the opponent's "living space" to the greatest extent, so that the opponent's own advantages cannot be effectively played.

The main task of the frontcourt players is to break through the opponent's line of defense, score goals, and win

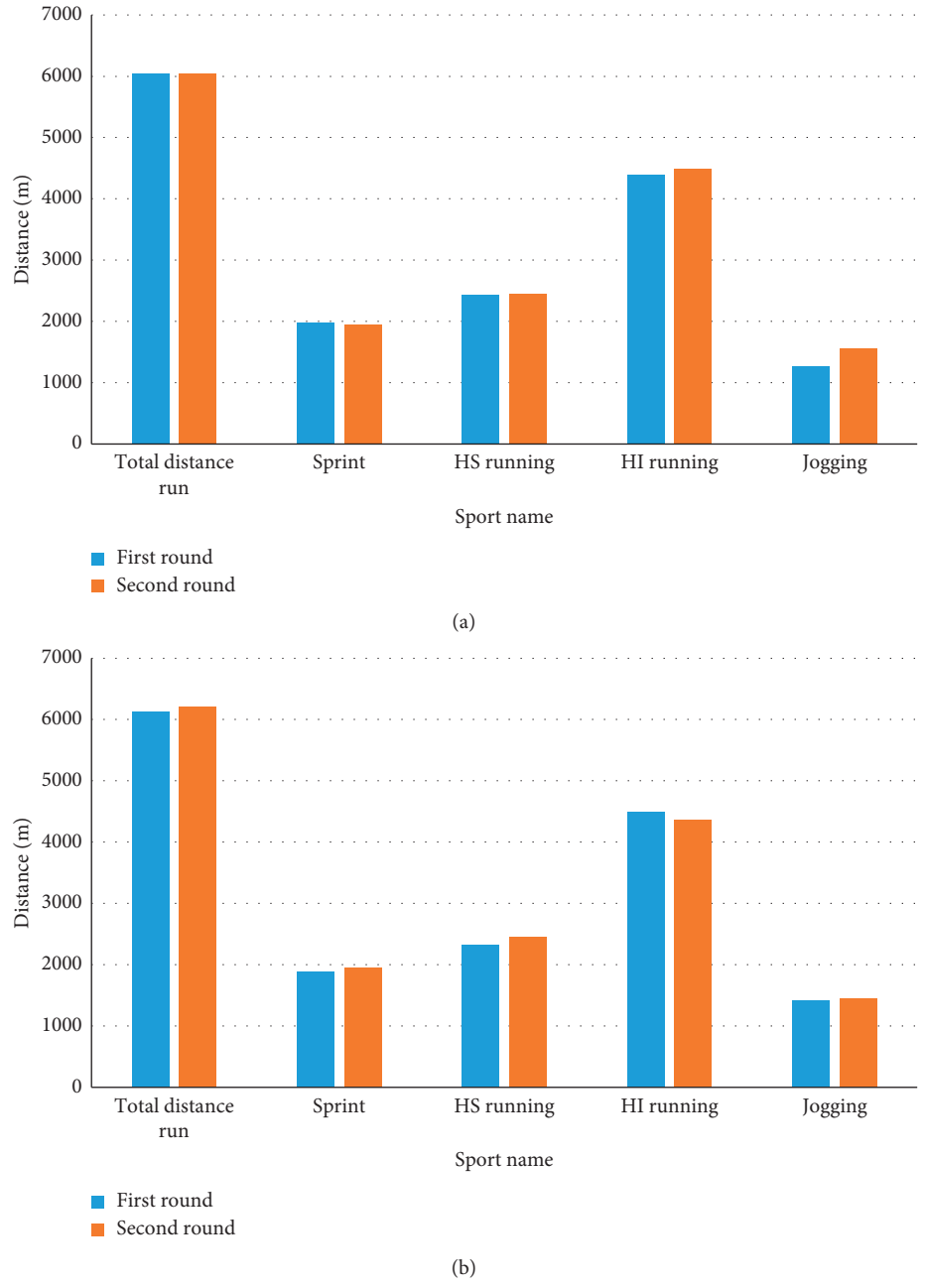

Figure 10: Statistics of the running distance per game.

the game. Therefore, any tactical activities undertaken by the strikers should revolve around this task. As shown in Figure 8, the physical structure characteristics of frontcourt players are shown.

It can be seen that the height of the players in the frontcourt is increasing, and the body should be strong. The reason is that in the fierce physical confrontation, in order to seize the opportunity and complete the coordination of various techniques and tactics, the frontcourt players are required to have a strong body as the foundation. Athletes are tall and, in a certain sense, are more likely to gain a space advantage than other players; especially in the process of competing for the high-altitude ball, a certain height advantage has already taken the lead in position. In the daily training, attention should be paid to the training of the agility and coordination of the players in the frontcourt position, so as to improve the ability of the players to shoot without losing the opportunity after getting rid of the defense. The running of the striker is often accompanied by the suppression of the opposing defender. Whether it is passing the ball or dribbling the ball, there will be direct physical confrontation with the defender. Therefore, in the usual training, it is closer to the reality of the game, which strengthens the confrontation of the practice and pays attention to the practice of the players' strength and speed.

The midfielder plays a linking role in the game, playing the role of passing the ball for the forwards in the attack, supporting the attack in the frontcourt, and completing the tactical cooperation with the teammates in the frontcourt. In the defense, this delays the speed of the opponent's advance in the own half and assists the players in the backcourt to strengthen the defense. Keeping their own goal is the main task of the backcourt players in the game. However, in the game, in order to form a local advantage in terms of numbers, the fullbacks often assist in the opponent's half, forming a situation of playing more and playing less. Figure 9 shows the physical characteristics that midfielders and backfielders should have.

The midfielders have certain positional characteristics, but there is no height index in the morphological indicators, indicating that the height has little influence on the midfield players but requires a certain degree of physical fulfillment. The midfielder's legs should be explosive, and, at the same time, they should have a certain speed. When the backcourt players are based on highly developed aerobic tolerance in terms of body performance, they must also have a good anaerobic energy supply capacity. In the training, on the basis of improving the aerobic metabolism of the players, we should combine the characteristics of the project and pay attention to the development of the speed endurance of the players. It applies various runs used in the competition (back run, side run, plunge or cut run, turn run, etc.) to the usual training.

In the training, attention should be paid to the improvement of the anaerobic metabolism of the players and the speed and strength of the players should be improved in a targeted manner.

The physical state of players on the field is often shown by running in the game, and the strength of running ability directly reflects the physical development level of a player. There are not many opportunities for players to really control the ball in the game, and most of the time in a game goes for tactical running or coping without the ball. Figure 10 shows the average running distance per game.

It can be seen that the players faced fierce competition in the game, the exercise intensity was large, and the physical energy consumption was also relatively large. The sufficient physical fitness of the players can ensure the high efficiency of the offense and the effectiveness of the defense.

4. Discussion

When coaches do tactical training, physical training can easily be overlooked. In the second half of the training, tactical training tends to take place in the training. The first half is usually individual strategy training and team strategy training. In the first half, the best training is warm-up and technical training. However, when it comes to tactical training, most teams let players learn new tactics first. They usually run or walk while strategizing. In order to learn the technique, the coach asks the athlete to passively defend from the beginning and learn the technique with the opponent. The athlete should gradually increase the speed and efficiency of the technique while simply learning the technique. However, this training method allows emerging athletes to practice basic techniques and minimize training conditions. Tactics are what the team needs to learn and improve over the long term, and they are the soul of the team. In order to maintain an athlete's fitness level and improve training skills, different tactics can use different training methods.

Breaking a press defense requires a clear-headed, decisive player who has limited time to pass the ball to the right area of the court and maintain reasonable offensive space. Teams that often use pressing defenses also put themselves on the cusp, because behind the pressing defense, it is more likely to be unguarded or there is the situation of playing more and less after being broken by the offensive team. When breaking the pressing defense, people should dribble the ball reasonably and try not to stop the ball at one time; otherwise, it is easy for the opponent to come forward and attack. Offensive players should be clear-headed, aware that the ball only has seconds to move from the backcourt to the frontcourt, and avoid defending the "hot zone," which is the corner or corner area. When passing and receiving the ball, players should not stand in place and wait for the ball but move forward to receive the ball, which forces the defender to move and easily creates a defensive neutral. The offensive player's eyes should not leave the ball. Otherwise, when a pinch attack occurs, the player's line of sight will be small and they will fight alone, making it easy for the defender to steal and drop the ball.

5. Conclusion

The goal of attack tactics used in sports is to defeat the opponent and win the game. This offensive tactic can be achieved through individual breakthroughs or teamwork, which requires players on the field to perform the same tactical actions based on the actual situation. Many sports games today are characterized by full attack, full defense, and full control over everything on the field. This paper focuses on tracking moving objects in video sequence images and mainly studies and analyzes online boosting algorithms based on statistical learning methods. In this paper, the preliminary prediction research is carried out. In view of the limited data sources and academic level, there are inevitably some omissions in the research. The analysis of the status quo analysis stage is not thorough enough, and it only shows the changes of relevant indicators and lacks internal judgment analysis. At the stage of theoretical research, this paper does not have a deep grasp of the theory. The SB algorithm is a multiclassifier tracking system, which requires a lot of time for training and updating and is not suitable for scenarios with high real-time requirements.

Data Availability

The experimental data used to support the findings of this study are available from the corresponding author upon request.

Conflicts of Interest

The authors declare that there are no conflicts of interest.

Acknowledgments

This work was supported by the Fundamental Research Funds for the Central Universities of China: Physical Education and Health Promotion (No. ZYGX2018007FRJH) and the Educational Reform Project of University of Electronic Science and Technology of China: Freshman Project Courses: Physical Enhancement and Functional Training (No. 2019PBLF029).

References

[1] A. Ahmadi, E. Mitchell, and C. Richter, "Toward automatic activity classification and movement assessment during a sports training session," *IEEE Internet of Things Journal*, vol. 2, no. 1, pp. 23–32, 2017.

[2] W. Tong and B. Li, "A systematic decision making for functional training in competitive sports training," *Journal of Intelligent and Fuzzy Systems*, vol. 40, no. 2, pp. 1–11, 2020.

[3] J. A. Pérez-Turpin, C. Elvira, and D. Cabello-Manrique, "Section III -sports training notational comparison analysis of outdoor badminton men's single and double matches," *Journal of Human Kinetics*, vol. 71, no. 2020, pp. 267–273, 2020.

[4] I. M. Sobko, Y. I. Chucha, I. A. Podmaryova, O. P. Nagovitsyna, and I. M. Zhuravlova, "Application of the video-tutorial "Challenge for Referees" in sports training of young basketball referees for the game season," *Health, sport, rehabilitation*, vol. 7, no. 1, pp. 42–53, 2021.

[5] L. Shao, "Research on sports training decision support system based on improved association rules algorithm," *Security and Communication Networks*, vol. 2021, no. 4, Article ID 5561970, 6 pages, 2021.

[6] F. Martinescu-Bdlan and C. M. Macovei, "Trends in modern sports training - basis of physical training for the cadets from the combat branch," *International conference KNOWLEDGE-BASED ORGANIZATION*, vol. 27, no. 2, pp. 150–154, 2021.

[7] S. Wei, P. Huang, R. Li, Z. Liu, and Y. Zou, "Exploring the application of artificial intelligence in sports training: a case study approach," *Complexity*, vol. 2021, no. 8, Article ID 4658937, 8 pages, 2021.

[8] Y. Xu, "A sports training video classification model based on deep learning," *Scientific Programming*, vol. 2021, no. 5, Article ID 7252896, 11 pages, 2021.

[9] S. Zhao, "Research on scientific sports training of students majoring in physical education," *Revista Brasileira de Medicina do Esporte*, vol. 27, no. 5, pp. 460–463, 2021.

[10] C. Zhang, M. Li, H. Wang, and N. Wang, "Auxiliary decision support model of sports training based on association rules," *Mobile Information Systems*, vol. 2021, no. 7, Article ID 7233800, 8 pages, 2021.

[11] T. Ba, "Performance analysis of sports training based on random forest algorithm and infrared motion capture," *Journal of Intelligent and Fuzzy Systems*, vol. 40, no. 12, pp. 1–11, 2020.

[12] E. Reutskaya and T. Poltoratskaya, "Peculiarities of statokinetic stability of skiers-racers at sports training stages," *SCIENCE AND SPORT: Current Trends*, vol. 8, no. 4, pp. 40–45, 2020.

[13] B. Ma, S. Nie, M. Ji, J. Song, and W. Wang, "Research and analysis of sports training real-time monitoring system based on mobile artificial intelligence terminal," *Wireless Communications and Mobile Computing*, vol. 2020, no. 6, Article ID 8879616, 10 pages, 2020.

[14] E. Reutskaya and T. Poltoratskaya, "Ratio of the speed components of ski racers at sports training stages in time trials," *SCIENCE AND SPORT: Current Trends*, vol. 8, no. 4, pp. 20–25, 2020.

[15] X. Wang, D. Huang, and X. Zhao, "Design of the sports training decision support system based on improved association rule, the apriori algorithm," *Intelligent Automation & Soft Computing*, vol. 26, no. 4, pp. 755–763, 2020.

[16] Z. Zhao, X. Liu, and X. She, "Artificial intelligence based tracking model for functional sports training goals in competitive sports," *Journal of Intelligent and Fuzzy Systems*, vol. 40, no. 1, pp. 1–13, 2020.

[17] A. B. Tozetto, M. Milistetd, C. Collet, T. Iha, J. Anello, and J. V. d. Nascimento, "Treinadores de basquetebol: Os desafios da prática No ambiente de formação esportiva," *Cuadernos de Psicología del Deporte*, vol. 19, no. 1, pp. 291–301, 2019.

[18] J. Wu, "Monitoring methods of different time structure level sports training based on the fusion of motion commitment theory model," *IPPTA: Quarterly Journal of Indian Pulp and Paper Technical - A*, vol. 30, no. 7, pp. 934–938, 2018.

[19] C. Arslanolu and A. Mor, "An analysis on the reading habits of university students studying physical education and sports training," *World Journal of Education*, vol. 8, no. 4, pp. 102–110, 2018.

[20] N. Kumyaito, P. Yupapin, and K. Tamee, "PERSONALIZED SPORTS TRAINING PLANS WITH PHYSIOLOGICAL CONSTRAINTS USING THE \varepsilon-CONSTRAINT METHOD WITH A GENETIC ALGORITHM," *Far East Journal of Electronics and Communications*, vol. 17, no. 2, pp. 475–496, 2017.

Hindawi
Scientific Programming
Volume 2022, Article ID 1297274, 9 pages
https://doi.org/10.1155/2022/1297274

Research Article

A Visual Recognition and Path Planning Method for Intelligent Fruit-Picking Robots

Hongli Li

Department of Electromechanical and Vehicle Engineering, Zhengzhou Institute of Engineering and Technology, Zhengzhou, Henan 450044, China

Correspondence should be addressed to Hongli Li; 20081057@zzut.edu.cn

Received 5 March 2022; Revised 19 March 2022; Accepted 23 March 2022; Published 14 April 2022

Academic Editor: Muhammad Zakarya

With the rapid development of economy and the increasing improvement of agricultural production level, people's demand for fruits is also increasing year by year. China is the largest fruit production and consumption country in the world. According to relevant statistics reported for China, by the end of 2019, the total amount of various fruits sold had reached about 270 million tons, with apples accounting for 48% of the global output and pears accounting for 69% of the national total output. However, China's fruit picking is still dominated by manual picking process, which takes a lot of manpower and time to complete, therefore resulting in low fruit picking efficiency. Some farmers are unable to complete fruit picking in a short time, resulting in a large number of fruits unable to be listed, resulting in huge losses. To solve this problem, this paper focuses on the visual recognition and path planning for intelligent fruit-picking robot. Using robot to complete fruit picking is the best way at present. This paper establishes a picking robot recognition and positioning system based on stereo vision, which is used to identify and locate the fruits planted in the orchard area. The coordinate error of the target point of the intelligent fruit-picking robot coordinate system is less than 10 mm, which has high accuracy. Then, the path of intelligent fruit-picking robot is planned based on visual feedback algorithm and biological stimulation neural network. Our empirical evaluations suggest that the proposed robot walks in the planting park in the shape of "zigzag" and realizes full-coverage path planning after 6 turns. The results show the efficiency of the intelligent method.

1. Introduction

The most important type of agricultural robot is the picking robot, which has great development potentials. However, there is no accurate definition of fruit and vegetable harvesting robot. Generally, the picking robot only completes the picking of vegetables and fruits and realizes the basic work of crop picking, packaging, and transportation by programming. It has strong automatic mechanical and perception abilities. It is an interdisciplinary frontier discipline, which involves electronics, machinery, information, agriculture, computer science, biology, and intelligent technology including artificial intelligence and machine learning techniques. At the same time, we should master the knowledge of mechanical structure, sensors, visual image technology, and other related fields in the context of decision making and implementation.

At present, agricultural production is also developing towards diversification, scale, and accuracy, and the cost of agricultural labor continues to increase, resulting in labor shortage and increased costs. Robot technology has become the main way to solve agricultural problems, in particular, when picking fruits for packaging and exporting. Through improving the automation of orchard fruits and vegetables, the automation of farmers' orchard planting and picking can be improved. At the same time, it can accurately identify and plan the picking path and greatly improve the efficiency of fruit and vegetable picking, which is of great value to promote the development of agricultural services and their modernization (i.e., intelligent agriculture).

The innovations of this paper in studying the visual recognition and path planning for intelligent fruit-picking robot are as follows: (1) establish a picking robot recognition system based on stereo vision, which uses a binocular stereo vision technology to identify and locate the fruit in the orchard. Furthermore, the method subsequently uses a fuzzy-based, two-dimensional entropy algorithm to identify the obstacles in the orchard, which can accurately identify and locate the specific positions of the fruit in the orchard—and it is a key part of the fruit picking. (2) Because the characteristics of the orchard plant planting are parallel rows and columns, therefore a biological stimulation neural network method is used to plan the optimal path of the global coverage of the intelligent fruit picking robot. The robot takes the shape of "zigzag" when picking fruits so that the picking robot can plan the optimal safe path in a short time and shorten the fruits' picking time. The following are the major contributions of this research.

(i) Establish a picking robot recognition and positioning system based on stereo vision.

(ii) Use fuzzy two-dimensional entropy algorithm to identify the obstacles in the orchard.

(iii) The biological stimulation neural network method is used to plan the optimal path of the global coverage of the intelligent fruit-picking robot.

The rest of the paper is organized as follows. In Section 2, we offer an overview of the related work. Section 3 is about the recognition and positioning system of picking robot based on stereo vision. In Section 4, trajectory planning of picking robot based on visual feedback is discussed. Section 5 illustrates the results of visual recognition and path planning of intelligent fruit picking robot. Finally, Section 6 concludes this paper along with future work.

2. Related Work

In the 1960s, Zhang and Chaisattapagon proposed to use robots for the purpose of picking fruits. Since then, fruit-picking robots have become increasingly mature with the development of decades [1]. It takes tens of seconds to pick successfully at first, but now it can be completed within 10 seconds [2]. The way of picking fruits is to separate fruit trees from fruits by mechanical vibration. This way has high picking efficiency. However, it will damage the fruits and it is difficult to ensure the quality of fruits [3]. In recent years, computer technology and electronic information technology have developed rapidly, especially artificial intelligence, machine learning, and image processing. Fruit picking robots are more intelligent [4]. Barnett et al. developed a fruit-harvesting auxiliary equipment based on Orsi ecological picking mobile platform [5]. This equipment is widely used in small- and medium-sized orchards and can assist in picking all kinds of fruits. It cannot be completed automatically in actual operation. Special personnel must lift the platform and mobile equipment. Moreover, similar devices should be operated by a computer application that has more control over the fruit-picking task and can guide them more intelligently through machine learning methods.

Wang et al. developed a shaking apple-picking robot [6], which surrounds the whole fruit tree from both sides and then vibrates the trunk area of the fruit tree with high frequency. The fruit falls from the fruit tree to the V-shaped collection device, and then the collection device is closed to complete the fruit picking. Chen et al. developed a negative-pressure clamping apple-picking robot [7]. The main body of the picking machine on this robot is a six-degree-of-freedom industrial robot, which can move the arm freely in a large area and install a micro camera at the end of the robot arm to collect the fruit position [8]. Feng et al. have developed a conceptual prototype of an apple-picking robot with a degree of freedom of 6 to automatically pick fruit in the orchard. The average cycle of picking fruit is 5–9 s [9]. The research time of picking robots in China is relatively short, and now the vast majority of picking robots cannot be applied in the market. Su et al. established the mobile system of apple-picking robot based on Voyager IIA and ARM11 + Windows CE and explored the visual obstacle detection technology in Apple Park. Furthermore, the proposed approach puts forward the path planning method of mobile robot based on biological stimulation neural network and uses a BP neural network to complete the navigation control algorithm. However, this technology cannot run in an embedded computer system [10, 11].

Li et al. deeply investigated and studied the forward kinematics and inverse kinematics of the mechanical arm and suggested an approach that completes the trajectory interpolation algorithm of the picking arm, which uses LQR for zoning control according to the basic constraints of trajectory planning, and completes the fuzzy trajectory tracking control. Based on the HOO stability control algorithm, Li et al. analyzed the control mode of the stable picking arm so as to effectively suppress the "shaking" problem of the apple-picking robot arm. However, the problem of arm motion planning and obstacle avoidance has not been deeply explored in the existing literature [12, 13]. Furthermore, machine learning-based methods are also not investigated in terms of fruit picking robots (location and position) and their accuracies.

3. Recognition and Positioning System of Picking Robot Based on Stereo Vision

3.1. Building an Independent Picking System. This paper constructs an intelligent fruit picking robot system, which consists of vision system [14], industrial robot, computer, and end effector. The vision system carried on the robot adopts the stereo vision product Bumblee2 manufactured by PGR company. The baseline length is 120 mm. The left and right lenses are perpendicular to the baseline and parallel to the optical axis. The lens adopts 1/3-inch Sony icx204 color CCD lens, which can be automatically synchronized, with a focal length of 3.8 mm. It connects the computer and IEEE-1394 to transmit data. It can search and locate the picking target in a certain area and is applied in the visual navigation of the rear mobile fruit picking robot. The end effector is

manufactured by German Schunk company, and the clamping force is guaranteed to be in a constant state. Finally, the system forms an open-loop visual control system. The control quantity of the robot controller is calculated based on the stereo vision information. It runs outside the control cycle, and the calculation times are only once, which is shown in Figure 1.

3.2. Identification and Location of Fruits. During fruit-picking process, the end effector of the intelligent fruit-picking robot determines the working position according to the fruits' target. Nowadays, various common methods of fruit picking are pure air suction picking, finger grasping picking, combined air suction, finger picking, and so on. [15–17]. In this paper, the electric gripper is selected to clamp the fruit, and then the fruit is picked by twisting the fruit handle. Therefore, the fruit center of gravity of the band actuator should be perpendicular to the working center of the gravity so that the fruit could be positioned according to the fruit center of gravity [18, 19].

The reliability and accuracy of fruit positioning in binocular stereo vision technology are disturbed by various factors, including various uncontrollable factors. If the real shape and ambient light lead to random distributions of invalid matching points during stereo vision matching, then it is difficult to obtain depth information. This can potentially be resulting in failure to complete fruit picking. In this paper, the depth of difficult matching points is set to 0.385 m through the stereo vision module [20]. Furthermore, approximately 70% of the fruits are spherical, which can avoid the above problems of stereo vision technology. The three-dimensional position information of different points on the target is used to construct the fruit ball model, and then the position of the fruit center of gravity is calculated by the least square method. The following is the calculation formula of the fruit ball model:

$$(x-a)^2+(y-b)^2+(z-c)^2=R^2. \tag{1}$$

If the coordinates of the spherical center in the camera coordinate system are (a, b, c), formula (1) can be converted to the following formula:

$$2ax+2by+2cz+R^2-\left(a^2+b^2+c^2\right)=x^2+y^2+z^2. \tag{2}$$

If there are n points, then they are expressed in the matrix form. The above formula can be illustrated as follows:

$$\begin{bmatrix} 2x_1 & 2y_1 & 2z_1 & 1 \\ 2x_2 & 2y_2 & 2z_2 & 1 \\ \cdots & \cdots & \cdots & \cdots \\ 2x_n & 2y_n & 2z_n & 1 \end{bmatrix} \begin{bmatrix} a \\ b \\ c \\ R^2-\left(a^2+b^2+c^2\right) \end{bmatrix} = \left[\, x_1^2+y_1^2+z_1^2 \;\; x_2^2+y_2^2+z_2^2 \;\; \cdots \;\; x_n^2+y_n^2+z_n^2 \,\right]^T. \tag{3}$$

The above formula is simplified as

$$Am=B. \tag{4}$$

m is calculated by the least-squares method:

$$m=\left(A^TA\right)^{-1}A^TB. \tag{5}$$

Through the above calculation, the spherical center coordinates are obtained.

In this paper, eight different points on the target are selected to calculate the target position, and the shape of the fruit is described as a circle. Based on Hough transform, the center coordinates (i, j) and radius R of different fruits on the image plane can be obtained. This method can accurately identify the center of the fruit and simply obtain the circumscribed rectangle of the outer circle of the fruit. The coordinates of the upper left point and the lower right point of the rectangle are $(x_{\min}, y_{\min})$, $(x_{\max}, y_{\max})$, respectively. Finally, the (x, y) points in the rectangular area are randomly selected. The entire process of fruit recognition program is shown in Figure 2.

3.3. Obstacle Recognition Based on Fuzzy Two-Dimensional Entropy. Different illumination and imaging resolution will interfere with the accuracy of target detection, resulting in the integration of pixels such as image boundary, edge, and region, showing an intermediate transition phenomenon, so the image has strong fuzziness in the natural environment. Image processing itself has the disadvantage of uncertain information. At the same time, there are many fuzzy information after image processing. Therefore, the fuzzy processing algorithm can be selected when dealing with the problem of identifying obstacles in the natural environment.

Assume that the size of a gray image is $M \times N$. The gray value of (m, n) pixel coordinates is represented by X_{mn}, L is the gray level series, and a is any fuzzy set A, μA (X_{mn}) is the fuzzy membership function of set a, that is, the degree of fuzzy set a to which the gray value of X_{mn} pixels on the image belongs.

The background or target on the image is represented by set A, which is used to segment the gray image threshold; that is, select a threshold to divide the image into two parts: target and background image. Assuming A_1 as the target and A_2 as the background, the following formula represents the image blur line H:

$$H=-P(A_1)\log P(A_1)-P(A_2)\log P(A_2). \tag{6}$$

The above formula $P(A_1)$ represents the probability of occurrence of A_1 fuzzy event, $P(A_2)$ represents the probability of occurrence of A_2 fuzzy event, and $P(A_1)+P(A_2)=1$.

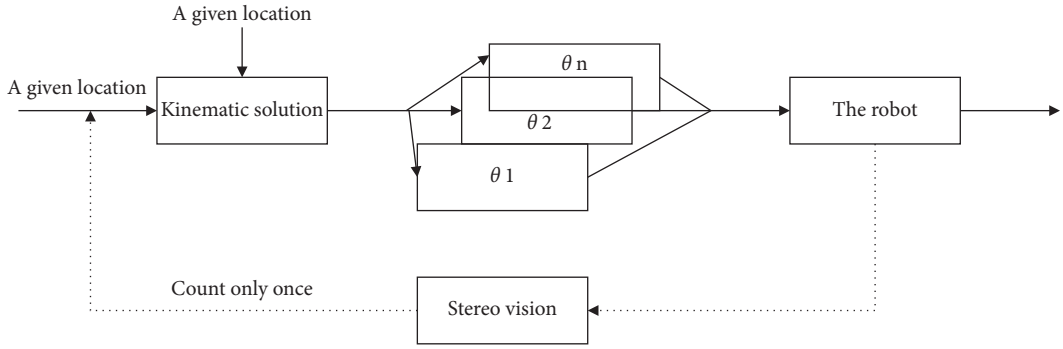

Figure 1: Open-loop visual control system.

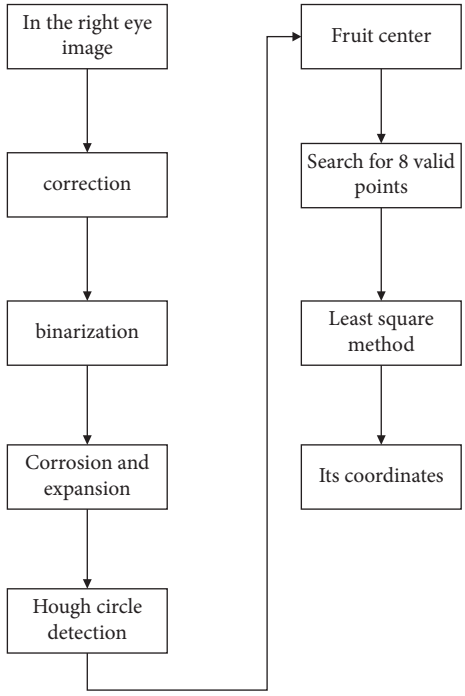

Figure 2: Flowchart of fruit identification and positioning.

If $P(A_1) + P(A_2) = 0.5$, the value of *di h* is the highest; that is, *di h* is the highest at the same time.

$$P(A_1) = \frac{1}{MN}\sum_{m=1}^{M}\sum_{n=1}^{N}\mu A_1(x_{mn}),$$
$$P(A_2) = \frac{1}{MN}\sum_{m=1}^{M}\sum_{n=1}^{N}\mu A_2(x_{mn}). \quad (7)$$

Upper formula $\mu_{A1}(x_{mn})$ represents the fuzzy membership function of the detection target, $\mu_{A2}(x_{mn})$ is the background fuzzy membership function, and $\mu_{A1}(x_{mn}) + \mu_{A2}(x_{mn}) = 1$.

4. Trajectory Planning of Picking Robot Based on Visual Feedback

4.1. Global Path of Picking Robot. Suppose the end effector of the fruit robot wants to pick n fruits, and its coordinates can be expressed as $\{g_1, g_2, \ldots, g_n\}$, where g_1 represents the initial departure and returns to *gi* after picking. It is assumed that the distance between any two points including the starting point and the target point is represented by $d(gi, gj)$. Then, the picking path planning problem is described as follows: Let $x = \{1, 2, \ldots, n\}$ be a subset of search integers, where X is the corresponding number of n fruits:

$$T_d(C) = d\left(g_{c_1}, g_{c_2}\right) + \sum_{n=2}^{n-1} d\left(g_{c_i}, g_{c_{i+1}}\right) + d\left(g_{c_n}, g_{c_j}\right). \quad (8)$$

In this paper, genetic algorithm is used to calculate the minimum value.

4.2. Mathematical Model of Genetic Algorithm. Genetic algorithm (GA) refers to taking the solution set of a problem as a population and improving the quality of the solution through genetic operations such as crossover, selection, and mutation. American scholars first proposed genetic algorithm, which has the advantages of strong universality, simple calculation process, and strong robustness. It can quickly deal with nonlinear and complex problems that traditional search algorithms cannot deal with. The other two characteristics of this genetic algorithm are global search and parallelism. That is, the following is the calculation expression of genetic algorithm:

$$SGA = (C, E, P_0, M, \Phi, \Gamma, T). \quad (9)$$

In the above formula, C represents the individual coding method, E denotes the individual fitness evaluation function, and P_0 represents the initial population. Similarly, M represents the population size, Φ denotes the selection operator, Γ stands for the crossover operator, and T represents the termination condition of the genetic operation. The basic flowchart of the genetic algorithm is shown in Figure 3.

4.3. Fruit-Picking Sequence Planning Based on Genetic Algorithm. This paper uses binocular stereo vision to recognize 9 different positions of fruits on the tree, and the positions are transformed into robotic positions, which are shown in Table 1 below (in terms of *x*-, *y*-, and *z*-axes). This should be noted that in the number column; 1 represents the initial position of the robot, and the remaining nine values

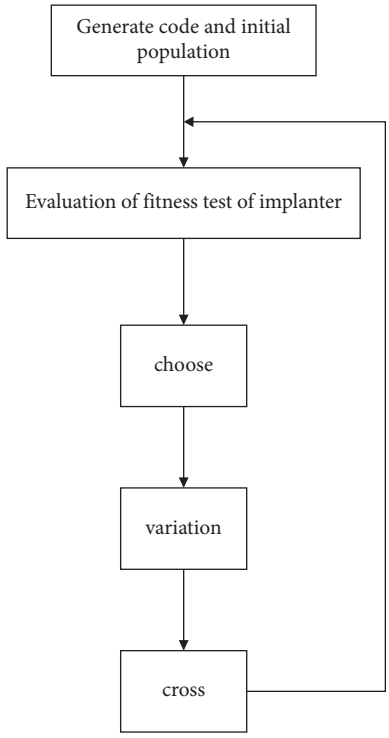

Figure 3: Flowchart of genetic algorithm.

Table 1: Fruit coordinate position.

Number	X (mm)	Y (mm)	Z (mm)
1	723.12	1.94	272.85
2	945.28	565.71	246.32
3	1218.37	821.76	284.64
4	1114.02	663.27	525.16
5	1176.55	848.75	289.75
6	849.22	656.74	536.49
7	1113.12	469.32	199.24
8	945.28	533.02	525.46
9	1164.08	545.37	480.02
10	1162.27	702.64	626.93

are numbered as fruit picking positions [21]. Furthermore, the value of M is 20, the value of q_c is 0.9, and the value of q_m is 0.1. We can substitute these predefined parameters and values into the above formula in order to calculate the best path, as given by $C = \{1, 8, 6, 10, 4, 9, 3, 5, 2, 7, 1\}$.

Figure 4 shows the picking path planning of intelligent fruit-picking robot; l is its shortest path, and the length is 2846 mm.

The basic picking path of the fruit intelligent picking robot is to arrange the coordinate origin of the fruit robot first, then pick the fruit from far to near, and then return to the initial position. The picking path based on this method is given by $C' = \{1, 2, 6, 8, 7, 9, 4, 10, 3, 1\}$. After calculation, the path is computed as given by $L^* = 3202.5$ mm. Therefore, L is greater than L^*, which shows that the genetic algorithm has certain significance for the path planning of the fruit robot. Moreover, this illustrates that it can improve the operation efficiency of the fruit picking robot, and the amount of work is also lower than that of other methods.

4.4. Path Planning Based on Biological Stimulation Neural Network

4.4.1. Neural Network Dynamic Model of Biological Stimulation. Based on the biological stimulation neural network, the connection relationship between neurons and external inputs in the dynamic environment is defined, and the targets and obstacles corresponding to the lowest end are distributed at the top of the neural activity state diagram. The neuron activities that are easy to be constrained by kinematics are used to spread so as to attract the robot in the global space. Obstacles in the neural activity state diagram can only be partially avoided by the robot [22]. The dynamic neuron activity state diagram based on neural network, combined with the incomplete kinematic constraints of the robot, can reasonably plan the robot path for autonomous obstacle avoidance [23].

In 1952, Huxley and Hodgkin first used circuit elements to build a small dendritic cell membrane calculation model based on biological nervous system. The following is the expression of dynamic voltage V_m passing through the cell membrane:

$$C_m \frac{dV_m}{dt} = -\left(E_p + V_m\right) g_p + \left(E_{Na} + V_m\right) g_{Na} - \left(E_k + V_m\right) g_k. \tag{10}$$

In the above formula, C_m represents the cell membrane capacitance, Ek represents the potassium ion saturation potential on the cell membrane, E_{Na} represents the sodium ion saturation potential in the cell membrane, and Ep represents the neutral leakage current saturation potential; g_k represents potassium ion conductivity, g_{Na} represents sodium ion conductivity, and g_p represents neutral channel conductivity.

4.4.2. Motion Control. The intelligent fruit-picking robot should complete the steering control and obstacle avoidance control when picking fruit in the planting park. Based on the analysis and derivation of error mechanics, the path planning control of the rear driving wheel of the robot is obtained. It is assumed that the reference speed of the robot is Vr and the angular speed is determined by ωr which both robot speeds are calculated by the following formulas [24]:

$$\begin{aligned} v &= c_1 e_D + v_r \cos e_\theta, \\ \omega &= \omega_r + c_2 v_r e_L + c_3 v_d \sin e_\theta. \end{aligned} \tag{11}$$

In the above equations, $C1$, $C2$, and $C3$ represent positive gain parameters, e_D represents driving direction, e_L represents new direction, and e_θ indicates steering angle and direction error.

4.4.3. Path Planning. Based on the biological stimulation neural network method, the intelligent fruit-picking robot

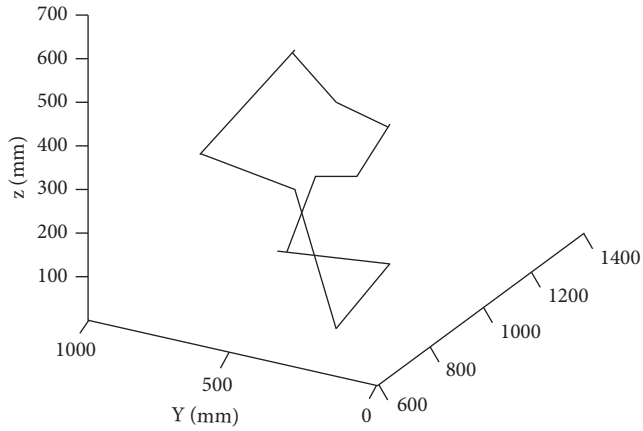

Figure 4: Optimal picking sequence diagram of fruit intelligent picking robot.

needs to walk in the botanical garden with complex environment under the condition of no control. Here, it is necessary to use biological stimulation neural network in the static plantation, and the number of static obstacles in each row of the park is less. The walking route of the intelligent fruit picking robot is "Zhi," and it traverses each row of plants planted until it stops at the position of the picking robot. The number of discrete topological tissue neurons in the biological stimulation neural network architecture is 32×32, assuming that the upper bounds B and D of external stimulation are both 1, ωij parameters in the latest connection weight μ. The value of μ is 0.7, the value of r_0 is 2, the calculated value of C is 0.35, and the value of neuron external input parameter E is 100. In Figure 5 below, two groups of obstacles with different sizes are selected, and the intelligent fruit-picking robot moves upward from the initial position of point $P(1, 1)$. The external input Ii of obstacle neurons in static environment is represented by E, and the values of other neurons are 0. If the intelligent fruit picking robot passes through any point, and the reset result of the external input of the neuron at this point is 0, it indicates that the picking work in the cost area has been completed.

In Figure 5 above, the intelligent fruit picking robot starts picking from the bottom to the top and then walks from the top to the bottom in a zigzag shape between planting lines. The steering angle values of the intelligent fruit picking robot are listed in Table 2. The results in the table show that the intelligent fruit robot has to undergo six turns after encountering two groups of obstacles during the picking period and to realize the full-coverage path planning [25].

5. Results of Visual Recognition and Path Planning of Intelligent Fruit-Picking Robot

5.1. Visual Recognition Analysis of Intelligent Fruit-Picking Robot. In this paper, the following translation matrix can be obtained by recording the end motion distance of the fruit intelligent robot with camera:

$$\begin{bmatrix} P_x & P_y & P_z \end{bmatrix}^T = \begin{bmatrix} -401.602 & 720.326 & 343.479 \end{bmatrix}. \quad (12)$$

The calibrated coordinates are obtained in the robot coordinate system, and then the end position is taught at the target position, and the robot base coordinates are read by the teaching pendant [26]. Based on the binocular stereo vision module, the fruit image is collected and stored. Next, the image coordinates of the calibration object center are marked through the system drawing tool, and then the two-dimensional coordinates (u, v) of the calibration object center are substituted into the stereo vision module to establish the three-dimensional library function and calculate the setting value of the camera coordinate system. In this experiment, ten calibration points were selected, which are shown in Table 3, and the mapping matrix T between the camera coordinates and the robot is obtained through using the least square method, as explained in earlier sections.

The mapping matrix of the intelligent fruit robot in the camera coordinate system is obtained by programming and calculating with MATLAB software, as follows:

$$T = \begin{bmatrix} 0.0182 & 0.0041 & 0.9923 & -401.62 \\ -0.9923 & 0.0295 & 0.0498 & 720.62 \\ -0.0009 & -0.9754 & 0.0127 & 343.429 \\ 0 & 0 & 0 & 1 \end{bmatrix}. \quad (13)$$

The mapping matrix is obtained after the verification of this experiment. The position of the teaching target point at the end of the fruit intelligent robot can be obtained by using the above calibration method, and the corresponding three-dimensional coordinate measurement value can be obtained. However, there is an error between the calculated value of the target point in the intelligent fruit robot coordinate system and the actual measurement value. This error is called calibration error, which is shown in Figure 6 below.

According to the experimental results, the maximum calibration error of different components on the target position coordinates of the fruit intelligent robot coordinate system is less than 10 mm. However, the error belongs to the comprehensive error, which also includes the error in the measurement process of the stereo vision module. The following are the two main factors that interfere with the calibration accuracy:

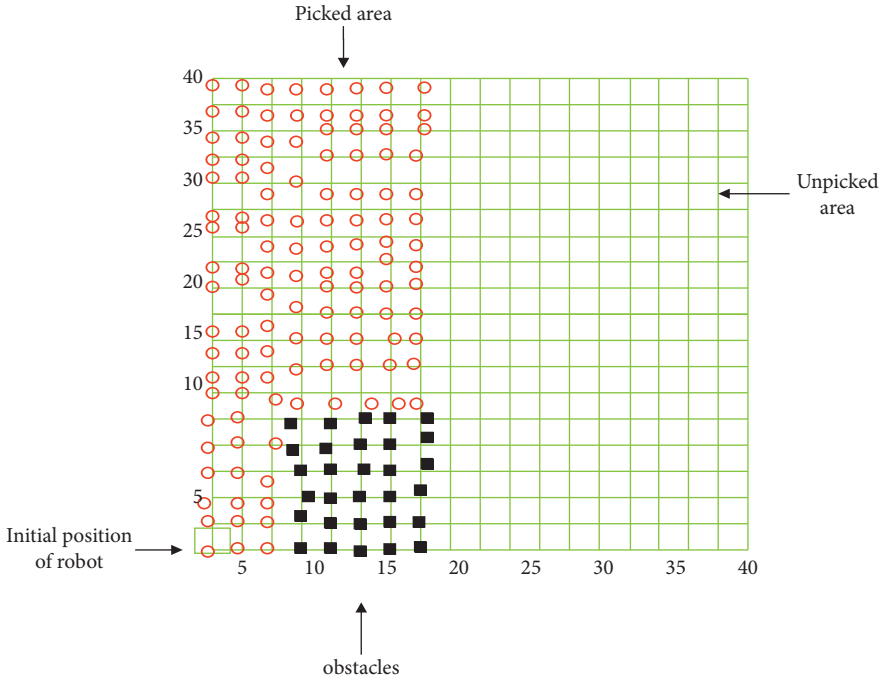

Figure 5: Full-coverage path planning.

Table 2: Robot motion angle.

The difference between the x-coordinates	The difference between the coordinates	θ
0	−1	5
0	1	1
1	−1	4
1	0	3
1	1	2

Table 3: Calibration point camera and robot coordinates.

Number	Camera coordinate system			Robot coordinate system		
	X_c (mm)	Y_c (mm)	Z_c (mm)	X_r (mm)	Y_r (mm)	Z_r (mm)
1	12.69	−14.62	1397.54	985.46	786.33	375.73
2	−203.12	−98.42	1364.35	936.65	978.32	451.14
3	8.26	−86.74	1382.11	983.52	769.43	443.26
4	−0.52	10.75	1535.45	1126.43	785.92	352.25
5	271.02	−64.17	1565.26	1156.45	520.48	425.32
6	386.99	−146.46	1594.21	1195.35	415.72	506.24
7	−34.51	−331.24	1394.71	979.43	806.92	688.73
8	272.69	−319.52	1469.17	1052.61	508.73	668.79
9	384.18	158.26	1365.27	952.47	398.37	202.87
10	232.16	56.34	1433.26	1024.15	558.37	302.86

(i) When the detection target is in the coordinate system of the fruit intelligent robot, teach the end center of the robot to the center of the target and then read the position of the robot, that is, the position of the target robot. At this time, it is difficult to coincide the target center and the end center, which interferes with the measurement accuracy and leads to considerable and nontrivial errors.

(ii) Camera 3D reconstruction and intelligent fruit-picking robot have high accuracy. However, when calibrating the system, this error will lead to gain in the calibration system and interfere with the accuracy of the calibration system. Therefore, after several groups of the measurement data, the error interference can be reduced by using the least-squares method.

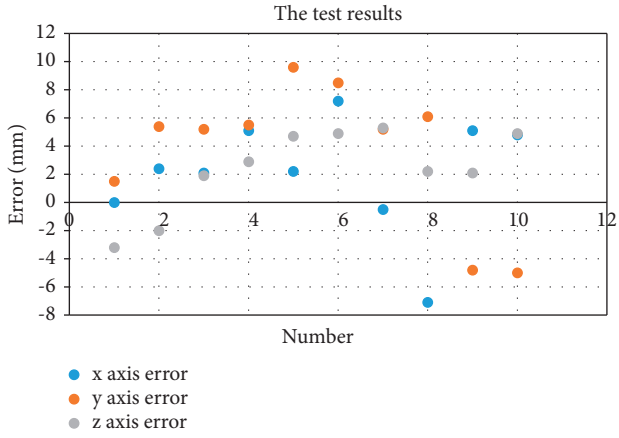

Figure 6: Test results of 10 calibrated points.

5.2. Visual Path Planning Analysis of Intelligent Fruit-Picking Robot. Due to the complexity of the park itself and the unpredictability of obstacles, it is necessary to combine with genetic algorithm and use the maximum fuzzy two-dimensional entropy to detect different types of obstacles in the orchard. The mathematical model of the genetic algorithm is established, and the fruit picking sequence is formulated according to the global picking path of intelligent fruit robot. The best picking path is calculated as $C = \{1, 8, 6, 10, 4, 9, 3, 5, 2, 7, 1\}$, of which the shortest picking path length is 2846 mm. Then, the path is planned based on the biological stimulation neural network dynamic model to realize the full path planning. The results show that the intelligent fruit robot has to go through 6 special projects to realize the full coverage of the orchard path.

When planning the full coverage path in the orchard planting area based on biological stimulation neural network, the optimal path and suboptimal path of the intelligent fruit picking robot from the starting point to the key location can be accurately obtained. When the fixed obstacles are known or there are no obstacles, then the intelligent fruit picking robot can fully cover the operation area, and its path shape is similar to the word "Zhi." This method is simple and efficient. During the path planning, it is necessary to establish a discrete topology map, which can reduce the analysis of the geometric parameters of the park, and the number of columns on the topology map can be determined only according to the number of rows in the park. Experiments show that this path planning method will not be affected by environmental obstacles. It only takes 50 ms to complete the path planning operation, and the biological stimulation neural network model does not need to learn, nor will it cause "deadlock," so it has strong universal applicability.

6. Conclusions and Future Work

At present, the problems of agriculture, rural areas, and farmers' income have attracted the attention of the state. China continues to adjust the agricultural industrial structure. The most obvious change is to expand the area of planting fruit trees. Fruit trees have become the second largest crop after grain lag. However, China's fruit and vegetable industry also faces many problems in the development process. The production technology is backward, the automation level is raised, the labor efficiency is low, and the fruit is not picked in time, which has a direct impact on the income of farmers. Aiming at this problem, this paper focuses on the visual recognition and path planning of fruit intelligent picking robot, establishes the recognition and positioning system of fruit picking robot based on three-dimensional four wonders, constructs the fruit autonomous picking system, uses binocular stereo vision technology to locate and identify the fruit, and uses fuzzy two-dimensional entropy to identify the obstacles. Then, the trajectory planning of the picking robot based on visual feedback is constructed, and the picking order is reasonably planned by using genetic algorithm. The best path is the best path $C = \{1, 8, 6, 10, 4, 9, 3, 5, 2, 7, 1\}$.

We evaluated and showed that the visual recognition system and path planning method of the intelligent fruit picking robot, established in this paper, can accurately identify the fruit position in the park and complete the picking task. In practice, the application of the robot can reduce the labor of fruit farmers and improve the efficiency of fruit picking. This takes trivial time to complete the path planning operation, and the biological stimulation neural network model does not need to learn, nor will it cause "deadlock," so it has strong universal applicability. In the future, we will integrate machine learning-based intelligent algorithms for decisions making of the fruit picking robots. Moreover, we will use more advanced methods to further improve the efficiency and accuracy of the robots in order to increase the farmer's profit and decrease the labor efforts.

Data Availability

The data can be requested from the corresponding author.

Conflicts of Interest

The authors declare that they have no conflicts of interest regarding the publication of this paper.

Acknowledgments

This study was supported by the Project of Young Backbone Teachers in Henan Province Colleges and Universities (2021GGJS182): Research on Control System of Intelligent Fruit-Picking Robot Based on Binocular Vision.

References

[1] N. Zhang and C. Chaisattapagon, "Effective criteria for weed identification in wheat fields using machine vision," *Transactions of the ASABE*, vol. 38, no. 3, pp. 965–974, 1995.

[2] X. Y. Cheng and X. Song, "Review on visual system of fruit and vegetable picking robot," *Journal of Zhejiang Agricultural Sciences*, vol. 60, no. 3, pp. 490–493, 2019.

[3] P. Satyam, P. Satyam, A. Ajay, and K. Davood, "Fuzzy tuned PID controller for envisioned agricultural manipulator,"

International Journal of Automation and Computing, vol. 18, no. 4, pp. 568–580, 2021.

[4] L. F. Luo, X. J. Zou, T. C. Cheng, and Z. Yang, "Design of virtual test system based on hardware-in-loop for picking robot vision localization and behavior control," *Transactions of the Chinese Society of Agricultural Engineering*, vol. 33, no. 4, pp. 39–46, 2017.

[5] J. Barnett, M. Duke, C. K. Au, and S. H. Lim, "Work distribution of multiple Cartesian robot arms for kiwifruit harvesting," *Computers and Electronics in Agriculture*, vol. 169, no. 2, Article ID 105202, 2020.

[6] C. Wang, Y. Wan, and G. Wang, "Development of control system for a picking robot used in plate flame cutting," *Research and Exploration in Laboratory*, vol. 36, no. 4, pp. 41–44, 2017.

[7] M. Chen, H. Zhang, and X. Wang, "Design of apple picking robot based on iterative learning PID algorithm," *Journal of Agricultural Mechanization Research*, vol. 42, no. 6, pp. 83–86, 2020.

[8] J. Li, Y. Mi, and G. Li, "CNN-based facial expression recognition from annotated RGB-D images for human-robot interaction," *International Journal of Humanoid Robotics*, vol. 16, no. 4, Article ID 19410021, 2019.

[9] Q. Feng, W. Zou, P. Fan, and X. Wang, "Design and test of robotic harvesting system for cherry tomato," *International Journal of Agriculture and Bioengineering*, vol. 11, no. 1, p. 5, 2018.

[10] Y. Su, L. Yang, and X. Song, "Design and experiment of intelligent mobile apple picking robot," *Journal of Agricultural Mechanization Research*, vol. 2016, no. 1, pp. 159–162, 2016.

[11] A. Abdi, M. H. Ranjbar, and J. H. Park, "Computer vision-based path planning for robot arms in three-dimensional workspaces using Q-learning and neural networks," *Sensors*, vol. 225, no. 5, p. 1697, 2022.

[12] S. Y Li and N Huang, "High precision control simulation of spherical fruit picking robot," *Computer Simulation*, vol. 36, no. 10, pp. 302–306, 2019.

[13] J. Xin, "Application of deep reinforcement learning in mobile robot path planning," in *Proceedings of the Chinese Automation Congress (CAC)2017*, 20-22 Oct.2017.

[14] M. Hamroun, K. Tamine, and F. Claux, "A new content-based image retrieval system using deep visual features," *International Journal of Image and Graphics*, vol. 2021, no. 4, Article ID 2150055, 2021.

[15] J. Wang, B. Li, Z. Li, I. Zubrycki, and G. Granosik, "Grasping behavior of the human hand during tomato picking," *Computers and Electronics in Agriculture*, vol. 180, no. 6, Article ID 105901, 2021.

[16] Y. Tang, M. Chen, C. Wang et al., "Recognition and localization methods for vision-based fruit picking robots: a review," *Frontiers of Plant Science*, vol. 11, p. 510, 2020.

[17] X. Cao, X. Zou, C. Jia, M. Chen, and Z. Zeng, "RRT-based path planning for an intelligent litchi-picking manipulator," *Computers and Electronics in Agriculture*, vol. 156, pp. 105–118, 2019.

[18] K. Wei and B. Ren, "A method on dynamic path planning for robotic manipulator autonomous obstacle avoidance based on an improved RRT algorithm," *Sensors*, vol. 18, no. 2, p. 571, 2018.

[19] H. Yang, L. Chen, Z. Ma et al., "Computer vision-based high-quality tea automatic plucking robot using Delta parallel manipulator," *Computers and Electronics in Agriculture*, vol. 181, Article ID 105946, 2021.

[20] J. Peng, X. F. Gao, and H. Q. Long, "A parameter measurement method for autonomous-rail rapid tram based on four-view stereo vision," *Journal of Chongqing University*, vol. 44, no. 4, pp. 29–36, 2021.

[21] Q. Q. Ping, Y. Liu, and X. M. Dong, "3-D reconstruction of texture less and high-reflective target by polarization and binocular stereo vision," *Journal of Infrared and Millimeter Waves*, vol. 36, no. 4, pp. 432–438, 2017.

[22] A. Mas U Mori, L. Sinapayen, and N. Maruyama, "Neural autopoiesis: organizing self-boundary by stimulus avoidance in biological and artificial neural networks," *Artificial Life*, vol. 2020, no. 4871, pp. 1–22, 2020.

[23] T. D. Griffith and J. E. Hubbard, "System identification methods for dynamic models of brain activity," *Biomedical Signal Processing and Control*, vol. 68, no. 3, Article ID 102765, 2021.

[24] Y. Lee and M. Yinman, "Adaptive interference suppression of phase-only thinned arrays via convex optimization," *IEEE Transactions on Antennas and Propagation*, vol. 68, no. 6, pp. 4583–4592, 2020.

[25] L. Paull, M. Seto, J. J. Leonard, and H. Li, "Probabilistic cooperative mobile robot area coverage and its application to autonomous seabed mapping," *The International Journal of Robotics Research*, vol. 37, no. 1, pp. 21–45, 2018.

[26] Y. Pan, C. Chen, D. Li, Z. Zhao, and J. Hong, "Augmented reality-based robot teleoperation system using RGB-D imaging and attitude teaching device," *Robotics and Computer-Integrated Manufacturing*, vol. 71, no. 4, Article ID 102167, 2021.

Hindawi
Scientific Programming
Volume 2022, Article ID 2195646, 10 pages
https://doi.org/10.1155/2022/2195646

Research Article

Secure and Efficient Data Storage Operations by Using Intelligent Classification Technique and RSA Algorithm in IoT-Based Cloud Computing

Faiqa Sajid,[1] **Muhammad Abul Hassan**,[2] **Ayaz Ali Khan**,[3] **Muhammad Rizwan**,[1,4] **Natalia Kryvinska**,[5] **Karovič Vincent**,[5] **and Inam Ullah Khan**[6]

[1]*Department of Computer Science, Kinnaird College for Women, Lahore 54000, Pakistan*
[2]*Department of Computing and Technology, Abasyn University, Peshawar 25000, Pakistan*
[3]*Department of Computer Science, University of Lakki Marwat, Lakki Marwat, Pakistan*
[4]*Secure Cyber Systems Research Group, WMG, University of Warwick, Coventry CV4 7AL, UK*
[5]*Information Systems Department, Faculty of Management Comenius University in Bratislava, Odbojárov 10, Bratislava 82005, Slovakia*
[6]*Department of Electronic Engineering School of Engineering & Applied Sciences (SEAS), Isra University, Islamabad Campus, Islamabad, Pakistan*

Correspondence should be addressed to Muhammad Abul Hassan; abulhassan900@gmail.com

Received 7 February 2022; Revised 7 March 2022; Accepted 16 March 2022; Published 14 April 2022

Academic Editor: Muhammad Zakarya

In mobile cloud services, smartphones may depend on IoT-based cloud infrastructure and information storage tools to conduct technical errands, such as quest, information processing, and combined networks. In addition to traditional finding institutions, the smart IoT-cloud often upgrades the normal impromptu structure by treating mobile devices as corporate hubs, e.g., by identifying institutions. This has many benefits from the start, with several significant problems to be overcome in order to enhance the unwavering consistency of the cloud environment while Internet of things connects and improves decision support system of the entire network. In fact, similar issues apply to monitor loading, resistance, and other security risks in the cloud state. Right now, we are looking at changed arrangement procedures in MATLAB utilizing cardiovascular failure information and afterward protecting that information with the assistance of RSA calculation in mobile cloud. The calculations tried are SVM, RF, DT, NB, and KNN. In the outcome, the order strategies that have the best exactness result to test respiratory failure information will be recommended for use for enormous scope information. Instead, the collected data will be transferred to the mobile cloud for preservation using the RSA encryption algorithm.

1. Introduction

Advancements in smart world have upgraded every industry. Intercommunication is the problem where desired results need to be obtained from implementing line models. Today's modern industry is comprised of complex system models which intend to improve over-all process. Sustained advancement in such industry required reliability and efficiency to Decision Support Systems (DSSs) [1].

The Internet is regarded as the most important invention since it allows users to make inter- and intra-connections among conventional and portable devices using various protocols [2]. Internet of things has newly emerged in last few decades. A large number of devices generate data in IoT environment and forward it for further processing. Main problem faced by devices attached with IoT environment is security which is not properly considered during manufacturing. Moreover, these devices have limited

memory, and data generated by each device are doubled of its memory size. IoT-based cloud computing is the integrated to process huge amount of data. Figure 1 briefly describes the merger of IoT and cloud computing to enhance the decision support system.

IoT-based cloud computing technology is providing the best possible practices which are focused on market research [3].

Cloud computing usually provides tools as entities on call, snappy transmission, and charge as a need to enhance user service. This technology offers utilities which include Platform as a Service (PaaS), Infrastructure as a service (IaaS), and Software as a service (SaaS). It is most continent way to provide computation services and can be accessed remotely [4]. In addition, the primary focal points are (i) offering on-demand solutions, (ii) compensation as invoice, and (iii) administration limits [5]. IoT-based cloud computing has a variety of applications such as web-based management. However, cloud storage requires specific databases to rely on the client's need; if the client wishes to hold their knowledge in free space, cloud computing exposes the server and then the knowledge (data) needs to be checked by Decision Support System for timely and accurate measurements.

Encryption techniques are being used to ensure privacy of data in Internet of Things (IoT) cloud and ensure confidentiality. Machine Learning (ML) Algorithms are employed including Decision Tree (DT), Support Vector Machine (SVM), Naïve Bayes (NB), *K*-nearest Neighbors (KNN), and Random Forest (RF) [6]. Each of the layout strategies displays a characteristic suitability and specificity that depends on the type of dataset [7]. Moreover, there are different assessment measurements for looking at the characterization techniques that every one of them could be helpful relying upon the issue. Fundamental problems for cloud computing are (i) digital unloading, (ii) centralized implementation, and (iii) dynamics which have been extensively explored in previous compositions. A few further changes have been introduced to overhaul protection for Clouds themselves, such as protection structure [8] based on TCG [9], stable redistribution [10–13], cloud network defence [14, 15], board tool and detachment [16, 17], and insurance [18, 19]. Main concern to IoT-cloud professional organizations is to ensure the confidentiality of records created and managed by mobile gadgets or cloud server [20]. Data/report confidentiality is very critical to the data/record holder because it may include some secret data.

Main contribution of this research study is as follows:

(i) Five different Machine Learning Algorithms are applied to classify the dataset

(ii) RSA algorithm is utilized for the data security

(iii) Fast Encryption and Decryption

Rest of the paper is organized as follows: Section 2 provides background study and related problem. Section 3 provides proposed methodology. Section 4 provides result and discussion, and conclusion is provided in Section 5.

2. Background Study

Machine Learning algorithms are being used for training to explain how the input variables apply to the category [5]. There are various identification approaches for data such as DT, SVM, NB, KNN, RF, LogR, LR, NB, ANN, LC, decision tree, and so on [6, 21]. The association of classifiers and usage of classifier is important [22]. Support Vector Machine (SVM) finds out hyperplane (*N*-characteristics) in *N*-dimensional space which distinguishes the data points. [23]. SVM has a few favourable circumstances in which it performs very well when the differentiation between bunches is self-evident and increasingly compelling for high dimensional spaces.. Because the number of tests is more than the number of measurements, it is persuasive.

There exist several drawbacks in SVM which do not deal with massive data sets. Every data point needs to access the sum of training dataset where SVM is considered the optimal choice in comparison with *K*-nearest neighbor (KNN). However, training tuples are linked to *n*-quality which usually refers to a stage in the domain of *n*-measures. Right now, the training tuples are put in a space of *n*-dimensional progression. The KNN classifier quickly determines sample space for the *k* preparation of tuples that are the most similar to dark tuples. The *K* tuples are the nearest neighbors of the darkest tuple [24, 25]. "Closeness" is known as the separation metric, e.g., the Euclidean separation. The distinction between Euclidean and two tuples or tuples $X1 = (x_{11}, x_{12}, \ldots, x_{1n})$ and $X2 = (x_{21}, x_{22}, \ldots, x_{2n})$ is derived from the following:

$$\operatorname{dist}(X_1, X_2) = \sqrt{\sum_{i=1}^{n} (x_{1i} - x_{2i})^2}. \quad (1)$$

DT is a tree-like flowchart layout where each inner hub is a feature check and other branch is the outcome [26]. Inside a tree the top hub is the root hub.

During development, choice measures for credits are utilized to pick the best possible asset while three basic determination measures for characteristics are the knowledge, benefit ratio, and Gain index. Information gain is depicted as follows:

$$\text{Gain (E, Y)} = \text{Entropy (E)} - \text{Entropy (E, Y)}, \quad (2)$$

where E is the target variable and *Y* is the feature to be split on.

Entropy (*E*, *Y*) describes the highlighted information. Tree pruning expects to perceive and take out these branches, with the objective of improving the precision of grouping on inconspicuous information. Random Forest (RF) can be utilized for selection process. Expectations across all trees were grouped to render the last forecast; class approach is utilized to collect information and indicate relapse expectations. The suggested techniques can be used for the progression of settle tests on ultimate conclusion.

Increase in base learner numbers (*k*) will decrease variance. However, *k* is lower due to that variance increases. However, for the entire cycle, bias remains constant. The

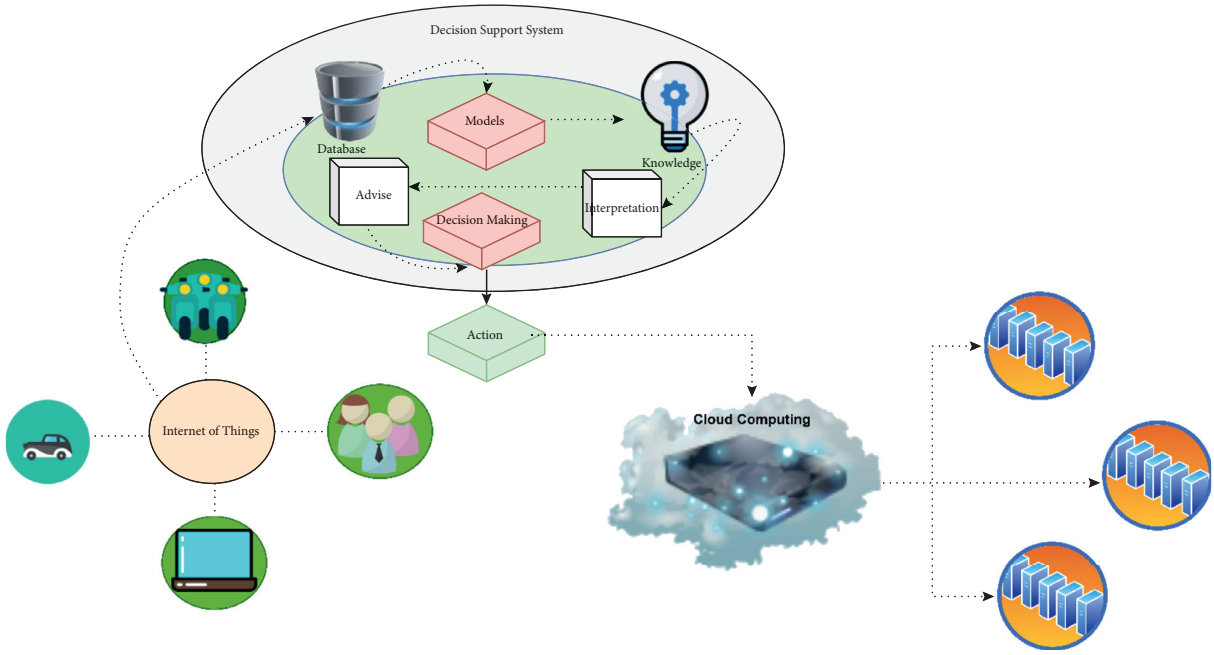

Figure 1: IoT-based cloud environment for the optimal decision support system.

cross-validation is used to find k as shown in the following equation:

$$\text{Random forest} = \text{DT (base learner)} + \text{bagging (Row sampling with replacement)} + \text{feature bagging (column sampling)} + \text{aggregation}\left(\frac{\text{mean}}{\text{median}}, \text{majority vote}\right). \tag{3}$$

Mobile computing has reduced the privacy and security concerns which usually mimic resource management [27]. Secure data organization is based on ethnicity-based intermediary which uses encryption while integrated phone applications have secured mobile data in better way. Users who store consumer data/records in IoT-based clouds use encryption and trustworthy computations. However, Diffie–Hellman key sharing, bilinear mapping, and the merkle hash tree compel the use of a stable knowledge ownership mechanism [28–31]. Table 1 describes multiple security risks which are elaborated in detail.

Provable Data Ownership (PDP) plot guarantees the clustering, confidentiality, and consistency of mobile consumer data processed on the IoT-based cloud. In Diffie–Hellman symmetric keys, key sharing is required where G1 and GT are cyclical multiplicative social activities with main recruitment q and g as generators of G1. The bilinear solution is e: G1 and G2 above GT, where G1 and GT are cyclical multiplicative social activities with main recruitment q and g as generators of G1. Merkle Hash Tree (MHT) is utilized as an analogous tree, with the leaves representing the actual results' hash calculation. The establishment of a tree must be validated by the verifier. Hyrax, a Hadoop method that facilitates cloud computing on smartphones, was created by Arockiam and Monikandan [32]. This provides a discerning approach to data exchange and suffers from a middle point of entry. Eugene in like manner executed a scattered media search and data sharing philosophy. Xu et al. [33] suggested methodology that promotes the enhancement of conventional encryption strategies by combining replacement ciphers and conversion ciphers. Both the replacement and the transposing methods used the alphabet for the cipher letter. In their proposed algorithm, plain text is initially translated to the appropriate ASCII code type of each alphabet. Rehman and Manickam [34] suggested an agent-aid paradigm by incorporating multiagent network and choice-making methodology to function load balancing problems in vast clouds. While the mentioned research, manage data sharing which boosts cloud computing efficiency through space-intensive applications, such as distributed data mining. In addition, natured inspired evolutionary computational technique (E-AntHocNet) and Fisheye State routing (FSR) can be considered for further improvements [35–37].

3. Methodology

The proposed model contains two stages. In the initial step, we pass our information to the five classification models. In

Table 1: Security risks with details.

Attacks	Explanation
Data revelation	Secure details of the owner shall be exposed to any unwanted user.
Tampering	At the point when any unapproved individual does a few changes in other client's information.
Rejection	At the point when an individual rejected in the wake of communicating something specific that he did not send it.
Virus	Those are particularly well-known threats. Those are symbols that will infect the show of a certain program.
Personality tricking	In this assault, a person mimics himself as someone who owns the details.

the second step, we can pass the highest precision model to the RSA algorithm which we proposed.

Figure 2 depicts the progression of the research that led to the development of the model. The proposed model consists of five techniques where data of patient or disease are sent directly to various classification techniques. Here, classification techniques that we use are SVM, NV, DT, RF, and KNN. SVM is accepted as the AI model utilized in characterization. Algorithm 1 shows the RSA after passing by all these techniques.

A support vector machine's objective is to achieve the most raised edge isolating hyperplane between two classes [24]. Hyperplane is never close to knowledge that focuses on different classes for greater supposition. Hyperplane has distant from the information targeting classification. Moreover, closest to the edge (classifier) is guidance for the vectors [38].

Naive Bayes utilized Bayes theorem and characterized those data, which is not known and trivial to each other. It further provides information of specific element and does not affect another in a class. In addition, likelihood of creating classification of clusters is very restrictive. For order of data, ground breaking calculation is used [25].

Random forests are an ensemble learning method for classification that involves creating a large number of option trees in a short amount of time and delivering a class. For individual trees, this strategy of classes (order) or mean forecast (relapse) is applied. Overfitting to their preparation set is caused by arbitrary tree propensity choices.

Decision Tree is based on supervised learning technique and utilized for the classification of data. Primary aim of DT is the possibility of target class. Parent node and its child nodes are used for clustering of data. DT checks for those nodes which is more gain among others [39].

These systems characterize data and generate outcomes. We consider the outcome in terms of precision. The most exact strategy is considered to be used in the future. Significances of these strategies will be examined in Result Section.

When one outcome is chosen from five possible outcomes, the information must be saved somewhere. As a result, we are sending our data to the cloud for the purpose of data compression. However, we require a secure method of sending data to the cloud. Because security is a top priority, we have implemented the RSA calculation [40] on the cloud to ensure that data are kept safe and secure.

Client data are encoded first and then stored in the mobile Cloud using the RSA technique. When necessary, the client submits a request for information to the Cloud supplier, who validates the customer and transmits the information. RSA is an encryption that prevents each message from being mapped to a number. RSA is made up of two parts: public and private keys.

3.1. Environment Setup. This research study focuses on the classification of dataset of heart patients using five different techniques. Tools which we are using for classification are SVM, NB, RF, DT, and KNN. These techniques have more roots of them, e.g., SVM have 6 types: Linear, Cubic, Quadratic, Fine Gaussian, Medium Gaussian, and Coarse Gaussian. We are using fine Gaussian SVM technique here because its accuracy is highest as compared with types. Decision Tree has 3 types further: complex tree, simple tree, and medium Tree. Among these types, complex tree has more accuracy so we are using fine tree for classification of data. The third technique which we are using is KNN. It has 6 types further: Weighted KNN, Cubic KNN, Cosine KNN, Coarse KNN, Fine KNN, and Medium KNN. So, we are using Fine KNN from k-nearest neighbor because it has more accuracy than other types of KNN. The fourth technique which we are using is Naïve Bayes. It has 2 types further: Gaussian Naïve Bayes and Kernel Naïve Bayes. So, we are using Kernel Naïve Bayes because it has more accuracy than other types of Naïve Bayes. At the last, we are using bagged trees in Random Forest because it has highest accuracy than others.

According to a recent medical assessment, if factors such as smoking, cholesterol, and diabetes are addressed in a country, people suffering from heart disease can reduce by about 15%. This Clevand data base was compiled by Robert Detrano and contains 303 occurrences of 76 attributes. Cleveland heart disease is the most commonly used dataset by data mining researchers in the UCI machine learning repository, with 76 variables. Only 11 variables have been employed by researchers to predict and analyse cardiac disorders. Table 2 shows that we have considered heart-attack dataset throughout the research. Total of 1311 instances are extracted from medical dataset. It has 11 numeric value attributes. One class has "0" value considered as negative and other class has "1" considered a positive for heart patients. The dataset originally had 76 features or qualities from 303 patients; however, published research only chose 11 features to be relevant in predicting heart disease. As a result, we will be working with a dataset of 303 patients and 11 characteristics.

Age, sex, cerebral palsy, resting blood pressure, cholesterol, fasting blood sugar test, electrocardiogram, maximum heart rate archieved, exhang, oldpeak, and outcome are attributes used in this paper shown in Table 3.

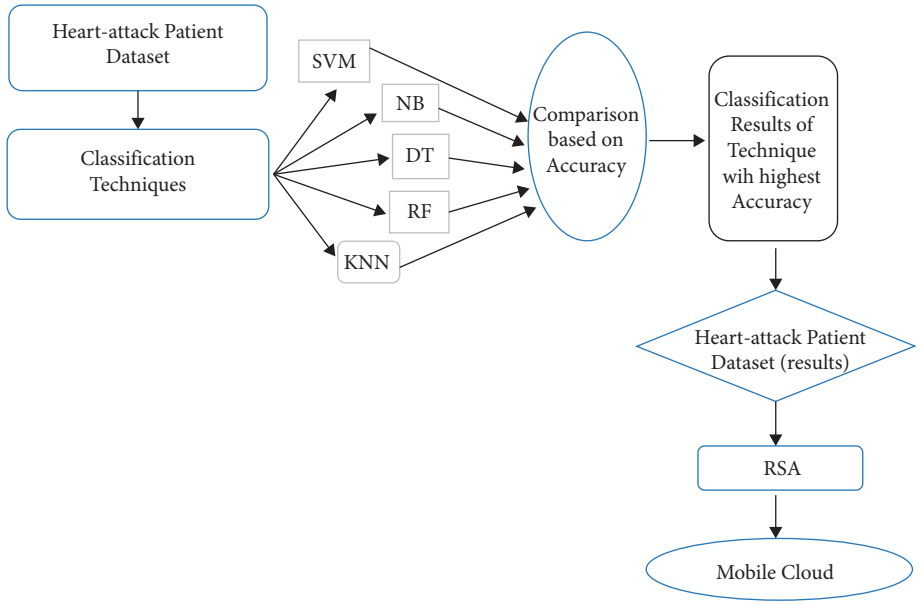

Figure 2: Model diagram of proposed technique.

(1) Start
(2) Choose P, Q where Prime $= \{P, Q\}$, $P \neq Q$
(3) Calculate S $\{S = P * Q\}$
(4) Calculate Φ (S), $\{\Phi(S) = (P-1)(Q-1)\}$
(5) Choose Random W {gcd $(\Phi(n), W = 1)$} and $1 < W < \Phi(S)$
(6) Calculate D, $\{d.e \equiv 1 \bmod \phi(S)\}$
(7) Public key $\{W, n\}$
(8) Private Key $\{D, n\}$
(9) End

Algorithm 1: Pseudo code of RSA.

Table 2: Dataset with details.

Dataset	No. of rows	No. of columns	Total data
Heart attack	1311	11	14421

Table 3: Attributes of dataset.

Attributes	Abbreviation
Age	—
Sex	—
Cerebral palsy	Cp
Resting blood pressure	Trestbps
Cholesterol	Chol
Fasting blood sugar test	Fbs
Electrocardiogram	Restecg
Maximum heart rate achieved	Thalach
Exhang	—
Oldpeak	—
Outcome	Num

For Table 4, arrangement, accuracy, scatter plot, confusion matrix, and ROC metrics are considered.

Client information is first encrypted and then stored in the Cloud via RSA. When the client requests information from the Cloud supplier, the Cloud supplier verifies client and then sends the information to the client.

In RSA, each message is assigned a whole integer, which is a square figure. RSA is made up of two parts: public and private keys. In our Cloud situation, everyone has access to the Public Key, but only the client with the first access to the data has access to the Private Key.

3.2. Encryption and Authentication of Data. To ensure data security, all data packets are encrypted and decoded using a private key, with asymmetric cryptography providing authentication. An upgraded RSA cryptographic method is presented as a solution.

3.2.1. Key Generation. We choose two distinct prime numbers: $a = 61$ and $b = 53$.

Process $n = a * b$, in this manner $n = 61 * 53 = 3233$.

Process Euler's totient work, $\emptyset\ (n) = (a-1) * (b-1)$. Thus, $\emptyset\ (n) = (61-1) * (53-1) = 60 * 52 = 3120$.

Picked any whole number e, with the end goal that $1 < e < 3120$ that is coprime to 3120. Here, we picked $e = 17$.

Process d, $d = e - 1 \pmod{\emptyset\ (n)}$; therefore, $d = 17 - 1 \pmod{3120} = 2753$.

Public Key is $(e, n) = (17, 3233)$ and Private Key is $(d, n) = (2753, 3233)$.

3.2.2. Encryption. Cloud co-op provides the client with the Public Key (17, 3233) for storing the information. Let suppose $m = 65$ for Client mapped information. This information is further encoded to the specialist co-op by utilizing Public Key $C = 6517 \pmod{3233} = 2790$ which is shared among both parties. The Cloud specialist co-op is currently storing these encoded data, i.e., figure content.

3.2.3. Decryption. When the customer requests the information, the Cloud specialist cooperative verifies the client and sends the encrypted data (if the client is legitimate).

At that time, the cloud client computes to decode the information, $m = \mathrm{Cd} \pmod{n} = 27902753 \pmod{3233} = 65$.

When the m esteem is gotten, client will get back the first information. Figure 3 describes the flow chart of RSA.

3.3. The RSA Algorithm for RSA Public and Private Key Pair Generation. Both key exchange and digital signatures can be done with the RSA technique. The mathematics behind RSA is extremely simple despite the fact that it is used with integers with hundreds of digits.

The steps below can be used to establish an RSA public and private key pair:

(i) P and q are two prime numbers. The modulus, $n = pq$, can be calculated using these numbers.

Table 4: Accuracy measures.

Measures	Explanation
Accuracy	Accuracy decides the precision of the calculation in foreseeing occasions
ROC curve	The ROC (receiver operating curve) bends are used to assess the ease of testing
Scatter plot	Scatter (x, y) makes a disperse plot with hovers at the areas determined by the vectors x and y
Confusion matrix	The confusion matrix shows the total number of perceptions in every cell

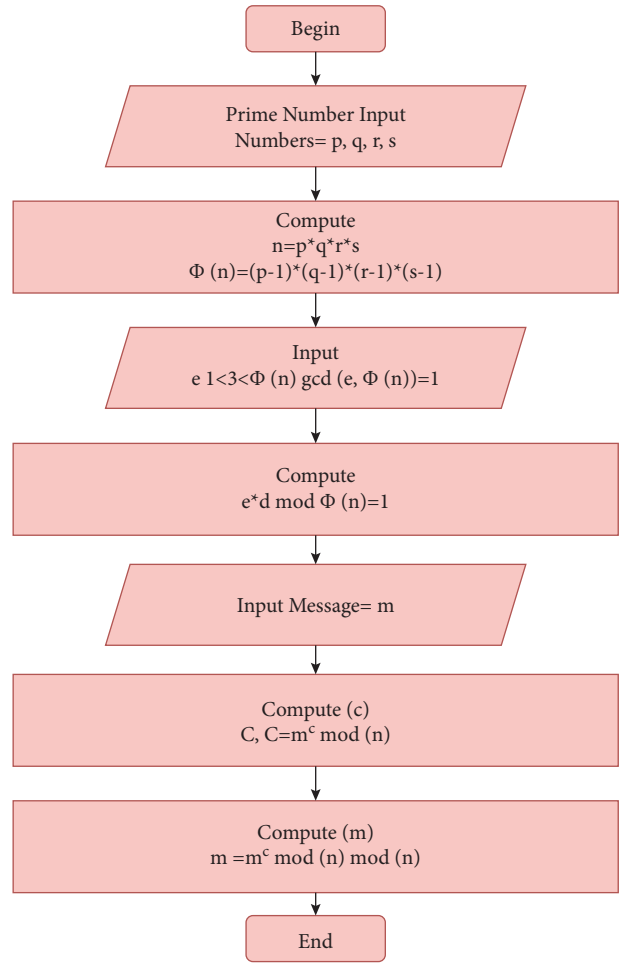

Figure 3: Flow chart depicted the RSA decryption algorithm.

(ii) Choose a third number, r, that is substantially prime to the product $(p\ 1)\ (q1)$; r is the public exponent.

(iii) Use the quotient $((rs-1))/((p-1)\ (q-1)$ to find an integer s. The private exponent is represented by the integer s.

(iv) The number pair (n, r) is the public key. Although these data are public, determining r from n and s is computationally impossible unless p and q are large enough.

(v) To encrypt a message, m generates the cipher-text C using equation 4 and the public key. $C = m^r \bmod (n)$ (4)

(vi) The receiver then uses the private key to decrypt the cipher-text using the following:

$$m = c^5 \bmod (n). \quad (4)$$

4. Results and Discussion

As previously stated, the proposed philosophy lashed back at the heart of informational collection understanding. Linear, Cubic, Quadratic, Fine Gaussian, Medium Gaussian, and Coarse Gaussian classifiers are processed by the SVM classifier with simplified parameters in order to find the ideal hyperplane that divides the pursuit space into two classes. SVM structured information into two classes using a reaction set for classifier in which 0 and 1 attributes are set on which assumption. Figure 4 shows the feature selection that was taken into account in the study.

Figure 4 depicts the feature selection which is age, sex, cerebral palsy, resting blood pressure, cholesterol, fasting blood sugar test, electrocardiogram, maximum heart rate archieved, exhang, and oldpeak considered in the study.

As we discussed in proposed methodology, total six techniques are used. First of all, data of disease are sent towards different classification techniques to classify data into two classes.

In SVM, there are further six types: Linear SVM, Quadratic SVM, Cubic SVM, Fine Gaussian SVM, Medium Gaussian SVM, and Coarse Gaussian SVM. We classify our data through all these six SVMs, and we found the best result from Fine Gaussian SVM as it has maximum accuracy among all SVMs.

In Naive Bayes, there are further two types: Gaussian Naive Bayes and Kernel Naive Bayes. We classify our data with these two Naive Bayes, and we found the best result from Kernel Naive Bayes as it has highest accuracy compared with Gaussian Naive Bayes.

In Decision Tree, there are further three types: Fine Tree, Medium Tree, and Coarse Tree. We classify our data with these three Decision Trees, and we found the best result from Fine Tree as it has highest accuracy compared with other two. We also classify our data through Random Forest. In KNN, there are further six types: Fine KNN, Medium KNN, Coarse KNN, Weighted KNN, Cubic KNN, and Cosine KNN. We classify our data with all these six KNN, and we found the best result from Fine KNN as it has highest accuracy among all KNN.

Table 5 determines classifier's performance on the basis of classified. Performance of SVM, NV, DT, RF, and KNN is calculated. The affectability, explicitness, exactness, and f-measure are calculated, and accuracy is checked, in order to analyze the classifier's performance. FP and FN are the proportions of negative instances incorrectly categorised as positive and positive cases incorrectly classed as negative, respectively.

On the basis of classified cases, Table 6 determines the performance of the classifier. Accuracy is determined and analysed based on these classified cases. Out of a total number of examples, the performance of SVM is measured in terms of Correctly Classified Instances and Incorrectly Classified Instances. Four different classifiers are true positive, true negative, false positive, and false negative values. SVM displays the largest true positive values, while KNN displays the lowest false negative values, DT displays the lowest false positive values, and RF displays the highest false negative values.

Measures used for classification are shown in Table 7 where TP and TN address true positive and true negative which are the degree of positive and negative cases that were really perceived independently. FP and FN address false

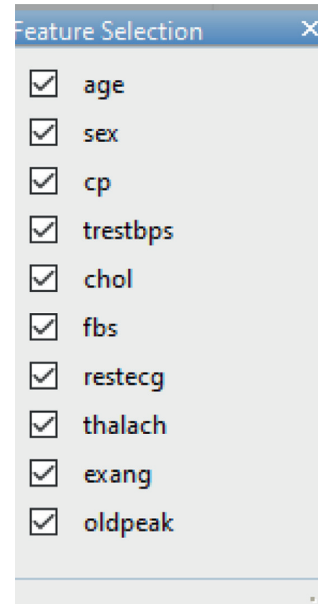

Figure 4: Feature selection.

Table 5: Classifier's performance on the basis of classified instances.

Classifiers	Correctly classified	Incorrectly classified
SVM	1308	2
KNN	1306	4
NB	1075	235
RF	1300	10
DT	1282	28

Table 6: True and negative values of classifiers.

Classifiers	TP	TN	FP	FN
SVM	742	566	2	0
KNN	742	564	4	0
NB	625	450	118	117
RF	742	558	10	0
DT	742	540	28	0

Table 7: Classifier's performance.

Sensitivity	TP/TP + FN
Specificity	FP/FP + TN
Precision	TP/TP + FP
F-measure	2 (Sen ∗ Pre)/ (Sen + Pre)
Accuracy	TP + TN/TP + FP + TN + FN

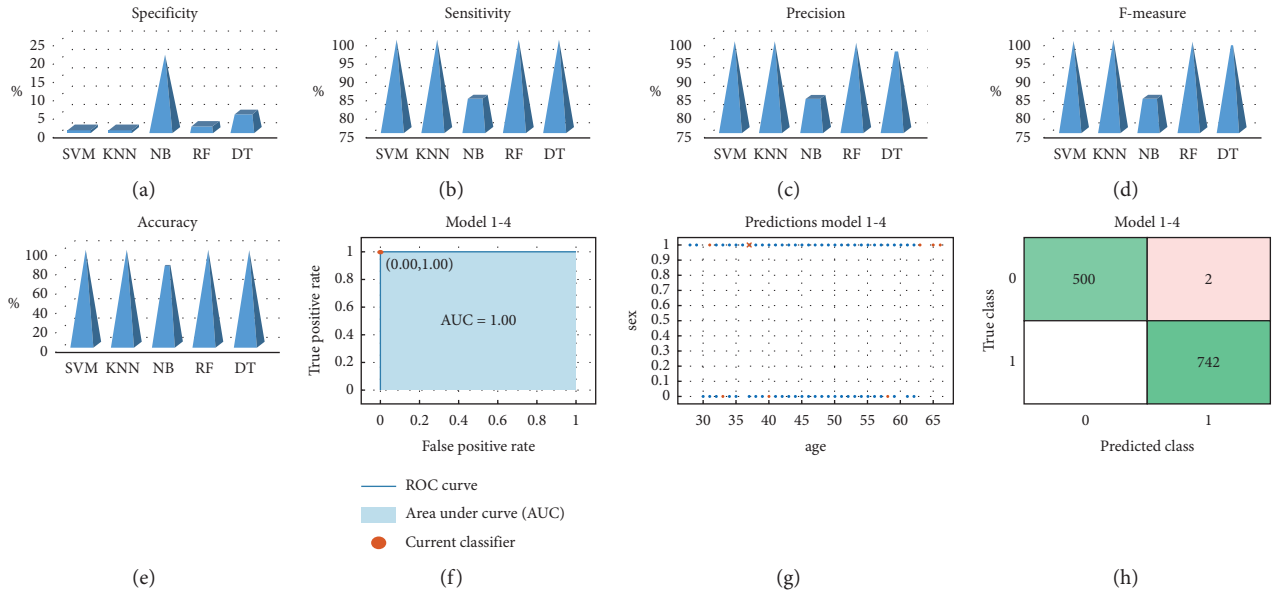

Figure 5: Performance measure comparison of five classification techniques. (a) Specificity. (b) Sensitivity. (c) Precision. (d) *F*-measure. (e) Accuracy. (f) ROC. (g) Scatter plot. (h) Confusion matrix.

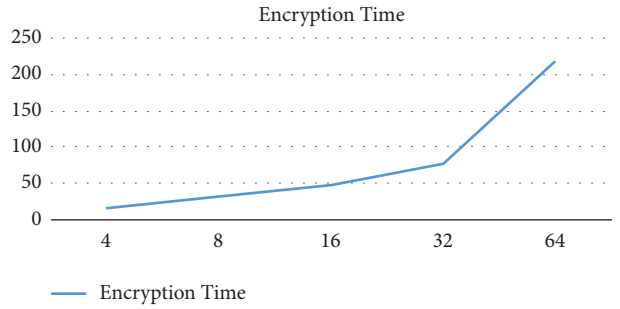

Figure 6: Encryption time using RSA algorithm.

Table 8: Prediction speed and training time of classifiers.

Classifiers	Prediction speed (obs/sec)	Training time (sec)
SVM	28000	23.01
KNN	16000	3.273
DT	12000	14.37
RF	8000	7.317
NB	14000	8.364

positive and false negative which are the degree of negative cases that were erroneously designated positive and the degree of positive cases that were erroneously named negative independently.

Figures 5(a)–5(d) and 6(e) illustrate the specificity, sensitivity, precision, f-measurement, and accuracy, which are used to calculate and estimate the effectiveness of the classifiers. Figure 5(a) shows that NB has the highest specificity. In Figures 5(b) and 5(c), NB has the lowest sensitivity and precision of 0.844 and 0.824, respectively. In Figure 5(c) and Figure 5(d), SVM achieves the highest precision and f-measure of 0.984 and 0.954, respectively. In Figure 5(e), the accuracy of several classifiers is shown in percentages, with SVM having the greatest accuracy of 0.974. SVM has the highest accuracy of all the classifiers. The percentage of correctly expressed positive and negative examples is denoted by TP and TN, respectively. Figure 5(f) depicts the categorization model's performance. In Figure 5(g), a scatter plot with horizontal and vertical axes is displayed. As illustrated in Figure 5, FP and FN are the proportions of negative instances incorrectly identified as positive and positive cases incorrectly classified as negative, respectively. SVM has a TP rate of 0.980, while KNN has a rate of 0.963, DT has a rate of 0.933, RF has a rate of 0.982, and NB has a rate of 0.802. SVM has an FP rate of 0.043, KNN of 0.030, DT of 0.14, RF of 0.050, and NB of 0.330.

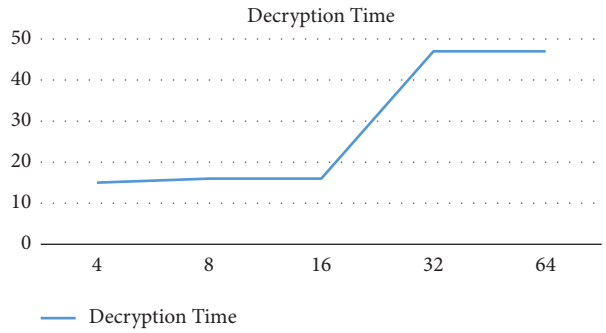

Figure 7: Decryption time using RSA algorithm.

The prediction speed and training time of each classifier are shown in Table 8, with SVM having the highest Prediction Speed observed per second (obs/sec) and KNN having the quickest training time.

Graph in Figure 6 represents a file of size 4 kb, 8 kb, 16 kb, 32 kb, and 64 kb taking 16 ms, 31 ms, 47 ms, 78 ms, and 218 ms encryption time using the RSA algorithm.

In RSA, exchange is the public key with the recipient is used for a decryption request. Hold it safe is a proprietary key that is never shared with any other person.

Graph in Figure 7 represents a file of size 4, 8, 16, 32, and 64 kb taking 15, 16, 16, 47, and 47 ms decryption time using the RSA algorithm.

If the key size is identical to the size of the packet to be sent across the network, an effective cryptosystem will produce the best results. Algorithm focused on parameters such as key length, block size, features, and functions. Because we realize data are held elsewhere in cloud storage, we need fast processing speed as well as fast protection. Here, the graph in Figure 6 indicates the success of the suggested case that how long it takes to encrypt the files.

5. Conclusions

An asset-restricted mobile PC saves data on an IoT-based cloud. However, constantly a significant inquiry regarding cloud specialist deals with the records appropriately while mobile cloud computing security is the fundamental concern. The proposed system gives a security system to make sure about the information in mobile cloud computing with the assistance of RSA calculation and other five different intelligent classification techniques.

A classification method based on the proposed methodology was presented to classify heart-attack data. First, dataset is generated for different parameters of heart attack. Second, based on these data, result is calculated in "0" and "1" form. Now, the generated data are sent straight to SVM, KNN, NB, RF, and DT for classification. The accuracies of the training dataset with classifiers are 99.80%, 99.6%, 82%, 99.2%, and 97.8% of SVM, KNN, NB, RF, and DT, respectively. SVM has high accuracy in comparison with other contemporary algorithms. In future, SVM could be utilized for grouping reason. The execution of the RSA calculation provides information assurance. Cloud security depends on reliable computing and encryption. Only the approved user can access the data in the proposed work. However, if any intruder (unauthorized user) tries to attack the system to collect sensitive data, the original information will be secure and cannot be recovered.

Data Availability

The data used to support the findings of the study are included within the article.

Conflicts of Interest

The authors declare that they have no conflicts of interest.

Acknowledgments

The authors specially thank Muhammad Abul Hassan for his continuous support and help throughout this research study. This research was supported by the Faculty of Management of Comenius University in Bratislava, Slovakia.

References

[1] M. L. Hoffmann Souza, C. A. da Costa, G. de Oliveira Ramos, and R. da Rosa Righi, "A survey on decision-making based on system reliability in the context of Industry 4.0," *Journal of Manufacturing Systems*, vol. 56, pp. 133–156, 2020.

[2] M. Abdel-Basset, G. Manogaran, A. Gamal, and V. Chang, "A novel intelligent medical decision support model based on soft computing and IoT," *IEEE Internet of Things Journal*, vol. 7, no. 5, pp. 4160–4170, 2019.

[3] P. Mell and T. Grance, *The NIST Definition of Cloud Computing*, NIST, Maryland, United States, 2011.

[4] M. Armbrust, A. Fox, R. Griffith et al., "A view of cloud computing," *Communications of the ACM*, vol. 53, no. 4, pp. 50–58, 2010.

[5] M. Kantardzic, *Data Mining: Concepts, Models, Methods, and Algorithms*, John Wiley & Sons Publishing, New Jersey, United States, 2003.

[6] Y. Kim, "Comparison of the decision tree, artificial neural network, and linear regression methods based on the number and types of independent variables and sample size," *Expert Systems with Applications*, vol. 34, no. 2, pp. 1227–1234, 2008.

[7] N. Santos, K. Gummadi, and R. Rodrigues, "Towards trusted cloud computing," *Proceedings of USENIX HotCloud*, 2009.

[8] "Tcg specification architecture overview," https://www.trustedcomputinggroup.org.

[9] K. Bowers, A. Juels, and A. Oprea, "Proofs of retrievability: theory and implementation," in *Proceedings of the ACM Workshop on Cloud Computing Security*, p. 43, Chicago Illinois USA, November 2009.

[10] W. Wang, Z. Li, R. Owens, and B. Bhargava, "Secure and efficient access to outsourced data," in *Proceedings of the ACM Workshop on Cloud Computing Security*, pp. 55–66, Chicago Illinois USA, November 2009.

[11] A. Yun, C. Shi, and Y. Kim, "On protecting integrity and confidentiality of cryptographic file system for outsourced storage," *P*, in *Proceedings of the ACM Workshop on Cloud Computing Security*, pp. 67–76, Chicago Illinois USA, November 2009.

[12] R. Chow, P. Golle, M. Jakobsson et al., "Controlling data in the cloud: outsourcing computation without outsourcing control,"

P, in *Proceedings of the ACM Workshop on Cloud Computing Security*, pp. 85–90, Chicago Illinois USA, November 2009.

[13] P. Lam, E. Bursztein, and J. Mitchell, "TrackBack spam: abuse and prevention," in *Proceedings of the ACM Workshop on Cloud Computing Security*, Chicago Illinois USA, November 2009.

[14] J. Sobey, T. Whalen, R. Biddle, P. V. Oorschot, and A. Patrick, "Browser interfaces and extended validation SSL certificates: an empirical study," in *Proceedings of the ACM Workshop on Cloud Computing Security*, Chicago Illinois USA, November 2009.

[15] J. Wei, X. Zhang, G. Ammons, V. Bala, and P. Ning, "Managing security of virtual machine images in a cloud environment," in *Proceedings of the ACM Workshop on Cloud Computing Security*, pp. 91–96, Chicago Illinois USA, November 2009.

[16] M. Christodorescu, R. Sailer, D. Schales, D. Sgandurra, and D. Zamboni, "Cloud security is not (just) virtualization security: a short paper," in *Proceedings of the ACM Workshop on Cloud Computing Security*, pp. 97–102, Chicago Illinois USA, November 2009.

[17] M. Chase, K. Lauter, J. Benaloh, and E. Horvitz, "Patient Controlled En- cryption: patient privacy in electronic medical records," in *Proceedings of the ACM Workshop on Cloud Computing Security*, p. 91, Chicago Illinois USA, November 2009.

[18] M. Raykova, B. Vo, S. Bellovin, and T. Malkin, "Secure anonymous database search," in *Proceedings of the ACM Workshop on Cloud Computing Security*, Chicago Illinois USA, November 2009.

[19] S. Liu, Yu Han, C. Miao, and C Alex, "A fuzzy logic based reputation model against unfair ratings," in *Proceedings of the 2013 International Conference on Autonomous Agents and Multi-Agent Systems*, pp. 821–828, International Foundation for Autonomous Agents and Multiagent Systems, St. Paul MN USA, May 2013.

[20] P.-N. Tan, M. Steinbach, and V. Kumar, *Introduction to Data Mining*, Addison-Wesley Publishing, Massachusetts, United States, 2006.

[21] I. U. Khan, A. Ryan, H. J. Alyamani et al., "RSSI-controlled long-range communication in secured IoT-enabled unmanned aerial vehicles," *Mobile Information Systems*, vol. 2021, 2021.

[22] D Sisodia, Shrivastava, and Jain, "ISVM for face recognition," in *Proceedings of the 2010 International Conference on Computational Intelligence and Communication Networks*, pp. 554–559, IEEE, Bhopal, India, 26-28 Nov. 2010.

[23] I. Rish, "An empirical study of the naive Bayes classifier," in *Proceedings of the IJCAI 2001 Workshop on Empirical Methods in Artificial Intelligence*, pp. 41–46, IBM, Vancouver, Canada, August 2001.

[24] S. Ray, *6 Easy Steps to Learn Naive Bayes Algorithm (With Code in Python)*, 2017, https://www.datasciencecentral.com/6-easy-steps-to-learn-naive-bayes-algorithm-with-code-in-python/.

[25] A. N Khan, S. U Mat Kiah, and S. A. Madani, "Towards secure mobile cloud computing: a survey," *Future Generation Computer Systems*, vol. 29, no. 5, pp. 1278–1299, 2013.

[26] W. Itani, A. Kayssi, and A. Chehab, "Energy-efficient incremental integrity for securing storage in mobile cloud computing," in *Proceedings of the Int. Conference on Energy Aware Computing*, Dec. 2010.

[27] W. Jia, H. Zhu, Z. Cao, L. Wei, and X. Lin, "SDSM: a secure data service mechanism in mobile cloud computing," in *Proceedings of the IEEE Conference on Computer Communications Workshops*, Apr. 2011.

[28] https://wiki.cloudsecurityalliance.org/guidance/index.php/Cloud_Computing_Architectural_Framework.

[29] M. L. Mat Kiah, "Towards secure mobile cloud: a survey," *Proceedings of Analyses paper*, vol. 29, p. 1278, 2012.

[30] J. Yang, H. Wang, J. Wang, C. Tan, and D. Yu1, "Provable data possession of resource constrained mobile devices in cloud computing," *Journal of Networks*, vol. 6, no. 7, pp. 1033–1040, 2011.

[31] E Eugene, *Hyrax: Cloud Computing on Mobile Devices", Dissertation of Thesis*, Carnegie Mellon University, Pittsburgh, 2009.

[32] Dr. L. Arockiam and S. Monikandan, "Data security and privacy in cloud storage using hybrid symmetric encryption algorithm," *International Journal of Advanced Research in Computer and Communication Engineering*, vol. 2, no. 8, 2013.

[33] Y. Xu, L. Wu, L. Guo, Z. Chen, L. Yang, and Z. Shi, "An intelligent load balancing algorithm towards efficient cloud computing," in *Proceedings of the AI for Data Center Management and Cloud Computing: Papers from the 2011 AAAI Workshop*, California, USA, August 7, 2011.

[34] S. U. Rehman and S. Manickam, "Denial of service attack in IPv6 duplicate address detection process," *International Journal of Advanced Computer Science and Applications*, vol. 7, pp. 232–238, 2016.

[35] I. U. Khan, I. M. Qureshi, M. A. Aziz, T. A. Cheema, and S. B. H. Shah, "Smart IoT control-based nature inspired energy efficient routing protocol for flying ad hoc network (FANET)," *IEEE Access*, vol. 8, pp. 56371–56378, 2020.

[36] M. Abul Hassan, S. Irfan Ullah, A. Salam, A. Wajid Ullah, M. Imad, and F. Ullah, "Energy efficient hierarchical based fish eye state routing protocol for flying ad-hoc networks," *Indonesian Journal of Electrical Engineering and Computer Science*, vol. 21, no. 1, pp. 465–471, 2021.

[37] M. A. Hassan, S. I. Ullah, I. U. Khan, S. B. Hussain Shah, A. Salam, and A. W. Ullah Khan, "Unmanned Aerial Vehicles Routing Formation using fisheye state routing for flying ad-hoc networks," in *Proceedings of the 4th International Conference on Future Networks and Distributed Systems (ICFNDS)*, pp. 1–7, New York, NY, United States, November 2020.

[38] D. Sisodia, L. Singh, and S. Sisodia, "Fast and accurate face recognition using SVM and DCT," in *Advances in Intelligent Systems and Computing*, vol. 2012, pp. 1027–1038, Springer, 2014.

[39] J. Han and M. Kamber, *Data Mining: Concepts and Techniques*, Elsevier, Second Edition, 2006.

[40] A. Ahmad and D. Ruelens, "Development of digital logic design teaching tool using MATLAB & SIMULINK," *IEEE Technology and Engineering Education (ITEE)*, vol. 8, no. 1, pp. 7–11, 2013.

Hindawi
Scientific Programming
Volume 2022, Article ID 9147444, 6 pages
https://doi.org/10.1155/2022/9147444

Research Article

Data Mining and Soft Computing in Business Model for Decision Support System

Foziah Gazzawe and Ryan Alturki

Department of Information Science, College of Computer and Information Systems, Umm Al-Qura University, Makkah, Saudi Arabia

Correspondence should be addressed to Foziah Gazzawe; fhgazzawe@uqu.edu.sa

Received 9 January 2022; Revised 18 March 2022; Accepted 31 March 2022; Published 12 April 2022

Academic Editor: Muhammad Usman

Several studies were taken to effectively determine the importance of data mining in business model development for decision support system. It was later discovered that most businesses have invested heavily in the data mining process which enables them to easily study and analyse the market environment and improve their domination in the market. Data mining is a process used by most firms to effectively collect information about certain topic. One factor that business model development usually focuses more on is the value of measurable performance and increased innovation in the market. The aim of the current research is to investigate the values and key roles played by data mining prospects in the business model development. It also revolves around current techniques used within business model development that are crucial in enhancing the position and competitiveness of a firm in the market. Although the data mining prowess varies in regards to the firm and effort used, the main concept remains on how to fully have the firm understand the effects and role played by data mining techniques in their overall business flow. In methodology, secondary sources are categorically used to enhance the overall flow of the study question by comparing them and analyzing them using the techniques provided. The results and analysis reveal that the effects of using data mining techniques are huge towards achieving success for various businesses. Moreover, the practical implications have categorically increased the notion of how influential the prospects of data mining can be when applied in businesses.

1. Introduction

The value of measurable performance and increasing market innovation is one area that business model development normally focuses on. Data mining has been one of the most influential prospects that have enabled firms to effectively increase their output in the market. This prowess gives the firms a complete control of managing how their clients perceive their overall business functions making it easy for them to fully take over all controls that affect the clients. There is also a huge difference that gives each firm applying this prospect to fully become adaptive in various schemes. Hence, when the market changes to reflect on other prospects that affects the society, it becomes easy to fully remain competitive without facing or undergoing any challenges of a breakdown or a fall in the business activities. Therefore, through data mining, the firm can easily incorporate specific client goals and specifications.

2. Business Model Development

A data mining is a process used by most firms to effectively collect information about certain topic. In most cases, these topics help firms to visionalize about their position in the market. Business models, according to the literature, can be regarded as "cognitive" gadgets, and their use necessitates the acquisition of extensive knowledge about customers, suppliers, and competitors. Recent experimental investigations have shown that the use of data-mining technologies has a favorable impact on business models, boosting strategic performance skills that drive competitive advantage. In research by [1] , the purpose was to strengthen studies on the

interaction between data-mining tools and business model design by examining whether organizational heterogeneity related to data-mining technologies might help or impede data-mining adoption in a real-world setting [1]. In another study, Lee and Jung [2] established prospects in which they tried to understand the relationship that exists between new big data of ships and the demand from clients. It was discovered that the presence of a new business model in the ship manufacturer industry established prospects that enhanced the growth of the business across the globe. The essence of the business model in this stage has also enabled various stakeholders to effectively increase their production process. One factor that business model development usually focuses more on is the value of measurable performance and increased innovation in the market [3].

Business model development requires creativity and innovation to be a regular aspect. It also involves understanding all the prospects about clients and how their behavior is crucial in enhancing the overall business activities of any firm. In their study, Breuer et al. [4] discovered that the society lacks a shared knowledge that enhances sustainability in a modelled business. Through this sustainability, enterprises can effectively understand the values bestowed towards data mining at their firms. In the current regime, the prospects of the changing market have forced researchers to embark on a study mission of trying to evaluate the effects of data mining on a broader market. A research conducted on the Indian market by Suma and Hills [5] tried to find reasons why data mining is efficient in understanding the demand for refurbished electronics. Through this business model setup, it becomes efficient for an individual to effectively focus more on the data accumulation and validation as a tool of creating new models of business opportunities. Data mining can also be used to predict the demand from clients and their likelihood to consume certain manufactured products. It can also be used to effectively shed light on all nonlinear factors that determine and describe online market [6].

2.1. Current Techniques Used within Business Model Development. The concept of business model development has evolved since ancient time. Traditionally, the techniques which were commonly used involved aspects such as brick and motor stores, advertising-based, direct sales, and franchising [7]. Despite their prowess in increasing the values of various industries, their efficiency has slowly been overpowered by the emerging techniques being introduced across the globe. A study by Sullivan et al. [8] conducted research on understanding the use of AI techniques as an alternative of boosting the business model in law firms. Through this approach, it was evident that the future is geared towards having AI services replace the roles being handled by humans. There are various techniques that are used in the business world today. According to Täuscher and Laudien [9], techniques such as subscription model, commission model, and advertising model are mostly preferred. Subscription model involves having clients to fully pay a recurring amount on a regular basis for particular services [10]. Brands which have fully implemented these services are movie and video streaming companies such as Netflix. Also, TV providers are also using this approach as the best option of conducting business. The advantages of this model are enabling the firms to retain the clients as well as simplifying the business process.

However, according to [11], the challenges of this model include management of subscribed clients. It becomes a difficult task for the firms to effectively manage the huge traffic that they experience simultaneously. Another huge challenge is the security of the payment done by the clients [12]. Another technique being used in the business world is the bundling model. Through this approach, a firm easily sells two products as a single unit [13]. Some of the firms that have specialized in this type of business include Adobe Creative Suite and AT&T. Besides, fast food firms also use this model to attract more clients to their business [14]. However, the main challenge that this model has is reduction in the profit model which makes the business to face losses in the long term [8]. Another common business model that companies have resorted to use is the freemium approach. In this model, a company offers its services for free but has a limit on services that the client can access [14]. Hence, after reaching the freemium limit, the client will be required to subscribe to more content in order to enjoy the services on board. The main challenge of this approach is that clients would easily opt for other services from competing companies [15].

2.2. Data Mining (Definition and Concept). Data mining is a concrete process that most firms use to effectively convert raw data into meaningful information. These firms target to achieve a certain range of competitiveness in the market by being directional and unique [16]. Therefore, they effectively engage their services in prospects that utilize most of their raw data to their benefits. In the long run, the firms end up having a robust system that gives them the power to effectively understand the needs of the clients. According to [17], data mining is a crucial process that firms use to effectively make lasting decisions for their activities. Through this process, the management fully understands the values and perceptions of all clients. It also accounts to how the products of the firm are received across the market. In different firms, the usage of data mining involves concepts such as forecasting, grouping, finding sequences, risk, and probability. When forecasting, a company estimates its sales while predicting server loads or down time. Grouping involves putting clients in clusters while predicting their affinities. In the risk and probability, most firms would easily use it to select the clients who can be used for targeted features such as mailings [18]. Since collected data seem to be made out of various sources, having a robust system that groups them would easily enhance the flow of business. In most cases, the firms use the space and values of data mining to make decisions that affect the values of the group. It is through such steps that people end up becoming effective and resourceful in their respective firms. In addition, the concepts and techniques used in data mining are useful

prospects that guide the company to fully understand their position in the market by analyzing how their clients respond to their products and goods. Another key factor of data mining is based on aspects such as integration, subject orientation, and time variant. These aspects help the firms to effectively understand their market and focus more on producing products that align with the requirements of the clients. Despite being a broad concept, the values demonstrated by the concepts in data mining are unidirectional and effective in enhancing all the activities conducted by the firm. Therefore, implementing data mining in any business is a key factor that helps firms to achieve success faster and grow while understanding the basic values that mean so much to their clients.

2.3. Data Mining Techniques and Application. There are many data mining techniques that can be used to effectively help boost the firm's performance in the market. These techniques are strategically set up to enable the firms to be successful in the market. The important factor when dealing with these big data is the essence of understanding how to use them for the good of the company. In most cases, the data mining techniques have become the ideal stopovers that have helped firms to remain competitive. In research by Majumdar et al. [19], data mining techniques were found to be an important element of accomplishing solutions to such a problem. An example of this is where big data is used is in agriculture, where there is a large number of factors such as soil differences, environmental influences, and commodity pricing. This is why it is vital that farmers use data methods when deciding. Examples of data mining techniques used in agriculture data include PAM, CLARA, DBSCAN, and Multiple Linear Regression. In another research, Alahmar [20] used data mining techniques to determine the length of hospital stay for patients. It was later discovered that using the stacked ensemble was an effective approach that was crucial in predicting short and long LOS for patients with both diabetic I and II. Hence, through the use of the stacked ensemble technique, the results automatically validated this approach and ensured that it can be applicable in various situations. Other important techniques that can be used in the world today include clustering, regression, classification, sequential patterns, and prediction. The application of these techniques in various institutions is one of the important factors behind the usage of data mining. Clustering ensures that the data recorded are sorted in a manner that enables the firm to understand how their clients value their services. Clustering also plays an important role in helping sort the available data into small groups that are easy to assess [21]. For instance, when dealing with records of people living in a certain region who uses a specific brand of petroleum jelly for their daily activities, using a cluster will ensure that those who prefer brand A and those who prefer brand B are categorically sorted and their needs are fully implemented. In this example, the clustered approach will allow the firm to put the clients in a certain category that will help in identifying more needs that are vital for the progress of the firm. In their study, Saxena et al. [21] used clustering techniques to effectively determine the similarity complex of customers in any business environment.

2.4. Potential of Data Mining to Support Business Model Development and Who Can Benefit from It. Data mining is employed by companies to discover connections in data to make improved business decisions. It can also be used to help investigate the patterns in sales, to predict customer loyalty, and to develop marketing methods. The following are some examples of data mining applications: market segmentation, fraud detection, interactive marketing, trend analysis, customer churn, direct marketing, and market basket analysis [22]. Market segmentation is the process through which businesses determine the common features of customers who purchase the same items from them. Through customer churn, the firms can easily predict which clients are most likely to abandon your firm for a competition [22]. In the essence of fraud detection, data mining is used to determine which transactions have the highest likelihood of being fraudulent. Moreover, trend analysis helps firms to determine clients and their probability of shopping with the firm [23].

Therefore, these prospects prove that the firms which deploy the data mining techniques benefit as compared to those that no longer use this approach. For instance, a bank may want to effectively determine if the use of its credit cards can be effective if the prices charged are reduced to halves. If this approach uses data mining, the firm would end up determining that their clients prefer services that are likely viable for their specific income [24]. Hence, in this example, the values of data mining remain to be high and would forever be the ideal approach used by firms in that region. In another study, Härting et al. [25] determined that business models and procedures have altered dramatically as a result of new advancements in digitization technologies such as Big Data and Data Science, and new business models have emerged in unprecedented numbers. Their research involved four potential prospects that aimed at improving the businesses by evaluating the weakest points while determining the best approaches that can be used to help them be more competitive in the market. A study by Sarkar et al. [26] used data mining techniques to effectively understand the occurrences of accidents at the workplace. It was later discovered that the values and prospects of the data mining technique were based on the availability of this drive from the management [27]. Hence, if the management has fully embraced the data mining technique, it becomes easy for the firms to grow and realize a huge potential in the market [23, 28].

3. Methodology

The data collected for this research study is secondary data. Secondary data is derived from second-hand sources or published sources. The data are collected from various sources such as journals, books, and scholarly articles. The reason for using secondary data in this research is because it supports the analysis of the data of this study for a long

period of time, and in addition to that, the researcher(s) can find additional data from the primary data that contribute to supporting the results of the current business models on the previous studies. As well, it would help with the use of this study outcomes to involve more results. Answering the research question will largely be done through analyzing the work which has been done on this topic so as to understand how businesses have been made use of data mining. The inclusion criteria for this review include papers on businesses which have employed data mining techniques. The research question will be answered through conducting a literature review including articles derived from different search engines, such as Google Scholar, DBLP, and IEEE Xplore. The findings are be displayed in Table 1, which compares the article use of data mining techniques.

In Table 1, we see that there are various articles which categorically reflect and value the usage of data mining techniques. For instance, research papers usually involve peer reviewed papers and would entail GIS spatial analysis. In the essence of raw data, the data mining tasks involved are data preprocessing. There is also the use of previous studies which focus on clustering and DBSCAN.

Research Question: What is the impact of data mining application in product/business model development?

4. Findings

The research question was answered using business papers that focused more on data mining techniques. Analysis of these samples was based on the approaches used which effectively increased the chances of collecting credible information about the research question. From the collected samples, it is evident that all infrastructures bestowed towards achieving a long-lasting goal would easily be influential in determining the analysis of the research question. Most of the studies used previous research that had focused on analyzing the data mining techniques. Hence, it becomes easy to effectively come up with joint analysis that helps businesses to effectively analyse their position in the market. Data mining has proved to be an important factor that businesses use to collect more information about their position in the market. It is clear that businesses which opt for any of the data mining approaches end up having and recording a mileage of success factors that effectively push them to be more successful. In business model development, data mining is also an important factor that can determine various prospects for the firm. Data mining techniques can also be utilised when inputting data to find the most effective performance strategy. A study by Majumdar [19] uses the PAM, CLARA, and DBSCAN data techniques to explore the best range of temperatures and wheat climate requirements to optimise crop productivity. Quality metrics are used to compare clustering algorithms. It was found that DBSCAN provided better clustering qualities than the PAM and CLARA techniques. Therefore, the importance of the current paper findings is to easily analyse how data mining techniques are important in enhancing the business prowess of any firm. Besides, businesses which employ the use of this approach would easily record improvements in their activities.

5. Discussion

5.1. Impact of Data Mining Techniques on Business Model Development. Business model development is a process that needs the combined input of all parties in a firm. Through this, it is easy for the firm to record their progress from one stage to another. Data mining could be used by a department store to aid in its target marketing mail campaign. Another way in which data mining techniques can be utilised is to determine which customers are likely to purchase more products based on the purchases they have made, through mined strong association rules [21]. This allows the organisation to send marketing and promotions to specific consumers who are likely to purchase items and improving sales. On the other hand, simplistic statistical analysis is incapable of handling vast amounts of data. There are various data techniques used in the research. A healthcare organisation, for example, can employ data mining to help with adjudication, claims, COB, and acceptance and rejection processes. Data mining functions including association, classification, and clustering are used. Organisation datasets can leverage the association to identify certain groups of claims that are likely to be submitted electronically, on paper, or through a web portal. The system may use this data to create numerous BI dashboards and analyses about the intake process [28]. In claim processing, data processing is also utilised to recover and uncover additional patterns. In another research, tenfold cross validation, two decision tree classifiers, classification and regression tree (CART), and C5.0 were implemented. Additionally, adaptive boosting, an ensemble technique, has been used to improve classification accuracy. The results reveal that for the prediction task, enhanced C5.0 produces more accuracy than the others. In addition, the rules derived provide insight into the situations. Another study focused on gradient boosting data technique. Multiple additive trees (MATs), or gradient boosting, is a novel improvement in data mining introduced by Friedman at Stanford University. It uses stochastic gradient boosting to extend and improve the decision tree (DT) model [28]. Boosting is a broad strategy for attempting to "boost" the efficiency of any given classification model by fitting a series of limited models and then combining them.

These techniques imply that the validity of the process used is essential in improving the outcome received. Therefore, when the new models are put in place, firms can easily meet the needs of their clients while maintaining their validity in the market. The outcome received proved how influential the process of data mining is and how it can effectively be used to transform the performance of a product from zero to greatness. Marketing firms use data mining to create data models and forecasts based on past data [29]. Promotions, marketing strategies, and pivots are all run by them. This leads to rapid growth and success. The retail business and marketing firms are on the same page. They believe in prediction models for their goods and services as a result of data mining. Better production and

Table 1: The current articles that use data mining techniques.

Article	Business resources	Database types	DM tasks	DM techniques/applications
[23]	Research papers	Peer-reviewed research papers	Inverse distance weighted (IDW)	GIS spatial analysis
[26]	Tenfold cross validation	Tenfold cross validation	Reactive and proactive data technique	Adaptive boosting
[27]	Raw data	Raw data	Data preprocessing	Data preprocessing
[21]	Previous studies	Previous studies	Clustering	Clustering
[19]	Previous studies	Previous studies	Data analysis	PAM, CLARA, DBSCAN, and multiple linear regression
[29]	Previous studies	Previous studies	Clustering	DBSCAN
[24]	Previous studies	Previous studies	Clustering	Clustering
[30]	Previous studies	Previous studies	Data analysis	CLARA
[28]	Previous studies	Previous studies	Data analysis	Association

Table 2: Advantages and disadvantages of current tool.

Tool	Advantage	Disadvantage
GIS spatial analysis	Helps in reading the characteristic of various places	It is costly to install.
Adaptive boosting	It effectively classifies text and images.	Conducting binary classification is difficult.
Data preprocessing	Eliminates redundancy of data	It is prone to bugs
Clustering	Contains greater scalability	It is difficult to recover in case the database fails

customer insights are possible in retail stores [3]. Historical data is used to calculate discounts and redemption coupons. Banks profit from data mining in terms of financial rewards and upgrades. They create a model based on consumer information and then examine the lending process, which is genuinely data driven. Manufacturers get their products. Table 2 shows the advantages and disadvantages of the tools used in data mining.

5.2. Future of Data Mining Techniques on Business Model Development. The outcomes have become a talking point that most enterprises use to define their prowess. The effective approaches used to collect insights help the firms to defend their worth and predict their position in the market. For all future prospects, using data mining techniques has proved to be effective because it allows the firms to fully predict how the behaviour of their product would impact competition from other entities [26]. Data mining techniques are especially useful over prior methods as they are more reliable and accurate in estimating future outcomes. Future inventory needs, shipments, and shop layouts can be managed through data mining techniques to increase sales [30]. This is useful for corporations as it aids with planning and using less resources. For instance, this technology is used to maximize occupancy and income of hotels, restaurants, and other hospitality settings through estimating the number of guests expected at a particular time period and planning accordingly.

6. Conclusions

The results show that improved C5.0 is more accurate than the others in the prediction task. The rules that are derived also provide insight into the situations. Another study looked into the technique of gradient enhancing data. Friedman at Stanford University presented multiple additive trees (MAT), also known as gradient boosting, as a new breakthrough in data mining. Data mining models have become important dynamics that are also being used in predictive aspects. It is now easy to predict the future and determine how the firm would perform if certain measures are put in place. The limitation of the current work is on the concept of using various studies that use different techniques. Besides, the future of data mining is intact, and there is a slight hope of having increased efficiency.

Data Availability

No data were used to support this study.

Conflicts of Interest

The authors declare that there are no conflicts of interest regarding the publication of this paper.

References

[1] N. Castellano and R. Del Gobbo, "Data-mining tools for business model design: the impact of organizational heterogeneity," *Lecture Notes in Information Systems and Organisation*, vol. 20, pp. 237–248, 2017.

[2] S. Lee and I. Jung, "Development of a platform using big data-based artificial intelligence to predict new demand of shipbuilding," *The Journal of The Institute of Internet, Broadcasting and Communication*, vol. 19, no. 1, pp. 171–178, 2019.

[3] T. Ayadat, D. Ahmed, S. Chowdhury, and A. Asiz, "Measurable performance indicators of student learning outcomes: a case study," *Global Journal of Engineering Education*, vol. 22, no. 1, pp. 40–50, 2020.

[4] H. Breuer, K. Fichter, F. L. Freund, and I. Tiemann, "Sustainability-oriented business model development: principles, criteria and tools," *International Journal of Entrepreneurial Venturing*, vol. 10, no. 2, pp. 256–286, 2018.

[5] V. Suma and S. M. Hills, "Data mining based prediction of demand in Indian market for refurbished electronics," *Journal of Soft Computing Paradigm (JSCP)*, vol. 2, no. 2, pp. 101–110, 2020.

[6] T. Van Nguyen, L. Zhou, A. Y. L. Chong, B. Li, and X. Pu, "Predicting customer demand for remanufactured products: a data-mining approach," *European Journal of Operational Research*, vol. 281, no. 3, pp. 543–558, 2020.

[7] D. Ibarra, J. Ganzarain, and J. I. Igartua, "Business model innovation through Industry 4.0: a review," *Procedia Manufacturing*, vol. 22, pp. 4–10, 2018.

[8] R. Sullivan, L. D. Jarvis, T. O'Gara, M. Langfitt, and C. Emory, "Bundled payments in total joint arthroplasty and spine surgery," *Current reviews in musculoskeletal medicine*, vol. 10, no. 2, pp. 218–223, 2017.

[9] K. Täuscher and S. M. Laudien, "Understanding platform business models: a mixed methods study of marketplaces," *European Management Journal*, vol. 36, no. 3, pp. 319–329, 2018.

[10] M. Villi and R. G. Picard, "Transformation and innovation of media business models," in *Making media*Amsterdam University Press, Amsterdam, Netherlands, 2019.

[11] Y. Li and T. Voege, "Mobility as a service (MaaS): challenges of implementation and policy required," *Journal of Transportation Technologies*, vol. 7, no. 2, pp. 95–106, 2017.

[12] R. K. Dzogbenuku, G. K. Amoako, D. K. Kumi, and G. A. Bonsu, "Digital payments and financial wellbeing of the rural poor: the moderating role of age and gender," *Journal of International Consumer Marketing*, vol. 34, no. 2, pp. 113–136, 2022.

[13] T. Kopczewski, M. Sobolewski, and I. Miernik, "Bundling or unbundling? Integrated simulation model of optimal pricing strategies," *International Journal of Production Economics*, vol. 204, pp. 328–345, 2018.

[14] J. Jiang, M. Yang, M. Kiang, and A.-F. Cameron, "Exploring the freemium business model for online medical consultation services in China," *Information Processing & Management*, vol. 58, no. 3, Article ID 102515, 2021.

[15] A. Beltagui, T. Schmidt, M. candi, and D. L. Roberts, "Overcoming the monetization challenge in freemium online games," *Industrial Management & Data Systems*, vol. 119, no. 6, pp. 1339–1356, 2019.

[16] A. I. Pascu, "Data mining. concepts and applications in banking sector," *Annals of' Constantin Brancusi' University of Targu-Jiu. Economy Series no.*vol. 1, 2018.

[17] H. Belwal, S. Tayal, Y. Sharma, and A. Sharma, "Data mining approaches for profitable business decisions," *Smart and Sustainable Intelligent Systems*, vol. 1, pp. 427–442, 2021.

[18] R. Asaad and R. M. Abdulhakim, "The concept of data mining and knowledge extraction R techniques." outcomes: a case study," *Global Journal of Engineering Education*, vol. 22, no. 1, pp. 40–50, 2020.

[19] J. Majumdar, S. Naraseeyappa, and S. Ankalaki, "Analysis of agriculture data using data mining techniques: application of big data," *Journal of Big data*, vol. 4, no. 1, pp. 1–15, 2017.

[20] A. Alahmar, E. Mohammed, and R. Benlamri, "Application of data mining techniques to predict the length of stay of hospitalized patients with diabetes," in *Proceedings of the2018 4th International Conference on Big Data Innovations and Applications (Innovate-Data)*, pp. 38–43, IEEE, Barcelona, Spain, August, 2018.

[21] A. Saxena, M. Prasad, A. Gupta et al., "A review of clustering techniques and developments," *Neurocomputing*, vol. 267, pp. 664–681, 2017.

[22] S. Donicar, "Market segmentation analysis in tourism: a perspective paper," *Tourism Review*, vol. 75, no. 1, 2019.

[23] B. Murugesan, S. Karuppannan, A. T. Mengistie, M. Ranganathan, and G. Gopalakrishnan, "Distribution and trend analysis of COVID-19 in India: geospatial approach," *Journal of Geographical Studies*, vol. 4, no. 1, pp. 1–9, 2020.

[24] F. Junliang, J. Zheng, L. Wu, and F. Zhang, "Estimation of daily maize transpiration using support vector machines, extreme gradient boosting, artificial and deep neural networks models," *Agricultural Water Management*, vol. 245, Article ID 106547, 2021.

[25] R. C. Härting, C. Reichstein, and M. Schad, "Potentials of Digital Business Models–Empirical investigation of data driven impacts in industry," *Procedia Computer Science*, vol. 126, pp. 1495–1506, 2018.

[26] S. Sarkar, A. Verma, and J. Maiti, "Prediction of occupational incidents using proactive and reactive data: a data mining approach," in *Industrial Safety Management*, pp. 65–79, Springer, Singapore, 2018.

[27] S. A. Alasadi and W. S. Bhaya, "Review of data preprocessing techniques in data mining," *Journal of Engineering and Applied Sciences*, vol. 12, no. 16, pp. 4102–4107, 2017.

[28] L. Zhang, J. Ren, H. Yuan et al., "Evaluation of smart healthcare systems and novel uv-oriented solution for integration, resilience, inclusiveness and sustainability," in *Proceedings of the 5th International Conference on Universal Village (UV)*, pp. 1–28, IEEE, Boston, MA, USA, October 2020.

[29] R. Dubey, A. Gunasekaran, S. J. Childe, C. Blome, and T. Papadopoulos, "Big data and predictive analytics and manufacturing performance: integrating institutional theory, resource-based view and big data culture," *British Journal of Management*, vol. 30, no. 2, pp. 341–361, 2019.

[30] A. Triayudi, S. Sumiati, T. Nurhadiyan, and V. Rosalina, "Data mining implementation to predict sales using time series method," *Proceeding of the Electrical Engineering Computer Science and Informatics*, vol. 7, no. 2, pp. 1–6, 2020.

Hindawi
Scientific Programming
Volume 2022, Article ID 1287979, 8 pages
https://doi.org/10.1155/2022/1287979

Research Article

A Text Detection and Recognition Algorithm for English Teaching Based on Deep Learning

Xia Luo[1] **and Huiyang Zhu**[2]

[1]*Wuchang Institute of Technology, Wuchang, Hubei 430065, China*
[2]*School of Foreign Languages, Hubei University of Science and Technology, Xianning, Hubei 437199, China*

Correspondence should be addressed to Huiyang Zhu; zhuhuiyang@hbust.edu.cn

Received 11 March 2022; Revised 26 March 2022; Accepted 29 March 2022; Published 8 April 2022

Academic Editor: Muhammad Zakarya

Traditional English teaching cannot make effective use of various resources, and the scheduling ability is poor. People cannot accurately obtain the information in the English textbook text in the learning process, resulting in some people who cannot better learn and master the English language. For this problem, this study adopts deep learning algorithm and establishes an English teaching text algorithm based on association semantic rules to mine the features between sentences and phrases in the text provided by English teachers. The proposed algorithm completes the feature extraction of the English teaching text and also analyzes the association analysis between semantics in English teaching text. In fact, its essence is to get English teaching association rules on the basis of information theory. By combining with semantic similarity information, English teaching text can be accurately detected and identified. The simulation results show that the proposed algorithm can accurately extract English teaching text information, and the accuracy and convergence speed during extraction are higher than other competing algorithms.

1. Introduction

At present, the rapid development of the network and computer technologies promotes the emergence of all kinds of network media, and the number of English teaching materials continues to increase. However, English texts appear in all kinds of news, media, and English teaching materials, making it increasingly difficult for people to read. People are eager to extract the text information of English teaching materials, understand the English content, and comprehensively improve the quality of English teaching materials in terms of reading and writing both. Based on the artificial intelligence and deep learning environments, this study uses the text detection algorithm based on PSE and the semantic rule mining algorithm to extract the semantic rule information of the English teaching materials. This can help to deeply excavate the keyword features in the English teaching materials and to combine the semantic analysis method to extract the text information and data mining. These text detection algorithms can help the readers to accurately identify the text information of the English teaching materials and play a guiding role in the English teaching. This is conducive to the overall improvement of English teaching quality.

Machine and deep learning techniques, including neural networks, are largely used in the prediction scenarios for real-world problems. This study detects and identifies the text information in English textbooks, realizes the sharing of English textbook text resources, and can also effectively improve the quality of English teaching. Its innovations are as follows. (1) A large number of text data in abstract English teaching can be deeply extracted corresponding to the information on the textbook text, so as to improve the quality and efficiency of teachers' English teaching to a certain extent. Subsequently, English learners can accurately grasp the feature distribution in English teaching texts and better manage and classify English teaching texts. (2) By detecting and identifying English teaching texts, we can better optimize the teaching quality and improve people's speed of reading English teaching texts. This study makes full use of

the concept of deep learning to extract English teaching text materials and formulates an English teaching text algorithm based on association semantic rules to mine the features between different sentences and phrases in the English teaching material text, so as to better extract the keyword semantic association data in the English teaching text. The following are the main contributions of the research conducted in this study:

1 We formulate an English teaching text algorithm based on the association semantic rules

2 We adopt a deep learning-based algorithm that establishes an English teaching text algorithm based on the association semantic rules to mine the features between sentences and phrases in the English language

3 Through combining with semantic similarity information, English teaching text can be accurately detected and identified

The rest of the study is organized as follows. In Section 2, we offer an overview of the related work. Section 3 is about the machine learning, in particular, deep neural networks, i.e., ANN and CNN. In Section 4, we design a deep learning-based algorithm. In Section 5, experimental setting and results are discussed. Moreover, experimental details along with performance evaluation metrics are also presented in this section. Finally, Section 6 concludes this study and illustrates several directions for further research and investigation.

2. Related Work

With the advent of the era of artificial intelligence, a major branch of the field of artificial intelligence is computer vision [1]. At the beginning of the twentieth century, a large number of scholars and experts focused on text detection. OCR was first used to detect text information, but the effect cannot meet the requirements. Since the rapid development of deep learning, more scholars use convolutional neural network (CNN) for text detection and study and explore the field of text detection through deep learning algorithm [2, 3]. From 2016 to 2017, a variety of different algorithms were proposed. When formulating the target detection scheme, the full convolution network (FCN) was used to strengthen the innovation, which greatly improved the level and ability of text detection [4].

In addition, some scholars introduce the end-to-end concept when training the model, so as to comprehensively improve the effect of text detection and recognition [5]. Ge et al. proposed CRNN algorithm. This algorithm makes full use of the concept of indefinite length speech sequence in speech recognition. This method is similar to the speech recognition. The text recognition model is established to solve the problem of phrase recognition or word recognition [6]. Xing et al. trained the background/text classifier of support vector machine (SVM), selected the original pixels as local features, classified all pixels, extracted the text information on the text confidence graph, and extracted the text region [7]. This all happens based on the confidence graph. Derendarz et al. suggested a symmetric text detector based on text symmetric features. Firstly, the symmetric text detector is used to extract the multiscale sliding window text saliency map in the input image. Then, the saliency map is fused according to the manual features, and finally, the convolutional neural network (CNN) classifier is used to delete the false detection information to complete the text detection [8]. Zhou et al. proposed a model in order to generate word level candidates by using edge box and the trained aggregation channel feature (ACF) detector and then trained the random forest two classifier based on the gradient histogram (HOG) feature to remove the false detection data and complete the text location [9].

Dewi et al. used the network similar to Yolo to extract the word level candidate box and filtered the text based on CNN classifier [10]. Jiang et al. transformed text detection into image segmentation based on the full convolution network (FCN) model. Furthermore, the authors segmented the region on the image on the text and then extracted the final text region by using local character features and global features [11]. AA et al. proposed r2am algorithm, which first uses CNN to extract the features on the input image, then inputs the features to the RNN with character level to complete the decoding operation, and then inputs the label. This algorithm uses the character attention mechanism to obtain the characteristic data, and it can recognize the text without a dictionary [12]. Guo et al. put forward the focus attention network (fan), which adds local supervision information to the attention module and can make the actual tag sequence and attention features align with each other. The proposed attention network can effectively deal with the problem of low attention accuracy on the attention module [13].

3. Neural Networks

3.1. Artificial Neural Network (ANN). The principle of artificial neural network is similar to the information processing process of the human brain, which is formed by a large number of artificial neurons connected with each other. Artificial neuron is the basic unit for processing information in artificial neural network. Figure 1 shows the basic processing flow of input signals to artificial neurons.

The output of an artificial neuron to the input signal a = [A1, A2, LAN] T is $t = f(U + b)$, and u is calculated by the following formula:

$$u = \sum_{i=1}^{m} w_i A_i, \tag{1}$$

where f represents the excitation function, ω_i represents synaptic weights on different neurons, A_i represents different components on input signal a, and b represents neuron bias parameters. In general, the excitation function is a nonlinear function, such as Tanh function and Sigmoid function.

Training neural network means that the neural network readjusts the parameters under the interference of the external environment and adopts other methods to deal with the external environment after conversion. In the process of

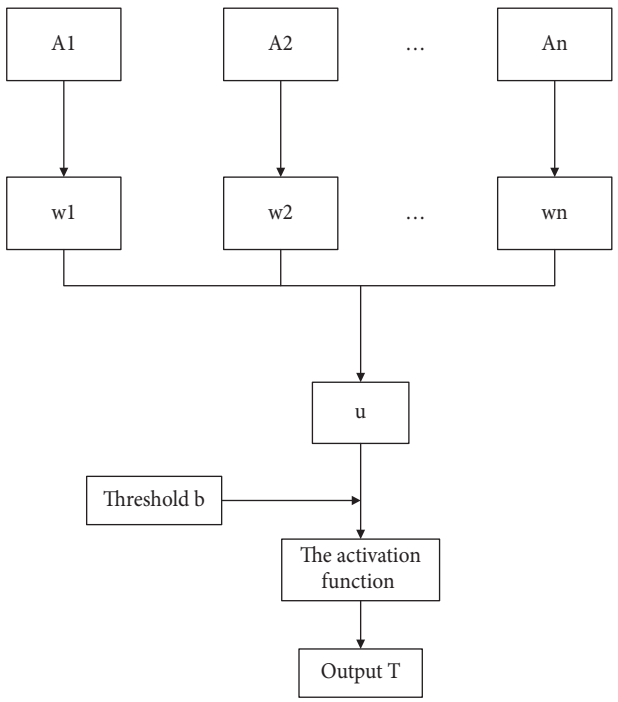

Figure 1: Artificial neuron model.

neural network prediction and classification, a supervised learning mode will be used, that is, a certain sample data will be selected for learning, and different variables on the network will be changed to make the results closer to the real value.

3.2. Convolutional Neural Network (CNN). The working mode of convolutional neural network is similar to feed-forward neural network, which is similar to the structure of traditional neural network [14]. Three-dimensional neurons can be used to reduce the parameters on the neural network, which greatly enhances the operation efficiency of the network. The components of convolutional neural network include the hidden layer, the input layer, and the output layer. The hidden layer includes the pool layer, the convolution layer, and the excitation function layer.

3.2.1. The Convolution Layer. A certain number of convolution kernel parameters together form a complete convolution, and the corresponding convolution kernel is determined according to the convolution bias term and weight vector. Various characteristic graphs are generated by the convolution kernel, and the number of convolution layers has a decisive impact on the number of convolution cores. The receptive field corresponding to the convolution kernel represents all the information involved in the convolution. The large receptive field indicates that the higher the amount of contextual semantic information available from the network. At the same time, the information on the text image corresponds to the information collected on the convolution kernel. Figure 2 is the convolution layer diagram.

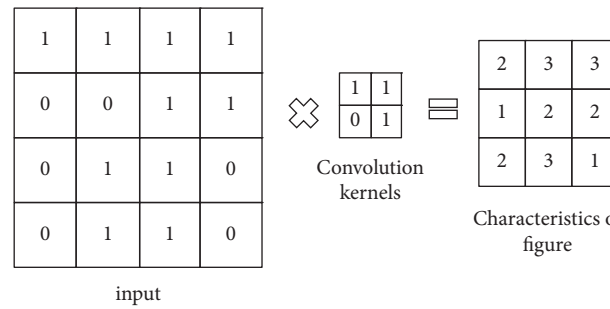

Figure 2: The schematic diagram of the convolution layer.

3.2.2. The Pool Layer. The basic principle of pooling is to simplify the amount of information and variables and speed up the operation of the network. The maximum pooling used in this study is to divide the input image into several different rectangular areas and use the ruler fixed scale filter to complete the maximum value calculation, so as to obtain the maximum value on each subarea. Figure 3 shows the maximum pooling operation process, and the connecting line in the figure represents the maximum pooling operation subarea.

3.2.3. Excitation Function Layer. There are many different types of neurons in a complete network. After continuous development, a large number of excitation functions [15] are generated. Now, the more widely used function types include ***tanh*** function, sigmoid function [16], upgraded ***prelu*** function, and ***relu*** function. In the past, ***tanh*** function and sigmoid function were selected as the excitation functions on convolution neural network, However, the gradient disappears between these two functions. At present, ***relu*** function is selected for in-depth training. Figure 4 shows ***relu*** function.

In the process of image processing by neural network, the image is usually multichannel. Each layer on the neural network is composed of multiple convolution cores, and the multichannel feature image is output. There are also many different channels in the convolution core. The corresponding channels are convoluted by the multichannel convolution core, and then, the pixel values on the corresponding pixel points are accumulated. After the convolution operation, a large number of characteristic images are output. Therefore, the number of channels of n-layer convolution core is equal to that of the input characteristic image.

4. Deep Learning-Based English Teaching Text Detection Algorithm

4.1. Text Detection Algorithm Based on PSE. This study adopts deep learning algorithm in the process of English teaching text detection and recognition to achieve the goal of Integrated English teaching text detection and recognition [17]. The text detection module is completed on the PSE detection framework, and the text recognition module is implemented on the CRNN recognition framework. Input

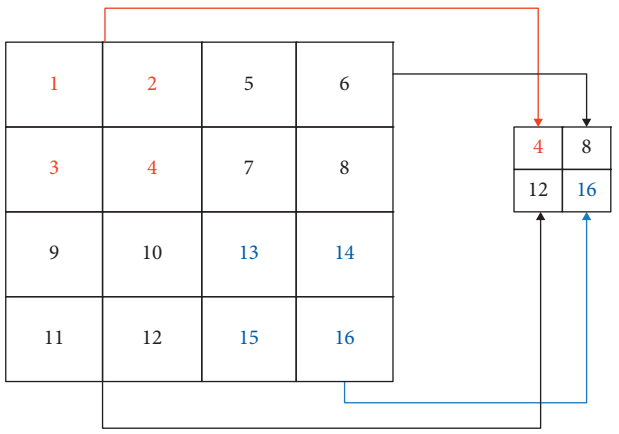

Figure 3: The maximum pool operation.

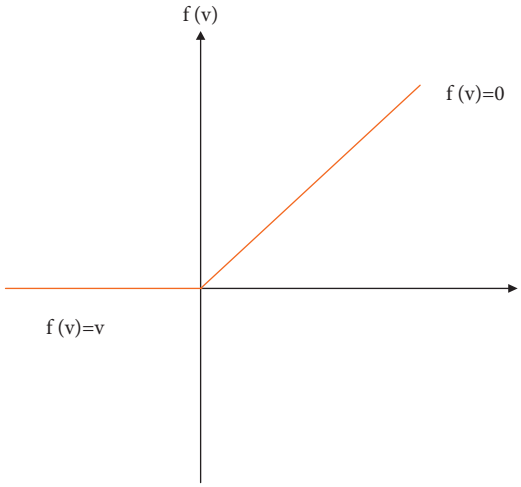

Figure 4: The Relu function.

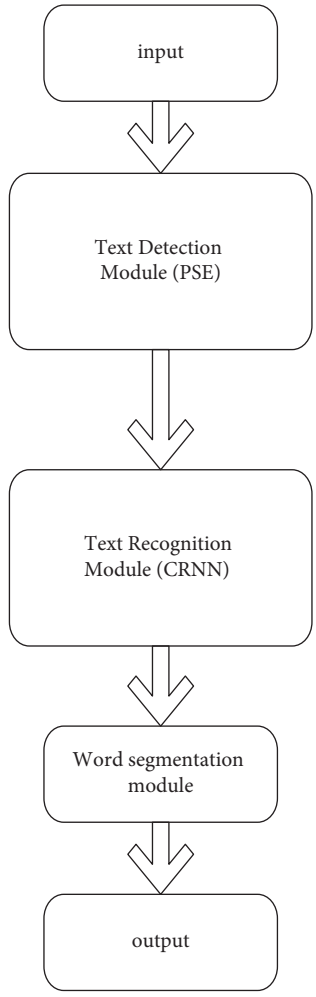

Figure 5: Integrated detection and identification architecture.

the English teaching text information into the detection framework, use the PSE text framework to detect the input text information to obtain the corresponding text box, and then input the text box with English teaching text information into the CRNN recognition box. Further identify the English teaching text content in the text box, and finally input the result information after word segmentation. Figure 5 shows the structure of English teaching text detection and recognition.

At present, the most common problems in the field of text detection include missed detection and false detection. This study focuses on the extraction and fusion of text feature information in English teaching. Loss function and network structure have a decisive impact on the quality of model effect, which is the core of in-depth learning. This study takes the accurate acquisition of row position information as the initial point, improves the network framework based on FPN feature extraction and feature fusion on the basis of considering the network structure, then introduces the empty space pyramid module based on ASPP, compares the experimental results obtained after the introduction of this module, and judges the feature extraction effect of this module. Then, start with the loss function, analyze and use the Dice coefficient loss function to compare the performance of different models under various balance coefficients, and select the best value in each model, so as to improve the accuracy of model detection results.

4.2. Text Content Extraction Algorithm for English Teaching

4.2.1. Extracting Features of the English Semantic Rules. This study designs an English teaching text extraction algorithm and proposes an English teaching text extraction algorithm based on the semantic rule mining. Based on this algorithm, the features between sentences and phrases in English teaching text are deeply mined, so as to achieve the purpose of relevance analysis of keyword semantics in the English teaching text. In order to complete the feature extraction, which can greatly improve the quality of the English teaching, a Boolean weight method is used. Here, the features are extracted based on the Boolean weighting method, that is, the later weight value of the word in a document is 1; on the contrary, the weight value is 0. The following is the basic formula:

$$wij = \left\{ \begin{array}{l} 1, f_{ij} \geq 1 \\ 0, f_{ij} \langle 1 \end{array} \right\}. \quad (2)$$

The above formula f_{ij} represents the frequency of word i in document d_j and w_{ij} represents the weighted vocabulary results. The weight level indicates the frequency of the text data which can also directly reflect the importance of the text data. The following formulas are the weight calculation method based on the information theory; the text summary extraction algorithm is based on the entropy weight:

$$\begin{cases} wij = \log(fij + 1) \times \left\{ 1 + \log\dfrac{1}{N} \sum_{k=1}^{N} \left[\dfrac{f_{ik}}{n_i} \log\left(\dfrac{f_{ik}}{n_i} \right) \right] \right\} \\ IDF = \log\left(\dfrac{N}{n} + 0.01 \right) \end{cases}. \tag{3}$$

During the extraction and recognition of English teaching texts, the number processing calculation should be completed in a standardized way. Based on the classification and measurement of document keywords on the premise of standardized processing, the importance of all keywords can be explained to achieve the purpose of identifying keywords. Based on information theory, this study effectively distinguishes semantic rules and association rules in English teaching texts and then obtains the final test mining results, which are expressed by the following formula:

$$x(L_{ac}) = 1 - \frac{L_{ac}}{\max(L_{ac}) + l}. \tag{4}$$

The maximum semantic correlation similarity can be obtained by characterizing the correlation between the maximum correlation coefficient and the number of texts by the following formula:

$$\max(L_{ac}) = \log_2 k, \tag{5}$$

where k represents the number of semantic categories and L_{ac} represents the extraction feature of semantic information related features, that is, the keyword entropy of each text; 1 is the standard constant coefficient:

$$\begin{cases} w_{ik}(d) = \dfrac{IDF_1}{IDF_{\text{const}}} \times a(L_{ac}) \\ IDF_1 = \text{coff}_1 + tf_{ik}(d) \times \log\left(\dfrac{N}{n_k} + 0.01 \right) \\ IDF_{\text{const}} = \text{coff}_{\text{const}} + \sqrt{\sum_{i=1}^{n} (tf_{ik}(d))^2 \times \left[\log\left(\dfrac{N}{n_k} + 0.01 \right) \right]^2} \end{cases}, \tag{6}$$

where $\text{coff}_{\text{const}}$ represents the fixed coefficient distribution of $\text{IDF}_{\text{const}}$ and coff1 represents the fixed coefficient of semantic feature IDF_1.

4.2.2. Accurate Extraction of English Teaching Text Information. Based on the actual distribution results of probability density, the extraction rates of different phase points in the corresponding region can be obtained. The following is the calculation formula:

$$Q_w(\omega) = \frac{\sum k_{wpg}(W_{pg})}{p \times q}. \tag{7}$$

The concept of related overview function is a set, which is the possibility of various proportions relative to the total point. Its formula is as follows:

$$C_N(r) = \frac{2}{N(N-1)} \sum_{i=1}^{N} \sum_{j=i+1}^{N} H\left(\tau - \left\| x_i - x_j \right\| \right). \tag{8}$$

The vector maximum difference of the similarity between two different English teaching texts can be obtained by expressing the similarity degree between two different texts by norm. The following is the basic formula:

$$\left\| x_i - x_j \right\| = \max_{1 \le k \le m} \left| x_{i-(k-1)\tau} - x_{j-(k-1)\tau} \right|. \tag{9}$$

The logarithmic distribution of the spatial feature distribution of semantic relevance is obtained, and the corresponding English textbook text results are extracted based on the concept of relevance semantics as follows:

$$C_m(r) = \frac{2}{N(N-1)} \sum_{i=1}^{N} \sum_{j=i+1}^{N} H\left(r - \left\| x_i - x_j \right\| \right). \tag{10}$$

The following formula is the confidence space corresponding to the distribution effectiveness of characteristic points of time-frequency distribution of English teaching text:

$$\sum_{i=1}^{c} \mu_{ik} = 1, \quad k = 1, 2, \ldots, n. \tag{11}$$

Therefore, finally, the clustering function of English teaching text information is optimized to complete the extraction of English teaching text information based on the location of semantic feature points of English teaching text summary.

4.3. Constructing Semantic Ontology Model for English Teaching Text. This study uses feature-oriented extraction and semantic ontology model to extract information from English teaching text database, effectively optimize the classification of English teaching text articles, strengthen teachers' class scheduling ability in the process of English teaching, and improve students' level of reading English textbook text information. Here, we need to establish a semantic ontology distribution structure model based on English textbook text analysis. The following are the English textbook text distribution nodes: $G_1 = (M_1^{\alpha}, M_1^{\beta}, Y_1)$ and $G_2 = (M_2^{\alpha}, M_2^{\beta}, Y_2)$; these two distribution nodes are undirected graph models, which hide the weight index of English textbook text distribution. The a_i attribute value is $\{C_1, C_2, \ldots, C_k\}$ and $G_1 \subseteq G_2 \leftrightarrow Y_1 \subseteq Y_2$ if $A = \{a_1, a_2, \ldots, a_n\}$ represents the confidence interval corresponding to the English teaching text. Through the integration of feature extraction module and hidden information transmission

channel, query interface and query vector set, and English teaching text query information output module, the distributed storage of English teaching text is established, and the English teaching text model is established based on ternary components. The formula is as follows:

$$C = Min\{\max(C_i)\},$$
$$\sum_{j'=1}^{p'} Z_{i,j,j_l} = 1, \quad \forall i \in (i,n), \forall j \in (1,n_i). \tag{12}$$

Based on the English teaching text ontology model, the Wigner Ville spatial distribution of the English text summary database is established [18]. The control library can obtain the information flow characteristics under various sampling intervals and reasonably divide the English teaching text set x into c types. The semantic ontology vector in the English teaching text can be divided into M sets in different directions. After preprocessing the English teaching and screening the English teaching text information, we can obtain the corresponding English teaching text extraction structure and complete the English teaching text algorithm design. At this time, we need to establish the English teaching text information flow model, modulate and demodulate the English teaching text classification information based on the English teaching text information flow, and complete the design of anti-interference filter, and accurately extract English teaching texts and classification information.

4.4. A Text Information Process Model for English Teaching. Based on the above saved English teaching text scheduling model, establish the English teaching text information flow model [19], extract the information and teaching text by using the information processing method, and establish a semantic feature base to explain the semantic information of English teaching text. The semantic feature base has n vector attribute sets, which can represent that the text module is a more complex envelope mode, which is calculated by the following formula:

$$\widetilde{y}(t) = \int\int_{\tau\varphi} b(\tau,\varphi)\exp[j2\pi\varphi t]\widetilde{f}(t-\tau)dtd\varphi, \tag{13}$$

where $f(t)$ represents the time-varying nonstationary parameters of different frequency components, b(τ, $\varnothing$) represents the extension function of English teaching text, and t indicates the time delay when extracting English teaching text. The following is the form of window function:

$$H(z) = \frac{N(z)}{D(z)}, \tag{14}$$

where n (z) is the frequency resolution of text semantic feature distribution, which is based on the ontology model of English teaching text, inz = $e^{\pm j\omega 0}$. The upper zero resolution is the lowest in the frequency domain, and D (z) represents the scale factor. The English teaching text information stored in the semantic feature ontology model belongs to the scalar time series, which is represented by the following:

$$x = \left[\ldots x_i \ldots x^i{}_j \ldots\right]^T \in R^{nN}. \tag{15}$$

Fusion of English teaching text information based on Fourier transform. The following is the Fourier transform process of extracting English teaching text information flow:

$$y(t) = \int\int_{a,b} \rho(a,b)\frac{1}{\sqrt{|a|}} f\left(\frac{t-b}{a}\right)\frac{dabd}{a^2}, \tag{16}$$

where ρ(a, (b)) represents the time-frequency combination, b represents the Fourier spectrum window, and a represents the scale parameter. There will be two Fourier spectrum windows in the English teaching text, which are controlled by feedforward and the edge state function of the semantic feature distribution of the English teaching text, which is calculated according to the following formula:

$$\begin{aligned}\dot{x} &= f_i(x_i,u_i)D\left(x_i,A_j(L)\right)\\ &= \min\left\{D\left(x_i,A_j(L)\right)\right\},\end{aligned} \tag{17}$$

where $u_i \in R^m$ represents the state space distribution function and $x_i \in R^n$ represents the state vector distribution of the English teaching text. Based on this, nonlinear feature sequence analysis and semantic association feature extraction are used to extract and mine English teaching text information.

5. Analysis of English Teaching Text Detection and Recognition Results

5.1. Experimental Environment. In this study, the performance of the algorithm in the process of English teaching text extraction is simulated. The hardware equipment of the experimental environment is i5 2.5 GHz Intel processor, 18 GB memory, and windows 7 64 bit operating system. The simulation software used in this algorithm is MATLAB 2016b. The basic parameters of equipment are Gmax = 30, D = 12, c = 3, NP = 30, F = 0.5, CR = 0.1, and m = 2. Set the initial English teaching text sampling frequency f_1 as 2.2 Hz and the termination sampling frequency f_2 as 0.24 hz; ω, the adaptive weight coefficient, is 0.56.

5.2. Results. According to the simulation parameters, as discussed in Section 5.1, we compared the proposed algorithm with the traditional FCM algorithm [20]. Our outcomes show the extraction accuracy of the English teaching text in Figure 6.

According to the analysis results shown in Figure 6, the accuracy of the English teaching text extracted by the method adopted in this study is higher than that of the FCM algorithm. Further in-depth analysis shows that the accuracy of response continues to improve after gradually increasing the number of iterations. We observed that the accuracy of this algorithm can reach 100% after 35 iterations, but the FCM algorithm needs about 50 iterations. By analyzing the data in the figure above, the accuracy of this method is about 78% and that of FCM algorithm is only 57% in 10 iterations. In addition, after continuously increasing the number of

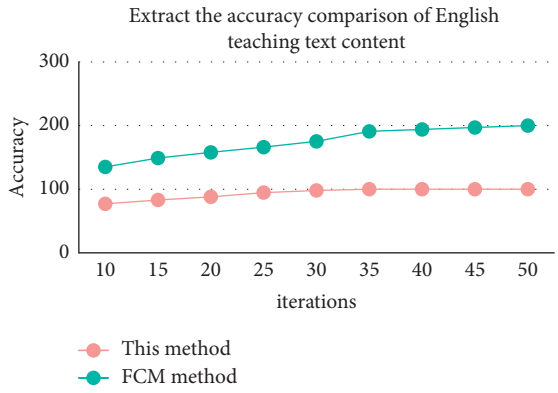

Figure 6: Comparison of accuracy of extracting English teaching text content.

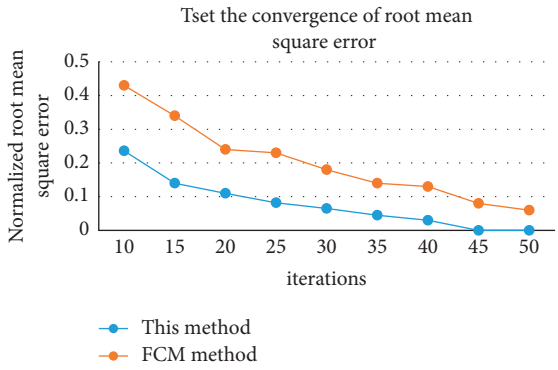

Figure 7: Test the normalized convergence result of root mean square error.

iterations, the accuracy of the algorithm adopted in this study also keeps rising steadily, which is more stable than FCM algorithm. The test index selected here is the speed of extracting English teaching text. The simulation results are shown in Figure 7. According to the results shown in Figure 7, this algorithm can complete the convergence in a short ten years and has strong real-time performance.

Through the above analysis, it is concluded that the English teaching text recognition and detection algorithm based on deep learning proposed in this study can extract the information in the English teaching text very accurately. The information in the extraction stage has high accuracy and strong convergence, which can realize the rapid detection and recognition of English teaching text and improve the comprehensive application of English teaching text. It can also be an important way for English teachers to improve teaching texts.

6. Conclusions and Future Work

In recent years, the text detection method based on deep learning has developed rapidly. Compared with the traditional text detection methods, the advantage of deep learning algorithm is to abandon the manual feature extraction method. However, this involves the process to learn and complete the feature extraction for a large number of sample data, so as to obtain a large number of feature information with high accuracy. In this study, we adopted a deep learning algorithm and established an English teaching text algorithm based on association semantic rules to mine the features between sentences and phrases in the text provided by the English teachers. Through experiments, we evaluated its detection speed and accuracy which were noted much higher than those of the traditional algorithms. The proposed algorithm can also be used for image detection in order to identify future trends in the field of image processing and computer vision.

In the future, we will develop more sophisticated algorithms for text detection which can result in higher accuracies. Similarly, deep learning methods are quite time consuming and the model training may take significant time. Therefore, methods such as aggregation can be used to improve the performance of the algorithm in terms of training and prediction time. Apart from CNN, other methods such as graph convolutional network (GCN), LSTM, ResNet, and attention networks can also be explored in the near future. The results demonstrated in this work are based on the Relu function; however, other functions would have different outcomes. Therefore, we will investigate various functions. The limitations of the network depth, kernel size, and filter number study can also be a good option for further improvement of this research. [21–28].

Data Availability

The data used to support the findings of the study can be obtained from the corresponding author upon request.

Conflicts of Interest

The authors declare that they have no conflicts of interest.

Acknowledgments

This work acknowledges an existing source which was presented as a conference in BDCPS : International conference on Big Data Analytics for Cyber-Physical-Systems. https://link.springer.com/book/10.1007/978-981-33-4572-0.

References

[1] S. Hocker, S. Shah, P. Vespa et al., "The future of neurocritical care research: proceedings and recommendations from the fifth neurocritical care research network conference," *Neurocritical Care*, vol. 32, no. 1, 2020.

[2] S. Y. Li, R. G. Li, Y. Xu et al., "WAF-based Chinese character recognition for spam image filtering," *Chinese Journal of Electronics*, vol. 27, no. 05, pp. 1050–1055, 2018.

[3] L. Gan, Q. J. Wu, Q. H. Huang, and R. J. Tang, "Quick selection of receiver function based on convolutional neural network," *Chinese Journal of Geophysics*, vol. 64, pp. 2394–2404, 2021.

[4] Q. W. Xu, H. Huang, X. F. Zhang, C. Zhou, and S. P. Wu, "Online fault diagnosis method for infrared image feature analysis of high-voltage lead connectors based on improved R-FCN," *Transactions of China Electrotechnical Society*, vol. 36, no. 7, pp. 1380–1388, 2021.

[5] J. Rohdin, A. Silnova, M. Diez et al., "End-to-end DNN based text-independent speaker recognition for long and short utterances," *Computer Speech & Language*, vol. 59, pp. 22–35, 2020.
[6] C.-M. Kim, R. C. Park, and E. J. Hong, "Breast mass classification using eLFA algorithm based on CRNN deep learning model," *IEEE Access*, vol. 8, Article ID 197312, 2020.
[7] F. Mohanty, S. Rup, B. Dash, B. Majhi, and M. N. S. Swamy, "Digital mammogram classification using 2D-BDWT and GLCM features with FOA-based feature selection approach," *Neural Computing & Applications*, vol. 32, no. 11, 2020.
[8] D. Derendarz, "Measurement of the flow harmonic correlations in pp, p+Pb and low multiplicity Pb+Pb collisions with the ATLAS detector at the LHC," *Nuclear Physics A*, vol. 982, pp. 479–482, 2019.
[9] J. Y. Zhou, D. Liang, and J. Tang, "Multi-channel human detection method based on prior Haar-Like features," *Transducer and Microsystem Technologies*, vol. 18, no. 9, pp. 122–125, 2019.
[10] H. Li, L. Deng, C. Yang, J. Liu, and Z. Gu, "Enhanced YOLO v3 tiny network for real-time ship detection from visual image," *IEEE Access*, vol. 9, no. 99, 1 page, 2021.
[11] Z. Y. Jiang, "Deep learning is used to solve the problem of image semantic segmentation," *Practical Electronics*, vol. 46, pp. 39-40, 2017.
[12] A. Aa and B. Rg, "Multi-oriented text detection in natural scene images based on the intersection of MSER with the locally binarized image," *Procedia Computer Science*, vol. 171, pp. 322–330, 2020.
[13] F. Guo, Y. X. Zhang, J. Tang, and W. Q. Li, "YOLOv3-A: a traffic sign detection network based on attention mechanism," *Journal on Communications*, vol. 27, no. 1, pp. 87–99, 2021.
[14] N. Li, B. Liu, and W. Wang, "An optimization algorithm based on single hidden layer feedforward neural networks," *Science Technology and Engineering*, vol. 19, pp. 136–141, 2019.
[15] S. M. Yang, Y. L. Wang, H. M. He, and Y. G. Li, "Active functions learning neural networke," *Journal of Jiangnan University(Natural Science Edition)*, vol. 14, pp. 689–694, 2015.
[16] Y. S. Lin, Y. L. Wei, Q. Q. Chen, W. Zhang, and Z. M. Qiu, "Optimization method for embedded platform," *Journal of Chinese Computer Systems*, vol. 42, pp. 2053–2058, 2021.
[17] K. Frost, J. Clothier, A. Huisman, and G. Wigglesworth, "Responding to a TOEFL iBT integrated speaking task: mapping task demands and test takers' use of stimulus content," *Language Testing*, vol. 37, no. 1, pp. 133–155, 2020.
[18] Y. N. Xu Yuan-Nan, Y. Zhao Yuan, L. P. Liu Li-Ping, Y. Zhang, and X.-D. Sun, "Target detection of saliency map based on pseudo Wigner-Ville distribution and Rényi entropy," *Acta Physica Sinica*, vol. 59, no. 2, pp. 980–988, 2010.
[19] Y. J. Zhang, J. L. Liu, and J. L. Ma, "Classification of multi topic extraction based on Chinese short information text message flow," *New Technology of Library and Information Service*, vol. 12, pp. 101–106, 2014.
[20] F. Zheng and J. L. Qin, "AGC system simulation and testing based on FCM clustering algorithm," *Electronics Test*, vol. 37, pp. 44-45, 2018.

Hindawi
Scientific Programming
Volume 2022, Article ID 3264378, 13 pages
https://doi.org/10.1155/2022/3264378

Research Article

M-DA: A Multifeature Text Data-Augmentation Model for Improving Accuracy of Chinese Sentiment Analysis

Liya Wang,[1] **Xinxin Xu**,[1] **Changhui Liu**,[2] **and Zhe Chen**[2]

[1]*College of Artificial Intelligence, Zhejiang Industry and Trade Vocational College, Wenzhou, Zhejiang 325003, China*
[2]*College of Computer Science and Engineering, Wuhan Institute of Technology, Wuhan 430205, China*

Correspondence should be addressed to Liya Wang; 1578938844@qq.com

Received 19 January 2022; Revised 16 February 2022; Accepted 9 March 2022; Published 4 April 2022

Academic Editor: Muhammad Usman

A neural network based on a word or character embedding is a mainstream model framework in text sentiment analysis and has achieved good results. However, there is a lack of learning about *POS-Tagging* and *Sequence-Tagging*. In this research, we propose a multifeature text data-augmentation model (M-DA) with a multiple-input single-output network structure to overcome this problem of Chinese text sentiment analysis. First, this paper sequentially obtains various sequences of Chinese text, including *word* sequence, *pos* sequence, *char* sequence, *char_pos* sequence, and *char_4tag* sequence, we use *char_pos* and the *char_4tag* to construct a new sequence (*4tag_pos*) and then use *4tag_pos* to mark the characters to obtain the reconstructed characters sequence (char_4tag_pos), so as to achieve the purpose of text enhancement. Then, the Word2Vec method is used to train the initial reconstruction of the character embedding. Finally, the BiLSTM network is used to capture the long-term dependence between the sequences, and the *dropout* technology and *attention* are used to improve the accuracy. In the course of the experiment, we also realized that it is better to use the original sequence and the sequence after text enhancement technology as the input of the BiLSTM network. Therefore, our proposed model also discusses the *concatenate* or *dot* method to fuse multiple sequences as the final embedding. Multigroup comparison experiments are conducted on the data set, and the results show that the proposed M-DA model is superior to the traditional deep learning technology in terms of accuracy, recall rate, f-measure, and accuracy, and the relative time cost is small.

1. Introduction

Natural Language Processing (NLP) has become an important direction in the field of artificial intelligence, which promotes the continuous development and breakthrough of language intelligence. Text sentiment analysis is the extraction of opinions and tendencies contained in texts with the characteristics of subjective consciousness [1, 2]. It is an important research direction in the field of natural language processing and is widely used in various industries [3]. With the continuous development of the Internet, Weibo, Zhihu, Douban, Tianya Forum, Jingdong, Meituan, Eleme, Taobao, etc., the many APPs and online comment platforms continue to increase. The Internet has deeply affected all aspects of life, and the number of Internet users has reached a high limit. While using the Internet to get information, individuals are also contributing to the creation of that information. Speeches, declarations, and other materials are being shared, and online information is exploding. Through text emotion analysis technology, users' views or emotional tendencies are mined from a large amount of user data [4]. Consumers can help themselves make purchase decisions according to the emotional tendencies of other users' comments.

Enterprise managers can understand the market demand through the emotional tendency of user comments, to update and improve the products in time. Government personnel can analyze public opinion based on users' opinions in popular events on social media, to correctly guide the spread of emotions of netizens, effectively control the trend of event development, or provide support for formulating related policies. Therefore, text sentiment analysis has a high

research value. A neural network based on a word or character embedding is a mainstream model framework in text sentiment analysis and has achieved good results. However, there is a lack of knowledge of *POS-Tagging*, *Sequence-Tagging*, etc. In this research, we propose a multifeature text data-augmentation model (M-DA) with a multiple-input single-output network structure to overcome the problem of Chinese text sentiment analysis.

The rest of the paper is organized as follows: Section 1 provides the related work, Section 2 provides the text data-augmentation steps and algorithm, Section 3 provides the language preprocessing. The BiLSTM model based on multifeature text data-augmentation is described in Section 4. Experimental analyses and results are explained in Section 5. The conclusion is given in S.

2. Related Work

Text sentiment analysis methods can be divided into two categories, based on sentiment dictionaries and machine learning methods. The method based on the sentiment dictionary is to first use the existing sentiment words in the dictionary to match the words in the sentence and then calculate the sentiment words in the sentence to obtain the comprehensive sentiment tendency of the sentence. Kamps et al. [5] used the WordNet dictionary to conduct word-level sentiment analysis. Hiroshi Kanayama et al. [6] proposed a fully automatic dictionary expansion method for domain-oriented sentiment analysis. However, this method does not consider the connection between words in the text and lacks semantic information, and the classification effect is too dependent on the quality of the dictionary. The successful application of machine learning in text sentiment analysis has effectively promoted the research and development of text sentiment analysis. Traditional machine learning methods require artificially labeled training sets and artificially designed features for emotional feature extraction and then use text classifiers for classification. Commonly used classifiers include naive Bayes, maximum entropy, support vector machines, etc. [7, 8]. Due to the performance of the classifier, the reliance on the number and quality of manually labeled training sets leads to excessive influence of human factors and huge human engineering. Later, methods based on deep learning appeared, and deep learning is an important branch of machine learning.

The recurrent neural network [9] is a popular model, and most studies use it as the method's basic module. Zhang et al. [10] used distributed word representation technology and RNN network for sentiment classification. Sequential deep learning model LSTM network [11] solves the problem of gradient disappearance or gradient dispersion in the RNN network [12]. BiLSTM [13] is composed of two LSTMs with opposite front and back directions to obtain contextual features. Zhou et al. [14] performed Chinese sentiment analysis by combining Word2Vec and Stacked Bi-LSTM model. In 2017, the Google machine translation team completely abandoned network structures such as RNN and CNN and only used the attention mechanism [15] for machine translation tasks and achieved good results. Luong et al. [16] proposed global and local attention mechanisms, which promoted the application of attention-based models in the field of NLP. Kokkinos et al. [17] proposed self-attention and applied self-attention to sentiment analysis tasks. Part of the research adds the attention mechanism screening feature at the end of the recurrent neural network. Fei et al. [18] combined the Bi-LSTM model with self-attention to form the SA-BiLSTM method. Long et al. [19] studied the sentiment analysis of Chinese text in social media by combining the BiLSTM network with the multi-head attention mechanism (MHAT). It shows that adding attention mechanism screening features can effectively improve the classification effect.

Text representation has been successfully applied to many downstream natural language processing (NLP) tasks as input features, which has a direct impact on the effect of deep learning models [20]. In 1986, Rumelhart et al. [21] first proposed the distributed representation of words used in deep neural language models. Bengio et al. [22] first used neural networks to build language models. Mikolov et al. [23] proposed the Word2Vec [24] technology based on the Log-Bilinear model [25] in 2013, which promoted the rapid development of *word* vectors. Despite the success and popularity of word embedding, most existing methods use each word as the smallest unit and ignore the morphological information of the word. When optimizing the cost function related to rare words and their context, the rare words cannot be represented well. To solve this problem, recently, Wieting et al. [26] proposed Charagram embedding, in which words or sentences are represented by character n-gram count vectors. This is an easy way to learn character-based combination models to embed text sequences. Sun et al. [27] proposed two new models to build better word representations by modeling external context and internal morphemes in a joint prediction method, called BEING and SEING. These two models can also be extended to learn phrase representations based on distributed morphology theory. Rei et al. [28] proposed a new architecture for combining alternative word representations. In the framework of sequence labeling, both character-level and word-level embedding are used. Rezaeinia et al. [29] showed that the improved *word* vector (IWV) is very effective for sentiment analysis. Rahimi et al. [30] proposed two new unsupervised models that integrate word polarity information and word cooccurrence into more tailored sentiment analysis features. Word polarity and cooccurrence are clustered together in the form of tension and tension factorization to generate word embeddings. Unlike other alphabet writing systems, the target of Chinese is three different levels of granularity of radicals, characters, and words. Yu et al. [31] proposed a method of joint embedding of Chinese words and their characters and radical subcharacter components and quantitatively evaluated the quality evaluation and word analogy tasks of word embedding learned by the model on word similarity. Peng et al. [32] inspired by aggressive hierarchical embedding [33] designed two fusion mechanisms to merge three granularities and achieved good results on Chinese

sentiment analysis tasks. In addition, Wu et al. [34] proposed using dictionary embedding and polarity reversal for sentiment analysis.

A Chinese character can be a word or part of a multisyllable word. However, in the above method, the vector calculation that is used to represent the document does not consider the position or part of speech of the words that are composed. So in this work, we propose a multifeature text data-augmentation model (M-DA). First, this paper sequentially obtains various sequences of Chinese text, including word sequence (*word*), part-of-speech sequence (*pos*), character sequence (*char*), word part-of-speech sequence (*char_pos*), and character position ;sequence (*char_4tag*), and then uses character position. The part-of-speech sequence constructs a new sequence (*4tag_pos*) and then uses 4tag_pos to mark the characters to obtain the reconstructed characters sequence (char_4tag_pos), to achieve the purpose of text enhancement. For example, after "十分" is divided into characters, "十" will be marked as the first character *B_m* of the quantifier, and "分" will be marked as the last character *E_m* of the quantifier. Then, the Word2Vec method is used to train the initial reconstruction of the word embedding. Finally, the BiLSTM network is used to capture the long-term dependence between the sequences, and the dropout technology and attention mechanism are used to improve the accuracy. In the course of the experiment, we also realized that it is better to use the original sequence and the sequence after text enhancement technology as the input of the BiLSTM network. Therefore, our proposed model also discusses the concatenate or dot method to fuse multiple sequences as the final embedding, to get our final multifeature text data-augmentation model (M-DA).

3. Text Data-Augmentation

Text Data-Augmentation is also called data-augmentation, which means that the value of limited data is equivalent to more data without a substantial increase in data. Data enhancement technology is already a standard configuration in the image field, and data enhancement is achieved through techniques such as image flipping, rotation, mirroring, and Gaussian white noise. In the field of NLP, Wei et al. [35] introduced NLP data enhancement technology, proposed an EDA model, and showed that the data-augmentation can prevent overfitting and improve the generalization ability of the model.

This paper considers that the knowledge of text *POS-Tagging* and *Sequence-Tagging* is usually very useful, so this paper proposes to use the position and part-of-speech sequence of the characters in the text to reconstruct the original character sequence, to achieve the purpose of data enhancement. Before obtaining the position and part-of-speech sequence (*4tag_pos)* of a word, it is necessary to obtain the word sequence (*word*), part-of-speech sequence (*pos*), character sequence (*char*), word part-of-speech sequence (*char_pos*), and character position sequence (*char_4tag*). Finally, use *4tag_pos* to reconstruct *char* as a new text sequence (*char_4tag_pos*).

Example: "It's really good. Breakfast makes me very satisfied." The text data-augmentation process is shown in Table 1.

The process of text data-augmentation is shown in Table 1. First, the *posseg* method in *jieba* is used to obtain *POS* at the same time as word segmentation. Then the words are divided into characters, and in the same way, the *POS* is iterated one by one to obtain the *POS* of the character (*char_pos*). Regarding text Sequence-Tagging, *2tag* oversimplifies the model and cannot obtain sufficient information; *6tag* makes the model complicated. It is good if the training sample is large enough, but the training set is too small to obtain accurate information through *6tag* [36]. Therefore, this paper uses *4tag* for marking. 'B' represents the beginning position of the word, 'M' represents the middle position of the word,' E′ represents the end position of the word, and 'S' represents a single character. By iterating the words, mark the characters one by one with the mark *4tag* to generate a new text sequence (*char_4tag*). Then, the *char_pos* and *char_4tag* are merged to obtain the position and *POS* information corresponding to the character (*4tag_pos*). Finally, we used *4tag_pos* to mark the characters to get the reconstructed text (*Char_4tag_pos*). The *position-POS* vector corresponding to the character will always follow the character, which can strengthen the semantic logic of the model. The enhanced dependencies in the text are shown in Figure 1. The quantifier "十分" (very) can highlight the main morphological features of things. The "B" marked character "十" is the beginning of the word, and the "分" marked character B belongs to the part of the word and the end position.

4. Language Preprocessing

Google's open-source tool Word2Vec converts text strings into numeric vectors, calculates the distance between words, and groups similar words according to their meanings. The CBOW model uses surrounding words to predict the center word, to use the prediction result of the center word, and to use the Gradient Descent method to continuously adjust the vector of the surrounding words. After the training is completed, each word will be used as the central word, and the *word* vectors of the surrounding words are adjusted so that the *word* vectors of all words in the entire text are obtained.

This paper uses the CBOW model based on Negative Sampling to construct the above seven sequence vectors. Take, for example, the vectorization of reconstructed text. Given the context of the reconstructed character w, w needs to be predicted. Therefore, for a given *Context(w)*, the reconstructed character w is a positive sample, and other reconstructed characters are negative samples. Assuming that a negative sample subset $\mathrm{NEG}(w) \neq \varnothing$ about *Context(w)* has been selected, and $\forall \tilde{w} \in \mathscr{D}$, define $L^w(\tilde{w}) \in \{1\ ,\ 0\}$ to represent the label of the word $\tilde{w}$. The label of positive samples is 1, and the label of negative samples is 0.

For a given positive sample (*Context(w), w*), the optimization goal of this model is to maximize the posterior probability of a given text.

Table 1: The process of text data-augmentation.

Word		*POS*	*Char*	*char_pos*	*char_4tag*	*4tag_pos*	*Char_4tag_pos*
Really very Good	真是很好	d	真	d	B	B_d	真B_d
		d	是	d	E	E_d	是E_d
		a	很	d	S	S_d	很S_d
		x	好	a	S	S_a	好S_a
				x	S	S_x	, S_x

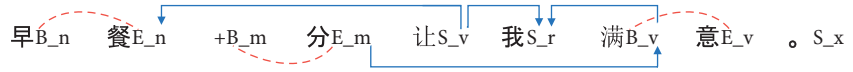

Figure 1: Enhanced dependencies in the text.

$$g(w) = \prod_{w \in \{w\} \bigcup \mathrm{NEG}(w)} p(u|\mathrm{Context}(w)). \tag{1}$$

$$p(u|\mathrm{Context}(w)) = \left[\sigma\left(x_w^T \theta^u\right)\right]^{L^w(u)} \cdot \left[1 - \sigma\left(x_w^T \theta^u\right)\right]^{1-L^w(u)}. \tag{2}$$

$$g(w) = \sigma\left(x_w^T \theta^w\right) \prod_{w \in \mathrm{NEG}(w)} \left[1 - \sigma\left(x_w^T \theta^u\right)\right]. \tag{3}$$

In equations (1)–(3), x_w represents the sum of the vectors of the reconstructed characters in *Context(w)*, and $\theta^u \epsilon \mathbb{R}^m$ represents an auxiliary vector corresponding to the word u, which is the parameter to be trained.

5. The BiLSTM Model Based on Multifeature Text Data-Augmentation

BiLSTM network is one of the commonly used neural networks in text tasks. This paper combines the proposed multifeature text data-augmentation model (M-DA) with the BiLSTM network to complete Chinese sentiment analysis tasks. The M-DA-BiLSTM model is a multiple-input single-output network structure. The schematic diagram of the model is shown in Figure 2.

For a given text sentence, use the reconstructed text method to obtain three types of text, such as *word*, *char*, *Char_4tag_pos*, and input the three types of text into the Word2Vec model for training and obtain the *word* vector w_i, $w_i \in R^{n \times k}$, and the character vector c_i, $c_i \in R^{n' \times k'}$, and reconstruct the character vector e_i, $e_i \in R^{n', \times k'}$, where n, n', n' is the vocabulary size (*dict_len*), k, k', k' is the vector dimension (*vec_dim*), and the obtained dictionary index is used to represent the sentence S. There are 3 ways of representation:

$$\begin{aligned} S1 &= \{\ldots, a_i, a_j, \ldots\}, \\ S2 &= \{\ldots, b_i, b_j, \ldots\}, \\ S3 &= \{\ldots, x_i, x_j, \ldots\}. \end{aligned} \tag{4}$$

5.1. Input Layer. Instantiate 3 Keras tensors; the shape values are all set to 128, which means that the input will be a one-dimensional vector with 128 elements in this dimension.

5.2. Embedding Layer. In this paper, we use the pretrained Word2Vec model for word embedding. The preprocessed data set provides a unique and meaningful sequence of words; each word has a unique ID. The embedding layer uses Word2Vec pretraining weights to initialize embedding weights and introduces external semantic information, which is often very helpful to the model. The input of an embedding layer should be a series of integer sequences, and all integers in the sequence will be replaced by corresponding columns in the corresponding *word* vector matrix, which is its *word* vector. For example, the *word* vector represents the sentence S as shown in Figure 3.

After passing through the dropout layer, change the mode of unified learning of weights and unified update of parameters in the previous network. In each training iteration, some parameters in the network are learned.

5.3. Concatenate Layer. Connect the layers of the input list. It takes a list of tensors as input, all shapes are the same except for the connected axis, and it returns a tensor connected as all inputs. The sentence S output at time t is shown in Figure 4.

5.4. BiLSTM Layer. It is a combination of forwarding LSTM and backward LSTM. The memory unit in LSTM is controlled by the forget gate f_t, the memory gate i_t, the temporary memory state $\tilde{c}_t$, the current memory state c_t, and the output gate o_t, and they are calculated by the hidden state h_{t-1} at the last moment and the current input s_t. See equations (5)–(7). In the calculation, the first hidden state needs to be used, but it does not exist and is generally set to a 0 vector in reality.

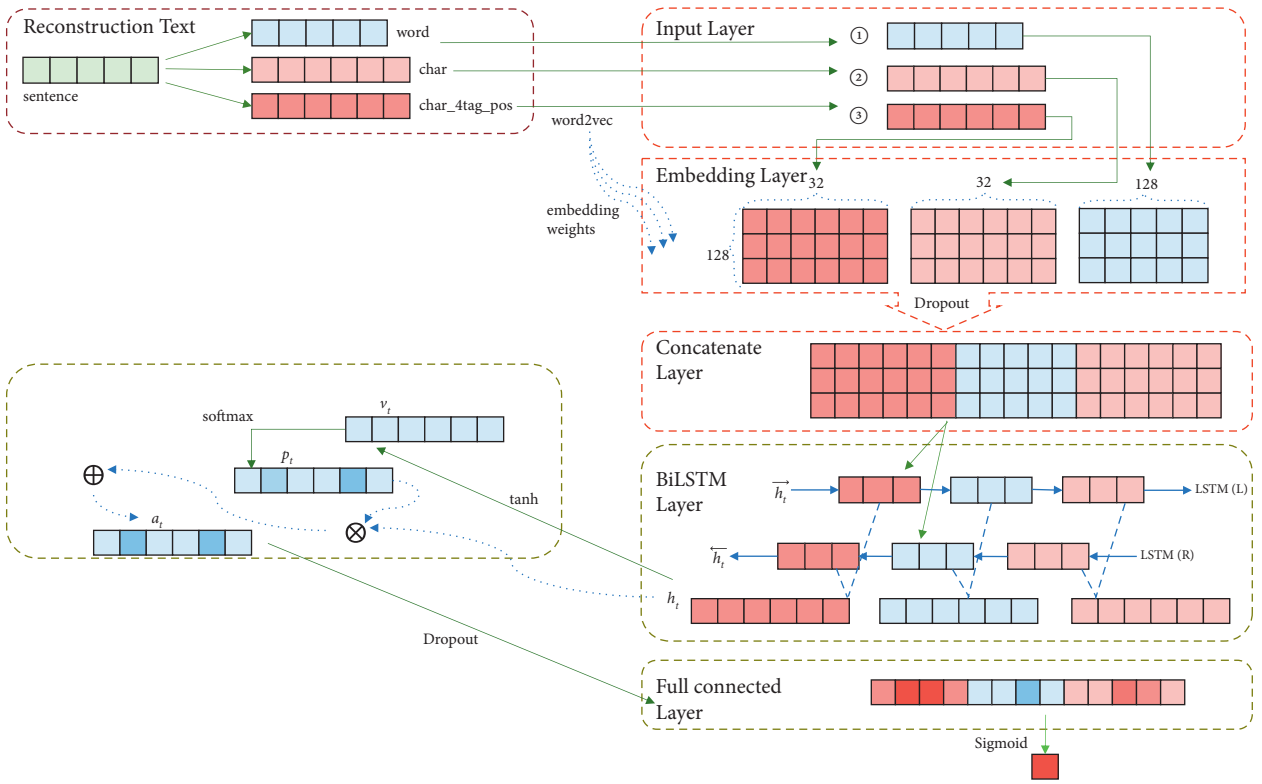

Figure 2: The M-DA-BiLSTM model.

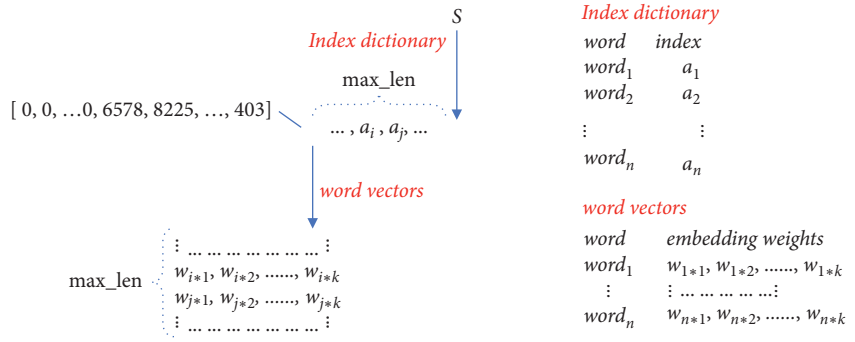

Figure 3: The word vector represents the sentence S.

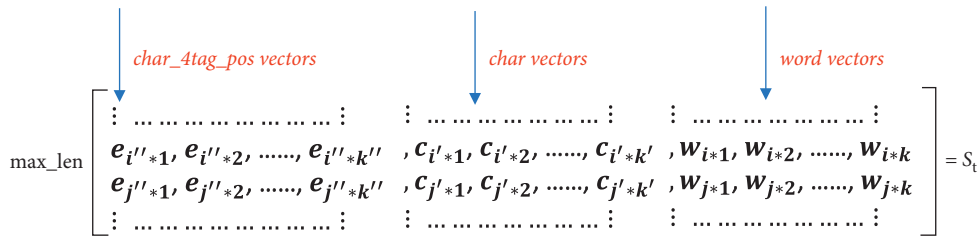

Figure 4: Sentence S output at time t.

$$\begin{bmatrix} f_t \\ i_t \\ \widetilde{c}_t \\ o_t \end{bmatrix} = \begin{bmatrix} \text{logistic} \\ \text{logistic} \\ \tanh \\ \text{logistic} \end{bmatrix} \left(\begin{bmatrix} W_f \\ W_i \\ W_c \\ W_o \end{bmatrix} s_t + \begin{bmatrix} U_f \\ U_i \\ U_c \\ U_o \end{bmatrix} h_{t-1} + \begin{bmatrix} b_f \\ b_i \\ b_c \\ b_o \end{bmatrix} \right). \quad (5)$$

$$C_t = i_t * \widetilde{C}_t + f_t * C_{t-1}. \quad (6)$$

$$h_t = o_t * \tanh(C_t). \quad (7)$$

W, U is the weight matrix, b is the bias vector, and tanh, logistic are the activation functions.

At time t, the hidden state output by the forward LSTM is $\overrightarrow{h_t}$, and the hidden state output by the backward LSTM is h_t ; then the hidden state h_t output by the BiLSTM is merged by the output of the forward and backward LSTM, as shown in

$$h_t = \overrightarrow{h_t} \oplus \overleftarrow{h_t}. \quad (8)$$

5.5. Attention. This paper uses attention to express the correlation between the words in the text sentence and the output result. First, generate the target attention weight v_t, then use the softmax function for probabilism of the attention weight to generate a probability vector p_t. Finally, the generated attention weight is assigned to the corresponding hidden layer state h_t. Different weights are applied to the state at each moment to ensure that the problem of information redundancy is solved while retaining valid information.

$$\begin{aligned} v_t &= \tanh(W * h_t + b), \\ p_t &= \frac{\exp\left(v_t^{\acute{u}} v_t\right)}{\sum_t \exp\left(v_t^{\acute{u}} v_t\right)}, \\ a_t &= \sum_t p_t h_t. \end{aligned} \quad (9)$$

5.6. Dense Layer. The parameter is 1, and the activation function is the sigmoid function. $h_w(x_i)$ is the probability that the predicted input x_i belongs to category 1, as shown in

$$\begin{aligned} h_w(x_i) &= p(y_i = 1 \mid x_i, w) = \text{sigmoid}\left(w^{\acute{u}} x_i\right) \\ &= \frac{1}{\left(1 + \exp\left(-w^{\acute{u}} x_i\right)\right)}. \end{aligned} \quad (10)$$

In the above equations, x_i is the sample feature vector, $y_i \in [0, 1]$ is the true label of the sample, and w is a trainable parameter.

The model uses a logarithmic loss function to update the parameter weight matrix w to complete the experience minimization, as shown in

$$L(w) = -\frac{1}{N} \sum_{i=1}^{N} \left(y_i \log h_w(x_i) + (1 - y_i) \log\left(1 - h_w(x_i)\right)\right). \quad (11)$$

The *summary* function is used to print the M-DA-BiLSTM model, as shown in Figure 5.

6. Experiments

The experimental data is a commonly used and public data set in this field, [37], the data set is Chinese shopping review text with binary sentiment tags, and the tag∈[0,1], where negative emotions are 0 and positive emotions are 1. Data evaluation objects include multiple types, including hotels, milk, books, and mobile phones. The division of the experimental data set is shown in Table 2.

In the experiment section, we will discuss experimental settings, evaluation indicators, comparison methods, and result analysis in detail.

6.1. Experimental Settings. The experimental environment configuration data are shown in Table 3.

Parameter settings will directly affect the classification effect of subsequent models. The specific parameter settings are shown in Table 4.

6.2. Evaluation Indicators. The four model evaluation indicators of accuracy, precision, recall, and F1 are commonly used standards for NLP model evaluation. Accuracy is an evaluation of the correct classification ability of the model. The higher the accuracy, the better the classification ability of the model. Precision is accuracy, and recall is an evaluation of recall. F1 is a weighted average of precision and recall and is a comprehensive evaluation index. The larger the value, the better the model, as shown in equations (12)–(15).

$$\text{Accuracy} = \frac{\text{TP} + \text{TN}}{\text{TP} + \text{FN} + \text{FP} + \text{TN}}. \quad (12)$$

$$\text{Precision} = \frac{\text{TP}}{\text{TP} + \text{FP}}. \quad (13)$$

$$\text{Recall} = \frac{\text{TP}}{\text{TP} + \text{FN}}. \quad (14)$$

$$F_1 = \frac{2 \times \text{Precision} \times \text{Recall}}{\text{Precision} + \text{Recall}}. \quad (15)$$

In the above formula, its specific meaning is shown in Table 5. TP represents positive emotions labeled by the model, which are positive emotions. FP is the positive emotion labeled by the model, which is negative. TN is a negative emotion labeled by the model, which is a negative emotion. FN represents the negative emotion labeled by the model, which is positive.

Layer (type)	Output Shape	Param #	Connected to
input_3 (InputLayer)	(None, 128)	0	
input_1 (InputLayer)	(None, 128)	0	
input_2 (InputLayer)	(None, 128)	0	
embedding_3 (Embedding)	(None, 128, 128)	372864	input_3 [0] [0]
embedding_1 (Embedding)	(None, 128, 32)	327424	input_1 [0] [0]
embedding_2 (Embedding)	(None, 128, 32)	263648	input_2 [0] [0]
dropout_3 (Dropout)	(None, 128, 128)	0	embedding_3 [0] [0]
dropout_1 (Dropout)	(None, 128, 32)	0	embedding_1 [0] [0]
dropout_2 (Dropout)	(None, 128, 32)	0	embedding_2 [0] [0]
concatenate_1 (Concatenate)	(None, 128, 192)	0	dropout_3 [0] [0] dropout_1 [0] [0] dropout_2 [0] [0]
bidirectional_1 (Bidirectional)	(None, 128, 200)	234400	concatenate_1 [0] [0]
dropout_4 (Dropout)	(None, 128, 200)	0	bidirectional_1 [0] [0]
attention_layer_1 (Attention_la	(None, 200)	40200	dropout_4 [0] [0]
dropout_5 (Dropout)	(None, 200)	0	attention_layer_1 [0] [0]
dense_1 (Dense)	(None, 1)	201	dropout_5 [0] [0]

Total params: 1, 238, 737
Trainable params: 1, 238, 737
Non−trainable params: 0

Figure 5: Network structure diagram of the M-DA-BiLSTM model.

Table 2: Experimental data settings.

Data	Train data	Validation set	Test set	Total
Number	16884	2000	2221	21105

Table 3: Experimental environment configuration.

Setting	Value (s)
Language	*Python*3.6
Processor	Intel(R) core(TM) i7-7700HQ CPU @ 2.80 GHz 2.80 GHz
Keras	2.2.4
TensorFlow	1.8.0
Numpy	1.16.2

Table 4: Parameter settings.

Parameter	Value
Vec_window	7
Char_vec_dim	128
Other_ vec_dim	32
Char_Dict_len	2912
Char_4tag_pos_Dict_len	10231
Word_Dict_len	8238
Max_len	128
Input_length	128
BiLSTM_layers	2
BiLSTM_dim	100
Dropout	0.2
Lr	0.001
Bach_size	32
Epochs	10

Table 5: Implications of relevant parameters for evaluation indicators.

Predict reality	Positive	Negative
Positive	TP	FN
Negative	FP	TN

6.3. Comparison Methods. The experiment uses the deep learning mainstream network BiLSTM and the classical language pretraining technology Word2Vec as the baseline model and sets the following series of comparative experiments.

(1) Word-BiLSTM [14]: The mainstream method BiLSTM network is used for sentiment analysis, and the model uses Word2Vec technology to train *word* vectors.

(2) Word-BiLSTM-attention [15, 18]: Compared with the model (1), the attention mechanism is conducive to the selection of important features.

(3) Char-BiLSTM-attention [26, 28]: For characters, the language pretraining models are used to convert characters into vector representations, which is also a popular method.

(4) Char_4tag_pos-BiLSTM-attention: The reconstructed text (*Char_4tag_pos*) proposed in this paper was used as input.

(5) (Char_4tag_pos: Word)-BiLSTM-attention: It is a network structure with multiple inputs and a single output. The input is the *Char_4tag_pos* vector and

the *word* vector, which are merged using the concatenate method and then input into the BiLSTM network.

(6) (Char_4tag_pos Dot Word)-BiLSTM-attention: Compared with model (5), the results of *Char_4tag_pos* vector and *word* vector using the Dot method are input into the BiLSTM network.

(7) (Char: 4tag_pos: Word)-BiLSTM-attention: It is a network structure with three inputs and a single output. The inputs are *Char*, *4tag_pos,* and *word* vector, and then the concatenate method is used to merge the three, so that the overall model can obtain more text representation information.

(8) (Char_4tag_pos: Word: Char)-BiLSTM-attention: Compared with model (7), the inputs are the *Char_4tag_pos*, *Char,* and *word* vectors, and then the concatenate method is used to merge the three. Observe that the *Char_4tag_pos* vector is better than the *4tag_pos* vector. This model is also the final model (M-DA-BiLSTM) proposed in this paper.

In this work, we propose a BiLSTM model (M-DA-BiLSTM) enhanced based on multifeature text data. In addition, the model uses dropout technology and attention mechanism to improve accuracy. The model uses text *4tag* sequence and *pos* sequence to reconstruct *char* to generate a new sequence (*Char_4tag_pos*) to achieve the purpose of text data enhancement for char. Here, we need to consider the following three situations.

The first is whether the text data enhancement method proposed in this paper has a positive effect when applied to the experimental data set. So we set up experimental groups 1, 2, 3, and 4, send the *Char_4tag_pos* vector directly to the network, and compare it with the mainstream model that uses *word* vector or *char* vector as input.

The second is whether the effect of using the enhanced text data sequence and the original sequence as input together is better than a single input. And what is the difference between different fusion methods? So we set up experimental groups 5 and 6, using concatenate or dot method to fuse Char_4tag_pos vector and word vector as input.

Third, what impact will more inputs and more features have on the model? And how do different subelements affect the model? So we set up experimental groups 7 and 8, using concatenate to fuse 4tag_pos, word and char and compare and fuse Char_4tag_pos, word, and char.

6.4. Result Analysis. On the test set, the four model evaluation indicators of accuracy, Precision, recall, and F-1 are used to evaluate the model after the training. The results are shown in Table 6, unit (%).

In Table 6, The Word-BiLSTM model is the mainstream model of sentiment analysis [14]. On its basis, The Word-BiLSTM-attention model uses the attention mechanism proposed in [15] to optimize the model. The Chinese have character-level granularity, which is different from English. The Char-BiLSTM-attention model uses the character-level vector proposed in [26] as the input of the neural network BiLSTM. By comparing with 3 groups of popular models, the *Char_4tag_pos*-BiLSTM-attention model has scores of 91.13% and 91.07% on the two comprehensive indicators accuracy and F1, which is better than the control group. The experiment verifies the feasibility and effectiveness of using the reconstructed *word* vector as the input of the BiLSTM network.

The models in Table 7 are all network structures with multiple inputs and a single output so that the model can obtain more textual information. The first two groups of models are the dual-input structure of *Char_4tag_pos* and *word* vector. They use two different methods to merge the two types of vectors. By comparing these two different merging methods, we can know that the *concatenate* method is 91.53% better than the *dot* method on the accuracy, and the *dot* method is 91.43% better than the *concatenate* method on F1. Therefore, Figure 6 shows the time cost of all comparison models. The abscissa (x-axis) is the epochs of iterations when training the model, and the ordinate (y-axis) is the time of each iteration, in seconds (s). It can be seen from Figure 6 that model 1 without attention has the smallest time cost, followed by single-input models 4, 2, and 3, then dual-input models 5, and three-input models 8, 7. The dual-input model based on the *dot* method has the greatest time cost. Comprehensive analysis shows that the scores of models 5 and 6 are the same inaccuracy. However, the time cost of the *dot* method is about three times that of *concatenate* method, so *concatenate* method is more practical than the *dot* method.

Compared with model 4, models 5 and 6 are better than the single-input structure of reconstructed *word* vector inaccuracy, which shows that the dual input of *Char_4tag_pos* and *word* vector can further optimize the model. Based on this, *Char_4tag_pos* is composed of the basic elements *char* and *4tag_pos*. So, we discussed the three inputs of *char*, *4tag_pos*, and *word* vector and used the merge method concatenate, which is less expensive in time.

By comparing model 7 with models 5 and 6, we can know that such a three-input model 7 achieves scores of 92.35% and 92.25% on the two comprehensive indicators accuracy and F1, and the results are better. The average time is only increased by about 20 s/epoch compared to the dual-input model 5, and it is much shorter than that of model 6.

Model 8 is the final model proposed in this paper. It is a three-input single-output network structure. The model scores 92.35%, 93.87%, and 92.25% on accuracy, precision, and F-1. The training model takes an average of 102 s/epoch. Compared with model 7, the reconstructed character vector is replaced with the *4tag_pos* vector as an input item, and the concatenate merging method can be used to further optimize the model under the premise that the time cost is as small as possible.

Figure 7 shows the distribution of the accuracy rate (val_acc) and the change of the loss rate (val_loss) of the 8 groups of comparative models on the validation set. Figure 7(a) uses a box plot to show the distribution of val_acc values during the entire model training process. The abscissa is the comparison model number, which has the

Table 6: The comparison results of a single model.

Model	Accuracy	Precision	Recall	F1
Word-BiLSTM	89.24	90.56	87.50	89.02
Word-BiLSTM-attention	90.45	90.28	90.60	90.44
Char-BiLSTM-attention	90.86	89.79	**92.10**	90.95
Char_4tag_pos-BiLSTM-attention	**91.13**	**91.36**	90.80	**91.07**

(i) The meaning of bold in "model" column: just to make the model name more visually prominent. (ii) The meaning of the bold values provided in the "Accuracy\Precision\Recall\F1" columns: just to highlight the highest value in each column.

Table 7: The comparison results of multifeature merging models.

Model	Accuracy	Precision	Recall	F1
(*Char_4tag_pos*: Word)-BiLSTM-attention	91.53	93.23	89.50	91.34
(*Char_4tag_pos* dot word)-BiLSTM -attention	91.40	90.82	**92.10**	91.43
(Char: *4tag_pos*: Word)-BiLSTM-attention	92.35	93.10	91.40	92.25
(*Char_4tag_pos*: Word: Char)-BiLSTM-attention	**92.66**	**93.87**	91.20	**92.53**

(i) The meaning of bold in "model" column: just to make the model name more visually prominent. (ii) The meaning of the bold values provided in the "Accuracy\Precision\Recall\F1" columns: just to highlight the highest value in each column.

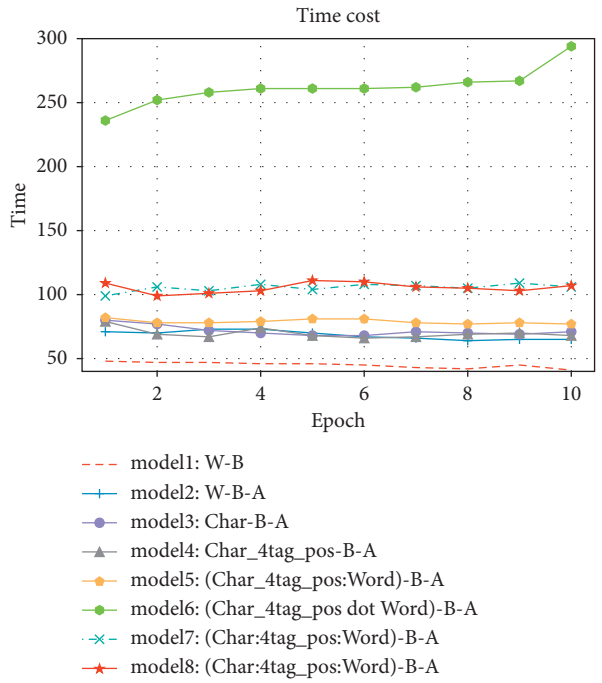

Figure 6: The time cost of model.

same meaning as the label in Figure 6, and the ordinate is the val_acc value. The biggest advantage is that it is not affected by outliers and can describe the discrete distribution of data in a relatively stable way. From Figure 7(a), model 4 is compared with the first three groups of models. In the single-input model, the reconstructed *word* vector contains the highest value as the input. Comparing models 5 and 6 with the first four groups, the median of the dual-input model is higher, and model 5 contains the highest value. Model 8 contains the highest value of val_acc and the highest median value, with a concentrated value distribution.

Figure 7(b) uses a line graph to show the change of val_loss during the training model. The abscissa is the number of iterations when the model is trained, and the ordinate is the loss rate predicted by the model on the validation set after each round of training. For the model loss rate, the smaller the better. From the visual point of view in the figure, model 1 has the highest loss rate, model 6 has the largest fluctuation, and the remaining 6 groups are more concentrated. Model 8 achieves the minimum value in the fourth iteration, and the curve is smooth. Based on the analysis in Figures 7(a) and 7(b), we can know that model 8 has the characteristics of fast convergence, high accuracy, and stability.

Figure 8 counts the prediction results of 8 groups of models on 2221 test samples from six indicators such as TP, FP, TN, FN, Right, and Wrong. The output result is the probability that the predicted sample is 1. For the

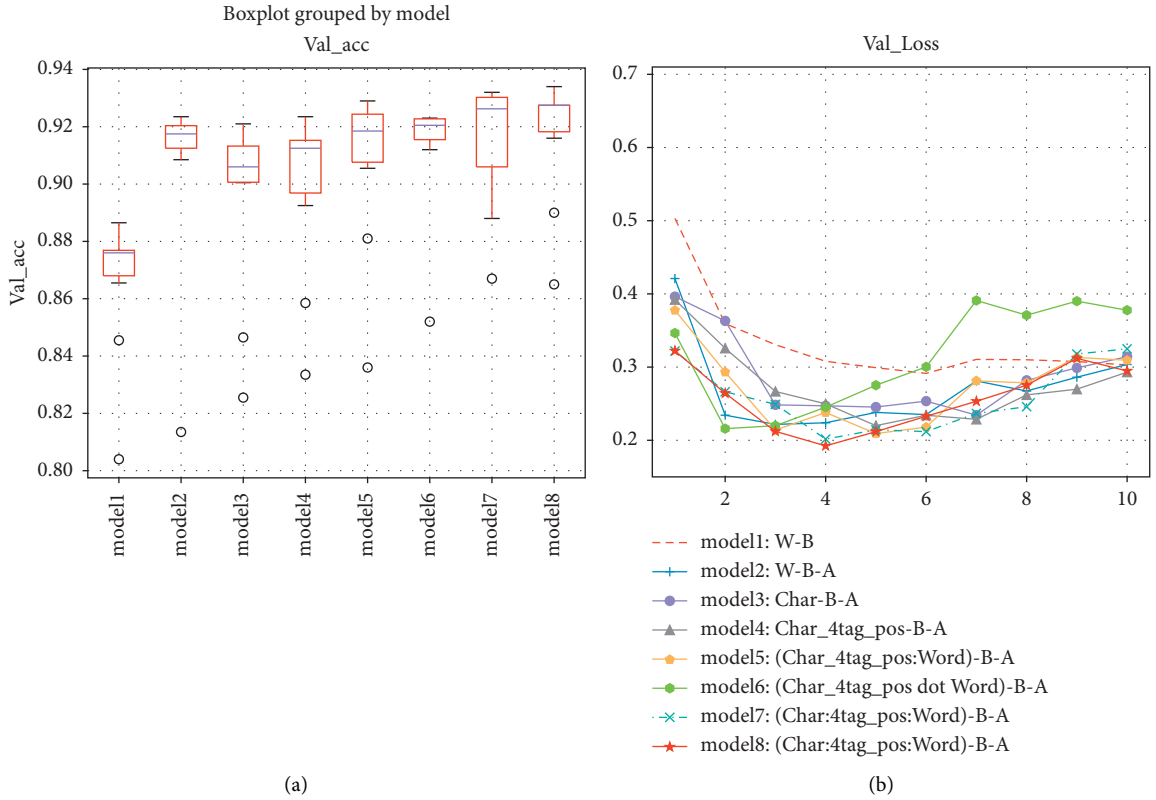

Figure 7: The change of Val_acc and Val_loss.

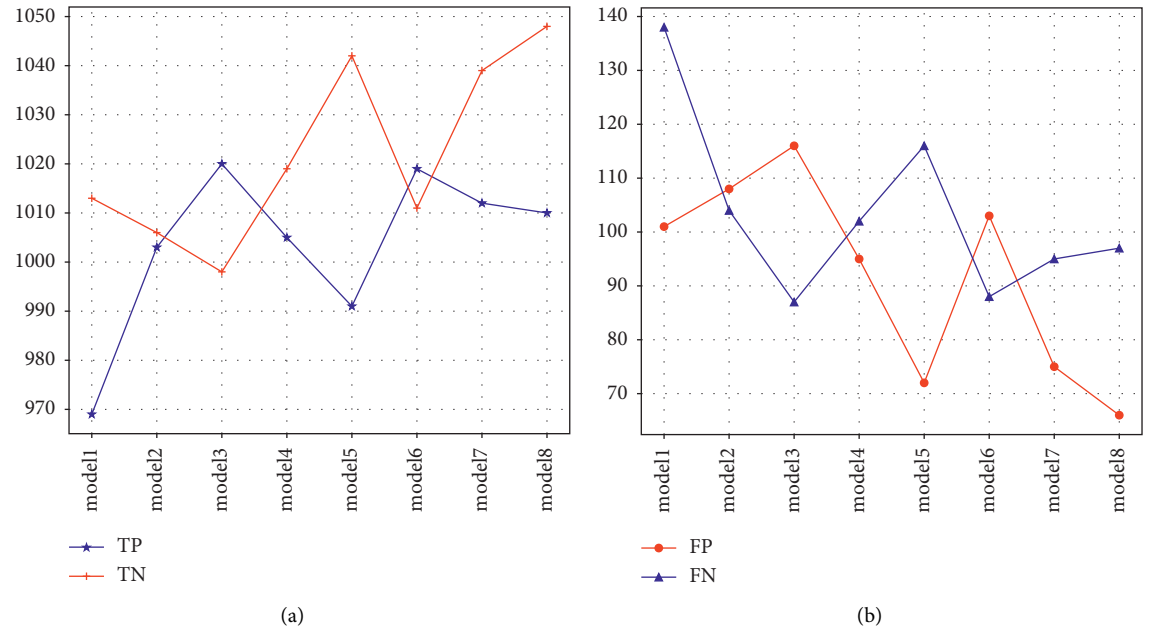

Figure 8: Continued.

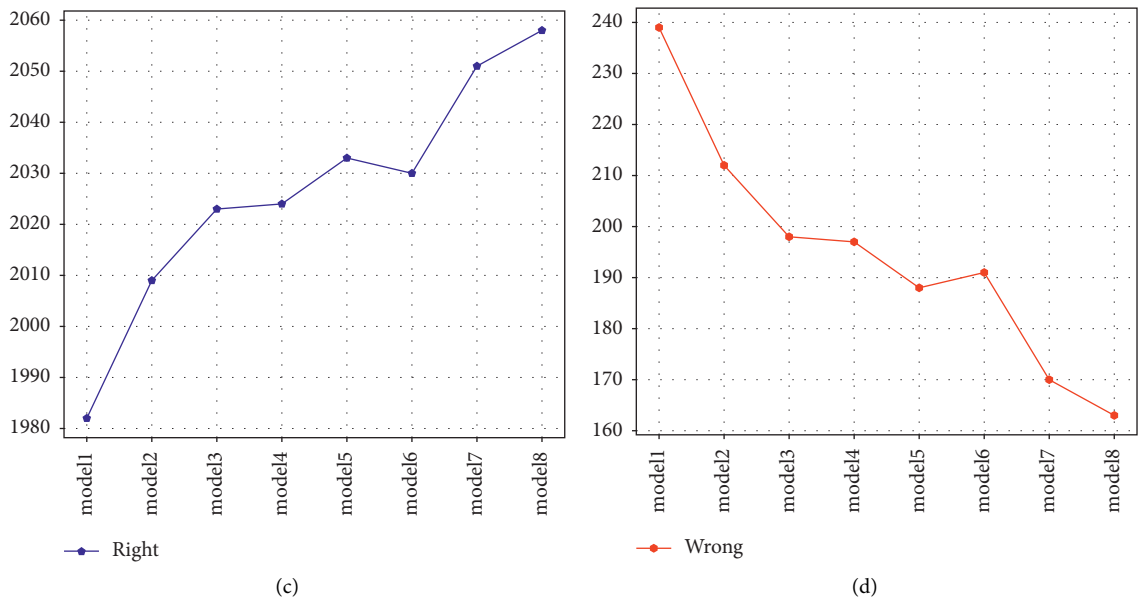

Figure 8: The statistical results of predicted values.

convenience of statistics, the output result greater than 0.5 is classified as 1, and the rest are 0. In Figure 8(a), TP represents the correct number of positive samples predicted by the model, and TN represents the correct number of negative samples predicted by the model. The higher the value, the better. In Figure 8(b), FP represents the number of negative sample errors predicted by the model, and FN represents the number of positive sample errors predicted by the model. The lower the value, the better. In Figures 8(c) and 8(d), Right is the number of samples that the model predicts correctly, and Wrong is the number of samples that the model predicts incorrectly. That is, Right = TP + TN, Wrong = FP + FN.

It can be seen from Figures 8(a) and 8(b) that, in the positive sample, model 3 performs better; in the negative sample, model 8 performs better. From the comprehensive indicators Right and Wrong in Figure 8(c) and 8(d), it can be seen that model 8 performs better on the entire sample. Model 8 is also the final model (M-DA-BiLSTM) proposed in this paper.

In summary, for the data set used in this paper, we verify the proposed M-DA-BiLSTM model. Here, we considered the following three situations:

In the first, we set up experimental groups 1, 2, 3, and 4, send the *Char_4tag_pos* vector directly to the network, and compare it with the mainstream model that uses *word* vector or *char* vector as input. It can be seen that the *Char_4tag_pos* vector is more appropriate on the experimental data in this paper, which indicates that the text data enhancement method proposed in this paper has a positive effect when applied to the experimental data set.

In the second, based on the results of experimental groups 1, 2, 3, and 4, we set up experimental groups 5 and 6, using concatenate or dot to fuse the Char_4tag_pos vector and the word vector as input. It can be seen that the effect of using the text data-enhanced sequence and the original sequence as the input is better than a single input, but the accuracy of the two fusion methods is equivalent, so we have analyzed the time cost, and the results show that the time cost of the concatenate method is small.

In the third, based on the results of experimental groups 5 and 6, we set up experimental groups 7 and 8, using concatenate to fuse 4tag_pos, word, and char, and compare and fuse Char_4tag_pos, word, and char. It can be seen that three-input is better than two-input, and Char_4tag_pos is more suitable as a subelement. However, the time cost of three inputs is nearly twice that of dual inputs. Therefore, training models with more inputs and more features will require higher and higher experimental hardware and software configuration.

7. Conclusion

In this work, we proposed a multifeature text data-augmentation model (M-DA). First, this work sequentially gathers several Chinese text sequences, including word, pos, char, char pos, and char 4tag (which we employ), and char pos produces a new text sequence (4tag pos). To achieve the goal of text enhancement, utilize 4tag pos to mark the characters and get the reconstructed characters sequence (char 4tag pos). Then, the Word2Vec method is used to train the initial reconstruction of the characters embedding. Finally, the BiLSTM network is used to capture the long-term dependence between the sequences, and the *dropout* technology and *attention* are used to improve the accuracy. In the course of the experiment, we realized that it is better to use the original sequence and the sequence after text enhancement technology as the input of the BiLSTM network. Therefore, the proposed model compares the experimental results of the concatenate or dot method and chooses to use concatenate. The method fuses multiple sequences as the final embedding, thereby further

improving the accuracy of text classification. This paper focuses on binary polarity detection in sentence-level sentiment analysis. In the future, we recommend investigating the effectiveness of our proposed M-DA-BiLSTM for other sentiment analysis tasks (such as aspect level or multiple sentiment analysis).

Data Availability

The data used to support the findings of this study are included in the article.

Conflicts of Interest

The authors declare that they have no competing interests.

References

[1] B. Pang, L. Lee, and S. Vaithyanathan, "Thumbs up? Sentiment classification using machine learning techniques," in *Proceedings of the ACL-02 Conference on Empirical Methods in Natural Language Processing*, pp. 79–86, Stroudsburg, PA, USA, July 2002.

[2] B. Pang and L. Lee, "Opinion mining and sentiment analysis," *Foundations and Trends in Information Retrieval*, vol. 2, no. 1-2, pp. 1–135, 2008.

[3] B. Liu, *Sentiment Analysis and Subjectivity. Handbook of Natural Language Processing*, N. Indurkhya and F. J. Damerau, Eds., , Taylor and Francis Group, Boca, FL, USA, Second edition, 2010.

[4] M. Hu and B. Liu, "Mining and summarizing customer reviews," in *Proceedings of the ACM SIGKDD Conference on Knowledge Discovery and Data Mining (KDD)*, pp. 168–177, Seattle WA USA, August 2004.

[5] J. Kamps and M. Marx, "Words with attitude," in *Proceedings of the First International Conference on Global WordNet*, pp. 332–341, CIIL, Mysore India, January 2002.

[6] H. Kanayama and T. Nasukawa, "Fully automatic lexicon expansion for DomainOriented sentiment analysis," in *Proceedings of the 2006 Conference on Empirical Methods in Natural Language Processing*, pp. 355–363, Association for Computational Linguistics, Stroudsburg, PA, USA, July 2006.

[7] B. Pang, L. Lee, and A Sentimental Education, "Sentiment analysis using subjectivity summarization based on minimum cuts," in *Proceedings of the Forty Second Annual Meeting on Association for Computational Linguistics*, pp. 271–278, Association for Computational Linguistics, Stroudsburg, PA, USA, July 2004.

[8] S. Liu, F. Li, F. Li, X. Cheng, and H. Shen, "Adaptive cotraining SVM for sentiment classification on tweets," in *Proceedings of the 22nd ACM International Conference on Conference on Information & Knowledge Management*, pp. 2079–2088, ACM, San Francisco CA USA, October 2013.

[9] A. Graves, A. R. Mohamed, and G. Hinton, "Speech Recognition with Deep Recurrent Neural networks," in *Proceedings of the Acoustics, Speech, and Signal Processing, 1988. ICASSP-88. 1988 International Conference on*, vol. 38, New York, NY, USA, April 1988.

[10] Y. Zhang, Y. Jiang, and Y. Tong, "Study of sentiment classification for Chinese microblog based on recurrent neural network," *Chinese Journal of Electronics*, vol. 25, no. 4, pp. 601–607, 2016.

[11] S. Hochreiter and J. Schmidhuber, "Long short-term memory," *Neural Computation*, vol. 9, no. 8, pp. 1735–1780, 1997.

[12] K. Cho, B. V. Merrienboer, C. Gulcehre et al., "Learning phrase represention using RNN Encoder Decoder for statistical machine translation," in *Proceedings of the 2014 Conference on Empirical Methods in Natural Language Processing (EMNLP)*, pp. 1724–1734, October 2014.

[13] M. Schuster and K. K. Paliwal, "Bidirectional recurrent neural networks," *IEEE Transactions on Signal Processing*, vol. 45, no. 11, pp. 2673–2681, 1997.

[14] J. Zhou, Y. Lu, H. N. Dai, H. Wang, and H. Xiao, "Sentiment Analysis of Chinese Microblog Based on Stacked Bidirectional LSTM," *IEEE Access*, vol. 7, p. 1, 2019.

[15] A. Vaswani, N. Shazeer, N. Parmar et al., "Attention Is All You Need," 2017, https://arxiv.org/abs/1706.03762.

[16] M. T. Luong, H. Pham, and C. D. Manning, "Effective Approaches to Attention-Based Neural Machine Translation," in *Proceedings of the 2015 Conference on Empirical Methods in Natural Language Processing*, pp. 1412–1421, September 2015.

[17] F Kokkinos and A Potamianos, "Structural attention neural networks for improved sentiment analysis," in *Proceedings of the Fifteenth Conference of the European Chapter of the Association for Computational Linguistics*, pp. 586–591, EACL, Valencia, Spain, January 2017.

[18] R. Fei, Y. Zhu, and Q. Yao, "A deep learning method based self-attention and Bi-directional LSTM in emotion classification," *Journal of Internet Technology*, vol. 21, no. 5, pp. 1447–1461, 2020.

[19] F. Long, K. Zhou, and W. Ou, "Sentiment analysis of text based on bidirectional LSTM with multi-head attention," *IEEE Access*, vol. 7, no. 99, p. 1, 2019.

[20] Q. Liu, M. J. Kusner, and P. Blunsom, "A Survey on Contextual Embeddings," 2020, https://arxiv.org/abs/2003.07278.

[21] D. E. Rumelhart, G. E. Hinton, and R. J. Williams, "Learning representations by back-propagating errors," *Cognitive Modeling*, vol. 10, no. 5, pp. 533–536, 1986.

[22] Y Bengio, H Schwenk, and J. S Senecal, "A neural probabilistic language model," *Journal of Machine Learning Research*, vol. 3, no. 6, pp. 1137–1155, 2003.

[23] T. Mikolov, K. Chen, G. Corrado, and J. Dean, "Efficient Estimation of Word Representations in Vector Space," 2013, https://arxiv.org/abs/1301.3781.

[24] T. Hayashi and H. Fujita, "Word embeddings-based sentence-level sentiment analysis considering word importance," *Acta Polytechnica Hungarica*, vol. 16, no. 7, pp. 7–24, 2019.

[25] A. Mnih and G. E. Hinton, "A scalable hierarchical distributed language model," in *Proceedings of the Twenty First International Conference on Neural Information Processing Systems*, pp. 1081–1088, NIPS, Vancouver British Columbia, Canada, December 2008.

[26] J. Wieting, M. Bansal, K. Gimpel, and K. Livescu, "Charagram: Embedding Words and Sentences via Character n-grams," in *Proceedings of the 2016 Conference on Empirical Methods in Natural Language Processing*, Austin, TX, USA, November 2016.

[27] F. Sun, J. Guo, Y. Lan, J. Xu, and X. Cheng, "Inside Out: Two Jointly Predictive Models for Word Representations and Phrase Representations," in *ProceeAAAI2016*, AAAI Press, Phoenix, AZ USA, February 2016.

[28] M. Rei, G. Crichton, and S. Pyysalo, "Attending to Characters in Neural Sequence Labeling Models," 2016, https://arxiv.org/abs/1611.04361.

[29] S. M. Rezaeinia, R. Rahmani, A. Ghodsi, and H. Veisi, "Sentiment analysis based on improved pre-trained word

embeddings," *Expert Systems with Applications*, vol. 117, pp. 139–147, 2019.

[30] Z. Rahimi and M. M. Homayounpour, "TensSent: a tensor based sentimental word embedding method," *Applied Intelligence*, vol. 6, pp. 1–16, 2021.

[31] J. Yu, X. Jian, H. Xin, and Y. Song, "Joint Embeddings of Chinese Words, Characters, and Fine-grained Subcharacter Components," in *Proceedings of the Conference on Empirical Methods in Natural Language Processing*, Copenhagen, Denmark, September 2017.

[32] H. Peng, Y. Ma, Y. Li, and E. Cambria, "Learning multi-grained aspect target sequence for Chinese sentiment analysis," *Knowledge-Based Systems*, vol. 148, no. MAY15, pp. 167–176, 2018.

[33] H. Peng, E. Cambria, and X. Zou, "Radical-based hierarchical embeddings for Chinese sentiment analysis at sentence level," in *Proceedings of the FLAIRS*, pp. 347–352, PaloAlto, CA, USA, May 2017.

[34] O. Wu, T. Yang, M. Li, and M. Li, "Two-level LSTM for sentiment analysis with lexicon embedding and polar flipping," *IEEE Transactions on Cybernetics*, pp. 1–13, 2020.

[35] J. Wei and K. Zou, "EDA: Easy Data Augmentation Techniques for Boosting Performance on Text Classification Tasks," 2019, https://arxiv.org/abs/1901.11196.

[36] M. Wenchao, L. Lianchen, and C. Anyan, "A comparative study on Chinese word segmentation using statistical models," in *Proceedings of the 2010 IEEE International Conference on Software Engineering and Service Sciences*, pp. 482–486, Beijing, China, July 2010.

[37] Github, "Chinese Shopping Reviews sentiment analysis," 2016, https://github.com/BUPTLdy/Sentiment-Analysis.

Hindawi
Scientific Programming
Volume 2022, Article ID 9535488, 7 pages
https://doi.org/10.1155/2022/9535488

Research Article

Early Warning of Regional Landslide Disaster and Development of Rural Ecological Industrialization Based on IoT Sensor

Xianjun Chen

Institute of Economics and Management, Chongqing Three Gorges Vocational College, Chongqing 404000, China

Correspondence should be addressed to Xianjun Chen; qqjl1111@outlook.com

Received 9 January 2022; Revised 23 January 2022; Accepted 28 January 2022; Published 29 March 2022

Academic Editor: Muhammad Usman

Regional landslide disaster is actually the instability caused by the movement of ground or slopes, etc. If a landslide occurs in a habitat area where people live, it can cause a great deal of damage. So, in order to improve the early warning effect of regional geological landslide disaster, the study abandoned the conventional geological probe data, directly used the tilt photography data provided by the fixed camera, introduced the camera clock synchronization control system supported by the high-sensitivity atomic clock timing function, and used the data warehouse hardware and computing host hardware. Combined with the spatial convolution neural network, fuzzy neural network (logarithmic depth iterative regression neural network, polynomial depth iterative regression neural network, transfinite learning machine, and binary neural network) and other technologies finally realize high geological disaster early warning sensitivity and long early warning advance. The system will become an alternative to the previous geological disaster early warning system based on the direct data of geological embedded probes.

1. Introduction

Zeng said in his study that rural ecological agriculture and ecotourism industry are important ways to realize new agriculture. However, the planting area and tourism reception area of ecological agriculture are generally located in mountainous landforms, and the quaternary development layer is thick in mountainous areas with good planting effect, which is easy to form landslides in extreme weather and extreme groundwater environment [1]. Sun and Zhang said in their study that common landslide types include collapse type, fault block type, creep type, layer displacement type, debris flow, and barrier lake [2]. Relevant studies provide accurate landslide early warning in large advance for data collection, data analysis, and data early warning of regional landslides.

In relevant studies, various machine learning algorithm modules are selected to perform in-depth mining on geological monitoring data so as to realize geological landslide early warning with sufficient advance, sensitivity, and specificity. Wang et al. used the combination model to analyze the susceptibility of landslide disasters and gave the susceptibility parameter factors so as to realize high-precision landslide early warning [3]. Liu et al. designed a big data model of a landslide disaster direct early warning factor and used the model to form a machine learning algorithm to realize landslide early warning with high sensitivity and large advance [4]. The research on regional landslide monitoring Internet of Things system is rare. Only one document has been published in mainstream journals in the recent 10 years. This document is the application suggestion of geological disaster monitoring and early warning sensor network technology proposed by Zhou [5]. That is, around 2011, the domestic geological disaster monitoring and early warning Internet of Things system has been basically matured, and the relevant technologies have been used to this day. Wang et al. took the Bailong River Basin as the research area, the evaluation model of regional landslide susceptibility was constructed, and its applicability and result rationality were explored [6]. Zhu et al. for landslides in the western mountainous areas, regional landslide sensitivity analysis was designed and validated, and evaluated it using environmental factor spatial features and heuristic fuzzy logistic model correlation [7]. Fang et al. used the logistic

regression algorithm to establish an early warning model for the regional landslide disasters in Qingchuan County, Sichuan Province [8,9]. Li et al. use data mining technology. The model was constructed by the artificial neural network algorithm to evaluate and predict the regional landslide [10].

Under the traditional Internet of Things signal system, this research focuses on the model combination mode of the machine learning algorithm, verifies its availability and reliability, and then discusses the engineering value of early warning data to ecological agriculture.

The rest of the paper is organized as follows: Section 2 focuses on the hardware design of regional landslide disaster early warning Internet of Things system, Section 3 throws light on innovation of the big data early warning algorithm based on machine learning, and Section 4 is about the simulation evaluation of the effectiveness of big data early warning algorithm. Similarly, Section 5 enlightens the importance of significance of a regional landslide disaster early warning system to the development of the rural ecological industry. Finally, Section 6 is the conclusion.

2. Hardware Design of Regional Landslide Disaster Early Warning Internet of Things System

The geological disaster early warning system for regional landslide uses the displacement and vibration data of rock stratum and soil layer to obtain relevant data in the traditional mode. However, in the principle of geology, stratum displacement can cause the displacement and vibration of rock stratum and soil layer, but the displacement and vibration of rock stratum and soil layer are difficult to have a logical relationship with the subsequent geomechanical changes. Therefore, although this kind of data is relatively direct, it is difficult to form an effective early warning. After the popularization of UAV tilt photography 3D modeling technology, considering the dependence of UAV on weather, fixed tilt photography probes are arranged at most key observation positions. Because the coordinates of the fixed tilt photographic probe can be accurately positioned by the total station and other measuring equipment, the monitoring modeling accuracy can reach the submillimeter level, which can intuitively show the subtle changes of the mountain surface, and the amount of data is much larger than the direct data monitoring results. This technology has become an important technical means of geological disaster monitoring in key areas. Moreover, the rock stratum monitoring data under the traditional mode have not been eliminated but entered the data warehouse as auxiliary data. The logic of the above data acquisition system is shown in Figure 1.

In Figure 1, we have the following: RD Meter: a probe device for obtaining geological monitoring data by analyzing the relative displacement between rock stratum and soil layer. Seismograph: equipment for receiving ground microvibration and obtaining geological monitoring data. Visible camera: the real-time photographing equipment based on visible light can be controlled by a remote clock synchronization signal to form three-dimensional modeling of multiangle tilt photography.

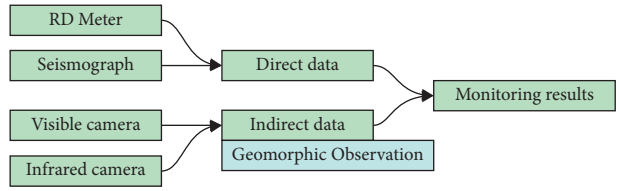

Figure 1: Data logic of geological disaster monitoring and early warning system.

Infrared camera: the equipment that cooperates with a visible camera to realize ground temperature data acquisition and synchronous three-dimensional modeling, and the equipment control mode is the same as that of the visible camera.

The above main data acquisition process based on camera involves clock synchronization control, data mining analysis, data warehouse, and other hardware functions, so the relationship between hardware devices (host, database, timer, etc.) is shown in Figure 2.

In Figure 2, we have the following: Red: the hardware equipment of the data warehouse is configured with a raid-based high-speed read-write high-capacity solid-state disk system, and the corresponding streaming media data management software is installed. Green: the data analysis host is configured with multiple high-performance CPU computing cores, the maximum capacity allowed by the motherboard is configured with a high-speed dynamic storage system, and multiple high-performance GPU computing cores are configured at the same time to form a multiboard floating-point computing support hardware. Blue: specially marked data processing thread. Brown: data input/output interface.

It should be emphasized that the timer module needs to provide a clock signal with a higher degree of synchronization to improve the observation accuracy. This accuracy needs to take into account the interference factors such as the time-consuming data transmission of the clock trigger signal line. In submillimeter measurement, the clock accuracy directly determines the modeling accuracy. Therefore, when conditions permit, the cesium atomic clock is used to control the core clock signal generator and the antineural network is used to control the transmission advance of the clock signal, which is limited by the length. Although the signal is important, this study focuses on the processing scheme of geological disaster monitoring and early warning signal, which is not discussed here.

3. Innovation of Big Data Early Warning Algorithm Based on Machine Learning

3.1. 2D Still Image Processing Part. The two-dimensional spatial convolution neural network combined with the log depth iterative regression fuzzy neural network is used to generate the fuzzy evaluation value of a single frame image, and the two-dimensional image on the time series generates the time series of fuzzy evaluation value. On this sequence, the transfinite learning machine is used to extract the comprehensive evaluation value of the static image. The logic of the big data algorithm is shown in Figure 3.

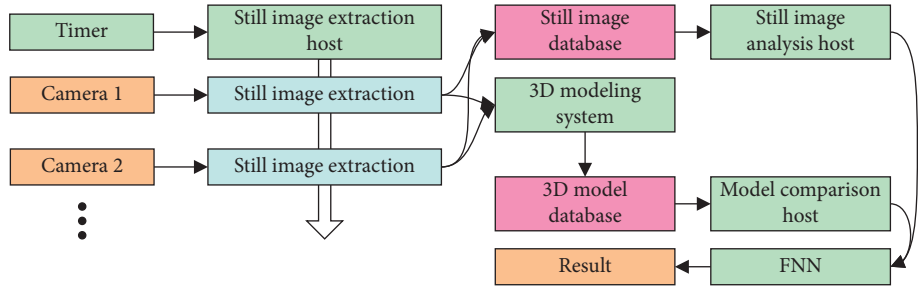

Figure 2: Hardware logic of geological landslide disaster monitoring and early warning system based on fixed camera tilt photography.

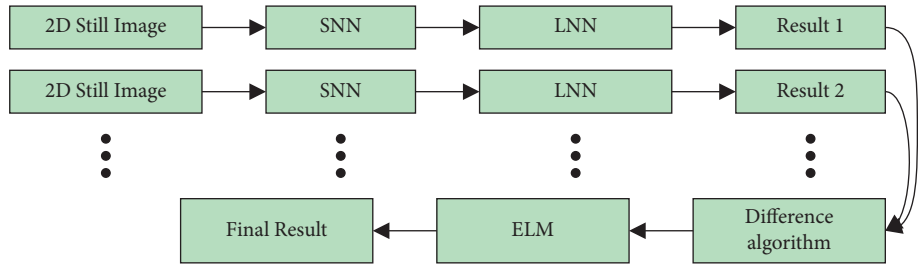

Figure 3: Static image processing model based on multiple neural network modules.

In Figure 3, we have the following: SNN: the two-dimensional spatial convolution neural network module is used to strengthen the detailed information of the two-dimensional image. LNN: the log depth iterative regression neural network is used to amplify the data details of high-density landing points near the zero point of the number axis, and compress and convolute the two-dimensional array data into a double precision floating-point data. ELM: it is used for the feature extraction of periodically changing data, fully known as extreme learning machine, which continues to compress and convolute multiple variables on the time series into a double precision floating-point variable.

The core algorithm function of the SNN module is the 2D spatial convolution function, as shown in the following formula:

$$y(d,e) = \int_{-\infty}^{+\infty} g(x)d(u-x)e(u-x)du\ . \tag{1}$$

Among them, $g(x)$ denotes the convolution kernel; $d(u-x)$ denotes the convoluted array expression of the first dimension; $e(u-x)$ denotes the convoluted array expression of the second dimension; x denotes the convolution control factor; u denotes the convolution pointer factor.

In the node of the log depth iterative regression neural network, the log depth iterative regression algorithm is used to construct the node basis function, as shown in the following formula:

$$y = \sum_{i=1}^{n} (A \cdot \ \log\ x_i + B). \tag{2}$$

Among them, x_i denotes the output value of the function node; A and B are the coefficient to be regression of the base function; n is the number of nodes of the upper neural network; before using the ELM, the above data needs to be converted, which calculates the ratio of the difference between two adjacent sequence elements and the previous element, which is shown in the following formula:

$$\widehat{A}_n = \frac{A_n - A_{n-1}}{A_{n-1}}. \tag{3}$$

Among them, $\widehat{A}_n$ denotes the n-th element of the difference sequence; A_n denotes the n-th element of the original sequence.

The essence of ELM is the depth iterative regression neural network based on trigonometric function. Although there are abundant selection objectives of ELM's basis function in relevant studies, the most basic trigonometric function depth iterative regression algorithm is adopted in this study, and its basis function is as follows:

$$y = \sum_{i=1}^{n} [A \cdot \ \sin(B \cdot x_i + C) + D]. \tag{4}$$

Among them, A, B, C, D denote the coefficients to be regressed; n denotes the number of nodes of the upper layer neural network. The meanings of other mathematical symbols are the same as those above.

3.2. 3D Model Comparison Processing Part. The comparative analysis algorithm of the three-dimensional model is basically similar to the comparative analysis algorithm of the above two-dimensional still image. Firstly, the double precision floating-point data sequence of deep iterative regression convolution is obtained by using the spatial convolution method and the logarithmic neural network method, and then the transfinite learning machine algorithm is used to further convolute the data sequence. Finally, a double precision floating-point variable is formed as the evaluation value of the three-dimensional

model. At the basis function selection level, the only difference is that the three-dimensional space convolution is used to replace the two-dimensional space convolution. The basis function of the three-dimensional space convolution neural network is shown as follows:

$$y(d,e,f) = \int_{-\infty}^{+\infty} g(x)d(u-x)e(u-x)f(u-x)du\ . \quad (5)$$

Among them, $g(x)$ denotes the convolution kernel; $d(u-x)$ denotes the convoluted array expression of the first dimension; $e(u-x)$ denotes the convoluted array expression of the second dimension; $f(u-x)$ denotes the convoluted array expression of the third dimension; x denotes the convolution control factor; u denotes the convolution pointer factor.

3.3. Fuzzy Neural Network Analysis. The logarithmic depth iterative regression neural network and transfinite learning machine neural network in the previous paper belong to the category of the fuzzy neural network. The fuzzy neural network forms a double precision floating-point variable by the convolution compression of bulk data, but the logarithmic neural network focuses on feature amplification and extraction of the high-density part of uneven data. The neural network of the transfinite learning machine focuses on the periodic change feature extraction of periodic variables. After two-dimensional image analysis and three-dimensional model analysis, the two outputs are double variable floating-point variables. The fuzzy neural network for subsequent data fusion adopts the FNN general mode, i.e., multinomial deep iterative regression neural network. Its data logic is shown in Figure 4.

In Figure 4, both FNN and FNN-pro use the sixth-order polynomial depth iterative regression function to design the neural network node basis function, as shown in formula (6), and the output function of the final early warning result adopts the binary fuzzy neural network node function as follows:

$$y = \sum_{i=1}^{n} \sum_{j=0}^{5} A_j x_i^j, \quad (6)$$

$$y = \sum_{i=1}^{n} \frac{1}{A \cdot e^{x_i} - B}. \quad (7)$$

Among them, A, B denote the coefficints to be regressed; A_j denotes the coefficient to be regressed of the j-th order polynomial; n denotes the number of nodes of the upper layer neural network. The meanings of other mathematical symbols are the same as those above.

The output result of the FNN module and the binarization module is a data located in [0, 1] interval and infinitely close to 0.000 or 1.000. When the data is near 0.000, it is considered that the corresponding early warning has not been issued. When the data is near 1.000, it is considered that the corresponding early warning has been issued. At this time, the alarm control system is used to trigger audible and visual early warning; at the same time, the mobile Internet is used to inform relevant managers and heads of management departments.

From the above algorithm analysis, it can be seen that the system belongs to a general neural network system, that is, the machine learning module driven by the neural network. By observing the camera information, it can judge the possible probability of regional landslide. The algorithm does not involve any calculation module of geology and geotechnical mechanics, so the system needs to use more data for training; however, it is not subjected to any current geological and geotechnical theory.

Different early warning directions, such as dividing different landslide early warning areas and setting different landslide early warning amounts, can build independent algorithm modules, each module can be trained independently, and finally, independent judgment is given. In the following study, the early warning efficiency of different early warning targets will be simulated and analyzed.

4. Simulation Evaluation of the Effectiveness of Big Data Early Warning Algorithm

The Simulink component is loaded under MATLAB to form a simulation environment. According to the above algorithm design, the early warning software for common early warning targets is constructed. The data source is all the available data of 26 deep mountain and deep valley ecological agriculture bases available in China from January 1, 2020 to December 31, 2021. Among them, 146 real landslide disasters were involved, and the prediction and early warning effectiveness of relevant landslide disasters were compared. The reference group provides the early warning results of the geological disaster early warning system based on the direct data of stratum monitoring provided by the State Seismological Bureau.

Firstly, the data before 146 geological landslides are classified according to the types of landslides, and the simulation software formed by the algorithm designed in this study is used to analyze and make early warning in the simulation environment. Compared with the early warning results of the previous system, Table 1 is obtained.

In Table 1, we have the following: Early warning advance: the interval between the issuance of early warning and the occurrence of disaster. Caving type here is no displacement of mountain foundation rock stratum, but there is large rock or a large amount of earthwork collapse. Displacement type: the basic rock stratum of the mountain is displaced and stripped, but the earthwork after stripping basically maintains the previous sequence. Torsion type: the basic rock stratum of the mountain body is displaced and stripped, and the earthwork after stripping disrupts the previous sequence. Debris flow type: the interaction of surface runoff and groundwater causes large-area erosive displacement of rock stratum.

In order to more intuitively observe the data in Table 1, visual processing is performed to obtain Figure 5.

According to the threshold requirements for industrial application of machine learning proposed by the Ministry of Industry and Information Technology, machine learning

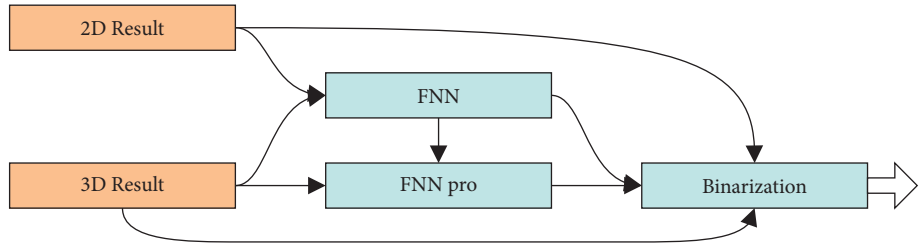

Figure 4: Fuzzy neural network module data logic diagram.

Table 1: Comparison of early warning sensitivity of different early warning systems under different early warning requirements (%) (data source: simulation analysis results).

Data source type	Disaster type	Early warning advance (s)			
		5	30	60	120
Camera based	Caving type	83.5	83.2	82.7	82.5
	Displacement type	98.6	97.3	96.5	95.7
	Torsion type	97.2	96.8	96.2	95.3
	Debris flow type	98.5	98.1	97.6	97.2
Direct data based	Caving type	67.4	52.5	31.2	16.8
	Displacement type	96.3	82.9	33.6	21.4
	Torsion type	95.7	81.4	31.7	18.5
	Debris flow type	96.9	81.8	32.3	19.7

software can be used as a grid connected data source for industrial application only when the sensitivity reaches more than 95%. In Figure 5, the sensitivity of the original system based on the direct data of geological monitoring decreases sharply with the increase of early warning, while the sensitivity of the simulation software formed by the algorithm designed in this study in the simulation environment does not decrease significantly with the increase of early warning. It is proved that the simulation system formed by the algorithm has higher availability than the original system.

Under the 120 s and 5 s early warning demand, the regional landslide that forms outside the collapse landslide is investigated, the sensitivity, specificity, and accuracy of the algorithm simulation system are compared and analyzed with the previous system, and Table 2 is obtained.

In Table 2, we have the following: Sensitivity: the ratio of the number of true positive early warning to the number of positive samples. Specificity: the ratio of the number of true negative warnings to the number of negative samples. Accuracy: the ratio of early warning data consistent with reality to all early warning data. T: in SPSS big data analysis software, the value of bivariate t check output is considered to be statistically different when $T < 10.000$. P: the log value of bivariate t-check output in SPSS big data analysis software is considered to have credible statistical significance when $P < 0.05$ and significant statistical significance when $P < 0.01$.

It can be seen that when the early warning advance is 120 s, there is a very significant statistical difference between the two groups of data, $T < 0.001$, $P < 0.001$; when the early warning advance is 5 s, there is a believable small statistical difference between the two groups of data, $T < 10.000$, $0.01 < P < 0.05$; It can be considered that the previous system

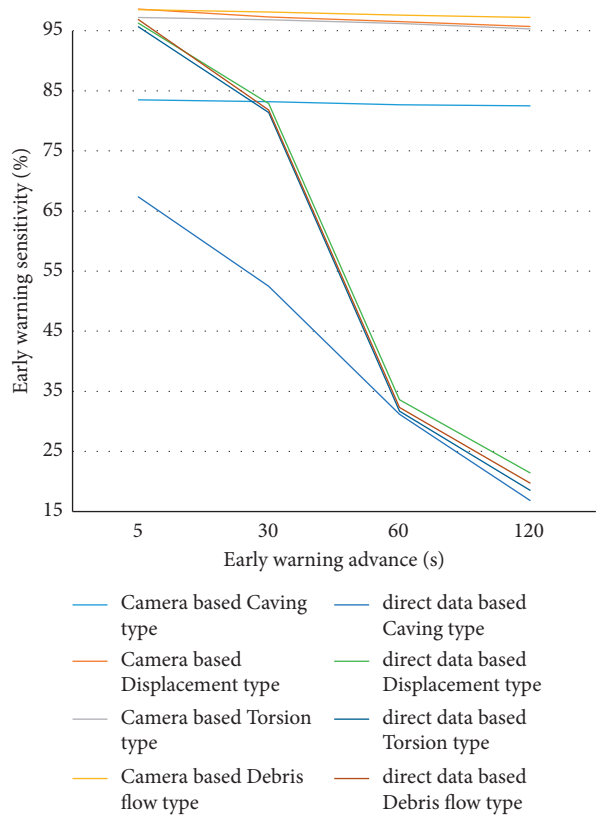

Figure 5: Comparison of early warning sensitivity of different early warning systems under different early warning requirements.

focuses more on short advance geological disaster early warning, and the system shows better early warning effect than the previous system under any advance conditions, especially with the increase of early warning advance.

Table 2: Comparison of sensitivity, specificity, and accuracy of the two algorithms in different early warning cycles (%).

Data source type	120 s			5 s		
	Sensitivity	Specificity	Accuracy	Sensitivity	Specificity	Accuracy
Camera based	98.3	96.6	95.8	97.8	98.2	98.1
Direct data based	19.8	24.6	21.7	96.1	97.5	96.7
T	0.000	0.000	0.000	8.726	9.443	8.954
P	0.000	0.000	0.000	0.017	0.025	0.019

5. Significance of Regional Landslide Disaster Early Warning System to the Development of Rural Ecological Industry

All eco agricultural production parks and tourism parks located near high mountains and deep valleys need to face the impact of geological disasters. Of the 146 landslides discussed in this study, they have caused direct economic losses, including 22 casualties (63 injuries and 2 deaths) and 37 losses of buildings and property, and the total number of abandoned or collapsed houses has reached 679 square meters. Regardless of the secondary losses caused by the decline in the number of tourists and insufficient reception capacity caused by the destruction of the landscape after the landslide disaster, only the direct economic losses are enough to bring economic burden to the operator.

In the research at home and abroad, when geological landslide disaster occurs, the early warning advance is about long and the emergency disaster relief capacity is about strong. Cooperating with the early warning mechanism (evacuation mechanism and protection mechanism) and optimizing the early warning algorithm to improve the advance of effective early warning is an important technical way to reduce the loss of ecological agriculture operators.

Sun Liming used the tilt photography method to quickly model the geological hazards of the barrier lake and realize the geotechnical analysis [11]. Yu Jiayong et al. used the tilt photography modeling method in the prediction and evaluation of geological disasters along a highway [12]. The above related studies show that the tilt photography method is an important method in the current geological disaster assessment and early warning. In particular, the tilt photography data acquisition system with fixed cameras is used in this study. Each camera is accurately positioned by the total station, and the shutter control of all cameras uses a high-precision timing synchronization system. With the support of big data and cloud computing hardware system, it can form submillimeter real-time 3D modeling with higher accuracy. Data analysis is based on a high-precision model, and the full use of the advantages of machine learning helps in analyzing incomplete data and hidden logic data to finally achieve the algorithm efficiency in the previous simulation.

The algorithm can basically achieve more than 95% of the early warning sensitivity under the demand of 120 s early warning advance. In the actual engineering implementation of domestic geological disaster early warning, it can be considered as having engineering value if it reaches 60% of the early warning data. In the simulation, under the 60% sensitivity target, the actual early warning advance of the system can reach more than 900 s, which is enough for the operator to organize effective evacuation of tourists.

6. Conclusion

This research comprehensively uses spatial the convolution neural network and the fuzzy neural network, and forms a multimodule deep iterative convolution neural network machine learning system based on the static image data and tilt photography data collected by visible light camera and infrared camera. Finally, it realizes the high early warning sensitivity and specificity of underground in the early stage of long early warning advance. However, the relevant algorithms in this research do not form packaged software but run in the simulation environment. The follow-up research will develop the application software for the algorithm and try it in the ecological agricultural industrial park with high geological disaster risk.

6.1. Future Work. This work can be further extended onto a major level using the spatial convolution neural network and the fuzzy neural network to form a multimodule deep iterative convolution neural network machine learning system based on the static image data and tilt photography data collected by visible light camera and infrared camera. This work can be useful as it realizes the high early warning sensitivity and specificity of underground at very early stages.

Data Availability

The data underlying the results presented in the study are included within the manuscript.

Conflicts of Interest

The author declares that there are no conflicts of interest.

Authors' Contributions

The author has read the manuscript and approved submit to your journal.

Acknowledgments

This work was supported by 2020 Science and Technology Youth Project of Chongqing Municipal Education Commission, "Research on the Development Mode of Rural Ecological Industrialization in Wanzhou under the Rural

Revitalization Strategy" fund: Big Data and Economic Development (no. KJQN202003507).

References

[1] X. Zeng, "Experimental analysis of the effect of optimizing the ecological environment on Promoting the development of rural agricultural Economy," *Shanxi Agricultural Economy*, no. 02, pp. 112–114, 2022.

[2] Z. Sun and R. Zhang, "Progress in the sensitivity analysis of landslide disaster in loess area," *Inner Mongolia Coal economy*, vol. 16, no. 12, pp. 123-124.

[3] G. Wang, N. Guo, B. Deng et al., "Analysis of landslide susceptibility and accuracy in different combined models," *Northwest geology*, vol. 54, no. 02, pp. 259–272, 2021.

[4] Y. Liu, R. Fang, Y. Su, and R. Xiao, "Research on regional landslide disaster early warning model based on machine learning," *Journal of Engineering Geology*, vol. 29, no. 01, pp. 116–124, 2021.

[5] P. Zhou, "Application status and development suggestions of sensor network technology for geological disaster monitoring and early warning," *Southern land and resources*, vol. 9, no. 10, pp. 12–14, 2011.

[6] G. Wang, N. Guo, and B. Deng, "etc.Analysis of landslide susceptibility and accuracy in different combined models," *Northwest Geology*, vol. 54, no. 02, pp. 259–272, 2021.

[7] Q. Zhu, M. Zhang, and Y. Ding, "etc.Fuzzy logic analysis method of regional landslide sensitivity," *Journal of Wuhan University (Natural Science Edition)*, vol. 46, no. 10, pp. 1431–1440, 2021.

[8] R. Ke Fang, Y. Liu, and Z. Huang, "Review of regional landslide risk assessment methods based on machine learning," *Chinese Journal of Geological Disasters and Prevention and Control*, vol. 32, no. 04, pp. 1–8, 2021.

[9] R. Ke Fang, Y. Liu, and Y. Su, "Regional landslide disaster early warning model in Qingchuan County, Sichuan Province, based on logistic regression," *Hydrogeological Engineering geology*, vol. 48, no. 01, pp. 181–187, 2021.

[10] L. Li, H. Yang, and J. Zhang, "etc.Research on regional landslide prediction based on artificial neural network," *Meteorological and Environmental Science*, vol. 43, no. 03, pp. 65–70, 2020.

[11] L. Sun, "Study on rapid sensing and simulation calculation method of landslide barrier in Alpine Canyon Area: Taking Baige barrier lake as an example," *Water conservancy and Hydropower Technology (Chinese and English)*, vol. 52, no. 07, pp. 44–52, 2021.

[12] J. Yu, X. Xue, C. Chen, R. Chen, K. He, and F. Li, "Three dimensional reconstruction of highway slope and disaster identification method based on UAV tilt photography," *Chinese Journal of highway*, vol. 17, no. 2, pp. 1–13, 2022.

Hindawi
Scientific Programming
Volume 2022, Article ID 1304826, 6 pages
https://doi.org/10.1155/2022/1304826

Research Article

Research on Static and Dynamic Fragile Node Identification Algorithms Based on Uncertainty in New Energy

Yingming Lin,[1] **Haohuai Wang**,[2] **Yang Liu**,[1] **Shiming Li**,[1] **Lei Li**,[3] **and Dongjian Gu**[3]

[1]*Power Dispatching and Communication Center of Guangdong Power Grid Company, Guangzhou 510600, China*
[2]*CSG Pwoer Dispatching Control Center, Guangzhou 510530, China*
[3]*Nari-Tech Nanjing Control Systems Ltd.,, Nanjing 211106, China*

Correspondence should be addressed to Yingming Lin; 631505040409@mails.cqjtu.edu.cn

Received 17 January 2022; Revised 10 February 2022; Accepted 15 February 2022; Published 24 March 2022

Academic Editor: Muhammad Usman

In order to identify the uncertain static and dynamic fragile nodes in new energy, the instability and randomness of new energy bring new challenges to the identification of vulnerable nodes in a power grid. Due to the characteristics of low cost and low energy consumption of new energy, people have paid much attention to the exploration and development of new energy. Due to the uncertainty of new energy, it is needed to properly analyze the uncertainty factors. To analyze the uncertainty factors in new energy using the framework of power big data artificial intelligence analysis based on cost-benefit analysis (CBA), it is required to carry out Fourier transform and extract the data characteristic matrix so that a vulnerability risk prediction index can be obtained by using a fuzzy convolution algorithm and binarization, and the safety form between the uncertainty factors in new energy and power stations can be evaluated. In this paper, a fuzzy neural network algorithm is proposed to identify the static and dynamic fragile nodes based on the uncertainty in new energy, so as to ensure the security and stability of the power generation system. The safety performance of the power station system is detected through different levels of early warning sensitivity. The simulation model of the above algorithm is constructed in MATLAB. The simulation results show that the proposed algorithm increases the sensitivity of the early warning system of the power station and the sensitivity of triggering the early warning system and improves the security of the power station system as a whole.

1. Instruction

Due to the increasing energy demand, new energy is considered the most attractive energy source. The new energy sources include wind energy, hydroelectric, ocean energy, geothermal energy, photovoltaic energy, etc. There are many studies on photovoltaic and wind energy sources due to the abundant availability of these sources everywhere on Earth. The objective is not only to get the energy but also to turn this obtained energy into proper use and to balance energy demand and supply.

In 2020, the Ministry of Finance, the National Development and Reform Commission, and the National Energy Administration issued several opinions on promoting the healthy development of nonaqueous renewable energy power generation, which defined in detail the concept of new energy, which is a renewable low emission energy type other than surface runoff potential energy (conventional hydropower station). Among them, wind power stations and photovoltaic power stations can be effectively developed under the current technical conditions. With the development of society, the requirement for an Internet power grid is increasing. Gradually, conventional energy is unable to meet the needs of industrial production. People are paying more and more attention to the environmental protection and regeneration characteristics of new energy to meet industrial needs, and new energy power generation has already entered the field of industrial production.

New energy, especially solar and wind energy, is highly uncertain due to dynamic climate conditions. A proper analysis of these uncertainties plays an important role in maintaining the stability and reliability of the system [1]. In

this context, a lot of work has been done. When new energy is connected to the power grid, due to the randomness of new energy, it has an impact on the stability of the power grid to a certain extent. In order to ensure the reliability of new energy connected to the power grid, the authors in [2] extract the minimum line during normal operation of the power grid by the Monte Carlo method to verify the fault repair time. The Monte Carlo method and the analytical method are commonly used methods for the reliability analysis of distribution networks [3, 4]. Experiments show that the newer energy is connected to the power grid, the higher the reliability of the power grid and the reserve capacity of the distribution station is directly proportional to the reliability of the power grid. In [5], the authors tested the reliability of a distribution network based on fuzzy spiking neural P system, considering the uncertainty of new energy access to the power grid and the deviation in the interactive power of tie lines between regions. Aiming at the problems existing in the cross-regional dispatching of new energy, the authors in [6] propose to design the decentralized collaborative debugging path of the multiregional interconnected systems according to the debugging level and solve the main problems and subproblems in the debugging problem respectively. The results show that this method effectively reduces the uncertain impact on the safe operation of interconnected systems and improves the economic benefits of interconnected areas.

The power system plays an important role in China's production and people's lives. Every year, the state invests a large amount of conventional energy for power generation. In order to reduce the impact on the environment and improve the utilization of renewable energy, in recent years, the state has continuously increased its investment in wind power and photovoltaic power generation and organized a large number of scientific researchers to study its principles in order to explore more effective control measures and to promote the development of national power.

New energy power generation promotes the transformation of the power system. With the strong support of policies, new energy power generation has formed a large-scale industry. Through the analysis of the national support policies for new energy in the past decade, it is found that the policies in the field of new energy have been continuously refined and expanded in the power generation related industrial chain in order to promote the all-round development of the new energy power generation industry through policy guidance [7].

New energy power generation is to alleviate the contradiction between supply and demand of the power system and reduce the consumption of conventional energy. However, compared with conventional energy power generation, new energy has a certain instability and has a certain impact on the power grid. How to intervene with these effects by scientific and technological means is a problem that is necessary to solve. In this study, a fuzzy neural network algorithm is used to identify the static and dynamic fragile nodes based on the uncertainty in new energy so as to ensure the security and stability of the power generation system.

The structure of the remaining paper is as follows: section 2 describes the periodic fluctuation of energy demand in all seasons and discusses how this fluctuation can be balanced. Section 3 discusses the uncertainty of new energies such as wind energy and photovoltaic energy. Section 4 gives the proposed algorithm based on the uncertainty of new energy. Section 5 provides the performance evaluation of the algorithm. Section 6 concludes this work.

2. Certainty of Social Energy Demand

Social energy demand shows a relatively fixed periodic law in different cycles and a linear law of continuous growth over a long timeline. That is, in the annual cycle, the energy demand in winter and summer is large, and the energy demand in spring and autumn is small. In the weekly cycle, the energy demand on weekdays is large, and the energy demand on rest days is small. In the single-day cycle, the energy demand during the day is large, and the energy demand at night is small.

Because of these laws, power supply enterprises have formulated the time-sharing electricity price policy of peak and flat valley, encouraged high energy-consuming enterprises to make use of power supply at night, set gradient electricity prices, encouraged residents to reasonably plan their total electricity consumption for the whole year, and gave greater electricity price discounts to residents with small total electricity consumption for the whole year. However, under this measure, it is still not possible to effectively balance the periodic fluctuation of power demand [8].

Therefore, there are two measures to balance this volatility. First, the power supply enterprise operates its own peak shaving and valley leveling power stations and uses high-power power stations such as liquefied natural gas (LNG) or fuel oil that can be started and stopped quickly to balance the change in power load in a short period. Water potential energy storage facilities or weight potential energy storage facilities are also established in the power supply network to achieve effective peak shaving and valley leveling during the fluctuation period of power supply and demand. Second, we encourage the power generation enterprises to respond to the peak shaving and valley shaving dispatching order of power supply, the control section of coal-fired power plants, hydropower plants, and other utilization equipment, and to install energy storage facilities for photovoltaic and wind power plants to obtain the buffer capacity of power supply and demand.

Energy determines economic development. With the gradual increase of the proportion of China's industry, the industrial sector has become the main energy growth sector for energy consumption. From the current situation, the growth of energy demand is sustainable, but energy is not

always renewable. There is a contradiction between the two, which promotes people's development and the exploration of new energy [9].

3. Uncertainty of Energy

In this section, the authors discuss the uncertainty of new energies such as wind energy and photovoltaic energy, their resources, and the problems associated with these resources.

3.1. Uncertainty of Photovoltaic Energy. Photovoltaic energy is subject to light intensity and light angle. The daily noon energy supply capacity is the strongest. Full load energy supply cannot be realized in the morning and evening, and there is no energy supply capacity at night. The curve is highly coupled with the energy demand curve of a single-day cycle, but there are also two problems:

First, the change curve of the energy supply capacity of a photovoltaic power station is relatively smooth, while the change of the energy one-day demand curve is closer to the trapezoidal curve.

Second, the energy supply capacity of a photovoltaic power station under strong light conditions in summer is strong, which corresponds to the peak power consumption in summer under the annual cycle, but its energy supply capacity under weak light conditions in winter is weak.

In addition, photovoltaic energy is seriously affected by cloudy, rainy, and hazy weather. A photovoltaic power generation system has a strong dependence on lighting resources. The time, intensity, and angle of sunlight directly affect the power output rate.

In Figure 1, the x-axis is labeled as hours in a day and the y-axis is labeled as energy demand. It can be seen that during the times around 0–8 and 19–24, the power demand is greater than that of photovoltaic power generation because the light energy is generally weak in this period. In the time period around 8–19, photovoltaic power generation is greater than or equal to the power demand because the light intensity in this period is strong and the light time is long.

In Figure 2, this curve is obtained from the difference between the curves of photovoltaic power generation and power demand in Figure 1. It can be clearly seen from Figure 2 that the photovoltaic power generation can meet the power demand only at about 8–18, which shows the shortboard of photovoltaic power generation. The excess part of photovoltaic power generation in this time period is wasted, so it needs to be stored for use in other time periods.

3.2. Uncertainty of Wind Energy. Wind energy is subject to wind energy intensity. Under the annual curve of the northern region, wind power is strong in spring and autumn, but the energy demand in spring and autumn is small in comparison to the actual power demand. Due to the influence of extreme weather in winter and summer, there may be windy weather caused by large pressure differences. Wind energy facilities need to reduce wind energy utilization by adjusting blade attack angles to avoid risks. Annual wind

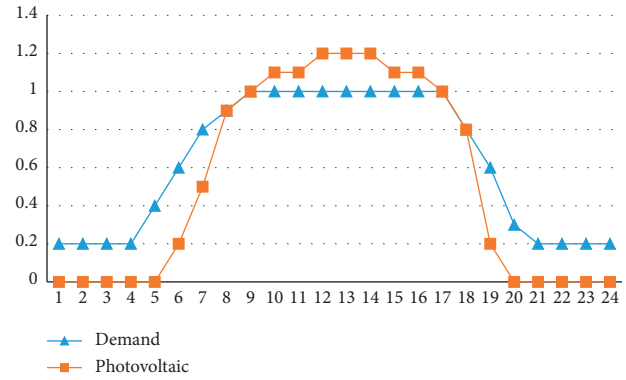

Figure 1: General combination relationship between photovoltaic power generation and power demand.

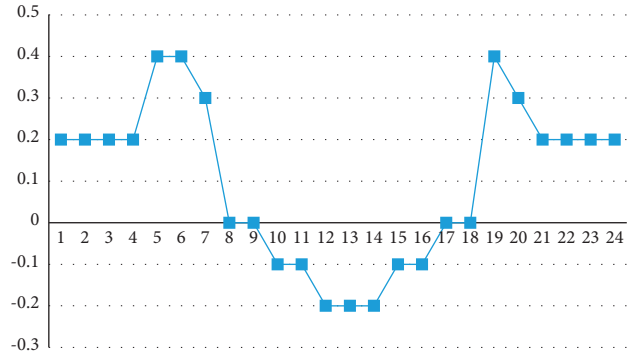

Figure 2: General difference relationship between photovoltaic power generation and power demand.

power generation and power demand are shown in Figures 3 and 4.

In Figure 3, the x-axis is labeled as months in a year and the y-axis is labeled as energy demand. It can be seen that the curves of wind power generation and power demand intersect each other in a year, the size of wind power generation is related to the alternation of seasons, and the power generation in the periods from March to May and August to December is greater than that of power demand.

In Figure 4, the difference between the power demand curve and the wind power generation curve data is used to obtain Figure 4. It can be clearly seen from Figure 4 that when the wind power generation capacity is large, the power demand is small, while when the wind power generation capacity is small, the power demand is large, which leads to the phenomenon of power generation waste and insufficient power demand.

4. Static and Dynamic Combination Algorithm Based on Uncertainty of New Energy

In the development of wind energy and photovoltaic energy, two development objectives should be ensured.

First, all wind energy and photovoltaic energy shall realize full power development under the conditions allowed by technical conditions; that is, the additional electric energy

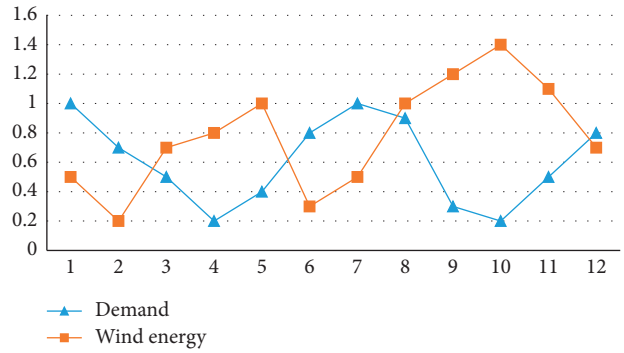

Figure 3: General combination relationship between wind power generation and power demand.

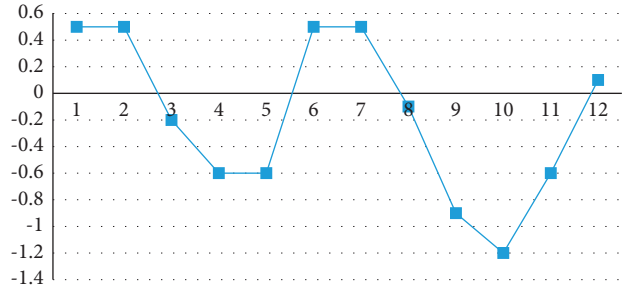

Figure 4: General difference relationship between wind power generation and power demand.

shall have sufficient energy storage facilities to balance the relationship between energy supply and demand.

Second, the charging and discharging efficiency of energy storage facilities should meet economic and business needs.

Under perfect conditions, the relationship between power generation capacity and energy storage capacity is given in the following formula:

$$\int_{-\infty}^{+\infty} S(t)\mathrm{d}t - \int_{-\infty}^{+\infty} C(t)\mathrm{d}t = \int_{-\infty}^{+\infty} \varepsilon(t)\mathrm{d}t + \int_{-\infty}^{+\infty} D(t)\mathrm{d}t, \quad (1)$$

where $S(t)$ is the time series function of power generation capacity, $C(t)$ is the power demand timing function, $D(t)$ is the time series function of energy storage capacity, and $\varepsilon(t)$ is the time series function of energy storage capacity loss. Based on this relationship, the vulnerability time series coefficient of the new energy power station is shown in the following formula:

$$\tau(t) = \frac{\int_{-\infty}^{+\infty} \varepsilon(t)\mathrm{d}t}{\int_{-\infty}^{+\infty} S(t)\mathrm{d}t}, \quad (2)$$

where $\tau(t)$ is the vulnerability time series coefficient of the new energy power station and other mathematical symbols are the same as in (1).

The vulnerability evaluation index of new energy power generation composed of the above formulas (1) and (2) can objectively reflect the vulnerability of new energy power stations equipped with energy storage facilities, but there are also some problems. That is, the four integral indexes in formula (1) and the two integral indexes in formula (2) have their own uncertainty, which are not typical periodic functions. Therefore, the actual evaluation $\tau(t)$ and the statistical ability of values are weak. Thus, subsequent data mining is required to guide production. Its main data mining direction is data prediction and early warning based on curve estimation.

Therefore, under the artificial intelligence analysis framework of power big data based on CBA, it is necessary to carry out a Fourier transform and extract the data characteristic matrix, and then use the fuzzy convolution algorithm and binarization method to obtain the vulnerability risk prediction index. The above algorithm architecture is shown in Figure 5.

The basis function of Fourier transform is shown in the following formula:

$$F(\omega) = \int_{-\infty}^{+\infty} A \cdot f(t)^{-ie\cdot 2\pi}\mathrm{d}t. \quad (3)$$

In the above equation, t is the traversal pointer of the sequence, ω is the traversal pointer of the frequency variable, A is the detection accuracy correction variable, $F(\omega)$ is the output function of Fourier transform, $f(t)$ is the input function of Fourier transform, and $-ie \cdot 2\pi$ is Fourier constant, where e is the natural constant.

The characteristic matrix obtained from the Fourier transform contains the strength of the main superimposed waveform, which is used to analyze uncertain data.

The node basis function of the fuzzy neural network based on sixth-order polynomial depth iterative regression is shown in the following formula:

$$y = \sum_{i=1}^{n}\sum_{j=0}^{5} A_j x_i^j, \quad (4)$$

where A_j is the coefficient to be regressed of the j-th order polynomial, that is, each node in the formula contains 6 coefficients to be regressed from A_0 to A_5, J is the polynomial order, and the meanings of other mathematical symbols are the same as those in the previously mentioned formulas.

The output data of the multicolumn neural network is the output data that lies in the [0, 1] interval. There is no distribution law for output data, so it needs to be binarized. An independent binarized neural network module is designed for each scheme to form a binarized multicolumn neural network. In a binarized neural network, binary values are used rather than floating values. which can be computed faster with less memory and power. The node basis function of the binarized neural network is as shown in the following formula:

$$y = \sum_{i=1}^{n} \frac{1}{A + B \cdot e^{x_i}}, \quad (5)$$

where e is the natural constant, and the approximate value here is $e = 2.718281828$; The meaning of other mathematical symbols is the same as formula (4).

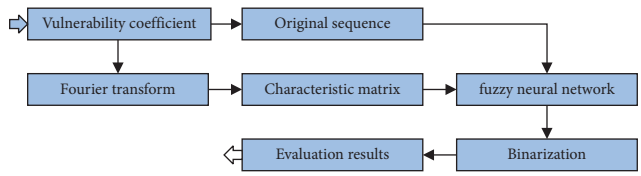

Figure 5: Logic architecture diagram of power big data artificial intelligence algorithm based on CBA.

Table 1: Comparison of early warning sensitivity based on early warning lead.

Sensitivity comparison	Early warning advance (s)				
	1	5	15	30	60
Direct curve estimation	97.24	83.65	52.91	27.63	8.59
Fuzzy neural network	97.93	96.32	95.87	93.19	91.03
t	8.972	5.105	2.593	0.031	0.000
P	0.019	0.008	0.002	0.001	0.000

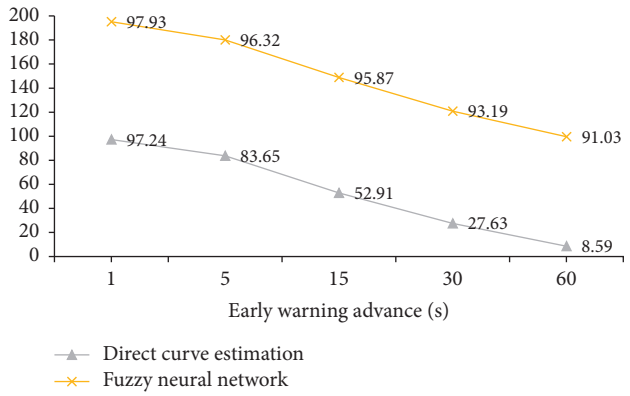

Figure 6: Comparison of early warning sensitivity under different early warning amounts.

5. Simulation Verification of Algorithm Efficiency

The Simulink module is loaded into MATLAB to build the simulation model for the above algorithm. The original data are the measured data of power supply company end grid connection of all 16 wind farms and 9 photovoltaic power plants in a city. When the neutral point offset reaches 50% of the cut-off setting value or the phase offset reaches 35% of the cut-off setting value, it is considered a high-risk state, and it is therefore necessary to give data early warning. The test points of early warning advance are set as 1 s, 5 s, 15 s, 30 s, and 60 s respectively.

We compare the vulnerability coefficient of formula (2) above $\tau(t)$. The prewarning sensitivity of the forward prediction value directly estimated by the nonlinear curve under MATLAB and the forward prediction value given under the artificial intelligence analysis framework of power big data based on CBA is shown in Table 1.

In Table 1, early warning advance is the time advance from the high-risk state when the early warning is given, and sensitivity is the proportion of true positive data in positive data. It can be seen from Table 1 that both the early warning sensitivity estimated by the direct curve obtained by using the software directly and the early warning sensitivity obtained by using the fuzzy neural network algorithm are reduced according to the increase in the test point time of the early warning advance. The difference between the two can be made more obvious by making the following Figure 6 according to the data in Table 1.

It can be seen in Figure 6 that the curve trend of early warning sensitivity obtained by curve estimation is the same as that obtained by the fuzzy neural network algorithm. The difference is that the early warning sensitivity obtained by the fuzzy neural network algorithm is high at the same test point, and the difference becomes more and more obvious with the increase of early warning advance. This shows that the fuzzy neural network algorithm can identify the high-risk state more accurately.

In Table 2, early warning trigger conditions are the proportional relationship between the measured value of data and the setting value of fault removal when the early warning is given, and sensitivity is the proportion of true positive data in positive data.

It can be seen from Table 2 that under different early warning trigger conditions, the early warning sensitivity trend obtained by either direct curve estimation or fuzzy neural network algorithm is the same, from high to low according to the early warning trigger conditions and from low to high. In order to facilitate a more straightforward comparison of the data differences between the two, the following Figure 7 is made according to the data in Table 2.

As it can be seen in Figure 7 the early warning sensitivity obtained by using the fuzzy neural network algorithm is high, and the lower the early warning sensitivity obtained with the harsh early warning trigger conditions. The early warning sensitivity obtained by using direct curve estimation is lower as compared with the fuzzy neural network algorithm, and the early warning sensitivity obtained with the harsh early warning trigger conditions decreases in a cliff-like manner. This shows that the direct curve estimation method cannot be used, but the early warning sensitivity obtained by using fuzzy neural network algorithm is relatively stable.

Table 2: Comparison of alert sensitivity based on alert trigger conditions.

Sensitivity comparison	Alert trigger condition				
	[0.30,1.00]	[0.25.0.30)	[0.20,0.25)	[0.10,0.20)	[0.00,0.10)
Direct curve estimation	98.19	96.38	88.76	53.17	4.38
Fuzzy neural network	98.97	98.54	96.14	95.08	91.65
t	9.346	6.728	3.172	1.008	0
P	0.016	0.008	0.004	0.001	0

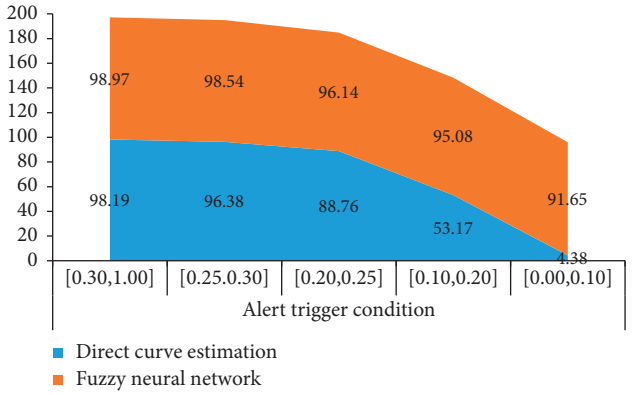

Figure 7: Comparison of early warning sensitivity under different early warning triggering conditions.

6. Conclusion

With the deepening of people's exploration of new energy, new energy power generation is gradually applied to the power system. Due to the interference of natural factors, it affects the quality of power and the security of the power system [10]. This study analyzes the uncertain factors of wind power and photovoltaics affected by the outside world. Through the identification of fragile nodes with the combination of static and dynamic uncertainty in new energy, Fourier transform is carried out, and a data feature matrix is extracted under the artificial intelligence analysis framework of power big data based on CBA. Then the vulnerability risk prediction index is obtained by using a fuzzy convolution algorithm and binarization method. The simulation results show that the proposed fuzzy neural network algorithm identifies the high-risk state more accurately and the early warning sensitivity obtained is relatively stable.

With the continuous development of science and technology, the exploration and cognition of new energy are further improved, and the application level in relevant fields is also improved to promote the safe and stable development of power systems [11].

Data Availability

Data source: self-statistics of the study.

Conflicts of Interest

The authors declare that there are no conflicts of interest with the publication of this paper and that all authors have seen the manuscript and have agreed to submit it to your journal.

References

[1] K. P. Kumar and B. Saravanan, "Recent techniques to model uncertainties in power generation from renewable energy sources and loads in microgrids - A review," *Renewable and Sustainable Energy Reviews*, vol. 71, pp. 348–358, 2017.

[2] C. Wang, H. Qiang, and S. Ying, "Reliability evaluation of distribution network based on new energy access," *Automation and instrumentation*, vol. 36, no. 11, pp. 6–10, 2021.

[3] G. T. Heydt and T. J. Graf, "Distribution system reliability evaluation using enhanced samples in a Monte Carlo approach," *IEEE Transactions on Power Systems*, vol. 25, no. 4, pp. 2006–2008, 2010.

[4] K. Hou, H. Jia, X. Xu, Z. Liu, and Y. Jiang, "A continuous time Markov chain based sequential analytical approach for composite power system reliability assessment," *IEEE Transactions on Power Systems*, vol. 31, no. 1, pp. 738–748, 2015.

[5] Y. Huang, T. Wang, J. Wang, and H. Peng, "Reliability evaluation of distribution network based on fuzzy spiking neural P system with self-synapse," *Journal of Membrane Computing*, vol. 3, no. 1, pp. 51–62, 2021.

[6] G. Zhu, L. Dong, and M. long, "Decentralized coordinated scheduling of multi area interconnected systems considering new energy uncertainty [J/OL]," *Journal of power system and automation*, vol. 1-10, 2022.

[7] L. Wu, "Research on quantitative evaluation of new energy power generation promotion policy based on PMC index," *Productivity research*, vol. 12, pp. 17–21, 2021.

[8] M. Zhao, Y. Liu, and Z. Guoqing, "Multi objective optimization of distributed energy supply network based on energy interconnection," *Electric power technology and environmental protection*, vol. 37, no. 6, pp. 40–50, 2021.

[9] J. Li, "Optimal allocation method of new energy considering system stability," *China Equipment Engineering*, vol. 23, pp. 166–168, 2021.

[10] Q. Li and F. Zhang, "Optimization algorithm of comprehensive intelligent energy evaluation index system based on multi factor model," *Sino foreign energy*, vol. 26, no. 12, pp. 18–25, 2021.

[11] S. Li and G. Zhu, "Analysis of energy transformation path under the vision of "double carbon"," *Nanjing Social Sciences*, vol. 12, pp. 48–56, 2021.

Hindawi
Scientific Programming
Volume 2022, Article ID 7602186, 10 pages
https://doi.org/10.1155/2022/7602186

Research Article

A Dynamic Evaluation Model of University Brand Value Based on Analytic Hierarchy Process

Mingchao Li[1,2] **and Bin Gong**[3]

[1]*School of Business, Macau University of Science and Technology, Macau 999078, China*
[2]*School of Marxism, Zhuhai College of Science and Technology, Zhuhai, Guangdong 519041, China*
[3]*Institute of Data Science, City University of Macau, Macau 999078, China*

Correspondence should be addressed to Mingchao Li; limingchao@jluzh.edu.cn

Received 25 February 2022; Revised 5 March 2022; Accepted 9 March 2022; Published 23 March 2022

Academic Editor: Muhammad Zakarya

In recent years, great changes have taken place in the economic environment, policies, competitive environment, and market of colleges and universities. Furthermore, factors including the reduction of number of students every year has led to the continuous decline in the number of students enrolled in colleges and universities. Facing this problem, it is essential that colleges and universities should build their own brand value and attract more high school graduates with the brand value of colleges and universities. Nowadays, higher education has been popularized and internationalized, and the competition among colleges and universities has gradually increased. In fact, colleges and universities can obtain high-quality school running resources by relying on their own loyalty, reputation and social status, and can also achieve greater development space in the field of education. Therefore, university managers began to pay attention to their own brand value. The brand value of colleges and universities cannot be directly reflected, but needs to be reflected from different aspects. For this problem, this paper uses analytic hierarchy process (AHP) to study the brand value of colleges and universities. By selecting many aspects as the indicators of the dynamic evaluation system of brand value of colleges and universities, this paper constructs a dynamic evaluation model of brand value of colleges and universities based on analytic hierarchy process. After analysis, the total score of the brand value of a university is 84.12 and the grade is "B." Based on the analysis of the results, it can be concluded that the overall score of the university is high and has a certain brand value. However, it is weak in talent training and academic reputation.

1. Introduction

The brand of colleges and universities is the foundation of standing in the society. If a college has no brand or low brand value, it is difficult to obtain good educational resources and students. Therefore, the brand value of colleges and universities is the foundation of expanding the scale of colleges and universities. Shaping the brand of colleges and universities requires long-term accumulation and the joint efforts of several generations. Once colleges and universities form their own brand value in the society, their influence and social appeal also increase rapidly. Therefore, this paper establishes a dynamic evaluation model of university value based on analytic hierarchy process, uses this model to accurately evaluate the university brand value from many aspects, and comprehensively promotes the promotion of university brand value.

The common problems of educational institutes including colleges and universities in China's system are low efficiency, high investment cost, and insufficient social influence, which have a serious impact on the brand value of colleges and universities. The extensive construction of colleges and universities reduces the brand value of colleges and universities, the serious lack of teachers also interferes with the brand value of colleges and universities, and the quality of students also reduces the brand value. Some colleges and universities arbitrarily adjust the name of colleges and universities, which reduces the brand value of colleges and universities and affects the image of colleges and universities in the society. The improvement of academic

reputation is conducive to the improvement of brand value of colleges and universities at home and abroad and plays a certain role in promoting academic research in China. At the same time, there is a relative lack of talent training, and the graduated college students lack management ability and innovation ability. This should be kept in mind that all academia including colleges and universities should improve students' creativity, formulate courses to spread students' thinking ability, give full play to students' imagination and creativity, and create a good research environment for students.

In this paper, we describe, in detail, the basic concepts and application steps based on analytic hierarchy process (AHP). Furthermore, we establish a dynamic evaluation system of university brand value based on AHP, combine with statistical analysis, and calculate the system through different levels of weight. Through evaluation, we judge the importance of university brand value according to the weight of each index. On the other hand, through the dynamic evaluation model of university brand value based on analytic hierarchy process, we select some college students to evaluate a university in China and use analytic hierarchy process to dynamically evaluate the university brand value, so as to improve the accuracy of the evaluation results. Based on the analysis of the results, it can be concluded that the overall score of the university is high and has a certain brand value. However, it is weak in talent training and academic reputation. The major innovations and contributions of this paper in the research process are as follows:

(i) Describe in detail the basic concepts and application steps based on analytic hierarchy process (AHP)

(ii) Establish a dynamic evaluation system of university brand value based on AHP and judge the importance of university brand value according to the weight of each index

(iii) Use analytic hierarchy process to dynamically evaluate the university brand value, so as to improve the accuracy of the evaluation results

(iv) We concluded that the overall score of the university is high and has a certain brand value; however, it is weak in talent training and academic reputation

The rest of the paper is organized as follows. In Section 2, we offer an overview of the related work. Section 3 is about the analytic hierarchy process (AHP) and its brief introduction along with applications. The AHP is the research methodology used in this research—used in two different case studies. Section 4 illustrates the dynamic evaluation model of university brand value based on analytic hierarchy process. Section 5 describes the dynamic evaluation of university brand value based on analytic hierarchy process. Moreover, experimental details based on our assumptions and evaluation are also presented in this section. Finally, Section 6 concludes this paper and offers several directions for further research and investigation.

2. Related Work

In the late 1980s, the American Institute of marketing held the world's first academic conference on "brand equity." Since then, some scholars have carried out research in the field of brand equity [1]. Anna et al. proposed that brand equity is the difference of the demander's brand knowledge under different marketing measures. Based on this perspective, it is pointed out that the brand has high brand value, and the demander can stimulate the purchase desire after identifying some well-known brands [2]. Brand knowledge includes brand impression and brand awareness. This definition is analyzed from the perspective of the demander and is the brand value based on the demander. Hu et al. believe that from this perspective, the research on brand assets and the judgment of the demander's response to marketing activities can promote enterprises to carry out marketing activities and guide managers to formulate marketing strategies based on this strategic orientation. An important component of the brand knowledge is based on brand awareness. The demander's ability to identify brand value, followed by brand impression, that is, the demander perceives the brand according to his own memory, and its association has brand significance, that is, the demander's special preference and intensity in marketing activities [3]. The brand value of colleges and universities is the relationship formed by the long-term interaction between the brand of colleges and universities, students, and employers. We should strengthen the ability to recognize the brand value of colleges and universities and strengthen the ability of students and relevant social personnel to recognize the brand value of higher education. Moreover, this will form a good interpersonal relationship with colleges and universities so as to form loyalty to the brand of colleges and universities and form a value higher than the physical assets of colleges and universities. These are considered as important competitive advantages of colleges and universities in brand value [4].

Nguyen et al. pointed out that it is necessary to improve brand awareness through external brand communication and brand embodiment [5]. Chun et al. analyzed from other perspectives and divided brand awareness into two research points: (i) brand memory and (ii) brand recognition [6]. Tribukait et al. studied the expectations and basic requirements of teachers' teaching, students' learning, and evaluation [7]. In [8], Uzun et al. deeply studied and investigated the sample information filled in by distance education students and undergraduate students and proposed to evaluate the quality of education service by using perception and teacher expectation. Xiaojuan et al. have concluded through research that the brand driving effect of colleges and universities can stimulate their own development, improve the image of schools and educational institutes in the region, and promote the development of the country [9].

Chen et al. constructed a "brand belief model" to classify the brand development into five different levels, namely: (i) product, (ii) company concept, (iii) conceptual brand, (iv) brand spirit, and (v) brand culture [10]. After long-term polishing in the market, the brand is raised to the field of

judgment spirit, which is also the highest level of brand development. At this time, the brand is integrated with brand spirit and brand culture. Li et al. believe that the university brand is a teaching concept, school running quality, and teaching characteristics accumulated and precipitated in the development process of the university, and is the recognition of the society for the university. The authors believe that the university should formulate the brand strategy from the core value, obtain a large number of school running resources, and provide students with better educational quality and services [11]. Moreover, Rangkuti et al. analyzed the influence of university brand on students' school choice from the perspective of high school students and formulated the brand elimination framework for students to choose universities for higher education [12]. Analytic hierarchy process (AHP) is a hierarchical and systematic multicriteria decision-making algorithm that combines quantitative and qualitative analysis. AHP is largely used in the state-of-the-art for decision making in various fields, but its effectiveness is relatively unexplored in modern educational systems [13]. In the next section, we describe the AHP algorithm in detail.

3. Analytic Hierarchy Process (AHP)

3.1. Concept of Analytic Hierarchy Process (AHP). Analytic hierarchy process (AHP) is a hierarchical and systematic multicriteria decision-making algorithm combining quantitative analysis and qualitative analysis. The basic characteristics of human rational thinking involve three aspects: judgment, decomposition, and synthesis. The research problems based on AHP also fully show the above contents [14]. The emergence of AHP method completely breaks the communication barrier between decision analysis and decision-makers. For a long time, decision-makers choose AHP method instead of making decisions through decision analysts, so as to effectively improve the reliability, effectiveness, and feasibility of decision-making schemes. Some problems that cannot be solved by quantitative analysis are very suitable for using AHP method, which is also the most ideal mathematical way to deal with this problem. When studying problems based on analytic hierarchy process, it should be completed according to the following steps. First, the hierarchical structure model is constructed, and then the judgment matrix of pairwise comparison is established; then consistency test and hierarchical single sorting are conducted [15]. Figure 1 shows the application flow chart of analytic hierarchy process.

3.2. Basic Steps of Analytic Hierarchy Process

3.2.1. Construct Hierarchical Structure Model. This paper analyzes the brand value of colleges and universities that need to be studied and hierarchizes the problems that need to be analyzed. According to different attributes, the target problem is re decomposed into multiple parts, and each part is called element. The elements under the same level are the criterion level for the lower level elements, which can dominate the lower level elements and are also dominated by the upper level elements. Based on this model, a hierarchical structure from top to bottom is constructed. At the top of the structure is the ideal result or expected goal of the analysis problem, which is called the goal layer. Generally, this layer has only one element. The criterion layer and subcriterion layer belong to the middle layer, in which there are multiple intermediate links related to the completion of the goal. Each scheme for implementing the decision is at the lowest layer, and the number of elements in each layer is no more than 9. On the contrary, it will increase the difficulty of pairwise comparison. If the number of criterion layers is large, multiple subcriterion layers can be formed by decomposing the criterion layer. When solving practical problems, the most critical part is to divide the hierarchy as investigated in [13, 16]. Figure 2 illustrates the hierarchy diagram.

3.2.2. Comparison and Judgment Matrix. Through constructing a hierarchical structure, the hierarchical relationship between different elements can be clearly expressed. For different decision makers, the importance of different criteria in the same layer to the target layer is different, especially when there are multiple factors in the lower layer of any criterion layer, the most important factor in the criterion layer cannot be determined at the first time, resulting in the decision maker being unable to take all factors into account, so as to make contradictory decisions. When dealing with this problem, a judgment matrix of pairwise comparison can be constructed by analytic hierarchy processes [17].

Suppose there are n factors $X = \{x_1, x_2, \ldots, x_n\}$ in z and compare the importance of n factors in z, select x_i and x_j, and a_{ij} represents the comparison result. After the comparison of each factor, $A = (a_{ij})\ n \times n$ to represent the matrix, and matrix A is called the judgment matrix between Z-X, In the AHP algorithm, the importance and relationship of each factor are reflected by the 1–9 scale method. In fact, the 1–9 scale represents the relationship among two or more than two factors based on the human thinking. The basic meaning along with different relationships of the 1–9 scale method is listed in Table 1.

The 1–9 scale method can accurately transform the way of human thinking to judge the importance of various things. When comparing and judging various things, the commonly used words are strong, a bit strong, very strong, and absolutely strong, etc. Therefore, if you want to make an in-depth judgment, you need to add the compromise method to the adjacent judgment level [18]. The 1–9 scale method can be applied in most judgment and decision making. After practical verification by psychologists, the results show that most people have 5 to 9 levels of discrimination ability in judging the same attribute of different things. Using the 1–9 scale can reflect the judgment ability of a considerable number of people [19, 20].

3.2.3. Hierarchical Single Ranking and Consistency Test. This process should be completed in the criterion layer, which requires the problem of arrangement vector between n elements. The most commonly used method to deal with

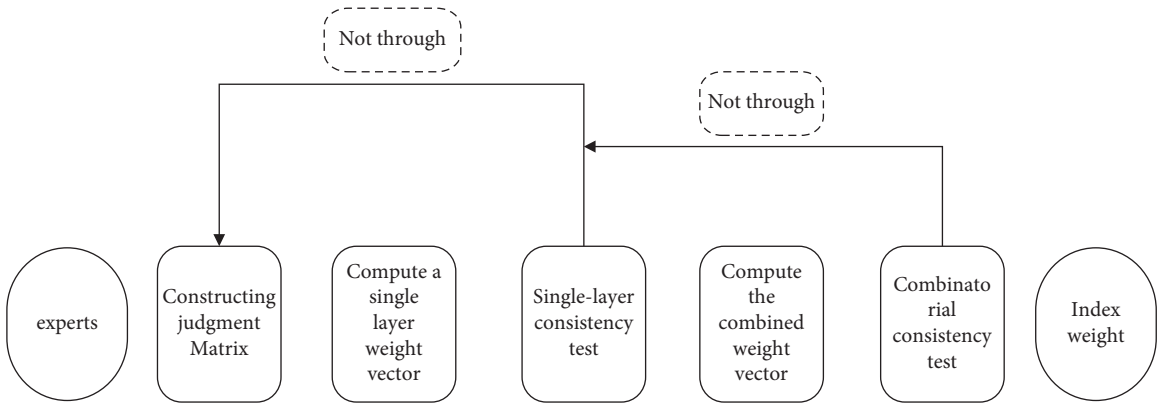

Figure 1: Flow chart of analytic hierarchy process.

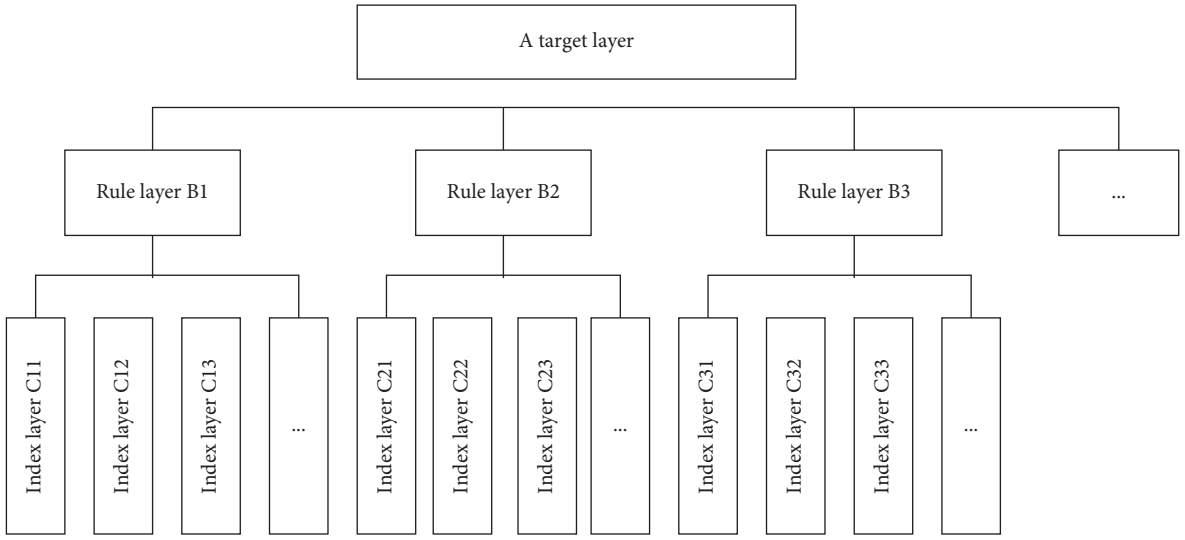

Figure 2: Hierarchy chart.

Table 1: Basic meanings of the 1–9 scale method.

Scale	Basic meaning
1	The importance of the two factors was the same
3	Comparing the two factors, the former is slightly more important than the latter
5	Comparing the two factors, the former is more important than the latter
7	Comparing the two factors, the former is far more important than the latter
9	Comparing the two factors, the former is far more important than the latter
2,4,6,8	The degree of importance is between two adjacent criteria

this problem is the eigenvalue method. The detailed process is as follows: judgment matrix A and λ Max corresponds to the feature vector W, after normalization, the importance ranking weight between the elements of the same layer and any elements of the upper layer can be obtained [16]. The above is the hierarchical single ranking.

The eigenvector W and the maximum eigenvalue are obtained by using the power method given by Algorithm 1. In the first step, W_0 represents the initial value vector, which is given by $w_0 = (1/n, 1/n, \ldots, 1/n)^T$. In second step, for all $k = 1,2,...,n$, the values of $\overline{w}_k = Aw_{k-1}$ is obtained, and w_{k-1} vector is obtained after normalization. In the third step, the premise of accuracy calculation, if $\max|w_{ki} - w_{(k-1)i}| < \varepsilon$, where w_{ki} is the i component in w_k, the settlement will be ended after meeting this requirement, otherwise jump to the second step. Finally, the calculation happens from the following equations.

$$\lambda \max = \frac{1}{n}\sum_{i=1}^{n}\frac{\overline{w_{ki}}}{w_{(k-1)i}}, \quad (1)$$

$$w_{kj} = \frac{\overline{w}_{ki}}{\sum_{j=1}^{n}\overline{w}_{kj}}. \quad (2)$$

4. Dynamic Evaluation Model of University Brand Value Based on AHP

4.1. Brand Value Evaluation Theory. The establishment of brand requires the joint construction of marketing activities, products, and needs. The brand can fully show the mutual needs between people and products and also has a direct impact on the selection of advertising channels and marketing activities [21]. In addition, the brand on assets also shows that it has some assets, which proves the brand value on three levels, namely, market level, demander level, and capital level. The income formed by the above activities is called brand value. Yu et al. pointed out that three perspectives can be unified in a theoretical framework. Based on the direct impact of nonmarketing strategies and enterprise marketing strategies on the brand, these nonmarketing strategies involve competitor strategies, 4P combination strategies, lifestyle, consumer values, market environment, etc., so as to arouse the demand of the demander, Therefore, the "ideas" of brand demanders have an impact on enterprise output and performance, including capital market performance and product market performance. Figure 3 shows the three-dimensional perspective of the brand value.

4.2. University Brand Value Service Model. The brand value of colleges and universities is directly related to the level of brand knowledge and understanding of the demander. Zhong et al. pointed out that brand awareness should be reflected from two different aspects: (i) external brand communication and (ii) enterprise brand [22]. Furthermore, the brand value should be reasonably divided into brand identification and brand memory, as shown in Figure 4.

Based on the achievements of scholars in the study of brand value and service value, the following university brand values are defined here [23]. The brand value of colleges and universities is that the brand of colleges and universities forms a kind of cognition of the brand of colleges and universities through long-term interaction and communication with employers and students, which can promote colleges and universities to have good preferences and contacts, so as to strengthen the brand popularity and loyalty of colleges and universities [24, 25].

4.3. Construction of Dynamic Evaluation Model of University Brand Value Based on Analytic Hierarchy Process

4.3.1. Constructing the Dynamic Evaluation System of University Brand Value Based on Analytic Hierarchy Process. The analytic hierarchy process (AHP) selected in this paper belongs to the subjective decision-making method. After the index weight is clear, it is decomposed into the hierarchical structure model into target layer, criterion layer, and index layer. When establishing the university brand value evaluation model based on analytic hierarchy process, we should first build different levels in this model, and then statistically analyze the factors at different levels, so as to clarify the overall goal of each factor, that is, the weight of university brand value, as shown in Figure 5.

4.3.2. Calculate Index Weight. According to the concept and application process of analytic hierarchy process given above, the weights of different indicators in the university brand value index system are calculated according to this process, as shown in Table 2.

(1) Primary Index Weight. Evaluation model of university brand value target level based on Analytic Hierarchy Process:

$$A = 0.53B_1 + 0.21B_2 + 0.12B_3 + 0.14B_4. \quad (3)$$

(2) Academic Reputation Index Weight. The academic reputation index weight of each index is calculated using Table 3.

Single-level evaluation model of academic reputation:

$$B1 = 0.42C_{11} + 0.27C_{12} + 0.31C_{13}. \quad (4)$$

(3) A Single-Level Evaluation Model of Academic Reputation. The teacher resource judgment matric and index weight are shown in Table 4.

Single level evaluation model of teacher resources:

$$B2 = 0.17C_{21} + 0.54C_{22} + 0.29C_{23}. \quad (5)$$

(4) Weight of Comprehensive Indicators of Teaching Quality. The teaching quality judgment matrix and index weight are shown in Table 5.

Single-level evaluation model of teaching quality:

$$B3 = 0.35C_{31} + 0.16C_{32} + 0.49C_{33}. \quad (6)$$

(5) Weight of Comprehensive Indicators of Talent Training. The talent training index and weight matrix are shown in Table 6.

Single-level evaluation model of talent training:

$$B4 = 0.59C_{41} + 0.25C_{42} + 0.16C_{43}. \quad (7)$$

Through the above calculation, it can be concluded that in the dynamic evaluation system of university brand value based on analytic hierarchy process, the weights of the first-class indicators academic reputation, teacher resources, teaching quality, and talent training are 0.54, 0.21, 0.12, and 0.14, respectively. Thus, accounting for the highest proportion of academic reputation, which has the greatest impact on the total index weight of the standard level. The weight of the second-level index academic reputation is 0.42, 0.27, and 0.31 for the number of national papers, the number

(1) Suppose W_0 represents the initial value vector, then $w_0 = (1/n, 1/n, \ldots, 1/n)^T$
(2) For $k = 1, 2, \ldots, n$, $\overline{w}_k = Aw_{k-1}$ is obtained, and w_{k-1} vector is obtained after normalization.
(3) On the premise of accurate accuracy calculation, if $\max|w_{ki} - w_{(k-1)i}| < \varepsilon$, where w_{ki} is the i component in w_k, the settlement will be ended after meeting this requirement, otherwise jump to the second step.
(4) Calculate next step using equations (1) and (2)

Algorithm 1: The power method to calculate eigenvector and eigenvalue.

Figure 3: Three-dimensional perspective of brand value.

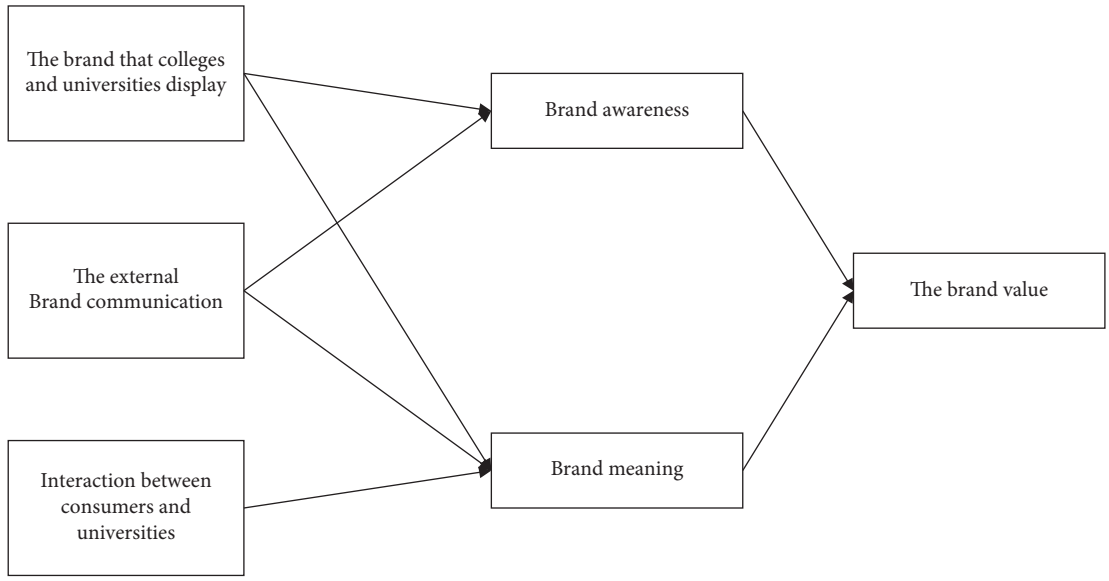

Figure 4: University brand value model.

of excellent papers at the school level, and the number of international awards for students, respectively. The index with the highest weight in academic reputation is the number of national papers. This should be noted that among the secondary indicators of teacher resources, the corresponding weights of teacher team structure, teacher strength, and doctoral teachers are 0.17, 0.54, and 0.29, respectively—where the teacher strength has the highest weight.

Moreover, among the secondary indicators of teaching quality, the corresponding indicators of the basic knowledge ability, professional and technical ability, and personal practical ability are 0.35, 0.16, and 0.49, respectively. We observed that among which the index with the highest weight is personal practical ability. Similarly, among the secondary indicators of talent training, the corresponding weights of the student employment, innovation ability, and management ability are 0.59, 0.25, and 0.16, respectively—in which the highest weight is allocated to the student employment. The specific weights are shown in Table 7:

The proportion of various indicators in the total target weight is shown in the bar chart in Figure 6. Among the primary indicators, the highest proportion is academic reputation, which accounts for 54%, followed by teacher resources, and the lowest proportion is teaching quality, which accounts for 12%. Among the secondary indicators, the highest weight is the employment of students, and the specific weight proportion is shown in Figure 6:

The analysis of the data, as shown in Figure 6, shows that the highest proportion of the total weight of secondary indicators is student employment C_{41}, accounting for 14.75%, and the lowest proportion is professional and

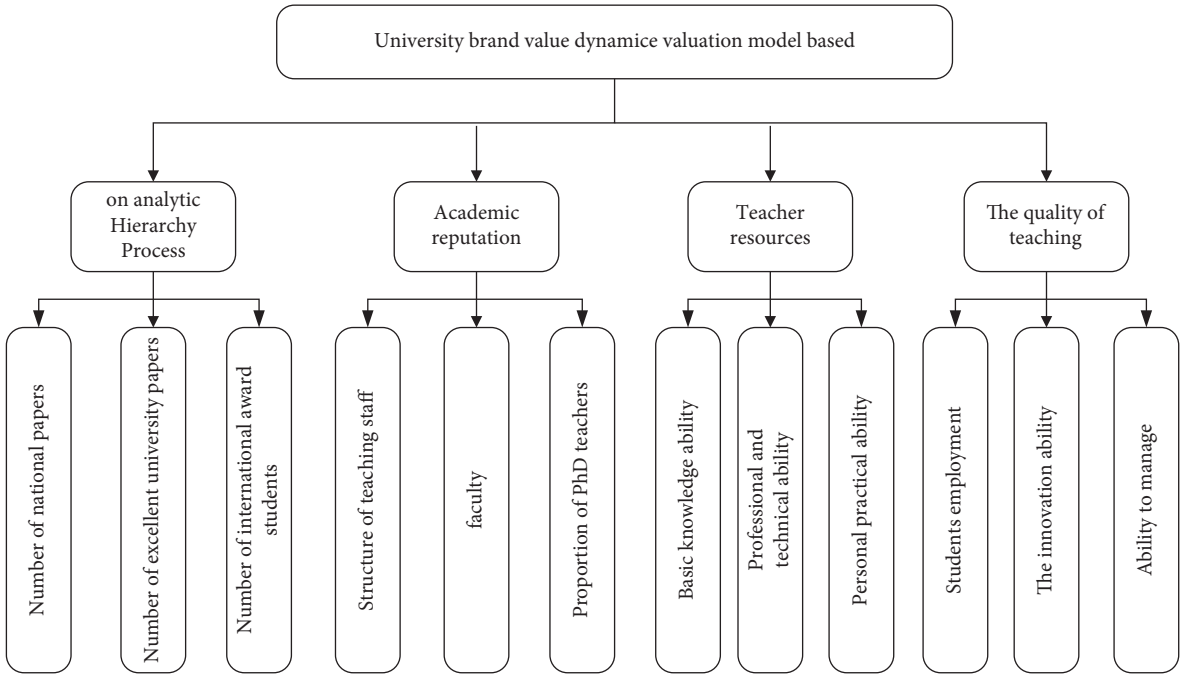

Figure 5: Evaluation system of university brand value based on analytic hierarchy process.

Table 2: Primary index judgment matrix and index weight.

A	B_1	B_2	B_3	B_4	The weight
B_1	1	2	1	3	0.53
B_2	2	1/3	2	1/3	0.21
B_3	1/2	1/2	1	1	0.12
B_4	2	1	1/2	1/2	0.14

Table 3: Academic reputation judgment matrix and weight of each index.

B_1	C_{11}	C_{12}	C_{13}	The weight
C_{11}	1	2	1/2	0.42
C_{12}	1/2	1	1/3	0.27
C_{13}	2	1/3	1	0.31

Table 4: Teacher resource judgment matrix and index weight.

B_2	C_{21}	C_{22}	C_{23}	The weight
C_{21}	1	1	1/2	0.17
C_{22}	3	1/2	1	0.54
C_{23}	2	1/3	2	0.29

Table 5: Teaching quality judgment matrix and index weight.

B_3	C_{31}	C_{32}	C_{33}	The weight
C_{31}	1	3	1/2	0.35
C_{32}	1/2	1	1	0.16
C_{33}	2	2	1/3	0.49

Table 6: Talent training index and weight matrix.

B_4	C_{41}	C_{42}	C_{43}	The weight
C_{41}	1	3	3	0.59
C_{42}	1/3	1	2	0.25
C_{43}	1/3	1/2	1	0.16

Table 7: Dynamic evaluation model of university brand value based on analytic hierarchy process (AHP).

Ability to manage	Rule layer	The weight	Index layer	The weight
University brand value dynamic evaluation system based on analytic hierarchy process	Academic reputation	0.54	Number of national papers	0.42
			Number of excellent university papers	0.27
			Number of international award students	0.31
	Teacher resources	0.21	Structure of teaching staff	0.17
			Faculty	0.54
			Proportion of PhD teachers	0.29
	The quality of teaching	0.12	Basic knowledge ability	0.35
			Professional and technical ability	0.16
			Personal practical ability	0.49
	Cultivation of talents	0.14	Students employment	0.59
			The innovation ability	0.25
			Ability to manage	0.16

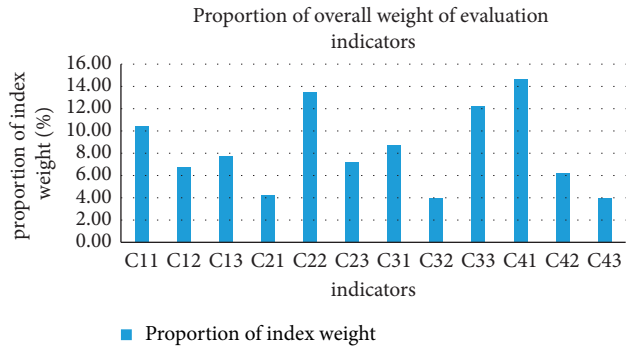

Figure 6: Proportion of overall weight of evaluation indicators.

technical ability C_{32} and management ability C_{43}, accounting for 4%. This shows that when evaluating the brand value of colleges and universities, students' management ability and professional, as well as, technical ability are not important indicators, and the weight is low in the evaluation.

5. Dynamic Evaluation of University Brand Value Based on Analytic Hierarchy Process

5.1. Data Sources. According to the results of this paper, the dynamic evaluation model and index system of the university brand value based on analytic hierarchy process are constructed. According to this method, the brand value of a 211 university in China is evaluated and analyzed by 20 independent students, and the scores are scored according to the evaluation criteria of the university brand value, as shown in Table 8. The comprehensive score can be calculated by normalizing the score and substituting it into the evaluation model. The following table shows the evaluation criteria of the brand value of colleges and universities. Note that we assume four levels, and this may vary with respect to the evaluation size and number of factors.

Table 8: Evaluation standard of brand value in colleges and universities.

Indicators	Level			
	A(>) 90	B(80–90)	C(60–80)	D(<60)
College brand value level	Higher	Good	General	The lower

5.2. Dynamic Evaluation Results of University Brand Value. Through the evaluation and scoring of 12 indexes by 20 independent students, we calculate the average value of each index given by all students and list the average scoring of each index, as shown in Table 8.

According to the average scores, as illustrated in Table 9, we can calculate the evaluation score of each index in the criterion layer using the following equations:

Academic reputation single level scoring: $B_1 = 0.42C_{11} + 0.27C_{12} + 0.31C_{13} = 0.42 \times 78.4 + 0.27 \times 81.9 + 0.31 \times 88.5 =$ **82.476**

Single level scoring of teacher resources: $B_2 = 0.17C_{21} + 0.54C_{22} + 0.29C_{23} = 0.17 \times 92.1 + 0.54 \times 89.6 + 0.29 \times 78.7 =$ **86.864**

Table 9: Average student evaluation.

Number	The evaluation index	Average
1	Number of national papers	78.4
2	Number of excellent university papers	81.9
3	Number of international award students	88.5
4	Structure of teaching staff	92.1
5	Faculty	89.6
6	Proportion of PhD teachers	78.7
7	Basic knowledge ability	91.8
8	Professional and technical ability	92.3
9	Personal practical ability	86.4
10	Students employment	79.5
11	The innovation ability	87.1
12	Ability to manage	82.2

Single level scoring of teaching quality: $B_3 = 0.35C_{31} + 0.16C_{32} + 0._{49C33} = 0.35 \times 91.8 + 0.16 \times 92.3 + 0.49 \times 86.4 = \mathbf{89.234}$

Single level scoring of talent training: $B_4 = 0.59C_{41} + 0.25C_{42} + 0._{16C43} = 0.59 \times 79.5 + 0.25 \times 87.1 + 0.16 \times 82.2 = \mathbf{81.832}$

Dynamic evaluation results of university brand value based on analytic hierarchy process (AHP): $A = 0.53B_1 + 0.21B_2 + 0.12B_3 + 0.14B_4 = \mathbf{84.12}$

By substituting the average evaluation scores of 20 students into the dynamic evaluation model of university brand value based on analytic hierarchy process, this paper calculates that the scores of criteria level indicators academic reputation, teacher resources, teaching quality, and talent training indicators are 82.476, 86.864, 89.234, and 81.832, respectively. Compared with the evaluation standards of university evaluation values listed in the above table, the results show that the level of the thought index is "B." After comprehensive calculation, the total score of brand value of the university is 84.12, which also belongs to "B" level. Based on the analysis of the results, it can be concluded that the overall score of the university is high and has a certain brand value. However, it is weak in talent training and academic reputation. Compared with other universities, the findings reveal that the number of academic papers published is less and its position in the academic field is slightly lower than other universities.

From the above two aspects, we conclude that the university should strengthen the academic ability of college students, encourage students to conduct scientific research, publish papers in relevant fields, and win honors in the international field. The improvement of academic reputation is conducive to the improvement of brand value of colleges and universities at home and abroad and plays a certain role in promoting academic research in China. At the same time, there is a relative lack of talent training, and the graduated college students lack management ability and innovation ability. Colleges and universities should improve students' creativity, formulate courses to spread students' thinking ability, give full play to students' imagination and creativity, and create a good research environment for students.

6. Conclusions and Future Work

The improvement of brand value of colleges and universities is reflected in the investment of education, the output of talents, and the training process. This paper uses analytic hierarchy process (AHP) to establish a dynamic evaluation system and model of brand value of colleges and universities and selects a number of indicators for evaluation, which can more truly reflect the brand value of colleges and universities. Combined with quantitative analysis and qualitative analysis, evaluate the brand value of colleges and universities as a whole, so that the results can reflect the real value of the data. In the process of empirical analysis, 20 students are selected to score several indicators affecting the brand value of colleges and universities, and the average score is calculated. This value is substituted into the established university brand dynamic evaluation model for calculation. The results show that the comprehensive score of the university is 84.12 and the grade is "B," which is one of the universities with high brand value in China. We observed that there is a relative lack of talent training, and the graduated college students lack management ability and innovation ability. Furthermore, colleges and universities should improve students' creativity, formulate courses to spread students' thinking ability, give full play to students' imagination and creativity, and create a good research environment for students. The indicators selected in this paper can comprehensively cover all aspects of the brand value of colleges and universities, so the results are of high value and can be applied in practice. In the future, we will evaluate the problem in a large space while considering large number of universities and students. Similarly, other factors should be considered that could more accurately classify the universities brand values.

Data Availability

The data can be requested from the corresponding author.

Conflicts of Interest

The authors declare that they have no conflicts of interest.

Acknowledgments

This study was supported by the Research on the Issue of National Identity Education in Guangdong Colleges and Universities Promoting the Return of Young Students in Hong Kong Under the Perspective of Branding Vision, Research Project of Party Building in Study Conference of Party Building in Guangdong Colleges and Universities in 2019 (project no: 2020MB015).

References

[1] J. Choi and S. Seo, "Do brand rumors matter? The role of brand equity and response strategy to brand rumor," *International Journal of Contemporary Hospitality Management*, vol. 33, no. 8, pp. 2862–2879, 2021.

[2] A. Badenhop and M. Frasquet, "Online grocery shopping at multichannel supermarkets: the impact of retailer brand equity," *Journal of Food Products Marketing*, vol. 27, no. 4, pp. 1–16, 2021.

[3] C. H. Huo and M. Pang, "The effect of consumers' perception of brand innovation on marketing productivity," *Research on Financial and Economic Issues*, vol. 37, no. 6, pp. 139–145, 2020.

[4] Y. P. Zhao, "A Brief analysis on the construction and value of Cultural creative brand in Chinese universities -- A case study of Hangzhou Normal University," *Media*, vol. 9, pp. 73-74, 2019.

[5] T. T. Nguyen and B. Grohmann, "The influence of passion/determination and external disadvantage on consumer responses to brand biographies," *Journal of Brand Management*, vol. 27, no. 3, 2020.

[6] T. Y. Chun, D. K. Lee, and N. H. Park, "The effect of marketing activities on the brand recognition, brand familiarity, and purchase intention on the SNS of fc," *The Journal of Asian Finance, Economics and Business*, vol. 7, no. 11, pp. 955–966, 2020.

[7] M. Tribukait, "Digital learning in European history education: political visions, the logics of schools and teaching practices," *History Education Research Journal*, vol. 17, no. 1, pp. 4–21, 2020.

[8] G. Ö. Uzun, A. Ç. Eş, and G. Evram, "Examination of attitudes of university students in distance education according to some variables," *Near East University Online Journal of Education*, vol. 3, no. 2, pp. 104–115, 2020.

[9] X. J. Zhai, Y. Zhang, and M. Shi, "An empirical study on the marketing of excellent cultural activities in academic libraries —taking nanjing university library as an example," *Journal of Academic Libraries*, vol. 38, no. 6, pp. 12–18, 2020.

[10] Z. K. Chen and T. Xu, "Daily-use ceramic brand design research based on kano model," *Jingdezhen Comprehensive College Journal*, vol. 35, no. 6, pp. 92–95, 2020.

[11] Z. Li, Z. Zhu, and H. Tian, "Research on brand heritage model construction and activation strategy based on brand asset theory," *E3S Web of Conferences*, vol. 179, no. 4, Article ID 02071, 2020.

[12] A. N. Rangkuti, L. A. Dalimunthe, and A. A. Lubis, "The development of statistics modules for the students of islamic colleges and universities in south tapanuli," *Al-Ta lim Journal*, vol. 27, no. 1, pp. 30–40, 2020.

[13] E. H. Forman and S. I. Gass, "The analytic hierarchy process-an exposition," *Operations Research*, vol. 49, no. 4, pp. 469–486, 2001.

[14] F. D. Ariyanti and A. C. Putri, "Selection of subcontractor vendor using analytic hierarchy process (AHP) method in construction company," *IOP Conference Series: Earth and Environmental Science*, vol. 794, no. 1, Article ID 012072, 2021.

[15] C. J. Zhang, "A class evaluation model of college students based on AHP," *China Science & Technology Panorama Magazine*, vol. 264, no. 9, 262 pages, 2014.

[16] P. Smutny and P. Schreiberova, "Chatbots for learning: a review of educational chatbots for the Facebook Messenger," *Computers & Education*, vol. 151, Article ID 103862, 2020.

[17] P. H. Dos Santos, S. M. Neves, D. O. Sant'Anna, C. H. D. Oliveira, and H. D. Carvalho, "The analytic hierarchy process supporting decision making for sustainable development: an overview of applications," *Journal of Cleaner Production*, vol. 212, pp. 119–138, 2019.

[18] Y. L. Ren, "Evaluation system for interactive asset performance management based on 1-9 scaling method," *Experimental Technology and Management*, vol. 34, no. 11, pp. 259–262, 2017.

[19] W. Ho and X. Ma, "The state-of-the-art integrations and applications of the analytic hierarchy process," *European Journal of Operational Research*, vol. 267, no. 2, pp. 399–414, 2018.

[20] F. Wang, Y. Lu, J. Li, and J. Ni, "Evaluating environmentally sustainable development based on the PSR framework and variable weigh analytic hierarchy process," *International Journal of Environmental Research and Public Health*, vol. 18, no. 6, p. 2836, 2021.

[21] A. Patsiotis, M. Atik, and T. Perrea, "The influence of m-marketing tools on consumer buying process: evidence from the dining sector," *International Journal of Retail & Distribution Management*, vol. 48, no. 10, pp. 1037–1056, 2020.

[22] X. Zhong, L. Ren, and T. Song, "Different effects of internal and external tournament incentives on corporate financial misconduct: evidence from China," *Journal of Business Research*, vol. 134, no. 2, pp. 329–341, 2021.

[23] M. Kaushik, "The impact of brand experience, service quality and perceived value on word of mouth of retail bank customers: investigating the mediating effect of loyalty," *Journal of Financial Services Marketing*, vol. 23, no. 1, pp. 12–24, 2018.

[24] Z. Liu, J. A. Duan, and V. Mahajan, "Dynamics and peer effects of brand revenue in college sports," *International Journal of Research in Marketing*, vol. 37, no. 4, pp. 756–771, 2020.

[25] C. M. Matli, T. Tlapana, and R. Hawkins-Mofokeng, "The role of branding in the choice of a university of technology," *International Journal of Research in Business and Social Science (2147-4478)*, vol. 10, no. 7, pp. 342–352, 2021.

Hindawi
Scientific Programming
Volume 2022, Article ID 7893940, 11 pages
https://doi.org/10.1155/2022/7893940

Research Article

A Machine Learning Based Intelligent Decision Support System for Flotation Dynamics in Simulation of Clay Minerals

Wanying Chen,[1] **Zhihong Li**,[1] **Bo Hao**,[1] **Jianchuan Gao**,[2] **and Minqiang Fan**[1]

[1]*School of Mining Engineering, Taiyuan University of Technology, Taiyuan 030024, China*
[2]*Coal Cleaning and Processing Department, Shanxi Coking Coal Group, Tai Yuan 030024, China*

Correspondence should be addressed to Zhihong Li; lizhihong9123@163.com

Received 5 February 2022; Revised 15 February 2022; Accepted 22 February 2022; Published 23 March 2022

Academic Editor: Muhammad Zakarya

In coal mines, process management is related with planning and flow of coal minerals from their mining points to journey's end. The process is dependent on the operational decisions, which should be completed during coal production. In these systems, simulation modelling is assumed a powerful tool for decision making. The simulation modelling can further be enhanced through applying artificial intelligence (AI) and machine learning (ML) methods. The communication of water with clay minerals upholds the water adsorption on the clay surface, which makes them complex systems. Therefore, evading the water absorption from the clay turns out to be a hard job. The computational trainings of clay minerals are needed to comprehend the dynamics of water distribution. Tradition of coal slurry treatment is completed by adding medicament of its mineral flocculation sedimentation. As a result of coal, slime water contains a lot of clay minerals that are rich in kaolinite versatility and it is difficult to settle. The flotation will be one of the kaolinite recycling. In this paper, clay minerals containing a variety of minerals were taken as samples, and sodium dodecyl sulfate and sodium oleate were used as collectors to explore the flotation effect through test and molecular dynamics simulation. A machine learning based intelligent decision support system is designed to improve the outputs of the simulation model. The results show that when the pH value is 8 and the amount of collector and sec-octanol are 150 g/t and 250 g/t, respectively, the flotation rate of fine mineral can reach 63.25%. According to the molecular dynamics simulation results, the addition of the collector can reduce the hydrophilicity of the kaolinite surface, and the physical adsorption of SDS only occurs on the (001) surface.

1. Introduction

The coal slurry preparation plant contains a large number of clay minerals, resulting in fine particle size, high viscosity, and complex interaction between particles. The slime water is difficult to settle [1], and the difficulty of treatment increases. Common clay minerals in coal include kaolinite, illite, and aemon mixed layer [2], among which kaolinite is widely used [3]. If it is enriched from tail coal for reuse, the utilization rate of tail coal can be improved, the difficult problems of environmental and slime water treatment can be solved, and considerable economic efficiency can be brought.

Flotation is the main method of fine mineral separation. Ionic collector is commonly used in kaolinite flotation. When dodecylamine was used as a collector [4], the good flotation effect under acidic conditions was due to the weakened adsorption difference between the cleavage planes and the occurrence of flocculation of mineral particles, which increased the adsorption density of dodecylamine [5]. The research results show that [6], due to the differences in the electrostatic forces between different tertiary amine cations and kaolinite surface, substituent effect and space effect of tertiary amine substituent group, and N atom bonding, the flotation results are different, and the results are similar to those of molecular dynamics simulation [7]. In the quaternary ammonium 123C system, metal ions and pH have a great influence on the floatability of kaolinite [8]. The results showed [9] that the adsorption capacity of CTAC, DTAC, and TTAC on kaolinite increased with the increase

of dosage of reagents. Aminoamide has a good collecting effect on pure kaolinite under acidic conditions, and the yield increases with the increase of dosage [10]. It is found that [11] flotation efficiency of flotation reagent varies with different concentration, pH, and temperature. Sodium oleate is a collector, and kaolinite with small particle size has better flotation efficiency [12]. Among them, reagents and kaolinite are mainly chemical adsorption, and pH and metal ions have great influence on the flotation effect of kaolinite [13–15].

The element composition of different surfaces of kaolinite is different, and the interaction between different reagents and different surfaces of the kaolinite can be well understood through molecular dynamics simulation, so as to explain the difference of the flotation efficiency between reagents [16–21]. Kaolinite is widely used in clay minerals. In this paper, the flotation performance and action mechanism of coal measure kaolinite by sodium dodecyl sulfate (SDS) and sodium oleate (NaOL) were investigated by flotation test and molecular dynamics simulation. The interaction between Na+ in SDS and O atoms in kaolinite, O in SDS anionic group, and H atoms in kaolinite belongs to ion-dipole interaction. The carboxylic acid ion of sodium oleate adsorbed with kaolinite (001) surface, and the hydrophobic alkane chain of oleate ion adsorbed with (00-1) surface [22, 23].

The communication of water with clay minerals upholds the water adsorption on the clay surface, which makes complex systems. Therefore, evading the water absorption from the clay turns out to be a hard job. The computational trainings of clay minerals are needed to comprehend the dynamics of water distribution. Moreover, process management in coal mines is related with planning, and flow of coal minerals from their mining points to journey's end. The process is dependent on the operational decisions, which should be completed during coal production. In these systems, simulation modelling is assumed a powerful tool for decision making. The simulation modelling can further be enhanced through applying artificial intelligence and machine learning methods [24–27]. Following are the major contributions of this paper.

(i) We explore the flotation effect through test and molecular dynamics simulation in clay minerals.

(ii) A machine learning based intelligent decision support system is designed and integrated in the simulation model.

(iii) A data aggregation technique is presented to improve the model training time.

(iv) The simulation modelling can further be enhanced through applying artificial intelligence and machine learning methods.

The remainder of the paper is structured as follows. In Section 2, we present an outline of the materials and methods. A brief debate over the machine learning, decision support system, and data aggregation is also included. Section 3 is related to the datasets and assessment metrics. In addition, experimental details and results are deliberated. Finally, Section 4 concludes this paper and offers several directions for further research and investigation.

2. Materials and Methods

2.1. Test Samples. The test samples were collected from clay minerals in Malan Coal Mine of Shanxi Coking Coal Group. The sample was in block and was ground to −0.074 mm by laboratory prototype, bagged, sealed, and reserved. Table 1 and Figure 1 show the chemical composition and mineral composition of the samples, respectively.

As can be seen from Table 1, SiO_2 and Al_2O_3 contents are the highest in the chemical composition of the samples, corresponding to quartz minerals and kaolinite and other clay minerals. It can also be seen from the diffraction peak and content percentage in Figure 1 that the main minerals in the sample are kaolinite and quartz.

2.2. The Reagents. Flotation collector is sodium dodecyl sulfate and sodium oleate (SDS, NaOL, 5% aqueous solution with water), regulator is HCl solution and NaOH solution, and foaming agent is sec-octanol; all agents are analytically pure.

2.3. Test Method

(1) *Flotation*: the XFG ii laboratory hanging cell flotation machine was used for the test, with the rotation speed of 1800 r/min. Moreover, periodically 6 g samples were taken each time, and put into 60 mL flotation cell. Next, by adding 50 mL tap water and mixing slurry for 2 min, we adjusted pH with HCL or NaOH. Subsequently, we added flotation collector and stirring for 3 min, and mixed foaming agent for 2 min and then blowing bubbles for 5 min. The flotation concentrate and tailings were dried and weighed to calculate the yield, and the element analysis was carried out to calculate the Al/Si ratio.

(2) *X-ray diffraction analysis*: Rigaku MiniFlex600 X-ray diffractometer was used for testing with a scanning range of 5°–85°.

(3) *Molecular dynamics simulation*: the molecular model of kaolinite and SDS was constructed and optimized by Material Studio software. The size of the simulated box was $44.67 \times 51.5 \times 120$ Å, and 30 pharmaceutical molecules were constructed. The thickness of the vacuum layer was 100 Å. The charge of kaolinite was calculated by QEq method, and the charge force field parameters of other molecules were allocated. Temperature is controlled at 298 K by Nose. The simulation time step is 1FS and the simulation time is 1000 ps. The electrostatic force was truncated by Ewald addition method, and the Van der Waals force was truncated by atom based method with a truncation radius of 12.5 Å. The balance part of 100 ps was used for subsequent analysis.

2.4. Decision Support System Framework. A decision support system (DSS) is an interactive, computer-based system that assists a user in making more effective decisions while solving semistructured geographical data. Satellite remote sensing and digital elevation modelling provide a systematic,

Table 1: Chemical composition of sample.

Name	SiO_2	Al_2O_3	Fe_2O_3	CaO	MgO	TiO_2	K_2O	Na_2O	MnO_2	P_2O_5	SO_3	Al/Si
Content	67.61	22.55	2.49	1.86	0.92	0.35	2.65	0.48	0.07	0.06	0.78	0.38

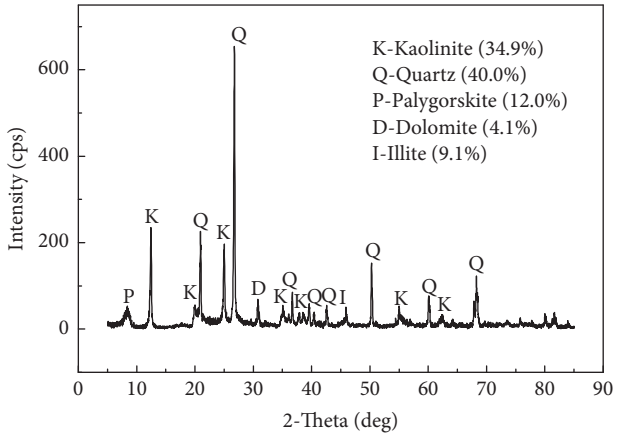

Figure 1: The XRD pattern of sample.

rational framework for advancing scientific knowledge of geophysical phenomena, which frequently lead to the detection of natural disasters or mineral wealth. Figure 2 illustrates the process of the simulation model and Figure 3 shows a decision support system framework for coal mines. As stated in Figure 2, after deciding the problem and objectives, the collected data will help to develop the simulation model. The model, as such, can offer a solution to the problem. The dataset is divided into training and testing parts, where the latter one is used to validate the solution against a set of objectives. The DSS system comprises several parts including machine learning, IoT sensors, and data aggregation module. These are discussed in subsequent sections.

2.4.1. Machine Learning. The mining industry's interest in using AI approaches in fields like geology and minerals processing has grown in recent years. In the realm of scientific inquiry, this pattern is repeated. Soft computing has been employed in the modelling, design, and optimization of mining operations, among other things. They can also help with the design, development, and operation of intelligent systems capable of adapting, learning, and operating autonomously in uncertain and imprecise environments. To extract useful models from empirical data, machine learning methods are used. These algorithms may be applied to metallurgical process optimization and design. On a larger scale, these approaches are used as soft sensors for the prediction of difficult-to-measure data. Modeling of metallurgical reactions or subprocesses engaged in integral processes such as flotation is one of the uses of these technologies. Machine vision is the study of ways for extracting useful information from high-dimensional pictures, and it has been utilized nearly exclusively in mining. In this paper, we used support vector machine (SVM) and long

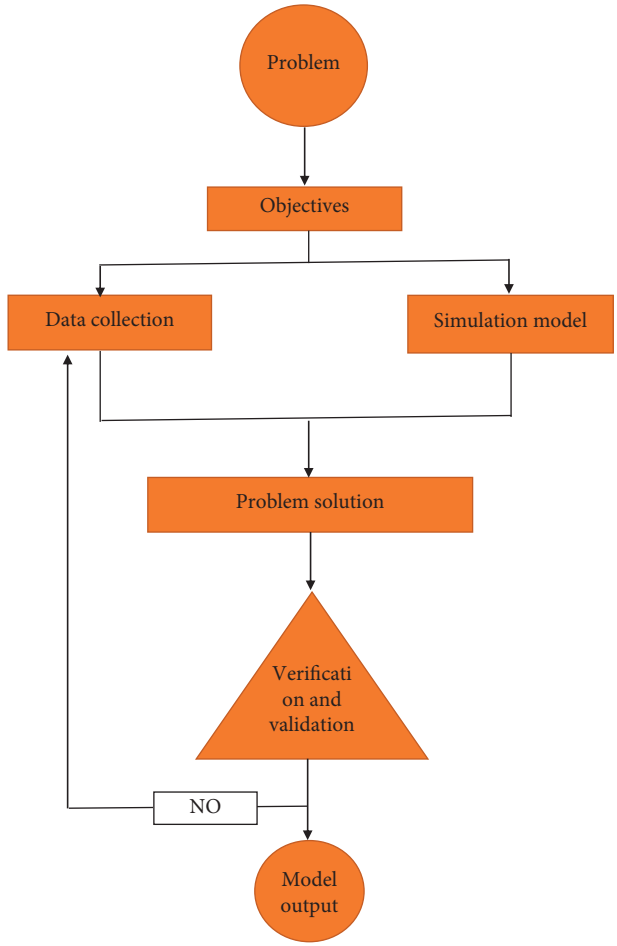

Figure 2: Process of the simulation process.

short-term memory (LSTM) approaches to further enhance the simulation model and improve decisions making.

2.4.2. Internet of Things. Internet of things (IoT) sensors are placed in the coal mineral site which are used to collect data. These sensors are distributed across the mining sites and required data is collected. The data is used to monitor the entire site and it can also be sent to the DSS for taking appropriate decisions. In addition, the data can also be utilized for safety purposes. Various IoT sensors that can measure physical surroundings and capture real-time environment changes make up the IoT sensor data layer. Temperature, pressure, humidity, level, accelerometer, gas, gyroscopes, motion sensors, image, optical sensors, radio-frequency identifier (RFID) sensors, and infrared (IR) sensors are some of the most prevalent IoT sensors. Similarly, management in coal mines is related with planning,

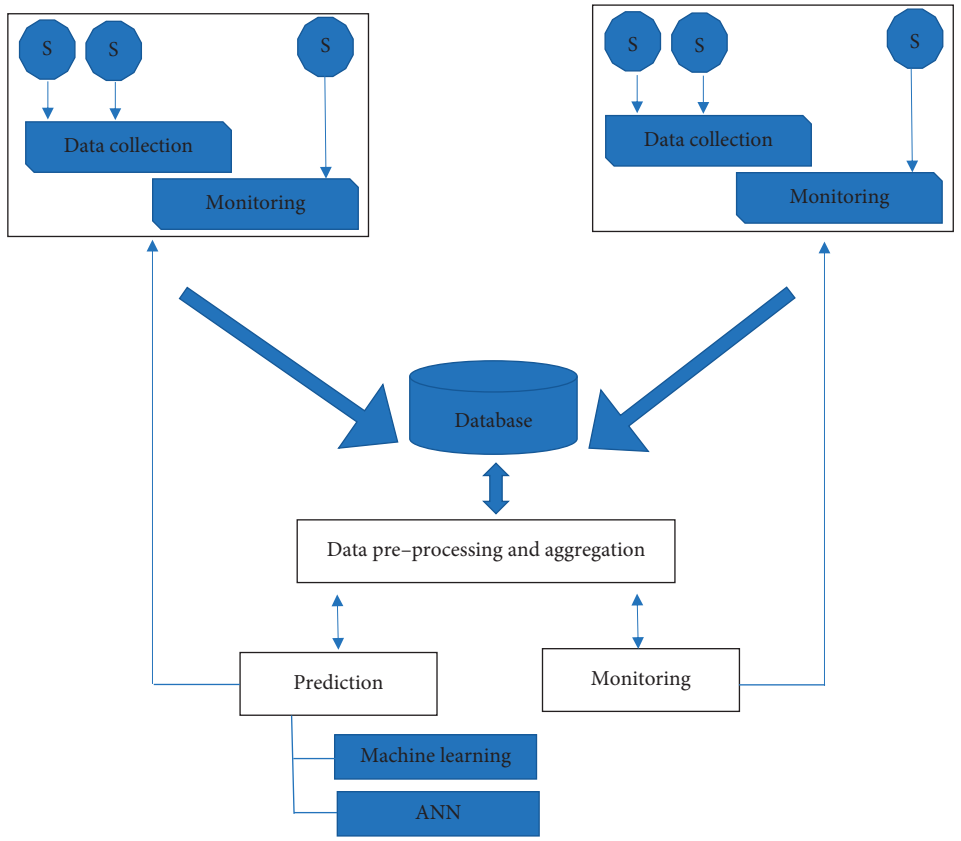

Figure 3: Decision support system framework for coal mines.

and flow of coal minerals from their mining points to journey's end. The process is dependent on the operational decisions, which should be completed during the coal production.

2.4.3. Data Preprocessing and Aggregation. The data is processed and certain methods are applied to remove redundancy. We use the well-known Euclidian distance equation to design an aggregation approach, as shown in Algorithm 1. The suggested algorithm compares two data points; in case they belong to the overlapping regions, one point is discarded and the other one is taken into account. This could be achieved through computing the Euclidian distance and then comparing the difference with a predefined threshold value. If the difference is less than or equal to the threshold value, then one point is discarded. Aggregation is a data preprocessing technique that reduces the burden on the decisions support system, as shown in Figure 3. The processed data is saved to a centralized database that can be used in the prediction and simulation of the coal mineral. Approaches like aggregation might be useful in removing duplicate data that, subsequently, reduces the training time. After preprocessing, the clean data is saved in the database for other tasks including prediction and monitoring. Different AI and ML algorithms are used in the prediction process.

3. Results and Discussion

3.1. Flotation Performance of Clay Minerals by Collectors. It should be noted that, in this study, NaOL and SDS were used as collectors. Moreover, due to their foaming properties and characteristics, the effects of adding and not adding foaming agents under different pH conditions were examined in the test. The relevant flotation test results are shown in Figure 4. Among them, the amount of collector without foaming agent is 500 g/t, the amount of collector with foaming agent is 150 g/t, and the amount of octanol in foaming agent is 250 g/t.

As can be seen from Figure 4, the flotation effect of SDS under the same conditions is significantly better than that of NaOL. When the pH value of NaOL is lower than 9, NaOL has no collecting effect on the sample, but when the pH value is higher than 10~11, NaOL has collecting effect, but the flotation rate of fine mineral is less than 20%. When SDS was used as collector, the flotation concentrate mineral yield was about 40%, significantly higher than that of NaOL collector, but the increase of fine mineral yield was slow when pH value was more than 7. The highest yields of NaOL and SDS were 52.89% and 64.51%, respectively, after the addition of sec-octanol foaming agent. The effects of two kinds of collecting agents were significantly improved. In particular, NaOL collector can obtain good flotation results under neutral and weak alkaline conditions.

Input: Original dataset denoted by points D_i and D_j
Output: Refined dataset denoted by two points D_i' and D_j'
for each element i, j in D_i, D_j
if $j \leq i$ or i D_i or j D_j
exit()
end if
$E_d(D_i, D_j) = \sqrt{(d_{ik} - \min_{jk})^2}$ where $d_{ik} \in D_i$ and $d_{jk} \in D_j$
if $E_d(D_i, D_j) \leq T_d$ **then**
Discard either D_i or D_j, to form D_i' or D_j'
end if

Algorithm 1: The data aggregation approach.

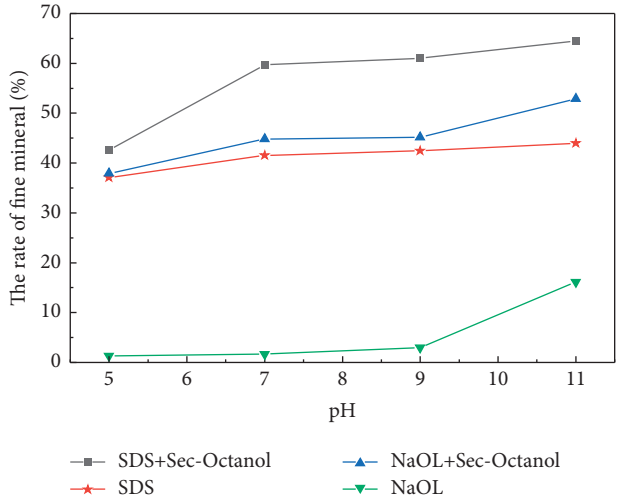

Figure 4: Effect of slurry pH value on sample flotation.

Figure 5 shows the influence of different collector dosage on flotation results of clay samples when pH = 8 (pH value of laboratory tap water) and the dosage of sec-octanol 250 g/t. It can be seen that when pH = 8, the dosage of foaming agent is unchanged, and the two collectors have the same flotation rule for samples; that is, with the increase of the dosage of collector, the flotation fine mineral rate gradually increases, and the fine mineral rate tends to be stable when the dosage of reagent is ≥ 150 g/t. The maximum yield of SDS is about 7% higher than that of the NaOL.

Tables 2 and 3 show the chemical composition analysis results of the flotation products, for SDS and NaOL, respectively; under the above conditions when pH = 8, the foaming agent dosage is approximately 250 g/t, and the collector dosage is 150 g/t.

As can be seen from Tables 2 and 3, under the action of two kinds of collectors, Al_2O_3 content in flotation concentrate is higher than tailings, SiO_2 content is lower than tailings. Except when SDS is used as collector, the Na_2O content in flotation concentrate is 0.2% lower than that in tailings. In other cases, the Na_2O and K_2O contents in concentrate are higher than those in tailings, while Na and K mainly exist in clay minerals.

Comparing the effects of the two collectors, it can be seen that the Al/Si ratio of the two reagents concentrate is greater

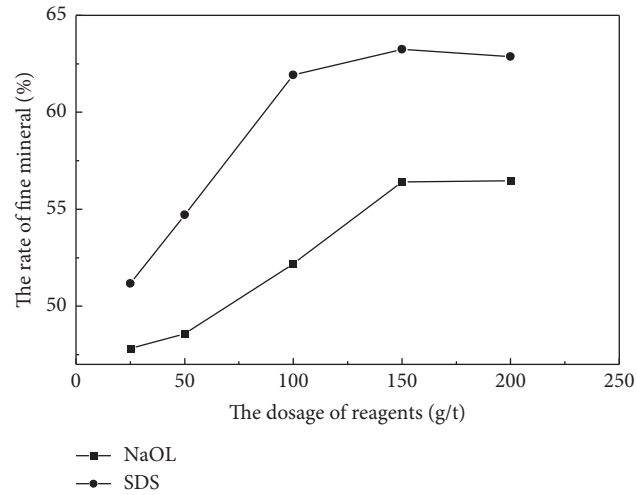

Figure 5: Influence of collector dosage on flotation results at pH = 8.

than that of the raw ore, and the Al/Si ratio of the tailings is smaller than that of the raw ore, indicating that the two reagents preferentially enrich clay minerals such as kaolinite, and the difference of the Al/Si ratio of the fine tailings when SDS is the collector is greater than that when NaOL is the collector, indicating that the selectivity of SDS is stronger than that of NaOL.

The phase analysis results of XRD spectra of flotation concentrate and tailings are shown in Table 4. It can be seen from Table 4 that the kaolinite collection ability of SODIUM SDS is greater than that of NaOL, but the quartz content in concentrate is also higher. The content difference between kaolinite and quartz in tailings of sodium lauryl sulfate is greater than that of NaOL and the difference is large, which indicates that the separation effect of SDS is greater than that of NaOL.

3.2. Molecular Dynamics Simulation of the Interaction between Collector and Kaolinite. Figure 6 shows the initial configuration and final adsorption model of two different collectors in water and kaolinite surface (001) and surface (00-1).

As can be seen from Figure 6, one end of sulfate ion in SDS interacts with kaolinite (001) crystal face and forms adsorption, but it is almost not adsorbed on kaolinite (00-1) crystal face. NaOL is adsorbed with its carboxylic ion to kaolinite (001) crystal face, while the hydrophobic alkane chain of oleate ion is adsorbed with the (00-1) crystal face, and the hydrophilic carboxylic ion head group is oriented towards the water phase. Tables 5 and 6 show the calculated energy of interaction between the kaolinite (001) crystal face and kaolinite (00-1) crystal face with each molecule, respectively.

The formula for calculating the interaction energy between the agent and kaolinite is

$EA + K = (E_{total} - EA - EK + W - EK - EA + W + EW + EA + K)/2$ [28].

Agent is A; kaolinite is K; water is W.

Table 2: X-ray diffraction phase analysis of SDS flotation products at pH = 8(%).

Name	SiO_2	Al_2O_3	Fe_2O_3	CaO	MgO	TiO_2	K_2O	Na_2O	MnO_2	P_2O_5	SO_3	Al/Si
Concentrate	64.17	25.72	2.53	1.60	0.94	0.40	3.04	0.47	0.07	0.06	0.83	0.45
Tailings	73.14	17.42	2.25	2.43	0.89	0.27	1.93	0.49	0.07	0.06	0.90	0.27

Table 3: X-ray diffraction phase analysis of NaOL flotation products at pH = 8(%).

Name	SiO_2	Al_2O_3	Fe_2O_3	CaO	MgO	TiO_2	K_2O	Na_2O	MnO_2	P_2O_5	SO_3	Al/Si
Concentrate	65.74	23.94	2.61	1.59	0.85	0.39	2.90	0.65	0.08	0.06	0.99	0.41
Tailings	72.94	17.74	2.46	2.11	0.95	0.28	2.07	0.41	0.08	0.06	0.76	0.28

Table 4: X-ray diffraction phase analysis of flotation products at pH = 8(%).

	Kaolinite	Quartz	Palygorskite	Illite	Dolomite
SDS concentration	41.3	36.0	8.5	10.9	3.3
SDS tailings	18.1	68.5	4.2	4.8	4.4
NaOL concentration	39.6	28.4	18.9	10.9	2.3
NaOL tailings	29.4	54.4	6.7	5.1	4.4

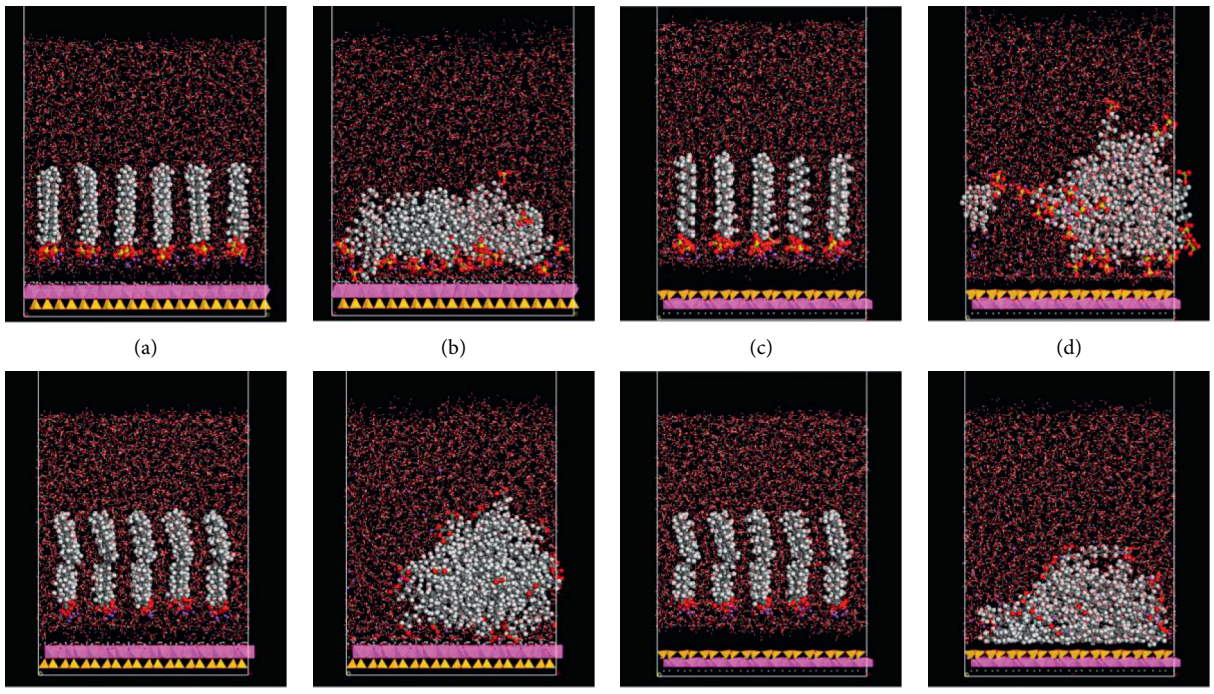

Figure 6: Initial configuration and final adsorption model of collector on kaolinite crystal surface (001) and (00-1). (a) Initial configuration of SDS-(001) crystal surface; (b) final adsorption model of SDS-(001) crystal surface; (c) initial configuration of SDS-(00-1) crystal surface; (d) final adsorption model of SDS-(00-1) crystal surface; (e) initial configuration of NaOL-(001) crystal surface; (f) final adsorption model of NaOL-(001) crystal surface; (g) initial configuration of NaOL-(00-1) crystal surface; (h) final adsorption model of NaOL-(00-1) crystal surface.

Table 5: Calculation of interaction energy between kaolinite (001) surface and each molecule.

Project	Nonbond energy	Composition of nonbond energy		
		Van der Waals	Long range correction	Electrostatic
Kaolinite interacts with water	−1702.12	208.74	−7.26	−1903.61
Kaolinite interacts with SDS	−190.64	−47.02	−1.53	−142.09
Kaolinite interacts with NaOL	−160.36	−22.11	−1.81	−136.44
Kaolinite adsorbed SDS to interact with water	−1613.70	223.19	−8.13	−1828.76
Kaolinite adsorbed NaOL to interact with water	−1669.59	182.626	−8.07	−1844.14

Table 6: Calculation results of the interaction energy between kaolinite (00-1) crystal face and each molecule.

Project	Nonbond energy	Composition of nonbond energy		
		Van der Waals	Long range correction	Electrostatic
Kaolinite interacts with water	−465.26	−291.40	−7.46	−166.41
Kaolinite interacts with SDS	−92.33	−22.90	−1.53	−67.90
Kaolinite interacts with NaOL	−264.53	−305.51	−1.81	42.50
Kaolinite adsorbed SDS to interact with water	−431.02	−279.30	−8.13	−143.60
Kaolinite adsorbed NaOL to interact with water	−283.55	−113.20	−8.07	−162.28

As can be seen from Table 5, the total adsorption energy of kaolinite (001) crystal face and water is −1702.12 kCal/mol, in which the electrostatic interaction energy is a large negative value, indicating that kaolinite (001) crystal face and water have a strong mutual attraction, while its van der Waals action energy is relatively small positive, playing a repulsion effect. The overall effect is strong adsorption dominated by electrostatic force. After SDS and NaOL adsorption, the total adsorption energy of kaolinite (001) crystal face with water is −1613.70 kCal/mol and −1669.59 kCal/mol, respectively, which are lower than the total adsorption energy of the original sample with water, indicating that the addition of agents can weaken the hydrophilicity of kaolinite (001) crystal face. The improvement effect of the SDS is better than the earlier approaches, i.e., NaOL for coal measure kaolinite.

It can be seen from Table 6 that the total adsorption energy of kaolinite (00-1) crystal face with water is −465.26 kCal/mol, which is more hydrophobic than that of (001) surface. Van der Waals force is the main force and electrostatic force is weak. The interaction force between kaolinite (00-1) crystal face and SDS is not strong, corresponding to the phenomenon that the agent molecules are almost not adsorbed on the surface of (00-1) after equilibrium, and the total adsorption energy of (00-1) crystal face and water changes very little, indicating that SDS is not adsorbed on this surface, nor does it change the hydrophilicity of this surface. Compared to kaolinite (00-1) crystal face with NaOL interaction, van der Waals interaction energy is stronger and has the effect of attracting, so as to make the simulation after balance, oleate ions of hydrophobic chain alkanes and (00-1) surface adsorption, and hydrophilic carboxylic acid ions head towards the water phase; the adsorption configuration cannot obviously improve the feeling on the surface of the water. Although the interaction energy between the surface and water decreased after the adsorption of NaOL agent, the hydrophobicity of the surface changed little under the adsorption configuration of NaOL agent. Figure 7 shows the relative concentration distribution curves of the kaolinite (001) crystal face-water, kaolinite (00-1) crystal face-water, kaolinite (001) crystal face-water-SDS, kaolinite (00-1) crystal face-water-SDS, kaolinite (001) crystal face-water-NaOL, and kaolinite (00-1) crystal face-water-NaOL.

In Figure 7(a), due to intermolecular interaction, water molecules migrate and are tightly adsorbed on the surface of kaolinite (001) crystal face [29], indicating that (001) surface is strongly hydrophilic. After the interaction with SDS and NaOL, it can be seen from (c) and (e) that Na and O plasma and atoms in the agent interact with the kaolinite surface and adsorb on the kaolinite surface, reducing the hydrophilicity of (001) crystal face. It can be seen from the radial distance in Figure 7(b) that when water molecules are adsorbed on the surface of (00-1), a thick drainage zone of water molecules is generated, indicating that this surface is a hydrophobic surface. As can be seen from the peak strength of agent molecules in Figures 7(d) and 7(f), NaOL is better adsorbed on the surface of (00-1) than SDS. In addition, the peaks of water molecules in kaolinite (00-1)-water-SDS system are still sharp and the peak strength is almost unchanged, indicating that the addition of SDS has a weak effect on the (00-1) surface, while the peak strength of water molecules in kaolinite (00-1)-water-NaOL system is greatly weakened, further indicating that the adsorption of NaOL on (00-1) is stronger. However, the surface (00-1) is a hydrophobic surface, and the adsorption of agents on this surface cannot improve the hydrophilicity of kaolinite, and the waste of agents will be caused under the same dosage of agents. Therefore, compared with SDS, the flotation effect of NaOL is relatively poor, which is the same as the flotation test result. Figure 6 shows the RDF of kaolinite (001) surface, SDS, and water.

As can be seen from Figure 8(a), the first peak of O atom in kaolinite and H atom in water appears at 0.155 nm, and the first peak of H atom in kaolinite and O atom in water appears at 0.203 nm, both within the length range of hydrogen bond, so kaolinite (001) crystal face is mainly adsorbed with water in the form of hydrogen bond. In Figure 8(b), the distance between hydroxyl H on kaolinite (001) crystal face and sulfate group in SDS is 0.161 nm, the distance between hydroxyl O on kaolinite (001) crystal face and Na+ in SDS is 0.211 nm, the distance between Na+ in kaolinite and O atom in kaolinite. The interaction of O in reagent anion group and H atom in kaolinite is ion-dipole interaction, which is the main source of adsorption force. Although Na + repels H atom on kaolinite surface (because H atom in hydroxyl group has certain positive charge in polarization), Na+ and THE O atom in kaolinite and the O in the reagent anion group have strong electrostatic interaction force of adsorption, which can be said to bridge the relationship between kaolinite and the reagent anion, making their adsorption firmer. Similarly, Figure 8(c) is the radial distribution function of kaolinite (00-1) crystal face and water. It can be seen that the first peak of O atom on kaolinite (00-1) crystal face and H atom in water is 0.175 nm and the peak strength is very weak, indicating that the probability of forming hydrogen bond between (00-1) crystal face and water is very low, so the interaction strength

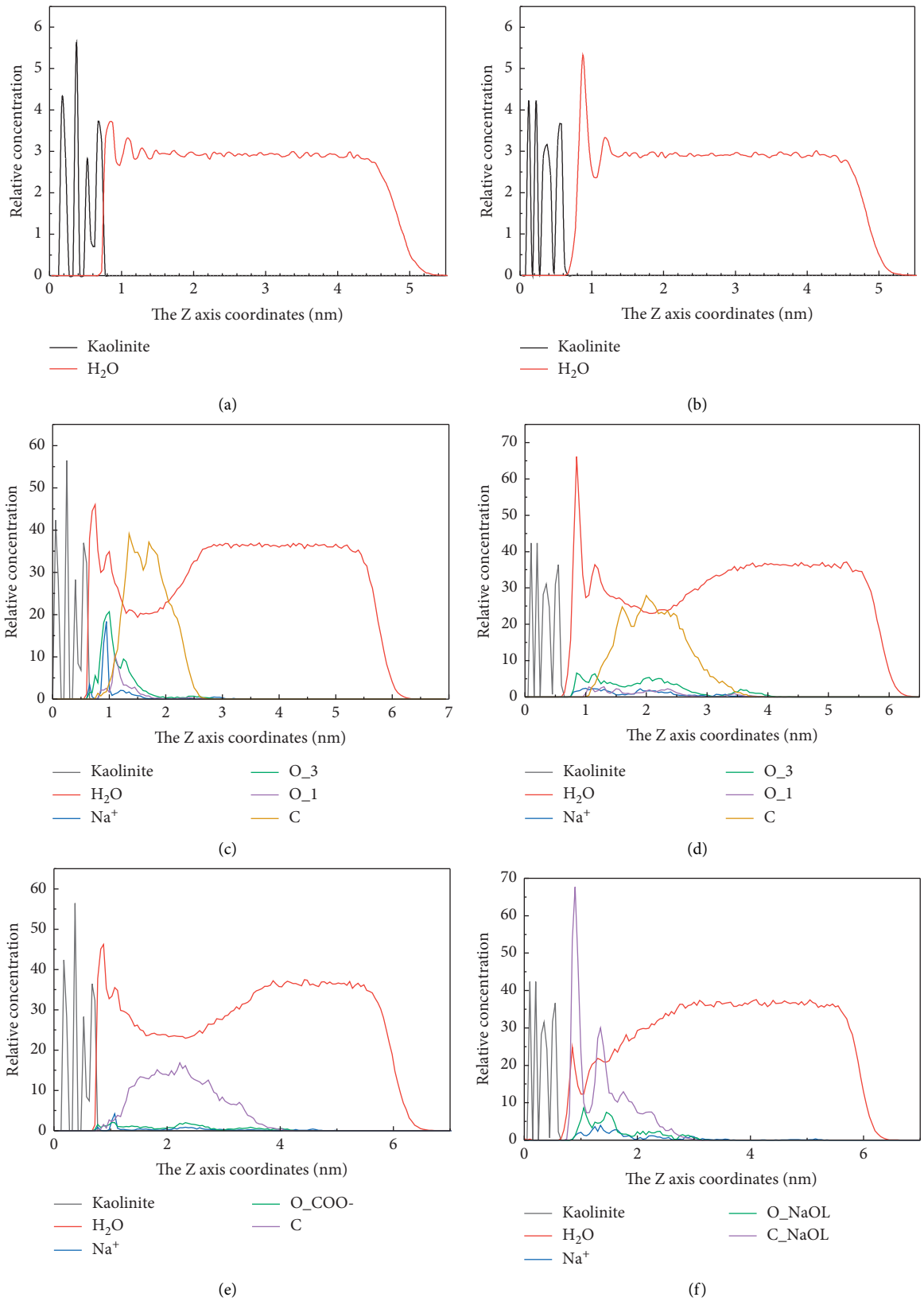

Figure 7: The relative concentration distribution of kaolinite, water, SDS, and NaOL. (a) Relative concentration distribution of kaolinite (001) crystal face-water; (b) relative concentration distribution of kaolinite (00-1) crystal face-water; (c) relative concentration distribution of kaolinite (001) crystal face-SDS-water; (d) relative concentration distribution of kaolinite (00-1) crystal face-SDS-water; (e) relative concentration distribution of kaolinite (001) crystal face-NaOL-water; (f) relative concentration distribution of kaolinite (00-1) crystal face-NaOL-water.

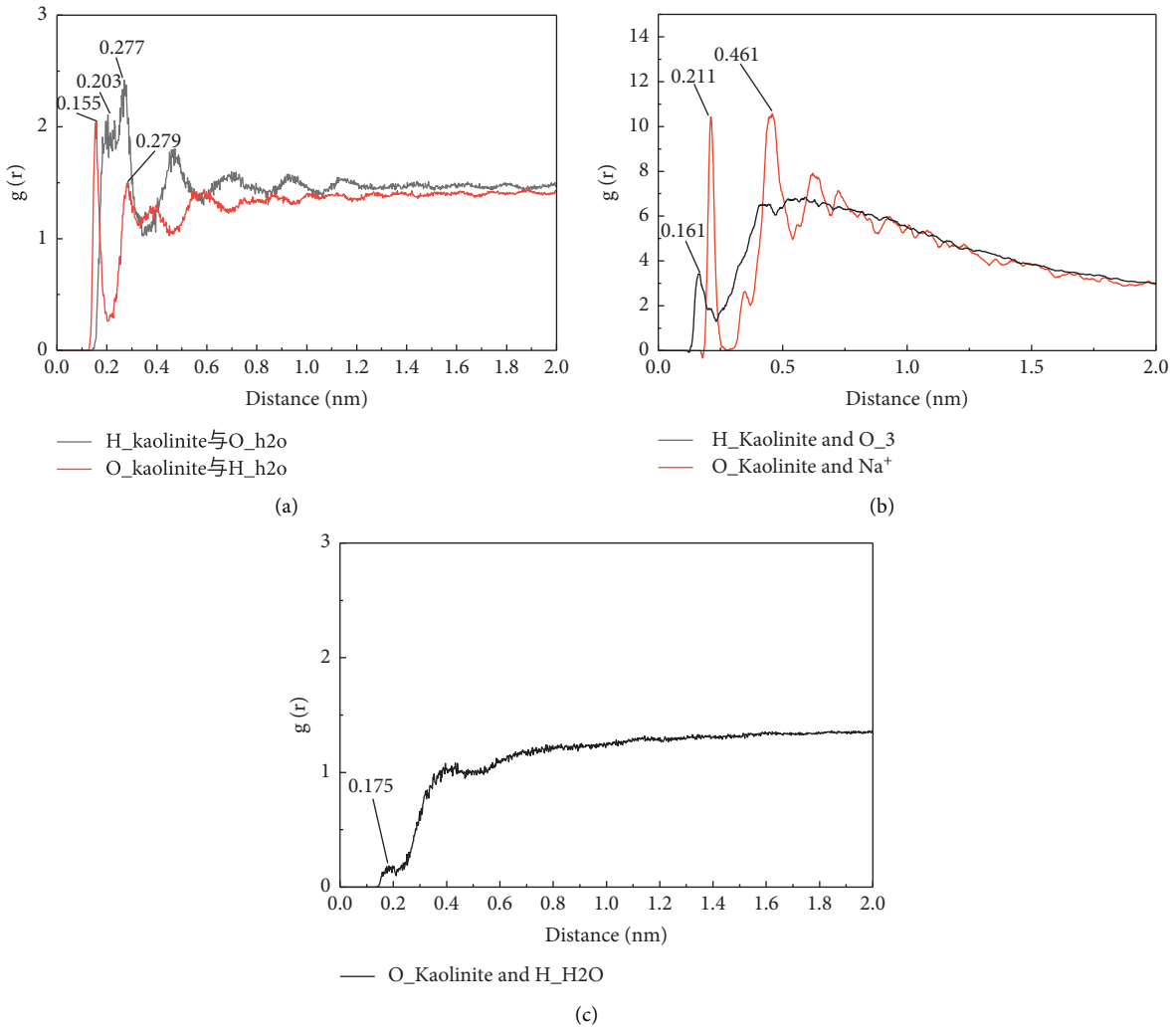

Figure 8: RDF of kaolinite, SDS, NaOL, and water. (a) RDF of kaolinite (001) crystal face and water; (b) RDF of kaolinite (001) crystal face-SDS-water; (c) RDF of kaolinite (00-1) crystal face and water.

is very weak [30]. These results and findings are the same as those of relative concentration and adsorption energy. In addition, sulfate base group and carboxylic acid ions are not adsorbed on this surface, so the radial distribution function of (00-1) crystal face and reagent has no peak formation, so it is no longer displayed, indicating that the hydrophilic groups of SDS and NaOL have no obvious adsorption on (00-1) crystal face.

The outcomes of the machine learning approaches and accuracy with and without aggregation approach are shown in Figures 9 and 10, respectively. In Figure 9, the aggregation approach significantly decreases the model training (42% to 47%) and prediction time (7.4% to 7.8%). The time is denoted in seconds. However, both SVM and LSTM are not significant to reduce the prediction times and are comparable. In Figure 10, the aggregation approach almost produced comparable results in terms of accuracy, i.e., RMSE and MAPE values. This means that our model has learned from the less data very well. The RMSE should be read as a number and the MAPE value is given in percentage. The lesser values represent a more accurate system and vice versa. In conclusion, the addition of the two agents can reduce the hydrophilicity of the kaolinite surface. The main source of the adsorption force is the interaction between Na+ in the agent and the O atom in kaolinite and the interaction between THE O atom in the anionic group of the agent and the H atom in kaolinite, which belongs to ion - dipole interaction.

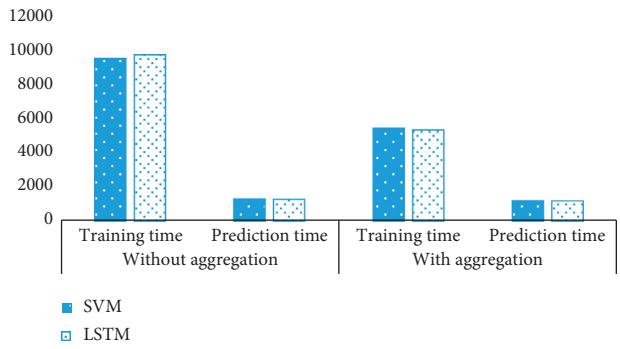

Figure 9: Model training and prediction time (seconds).

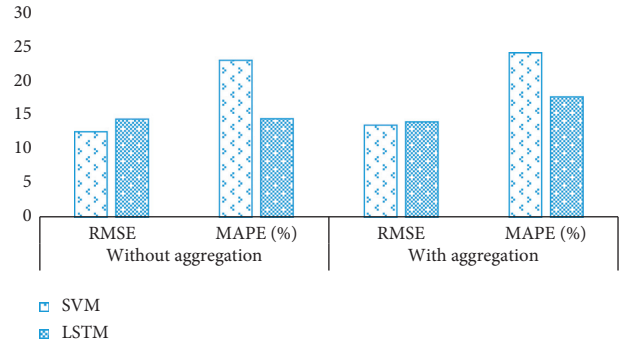

Figure 10: Accuracy of the proposed decision support system in terms of RMSE and MAPE.

4. Conclusions and Future Work

In this paper, clay minerals containing a variety of minerals were taken as samples, and sodium dodecyl sulfate and sodium oleate were used as collectors to explore the flotation effect through test and molecular dynamics simulation. A machine learning based intelligent decision support system is designed to improve the outputs of the simulation model. The flotation effect of SDS is better than that of NaOL for coal measure kaolinite. The addition of foaming agent can greatly reduce the dosage and improve the yield. When pH = 8 and the dosage of sec-octanol is 250 g/t and that of SDS is 150 g/t, the flotation rate of refined minerals by SDS can reach 63.25%. According to the molecular dynamics simulation, kaolinite (001) crystal face is hydrophilic, and (00-1) crystal face is hydrophobic. The interaction energy between kaolinite and water decreases after the interaction with the agent, indicating that the addition of the agent can weaken the hydrophilic kaolinite crystal surface. The sodium oleate is adsorbed with its carboxylic ion to kaolinite (001) crystal face, while the hydrophobic alkane chain of oleate ion is adsorbed with (00-1) crystal face, and the hydrophilic carboxylic ion head group is oriented towards water phase. One end of sulfate ion in SDS interacts with the crystal face of kaolinite (001) and forms adsorption, but it almost does not adsorb on the crystal face of kaolinite (00-1).

Furthermore, the coal mineral simulation model can be further improved through integrating a decision support system and machine learning technique. We observed that decision making is significantly enhanced while reducing the model training time when a data aggregation mechanism is applied. In the future, we will further investigate the impact of other machine learning approaches and, in particular, how the proposed decision system will be integrated in a real world scenario.

Data Availability

The raw/processed data required to reproduce these findings cannot be shared at this time as the data also forms part of an ongoing study.

Conflicts of Interest

The authors declare that they have no conflicts of interest.

Acknowledgments

This work was supported by Study on Coordinated Dewatering and Stable Clean Combustion Mechanism of Urban Sludge-Coal Slime Based on Mild Oxidation (U1910214).

References

[1] F. F. Min, J. Chen, and L. Y. Liu, "State-of-the-art and developing trend of the new technologies for treating difficult-to-settle coal slurry," *Journal of Coal Preparation Technology*, vol. 5, pp. 4–9, 2018.

[2] J. T. Liu, M. Q. Zhang, and Y. Zeng, "Effects of different type clays on the dispersion of fine particles in coal slurry," *Journal of China University of Mining & Technology*, vol. 39, no. 1, pp. 59–63, 2010.

[3] L. S. Yi, Q. R. Li, L. N. Qi, and H. Li, "Study on technological mineralogy of the kaolin from Ningxiang," *Multipurpose Utilization of Mineral Resources*, vol. 2, pp. 78–80, 2016.

[4] F. Q. Lu, B. H. Hou, and M. X. Zhang, "Study on flotation characteristics of coal series minerals in dodecylamine system," *Journal of Chifeng University (Natural Science Edition)*, vol. 36, no. 5, pp. 39–41, 2020.

[5] H. P. Li, Y. H. Hu, D. Z. Wang, and J. Xu, "Mechanism of interaction between cationic surfactant and kaolinite," *Journal of Central South University (Science and Technology)*, vol. 2, pp. 228–233, 2004.

[6] X. F. Cao, C. M. Liu, and Y. H. Hu, "Research on the flotation of kaolinite using a series of dodecyl tertiary amines," *Strategic Study of CAE*, vol. 13, no. 1, pp. 93–97, 2011.

[7] C.-m. Liu, A.-s. Feng, Z.-x. Guo, X.-f. Cao, and Y.-h. Hu, "Dynamics simulation of tertiary amines adsorbing on kaolinite (001) plane," *Transactions of Nonferrous Metals Society of China*, vol. 21, no. 8, pp. 1874–1879, 2011.

[8] Y. L. Zhou, Y. H. Wang, Y. H. Hu, D. X. Sun, and M. J. Yu, "Influence of metal ions on floatability of diaspore and kaolinite," *Journal of Central South University (Science and Technology)*, vol. 40, no. 2, pp. 268–274, 2009.

[9] H. Jiang, G. Y. Xiang, S. Ahmed Khoso, J. H. Xie, K. Huang, and L. H. Xu, "Comparative studies of quaternary ammonium salts on the aggregation and dispersion behavior of kaolinite and quartz," *Minerals*, vol. 9, no. 8, 2019.

[10] S. M. Zhao, D. Z. Wang, Y. H. Hu, J. Xu, and X. L. Zhao, "A series of aminoamides used for flotation of kaolinite," *Journal of University of Science and Technology Beijing (English Edition)*, vol. 3, pp. 208–212, 2005.

[11] M. Fan and X. Y. Wang, "The surface properties of kaolinite and flotation characteristics," *Modern Chemical Research*, vol. 9, no. 3, pp. 52–57, 2012.

[12] J. Guo, M. Li, Q. M. Fang, and Y. P. Hu, "The influence of particle size on separation of diaspore and kaolinite," *Multipurpose Utilization of Mineral Resources*, vol. 5, pp. 17–21, 2003.

[13] G. F. Zhang, Q. M. Feng, Y. P. Lu, and L. M. Ou, "Mechanism on diaspore and kaolinite collected by sodium oleate," *The Chinese Journal of Nonferrous Metals*, vol. 2, pp. 298–301, 2001.

[14] L. H. Xu, F. Q. Dong, H. Q. Wu, H. Jiang, Z. Wang, and J. H. Xiao, "Solution chemistry mechanism of sodium oleate on kaolinite," *Journal of wuhan university of thehnology*, vol. 34, no. 12, pp. 119–123, 2012.

[15] B. H. Hou and L. Y. Liu, "Effect of Ca2+ on kaolinite and quartz flotation at different pH values in the presence of

sodium oleate," *Journal of Coal Engineering*, vol. 52, no. 4, pp. 149–154, 2020.

[16] L. Xu, Y. Hu, F. Dong, Z. Gao, H. Wu, and Z. Wang, "Anisotropic adsorption of oleate on diaspore and kaolinite crystals: implications for their flotation separation," *Applied Surface Science*, vol. 321, pp. 331–338, 2014.

[17] L. H. Xu, H. Jiang, F. Q. Dong, H. Q. Wu, Z. Wang, and J. H. Xiao, "The effect of DTAC on flotation of kaolinite with different particle size," *Journal of China University of Mining & Technology*, vol. 42, no. 5, pp. 832–837, 2013.

[18] B. Liu, M. Dai, I. Ali et al., "Molecular insights on the influence of temperature and metal ions on the hydration of kaolinite (001) surface," *Molecular Simulation*, vol. 47, no. 12, pp. 1029–1036, 2021.

[19] T. Yue, W. Sun, and P. Chen, "Mechanism of reverse flotation desilication forbauxite by quaternary ammonium salt collector," *The Chinese Journal of Nonferrous Metals*, vol. 24, no. 11, pp. 2872–2878, 2014.

[20] P. Chen, W. Sun, and T. Yue, "Dynamics simulation of tributyltetradecylphosphonium chloride on kaolinite (001) plane," *Journal of China University of Mining & Technology*, vol. 43, no. 2, pp. 294–299, 2014.

[21] L. N. Guo, Z. H. Li, Z. L. Zhu, Y. L. Liu, and M. Q. Fan, "Study and dynamics simulation of cationic collecting performance on kaolinite," *China Mining Magazing*, vol. 26, no. 5, pp. 112–116, 2017.

[22] R. Wilson, P. H. J. Mercier, B. Patarachao, and A. Navarra, "Partial least squares regression of oil sands processing variables within discrete event simulation digital twin," *Minerals*, vol. 11, no. 7, p. 689, 2021.

[23] S. Bandera, C. O'Sullivana, P. Tangney, and S. Angioletti-Uberti, "Coarse-grained molecular dynamics simulations of clay compression," *Computers and Geotechnics*, vol. 138, Article ID 104333, 2021.

[24] M. Shishvan and J. Benndorf, "Operational decision support for material management in continuous mining systems: from simulation concept to practical full-scale implementations," *Minerals*, vol. 7, no. 7, p. 116, 2017.

[25] M. Kozielski, M. Sikora, and Ł. Wróbel, "DISESOR-decision support system for mining industry," in *Proceedings of the Federated Conference on Computer Science and Information Systems (FedCSIS)*, September 2015.

[26] Y. Zhang and C. Xiao, "Molecular dynamics simulation of clay hydration inhibition of deep shale," *Processes*, vol. 9, no. 6, p. 1069, 2021.

[27] L. A. Cisternas, F. A. Lucay, and Y. L. Botero, "Trends in modeling, design, and optimization of multiphase systems in minerals processing," *Minerals*, vol. 10, no. 1, p. 22, 2020.

[28] X. Lyu, X. You, M. He et al., "Adsorption and molecular dynamics simulations of nonionic surfactant on the low rank coal surface," *Fuel*, vol. 211, pp. 529–534, 2018.

[29] M. Yuan, W. Nie, H. Yu et al., "Experimental and molecular dynamics simulation study of the effect of different surfactants on the wettability of low-rank coal," *Journal of Environmental Chemical Engineering*, vol. 9, no. 5, Article ID 105986, 2021.

[30] C. Qi, H. Manzano, D. Spagnoli, Q. Chen, and A. Fourie, "Initial hydration process of calcium silicates in Portland cement: a comprehensive comparison from molecular dynamics simulations," *Cement and Concrete Research*, vol. 149, Article ID 106576, 2021.

Hindawi
Scientific Programming
Volume 2022, Article ID 9959153, 9 pages
https://doi.org/10.1155/2022/9959153

Research Article

3D Face Geometry Optimization Using Artificial Intelligence and Computer Graphics

Dan Liu

College of Art, Wuhan Business University, Wuhan, Hubei 430022, China

Correspondence should be addressed to Dan Liu; 20150560@wbu.edu.cn

Received 30 January 2022; Revised 25 February 2022; Accepted 28 February 2022; Published 22 March 2022

Academic Editor: Muhammad Zakarya

Human face plays an indispensable role in emotional expression and information exchange, which attracts large number of researchers to study face recognition. Nowadays, with the rapid development of computer graphics, artificial intelligence, and other technologies, the ability of the human vision system to recognize facial expressions and facial organs is enhanced. More and more experts think about how to make the computer vision system have this capability. By combining artificial intelligence and computer graphics, this paper studies how to optimize the 3D face network model and extract geometric features for 3D face recognition. We propose a 3D face network model based on Poisson equation to realize face hole recognition and boundary preprocessing. Besides, we also establish the 3D face surface equation and equal face value extraction and enhance the face feature based on facial semantic information. We study the hole repair of 3D face model based on Poisson equation integrating semantic information and achieve the purpose of optimizing the 3D face model. After the optimization, the method is compared with mesh repair and Poisson repair, which demonstrates that our Poisson-based 3D face hole repairing model obtains the best results among compared methods.

1. Introduction

In recent years, the research focus is to reconstruct realistic 3D face models. With the rapid development of artificial intelligence and computer graphics, 3D face models have been widely used in various fields, such as human-computer interaction, remote conference, multimedia communication, and virtual movie roles. In the field of computer graphics, data processing and geometric optimization of 3D face model have also become hot research issues. In the field of artificial intelligence, face recognition technology is also gradually developing to the field of 3D face application. The real 3D face image data are collected and reconstructed through the high-precision 3D face camera [1], and a 3D face model similar to the real one is obtained. However, the collected three-dimensional information often lacks measurement data, resulting in the lack of holes in the reconstructed three-dimensional model, which cannot be applied in practice. Therefore, artificial intelligence and computer graphics should be used to optimize the 3D face geometric model.

Through combining artificial intelligence and computer graphics, this paper studies how to optimize the 3D face network model and extract geometric features for 3D face recognition. In essence, we propose a 3D face network model based on Poisson equation to realize face hole recognition and boundary preprocessing. Besides, we also establish the 3D face surface equation and equal face value extraction and enhance the face feature based on facial semantic information. We study the hole repair of 3D face model based on Poisson equation integrating semantic information and achieve the purpose of optimizing the 3D face model. The major innovations of the research conducted in this paper are as follows:

(1) We use the artificial intelligence technology and 3D scanner to establish 3D face projection map; the face feature point detection and face detection are conducted on 2D image based on the convolution neural network. We extract face features to formulate the conformal mapping two-dimensional feature map based on the face model co-mapping algorithm; the method introduces multiple geometry feature fusion approach to analyze various 3D face feature information and conducts feature fusion by feature concatenation and weighted overlay.

(2) We fuse the face semantic information with Poisson equation to optimize the 3D face network. For the hole problems in the model, the hole detection is implemented, and the edge hole boundary network is marked. The Poisson surface is established based on the principle of Poisson equation, and the feature of Poisson algorithm is enhanced by using face semantic information to achieve the purpose of repairing the 3D face model. The holes in the 3D face network model are repaired based on Poisson equation.

The rest of the paper is organized as follows. In Section 2, we offer an overview of the related work. Section 3 is about 3D face recognition based on geometric features. In Section 3 face mesh model optimization based on Poisson equation is discussed. Analysis of experimental results of 3D face geometry optimization methods is explained in Section 5. Moreover, experimental details are also presented. Finally, Section 6 concludes this paper along with directions for future research.

2. Related Work

3D face recognition was proposed from the late 1980s to the early 1990s [2]. In this period, the three-dimensional data acquisition equipment was backward and the computing power of the processor was poor, so this research could not be fully carried out, and the number of selected datasets was small, which could not be applied in practice. Nowadays, with the rapid development of computer technology, various advanced storage devices and 3D data acquisition devices have been developed to promote the rapid development of 3D image face recognition technology. In the twenty-first century, experts at home and abroad have focused on 3D face recognition technology. Zulkifli et al. [3] studied the thinking mode of face feature and proposed an extraction method based on characteristic head and face features. Its essence is to represent frontal face with a 3D space function and then locate it on a 2D plane to estimate the function parameters by projecting the shape function into a 2D gray image, making full use of the prior knowledge of face structure to effectively deal with many problems in the process of shape restoration by projection. [4] proposed a novel face imaging model which is based on the gray plane method. In detail, this model can establish a deformable 3D mesh surface, which transforms the face matching problem into an elastic matching problem between changeable surfaces. At the same time, through the surface deformation which can be completed by the finite element analysis method, we can judge if the identities of different people in the image are the same based on the actual deformation situation.

[5] proposed a multi-pose face recognition method under different lighting conditions based on a three-dimensional deformation model. The remarkable feature of this method is to use the three-dimensional information of face to recognize the face and better deal with the impact of changing lighting and face pose on the recognition accuracy in face recognition. This method is a synthetic analysis technology. Based on three-dimensional face texture statistics and face shape deformation model [6], the camera model and illumination model during image acquisition are established by using graphics simulation, so that the characteristics of face shape and texture are completely separated from various external parameters, which refer to illumination, camera configuration, etc. This can improve the accuracy of face recognition. Eun et al. [7] used cylinders to represent the three-dimensional head and used projection photography to evaluate the head posture. Hua et al. [8] combined expectation maximization algorithm, AAM algorithm, and 3dmm algorithm to predict the pose of a single face image.

3. 3D Face Recognition Based on Geometric Features

3.1. Principles and Characteristics of Face Modeling. The three-dimensional scanner [9] is a high-precision instrument in the optical field. Its principle is to obtain the three-dimensional coordinates of the human face by using the triangulation method, emit light through the laser, pass through the parallel equidistant straight line to form an amplitude grating, and form a linear interference fringe to map to the human face. The fringe is deformed due to the change of the depth and curvature of the object surface. The deformed fringe image can be captured by the CCD camera [10], and the laser beam CCD and the laser beam emission angle can be combined to form an internal imaging device, and the position coordinates or distance data of the detected point can be obtained based on the triangular geometric relationship. The center point of CCD camera lens is the origin of measurement coordinate system. The imaging point of the face to be measured is represented by (x, y, z), f represents the focal length of the camera, B represents the distance between the camera and the laser projection center, and *?* represents the angle between the center of the light source and the monitored point forming a straight line and the x-axis. Based on the 3D face scanner, the face projection in Figure 1 is constructed.

The system parameters in the figure above are b, f, and θbased on the camera calibration technology; u and V represent the pixel coordinates on the CCD camera, and the following relationship exists on the XOZ plane:

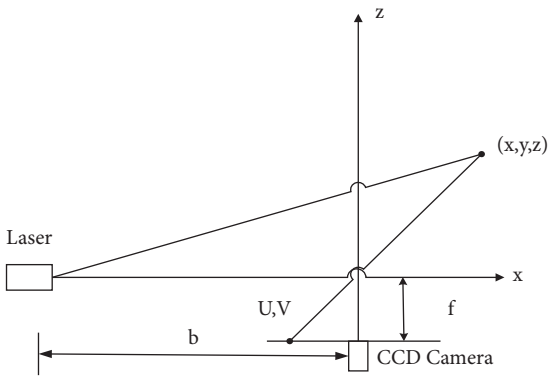

Figure 1: The projection of 3D scanner.

$$\frac{f}{u} = \frac{z}{x},$$
$$\frac{b+x}{z} = \cos\theta. \tag{1}$$

The YOZ plane has the following relationships:

$$\frac{f}{v} = \frac{z}{y},$$
$$\frac{x}{y} = \frac{u}{v}. \tag{2}$$

The three-dimensional coordinates of the following measured points (x, y, z) can be obtained:

$$[x, y, z] = \frac{b}{f\cos\theta - u}[u, v, f]. \tag{3}$$

3.2. Face Model Co-Mapping Algorithm. In the mapping process, the conformal mapping algorithm converts the Gaussian curvature angles of different points of the 3D face point cloud into the adjacent triangular mesh measurement [11]. Firstly, define the internal angle at the fixed point V_i as f_{ijk}. Define the side length of the triangular mesh of the center of two circles in the circle packing as the inversion distance Iij; Ki represents the Gaussian curvature of the fixed point position.

By carefully observing the facial features, the highest point in the face model is the nose position, and a three-dimensional spatial coordinate system is constructed. The nose coordinate is represented by the maximum value on the Z axis. If P is the tip of the nose, the starting point selected in the solution process based on Ricci flow algorithm is p, and the 3D face cloud model is mapped into a 2D face image. Figure 2 shows the face model co-mapping algorithm process [12].

(1) The initial Riemannian metric radius of all orders on the 3D model is calculated based on the initial triangular mesh edge length. The following is the calculation formula:

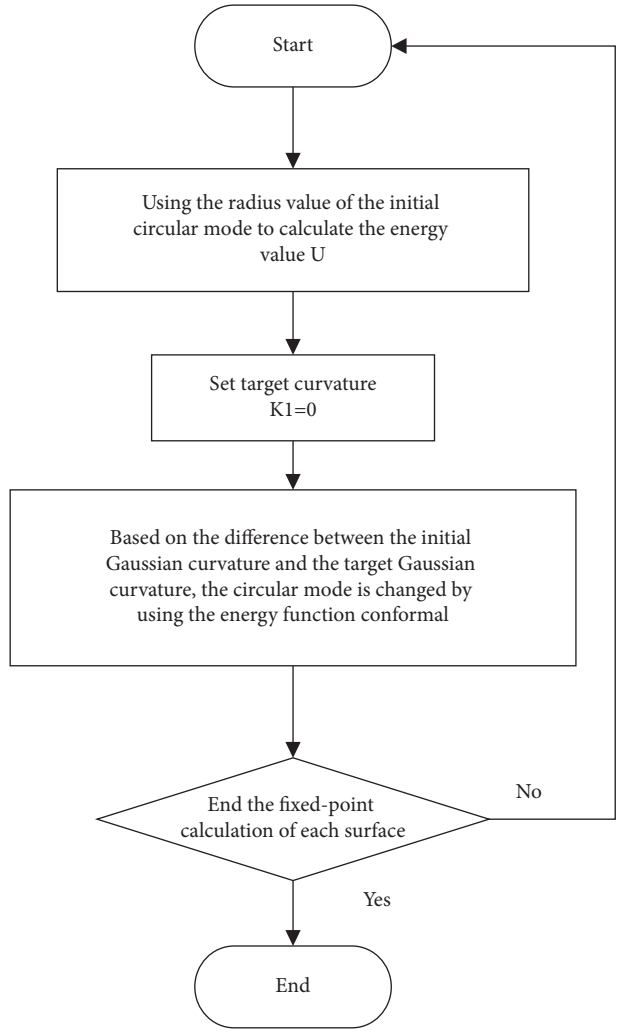

Figure 2: The face model co-mapping algorithm flow.

$$r_i^{jk} = \frac{I_{ji} + I_{ik} - I_{jk}}{2}. \tag{4}$$

After calculation, the radius of the fixed point Vi position is $r_i = \min r_i^{jk}$.

(2)Using the triangular mesh edge length and the initial circular pattern radius, the inversion distance of all edges is obtained by cosine theorem. The conformal mapping algorithm only changes the circular pattern radius, but the inversion distance does not change.

$$I\left(C_i, C_j\right) = \frac{I_{ij}^2 - r_i^2 - r_j^2}{2r_i r_j}. \tag{5}$$

(2)Calculate all internal angles in the grid, and the formula is as follows:

$$\theta_k^{ij} = \cos^{-1}\frac{I_{jk}^2 + I_{ki}^2 - I_{ij}^2}{2I_{jk}I_{ki}}. \tag{6}$$

(3)Calculate the discrete Gaussian curvature Ki of all vertices, and its formula is as follows:

$$Ki = \left\{ \begin{array}{l} 2\pi - \sum f_{i,j,k\epsilon} F^{\theta_i{}^{jk}}, \sum v_i \notin \vartheta \\ \pi - \sum f_{i,j,k\epsilon} F^{\theta_i{}^{jk}}, \sum v_i \notin \vartheta \end{array} \right\}. \tag{7}$$

(4)The initial energy is defined according to the initial circle radius defined by each vertex, which is calculated by the following formula:

$$u_i = \log r_i. \tag{8}$$

(5)Define the Gaussian curvature of all points on the surface as K′, define the target Gaussian curvature as O, and adjust the energy value on each point according to the difference between the target curvature and the initial Gaussian curvature to adjust the circle radius. The calculation formula is as follows:

$$u_i' = u_i + (K' - K). \tag{9}$$

(6)Based on the radius between the new circle mode and the adjacent circle mode and the reverse distance of the edge where the two points are located, the edge length of the triangular mesh is calculated, and the following is the calculation formula:

$$I_{ij} = r_i^2 + r_j^2 + 2I_{ij} r_i r_j. \tag{10}$$

This should be noted that after traversing all the points in the 3D model, the conformal plane metric of the triangular network in the original 3D face model can be obtained. Based on the corresponding concerns in the triangular mesh of the original 3D model, the plane metric can be rearranged in the 2D plane disk to obtain the conformal mapping 2D feature map.

3.3. Multiple Geometric Feature Fusion Algorithms. The recognition ability of different face features is also different, and the role of face recognition is also different. There is less information in a single feature and strong information limitations. By fusing a variety of feature information and comprehensively analyzing [13] various feature data, the original data can be retained to the greatest extent. Based on the in-depth analysis of various features, this paper proposes a face recognition algorithm integrating a variety of different features. Because different channels express different information in different ways and there are differences in the amount of information, each channel should be normalized and the weight should be evenly distributed to each channel.

In terms of fusion, the most widely used methods are weighted superposition and feature concatenation [14]. After feature concatenation, it has a high feature vector dimension. Here, the following weighted superposition methods are used to realize multivariate feature fusion:

$$E(u) = \sum_{i=1}^{N} \omega_i \, E(u_i), \tag{11}$$

where ωi is the role of different types of recognition features in recognition devices.

4. 3D Face Mesh Model Optimization Based on Poisson Equation

4.1. Poisson Equation. Poisson equation [15] belongs to partial differential equation. Poisson surface is reconstructed by combining implicit fitting, local features, and global features, Poisson equation is calculated, a three-dimensional model is established to represent the hidden layer surface, and the surface model with geometric entity information is obtained by equivalent extraction. Combined with Poisson equation reconstruction method, it can better deal with the surface smoothness and surface detail features on the closed feature model [16].

When dealing with the scaling function $V : R^3 \longrightarrow R^3$, this method is realized by using the specified vector domain $V : R^3 \longrightarrow R^3$. On a certain basis of the solid model δM, the solid surface is represented by $\min_x \|\nabla x - \overrightarrow{V}\|$, and the gradient of the scaling function makes it infinitely close to the composition of the vector domain. The minimum value of the scaling function is calculated as follows:

$$E(x) = \int \|\nabla x(p) - \overrightarrow{V}(p)\|^2 \mathrm{d}p. \tag{12}$$

Since the vector field v cannot be integrated directly, it is necessary to convert the problem into the problem of calculating Poisson equation, and the following divergence operator formula is introduced:

$$\Delta x = \nabla \cdot \nabla x = \nabla \cdot V. \tag{13}$$

4.2. 3D Face Mesh Hole Repair Based on Poisson Equation. Figure 3 shows the flowchart of 3D face mesh hole repair algorithm based on Poisson equation.

4.2.1. Hole Identification and Boundary Pretreatment. The closed ring formed by the head and tail connecting boundary is a hole. As evident from the state of the art, different types of holes have boundary structures with high similarity. The shape of the hole can be obtained by identifying the boundary edge. In a complete triangular mesh structure, each edge has two corresponding triangular patches. The hole boundary is a triangular network, and any edge in the triangular network belongs to only one triangular network. Based on this property, different hole regions can be identified. As shown in Figure 4, the hole area is a blank position. The information of the original point set of the hole boundary is relatively sparse. During the reconstruction, the hole boundary will produce long and narrow triangular patches that are inconsistent with the properties of Delaunay triangle [17,18]. To further refine the triangular patches of the hole boundary area, we

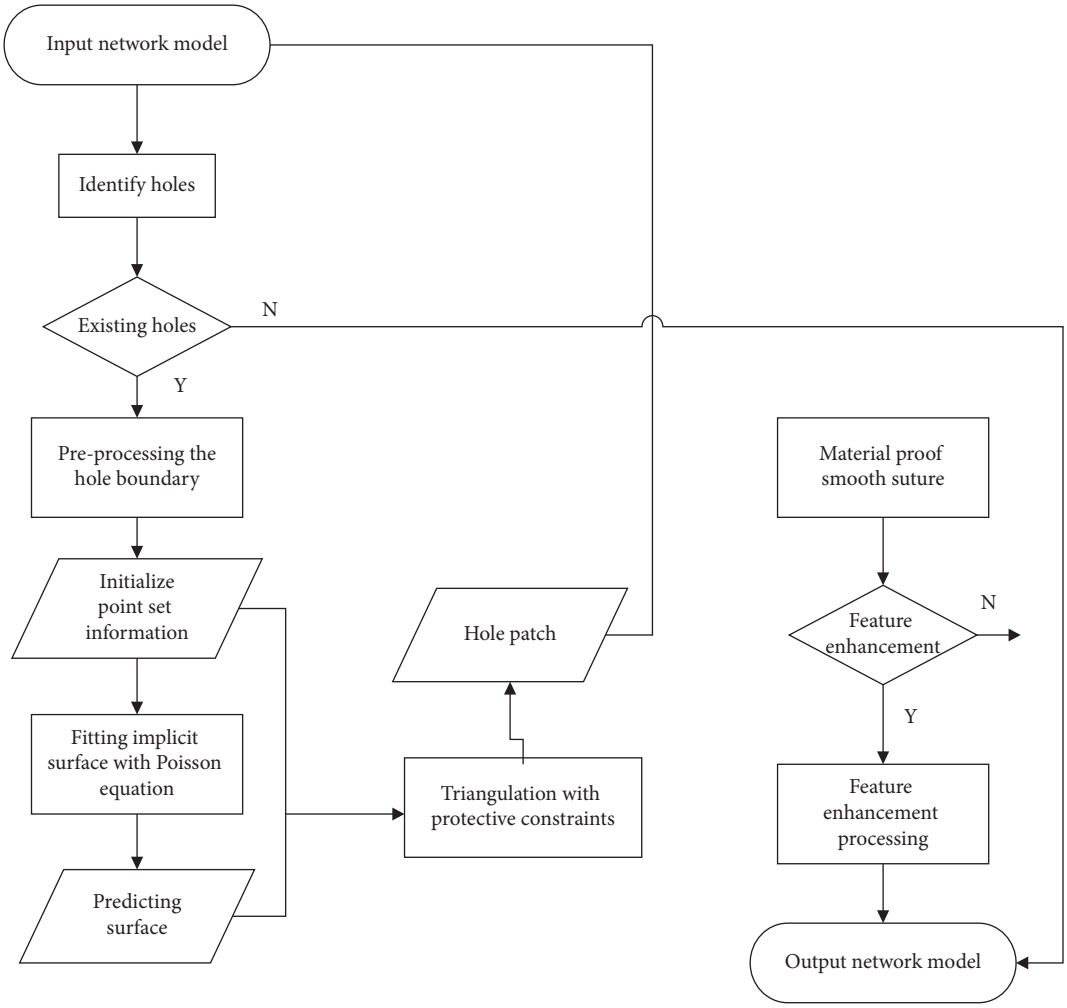

Figure 3: The flowchart of 3D face mesh hole repair algorithm based on Poisson equation.

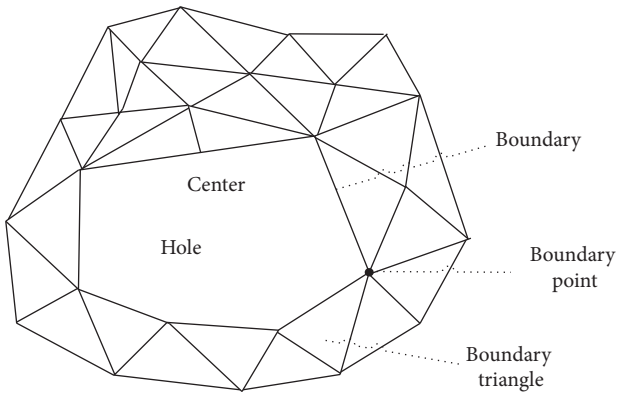

Figure 4: Concepts and boundary pretreatment of triangular mesh holes.

can make full use of the hole boundary area data and the stitching process to provide a better interface and enhance the transition effect [19].

4.2.2. Establishing Surface Equation. The algorithm runs based on the network model vertex information and the original point cloud information and obtains the network model vertex information according to the topology. A three-dimensional surface represents the changes in the surface at different locations, i e., constants. The normal vector in the point on the surface of the model is the same as the gradient of the function [20]. If M represents the input network model, all directed point sets C □ m {C1, C2,. . ., CN} of M in R^3 space are obtained, and Nci is the internal normal vector of directed point Ci. The vector field of this

point set is represented by V, and the x implicit three-dimensional surface equation is obtained by fitting the point vector set. By converting this problem into $\min\|\nabla x - V\|$, the surface equation can be closer to the vector domain. This problem is converted into a Poisson equation problem, as follows:

$$\Delta x = \nabla \cdot \nabla x = \nabla \cdot V. \tag{14}$$

The octree segmentation algorithm is introduced into the segmentation space in this algorithm to solve the discretization problem. Then, the 3D surface vector field uses the small surface patch information and area obtained by 3D surface segmentation, which is calculated by the following formula:

$$\nabla (xM \times F)(q) = \sum_{c \in C} \int Fp(q) N_M(P) \mathrm{d}p. \tag{15}$$

In the above formula, the offset between q and p is represented by Fp (q) = F(q-p), C is the set of input points, so as to establish octree O, and the sample points are saved in the leaf node. Define Fo at node o:

$$F_\circ(q) = F\left(\frac{q - m_\circ}{\omega_\circ}\right)\frac{1}{\omega_\circ^3}. \tag{16}$$

The node closest to the eight positions of node C is represented by NgbrD (c), ωo, c is the weight of all interpolation points, and then the three-dimensional surface vector domain is approximately represented by the following:

$$V(q) = \sum_{c \in C} \sum_{\circ \in NgbrD^{(c)}} \omega_{\circ,c} F \circ (q) N_c. \tag{17}$$

4.2.3. Equal Face Value Withdrawal. After obtaining the most ideal fitting equation of X three-dimensional surface, we should extract the equation isosurface and further obtain the three-dimensional surface. If the point on the isosurface meets the requirements of function F(ci) = 0, F(ci) < 0, it indicates that the point is located in the surface, and if f (ci) > 0, it indicates that the point is located outside the surface. In this paper, MC (marching cubes) algorithm is used to extract the equivalent value, and the R threshold is set to ensure that the extracted equivalent surface is consistent with the original model surface, and the average value of each point is calculated, which can reduce$x$. Scaling affects the effect of extracting isosurfaces [21].

$$\begin{aligned} r &= \frac{1}{|C|}\sum_{c \in C} \overline{x}(c), \\ \partial M &= \left\{q \in R^3 | \overline{X}(q) = r\right\}. \end{aligned} \tag{18}$$

4.2.4. Hole Patch Generation and Stitching. Based on the above process, the prediction surface is obtained. In this algorithm, Delaunay triangulation is used to segment the surface with protection constraints to obtain the meshed prediction surface. Subdivide the hole area, and the hole indefinite M'can be obtained without refining the triangular mesh area. Strengthening the protection constraint is to reduce the quadratic angle triangulation triangular network model, which can save a lot of time and retain the original state of the network. Finally, the following hole patches are obtained by matching the predicted surface with the neighborhood triangle of the hole area. The protected areas are defined as

$$P = \left\{p \in R^3 : |\mathrm{dis}(M, p)| < r\right\}. \tag{19}$$

The distance between points m and P of the triangular network is represented by dis (m, P) and the threshold radius is represented by R. Assuming that the hole patch is the average triangular mesh side length, the known information can be stitched better by subdividing the hole patch, protecting the constrained triangular mesh, and reserving the interface at the boundary position. Figure 5 shows different situations of stitching.

4.2.5. Feature Enhancement. Based on the semantic information of face features [22], the feature vector p of 3D face region is obtained by multiplying the patch matrix vector of 3D feature region by the weight of hidden layer of face feature classification. According to the Poisson surface equation and isosurface extraction constructed above, the hole surface is obtained by Delaunay triangular section algorithm, and then the feature points near the hole are extracted to construct the feature point set. Combined with the above missing data and mixed feature model, the hole eigenvalue is improved [23]. If the hole is in the face feature area, assume that the complete part is S = (S1, S2,. . .,Sn)^T, and transform the feature point feature matrix to obtain S':

$$SxP = S'. \tag{20}$$

The triangular mesh patch is deformed and combined with Poisson equation with Dirichlet boundary conditions, as follows:

$$\begin{aligned} \Delta f &= divh, \\ f_{\partial\Omega} &= |f^*|_{\partial\Omega}, \end{aligned} \tag{21}$$

where F represents unknown scalar function, divh represents h divergence, and f* represents scalar function constrained by boundary conditions. Finally, seamlessly stitch the original model and feature enhancement hole patch to end the hole patch. Function expansion module is shown in Figure 6.

5. Analysis of Experimental Results of 3D Face Geometry Optimization

5.1. 3D Face Network Model Quality Evaluation System. Here, we need to detect holes first, so we design and develop a three-dimensional face network model quality detection system [24], which can obtain holes through boundary properties. There are many formats of 3D models. When designing algorithms, we should convert different formats and realize reading operation. By analyzing the data structure

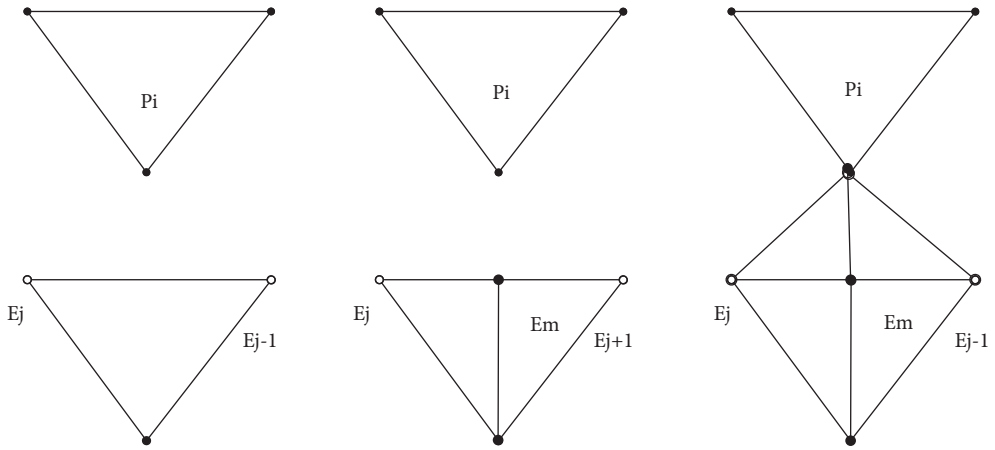

Figure 5: Different sutures.

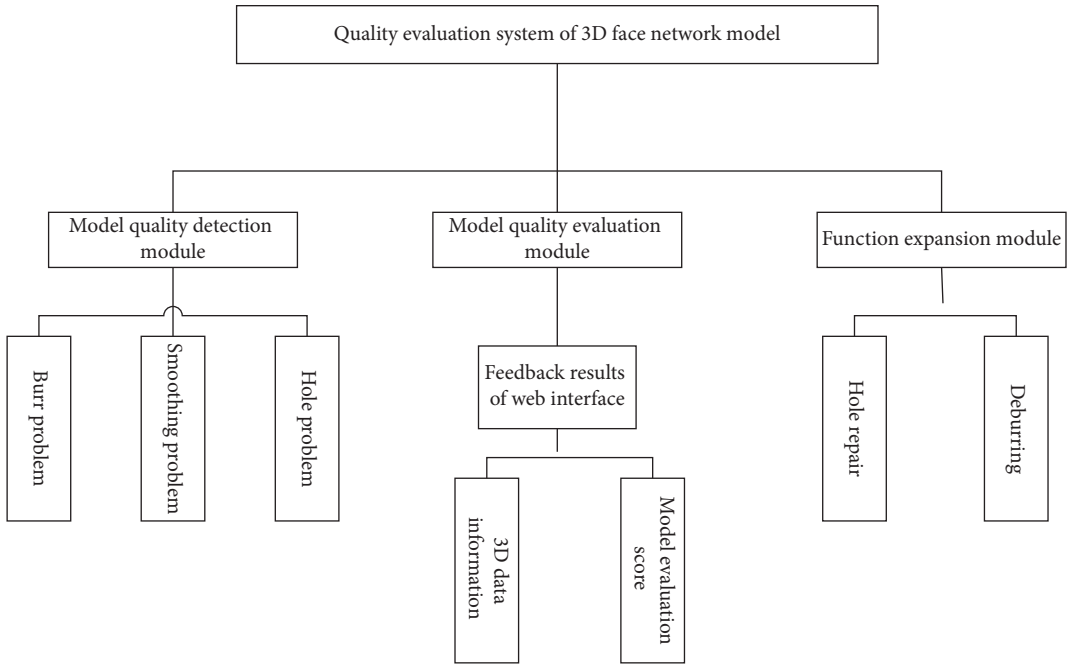

Figure 6: System function module diagram.

of the 3D face model, we can better process the model. Starting from the model properties existing in the reconstruction model, this paper designs the following three-dimensional face network model quality evaluation system.

The system reflects the quality model of 3D face model reconstruction. In the system, the detection module should analyze the number of holes, the smoothness of the model, and whether there are burrs on the model. Eventually the data are taken as the evaluation standard. When detecting the number of holes, it is necessary to read and analyze the data on the 3D face model to obtain the 3D point cloud information. It is convenient to distinguish triangular patches by using the inner and outer boundary extraction algorithms to obtain the corresponding number of holes.

The HTML page reflects the model quality evaluation module, displays the read three-dimensional information on the page, and evaluates the model score. The model quality evaluated in this way lacks integrity. It is necessary to expand the number of holes, form a specific evaluation criterion, and then formulate an accurate evaluation quality to optimize the frame page.

Function Expansion Module. This module is used for quality detection, which is conducive to promoting three-dimensional reconstruction and greatly improving data integrity. The extended function is related to the classification management of various quality models, such as repairing holes and removing debris information. In this paper, the quality evaluation framework of 3D face reconstruction is used to provide management basis for the construction of 3D face database.

5.2. Hole Repair Analysis of 3D Face Mesh Model Based on Poisson Equation. The original 3D face network model is

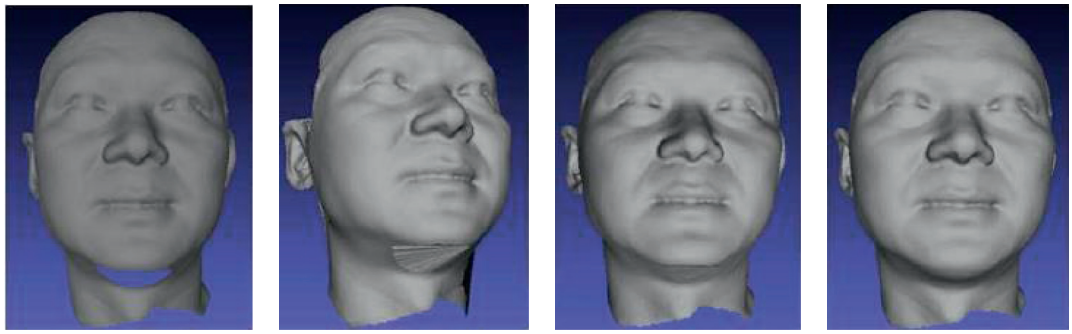

(a) (b) (c) (d)

Figure 7: Hole repair results of 3D face mesh model.

Table 1: Comparison of three hole repair methods of 3D face mesh model.

Model repairing method	Hole number	Unrepaired point number	Repaired point number	Unrepaired grid number	Repaired grid number	Time/ms
Mesh repairing	1	104029	105482	206132	206912	2691
Original Poisson	1	104029	106723	206132	210576	1972
Poison hole repairing	1	104029	104864	206132	207321	1436

compared, and the results of mesh hole repair by various methods are shown in Figure 7. As shown in the figure, the mesh repair method cannot completely retain the surface features on the mesh. Poisson equation adopted in this paper has the best effect and can significantly improve the surface smoothness of the hole model.

According to the above table, the number of original vertices of the network model is 104029 and the number of triangular meshes is 206132. After repair, the number of fixed points and meshes has changed significantly, and there is a certain difference in time consumption. Combined with the repair results in Figure 7 above and compared with the original Poisson repair method, this algorithm integrates the face semantic information and establishes a new feature enhancement algorithm based on Poisson equation to repair holes. When the number of networks and vertices meets the requirements, the repair effect is the best.

6. Conclusions and Future Work

In this paper, the 3D face model with high authenticity in the measured data is obtained by 3D reconstruction. However, the reconstructed model data are incomplete and have some defects. Therefore, the optimization and repair of the face model is very important in 3D face model and can also effectively improve the robustness and availability of the 3D face model. The traditional way uses geometric heuristic method to repair. Starting from the face features, this paper uses semantic information to greatly improve the repair quality of the 3D face model, and the repair model accuracy is also improved significantly. By combining artificial intelligence and computer graphics, this paper proposed a 3D face recognition system based on geometric features and used this algorithm to extract and segment the feature semantics of the 3D face model as an important basis for repairing the 3D face mesh. The feature enhancement of the 3D face network model based on Poisson equation is used to repair the holes, detect the 3D face holes, mark the boundary network, and clarify the location of the specific holes.

Using the principle of Poisson equation and isosurface extraction technology, combined with the face detection model, the hidden layer weight in the convolution neural network is extracted to obtain the feature vectors of different regions. The feature vector is introduced into the Poisson equation to enhance the surface fitting features, so as to realize the hole repair of the 3D face network model based on Poisson equation, which integrates the face semantics, and the 3D face network model is also significantly optimized. In the future, we will consider integrating machine learning-based methods to improve the system performance.

Data Availability

The data used to support the findings of this study are available from the corresponding author upon request.

Conflicts of Interest

The author declares that there are no conflicts of interest.

Acknowledgments

This study was supported by the Research on the innovation and reform of talent training mode under the background of "mass entrepreneurship and innovation"—Take the "art and design" major as an example (no. 2017107).

References

[1] P. Ekberg, B. Daemi, and L. Mattsson, "3D precision measurements of meter sized surfaces using low cost illumination

and camera techniques," *Measurement Science and Technology*, vol. 28, no. 4, Article ID 0454, 2017.

[2] S. Da, R. A. Gilderlane, and M. S. Jose, "Thé G A P Triaxial slicing for 3-D face recognition from adapted rotational invariants spatial moments and minimal keypoints dependence," *IEEE Robotics and Automation Letters*, vol. 1, 2018.

[3] N. N. Zulkifli, N. Halim, N. Yahaya, and H. Van Der Meijden, "Patterns of critical thinking processing in online reciprocal peer tutoring through facebook discussion," *IEEE Access*, vol. 16, no. 99, p. 1, 2020.

[4] C. Nastar and N. Ayache, "A physically based analysis of deformations in 3D images," in *Proceedings of the SPIE - The International Society for Optical Engineering*, San Diego, CA, USA, March 2011.

[5] V. Blanz, P. Gr Other, P. J. Phillips, and T. Vetter, "Face recognition based on frontal views generated from non-frontal images," in *Proceedings of the IEEE Conference Computer Vision Pattern Recognition*, vol. 2, pp. 454–461, San Diego, CA, USA, June 2005.

[6] Z. Kang, M. Sadeghi, and R. Horaud, "Face frontalization based on robustly fitting a deformable shape model to 3D landmarks," 2020, https://arxiv.org/abs/2010.13676.

[7] H. J. Eun, Y. M. Seo, and Y. G. Park, "Effect of a two cylinder vertical location on the three-Dimensional natural convection between a parallel channel," *Transactions of the Korean Society of Mechanical*, vol. 38, 2018.

[8] J. Hua, T. Hao, and L. Zeng, "An improved estimation algorithm of space targets pose based on multi-modal feature fusion," *Mathematics*, vol. 9, 2021.

[9] P. Knoops, C. Beaumont, A. Borghi et al., "Comparison of three-dimensional scanner systems for craniomaxillo facial imaging," *Journal of Plastic, Reconstructive & Aesthetic Surgery*, vol. 70, no. 4, pp. 441–449, 2017.

[10] D. Wang, D. Xu, Z. Tao, and H. Kuang, "A fast auto-focusing technique for the long focal lens TDI CCD camera in remote sensing applications," *Optics & Laser Technology*, vol. 45, 2013.

[11] L. Kuang and M. Chang, "3D model deformation algorithm for quasi-conformal mapping," *China Science paper*, vol. 24, 2021.

[12] S. Y. Dong, "Surface matching algorithm based on hyperbolic ricci flow," *Computer Applications and Software*, vol. 62, 2015.

[13] M. Abouhawwash, "Sentimental analysis of COVID-19 related messages in social networks by involving an N-gram stacked auto encoder integrated in an ensemble learning scheme," *Sensors*, vol. 21, 2021.

[14] A. Baykasolu, F. B. Ozsoydan, and M. E. Senol, "Weighted superposition attraction algorithm for binary optimization problems," 2020.

[15] J. Q. Jin and W. W. Yang, "Convolution pyramids based rapid screened Poisson equation solver," *Journal of Computer-Aided Design & Computer Graphics*, vol. 32, no. 8, 2020.

[16] A. Nüchter, "Dynamic point cloud compression based on projections, surface reconstruction and video compression," *Sensors*, vol. 22, 2021.

[17] Q. L. Yuan and X. Q. Wu, "3D surfaces reconstruction algorithm via detaching Delaunay triangular mesh and search-ball approach," *Journal of Graphics*, vol. 39, 2018.

[18] Y. Zhu, L. Xun, Z. Claudia, L.-G. Carlos, and A. Gustavo, "Feature extraction and matching of 3D face model based on facial landmark detection," in *Proceedings of the 2020 International Conference on Virtual Reality and Visualization (ICVRV). IEEE*, Recife, Brazil, November 2020.

[19] B. Gecer, P. Stylianos, K. Irene, and Z. Stefanos, "Ganfit: generative adversarial network fitting for high fidelity 3d face reconstruction," in *Proceedings of the IEEE/CVF conference on computer vision and pattern recognition*, 2019.

[20] H. E. Hua, L. I. Zongchun, and Y. Rongxin, "On the consistent normal vector adjustment of point cloud using surface variation," *Acta Geodaetica et Cartographica Sinica*, vol. 48, 2018.

[21] E. Richardson, M. Sela, and R. Kimmel, "3D face reconstruction by learning from synthetic data," in *Proceedings of the 2016 4th International Conference On 3d Vision (3DV). IEEE*, Stanford, CA, USA, October 2016.

[22] Z. W. Bai and T. T. Yi, "Face image inpainting method based on multi-scale feature fusion," *Computer Engineering*, vol. 47, no. 5, 2021.

[23] L. Tang, S. Zheng, and Z. Zhou, "Estimation and inference of combining quantile and least-square regressions with missing data," *Journal of the Korean Surgical Society*, vol. 57, Article ID S1226319217300637, 2017.

[24] S. Zhang, D. Zhou, and Z. Qiang, "A method of data registration for 3D point clouds combining with motion capture technologies," in *Proceedings of the Asian Conference on Intelligent Information and Database Systems*, March 2016.

Hindawi
Scientific Programming
Volume 2022, Article ID 5761363, 10 pages
https://doi.org/10.1155/2022/5761363

Research Article

Evaluation of Women's Entrepreneurship Education Based on BP Neural Network

Xi Zhao,[1,2] Chunyi Lin,[3] Shuangguo Wang,[4] and Henan Zhao[5]

[1]*Business School, Qingdao University, Qingdao, Shandong 266071, China*
[2]*School of Economics and Management, Hefei University, Hefei, Anhui 230601, China*
[3]*School of Humanities, Fujian University of Technology, Fuzhou, Fujian 350118, China*
[4]*School of Business, East China University of Science and Technology, Shanghai 200237, China*
[5]*School of Foreign Languages, Hefei University, Hefei, Anhui 230601, China*

Correspondence should be addressed to Chunyi Lin; chunyilin@fjut.edu.cn

Received 12 February 2022; Revised 27 February 2022; Accepted 2 March 2022; Published 21 March 2022

Academic Editor: Muhammad Zakarya

Entrepreneurship education is the key to cultivating the entrepreneurial spirit of national talents. The goal of entrepreneurship education is to cultivate a large number of pioneering talents, and women's entrepreneurship education is particularly important. The government, enterprises, schools, and all sectors of society start from multiple channels to let students strengthen their entrepreneurial awareness and improve their entrepreneurial ability. This paper uses the most advanced BP neural network algorithm to study and evaluate women's entrepreneurship education. This paper briefly introduces the concept and model of the artificial neural network and establishes a BP neural network model while improving the classical BP neural network. Then, we list the application process of the BP neural network model in evaluating women's entrepreneurship education. We select college students for empirical analysis, determine the number of neurons, and select 9 items as the evaluation index of women's entrepreneurship education. Using valid assumptions, we further determine the model learning rate and momentum factor. Finally, the results show that the actual evaluation results based on the BP neural network are basically the same as the expected results, and the maximum relative error between the actual value and the expected value is approximately 1.64 %, and the comprehensive evaluation value is 92 points. The proposed algorithm can effectively avoid the problems of instability and slow convergence of the traditional model and can comprehensively improve the accuracy of the evaluation results of women's entrepreneurship education.

1. Introduction

The quality of entrepreneurship education is directly related to the effect of national basic education, and women's entrepreneurship education is directly related to the future development of the country. Recently, entrepreneurship education has attracted extensive attention from all walks of life in academia and industries [1]. In the context of artificial intelligence, the BP neural network is a multilayer feedforward neural network in artificial neural network. Based on the gradient descent method, using the network output error, it can adjust and modify the network connection weight and reduce the error modulation. The research on the evaluation of women's entrepreneurship education is mainly subjective and theoretical, therefore lacking a certain programmatic evaluation design. Furthermore, most of them adopt a centralized mode, guarantee system, and evaluation system and have not studied a complete evaluation system for the women's entrepreneurship education. The goal of entrepreneurship education is to cultivate a large number of pioneering talents, and women's entrepreneurship education is particularly important.

In this paper, the BP neural network algorithm is used to solve this problem. The establishment of a BP neural network model can improve the accuracy of the evaluation results of women's entrepreneurship education. The results

obtained have certain advantages for colleges and universities in formulating teaching strategies and adjusting teaching directions. It can also help colleges and universities focus on students' entrepreneurship education and strengthen women's entrepreneurship education in China, comprehensively improving the ability and level of women's entrepreneurship education. In this paper, we briefly introduce the concept and model of the artificial neural network and establish a BP neural network model while improving the traditional BP neural network. We then describe the application process of the BP neural network model in evaluating women's entrepreneurship education. This paper uses the improved BP neural network model to evaluate women's entrepreneurship education, which can effectively avoid the problems of instability and slow convergence of the traditional model and can comprehensively improve the accuracy of the evaluation results of women's entrepreneurship education. The major innovations of the research conducted in this paper, in terms of women's entrepreneurship education, can be summarized as follows:

(i) We describe the concept, topology, and network structure of the BP neural network in detail, so that we can accurately grasp the structure of the BP neural network.

(ii) We build a BP neural network model, evaluate women's entrepreneurship education based on the model, and select 9 items as the evaluation indicators of women's entrepreneurship education.

(iii) The indicators involve colleges and universities, society, the government, and women entrepreneurs themselves, covering all aspects, which can more accurately grasp the role of all aspects in women's entrepreneurship education and help to accurately analyze the evaluation results of women's entrepreneurship education.

The rest of the paper is organized as follows: in Section 2, we offer an overview of the related work. Section 3 is about the BP neural network based model. Section 4 illustrates the valuation of women's entrepreneurship education based on the BP neural network. Section 5 describes the empirical analysis of women's entrepreneurship education evaluations based on the BP neural network. Moreover, experimental details are also presented. In Section 4, results are discussed. Finally, Section 6 concludes this paper and offers several directions for further research and investigation.

2. Related Work

The evaluation of innovation education has become an important index for cultivating college talents in various countries, and the accuracy of the evaluation results has attracted attention in various fields. With the rapid development of the BP neural network algorithm, more and more people have begun to use the BP neural network in the evaluation of entrepreneurship education. Mars and Hoskinson pointed out that the evaluation of entrepreneurship education should abandon the traditional "rote learning" content, judge students' thinking ability and reaction ability at a deeper level, and analyze and judge students' entrepreneurship ability through case analysis and formulating business plans [2]. Maritz et al. proposed that the evaluation of entrepreneurship education is the core of education evaluation, and the level of graduate entrepreneurship education can be evaluated according to the GIM plan. The evaluation indicators mainly include innovation intention, personal behavior, skill return, and knowledgeability [3]. Ota et al. described in detail the education evaluation system adopted by Indian entrepreneurship, and proposed that Indian business schools take entrepreneurship as a basic course in business education, which involves joint entrepreneurship, self-entrepreneurship, and internal entrepreneurship. The knowledge of the system is conducive to knowledge creation [4].

Matlay et al. established a complete evaluation system of entrepreneurship education practice, and proposed that the United States and the United Kingdom have a small distance in entrepreneurship education. Compared with postgraduates and undergraduates, they focus on the cultivation and practice of entrepreneurship education ability in the postgraduate learning stage [5]. Papadopoulos et al. formulated ten teaching cases according to the database syllabus of seven universities established in Denmark and constructed the evaluation model of entrepreneurship education by analyzing the cases. The main forms are formative evaluation, summative evaluation, and learner-centered evaluation [6]. Fan et al. and others designed the evaluation indicators of entrepreneurship education at the undergraduate stage of colleges and universities, and the selected indicators mainly include ability level, incentive support, ability level, allocation of teachers, and resource allocation [7]. Tang and Liu and others pointed out that through background evaluation to judge entrepreneurial resources, the environment, needs, and opportunities, input evaluation as the basic demand condition, and the evaluation process is the implementation process of supervision, inspection, and feedback. Achievement evaluation is used to evaluate the results achieved, in particular, including acceptance, subject satisfaction, and so on [8]. Wang and Tian classified entrepreneurship evaluation into two dimensions: (i) subjective evaluation and (ii) objective evaluation. The subjective evaluation indicators include the innovation ability and innovation demand. The objective indicators include education process, education input, and education output. Based on these two indicators, the evaluation validity and reliability are guaranteed to be in balance [9]. Based on the CIPP model, Guan and Sun formulated 11 primary indicators and 22 secondary indicators based on input resources, entrepreneurial environment, and achievement performance, and the primary indicators and secondary indicators are input into the model to judge the achievement of entrepreneurship education [10].

3. BP Neural Network-Based Model

3.1. Artificial Neuron Model. The concept of an artificial neural network (ANN) is to regard the biological simulation process as the basic feature, and the computing structure

reflecting the local characteristics of the human brain is an artificial neural network. u_i represents the output result of a combined input signal, v_i represents the local sensing area of a neuron, x_i represents the input signal of neuron i, and W_{ij} represents the synaptic strength [11, 12].

$$u_i = \sum_j w_{ij} x_j. \tag{1}$$

In the above formula, y_i represents the output value of neuron i and $f(.)$ represents the excitation function. Because there are many types of functions, the following are common functions:

$$y_i = \left(\sum_i w_{ij} x_j + b_j \right). \tag{2}$$

3.1.1. Threshold Function. The threshold function judges the neuron state according to the neuron output result. If the neuron output result is 1, it indicates that the neuron is excited, and if it is 0, it indicates that the neuron is inhibited.

$$\begin{aligned} f(v) &= \begin{cases} 1, & \text{if} \quad v \geq 0, \\ 0, & \text{if} \quad v < 0, \end{cases} \\ f(v) &= \begin{cases} 1, & \text{if} \quad v_i \geq 0, \\ -1, & \text{if} \quad v_i < 0. \end{cases} \end{aligned} \tag{3}$$

3.1.2. Piecewise Linear Function. The piecewise linear function is defined as follows:

$$f(v) = \begin{cases} 1, & \text{if} \quad v_i \geq +1, \\ v, & \text{if } v_i + 1 > -1, \\ -1, & \text{if} \quad v_i \leq -1. \end{cases} \tag{4}$$

3.1.3. Sigmoid Function. There are many differences between the sigmoid function and other functions. The sigmoid function [13] can also be called an S-type function, which is a widely used excitation function. The following is the basic formula:

$$f(v) = \frac{1}{1 + \exp(-av)}. \tag{5}$$

3.2. Introduction to Artificial Neural Network. An Artificial neural network belongs to a modular adaptive nonlinear dynamic system, and its components include multiple neurons [14]. The system has strong adaptability and autonomous learning ability and shows the characteristics of nonlimitation and nonlinearity. Based on the achievements of the modern neural field, an artificial neural network is proposed. The principle is to simulate the processing mode of a brain neural network. Based on different information memory modes, a new machine is designed, which is similar to the human brain and can automatically process all kinds of information. The basic processing unit of an artificial neural network is the neuron, and the neuron structure is shown in Figure 1 below [15].

Figure 1 shows that x_i represents the input signal, W_{ij} is the weight of the connecting neuron between the i and the j, θ_j represents the threshold value of the j neuron, s represents the set external input signal, and y_j represents the output signal. Based on this model, the following represents the transformation of the j neuron:

$$y_j = f\left(\sum_i w_{ij} x_i - \theta_j + S_j \right). \tag{6}$$

As a multilayer feedforward neural network, the BP neural network has a strong nonlinear mapping ability. Each layer of the neural network model is only connected to adjacent neurons and has no relationship with internal neurons. The components of neurons include the hidden layer, input layer, and output layer. In a typical BP neural network learning algorithm, the objective function is the sum of squares of network errors, and the minimum value of the objective function is calculated through the gradient algorithm. The principle is error correction. The gradient descent method is used to output the error from the network, realize backpropagation, modify and adjust the network connection weight, and reduce the error modulation to the minimum, and the neural network learning process is listed in Figure 2.

3.3. Artificial Neural Network Model. Artificial neural network model has a remarkable feature of diversity. Based on the principle of model classification, it adopts a variety of ways to summarize the types of models. Firstly, it is the network topology type [16], connecting various neurons to generate different network topologies, and then further divided into hierarchical structures. The structure is readjusted according to the hierarchy. The interconnection structure is characterized by connecting each layer. The second is the network information flow type, while the feedforward network transmits information in the order from front to back, while the feedback network transmits information in the direction from back to front, which is shown in Figure 3.

3.4. BP Neural Network Model. In 1986, Rumelhart and McClelland used the multilayer network learning algorithm in a neural network in 1986 [17]. The algorithm is the error backpropagation algorithm, that is, the BP algorithm. The algorithm belongs to a special program, and neural networks are one of the most cutting-edge disciplines at present. Combining the two becomes BP neural network. Based on the law and characteristics of function, a neural network can automatically learn more complex data experience and information. For complex functions, especially nonlinear functions, the characteristics of neural networks can be more prominent. The basic characteristics of neural networks are self-organization, self-adaptive, and self-study habits. Based

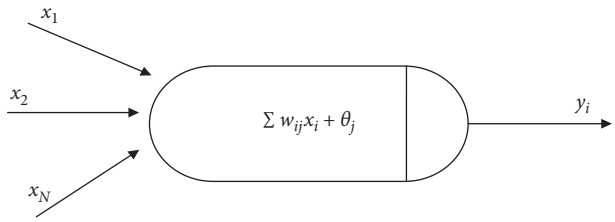

Figure 1: Neuron structure.

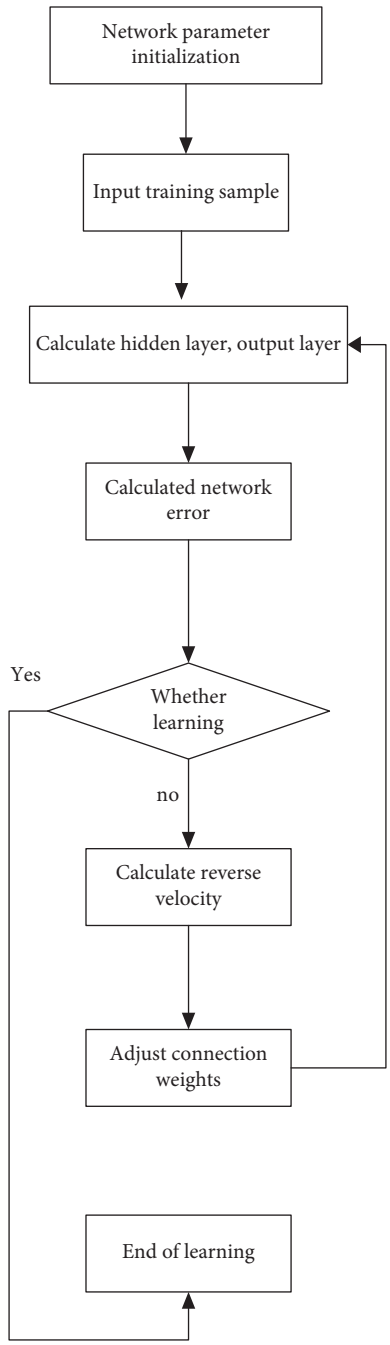

Figure 2: Neural network learning flow chart.

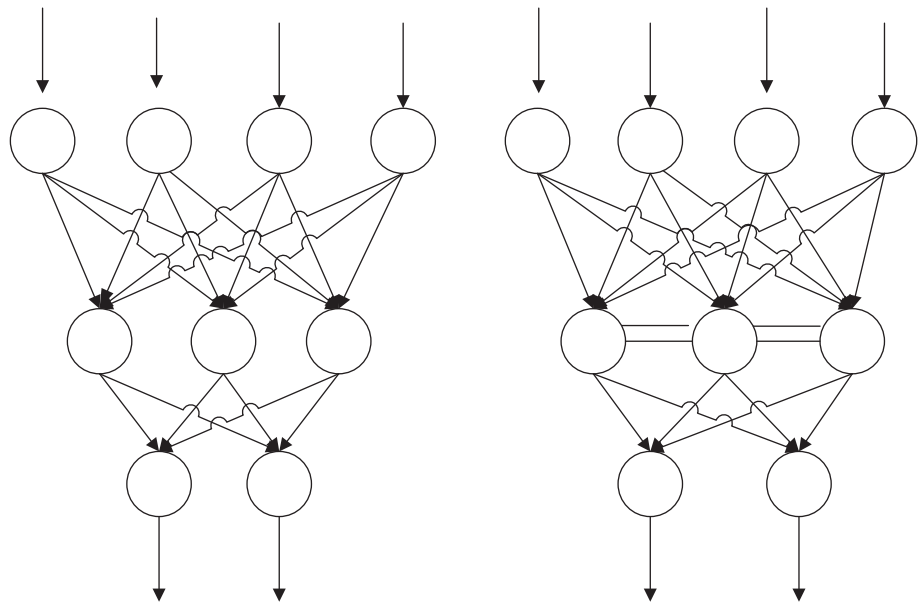

Figure 3: Comparison of the single-layer network structure with the interconnection hierarchical network structure.

on the functional characteristics and basic laws, the neural network deeply analyzes some complex problems and seeks the best way and strategy to deal with the problems. Figure 4 shows the topology of the BP neural network.

4. Evaluation of Women's Entrepreneurship Education Based on BP Neural Network

4.1. BP Neural Network Structure. A BP neural network is composed of three parts: the front end, the middle, and the end, which correspond to the input layer, the hidden layer, and the output layer. The beginning of the imported the input is the input vector, whose formula is $x = (x_1, x_2, \ldots, x_i, \ldots, x_n)^T$, and it is assumed that $x_0 = -1$; The middle part of the neural network is the hidden layer, which will interfere with the training speed. The result of the derived data is the output vector, and its formula is $y = (y_1, y_2, \ldots, y_i, \ldots, y_n)^T$. the assumption of $y_0 = -1$ can be added. The introduction of the threshold by the output layer will directly affect the end neural network. $O = (O_1, O_2, \ldots, O_i, \ldots, O_n)^T$ represents the output vector of the output layer. The weight matrix between the input layer and the hidden layer is mainly used to receive data, while the function of the hidden layer is the adjustment and change process. The weight matrix generated by the two processes directly affects the BP neural network. $v = (v_1, v_2, \ldots, v_k, \ldots, v_n)^T$ represents the output matrix. Since the output layer is the data export port, its output result directly affects the BP neural network, $w = (w_1, w_2, \ldots, w_k, \ldots, w_n)^T$ is the matrix expression of the BP neural network.

The mathematical relationship between various parts of the network has significant advantages. The front end is the input layer, and net_k and O_k are the front ends. The following are the input layer formulas for the front ends:

$$\begin{aligned} O_k &= f(\text{net}_k), \quad k = 1, 2, \ldots, n, \\ \text{net}_k &= \sum_{j=0}^{m} w_{jk} y_j \quad k = 1, 2, \ldots, n. \end{aligned} \tag{7}$$

The middle part of the network is the hidden layer, and net_j and y_j have an impact on the middle part [18]. The formula is as follows:

$$\begin{aligned} y_j &= f(\text{net}_j), \quad j = 1, 2, \ldots, m, \\ \text{net}_j &= \sum_{i=0}^{m} j v_{ij} x_i, \quad j = 1, 2, \ldots, m. \end{aligned} \tag{8}$$

A common category of functions is the unipolar sigmoid function. The transfer function $f(x)$ can be used in the neural network. At the same time, $f(x)$ can also select the corresponding unipolar sigmoid function according to the demand:

$$f(x) = \frac{1}{1 + e^{-x}}. \tag{9}$$

The BP training algorithm is based on the BP neural network. The algorithm is introduced and trained. The basic process of the algorithm is to set parameters and variables first, where n represents the number of samples, and the input vector is $x_k = [x_{k1}, x_{k2}, \ldots, x_{km}]$, $(k = 1, 2, 3, \ldots, n)$. The formula is as follows:

$$w_{MI}(n) = \begin{bmatrix} w_{11}(n) & w_{12}(n) & \ldots & w_{1I}(n) \\ w_{21}(n) & w_{22}(n) & \ldots & w_{2I}(n) \\ \ldots & \ldots & \ldots & \ldots \\ w_{M1}(n) & w_{M2}(n) & \ldots & w_{MI}(n) \end{bmatrix}. \tag{10}$$

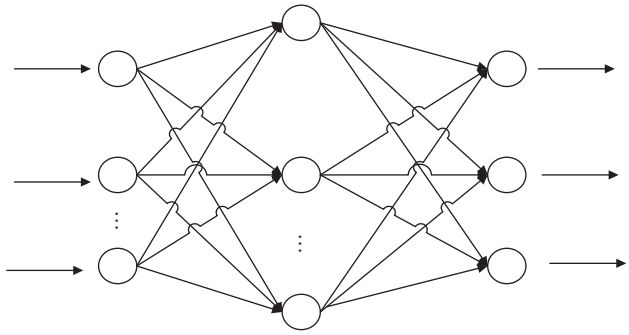

Figure 4: Topological structure of BP neural network model.

The formula is the weight vector between the middle part I and the beginning of the n^{th} iteration.

$$w_{LJ}(n) = \begin{bmatrix} w_{11}(n) & w_{12}(n) & \dots & w_{1J}(n) \\ w_{21}(n) & w_{22}(n) & \dots & w_{2J}(n) \\ \dots & \dots & \dots & \dots \\ w_{I1}(n) & w_{I2}(n) & \dots & w_{IJ}(n) \end{bmatrix}. \tag{11}$$

The above formula is the weight vector between the two intermediate parts I and J in the nth iteration.

$$w_{LJ}(n) = \begin{bmatrix} w_{11}(n) & w_{12}(n) & \dots & w_{1J}(n) \\ w_{21}(n) & w_{22}(n) & \dots & w_{2J}(n) \\ \dots & \dots & \dots & \dots \\ w_{I1}(n) & w_{I2}(n) & \dots & w_{IJ}(n) \end{bmatrix}. \tag{12}$$

The above is the weight vector between the middle part J and the end in the nth iteration. After n cyclic iterations, the output result is generated, and the actual output value is $y_k(n) = [y_{k1}(n), y_{k2}(n), \dots, y_{kn}(n)]$, $(k = 1, 2, 3, \dots, n)$, and the expected output result is $d_k = [d_{k1}, d_{k2}, \dots, d_{k3}]$, $(k = 1, 2, 3, \dots, n)$.

Secondly, during the initialization of the network, the nonzero random number is assigned to $w_{MI}(n)$, $w_{IJ}(n)$, $w_{JP}(n)$, and the value of n is assumed to be 0 [19].

Thirdly, the data of sample x_k is input, and the basic data of the neural network is sample data, which directly affects the network effect. It is necessary to assume that the value of n is 0.

Fourth, the middle and end weights and output vectors are interrelated.

$$v_p(np) = y_{kp}(n), \quad p = 1, 2, \dots, p. \tag{13}$$

Fifth, $E(n)$ is calculated based on the error between $y_k(n)$ and d_k. If it is consistent with the set error, you need to jump to the eighth step. If it is inconsistent with the required error, you can directly jump to the next step.

Sixth, the number of iterations of BP neural network parameters is calculated, and then the number of $n+1$ iterations is compared. If the latter is less than the former, it needs to be readjusted to enter the eighth. If the former is less than the latter, it needs to adjust the local gradient of neurons δ.

$$\delta_p^p(n) = y_p(n)\big(1 - y_p(n)\big)\big(d_p(n) - y_p(n)\big). \tag{14}$$

Seventh, the weight interference between the front end, middle, and end of the BP neural network is serious, so we should first calculate the specific weight and then readjust the weight according to the training error.

Eighth, take some time to train the neural network. If it is finished, you need to quit the training. If it is not finished, you need to readjust until the third step above.

4.2. Improved BP Neural Network. The BP neural network has significant advantages, but it also has inevitable problems, which are described in detail below:

(1) There is a great contradiction between the global optimal value and the local minimum value, so the ideal global optimal value cannot be obtained.

(2) It needs more neural network training time, but the disadvantage is that the convergence speed is slow and the efficiency is difficult to improve.

(3) Based on the theoretical guidance, the prediction results obtained by the neural network can be ensured to be very accurate, especially the number of hidden layer nodes should be determined according to the theoretical guidance.

(4) The contradiction between forgetting old samples and learning new samples: the disadvantage of a neural network is that the previous samples will be forgotten while learning new samples. In order to deal with the above problems, the algorithm should be modified and adjusted again. The measures taken are as follows:

(i) Add a new momentum term: there is a direct correlation between the BP neural network inversion and learning rate η. High η value indicates that the convergence speed of the network is fast, but it will lead to the decline of stability; smaller η value will solve the problem of poor stability, but the corresponding convergence speed will also decrease. Therefore, the momentum term is introduced, α is the momentum term, and it is added to the BP neural network to form a new BP algorithm.

$$\Delta w_{ij}(n) = \alpha \Delta w_{ij}(n-1) + n\delta_j(n)v_i(n). \tag{15}$$

In the above formula, T represents the variable time series, and the value of t is $0 - n$, which can be obtained:

$$\Delta w_{ij}(n) = \eta \sum_{t=0}^{n} a^{n-t}\delta_j(t)v_i(t). \tag{16}$$

(ii) Adjusting the learning rate: assume η represents the learning rate. After reducing the weight, the overall error decreases, $\eta = \theta\eta$ $(\theta < 0)$. According to the change degree of learning efficiency, the weight will also be changed to reduce the overall

error and fully reflect the effect of the adjusting learning rate.

(iii) The odd function is used as the excitation function: the most common type of function is the odd function. Selecting an odd function as an excitation function can speed up the operation speed of the BP neural network algorithm. The following are hyperbolic tangent functions in odd functions:

$$f(u) = a\tanh(bu) = a\left[\frac{1-\exp(-bu)}{1+\exp(-bu)}\right] = \frac{2a}{1+\exp(-bu)} - a. \tag{17}$$

This paper uses the improved BP neural network model to evaluate women's entrepreneurship education, which can effectively avoid the problems of instability and slow convergence of the traditional model and can comprehensively improve the accuracy of the evaluation results of women's entrepreneurship education. The BP neural network simulates the thinking mode of the human brain, and its adaptability, learning ability, and memory are strong. There is no need to build a model in advance for evaluation through this mode. As long as the expert evaluation sample data is input, a large amount of relevant data can be accumulated after learning and training. This method can accurately explain the relationship between various parameters and finally get the ideal evaluation result.

5. Empirical Analysis of Women's Entrepreneurship Education Evaluation Based on BP Neural Network

5.1. Number of Neurons in Each Layer of the BP Neural Network

5.1.1. Number of Neurons in the Input Layer. When studying the evaluation of women's entrepreneurship education based on the BP neural network, this paper sets multiple evaluation indicators, mainly including nine indicators: family entrepreneurship background, whether there is entrepreneurship experience, social practice time, women's entrepreneurship ability, university entrepreneurship environment, teacher team construction, women's entrepreneurship investment, government support policies, and social assistance. Therefore, the number of neurons n is 9.

After determining the number of neurons in the output layer and hidden layer, the actual output result of the network is unique, so the number of neurons in the output layer is also unique, so the value of M is 1 [20]. By comparing the numbers of hidden layer neurons and input and output layer neurons, it can be determined that the external environment will cause direct interference to them. If the quantity decreases, the corresponding amount of information also decreases. If the quantity increases, the fault tolerance will be reduced, the training cycle will be prolonged, and the optimal value will appear. The following is the empirical formula:

$$l = \sqrt{n+m+a}. \tag{18}$$

The numbers of neurons listed in Table 1 are 3, 4, 5, 6, 7, 8, and 9, respectively. At this time, the training error continues to decrease and there is a certain correlation between them. After analysis, the number of neurons 9 is the most ideal.

5.1.2. Model Learning Rate. Learning efficiency has a decisive impact on the efficiency [21] of training and testing neural networks, and the equivalent learning efficiency is η. If the η value is too high, the weight is large and the convergence speed is fast, which makes the network fluctuate greatly. Low η value will reduce the network efficiency and the convergence speed. For this problem, we can introduce motion vector α . Based on the evaluation results of this paper, the training times and errors in Table 2 are analyzed, and the learning rate is 0.01.

5.1.3. Momentum Factor α. The momentum factor plays a major role in the neural network, especially during the training period. Furthermore, the momentum factor can reduce the local maximum and local minimum problems of the network [22]. Through the experiments, it is concluded that the best value of the momentum factor is 0.85. When the neural network is used to evaluate the effect of women's entrepreneurship, the most ideal value is 9.0.

5.2. Implementation of Women's Entrepreneurship Education Evaluation Based on BP Neural Network. When implementing the evaluation of women's entrepreneurship education based on the BP neural network, this paper selects a university student majoring in statistics to carry out empirical analysis and uses expert scoring and a questionnaire to evaluate the quality of women's entrepreneurship education in colleges and universities. By collecting the entrepreneurship teaching quality of statistics majors in the same type of colleges and universities as the evaluation data, represented by U_i, it is assumed that U_1, U_2, U_3, and U_4 are the training samples of the model, and the detection samples are U_5, U_6, U_7, and U_8, and then the neural network simulation is realized through MATLAB software ε. The learning accuracy is 10^{-4}, and the learning factor is η. The value of η is 0.3. Based on this value, the weight matrix between the following hidden layer and the input layer is obtained:

Table 1: Relationship between the number of neurons in the hidden layer and error.

Number of hidden layer neurons	The training error	Test error
3	1.263	1.06
4	0.798	0.83
5	0.642	0.74
6	0.581	0.68
7	0.568	0.69
8	0.453	0.66
9	0.391	0.65

Table 2: Comparison results of different learning rates.

Learning rate	0.005	0.01	0.02	0.03	0.04	0.05	0.06	0.07
Number of training	18	10	19	22	29	35	44	49
Error (e-001)	6.89	3.13	5.89	9.92	3.62	9.99	8.79	10.12

$$\begin{bmatrix} 0.0012 & -0.0123 & -0.0159 & -0.0005 & \dots & -0.0069 & 0.0014 & -0.0119 \\ -0.5561 & -0.0176 & -0.5527 & -0.3601 & \dots & -0.9137 & -0.9014 & -0.3595 \\ -0.0301 & 0.0087 & -0.0725 & -0.0045 & \dots & -0.1182 & 0.0049 & -0.0476 \\ \dots & \dots & \dots & \dots & \dots & \dots & \dots & \dots \\ 0.1506 & 0.0752 & 0.0841 & 0.0392 & \dots & 0.1527 & 0.0965 & 0.0572 \\ -0.0079 & 0.0153 & -0.0032 & 0.0117 & \dots & 0.0073 & 0.0354 & 0.0289 \end{bmatrix}. \tag{19}$$

The following is the weight matrix between the output layer and the hidden layer:

$$\begin{pmatrix} -0.1045 & -0.1796 & 4.5012 & 0.5016 & -0.8106 & 4.4927 & 2.1609 & -1.3017 \\ -2.8342 & 8.9274 & -5.2207 & & & & & \end{pmatrix}. \tag{20}$$

Based on the parameters of the BP neural network model and the actual training results, the results show that the overall verification process and effect of the BP neural network are ideal. The analysis of Figure 5 shows that the value of R during the fitting regression of the training process is 0.9602, and the value of R on the fitting regression of the verification process is 0.9207. The closer the value of R is to 1, the better the fitting effect is. Therefore, the rationality and scientificity of the model and data are also tested.

5.3. Test BP Neural Network. According to the analysis of the data in Figure 6, after the BP neural network is improved and the training is completed, the data in the BP neural network need to be randomly selected to test the BP neural network model to obtain the evaluation results of women's entrepreneurship education. The overall analysis of the evaluation of women's entrepreneurship education based on the network's expected value and actual output results shows that the expected value is generally consistent with the actual value. There is no large fluctuation, which fully reflects the high reliability of the BP neural network, and the data collected and analyzed are very reasonable. Through the test of the BP neural network, according to the actual output results, we can get the expected effect, and the maximum relative error between the actual value and the expected value is 1.64%.

5.4. Analysis of Evaluation Results of Women's Entrepreneurship Education Based on BP Neural Network. By analyzing the evaluation results of women's entrepreneurship education based on the BP neural network, the actual value obtained is similar to the expected results, and each score result corresponds to the nine index data of students' evaluation of women's entrepreneurship education. According to each score, a women's entrepreneurship ability can be reflected. The comprehensive evaluation result of women's entrepreneurship education is 92 points. The evaluation results are analyzed in detail below.

(1) A high evaluation score indicates that the student has a high degree of education in female entrepreneurship education. Colleges and universities provide him with an ideal entrepreneurial environment. The school has a strong faculty. The government supports female entrepreneurship in terms of policies. It also has a large number of autonomy from

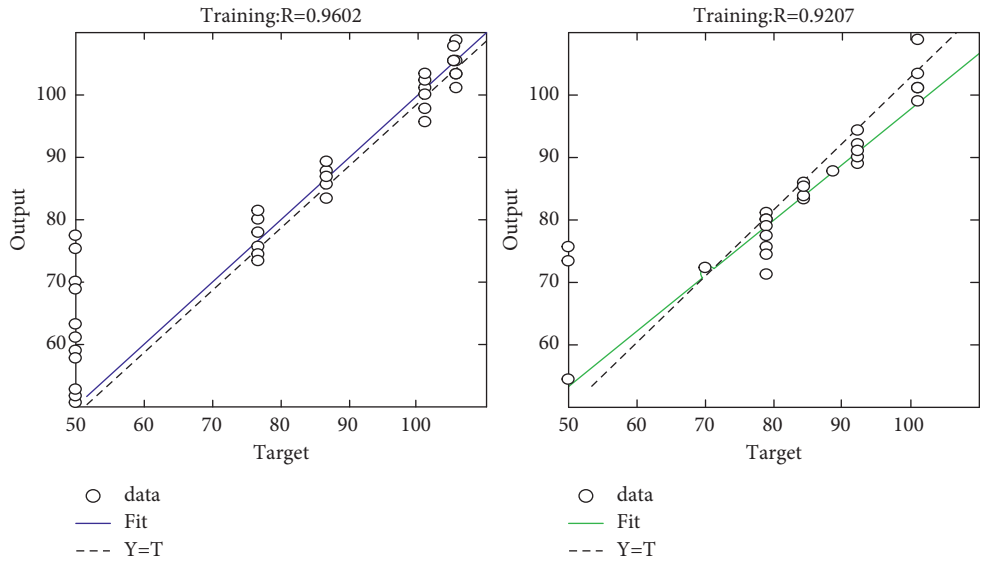

Figure 5: Comparative analysis results of neural network fitting regression.

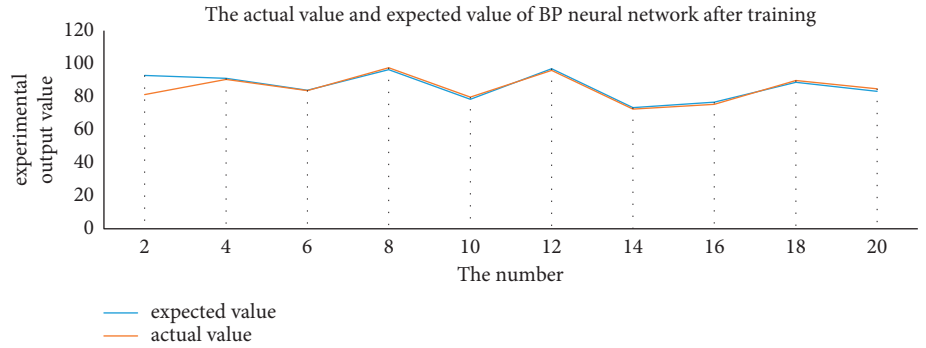

Figure 6: Comparison between the actual value and the expected value predicted by the neural network.

society, a rich entrepreneurial experience, and practical experience. Families also support women's entrepreneurship and provide them with some capital and experience. According to the data collected by the BP neural network, the university has achieved ideal results in women's entrepreneurship education, which can cultivate a large number of female entrepreneurs with entrepreneurial experience and provide more female talents to society.

(2) Some students score less than 90 points, indicating that they have the experience of participating in women's entrepreneurship education. Colleges and universities also provide them with a certain entrepreneurial environment, but their entrepreneurial ability is relatively insufficient. According to the data stimulated by the BP neural network model and simulation experiments, the university should continue to improve women's entrepreneurial ability and create a good entrepreneurial environment in women's entrepreneurship education.

(3) The evaluation results of some students are less than 80 points, indicating that they lack sufficient entrepreneurial ability and relevant entrepreneurial experience, and the school teaching staff and entrepreneurial environment are insufficient. Therefore, colleges and universities should strengthen the construction of teaching staff from this aspect and invest more funds to support women's entrepreneurship.

6. Conclusions and Future Work

This paper uses the BP neural network model to train and test it, selects the students of a certain university in China to study the quality of women's entrepreneurship education based on the BP neural network, and evaluates it. The final comprehensive evaluation result is 92, which shows that the university has a high level of women's entrepreneurship education, but there are still some deficiencies. This paper focuses on analyzing the structure of the BP neural network, establishing the BP neural network model and improving the BP neural network model. Based on the BP neural network model, we comprehensively evaluate women's innovation education, select 9 indicators as important indicators to

evaluate women's entrepreneurship education, and determine the learning speed and momentum factor of the model. Through empirical analysis, the comprehensive evaluation results of women's entrepreneurship education based on the BP neural network model are obtained. The results obtained in this way are more accurate, and it has become a more widely used way to evaluate women's entrepreneurship education. However, there is little research on education quality in China. The BP neural network model established in this paper is only a theoretical model and has not been widely used in practice. It needs to be practiced and applied in the later stages. We will consider these limitations as the focus of our future research. We will also consider more advanced algorithms such as CNN and attention networks [23].

Data Availability

The data used to support the findings of this study can be requested from the corresponding author.

Conflicts of Interest

The authors declare that they have no conflicts of interest.

Acknowledgments

This research was funded by the China Postdoctoral Science Foundation ("Research on the Evaluation and Optimization Policy of Female WeChat Business Entrepreneurship Environment from the Perspective of Social Capital," No. 2017M622122) and the Qingdao Postdoctoral Applied Research Project ("Research on the Characteristics of Female WeChat Business Entrepreneurship from the Perspective of Social Capital," 2016045).

References

[1] Y. Cao and H. Jiang, "An empirical study on the quality of entrepreneurship education based on performance excellence management," *Eurasia Journal of Mathematics, Science and Technology Education*, vol. 13, no. 8, pp. 5663–5673, 2017.

[2] M. M. Mars and S. Hoskinson, "opportunities and challenges: research and innovation in the life sciences," *Research on Adaptive Back-Stepping Integral Control of Class of Dynamic System*, vol. 23, pp. 125–140, 2013.

[3] A. Maritz, A. de Waal, S. Buse, C. Herstatt, A. Lassen, and R. Maclachlan, "Innovation education programs: toward a conceptual framework," *European Journal of Innovation Management*, vol. 17, no. 2, pp. 166–182, 2014.

[4] R. Ota, S. Agrawal, and P. Sarkar, "A roadmap for achieving health equity in India: a proposed framework and assessment of the determinants of health equity," *Indian Journal of Community Health*, vol. 30, no. 3, pp. 189–195, 2018.

[5] H. Matlay, L. Pittaway, and C. Edwards, "Assessment: examining practice in entrepreneurship education," *Education + Training*, vol. 54, no. 8/9, pp. 778–800, 2012.

[6] P. M. Papadopoulos, R. Burger, and A. Faria, "Innovation and entrepreneurship in education," *Advances in Digital Education and Lifelong Learning*, Emerald Publishing Limited, Bingley, UK, 2016.

[7] W. X. Fan, Y. Ma, and C. J. Liu, "analysis of influence factors of postgraduates' innovation and entrepreneurship education——an empirical study based on SEM," *Heilongjiang Researches on Higher Education*, vol. 27, no. 1, 2017.

[8] C. P. Tang and J. Liu, "Construction engineering practice teaching quality evaluation index system of building," *Journal of Juamjusi Education Institute*, vol. 18, no. 3, 2015.

[9] S. Wang and H. F. Tian, "Research on evaluation index system of innovation and entrepreneurship education in higher vocational colleges," *Heilongjiang Researches on Higher Education*, vol. 49, no. 1, 2017.

[10] Z. Guan and X. F. Sun, "Research on the construction of evaluation system of innovation and entrepreneurship education in agricultural vocational colleges," *Journal of Ningbo Polytechnic*, vol. 22, no. 5, 2018.

[11] Y. H. Liu, "Neural network, the C programming and the mine safety predicting simulation," *Computer Engineering & Software*, vol. 34, no. 5, 2013.

[12] X. Xia, "Interaction recognition and intervention based on context feature fusion of learning behaviors in interactive learning environments," *Interactive Learning Environments*, vol. 37, pp. 1–18, 2021.

[13] C. Y. Pei, S. Nordholm, and H. D. Hai, "Optimization and evaluation of sigmoid function with a priori SNR estimate for real-time speech enhancement," *Speech Communication*, vol. 55, no. 2, pp. 358–376, 2013.

[14] X. H. Li, "Research on adaptive back-stepping integral control of class of dynamic system," *Computer Simulation*, vol. 30, no. 9, 2013.

[15] Z. W. Yeh, C. H. Hsu, A. White et al., "POPPINS: a population-based digital spiking neuromorphic processor with integer quadratic integrate-and-fire neurons," 2022, https://arxiv.org/abs/2201.07490.

[16] E. Gal, M. London, A. Globerson et al., "Rich cell-type-specific network topology in neocortical microcircuitry," *Nature Neuroscience*, vol. 20, 2017.

[17] K. Takahashi, M. Kurokawa, and M. Hashimoto, "Multi-layer quantum neural network controller trained by real-coded genetic algorithm," *Neurocomputing*, vol. 134, pp. 159–164, 2014.

[18] Q. Gao and M. A. Yan-Mei, "Research and application of the level of the deep belief network (DBN)," *ence Technology and Engineering*, vol. 16, 2016.

[19] D. Singh and G. J. Sreejith, "Initializing ReLU networks in an expressive subspace of weights," 2021, https://arxiv.org/abs/2103.12499.

[20] T. Horita and I. Takanami, "An FPGA-based multiple-weight-and-neuron-fault tolerant digital multilayer perceptron," *Neurocomputing*, vol. 99, no. JAN.1, pp. 570–574, 2013.

[21] S. P. Mebin, V. Gnanamoorthi, and G. Devaradjane, "Prediction efficiency of artificial neural network for crdi engine output parameters," *Transportation Engineering*, vol. 3, Article ID 100041, 2020.

[22] S. Chen, Y. Jun, L. Qian, H. Di, and L. T Fu, "Interval neural network modeling method based on adaptive momentum factor," *Journal of Sichuan University (Natural Science Edition)*, vol. 54, 2017.

[23] Y. Guo, "Credit risk assessment of P2P lending platform towards big data based on BP neural network," *Journal of Visual Communication and Image Representation*, vol. 71, Article ID 102730, 2020.

Hindawi
Scientific Programming
Volume 2022, Article ID 8720831, 12 pages
https://doi.org/10.1155/2022/8720831

Research Article

Relationship between Surface Subsidence Range and Geological Mining Conditions Using Numerical Simulation and Machine Learning

Yanjun Zhang,[1] **Fushuai He**,[2] **Jiayuan Kong**,[3] **Yuanhao Zhu**,[1] **and Lingfei Wang**[4]

[1]*College of Geoscience and Surveying Engineering, China University of Mining and Technology-Beijing, Beijing 100083, China*
[2]*Power China Zhongnan Engineering Corporation Limited, Changsha 410000, China*
[3]*School of Mining Engineering, Taiyuan University of Technology, Taiyuan 030024, China*
[4]*Statistics Bureau of Xinzhou City, Xinzhou 034000, China*

Correspondence should be addressed to Yanjun Zhang; bqt2100204049@student.cumtb.edu.cn

Received 8 February 2022; Revised 17 February 2022; Accepted 24 February 2022; Published 20 March 2022

Academic Editor: Muhammad Zakarya

With the increase of mined-out areas and geological disasters, it is necessary to study the influence range of mining. Moreover, with the growth in the amount of data, machine learning methods are commonly used to predict the surface subsidence. The 10 mm subsidence boundary is an important indicator to determine the influence range, and FLAC^{3D} is suitable for solving the nonlinear large deformation problems. Therefore, it can be used to explore the relationship between the influence range of the surface movement (L) and geological mining conditions. Taking working faces A and B of two mines, through the establishment of a numerical model, the relationship between L and bedrock thickness, loose layer thickness, working face mining length, and overlying rock lithology is explored by using the control variable method. Moreover, the variation law is analyzed theoretically and mechanically. The results show that L is positively correlated with the thickness, while negatively correlated with the mining length. Similarly, L shows a slight increase after the key layer becomes weak. This study provides a scientific basis for reasonable coal mining and protection of surface buildings in the mining area. Integrating machine learning into the numerical model further increases the model throughput. The findings show that machine learning models had high accuracy in predicting surface subsidence, with the random forest trees and regression models having lower time and high accuracy, respectively.

1. Introduction

Coal mining has caused varying degrees of damage to the surface, seriously affecting the safety of ground buildings. FLAC^{3D} is a finite element difference software based on the Lagrange algorithm, which has unique advantages in simulating stability, vibration, and large nonlinear deformation problems. At present, FLAC^{3D} has been widely used in grouting reinforcement and filling mining [1, 2], slope stability [3], goaf stability analysis [4, 5], and mining subsidence [6, 7] and has become increasingly mature. In terms of mining subsidence, many scholars have explored the laws of rock, surface movement, and deformation under various geological mining conditions by means of numerical simulations. For example, Liu et al. [8] used FLAC^{3D} to explore the subsidence law of coal mining under the condition of large mining width and obtained higher simulation accuracy compared with the measured value. Similarly, Yu et al. [9] used FLAC^{3D} numerical simulation as a technical means to explore the law of surface movement and deformation of thick loose layers with large mining heights. The authors obtained the conclusion that the surface subsidence is proportional to the overburden lithology and the subsidence velocity is inversely proportional to the overburden lithology.

Likewise, Zhang et al. [10] used FLAC^{3D} to simulate the influence of increasing mining working face and mining depth on the substation and its surrounding areas and

obtained a series of results. Taking Xieqiao Mine as the research background, Pang and Xu [11] obtained the influence range of the surface movement by constructing the FLAC^{3D} coal seam mining model. Moreover, they summarized the migration law of overlaying rock under different advancing distances. However, these scholars have only studied the range of surface movement for a single special geological and mining factor and lack comprehensive consideration of multiple factors to study the range of surface movement. It is believed that the thickness of the loose layer and bedrock, the lithology of the overlying rock, and the mining length of the working face are some of the most important factors that can significantly affect the law of surface movement and deformation [9–12].

In view of this, the establishment of the FLAC^{3D} three-dimensional numerical model, we use the control variable method to explore and investigate different trends in the influence range of surface movement. Furthermore, we study the trends in the change of bedrock and loose layer thickness, the mining length of the working face, and the physical, as well as the mechanical properties of the overlying rock. Moreover, with the growth in the amount of data, machine learning methods are usually used to predict the surface subsidence. Through simulation study, we obtain the correlation equation between the influence range of surface movement (10 mm subsidence boundary) and the geological mining conditions. Subsequently, this provides reference for coal mining under three different conditions and for the protection of buildings in the mining area. The following are the major contributions of the research conducted in this paper:

(i) We study the influence range of mining
(ii) The variation law is analyzed theoretically and mechanically
(iii) The study provides scientific basis for reasonable coal mining and protection of surface buildings in mining area
(iv) Machine learning method is integrated into the numerical model to predict the surface subsidence

The rest of this paper is organized as follows: In Section 2, we offer an overview of the materials and methods. Section 3 offers a brief discussion over the machine learning methods. Section 4 is about the datasets and evaluation metrics. Moreover, experimental details are presented. In Section 5, results are discussed. We summarize the major findings and outcomes of this research in Section 6. Finally, Section 7 concludes this paper with directions for further research and investigation.

2. Materials and Methods

2.1. Overview of the Study Area. The mining coal seam of working face A is 4 # coal seam. The size of the working face is 1000 m × 200 m. The average inclination angle of the coal seam is 2°, belonging to near-horizontal coal seam. The average mining depth is 500 m, and the average mining thickness is 2.3 m. The thickness of loess is 20 m. The working face adopts fully mechanized top coal caving and uses a long-wall retreating mining method. The all caving method is used to manage the roof. In order to avoid accidental results, this paper also selects another working face B under different geological conditions to explore. The mining coal seam of working face B is 3 # coal seam. The size of the working face is 1000 m × 200 m. The coal seam is near-horizontal coal seam. The average mining depth is approximately 313.5 m, and the average mining thickness is 4.4 m. The thickness of loess is 15.5 m. The working face adopts fully mechanized top coal caving and uses a long-wall retreating mining method. The all caving method is used to manage the roof. The layout of the observation station is shown in Figure 1.

2.2. The Influence Range of Surface Movement. After coal mining, the stress balance around the goaf is damaged, and the rock strata move, deform, and destroy. When the goaf area reaches a certain range, the influence of underground mining is transmitted to the surface, which can cause surface movement and deformation. Subsequently, this can form a surface movement basin larger than the goaf area [13–15]. The horizontal distance from the boundary point on the main section of the moving basin (10 mm subsidence boundary) to the boundary of the coal pillar side is called the influence range of the surface movement (denoted by L in this paper) [16, 17]. Figure 2 shows the influence range of the surface movement.

2.3. FLAC^{3D} Numerical Simulation

2.3.1. Principles of the FLAC^{3D}. FLAC^{3D} is a simulation calculation software developed by Itasca in the United States, which can simulate the stress characteristics of the three-dimensional structures such as soil and rocks. The software is based on the Lagrange algorithm and uses the finite difference explicit algorithm to obtain the time step solution of all the motion equations (including internal variables) of the model, which can track the progressive failure and collapse of the material. FLAC^{3D} is suitable for simulating the mechanical behavior of rock and soil materials, especially for simulating large deformation and distortion, which can accurately analyze the movement and deformation laws of rock and surface after coal seam mining. Further details of the software can be found in [18, 19].

In order to establish the calculation model, it is necessary to mesh division, select the constitutive model, and give boundary conditions to obtain the initial equilibrium state of the model. Then, the engineering simulation analysis is carried out through excavation or changing the boundary conditions [20, 21].

2.3.2. Model Establishment. The three-dimensional numerical model is established based on the actual stratum structure of working face A. The model size is 3000 m × 1000 m × 515.3 m, and the excavation size is 1000 m × 200 m × 2.3 m. The model adopts the

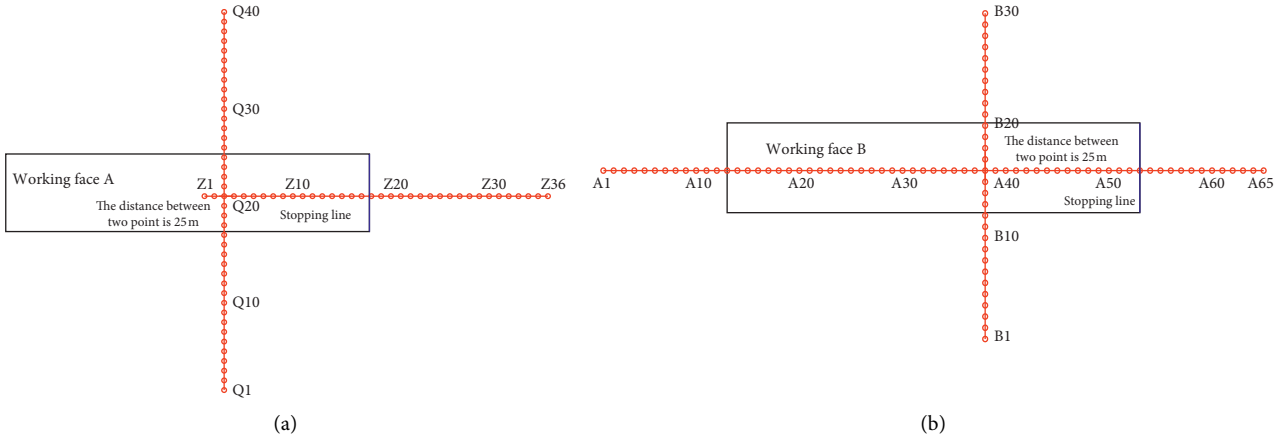

Figure 1: Layout diagram of the observation station. (a) Working face A; (b) working face B.

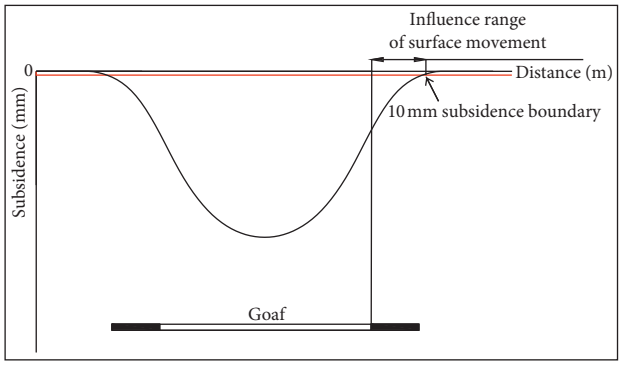

Figure 2: Influence range of the surface movement.

Mohr–Coulomb calculation criterion; the boundary adopts displacement constraint mode; the x-direction boundary adopts x-direction constraint; the y-direction boundary adopts y-direction constraint; the bottom constraint has three directions of displacement; the top surface is a free surface; and the initial stress field is calculated according to the gravity stress field of rock mass [22, 23]. Table 1 illustrates the physical and mechanical parameters of each layer that are used as parts of the model. The FLAC^{3D} model is shown in Figure 3.

The numerical simulation model is constructed according to the geological conditions and distribution of the coal and rock strata in working face B, as shown in Figure 4. The model size is 3000 m × 1000 m × 327.9 m, and the excavation size is 1000 m × 200 m × 4.4 m. The Mohr–Coulomb calculation criterion is still used in the model. The physical and mechanical parameters of each layer of the model are shown in Table 2.

2.3.3. Simulation Accuracy Analysis. Taking working face A as an example, the subsidence value of surface movement is extracted from the FLAC^{3D}, and the simulation accuracy of some points with a larger subsidence value is listed in Table 3. This should be noted that the surface subsidence value is the result extracted after the numerical model is balanced, so it can be equated with the subsidence value after the actual coal seam mining is stable. According to the surface movement data, compared with the measured subsidence value after stability, the maximum absolute error of the simulation is less than 50 mm, and the maximum relative error is less than 5%. The absolute error and relative error are small enough (considerably), indicating that the FLAC^{3D} numerical simulation results are significantly accurate [24].

3. Machine Learning

In this paper, the localities of the surface subsidence area were first documented by means of a wide inspection. A four-dimensional distribution of subsidence was then delivered for constructing and assessing learning models. The statistics logged into the dataset were subdivided into twofold segments of training (70 percent) and testing (30 percent) datasets. The link between surface sinking sites and the effective variables was evaluated in the research region, and drawings of the features causing land subsidence were generated by means of basic information (geographical and satellite pictures) in a raster format. A land subsidence map of the vulnerability zoning was created for further study, and the findings were assessed using simple regression (SR), boosted regression tree (BT), random forest trees (RFT), and support vector machine (SVM) models [25]. The assessment findings showed that machine learning models had high accuracy in predicting surface subsidence, with the BRT and SR models having high accuracy, respectively. Therefore, machine learning algorithms may be used for land use planning and groundwater management. The model is shown in Figure 5.

Regression-based machine learning models describe the link and association among various variables by drawing a trend line from to the observed data. In a linear model of regression, a straight line is employed. However in nonlinear or logistic models of regression, a bent line is drawn. In case of the variables (independent) amendment, you may use regression to anticipate how the variable (dependent) will change. Simple linear regression models are useful to assess the association and link among two or more than two variables (quantitative). Decision trees are supervised

Table 1: Physical and mechanical parameters of working face A.

Lithology	Thickness (m)	Density ($kg \cdot m^{-3}$)	Bulk modulus (MPa)	Tension (MPa)	Cohesion (MPa)	Friction angle (°)
Loess	20	1825	75	0.82	0.02	17
Siltstone	200	2640	2568	5.96	11	30
Mudstone	110	2566	2200	4.35	9.56	22
Medium grained sandstone	170	2610	3169	7.84	14.4	26
Coal	2.3	1349	876	0.73	2.38	25
Fine-grained sandstone	13	2660	2860	6.12	12.7	21

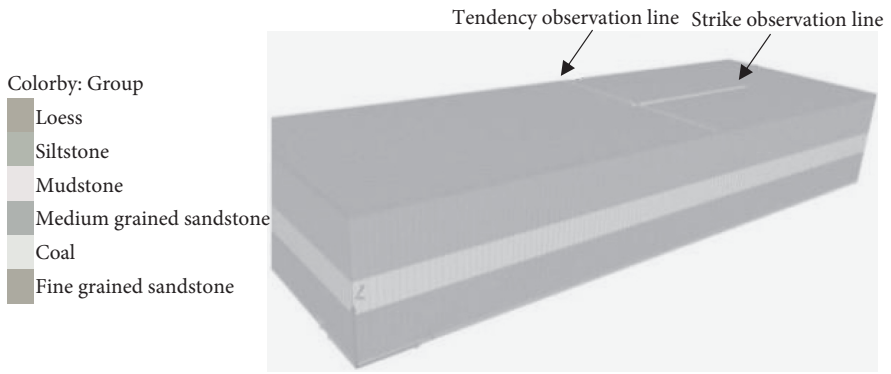

Figure 3: Numerical model of working face A.

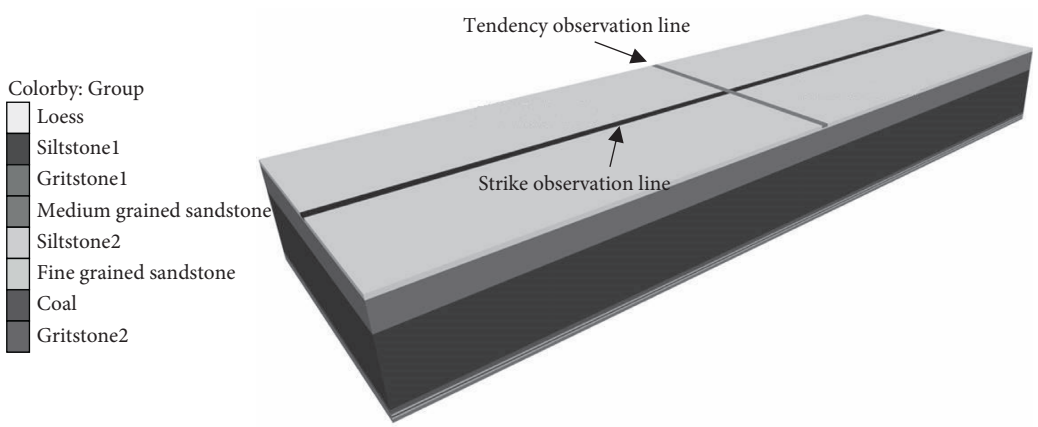

Figure 4: Numerical model of working face B.

Table 2: Physical and mechanical parameters of working face B.

Lithology	Thickness (m	Density ($kg \cdot m^{-3}$)	Bulk modulus (MPa)	Tension (MPa)	Cohesion (MPa)	Friction angle (°)
Loess	15.5	1713	68	0.81	0.03	15
Siltstone 1	60	2640	2520	5.2	10.1	38
Gritstone1	214.8	2633	3062	7.72	11.8	32
Medium grained sandstone	13.7	2598	2886	6.8	11.4	29
Siltstone 2	4.6	2640	2520	5.2	10.1	38
Fine grained sandstone	4.9	2651	2650	5.56	10.5	28
Coal	4.4	1579	893	0.74	2.5	27
Gritstone 2	10	2633	3062	7.72	11.8	32

Table 3: Comparison of simulated and measured subsidence.

Number	Measured subsidence (mm)	Simulated subsidence (mm)	Absolute error (mm)	Relative error (%)
Z1	1313	1316	3	0.2
Z2	1273	1303	30	2.4
Z3	1242	1286	43	3.5
Z4	1238	1264	26	2.1
Z5	1214	1239	25	2.1
Z6	1181	1210	28	2.4
Z7	1172	1176	4	0.3
Z8	1118	1139	21	1.9
Z9	1075	1098	23	2.1

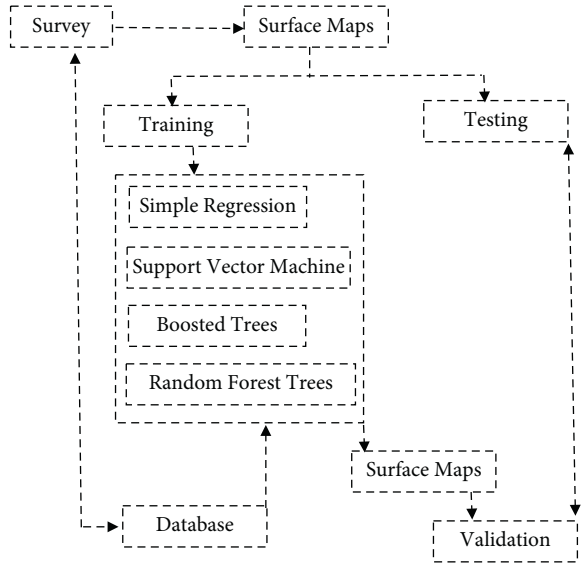

Figure 5: The proposed model for machine learning and model training.

learning techniques that may be used for classification as well as regression. The basic concept behind decision trees is to find the descriptive features that hold the maximum (related) information about the features of the target and subsequently divide the dataset along their values. This division essentially leading in values of the target feature that are as uncontaminated as reasonable for the fundamental datasets. Note that SVM models conduct vigorous regression for quantitative responses through grouping predictors in the observation space and commissioning a collection of inner products to exploit the correlations between observations. A cooperative of unpruned decision trees, individually created by using a sample of the bootstrap in the dataset (training) and randomly picked subgroups of variables (predictors) as candidates for separating tree nodes are used in the random forest regression.

4. Results

4.1. Relationship between L and Bedrock Thickness. Under the conditions of good simulation results above, the control variable method was used to explore the relationship between the influence range of the surface movement and its relationship with other factors by changing the thickness of the bedrock. During experimentations, one of the premises was that the mining length was 1000 m, and the thickness of the loose layer and the lithology of overlaying rock remained unchanged. In the experiment, the thickness of mudstone in working face A and the thickness of siltstone in working face B were changed, respectively, and the thickness variation range was 0 m–120 m. The calculation results were extracted from FLAC^{3D}, and the relationship between the variation of the influence range of surface movement ΔL and the variation of rock thickness Δm is shown in Figure 6.

From the experimental results in Figure 6, it can be obtained that the linear relationship between ΔL and Δm is approximately linear, and the influence range of the surface movement increases with the increase of bedrock thickness, which is a positive correlation. After abstraction, the linear regression equation of ΔL and Δm in working face A is $\Delta L = 0.68\Delta m$, and the linear regression equation of ΔL and Δm in working face B is $\Delta L = 1.23\Delta m$.

4.2. Relationship between L and Thickness of Loose Layer. Under the premise that the mining length was 1000 m and the bedrock thickness and the overlaying rock lithology remained unchanged, the thickness of the loose layer was changed to explore its influence on the range of surface movement. The thickness of the loose layer in working face A increased from 0 m to 120 m, and the thickness of the loose layer in working face B increased from 0 m to 124.5 m. The relationship between the variation of the range of surface movement ΔL and the variation of the thickness of the loose layer Δh is shown in Figure 7.

It can be seen from Figure 7 that the overall relationship between ΔL and Δh is approximately linear. The influence range of the surface movement increases with the increase of the thickness of the loose layer, which is a positive correlation. After abstraction, the linear regression equation of ΔL and Δh in working face A can be fitted as follows: $\Delta L = 0.71\Delta h$, but the influence range of surface movement increases abruptly when the loose layer is 120 m. The linear regression equation of ΔL and Δh in working face B is $\Delta L = 0.42\Delta h$.

4.3. Relationship between L and Mining Length. The relationship between the influence range of the surface movement and the mining length of the working face was studied by changing the excavation length of working faces A and B

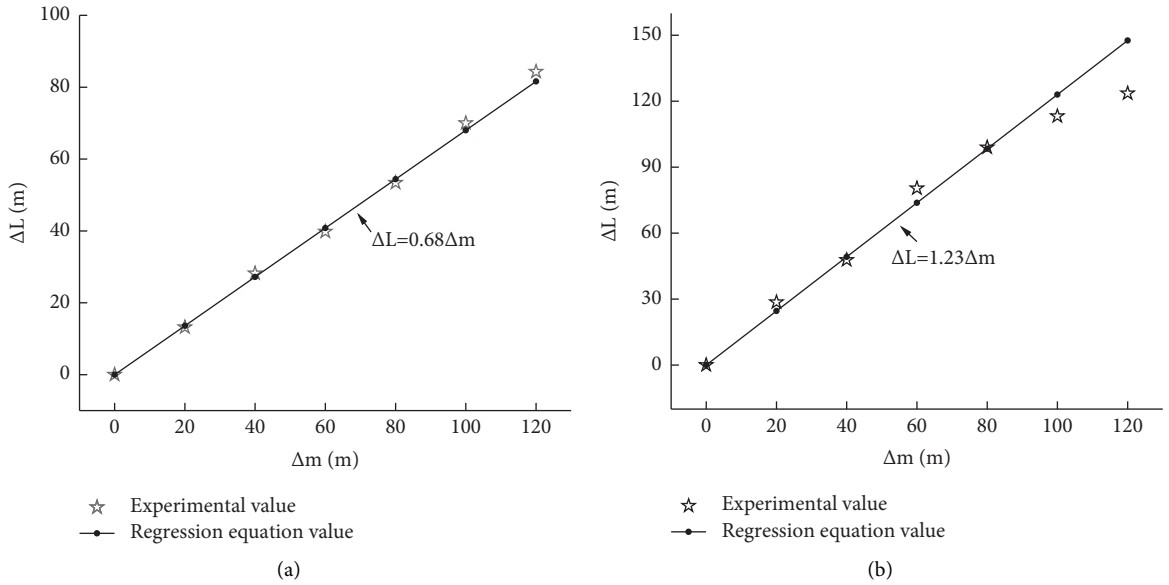

Figure 6: Relationship between variation of influence range of the surface movement and variation of bedrock thickness. (a) Working face A and (b) working face B.

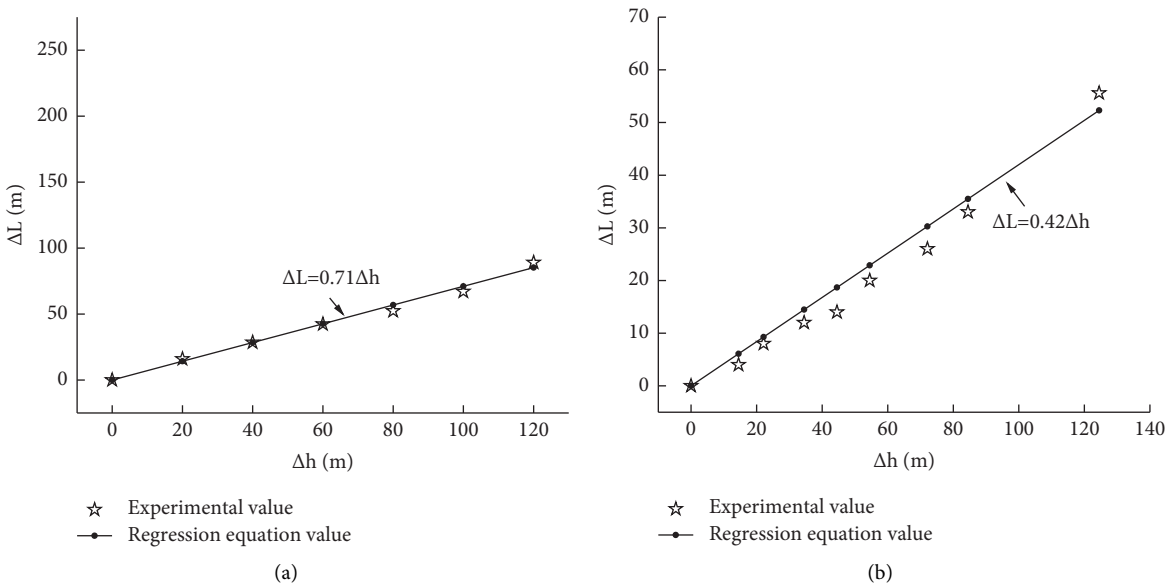

Figure 7: Relationship between variation of influence range of surface movement and variation of loose layer thickness. (a) Working face A and (b) working face B.

(according to the starting distance of 0.25–0.5 times the mining depth, the initial lengths of working faces A and B were determined to be 300 m and 200 m, respectively). The thickness of bedrock, loose layer, and lithology of the overlying rock were unchanged. The advancing distance of working face A was 100 m each time and that of working face B was 200 m each time. The excavation results were counted and the relationship between the variation of the influence range of surface movement ΔL and the variation of mining length Δs is plotted as shown in Figure 8.

It can be seen from Figure 8 that the two working faces show the same regularity. The influence range of the surface movement is negatively correlated with the mining length, and ΔL and Δs show a linear relationship as a whole. After abstraction, the linear regression equation of ΔL and Δs in working face A is $\Delta L = -0.11\Delta s$, and the linear regression equation of ΔL and Δs in working face B is $\Delta L = -0.05\Delta s$.

4.4. Relationship between L and Overlaying Rock Lithology. On the basis of the mining length of 1000 m, the thickness of the rock layer and the thickness of the loose layer were kept unchanged, and the physical and mechanical parameters of the rock layer were changed to explore the relationship

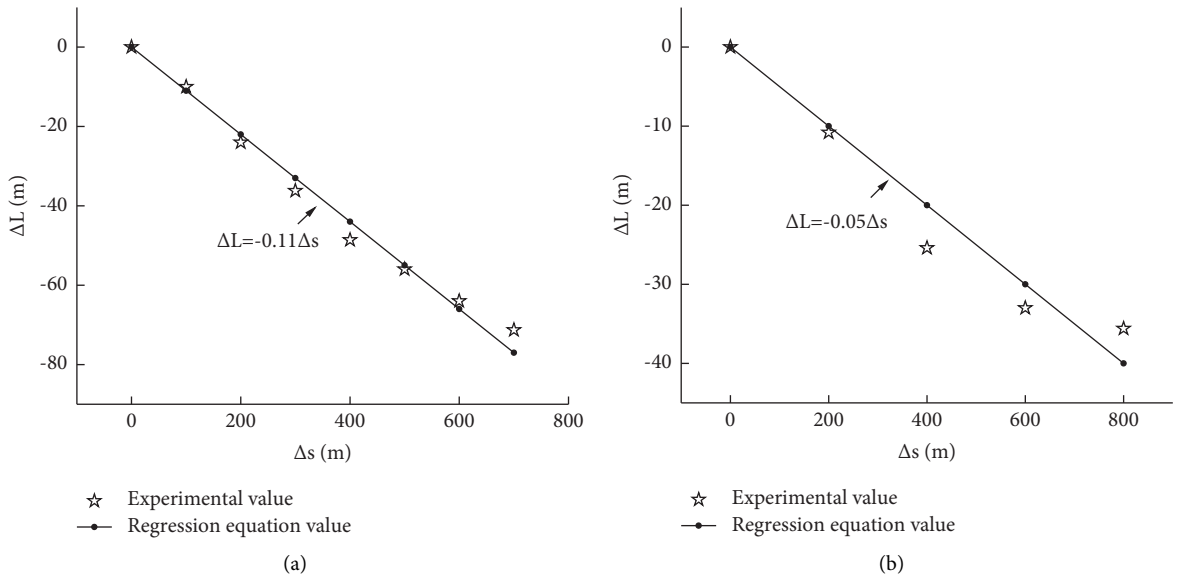

Figure 8: Relationship between variation of influence range of the surface movement and variation of mining length. (a) Working face A and (b) working face B.

between the influence range of the surface movement and the lithology of the overlaying rock. In order to have a representative choice to change the key layer parameters, the original hard key layer was replaced by sandy mudstone and mudstone. In the experiment, the medium grained sandstone layer of working face A and the gritstone 1 layer of working face B were changed, respectively. The physical parameters of the changed and replaced rock are shown in Table 4.

The influence range of the surface movement under the corresponding strata of working face A and B is shown in Table 5, respectively. Through Table 5, it is known that the influence range of the surface movement increases by 4% and 6.6%, respectively. Furthermore, after replacing medium grained sandstone in working face A with sandy mudstone and mudstone, while the influence range of the surface movement increases by 2.5% and 3.4%, respectively, after replacing strata in working face B. The influence range of the surface movement is slightly affected by the rock mechanical properties as well.

4.5. Relationship between L, Geological Conditions, and Mining Conditions. From the above experiments, it can be seen that the influence range of the surface movement L is linear with the thickness of bedrock, the thickness of loose layer, and the mining length. At the same time, it will be affected by the mechanical properties of the rock. The relationship between L and geological mining conditions is as follows:

$$L = am + bh + cs + \mathrm{d}, \tag{1}$$

where a, b, and c represent the overlaying rock thickness, loose layer thickness, and mining length slope parameters, respectively. They are related to geological and mining conditions; d is the correction number related to the mechanical properties of the rock strata.

The a, b, and c coefficients have been obtained by using the control variable method in Sections 4.1–4.3, and the simulation results in Section 4.4 can be substituted into the relational expression. The relational expression of working face A between L and geological mining conditions is as follows: $L = 0.68m + 0.71h - 0.11s + \mathrm{d}$, combined with geological mining parameters, when the key layer is medium grained sandstone, $d = 239.4$ m; when replaced by sandy mudstone, $d = 258.4$ m; when replaced by mudstone, $d = 270.4$ m. The relationship of working face B between L and geological mining conditions is $L = 1.23m + 0.42h - 0.05s + \mathrm{d}$, when the key layer is gritstone, $d = 31$ m; when replaced by sandy mudstone, $d = 40$ m; when replaced by mudstone, $d = 43$ m, it can be seen that d increases gradually as the rock becomes weak.

4.6. Machine Learning to Predict Surface Subsidence. We used four machine learning approaches to predict the surface subsidence, i.e., simple regression, support vector machines, boosted trees, and random forest trees. Figure 9 shows the time needed for training the model and prediction durations. The random forest tree was almost comparable to the SVM in terms of training time, but we observed lower prediction durations than the SVM, regression, and boosted trees (i.e., 3.56% to 7.33%). The durations are shown in seconds. Figure 10 shows the accuracy of various methods in RMSE and MAPE. The accuracy of the prediction approach is measured using the well-known parameters, i.e., root mean square error (RMSE) and MAPE. The MAPE values are shown in percentages where the lower ones are better than the higher values. Again, the RMSE and MAPE values confirm the efficiency of the random forest trees than the regression and SVM. As mentioned in Section 3, the entire dataset was divided into training (70 percent) and testing (30 percent) and the accuracy is computed with respect to the latter one.

Table 4: Changing physical and mechanical properties of rock.

<!—Col Count:6-->Lithology	Thickness (m)	Density (kg·m^{-3})	Bulk modulus (MPa)	Tension (MPa)	Cohesion (MPa)
Medium grained sandstone	2610	3169	7.84	14.4	26
Gritstone1	2633	3062	7.72	11.8	32
Sandy mudstone	2570	2400	4.8	9.86	23
Mudstone	2566	2200	4.35	9.56	22

Table 5: Changes of influence range of surface movement.

Working face	Lithology	The influence range of surface movement	Working face	Lithology	The influence range of surface movement
A	Medium grained sandstone	470	B	Gritstone1	354
A	Sandy mudstone	489	B	Sandy mudstone	363
A	Mudstone	501	B	Mudstone	366

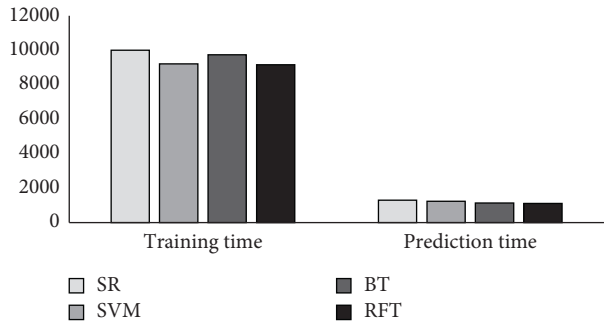

Figure 9: The training and prediction times of various techniques (seconds) (lower values denote more efficient schemes than the higher values and vice versa).

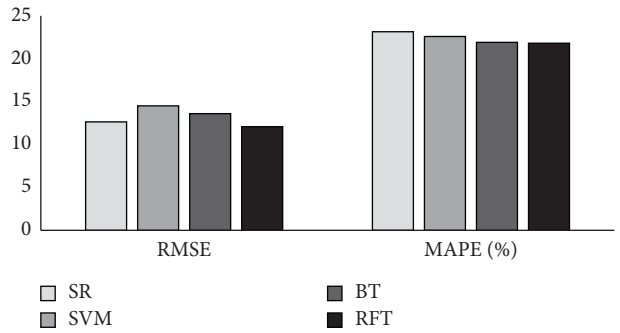

Figure 10: Accuracy of various techniques in terms of RMSE and MAPE.

5. Discussion

5.1. Analysis of Relationship between L and Bedrock Thickness. From the above, it can be seen that the simulation results of two working faces in different regions are similar, which confirms that the study of surface movement and deformation by FLAC is credible and correct. Therefore, only one of the working faces is selected to discuss in the following sections. Under the condition that the mining length is 1000 m and the lithology of the overlaying rock and the thickness of the loose layer are unchanged. Furthermore, taking working face B as an example, the subsidence value obtained by changing the thickness of siltstone is plotted as the subsidence curve, as shown in Figure 11.

It can be seen from Figure 11 that with the increase of siltstone thickness, the maximum surface subsidence value gradually decreases. However, the surface influence range slightly increases, and the basic shape of the curve is similar and gradually becomes flat. The increase of bedrock thickness improves the stability of rock strata and makes the surface subsidence value smaller. At the same time, the thickness of the bedrock makes the mining depth larger. According to the positive correlation between the surface influence range and the mining depth, the larger the mining depth is, the larger the surface influence range is, which is consistent with the experimental results of the larger influence range of the surface movement with the increase of bedrock thickness.

5.2. Analysis of Relationship between L and Loose Layer Thickness. Under the premise of mining length 1000 m, rock thickness, and rock lithology unchanged, taking A working face as an example, changing the thickness of the loose layer, the curve diagram of each subsidence result is drawn as Figure 12.

It can be seen from Figure 12 that the shape change of the subsidence curve of 0–100 m in the loose layer is small, and the subsidence curve changes significantly at 120 m, which is manifested as the increase of subsidence value and the increase of surface influence range. This may be due to the excessive load caused by the thick loose layer that destroys the stability of the bedrock and makes surface subsidence occur again. The influence range of the surface movement increases with the increase of the thickness of the loose layer, which is consistent with the characteristics of wide influence range under the geological conditions of a thick loose layer. The experiment further confirms the known law of surface movement and deformation.

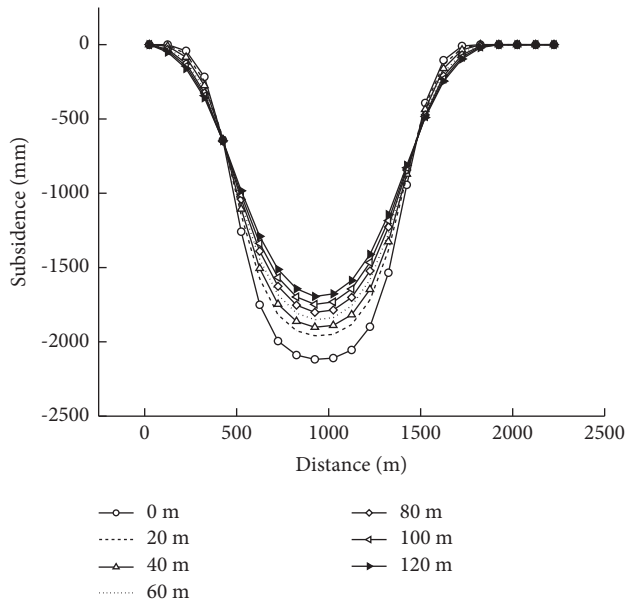

Figure 11: Subsidence curve of siltstone thickness variation.

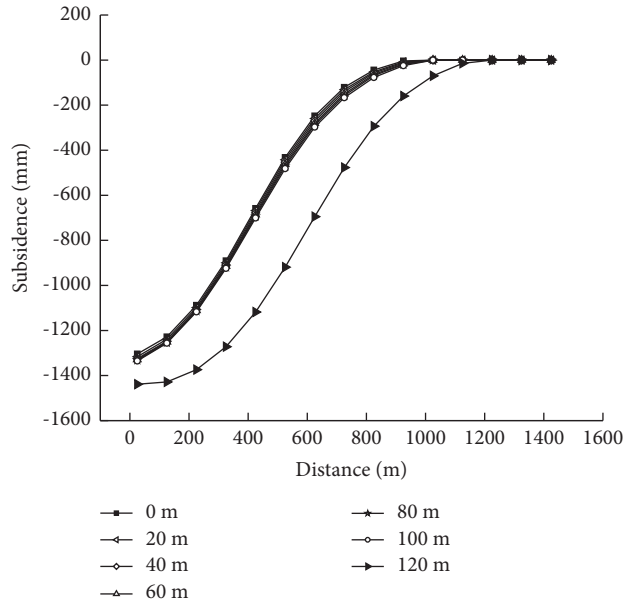

Figure 12: Subsidence curve of loose layer thickness variation.

5.3. Analysis of Relationship between L and Mining Length. Taking working face B as an example, the subsidence curve is drawn as shown in Figure 13 after extracting and counting the obtained surface movement deformation values. As can be seen from Figure 13, the maximum subsidence point is moving forward as the working face advances, and the subsidence value is increasing, eventually forming a bowl basin on the surface. When the excavation is 200 m, 400 m, and 600 m, respectively, the angle between the tangent and the horizontal line near the inflection point of the subsidence curve is 31°, 47°, and 50°, respectively. During the propulsion process, the angle between the tangent and the horizontal line near the inflection point increases continuously, the angle growth decreases gradually, and the subsidence curve becomes steeper and steeper, which is consistent with the decreasing and gradually stable influence range of the surface movement.

The stress nephogram of 200 m, 400 m, and 600 m excavation are shown in Figures 14(a)–14(c). Through the stress nephogram, it can be found that the rock mass forms a pressure arch after the mining is completed. With the increase of the excavation length, the vault part continues to extend, and the reasonable axis of the arch under the vertical uniform load is a quadratic parabola. Therefore, the stability of the actual pressure arch is reduced, which leads to a greater mining length. Moreover, the more intense the surface movement basin activity is, the steeper the subsidence curve is. Similarly, the steeper the subsidence curve is, then smaller the influence range of the surface movement is. This reasonably explains the principle that the influence range of the surface movement changes with the mining length.

5.4. Analysis of the Relationship between L and Overlaying Lithology. Under the condition of controlling the mining length of 1000 m and the thickness of rock and loose layer unchanged, the subsidence curves of each experimental results of working face A and B are shown in Figure 15. It can be observed from Figure 15(a) that the subsidence value essentially increases obviously after replacing the hard core layer of medium grained sandstone in working face A with soft sandy mudstone and mudstone, respectively. Moreover, the maximum subsidence value is close to the thickness of coal seam excavation (2300 mm), which indicates that without the support of the key layer, the rock strata will be completely collapsed and compacted. This means that it will have a great impact on the ground, and the corresponding parameter d is also large (about 250 m). It can be seen from the subsidence curve, as shown in Figure 15(b), that after replacing the hard key layer of working face B with sandy mudstone and mudstone, the subsidence value increases significantly but the maximum subsidence does not reach the mining thickness (4400 mm). The reason is that there are also siltstone key layers in addition to gritstone. The support effect of this nonsingle key layer has a good protective effect on surface movement and failure, and the parameter d is small (about 40 m).

6. Major Findings and Outcomes

The major findings of this study can be summarized as follows:

(1) Under the condition of constant mining length, overlaying rock lithology and loose layer thickness, we observed that the influence range of the surface movement is also regularly increased with the increase of bedrock thickness. The positive correlation curve shape of the two is in line with the linear function, and the slope is related to the geological and mining conditions.

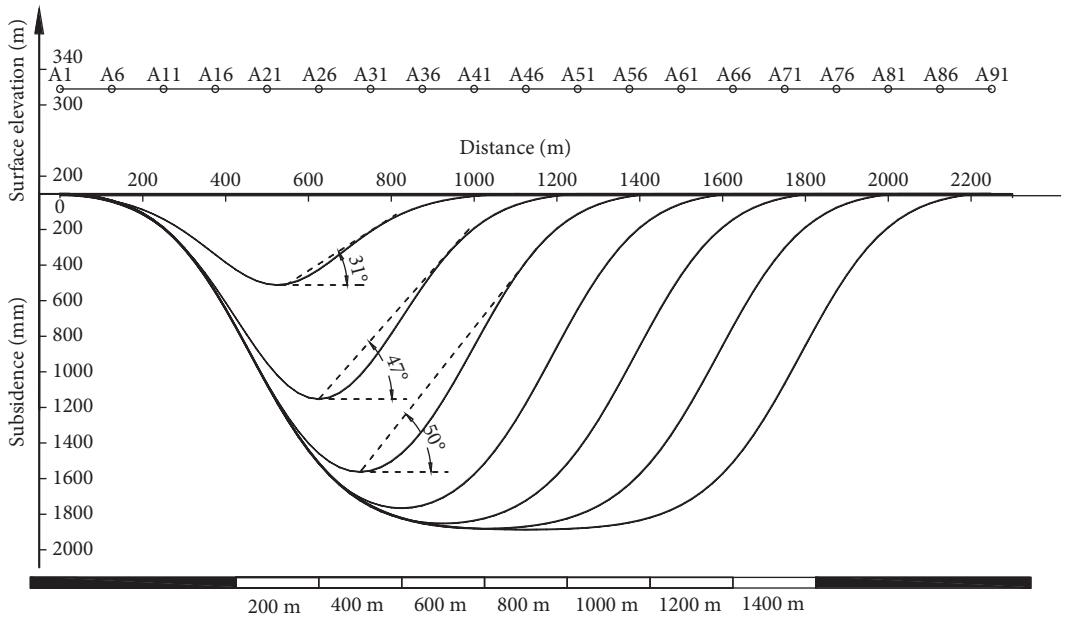

Figure 13: Subsidence curves under different mining lengths.

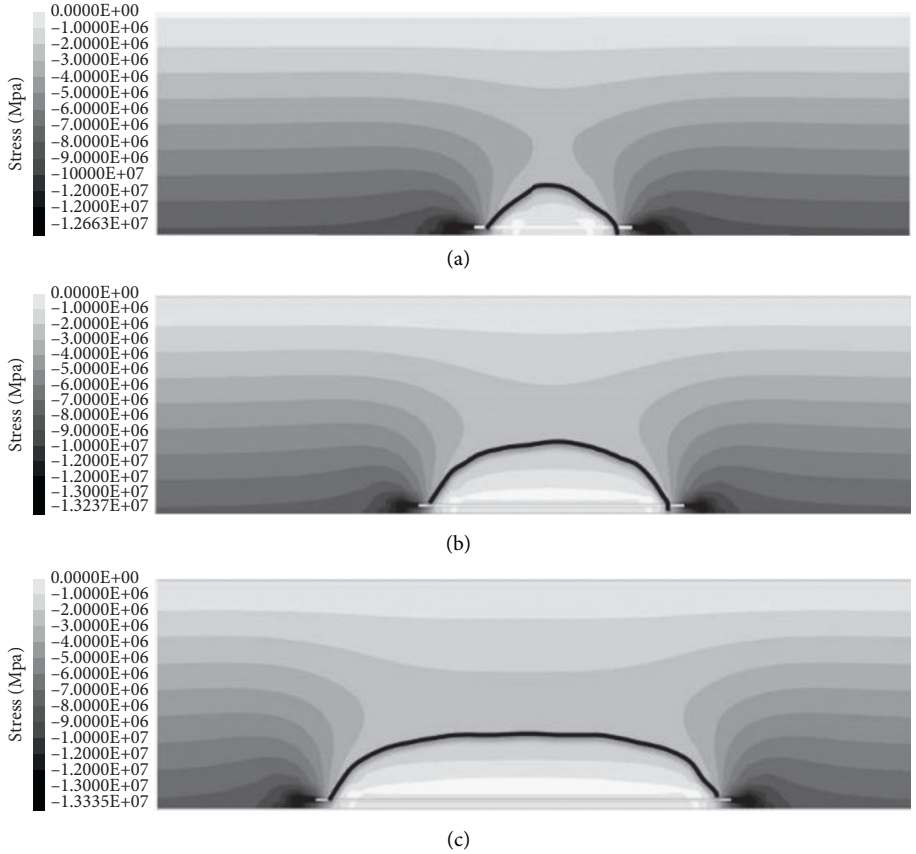

Figure 14: Stress nephogram under different excavation lengths: (a) advanced to 200 m, (b) advanced to 400 m, and (c) advanced to 600 m.

(2) Under the condition that the mining length, bedrock thickness, and overlaying rock lithology remain unchanged, the influence range of the surface movement increases with the increase of the thickness of the loose layer. This shows a positive correlation and a linear relationship. However, when the

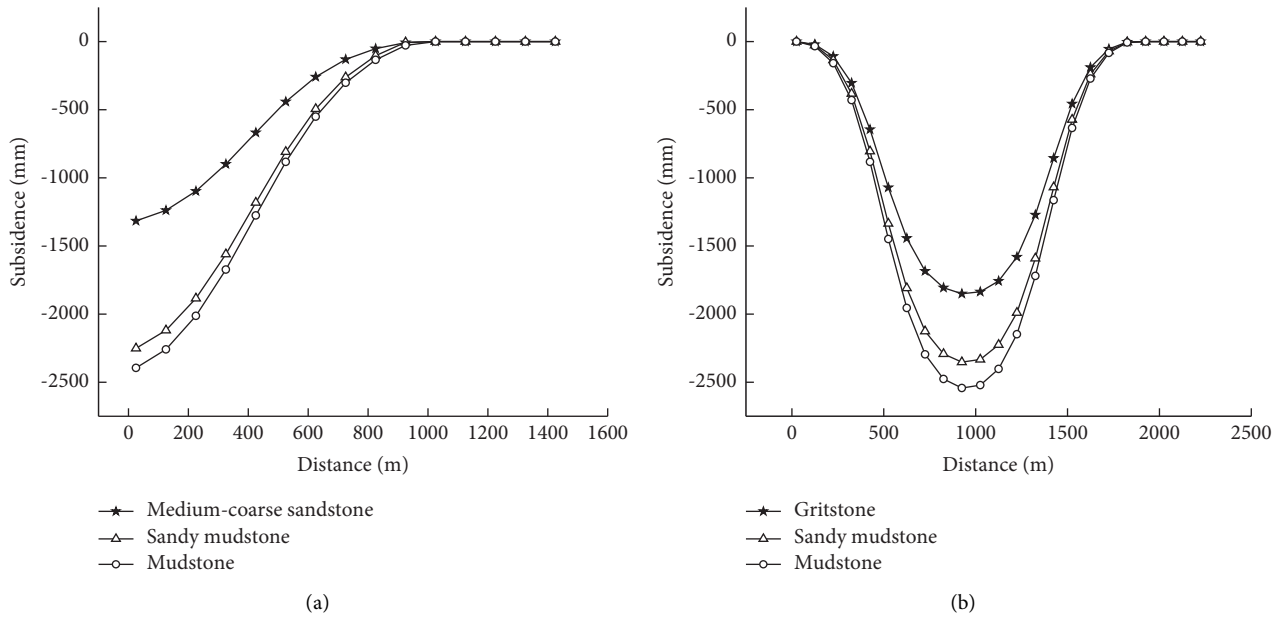

Figure 15: Comparison of subsidence curves of changing rock mechanical parameters. (a) Working face A; (b) working face B.

loose layer reaches a certain thickness, it will lead to too much load to destroy the stability of the bedrock, therefore, essentially causing the secondary subsidence of the surface, and resulting in a sudden increase in the influence range of the surface movement.

(3) On the premise of certain geological and mining conditions, the influence range of the surface movement is negatively correlated with the mining length, and the slope is related to geological and mining conditions. The stress nephogram shows that the pressure arch is formed after the mining. The stability of the pressure arch decreases with the increase of the excavation length, and the subsidence curve becomes steeper, resulting in a smaller influence range of the surface movement.

(4) On the basis of a certain mining length and a constant thickness of the bedrock and loose layer, after replacing the key layer with a relatively weak rock, the influence range of the surface movement shows a slight increase. Based on the four factors, the relationship between the influence range of the surface movement and the geological and mining conditions is given, and the value of parameter d is obtained by substituting it into the formula, and d increases gradually with the weakening of the rock strata.

(5) Integrating machine learning in the numerical model further increases the model throughput. The findings show that machine learning models had high accuracy in predicting surface subsidence, with the random forest trees and regression models having lower time and high accuracy, respectively.

7. Conclusions and Future Work

In this paper, we studied the influence range of mining and analyzed the variations law theoretically and mechanically. The study provided a scientific basis for reasonable coal mining and protection of the surface buildings in the mining area. We also used machine learning methods which were integrated into the numerical model to predict the surface subsidence. On the basis of a certain mining length and a constant thickness of the bedrock and loose layer, after replacing the key layer with a relatively weak rock, the influence range of the surface movement shows a slight increase. We explored the relationship between the influence range of surface movement (L) and geological mining conditions. Through the establishment of a numerical model, the relationship between L and the bedrock and loose layer thickness, working face mining length, and overlying rock lithology is explored by using the control variable method. The results show that L is positively correlated with the thickness and negatively correlated with the mining length.

In the future, we will further investigate the relationship between the influence range of surface movement (L) and geological mining conditions while taking additional parameters into account. The study is based on small amount of dataset, and further data collection approaches should be used to use vast amount of datasets. On the other hand, we will develop machine learning and Internet of Things (IoT) based algorithms to increase the prediction capability of surface subsidence.

Data Availability

The raw/processed data required to reproduce these findings cannot be shared at this time as the data also form part of an ongoing study.

Conflicts of Interest

The authors declare that they have no conflicts of interests.

Acknowledgments

This research was supported by the Shanxi Graduate Education Innovation Project of China under the grant number (2019SY126).

References

[1] X. L. Li, J. Wu, and Y. B. Tian, "The application of FLAC3D in goaf grouting reinforcement," *Safety In Coal Mines*, vol. 44, no. 12, pp. 201–203, 2013.

[2] B. Wang, G. L. Guo, H. Z. Li, and Q. B. Guo, "Numerical simulation on the ratio of backfilling design for lower coal seam backfilling mining," *Metal Mine*, vol. 45, no. 9, pp. 69–72, 2016.

[3] X. J. Liu, "Generating technology of complex geological body FLAC3D model based on GOCAD," *Chinese Journal of Geological Hazard and Control*, vol. 22, no. 4, pp. 41–45, 2011.

[4] Z. H. Shang, S. H. Tang, and W. Y. Jiao, "Failure probability of goaf in large-scale based on simulation of FLAC^{3D}," *Rock and Soil Mechanics*, vol. 35, no. 10, pp. 3000–3006, 2014.

[5] C. Q. Cheng, L. B. Dong, and S. D. Xu, "Simulation and optimization of deep stope mining sequence in hongtoushan copper mine," *Metal Mine*, vol. 45, no. 9, pp. 66–68, 2016.

[6] Q. Ni, N. D. Che, W. R. Yu, J. S. Hou, J. R. Gao, and N. N. Liu, "Deformation analysis and construction optimization of deep foundation pit based on excavation method," *Science Technology and Engineering*, vol. 21, no. 16, pp. 6838–6847, 2021.

[7] X. L. Wang and J. Wang, "Research status and development of numerical simulation on failure characteristics of overburden," *Science Technology and Engineering*, vol. 21, no. 7, pp. 2551–2562, 2021.

[8] J. Liu, B. Y. Hao, and H. Huang, "Study on FLAC^{3D} simulation of mining subsidence laws in working face with large mining width," *Coal Technology*, vol. 33, no. 11, pp. 132–134, 2014.

[9] X. Y. Yu, C. Mu, and D. D. Zhang, "Study on law of surface movement and deformation in thick loose layer with large mining height," *Safety In Coal Mines*, vol. 51, no. 4, pp. 235–239, 2020.

[10] T. J. Zhang, Y. Yu, L. Zhang, and Q. Wang, "Numerical simulation analysis of mining subsidence of mine by FLAC^{3D}," *Coal Technology*, vol. 37, no. 2, pp. 11–14, 2018.

[11] H. Pang and L. J. Xu, "Research on prediction method of surface subsidence in mining area based on FLAC^{3D}," *Coal Technology*, vol. 37, no. 1, pp. 204–206, 2018.

[12] H. F. Hu, *Study on Influence Law and Prediction of Surface Movement of Composite media with Different Soil-Rock Ratio*, Taiyuan university of technology, Taiyuan, 2012.

[13] Y. Zhang, Y. Yan, H. Dai, Y. Zhu, and T. Wu, "Stability and force chain characteristics of "inclined step cutting body" in s," *Applied Sciences*, vol. 11, no. 21, Article ID 10276, 2021.

[14] X. Lian, Y. Zhang, H. Yuan, C. Wang, J. Guo, and J. Liu, "Law of movement of discontinuous deformation of strata and ground with a thick loess layer and thin bedrock in long wall mining," *Applied Sciences*, vol. 10, no. 8, p. 2874, 2020.

[15] M. F. Cai, "Key theories and technologies for surrounding rock stability and ground control in deep mining," *J Min Strat Control Eng*, vol. 2, Article ID 033037, 2020.

[16] K. Z. Deng, Z. X. Tan, Y. Jiang, H. Y. Dai, and Y. Shi, *Deformation Monitoring and Subsidence Engineering*, China University of Mining and Technology Press, Xuzhou, 2014.

[17] G. Q. He, L. Yang, G. D. Ling, F. C. Jia, and D. Hong, *Mining Subsidence Theory*, China University of Mining and Technology Press, Xuzhou, 1991.

[18] Y. Cai, X. Li, W. Xiao, and W. Zhang, "Simulation of mining-induced ground damage using orthogonal experiments to determine key parameters of super-large coalface: a case study in sc," *Applied Sciences*, vol. 10, no. 7, p. 2258, 2020.

[19] S. J. Qin, H. S. Zhang, and G. D. Li, "Analysis on comparison between coal mining subsidence prediction and probability integration based on FLAC^{3D}," *Coal Engineering*, vol. 46, no. 6, pp. 96–98, 2014.

[20] R. J. Finno, F. T. Voss, E. Rossow, and J. T. Blackburn, "Evaluating damage potential in buildings affected by excavations," *Journal of Geotechnical and Geoenvironmental Engineering*, vol. 131, no. 10, pp. 1199–1210, 2005.

[21] C. Liu, H. Li, and H. Mitri, "Effect of strata conditions on shield pressure and surface subsidence at a longwall top coal caving working face," *Rock Mechanics and Rock Engineering*, vol. 52, pp. 1523–1537, 2019.

[22] Q. Cheng, Y. Shi, and L. Zuo, "Numerical simulation and analysis of surface and surrounding rock failure in deep high-dip coal seam mining," *Geotechnical & Geological Engineering*, vol. 37, no. 5, pp. 4285–4299, 2019.

[23] C. Jia, X. Yang, J. Wu, P. Ding, and C. Bian, "Monitoring analysis and numerical simulation of the land subsidence in linear engineering areas," *KSCE Journal of Civil Engineering*, vol. 25, no. 7, pp. 2674–2689, 2021.

[24] W. Guo and F. Xu, "Numerical simulation of overburden and surface movements for Wongawilli strip pillar mining," *International Journal of Mining Science and Technology*, vol. 26, no. 1, pp. 71–76, 2016.

[25] W. Cao, X. Wang, P. Li, D. Zhang, C. Sun, and D. Qin, "Wide strip backfill mining for surface subsidence control and its application in critical mining conditions of a coal mine," *Sustainability*, vol. 10, no. 3, p. 700, 2018.

Hindawi
Scientific Programming
Volume 2022, Article ID 3585162, 7 pages
https://doi.org/10.1155/2022/3585162

Research Article

A Dynamic Multitarget Detection Algorithm in front of Vehicle Based on Embedded System and Internet of Things

Huili Dou[1] **and Guohua Wang**[2]

[1]*Institute of Rail Transit, Zhejiang Institute of Communications, Hangzhou, Zhejiang 310012, China*
[2]*Transportation Mechanical and Electrical Engineering Institute of Planning & Design, Zhejiang Provincial Institute of Communications Planning, Design and Research Co., Ltd., Hangzhou, Zhejiang 310030, China*

Correspondence should be addressed to Huili Dou; wanggh@zjic.com

Received 18 January 2022; Revised 13 February 2022; Accepted 18 February 2022; Published 20 March 2022

Academic Editor: Muhammad Usman

There are few studies for the classification detection and dynamic multitarget detection of the targets in front of vehicles. In order to solve this problem, a dynamic multitarget detection algorithm is proposed. First, a dynamic multitarget detection with displacement at any time is suggested; secondly, a multitarget detection algorithm based on improved You Only Look Once version 3 (YOLOv3) is proposed for the detection of multitarget high probability risk events in front of the vehicle. The YOLOv3 algorithm model is a lightweight backbone network that uses embedded real-time detection technologies. In this paper, we use a lightweight Mobilenetv2 to replace Darknet-53 for feature extraction. Moreover, an optimizer is used for multiobjective feature extraction, group normalization, and multiobjective feature extraction. The results show that in comparison with the original YOLOv3 algorithm, the detection leakage rate of the improved YOLOv3 multitarget detection algorithm is less than 5%, and the amount of model parameters in this paper is reduced by 95% as compared to the traditional data and CPU intertime is reduced to 78%.

1. Introduction

The introduction of smart Internet of Things technology within the traffic management system is essential in light of the rapid expansion of urban modernization [1]. It is inseparable from the support of developing innovations to effectively adapt to the complex and changing traffic management needs. Sophisticated computer system, Internet of Things innovation, telecommunication, automatic control technology, and other technologies have been used to create an intelligent traffic management system. Its features include real-time, accurate, and efficient monitoring. To achieve efficient traffic control, the objective of a smart transportation system is to create an evolutionary combination of three parts of traffic involvement: driver, vehicle, and road [2].

Target detections major function and task are to accurately locate the relevant target object information in an image using location and recognition. The main purpose of the Internet of things is to provide network capabilities to the equipment and supplies used in our daily life to form information networking and interconnections and maintain the coverage of an information network service [3]. Vehicle signal recognition and vehicle information image acquisition in the Internet of things mode mainly focus on dynamic multitarget acquisition, which is the mainstream improvement direction of multitarget detection technology algorithm at present [4]. Traditional target detection technologies, such as hog feature technology combined with support vector machine (SVM), have some problems: first, the region selection strategy of sliding window is lacking pertinence, high time complexity, and window redundancy [5]; the second problem is that the combination of manual design features and object detection has no good robustness [6]. Multitarget detection can achieve a technical breakthrough and improve the intelligent level of automobile driving faster by using an algorithm with

international advanced experience, which is based on the advantages of embedded systems and the deep learning convolution neural network of Internet of things [7]. For using a unified algorithm architecture of pedestrian and vehicle joint recognition technology, it is necessary to adopt highly significant regional or redundancy strategies to select specific targets [8]. Through the multitarget online self-learning tracking and multitarget tracking method, the multitarget recognition in front of the vehicle can be realized, and the technology can automatically upgrade the recognition algorithm to make the system track the target more stably [9]. Some scholars have studied a basic network architecture of single-shot detector (SSD) network and visual geometry group (VGG)-16. The assumption is replaced by residual network Resnet-26, which improves the detection algorithm and the real-time accuracy of traffic detection [10]. Some scholars applied the full convolution network technology to the three-dimensional scanning data to combine the three-dimensional point dimension with the two-dimensional grid as the feature extraction method by forming different 2D end-to-end full convolution networks through the candidate regions and detect the vehicle target and frame and achieved good results. Scholars of vehicle technology proposed to design a feature convolution kernel library composed of multiple forms and color Gabor [11] to train and screen the optimal feature extraction convolution kernel group by replacing the low-level convolution kernel group of the original network, so as to improve the detection accuracy [12]. In the upgrading iteration from single image detection to multitarget image detection, the adaptive threshold strategy is added to reduce the missed alarm rate and false alarm rate and realize the target detection in complex traffic scenes [13]. In addition, there are some innovative researches including traffic hazard's warning sign recognition technology, which turns target detection in complex traffic environment into a method of detection together with signs, forming an effective network combination method.

The above studies solve and put forward relevant methods and specific improvement directions from different angles and technical levels. The main research value of the dynamic multitarget detection algorithm in front of the vehicle in the embedded system combined with the Internet of things lies in the following: a lot of research focuses on how to improve the algorithm, and the detection algorithm of multiple targets is upgraded. The improvement of multitarget detection technology must insist that the multitarget detection algorithm can meet the specific requirements and operation value. Combined with the traffic development trend, single category target detection can no longer meet the needs of the traffic scene in front of the vehicle. The complexity of all target detection has become complex and diverse, and the detection accuracy still needs to be improved. In the next few years, road traffic will be more complex, and it is necessary to find approaches of how to effectively and accurately identify the process of the development using the Internet of things. Thus, the Internet will become more critical when it comes to identifying multiple targets, such as a variety of different vehicles, mixed pedestrians and objects, electric motorcycles, and two-wheeled vehicles which often appear and become dangerous targets, so it is necessary to upgrade and iterate the multi-objective algorithm of vehicle automatic driving technology detection.

By considering the statement of the above problems and according to the analysis of this paper, the target needs to be inspected in front of the vehicle in a complex traffic environment and divided into vehicle dynamic target and vehicle static target. The dynamic target is the displacement in front of the vehicle at any time. The main body applicable to the road includes four-wheel vehicles and two-wheel vehicles. Cars, trucks, and buses are in category of four-wheel vehicles while bicycles, motorcycles, and people are placed in the category of two-wheel vehicles. There are many potential safety problems for pedestrians and cyclists. The static target is about the target that the front of the vehicle will not be displaced. The road auxiliary reference is the traffic signal. The single-stage detection algorithm YOLOv3 algorithm is a basic algorithm aiming at the problem that the model is large and is not suitable for embedded devices; the interfree problem is improved during CPU detection.

The rest of this paper is organized as follows. In Section 2, the basic principle of the proposed algorithm and its optimization is presented. In Section 3, the experimental results are discussed. Finally, this paper is concluded in Section 4.

2. Algorithm Principle and Optimization

The multitarget detection algorithm based on deep learning can be divided into regions with convolutional neural networks (r-CNN) series in terms of detection mode. Its multitarget detection method can adopt the two-stage algorithm via the single-stage detection algorithm represented by YOLO series. The two-stage detection algorithm concept is as follows: first, employ algorithm for location information [14]; secondly, produce classification for category information. According to the proposed model, the focus is on real-time detection [15]. The single-stage detection method introduces a novel concept: the dynamic multitarget image in front of the vehicle is transformed into network output [16] by returning the category of bounding box position in the output layer [17] and transforming multitarget detection problem to regression problem by improving the detection speed [18–20].

2.1. YOLOv3 Algorithm. YOLO is a series of algorithms. YOLOv3 is the third version of YOLO algorithm. The proposed research work has a network structure that describes the YOLOv3 algorithm's principle; the network structure diagram is shown in Figure 1.

YOLOv3 architecture does not use classic backbone network structures such as VGG-16 and Resnet-50. The ImageNet classification is used as the backbone network for object detection. ImageNet is recognized as authoritative datasets for evaluating the capabilities of deep convolutional neural networks. Many new networks are developed to improve the performance of existing networks. The

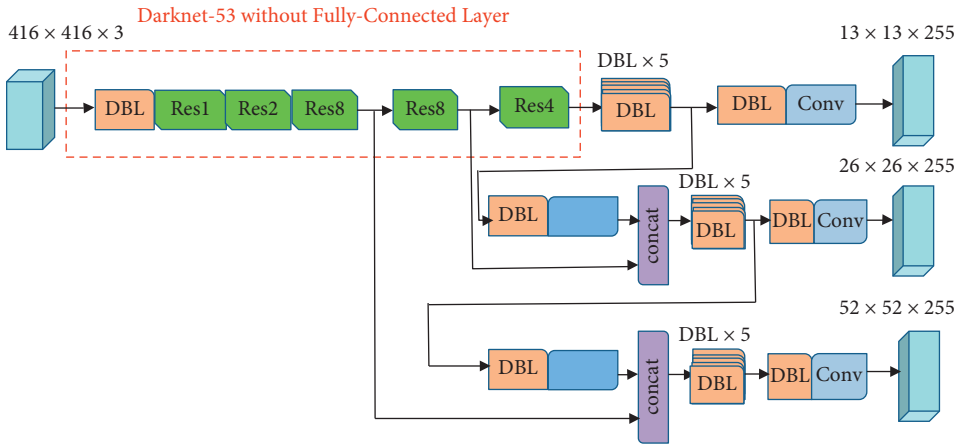

Figure 1: YOLOv3 schematic diagram of algorithm.

proposed model produces a backbone network as the combination of Darknet-53 feature extraction method. The structure of network is shown in Figure 2. The structure of basic YOLOv3 has neither pool layer nor the full connection layer. The front propagation process is size transformation and is realized by changing the step size of convolution layer. The image edge is reduced to half size and the area is reduced to 1/4 of its original size. Using five samples, the characteristic image is 1/32 of the original image. The YOLOv3 algorithm adopts the fixed pattern noise (FPN) idea [21, 22] in the construction by using multiscale targets of different sizes for detection, and as an output, three characteristics of different scales, 13×13, 26×26, and 52×52, are produced, which makes the detection effect of YOLOv3 more significant than that of Yolo algorithm.

By comparing the YOLOv3 algorithm with the fast r-CNN two-order detection algorithm, the former has obvious advantage in terms of detection speed, but there are some shortcomings: the trained model is large, not suitable for embedded devices, and the influence time in the detection under the CPU is high. In order to solve this problem, the following methods are adopted for the optimization of YOLOv3 algorithm. Model optimization is carried out through the aspects of backbone network optimization and model pruning optimization. This paper considers two aspects of optimization, backbone network optimization adjustment and normalized optimization adjustment, as shown in Figure 3.

2.2. Lightweight Improved Model. MobileNetv2 is utilized as the backbone network to replace Darknet-53 for feature extraction in the lightweight model's design. MobileNet has been optimized into Mobilenetv2 [23–25]. The model is useful for resolving the compatibility issue between mobile terminals and embedded devices. MobileNet builds depth neural networks using depth separable convolution, based on the streamlined design. In Figure 3, the first layer is a convolution layer, followed by depth convolution and point-by-point convolution layers. The used lightweight model architecture is the segregated deep neural network.

Set the input feature mapping according to the model F, its size is (DF, DF, M), the standard convolution K used is (DK, DK, M, N), and the output feature map is G, size (DG, DG, N). The standard convolution is calculated by

$$G_{k,l,m} = \sum_{i,j,m,n} F_{k+i-1,l+j-1,m}. \tag{1}$$

The number of inserted channels is M and the number of output channels is N. The corresponding calculation quantity is expressed as

$$\Omega = D_K \cdot D_K \cdot M \cdot N \cdot \cdot DF \ \cdot D_F. \tag{2}$$

The modified standard convolution is K=(D_K, D_K, M, N). Then, it is divided by depth convolution and point-by-point convolution. Specifically, depth convolution is responsible for filtering, and its size is (D_K, D_K, 1, M) and its output characteristic is (D_G, D_G, M). The point-by-point convolution is responsible for the conversion channel, and its size is (1, 1, M, N) and its output is (D_G, D_G, N). The convolution formula of depth convolution is

$$G_{k,l,n} = \sum_{i,j,m} K_{i,j,m,n} \cdot F_{k+i-1,l+j-1,m}. \tag{3}$$

In (3), K is the depth convolution and convolution kernel is (D_K, D_K, 1, M). Among them, m_{th} is the application of convolution kernel in F and m_{th} is the channel, G and m_{th} outside.

The calculated equation of depth convolution and point-by-point convolution is

$$\Omega = D_K \cdot D_K \cdot M \cdot N \cdot D_F + M \cdot N \cdot D_F. \tag{4}$$

From the perspective of comprehensive calculation, the reduction of comprehensive calculation is more obvious. Through the derivation of the above formula, it can be found that the amount of parameters can be significantly reduced by using depth separation convolution. Thus, MobileNet is improved in aspect of linear bottleneck and inverted residual block, as shown in Figure 4.

The algorithms of RELU6 and PW1x1 are introduced in MobileNets, built in the previous portion. For feature

	Type	Filters	Size		Output	
	Convolutional	32	3	3	256	256
	Convolutional	64	3	3/2	128	128
1	Convolutional	32	1	1		
	Convolutional	64	3	3		
	Residual				128	128
	Convolutional	128	3	3/2	64	64
2	Convolutional	64	1	1		
	Convolutional	128	3	3		
	Residual				64	64
	Convolutional	256	3	3/2	32	32
8	Convolutional	128	1	1		
	Convolutional	256	3	3		
	Residual				32	32
	Convolutional	512	3	3/2	16	16
8	Convolutional	256	1	1		
	Convolutional	512	3	3		
	Residual				16	16
	Convolutional	1024	3	3/2	8	8
4	Convolutional	512	1	1		
	Convolutional	1024	3	3		
	Residual				8	8
	Avgpool	Global				
	Connected	1000				
	SoftMax					

Figure 2: YOLOv3 algorithmic network.

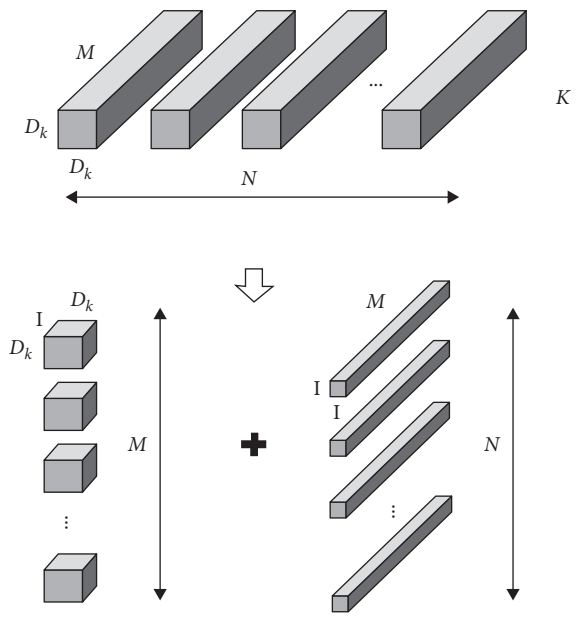

Figure 3: YOLOv3 optimal adjustment of standard convolution to depth convolution.

extraction, the point-to-point convolution feature approach is used with deep convolution [26]. Because calculating the characteristics of DW convolution defines its ability to adjust the number of channels, flowing from the top layer to the output, the improvement primarily involves PW convolution added to DW convolution as illustrated in Figure 5. The number of channels flowing to the upper layer is small. DW can only extract features in low-dimensional space, which is

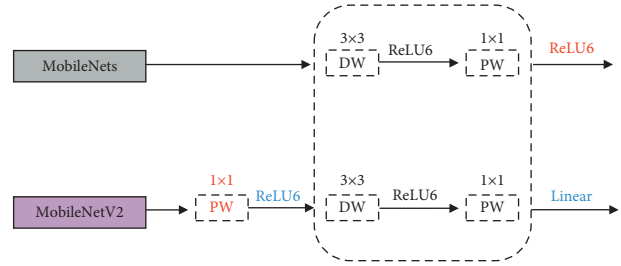

Figure 4: MobileNets microstructure.

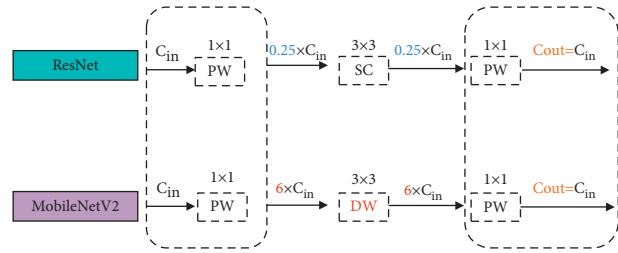

Figure 5: MobileNetV2 microstructure.

not good. Therefore, PW activation function can be added before each DW, generally linear bottleneck, because the activation function can effectively increase nonlinearity in high-dimensional space and destroy features in low-dimensional space. The function of the second PW is dimension reduction.

2.3. Normalization Adjustment. In training of depth convolution neural network, the problems of network deepening, difficult training, and slow convergence arise [27]. BN and GN are shown in Figure 6.

The gradient will disappear when the parameters reach to low level of neural network. Based on BN, the optimization algorithm adds the group normalization method to normalize the same group of the same feature map, while the group is divided into channel dimension. Therefore, the normalization operation is independent from the size of the batch and avoids its influence.

3. Experimental Analysis and Visualization

The experimental platform is divided into two portions, the hardware platform and the software platform. NVIDIA GeForce GTX 1080ti (double) GPU; Intel Core i7-7700 CPU; 32 GB disc Tensorflow1.13.1 GPU deep learning framework; PyCharm Community IDE; Linux-Ubuntu 16.04; and 10 types of targets in the bdd100k data set are analyzed, Python script files are generated, and the seven types of target image data and label files studied in this paper are extracted, all with the goal of studying the dynamic multitarget in front of the vehicle.

3.1. Experiment Data Set. The experimental datasets are shown in Table 1. The statistics of data set adopts instance object, BDD100 K, and team-test. Datasets in the experiment are car, bus, truck, bike, motor, rider, and person.

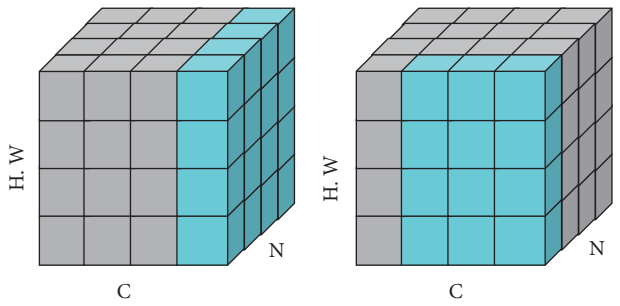

Figure 6: Normalization operation.

Table 1: Data sets used in the experiment.

Instance object	BDD100 K	Team-test
Car	1134567	11876
Bus	17890	1 198
Truck	43689	1092
Bike	11783	913
Motor	4535	716
Rider	6576	6021
Person	138762	7023

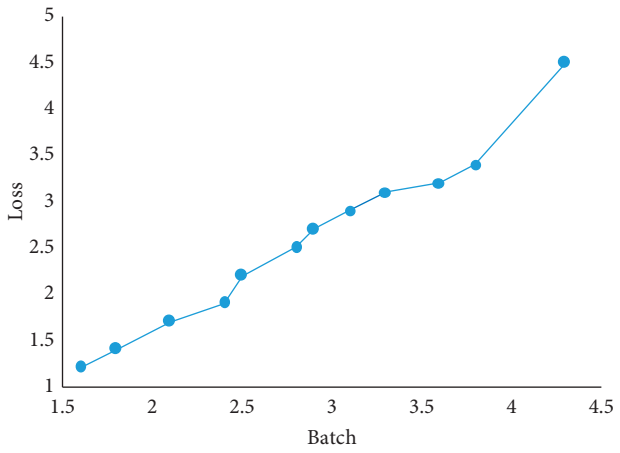

Figure 7: Visual analysis diagram.

3.2. Visual Analysis. Visual analysis is carried out using YOLOv3 algorithm and the optimized YOLOv3 algorithm, respectively. The loss change value of models is recorded, as shown in Figure 7.

After a comparison analysis, it can be shown that using different algorithms introduced in the training process, the optimized algorithms curve change is steeper, the decrease in the curve descent process is slower, and the mitigation algorithm's effectiveness is lowered. Missed detection rate and false detection rate of the target detection test set in the field of unmanned technology environment perception are considered incredibly essential evaluation indicators in the target detection model, which directly increases the model's trustworthiness.

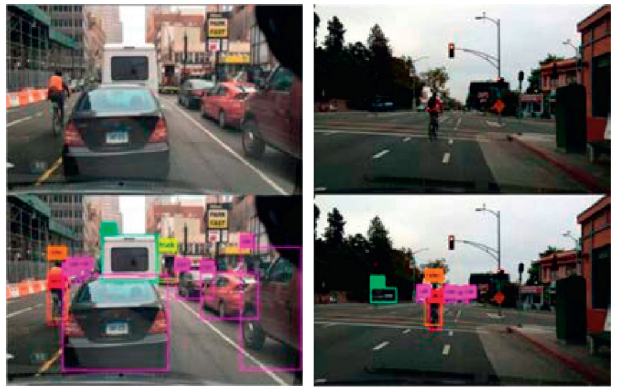

Figure 8: Visualization of real scene detection effect of test object 1.

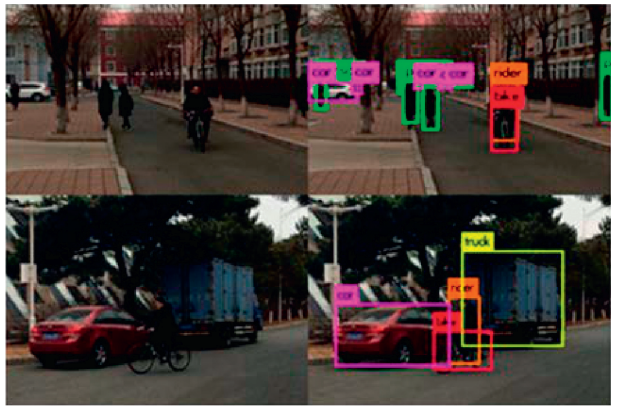

Figure 9: Visualization of real scene detection effect of test object 2.

3.3. Visualization of Target Detection. The visualization of target detection effect is shown in Figures 8 and 9, the algorithm YOLOv3 MobileNetV2 obtains YOLOv3, and the model visualizes the dynamic multitarget detection in front of the test object vehicle.

In the real scene detection effect, I Xian multitarget detection can be carried out, including all detection objects such as cars, trucks, bicycles, pedestrians, and motorcycles. The effect of multitarget detection in front of vehicles has been significantly improved, which is proved in experiments. The algorithm YOLOv3 MobileNetV2 obtains YOLOv3. The model has significantly improved the visualization of dynamic multitarget detection in front of the test object vehicle.

4. Conclusion

A dynamic multitarget detection algorithm in front of vehicle based on improved YOLOv3 is proposed in this paper. The lightweight network MobileNetv2 is used as a replacement of Darknet-53 to form the backbone network for feature extraction; the normalization and optimizer are adjusted to accelerate the convergence of the network. The optimization algorithm trained the two models and from the

perspectives of loss visualization, missed detection rate and false detection rate, model size, and effect time, the fundamental algorithms are compared and analyzed. The experiments show that the optimization model constructed in this paper improved by 0.5% in the map, the parameter quantity is reduced to about 89% compared with the YOLOv3 basic model, and the influence time under the CPU is reduced to about 70%. The visualization of test set and actual scene detection qualitatively verifies that the proposed algorithm has a good detection effect for dynamic multitarget detection in front of the vehicles. From the current research in the field of intelligent networked vehicle environment perception, the image level research is using camera as a sensor, including target detection, target tracking, and semantic or instance segmentation. There is still room for improvement in accuracy and speed, the common practice in the industry is sensor fusion, which matches and fuses the cloud information obtained by radar with the image information obtained by the camera to achieve higher perception accuracy. The significance of this paper is that it can optimize the speed of camera sensor target detection, saved computing time, and space for the subsequent fusion. In this paper, the algorithm is only for those embedded systems that are based on the environmental detection and has not been transplanted to the other embedded platforms, and the robustness of the model has not been specifically analyzed. The follow-up research will focus on this aspect.

Data Availability

The datasets used and/or analyzed during the current study are available from the corresponding author on reasonable request.

Conflicts of Interest

The authors declare that they have no conflicts of interest.

References

[1] M. Ibrar, A. Akbar, R. Jan et al., "Artnet: Ai-based resource allocation and task offloading in a reconfigurable internet of vehicular networks," *IEEE Transactions on Network Science and Engineering*, vol. 9, no. 1, pp. 67–77, 2020.

[2] Z. Wang and Y. Ma, "Detection and recognition of stationary vehicles and seat belts in intelligent Internet of Things traffic management system," *Neural Computing & Applications*, vol. 34, no. 5, pp. 3513–3522, 2021.

[3] A. J. Moshayedi, A. Kolahdooz, and L. Liefa, *Unity in Embedded System Design and Robotics: A Step-by-step Guide*, CRC Press, Routledge, 2022.

[4] Y. Ye, Q. Wang, and J. Wang, "Green city air monitoring and architectural digital art design based on IoT embedded system," *Environmental Technology & Innovation*, vol. 23, Article ID 101717, 2021.

[5] J. D. J. C. Robles, I. Torres-Zúñiga, J. G. Avina-Cervantes, and M. A. Ibarra-Manzano, "FPGA-based architecture to estimate the input glucose in a dark fermenter using a super-twisting observer," *Microprocessors and Microsystems*, vol. 85, Article ID 104297, 2021.

[6] P. Singh and N. Senroy, "Steady-State models of STATCOM and UPFC using flexible holomorphic embedding," *Electric Power Systems Research*, vol. 199, Article ID 107390, 2021.

[7] N. Niu, F. Fu, B. Yang et al., "DLBF: A low overhead wear leveling algorithm for embedded systems with hybrid memory," *Microelectronics Reliability*, vol. 123, Article ID 114154, 2021.

[8] B. Zeng, Z. Zhang, X. Zhang, and J. Xiang, "Design of refueling control system with multi-controlterminal based on network," *Electronics*, vol. 10, no. 13, p. 1559, 2021.

[9] W. Huang, C. Zhang, X. Wu, J. Shen, and Y. Li, "The detection of defects in ceramic cell phone backplane with embedded system," *Measurement*, vol. 181, Article ID 109598, 2021.

[10] R. Tabish, J.-Y. Wen, R. Pellizzoni et al., "An analyzable intercore communication framework for high-performance multicore embedded systems," *Journal of Systems Architecture*, vol. 118, Article ID 102178, 2021.

[11] J. Shi, J. Bian, J. Richter et al., "MODES: Model-based optimization on distributed embedded systems," *Machine Learning*, vol. 110, no. 6, pp. 1527–1547, 2021.

[12] E. Cardillo, C. Li, and A. Caddemi, "Embedded heating, ventilation, and air-conditioning control systems: From traditional technologies toward radar advanced sensing," *Review of Scientific Instruments*, vol. 92, no. 6, Article ID 061501, 2021.

[13] M. Calixto-Rodriguez, J. S. V. Martínez, M. A. Meneses-Arcos et al., "Design and development of software for the SILAR control process using a low-cost embedded system," *Processes*, vol. 9, no. 6, p. 967, 2021.

[14] J. Kim and J. Cho, "Low-cost embedded system using convolutional neural networks-based spatiotemporal feature map for real-time human action recognition," *Applied Sciences*, vol. 11, no. 11, p. 4940, 2021.

[15] Z. Zhang, X. Wang, Q. Hao et al., "High-efficiency parallel cryptographic accelerator for real-time guaranteeing dynamic data security in embedded systems," *Micromachines*, vol. 12, no. 5, p. 560, 2021.

[16] J. H. Choi, K. M. Kim, and J. W. Kwak, "TA-CLOCK: Tendency-aware page replacement policy for hybrid main memory in high-performance embedded systems," *Electronics*, vol. 10, no. 9, p. 1111, 2021.

[17] S. Luo, L. Zhang, and Y. Fan, "Dynamic multi-objective scheduling for flexible job shop by deep reinforcement learning," *Computers & Industrial Engineering*, vol. 159, Article ID 107489, 2021.

[18] W. Yin, Z. Ming, and T. Wen, "Scheduling strategy of electric vehicle charging considering different requirements of grid and users," *Energy*, vol. 232, Article ID 121118, 2021.

[19] Z. Li, C. Peng, G. Yu, X. Zhang, Y. Deng, and J. Sun, "Detnet: A backbone network for object detection," arXiv preprint arXiv:1804.06215, 2018.

[20] A. Thamallah, A. Sakly, and F. M'Sahli, "Dynamic multiobjective matrix control for a class of switched systems," *Transactions of the Institute of Measurement and Control*, vol. 43, no. 10, pp. 2229–2245, 2021.

[21] H. Liu, Y. Wang, S. Liu, Q. Liu, Y. Xie, and X. Ma, "May. Research on multi-objective optimal scheduling strategy of photovoltaic and energy storage based on dynamic programming," *IOP Conference Series: Earth and Environmental Science*, vol. 781, no. No. 4, IOP Publishing, Article ID 042011, 2021.

[22] M. Chen and Y. Ma, "Dynamic multi-objective evolutionary algorithm with center point prediction strategy using ensemble Kalman filter," *Soft Computing*, vol. 25, no. 7, pp. 5003–5019, 2021.

[23] W. Yankai, W. Shilong, L. Dong, S. Chunfeng, and Y. Bo, "An improved multi-objective whale optimization algorithm for the hybrid flow shop scheduling problem considering device dynamic reconfiguration processes," *Expert Systems with Applications*, vol. 174, Article ID 114793, 2021.

[24] B. H. Nguyễn, T. Vo-Duy, C. H. Antunes, and J. P. F. Trovão, "Multi-objective benchmark for energy management of dual-source electric vehicles: An optimal control approach," *Energy*, vol. 223, Article ID 119857, 2021.

[25] A. Ahrari, S. Elsayed, R. Sarker, D. Essam, and C. A. C. Coello, "A heredity-based adaptive variation operator for reinitialization in dynamic multi-objective problems," *Applied Soft Computing*, vol. 101, Article ID 107027, 2021.

[26] H. Karimi, R. Bahmani, and S. Jadid, "Stochastic multi-objective optimization to design optimal transactive pricing for dynamic demand response programs: A bi-level fuzzy approach," *International Journal of Electrical Power & Energy Systems*, vol. 125, Article ID 106487, 2021.

[27] L. Zhang, J. Lu, and Z. Yang, "Optimal scheduling of emergency resources for major maritime oil spills considering time-varying demand and transportation networks," *European Journal of Operational Research*, vol. 293, no. 2, pp. 529–546, 2021.

Hindawi
Scientific Programming
Volume 2022, Article ID 4959930, 19 pages
https://doi.org/10.1155/2022/4959930

Research Article

Development of Public Administration Research with a Bibliometric Analysis

Zepeng Yu

Department of Information Resources Management, School of Public Affairs, Zhejiang University, Hangzhou 310058, Zhejiang, China

Correspondence should be addressed to Zepeng Yu; yuzp@zju.edu.cn

Received 16 December 2021; Revised 8 February 2022; Accepted 11 February 2022; Published 18 March 2022

Academic Editor: Muhammad Usman

Recently, several studies adopted bibliometric methodology to estimate the development of the field of public administration (PA). However, only a small scope of journals was covered in their analyses. Few of those investigated the evolution of the entire field. To make a progress, this paper included a 19-year timespan, 53 journals, and more than 20,000 items for analysis in a bibliometric way. Both the activity and the quality indicators of research results were applied from the bibliometric perspective with 3-year and 5-year citation windows at three aggregation levels including journal, country, and institution by using publications in PA indexed in Social Sciences Citation Index (SSCI). "Resident" journal is proposed as a new concept to explore differences between traditional and emerging research forces. The results suggest that resident journals maintain a large advantage over other journals in terms of higher quality journal indicators and citation impact indicators. Moreover, international and national collaboration shows a growth tendency, especially for the international type. The majority of active institutions are from the US and the UK, which indicates their dominant position over others. This study provides more comprehensive comparisons through large-scale data and acknowledged methods to explore the development of PA field research.

1. Introduction

As a practice-oriented field, public administration has the characteristics of comprehensiveness and interdisciplinary, which means that PA field usually absorbs the knowledge, concepts, theories, and methods from other fields. To better describe and analyze the research results in this field, several studies tried to introduce bibliometric methodology to estimate the development of PA.

One common carrier of the progress of a discipline or a field is a journal, which indicates the cohesion of authors and topics around a novel area of inquiry [1]. By exploring the evolution of important journals in the field, we can begin to weave the history of a field. For instance, bibliometric methods are employed to inspect the path of the field of PA via an analysis of articles published in the journal named Public Administration Review (PAR) from 1940 to 2013 [2]. PAR is well-matched for this analysis given its historical position as one of the oldest of the 53 journals in PA field indexed in the Web of Science (WoS).

In the fields of library and information science, there are three most common terms: bibliometrics, scientometrics, and informetrics [1]. Although the three have different research objects and purposes, they have the same origin and are based on common principles, methods, and tools. Among the three terms, bibliometrics and scientometrics are the most similar, and the research fields overlap to a considerable extent, but there are also some differences. Bibliometrics is a series of methods for researching and measuring bibliographic information, while scientometrics focuses on the quantitative aspect of scientific research. From the perspective of research objects and content, scientific and technological research results are often recorded in the literature, which means that those literatures become the intersection of bibliometric and scientometric research. However, the research object of bibliometrics is always scientific and academic literature, while scientometrics also pays attention to the activities of scientific researchers, scientific research management, the role of science and technology in the national economy, and technology policy.

This study tries to introduce bibliometric and scientometric methodology to PA. The number of journals is expanded to 53 journals of the entire PA field, and the period is extended to 19 years. In addition, 19-year annual lists of journals in PA in Journal Citation Report (JCR) are used as the criteria to select journals. Although these lists change yearly, it is found that some journals always stay in the lists. To differentiate these journals from the others, these stable journals are termed as "resident" and the others as "nonresident." This study also provides some insight into the impact of publications that appeared in three datasets (i.e., resident, nonresident, and total journals).

To provide a comprehensive and accurate definition of influence, this study estimates publications in a bibliometric way. Both the activity and the quality of research are used. The former is measured by the productivity of publications, and the latter results from Journal Impact Factors (JIF) quartile indicators and citation impact indicators. More importantly, the extended scope makes it possible to discuss the contribution of countries and institutions in PA. Specifically, this study focuses on three aggregation levels (including journal, country, and institution levels) of publications in PA to answer the following questions:

(i) Can resident journals datasets represent the entire field of PA?

(ii) What are the active countries in PA? Does the proportion of coauthorship remain low as previous studies mentioned?

(iii) What are the active institutions in PA? Are they consistent with the active institutions mentioned in previous studies?

As a diachronic analysis, this study focuses on several bibliometric features, including paper productivity, active countries and institutions, authorship patterns, and citation patterns.

The subsequent sections of this paper are organized as follows. Section 2 gives a review of relevant research in PA and illustrates some of the existing classic studies in bibliometrics. Section 3 presents the data and methods employed in the study. Section 4 shows the results, the fifth section is about the discussion, and the final section concludes the research.

2. Literature Review

In the PA field, there is a typical and traditional practice that attempts to determine the impact of literature in a subjective way to evaluate research results. However, scholars represented by Bozeman criticized the practice [3]. They argued that obtaining opinions on research results from the subjective evaluations of a small number of scholars is likely to be subject to subjective bias, and the results may also vary widely among respondents. The debate reflects the dilemma of traditional methods of evaluating research results in PA. In this regard, Bozeman proposed another improved idea, which is to introduce relevant methods in bibliometrics into the evaluation of research results and describe the characteristics of research results in an objective way.

In terms of research objectives, bibliometrics mainly focuses on the regularity of documents in the process of utilization and communication, while scientometrics focuses more on analyzing the regularity of the amount of scientific information generation, dissemination, and utilization, to better understand the mechanism of scientific research.

Inspired by the call of Bozeman [3], some studies began to adopt bibliometric methods to PA. For instance, Powell [4] analyzed five leading journals in the field of social policy. It was reported that more than half of the articles were written by authors from the UK, and most of the rest came from other parts of Europe. Ni et al. [2] analyzed 3,934 articles published in PAR journals from 1940 to 2013. They reviewed the research progress of the journal for more than 70 years through citation analysis, collaborative network analysis, keywords analysis, and other technologies. It was a substantial attempt of bibliometric methods in PA. However, only one journal was covered in their work, which was hard to provide a comprehensive evaluation of PA.

Currently, the application of bibliometric methods to PA mainly stays at the level referred to one or several journals, but few studies have analyzed the entire field. This study reviewed six studies published from 2010 to 2017 as shown in Table 1.

There was only one study by Corely and others [5] that sorted out the entire PA field, whose focus was merely on output and authorship analysis. In general, a bibliometric research has a focus on several analyses on productivity, authorship, citation, and social network. However, only one research conducted by Ni et al. [2] involved all the above analyses. It is essential to find some bibliometrics and scientometrics methods that might be applied in PA. Mingers and Leydesdorff [1] presented a comprehensive review of the theory and practice of scientometrics. In terms of the analysis of collaboration and citation impact, some researchers suggested that the research unit should be distinguished in different aggregation levels [10–12]. These units range from macro-level to micro-level, including countries, institutions, research groups, and individual researchers.

Publications coauthored by more than one research unit can be analyzed to examine the research collaboration between the research units. Based on the bibliometric data of about 4.5 million articles in 56 subject categories in SSCI, Henriksen [13] found that the average number of authors, as well as the proportion of coauthored and internationally coauthored publications, increased in most categories. However, there are large variations among disciplines to the extent of the increasing proportion of coauthorship. The coauthorship has generally increased in the category with a high proportion of international coauthorship, but the increased international coauthorship is not the only factor that affects the growth of the author's collaboration.

Citation analysis based on citations received by scientific publications typically uses citation impact indicators to assess the scientific influence. Waltman [12] gave an in-depth review of the literature on citation impact indicators. Citation impact indicators are based on analysis of citations obtained from all

Table 1: The application of bibliometrics in some research in PA in 2010–2017.

Authors	Publication year	Time span	Coverage	Indicators
Corley and Sabharwal [5]	2010	1973–2007	23 journals	No. of publications, no. of citations of authors, impact factor of authors
Raadschelders and Lee [6]	2011	2000–2009	1 journal, PAR	No. of publications, proportions of publications,
Gulrajani and Moloney [7]	2012	1996, 1999, 2002, 2005, 2008	10 journals	No. of publications, proportions of publications
Adams et al. [8]	2014	1980s, 2007–2010	2 journals in public policy	No. of publications, no. of citing items, no. of cited items, proportion of gender
Adams et al. [9]	2016	2009–2013	7 journals in public policy	No. of citing items, no. of cited items
Ni et al. [2]	2017	1940–2013	1 journal, PAR	No. of publications, proportion of publications, no. of authors, proportion of coauthored items.

publications published by a research unit. Well-known examples of impact indicators are JIF and h-index [14, 15].

Citation impact indicators can be classified into size-dependent and size-independent indicators. Size-dependent indicators are designed to provide an overall performance measure. These indicators will never decrease when new publications are added. On the other hand, size-independent indicators are intended to provide an average performance measure for each publication, which is often used to compare units with different sizes, such as comparing between a small research unit and a large one [12]. Mean-based indicators are one type of size-independent indicator, including impact factors, mean normalized citation score (MNCS), and relative citation rate (RCR), but all of them are criticized in the literature [16]. The citation distribution of a publication set tends to be highly skewed, so the average number of citations may be heavily influenced by one or a few most cited publications [17, 18].

Percentile-based methods (quartiles, percentiles, percentile rankings, or percentile ranking classes) have been proposed as a nonparametric alternative to parametric mean-based approaches [19]. Percentiles are based on an ordered set of citation counts in a reference set, whereby the proportion of publications at or below the citation counts of a certain publication is used as an indicator for its relative citation impact. For a given publication, the average citation counts are not used to normalize it. On the contrary, publications similar to it are grouped into a reference set, and the citation impact is calculated by its rank in the citation distribution of the set [20].

The Leiden Ranking is a famous university ranking at the institution level based on bibliometrics, made by the Centre for Science and Technology Studies (CWTS) of Leiden University. Nearly 1,000 major universities worldwide have been covered by the 2018 edition of the ranking. Because of the mature way of ranking, this paper will select some methods and indicators of the Leiden Ranking (e g., $PP_{top\ 1\%}$ and $PP_{top\ 10\%}$) for research evaluation at the country and institution levels [18].

3. Methods

3.1. Data Collection. The study is based on data from the Web of Science (WoS) database from Clarivate Analytics. There are two document types (i.e., article and review) included, which are regarded as citable items for citation analysis. Publications in a 19-year period indexed in SSCI of WoS are used for analysis. Timespan is set from 1998 to 2016 for two reasons. Firstly, the institution with which the authors affiliate only purchases SSCI starting from 1998. Secondly, data in a 19-year period can serve to trace and analyze the evolution of the field.

JCR in WoS is used to determine the field of PA and the scope of journals. According to journal lists of JCR 1998–2016, journals in PA have changed almost every year. With journals added and removed in the period, the number of journals increases from 24 in 1998 to 47 in 2016, and 53 journals are involved totally. The 53 English language journals were all included in this study to cover all journals in PA.

In JCR 1998–2016, the list of journals in PA varies over time, and some journals on the list also experienced several changes (e.g., the full name of journal *Governance* changed in the year 2008, while ISSN of *Journal of Homeland Security and Emergency Management* changed since 2012) in this period. To recognize those journals clearly, 54 ISSNs are used to retrieve and screen data in SSCI. The process is shown in Figure 1.

According to the steps mentioned above, 23,243 items (including 22,690 articles and 553 reviews) were downloaded on Jan 13th, 2018. The criteria to determine whether a publication belongs to PA are that the journal where the publication was published should be in the PA journal list in its publication year. For example, an article published in the Policy Studies in 2010 was not included in the dataset of this study, because the journal was included in the PA journal list since the year 2011. According to the above criteria, filtered data contains 20,980 items, involving 20,480 articles and 500 reviews. For statistical analysis, a statistical software, Statistical Product and Service Solutions (SPSS) v23.0, was utilized.

3.2. Journal Classification. In this paper, two methods were used to classify journals. The first is based on the appearance of journals in the annual lists of PA. Although the lists have changed almost every year, still it was found that 24 journals

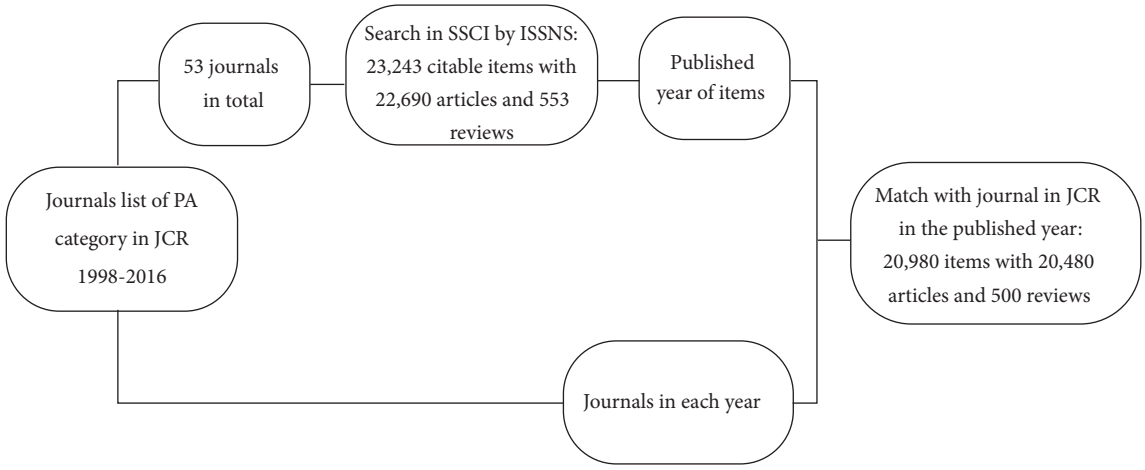

Figure 1: Retrieving and screening process.

have been staying on the lists for the past decade (i.e., 2007–2016). To distinguish them from others, they were labeled as "Resident" journals, while the other 29 journals were named as "nonresident" journals. All publications were grouped into three datasets as follows:

(i) Dataset I: dataset with data from 53 journals in total

(ii) Dataset II: dataset with data from 24 resident journals

(iii) Dataset III: dataset with data from 29 nonresident journals

The subsequent analysis listed the contributions of countries and institutions in the three datasets to reflect their performance. A list of the 53 journals is illustrated in Table 2 and resident journals are specifically noted with a symbol †.

The second classification is related to the JIF values of journals in JCR 1998–2016. Journals were assigned to the four quartiles 1, 2, 3, and 4, based on their JIF rankings in PA. Referring to the study by Zhou and Lv [21], journals in higher rankings (i.e., Q1 and Q2) were named as higher quality journals and those in Q3 and Q4 as lower-quality journals when it was essential. Publications on higher quality journals can be considered of higher quality, although not always true. The reason is that not all publications in a higher quality journal are of higher quality than those in a lower-quality journal. Therefore, we assumed that a country with more publications in higher quality journals has more competitive capacity. The JIF quartile indicator was used to reflect the influence of major contributors.

3.3. Research Unit. In practice, the record in the WoS often contains an author information field and an affiliation field. The names of authors and the addresses corresponding to authors are recorded in the affiliation field. An address often contains information about a country, an institution, and even a postcode. To make full use of the information, the research unit in this study mainly involves two aggregation levels: country and institution. The active countries and institutions were analyzed as the active players in PA.

The affiliation of authors is based on the corresponding information in the address field of WoS data. Two countries need to be further clarified. The first is the UK. The address of an author from England, Scotland, Wales, and Northern Ireland was classified into the UK. The second one is China. An author who comes from mainland China, Hong Kong, and Macao was regarded as the one from the Peoples Republic of China, or China in short. Because the year 1998, which this study starts from, is later than 1997 (the year when Hong Kong returned to China), the earliest publication from Macao was published in 2000 later than 1999 (the year when Macao returned to China).

In the identification and correction process for institutions, different variants of an organization's name were identified, including abbreviations, misspellings, historical name changes, and classified into the same institution. Additionally, as mentioned by Ni et al. [2], there is a confusion of organization between system-level and campus-level. To facilitate the distinction, we correct the organizations with the reference to some popular university rankings. The records with system-level organizations were identified and split into campus-level institutions.

There are two typical instances. (i) The University of London is a system-level institution whose records are assigned to campus-level institutions, such as the London School of Economics and Political Science (LSE), University College London (UCL), and Imperial College London. (ii) The records affiliated to Indiana University System are split as campus-level institutions, including Indiana University Bloomington and Indiana University Purdue University Indianapolis (IUPUI).

Referring to some research [10, 22], publications can be divided into two categories: single-authored and coauthored. In addition, publications can also be divided into two categories: national and international. By combining these two dimensions, four types of publications are classified. Together with the type of publications without affiliation information, five types of items are shown in Table 3.

Despite the perfect records in the WoS in recent years, there are still problems in early records, which did not

Table 2: Journals' ranks in the field of public administration in JCR from 1998–2016 (in rank order by JCR 2016).

Rank	JCR abbreviated title	1998	1999	2000	2001	2002	2003	2004	2005	2006	2007	2008	2009	2010	2011	2012	2013	2014	2015	2016
1	J PUBL ADM RES THEOR †						14	7	1	2	1	2	2	2	2	2	1	1	1	1
2	PUBLIC ADMIN REV †	8	5	3	4	4	7	8	5	3	3	3	9	14	16	20	16	6	5	2
3	J POLICY ANAL MANAG †	5	4	6	3	3	1	2	8	4	2	5	4	1	12	3	3	2	3	3
4	J EUR PUBLIC POLICY †		2	1	1	2	6	5	12	7	4	1	6	7	8	9	11	7	7	4
5	PUBLIC ADMIN †	7	8	7	11	6	3	3	7	5	7	6	8	12	4	12	4	11	8	5
6	REGUL GOV															5	12	8	4	6
7	CLIM POLICY †							10	4	19	12	9	5	6	11	7	6	9	6	7
8	GOVERNANCE †	3	7	5	7	1	4	1	2	10	9	8	3	4	6	6	8	4	2	8
9	PUBLIC MANAG REV †										21	12	14	11	15	17	10	16	9	9
10	POLICY STUD *J* †	19	21	16	19	23	24	20	14	11	18	19	23	13	3	16	2	5	10	10
11	POLICY POLIT †	4	6	10	5	5	5	9	9	8	8	20	22	25	22	25	13	18	19	11
12	J PUBLIC POLICY														20	14	18	19	23	12
13	ENVIRON PLANN C †	10	9	8	8	13	9	16	18	12	16	13	11	15	9	15	15	10	11	13
14	POLICY SCI †	16	11	24	14	17	10	12	15	14	15	10	16	8	1	13	9	3	12	14
15	INT PUBLIC MANAG J													3	24	8	25	22	16	15
16	J EUR SOC POLICY											7	7	5	7	4	5	12	13	16
17	REV POLICY RES													10	23	10	20	15	20	17
18	SCI PUBL POLICY															18	21	17	16	18
19	PUBLIC POLICY ADMIN																			19
20	REV PUBLIC PERS ADM													19	33	20	14	14	18	20
21	J SOC POLICY †	2	3	2	6	7	2	6	6	6	5	14	12	16	10	11	7	21	21	21
22	AM REV PUBLIC ADM †	15	24	17	14	16	22	15	13	16	12	16	15	17	14	22	22	13	15	22
23	INT REV ADM SCI †	14	22	22	17	20	16	21	22	21	22	15	17	21	18	31	24	27	33	23
24	J ACCOUNT PUBLIC POL													25	13	24	19	32	14	24
25	SOC POLICY ADMIN												13	20	28	19	17	23	22	25
26	NONPROFIT MANAG LEAD														27	37	38	34	35	26
27	PUBLIC MONEY MANAGE †	17	10	9	9	10	11	11	10	17	11	23	26	23	25	22	27	33	32	27
28	POLICY SOC																33	37	24	28
29	ADMIN SOC †	12	12	19	10	12	15	22	11	9	10	11	10	18	19	35	26	26	26	29
30	AUST *J* PUBL ADMIN †	18	15	20	24	18	20	23	19	20	23	18	21	24	29	32	35	38	34	30
31	J COMP POLICY ANAL														31	34	36	30	36	31
32	PUBLIC PERS MANAGE †	23	18	23	23	15	21	24	24		25	24	29	34	34	41	42	42	38	32
33	LOCAL GOV STUD †										20	20	18	29	35	26	28	24	29	33
34	CONTEMP ECON POLICY †	6	13	14	18	11	13	17	17	15	17	22	20	28	26	27	32	36	37	34
35	PUBLIC ADMIN DEVELOP †	20	16	13	12	9	8	14	16	13	14	25	24	22	21	28	23	20	28	35
36	PUBLIC PERFORM MANAG														32	33	39	28	25	36
37	LEX LOCALIS														39	39	30	25	30	37
38	CAN PUBLIC POL †	13	19	18	21	14	18	18	20	18	26	26	28	32	37	29	28	29	39	38
39	POLICY STUD-UK														17	36	37	35	27	39
40	HUM SERV ORG MANAGE																		41	40
41	J HOMEL SECUR EMERG											17	19	31	29	38	40	39	40	41
42	TRANSYLV REV ADM SCI													33	40	40	31	41	43	42
43	CAN PUBLIC ADMIN †	24	14	21	22	21	17	26	25	23	27	28	30	30	36	42	41	40	42	43
44	GEST POLIT PUBLICA												27	38	42	45	44	46	46	44

Table 2: Continued.

Rank	JCR abbreviated title	1998	1999	2000	2001	2002	2003	2004	2005	2006	2007	2008	2009	2010	2011	2012	2013	2014	2015	2016
45	REV CLAD REFORMA DEM													35	41	44	43	44	45	45
46	CIV SZLE												31	36	43	43	45	43	44	46
47	AMME IDARESI DERG												32	38	45	47	46	45	47	47
48	J COLLECT NEG PUB SE	22																		
49	PHILOS PUBLIC AFF	1	1	4	2	8	12	4	3	1	6	4	1	9	5	1				
50	SOC SECUR BULL	9	20	15	16	24		13												
51	INNOVAR-REV CIENC AD													37	44	46				
52	PUBLIC INTEREST	11	17	12	13	19	23	19	21		19									
53	ADMIN SOC WORK	21	23	11	20	22	19	25	23	21	24	27	25	27	38	30	34	31	31	

Notes: A journal with symbol † means a resident journal.

Table 3: Definition of five types of authorship.

	Type of authorship	Indicators
I	Internationally coauthored publication	P_{IC}
II	Nationally coauthored publication	P_{NC}
III	Internationally single-authored publication	P_{IS}
IV	Nationally single-authored publication	P_{NS}
V	Publication with no affiliation information	P_{NA}

contain author or affiliation information. Therefore, two cases of data were marked and processed as follows.

Case 1. There were three items that contained an empty author information field. After analyzing each item, it was found that all of them were written by Perri Six, a noted social scientist in the UK. After manual identification, the three publications were included in this study.

Case 2. The items contained an empty affiliation field, resulting in the number of some countries being counted as zero. It means that these countries were excluded when analyzing active countries and institutions but included in other analyses at the journal level. The total number of such items was 949, accounting for 4.08% of the total number.

The lack of affiliation information is due to two reasons: first, there were two main objective reasons that the authors of a publication forgot to add affiliation information when it was submitted, or the database did not save this information at an earlier time. Second, subjective reasons are much more complicated, including the author's judgment on the contribution of a publication and considerations for protecting personal privacy. We cannot manually add it, even if an author's affiliation is specific at a certain time, since it is likely to be the author's deliberate choice to hide affiliation information, and the institutional contribution to the publication should be subjectively judged by its authors.

3.4. Citation Analysis. Citation analysis is a common method of research evaluation, using some indicators such as total citations, citations per publication, and the proportion of highly cited publications. This study focused on the citation impact of resident journals and the total journals dataset to evaluate the performance of some countries as a way to reflect influence.

The citation window is a time window for counting the citations of a publication. There are different citation patterns in different fields. A 3-year window is a good trade-off choice among different fields [23]. Bornmann, et al. [19] suggested that a reliable approximation for long-term citation impact (e.g., correlation coefficient $r \geq 0.8$) requires a citation window of at least 5 years. Waltman [12] believes that the general approach is to use a 5-year window. Given that PA is a discipline in the social sciences, both 3-year and 5-year windows were adopted to better reflect the citation patterns in PA.

Citation data included in this study is from the WoS in the period 1998–2017. According to the definition of citation window, only the data in 1998–2015 is available when the 3-year window is used, and only the data in 1998–2013 is included when the 5-year window is used.

This work used both mean-based and percentile-based indicators. Citation per publication (CPP) is a frequently used mean-based indicator that intuitively reflects the average citations that a set of publications received from publications. A set of publications can be defined at different aggregation levels and periods. The citation impact of the research unit can be illustrated by analyzing its corresponding set of publications.

The proportion of highly cited publications is a form of percentile-based indicator. Reference sets used in the percentile-based approach are defined as a set of publications in the same field, same publication year, and same document type. A percentile-based indicator is usually defined and named by a specific threshold for the indicator, including top 1%, 5%, and 10%. According to the calculation of percentiles drawn from the Leiden rankings [24], all the three indicators are included, labeled as $PP_{topx\%}$.

4. Results

To provide a clear picture to answer the questions mentioned in the first section, this part is organized into five subsections. The first three subsections are about productivity, and the following sections focus on research quality.

4.1. Overview on Productivity. Figure 2 illustrates the annual changes of journals and publications in PA. In general, the number of journals rises from 24 in 1998 to 47 in 2016, while the number of publications also grows from 734 in 1998 to 1697 in 2016. However, both the number of journals and publications increased steadily with a slight fluctuation in the period of 1998–2006. Then, the two numbers increased rapidly from 2007 to 2011 but have returned to a steady-state since 2012.

The cases in datasets of resident and nonresident journals are also shown in Figure 2. In the last decade, although the number of resident journals did not change, the number of publications has shown a decelerated growth trend. It suggests that some resident journals are also expanding their size of publications cautiously. However, the number of publications in nonresident journals has grown substantially with the increasing number of journals. It indicates that articles in non-resident journals are the main driving force for the growth of the number of publications.

About the changing number of publications (Figure 2), the 19 years can be divided into three stages, namely, 1998–2006, 2007–2011, and 2012–2016. During the first and third stages, the number of journals and publications is stabilized, while those in the second stage 2007-2011 experience a dramatic growth.

According to the affiliation information in the address field, the number of authors and countries is counted. Figure 3 shows the annual evolution of the average number of authors and countries for each publication. The values of

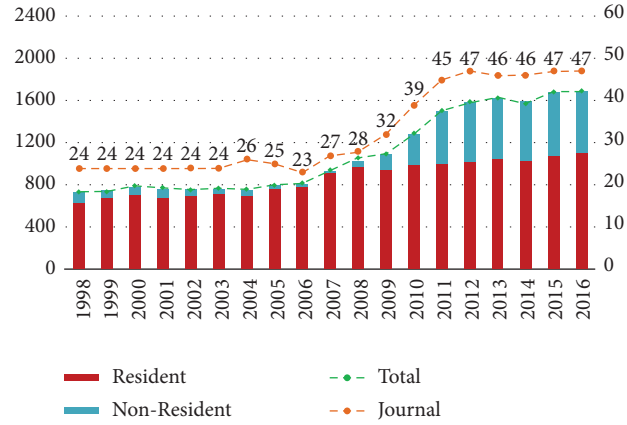

Figure 2: The number of papers and journals in PA.

Figure 3: The number of authors and countries/territories per publication for three datasets.

authors and countries in the field increased from 1.53 to 0.95 in 1998 to 2.19 and 1.28 in 2016. It implies an increasing collaboration in PA for the increasing use of statistics and register/survey data [13]. In 1998–2002, the average number of countries was less than 1, which was due to the lack of address information in some of the data. In subsequent analysis, it can be observed that the lack of address information decreases year by year.

Generally speaking, although the number of publications as the denominator increases, all the quotients show a growing trend. The average number of authors, however, grows faster than that of countries. The actual growth rate of the average number of countries will be slower when the impact of missing data is removed. During those 19 years, the performance of the resident journals dataset changed in line with that of the total journals dataset. In contrast, the performance of nonresident journals is fluctuating, but its trends became stable after 2012 and are close to overall performance. The previous volatility was mainly due to the small size of nonresident journals that are vulnerable to extreme values.

4.2. Active Players. The top 20 countries that published papers in the 19 years are shown in Table 4. It is clear that the US and the UK are the major contributors, which account for 58% of the total published papers. The percentages of publications from the countries ranking 2–5 published in resident journals are greater than the world average (78.3%), which indicates that they focused more on publishing papers in resident journals. On the contrary, those of the US in the three stages are lower than the world average ($86.1 < 91.4$, $79.8 < 81.9$, $63.3 < 64.5$), which suggests that American authors have contributed more to nonresident journals than the resident journal. However, from the perspective of three

Table 4: Top 20 countries/territories publishing in PA.

Rank	Nation	Publications	%world	%resident/total Period	1998–2006	2007–2011	2012–2016
1	USA	7935	37.82	76.6	86.1	79.8	63.3
2	UK	4244	20.23	88.2	99.3	89.8	75.6
3	Canada	1582	7.54	86.6	96.7	89.5	74.4
4	Australia	1317	6.28	83.8	99.5	87.6	70.8
5	Netherland	1056	5.03	82.3	100	89.4	72.3
6	Germany	813	3.88	76.1	99.4	78.4	66.7
7	China	584	2.78	73.1	97.7	79.3	64.3
8	Denmark	437	2.08	75.1	100	77.8	66.7
9	Spain	434	2.07	69.1	100	82.2	55.4
10	Sweden	373	1.78	74	100	82.9	60.2
11	Italy	352	1.68	72.4	100	75.2	65.3
12	South Korea	352	1.68	67.3	96.9	81	58.5
13	Belgium	34	1.59	73.4	97.1	78.6	66.3
14	Norway	306	1.46	81.4	100	90.1	70.2
15	Switzerland	286	1.36	80.8	100	85.3	72.8
16	France	240	1.14	84.6	100	90.7	74.6
17	Israel	234	1.12	68.4	76.8	65.5	64.5
18	Romania	205	0.98	3.4	100	7.2	0.7
19	New Zealand	181	0.86	85.1	98.5	87.8	68.8
20	Singapore	160	0.76	65.6	100	88.5	54.4
	World	20980	100	78.3	91.4	81.9	64.5

stages, the shares of publications of resident journals in almost all countries are declining, which implies that the gap between resident and nonresident journals is narrowing. Some countries show a preference for resident journals, whose percentages of resident journals in the three stages are higher than the world average. For example, countries ranking 2–5, as well as Norway, Sweden, France, and New Zealand, always focus more on publishing in resident journals.

From 1998 to 2016, the top 20 institutions are given in Table 5. All of the 20 institutions are universities, which indicates that the role of the university is far stronger than other types of institutions.

The distribution of the top 20 institutions among countries is highly skewed. The number of institutions from the US and the UK is 10 and 5, respectively. There are only two institutions in the Netherlands, and one in Australia, Canada, and China.

According to the interval mean of the percentage of items from resident journals, 15 of the 20 institutions have mainly published publications in resident journals. Unlike previous studies with data from a single journal PAR, we found that the most active institution in past 19 years is Cardiff University from the UK, which is different from their result [2]. The aggregation effect of the university system on publications productivity and citations will not be reflected in our research, because we have split the system-level institutions into the campus-level. However, Indiana University, Bloomington, is still an important part of the system and is ranked 9th. A similar situation occurs at the University of Wisconsin, Madison. The institutions that appeared on both two lists are all from the US, including the University of Georgia, Harvard University, Texas A&M University, Syracuse University, and American University.

4.3. Authorship Style Analysis. The proportions of different types of publications (Table 3) in the three datasets are presented in Figure 4. Overall, both internationally and nationally coauthored publications have increased, from 3.81% to 34.06% (in 1998) to 21.80% and 46.43% (in 2016), respectively. In contrast, the proportion of national single authorship decreases from 50.82% in 1998 to 30.34% in 2016. The collaboration in PA is growing, and the international collaboration increases significantly. The phenomenon also occurs in several fields of social sciences, which tend to use quantitative research methods, experiments, and labor division [13]. The total proportion of coauthorship is 68.23% in 2016, which is still lower than that in 2013 in the fields of Business and Economics as shown in the study by Henriksen [13]. In addition, the case of the missing address information reduces from 10.35% in 1998 to 0.29% in 2016, which implies that the quality of the records indexed by WoS becomes better. It is worth noting that the share of international single authorship shows a fluctuation but stabilized at around 1%. The main reason is that these authors are affiliated with more than one country [2].

Figure 4 illustrates that the changes in resident journals are similar to those in all journals, while the nonresident journals are quite different. To verify the judgment, the Paired Samples T-test and the Wilcoxon Rank test were used to investigate three indicators: the proportions of internationally and nationally coauthored publications as well as those of national single authorship. At first, the international items of resident and total journals dataset are paired. Then, the differences are calculated, and a T-test is performed by SPSS. The other two indicators are tested likewise.

Table 6 illustrates the outputs of the Paired Samples T-test. The p values of the three types are all greater than 0.05, indicating that the null hypothesis is acceptable (i.e., there is no statistically significant difference between the two datasets).

Table 5: Top 20 institutions publishing in PA.

Rank	Nation	Institution	Publications	%resident/total %world	Period	1998–2006	2007–2011	2012–2016
1	UK	Cardiff Univ.	307	1.46	91.2	100	97.7	77.4
2	UK	London Sch. of Eco and POL SC	296	1.41	83.4	100	74.5	76.2
3	USA	Univ. Georgia	294	1.4	83	90	90	68.1
4	UK	Univ. Birmingham	282	1.34	89.7	100	88.8	78.9
5	UK	Univ. Manchester	237	1.13	87.8	100	96.6	62.3
6	Netherland	Erasmus univ. Rotterdam	223	1.06	79.4	100	84.6	73.1
7	Australia	Natl Univ.	222	1.06	85.6	98.4	89.9	73
8	Canada	Univ. Toronto	218	1.04	77.1	88.9	88.2	55.8
9	USA	Indiana univ. Bloomington	204	0.97	79.9	98.2	83.9	65.1
10	USA	Harvard Univ.	186	0.89	71.5	78	62.5	69.6
11	USA	Texas a&*M* Univ.	179	0.85	84.9	100	83	69.4
12	Netherland	Univ. Utrecht	173	0.82	82.7	100	89.5	75.3
13	UK	Univ. Oxford	172	0.82	89	98.1	91.5	78.3
14	USA	Rutgers State Univ.	169	0.81	75.7	83	86	62.1
15	USA	Arizona State Univ.	163	0.78	70.6	86.7	75.4	60.5
16	China	City Univ. Hong Kong	156	0.74	75	100	79.6	64.6
17	USA	Univ. Wisconsin Madison	155	0.74	86.5	93	90.9	77.2
18	USA	Syracuse Univ.	152	0.73	89.5	100	87.5	75
19	USA	Univ. Washington	147	0.72	84.9	91	93.5	64.1
20	USA	American Univ.	146	0.70	81.6	100	78.5	71.7
	World		20980	100	78.3	91.4	81.9	64.5

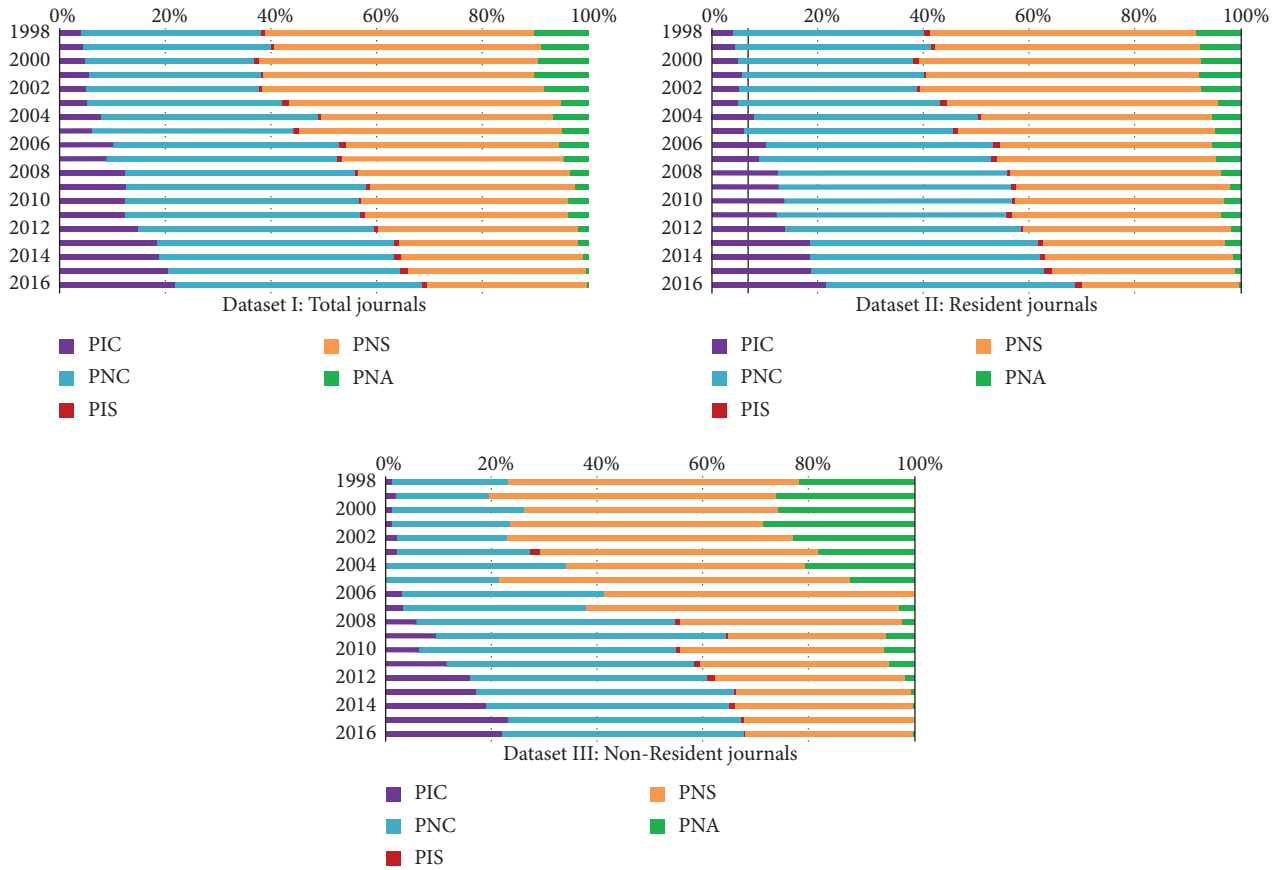

Figure 4: Proportion of publications five types of authorship in three datasets.

Table 6: Paired samples *T*-test for proportions of three types of authorship.

Variable	Mean	Sd	T	Df	Sig(2-tailed)
R_PIC-t_PIC	0.00276	0.00635	1.898	18	0.074
R_PNC-t_PNC	0.00146	0.01135	0.56	18	0.582
R_PNS-t_NS	0.00107	0.00726	0.639	18	0.531

Table 7: Wilcoxon rank test for proportions of three types of authorship.

Variable	Negative ranks		Positive ranks		Ties		Z	Asymp.Sig (2-tailed)
	N	Mean	N	Mean	N	Mean		
R_PIC-t_PIC	16	9.56	3	12.33	0	0	-2.334	0.02
R_PNC-t_PNC	11	10.18	8	9.75	0	0	-0.684	0.494
R_PNS-t_PNS	9	11.89	10	8.3	0	0	-0.483	0.629

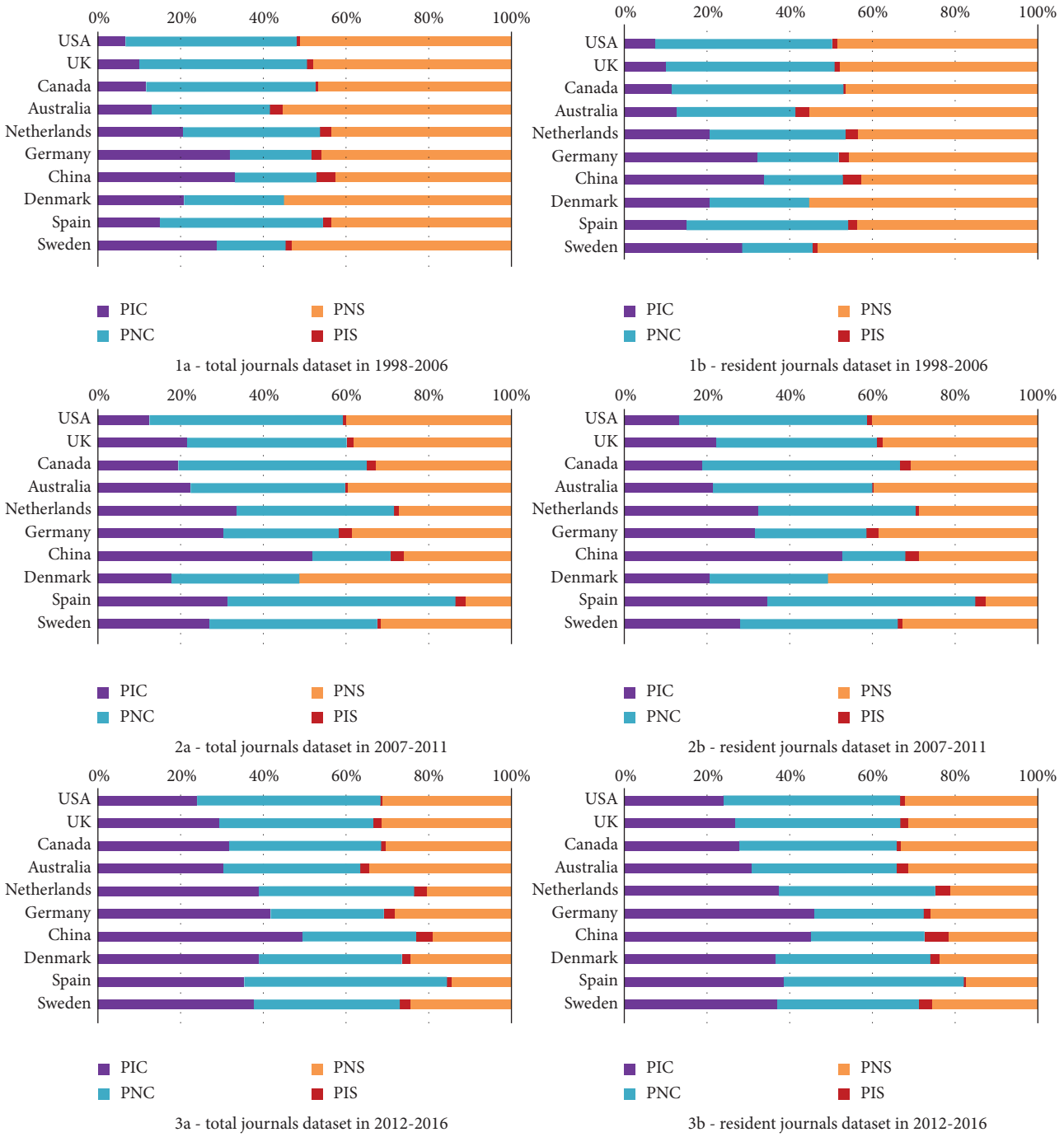

Figure 5: Authorship patterns of top 10 countries published in the datasets I and II in three stages.

Table 7 shows the results of the Wilcoxon rank test with three types of p values of 0.020, 0.494, and 0.629, respectively. It means that, for internationally coauthored papers, there is a statistically significant difference between the indicators of the two datasets, while the others are not different.

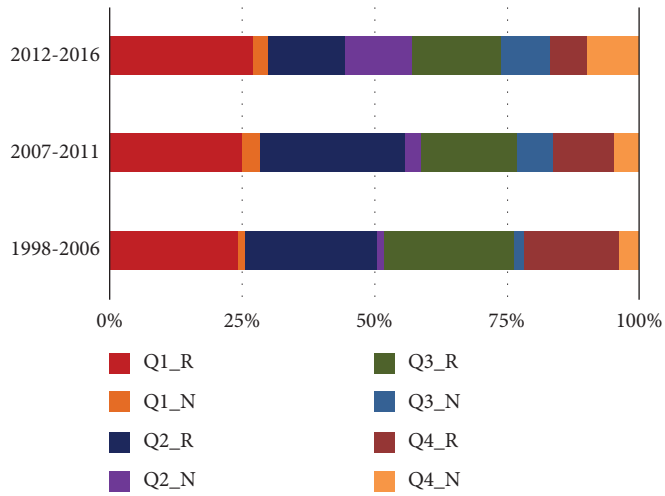

Figure 6: Publications in JIF quartile from resident and nonresident journals.

Based on the results of Table 6 and 7, it indicates that the difference between the two datasets is small with respect to the national coauthorship and single authorship indicators. However, there is a gap between the two datasets in terms of internationally coauthored papers, and the reasons are explained in the subsequent analysis.

According to the productivity of the 20 countries in Table 4, this article focuses on the top 10 countries in the analysis below. The number of papers in these 10 countries accounts for more than 70% of the world (73.65% for all journals and 77.69% for resident journals). Types of authorship of the top 10 countries in total and resident journals dataset are detailed in Figure 5.

Figure 5 shows that there is almost no difference between the two datasets. However, there are some particular performances in the three stages. In terms of the international coauthorship indicator, China and Spain showed an increase and then a decrease, while the proportions of the other eight countries increase to various extents. National single authorship of nine countries except Spain presents a downward trend. Overall, in the first stage, nationally single-authored publications play major roles in these countries. In the final stage, the major roles are gradually replaced by coauthorship. The result is also in line with our judgment from Figure 4. However, the dominant forms of collaboration are different as shown in 3a and 3b of Figure 5: the top 4 countries are dominated by nationally coauthored papers, while the countries ranking 5–10 are led by international collaboration.

It is noted that, in 3a and 3b of Figure 5, the differences in the proportion of internationally coauthored papers between the two datasets in the UK, Canada, Germany, and Spain are more obvious. These countries have wider proportions of international coauthorship in resident journals, which indicates a gap between the two datasets. It can be seen that these countries prefer to conduct international collaboration in resident journals. Considering that the top 10 countries are responsible for more than 70% of the papers, the results also partially explain the differences in the outputs of Table 6 and 7.

4.4. Publications in JIF Quartile. The distribution of publications of JIF quartiles is illustrated in Figure 6. Data from resident and nonresident journals are characterized by different fillers and colors. In the early period, resident journals account for a large proportion of the four quartiles. However, in the third stage, the resident journals only occupy an absolutely leading position in the Q1 zone, accounting for 90.24%. In Q2, Q3, and Q4 zones, they only accounted for 52.76%, 63.32%, and 39.33%, respectively. It implies that publishing a paper in a resident journal may obtain a higher impact factor.

According to data from the total and resident journals dataset, the performance of the top 10 countries in JIF quartiles is presented in detail in Figure 7. Germany, Denmark, and Sweden published more in Q1 and Q2 zones, which indicates that scholars from these countries are more able to publish papers in higher quality journals. On the contrary, papers in Canada and Australia are mainly published in lower quality journals. Resident journals dataset differs from all journals dataset, especially in the second and third stages. Most countries perform better in the resident journals dataset than in the total journals dataset, except for the second stage of the Netherlands and the third stage of Canada.

4.5. Citation Analysis. In this paper, we use both CPP and $PP_{top\ x\%}$ indicators to investigate the impact of the three datasets.

4.5.1. Citation per Publication (CPP). Based on two citation windows, the annual change of the CPP indicator is presented in Figure 8. Each of the six CPPs illustrates a growth, although with some fluctuations. It indicates that the opportunity to be cited is growing because of the increasing number of publications in WoS. The changes in the resident journals dataset are almost identical to those in the total journals dataset in both citation windows. Resident journals performed better than the overall journals significantly since

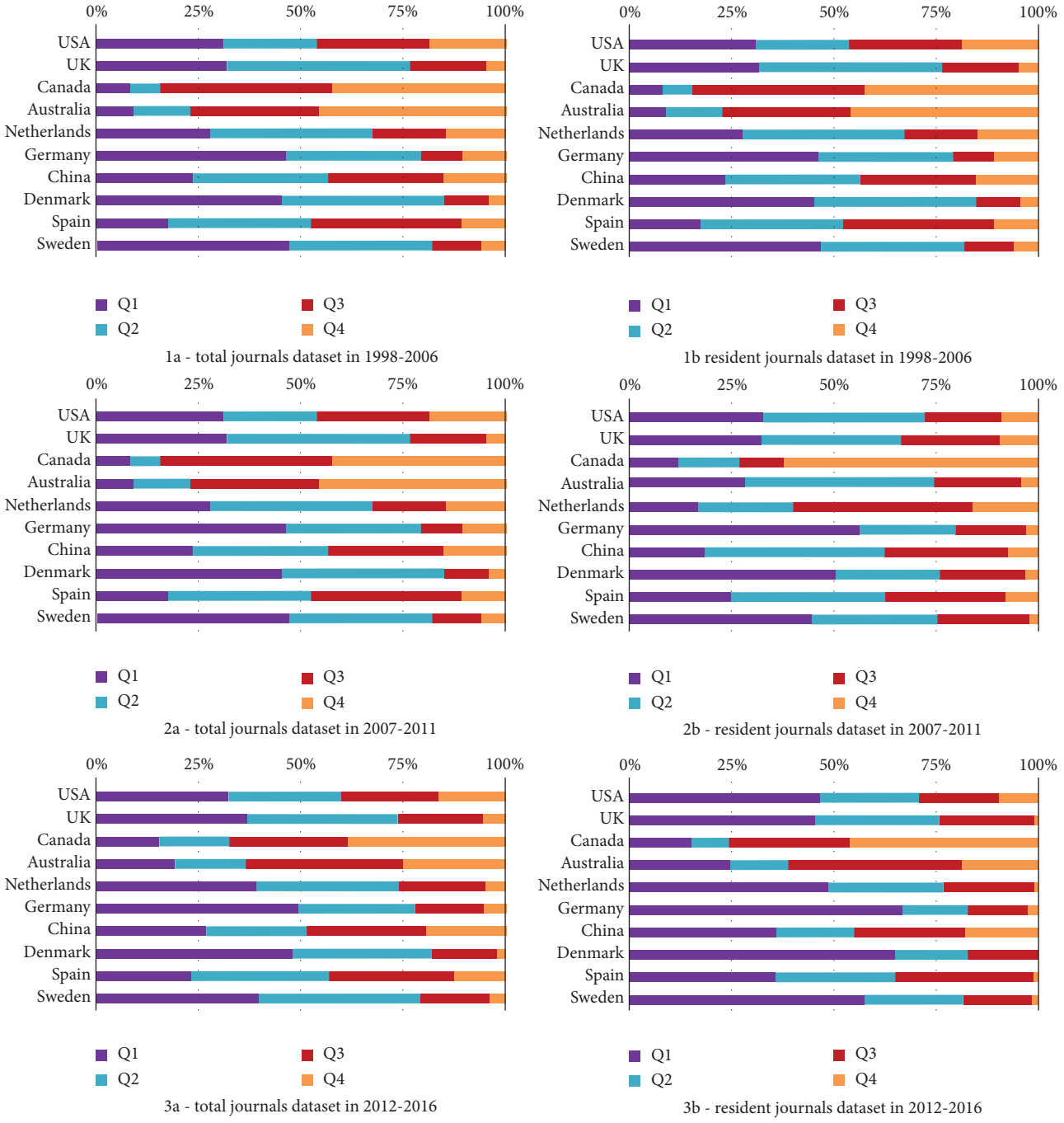

Figure 7: Publications in JIF quartile of top 10 countries publishing in the datasets I and II.

2009, which can also be reflected in the widening gap between resident journals and nonresident journals.

According to data from the total and resident dataset, the CPPs for the top 10 countries are shown in Figure 9. Because of the patterns presented in Figure 2, we calculated the CPPs in three stages. The first two are 1998–2006 and 2007–2011 in line with the prior analysis, but the third is different. Since the citable data are limited by the choice of the citation window, the 3-year window corresponds to data in 2012–2015, and the 5-year window corresponds to the period 2012–2013.

Figure 9 shows that indicators in the resident journals dataset are higher than those in the total journals dataset. The differences between the countries presented by the two citation windows are not clear. A subtle difference is reflected between Germany and Sweden, where the former performs better in the 3-year window, and the latter is better in the 5-year window.

In general, it does not mean that countries with greater productivity perform better. For example, the CPP of the United States with the largest number of publications is located in the medium of the top 10 countries. In contrast,

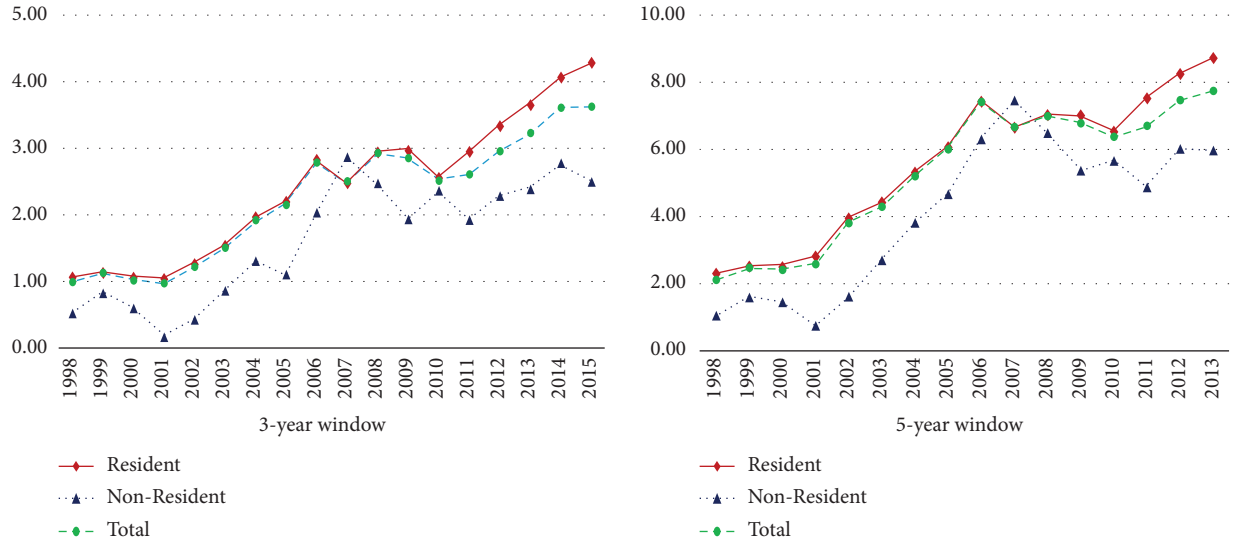

Figure 8: CPP for three datasets based on 3-year and 5-year windows.

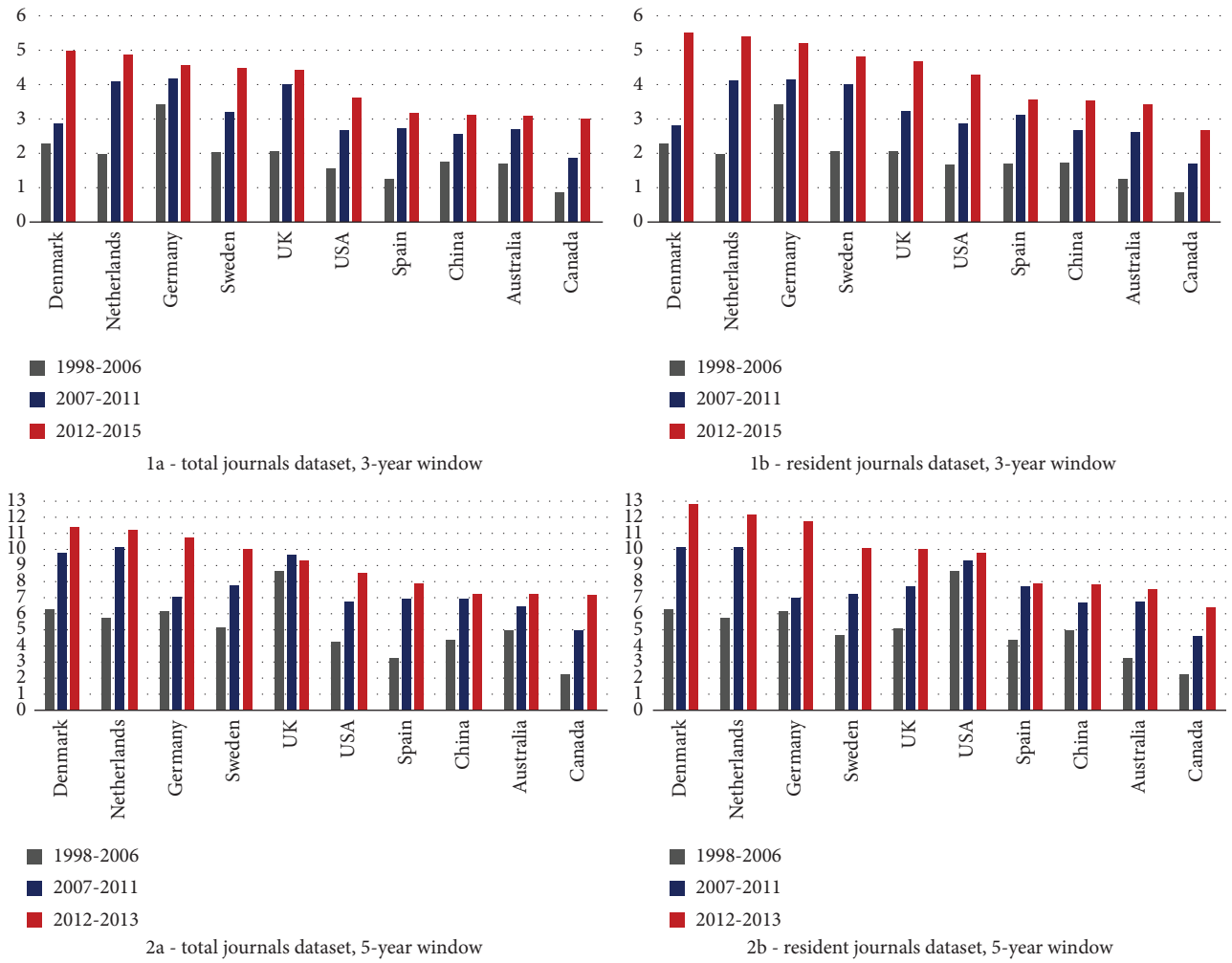

Figure 9: CPP of top 10 countries publishing in the datasets I and II.

Figure 10: The proportion of highly cited publications in resident journals by total journals (%).

CPPs of the UK, the Netherlands, Germany, Denmark, and Sweden are higher, which implies a better quality of publications in these countries. Figure 7 indicates that the higher quality of Germany, Denmark, and Sweden is mainly because they publish more in the Q1 zone, while the UK and the Netherlands have a high proportion of papers in the Q1 and Q2 zones.

4.5.2. Highly Cited Publications. Top 1%, 5%, and 10% are employed to better explore the citation patterns. To present the gap between resident and nonresident journals dataset, the percentage of publications in resident journals to the total journals is calculated, and the changes in the proportion of highly cited publications in resident journals are shown in Figure 10. Overall, the percentage of highly cited papers in resident journals accounts for more than 65% of the total, which means that resident journals are the major contributors of highly cited papers. However, the overall trend of these ratios is decreasing, reflecting a narrowing gap between resident journals and nonresident journals.

Based on 3-year and 5-year windows, the number of the top 1%, 5%, and 10% most cited publications of the top 10 countries is counted separately. According to the Leiden ranking, the values are recorded as $P_{top\ 1\%}$, $P_{top\ 5\%}$, and $P_{top\ 10\%}$. The normalized indicators recorded as $PP_{top\ 1\%}$, $PP_{top\ 5\%}$, and $PP_{top\ 10\%}$, can measure the proportion of the most cited papers in the total number of papers published per country. For example, in 2b of Figure 11, according to the 3-year window from 2012 to 2015, the number of the top 5% cited papers and the total number of papers produced by the United States are 224.5 (not an integer due to the fractional counting method) and 2139. $PP_{top\ 5\%}$ indicator = 224.5/2139 = 10.5% > 5%. It means that the top 5% cited papers of the US are greater than the world average.

The normalized indicators are shown in Figures 11 and 12, which correspond to the 3-year and 5-year windows, respectively. There is no significant difference in the growth or decrease trend of the two datasets in the three stages, but the growth rate is different. In general, the resident journals dataset performs better than all the journals datasets. Due to the choice of different windows, there will be some unique results. To ensure reliability, we mainly focus on the common phenomena in the two windows.

For the $PP_{top\ 1\%}$ indicator, it can be seen that the United States, the United Kingdom, the Netherlands, Denmark, and Sweden have consistently exceeded the world average for three stages. Germany and Spain have experienced significant fluctuations, but there is still a downward tendency. Notable improvement has been made in Canada and the Netherlands. Although China has made progress, the extent is still small. The values of China reach the world average in the year 2012 and 2013 for the 5-year window but not for the 3-year window. It shows that China still has a gap with other countries in producing higher-level publications.

For the $PP_{top\ 10\%}$ indicator, the gap between the top 10 countries is not as large as the $PP_{top\ 1\%}$ indicator. The US, the UK, the Netherlands, and Germany have consistently exceeded the world average in three periods. It is noteworthy to describe the situation of Germany. Regardless of the fact that Germany does not perform well on the $PP_{top\ 1\%}$ indicator, it performed better than the world average in terms of the other two indicators. The fact may indicate that Germany has muscular strength but may lack Olympic players. Contrary to the situation in Germany, China's performance in the $PP_{top\ 10\%}$ indicator is not as good as the $PP_{top\ 1\%}$ indicator, indicating that China's capacity still needs to be strengthened. As a transition indicator, the result of $PP_{top\ 5\%}$ shows more similarity with that of $PP_{top\ 10\%}$ than $PP_{top\ 1\%}$.

In general, the US, the UK, and the Netherlands are always the main players in publishing highly cited papers.

5. Discussion

The resident journal is an interesting phenomenon observed in this study when examining the journal lists of specific subject categories of JCR. Resident journals and nonresident

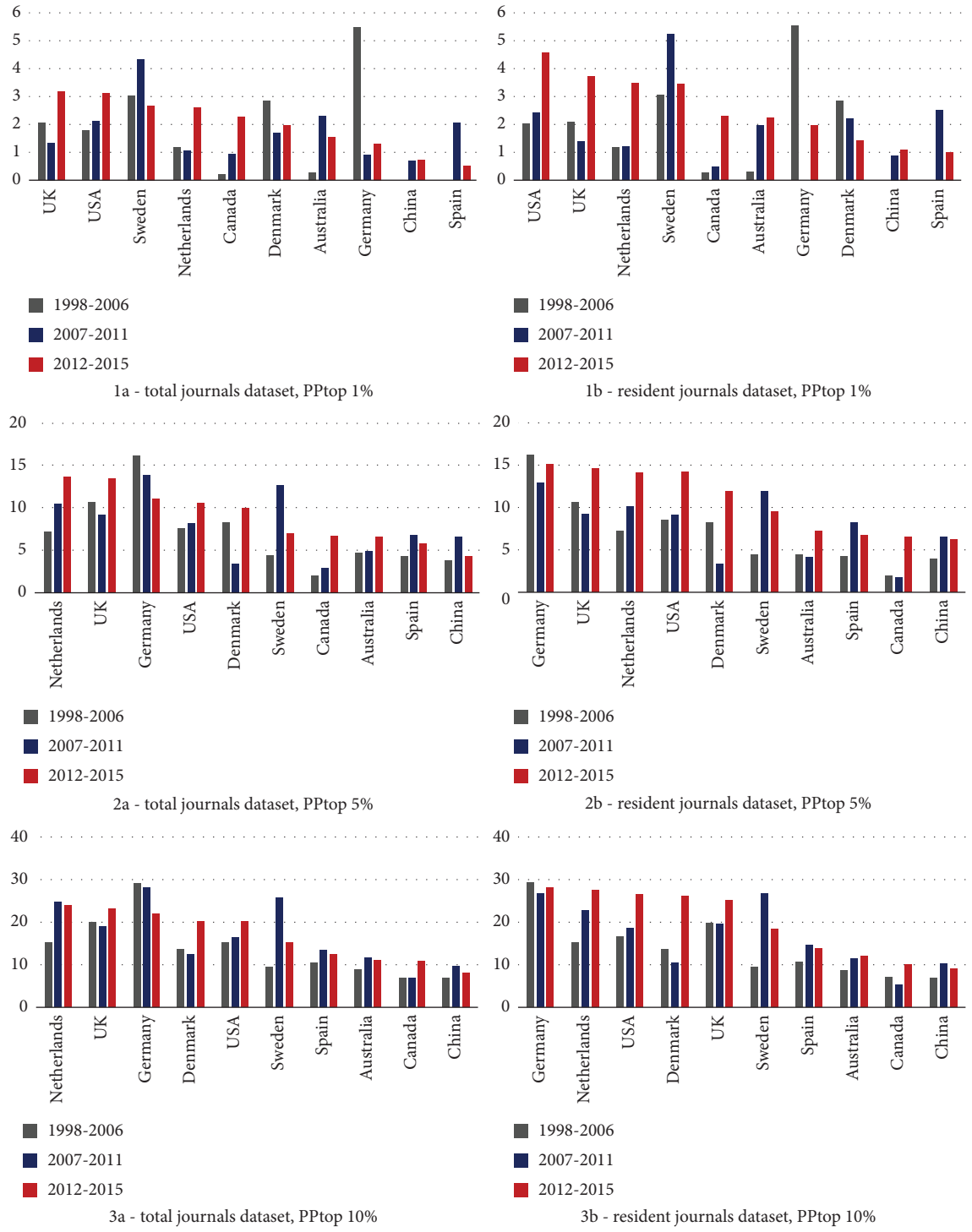

Figure 11: $PP_{top\ x\%}$ of top 10 countries publishing in the datasets I and II based on 3-year window.

journals may represent traditional and emerging forces in the discipline, respectively. These forces are ostensibly represented by journals, but they may potentially reflect the objective patterns and subjective capacities of individual researchers, institutions, and countries.

The application of a 10-year window as a threshold for the definition suggests that resident journals are essentially a concept based on the time span, which means that the set will vary as time windows change. However, as mentioned earlier, the dataset of journals in PA has expanded dramatically since 2007 and did not stabilize until around 2012. Therefore, choosing the 10-year window, which includes a five-year growth period and a five-year stabilization period, can better reflect the evolution tendency between traditional

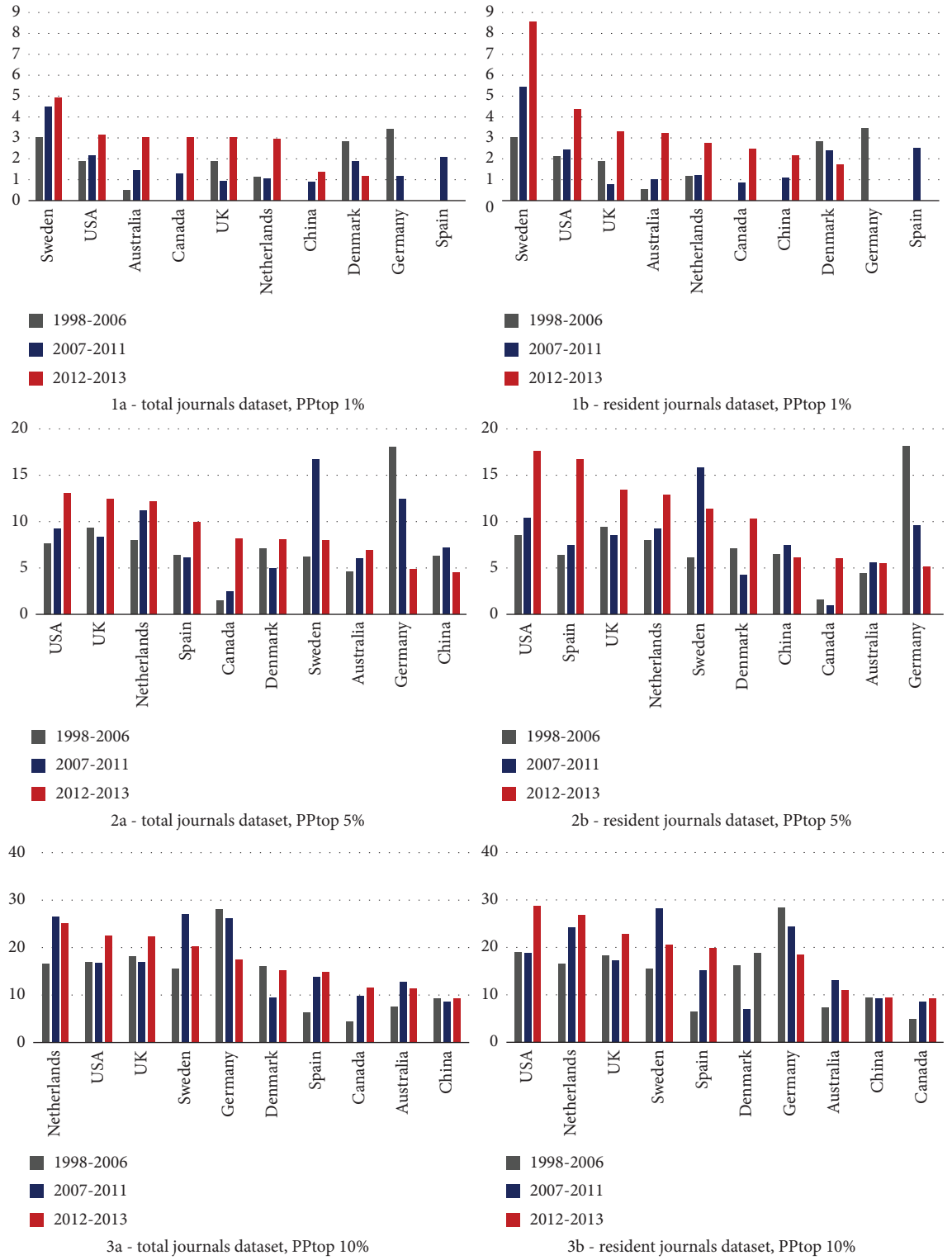

Figure 12: $PP_{top\ x\%}$ of top 10 countries publishing in the datasets I and II based on 5-year window.

and emerging forces during the expansion period of the journal list in PA.

For some indicators related to productivity (such as the number of publications, the number, and proportion of authorship), the difference between residents and other journals is not very significant. However, for indicators related to research quality, resident journals outperformed others. The results of the work indicate that the resident journal, which represents the traditional forces, still dominates PA. The resident journals in this field have better representativeness, regardless of productivity, national and institutional contributors, collaboration patterns, JIF

quartile indicators, and citation impact. Moreover, it can be seen from the research unit analysis that resident journals have many immovable contributors to inactive countries and institutions.

Overall, the questions raised in Section 1 can be answered as follows.

At the journal level, resident journals have greater influence in PA compared with nonresident journals. However, the gap between them is narrowing at some indicators. Publications in resident journals dataset and total journals show great similarities, indicating that resident journals have certain representativeness, but recently this similarity is weakening.

At the country level, it shows that the activity measured by the productivity of publications is not strictly linked to the quality of research represented by higher quality journals and citation impact. Similar to the results of previous studies, the proportion of collaboration in PA is still lower than that in some disciplines in social sciences, but both international and national collaborations have a growth tendency.

At the institution level, the distribution of active institutions in PA is highly skewed among countries. Most of the active institutions are from the US and the UK, which indicates that these two countries still hold the dominant advantage. These active institutions are less dependent on resident journals over time.

It is noteworthy that the finding also supports some conclusions of previous studies. For example, the contribution of collaboration (including those that are international and national) generally shows an increasing trend. However, compared with some fields in social sciences, the share of coauthorship in PA is still low. In addition, in the research of the journal PAR [2], many of the top 15 institutions also appeared in the above list of institutions (Table 5).

6. Conclusion

Bibliometrics is a series of statistical methods for researching and measuring bibliographic information. More specifically, bibliometrics describes the characteristics of research results in an objective way, which can address the subjective bias from a typical and traditional evaluation in PA field. To provide a comprehensive and accurate definition of influence, this study estimated publications in a bibliometric way. Both the activity and the quality indicators of research results were applied to various articles published in a 19-year period. A 3-year and a 5-year citation window were employed at three aggregation levels including journal, country, and institution by using publications in PA indexed SSCI. The scope of this study has expanded from single or several journals to 53 journals, covering the entire field of PA. Various methods and indicators from scientometrics and bibliometrics were used to reflect influence, and a larger-scale empirical analysis was conducted in this study than previous studies.

A new concept named "resident" journal is proposed to explore differences between traditional and emerging research forces. The results suggest that resident journals maintain a large advantage over other journals in terms of higher quality journal indicators and citation impact indicators. Moreover, international and national collaborations show a growth tendency, especially for the international type. The majority of active institutions are from the US and the UK, which indicates their dominant position over others. This study provides more comprehensive comparisons through large-scale data and acknowledged methods to explore the development of PA field research.

Data Availability

The datasets used and/or analyzed during the current study are available from the corresponding author upon request.

Conflicts of Interest

The author declares that he has no conflicts of interest.

Authors' Contributions

Zepeng Yu designed the study, analyzed data, wrote the manuscript, and contributed to writing of the manuscript.

Acknowledgments

The author is grateful to professor Loet Leydesdorff for the software "isi.exe" to extract and analyze data. This study was grateful to Clarivate Analytics for raw data of the journals in the field of public administration.

References

[1] J. Mingers and L. Leydesdorff, "A review of theory and practice in scientometrics," *European Journal of Operational Research*, vol. 246, no. 1, pp. 1–19, 2015.

[2] C. Ni, C. R. Sugimoto, and A. Robbin, "Examining the evolution of the field of public administration through a bibliometric analysis ofPublic administration review," *Public Administration Review*, vol. 77, no. 4, pp. 496–509, 2017.

[3] B. Bozeman, "The problem of beauty contest scholarship in public administration-and a possible alternative," *Administration & Society*, vol. 44, no. 8, pp. 1019–1026, 2012.

[4] M. Powell, "Citation classics in social policy journals," *Social Policy and Administration*, vol. 50, no. 6SI, pp. 648–672, 2016.

[5] E. A. Corley and M. Sabharwal, "Scholarly collaboration and productivity patterns in public administration: analysing recent trends," *Public Administration*, vol. 88, no. 3, pp. 627–648, 2010.

[6] J. C. N. Raadschelders and K. Lee, "trends in the study of public administration: empirical and qualitative observations from public administration review, 2000-2009," *Public Administration Review*, vol. 71, no. 1, pp. 19–33, 2011.

[7] N. Gulrajani and K. Moloney, "Globalizing public administration: today's research and tomorrow's agenda," *Public Administration Review*, vol. 72, no. 1, pp. 78–86, 2012.

[8] W. C. Adams, D. L. Infeld, L. F. Minnichelli, and M. W. Ruddell, "Policy journal trends and t," *Policy Studies Journal*, vol. 42, no. SI, pp. S118–S137, 2014.

[9] W. C. Adams, D. L. Infeld, K. L. Wikrent, and O. B. Cisse, "network bibliometrics of public policy journals," *Policy Studies Journal*, vol. 441, no. SI, pp. S133–S151, 2016.
[10] L. Waltman and N. J. van Eck, "Field-normalized citation impact indicators and the choice of an appropriate counting method," *Journal of Informetrics*, vol. 9, no. 4, pp. 872–894, 2015.
[11] J. Ruiz-Castillo and L. Waltman, "Field-normalized citation impact indicators using algorithmically constructed classification systems of science," *Journal of Informetrics*, vol. 9, no. 1, pp. 102–117, 2015.
[12] L. Waltman, "A review of the literature on citation impact indicators," *Journal of Informetrics*, vol. 10, no. 2, pp. 365–391, 2016.
[13] D. Henriksen, "The rise in co-authorship in the social sciences (1980-2013)," *Scientometrics*, vol. 107, no. 2, pp. 455–476, 2016.
[14] E. Garfield, "The Impact Factor and using it correctly," *Unfallchirurg, Der*, vol. 101, no. 6, pp. 413-414, 1998.
[15] J. E. Hirsch, "An index to quantify an individual's scientific research output," *Proceedings of the National Academy of Sciences*, vol. 102, no. 46, pp. 16569–16572, 2005.
[16] G. Abramo and C. A. D'Angelo, "A farewell to the MNCS and like size-independent indicators," *Journal of Informetrics*, vol. 10, no. 2, pp. 646–651, 2016.
[17] L. Bornmann, L. Leydesdorff, and R. Mutz, "The use of percentiles and percentile rank classes in the analysis of bibliometric data: o," *Journal of Informetrics*, vol. 7, no. 1, pp. 158–165, 2013.
[18] L. Waltman, C. Calero-Medina, J. Kosten et al., "The Leiden ranking 2011/2012: data collection, indicators, and interpretation," *Journal of the American Society for Information Science and Technology*, vol. 63, no. 12, pp. 2419–2432, 2012.
[19] L. Bornmann, L. Leydesdorff, and J. Wang, "Which percentile-based approach should be preferred for calculating normalized citation impact values? An empirical comparison of five approaches including a newly developed citation-rank approach (P100)," *Journal of Informetrics*, vol. 7, no. 4, pp. 933–944, 2013.
[20] L. Leydesdorff and L. Bornmann, "Integrated impact indicators compared with impact factors: an alternative research design with policy implications," *Journal of the American Society for Information Science and Technology*, vol. 62, no. 11, pp. 2133–2146, 2011.
[21] P. Zhou and X. Lv, "Academic publishing and collaboration between China and Germany in physics," *Scientometrics*, vol. 105, no. 3, pp. 1875–1887, 2015.
[22] C. R. Sugimoto, C. Ni, and V. Lariviere, "On the relationship between gender disparities in scholarly communication and country-level development indicators," *Science and Public Policy*, vol. 42, no. 6, pp. 789–810, 2015.
[23] W. Glänzel and H. F. Moed, "Journal impact measures in bibliometric research," *Scientometrics*, vol. 53, no. 2, pp. 171–193, 2014.
[24] L. Waltman and M. Schreiber, "On the calculation of percentile-based bibliometric indicators," *Journal of the American Society for Information Science and Technology*, vol. 64, no. 2, pp. 372–379, 2013.

Hindawi
Scientific Programming
Volume 2022, Article ID 8376325, 11 pages
https://doi.org/10.1155/2022/8376325

Research Article

Deep Learning Models and Social Governance Guided by Fair Policies

Kai Wang[1] **and Zhen Wang**[2]

[1]*College of Humanities and Social Sciences, Jiangxi Open University, Nanchang, Jiangxi, China*
[2]*College of Psychology, Jiangxi Normal University, Nanchang, Jiangxi, China*

Correspondence should be addressed to Zhen Wang; 004694@jxnu.edu.cn

Received 6 December 2021; Revised 29 December 2021; Accepted 3 January 2022; Published 18 March 2022

Academic Editor: Muhammad Usman

With the rapid advancement of information technology, artificial intelligence and machine learning have become the central technology tools for information sharing. To speed up the efficiency of information resource transmission of national government departments and improve the informatization level of government social management and public service systems, the persona system is designed using an artificial neural network, and a social service and management resource pool system is developed. The behavior data randomly generated by users in daily life is collected and cleaned, and training samples are extracted for training an artificial neural network. Next, the demographic attribute tags and interest tags are modelled, and the social service and management resource pool system is built and tested. Results show that for the population attribute label construction, the index value using the app name is mapped to 0 or 1, and the sample sampling ratio is set to 1.0. The proposed model achieved the overall accuracies of 85.2%, 74.5%, and 99.0% for the prediction of constructed age, academic qualifications, and interest label, respectively. The constructed system greatly deepens the visualization of the characteristics of social governance elements. The system can enhance the level of resource sharing by government departments and provide the foundation for spatial decision-making in smart social governance.

1. Introduction

The sharing of program information among government agencies can help achieve important public benefits of increased productivity, improved policymaking, and integrated public services. Government information sharing allows information exchange between different government agencies as well as between public and private institutions. Sharing information enables enhanced efficiency, a better quality of processes and services, and improved transparency. The implementation of information sharing initiatives requires different types of initiatives such as technical, organizational, institutional, and political [1]. In the government resources, sensor information, public information, and Internet information continue to gather. More and more institutions or individuals use machine learning, accurate data analysis, and other controllable technologies to accurately analyze the elements of social governance. Nowadays, persona technology is increasingly used in social media, e-commerce, mobile Internet, and e-government [2].

More and more researchers have researched the application of portrait technology in social governance. Elgammal et al. [3] pointed out that corporate governance and corporate social responsibility are driven by ethical practices. The relationship between corporate ethics and corporate social responsibility has been studied by many researchers. They showed that there is a significant correlation between corporate ethics and corporate social responsibility and ethical practices have a positive impact on corporate social responsibility. Qiang et al. [4] described that China, with a population of 1.4 billion, is experiencing perhaps the largest urbanization and modernization in human history. In this context, in 2014, the multidisciplinary research team of Tsinghua University launched a social governance

experiment in Qinghe Street, Beijing. The goal of the project was to discover and solve social problems in urban communities and to study changes in community governance models in large cities. As an innovative model of social governance, this new rural cooperative medical system has important theoretical and practical significance. Widyawati [5] pointed out that the convergence of government information and sensor information can promote the continuous development of precision social governance.

Personas are progressively used in policymaking to aid in planning more human-centred policies and services to the population [6]. In the transportation field, personas are mostly applied concerning diverse mobility behavior patterns to provide services for different types of travellers, e.g., based on vehicle driving behavior patterns defined by motives for car use or the number of annual vehicle kilometres travelled, to allow for various levels of energy consumption [7]. Other approaches use personas for expressing different types of public transport passengers, drivers, or ride-sharing customers for considering different preferences and expectations regarding vehicle design or user experience, e.g., by combining different levels of openness towards various features. Personas are a powerful tool for communication in design teams, as the technique forces designers to consider social and political aspects of design that otherwise often go unexamined. Personas also provide a shared basis for communication, e.g., between clients and designers. Aries and Faily [8] proposed the development and application personas based on empirical data relevant to the business, providing a useful means to identify audience awareness needs, communicate with a predefined security theme for the program cycle. However, the personas generated were generally based on more technical roles. Collection of data from less technical roles providing a balanced spread of the business audience would be more appropriate when fully applying this methodology in a real-world scenario of a persona-centred ongoing information security awareness solution for the workplace. Schoch et al. [9] created personas to understand social barriers and used them for prototyping a web app. One of the major limitations of personas is that they can hardly account for change, especially fast change. Even the well-constructed personas may become partially inaccurate after some time, resulting in the need for additional effort, time, and expense to repair inconsistencies and lost credibility.

More and more researchers use personas and information dynamic perception technology and deep learning technology to accurately analyze the elements of social governance. However, this research work still has certain shortcomings. In this study, a persona system is designed using machine learning techniques, and a social service and management resource pool system is developed. The behavior data training samples generated by different users in their routine life is collected, cleaned, and used to train an artificial neural network. Moreover, the demographic attribute and interest tags are modelled, and the social service and management resource pool system is implemented and evaluated. The model achieved overall prediction accuracies of 85.2%, 74.5%, and 99.0% for age, education background, and interest tags, respectively. In addition, the constructed system links the data exchange channels of various departments in the government, enabling users to realize the interconnection and sharing of information through basic service interfaces.

The rest of the paper is ordered as follows: Section 2 provides detail about the construction of the persona model for social governance. Section 3 illustrates the obtained results and analysis, and the conclusion is presented in section 4.

2. Construction Method of the Persona Model of Social Governance Elements

2.1. User Persona Technical Analysis. User personas link user data and big data applications. The purpose of user personas is to tag target users with a series of user tags such as age, gender, and educational background. The user is a complex whole, and it is difficult to describe it by a single term. Therefore, one label in the user persona is only used to describe one dimension of the user. A user needs to be described with multiple tags. The characteristic of user persona lies in the use of mathematical methods to describe the characteristics of a person in a particular business and can be interpreted by machines [10]. Machine-generated models are difficult to use for training on unprocessed log data. If the data is labeled before the model training, the data distribution can be easily analyzed, and the data operation can also be transformed. It is essential to categorize the data characteristics in the user persona and present it in a highly interpretive, multidimensional, and labeled form to meet various business needs. The purpose of user personas can be divided into two points. One is to classify users. For example, merchants can make personalized recommendations to users according to different types of users, so that users are stickier to products. The other is to analyze the characteristics of users, tap potential users, and expand the business. The role of user personas is very important. The core job of user persona is labeling, which can be processed by people and is convenient for computer processing [11]. The user persona model is shown in Figure 1. Likewise, the persona model of a person formed according to the life of a person is shown in Figure 2, and the process of establishing a user label system is shown in Figure 3.

In Figure 1, user personas are divided into five aspects.

(i) Target: it uses specific mathematical methods to describe the characteristics of a person in a specific business

(ii) Way: the machine can interpret the way

(iii) Organization: it is to organize the data

(iv) Standard: it is to build a knowledge system related to a specific business

(v) Validation: it uses quantitative indicators to evaluate the model

Figure 2 shows that the persona model of a person is related to time. The person shown in Figure 2 was born on XX Street in 1990, went to elementary school in 1996, joined

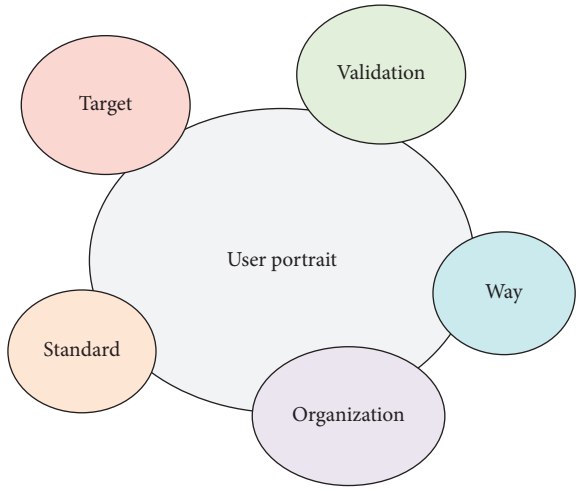

Figure 1: Five aspects of user personas.

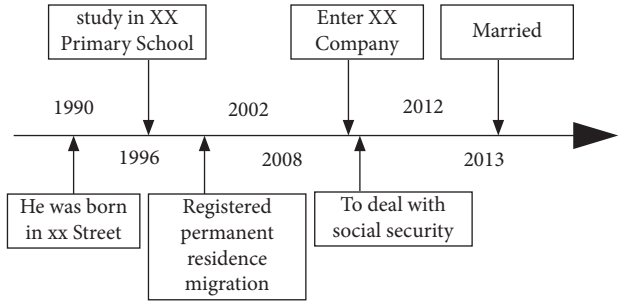

Figure 2: A persona model of a person.

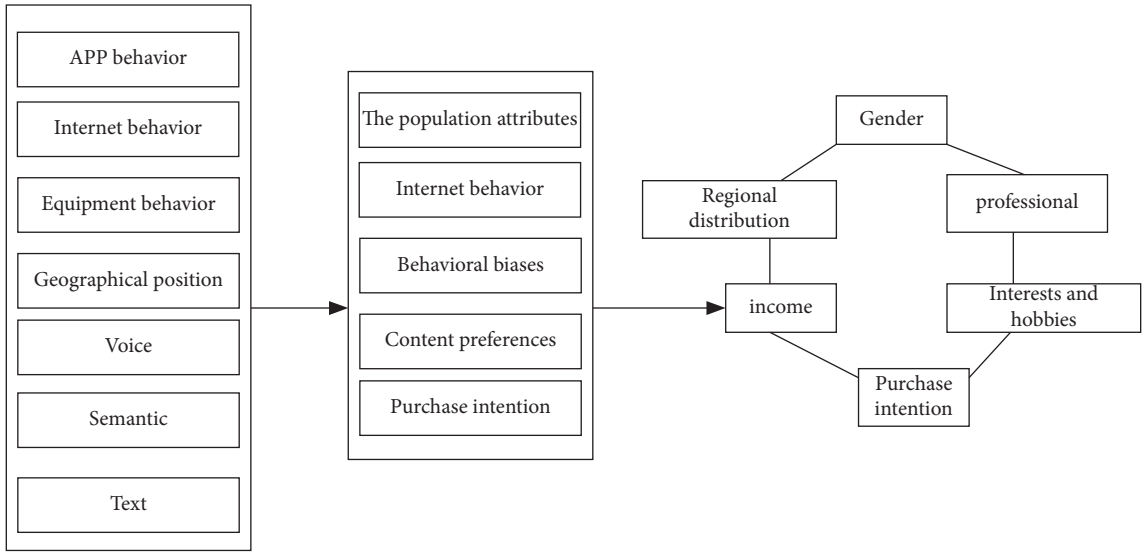

Figure 3: User label system establishment.

a company in 2012, and got married in 2013. Figure 3 shows that the construction of the user tag system is divided into three stages. The first stage is basic data, app behavior, Internet behavior, location behavior, geographic location, voice, semantics, and text. The second stage is user tag mining, demographic attributes, online behavior, interest preferences, content preferences, and purchase intentions. The third stage is user persona, gender, age, geographical distribution, hobbies, purchase intention, purchase, and occupation [12]. Satisfying business needs is a prerequisite for establishing user personas. To build a user profile, it is necessary to clarify the data rows used in the construction of

the target to lay the foundation for the specified label. User persona tags are divided into two categories, the first category is static tags, and the second category is dynamic tags. The demographic attribute tags in static tags are relatively stable and generally do not change [13]. They are often used to describe the most basic characteristics of users. There are dependencies between static tags. Using original data, what can be constructed is fact tags. Through simple statistical methods, higher-level preference tags can be constructed. Using deep learning techniques in machine learning tools can also predict labels. User persona technology is adopted to construct a persona model of social governance elements. The profile model of social governance elements is shown in Figure 4.

Figure 4 shows that the persona model of social governance elements has a three-tier structure. The function of the underlying structure is to build a persona model, which is specifically divided into basic attributes, location characteristics, behavior characteristics, and relationship networks. The middle structure is analysis algorithms, which are natural language processing, machine learning, clustering algorithms, and prediction algorithms. The top-level structure is the basic data, which are residence, life, production, and medical care. The user label system is shown in Figure 5, which shows that population attributes are divided into basic attributes and geographic locations. The basic attributes can be divided into gender, age, and educational background. Industry preferences can be divided into automobiles, real estate, tourism, and finance.

The priority of various label construction is shown in Figure 6. It shows that from the bottom to the top are the original data, fact labels, model labels, and high-level labels. Among them, fact tags can be divided into usage times, historical trends, active days, and complaints times. Model tags are divided into demographic attributes, industry interests, geographic locations, and product preferences, and advanced tags are divided into population attributes and potential loss.

Jieba is a common method of word segmentation [14]. The working principle is to combine the possible words in the generated sentence into a ring graph. Next, dynamic programming is used to calculate word frequency probability. Finally, the hidden Markov model (HMM) is employed to recognize unregistered words [15]. The schematic diagram of the Jieba word segmentation principle is shown in Figure 7:

A complete back propagation (BP) neural network consists of an input layer, an output layer, and multiple hidden layers. In the BP neural network, the neurons between the hidden layers are connected, but the input layer and the hidden layer, and the hidden layer and the output are fully connected [16]. The BP neural network is composed of three processes:

(i) When the input signal enters the BP neural network, the signal flows through the input layer to the hidden layer and passes to the output layer. When the signal is transmitted to the neuron on the hidden layer, it is transmitted to the next hidden layer after the action of the neuron on the hidden layer, finally passed to the output layer.

(ii) The difference between the actual output and the expected output of the network is used as the error

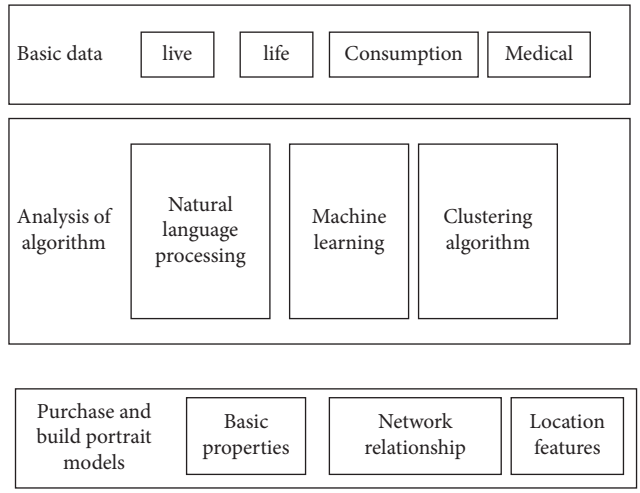

Figure 4: Information persona model of social governance elements.

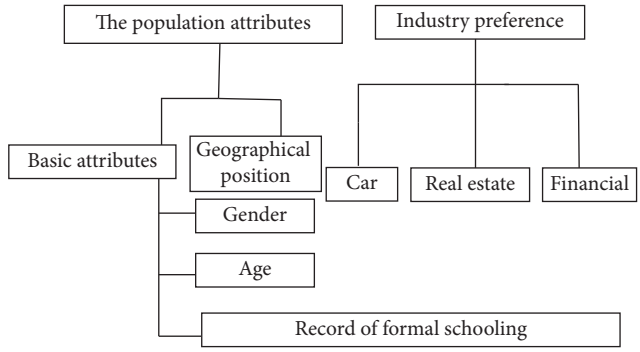

Figure 5: User tag system.

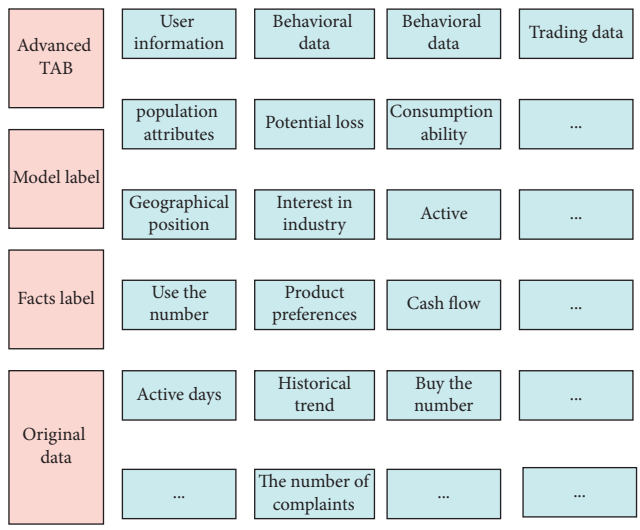

Figure 6: The priority of various label construction.

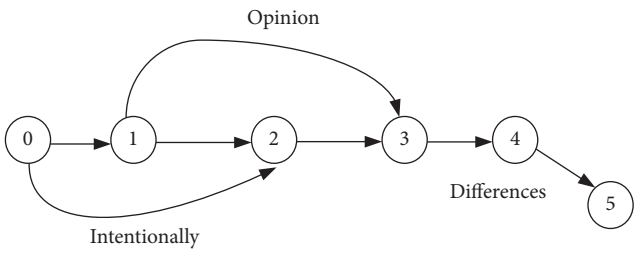

Figure 7: Schematic diagram of the Jieba word segmentation principle.

signal, and the output layer of the neural network is used to modify the connection weights layer by layer through the hidden layer item output layer.

(iii) The first two steps were performed repeatedly until the global error of the network reaches the threshold.

As the network depth continues to deepen, the increase in the accuracy of network training will tend to be flat. From AlexNet to VGGNet, the number of network model layers continues to increase, and the effect is getting better and better. As the number of network layers increases, the network will have problems such as overfitting, degradation, gradient explosion, and gradient disappearance. To solve these problems, the residual network is often optimized [17]. Although the depth of this network is deeper than that of ordinary convolutional neural networks (CNNs), the computational efficiency is higher than that of ordinary CNNs. The key point of the residual network is to let the information flow through the shortcut connection to the shallow layer. The residual network solves the problems of network degradation and gradient explosion caused by the increase of the number of layers in the CNN. The recurrent neural network (RNN) performs very well in the field of neurolinguistic programming (NLP) [18]. In the RNN model, each input node corresponds to a hidden node, and the hidden nodes form a linear sequence, and the information is passed from the front to the back. A recurrent neural network is a neural network with a feedback structure. Its output is not only related to the weight of the current input network but also related to the input of the previous network. The RNN has the concept of time sequence, and the state at the next moment is affected by the state at the current moment. Some researchers have called recursive networks as deep networks [19]. Its depth can be expressed in three aspects. The first aspect is the input depth, the second is the output depth, and the third is the time step. An expanded RNN structure is shown in Figure 8.

The computation of the forward propagation of the RNN network is shown in the following equations:

$$a_k^t = \sum_{h=1}^{H} w_{hk} b_h^t, \tag{1}$$

$$a_h^t = \sum_{i=1}^{I} w_{ih} x_i^t + \sum_{h'=1}^{H} w_{h'h} b_{h'}^{t-1}, \tag{2}$$

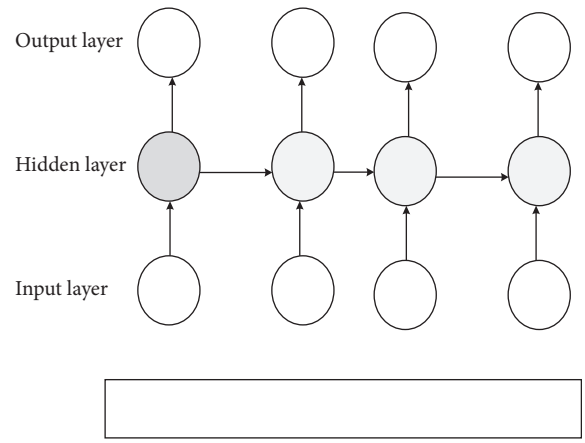

Figure 8: Schematic diagram of the RNN model.

$$b_h^t = \theta_h\left(a_h^t\right), \tag{3}$$

where b is the calculated value of the activation function, a is the value calculated by the aggregation, w represents the link parameter between different nodes, the output layer is w_k, and the hidden layer is w_h.

The computation process of the backward propagation of the RNN network is shown in the following equations:

$$\delta_h^t = \theta'\left(a_h^t\right)\left(\sum_{k=1}^{K} \delta_k^t w_{hk} + \sum_{h'=1}^{H} \delta_{h'}^{t+1} w_{hh'}\right), \tag{4}$$

$$\delta_j^t = \frac{\partial L}{\partial a_j^t}, \tag{5}$$

$$\frac{\partial L}{\partial w_{ij}} = \sum_{t=1}^{T} \frac{\partial L}{\partial a_j^t} \frac{\partial a_j^i}{\partial w_{ij}} = \sum_{t=1}^{T} \delta_j^t b_i^t. \tag{6}$$

In equations (4), (5), and (6), w_{hk} is the weight matrix of $l \times n$, connecting l hidden layer units to n output layer units, $w_{hh'}$ denotes the $n \times n$ weight matrix, connecting k hidden layer units to l output layer units, δ_j^t means the hidden layer vector, w_{ij} represents the fixed parameter, a_h^t is the fixed coefficient, b_i^t is the weight, and L is the parameter in the matrix unit.

The advantage of the RNN neural network is that the concept of timing is added to the neural network. This makes it possible to set different inputs of the RNN neural network according to the time node. In the RNN neural network, data can also be multi-input. The disadvantage of RNN is that it cannot solve the problem of long-term network dependence, gradient disappearance, and explosion. For this reason, the long short-term memory (LSTM) network is proposed in multiple studies [20, 21]. One neuron in the LSTM model contains one cell state and three gate mechanisms. The cell state in the LSTM model is the basis of the LSTM model, and its function is equivalent to the model memory. With the change of time, the cell state also changes to a certain extent. The LSTM model uses forget gates, update gates, and output gates to protect and control the state of cells. The information recorded in the LSTM network is updated and determined by the gate mechanism.

Vasvani et al. [22] proposed a structural transformer that processes sequence models by the attention mechanism. BERT (bidirectional encoder representations from transformers) applies the bidirectional training of the transformer. The transformer in the BERT network refers to the complete encoder-decoder framework. The complete encoder-decoder framework includes mutihead self-attention, layer norm, skip connection, and transformer structure. The visual attention mechanism is a signal processing mechanism similar to the human brain. Humans can select local areas of focus by observing the overall picture. Then, more attention is focused on the focus area than the normal area to get more detailed features and suppress other useless information. According to the big categories, the attention mechanism can be divided into soft attention mechanism and hard attention mechanism. The calculation method of the soft attention mechanism is to pack all the components and perform weighting operations on the retained components [23]. The calculation method of hard attention is to select some components for weighting. A schematic diagram of this attention mechanism is shown in Figure 9.

The essential idea of the attention mechanism is to treat the constituent elements in the input as the composition of key-value pairs of data. The key-value pair data correspond to the element query in the output. By calculating the similarity between the query element and each key, the weight coefficient of each key corresponding to the key value can be obtained. Multiple key values is summed to obtain the final attention mechanism value. For multivariate time series forecasting, the introduction of an attention mechanism can focus on the relevant variable dimensions that are dependent on the forecast time series, instead of all input sequences.

The BERT model is a pretrained model with excellent performance. When using it, there is no need to use a large amount of data to train it and fine-tune the pretraining model to be used for downstream NLP tasks. The schematic diagram of the BERT model is shown in Figure 10, and the transformer encoding is shown in Figure 11, respectively.

The transformer encoding is divided into the following three processes:

Token embeddings: it is responsible for converting each word into a vector of fixed dimensions. BERT uses the WordPiece vocabulary for tokenization.

Segmentation embeddings: it is responsible for separating two sentences with symbols. Each word in the first sentence is assigned 0, and the token of the second sentence is assigned 1.

Position embeddings: it helps to add position coding.

2.2. Research on Logistic Regression and Support Vector Machine (SVM) Model. Spark is designed to perform iterative work, which is consistent with the training process of machine learning algorithms. MLlib is a spark's machine learning library. It supports classification, clustering, regression, and collaborative filtering. Classification is the most extensive in commercial applications. MLlib classification and regression-related algorithms are shown in Table 1. The loss function and its subgradients in MLlib are shown in Table 2, and the core content of the MLlib algorithm library is shown in Figure 12, respectively.

The models used are LSVM and logistic regression. The convex optimization method is used to optimize the objective function, as given in the following equation:

$$\mathcal{F}(w)\colon \lambda R(w) + \frac{1}{n}\sum_{i=1} L(w; x_i, y_i). \tag{7}$$

The objective function optimized by the logistic regression algorithm is shown in the following equation:

$$L(w) = \sum_{i}\left[-y_i \log\left(1 + e^{-w^t x_i}\right) - (1 - y_i)\log\left(1 + e^{w^t x_i}\right)\right]. \tag{8}$$

In equation (8), x_i is the i-th data vector, y_i indicates the category of x_i, and $w \in R^n$ denotes the desired vector and $y_i \in \{0, 1\}$ is the category of $x_i w \in R^n$ and is the desired vector. The method of calculating the classification accuracy of LSVM is to find a hyperplane in a high-dimensional space. This hyperplane is used to classify the points in the space and calculate the distance between the points and the hyperplane to evaluate the classification accuracy. The loss function of the SVM algorithm is computed as

$$\sum_{i=1}^{N}\left[1 - y_i\left(wx_i + b\right)\right]_+ + \lambda\|w\|^2. \tag{9}$$

2.3. Method of Establishing the Framework of the Resource Pool of Social Governance Elements. Since user data systems require a lot of data processing work, common big data processing systems such as MapReduce and Spark are used. A common big data processing platform is the Hadoop distributed file system (HDFS). The user's behavior on the app is collected and stored in the Hadoop distributed file system. YARN is used to manage data resources. It was introduced in Hadoop 2.0 to remove the bottleneck on job tracker which was present in Hadoop 1.0. The data processing flow is as follows: the client first sends a request and according to the corresponding protocol, the server log is stored [24]. The server log is retrieved using a script file. The engine calls the program package to load the content in the temporary file, stores the structured data in different folders, and stores the parsed data on HDFS. In the establishment of the label, the gender label and the educational background label in the population label are selected. Among them, the gender label is divided into male and female. The academic qualifications are labeled as lower, middle, and higher. The data used comes from real data from a statistical company. Two million data points are used as the gender label seed, and the behavior data in the app is intersected. 270,000 data points are retained as training samples, and 2.2 million degree labels are used as training samples. Because there are many subcategories of the interest tag, the loan category under the finance tag is selected. In this way, the framework of the social governance element resource pool was established. First, a classification system needs to be established. By sorting out 200 million pieces of information shared by

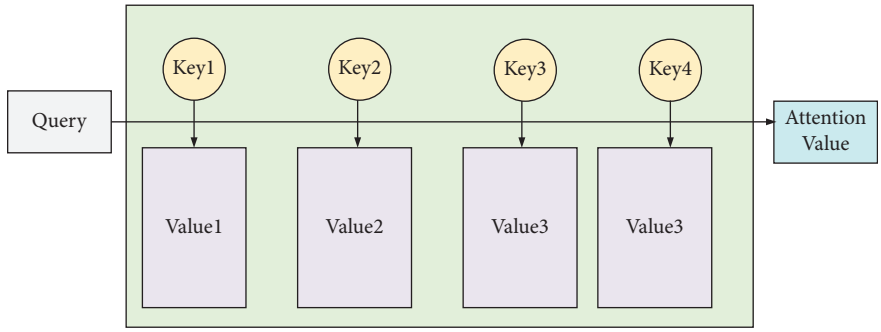

Figure 9: Schematic diagram of attention mechanism.

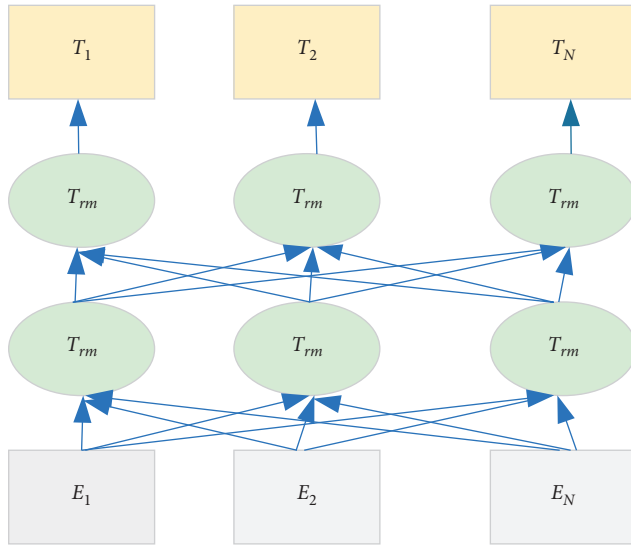

Figure 10: Schematic diagram of the BERT model.

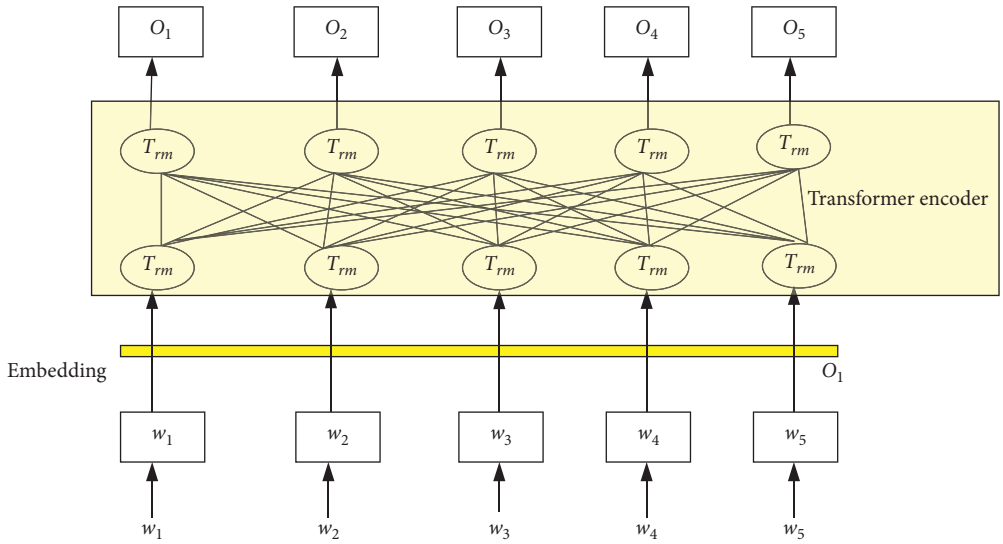

Figure 11: Transformer encoder.

30 departments, forming an information resource directory, and establishing multiple classifications and labeling systems. Next, the rules are constructed. To study the situation of the functional department data, the data analysis method is used to obtain the similarities and differences of the population and the degree of matching. The authoritative

Table 1: MLlib classification and regression-related algorithms.

Problem type	Algorithm
Binary classification	Linear support vector machine (LSVM), logistic regression, decision tree, random forest, gradient descent decision tree (GBDT), and naive Bayes model (NBM)
Multiple classifications	Logistic regression, decision tree, random forest, and NBM
Return	Linear least squares, lasso, ridge regression, decision tree, random forest, GBDT, and isotonic regression

Table 2: Loss function and its subgradients in MLlib.

	loss fuction $L(w, x, y)$	gradient or subgradient
Hinge loss	$\max\{0, 1 - yw^T\mathbf{x}\},\ y \in \{-1, +1\}$	$\begin{cases} -yx & \text{if } yw^T x < 1 \\ 0 & \text{otherwise} \end{cases}$
Logistic loss	$\log(1 + \exp(-yw^T x)),\ y \in \{-1, +1\}$	$-y(1 - 1/1 + \exp(-yw^T x))$
Squared loss	$1/2(w^T x) - y)^2,\ y \in R$	$(w^T x - y)x$

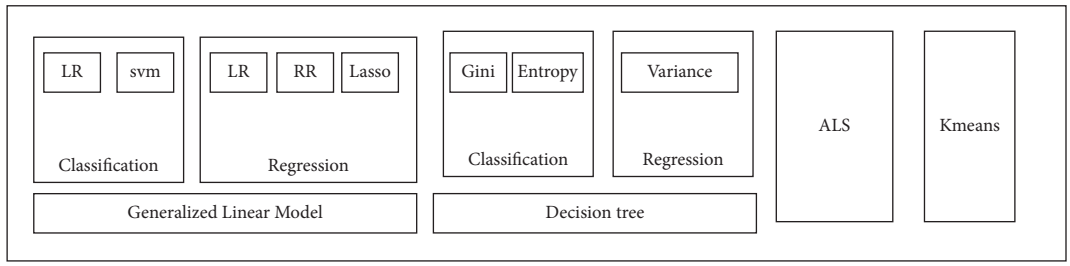

Figure 12: The core content of the MLlib algorithm library.

data of the authoritative department is the rule basis of the model, which is used to compare and match all information fields. The resource pool of social governance elements by the user profile model consists of three parts: construction of resource pool data warehouse and storage mechanism, the design of persona model of social governance elements, and the design of label system rules. The experimental programs are divided into four types:

Solution 1: count the names of used apps and create an index table

Solution 2: count the number of times and use the number filling feature

Solution 3: map the secondary classification directory and establish a feature index

Solution 4: same as Solution 3, except that the number of uses of the secondary directory is accumulated and filled

3. Results

3.1. Analysis of Population Attribute Mining. Experiments found that using the app name mapping index table and filling it with 1 is the best choice. During the experiment, the sampling ratio and the model are changed, and the results are shown in Table 3. It is evident that for a sampling ratio of 1, the LR obtained an accuracy (AUC) of 0.82%, and precision (PRE) of 0.77%, respectively. When the sampling ratio is reduced to 0.4, the model reported 0.81% AUC and 0.77% PRE, respectively. In the case of SVM, when the sampling ratio is 0.2, the highest AUC and PRE reported are 0.73% and 0.66%, respectively. However, the performance of the SVM model is not as good as the LR model.

The result of education qualification prediction is shown in Figure 13.

Figure 13 shows that the overall accuracy rate of academic qualification prediction reaches 74.5%, and the constructed system has the highest accuracy rate for predicting low academic qualifications. In the survey samples, the proportion of people with high education is relatively low, the proportion of people with high education in the training set is low, and the model learns fewer characteristics of people with high education. The accuracy rate of the constructed system for predicting high degrees is lower than that for a low degree.

3.2. Model Performance Analysis. To compare the performance of different machine learning models, the comparative results of each deep learning model on the verification set on each epoch are shown in Figure 14.

It can be seen that the accuracy of the BERT in the first epoch is 92%, and the accuracy of the BERT in the fifth epoch is 0.94%. The accuracy of the CNN in the first and second epochs are 89% and 0.90%, respectively. Likewise, the accuracy of bidirectional long short-term memory (Bi-LSTM) + attention in the first epoch is 85%, and that in the fifth epoch is 87%, respectively. Similarly, the accuracy of the transformer block in the first epoch is 81% and in the fifth epoch is 84%. Comparing the performance of the four models, it is evident that the BERT model provides the

Table 3: Results of changing the sampling ratio and model.

Model	Sample sampling ratio	AUC	PRE
LR	1	0.82	0.77
	0.4	0.81	0.77
	0.2	0.89	0.85
	0.1	0.89	0.86
	0.01	0.91	0.82
SVM	1	0.72	0.66
	0.5	0.72	0.66
	0.2	0.73	0.66

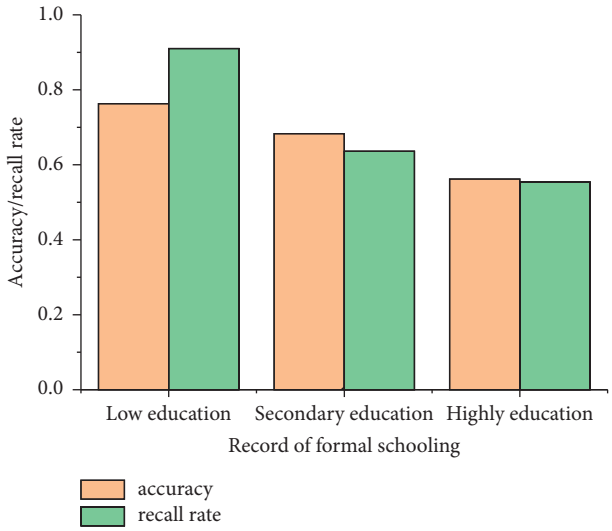

Figure 13: Educational qualification prediction results.

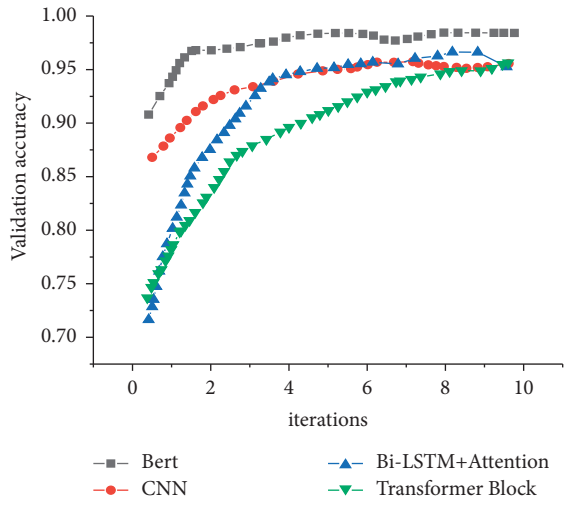

Figure 14: Accuracy of deep learning model validation set.

highest performance. In addition, the CNN also has a good performance on the dataset. Although the accuracy of the CNN is slightly lower than the BERT model, the training speed t is faster. The test results of the deep learning model are shown in Figure 15, and the training process of each model is shown in Figure 16.

Figure 16 shows that there is no need to use complex functions to construct location information on a smaller dataset; therefore, the BERT pretrained model is used. The migration fine-tuning model on the Chinese intention recognition subtask has a very good effect and can accurately judge the user's intention.

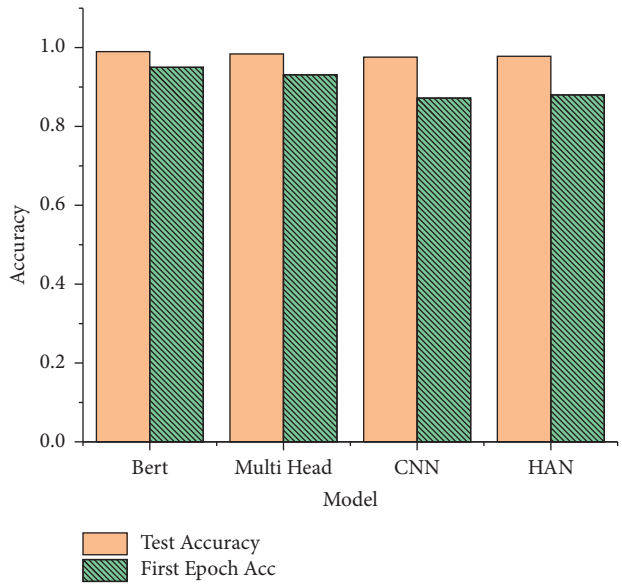

Figure 15: Deep learning model test set results.

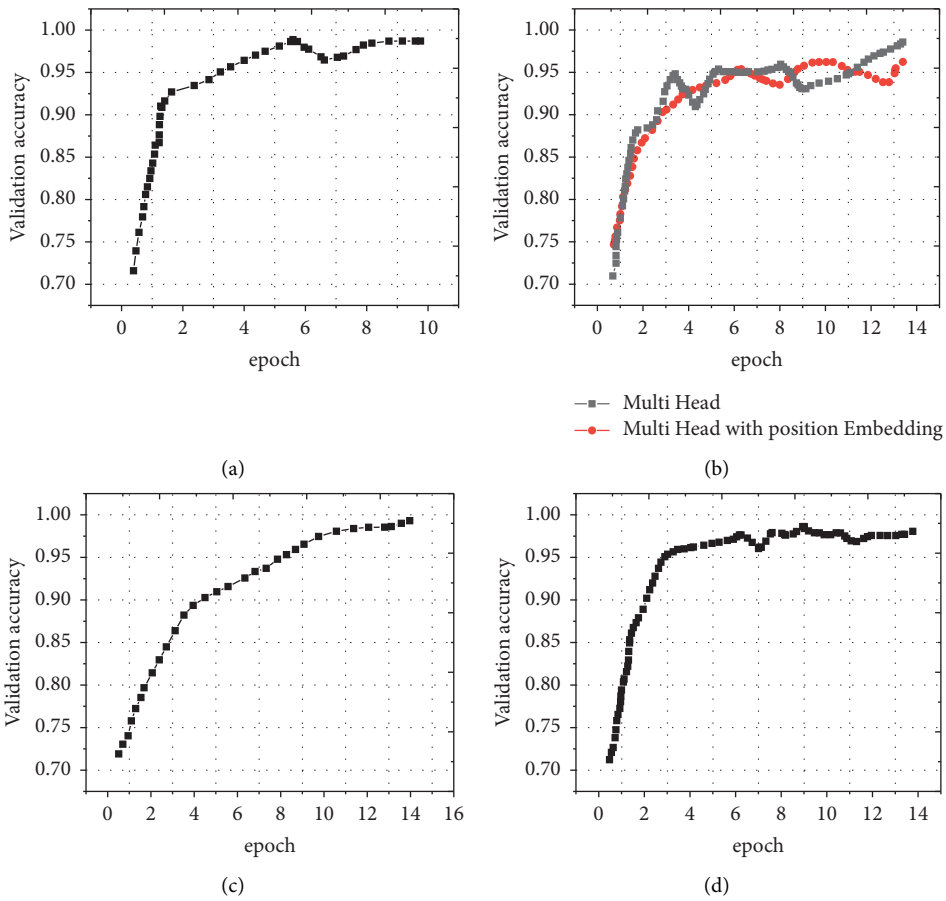

Figure 16: The training process of each model. (a) Bert. (b) Transformer. (c) Bi-LSTM + attention. (d) CNN.

4. Conclusions

With rapid development, artificial intelligence has become the central technique for intelligent resources information. In this study, the persona system is designed to speed up the efficiency of information resource transmission of national government departments and improve the informatization level of government social management, and a social service

and management resource pool system is proposed. Based on the collected data, the tags for demographic attributes and interest are modelled and the social service and management resource pool system is built and tested using a deep learning model. In the experiment, the overall accuracies of the constructed age, academic qualifications, and interest label reported are 85.2%, 74.5%, and 99.0%, respectively. The constructed system greatly deepens the visualization of the characteristics of social governance elements. Its visualization and vividness have been significantly enhanced, the level of resource sharing by government departments has been greatly improved, and the foundation for spatial decision-making in smart social governance has been laid.

Data Availability

The datasets used and/or analyzed during the current study are available from the corresponding author upon reasonable request.

Conflicts of Interest

The authors declare that they have no conflicts of interest.

References

[1] J. D. Watson and F. H. C. Crick, "Molecular structure of nucleic acids: a structure for deoxyribose nucleic acid," *Nature*, vol. 171, no. 4356, pp. 737-738, 1953.

[2] E. P.-y. Yu, C. Q. Guo, and B. V. Luu, "Environmental, social and governance transparency and firm value," *Business Strategy and the Environment*, vol. 27, no. 7, pp. 987–1004, 2018.

[3] W. Elgammal, A.-N. El-Kassar, and L. Canaan Messarra, "Corporate ethics, governance and social responsibility in MENA countries," *Management Decision*, vol. 56, no. 1, pp. 273–291, 2018.

[4] L. Qiang Li, Z. Hao Wang, and W. Lu Zheng, "Bringing society back in: the new Qinghe experiment and social governance in China," *Korea Journal*, vol. 58, no. 1, pp. 70–95, 2018.

[5] L. Widyawati, "A systematic literature review of socially responsible investment and environmental social governance metrics," *Business Strategy and the Environment*, vol. 29, no. 10, pp. 73–95, 2020.

[6] R. K. Bhaskaran, I. Ting, S. K. Sukumaran, and S. D. Sumod, "Environmental, social and governance initiatives and wealth creation for firms: an empirical examination," *Managerial and Decision Economics*, vol. 41, no. 10, pp. 3–5, 2020.

[7] M. H. Shakil, "Environmental, social and governance performance and stock price volatility: a moderating role of firm size," *Journal of Public Affairs*, vol. 4, no. 1, pp. 12–20, 2020.

[8] D. Ki-Aries and S. Faily, "Persona-centred information security awareness," *Computers & Security*, vol. 70, pp. 663–674, 2017.

[9] E. Schoch, A. M. L. A. Choi, H. Lee, S. Connor, and E. J. Rose, "The food locker: An innovative, user-centered approach to address food insecurity on campus," in *Proceedings of the 37th ACM International Conference on the Design of Communication*, Association for Computing Machinery, Portland, OR, USA, October 2019.

[10] R. Bodin, M. M García, and G. Robins, ""Reconciling conflict and cooperation in environmental governance: a social network perspective," *Annual Review of Environment and Resources*, vol. 45, no. 1, pp. 18–29, 2020.

[11] L. E. Delgado, C. C. Zúiga, R. A. Asún et al., "Toward social-ecological coastal zone governance of Chiloé Island (Chile) by the DPSIR framework," *The Science of the Total Environment*, vol. 785, no. 13, Article ID 143999, 2020.

[12] Z. Umar, D. Kenourgios, and S. Papathanasiou, "The static and dynamic connectedness of environmental, social, and governance investments: International evidence," *Economic Modelling*, vol. 93, no. 3, pp. 112–124, 2020.

[13] J. Huang, B. Liu, and J. Tao, "Learning long-term temporal contexts using skip RNN for continuous emotion recognition," *Virtual Reality & Intelligent Hardware*, vol. 3, no. 1, pp. 55–64, 2020.

[14] J. C. Timoneda, "Estimating group fixed effects in panel data with a binary dependent variable: how the LPM outperforms logistic regression in rare events data," *Social Science Research*, vol. 93, no. 1, Article ID 102486, 2020.

[15] M. A. Qureshi, S. Kirkerud, K. Theresa, and T. Ahsan, "The impact of sustainability (environmental, social, and governance) disclosure and board diversity on firm value: the moderating role of industry sensitivity," *Business Strategy and the Environment*, vol. 29, no. 1, p. 2486, 2020.

[16] V. Casino, L. House-Peters, J. W. Crampton, and H. Gerhardt, "The social life of robots: the politics of algorithms, governance, and sovereignty," *Antipode*, vol. 52, no. 1, p. 6, 2020.

[17] N. Licht, "Wandel von Sozialpolitik im Kontext von Global Social Governance: Das Beispiel Peru," *Studies*, vol. 99, no. 12, p. 63, 2020.

[18] F. Li, Y. Ji, W. Liu, B. P. S. Rawat, P. Cai, and H. Yu, "Fine-tuning bidirectional encoder representations from transformers (BERT)-based models on large-scale electronic health record notes: an empirical study," *JMIR Medical Informatics*, vol. 7, no. 3, p. 3, 2019.

[19] Z. Ren, Q. Shen, X. Diao, and H. Xu, "A sentiment-aware deep learning approach for personality detection from text," *Information Processing & Management*, vol. 58, no. 3, Article ID 102532, 2021.

[20] Y. Zhou, Y. Yang, H. Liu, X. Liu, and N. Savage, "Deep learning based fusion approach for hate speech detection," *IEEE Access*, vol. 8, no. 8, pp. 128923–128929, 2020.

[21] K. Shankar, S. K. Lakshmanaprabu, D. Gupta, A. Maseleno, and V. H. C. de Albuquerque, "Optimal feature-based multi-kernel SVM approach for thyroid disease classification," *The Journal of Supercomputing*, vol. 76, no. 28, pp. 1–16, 2020.

[22] M. Khan, M. Q. Reza, A. K. Salhan, and S. P. S. M. A. Sirdeshmukh, "Classification of oils by ECOC based multi-class SVM using spectral analysis of acoustic signals," *Applied Acoustics*, vol. 183, no. 3, Article ID 108273, 2021.

[23] Y. Wang, D. Wang, and Y. Tang, "Clustered hybrid wind power prediction model by ARMA, PSO-SVM and clustering methods," *IEEE Access*, vol. 8, no. 1, p. 1, 2020.

[24] T. L. Bailey, "MD-SVM: a novel SVM-based algorithm for the motif discovery of transcription factor binding sites," *Bioinformatics*, vol. 28, no. 1, pp. 56–62, 2019.

Hindawi
Scientific Programming
Volume 2022, Article ID 5951844, 10 pages
https://doi.org/10.1155/2022/5951844

Research Article

A Study on the Application of Computer-Aided Dual-Coding Theory in English Vocabulary Teaching

Li Luo

Humanities Institute, Chongqing Metropolitan College of Science and Technology, Yongchuan, Chongqing 402160, China

Correspondence should be addressed to Li Luo; luoli@cqcst.edu.cn

Received 27 January 2022; Revised 11 February 2022; Accepted 18 February 2022; Published 16 March 2022

Academic Editor: Muhammad Usman

Learning English needs a huge amount of vocabulary recalls as well as multiple grammatical structures and practices. With the development and improvement of the humanization and quality of English teaching, the multidimensional teaching of English has formed a powerful learning model and teaching method. The teaching of dual-coding theory assisted by computer teaching software mainly focuses on the dual activation representation of language combined with nonverbal graphic recognition to complete the recognition of information. According to the dual-coding hypothesis, in Gilford's intelligence theory, the capacity of spatial and information recognition and reading is highly significant. With the large amount of visual recognition and information acquisition, images involve spatial domain information reading, which is a learning method based on the principle of information feature recognition. Based on the principle of dual-coding theory, it is a very effective way to present information and recall specific information in the form of vision and language. In this study, the application research for the purpose of English vocabulary teaching is adopted that has strong innovative and practical characteristics. According to the steps and contents of English vocabulary learning, the study is carried out step by step from the context in detail, so it continuously improves the learning quality and efficiency of English vocabulary teaching. Vocabulary teaching can help the students better improve their cognitive level of vocabulary and meet the vocabulary test requirements of the new institution entrance examination. Further, how to improve the effect of senior high school English vocabulary teaching is a major topic in the field of senior high school English teaching. In order to sort out this issue, I proposed a computer-aided dual-coding theory to help quickly understand vocabulary usage in order to increase learning efficiency. The Paivio–Desrochers model is used in this study. In addition, this study also attempts to explore the application of dual-coding theory in senior high school English vocabulary teaching.

1. Introduction

According to the dual-coding theory (DCT), human brain uses both verbal and visual information for the storage and representation of information, but the human mind processes this information differently with the help of two separate channels [1]. The dual-coding theory (a theory of cognition) was proposed by the Canadian psychologist Allan Paivio of the University of Western Ontario in 1971. Paivio based his hypothesis on the idea that the development of mental images enhances learning [2]. He put forward the dual-coding theory of long-term memory. Based on long-term memory, memory methods are divided into two systems: image system and semantic system. Representation and semantics are two parallel and related cognitive systems. Representation system uses representation code to store information and semantic system stores information with the help of semantic code [3]. People's visual representations are particularly developed, and they can be activated by relevant inspirations, respectively. Semantic code is an abstract representation of meaning. Some discrete materials are organized due to meaningful connections, making memory relatively easy [4].

Paivio found in his experiment that the fastest recognition is made by the help of dual memory of images and words. The fast and direct image is produced by the content recalled from pictures and words [5]. The combination of information and tools has certain advantages. The brain's memory effect and speed of image materials are slightly better than those of simple semantic memory. The theory

describes the human cognitive process, which includes two different but interrelated input channels: verbal and nonverbal systems. One processing system is responsible for processing based on language and the other processing system is responsible for processing based on images. In other words, one is responsible for the handling of information and the other is responsible for the storage and extraction of information [6]. Yan and Filieri [7] make a 5-minute experiment. In this experiment, (A) is used to recall the pictures and words together while (B) is used to remember the words and visuals separately. Yan et al. [8] also conducted such an experiment, using a primate gorilla with the same brain as human beings, but with a smarter brain. When gorilla remembers a picture for only 0.3–0.5 seconds, the memory effect of sound plus picture is more significant.

According to the dual-coding theory, there are two processing systems with independent but interrelated functions in the human brain: one processing system is based on language, and the other processing system is based on image [9]. Image system is specific for representing and processing nonverbal objects and events. It is composed of image representations with associative relationship. Cognition is supported by two special representation systems, which come from experience and have obvious differences in expressing and processing information about nonverbal objects, events and linguistic information [10]. Combined with English research, in the current process of English vocabulary teaching, more and more students begin to feel the pressure of vocabulary memory and application, which also highlights the shortcomings of current English vocabulary teaching. In other words, for getting a deep insight about a language and to speak fluently, vocabulary memorization and understanding is playing a vital role in this regard [11]. On the basis of DCT, we understand that in senior high school English vocabulary teaching, we should not only pursue the image of vocabulary itself in form, but also further strengthen the processing of its overall change around the change of vocabulary and the application of vocabulary [12]. Through this changing teaching, we can improve students' level and ability of vocabulary perception so as to deepen their impression and complete the predetermined vocabulary teaching objectives. For example, for the changing forms of verbs, a good memory bridge is formed with the help of certain context to help students input vocabulary and encode vocabulary so as to lay the foundation for the subsequent retrieval of vocabulary information [13].

In order to promote the students' vocabulary processing cognitively, this study determines that the dual-coding theory can improve English vocabulary learning, improve the overall language vocabulary level, and enrich their own vocabulary reserves through word roots, affixes, and other ways. In this way, an overall dual-coding framework is formed, which creates favorable conditions for subsequent vocabulary application and vocabulary extraction [14]. In the process of guiding students' cognitive processing, we should also start from students' cognitive behavior characteristics and cognitive tendency, create a more favorable language cognitive environment for students through the enrichment of language culture and relevant background knowledge materials, and also play the role of the combination of vocabulary cognition and dual-coding theory. By creating a good cognitive incentive system, students are encouraged to actively explore, actively construct, and actively double code so as to provide a good foundation for senior high school English vocabulary teaching in the future [15]. In the process of encouraging students, we can appropriately adopt the way of word memory competition, let students improve the effect of word memory with the help of game level interaction, and realize the effectiveness and persistence of coding through rich and colorful double construction activities [16].

Finally, the evaluation system of vocabulary teaching needs to be improved. Nowadays, the process of English vocabulary teaching, relevant evaluation indicators, and contents of vocabulary teaching are mainly through reading comprehension and grammar [16]. Test modes like fill in the blanks and other related specific questions of word base lack English vocabulary teaching. Fill in the blanks and other related specific questions, which is lack of word-based test methods and test modes. Therefore, how to proceed from the current situation and further explore the idea of overall English vocabulary teaching evaluation is particularly important. In short, from the above analysis, it can be seen that in the current process of English vocabulary teaching the use of dual-coding theory and technology is applied to the process of English vocabulary teaching. The research on these methods, strategies, and environmental evaluation system of vocabulary teaching is still in the initial stage, and there is still a lot of study space. Using this innovative research method, we want to put forward specific research ideas and processes, which lays a foundation for follow-up research. The main contributions are as follows: (1) in this paper, we describe Paivio–Desrochers dual-coding theory and dual-coding theory of multimedia learning. (2) We summarized the applications of computer-aided dual-coding theory in English vocabulary teaching. (3) We closed our study with a summary of the predictions concerning the role of spatial ability in learning from words and pictures.

The rest of the paper is organized as follows. Section 2 illustrates the related work, Section 3 demonstrates the material and methods, and Section 4 represents the results and discussion. Finally, the research study is concluded in Section 5.

2. Related Work

Vocabulary is regarded as a complete set of words and phrases and is one of the three constructive parts of linguistic. It is a societal phenomenon that has occurred in the past. Liu and Ge [17] stated that the main difference between the English language native speakers and the nonnative speaker is the vocabulary of English, which indeed is very necessary for the fluency and better understanding of the English language. Without saying the vocabulary has less importance. In an English as a Second Language (ESL) class, teaching and understanding vocabulary requires a lot of time and effort. People are frequently disheartened from the

learning outcomes [18]. Therefore, people need a system that improves English vocabulary. So, this paper introduces a study on the application of computer aided dual coding theory in English vocabulary teaching. Fu and Xu [19] have worked on micro-English vocabulary system, which consists of the following sections:

(1) *Mobile Learning*

Mobile learning is a new learning mode in education that is built on today's mobile communication and computer technologies. The word "mobile" refers to the digitalize embodiment of interactive learning content [20]. Mobile learning is less reliant or limited than Web-based learning, and hence it overcomes the constraints of time and place. When and whenever feasible, the learning mode provides learners with new experiences.

(2) *Microlearning*

Adult learners are becoming more interested in microlearning, particularly in professional training. The term "micro" refers to microdevices that are modest, light, or small in size. It refers to little learning content as well as smaller learning media with a brief learning duration. Microlearning is concerned with the acquisition, storage, production, and transmission of tiny blocks of knowledge via a small and portable device. It provides a comfortable and enjoyable learning atmosphere and experience for students [21].

(3) *Mobile Microlearning*

Mobile microlearning is derived from on-demand learning, which is made by merging mobile technology (wireless and tiny devices) with microlearning mode. Mobile microlearning is found in a variety of learning environments. Mobile microlearning consists of two advanced features: first, flexibility in learning activities at any time and place and second, interactivity between learners and educators in both instances and relaxation [22].

2.1. Dual-Coding English Vocabulary Theory. Paivio presented the dual-coding hypothesis in 1971. According to the Paivio hypothesis, the value of linguistic and nonlinguistic items is equal. He claims that human cognition is very specific when we process both verbal and nonverbal objects [23]. A verbal system processes not only writing and speech, but it also acts as a symbol for nonlinguistic objects like events and behaviors. The connotation of dual-coding theory and its assumption has two cognitive subsystems: one is dedicated to the representation and processing of nonverbal things and events (i.e., images), while the other is used for language processing [24]. The theory grips that it is very important for later information recognition to store lexical information by dual-coding language. The application of dual-coding theory can stimulate student's image thinking and help them to gain new information with the help of the original knowledge reserve [25]. Dual-coding theory plays an extremely important role in student's vocabulary memory, problem solving, concept learning, and overall language cognition. Figure 1 describes the concept of the dual-coding theory.

Figure 1explains the processing of our cognitive system, which consists of verbal and nonverbal systems. It also consists of three levels of processing, which includes representational processing, referential processing, and associative processing. The top of the model shows that people's cognitive process initially begins with sensory systems of verbal and nonverbal stimuli from the real environment [26]. As shown in the figure, the organization of the verbal system is sequential and hierarchical. It indicates that the verbal system works like a network. On the other side, the images in the nonverbal system are constructed in an overlapping and nested way.

2.2. Dual-Coding Theory of Multimedia Learning. Multimedia learning occurs when students create knowledge from the information offered in two or more modes, such as a graphically shown animation and audibly presented narrative. In a precise sense, our definition applies to the word "multimodal" (which refers to the concept that the learner uses more than one sense modality) rather than "multimedia" (which refers to idea that the instructor uses more than one presentation medium) [27]. Two separate sense modalities are visual and verbal processing, and two different presentation mediums are animation and narration. It is also worth noting that, in some cases, verbal content can elicit the development of visual representations and that visual material can elicit the construction of verbal representations.

A dual-coding theory of multimedia learning is summarized in Figure 2. Our version of dual-coding theory (Paivio, 1971, 1986; Clark and Paivio, 1991), which we adapted and modified from Paivio's theory (Paivio, 1971, 1986; Clark and Paivio, 1991), provides a three-process account of how visually and verbally presented material may be integrated within the learner's working memory during learning [28]. A verbal explanation, such as an oral narration, is delivered to the student in the top-left area of the picture. The learner creates a mental model of the system presented in the spoken explanation in working memory. Building a verbal representational link is the cognitive process of moving from an external to an internal representation of linguistic content (or verbal encoding) [25]. A visual explanation, such as an animation, is offered to the student in the bottom-left area of the picture. The learner creates a mental model of the visually presented system in working memory. Building a visual representational connection (or visual encoding) is the cognitive process of transitioning from an external to an internal representation of visual information, as illustrated by the second arrow. The development of referential links between the two mental representations, i.e., the mapping of structural relations between the two representations of the system, is denoted by the third arrow.

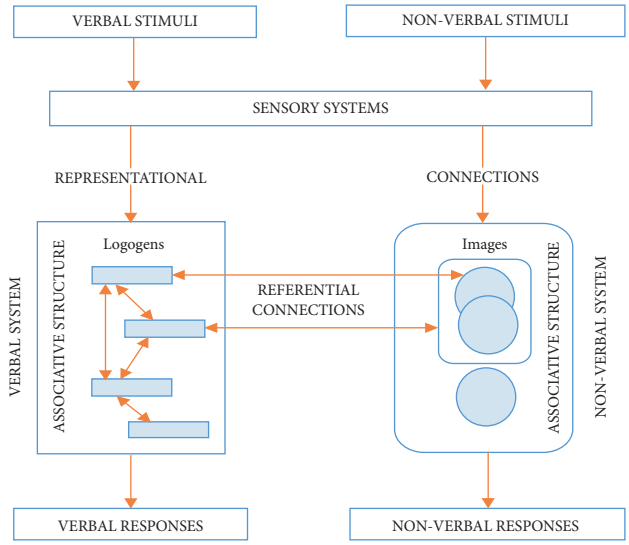

Figure 1: Proposed diagram of dual-coding theory.

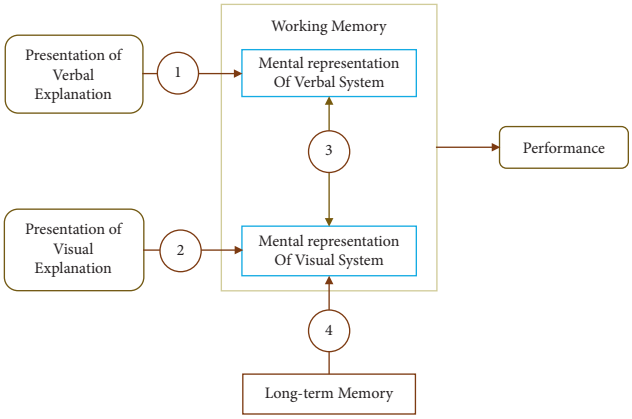

Figure 2: Dual-coding model of multimedia learning.

Figure 2 consists of the following: establishing verbal representational connections is number 1, constructing visual representational connections is number 2, building referential connections is number 3, and retrieval from long-term memory is number 4.

From the overall analysis, there are still several problems in English vocabulary teaching. First of all, the vocabulary teaching method is relatively single. From the summary of existing researches, it is found that the current process of English vocabulary teaching is still working on traditional teaching methods along with the relatively single vocabulary teaching [26]. To some extent, this affects students' motivation and interest in vocabulary learning and cannot form a more effective vocabulary reserve. Therefore, in the future development of English vocabulary teaching, we should also optimize and improve the necessary vocabulary teaching methods.

Secondly, the strategies of English vocabulary teaching need to be improved. In the current process of English vocabulary teaching, vocabulary teaching strategies are the main expression of vocabulary teaching methods [27]. The overall process of English vocabulary teaching and its strategy is to stimulate student's cognitive initiative and improve student's motivation of vocabulary learning with the help of dual-coding theory to meet the predetermined vocabulary learning objectives [29]. In addition, the vocabulary teaching environment needs to be optimized. As we know, in the process of vocabulary teaching, the teaching environment can have a certain impact on the overall students' vocabulary learning and teachers' vocabulary teaching. At present, there are still some deficiencies in the hardware environment of vocabulary teaching and the software environment of vocabulary teaching [30]. This is another major factor affecting English vocabulary teaching.

From the overall perspective of research, the combination of computer-aided dual-coding theory into English vocabulary learning is an important effect, which can improve the effect of English vocabulary teaching. When studying the application of dual-coding theory, this paper adopts the memory method of picture and text, which can better and more effectively improve the quality of English vocabulary teaching.

3. Materials and Methods

3.1. Proposed Research Architecture Based on Allan Paivio's Dual-Coding Theory. According to the idea stated in a literature review, students who accepted dual coding and picture creation interventions had a greater degree of vocabulary learning. The efficiency of computer-aided dual-coding theory in English vocabulary teaching based on DCT as a unique teaching approach is investigated in this research. The impact of computer-assisted learning on students' learning vocabulary is examined using a framework based on DCT [31]. Figure 3 illustrates the proposed research architecture, which is based on Allan Paivio's dual-coding theory.

The above diagram represents our cognitive system. There are two cognitive subsystems: one dedicated to the representation and processing of nonverbal objects and events (images) and the other to language.

The applications of dual-coding theory focus on different issues. In the field of English vocabulary, the application value of this paper mainly analyzes the direction of vocabulary potential memory and puts forward specific problems and contents [32]. The fundamental development of vocabulary and the use of visuals will be integrated and configured on the basis of a statistical relationship, which is analyzed in the following equations:

$$\rho(i) = \frac{n_i}{n}, \quad i = 0, 1, 2, \ldots\ldots, L-1. \tag{1}$$

In equation (1), ρ is risk model for the application of dual-coding theory in English vocabulary teaching, i is used for risk coefficient whose range is from 1 to $L-1$. The greater value of i indicates that the risk is high. In this relationship, n_i value is used for risk judgment, (n_i/n) is used for risk proportion function, and the value of n represents the overall risk.

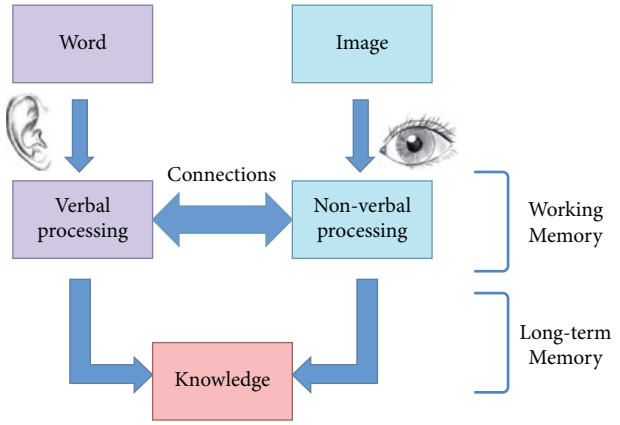

Figure 3: The proposed research architecture.

$$E_{k\,(k=1,2,3\ldots L-1)}. \tag{2}$$

In equation (2), E_k represents the overall valuation of phased risk, where E stands for valuation, and K is the number of stages. That consists of the early stage, the middle stage, and the later stage. According to the development trend of the application of dual-coding theory in English vocabulary teaching, it can be divided into more stage areas, which will not be considered for the time being, but there is possibility in the formula. So, it is expressed as E_k, and the K value ranges from 1 to $L - 1$.

Dual-coding theory has more important application value than simple language memorization. Dual-coding theory can further mobilize students' cognitive system. Through the dual processing of vocabulary language and intention, it can also help students improve the memory effect of vocabulary with the coordination of left and right brain. The difficulty of vocabulary memory and the mutual connection of pictures and words are recorded in Table 1.

According to Figure 4, with the increase of the number of images, the text content also increases correspondingly, and the difficulty of memory gradually decreases. This shows that while guiding students to increase vocabulary, they can also improve their familiarity with vocabulary and correct the spelling, application, and function of vocabulary. Therefore, the input of vocabulary information through dual coding not only help students construct the long-term memory of vocabulary, but also help students experience practical fun in the actual process, so as to avoid the phenomenon of burnout and low interest in the past vocabulary.

3.2. The Principles of Dual-Coding Theory in English Vocabulary Teaching. In order to effectively apply dual-coding theory in the future to English vocabulary teaching, the dual-coding theory combined with English teaching should follow some basic principles, which include the following: first of all, the principle of interest according to the learning of English vocabulary teaching, vocabulary teaching should be carried out in combination with students' cognitive characteristics and cognitive laws. Interest is not only the key teaching point around students' memory, but also an important base for actual vocabulary memory. Therefore, according to the theoretical requirements of dual-coding theory, the teachers should provide good cognitive stimulation and guidelines to students. Second, the principle of development of dual-coding theory should be combined with the basic content of English vocabulary memory for effective learning. The records of English vocabulary in memory must build a better development foundation with the help of dual-coding theory.

Starting with the relevant basic theories such as "zone of proximal development," this paper improves the cognitive quantity and difficulty of students' English vocabulary. Through the application of this developmental principle, we can better help students improve their overall cognitive level of language and vocabulary. Third, according to the principle of pertinence, different students have certain personalized differences in the application of dual-coding theory. Especially with the continuous improvement of students' requirements for the application of English vocabulary, it is particularly important to formulate corresponding personalized English vocabulary learning strategies and give full production to the processing effect of double coding on language materials. Based on the principle of pertinence, we need to follow the guiding ideology of personalized and differentiated teaching so as to better optimize the overall teaching structure and meet the needs of realizing the objectives of English vocabulary teaching.

Table 1: The statistics of dual-coding theory in vocabulary memory.

Difficulty statistics (%)	Images	Word
75	1	10
65	3	20
45	6	38
32	8	46

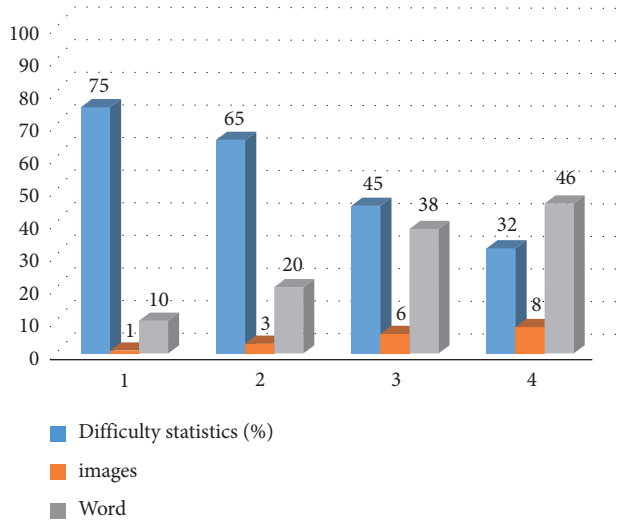

Figure 4: The statistical results of dual-coding theory in vocabulary memory.

The fourth one is the principle of innovation. In the field of English vocabulary teaching, we should pay attention to the innovation of teaching methods, teaching strategies, and teaching modes from the actual goal of English vocabulary or the application goal of English vocabulary teaching. At a certain level, dual-coding theory provides theoretical support for English vocabulary teaching. In the field of specific practical process, we should further innovate the relevant teaching system and teaching methods based on the objectives of English vocabulary teaching.

4. Results and Discussion

In this section, the experimental results are discussed. The acquisition of a specific vocabulary word while reading a story is best when there are both verbal and visual information. Based on the basic connotation of dual-coding theory and the relevant research results, this paper discusses the future application strategies from the following aspects. According to the application-oriented analyzing of double coding, the parsing type is classified into the following formula:

$$\sum_{i=0}^{L-1} \rho(i) = \sum_{i=0}^{L-1} \frac{n_i}{n} \times E_{k(k=1,2,3,\ldots,L-1)} \leq 1. \quad (3)$$

Here, $\rho(i) = n_i/n, \quad i = 0, 1, 2, \ldots\ldots, L-1$, is used to verify and analyze the overall judgment of the model. $\sum_{i=0}^{L-1} n_i/n$ indicate memory coefficient and evaluation of phased memory difficulty and $E_{k(k=1,2,3\ldots L-1)}$ determine products; if the value is less than 1, the difficulty is low. From this, we can conclude that the relative value of the obtained memory effect will be relatively high. On the contrary, when the value is larger or it is closer to 1, then the difficulty will be greater, and the relative benefit will be reduced. If it is equal to 1, the difficulty is 100% and the benefit is 0. Figure 5describes the block diagram of dual-coding theory.

The above diagram represents the Paivio and Desrochers bilingual dual-coding theory for languages (L_1 and L_2) with corresponding verbal systems (V_1 and V_2), and an image system which connects these systems to each other. According to bilingual dual-coding theory, there exist separate but interconnected logogen systems for two languages (L_1 and L_2), and each of which also connects to a nonverbal image system as shown in Figure 5. The dual-coding analysis of the combination of text and text, the methods and internal relations of learning vocabulary in the research strengthens the volume of the research results and their integration value. By designing the effectiveness of the dual-coding theory, we pay attention to the visualization of vocabulary teaching and language teaching. In this research work, we study the teaching effects under different models.

4.1. Picture and Text Loose-Decoration-Matching Style. The text corresponding to the picture in Figure 6is to learn as much as possible about the eight planets of our Solar System. Remember that NASA (USA) has already sent spaceships to explore Jupiter and Mars, which can be found out from books and the Internet sources. Think about which planet you would like to explore. Which planet have you prepared to choose and why you choose it? The basic characteristics of the planet are, for example, the position and surface size, what has already been found out about the planet, and what you hope to find out when you visit it. The picture shows a general view of outer space of Solar System not specifically referring to a planet. Although Jupiter is mentioned in the picture on the right, but it is highlighted by the four satellites around it, and the focus is not on Jupiter. In this image of Solar System, planets Jupiter and Mars are dominant and the pictures can represent any planet. Therefore, the author believes that the pictures here mainly play a decorative role and are created to adapt the style of the text, as shown in Figure 6.

4.2. The Loose Style of Picture and Text-Arousing Emotion Alienation. Figure 7 shows an illustration belongs to the exercise part of the textbook, and its corresponding text is to go over the following passage guessing the meaning of the unknown words. Listen to Part A once more and fill in the blanks. Write one word for each blank. It can be seen from the instructions of this paragraph that the author hopes to stimulate the listener's association through the picture, but the subject of the text refers to birds. The text also mentions that the use of oil makes some changes in the feathers of birds, but the picture does not reflect the role of oil. This picture makes the reader feel at a glance that the subject in the picture is forced to execute certain instructions and struggling, which makes the reader feel a tense atmosphere. Therefore, there is a sense of tension in the relationship between the picture and the text. The film does not present a completely irrelevant scene, so the relationship between picture and text is alienated.

4.3. Picture and Text Loose Control Agreement Style. The text corresponding to Figure 8 is that if you meet a foreigner who comes up choose to you talk, what countries might he be from? If a girl in wearing shorts goes into a Muslim house and a man pointing at her shoes and shorts, then what should she do? It can be seen from the text that its main content is foreign-related etiquette, which has a wide range. Looking at the picture again, although the front shows the faces of two Westerners, we cannot be sure whether they belong to foreigners or natives with their backs to the faces of readers, and the handshake can be entered when we meet; it can also be a handshake when reaching a certain agreement and business cooperation. Moreover, there are computers and documents in the picture. At first glance, it looks more like negotiating business, and the scope is significantly narrower than that of foreign etiquette. Therefore, the author believes that the picture has a certain correlation with the text, but its main purpose should be to retain the reader's attention so that the reader is not tired of boring words and does not have the function of restatement of the text or inducing the reader's point of view.

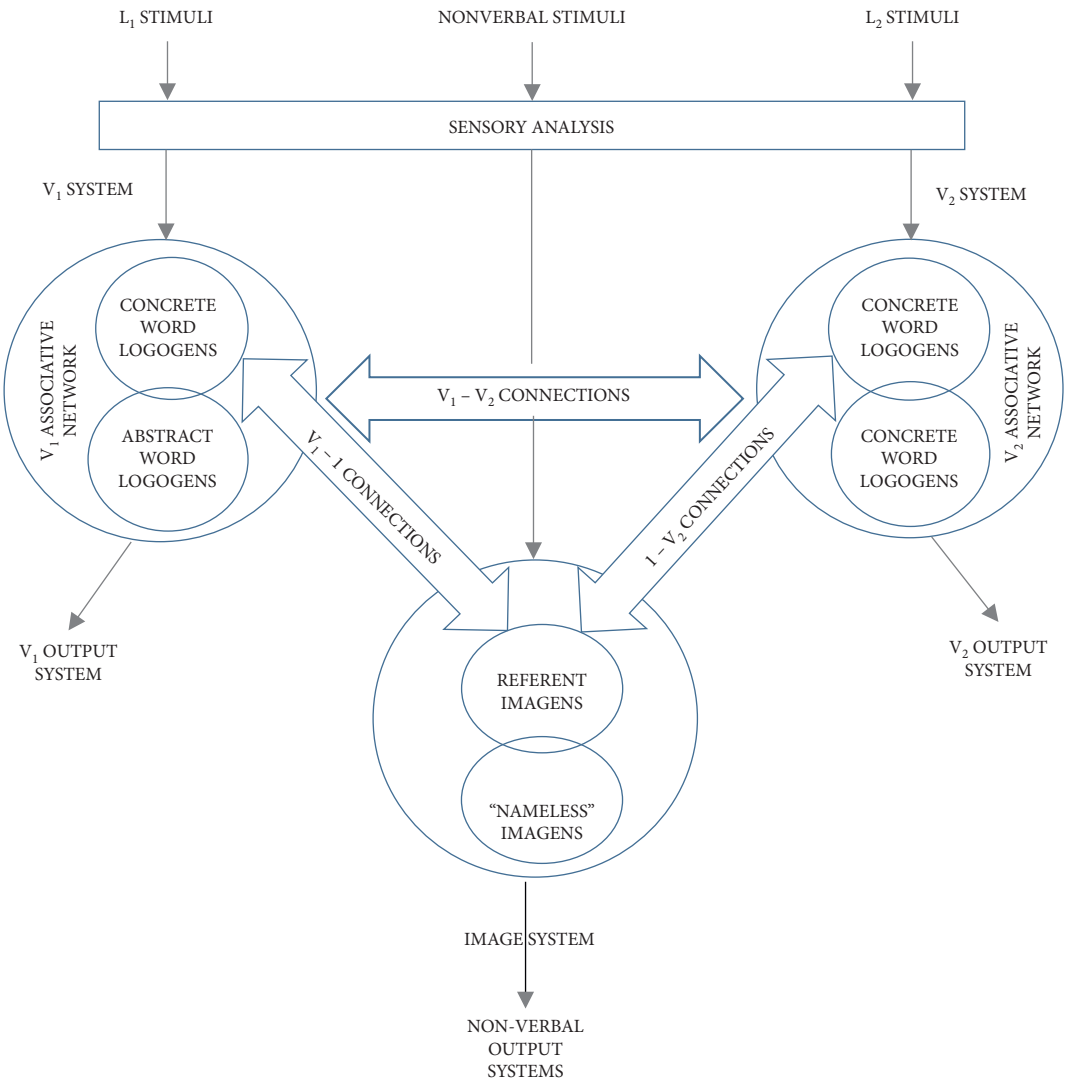

Figure 5: Bilingual dual coding model, from Paivio and Desrochers.

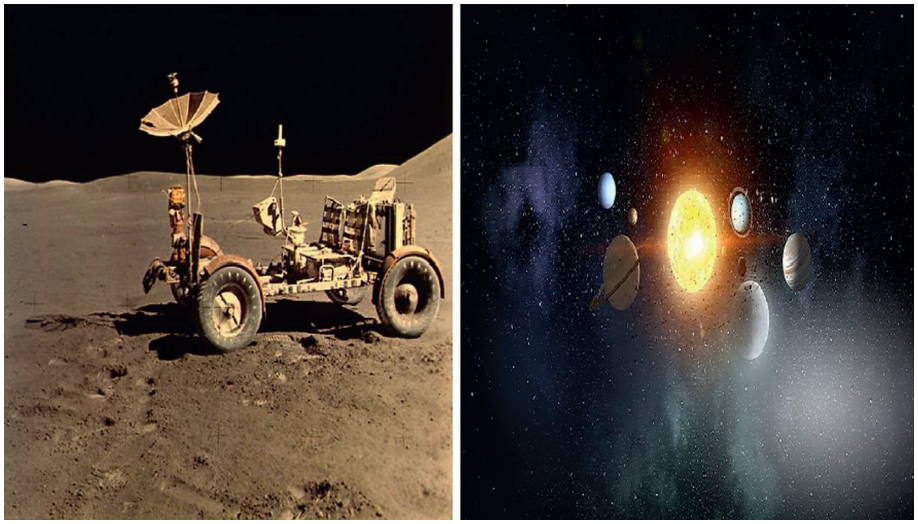

Figure 6: Picture and text loose-decoration-matching style.

Figure 7: Picture and text loose-inspire emotion-alienate style.

Figure 8: Picture and text loose-control-agreed style.

Figure 9: Close relationship between picture and text, organization, and positioning style.

4.4. The Close Relationship between Picture and Text-Organization-Positioning Style. The corresponding text is from the Atlas; we could see that the Mekong River begins in a glacier on a Tibetan Mountain. It becomes rapids as it passes Yunnan Province. It became slow when it enters to Southeast Asia. At last, the river delta enters to the South China Sea. The text describes to the reader the location of the Mekong River, which originates from the Qinghai Tibet Plateau and the flow of water is slow, cold, and clear. When passing through Yunnan Province, then the flow of water

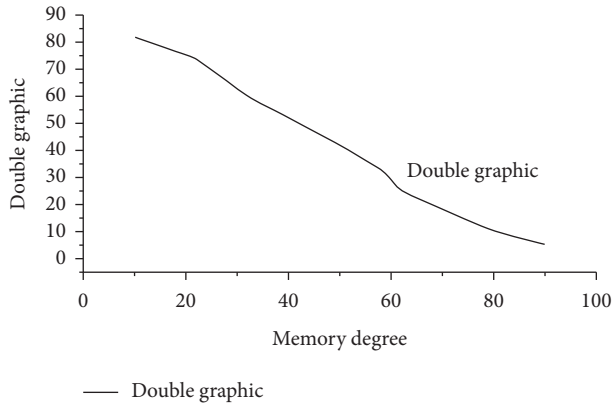

Figure 10: Correlation diagram between the effect of graphic memory and the degree of memory.

becomes fast, with Grand Canyon and waterfall. When entering Southeast Asia, the speed slows down and finally enters to South China Sea. The purpose of illustration is to present the Mekong River Basin and specific location to students so that readers can locate their eyes on the map and make it clear to readers at a glance. The illustrations have a strong organizational role and belong to the positioning in the relationship between pictures and texts.

By analyzing the different results of the experiment, it can be seen that the effect of English vocabulary teaching from the perspective of dual-coding theory is improving, and the effect of accompanying graphic memory is increasing. The experimental results are shown in Figure 9.

In Figure 10, the horizontal axis represents the degree of memory and the vertical axis is the number of double pictures and texts. According to the increase of the number of pictures and texts, the degree of memory continues to improve and the difficulty of memory becomes lower, which shows that the better the effect of double combination of pictures and texts, the stronger the degree of memory.

5. Conclusion

Based on the basic connotation of dual-coding theory and illustration of lessons from relevant research results, this paper discusses the application strategies in the future from different aspects. First of all, this article gives attention to the visualization of vocabulary teaching. In the process of language teaching, divergent thinking and image thinking can help students to extend their impression so as to improve their cognitive level. In the process of improving the visualization of vocabulary teaching, students should be helped to associate at the functional level from the image of vocabulary. Secondly, it guides students' cognitive processing of vocabulary. In the future high school English vocabulary teaching process, we should change the traditional rote teaching methods and constantly strengthen the content of vocabulary teaching and the cognitive processing of vocabulary teaching around the students' language cognitive characteristics and the application requirements of dual-coding theory. Actively guide students to expand and extend words through the words they know. Thirdly, pay attention to student motivation. Dual-coding theory is an important guiding theory of English vocabulary teaching in senior high school. In the specific process of practice, we should constantly focus on students' vocabulary cognitive characteristics and improve students' awareness of active participation. In particular, starting from the goal of English vocabulary teaching in senior high school, we should strengthen the necessary incentive conditions, incentive methods, and the realization of incentive objectives. The experiment of cognitive memory based on dual-coding theory proves that fine processing coding helps vocabulary enter long-term memory. Dual-coding theory plays a very important practical role in English vocabulary teaching. How to further develop the value of dual coding theory and meet the requirements of English vocabulary teaching in the new era is a major topic in the whole academic field. This paper mainly analyzes the basic connotation of dual-coding theory and the ways and methods of its application in English vocabulary teaching in the future. It is hoped that this study can help to promote the improvement of the overall teaching theory and practice of English vocabulary teaching.

Data Availability

The datasets used and/or analyzed during the current study are available from the corresponding author upon reasonable request.

Conflicts of Interest

The authors declare that they have no conflicts of interest regarding the publication of this paper.

References

[1] M. Rodríguez and M. Sadowki, "Effects of rote, context, keyword, and context/keyword methods on retention of vocabulary in EFL classrooms," *Language Learning*, vol. 50, no. 2, pp. 385–412, 2000.

[2] C. Kanellopoulou, K. L. Kermanidis, and A. Giannakoulopoulos, "The dual-coding and multimedia learning theories: film subtitles as a vocabulary teaching tool," *Education Sciences*, vol. 9, no. 3, p. 210, 2019.

[3] S. Li, Y. Wang, R. Filieri, and Y. Zhu, "Eliciting positive emotion through strategic responses to COVID-19 crisis.Evidence from the tourism sector," *Tourism Management*, vol. 90, pp. 110–123, 2021.

[4] Y. Chen, Z. Lin, R. Filieri, and R. Liu, "Mobile social media and the enjoyment of tourism experience: a broaden-and-build perspective," *Asia Pacific Journal of Tourism Research*, vol. 26, pp. 199–210, 2021.

[5] R. Filieri, Z. Lin, G. Pino, S. Alguezaui, and A. Inversini, "the role of visual cues in eWOM on consumers' behavioral intention and decisions," *Journal of Business Research*, vol. 135, pp. 120–129, 2021.

[6] R. Filieri, A. Yen, and Q. Yu, "An exploration of the declaration of love towards a destination on Instagram," *Tourism Management*, vol. 85, pp. 132–141, 2021.

[7] M. Yan and R. Filieri, "Continuance intention of online technologies: a systematic literature review," *International*

Journal of Information Management, vol. 58, pp. 178–189, 2021.

[8] Yan, M. Filieri, R. Raguseo, E. Gorton, and Matthew, "Mobile apps for healthy living: factors influencing continuance intention for health apps," *Technological Forecasting and Social Change*, vol. 166, pp. 198–204, 2021.

[9] R. Filieri, E. Raguseo, and C. Vitari, "extremely negative ratings and online consumer review helpfulness: the moderating role of product quality signals," *Journal of Travel Research*, vol. 60, pp. 210–223, 2021.

[10] R. Filieri, A. Javornik, H. Hang, and A. Niceta, "Environmentally framed eWOM messages of different valence: the role of environmental concerns, moral norms, and product environmental impact," *Psychology and Marketing*, vol. 38, pp. 278–291, 2021.

[11] J. Mathematics, "New mathematics research from bohai university discussed (the effects of computer-assisted learning based on dual coding theory)," *Computer Weekly News*, vol. 18, pp. 92–105, 2021.

[12] L. Anielle and W. Gabriele, "Autonomy support enhances performance expectancies, positive affect, and motor learning," *Psychology of Sport and Exercise*, vol. 31205 pages, 2021.

[13] L. Geert, K. Thijs, and E. Babak, "A survey on deep learning in medical image analysis," *Medical Image Analysis*, vol. 42, 2017.

[14] O. Atsuya and Y. Genki, "Computational mechanics enhanced by deep learning," *Computer Methods in Applied Mechanics and Engineering*, vol. 327, pp. 112–132, 2021.

[15] A. Myrtede, M. David, and K. Gramopadhye, "Comparing learning outcomes in physical and simulated learning environments," *International Journal of Industrial Ergonomics*, vol. 68, pp. 132–139, 2021.

[16] X. Li, "Mobile learning models of foreign language teaching," *E-Education Research*, vol. 191, pp. 109–111, 2009.

[17] Y. Liu and S. Ge, "Classroom appearance at any time with M-Learning," *Information Technology Education*, vol. 56, no. 6, pp. 20-21, 2003.

[18] Z. Zhu, H. Zhang, and X. Gu, "Micro-learning: a practical model of informal learning," *China Educational Technology*, vol. 106, no. 2, pp. 10–13, 2008.

[19] D. Fu and FuY. Xu, "Ubiquitous learning environment supported by pervasive computing," *China Educational Technology*, vol. 68, no. 7, pp. 94–98, 2007.

[20] H. T. Kwok and H. Lam, "The role of textbook learning resources in e-learning: a taxonomic study," *Computers & Education*, vol. 118, pp. 165–178, 2021.

[21] C. Elisabeth, F. Valda, and R. Hazel, "Simulation videos presented in a blended learning platform to improve Australian nursing students' knowledge of family assessment," *Nurse Education Today*, vol. 66, pp. 201–212, 2021.

[22] Z. Yuwen, H. Changqin, and H. Qintai, "Personalized learning full-path recommendation model based on LSTM neural networks," *Information Sciences*, vol. 12–23, 2021.

[23] P. Sanjay, M. Chuizheng, and C. Zhengping, "Benchmarking deep learning models on large healthcare datasets," *Journal of Biomedical Informatics*, vol. 83, pp. 299–312, 2021.

[24] F. Oliver, H. Yuki, and J. Tan, "Deep learning for healthcare applications based on physiological signals: a review," *Computer Methods and Programs in Biomedicine*, vol. 161, pp. 199–212, 2021.

[25] M. Jason and H. Harrison, "Understanding students' preferences toward the smart classroom learning environment: development and validation of an instrument," *Computers & Education*, vol. 122, pp. 167–187, 2021.

[26] B. Ruth, V. Michiel, and D. W. Bram, "The design of blended learning in response to student diversity in higher education: instructors' views and use of differentiated instruction in blended learning," *Computers & Education*, vol. 120, pp. 134–145, 2021.

[27] T. Toshiyuki, T. Koichi, and S. Takeji, "[P266] Patient-optimized deep learning for robust tumor tracking," *Physica Medica*, vol. 52, pp. 1113–11143, 2021.

[28] K. Andreas and X. Francesc, "Prenafeta-Boldú Deep learning in agriculture: a survey," *Computers and Electronics in Agriculture*, vol. 147, pp. 252-253, 2021.

[29] B. Deblina, P. Anand, and H. Jeong, "An immersive learning model using evolutionary learning," *Computers & Electrical Engineering*, vol. 65, pp. 188–197, 2021.

[30] D. Hongying, L. Yi, and L. Ping, "Active learning for modeling and prediction of dynamical fluid processes," *Chemometrics and Intelligent Laboratory Systems*, vol. 183, pp. 145–154, 2021.

[31] H. Zilong, T. Jinshan, and W. Ziming, "Deep learning for image-based cancer detection and diagnosis," *A survey.-Pattern Recognition*, vol. 83, pp. 134–145, 2021.

[32] S. Samantha and J. Cohen, "Neural engagement with online educational videos predicts learning performance for individual students," *Neurobiology of Learning and Memory*, vol. 35, pp. 111–123, 2021.

Hindawi
Scientific Programming
Volume 2022, Article ID 7744067, 8 pages
https://doi.org/10.1155/2022/7744067

Research Article

Construction of Mathematical Modeling for Teaching Evaluation Index System Based on the Delphi AHP Method

Zhihong Zhang

College of Mechanical and Electrical Engineering, Zhengzhou Tourism College, Zhengzhou Henan 451464, China

Correspondence should be addressed to Zhihong Zhang; zhangzhihong@zztrc.edu.cn

Received 14 February 2022; Revised 25 February 2022; Accepted 28 February 2022; Published 15 March 2022

Academic Editor: Muhammad Zakarya

China plays an important role in the global basic education of mathematics. Moreover, China has a lot of educational experience and methods and trains many excellent talents in the field of mathematics. However, there are still various disadvantages in the process of mathematics teaching. The traditional exam-oriented education makes the talent thought of mathematics education lack openness. Teachers also focus on difficult problems, partial questions, and exam questions during teaching. When teaching, teachers cannot contact students' daily life, which has low value. Mathematics teaching methods are too rigid and lack attraction. Most teachers focus on contents in textbooks while students cannot understand the value of mathematics in learning. This results in the decline of most students' interest in mathematics courses. To solve this problem, mathematical modeling teaching is put forward. China has a short application time in this field, and mathematical modeling is complex and systematic. When dealing with mathematical modeling problems, we must be able to skillfully use the basic knowledge learned and also involve the knowledge of other disciplines, so we must realize the integration of the knowledge of various disciplines. In addition, mathematical modeling teaching attaches great importance to students' communication ability, mathematical interpretation ability, and teamwork ability. Teachers can improve students' ability; however, our teachers' abilities in mathematical modeling teaching are uneven and there are no relevant standards. Therefore, it is necessary to establish an evaluation index system to accurately judge teachers' abilities. Based on this, this study uses the Delphi AHP method to construct the evaluation index system and selects four criteria level indexes and 12 index level indexes to judge teachers' mathematical modeling teaching ability.

1. Introduction

At present, China's education reform has entered a new period, with a variety of new education and teaching modes, and the emergence of Delphi and analytic hierarchy process (AHP) speeds up the pace of education reform. This method can more accurately evaluate the weight, importance, and role of various indicators in the process of mathematical modeling teaching. Through mathematical modeling teaching, students' mathematical ability and thinking ability can be strengthened. However, at present, most of the research is on mathematical modeling teaching for middle school students, college students, and graduate students, and there is less content on evaluating mathematical modeling teaching [1]. However, our teachers' abilities in mathematical modeling teaching are uneven, and there are no relevant standards. It is urgent to use the most advanced methods to evaluate the quality of teaching modeling. This is used to judge the teaching quality and future development direction of the mathematical modeling in schools and colleges.

The ability of students and individuals during mathematical modeling is not only the ability of mathematical modeling but also the necessary ability to successfully perform modeling tasks. When analyzing the teaching ability of mathematical modeling in colleges and universities, this study starts from four aspects, namely, modeling options, teaching monitoring, modeling process, and cooperative learning. This ideological index is used as the criterion layer of the evaluation index system of mathematical modeling teaching established in this study and further defines the 12 indexes of the index layer. By

calculating the weight of each index, the importance of each index in the teaching modeling evaluation index system is judged according to the weight of the index.

The innovations and contributions of this study in the process of studying the evaluation index system of mathematical modeling teaching are

(1) Describe in detail the two methods used in this study, namely, the Delphi method and analytic hierarchy process (AHP), list the setting and specific operation process of expert group personnel in the Delphi method, and explain the way to modify expert opinions.

(2) This study focuses on the analysis of the mathematical modeling process and explains in detail the three mathematical modeling models that are widely used.

(3) We use the Delphi AHP method to construct the evaluation index system and select four criteria level indexes and 12 index level indexes to judge teachers' mathematical modeling teaching ability.

(4) The 1–5 scale method of analytic hierarchy process (AHP) is selected to construct the judgment matrix and establish the evaluation index system and model of mathematical modeling teaching. The selected indexes can fully cover all aspects.

The rest of the paper is organized as follows. In Section 2, we offer an overview of the related work. Section 3 is about the Delphi method. Mathematical modeling is presented in Section 4. In Section 5, the proposed system is discussed. Moreover, results are also illustrated in this section. Finally, Section 6 concludes this study and offers several directions for further research and investigation.

2. Related Work

Mathematical modeling was first formed from practical applied mathematics [2]. As early as the 1970s, the mathematical modeling course was carried out in the UK, and the mathematical modeling course is mainly used by doctoral and master students. After years of development, it has been extended to undergraduates and primary and secondary school students. In 1985, the United States launched a global undergraduate mathematical modeling competition, that is, MCM competition. The increasing scale of the competition in the world strengthened more college students' mathematical awareness and improved their mathematical practice ability [3]. By 1989, the United States took mathematical modeling as one of the main reform projects in the mathematical reform [4]. China's mathematical modeling has gone through many processes. It was the first to carry out mathematical modeling competition nationwide and developed into setting up mathematical modeling courses in colleges and universities [1]. At present, mathematical modeling courses are added to the national curriculum system. In 1992, China launched the largest mathematical modeling competition for college students and took the competition content as an important project to cultivate college students' competition ability. Since then, most engineering, science, and even some liberal arts colleges in China have also set up mathematical experiment courses and mathematical modeling teaching courses. The education department adds the mathematical experiment course and mathematical modeling course into the university teaching curriculum system as elective courses or compulsory courses [5].

Wang et al. believe that mathematical modeling ability refers to students' creativity, design ability, and ability to build mathematical models [6]. Using teaching activities can fully reflect students' personal mathematical ability. ICMI study (14) defines mathematical modeling ability as the ability to translate various questions, variables, assumptions, relationships, and other assumptions into mathematical language, evaluate and explain the mathematical ability to answer them, and test the scope and nature of the model by investigating assumptions, so as to judge the ability suitable for the model [7]. In the 21st century, the field of mathematics education began to study the mathematical modeling ability. During the research period, scholars such as Jun F et al. reasonably distinguished six different mathematical modeling abilities, such as clarifying objectives, simplifying assumptions, describing problems, clarifying parameter constants, and variables, selecting models and returning to practical problems [8]. Wang et al. (2020) analyzed the five different stages of mathematical modeling and pointed out that "the five subabilities of mathematical modeling ability mainly include logical reasoning ability, reading comprehension ability, calculation ability, mathematical ability, and self-learning ability [9]." Mathematical modeling ability is a very complex mathematical ability, which usually needs a mixture of multiple mathematical activities, including mathematical ideas, mathematical methods and knowledge, and the ability to deal with practical problems [10]. Therefore, while improving personal mathematical modeling ability, we should also strengthen our own mathematical ability [11].

3. Index System Based on the Delphi AHP Method

3.1. Delphi Method. Delphi method was first used in the expert group of problem definition and screening. It usually needs to complete three rounds of consultation [12]. Figure 1 shows the research process of the Delphi method [10, 13].

At present, the ideal number of consultants of the expert group has not been determined. Usually, the number of expert groups is in the range of 10 to 30. Generally, the first round of questionnaire consultation is highly open, and some primary information can be provided to the expert group personnel. After receiving the information, the expert group personnel should expand from their personal professional knowledge. However, in some studies, experts will redefine and classify questions, so there is no need to carry out the first round of consultation and start directly from the second round, which is called the modified Delphi method. After entering the second round, the expert group shall rearrange and score specific items. The standards followed

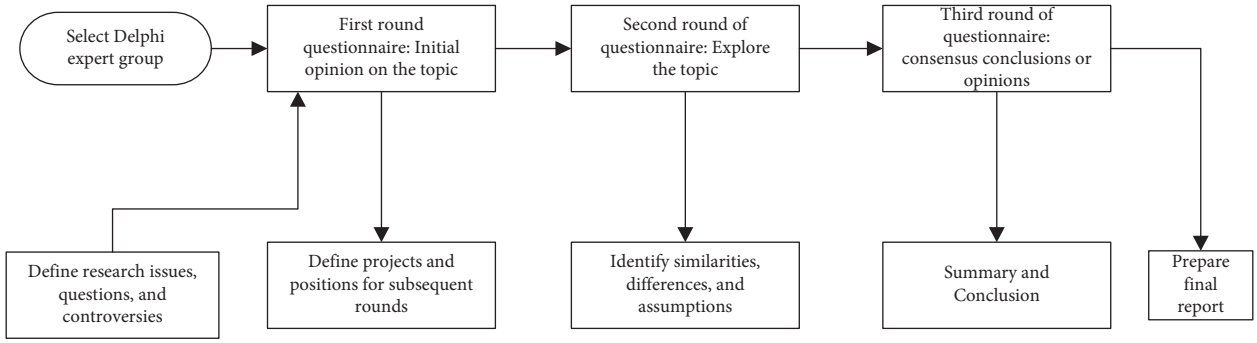

Figure 1: Operation process of the Delphi method.

by the feedback results are median, mean, and coefficient of variation (CoV). Experts can directly express their opinions on evaluation indicators. Complete or carry out the third round of inquiry to get an accurate project ranking and score.

Based on the constructed evaluation index system, the weight opinion consultation form and expert opinion consultation form are prepared, and the expert opinions are revised in two rounds through the modified Delphi method. On the basis of expert feedback results, the index system is modified, added, and deleted again to make the content of the index system more perfect.

3.2. Analytic Hierarchy Process. In the 1970s, T.L. Saaty proposed a multicriteria decision-making method combining quantitative and qualitative analysis, namely, analytic hierarchy process (AHP) [14]. In this method, experienced and knowledgeable experts in the field qualitatively compare the importance of decision-making objectives at all levels, and then, researchers use the scaling method to calculate the value. Based on various index systems, this study compiles the weight questionnaire of mathematical modeling teaching evaluation index system, and experts use the 1–5 scale method to evaluate the importance of different levels of indicators. Finally, Yaahp software is used to analyze the expert evaluation data to calculate the weight of different levels of indicators [15].

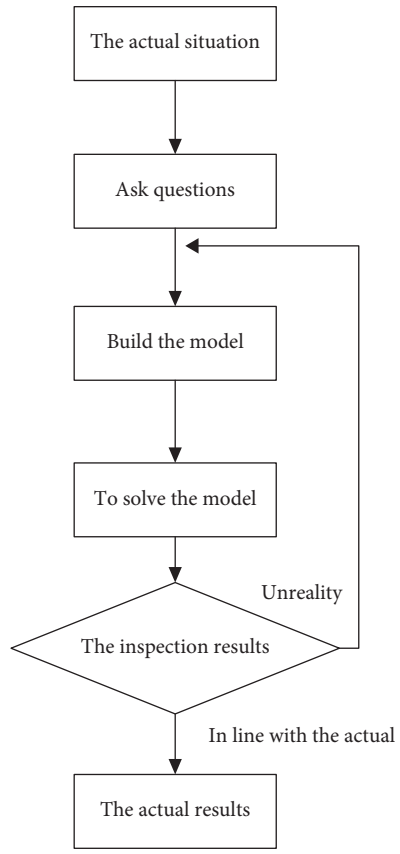

Figure 2: Flowchart of mathematical modeling.

4. Mathematical Modeling

4.1. Mathematical Modeling Process. Figure 2 is the mathematical modeling flowchart of China's senior high school mathematics curriculum. The figure describes in detail all links of mathematical modeling, mainly including asking questions according to the actual situation, how to build a mathematical model according to the questions raised, how to answer the mathematical model questions, and how to test the results. If the results are difficult to explain the actual situation problems, the constructed model should be improved and modified. Mathematical modeling also includes the content of the improved model [16].

There is no direct relationship between mathematical modeling activities and the development of mathematical knowledge system, so the teaching of mathematical modeling activities shall not focus on specific knowledge and content [17]. During mathematics teaching, the time of mathematical modeling activities can be reasonably arranged according to the actual needs to ensure that the number of class hours exceeds 4. The original intention of compiling the textbook is to improve students' mathematical level. The basic structure selected is "teaching modeling activity Case + mathematical modeling activity a + mathematical modeling activity B." The purpose of "mathematical modeling activity case" is to use the way of classroom teaching to let students really feel the mathematical modeling process and complete the preparation of mathematical teaching activity report, so as to better understand this activity and master a lot of experience in mathematical

modeling activities. Based on students' personal experience, teachers can expand the contents outside the teaching materials and formulate mathematical modeling tasks consistent with students [18].

4.2. Mathematical Modeling. At present, the well-known mathematical modeling model is "four stage modeling process," which is described in detail below:

(i) Analyze the problem: analyze the background materials related to the problem and find the factors leading to the problem.

(ii) Simplified hypothesis: clarify the factors that interfere with the research object, focus on the analysis of the main factors, and simplify the secondary factors, which can reduce the difficulty of problem analysis and grasp the essence of the problem more deeply.

(iii) Modeling and solving: build a mathematical model based on analysis and solve the model by computer program or mathematical method.

(iv) Modification and verification: check the model, judge whether it is consistent with the reality, and then further explain it, and apply it in real life and production to form economic and social benefits. The details are shown in Figure 3.

Mathematical modeling five-step model is also widely used in practice, and the result is relatively simple, which is favored by a large number of scholars at home and abroad [19]. Especially, in the process of mathematical modeling in middle school, mechanism analysis is a common modeling method. The following describes the five-step model in detail and studies the process of building the model based on mechanism analysis. Figure 4 shows the five step model of mathematical modeling.

Blum and other experts proposed the modeling process, that is, the initial form of the seven-step mathematical modeling model [20]. The detailed process is listed in Figure 5.

5. Construction of the Evaluation Index System of Mathematical Modeling Teaching Based on the Delphi AHP Method

5.1. Establishment of Mathematical Modeling Teaching Evaluation System. By sorting out and analyzing the literature on mathematical modeling teaching, mathematical modeling, and teaching evaluation indicators, combined with teaching materials and expert opinions, this study determines the basic teaching concept of mathematical modeling and extracts the teaching characteristics and mathematical modeling. Based on the developmental teaching evaluation, according to the developmental teaching evaluation index and mathematics teaching quality evaluation system (MQI), take it as the main evaluation tool and establish the mathematical modeling teaching evaluation index system from the three points of student subject, teacher leadership, and teaching effect, which is shown in Figure 6 [21].

5.2. Construction of Judgment Matrix. Based on the 1–5 scale method of analytic hierarchy process (AHP), the feedback opinions of all experts are assigned, and the corresponding judgment matrix of each expert is constructed [22]. There are 13 expert feedback results obtained in this study. The criteria level index judgment matrix is listed in Table 1.

After constructing the judgment matrix, check the consistency of the judgment matrix, and check whether there is a logical inconsistency between the feedback data provided by experts. In the analytic hierarchy process, the consistency of the judgment matrix is tested according to the random consistency proportion C scale. The results show that the CR result is less than 0.1, which cannot ensure that the judgment matrices given by all experts meet the consistency requirements. If there is inconsistency in some judgment matrix data, the judgment matrix data can be automatically corrected and stopped until the consistency requirements are met. The consistency correction algorithm of automatic selection judgment matrix is deeply explored to test whether the judgment results given by various experts are consistent or not.

After analysis and judgment, 21 judgment matrix data inconsistencies appear in the judgment matrix established in this study. Among these judgment matrices, 12 adopt the "minimum change" algorithm to correct them, which meets the consistency requirements after correction. The other five matrices also meet the consistency requirements by using the "optimal direction" algorithm. There is no need to further study and process the above judgment matrix data. The remaining three judgment matrices need to modify the contents of two data items, accounting for 20% of the total data items. Only a small part of the data needs to be corrected without in-depth processing of the judgment matrix data. There is also a judgment matrix to correct three of the data, accounting for 30% of all the data, so the judgment matrix cannot be used. Here, only the consistency test results of the judgment matrix given by experts are listed, which are shown in Table 2.

5.3. Calculation of Index System Weight. Yaahp software, as auxiliary software of analytic hierarchy process, is developed based on Yaahp software. By comparing Yaahp software, Yaahp software has the advantage of supporting various scale types, including 1–5 scale, 1–9 scale, 1–2 scale, and 1–3 scale. This study uses the 1–5 scale method on Yaahp software to study the expert scoring data and calculate the weight of the evaluation index system of mathematical modeling teaching. The following is the detailed process:

(1) First, establish the hierarchical structure model. Based on mathematical modeling and mathematical evaluation index system, clarify the control criteria and control objectives and complete the drawing of hierarchical model based on this.

(2) Secondly, construct judgment matrix. This study selects the 1–5 scale method to count the weight score results given by experts and constructs the index judgment matrix of experts for different levels.

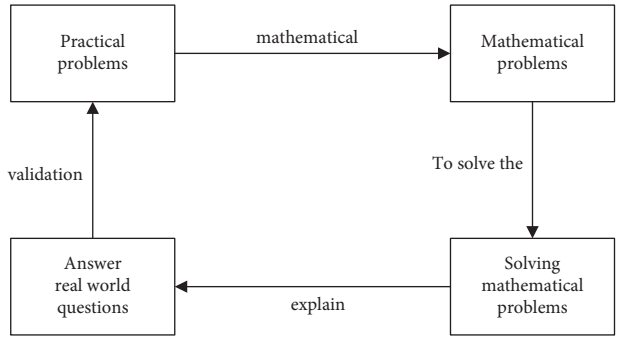

Figure 3: Four stage modeling model.

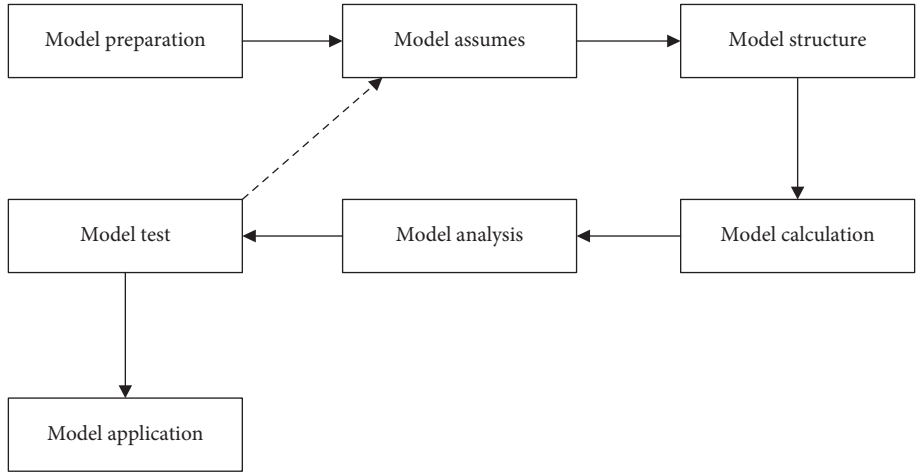

Figure 4: Five-step mathematical modeling.

(3) Again, check the consistency of the judgment matrix. Evaluate the judgment matrix data given by experts to judge whether it meets the consistency requirements. Yaahp software comes with two automatic repair consistency algorithms, namely, the optimal direction algorithm and the minimum selection algorithm. This method is used to automatically repair the judgment matrix of inconsistent data. Based on the judgment matrix described by Yaahp software and the given processing decision, it is judged whether to further process the judgment matrix.

(4) Finally, analyze the weight data. The common ways to calculate the judgment matrix are (i) sum method, (ii) power method, and (iii) root method. Combined with the group decision-making expert data and element weight, the calculation results are obtained, and the results are deeply analyzed to obtain the single ranking and final total ranking of different levels of indicators.

Based on the hierarchical single sorting, the combined weights of different indicators can be obtained by multiplying the aggregated secondary indicator weights and the corresponding primary indicator weights. The detailed calculation results are listed in Table 3.

5.4. Construction of the Evaluation Model. After all the weights of the evaluation index system of mathematical modeling teaching based on the Delphi AHP method have been determined, the following mathematical modeling teaching evaluation models are established by using the weighted average method [23]:

$$S = \sum_{i=1}^{12} W_i T_{jk}, \tag{1}$$

where W_i represents the combined weight of the i secondary index, S represents the total score of mathematical modeling teaching, and T_{ik} T_{jk} represents the score of secondary index, evaluates the overall level of mathematical modeling teaching based on the total score, and makes up for the problems and deficiencies existing during mathematical modeling teaching according to the score of each index.

According to the feedback of experts, this study establishes the evaluation index system of mathematical modeling

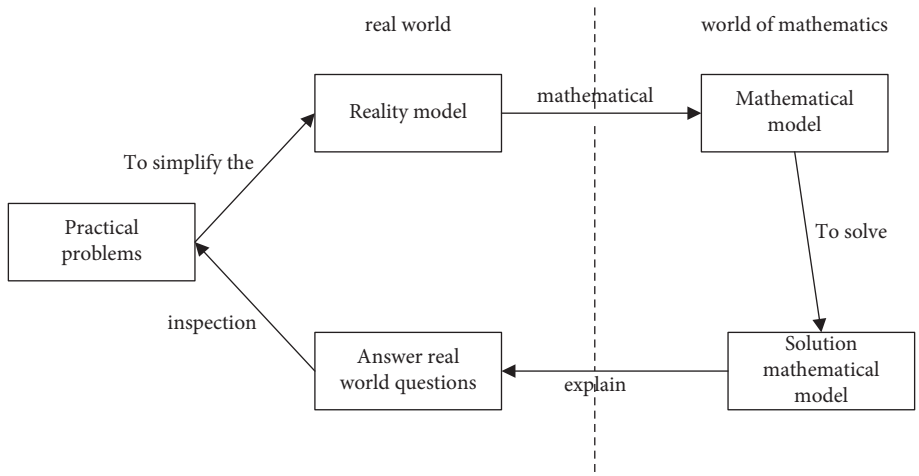

Figure 5: Seven-step model of Blum mathematical modeling.

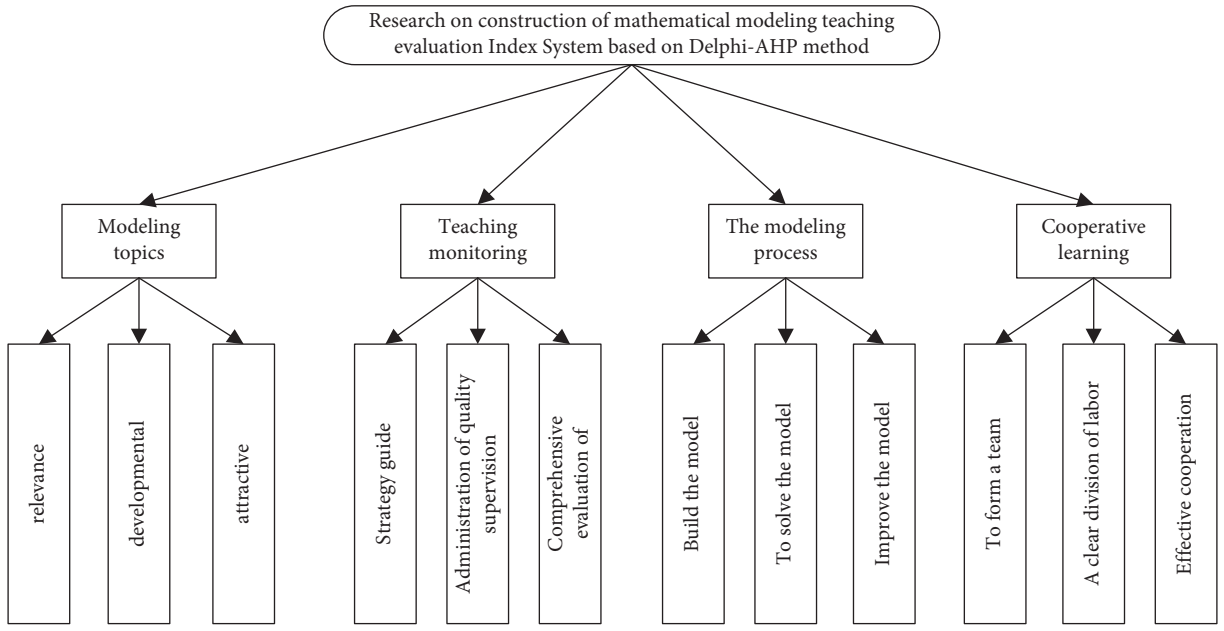

Figure 6: Evaluation index system of mathematical modeling teaching based on the Delphi AHP method.

Table 1: Criteria layer index judgment matrix.

T	Modeling topics T_1	Teaching monitoring T_2	The modeling process T_3	Cooperative learning T_4
Modeling topics T_1	1	3	1	3
Teaching monitoring T_2	1/2	1	1/3	1
The modeling process T_3	1	2	1	2
Cooperative learning T_4	1/3	1	1/3	2

Table 2: Consistency test results of index judgment matrix of any expert at all levels.

Judgment matrix	The maximum characteristic root λ max		Consistency ratio CR		Consistency test
	Before correction	The revised	Before correction	The revised	
T	—	5.032	—	0.0097	<0.1
T_1	3.24	3.14	0.21	0.0998	<0.1
T_2	—	5.36	—	0.0724	<0.1
T_3	—	5.06	—	0.0132	<0.1
T_4	—	3.07	—	0.0528	<0.1

Table 3: Weight distribution of indicators at all levels.

Level indicators	The weight	The secondary indicators	The weight	The combination weights
Modeling topics T_1	0.276	Relevance T_{11}	0.457	0.127
		Developmental T_{12}	0.316	0.082
		Attractive T_{13}	0.245	0.064
Teaching monitoring T_2	0.192	Strategy guide T_{21}	0.332	0.057
		Administration of quality supervision T_{22}	0.197	0.032
		Comprehensive evaluation of T_{23}	0.172	0.029
The modeling process T_3	0.376	Build the model T_{31}	0.283	0.087
		To solve the model T_{32}	0.164	0.053
		Improve the model T_{33}	0.127	0.036
Cooperative learning T_4	0.156	To form a team T_{41}	0.326	0.051
		A clear division of labor T_{42}	0.374	0.057
		Effective cooperation T_{43}	0.335	0.052

teaching based on the Delphi AHP method, calculates the weight of each index by using the above method, and obtains the total score by solving formula (1). The calculation formula is as follows:

$$S = 0.12T_{11} + 0.08T_{12} + 0.06T_{13} + 0.05T_{21} + 0.03\,T_{22} + 0.03T_{23} + 0.08T_{31} + 0.05T_{32} + 0.03T_{33} + 0.05T_{41} + 0.05T_{42} + 0.05T_{43}. \quad (2)$$

5.5. Discussion on Evaluation Results. In this study, the current mainstream statistical algorithm Delphi and analytic hierarchy process (AHP) are used to establish the evaluation index system of mathematical modeling teaching, which enriches the field of teaching modeling evaluation, promotes the sustainable development of this field, and formulates the corresponding judgment standards to measure the evaluation of mathematical modeling teaching. Starting from the research on teaching modeling evaluation, the carrier of most of the current research is the division of mathematical modeling level and modeling process. A variety of practical evaluation tools are designed from the perspective of students, focusing on students' modeling ability and cultivating students' personal quality. This study focuses on mathematical modeling teaching and selects criteria level indicators for modeling topic selection, teaching monitoring, modeling process, and cooperative learning. The indicators on the indicator level mainly include appropriateness, development, attraction, strategy guidance, quality supervision, comprehensive evaluation, model establishment, model solving, model improvement, component team, clear division of labor, and effective cooperation, with a total of 12 indicators. Based on this index, the evaluation index system and evaluation model of mathematical modeling teaching are established. The basic idea of this study is the teaching process of mathematical modeling. According to the achievements of scholars, the teaching of mathematical modeling is divided into three stages: learning and skillfully using mathematical model, understanding the modeling process, and the practical application of mathematical modeling.

In this study, the evaluation index system of mathematical modeling teaching based on the Delphi AHP method is established. The calculated primary index weights are 0.276, 0.192, 0.376, and 0.156, respectively. The importance of each index is judged according to the weight value. The most important index is the modeling process, followed by modeling options, then modeling monitoring, and finally cooperative learning. Among the secondary indicators, the most important is appropriateness, with a weight of 0.12, followed by clear division of labor, effective cooperation, strategic guidance, team formation, and development. The weights of the above six indicators exceed 0.05. After accumulating each indicator, the proportion in the total indicator weight is 1/2 left and right.

In the evaluation index system, the value range of Cronbach coefficient of different dimensions is 0.81 to 0.95, the first-order Cronbach coefficient is 0.92, and the second-order Cronbach coefficient is 0.98, indicating that the reliability test level and reliability of the evaluation index system of mathematical modeling teaching based on the Delphi AHP method are high, and the corresponding half reliability coefficients are 0.91 and 0.97. The i-cvi [22] of each index is taken in the range of 0.8 to 1. The internal consistency reliability is calculated by SPSS software, and the results are more than 0.9. Therefore, the evaluation index system has high reliability.

6. Conclusions and Future Work

With the development of science and technology and the promotion of the rapid reform of education, the traditional mathematics teaching model has been unable to meet people's needs. This promotes the comprehensive application of mathematical modeling teaching methods in various countries. However, there is a large gap in each teacher's mathematical modeling teaching ability, so it is impossible to accurately evaluate the teacher's ability. Aiming at this

problem, this paper studies the evaluation of mathematical modeling teaching by combining Delphi and analytic hierarchy process (AHP), selects modeling options, teaching monitoring, modeling process, and cooperative learning as the criterion level indicators, establishes the evaluation index system of mathematical modeling teaching based on Delphi AHP, and describes Delphi and analytic hierarchy process (AHP) in detail. This study introduces the teaching process of mathematical modeling, which lays the foundation for the establishment of mathematical modeling. After calculation, the weights of the first-class indicators of this model are 0.276, 0.192, 0.376, and 0.156, respectively. The importance of the indicators is arranged according to the weight. Among them, the modeling process is the most important, followed by modeling options and modeling monitoring, and finally cooperative learning. In the future, we aim to clarify the importance of each indicator in evaluating mathematical modeling teaching, so as to judge teachers' mathematical modeling teaching ability.

Data Availability

The data can be obtained from the corresponding author upon request.

Conflicts of Interest

The author declares no conflicts of interest.

References

[1] M. Z. Lai and Y. C. Shu, "Mathematical modeling provides a combination of mathematics and real life [J]," *Journal of Mathematics Education*, vol. 26, no. 6, 2017.

[2] L. Wang and G.-S. G. S. Kuo, "Mathematical modeling for network selection in heterogeneous wireless networks — a tutorial," *Communications Surveys and Tutorials, IEEE*, vol. 15, pp. 271–292, 2013.

[3] Y. Yao, J. Qiu, and Z. Wang, "Improving the innovation and entrepreneurship of college students through the mathematical modeling competition [J]," *Computer Era*, vol. 18, 2019.

[4] L. Chang, "Review of domestic and foreign research on higher order (mathematical) thinking [J]," *Journal of Mathematics Education*, vol. 25, no. 5, 2016.

[5] R. Yang and S. W. Zhou, "Cultivating students' practical and innovative ability by taking mathematical modeling competitions as starting point [J]," *Experimental Technology and Management*, vol. 38, no. 3, 2021.

[6] Z. Y. Wang, *The Exploration of Cultivating Students' Ability of Mathematical Modeling in High School Mathematics Teaching*, G633.6G632.3, 2005.

[7] C. Margolinas, *Task Design in Mathematics Education. Proceedings of ICMI Study 22*, Icmi Study, 2013.

[8] F. U. Jun, H. Zhu, and X. C. Wang, "Practice and deep thought of training innovative ability in mathematical model building teaching [J]," *Journal of Mathematics Education*, vol. 36, 2007.

[9] J. J. Wang, "Research on application of problem guiding method in mathematics teaching in senior high school [J]," *Kaoshi Zhoukan*, vol. 16, 2020.

[10] H.-D. Li, L. Zhang, and C.-L. Lin, *An Intelligent Model for Assessing Abilities of University Teachers Based on AHP and Delphi Method*, 2021.

[11] S. Z. Wang, "Development process and prospect of mathematical modeling in Chinese school section [J]," *Journal of Mathematics Education*, vol. 26, no. 6, 2017.

[12] C. Wang and S. Qin, "A study of data statistical processing method of Delphi method and its application [J]," *Journal of Inner Mongolia Finance and Economics College*, vol. 24, 2011.

[13] L. Shen, J. Yang, X. Jin, L. Hou, S. Shang, and Y. Zhang, "Based on Delphi method and analytic hierarchy process to construct the evaluation index system of nursing simulation teaching quality," *Nurse Education Today*, vol. 79, pp. 67–73, 2019.

[14] M. Gardašević-Filipović and Z. Šaletić Dragan, "Multicriteria optimization in a fuzzy environment: the fuzzy analytic hierarchy process [J]," *Yugoslav Journal of Operations Research*, vol. 20, no. 1, 2010.

[15] M. D. Roshaidie, W. Liang, C. Jun, K. H. Yew, and F.-t Zahra, "Importance of secure software development processes and tools for developers [J]," *Software Engineering*, vol. 12, 2020.

[16] A. Plotnitsky, "On "decisions and revisions which a minute will reverse": consciousness, the unconscious and mathematical modeling of thinking," *Entropy*, vol. 23, no. 8, p. 1026, 2021.

[17] A. Elizarov, A. Kirillovich, E. Lipachev, and O. Nevzorova, "OntoMath digital ecosystem: ontologies, mathematical knowledge analytics and management [J]," *Digital Libraries*, vol. 56, 2017.

[18] M. Alaa, I. S. M. A. Albakri, C. K. S. Singh et al., "Assessment and ranking framework for the English skills of pre-service teachers based on fuzzy Delphi and TOPSIS methods," *IEEE access*, vol. 7, pp. 126201–126223, 2019.

[19] Y. Sun, "Exploration of conventional training strategies for primary school students' mathematics learning based on cooperative modeling [J]," *Journal of Educational Development*, vol. 8, 2011.

[20] Y. S. Yu, "Research on mathematical modeling thought in probability statistics of economic management -- comment on fundamentals of economic management and finance and taxation [J]," *Journal of Machine Design*, vol. 37, no. 1, 2020.

[21] M. F. Li, X. Zhou, and Z. Y. Yang, "Quality analysis of 5 ~ 6-year-old children's mathematics group Activities: based on the MQI evaluation system [J]," *Studies In Early Childhood Education*, vol. 3, 2020.

[22] G. Yu, S. Niu, J. Ma, and Y. Song, "An adaptive prediction-correction method for solving large-scale nonlinear systems of monotone equations with applications," *Abstract and Applied Analysis*, vol. 2013, no. 3, pp. 1–13, 2013.

[23] S. Sabilan, M. I. Hamzah, and A. H. Tamuri, *Validity and Reliability of Evaluation Instrument on Islamic Education Teachers' Training Based on I-Cvi and Efa*, 2020.

Hindawi
Scientific Programming
Volume 2022, Article ID 7868591, 12 pages
https://doi.org/10.1155/2022/7868591

Research Article

The Acceptance Status of Traditional Moral Culture in Colleges and Universities Using Convolutional Neural Network

Bingduan Liu

School of Art and Design, Wuhan Institute of Technology, Wuhan 430205, China

Correspondence should be addressed to Bingduan Liu; studytochina@wit.edu.cn

Received 10 December 2021; Accepted 27 December 2021; Published 24 February 2022

Academic Editor: Muhammad Usman

In today's world, competition among countries is not just a contest of hard force, but also a contest of soft power. China has a five-thousand-year-old history and civilization, with a strong traditional moral culture at its core. The university stage is an important time for college students to develop their worldview, outlook on life, and values. In this context, excellent traditional and moral culture education plays an important role and significance in their development. College students are the country's future builders and an important force to inherit China's excellent moral culture. The rapid development of the modern Internet era has made the channels for college students to understand and accept the cultures of various countries more and more diverse and convenient. Actively borrowing their essence can help promote the development of Chinese culture, but we must also pay attention to active defense and resistance against the dregs of culture. This paper discusses the current situation and problems of the acceptance status of excellent traditional moral culture among college students and analyses the factors that restrict the acceptance of excellent traditional moral culture among college students to conduct a large-scale study on the acceptance status of traditional moral culture in colleges and universities. A model based on convolutional neural networks is suggested for predicting college students' embrace of traditional moral values. By learning and describing their activities and preferences on the Internet, the model assesses and creates college students' acceptance status for conventional moral culture. Extensive tests indicate that the suggested technique can successfully assess college students' acceptance status for traditional moral culture, and the model's superior performance is supported by test results.

1. Introduction

With the increasingly harsh rivalry among nations' comprehensive national strength, the competition of countries' soft power is receiving more and more attention and importance in today's peaceful development. As the motherland's future leaders, college students' attitudes toward and acceptance of outstanding traditional moral culture play a critical role in preserving history and culture and actively advancing excellent moral culture. In this new period of fast economic globalization, China's great traditional moral culture is now confronted with a challenging foreign and local environment. College students should actively accept Chinese excellent traditional moral culture and, in light of China's current national circumstances, grasp the international development trend to better transform and carry forward Chinese excellent traditional moral culture and promote China's soft power development [1].

With the advent of the Internet era, college students are exposed to a plethora of international and domestic cultural information, including many foreign excellent and dreary cultures, which has a direct impact on the moral and cultural outlook of college students and naturally leads to clashes with traditional Chinese culture [2]. The author plotted the hotness trend of the search phrase Chinese traditional moral culture in Google from 2004 to 2021, as shown in Figure 1, and we can see that the hotness trend is steadily diminishing, suggesting that the Internet's attention to Chinese traditional moral culture is constantly declining. College students bear the important responsibility of inheriting excellent traditional moral culture as the driving force of future socialist modernization construction, and their attitude toward

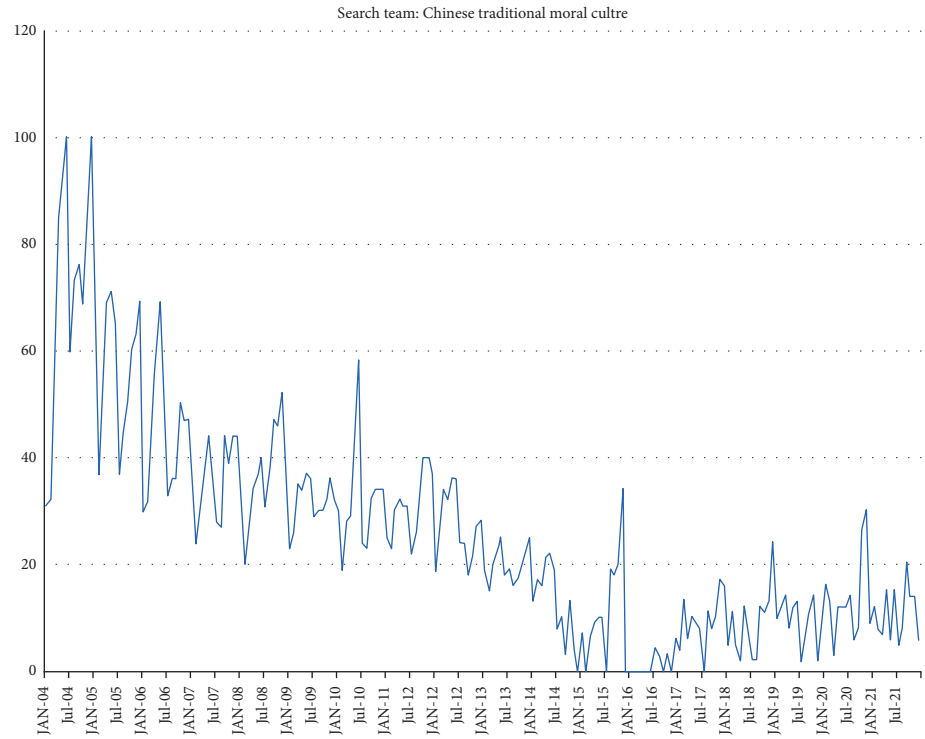

Figure 1: Google hot trends chart.

accepting excellent traditional moral culture is extremely important and should be given more and more attention and concern. The acceptance state of outstanding traditional moral culture among college students is the study object of this work, which examines the acceptance state, degree, and routes of current college students to excellent traditional moral culture. The purpose of this paper is to examine the acceptance status [3], degree, and channels of excellent traditional Chinese moral culture among contemporary college students to carry forward excellent traditional Chinese moral culture, build an advanced culture with the times, and strengthen China's soft power construction. The university stage is critical for the formation and improvement of one's worldview, outlook on life, and values, and in an era when the world is moving toward a knowledge-based economy and a technology-based national strategy, university students are the country's hope for prosperity and strength. Acceptance and inheritance of good traditional moral culture by college students is highly regarded by people from all walks of life, and it is critical to assemble the Chinese nation's solid will and renew the great national spirit to realize the Chinese nation's great rejuvenation. Acceptance of outstanding traditional moral culture by college students is also important for improving their overall strength and cultural literacy [4]. Confucianism, Taoism, and Buddhism, which are at the heart of China's great traditional moral culture, may assist college students in overcoming the challenges and problems they face in everyday life and their studies, as well as nurturing high connotations in college students. As a result, the purpose of this article is to create awareness of the need of adopting and cultivating outstanding traditional Chinese moral culture among college students, so that they may comprehend the relevance of doing so in their future studies, lives, and job [5].

Traditional moral culture education for college students is an education that aids in the development of outstanding moral character among college students. The fast growth of the Internet, particularly social networking sites, presents both possibilities and problems for conventional moral culture teaching for college students. Colleges and universities may take advantage of the central role of social networks in college students' everyday lives to develop a new model of the traditional moral culture education and actively guide the development of excellent traditional moral and cultural character in college students. One of the most important characteristics of high-quality talents is a noble character, which allows for a wide spectrum of synergistic growth. Noble personal character and values are beneficial to people's peaceful contact with others in the process of self-control, while also encouraging harmonious social growth, in social activities. Colleges and universities should make extensive use of social media to encourage the formation of traditional moral culture among students [6]. It gives college students a suitable teaching platform for traditional moral culture instruction. Traditional moral culture education in schools is limited to the teaching of textbook contents, and students mechanically complete learning tasks. As a result of the negative effects of exam-oriented education, colleges and universities place a greater emphasis on instilling theoretical knowledge of traditional moral culture in students, which to some extent inhibits students' interest, reduces teaching efficiency and results, and is not conducive to student play. Social networks, on the other hand, ignore these flaws and

place a greater focus on the central role of students, offering a platform for college students to learn more about conventional moral culture's ideological and theoretical knowledge as well as new thinking patterns [7]. It provides a variety of educational tools for college students' traditional moral culture instruction. The diverse information distribution contents of social networks contribute to the enrichment of conventional moral culture instructional resources. Educators can help college students' ideologies become less confined by providing them with relevant knowledge and news, as well as assisting them in taking a step back to consider their benefits and disadvantages from a higher perspective. At the same time, college students may pick their learning materials at any time and from any location, enhancing their creative awareness and desire to study.

Social networks are more significant in the everyday lives of college students in the contemporary era of social networks, and they have a profound impact on their consciousness and conduct. As a result, the study of traditional moral culture acceptance in colleges and universities in a social network setting provides the foundation for providing traditional moral culture education to college students. However, in the social network setting, college students' behaviors and preferences are abstract and difficult to quantify, and their acceptance status of conventional moral culture is similarly oblique and implicit. This research offers a model based on convolutional neural networks to correctly assess the acceptance status of traditional moral culture in colleges and universities. The model first obtains college students' preferences in social networks and characterizes them as digital features, then extracts high-level semantic information from digital features using a convolutional neural network, and finally uses a classifier to discriminate college students' acceptance status for traditional moral culture. Extensive studies reveal that the suggested technique properly identifies college students' acceptance status for traditional moral culture, laying the groundwork for furthering traditional moral culture instruction in colleges and universities in the social network environment. Main contributions of this research work are listed below:

(i) Due to several factors such as social evolution and cultural conflicts, school reform and teacher quality, family moral education environment, and college students' self-restraint ability, this work finds that the existing problems primarily include a lack of awareness among college students themselves, an imperfect education mechanism, and a lack of practical activities.

(ii) Based on their actions and preferences in social networks, the suggested model predicts college students' acceptance status of Chinese good traditional moral culture.

(iii) Finally, studies in the test set demonstrate the validity and accuracy of the proposed model by constructing a dataset with actual questionnaires, laying the groundwork for future instruction on Chinese superb traditional moral culture for college students' groups.

The rest of the paper is organized as follows: Section 2 explains the related work, Section 3 presents the methodology for the proposed model, Section 4 explains experimentation and evaluation results that the author has obtained during work, and finally, the author concluded the work in separate section as Section 5.

2. Related Work

In this section, the author discusses works related to the research topic. Here social networks and challenges posed by social networks and convolutional neural networks are first explained.

2.1. Social Networks. Simply said, social networks are webs of social interactions and personal connections. Consider how you met your pals and how you got to know them. Perhaps you met them in primary school, or perhaps you met them via a pastime or through your church. In either case, you were exposed to social networks, which entail meeting new people in a social setting and forming strong personal relationships over time. While social networking concentrates upon allowing like-minded people to communicate with one another through websites and web-based apps, social networking sites include Facebook, MySpace, Twitter, and LinkedIn. The word "social network" has a fairly broad definition since it is still a relatively new technology that is prone to fast development. As indicated in Figure 2, there are three main types of social networks, and an integrated social business strategy uses all three to increase communications with various groups of people.

(i) Public social networks: these networks, like Facebook and Twitter, are useful for connecting with consumers and prospects. These networks solve simple issues.

(ii) Social extranets: these networks include customer communities, which allow for deeper engagement and cooperation with customers, as well as private business-to-business networks, which allow for communication with partners and B2B customers. In these networks more focus is on engagement.

(iii) Employee networks: these are used for internal corporate communication. Most of these networks share knowledge and response better that above.

2.2. The Challenges Posed by Social Networks. For China's education model, the emergence and development of social networks have also promoted the reform and innovation of China's traditional education model to a certain extent and played a positive role in promoting the construction of China's advanced culture [8]. The form of education in the era of social network is no longer restricted by geography, the circle of friends can be extended to all corners of the world, and college students can use their virtual identities to communicate and study with the outside world, confide their inner feelings without any worries, and relieve the

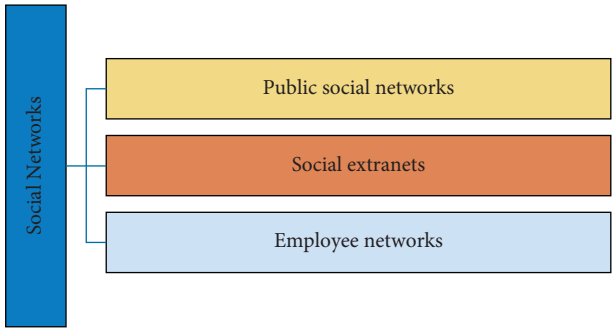

Figure 2: Types of social networks.

pressure brought by their study life [9]. This enriches the lives of college students and satisfies their spiritual needs. The social network environment focuses on the development of personal ability and ignores the beneficial effect of personal cultivation and traditional moral culture on their own progress. Under the influence of this negative concept, college students mistakenly believe that the development of society needs only people with higher personal expertise and skills, which leads college students to neglect the formation of traditional moral culture and lack of binding force on their personal behavior in the process of learning professional knowledge. Therefore, students set their main goals on professional knowledge, computer knowledge, foreign languages, etc. and participate in various club activities to improve their ability to do things and social skills, but they are not motivated to study the content of traditional moral and cultural education. This leads to some college students' rude speech and behavior, noncompliance with public order, and poor self-restraint ability. At the same time, because college students lack certain social experience, have little sense of right and wrong, and do not have enough immunity to the external environment, they are easily influenced by the bad social values, and their ideology and behavior consciousness deviate from the moral standards. As the main group of social media and social networking sites such as microblogs and WeChat, college students are easily influenced by some bad information in social networks, thus distorting their not yet fully mature outlook on life, values, and worldview [10]. For example, the most common kind of negative energy circulating on the network nowadays, namely, the show of wealth, the excessive worship, and enjoyment of material enjoyment, can easily influence the values of college students and focus one-sidedly on the psychological satisfaction brought by material conditions, which leads college students to excessively pursue material benefits in the learning process.

In addition to affecting the learning effect, more importantly, it is not conducive to the formation of good personal cultivation of college students. It is not conducive to the formation of good traditional moral culture of college students. The initial formation of people's traditional moral concept comes from parental education and family environment influence, which is the basis for further improvement of moral concepts after entering society. However, contemporary college students generally [11] have the phenomenon of weak moral concepts in their families. For example, college students fall in love, due to the characteristics of the wide coverage of social networks, the concept of love of college students is influenced by the Western open ideology, and deviations in the concept of love and morality appear. To satisfy their material life or fill their inner emptiness, some students fall in love with an extremely irresponsible attitude, and what is more outrageous is that some students decide the love object through games, do not take feelings as the starting point, choose the love object at will or change the love object frequently, are not bound by ethics and morality, and show their personal ability through love. The spread of bad social concepts in social networks largely affects the behavioral norms and social ethics of college students and is not conducive to the formation of good traditional moral concepts of college students [12]. It is not conducive to the formation of responsible social and public consciousness of college students.

2.3. Convolutional Neural Networks. The convolutional neural network (CNN) is a deep learning architecture inspired by the visual system. Hubel and Wiesel discovered it in 1962 while studying the primary visual cortex of cats. Receptive fields are tiny subregions of the visual field that are responsive to cells in the cortex [23]. These cells are responsible for detecting light in the receptive fields. In 1980, Fukushima introduced Neocognitron, which was based on Hubel and Wiesel's work and was the first computer-simulable model. This Neocognitron is regarded as the forerunner of CNNs, and it was based on the hierarchical structure of neurons for image processing. By creating an artificial neural network with a multilayer termed LeNet-5, the author of [24] laid the groundwork for CNNs. The backpropagation technique was used to train this artificial neural network, which was employed to do handwritten digit categorization. It was possible to recognize patterns from raw pixels after training with this approach. Despite its numerous advantages, LeNet-5 has not been effective in handling complicated issues such as video categorization.

Artificial neural network (ANN) is a hot research topic that emerged in the field of artificial intelligence in the 1980s [13]. It abstracts the neuronal network of the human brain from the perspective of information processing, builds some simple models, and forms different networks according to different connections. It is often directly referred to as a neural network or neural-like network in engineering and academic circles. A neural network is an operational model consisting of a large number of nodes (or neurons) connected. Each node represents a specific output function, called the activation function-n. Each connection between two nodes represents a weighted value of the signal passing through that connection, called weight, which is equivalent to the memory of an artificial neural network. The output of the network varies depending on the connection method, weight, and excitation function of the network. The network itself is usually an approximation of some algorithm or function in nature, or it may be an expression of a logical strategy. In the last decade or so, the

research work of artificial neural networks has been deepening and has made great progress, and it has successfully solved many practical problems that are difficult to be solved by modern computers in the fields of pattern recognition, intelligent robotics, automatic control, prediction estimation, biology, medicine, economy, etc., and has shown good intelligent properties. With the rapid development of neural networks, their definitions have also emerged. As early as 1989, YannLeCun and his colleagues published the results of convolution neural networks (CNN) [14], a deep neural network with a convolutional structure, usually with at least two nonlinear trainable convolutional layers and two nonlinear fixed convolutional layers (also known as pooling). The structure of CNNs is inspired by the famous Hubel-Wiesel model of biological vision, especially to simulate the behavior of Simple Cell and Complex Cell in layers V1 and V2 of the visual cortex. The evolutionary path of CNN can be summarized into 4 paths: (1) deeper network; (2) enhanced convolutional mode, and fusion of the above two ideas; (3) from classification to detection; and (4) addition of new functional modules. More and more CNN models are now evolving step by step from giant networks to lightweight networks, and the model accuracy is getting higher and higher. The focus of the industry has now shifted from accuracy improvement (because they are all already high) to a balance of speed and accuracy [14], all wanting the models to be fast and accurate. Therefore, from the original AlexNet [15] and VGG-Net [16] to the smaller Inception and ResNet [17] series and then to the current MobileNet [18] and ShuffleNet [19] that can be ported to mobile, we can see some trends as follows. Convolutional kernels: (1) large convolutional kernels are replaced by multiple small convolutional kernels; (2) single-size convolutional kernels are replaced by multisize convolutional kernels; (3) circumscribed shape convolutional kernels tend to use deformable convolutional kernels; (4) 1×1 convolutional kernels are used. Convolutional layer channels: (1) standard convolution is replaced by depth-wise convolution; (2) grouped convolution is used; (3) channel shuffle is used before grouped convolution; (4) channel weighting is calculated. For convolutional layer connection: (1) use skip connection to make the model deeper; (2) densely connect so that each layer incorporates the feature outputs of the other layers. Convolutional neural networks are still evolving and innovating, but each advancement is an improvement and innovation based on the previous neural network structure, which makes up for the shortcomings of the existing network. After AlexNet [15], there are two major directions of innovation, one is the improvement of the network structure and the other is the improvement of the network depth. However, the current neural network has a huge number of parameters, and the requirement of computational power is still very high. How to choose the appropriate hyperparameters, such as learning rate, kernel size of convolutional filtering, number of layers, etc., requires a lot of technology and experience, which is also the future development direction of convolutional neural networks and needs more in-depth research.

3. Method

In this section, the author explains the methodology that was adopted for the proposed research work.

3.1. Data Collection. The study of different college students' acceptance status of traditional moral culture in colleges and universities using social media data is mainly conducted by text data mining techniques based on convolutional neural networks. First, based on the Weibo and WeChat accounts raised by volunteers, crawler technology is used to obtain textual information related to Weibo and WeChat users, which is used to build a database and train a model.

In recent years, the emergence and development of microblog social platforms have led to a dramatic change in the way people use the Internet, transforming from simple web browsing and information searching to information mining, communication, and sharing. Especially since 2010, microblogs have rapidly penetrated among Internet users by virtue of their platform's openness, terminal scalability, and content simplicity and gradually developed into an important social media, becoming an important medium for college students to obtain real-time news, social sharing, and social participation. After the processing work of deduplicating and summarizing microblog information by date, the content of microblog texts posted, commented, retweeted, and liked by a certain college student is the core data of this study, as shown in Table 1.

At present, millions of WeChat public resources are accumulating information and quality content, which has become the main way for a considerable number of users to obtain information. However, due to the limitations of WeChat's social properties and the fact that it is not the same as traditional web pages that link to each other through hyperlinks, these massive quality resources have not been effectively released and have existed in an "island" in the current Chinese Internet world. The core indicators of this study are the number of tweeted articles in the public number subscribed by a college student, the text posted in the circle of friends, and the collected articles, after summarizing the information of WeChat. For these core indicators, after finishing the calculation, this paper designs the main basis of WeChat pushed articles, the content posted by users, and the text content collected by users, as shown in Table 2.

3.2. Model Architecture. In this section, the author explains architecture of the model. The flowchart of traditional moral culture acceptance state model in colleges and universities based on convolutional neural network is shown in Figure 3.

In this paper, the test data obtained from microblogs and WeChat are cleaned, truncated, and sequence-labelled, and the preprocessed data are input into a BERT model [20], and its output is connected to a convolutional neural network model for identifying the acceptance status of traditional moral culture by college students. The model used in this paper contains two structures: the BERT model and the convolutional neural network model [21]. The two models

Table 1: Weibo indicators.

Indicator name	Description
Post content	Content of Weibo posted by each university student
Comments	Content of Weibo posts per student
Retweets	Retweets by each student
Likes	Content of Weibo liked by each student

Table 2: WeChat indicators.

Indicator name	Description
Push content	Content pushed to users by WeChat
Publish content	Content posted by users on WeChat
User favorites	Content collected by users on WeChat

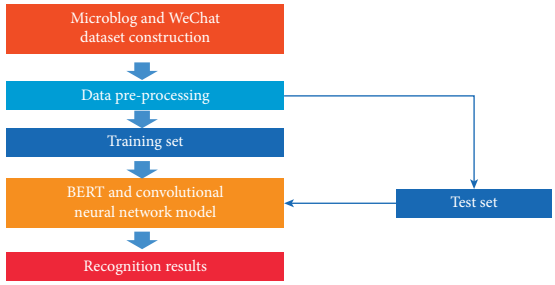

Figure 3: Flowchart.

are connected hierarchically. The overall structure of the model is shown in Figure 4.

3.3. BERT Model. The model structure of BERT is a multilayer bidirectional converter structure, and unlike other recent language representation models, BERT [21] aims to pretrain deep bidirectional representations by jointly regulating the context in all layers. In the encoding process of the converter, the data are first passed through the self-attentive module to obtain a weighted feature vector:

$$Z = \text{Attention}(Q, K, V) = \text{soft max}\left(\frac{QK^T}{\sqrt{d_k}}\right)V, \quad (1)$$

where Q, K, and V are obtained from 3 embedding vectors, respectively. The feature vector Z is passed through the feedforward neural network to obtain the word encoding.

$$\text{FFN}(Z) = \max\left(0, ZW_1 + b_1\right)W_2 + b_2. \quad (2)$$

The input of BERT is composed of three parts: (1) character embedding represents the embedding of the current word; (2) paragraph embedding represents the index embedding of the sentence where the current word is located; (3) location embedding represents the index embedding of the location of the current word. The input is "I won the lottery today, I'm buying dinner," and the output of BERT is a vector representation of the input words with the full-text semantic information, which is a pretraining model using the mask language model and the next sentence prediction model. Masked language model: 15% of the characters in the input vector are masked out randomly. When training the model, a vector is fed into the model several times for parameter learning, and instead of masking out the words each time, the words to be masked out are replaced with "[Mask]" in 80% of the time, with any other words in 10% of the time, and with the original marker.

3.4. Convolutional Neural Networks. The word vector with global features output from BERT is used as the input of the convolutional neural network, which is different from image convolution, which uses a two-dimensional vector, and text convolution, which uses a one-dimensional vector. This paper adopts the structural model of a one-dimensional convolutional layer with a maximum pooling layer classification layer and adds a discard layer to prevent overfitting and overparameterization during the training of the model [22]. After preprocessing a text sequence of length n, the feature mapping of each word is obtained by encoding the BERT pretraining model as follows:

$$e_{x_i} = E[x_i], \quad (3)$$

where x_i denotes the word vector corresponding to character i at position i, and $E[x_i]$ denotes the dense vector of word vectors trained in the model. The feature mapping of the sequence is denoted as

$$e_{i:n} = e_{x_1} \oplus e_{x_2} \oplus \cdots \oplus e_{x_n}. \quad (4)$$

e_{x_1} denotes the vector that is in the first position in the sequence and $*$ denotes the concatenation operator. The word vector is passed through a one-dimensional convolutional layer to obtain the feature mapping c_i.

$$c_i = f\left(w_i^* e_{x_i} + b\right), \quad (5)$$

where w_i denotes the weight and b denotes the bias. The feature mapping is expressed as

$$c = [c_1, c_2, \ldots, c_n]. \quad (6)$$

After maximizing the pooling layer to obtain the feature vector:

$$\hat{c} = \max(c). \quad (7)$$

The classification results after the fully connected layer:

$$P\left(y|x_1, x_2, \ldots, x_n\right) = \text{soft max}(\hat{c}). \quad (8)$$

4. Experimentation and Evaluation

4.1. Dataset. In order to construct the dataset, the author first designed the Questionnaire on the Acceptance Status of Excellent Traditional Moral Culture among College Students. This questionnaire is divided into three parts: objective information, subjective questions, and social network information, involving contemporary college students' attitudes toward, mastery of, and opinions and suggestions on excellent traditional Chinese moral culture, and mainly includes the

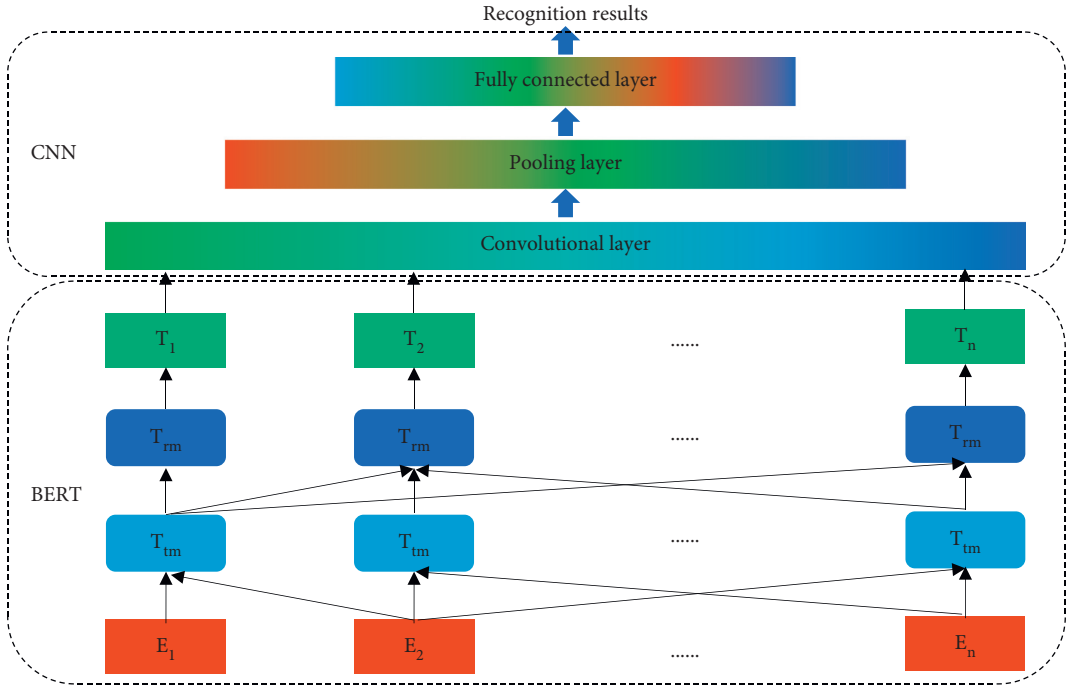

Figure 4: Model architecture.

following types of questions: (1) Overall acceptance status of excellent traditional moral culture among college students, denoted as C1. (2) Acceptance status of political morality such as serving the country with fidelity and national temperament, denoted as C2. (3) The acceptance status of righteousness and profit cultivation, such as self-restraint and righteousness, is expressed as C3. (4) The acceptance status of social morality, such as honesty and knowledge of reward, modesty, and benevolence, is expressed as C4. (5) The acceptance status of human morality, such as family harmony and filial piety, is expressed as C5. (6) The acceptance status of enterprising spirit, such as pragmatism and self-improvement, is expressed as C6. The questions are closely matched with the life of college students and have high practicality. The objective information and subjective questions constitute the labels of each college student's acceptance status of traditional moral culture in colleges and universities, and the social network information constitutes the sample data of college students' acceptance status of traditional moral culture in colleges and universities. The social network information was crawled using crawler technology to crawl relevant text data. The survey questionnaires were distributed to undergraduate and graduate students in several universities, with a total of 500 volunteers. To ensure that the questionnaires could be effectively collected, a combination of field and correspondence distribution was used between May 30, 2021, and July 10, 2021, and a stratified sampling method was used to distribute questionnaires to several school students (see Table 3), and a total of 500 questionnaires were distributed and 473 were collected, removing invalid questionnaires and making a total of 462 valid questionnaires. The dataset was divided into 312 training samples, 50 validation samples, and 100 test samples.

4.2. Experimental Setup. The proposed method operating system is Linux 16.0, programming environment is python3.6 pytorch-gpu, GPU is GXT 2080TI, memory is 64G, and CPU is Intel (R) Core (TM) i5-9300H 2.4 GHz. the model optimization method uses Adam gradient descent and cross entropy loss function method, the learning rate is set to 0.0004 by debugging, the batch size is set to 32, and the discard layer parameter is set to 0.4 in order to avoid overfitting and overparameterization of the model during training.

4.3. Experimental Results. The loss curves during the model iterations are shown in Figures 5 and 6. As seen in Figure 6, the model is trained for 5 times (300 iterations) when the loss curve plateaus and the classification effect is optimal. The model's test accuracy increases with the number of trainings with the same number of test sets as shown in Figure 7. Figure 7 shows that the model accuracy gradually increases with the increase of training data, and it is difficult to achieve the desired model accuracy with a small number of datasets, and the accuracy of the model needs a large amount of data support.

4.3.1. C1 Category Acceptance Status. The survey results show that college students' overall acceptance of good traditional morality is average, and their overall willingness to accept is generally not strong, while their knowledge mastery is good, but they fail to reach the most ideal acceptance state in terms of interpretation, screening, and practice. When answering the question "What is your overall evaluation of your own acceptance of good traditional moral culture," as

Table 3: Survey statistics table.

Student type	Number of distribution	Number of recycling	Recycling rate (%)	Effective number	Effective recycling rate (%)
Undergraduates	350	329	94.0	322	97.8
Graduate students	150	144	96.0	140	97.2

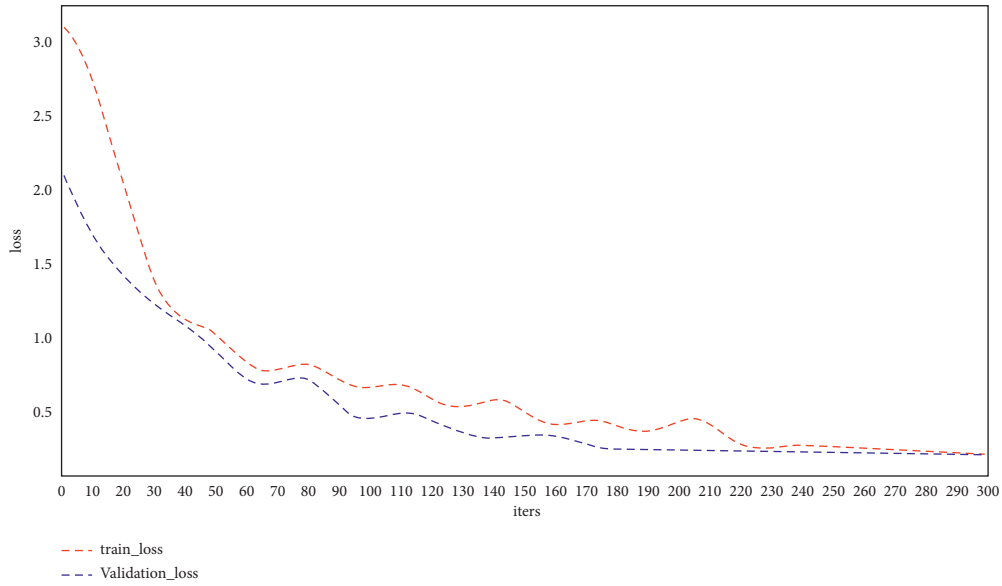

Figure 5: Training and validation loss trend graphs.

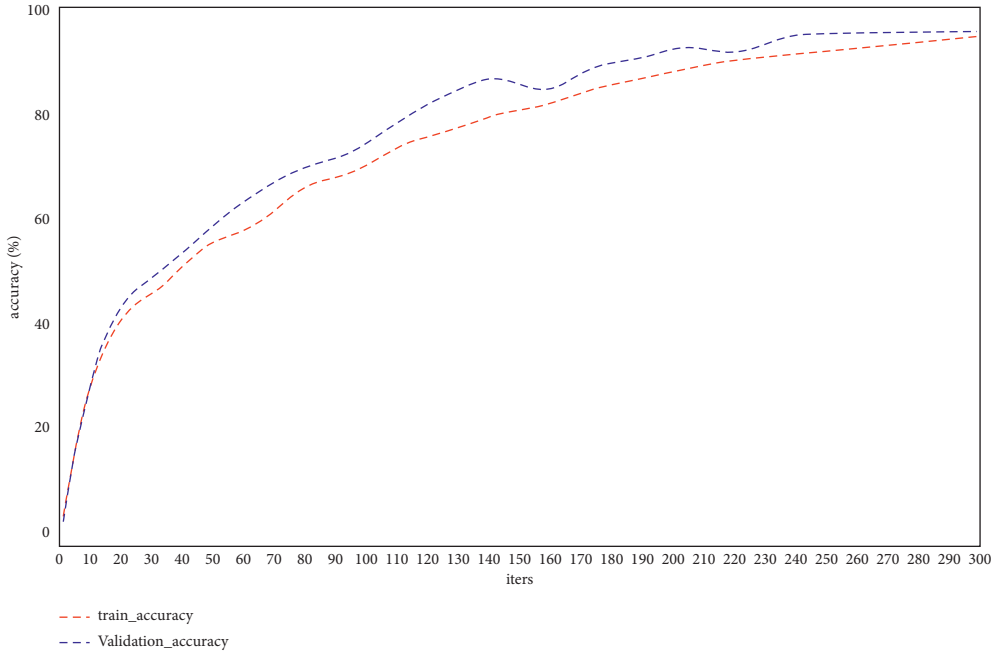

Figure 6: Training and validation accuracy trend graph.

many as 43% of the students chose "average," 8% chose "poor," 39% chose "good," and only 10% of college students think their own acceptance of good traditional culture is excellent. The overall acceptance result predicted by the model is almost the same as the actual one.

4.3.2. C2 Category Acceptance Status. From the data in Table 4, it can be seen that 71% of college students chose to accept it in their hearts, which shows that the overall patriotism of college students is relatively strong, but the percentage of those who can practice it is only 13%. Indeed,

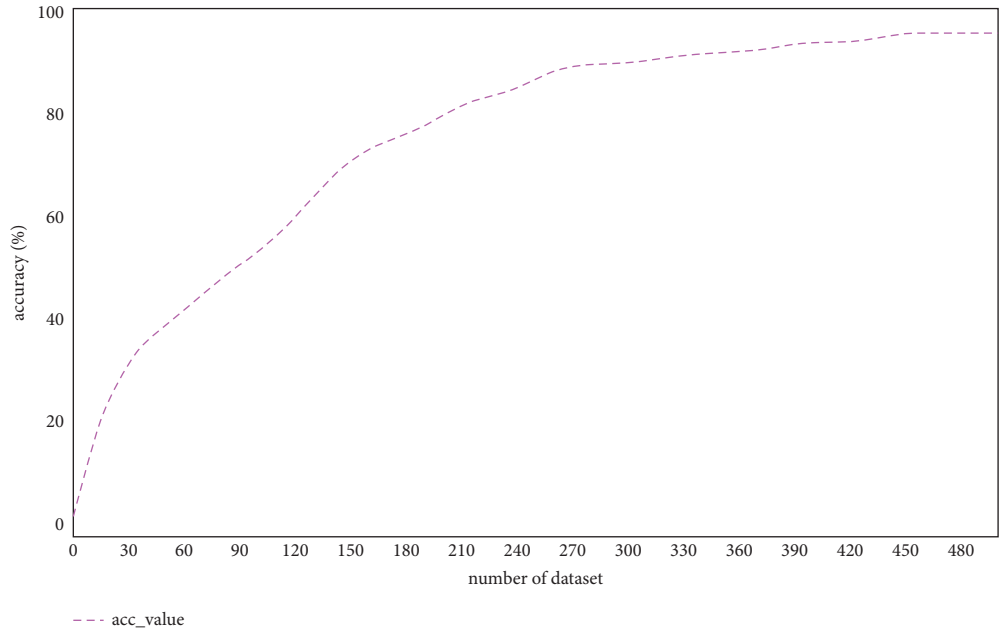

Figure 7: Data volume and accuracy trend graph.

Table 4: C2 statistics table.

	Resist	Understand	Agree	Acceptance	Behavioral practices
Number of people	1	3	12	71	13
Percentage	1	3	12	71	13
Number of model output	1	2	11	72	14

being in the peace era, there are not many opportunities provided for college students to go to the battlefield.

4.3.3. C3 Category Acceptance Status. From the data in Table 5, the total number of college students who chose "accept it in their hearts" and "practice it" is 77, which is slightly lower than "serve the nation with loyalty and national integrity." However, the proportion of those who can set an example and put it into practice has increased to a certain extent. 23% of college students still chose "familiar with" or "below"; in particular, the proportion is higher among the junior students.

4.3.4. C4 Category Acceptance Status. From the data in Table 6, it is clear that the number of college students who accept "honesty, knowledge, humility, and love" is significantly lower than the first two, and the number of those who can put it into practice is also reduced accordingly. Some pessimists have argued that honesty is leaving our time and the world is full of frauds and lies.

4.3.5. C5 Category Acceptance Status. From the data in Table 7, it can be seen that, among the above four statistics, college students accept the highest degree of human morality such as "family harmony and filial piety" and are able to put it into practice. As we know, most of the college students choose to buy gifts to express their filial respect to their parents and elders, which is a way to express their feelings but not enough.

4.3.6. C6 Category Acceptance Status. From the data in Table 8 and the comparison of college students' school performance, the author found that most of the students who chose to practice behavior ranked in the top third of their grade, which fully illustrates the importance of practice for improving college students' own ability. Most of the respondents who chose to accept it said that they agree with the expected benefits brought by the efforts, but they are always unable to devote themselves to their study or work due to various distracting factors, and their attention is very easily distracted, and they often end up in a tiger's head and stop halfway.

4.3.7. Graphical Representation. Figure 8 depicts a graphical depiction of the acceptance status of the C2 category. In this figure, the author has taken the number of persons who participated in the experimental work, their percentage, and the number of models output. This shows that just one person resisted, three people understood, twelve agreed, and seventy-one accepted it with thirteen behavioral practices. Furthermore, in the author's model output one resisted, two understood, eleven agreed, and seventy-two accepted behavior patterns.

Table 5: C3 statistics table.

	Resist	Understand	Agree	Acceptance	Behavioral practices
Number of people	2	5	16	57	20
Percentage	2	5	16	57	20
Number of model output	2	5	15	56	22

Table 6: C4 statistics table.

	Resist	Understand	Agree	Acceptance	Behavioral practices
Number of people	3	4	28	54	11
Percentage	3	4	28	54	11
Number of model output	2	3	26	56	13

Table 7: C5 statistics table.

	Resist	Understand	Agree	Acceptance	Behavioral practices
Number of people	1	2	7	45	45
Percentage	1	2	7	45	45
Number of model output	0	1	8	46	45

Table 8: C6 statistics table.

	Resist	Understand	Agree	Acceptance	Behavioral practices
Number of people	3	4	23	45	25
Percentage	3	4	23	45	25
Number of model output	2	3	21	47	27

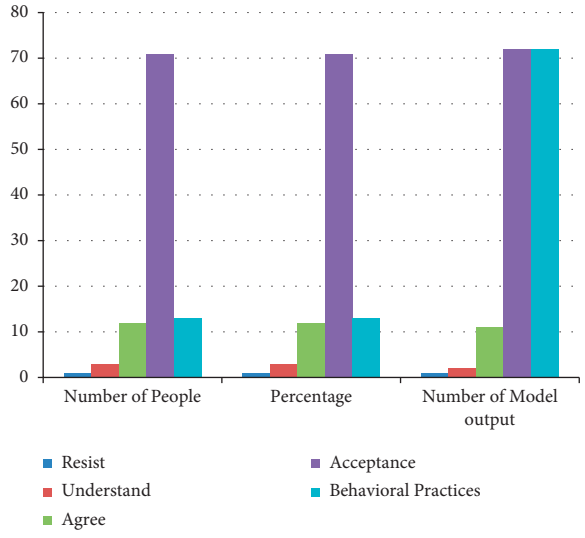

Figure 8: Representation of the acceptance status of the C2 category.

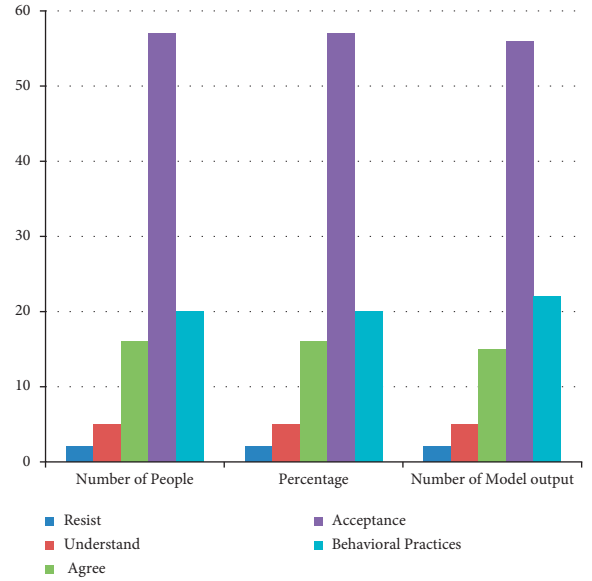

Figure 9: Representation of the acceptance status of the C3 category.

Figure 9 shows a graphical depiction of the acceptance status of the C3 category. Here the author has taken the number of persons who participated in the experimental work, their percentage, and the number of models output. This shows that just two people resisted, five people understood, sixteen agreed, and fifty-seven accepted it with twenty behavioral practices. Similarly, two percent resisted, five percent understood, sixteen agreed, and fifty-seven accepted it with twenty behavioral practices. Furthermore, in the author's model output two resisted, five understood, fifteen agreed, and fifty-six accepted with twenty-two behavior patterns.

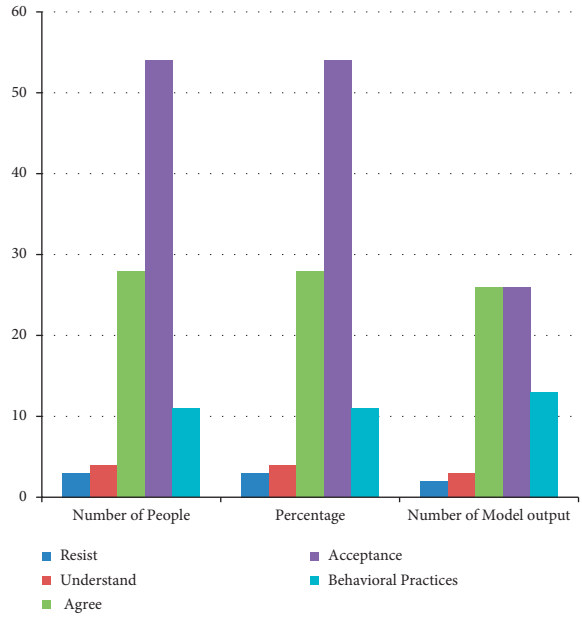

Figure 10: Representation of the acceptance status of the C3 category.

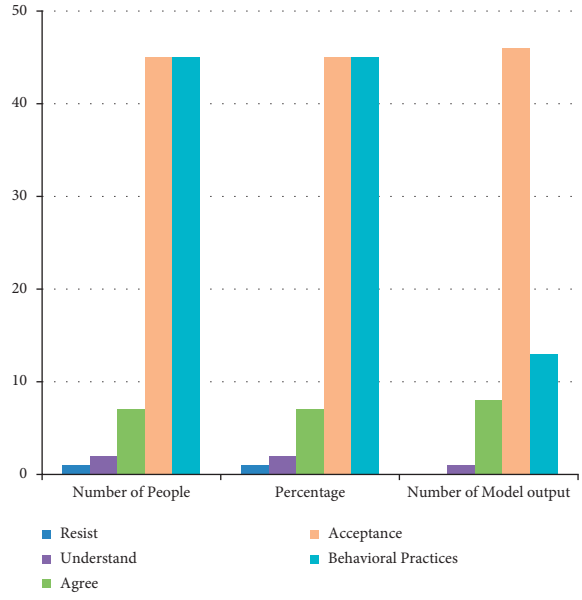

Figure 11: Representation of the acceptance status of the C5 category.

Figure 10 shows a graphical depiction of the acceptance status of the C4 category. Here, the author has taken the number of persons who participated in the experimental work, their percentage, and the number of models output. This shows that three people resisted, four understood, twenty-eight agreed, and fifty-four accepted it with eleven behavioral practices. Similarly, three percent resisted, four percent understood, twenty-eight agreed, and fifty-four accepted it with eleven behavioral practices. Furthermore, in the author's model output two resisted, three understood, twenty-six agreed, and fifty-six accepted with thirteen behavior patterns.

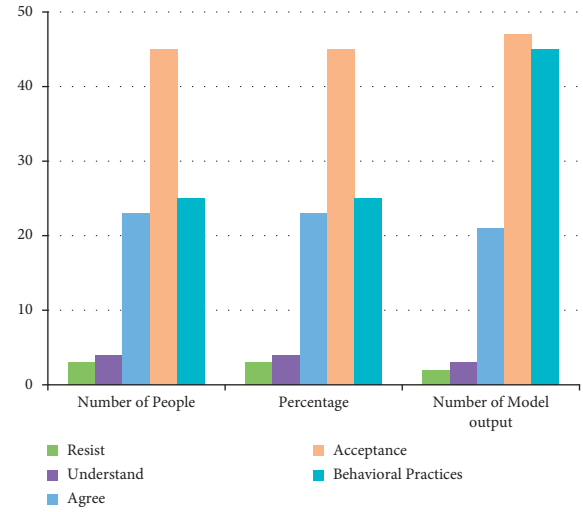

Figure 12: Representation of the acceptance status of the C6 category.

Figure 11 shows a graphical depiction of the acceptance status of the C5 category. Here the author has taken the number of persons who participated in the experimental work, their percentage, and the number of models output. This shows that only one person resisted, two understood, seven agreed, and forty-five accepted it with forty-five behavioral practices. Similarly, one percent resisted, two percent understood, seven agreed, and fifty-five accepted it with forty-five behavioral practices. Furthermore, in the author's model output zero resisted, one understood, eight agreed, and forty-six accepted with forty-five behavior practices.

Figure 12 shows a graphical depiction of the acceptance status of the C6 category. Here the author has taken the number of persons who participated in the experimental work, their percentage, and the number of models output. This shows that three people resisted, four understood, twenty-three agreed, and forty-five accepted it with twenty-five behavioral practices. Similarly, three percent resisted, three percent understood, twenty-three agreed, and forty-five accepted it with twenty-five behavioral practices. Furthermore, in the author's model output two resisted, three understood, twenty-one agreed, and forty-seven accepted with twenty-seven behavior practices.

5. Conclusion

In this paper, the author conducted a study on the theme of college students' acceptance of Chinese excellent traditional moral culture, and the acceptance state here is not a broad discussion of acceptance in philosophy, but a separate analysis of the "state" of it, using various methods such as logical analysis, questionnaire survey, and mathematical statistics, based on fully absorbing the existing research results. To begin with, the adoption of good traditional Chinese moral culture among college students is a significant issue. To begin with, the adoption of good traditional moral culture by college students is important not only for the

development and promotion of socialist core values but also for encouraging college students to become suitable socialist successors. Second, the author discovered that the main issues are a lack of awareness among college students, an imperfect education mechanism, and a lack of practical activities, which are caused by a variety of factors such as social evolution and cultural conflicts, school reform, and teacher quality, family moral education environment, and college students' ability to self-restraint. This paper proposes a model based on a convolutional neural network that predicts college students' acceptance status of Chinese excellent traditional moral culture based on their behaviors and preferences in social networks to address the problem that it is difficult to identify college students' acceptance status of Chinese excellent traditional moral culture. Experiments were done in the test set by assembling the dataset with actual questionnaires to establish the validity and accuracy of the proposed model, laying the groundwork for future instruction on Chinese superb traditional moral culture for college students' groups.

Data Availability

The datasets used during the current study are available from the corresponding author on reasonable request.

Conflicts of Interest

The author declares that he has no conflicts of interest.

References

[1] Y.-t. Zhu, "The birth of traditional Chinese ethics in west zhou (1046-771 BC)," *A Panoramic History of Traditional Chinese Ethics*, Springer, Singapore, 2021.

[2] G. Lin, "Research on the application of traditional Chinese medicine culture in the construction of teachers' ethics system in medical colleges-take Zhangzhou health vocational college as an example," *Frontiers in Educational Research*, vol. 3, no. 14, 2020.

[3] Y. Yan, "The drive for success and the ethics of the striving individual," *Ordinary Ethics in China*, Routledge, Milton Park, UK, pp. 263–291, 2020.

[4] G. Shan, "From intrinsic value to the emotion of wonder," *Environmental Ethics*, vol. 40, no. 1, pp. 81–91, 2018.

[5] Z. Yu, J. Pei, M. Zhu, J. Zhang, and J. Li, "Multi-attribute adaptive aggregation transformer for vehicle re-identification," *Information Processing and Management*, vol. 59, no. 2, Article ID 102868, 2022.

[6] J. Zhu, T. Stone, and M. Petrini, "The ethics of refusing to care for patients during the coronavirus pandemic: a Chinese perspective," *Nursing Inquiry*, vol. 28, no. 1, Article ID e12380, 2021.

[7] M. Wen, S. Zhang, and D. McGhee, "Utilizing the moral nobility of older Chinese women in governance: the uses of humility, empathy, and an ethics of care in moral clinics in Huzhou city," *British Journal of Sociology*, vol. 71, no. 2, pp. 300–313, 2020.

[8] Y. Lian-yun and P. Jing, "Construction of life-practice moral education based on traditional Chinese morality with life connotation," *Frontiers of Education in China*, vol. 1, no. 3, pp. 456–461, 2006.

[9] Y. Yan and P. Chen, "The influence of traditional Chinese culture on the University student's ecological moral education," *Journal of Jiangsu Polytechnic University (Social Science Edition)*, vol. 1, 2010.

[10] L. Zhang, Y. Wang, M. Xiao, Q. Han, and J. Ding, "An ethical solution to the challenges in teaching anatomy with dissection in the Chinese culture," *Anatomical Sciences Education*, vol. 1, no. 2, pp. 56–59, 2008.

[11] D. Y. F. Ho, W. Xie, X. Liang, and L. Zeng, "Filial piety and traditional Chinese values: a study of high and mass cultures," *PsyCh Journal*, vol. 1, no. 1, pp. 40–55, 2012.

[12] H. L. Yang and W. P. Wu, "The effect of moral intensity on ethical decision making in accounting," *Journal of Moral Education*, vol. 38, no. 3, pp. 335–351, 2009.

[13] R. Hayhoe, "The evolution of modern Chinese educational institutions," *Contemporary Chinese education*, Routledge, Milton Park, UK, pp. 26–234, 2017.

[14] J. Wen, E. Thibeau-Sutre, M. Diaz-Melo et al., "Convolutional neural networks for classification of Alzheimer's disease: overview and reproducible evaluation," *Medical Image Analysis*, vol. 63, Article ID 101694, 2020.

[15] B. Chapaliuk, "Overview of the three-dimensional convolutional neural networks usage in medical computer-aided diagnosis systems," *American Journal of Neural Networks and Applications*, vol. 6, no. 2, pp. 22–28, 2020.

[16] A. Palvanov and Y. Cho, "VisNet: deep convolutional neural networks for forecasting atmospheric visibility," *Sensors*, vol. 19, no. 6, p. 1343, 2019.

[17] B. Park, H. Park, S. M. Lee, J. B. Seo, and N. Kim, "Lung segmentation on HRCT and volumetric CT for diffuse interstitial lung disease using deep convolutional neural networks," *Journal of Digital Imaging*, vol. 32, no. 6, pp. 1019–1026, 2019.

[18] M. Islam, G. Chen, and S. Jin, "An overview of neural network," *American Journal of Neural Networks and Applications*, vol. 5, no. 1, pp. 7–11, 2019.

[19] L. Lazebnik, "Convolutional neural network architectures: from LeNet to ResNet," *Presentation, University of Illinois, accessed*, vol. 20, 2018.

[20] K. He, X. Zhang, S. Ren, and S. Jian, "Deep residual learning for image recognition," in *Proceedings of the IEEE Conference on Computer Vision and Pattern Recognition*, pp. 770–778, Las Vegas, NV, USA, December, 2016.

[21] Z. Lu, P. Du, and J.-Y. Nie, "VGCN-BERT: augmenting BERT with graph embedding for text classification," *Lecture Notes in Computer Science*, vol. 12035, pp. 369–382, 2020.

[22] Z. J. Wang, R. Turko, O. Shaikh et al., "CNN explainer: learning convolutional neural networks with interactive visualization," *IEEE Transactions on Visualization and Computer Graphics*, vol. 27, no. 2, pp. 1396–1406, 2020.

[23] D. H. Hubel and T. N. Wiesel, "Receptive fields, binocular interaction and functional architecture in the cat's visual cortex," *The Journal of Physiology*, vol. 160, no. 1, pp. 106–154, 1962.

[24] Y. LeCun, B. E. Boser, J. S. Denker et al., "Handwritten digit recognition with a back-propagation network," in *Advances in Neural Information Processing Systems*Morgan Kaufmann Publishers Inc., San Francisco, CA, USA, 1990.

Hindawi
Scientific Programming
Volume 2022, Article ID 9285258, 9 pages
https://doi.org/10.1155/2022/9285258

Research Article

An IoT-Based Intelligent Geological Disaster Application Using Open-Source Software Framework

Yang Liu and Jin Zhang

School of Mining Engineering, Taiyuan University of Technology, Taiyuan 030024, Shanxi, China

Correspondence should be addressed to Yang Liu; lyzxgood@qq.com

Received 1 January 2022; Revised 16 January 2022; Accepted 3 February 2022; Published 24 February 2022

Academic Editor: Muhammad Zakarya

With the development of Internet of Things (IoT) and machine learning technologies, mobile geographic information systems (GISs) have developed rapidly. Moreover, mobile GIS applications serve all walks of life including remote sensing, geological disaster management, and decision support systems. This article discusses the main development methods of the Android system for mobile GIS, analyzes the characteristics of different development methods, and mainly introduces the technology of developing mobile GIS based on free and open-source software (FOSS) framework. Finally, we present a data collection framework for an Android application development, based on QGIS, QFiled, GeoServer, PostgreSQL, and GeoPackage. The mobile GIS can collect important data. Furthermore, the data collection framework uses a data aggregation technique to filter and remove redundant data. Machine learning approaches are integrated in the GIS to make it intelligent. The application, in the Xishan mining area of Taiyuan, proves that the proposed framework can complete the collection and storage of geological disaster data, which has certain practical significance. Our experimental results show that the data aggregation method is approximately 42.3–44.09 percent (training times) more efficient than the no aggregation approach. Moreover, the attention network may produce an additional overhead in the prediction process, depending on the model. This overhead is observed between 0.58% and 2.83% for the LSTM model.

1. Introduction

The evaluation of geological disasters is the basis for prevention and control of geological disasters. Traditional field surveys of geological disasters are based on paper maps and image data, using GPS, cameras, and other equipment to collect data and then organize and manage the data indoors. The workload of this process is large, and the interaction of each link is poor. Moreover, it is easy to make mistakes, which may lead to low work efficiency. Now, the digital survey of geological disasters has become the norm, but the original smart devices provided limited functions, such as communication, multimedia, and memos. With the rapid development of hardware and software, only mobile devices can essentially meet more advanced requirements than the traditional geological disaster surveys. Digital surveys have been applied to varying degrees in many fields such as geological surveys, land surveys, forestry surveys, and mineral resources surveys.

Mobile GIS is a comprehensive system with geospatial database as data support. This is possible through using geographic application server that can (i) provide map and geographic application services, (ii) establish data transmission between mobile client and server through wireless network communication technology, and (iii) provide mobile terminal as data collection and application tool. Mobile GIS has the characteristics of convenient mobility, real-time data, terminal independence, location relevance, information diversity, and distributed data sources. It gradually enters all walks of life and affects people's lives. At present, GIS has entered the era of cloud computing, Internet of things, and machine learning. Machine learning and IoT can play a vital role in developing intelligent applications and GISs.

Mobile GIS in the era of cloud computing and IoT is a cloud + terminal application model. The cloud focuses on map services, data storage, analysis, and calculation, IoT can help in collecting important data, and the mobile terminal pays more attention to data display and user interaction. In addition, the server and mobile terminals can be extended and developed, and the required data and functions can be integrated into the application. Whether from the perspective of rigid demand or new applications, mobile GIS will have a broader market space [1].

This article is based on the open-source Android platform, combined with mobile map technology, communication technology, machine learning, and data storage technology. Aiming at the problem that the field geological disaster survey work is greatly affected by environmental factors, a task-based geological disaster survey APP based on an open-source framework is developed. The framework makes full use of open-source software to realize the collection, browsing, and display of geological disaster information, provide convenient working methods for geological disaster investigation, and improve the efficiency of geological disaster data collection though aggregation and machine learning [2]. The main contributions in this paper are as follows:

(i) Open-source Android platform is combined with mobile map, communication, and data storage technologies

(ii) A task-based geological disaster survey application based on an open-source framework is developed

(iii) Open-source software is made full use to realize the collection, browsing, and display of geological disaster information

(iv) The efficiency of geological disaster data collection through data aggregation and machine learning techniques is improved

The rest of the paper is organized as follows. In Section 2, we offer an overview of open-source platform and various key enabling technologies. Section 3 offers a brief introduction to open-source software platforms. In Section 4, the implementation technology of an IoT-based geological disaster survey APP is described. In Section 5, the application is discussed in detail along with the aggregation algorithm. Moreover, we evaluate the proposed framework using a disaster dataset. In Section 6, results are discussed. Moreover, various machine learning techniques are evaluated on the aforementioned dataset to study validity of the framework. Finally, Section 7 concludes this paper and offers several directions for further research and investigation.

2. Background and Related Work

Geological disasters mainly occur in areas with unstable geological conditions, such as plate junctions, and mountainous areas. Due to the large topography, frequent seismic activities, and abundant rainfall, it is easy to cause landslides, collapses, mudslides, and other geological disasters. The mountain itself has a weak network signal, and the occurrence of disasters further affects the signal strength [2, 3].

There are three main modes for the development of mobile geological disaster collection APP such as (i) based on the secondary development platform provided by GIS vendors, (ii) based on mobile map API development provided by map service providers, and (iii) independent bottom development.

Yu et al. [4] used ESRI's ArcPad Application Builder secondary development software to develop customized functions for geological disaster data collection. The system has functions such as GPS or manual positioning points on the map, disaster point attribute information entry, and data storage. At the same time, the data interaction between outdoor information and indoor ArcGIS software is realized [5]. In order to solve the problems of geological disaster field investigators in identifying disaster points, photo description and positioning difficulties, and so on, three-dimensional real-world GIS was applied to the field data collection work, and the location and time of the photo shooting were correlated. Work provides support and convenience. Jiang [6] used embedded GIS technology to study the key technologies of spatial data organization and transmission, designed a mobile GIS land law enforcement dynamic inspection system, and applied it to land law enforcement inspection work, effectively improving the efficiency of land law enforcement inspection process.

Zhu [7] developed a system based on the Android system that can meet the requirements of the field collection of forest resources, using OpenLayers open-source GIS to realize coordinate positioning, data display, attribute editing, and import and export of spatial data. The system can meet the business needs of the field investigation of forest resources and at the same time provide a reference for other related research. Zhang [8] designed and developed an Android-based mobile returning farmland to forest operation design and verification system. It uses UCMap for secondary development and realizes vector map loading, spatial data editing, operation design, and verification and acceptance data form entry management and positioning. Yuan [9] developed a mobile GIS agricultural information acquisition system through the Android platform. Remote sensing images and vector data are released through ArcGIS Server 10.3. The system realizes the collection, editing, uploading, and GPS positioning of agricultural land attribute data, which improves work efficiency and accuracy.

Kong [1] has developed an intelligent inspection system APP for the Android system, which realizes the functions of location service, navigation, and positioning, three-dimensional map display, and so on, which improves the work efficiency of workers, reduces costs, and facilitates the management of workers. Huang [10] combined Android development technology, cloud computing, network services, and other related technologies to develop a geological cloud-based hydrogeology and water resources survey field data collection system, which realized the location, display, attribute data entry, upload, and other functions of the survey point.

However, the secondary development platform provided by GIS vendors greatly simplifies the development process

and has powerful functions, simple operation, and short development time [2]. However, its cost is extremely high, which is a high price for individuals or small manufacturers. Development based on the mobile map API provided by the map service provider is relatively easy to get started, and the development documents are detailed. However, as a map service provider, the functions and services it can provide are limited and cannot meet the GIS application requirements of special industries. Independent bottom-level development requires developers to independently research and design all interfaces, functions, and algorithms, which seems to reduce costs, but it takes time and tests capabilities. Products developed are difficult to compete with those developed by professional GIS vendors. The cost spent in the development process may be greater than the investment in commercial software.

3. Android GIS Open-Source Platform

OSMDroid is a map application development kit provided by the open-source map OpenStreetMap (OSM) based on the Android platform and can use OSM online maps [3, 11].

QGIS is an open-source desktop geographic information system, developed based on Qt and System in a Package (SIP), and belongs to the official plan of the Open-Source Geospatial Foundation (OSGeo). Developers can adjust themselves under the authorization of the General Public License (GNU) Program code, and all developers can modify the program freely [12–14].

Based on Android client and GeoServer map server, the Android client part includes two parts: the map view and the communication module. As the map server, GeoServer mainly provides some map services, such as map browsing, query analysis, and thematic maps. The mobile terminal communicates with the server through HTTP, Socket, and so on.

3.1. Key Technologies

3.1.1. Development Technology. Qt is a C++-based cross-platform application development framework. After Qt5.2 version, Qt has a series of libraries, tools, plug-ins, and so on that support Android development. It includes the Qt Creator plug-in and tool set for compiling, packaging, deploying, and debugging Qt applications for the Android platform; it also includes a set of Java class libraries and Qt JNI class libraries for connecting the Java layer and C++ layer on Android. An Android program developed with Qt consists of two parts: one part is the Android part, including Android Manifest, QtApplication.java, QtActivity.java, MinistroService files, and some other resources required by the application, and the other part is the native part, including the Qt library and the cross-compiled dynamic library (.so) file [12–14]. Three-party open-source libraries similar to GDAL raster image processing library, GEOS spatial analysis library, SQLite database, expat parsing XML document, Proj map projection library, and so on are all written in C++, so you need to use Qt Creator to call the Android NDK cross-compilation tool, compile all the C++ libraries into dynamic link library files supported by Android, and then combine with Android in Qt to form a mobile application with rich GIS functions [5].

3.1.2. Mobile Database. GeoPackage is an open data format developed by OGC for storing geographic information. Its storage form is independent of the platform and is implemented internally using SQLite database. GeoPackage supports a maximum storage of 140TB, which can store vector data and raster tile data such as remote sensing image pyramids, map tile matrix sets, and attribute data. GeoPackages' vector data model uses points, lines, and polygons to describe geographic phenomena. A point is a single position in space, with X and Y coordinates, and can also have Z and M values; a curve is the basic type of all one-dimensional geometric types, it has a length but no area, and a line connects two or more in space A curve with a single point; a multisurface is the basic type of all two-dimensional geometric types. It has an area, and a polygon is composed of closed lines. The vector feature data are stored in one table, the attribute data related to the feature are stored in another table, and the graphics and attributes are connected by ID. In the raster data model, regular grid cells are used to describe the surface of the earth. Each cell contains a value that represents a certain category and can also store the attributes of the category. The position of the cell is determined by the coordinates of the top left corner vertex. The attribute information is stored in the user-defined attribute table in GeoPackage. These tables may contain attributes such as IDs or geolocation addresses that allow them to be associated with rows in other attribute tables, feature tables, or tile tables [6].

4. Implementation Technology for Task-Based Geological Disaster Survey APP

4.1. Architecture. The open-source-based mobile GIS platform architecture consists of three parts: data layer, service layer, and application layer. The server uses GeoServer, the mobile database uses GeoPackage, the server database uses PosrgreSQL, the desktop client uses QGIS, and the mobile client uses QFiled. With the development of cloud computing, ordinary server can no longer meet the demand, so the latest mobile GIS platform architecture server should deploy the GIS platform on the "cloud" infrastructure in order to provide more extensive and efficient services. The overall architecture diagram of the proposed open-source framework is shown in Figure 1.

4.2. Task-Based Project Configuration. The open-source framework allows users to configure the survey interface and survey content according to their needs before geological disaster surveys and can determine the completion of tasks through statistics. The survey content and survey area assigned to each person in the task-based field geological disaster survey are different, so in addition to the difference in the task name, there will be special text descriptions to describe the overall overview and targeted content of the

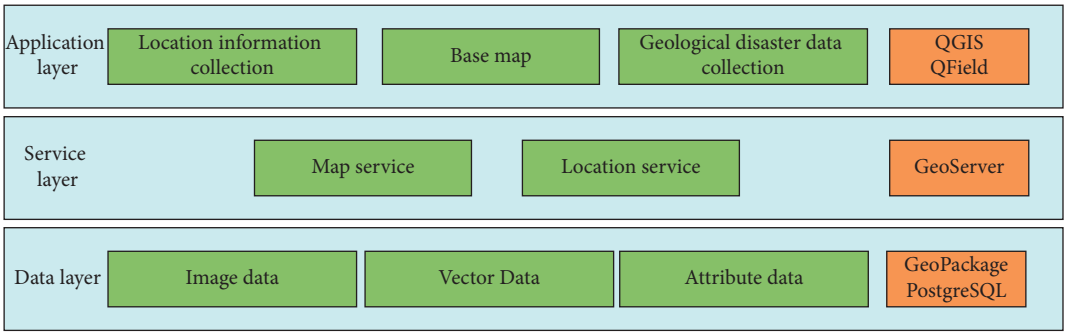

Figure 1: Overall architecture diagram of the proposed open-source framework.

task, help users understand the content and purpose of the task more quickly, and carry out their work more effectively.

In the field survey, there are not only textual surveys but also on-site photographs to record the disaster scene. Photos are associated with their corresponding elements as attributes. The corresponding photos can be found according to the path of the photos in the attribute table, and corresponding descriptions can be added to the photos, such as the latitude and longitude when the photo was taken, and the shooting time.

A disaster location requires not only the recording of disaster points to be read but also the outline of the disaster area elements. In order to avoid missing data or duplication, the two tables are associated, and the data are collected separately and finally integrated into one table. The two tables are related through the ID field. The ID field value is used to uniquely identify a record in the table and cannot be empty.

After the task is completed, it is necessary to check the quantity and quality of the task completed. Therefore, when the project is deployed, set constraints on special fields to limit the scope of the collected data or use function statistics to collect the number of disasters, the area, and the length of the collection trajectory.

4.3. System Function. According to the business requirements of the field survey of geological disasters, the main functional modules of the system design include basic map, data collection, and GPS positioning. The functional structure diagram of the system is shown in Figure 2:

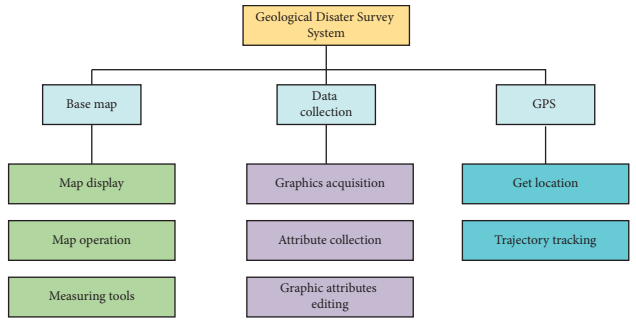

Figure 2: The functional structure diagram of the geological disaster survey system.

4.3.1. Base Map. QgsMapCanvas is a class used to display all GIS data types on the canvas. QgsMapTool is the base class of all map tools. For example, the map pan and zoom functions are implemented based on the QgsMapToolTouch class and the QgsMapToolZoom class. The Qgsgeometry is a container of geometric objects. The actual geometric objects are stored in the container as QgsAbstractGeometry, which can be accessed through the *get()* method or set using the *set()* method, allowing access to the underlying primitive geometric objects, such as points, lines, polygons, curves, or others Geometry subclass. QgsDistanceArea can perform measurement on an existing QgsGeometry object, use *measure()* with QgsGeometry as a parameter, and calculate the distance or area. QgsMapLayer is the base class of all map layer types.

4.3.2. Data Collection. QgsMapToolEdite and QgsMapToolIdentify inherit from QgsMapTool. QgsMapToolEdite is the base class of map tools used to edit vector geometry, and QgsMapToolIdentify is used to identify map tools in layers. The QgsFeature class encapsulates a single feature, including its id, geometry, and field/value attribute list.

4.3.3. GPS Positioning. The current location can be obtained through the GPS module embedded in the smart device. The QgsGPSConnection class is used to connect to the GPS device, and QgsGPSConnection:currentGPSInformation() can return the current GPS information, such as longitude and latitude.

4.3.4. Machine Learning. We use LSTM approach to extract appropriate features for further analysis on the collected dataset. First, we collect data and then manipulate it based on data aggregation technique. Figure 3 displays the IoT sensor data processing, fusion, and analysis layers' basic architecture. Various IoT sensors that can measure physical surroundings and capture real-time environment changes make up the IoT sensor data layer. Temperature, pressure, humidity, level, accelerometer, gas, gyroscopes, motion sensors, image, optical sensors, Radiofrequency Identifier (RFID) sensors, and Infrared (IR) sensors are some of the most prevalent IoT sensors. The microprocessing unit,

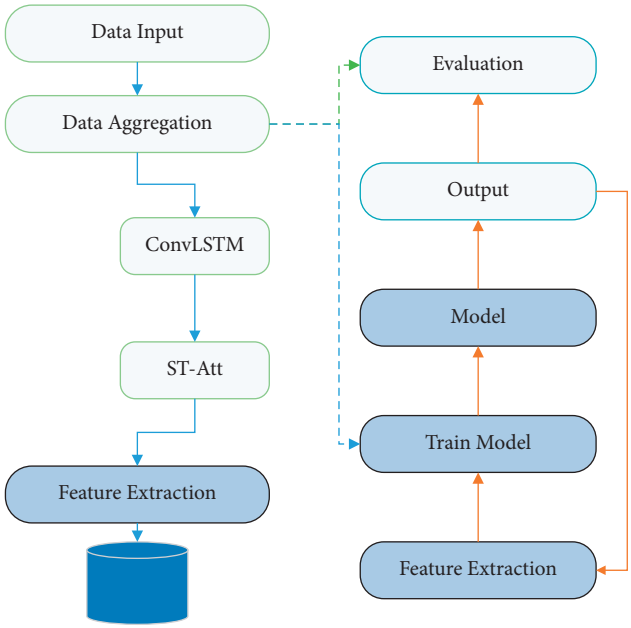

Figure 3: The proposed model.

storage unit, control unit, power system, and wireless communication interfaces are the most common IoT sensors.

5. The Proposed Model

5.1. Study Area. The study area is the Xishan mining area in Taiyuan City, Shanxi Province, which is geographically located at 112°14′ ~ 112°32′east longitudes and 37°46′ ~ 37°57′north latitudes. The study area is shown in Figure 4. The mining area is mostly in the middle mountain area, which is roughly divided into high mountain area, middle mountain area, hilly area, and alluvial plain area. Due to long-term coal mining activities in the area, many geological disasters have occurred, such as landslides, ground fissures, mudslides, and collapses. In recent years, the Xishan mining area has been continuously transformed, and the coal mining subsidence area and the ecology of the mining area have been treated, and it has also developed into a tourist base. Although geological disasters in mining areas are subject to certain control, new geological disasters will also appear at the same time. Therefore, it is necessary to conduct geological disaster surveys in a timely manner to determine the status of disasters and protect the transformation results of mining areas. The proposed framework can be easily used for the above purpose.

5.2. Function. According to the business requirements of the field survey of geological disasters, the main functional modules of the system design include basic maps, data collection, and GPS positioning.

5.2.1. Base Map. Mainly the visualization and operation of the map are realized. Map operation buttons or touch functions are used to zoom in, zoom out, and pan the map.

Figure 4: Remote sensing image of the study area.

The measurement tool module includes length and area measurement.

5.2.2. Data Collection. The data types that need to be collected in field investigation tasks are divided into three types: point, line, and surface. In the survey, geometric figures can be drawn through screen drawing or GPS positioning, and corresponding attribute data and multimedia can be added after drawing. In addition to adding elements, data collection also includes element deletion and element editing, which can modify the attribute data of geometric elements, edit nodes of line and area elements, and divide area elements. We also use an aggregation approach, as discussed in next section, to study the impact of deletion from the original data. However, attributes are kept unchanged.

5.2.3. Data Aggregation Algorithm. The data collected through various sensors overlapping similar regions may consist of redundant data. A method is required to store only useful data. In the IoT environment, many sensors are used to collect data, and the coverage region is likely to overlap. Duplicate, useless data may be collected as a result of this overlap, putting a burden on the storage medium and subsequently on the machine learning model. In addition to lengthening latencies, time spent on training and, as a result, predicting can be wasted. As a result, the vast amount of data gathered may contain duplicate values, producing network congestion and impairing the prediction process. As a result, duplicate data must be removed using a procedure. If $D_{\min}/D_{\max}$ is less than the predefined threshold value, the data are redundant, and only one of the i or j values is kept, while the other is destroyed. If $D_{\min}/D_{\max}$ is greater than or equal to the threshold value, then the data are dissimilar; consequently, both data points must be taken into account during the assessment process [15, 16].

$$D_{\min} = \sqrt{\left(\min_j - \min_i\right)^2}, \forall i, j = 1...n,$$
$$D_{\max} = \sqrt{\left(\max_j - \max_i\right)^2}, \forall i, j = 1...n. \quad (1)$$

Aggregation is most effective during the data collecting stage. Algorithm 1 illustrates the aggregation procedures. For each data point, we compute the Euclidean distance from Step 1 to Step 4. In Steps 5–7, we compare its value to a predefined threshold value; if the conditions are met, the

Input: Raw data in form of data set-I, that is, M_i and M_j
Output: Refined data in form of data set-II, that is, M_i' and M_j'
(1) **repeat**
(2) //Repeat the following steps for each element $i \in M_j$ where $j > i$;
(3) $E_d(M_i, M_j) = \sqrt{(m_{ik} - \min_{jk})^2}$ where $m_{ik} \in M_i$ and $m_{jk} \in M_j$
(4) **if** $E_d(M_i, M_j) \leq t_d$ **then**
(5) Remove either M_i or M_j, to form M_i' or M_j'
(6) **end if**
(7) **else**
(8) Do nothing
(9) **end if**
(10) **until** $i \notin M_i$or $j \notin M_j$;

Algorithm 1: The data aggregation technique.

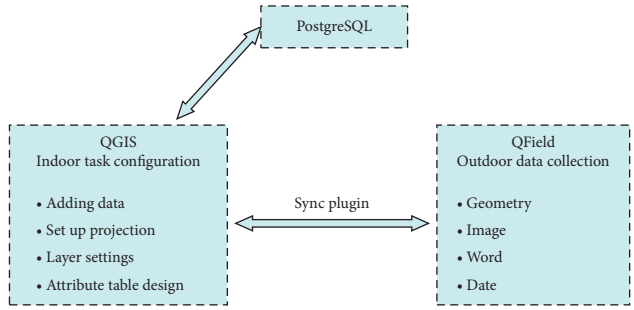

Figure 5: The work flow chart that shows the overall process.

123	0	fid	1.2	15	Landslide gradient		
123	1	Landslide number	1.2	16	Main sliding direction	29	Disaster level
abc	2	Landslide name	t/f	17	Physical delineation	30	Number of threats (person)
abc	3	Sliding type	1.2	18	Front elevation	31	Threatening property (ten thousand y
abc	4	Formation lithology	1.2	19	Trailing edge elevation	32	Risk level
abc	5	Slope structure type	1.2	20	Long	33	Disaster-bearing body survey
abc	6	(Potential) slippery surface type	1.2	21	Width	34	Prevention
abc	7	Macro stability	1.2	22	Average thickness of landslide	35	Type of control
abc	8	Active status	1.2	23	Landslide area	36	Suggestions on prevention and treatr
abc	9	Expansion method	1.2	24	Landslide volume	37	Remote sensing interpretation point
abc	10	Landslide era	abc	25	Scale level	38	Survey point
	11	Landslide time	abc	26	Live photos	39	Mapping point
abc	12	Predisposing factors	123	27	The number of deaths (persons	40	Disaster prevention plan/group monit
abc	13	Landslide shape (planar)	1.2	28	Direct loss (ten thousand yuan)	41	Qualitative risk assessment
abc	14	Landslide shape (section)					

Figure 6: Landslide survey form used in the evaluation.

data point is removed; otherwise, we move on to the next data point. It is important to note that before using the Euclidean distance measure, the data sets must be normalized. To assure the applicability of the aforementioned distance measure, a simplified normalizing function must be applied. In this paper, we employed the normalization strategy as described by the following equation [15, 17]:

$$M_i^{\text{norm}} = \frac{M_i - M_{\min}}{M_{\max} - M_{\min}}, \quad (2)$$

where $M_{\min}$ and $M_{\max}$ are the minimum and maximum values across all data points, respectively, and M_i^{norm} is a normalized value for M_i. For example, if we want to normalize the provided data points in a dataset between 0 and 1, we will use $M_{\min} = 0$ and $M_{\max} = 1$.

5.2.4. GPS Positioning. The GPS module embedded in the smart device can be used to obtain the current position, and it can also be used to track straight lines and polygons and

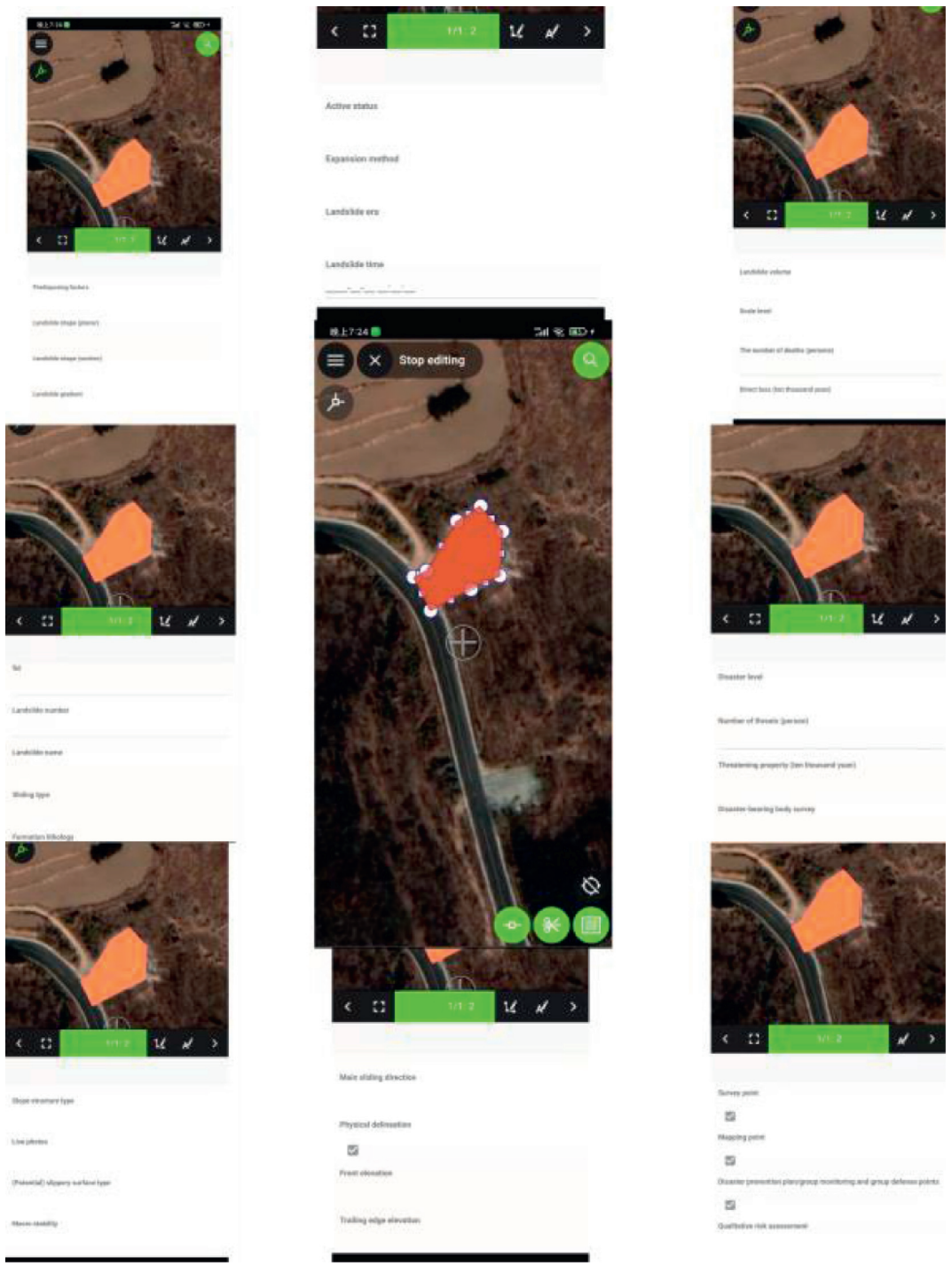

Figure 7: Landslide disaster data collection interface.

record continuous GPS points to achieve track recording by setting the time interval and minimum distance.

5.3. Work Process. The desktop is responsible for the project configuration before the field survey and the data storage and processing after the survey. In QGIS, the image data of the mining area are used as the base map, the vector data of the data collection area are configured, the appropriate map projection is selected, and the layers to be edited are set according to the research problem and the actual situation. Then, the synchronization plug-in is used to assign different projects to different personnel to realize offline tasking of data collection. Import the project to the mobile terminal, open Qfield, and compare the image map with the field to quickly find the boundary of the acquisition area. Select the layer to be edited, complete the data collection by GPS or screen drawing, and then enter the attribute information, and you can directly

edit the nodes and modify the attributes of the existing changed elements. After the task is completed, synchronize the project package back to the desktop, perform attribute inspection and topology inspection in QGIS, and import the data into the PostgreSQL database for storage after the inspection is qualified. The overall process is shown in Figure 5.

5.4. Project Preparation. The scope of the project is determined, the desktop QGIS is used for format conversion, projection settings, and layer settings for the image data, and disaster data and other related data of the research area are addressed. The configured project is packaged and imported into the geological disaster field acquisition system. The technical requirements for geological disaster risk survey evaluation (1 : 50,000) in the technical specifications are referred for the first national comprehensive risk survey of natural disasters, and the six geological disasters survey tables are designed for landslides, collapse, mudslides, ground collapse, ground subsidence, and ground fissures, such as shown in Figure 6.

5.5. Data Collection. Using QField, combined with the packaged project package, the geometric elements and attribute information of geological disasters are collected in the field. The collection process is shown in Figure 7.

5.6. Data Storage. After completing the data collection, save the project and export it to the computer, also import the modified data back to QGIS through the QFieldSync plug-in, and complete the data storage in QGIS or directly store the data on the server of the PostgreSQL/PostGIS database during the project configuration stage, so that the data can be accessed directly through the Internet, and it supports multiperson editing. Others can see the editing content of others in real time. This method also requires that redundancy is maintained while ensuring appropriate methods for updating the dataset. The project package is packaged into the mobile device.

6. Results and Discussion

In this section, we discuss the outcomes of the machine learning technique and data aggregation in terms of training and prediction duration. The results for two approaches, i.e., ARIMA and LSTM are shown in Figures 8 and 9, respectively. This can be seen that both approaches can predict more efficiently when combined with the attention networks. Moreover, with aggregation, the data amount is significantly reduced, therefore, increasing the model training time, with almost comparable accuracy in terms of RMSE and MAPE values [15]. We noted that the attention network reduces the accuracy for ARIMA; however, for LSTM, the accuracy improvement can be as high as 50.19%. For aggregation approach, the accuracy is affected due to the amount of data available for training the model. The impact was observed between 0.58% and 2.83% when data are aggregated as shown in Figure 9.

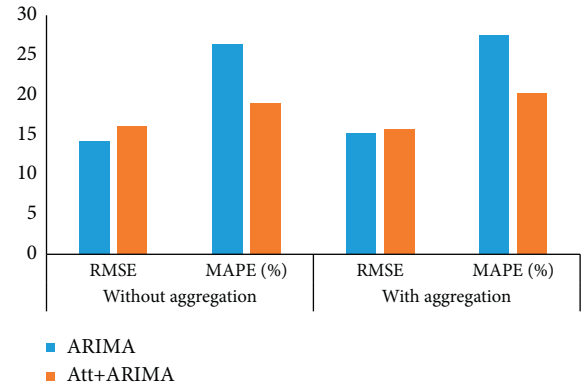

Figure 8: RMSE and MAPE metrics for ARIMA (without and with aggregation approach).

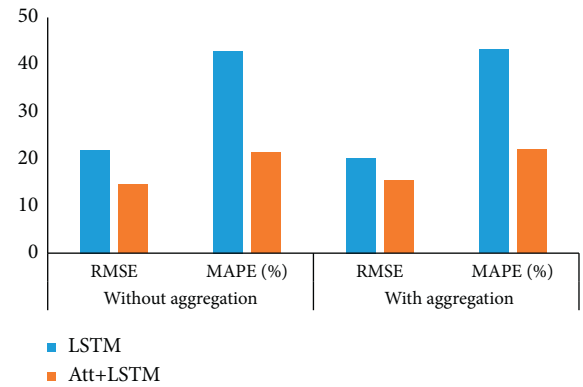

Figure 9: RMSE and MAPE metrics for LSTM (without and with aggregation approach).

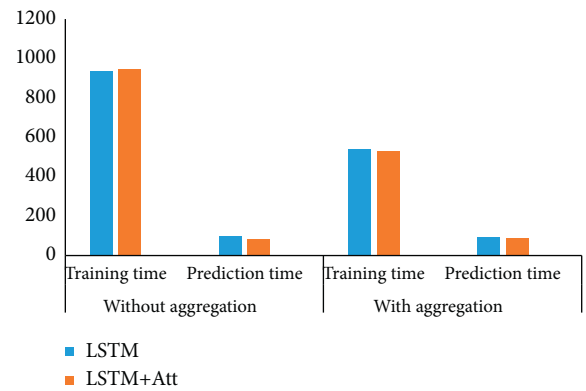

Figure 10: Training and prediction times (seconds).

As shown in Figure 10, the data aggregation method is approximately 42.3–44.09 percent (training times) more efficient than the no aggregation approach. The attention network mechanism is more effective for prediction (~9.08%) rather than training the model. For training the model, the attention network has an additional overhead, and we observed an increase in training durations.

The open-source GIS function is constantly improved and has strong scalability. Developers can add different

modules according to their needs. In the future, open-source software will definitely provide more reliable services and help for the government, enterprises, and individuals. Independent bottom-level development is time-consuming and labor-intensive, requires high developer capabilities, and is difficult to guarantee quality [18].

7. Conclusions and Future Work

The secondary development platform provided by GIS vendors simplifies the development process, but it is expensive. The free map SDK provided by map service providers is easy to develop, but it has few professional functions and is mainly used to serve the lives of the general public. In this paper, we proposed a task-based geological disaster survey APP. The APP has a geographic information system interface. Users can quickly obtain information, reduce the chance of error, support users to publish their own data, and can be extended for different applications. The data collection work of the industry can also realize the simultaneous investigation of multiple people across regions. The practical application in the Xishan mining area of Taiyuan proves that the framework can complete the collection and storage of geological disaster data, which has certain practical significance.

In the future, we plan to implement more complex machine learning methods such as neural networks, deep neural networks, and convolutional neural networks. Moreover, we will use a different and more robust aggregation and fusion methods to verify the validity of the proposed model. More features of the data might be used to study the impact of data deletion and changing over the obtained results. Besides, transmission delays when the data are stored over the cloud and network edges will also be studied in our future work. These delays will have a significant impact on the application performance and, therefore, the results. Further research will be carried out to investigate how the framework should be implemented and used in real-life [19].

Data Availability

The raw/processed data required to reproduce these findings cannot be shared at this time as the data also form part of an ongoing study.

Conflicts of Interest

The authors declare that they have no conflicts of interest.

References

[1] B. Kong, *Design and Implementation of Intelligent Inspection System Based on mobile GIS [D]*, Shandong University of Science and Technology, Qingdao, China, 2017.

[2] Y. Xie and L. Dai, "Research and implementation of offline land resources "a map" system based on ArcGIS for Android and Spatialite," *Value Engineering*, vol. 39, no. 05, pp. 224–226, 2020.

[3] D. A. Sansare and S. Y. Mhaske, "Natural hazard assessment and mapping using remote sensing and QGIS tools for Mumbai city, India," *Natural Hazards*, vol. 100, no. 3, pp. 1117–1136, 2020.

[4] F. Yu, Y. Xia, K. Yang, and Y. Zhang, "Application research of mobile GIS technology in the field of geological disaster data collection," *Chinese Journal of Geological Hazard and Control*, vol. 17, no. 02, pp. 102–106, 2006.

[5] Z. Wang, M. Xie, C. Dong, M. Hu, and X. Liu, "Research on three-dimensional auxiliary system for field survey of geological hazards based on 3S technology," *Engineering Investigation*, vol. 39, no. 12, pp. 42–45+62, 2011.

[6] W. Jiang, *Design and Implementation of Embedded GIS for Land Survey Based on Android Platform*, Southeast University, Nanjing, China, 2013.

[7] Yu Zhu, *Research and Construction of a Field Collection System for forest Resource Data Based on Android [D]*, Beijing Forestry University, Beijing, China, 2014.

[8] J. Zhang, *Design and Verification System for Returning farmland to forest Based on mobile GIS [D]*, Beijing Forestry University, Beijing, China, 2013.

[9] L. Yuan, *Design and Implementation of Agricultural Information Collection System Based on mobile GIS [D]*, Hubei University, Wuhan, China, 2017.

[10] L. Huang, *Design and Implementation of Field Data Acquisition System for Hydrogeology and Water Resources Survey Based on Geological Cloud [D]*, Chinese Academy of Geological Sciences, Beijing, China, 2019.

[11] S. Partha and M. Naman, "A smartphone-based application for "localized" GIS data aggregation in absence of internet," in *Proceedings of the 20th International Conference on Distributed Computing and Networking*, Bangalore, India, January 2019.

[12] J. Smołka, B. Matacz, E. Łukasik, and M. Skublewska Paszkowska, "Performance analysis of mobile applications developed with different programming tools," *MATEC Web of Conferences*, vol. 252, no. 4, Article ID 05022, 2019.

[13] B. Wang, *Development and Research of mobile GIS Application Based on Qt for Android [D]*, Zhengzhou University., Zhengzhou, China, 2016.

[14] M. Lettner, M. Tschernuth, and R. Mayrhofer, "Mobile platform architecture review: android, iPhone, Qt," in *Proceedings of the International Conference on Computer Aided Systems Theory*, February 2011.

[15] A. Ali, Y. Zhu, and M. Zakarya, *A Data Aggregation Based Approach to Exploit Dynamic Spatio-Temporal Correlations for Citywide Crowd Fows Prediction in Fog Computing*, pp. 1–33, Multimedia Tools and Applications, Berlin, Germany, 2021.

[16] A. Ali, Y. Zhu, and M. Zakarya, "Exploiting dynamic spatio-temporal correlations for citywide traffic flow prediction using attention based neural networks," *Information Sciences*, vol. 577, pp. 852–870, 2021.

[17] X. Lin and J. Zhang, "Object-based morphological building index for building extraction from high Resolution. Remote sensing imagery," *Acta Geodaetica et Cartographica Sinica*, vol. 46, no. 6, pp. 724–733, 2017.

[18] V Badrinarayanan, A Kendall, and R. Cipolla, "SegNet: a deep convolutional encoder-decoder architecture for image segmentation," *IEEE Transactions on Pattern Analysis and Machine Intelligence*, vol. 39, no. 12, pp. 2481–2495, 2017.

[19] M. Chen, J. Wu, L. Liu et al., "DR-net: an improved network for building extraction from high resolution remote sensing image," *Remote Sensing*, vol. 13, no. 2, p. 294, 2021.

Hindawi
Scientific Programming
Volume 2022, Article ID 3291127, 7 pages
https://doi.org/10.1155/2022/3291127

Research Article

Intelligent Algorithm Risk and Prevention Mechanism of College Students' Ideology under the Background of Artificial Intelligence

Huang You Yu

College of Artificial Intelligence, Zhejiang Collage of Security Technology, Wenzhou 325016, Zhejiang, China

Correspondence should be addressed to Huang You Yu; huangyouyu24@163.com

Received 12 January 2022; Accepted 26 January 2022; Published 23 February 2022

Academic Editor: Muhammad Usman

With the rapid development of economic, the artificial intelligence network ideology of mobile Internet of things has become the core part of network security. It is also the most direct embodiment of a national ideology in the network era, and the risk prevention of ideology in colleges and universities is an important part of security work. The values, diversity, and related ideological and moral changes of college students' ideology are facing complex and severe challenges. In the age of mobile Internet of things, it is especially vital to strengthen and improve the responsibility of ideological values construction of the college students and constantly develop the risk operation and prevention management mechanism of college Internet of things.

1. Introduction

With the rapid development of mobile Internet information technology, especially the upgrading of network technology in the "big data" cyberspace, the expansion of media, and the growth of Internet users, Internet technology has become an important modern media means. Under the background that people gradually rely on Internet information, netizens are vulnerable to some wrong values, resulting in the interference and penetration of various foreign network consciousnesses on Netizens' thoughts, which are more and more difficult to control and prevent.

Network ideology is a type of network social practice that is unique. It not only follows the rules of general philosophy but also possesses a relatively unique feature of network operation. Colleges and universities play a key role in the growth of national successors, as well as in the formation of network ideology. We should focus on increasing the immune function of college students' ideological infiltration in the process of guiding and educating them. Li Bowen et al. pointed out in the analysis of the problems and countermeasures of network ideology education in colleges and universities that it should strengthen the education of network ideology, adopt effective strategies for these problems, and strive to fundamentally enhance the recognition of college students' mainstream ideology [1]. Shao Xuping said in the dialogue on the proper direction of ideological education in colleges and universities in the Internet era that the change of network media has led to the change of human society and the change of international political and economic order, and ideological education in colleges and universities has also been faced with unprecedented challenges [2]. Ning Xiaoke et al. said in their systematic analysis of the ideological security governance mechanism of China's colleges and universities in the era of big data that building the ideological security governance mechanism of China's colleges and universities by using big data technology is a systematic project, a practical need to stand firmly at the forefront of ideological work, and an important way to enhance the ideological security of colleges and universities. It is also an inevitable requirement for the innovation of ideological security governance methods in colleges and universities [3]. Ni Li said that, as an accurate paradigm of information dissemination, the technical essence of the algorithm and its hidden algorithm power determine its ideological attribute of accurate control. In the face of the new pattern of transmission power and the algorithm risk of ideology caused by the algorithm, colleges and universities should build a prevention mechanism, from passive control to active avoidance and preprevention [4].

This paper analyzes and discusses the application of the algorithm risk and prevention mechanism of ideology in the mobile Internet era on the University platform and believes that the mobile Internet era will have an increasing impact on the ideology of college students. Developing an algorithm risk and preventive mechanism for college network ideology can help to protect students' network information from hidden threats on the school intranet. Strict control of the educational ideology in colleges and universities is of key importance.

2. Main Module of Machine Learning Based on Fuzzy Neural Network

To analyze the application of algorithmic, the risk and prevention mechanism of university ideology in the mobile Internet era, the machine learning concept of fuzzy neural network is introduced to endow its robot ontology learning perception. Fuzzy neural network technology is a network technology integrating the strong structural knowledge expression ability of fuzzy logic reasoning and the autonomous learning ability of neural network. It is the result of the organic combination of fuzzy logic reasoning and neural network application [5]. By altering the connection weight between network neurons, machine learning of fuzzy neural networks may successfully reproduce human learning. It possesses self-adaptive, self-learning, and self-organization capabilities. Selecting appropriate fuzzy neural network modules and corresponding function formulas can reduce the number of errors between networks. Using the fusion technology of fuzzy system, the capture and evaluation scheme of ideological information in colleges and universities based on fuzzy neural network is analyzed, as shown in Figure 1:

In Figure 1, the student-related interactive information of the university network platform system can be directly praised, browsed, forwarded, and replied by the students. The forwarded and replied to information data will be uniformly entered into the source information base. The information of the source information base can enter machine learning through the extranet information or directly into machine learning after correlation analysis. The linear fuzzy processing provides relevant information to machine learning module for elevation. In linear fuzzy processing, the information is weighted to claim the results. The point praise and browsing behavior data of students' interactive information can be directly entered into the machine learning module, and the required evaluation results can be obtained after linear fuzzy processing.

In the current study, the polynomial depth iterative regression along with the defuzzification method of linear fuzzy network is selected. The polynomial depth iterative regression delivered connection between independent and dependent values, while the defuzzification method of linear fuzzy network provides quantifiable values to obtain results [6, 7].

Machine learning module based on sixth-order polynomial depth iterative regression basis function is as follows:

$$y = \sum_{i=1}^{n} \sum_{j=0}^{5} A_j x_i^j, \tag{1}$$

where A_j is the coefficient to be regressed of the jth order polynomial. That is, each node in the formula contains 6 coefficients to be regressed from A_0 to A_5, and j is the polynomial order.

Defuzzification module based on linear fuzziness is

$$F = S(t_n) \cdot S\left(\frac{t_n - t_{n-1}}{t_{n-1}}\right), \tag{2}$$

where $S\{t_{n'}\}$ represents the real-time value and $S\{t_n - t_{n-1}/t_{n-1}\}$ represents the difference ratio. The linear fuzzy matrix is input to the single-layer binarization, and the output result on a [0, 1] interval is output: [0.9,1.0] is red; (0.8,0.9] is orange; (0.7,0.8] is yellow; (0.6,0.7] is blue; [0.0,0.6] is no warning.

3. Division of Data Sources and Calculation of Time-Domain Integral of Results

The campus is a reduced version of a social group, with the interweaving of various interpersonal relationships. In the era of Internet mobile communication, the students' way of thinking has changed and got advance now, which dominates the trend of the younger generation.

Short videos, We Media, and school intranet have become the entertainment methods of school students. While recording their life clues, they also expose their personal information and daily path to software app. The more personal information resources are collected, the easier it is to define the individual. Furthermore, different software systems share the user's personal information. After image and sound extraction, face recognition, voice communication system recognition, landmark recognition, key background music recognition, and personal data will be basically formed [8, 9].

The legitimacy of data capture is agreed to avoid capturing nonpublic information and encourage the opening of semipublic information. In recent years, more and more system software obtains the approximate geographical location of users by sharing users, resulting in the violation of users' privacy by bad apps, as shown in Figure 2.

The new key point recognition process of image information and sound uses the spatial convolution algorithm, and its basis function is shown in (3).

In order to achieve the above image processing objectives, the spatial convolution basis function is applied:

$$y = \int_{-\infty}^{+\infty} g(x) j(a - x) dx, \tag{3}$$

where *g(x)* is the original image, *j(a-x)* is the convolution kernel, x is the traversal variable, a is the auxiliary positioning variable, and y is the output value of neural network.

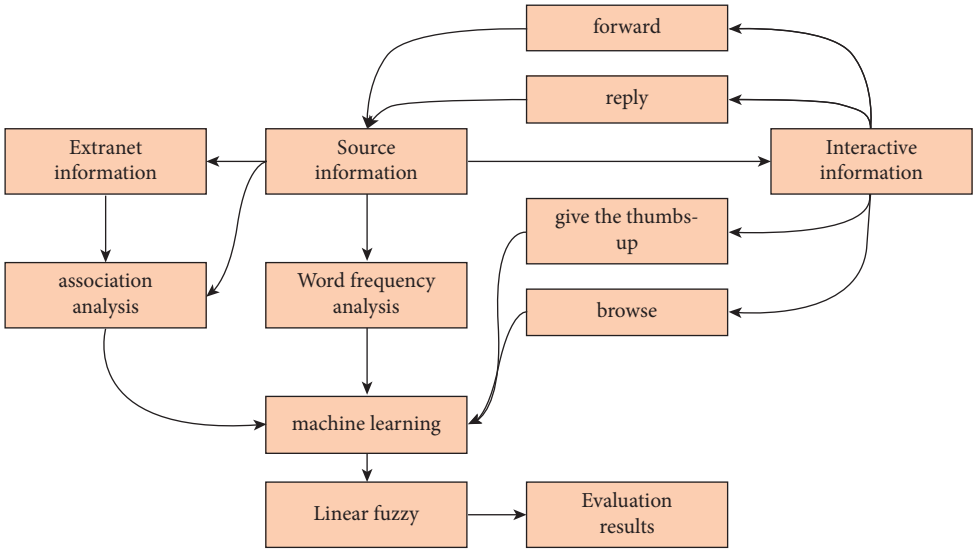

Figure 1: Capture and evaluation scheme of ideological information in colleges and universities.

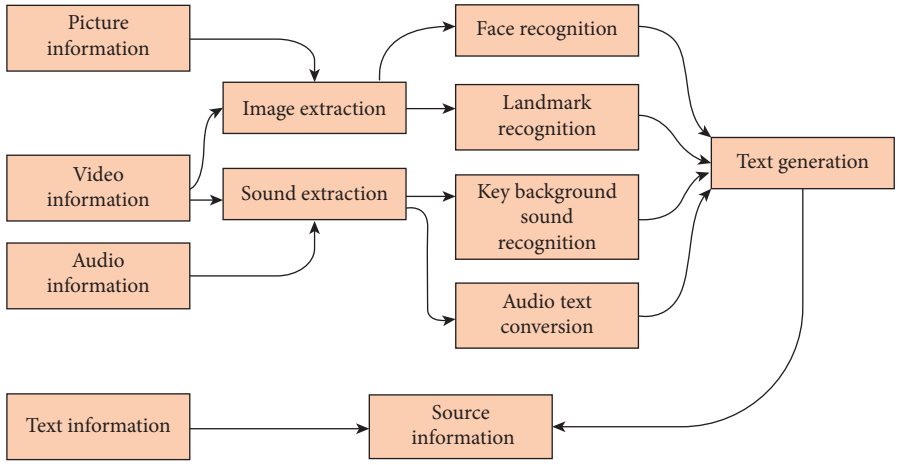

Figure 2: Data preparation process of data source.

4. Data Association Analysis Driven by News Fusion Technology

Hierarchical one to many data fission association: each information corresponds to multiple forwarding, likes, collections, browsing, and other operations. It focuses on the forwarding action of information and tracks all associated operations in the forwarding process.

For capturing and securing information of strong contacts and weak contacts, the spatial propagation clustering method signifies each node as the linear composition of other nodes. For this purpose, it takes the global linearity of the data and does the random extraction of multiple tuples from the captured data as the initial centers of multiple clusters. Then, the distance between other data and these initial centers is calculated by it. Each tuple is classified into the nearest group, to go through the distribution of clustering groups.

AP algorithm takes all nodes as a potential cluster center, mainly uses the similarity between two nodes in the dataset for iterative calculation, and finds the optimal similar cluster center through the propagation between nodes. The similarity is expressed as the negative number of the square of the Euclidean distance between two nodes. The formula of the similarity matrix between input nodes is as follows:

$$S(i, j) = -\left\| x_i - x_j \right\|. \tag{4}$$

In the AP algorithm, the center point $P = \text{median}(s)$ needs to be confirmed, which is used to refer to the value of the offset center. It defaults to the average value of the similarity matrix. The algorithm adds A (Availability) algorithm and R (responsibility) algorithm to the calculation process. The data in the two matrices are superimposed and updated continuously in the iterative calculation process.

Among them, $A = (a(i,j))_{max}, a(i,j)$ is the information value sent from node j to node i, which is defined as the optimization degree of node i selecting node j as the cluster center; $R = (r(i,j))_{max,} r(i,j)$ is the information value sent by node i to node j, which is defined as the optimization degree of node i selecting node j as the cluster center. The iterative formulas of input attribution matrix and attraction matrix are as follows:

$$\begin{aligned} r(i,k) &= s(i,k) - \max\{a(i,j) + s(i,j)\} j \in \{\{1,2,...,N | j \neq k\}\}, \\ r(k,k) &= p(k) - \max\{a(k,j) + s(k,j)\} j \in \{\{1,2,...,N | j \neq k\}\}, \\ &\begin{cases} a(i,k) = \min\left\{o, r(k,k) + \sum\{\max\{o, r(j,k)\}\}\right\} \\ j \in \{1,2,...N \mathrm{I} j \neq i, j \neq k\} \end{cases}, \\ a(k,k) &= \sum\{\max\{o, r(j,k)\}\} j \in \{\{1,2,...,N | j \neq k\}. \end{aligned} \tag{5}$$

In order to prevent drift, a damping factor is added to the matrix of attribute similarity λ. To increase the stability of the algorithm, the input formula is as follows:

$$\begin{aligned} r(i,k)^{t+1} &= \lambda . r(i,k)^{t} + (1-\lambda) . r(i,k)^{t-1}, \\ a(i,k)^{t+1} &= \lambda . a(i,k)^{t} + (1-\lambda) . a(i,k)^{t-1}. \end{aligned} \tag{6}$$

According to the iterative calculation method of the above formula, we calculate the matrix of attribution and attraction to maximize the clustering objective function. The clustering function is as follows:

$$\mathrm{S}(\mathrm{C}) = \sum_{i=1}^{N} s(i, c_i) + \sum_{k=1}^{N} \delta_k(C), \tag{7}$$

where c_i is the cluster center point of node i, C is composed of c_i is a vector consisting of i, i is 1, 2, N (n is the number of nodes), and S(C) is the sum of the similarity of all nodes to their respective cluster centers. The input formula of $\delta_k(C)$ is as follows:

$$\delta_k(C) = \begin{cases} -\infty, C_k \neq kAn\ d\exists i, C_i = k, \\ 0, \quad other. \end{cases} \tag{8}$$

This formula is used as the constraint term of consistency. If there is a node i, select k as the central point of its clustering, that is, $C_i = k$ is established, node k must choose itself as the cluster center, that is, $C_\lambda = k$. Otherwise, the value of the function is -∞ so that node i no longer selects k as its own clustering center in the next iteration.

After iteration, the cluster center point is selected again by calculating the value of $A + R$. When $(r(k,k) + a(k,k)) > 0$, node k becomes the cluster center point. The formula of cluster center point C_i in each node is as follows:

$$c_i = arg \max_k \{a(i,j) + r(i,k)\}. \tag{9}$$

The expression of the formula selects the cluster center with the largest sum of attribution and attraction for each node as its own cluster center.

5. Verification Results of Educational Practice

From 2018, it will be deployed to guide college students' ability to control the algorithm because it is the main link to deal with the risk of college ideological algorithm; cultivate college students' ability and literacy to use the algorithm, and the algorithm will help improve college ideological education and give play to the ability to guide college students' ideas and gather ideological consensus [10]. The necessity and results of the risk and prevention mechanism of the algorithm are verified from three aspects: students' examination results, the effect of discipline management, and students' employment.

5.1. Comparison of Students' Test Scores. Statistical analysis is made on the examination situation of students from 2017 to 2021, that is, from the aspects of pass rate, excellent rate, achievement improvement rate, and teachers' teaching evaluation, so as to verify the effectiveness of this research algorithm.

In Table 1, since the implementation of the algorithmic risk and prevention mechanism of ideology in Colleges and universities in 2018, the passing rate, excellence rate and achievement improvement rate of students have increased year by year, and the satisfaction with teachers' teaching evaluation has also increased year by year, which shows that with the increase of implementation time, students' examination scores have also improved, which are positively correlated.

In order to make the data in Table 1 look more simple and clear, we make broken line, as shown in Figure 3.

In Figure 3, it can be clearly seen that the passing rate and excellent rate of students increase with the increase of years; especially, when the ideological algorithm risk and prevention mechanism of the study is used in 2018, the growth rate is the highest.

5.2. Comparison of the Effect of Student Discipline Management. The discipline management of students in colleges and universities is a very important link. College life is relatively loose. If there is no restriction, it is easy to be affected by the external environment, resulting in the neglect of studies. The algorithm helps to improve ideological education in colleges and universities, helps schools to restrict and manage themselves, and makes effective use of time to learn professional knowledge.

In Table 2, according to the data from 2017 to 2021, when the algorithm was not deployed and implemented in 2017, students' discipline was poor, and there were many phenomena such as missing classes, exams, and being late. However, the use of the algorithm in 2018 enhanced students' sense of identity with the mainstream ideology and made students more self-discipline and discipline. Therefore, since the application of the algorithm in 2018, students' enthusiasm for class has increased, so the late rate and absence rate have decreased year by year. At the same time, the number of people who abide by the examination discipline has increased, so the absence rate and cheating rate have also decreased year by year.

Table 1: Comparison of students' test scores.

Year	Pass rate (%)	Excellent rate (%)	Performance improvement rate (%)	Satisfaction with teaching evaluation results (%)
2017	61.35	5.64	16.35	63.57
2018	67.51	7.65	21.84	70.23
2019	80.93	15.67	33.62	85.64
2020	85.25	19.74	39.41	88.62
2021	89.56	23.11	43.83	91.61

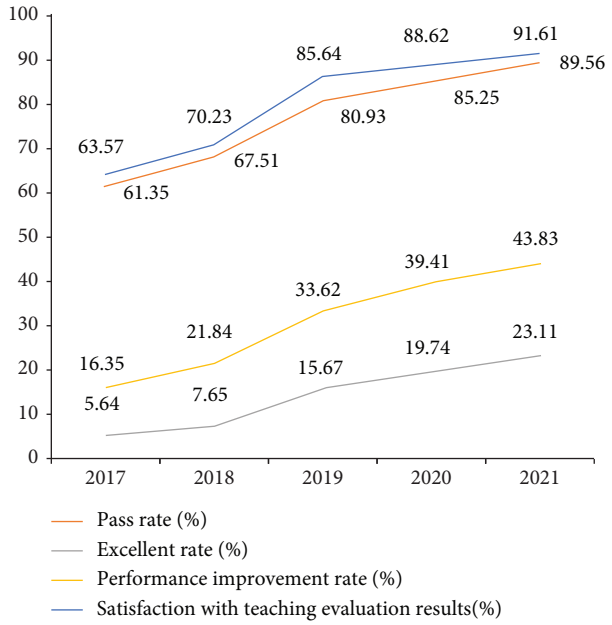

Figure 3: Student performance during 2017–2021.

Table 2: Comparison of the effects of student discipline management.

Year	Absenteeism rate (%)	Late rate (%)	Absence rate (%)	Cheating rate (%)
2017	26.52	24.57	17.94	32.57
2018	21.36	20.81	14.35	26.34
2019	12.68	11.02	8.37	17.58
2020	10.57	7.68	6.41	11.69
2021	6.94	4.23	3.72	7.54

5.3. Comparison of Student Employment. The school is the cradle of distribution of knowledge to students, with the purpose of improving employment. Because the laziness of study causes the inconsistency of professional knowledge and expertise, the employer cannot pass the assessment, and the employment intention is not clear. Through this algorithm, students can be educated and guided to have a correct ideological understanding, to correct their learning attitude and their own habits and management, expand their knowledge in other fields, and improve their comprehensive quality while receiving professional knowledge.

In Table 3, it can be seen from the employment data of students from 2017 to 2021 that when the deployment and implementation of the algorithm were not carried out in 2017, the one-time employment rate of students reached 85.67%, the one-time turnover cycle was also short, only 3.54%, and students' employment satisfaction and enterprises' satisfaction with students were not too high. However, since 2018, various indicators of student employment have improved significantly. The one-time employment rate has increased to 98.41%, and the time of one-time resignation cycle has become longer, reaching 26.87%, which shows that the employment situation is relatively stable.

Figure 4 covers all the verification indicators. It can be seen from Figure 3 that, in 2017, all indicators are not favorable. It improved in 2018 following the deployment and implementation of the design algorithm. A year after the implementation in 2019, all indicators have shown swift improvement demonstrating that the algorithm has a considerable impact on college students' ideological security education.

6. Summary

In contemporary society, the network has become the most important tool for people to communicate and disseminate information resources. In the age of mobile Internet, this

Table 3: Comparison of student employment.

Year	Primary employment rate (%)	One turnover cycle (month)	Employment satisfaction rate (%)	Enterprise satisfaction rate (%)
2017	85.67	3.54	73.91	80.02
2018	88.54	9.31	79.26	84.36
2019	96.57	18.25	88.94	92.21
2020	97.84	23.54	93.97	95.35
2021	98.41	26.87	95.68	97.68

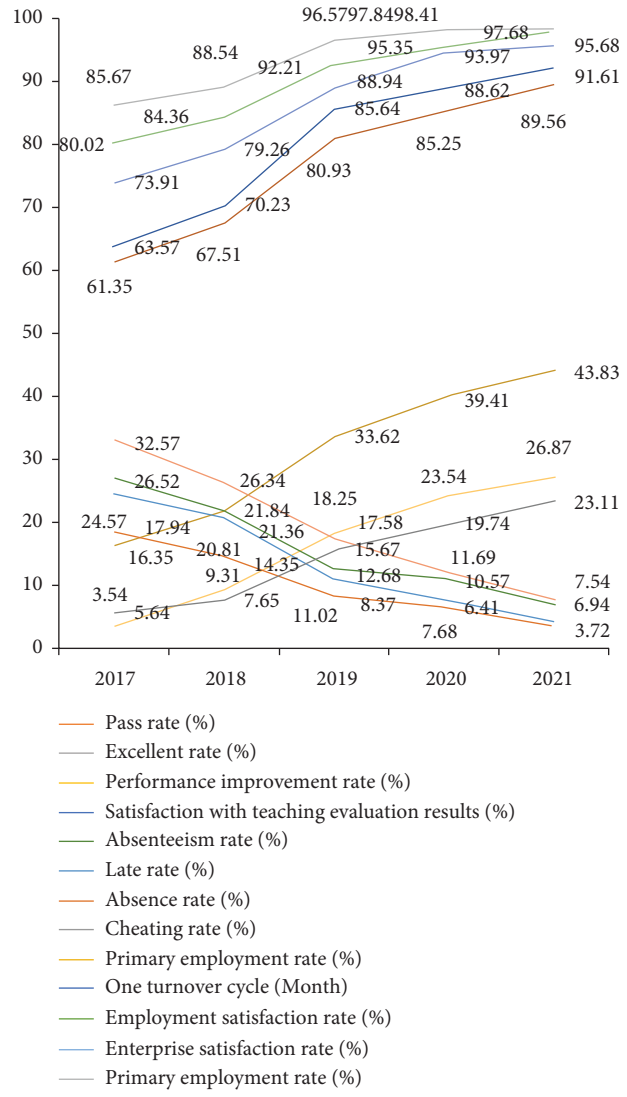

Figure 4: Verification results of educational practice.

study, therefore, designs the algorithm risk and prevention mechanism of college Ideology so that college students can master the discourse power of college ideology security independently making the system of college ideology security discourse power more understandable and reliable. From the perspectives of students' examination outcomes, discipline management effect, and student employment, this study verifies the practicality and superiority of the design. The design can be deeply integrated through the combination of mobile Internet and ideological security education in colleges and universities, which is conducive to the smooth development of ideological security education in colleges and universities, and can be popularized and used among all colleges and universities. However, the research algorithm design will be optimized and improved in the follow-up to better serve the mainstream ideological security education for students in colleges and universities [11].

Data Availability

The data underlying the results presented in the study are available within the article.

Disclosure

The authors confirm that the content of the manuscript has not been published or submitted for publication elsewhere.

Conflicts of Interest

There are no potential conflicts of interest in this study.

Authors' Contributions

All authors have seen the manuscript and approved to submit to the journal for publication.

References

[1] B. Li, Y. Jiang, and H. Zhong, "Problems and Countermeasures of network ideological education in Colleges and universities," *Journal of Heilongjiang Institute of teacher development*, vol. 40, no. 11, pp. 20–22, 2021.

[2] X. Shao and D. Huang, "Dialogue: the inevitable direction of ideological education in colleges and universities in the internet age," *Party building and ideological education in schools*, vol. 36, no. 14, pp. 70–72, 2021.

[3] X. Ning and X. Yang, "Systematic analysis on Ideological Security Governance Mechanism of colleges and universities in China in the era of big data," *Journal of Systems Science*, vol. 1-5, pp. 12–31, 2021.

[4] L. Ni, "Algorithmic risk and prevention mechanism of College Ideology in the era of artificial intelligence," *Journal of Shandong Youth Political College*, vol. 37, no. 04, pp. 18–24, 2021.

[5] X. Zhang, m Zhang, and H. Wang, "Research on maintaining the ideological security of Universities under the perspective of "Internet plus" -- Based on the perspective of spreading the socialist core values," *Jilin education*, vol. 41, no. 35, pp. 64-65, 2020.

[6] d Liu, "Ideological discourse power mechanism in Colleges and Universities: basic connotation, constituent elements and operational value," *Guide to ideological and theoretical education*, vol. 16, no. 12, pp. 118–121, 2018.

[7] B. Ruan, "Restrictive factors and solutions to the implementation of ideological responsibility system in Colleges and universities," *Ideological and theoretical education*, vol. 24, no. 06, pp. 106–111, 2019.
[8] R. Huang, "Tang dengran Practical thinking on the construction of ideological work team in Colleges and universities in the new era," *Party building and ideological education in schools*, vol. 19, no. 13, pp. 9–13, 2019.
[9] J. Liu and Q. Dong, "Discussion on improving the discourse system and mastering the discourse power of ideological work in Colleges and universities," *Research on ideological education*, vol. 35, no. 09, pp. 35–39, 2015.
[10] X. Guo, "Algorithm risk of intelligent communication and its governance path," *National governance*, vol. 32, no. 22, pp. 40–45, 2020.
[11] G. Gao, "Challenges and Countermeasures of network ideological security in Colleges and universities from the perspective of algorithm recommendation," *Journal of Shandong Youth Political College*, vol. 37, no. 05, pp. 48–54, 2021.

Hindawi
Scientific Programming
Volume 2022, Article ID 1603273, 11 pages
https://doi.org/10.1155/2022/1603273

Research Article

U-Net: A Smart Application with Multidimensional Attention Network for Remote Sensing Images

Yao Wang, Jiayuan Kong, and Hesheng Zhang

School of Mining Engineering, Taiyuan University of Technology, Taiyuan 030024, China

Correspondence should be addressed to Hesheng Zhang; zhanghesheng@tyut.edu.cn

Received 7 January 2022; Revised 21 January 2022; Accepted 31 January 2022; Published 21 February 2022

Academic Editor: Muhammad Zakarya

Building segmentation is an important step in urban planning and development. In this work, we propose a new deep learning model, namely Multidimension Attention U-Net (MDAU-Net), to accurately segment building pixels and nonbuilding pixels in remote sensing images. Furthermore, we introduce a novel Multidimension Modified Efficient Channel Attention (MD-MECA) model to enhance the network discriminative ability through considering the interdependence between feature maps. Through deepening the U-Net model to a seven-story structure, the ability to identify the building is enhanced. We apply MD-MECA to the "skip connections" in traditional U-Net, instead of simply copying the feature mapping of the contraction path to the matching extension path, to optimize the feature transfer more efficiently. The obtained results show that our proposed MDAU-Net framework achieves the most advanced performance on publicly available building data sets (i.e. the precision over the Massachusetts buildings data set and WHU data set are 97.04% and 95.68%, respectively). Furthermore, we observed that the proposed framework outperforms several state-of-the-art approaches.

1. Introduction

With the rapid development of China's remote sensing satellite industry, building segmentation in remote sensing image is an important research field in the image interpretation problems. Extracting feature information from remote sensing images is related to urban planning and development. Therefore, timely updating of image information will have an impact on everything that depends on these systems [1]: for example, mapping, disaster analysis, and emergency response. For a long time, the acquisition of feature information in remote sensing images relies on the traditional manual visual interpretation method, which is time consuming and laborious, which restricts the development and application of high-resolution images. Therefore, the use of remote sensing images accurately, quickly, and automatically extraction of target features has attracted widespread attention of many researchers all over the world.

Many researchers have recommended a countless number of programmed building segmentation approaches for remote sensing images. However, the interdependence among the feature channels is often not discussed. Later, by presenting the attention segment, in the context of deep learning-based approaches, the features of dissimilar spaces and channels can be advanced to enrich the essential features and suppress the features that are not significant to the task. U-Net structure is widely used in the field of medical image segmentation. The channel attention mechanism can adjust the characteristic response value of each channel adaptively. The importance of different feature channels obtained by automatic learning is used to enhance the important features and suppress the features that are not important to the segmentation task. This method can be integrated into the U-Net model to improve its performance.

In this work, we introduce a multidimensional channel attention, which uses the average pool and the maximum pool features in multidimensional channel to further improve the performance of building segmentation in remote sensing images. In this study, we propose a new Multidimension Channel Attention Network model, called MDAU-Net, based on deep learning, which has achieved the latest performance in remote sensing image building

segmentation. We demonstrate through experimental results that the proposed MDAU-Net model achieves the best performance on two real data sets. Furthermore, the proposed model greatly reduces the network complexity in computer vision tasks (including image classification, object detection, and instance segmentation) while maintaining the performance. Specifically, we have the following contributions:

(1) Deepen the structure of U-Net, using 7-layer convolution and downsampling module for feature extraction and making full use of different levels of building feature details, so as to achieve the purpose of more fine segmentation of buildings

(2) We apply MD-MECA in order to "skip connections," so as to give weight to each feature map in the shrinking path in the feature transfer step, instead of copying them equally to the corresponding expansive path

(3) Batch normalization [2] is used after the feature stitching of the upsampling part, and Dropblock [3] is used after convolution to solve the over fitting problem in the network training process

(4) On the basis of the above work, we propose MDAU-Net and evaluate it on Massachusetts [4] and WHU data sets [5]

The rest of the paper is organized as follows. In Section 2, we offer an overview of the related work. Section 3 is about the proposed methodology. In Section 4, data sets and evaluation metrics are discussed. Moreover, experimental details are also presented. In Section 5, results are discussed. Moreover, various machine learning techniques are evaluated on the aforementioned data set to study validity of the proposed model. Finally, Section 6 concludes this paper and offers several directions for further research and investigation.

2. Related Work

In the past few decades, researchers have proposed a great number of automatic building segmentation methods for remote sensing images. For example, Zhong et al. [6] used k-means clustering, Kohonen et al. [7] used self-organizing mapping network, and Lin et al. [8] introduced the object-oriented Morphological Building Index (MBI). However, these methods are very dependent on the geometric texture of buildings and cannot adapt to the buildings under different conditions in the image. The sensitivity of their features and spectra is not enough to capture, similar objects are prone to mix and produce adhesion phenomenon, and the robustness is not enough good [9, 10].

Recently, deep learning-based methods have been used for automatic segmentation of buildings in remote sensing images and achieved excellent results. The deep learning method based on convolutional neural networks (CNN) proposed by Krizhevsky et al. [11] is usually used in various computer vision tasks. Long et al. [12] proposed full convolutional networks (FCN), which can classify images at the pixel level. Compared with the FCN structure, the SegNet structure proposed by Badrinalayanan et al. [13] transfers the maximum pooling index to the decoder, which improves the segmentation resolution and saves more storage space. Later, in order to improve the use of feature information in images, Ronneberger et al. [14] proposed the U-Net spanning connection structure, which has been widely used in image segmentation. This structure realizes the fusion of multiscale image information and improves the segmentation performance [15].

Although these deep learning-based methods have achieved significant results, the interdependence between the feature channels is often ignored. Later, by introducing the attention module, the features of different spaces and channels can be refined to enhance the important features and suppress the features that are not important to the task. At present, many researchers have applied attention module to the image extraction and have achieved good results [16, 17, 18].

3. Proposed Methodology

3.1. A.U-Net. U-Net structure was proposed by Ronneberger et al. [14] in May 2015 and was initially widely used in the field of medical image segmentation. As a very classic full convolutional network model, it is widely used in the field of remote sensing image segmentation at present. Its network structure is shown in Figure 1.

U-Net is divided into two parts, the left part is the feature extraction part, also known as the lower sampling part, the right part is the upper sampling part. In the feature extraction part, the deep semantic features of the image are extracted through convolution and pooling [19].

Each process includes the image is transformed into a matrix with the number of channels increased by 64 after two convolutions, and then the maximum pooling operation is carried out to reduce the length and width of the image to half of the original. In accordance with the same process, after four times of subsampling, the image becomes a $32 \times 32 \times 512$ matrix, and after two 3×3 convolution operations, the final feature map is obtained. For the upsampling part, the calculation starts from the information at the bottom of the network. After each 2×2 deconvolution, it is spliced with the downsampling feature map of the same layer, fused with the channel number corresponding to the feature extraction part at the same scale, and then the upsampling is completed once after two 3×3 convolution operations. Through the combination of feature images obtained by feature extraction, information is supplemented to optimize the segmentation results.

3.2. MECA and MD-MECA. Inspired by the recently proposed CAR-UNet (Channel Attention Residual U-Net) [20], Modified Efficient Channel Attention (MECA) module in CAR-UNet was improved. MECA module structure is shown in Figure 2, which greatly reduces the network complexity in image classification, object detection, and instance segmentation while maintaining performance. In

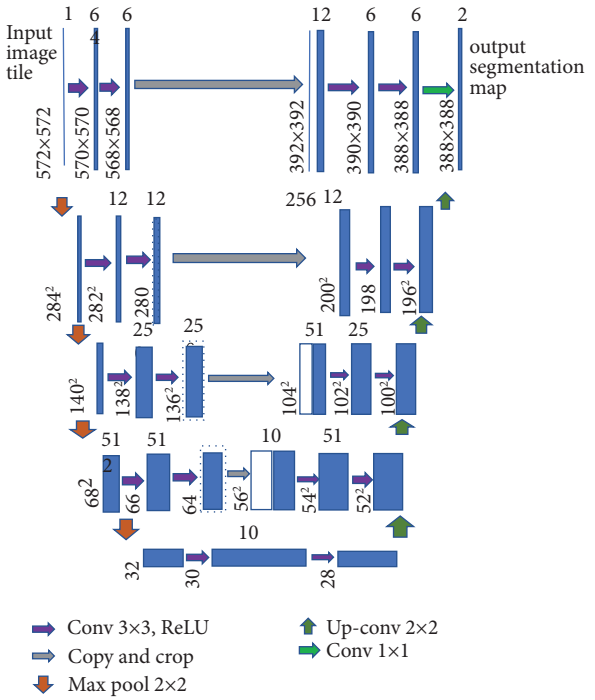

Figure 1: The classical U-Net network architecture.

this paper, the optimized module is named MD-MECA (Multidimension Modified Efficient Channel Attention). By adding MD-MECA to the encoding transfer features of U-Net architecture to the decoding module, compared with the original U-Net, the structure optimized the feature graph during the transmission of the feature graph, supervised the information of the feature graph of the encoding part in different ways, and then passed it to the decoding part for information supplement.

Channel attention (CA) was first used as a Squeeze-and-Excitation Networks for classification, which modeling by using the relationship between the channels [21]. It can adjust the characteristic response value of each channel adaptively. The importance of different feature channels obtained by automatic learning is used to enhance the important features and suppress the features that are not important to the segmentation task. And recent works showed that the channel attention mechanism has great potential in improving the performance of deep convolutional neural networks (CNN). Guo et al. [20] proposed a CAR-Unet (Channel Attention Residual U-net) network model for retinal vascular segmentation and achieved good results. The MECA module in CAR-Unet network model is based on an effective channel attention ECA module proposed by Wang et al. [22] and adopts both average pooling layer and maximum pooling layer to obtain more detailed channel attention, so as to better collect spatial information.

MECA module uses convolution to avoid dimensionality reduction in SE network blocks, thus greatly reducing the complexity of the model while maintaining superior performance. The MECA module is an embedding channel monitoring module, which extracts global features by using different global pooling calculations: average pooling can extract spatial information, while maximum pooling can obtain unique object characteristics, which can attract more detailed channel attention. Therefore, MECA module combines the global features extracted from the two to obtain a more refined channel monitoring weight and carries out channel attention monitoring based on C channel to obtain the weight parameters between different channels [23].

The feature graph in MECA module has different dimensions H, W, and C, which stand for the height, width, and the number of channels of the input feature F. Therefore, the MECA module can be strengthened by multiangle and all-aspect supervision, so that the feature graph can represent more detailed target information. Inspired by this, MECA (Modified Efficient Channel Attention) module in CAR-UNet was improved. Based on the dimension characteristics of the feature map, this paper optimized the MECA module and named the optimized module MD-MECA (Multidimension Modified Efficient Channel Attention Networks): on the basis of the C channel dimension, H and W channels are added simultaneously, and the same attention supervision module is designed, respectively, to obtain the supervision weight parameters of different dimensions. Then, MD-MECA module was added to the deeper U-Net network structure during the process of encoding, transmission, and decoding [24, 25]. Compared with the original U-Net, the structure optimized the feature graph during the transmission of the feature graph, supervised the feature graph of the coding part in different ways, and then transmitted to the decoding part for information supplement.

The module structure of MD-MECA is shown in Figure 3: the supervision weight based on each dimension is extracted, respectively, with the supervision structure of MECA. Formally, input feature $F \in R^{H\times W\times C}$ through the channel-wise max pooling and average poling can generate $F_{mp} \in R^{1\times 1\times C}$ and $F_{ap} \in R^{1\times 1\times C}$, respectively, e.g., at the c^{th} channel:

$$F_{mp}^{c} = \text{Max}\left(F^{c}(i,j)\right), 0 < c < C, 0 < i < H, 0 < j < W,$$
$$F_{ap}^{c} = \frac{1}{H\times W}\sum_{u=1}^{W}\sum_{j=1}^{W} F^{c}(i,j), 0 < c < C, \tag{1}$$

where $\text{Max}(\cdot)$ represents the maximum value, and $P^{c}(\cdot)$ represents the pixel value at a specific position in channel c. The two calculated values are then transmitted to a 1D convolutional neural network with shared weights to generate a channel monitoring mechanism $M^{c} \in R^{1\times 1\times C}$ Then, the MECA module combines the eigenvectors of the convolutional layer output by channel addition, and the calculation is as follows:

$$M(F) = \sigma\left(\text{Conv1 } D\left(F_{ap}\right) + \text{Conv1 } D\left(F_{mp}\right)\right), \tag{2}$$

where Conv1D(•) represents the 1D convolutional layer and $\sigma(\bullet)$ denotes the Sigmoid function. Similarly, the monitoring weight based on H dimension and W dimension of feature map is obtained in the same calculation method, and then

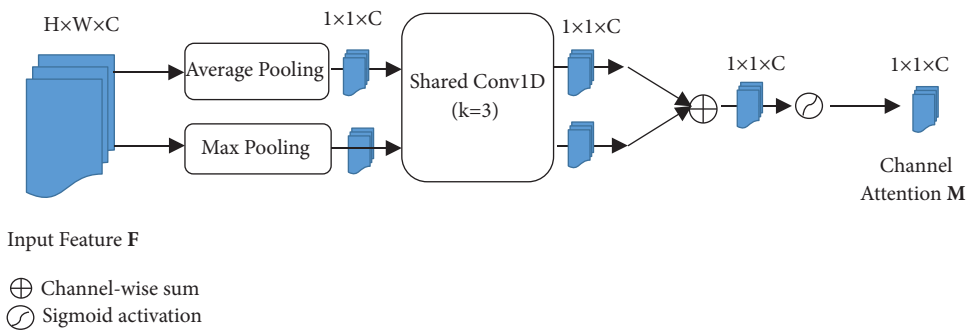

Figure 2: Diagram of the classical MECA technique.

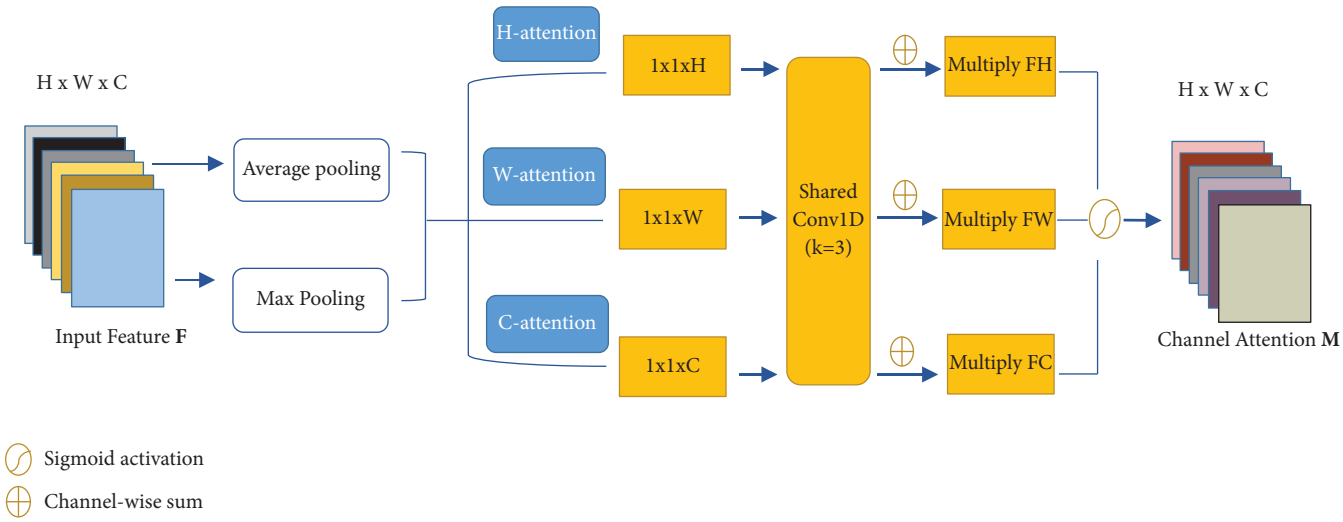

Figure 3: Structure of the proposed MD-MECA module.

the feature map is supervised in three dimensions, and then the required feature map is obtained by adding and combining them pixel by pixel.

Through the above method, the experiment has carried on the different dimension and the level optimization to the image feature image. By adding MD-MECA to the coding transfer features of U-Net architecture to the decoding module, the detailed texture features and semantic features transmitted by the coding part are refined. Therefore, the features obtained by the decoding part have better characterization ability to the target and can better segment the remote sensing image.

3.3. Batch Normalization and DropBlock. The Google team came up with a Batch Normalization method in 2015. In the deep network, if the network activation output is large, the gradient will be small and the learning rate will gradually slow down. In this way, the deeper the network structure is, the shallow layer of the gradient will be small and the learning rate will be slow. The higher the deep gradient, the faster the learning rate. For such a network structure, it loses its deep meaning. In order to solve this problem, the use of BN layer in the network can solve gradient disappearance and gradient explosion, improve the training speed and network convergence speed, and effectively prevent overfitting problems.

Overfitting is a serious problem in deep neural networks. The more complex the network structure is, the processing speed is slow, so it is difficult to deal with the overfitting of different complex neural networks in the test. Dropout proposed by Srivastava et al. [26] is also a technology to solve this problem. Its key idea is to temporarily discard neural units from the neural network in accordance with certain probability during training. Dropout has a significant effect in the full connection layer, but elements of adjacent positions in the feature graph of the convolutional layer share semantic information in space. Therefore, although a unit is discarded, its adjacent elements can still keep the semantic information of this location, and the information can still circulate in the convolutional neural network. Therefore, to solve this problem, this paper introduces a structural form of the dropout method, i.e., DropBlock. The DropBlock technology is a regularization technology used in convolutional neural network proposed by researchers of Google Brain in 2018. It can discard units in adjacent regions of feature graph at the same time to improve accuracy.

3.4. Network Architecture. The detailed architecture of Multidimension Attention U-Net (MDAU-Net) is displayed in Figure 4. Structure of MDAU-Net is derived from U-Net, the structure adopts multilevel subsampling structure module, which increases the model depth to increase the nonlinear mapping, thus enhancing the feature fitting ability. The experimental structure is designed with a 7-layer lower sampling module; each module consists of a 3×3 convolutional layer (ReLU) plus a 2×2 Maxpooling layer. For the input data with the size of 1024×1024, the image is extracted with the size of 8×8, and the size is 1/64 of the original image after 7 times of pooling at the coding end under the sampling structure. At the same time, 7 (seven) feature graph modules of different levels are obtained. In the upsampling part, seven (7) stages of upsampling calculation were also carried out. Furthermore, each layer was combined with the feature map of the downsampling coding part to supplement information and optimize the segmentation contour texture features. At the same time, MD-MECA module is added to the feature image transfer part of the coding part of each layer, and the feature image sent by the coding part is optimized through multidimensional supervised calculation to highlight the geometric features and suppress the background features.

For remote sensing image features, the shallow layer features have sufficient texture features, which is helpful to the contour restoration of segmentation algorithm. High-level semantic features help to distinguish target categories. Therefore, it is necessary to combine the features of the two to complete the feature information as much as possible. In the MDAU-Net network structure proposed in this paper, the multilevel coding and decoding structure is adopted, and the feature graphs of different levels in the coding part are made full use of to build a deeper network, and the features are extracted and combined in a fine way, so as to obtain better prediction effect.

4. Data sets and Evaluation Metrics

4.1. Data sets

4.1.1. Experimental Data. In order to avoid the impact of the uniqueness of the data set on the experimental results, the Massachusetts building data set and WHU data set were selected as the experimental data. Because the annotation accuracy and spatial resolution of different data sets are different, the conclusion is more convincing.

In this paper, 600 images in each data set were selected for training, 100 images for testing, and 100 images for verification. The input image size was 512 pixels ×512 pixels.

(1) Flip conversion: flip the image along the vertical or horizontal direction

(2) Random rotation transformation: randomly rotate the image by several angles

(3) Random clipping: local images at different positions can be obtained through random clipping of images

(4) Contrast transformation: the contrast transformation factor is randomly set for the image to adjust the image contrast

Among them, Figure 5(a) is the original image without processing; Figures 5(b)–5(d) is the clockwise rotation of 90°, 180°, and 270°, respectively; Figures 5(e) and 5(f) are the vertical and horizontal mirror flipping; Figure 5 5(g) is the contrast transformation; and Figure 5(h) is the random cropping. A total of 4000 images and labels were obtained after the geometric modification method data were expanded. Finally, in each data set, there are 1400 images as the training set, 400 images as the test set, and 200 images as the verification set.

4.1.2. Evaluation Metrics. Recall, Precision, F1-measure, and IoU were used to evaluate the experimental results. Recall rate is the ratio of correctly predicted positive samples to the total number of true positive samples. Accuracy refers to the ratio of correctly predicted samples to the total predicted samples, F1 value refers to the harmonic average of accuracy and recall rate, while IoU is the intersection of pixels labeled as building in the predicted results and ground truths, divided by the union of pixels labeled as building in the predicted results and ground truths. The calculation formula is as follows:

$$\begin{aligned} P_{rec} &= \frac{\mathrm{TP}}{\mathrm{TP} + \mathrm{FN}}, \\ P_{pre} &= \frac{\mathrm{TP}}{\mathrm{TP} + \mathrm{FP}}, \\ F1 &= 2 \times \frac{P_{pre} \times P_{rec}}{P_{pre} + P_{rec}}, \\ IoU &= \frac{\mathrm{TP}}{\mathrm{TP} + \mathrm{FP} + \mathrm{FN}}, \end{aligned} \tag{3}$$

where *TP* represents the correct number of pixels extracted, *FP* represents the number of pixels extracted with errors, and *FN* represents the number of missing pixels.

4.1.3. Implementation Details. In order to verify the feasibility of MDAU-Net proposed in this paper in remote sensing images and the superiority of the improved network MDAU-Net compared with U-Net network and CAR-UNet network, the same group of training samples and test samples were used for comparative experiments, and the experimental computer operating system was Windows. Based on the design of PyTorch deep learning framework of version 1.4.0, the CPU is configured as E2650, graphics card NVIDIA 1080Ti ×2, GPU is configured as GeForce GTX 1080, and video memory is 8G. Experimental parameters are shown in Table 1.

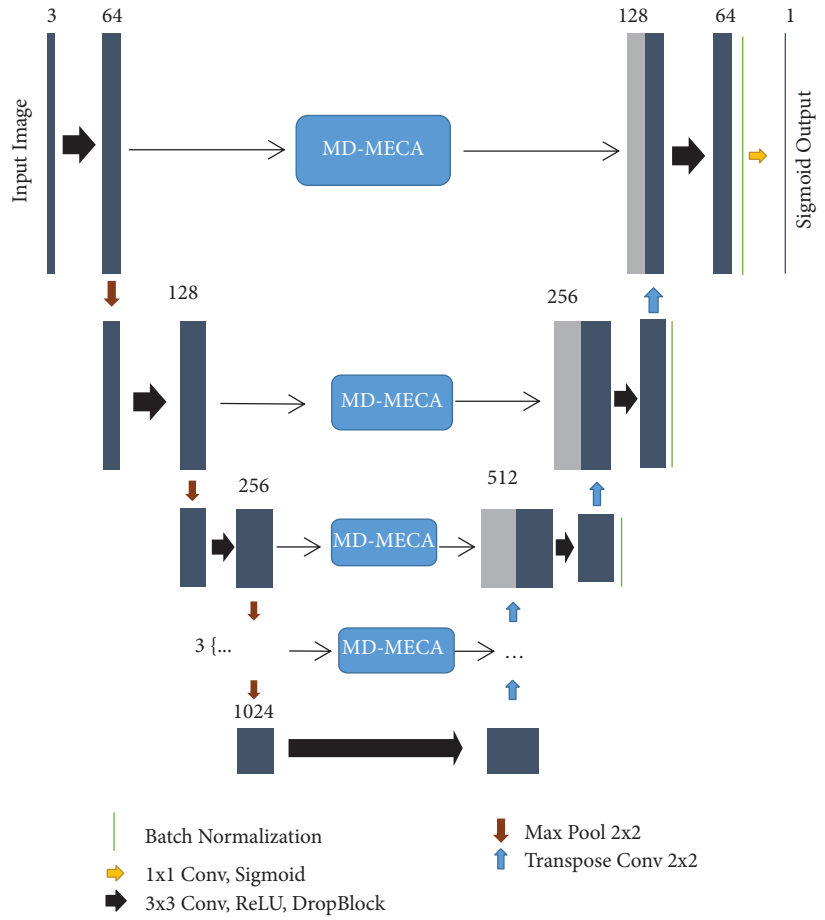

Figure 4: The MDAU-Net architecture (proposed model).

(a) (b) (c) (d) (e) (f) (g) (h)

Figure 5: Data expansion processing results (a) image, (b) rotate 90°, (c) rotate 180°, (d) rotate 270°, (e) flip vertical, (f) flip horizontal, (g) transform contrast, and (h) random cutting.

Table 1: Experimental parameters.

name of the parameter	Parameter values
Learning rate	1×10^{-3}
Optimizer	Adam
Loss function	Binary cross entropy
Batch size	2
Epochs	100
Dropout rate	0.15
Block size	7

5. Experiments and Results

5.1. Ablation Study

5.1.1. The Influence of Layer Number of Network Structure. Firstly, based on U-Net network model, the influence of model depth on experimental results is studied. The experiment was conducted on the Massachusetts building data set and the WHU data set, respectively. Tables 2 and 3 show the effect of different model depths on the experimental performance.

Table 2: Comparison of results of different deep network experiments on Massachusetts data set.

Methods	Layer number	Recall (%)	Precision (%)	F1-measure (%)
U-Net	4	86.36	91.94	89.06
U-Net5	5	89.92	92.54	91.21
U-Net6	6	92.41	94.87	93.62
U-Net7	7	94.38	96.62	95.49
U-Net8	8	92.53	94.33	93.42

Table 3: Comparison of results of different deep network experiments on WHU data set.

Methods	Layer number	Recall (%)	Precision (%)	F1-measure (%)
U-Net	4	84.62	90.64	87.53
U-Net5	5	88.74	91.32	90.01
U-Net6	6	91.28	93.63	92.44
U-Net7	7	95.14	95.81	95.47
U-Net8	8	92.46	94.19	93.32

As can be seen from the experimental results, with the increase of the number of network layers, each accuracy index will increase, but when the number of network layers reach 8, the influence of overfitting problem is very serious. By comparison, it can be found that U-Net7 has the best building extraction effect among the five network models. In different data sets, U-Net7 has the highest recall rate, accuracy and F1 values, which reach 96.62% and 95.81% respectively. Therefore, it can be concluded from the experimental results that the more layers of the network structure, the higher the accuracy of the experimental results. With the deepening of the network layer, although the receptive field will increase, the number of down sampling will increase, resulting in the loss of detail information. Meanwhile, the overfitting problem will increase with the deepening of the network, thus the experimental accuracy will be affected. Based on the above considerations, U-Net7 is selected as the best basic network model for the experiment.

5.1.2. The Impact of Batch Normalization and DropBlock. Based on the selected U-Net7 network model, the experiment explores the impact of Batch Normalization and DropBlock on the experimental results.

Tables 4 and 5 show the precision comparison of experimental results on Massachusetts data set and WHU data set after the introduction of BN layer and DropBlock, respectively, in U-Net7 network structure model. It can be seen that the selection of different data sets has a direct impact on the prediction results; however, under the same experimental conditions and data sets, the proposed U-Net7 network combined with BN and DropBlock at the same time, compared with the U-Net7 network combined with BN or DropBlock alone, the accuracy index has been improved to a certain extent, and the building extraction has reached high accuracy

Table 4: Massachusetts data set comparison of network models' experiment results.

Network structure	Recall (%)	Precision (%)	F1-measure (%)
U-Net7+BN	95.36	96.94	96.14
U-Net7+DropBlock	94.42	95.82	95.11
U-Net7+BN + DropBlock	96.68	97.04	96.86

Table 5: WHU data set Comparison of network models' experiment results.

Network structure	Recall (%)	Precision (%)	F1-measure (%)
U-Net7+BN	94.21	94.83	94.52
U-Net7+DropBlock	94.26	95.12	94.69
U-Net7+BN + DropBlock	94.63	95.68	95.15

requirements. The accuracy rates are 97.04% and 95.68%, respectively, indicating that BN and DropBlock can effectively solve the gradient disappearance and gradient explosion, reduce the overfitting problem, and improve the accuracy of building identification. The feasibility and potential of this method in remote sensing image target extraction are proved.

5.2. Comparison to State-of-the-Art Methods. Based on the experimental data set, the classical U-Net network, CAR-UNet network, and MDAU-Net network were trained, respectively, and the experimental results were compared in detail after testing.

The three index values of the three methods in the two test data sets are shown in Table 6. The statistical data in Table 6 show that in the two tests, the three index values of the method in this paper are better than the corresponding index values of U-Net and CAR-UNet. Taking the Massachusetts data set as an example, the accuracy rates of the method, U-Net, and CAR-UNet are 97.04%, 94.82%, and 92.34%; recall are 87.68%, 82.42%, and 82.36%; IoU are 78.35%, 72.31%, and 70.96%, respectively. It can be seen from Table 6 that the selection of data sets has a direct impact on the predicted results. However, under the same experimental conditions and data sets, the accuracy indexes of the MDAU-Net network proposed in this paper are improved to some extent compared with the U-Net network and CAR-UNet network and meet the high accuracy requirements for target extraction.

Part of the visualization results are shown in Figures 6 and 7. The visual effect shows that although there are a few extraction errors, the overall building extraction effect is good. It can be seen from the results that the overall effect of MDAU-Net extraction of the target is better than that of U-Net and CAR-UNet network structures, and the result image extracted by MDAU-Net is closer to the label map. As can be seen from the figure, the extraction of irregular buildings in the image is incomplete, and the overall extraction effect is not good. Adhesion phenomenon exists in small -scale buildings; In addition, there are a few extraction

Table 6: Quantitative evaluation results of building detection for different methods.

Data sets	Test area	IoU			Recall			Precision		
		U-Net	CAR-UNet	MDAU-Net	U-Net	CAR-UNet	MDAU-Net	U-Net	CAR-UNet	MDAU-Net
Massachusetts building data set	1	69.74	68.96	76.95	83.46	80.23	86.46	88.48	91.34	96.32
	2	66.98	69.73	77.82	80.27	81.32	85.24	94.24	93.21	95.11
	3	73.26	74.22	80.93	81.64	78.43	88.72	93.31	90.23	96.68
	Mean	**70.96**	**72.31**	**78.35**	**82.36**	**82.42**	**87.68**	**92.34**	**94.82**	**97.04**
WHU data set	1	69.42	69.83	76.42	83.24	81.47	82.03	90.18	90.21	93.02
	2	68.33	65.24	73.92	80.66	82.56	87.49	89.32	91.37	92.83
	3	74.26	73.82	78.46	81.24	80.33	89.32	86.87	93.06	94.37
	Mean	**71.53**	**72.41**	**77.97**	**82.21**	**83.26**	**90.63**	**88.94**	**93.12**	**95.68**

Bold shows the values of IOU, recall, and precision on the whole dataset.

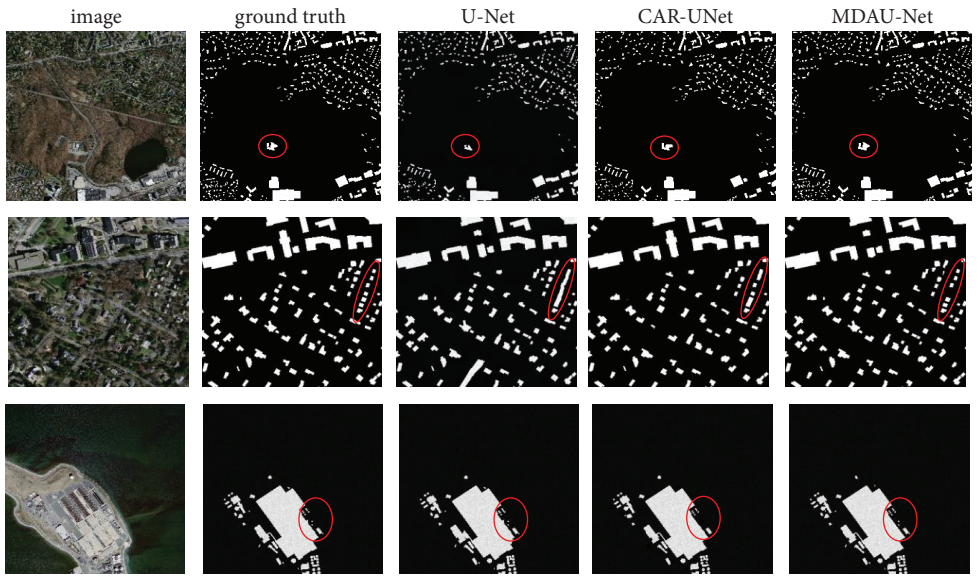

Figure 6: Experimental comparison of extraction results from the Massachusetts data set.

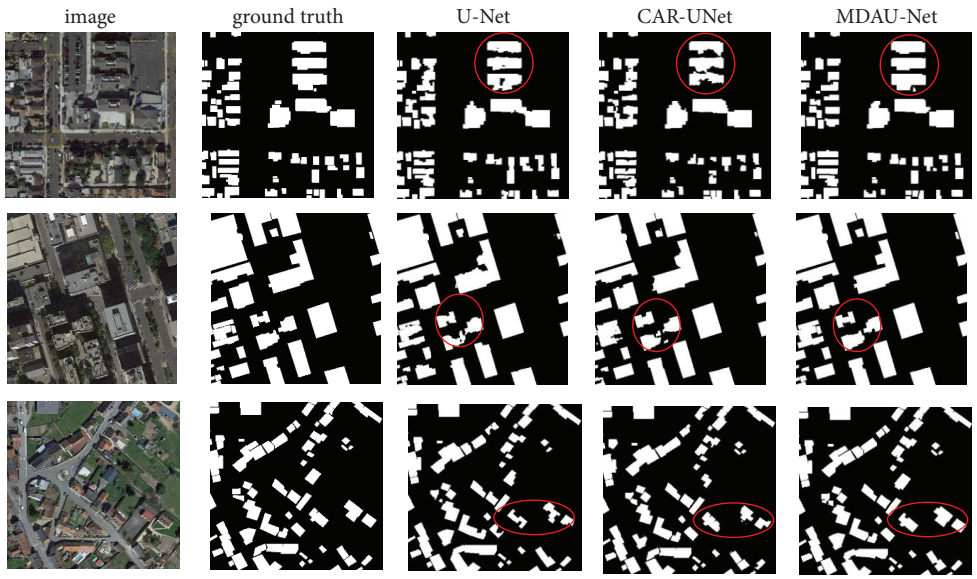

Figure 7: Experimental comparison of extraction results from the WHU data set.

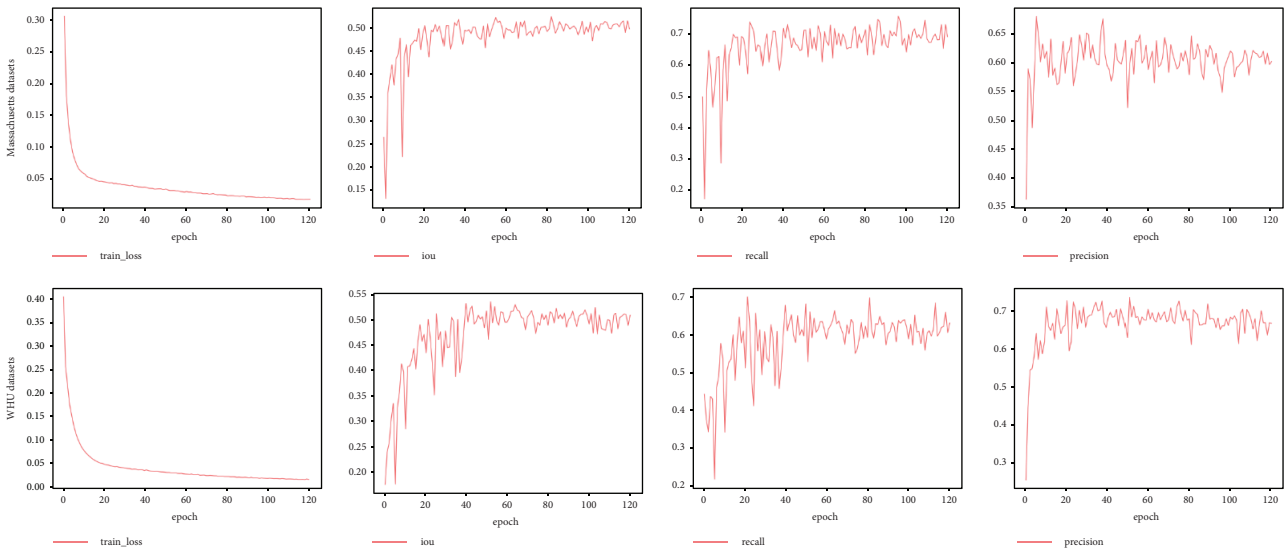

Figure 8: Accuracy of the proposed MDAU-Net model using evaluation graph on both Massachusetts and WHU data sets.

errors in this method, mainly in that it is easy to mistake the bright hardened ground and bare ground as buildings in the test image; and the cement hardened ground is connected with the building, so it is difficult to eliminate this false extraction through postprocessing. However, in the case of irregular building boundaries and a large number of isolated points, the MDAU-Net network structure proposed in this paper can effectively extract targets comprehensively, and the extraction effect is better in dense buildings or shaded areas, especially for some small buildings or irregular buildings with good recognition effect. It can be seen that the improved network model is more complete in extracting the target details, segmenting the target edges accurately, and has a better recognition effect on some subtle feature details.

Figure 8 shows the change curves of train loss, IoU, recall, and precision of this method in the training process of Massachusetts data set and WHU data set. The horizontal axis represents the number of training steps, as shown in Figure 8. After 100 steps of training, the change rate of loss value gradually decreased and later became stable. It shows that the network type has good stability. In Figure 8, IoU, recall, and precision of two different data sets all increased step by step with the increase of training steps. The precision reached 97.04% and 95.68% in the end.

In other experiments, Softmax, Sigmoid, and ReLU were the three types of activation functions we employed [9, 27, 28, 29]. Over the acquired findings, we noticed significant variations that may be attributed to the data sets. Because the Massachusetts data set is so big, there were more variances than in the WHU data set. This indicates that the proper activation function should be employed based on the data set and image attributes. Furthermore, each activation function generates distinct and significantly different results when paired with a certain training model. When compared to the standard U-Net and MECA methods, the MDAU-Net model has a tiny overlap. Smaller overlaps guarantee that the model delivers outcomes that are more similar to one another, i.e., stray less from one another.

6. Conclusions and Future Work

In this paper, we presented a Multidimension Attention Network model for building segmentation in remote sensing images. The method considers the relationship between feature channels and introduces a new channel attention mechanism to enhance the network discrimination ability. Specifically, we increase multiple dimensions through the recently proposed modified efficient channel attention (MECA). Then, we apply MD-MECA to "skip connections," assigning weights to the element map from the shrink path rather than equally copying to the corresponding expansive path. The DropBlock is added after the convolutional layer and BN is added in the decoding path, which improves the accuracy of the segmentation algorithm in remote sensing images and effectively solves the problems of missed detection, wrong detection, and irregular edge in the segmentation and extraction of buildings in remote sensing images.

It is compared with the classical U-Net network structure and car U-Net network structure. The results show that the recall, accuracy, F1 value, and IoU of this method have been significantly improved, and the final extraction effect can detect and classify buildings more accurately. Our experiments show that the algorithm achieves the highest performance of building segmentation on two data sets, i.e., Massachusetts and WHU. However, we observed that the activation function used in this method cannot activate all neurons and the improvement accuracy is limited. Therefore, the optimization of the model structure and the search for the optimal activation function are further research work [30].

Data Availability

The raw/processed data required to reproduce these findings cannot be shared at this time as the data also form part of an ongoing study.

Conflicts of Interest

The authors declare that they have no conflicts of interest.

Acknowledgments

This work was supported by the Shanxi Province Key R&D Plan (International Science and technology cooperation) (project 201903D421089) and Shanxi Postgraduate Education Innovation Project, Research on discontinuous deformation law of mining surface based on particle flow theory (2019SY126).

References

[1] C. Liu, X. Huang, Z. Zhu, H. Chen, X. Tang, and J. Gong, "Automatic extraction of built-up area from ZY3 multi-view satellite imagery: analysis of 45 global cities," *Remote Sensing of Environment*, vol. 226, no. 226, pp. 51–73, 2019.

[2] S. Ioffe and C. Szegedy, "Batch normalization: accelerating deep network training by reducing internal covariate shift," 2015, https://arxiv.org/abs/1502.03167.

[3] G. Ghiasi, T. Lin, and Q. Le. DropBlock, "A regularization method for convolutional networks," 2018, https://arxiv.org/abs/1810.12890.

[4] V. Mnih, *Machine Learning for Aerial Image Labeling*, pp. 84–88, University of Toronto, Toronto, Canada, 2013, PhD_Thesis.

[5] S. Ji, S. Wei, and M. Lu, "Fully convolutional networks for multisource building extraction from an open aerial and satellite imagery data set," *IEEE Transactions on Geoscience and Remote Sensing*, vol. 57, no. 1, pp. 574–586, 2019.

[6] Y. Zhong and L. Zhang, "Initialization methods for remote sensing image clustering using K-means algorithm," *Systems Engineering and Electronics*, vol. 32, no. 9, pp. 2009–2014, 2010.

[7] T. Kohonen, "The self-organizing map," *Proceedings of the IEEE*, vol. 78, no. 9, pp. 1464–1480, 1990.

[8] X. Lin and J. Zhang, "Object-based morphological building index for building extraction from high Resolution.Remote sensing imagery," *Acta Geodaetica et Cartographica Sinica*, vol. 46, no. 6, pp. 724–733, 2017.

[9] C. Li, C. Xu, Z. Cui, D. Wang, T. Zhang, and J. Yang, "Feature-attentioned object detection in remote sensing imagery," in *Proceedings of the 2019 IEEE International Conference on Image Processing (ICIP)*, pp. 3886–3890, Taipei, Taiwan, September 2019.

[10] D. Yu, R. Zhang, and S. Qin, "Cascade saliency attention network for object detection in remote sensing images," in *Proceedings of the 2020 25th International Conference on Pattern Recognition (ICPR)*, pp. 217–223, Milan, Italy, January 2021.

[11] A. Krizhevsky, I. Sutskever, and G. Hinton, "Imagenet classification with deep convolutional neural networks," *Advances in Neural Information Processing Systems*, vol. 25, pp. 1097–1105, 2012.

[12] J. Long, E. Shelhamer, and T. Darrell, "Fully convolutional networks for semantic segmentation," in *Proceedings of the IEEE conference on computer vision and pattern recognition*, pp. 3431–3440, Boston, MA, USA, June 2015.

[13] V. Badrinarayanan, A. Kendall, and R. Cipolla, "SegNet: a deep convolutional encoder-decoder architecture for image segmentation," *IEEE Transactions on Pattern Analysis and Machine Intelligence*, vol. 39, no. 12, pp. 2481–2495, 2017.

[14] O. Ronneberger, P. Fischer, and T. Brox, "U-net: convolutional networks for biomedical image segmentation," *Lecture Notes in Computer Science*, in *Proceedings of the International Conference on Medical image computing and computer-assisted intervention*, pp. 234–241, Munich, Germany, October 2015.

[15] S. T. Seydi, M. Hasanlou, and M. Amani, "A new end-to-end multi-dimensional CNN framework for land cover/land use change detection in multi-source remote sensing datasets," *Remote Sensing*, vol. 12, no. 12, p. 2010, 2020.

[16] M. Chen, J. Wu, L. Liu et al., "DR-net: an improved network for building extraction from high resolution remote sensing image," *Remote Sensing*, vol. 13, no. 2, p. 294, 2021.

[17] A. Abdollahi, B. Pradhan, and A. M. Alamri, "An ensemble architecture of deep convolutional segnet and unet networks for building semantic segmentation from high-resolution aerial images," *Geocarto International*, vol. 18, no. 3, 2020.

[18] F. I. Diakogiannis, F. Waldner, P. Caccetta, and C. Wu, "ResUNet-a: a deep learning framework for semantic segmentation of remotely sensed data," 2019, https://arxiv.org/abs/1904.00592.

[19] B. Wang, L. Wang, J. Chen, Z. Xu, T. Lukasiewicz, and Z. Fu, "W-net: dual supervised medical image segmentation model with multi-dimensional attention and cascade multi-scale convolution," 2020, https://arxiv.org/abs/2012.03674.

[20] C. Guo, M. Szemenyei, Y. Yi, Y. Hu, W. Wang, and W. Zhou, "channel attention residual U-net for retinal vessel segmentation," 2020, https://arxiv.org/abs/2004.03702.

[21] J. Hu, L. Shen, and G. Sun, "Squeeze-and-excitation networks," in *Proceedings of the IEEE Computer Vision and Pattern Recognition*, pp. 7132–7141, Salt Lake City, UT, USA, June 2018.

[22] Q. Wang, B. Wu, P. Zhu, P. Li, W. Zuo, and Q. Hu, "ECA-net: Efficient channel attention for deep convolutional neural networks," in *Proceedings of the IEEE/CVF Conf. Comput. Vis. Pattern Recognit. (CVPR)*, Seattle, WA, USA, June. 2020.

[23] X. Qi, K. Li, P. Liu, X. Zhou, and M. Sun, "Deep attention and multi-scale networks for accurate remote sensing image segmentation," *IEEE Access*, vol. 8, Article ID 146627, 2020.

[24] X. Lai, W. Yang, and R. Li, "DBT masses automatic segmentation using U-net neural networks," *Computational and mathematical methods in medicine*, vol. 2020, Article ID 7156165, 10 pages, 2020.

[25] J. Kong, Y. Gao, Y. Zhang, H. Lei, Y. Wang, and H. Zhang, "Improved attention mechanism and residual network for remote sensing image scene classification," *IEEE Access*, vol. 9, no. 2021, Article ID 134800.

[26] N. Srivastava, G. Hinton, A. Krizhevsky, I. Sutskever, and R. Salakhutdinov, "Dropout: a simple way to prevent neural networks from overfitting," *Journal of Machine Learning Research*, vol. 15, no. 1, pp. 1929–1958, 2014.

[27] A. Ali, Y. Zhu, and M. Zakarya, "Exploiting dynamic spatio-temporal correlations for citywide traffic flow prediction using attention based neural networks," *Information Sciences*, vol. 577, pp. 852–870, 2021.

[28] X. Tang, H. Zhang, J. Ma, X. Zhang, and L. Jiao, "Supervised adaptive-RPN network for object detection in remote sensing images," in *Proceedings of the IGARSS 2020-2020 IEEE International Geoscience and Remote Sensing Symposium*, pp. 2647–2650, Waikoloa, HI, USA, 26 September.-2 October 2020.

[29] L. Hou, J. Xue, K. Lu, L. Hao, and M. M. Rahman, "A single-stage multi-class object detection method for remote sensing images," in *Proceedings of the 2019 IEEE Visual Communications and Image Processing (VCIP)*, pp. 1–4, Sydney, Australia, December 2019.

[30] S. Dong and Z. Chen, "Block multi-dimensional attention for road segmentation in remote sensing imagery," *IEEE Geoscience and Remote Sensing Letters*, vol. 19, 2021.

Hindawi
Scientific Programming
Volume 2022, Article ID 4037625, 14 pages
https://doi.org/10.1155/2022/4037625

Research Article

A Deep Neural Network-Based Target Recognition Algorithm for Robot Scenes

Lijing Liu

School of Engineering, Hong Kong University of Science and Technology, Hong Kong 999077, China

Correspondence should be addressed to Lijing Liu; liulijing1997@cumt.edu.cn

Received 7 December 2021; Revised 22 December 2021; Accepted 28 December 2021; Published 11 January 2022

Academic Editor: Muhammad Usman

Intelligent robots are a key vehicle for artificial intelligence and are widely employed in all aspects of everyday life and work, not just in the industry. One of the talents required for intelligent robots to complete their jobs is the capacity to identify their environment, which is a crucial obstacle to be overcome. Deep learning-based target identification algorithms currently do not fully leverage the link between high-level semantic and low-level detail information in the prediction step and hence are less successful in recognizing tiny target objects. Target recognition via vision sensors has also improved in accuracy and efficiency because of the development of deep learning. However, due to the insufficient usage of semantic information and precise texture information of underlying characteristics, tiny target recognition remains a difficulty. To address the aforementioned issues, we propose a target detection method based on a jump-connected pyramid model to improve the target detection performance of robots in complex scenarios. In order to verify the effectiveness of the algorithm, we designed and implemented a software system for target detection of intelligent robots and performed software integration of the proposed algorithm model with excellent experimental results. These experiments reveal that, when compared to other algorithms, our suggested algorithm's characteristics have higher flexibility and robustness and can deliver a higher scene classification accuracy rate.

1. Introduction

Intelligent robots have become widely employed in many industries as a result of the fast expansion of the economy in recent years, as well as the rapid emergence of artificial intelligence [1]. The use of these technologies has increased the efficiency of automated manufacturing while also satisfying the demand for services in a variety of sectors, hence improving human life quality [2]. Intelligent robots' "intelligence" is based on their capacity to detect their surroundings and interact with people and objects [3]. Robots can utilize machine vision systems to grasp information in the same way that humans rely largely on their eyes to understand the world and their environment. The capacity to swiftly and reliably locate and distinguish things in pictures is one of the most significant areas of research.

Coverage, surveillance, search, patrolling, monitoring, and pursuit-evasion are only a few of the decisional issues that target detection and tracking involve. The use of intelligent robotic target detection technology offers a wide range of applications [4]. In the sphere of security, security robots may undertake real-time video monitoring of public locations [5] such as residential neighborhoods, supermarkets, banks, and junctions. Tour guide robots [6] in the service industry may detect and identify targets in real time, such as automobiles traveling on campuses or scenic places, pedestrians arriving and exiting, and attraction signs and signage, to provide guests with prompt politeness and advice. In industry, target detection technology [7] for industrial robots may be utilized for tasks like workpiece identification and component damage detection, which not only saves time but also enhances productivity. Figure 1 depicts an intelligent power inspection robot that replaces manual labour to accomplish automatic detection and intelligent analysis of the state of power equipment, therefore enhancing the grid's and equipment's safety. This has enhanced the grid's and electrical equipment's dependability significantly.

Figure 1: Electric power intelligent inspection robot.

The objective of target detection entails both identification and localization [8]. This signifies that all of the target categories to be detected in the image have been recognized, and their locations have been computed. It is critical to verify that the target is fully and precisely recognized and that the target's position is exact enough. In general, the target's class must be recognized, the label must be identified, and the target's position box must be defined by the top left and bottom-right coordinates. Although there are usually just a few target instances in a picture, the number of alternative places and sizes to examine is tremendous. In some detection tasks, the bounding box of the target must be established [9] and also the position of pose information or certain tiny local targets must be detected [10]. Once the location of a water glass has been determined, features such as the orientation of the handle must be sought to offer the positional pose information required to grasp the target.

Many classic target detection approaches [11] work well for fixed targets of a given kind or detection tasks in specific settings, but they are ineffective for detecting many targets in complicated surroundings. At the same time, detection speed is a crucial measure, and real-time target detection is required in many applications, which classical target detection algorithms are unable to satisfy. Deep learning's superior performance in image identification, particularly convolutional neural networks, has made deep learning-based target detection and recognition a prominent study issue in recent years. A deep neural network-based target identification system for robot situations has been developed to provide outstanding target recognition performance and universality. The following are some of the contributions:

(i) Firstly, we address the problems in the application of target detection algorithms for mobile robots

(ii) Secondly, we propose a target detection method based on a jump-connected pyramid model to improve the target detection performance of robots in complex scenarios

(iii) Thirdly, we design and implement a software system for target detection of intelligent robots and perform software integration of the proposed algorithm model with excellent experimental results

(iv) Finally, we verify the effectiveness of the algorithm, experiments were carried out on several different datasets, and the results confirmed the effectiveness of the algorithm

The remainder of our work is organized as follows: Section 2 shows the related works, Section 3 represents the methodology that we have adopted for our work, Section 4 explains the experimental work and graphical representation, and in Section 5, we conclude our work.

2. Related Work

In this section, we discuss works of researchers related to our proposed work.

2.1. Current Status of Research on Target Detection Methods. Target detection has been a major research topic in the field of computer vision. Target detection is used to determine where targets are in space and which category they belong to: pedestrian detection [12], face detection [13], vehicle detection [14], intelligent surveillance [15], and autonomous driving [16]; among other applications, target detection is now widely used in our daily lives [17]. Traditional target identification methods are divided into three parts, as shown in Figure 2: According to this figure, potential regions in a given picture, also known as candidate windows, are selected, and then features from the targeted area of the image are extracted using a features extraction procedure. After that, other categorization methods are used. They categorize the targeted region based on the results of focused detection. These classifiers are also used to train a classifier for classification using the obtained information.

2.1.1. Candidate Area Selection. Targets can appear in any area in the image and be huge or little, and their forms and dimensions are not set in the image in the real world. To traverse the entire image without missing any possible locations, a sliding window approach is used, in which different sizes and aspect ratios are assigned to the windows, causing them to slide across the image from left to right and from top to bottom, and then these windows are used for the subsequent feature extraction work.

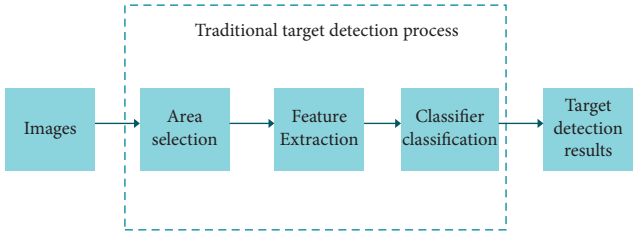

Figure 2: Traditional target detection flow chart.

2.1.2. Feature Extraction. The process of translating raw data into numerical features that can be processed while keeping the information in the original dataset is known as feature extraction. It produces better outcomes than applying machine learning to raw data directly. Many great feature operators have been extracted throughout years of study, such as Scale Invariant Feature Transform (SIFT), Histogram of Oriented Gradient (HOG), and others, in addition to typical features such as color, texture, shape, and gradient.

2.1.3. Classifiers. The technique of guessing the class of given data points is known as classification. Targets, labels, and categories are all terms used to describe classes. The job of estimating a mapping function (f) from input variables (X) to discrete output variables is known as classification predictive modeling (y). In machine learning, a classifier is an algorithm that automatically sorts or categorizes data into one or more "classes." Support Vector Machine (SVM), AdaBoost, and other classifiers are commonly utilized.

2.2. The Current State of Research in Deep Learning for Robotic Target Detection. At present, deep learning-based target detection algorithms fall into two main categories: one is the R-CNN family of target detection frameworks based on combining candidate regions (region proposal); the other is an algorithm that converts target detection into a regression problem.

The two-stage strategy is another name for the candidate region-based approach. This is because the whole network is split into two stages: first the extraction of candidate frames from the region of interest and then regression on the target's class and position. CNNs (convolutional neural networks) are an important part of candidate region-based algorithms. Since then, ResNet [18] and Inception v4 [19] have lowered target detection classification error to less than 4%. The two-stage based target detection method has demonstrated considerable gains in speed and accuracy for the job of picture classification using the new feature extraction model. Because of the completely connected layer of the CNN, the App-Net algorithm model developed by He et al. [20] overcomes the problem that the input pictures must be of the same size. Ross Girshick et al. [21] introduced the R-CNN algorithm concept in 2014. This algorithm is also the heart and soul of the R-CNN algorithm family. The R-CNN method calculates the candidate area input frame for the network model using the selective search [22] algorithm and utilises it as the input for the network model after normalisation. However, while collecting features from candidate frames in candidate areas, the R-CNN method performs a lot of duplicate calculations, slowing down the network model's overall detection performance. Ren et al. [23] introduced the Faster R-CNN target identification method based on the R-CNN, which is a network model that contains an RPN (Region Proposal Network), to address this problem. Instead of using the selective search technique, the RPN maps the candidate frames to the input picture, speeding up the detection process. Target detection has always followed the "region proposal + classification" concept, from R-CNN to Faster R-CNN [24], and this family of algorithmic models has effectively increased the detection accuracy and speed of convolutional neural networks for target detection.

Another method is the regression-based method, also known as the single-stage method. The regression-based detection method divides the feature map into S∗S grids and performs direct bounding box prediction in each grid, followed by category prediction and position regression. The YOLO algorithm [25] is the first algorithm to propose the idea of "single stage." The YOLO algorithm uses a regression-based approach. Unlike the two-stage algorithm model, the YOLO algorithm slices the image into S∗S grids and detects the possible target objects in the center of each grid. Each grid predicts two scales of bounding box information and the corresponding object class information. Instead of using a two-stage candidate region approach, the YOLO algorithm slices the image into a grid format and predicts the target object at the center of the grid at multiple scales. Compared with the candidate region-based target detection method, the YOLO algorithm significantly improves the detection speed of the network model while ensuring the accuracy and basically achieves the requirement of real-time detection. However, although the YOLO algorithm significantly improves the detection speed, the grid mechanism used in the YOLO algorithm is less effective in detecting small targets that fall in the center of the grid in complex scenarios with multiple targets. Moreover, compared to the two-stage target detection based on candidate regions, the localization of bounding boxes is poor, and the accuracy of localization is much lower than that of the Faster R-CNN algorithm model. Moreover, the detection effect is not as good as expected for objects with more regular shapes of the target objects. In response to the problems of the YOLO algorithm model, SSD algorithm model [26] is based on the YOLO algorithm, by combining the ideas of RPN algorithm [27], using the prediction on multiscale feature layers, and using the idea that different scales of the feature map feel different fields, respectively, on the high-level and low-level feature map prediction. The algorithmic model effectively improves the shortcomings of the YOLO algorithm, achieving detection accuracy (mAP) of 73.2% and a detection speed of 59 frames per second. However, SSD does not take small targets into account sufficiently, so detection of small targets is unsatisfactory, and region regression is difficult to converge when there are no candidate regions.

In conclusion, despite the rapid advancement of target detection algorithms, the problem of low detection accuracy

of tiny targets frequently encountered during the work of deep learning-based target detection techniques when applied to real-world settings such as robots requires more investigation.

2.3. Deep Learning Approach. Deep learning's success in picture classification and semantic segmentation [28–30] prompted scientists to apply it to RGB-D data processing. However, the techniques differ in terms of how depth data is sent into the network. The first method is to transmit the depth stream to the neural network as a fourth channel alongside the RGB. The benefit of this technique is that a lot of work has already been done on 2D RGB picture categorization. For this application, converting three-channel input to four channels is pretty simple. As a result, the challenge of how to encode depth data arose. The Horizontal Height Angle (HHA), for example, stores depth information in three channels [31]. The HHA is made up of data derived from depth horizontal disparity, height above ground, and the angle between the pixel's local surface normal and gravity's direction.

Deep neural networks are used in the work in [32] to extract features and categorize RGB-D photos. As a feature extractor, the suggested architecture employs a pretrained convolutional neural network (CNN). The network structure of [33] is as follows: five convolutional layers, three max-pooling layers to minimize the output dimensionality of the first, second, and fifth convolutional layers, two fully connected layers at the network's conclusion, and a softmax layer for classification. As an activation function, the Rectified Linear Unit (ReLU) is utilized. The network was trained for 1000 category classification tasks using the ImageNet dataset [34]. To adapt RGB-D pictures to CaffeNet, Schwarz et al. preprocessed RGB images by merging them with segmentation masks given with the dataset. This method converts RGB pictures to the fixed 227 by 227 dimensions that CaffeNet requires. The same approach is used to process depth pictures. The authors offer a unique approach for depth picture colorization that CaffeNet may use to transform it to a three-channel representation. The data from the RGB and depth photos are then merged and used to classify objects using a Support Vector Machine (SVM).

The work of [35] takes an approach similar to that of [32] and enhances performance only via the use of neural networks. The concept of starting with a pretrained model remains the same, but its design combines two models to do classification. Similarly, the network is divided into two streams, each of which is based on CNN that has been pretrained. The first channel is used to extract features from an RGB picture. The second extract is another collection of characteristics from the same data frame's depth data. To achieve classification, the two sets of features were combined and fed to a fully connected neural network. SafeNet is also used in both streams. Unlike earlier research, however, the authors fine-tune both streams on the RGB-D dataset [36]. The training process starts with the initialization of two streams using pretrained weights from CaffeNet, which was trained on the ImageNet dataset. On the RGB-D dataset, the second step is to train two streams separately. Combining the two streams and training the final classification layers represent the final phase.

2.4. Current State of Research in Small Target Detection. Although deep convolutional neural networks have made great progress in target detection, the detection of small targets still suffers from low detection accuracy. In response, some scholars have proposed new detection network models. In 2016, Bell et al. proposed an Inside-Outside Net (ION) detection model based on the inside and outside information of the region of interest [37]. In 2017, based on the Faster R-CNN network, Lin et al. [38] proposed a Feature Pyramid Network (FPN) with lateral connections, which utilises multiscale features and a top-down structure to achieve target detection. However, FPN only uses the top-level features for detection, ignoring the detailed information that is important for small target detection. To address the problems of the SSD algorithm for small target detection, Fu et al. [39] proposed a Deconvolutional Single Shot Detector (DSSD) algorithm, which changed the base network of the SSD algorithm to ResNet-101 [40], to enhance the feature extraction capability of the network. By combining multi-scale information, the detection accuracy of the model is improved. However, the above network ignores the connection between low-level features and high-level features and does not consider the perceptual field size of the convolutional operation, so that the convolutional operation with the same size of convolutional kernels for objects of different scales cannot extract the object information well.

3. Methodology

3.1. Target Recognition Algorithm for Robot Scenes Using a Deep Neural Network. Mobile robots must be able to properly navigate in complicated situations, detect and track items, avoid obstacles, establish their location, and rebuild 3D visual representations of their surroundings using cameras and other sensors. They may also be asked to provide humanitarian assistance and conduct industrial inspections. A service robot would often be expected to undertake search and rescue, give humanitarian aid in the care of the elderly via monitoring, and deliver timely information about their activities. Another possibility is the growing interest in unmanned aerial vehicles (UAVs) and vision-assisted driving. Traditionally, these functions have been provided by vision-based systems using stereovision or multiview coding. 14 tracking filters such as the Kalman filter, probabilistic data association filter, and multiple sensor fusion and state estimation are commonly used. Simultaneous localization and mapping (SLAM) provide a means of creating an environmental map identifying important obstacles, 3D surface reconstruction, and navigation and understanding the external world for indoor localization and navigational tasks with no external reference support like GPS or wireless location support. The authors of [41] described a real-time approach for reconstructing 3D surfaces from a set of known perspectives using an event-based

camera. Although visual-inertial/odometry (VI/VIO) relies on cameras and inertial measuring units (IMUs) to assess a robot's state (position, orientation, and velocity), it may also be used for other tasks including control, obstacle detection, and avoidance, as well as path planning. References [42, 43] are excellent resources for a thorough examination of SLAM.

3.2. A Small Target Detection Method Based on a Jump Connection Pyramid Model. Because of the camera distance and angle, intelligent mobile robots are in the process of moving, resulting in a large number of small target items that must be identified while moving. For example, the inspection robot must gather information on failure locations, instruments, and equipment, among other things, throughout the inspection process, which necessitates the exact recognition of tiny targets in the picture through implementation. As a result, improving the identification of tiny targets by intelligent service robots in environmental awareness is critical. Target detection based on convolutional neural networks has reached great detection accuracy and detection speed thanks to the widespread usage of deep convolutional neural networks for target detection. Small target identification, on the other hand, remains a hurdle. Small targets are frequently neglected during feature extraction, since they make up such a small amount of the image. Furthermore, conventional deep convolutional neural network target identification methods in the network prediction phase do not fully exploit the link between the semantic information of higher-level features and the detailed information of lower-level features.

We present a tiny target identification approach based on the jump-connected pyramid model to overcome these issues. The majority of the innovation is in two areas: To begin, a jump-connected pyramid model is presented as a way to combine the semantic information of high-level characteristics with the detailed information of low-level features in the network. Different steps of deconvolution are used to downscale the disconnected high-level features to the same size as that of the low-level features, and a 1×1 convolution layer is employed to minimize the dimensionality of the high-level features. Finally, the fused features are subjected to classification and position regression. Second, three parallel transversal network topologies are employed in the network model to better extract feature information corresponding to varied sizes of objects.

3.3. Convolutional Neural Network Fundamentals. The technique in this paper's deep network model is mostly based on convolutional neural networks. As a result, before we go over the overall structure of the proposed network model, as well as the detailed structure of each part and the training of the model, we will go over the principles and composition of convolutional neural networks, forward and backward propagation of convolutional neural networks, and the basic loss function principles. Deep neural networks are built on the foundation of convolutional neural networks (CNNs), which are widely utilized in computer vision, speech recognition, natural language processing, and bioinformatics. Convolutional neural networks, in particular, for computer vision, combine convolution and pooling to efficiently minimize the number of weight parameters, even with the direct input of multidimensional pictures, without requiring a large amount of processing effort. Furthermore, several types of transformation, such as translation, angle, and scale transformation scaling, are extremely invariant to convolutional neural networks. As a result, the target detection technique proposed in this study uses a convolutional neural network structure.

Convolutional neural networks work by mimicking the way humans process information, combining underlying features of an image through multiple layers of convolutional pooling to form higher-level features that represent more abstract information such as categories. Convolutional neural networks consist of a convolutional layer, a pooling layer, and a fully connected layer. The network structure consists of a convolutional layer, a pooling layer, and a fully connected layer. In detail, a convolutional neural network generally starts with alternating convolutional and pooling layers, with the last few layers near the output layer being the fully connected layers, as shown in Figure 3.

Because the layers of the convolutional neural network are completely linked, there are a lot of training parameters, which restricts the depth and complexity of the network model. The information links in each space of the picture, on the other hand, are confined. To obtain global information about an image, it is not necessary to have information about the perceptual field of the entire image but only about a portion of it, and then the global information can be obtained by combining the information of all the local perceptual fields, reducing the number of training parameters even further.

3.4. General Framework of the Model. To solve the current problem of low accuracy of small target detection based on deep learning, we propose a small target detection method based on the jump-connected pyramid model, whose overall structure is shown in Figure 4.

Our model uses VGG16 as the feature extraction network and adds a global receptive field (GRF) module to the feature extraction structure to extract the global feature information of the network. In the prediction stage of the network model, a Skip Feature Pyramid Network is used to fuse the higher-level semantic feature information with the lower-level feature detail information, and nonmaximum suppression is used to obtain the final prediction results. As shown in the figure, the input of the network model is a fixed size color image, and convolution 4_3, convolution 5_3, convolution 6_2, and fully connected layer 7 are the convolutional layers of the VGG16 based network at different scales.

3.5. Jump Connection Pyramid Module. Figure 5 depicts the proposed jump pyramid paradigm in this work. Figure 5(a) depicts the YOLO algorithm's model structure, which predicts using just the final layer of feature layers, with the benefit of increased detection speed but the downside of

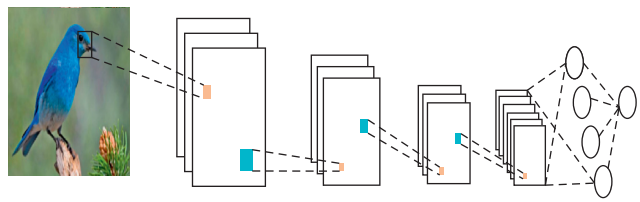

Figure 3: CNN feature structure.

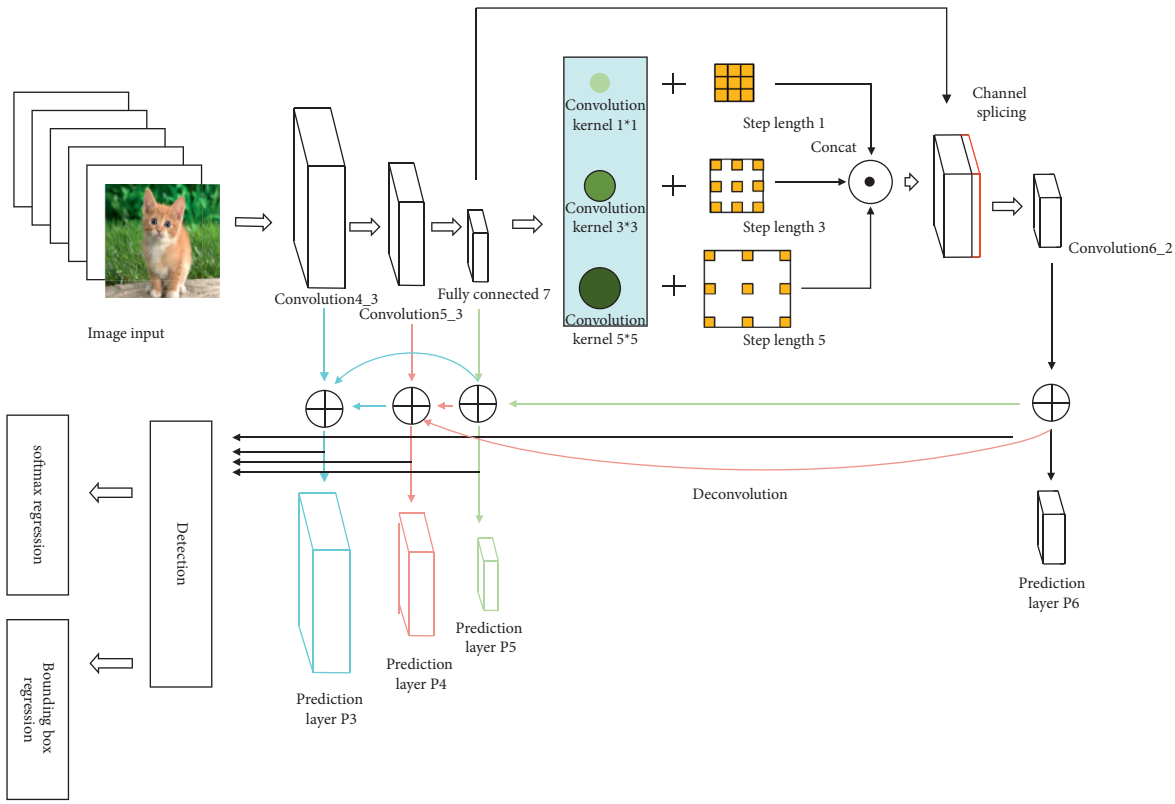

Figure 4: Block diagram of a small target detection model based on a jump connection pyramid.

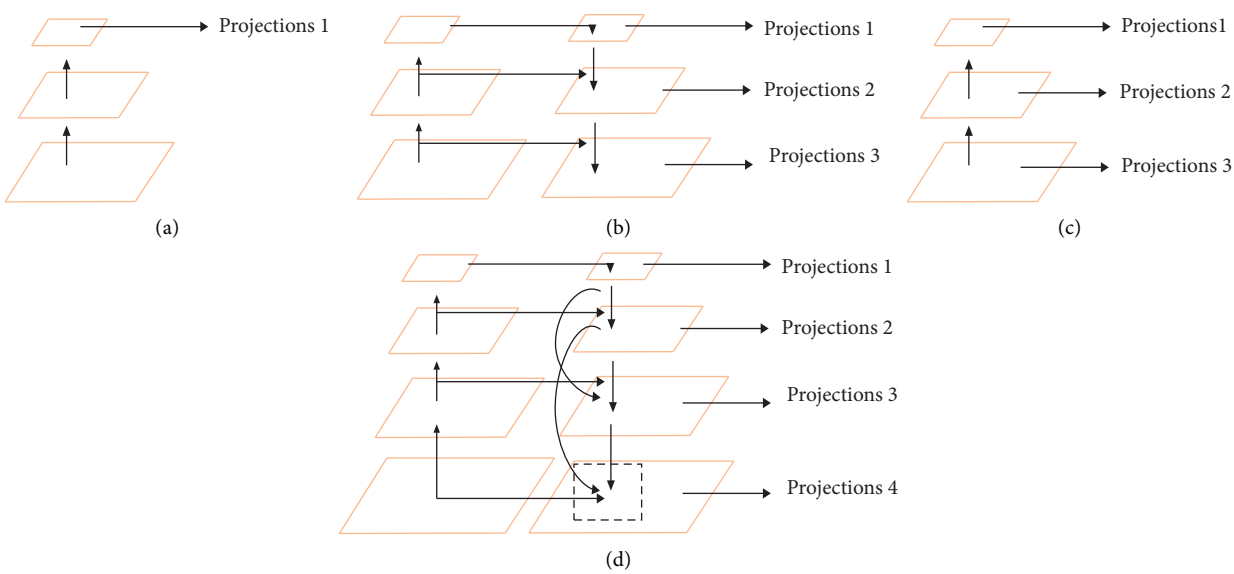

Figure 5: Different structural forms of predictive networks.

poorer detection accuracy. Figure 5(b) is an enhancement to the single-layer feature layer prediction model in Figure 5(a), which predicts higher-level feature layers and hence improves detection outcomes. A top-down pyramid model with distinct feature layers is shown in Figure 5(c). This algorithmic approach takes into account information from nearby feature maps but overlooks the link between higher-level semantic information and lower-level specific feature information. Figure 5(d) shows a jump-connected pyramid model that employs different levels of deconvolution for upsampling and a pixel-by-pixel summation approach to fuse the information between nonadjacent feature maps to address these issues.

In deep convolutional neural networks, the deeper the network model is the more abstract feature information is contained in the image feature layers. For the detection of small targets, the detailed features contained in the lower layer feature maps are equally important for target prediction. Therefore, a jump-connected pyramid model is proposed to fuse the information from the upper and lower feature maps. Furthermore, this allows the use of scale information from different feature layers.

The specific fusion method is shown in Figure 6. First, the high-level feature maps in the selected feature extraction network are passed through a 256-channel 3×3 convolution kernel, changing the number of channels in the different feature layers to the same to facilitate subsequent fusion calculations. After obtaining the same number of feature layers, the adjacent feature maps are upsampled using a 2×2 deconvolution operation with a step size of 2. Nonadjacent feature maps are also upsampled using a 4×4 deconvolution step. The specific deconvolution operation is shown in the following equation:

$$o = \left[\frac{i - f + 2p}{s}\right] + 1, \tag{1}$$

where i is the size of the input feature map; f is the size of the convolution kernel; s is the step size of the deconvolution; and p is the number of pixels filled. The resulting feature map is used as the fused feature map by summing over each pixel.

3.6. Global Feel Wild Module. The top-down network structure is commonly used in current models based on deep convolutional neural networks. This structure neglects the different perceptual fields for different sizes of objects. To address the above problem, a parallel aggregation structure is proposed to enhance the global feature extraction of the overall model by using different step sizes of null convolution and different sizes of convolution kernels. The structure of the global perceptual field module is shown in Figure 7, which can effectively extract features from objects of different scales and sizes.

In the network model, we use the structure of null convolution to improve the perceptual field of the convolutional neural network. Assuming an input feature map of x, a filter of w, and a sampling step of r, for each coordinate i of the output feature map y, the expression for the null convolution is as follows:

$$y[\mathrm{i}] = \sum_k x[i + r \cdot k] w[k]. \tag{2}$$

For a null convolution with a sampling step of r and a convolution kernel size of $k \times k$, the perceptual field size is calculated as follows:

$$k_e = k + (k - 1)(r - 1). \tag{3}$$

The change in perceptual field size can be seen as $k \times k \longrightarrow k_e \times k_e$.

The global perceptual field module's detailed structure is as follows. To begin, by altering the number of channels in the feature map, a 1×1 convolutional layer is utilized to lower the computational burden of the feature model. The visual feature information is then retrieved at various scales utilizing convolution kernels of 1, 3, and 5 sizes, as well as cavity convolution of 1, 3, and 5 sizes. The feature maps are stitched together in channels after that. Using a 1×1 convolution kernel, the number of channels is altered to the same as that of the original feature map, and the corresponding pixels of the original feature map are overlaid. This not only enhances the feature extraction of tiny target objects but also increases the information in the global perceptual field.

3.7. Loss Functions. To balance the problem of large differences in the number of positive and negative samples in the dataset, this section uses negative sample mining to solve the problem of imbalance in the extreme foreground-background categories. In the training process of the network model, instead of using all negative sample bounding boxes and randomly selecting negative sample bounding boxes, the loss of negative samples is ranked and the ratio of positive to negative samples is 3 : 1. Before the final prediction, the bounding boxes generated by the network prediction are bifurcated to filter out the foreground and background. This reduces the number of negative samples. The loss function of the network is shown in the following equation:

$$\begin{aligned} L(\{p_i\}, \{x_i\}, \{c_i\}, \{t_i\}) = {} & \frac{1}{N_{\mathrm{conv}}} \left(\sum_i l_b(p_i, [l_i^* \geq 1]) + \sum_i [l_i^* \geq 1] \cdot l_r(x_i, g_i^*) \right) \\ & + \frac{1}{N_p} \left(\sum_i l_m(c_i, l_i^*) + \sum_i [l_i^* \geq 1] \cdot l_r(t_i, g_i^*) \right), \end{aligned} \tag{4}$$

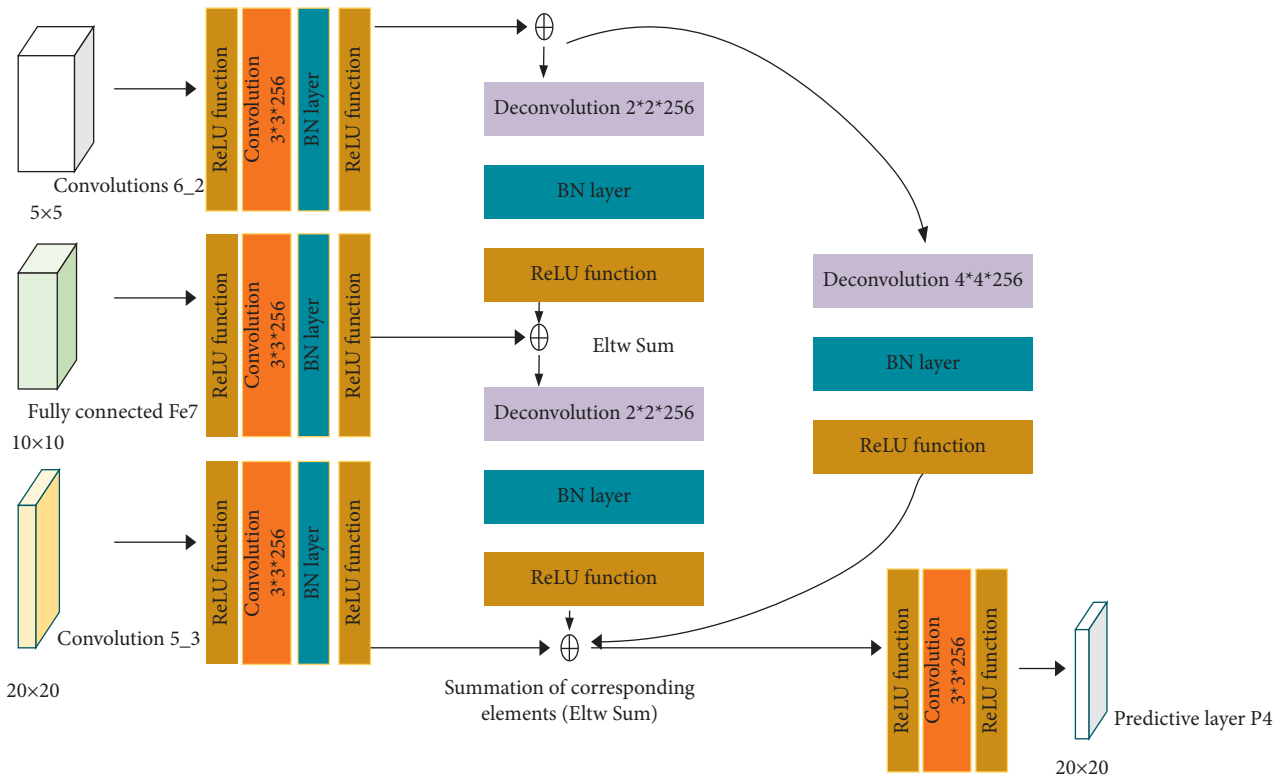

Figure 6: The detailed structure of the jump-connected pyramid.

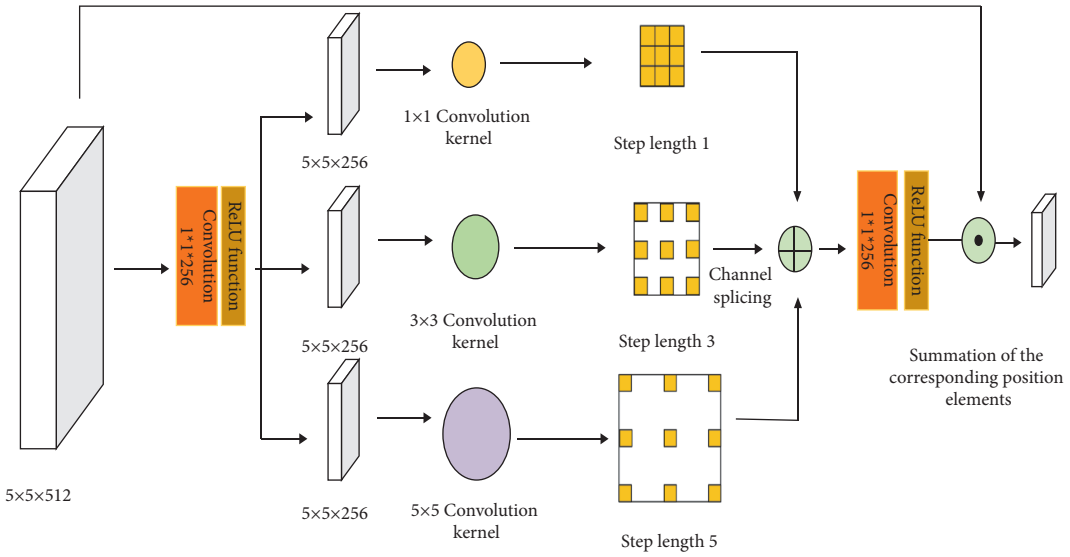

Figure 7: Global Feel Wild module structure.

where i is the index of the bounding box in each training batch of the training set; l_i^* is the corresponding category label of each image annotation in each batch of images; g_i^* is the coordinate label information corresponding to each image annotation; p_i and x_i denote the presence and absence of the target object and the corresponding coordinate information in the bounding box predicted by the network; c_i and t_i are the classes of the objects in the predicted target bounding box and the corresponding coordinate information; N_{conv} and N_p are the numbers of positive sample enclosing boxes in the feature extraction network and the prediction network, respectively; l_b is the cross-entropy loss of the binary classification of the output of the feature extraction network, that is, the determination of whether there is a target in the enclosing box; l_m is the confidence level for the multiclassification task. Similar to the Fast R-CNN algorithm, l_r is the smoothed L1 regression loss. The corresponding loss of the model is only calculated if

the prediction is true when $l_i^* \geq 1$ in the enclosing box. The specific loss function for one of the position loss functions l_r is as follows:

$$l_r(x, g^*, l^*) = \sum_{i \in Pos}^{N} \sum_{m \in \{cx,cy,w,h\}} [l^* \geq 1] \text{smooth}_{L1}\left(x_i^m - \widehat{g}_j^m\right),$$

$$\widehat{g}_j^{cx} = \frac{\left(g_j^{cx} - d_i^{cx}\right)}{d_i^w},$$

$$\widehat{g}_j^{cy} = \frac{\left(g_j^{cy} - d_i^{cy}\right)}{d_i^h},$$

$$\widehat{g}_j^{w} = \log\left(\frac{g_j^w}{d_i^w}\right),$$

$$\widehat{g}_j^{h} = \log\left(\frac{g_j^h}{d_i^h}\right), \tag{5}$$

where (cx, cy, w, h) are the predicted center coordinates of the bounding box and the corresponding width and height, respectively. $(\widehat{g}^{cx}, \widehat{g}^{cy}, \widehat{g}^{w}, \widehat{g}^{h})$ denote the center coordinates of the image annotated coordinates of the center of the bounding box and the corresponding width and height, $(d^{cx}, d^{cy}, d^{w}, d^{h})$ denote the center coordinates of the default bounding box as well as the width and height, and $(x^{cx}, x^{cy}, x^{w}, x^{h})$ denote the center coordinates of the predicted bounding box as well as the width and height.

4. Experiments and Analysis of Results

The algorithmic model in this research was pretrained on the ILSVRCCLS-LOC dataset and employed the VGG16 network as the basis feature extraction network. The method in this part was tested on the PASCAL VOC and MS COCO datasets, respectively, to ensure that the algorithm model was effective. The PASCAL VOC and MS COCO databases provide 20 and 80 categories, respectively, with each category having its own category information and location label information.

4.1. Experimental Analysis of the PASCAL VOC Dataset. The network model was trained on the PASCAL VOC2007 and PASCAL VOC2012 datasets and tested on the PASCAL VOC2007 dataset. Figure 8 shows some example images of the PASCAL VOC dataset. The algorithm model presented in this section was trained for a total of 140K iterations. The learning rate was set to 10^{-3} for the first 80K iterations, decreasing to 10^{-4} for 80K to 100K iterations, 10^{-5} for 100K to 120K iterations, and 10^{-6} for 120K to 140K iterations.

As shown in Table 1, the experimental results of the algorithm model in this section on the PASCAL VOC2007 dataset are compared with those of the mainstream methods. As can be seen from the table, the final detection results vary depending on the size of the input images. The algorithm model obtained the detection accuracy on the PASCAL VOC2007 dataset by calculating the average accuracy of the test set. When the input image size is 320×320, the accuracy of the algorithm model in this section is 80.1%, with a speed of 31.2 frames per second. When the input image is 512×52, the average accuracy of the detection is 81.9% and the speed is 18.2 frames per second. Our algorithmic model is 1% more accurate than the STDN algorithm with the highest accuracy, but the speed of detection is 10.4 frames per second lower. The accuracy of the algorithm model and the speed of detection of the algorithm model are highly dependent on the size of the input image. When the size of the input image is large, the number of corresponding pixels in the image will increase, and the corresponding targets in the image will occupy more pixels, which will increase the computational consumption of the feature extraction phase of the network model and affect the detection efficiency of the network model. The algorithm model in this section improves the detection accuracy of the network model with less reduction in rate and also validates the effectiveness of our proposed algorithm model in improving the accuracy of small targets.

Table 2 shows the results of this part for the PASCAL VOC2007 test set. The average accuracy rates for each of the 20 categories are shown in the table. This method's detection rate for tiny targets is substantially higher than that of other standard detection methods, as seen in the table. For all categories, the average accuracy is 1% greater than the best algorithm. Small objects such as birds, sheep, and plants had greater accuracy than other networks by 2.5 percent, 3.2 percent, and 2.7 percent, respectively. The experimental findings in this study demonstrate the algorithm's usefulness.

4.2. Design of a Target Detection System for Intelligent Mobile Robot Scenarios. Intelligent mobile robots perform the task of target detection through three main processes: sensing, decision-making, and control. The intelligent mobile robot uses sensors on its body to obtain information about the external environment, which is then processed and transmitted to the robot's decision-making system, where the decision-making process makes the appropriate decision and the final decision command controls the mobile robot to complete the corresponding task.

In order to better validate the effectiveness of the proposed scene target detection algorithm for mobile robot environment awareness, we have developed and designed a prototype software system for realistic scene detection using C++ MFC and Python technology. The software is organized as follows: firstly, a requirements analysis is carried out to determine the specific functions to be implemented; then, a prototype target detection system based on the C++ MFC software environment is designed and implemented. Compared to MATLAB and Java, the MFC development environment is more efficient and allows for simpler and more user-friendly programming of the window interface while still meeting the design requirements. The flow chart of the system is shown in Figure 9.

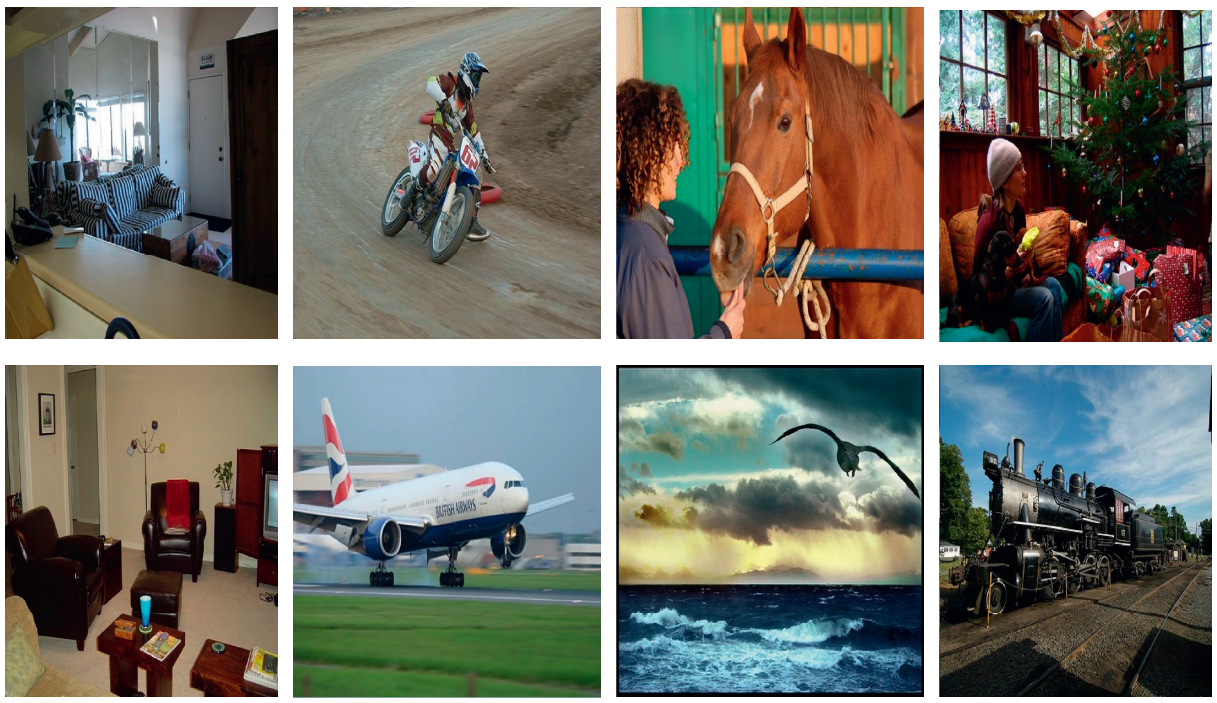

Figure 8: Example image of a PASCAL VOC dataset.

Table 1: Detection results of different network models for PASCAL VOC2007.

Methods	Basic network	Accuracy	Detection speed	Image size
Faster	VGG16	73.2	7	1000 × 600
Faster	Residual-101 [10]	76.4	2.4	1000 × 600
R-FCN	Residual-101	80.5	9	1000 × 600
DSOD300	DS/64-192-4	77.7	17.4	300 × 300
YOLOv2	Darknet-19	78.6	40	544 × 544
SSD300	VGG16	77.5	46	300 × 300
DSSD32	Residual-101	79.5	9.5	321 × 321
STDN321	DenseNet-169	79.2	41.5	321 × 321
Ours320	**VGG16**	**80.1**	**31.2**	**320 × 320**
SSD512	VGG16	78.6	19	512 × 512
DSSD513	Residual-101	81.5	5.5	513 × 513
STDN513	DenseNet-169	80.9	28.6	513 × 513
Ours512	**VGG16**	**81.9**	**18.2**	**512 × 512**

Bold values represent the experimental results of our method.

4.3. Recognition of the Target. We use the RTX 2080ti as the equipment, TensorFlow as the experimental framework, and the COCO database to test the improved YOLO approach. Because the experimental scenario is an office, the COCO dataset was used for a thorough examination. If you need to add a specific target for identification, just upload the relevant information and change the network structure as needed. Figure 8 displays the implementation's final result. There are 90 categories in the dataset, with many small targets, many single-picture targets, and noncentral distribution for the bulk of the items. It is better suitable for daily usage and more difficult to detect. Despite the poor quality of the experimental apparatus, as illustrated in Figure 8, good experimental results are obtained. The algorithm can analyze 416 × 416 images at 29 frames per second with up to 55.3 percent mAP@0.5, which is similar to RetinaNet but four times faster.

4.4. Experimental Analysis of the MS COCO Dataset. The MS COCO dataset tests were undertaken to further evaluate the efficiency of the algorithmic model presented in this section. The MS COCO dataset offers more categories and training pictures than the PASCAL VOC dataset, and it contains data from a variety of complicated scenarios. Table 3 shows the detection results for the MS COCO dataset. The findings for the underlying feature network and several picture sizes are shown. For an input picture

Table 2: PASCAL VOC2007 test results for different categories.

Methods category	Faster	ION	MR-CNN	YOLOv2	SSD300	SS512	STDN321	STDN513	Ours320	Ours 512
Aero	76.5	79.2	80.3	86.3	79.5	84.8	81.2	86.1	84.5	**88.5**
Bike	79	83.1	84.1	82	83.9	85.1	88.3	**89.3**	85.4	86.4
Bird	70.9	77.6	78.5	74.8	76	81.5	78.1	79.5	80.1	**84**
Boat	66.5	65.6	70.8	59.2	69.6	73	72.2	74.3	73.8	**75.8**
Bottle	52.1	54.9	68.5	51.8	50.5	57.8	54.3	61.9	60	**69.4**
Bus	83.1	85.4	88	79.8	87	87.8	87.6	88.5	87.7	**88.9**
Car	84.7	85.1	85.9	76.5	85.7	88.3	86.7	88.3	88.2	**89.2**
Cat	86.4	87	87.8	**90.6**	88.1	87.4	88.7	89.4	89	89.5
Chair	52	54.4	60.3	52.1	60.3	63.5	63.5	**67.4**	63.8	66.7
Cow	81.9	80.6	85.2	78.2	81.5	85.4	83.2	85.5	84.7	**86.4**
Table	65.7	73.8	73.7	58.5	77	73.2	79.4	**79.5**	77.2	73.2
Dog	84.8	85.3	87.2	**89.3**	86.1	86.2	86.1	86.4	86	87.6
Horse	84.6	82.2	86.5	82.5	87.5	86.7	**89.3**	89.2	86.4	88.2
M. bike	77.5	82.2	85	83.4	83.9	83.9	88	**88.5**	86.7	87.5
Person	76.7	74.4	76.4	81.3	79.4	82.5	77.3	79.3	82.5	**84.9**
Plant	38.8	47.1	48.5	49.1	52.3	55.6	52.5	53	56.1	**58.3**
Sheep	73.6	75.8	76.3	77.2	77.9	81.7	80.3	77.9	81.3	**84.9**
Sofa	73.9	72.7	75.5	62.4	79.5	79	80.8	**81.4**	80.4	78.3
Train	83	84.2	85	83.4	87.6	86.6	86.3	86.6	88.5	**87.8**
Tv	72.6	80.4	81	68.7	76.8	80	82.1	**85.5**	79.8	80.8
mAP	73.2	75.6	78.2	76.8	77.5	79.5	79.3	80.9	80.1	**81.9**

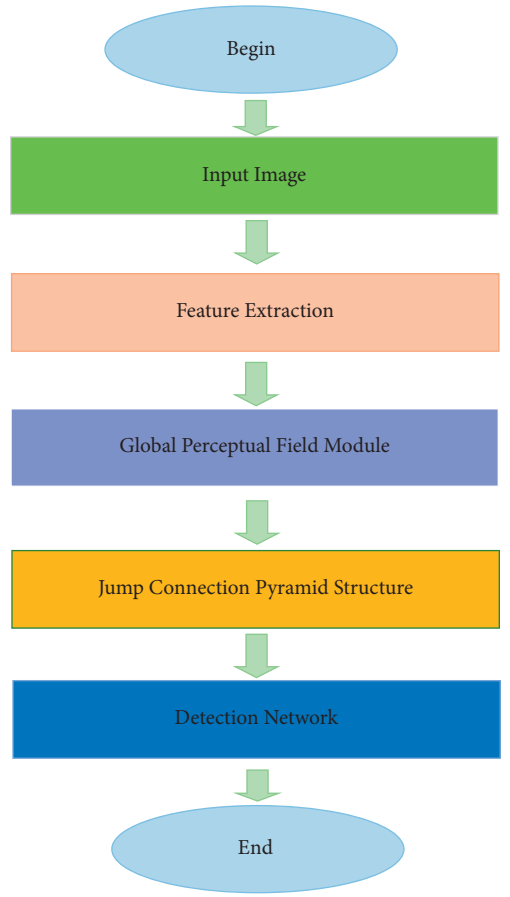

Figure 9: Flow chart of small target detection for robot scenes.

Table 3: MS COCO dataset test results.

Methods	Basic network	AP0.5 : 0.95	$AP_{0.5}$	AP0.75	APS	APM	APL	AR1	AR10	AR100	ARs	AR_M	AR_L
Faster	VGG16	21.9	42.7	—	—	—	—	—	—	—	—	—	—
ION	VGG16	23.6	43.2	23.6	6.4	24.1	38.3	23.2	32.7	33.2	10.1	37.7	53.6
R-FCN	Residual-101	29.2	51.5	—	10.3	32.4	43.3	—	—	—	—	—	—
DSOD	DS/64/192/4	29.3	47.3	30.6	9.4	31.5	47	27.3	40.7	43	16.7	47.1	65
YOLOv2	Darknet	21.6	44	19.2	9	28.9	41.9	24.8	37.5	39.8	14	43.5	59
SSD300	VGG16	25.1	43.1	25.8	6.6	25.9	41.4	23.7	35.1	37.2	11.2	40.4	58.4
DSSD321	Residual-101	28	46.1	29.2	7.4	28.1	47.6	25.5	37.1	39.4	12.7	42	62.6
STDN321	DenseNet	28	45.6	29.4	7.9	29.7	45.1	24.4	36.1	38.4	12.5	42.7	60.1
Ours320	**VGG16**	**28.2**	**47.7**	**29.1**	**10.3**	**31.4**	**43.7**	**25.8**	**38.9**	**41.2**	**16.9**	**47.2**	**61**
SSD512	VGG16	28.8	48.5	30.3	10.9	31.8	43.5	26.1	39.5	42	16.5	46.6	60.8
DSSD513	Residual-101	33.2	53.3	35.2	13	35.4	51.1	28.9	43.5	46.2	21.8	49.1	66.4
STDN513	DenseNet	31.8	51	33.6	14.4	36.1	43.4	27	40.1	41.9	18.3	48.3	57.3
Ours512	**VGG16**	**33.1**	**52.3**	**32.4**	**15.6**	**34.6**	**42.7**	**28.3**	**42.6**	**45.6**	**25.9**	**50.8**	**60.1**

Bold values represent the experimental results of our method.

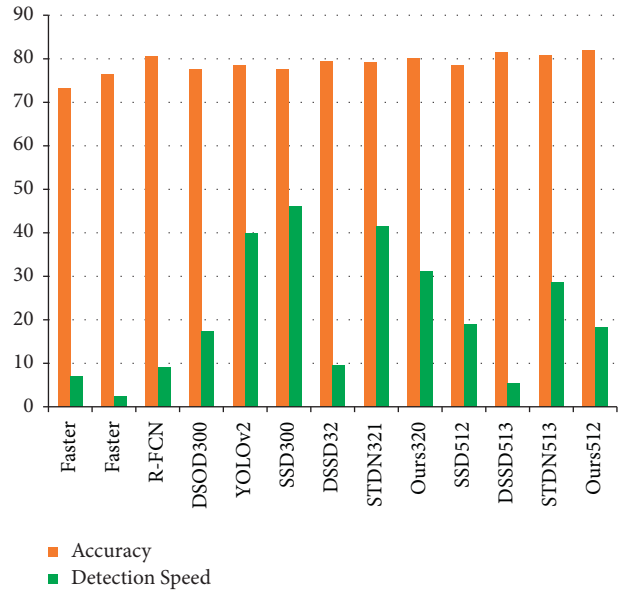

Figure 10: Detection results for PASCAL VOC2007.

size of 320 × 320 and an evaluation metric of AP0.5 : 0.95, the detection method in this section has a 28.2% accuracy. The detecting algorithm's accuracy is 33.1% when the input picture size is 512 × 512 pixels. The detection algorithm in this section has a recall and accuracy of 2.4 percent and 1.2 percent, respectively, greater than the STDN algorithm model, where APS denotes the detection accuracy of tiny targets. The MS COCO dataset has more categories and more sophisticated visual information than the PASCAL VOC dataset. As a result, the detection accuracy is quite poor on average, and there are disparities in the detection results based on different criteria. The maximum detection accuracy was likewise attained for the metrics examined for the detection of tiny objects. As a consequence, the experimental findings support the efficacy of the method presented in this study.

Figure 10 compares the accuracy and detection of all of the approaches we tested for PASCAL VOC2007. The accuracies of Ours320 and Ours512 are 80.1% and 81.9%, respectively, according to this graph, which are the greatest accuracies of all approaches. Similarly, these two approaches had the greatest detected speed among the chosen methods, with 31.2 and 18.2 seconds for Ours320 and Ours512, respectively.

Figure 11 shows the comparison among our selected 10 methods, that is, Faster, ION, MR-CNN, YOLOv2, SSD300, SSD512, STDN321, STDN513, Ours320, and Ours512, respectively, against method categories. From this figure, it is clear that Ours512 is better than other methods that we have selected.

Figure 12 depicts a comparison of the results obtained from the MS COCO dataset test. It is obvious from this figure that Ours320 and Ours512 are superior to the other approaches we considered.

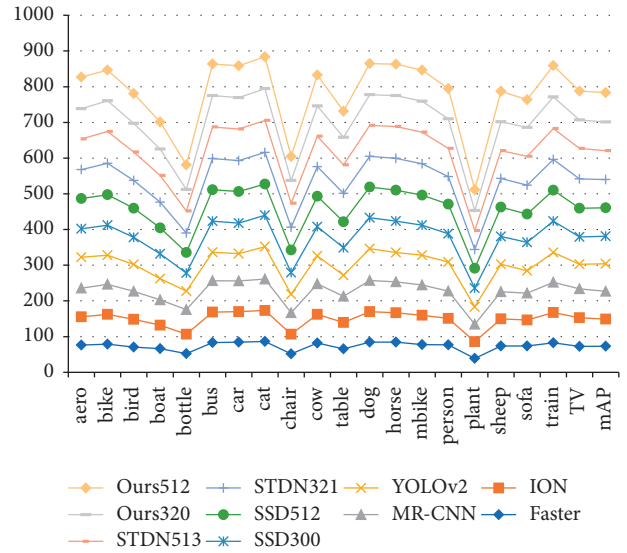

Figure 11: Test results for different categories.

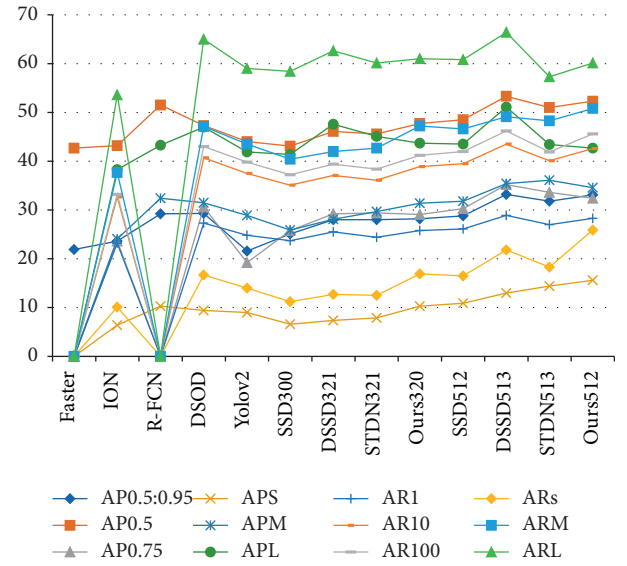

Figure 12: MS COCO dataset test results.

5. Conclusion

Target detection and placement based on deep learning algorithms has been a popular issue in the field of pattern recognition in recent years. People not only want to be free of easy and repetitive tasks, but they also want robotic intelligence to be able to satisfy the needs of humans autonomously, lessening the load on families and society and enabling a variety of intelligent services. We examine challenges in the application of target identification algorithms for mobile robots in this research, with the goal of improving intelligent mobile robots' perception of external environmental information and making intelligent inspection robots more suited to actual surroundings. A jump-connected pyramid model is used to suggest a target detection approach. The high-level feature map semantic information in a deep learning-based target algorithm model is extremely abstract for the target's features, but the low-level feature map information includes comprehensive information. To merge many layers of high-level semantic feature information with the detailed information of low-level feature maps, a jump-connected pyramid structure is proposed. Furthermore, the global feature information is recovered utilizing different sizes of convolution kernels and varied step sizes of complete convolution in the network model to better extract feature information related to objects at different scales. Experiments were carried out on numerous different datasets to validate the algorithm's performance, and the findings verified the algorithm's effectiveness. Furthermore, these findings suggest that the proposed model performs much better than previous algorithm models in terms of tiny target identification accuracy.

Data Availability

The datasets used in this study are available from the corresponding author upon reasonable request.

Conflicts of Interest

The author declares that he has no conflicts of interest.

References

[1] R. Sarc, A. Curtis, L. Kandlbauer, K. Khodier, K. E. Lorber, and R. Pomberger, "Digitalisation and intelligent robotics in value chain of circular economy oriented waste management - a review," *Waste Management*, vol. 95, pp. 476–492, 2019.

[2] G. Ren, T. Lin, Y. Ying, G. Chowdhary, and K. C. Ting, "Agricultural robotics research applicable to poultry production: a review," *Computers and Electronics in Agriculture*, vol. 169, Article ID 105216, 2020.

[3] H. Hassani, E. S. Silva, S. Unger, M. TajMazinani, and S. Mac Feely, "Artificial intelligence (AI) or intelligence augmentation (IA): what is the future?" *A&I*, vol. 1, no. 2, pp. 143–155, 2020.

[4] Y. Tang, M. Chen, C. Wang et al., "Recognition and localization methods for vision-based fruit picking robots: a review," *Frontiers of Plant Science*, vol. 11, p. 510, 2020.

[5] E. E. Joh, "Private security robots, artificial intelligence, and deadly force," *U.C. Davis L. Review*, vol. 51, p. 569, 2017.

[6] C. Kahraman, M. Deveci, E. Boltürk, and S. Türk, "Fuzzy controlled humanoid robots: a literature review," *Robotics and Autonomous Systems*, vol. 134, Article ID 103643, 2020.

[7] A. Rogowski and P. Skrobek, "Object identification for task-oriented communication with industrial robots," *Sensors*, vol. 20, no. 6, p. 1773, 2020.

[8] L. Liu, M. Pietikäinen, J. Qin, O. Wanli, and V. G. Luc, "Efficient visual recognition," *International Journal of Computer Vision*, vol. 128, no. 8, pp. 1997–2001, 2020.

[9] Y. Xue and Y. Li, "A fast detection method via region-based fully convolutional neural networks for shield tunnel lining defects," *Computer-Aided Civil and Infrastructure Engineering*, vol. 33, no. 8, pp. 638–654, 2018.

[10] S. Moradi, P. Moallem, and M. F. Sabahi, "Fast and robust small infrared target detection using absolute directional mean difference algorithm," *Signal Processing*, vol. 177, Article ID 107727, 2020.

[11] H. Zhu, S. Liu, L. Deng, Y. Li, and F. Xiao, "Infrared small target detection via low-rank tensor completion with top-hat

regularization," *IEEE Transactions on Geoscience and Remote Sensing*, vol. 58, no. 2, pp. 1004–1016, 2019.

[12] Y. Tian, L. Ping, and X. Wang, "Pedestrian detection aided by deep learning semantic tasks," 2015, https://arxiv.org/abs/1412.0069.

[13] G. Levi and T. Hassner, "Age and gender classification using convolution neural networks," in *Proceedings of the .2015 IEEE Conference on Computer. Vision and Pattern Recognition Workshops*, pp. 34–42, CVPRW, Boston, MA, USA, 2015.

[14] Y. Zhou, Q. L Liu, L. Shao, and M. Mellor, "DAVE: a unified framework for fast vehicle detection and annotation," 2016, https://arxiv.org/abs/1607.04564.

[15] L. T. Nguyen-Meidine, E. Granger, M. Kiran, and L. A. Blais-Morin, "A comparison of CNN-based face and head detectors for real-time video surveillance applications," 2018, https://arxiv.org/abs/1809.03336.

[16] X. Chen, H. Ma, J. Wan, B. Li, and T. Xia, "Multi-view 3D object detection network for autonomous driving," 2016, https://arxiv.org/abs/1611.07759.

[17] J. Han, D. Zhang, G. Cheng, N. Liu, and D. Xu, "Advanced deep-learning techniques for salient and category-specific object detection: a survey," *IEEE Signal Processing Magazine*, vol. 35, no. 1, pp. 84–100, Jan. 2018.

[18] K. He, X. Zhang, S. Ren, and J. Sun, "Deep residual learning for image recognition," in *Proceedings of the IEEE Conference on Computer Vision and Pattern Recognition (CVPR)*, pp. 770–778, Las Vegas, NV, USA, June 2016.

[19] C. Szegedy, S. Ioffe, V. Vincent, and A. A. Alemi, "Inception-v4, inception-ResNet and the impact of residual connections on learning," in *Proceedings of the Thirty-First AAAI Conference on Artificial Intelligence*, pp. 4278–4284, AAAI Press, February 2017.

[20] K. He, X. Zhang, S. Ren, and J. Sun, "Spatial pyramid pooling in deep convolutional networks for visual recognition," *IEEE Transactions on Pattern Analysis & Machine Intelligence*, vol. 37, pp. 1904–1916, 2014.

[21] G. Gkioxari, R. Girshick, and J. Malik, "Contextual action recognition with r∗ cnn," in *Proceedings of the IEEE international conference on computer vision*, pp. 1080–1088, Santiago, Chile, December 2015.

[22] P. Bharati and A. Pramanik, "Deep learning techniques-R-CNN to mask R-CNN: a survey," *Computational Intelligence in Pattern Recognition*, Springer, Berlin, Germany, pp. 657–668, 2020.

[23] S. Ren, K. He, R. Girshick, and J. Sun, "Faster R-CNN: towards real-time object detection with region proposal networks," *IEEE Transactions on Pattern Analysis and Machine Intelligence*, vol. 39, no. 6, pp. 1137–1149, 2017.

[24] X. Sun, P. Wu, and S. C. H. Hoi, "Face detection using deep learning: an improved faster RCNN approach," *Neurocomputing*, vol. 299, pp. 42–50, 2018.

[25] Y. Tian, G. Yang, Z. Wang, H. Wang, E. Li, and Z. Liang, "Apple detection during different growth stages in orchards using the improved YOLO-V3 model," *Computers and Electronics in Agriculture*, vol. 157, pp. 417–426, 2019.

[26] W. Liu, D. Anguelov, D. Erhan et al., "SSD: Single Shot Multibox detector," *European Conference on Computer Vision*, Springer, Berlin, Germany, pp. 21–37, 2016.

[27] Y. Xiao, X. Wang, P. Zhang, F. Meng, and F. Shao, "Object detection based on faster R-CNN algorithm with skip pooling and fusion of contextual information," *Sensors*, vol. 20, no. 19, p. 5490, 2020.

[28] K. He, X. Zhang, S. Ren, and J. Sun, "Deep residual learning for image recognition," in *Proceedings of the IEEE Conference on Computer Vision and Pattern Recognition*, pp. 770–778, Las Vegas, NV, USA, June 2016.

[29] K. Simonyan and A. Zisserman, "Very deep convolutional networks for large-scale image recognition," 2014, https://arxiv.org/abs/1409.1556.

[30] A. Krizhevsky, I. Sutskever, and G. E. Hinton, "ImageNet classification with deep convolutional neural networks," in *Advances in Neural Information Processing Systems*, vol. 25, pp. 1097–1105, Curran Associates, Inc., Dutchess County, NY, USA, 2012.

[31] S. Gupta, R. Girshick, P. Arbeláez, and J. Malik, "Learning rich features from RGB-D images for object detection and segmentation," in *Proceedings of the European Conference on Computer Vision*, pp. 345–360, Springer, Berlin, Germany, July 2014.

[32] M. Schwarz, H. Schulz, and S. Behnke, "RGB-D object recognition and pose estimation based on pre-trained convolutional neural network features," in *Proceedings of the 2015 IEEE International Conference on Robotics and Automation (ICRA)*, pp. 1329–1335, Seattle, WA, USA, May 2015.

[33] Y. Jia, E. Shelhamer, J. Donahue et al., "Caffe: convolutional architecture for fast feature embedding," in *Proceedings of the 22nd ACM International Conference on Multimedia*, pp. 675–678, Orlando, FL, USA, November 2014.

[34] O. Russakovsky, J. Deng, H. Su et al., "ImageNet large scale visual recognition challenge," *International Journal of Computer Vision*, vol. 115, no. 3, pp. 211–252, 2015.

[35] A. Eitel, J. T. Springenberg, L. Spinello, M. Riedmiller, and W. Burgard, "Multimodal deep learning for robust RGB-D object recognition," in *Proceedings of the 2015 IEEE/RSJ International Conference on Intelligent Robots and Systems (IROS)*, pp. 681–687, Hamburg, Germany, September2015.

[36] K. Lai, L. Bo, X. Ren, and D. Fox, "A large-scale hierarchical multi-view RGB-D object dataset," in *Proceedings of the 2011 IEEE International Conference on Robotics and Automation*, pp. 1817–1824, Shanghai, China, May 2011.

[37] S. Bell, C. L. Zitnick, K. Bala, and G. Ross, "Inside-outside net: detecting objects in context with skip pooling and recurrent neural networks," in *Proceedings of the IEEE conference on computer vision and pattern recognition*, pp. 2874–2883, Las Vegas, NV, USA, June 2016.

[38] T. Y. Lin, P. Dollár, R. Girshick, K. He, B. Hariharan, and S. Belongie, "Feature pyramid networks for object detection," in *Proceedings of the IEEE conference on computer vision and pattern recognition*, pp. 2117–2125, Honolulu, HI, USA, July 2017.

[39] C. Y. Fu, W. Liu, A. Ranga, A. Tyagi, and A. Berg, "Dssd: Deconvolutional single shot detector," 2017, https://arXiv:1701.06659.

[40] Z. Wu, C. Shen, and A. Van Den Hengel, "Wider or deeper: revisiting the ResNet model for visual recognition," *Pattern Recognition*, vol. 90, pp. 119–133, 2019.

[41] H. Rebecq, G. Gallego, and E. Mueggler, "EMVS: event-based multi-view stereo-3d reconstruction with an event camera in real-time," *International Journal of Computer Vision*, vol. 126, no. 12, pp. 1395–1414, 2018.

[42] G. N. Desouza and A. C. Kak, "Vision for mobile robot navigation: a survey," *IEEE Transactions on Pattern Analysis and Machine Intelligence*, vol. 24, no. 2, pp. 237–267, 2002.

[43] C. Cadena, L. Carlone, H. Carrillo et al., "Past, present, and future of simultaneous localization and mapping: toward the robust-perception age," *IEEE Transactions on Robotics*, vol. 32, no. 6, pp. 1309–1332, 2016.